



W. W. F. Klingsch
C. Rogsch
A. Schadschneider
M. Schreckenberg
Editors

Pedestrian and Evacuation Dynamics 2008

 Springer

Pedestrian and Evacuation Dynamics 2008

Wolfram W.F. Klingsch • Christian Rogsch •
Andreas Schadschneider • Michael Schreckenberg
Editors

Pedestrian and Evacuation Dynamics 2008

 Springer

Editors

Wolfram W.F. Klingsch
Baustofftechnologie und Brandschutz
Bergische Universität Wuppertal
Pauluskirchstr. 7
42285 Wuppertal, Germany
klingsch@uni-wuppertal.de

Andreas Schadschneider
Institut für Theoretische Physik
Universität zu Köln
Zülpicher Str. 77
50937 Köln, Germany
as@thp.uni-koeln.de

Christian Rogsch
Baustofftechnologie und Brandschutz
Bergische Universität Wuppertal
Pauluskirchstr. 7
42285 Wuppertal, Germany
christian@rogsch.de

Michael Schreckenberg
Physik von Transport und Verkehr
Universität Duisburg-Essen
Lotharstr. 1
47048 Duisburg, Germany
schreckenberg@ptt.uni-due.de

ISBN 978-3-642-04503-5

e-ISBN 978-3-642-04504-2

DOI 10.1007/978-3-642-04504-2

Springer Heidelberg Dordrecht London New York

Library of Congress Control Number: 2009941802

Mathematics Subject Classification (2000): 49-XX, 4906, 65-XX, 65C05, 65C20, 68-XX, 68Q80, 68U05, 68U07, 68U10, 68U20, 68U35, 82-XX, 82C21, 90-XX, 90BXX, 91-XX, 91CXX, 93-XX, 93E25

© Springer-Verlag Berlin Heidelberg 2010

This work is subject to copyright. All rights are reserved, whether the whole or part of the material is concerned, specifically the rights of translation, reprinting, reuse of illustrations, recitation, broadcasting, reproduction on microfilm or in any other way, and storage in data banks. Duplication of this publication or parts thereof is permitted only under the provisions of the German Copyright Law of September 9, 1965, in its current version, and permission for use must always be obtained from Springer. Violations are liable to prosecution under the German Copyright Law.

The use of general descriptive names, registered names, trademarks, etc. in this publication does not imply, even in the absence of a specific statement, that such names are exempt from the relevant protective laws and regulations and therefore free for general use.

Cover illustration: Norbert Sdunzik

Cover design: WMXDesign GmbH, Heidelberg

Printed on acid-free paper

Springer is part of Springer Science+Business Media (www.springer.com)

Preface

Proper management of evacuation processes is one of the basic requirements within life safety concepts, and it helps to prevent critical situations from getting out of control. Super high-rise buildings, deep underground stations or shopping areas, airplanes for the mass transportation, sport stadiums or meeting places with tens of thousands of visitors—they all call for new dimensions in safe evacuation planning. Research results in evacuation dynamics give answers to these challenges.

PED-conferences are the prime address for all research in this field. The increasing number of participants from different fields of research reflect their importance. After PED-conferences in Germany (Duisburg, 2001), Great Britain (Greenwich, 2003) and Austria (Vienna, 2005), the PED 2008 Conference in Wuppertal/Germany reached new heights with more than 120 participants from 20 countries and nearly 100 presentations. The wide field of topics discussed in presentations also reflects deeper understanding of fundamental effects as well as the stronger interactions between different research areas. New test designs offer new important basic data, new analysis procedures open a better understanding of complex interactions, new model designs allow more realistic simulations, and the input from architectural design and the medical references on physical limitations help to realize a safe evacuation design. On the one hand all these data give an outlook of future possibilities and sometimes they open an astonishing new understanding of seemingly well-known data. On the other hand, they make clear the limitations of our current knowledge. Integration of evacuation analysis into fire safety concepts is without doubt an important step to improve the quality of life safety planning. But incorporation of tools for calculating toxic gas concentrations, for example, should be accepted only with caution, as too little reliable information about the chemistry of fire sources and its modeling is available.

The PED 2008 Conference Proceedings offer a wealth of the latest information on all fields of pedestrian evacuation and will be an important source for all researchers working in their different disciplines.

Finally, we would like to thank all people who, mostly behind the scenes, have helped to make the conference a success. Special thanks go to Mrs. Birgit Dahm-Courths for the excellent job she has done in preparing these proceedings, and to Mrs. Sabine Mehring for the excellent assistance before and during the whole conference. Furthermore, we would like to thank Wahed Azimi, Tobias Rupprecht, Dimitrios Toris, Nina Wellenberg, and Andreas Winkens for their “helping hands”, without whose support this conference could not have been realized.

Wuppertal, Köln, Duisburg
July 2009

Wolfram W.F. Klingsch
Christian Rogsch
Andreas Schadschneider
Michael Schreckenberg

Contents

Part I Experiment and Evacuation

The UK WTC9/11 Evacuation Study: An Overview of the Methodologies Employed and Some Preliminary Analysis <i>Edwin R. Galea, Lynn Hulse, Rachel Day, Asim Siddiqui, Gary Sharp, Karen Boyce, Louise Summerfield, David Canter, Melisa Marselle, and Paul V. Greenall</i>	3
Evacuation Movement in Photoluminescent Stairwells <i>Guylène Proulx and Noureddine Bénichou</i>	25
Automatic Extraction of Pedestrian Trajectories from Video Recordings <i>Maik Boltes, Armin Seyfried, Bernhard Steffen, and Andreas Schadschneider</i>	43
Stairwell Evacuation from Buildings: What We Know We Don't Know <i>Richard D. Peacock, Jason D. Averill, and Erica D. Kuligowski</i>	55
Evacuation of a High Floor Metro Train in a Tunnel Situation: Experimental Findings <i>Monika Oswald, Hubert Kirchberger, and Christian Lebeda</i>	67
Using Laser Scanner Data to Calibrate Certain Aspects of Microscopic Pedestrian Motion Models <i>Dietmar Bauer and Kay Kitazawa</i>	83
Pedestrian Vision and Collision Avoidance Behavior: Investigation of the Information Process Space of Pedestrians Using an Eye Tracker <i>Kay Kitazawa and Taku Fujiyama</i>	95

FDS+Evac: An Agent Based Fire Evacuation Model
Timo Korhonen, Simo Hostikka, Simo Heliövaara, and Harri Ehtamo .. 109

Comparisons of Evacuation Efficiency and Pre-travel Activity Times in Response to a Sounder and Two Different Voice Alarm Messages
David Purser 121

Design of Voice Alarms—the Benefit of Mentioning Fire and the Use of a Synthetic Voice
Daniel Nilsson and Håkan Frantzich 135

Enhanced Empirical Data for the Fundamental Diagram and the Flow Through Bottlenecks
Armin Seyfried, Maik Boltjes, Jens Kähler, Wolfram Klingsch, Andrea Portz, Tobias Rupprecht, Andreas Schadschneider, Bernhard Steffen, and Andreas Winkens 145

Parameters of Pedestrian Flow for Modeling Purposes
Valerii V. Kholshchikov and Dmitrii A. Samoshin 157

Emergency Preparedness in the Case of a Tsunami—Evacuation Analysis and Traffic Optimization for the Indonesian City of Padang
Gregor Lämmel, Marcel Rieser, Kai Nagel, Hannes Taubenböck, Günter Strunz, Nils Goseberg, Thorsten Schlurmann, Hubert Klüpfel, Neysa Setiadi, and Jörn Birkmann 171

Case Studies on Evacuation Behaviour in a Hotel Building in BART and in Real Life
Margrethe Kobes, Nancy Oberijé, and Martina Duyvis 183

Analysis of Empirical Trajectory Data of Pedestrians
Anders Johansson and Dirk Helbing 203

Model-Based Real-Time Estimation of Building Occupancy During Emergency Egress
Robert Tomastik, Satish Narayanan, Andrzej Banaszuk, and Sean Meyn 215

Experiments on Evacuation Dynamics for Different Classes of Situations
Jarosław Was 225

Prediction and Mitigation of Crush Conditions in Emergency Evacuations
Peter J. Harding, Martyn Amos, and Steve Gwynne 233

Start Waves and Pedestrian Movement—An Experimental Study
Christian Rogsch 247

Clearance Time for Pedestrian Crossing
Craig R. Childs, Taku Fujiyama, and Nick Tyler 249

Ship Evacuation—Guidelines, Simulation, Validation, and Acceptance Criteria
Hubert Klüpfel 257

Empirical Study of Pedestrians’ Characteristics at Bottlenecks
Andreas Winkens, Tobias Rupprecht, Armin Seyfried, and Wolfram Klingsch 263

RFID Technology Applied for Validation of an Office Simulation Model
Vincent Tabak, Bauke de Vries, and Jan Dijkstra 269

Study on Crowd Flow Outside a Hall via Considering Velocity Distribution of Pedestrians
Xiang Shu Liu, Jia Xiu Pan, Liang Yujuan, and Yu Xue 277

Analysis on the Propagation Speed of Pedestrian Reaction: Velocity of Starting Wave and Stopping Wave
Akiyasu Tomoeda, Daichi Yanagisawa, and Katsuhiko Nishinari 285

Part II Simulation and Modeling

Toward Smooth Movement of Crowds
Katsuhiko Nishinari, Yushi Suma, Daichi Yanagisawa, Akiyasu Tomoeda, Ayako Kimura, and Ryousuke Nishi 293

Modeling Evacuees’ Exit Selection with Best Response Dynamics
Harri Ehtamo, Simo Heliövaara, Simo Hostikka and Timo Korhonen 309

Front-to-Back Communication in a Microscopic Crowd Model
Colin Marc Henein and Tony White 321

Comparison of Various Methods for the Calculation of the Distance Potential Field
Tobias Kretz, Cornelia Bönisch, and Peter Vortisch 335

Agent-Based Simulation of Evacuation: An Office Building Case Study
Yiqing Lin, Igor Fedchenia, Bob LaBarre, and Robert Tomastik 347

A Genetic Algorithm Module for Spatial Optimization in Pedestrian Simulation
Lukas Kellenberger and Ruedi Müller 359

Opinion Formation and Propagation Induced by Pedestrian Flow
Yu Xue, Yan-fang Wei, Huan-huan Tian, and Li-juan Liang 371

Passenger Dynamics at Airport Terminal Environment
Michael Schultz, Christian Schulz, and Hartmut Fricke 381

Application Modes of Egress Simulation
Steve M.V. Gwynne and Erica D. Kuligowski 397

Investigating the Impact of Aircraft Exit Availability on Egress Time Using Computer Simulation
Edwin R. Galea, Madeleine Togher, and Peter Lawrence 411

Bounded Rationality Choice Model Incorporating Attribute Threshold, Mental Effort, and Risk Attitude: Illustration to Pedestrian Walking Direction Choice Decision in Shopping Streets
Wei Zhu and Harry Timmermans 425

A SCA-Based Model for Open Crowd Aggregation
Stefania Bandini, Mizar Luca Federici, Sara Manzoni, and Stefano Redaelli 439

Hardware Implementation of a Crowd Evacuation Model Based on Cellular Automata
Ioakeim G. Georgoudas, Georgios C. Sirakoulis, and Ioannis T. Andreadis 451

Applying a Discrete Event System Approach to Problems of Collective Motion in Emergency Situations
Paolo Lino and Guido Maione 465

SIMULEM: Introducing Goal Oriented Behaviours in Crowd Simulation
Sébastien Paris, Delphine Lefebvre, and Stéphane Donikian 479

Conflicts at an Exit in Pedestrian Dynamics
Daichi Yanagisawa, Akiyasu Tomoeda, and Katsuhiko Nishinari 491

Improving Pedestrian Dynamics Modeling Using Fuzzy Logic
Phillip Tomé, François Bonzon, Bertrand Merminod, and Kamiar Aminian 503

Modeling the Link Volume Counts as a Function of Temporally Dependent OD-Flows
Dietmar Bauer 509

Effect of Subconscious Behavior on Pedestrian Counterflow in a Lattice Gas Model Under Open Boundary Conditions
Kuang Hua, Song Tao, Li Xingli, and Dai Shiqiang 517

Hand-Calculation Methods for Evacuation Calculation—Last Chance for an Old-Fashioned Approach or a Real Alternative to Microscopic Simulation Tools?
Christian Rogsch, Henning Weigel, and Wolfram Klingsch 523

Adding Higher Intelligent Functions to Pedestrian Agent Model
Toshiyuki Kaneda, Takumi Yoshida, Yanfeng He, Masaki Tamada, and Yasuhiro Kitakami 529

“FlowTech” and “EvaTech”: Two Computer-Simulation Methods for Evacuation Calculation
Ilya Karkin, Vladimir Grachev, Andrey Skochilov, and Vladimir Zverev . 537

Large Scale Microscopic Evacuation Simulation
Gregor Lämmel, Marcel Rieser, and Kai Nagel..... 547

Numerical Optimisation Techniques Applied to Evacuation Analysis
Rodrigo Machado Tavares and Edwin R. Galea 555

A Multi-Method Approach to the Interpretation of Pedestrian Spatio-Temporal Behaviour
Alexandra Millonig and Georg Gartner..... 563

The Microscopic Model and the Panicking Ball-Bearing
Colin Marc Henein and Tony White 569

Design of Decision Rules for Crowd Controlling Using Macroscopic Pedestrian Flow Simulation
Stefan Seer, Norbert Brändle, and Dietmar Bauer..... 577

3-Tier Architecture for Pedestrian Agent in Crowd Simulation
Gao Peng and Xu Ruihua 585

Optimising Vessel Layout Using Human Factors Simulation
Steven J. Deere, Edwin R. Galea, and Peter J. Lawrence..... 597

Agent-Based Animated Simulation of Mass Egress Following an Improvised Explosive Device (IED) Attack
Douglas A. Samuelson, Matthew Parker, Austin Zimmerman, Stephen Guerin, Joshua Thorp, and Owen Densmore 605

A Novel Kinetic Model to Simulate Evacuation Dynamics
Sergei Burlatsky, Vladim Atrazhev, Nikolay Erikhman, and Satish Narayanan 611

Egress Route Choice Modelling—Concepts and Applications
Volker Schneider and Rainer Könnecke 619

Architectural Cue Model in Evacuation Simulation for Underground Space
Chengyu Sun, Bauke de Vries, and Qi Zhao 627

Integrating Strategies in Numerical Modelling of Crowd Motion
Juliette Venel 641

Small-Grid Analysis of Evacuation Processes with a Lattice Gas Model for Mixed Pedestrian Dynamics
Yan-fang Wei, Yu Xue, and Shi-qiang Dai 647

Evacuation Simulation and Human Behaviour Models in Tall Buildings
Marja-Liisa Siikonen and Janne S. Sorsa 653

Proof of Evacuation Routes and Safety Exits: Time Data as the Main Criteria for the Evaluation of Escape Routes and Safety Exits?
Nathalie Waldau, Marita Kersken-Bradley, and Thilo Hoffmann 659

Dependence of Modelled Evacuation Times on Key Parameters and Interactions
David Purser 667

A Modification of the Social Force Model by Foresight
Bernhard Steffen 677

Models for Crowd Movement and Egress Simulation
Hubert Klüpfel 683

Modelling Pedestrian Escalator Behaviour
Michael J. Kinsey, Edwin R. Galea, Peter J. Lawrence, Darren Blackshields, Lynn Hulse, Rachel Day, and Gary Sharp 689

Introducing a Coupled Model for Simulating Crowd Behaviour	
<i>Alicia Guadalupe Ortega Camarena and Dominik Jürgens</i>	697
Evacuation Modelling of Fire Scenarios in Passenger Trains	
<i>Jorge Capote, Daniel Albear, Orlando Abreu, Mariano Lázaro, and Arturo Cuesta</i>	705
Pedestrian Dynamics with Event-Driven Simulation	
<i>Mohcine Chraïbi and Armin Seyfried</i>	713

Part III Psychology

The Need for Behavioral Theory in Evacuation Modeling	
<i>Erica D. Kuligowski and Steve M.V. Gwynne</i>	721
NO-PANIC. “Escape and Panic in Buildings”—Architectural Basic Research in the Context of Security and Safety Research	
<i>Christa Illera, Matthias Fink, Harry Hinneberg, Karin Kath, Nathalie Waldau, Andrea Rosič, and Gabriel Wurzer</i>	733
Was It Panic? An Overview About Mass-Emergencies and Their Origins All Over the World for Recent Years	
<i>Christian Rogsch, Michael Schreckenberger, Eric Tribble, Wolfram Klingsch, and Tobias Kretz</i>	743
Hierarchical Structure of the Mass and Group-Level Behaviors in Urban Rail Transfer Stations	
<i>Xiaolei Zou, Ruihua Xu, and Peng Gao</i>	757
The Use of a Structure and Its Influence on Evacuation Behavior	
<i>Steve M.V. Gwynne and Dave Boswell</i>	773

Part IV Miscellaneous

Inhalation Injury of Lung and Heart After Inhalation of Toxic Substances	
<i>Herbert Löllgen and Dieter Leyk</i>	781
Quantitative Comparison of International Design Standards of Escape Routes in Assembly Buildings	
<i>Burkhard Forell, Ralf Seidenspinner, and Dietmar Hossler</i>	791

Visualizing the Human Form for Simulation and Planning
Gabriel Wurzer 803

A Real-Time Pedestrian Animation System
Christian Schulz, Michael Schultz, and Hartmut Fricke 811

**Modeling of Escape Routes According to Occupancy,
Economy, and Level of Safety in Slovak Republic**
Martin Lopusniak 819

List of Participants 825

Experiment and Evacuation

The UK WTC9/11 Evacuation Study: An Overview of the Methodologies Employed and Some Preliminary Analysis

Edwin R. Galea¹, Lynn Hulse¹, Rachel Day¹, Asim Siddiqui¹, Gary Sharp¹, Karen Boyce², Louise Summerfield², David Canter³, Melisa Marselle³, and Paul V. Greenall³

¹ Fire Safety Engineering Group, University of Greenwich, London, UK
e-mail: e.r.galea@gre.ac.uk

² FireSERT, University of Ulster, Belfast, UK
e-mail: ke.boyce@ulster.ac.uk

³ Centre for Investigative Psychology, University of Liverpool, Liverpool, UK
e-mail: d.canter@liverpool.ac.uk

Summary. This paper briefly describes the methodologies employed in the collection and storage of first-hand accounts of evacuation experiences derived from face-to-face interviews with evacuees from the World Trade Center (WTC) Twin Towers complex on 11 September 2001 and the development of the High-rise Evacuation Evaluation Database (HEED). The main focus of the paper is to present a preliminary analysis of data derived from the evacuation of the North Tower.

1 Introduction

The evacuation of the WTC complex in 2001 is one of the largest full-scale evacuation of people in modern times with over 14,000 people escaping from the buildings. The survivors' evacuation experiences provide valuable insights into the factors that helped and hindered egress within the rapidly changing high-rise building environment. Thus understanding survivors' evacuation experiences is a vital component in unravelling the complex inter-related processes that drive high-rise building egress. It is now widely acknowledged that there are three broad stages through which any egress proceeds; making sense of the situation, planning to leave, and then finding and using a route out of the building [1]. It has also long been recognised that there are important social processes that influence decision making and thereby modify egress patterns. Analysis of the accounts of those evacuating from the WTC towers not only enables us to develop a more detailed understanding of what processes underlie each of the main evacuation stages but, due to the large number of

people involved, it enables us to explore the impact of aspects of social and organisational factors on the effectiveness of the whole evacuation.

The project described in this paper called HEED—High-rise Evacuation Evaluation Database—is funded by the UK Engineering and Physical Science Research Council (EPSRC—project GR/S74201/01 and EP/D507790). It involves a collaboration between the Universities of Greenwich, Ulster and Liverpool and aims to collect first hand evacuation experiences of survivors from the WTC twin towers evacuation. Some 271 evacuees have been interviewed. Details of the project can be found on the HEED website www.wtc-evacuation.com. Several studies have already investigated the evacuation of the WTC [2–4] using published accounts from survivors, questionnaires and focus groups. However, the main features which distinguish HEED from other projects are:

- a more open approach to data collection through the development of an interview process that attempts to extract a richness of data not previously evident in other projects;
- an attempt to understand more fully the social and organisational factors that influence evacuation activity, e.g., the influence of groups, organisational structure and perception of risk;
- an attempt to quantify crowd densities and understand how these contributed to observed behaviour and human performance;
- accessibility of the data, and full interview transcripts, through the development of an online relational database which will be accessible in the future by *bona fide* users.

The main aim of the HEED project is to distill, organise and present 9/11 survivor interview accounts into the HEED relational database. The objectives of project HEED are to:

- collect and collate human experiences in the WTC disaster and structure this into a database to provide an interactive research tool;
- ensure that the data collected is transformed into information that is of immediate, medium and long term use to the managers, designers, enforcement agencies and owners of medium- and high-rise buildings, the research community involved in the development of computer based evacuation models and all those interested in understanding the social process that structure emergency and related situations;
- provide easy, free and immediate access to the database for *bona fide* users;
- use the information collected and collated to perform preliminary analyses of the data to identify some of the key factors that influence the design and management of medium- to high-rise buildings and to test some of the social psychological models of human actions in such circumstances;
- investigate the WTC evacuation using evacuation models and using the HEED data suggest how these models could be improved.

1.1 Research Themes

The HEED study identified an extensive range of human factors research issues of relevance to fire safety engineering. These included:

- **Cue recognition and response:** It is important to understand the participants' entire experience from the time they received a cue and examining such areas as, What cues did they receive? How were they interpreted? How did they respond? Currently, engineers use arbitrary values to represent occupant response times, often simply taking, for example, 0 to 2 minutes. In this study we aim to determine a representative range of response times and understand the interaction between response times and other factors, such as proximity of incident, risk perception, group membership, etc.
- **Conditions during egress:** We aim to explore whether the participant experienced any difficulties during egress (e.g. congestion)? What did it cause them to do? Did they walk or run and at what speed and why?
- **Fatigue:** All engineering analysis of high-rise building evacuation currently either ignores the impact of fatigue or treats it in a crude and arbitrary manner. Was fatigue an issue in the WTC evacuation, did it exert an influence on the overall evacuation and if so, in what way? We wished to determine the extent to which participants had to stop for a rest, and if so, where, for how long, and with whom?
- **Travel speeds:** A very basic piece of data essential in all engineering evacuation analysis is the travel speed of people on stairs. Obviously, if this key parameter is incorrectly represented the entire evacuation analysis becomes invalid. There is some evidence to suggest that the travel speeds in the WTC evacuation were significantly lower than those typically used in engineering analysis [2, 3]. What was the speed of people on the stairs and what contributed to it? How was the travel speed related to crowd densities, population demographics, etc?
- **Perception of risk:** This is an area which has been little explored in the fire literature. This research aimed to capture participants' level of perceived risk during their evacuation from the Twin Towers. Subsequent analysis will enable a better understanding of, for example, the relationship between response times and perceived risk and types of cues and perceived risk.
- **Group formation:** All engineering evacuation analysis currently assumes that occupants evacuate as individuals. This belief is implicit in all building design. This key assumption has an important influence on the unfolding evacuation dynamic and potentially on the overall efficiency of the evacuation. We wished to determine the participant's experiences as a member of one or more groups as they evacuated the WTC, and understand the group's lifecycle from the participant's perspective. How did the group form? What were the factors driving formation and dissolution? What was the nature of the group membership? How did the group operate?

- **Choosing and locating an exit route:** The key to understanding movement in an emergency is to discover why people choose a particular route. Was their exit route pre-planned? Was it the closest? Familiar? Used in fire drill? What were the reasons behind some participants choosing to evacuate by the elevator?
- **Merging flows and deference behaviours:** In high-rise building evacuations a key behaviour is the nature in which people on the floor merge with people on the stairs as this determines how the evacuation unfolds and how quickly any particular floor can empty into the staircase. We wished to explore fundamental questions concerning this behaviour, for which engineers do not have clear answers e.g., Did people on the stairs defer to people entering the staircase from the floor and allow them to enter? Did the floor and stair occupants take turns and allow a one-for-one merging/filtering or does one flow win out over the other for long periods of time?
- **Experience and training:** A number of people in the 9/11 evacuation had previous experience of evacuating the building during the earlier terrorist bomb attack of 1993. Additionally, many people had second hand experience of the 1993 evacuation through friends, family and colleagues. How did their first and second hand experience impact upon their evacuation? What training had people undergone in case of emergency situations and had they learned behaviours from this and other evacuation experiences.
- **Management and organisational structure:** The different ways in which the diverse organisations marshalled and instructed their employees to leave is also explored in order to determine its implications for various engineering provisions. For example, how bureaucratic was the company the participant worked for? Did this have any impact on the nature of the participant's emergency response? Did managers instruct their staff members to evacuate? Why or why not? Did employees inform managers of their decision to evacuate? Did their manager/superior communicate with them?

Analysis of the collected data is not yet completed. In this paper we present some preliminary analysis of data relating to the North Tower (WTC1) addressing the first five research themes. The analysis should not be considered complete and is subject to change as more data is analysed.

2 Research Protocols

This investigation focused on those persons who evacuated from WTC1 or WTC2 on 9/11. The research protocols—which received Institutional Review Board (IRB) approval from John Jay College of Criminal Justice in New York (JJ), the New York City Department of Health and Mental Hygiene (NYC

DOHMH) and Pace University—are outlined in brief below. A more detailed account may be found in [5].

2.1 Recruitment

Participants for the interviews were recruited mainly from the World Trade Center Health Registry (WTCHR), compiled by the NYC DOHMH. The WTCHR is a voluntary list of individuals who were exposed to the environmental effects of 9/11. Individuals who wished to take part in the study were invited to register on the project’s website (www.wtc-evacuation.com), and invited to complete a web based Pre-Interview Questionnaire. In total, 3,064 invitation letters were sent via the DOHMH. A 9.3% response rate was obtained from the DOHMH mailshot and 287 people registered to take part in our study. In total 271 interviews were conducted during five extended interview periods by the researchers in New York.

2.2 Interview Structure and Content

The interview schedule comprised a combination of free-flow narrative and a semi-structured interview. Participants were asked to tell their story in their own words. The purpose of this was to enable participants to relax and facilitate memory recollection and uncover experiences and situations in the WTC evacuation that might not previously have been considered by the researchers. The free-flow narrative was followed by a semi-structured interview, during which the interviewer confirmed and expanded upon details previously provided in the free flow and sought to ascertain more specific information regarding the participant’s entire experience relevant to the specific areas of research interest.

Throughout the interview, interviewers attempted to extract from the participant as much contextual information relating to time and location of the described experiences. For example, it was considered important to determine an estimate for the actual time (absolute) that something occurred, and the time taken for certain events to occur, e.g., waiting in line, fire fighters to pass. Interviewers also attempted to establish where the participant was when this occurred (floor level, location on floor). Where absolute times could not be determined they tried to determine the times that things were occurring relative to global time markers, e.g., time WTC2 hit, time WTC2 collapsed. This information was crucial to address specific engineering research questions related to, e.g., response times, travel speeds, etc.

To quantify participants’ experiences of crowd densities during the stair descent, computer generated animations of people descending stairs based on the classic Fruin densities (also often referred to as Level of Service or LoS) [6] were periodically administered. These animated images were introduced whenever the participant entered or exited a stairwell, and whenever they

mentioned crowding on the stairs. This information, together with information on time periods where important events occurred on stairs, assists in identifying travel speeds on stairs and associated crowd densities. During the interview, participants were also asked to complete risk perception and organisational structure questionnaires. The risk perception questionnaire comprised a general question on how at risk they felt at the time (rated on a seven point scale, from 1 'no risk' to 7 'very high risk') and why, followed by a series of statements related to different risk attributes, identified from risk perception studies, e.g., information available, control, dread, etc., to which they had to rate their level of agreement. Participants were asked to complete the risk perception questionnaire up to four different times during their evacuation, i.e. at WTC1 impact (or when the participant noticed something unusual happening), when the participant was deciding to evacuate, when the participant knew that WTC2 had been hit (if applicable) and when the participant knew WTC2 had collapsed (if applicable). In the organisational structure questionnaire, the participant was asked to rate their level of agreement on a 5-point scale with each of 10 statements related to the how the company functioned, e.g., 'In my job, my authority was precisely defined'; 'In my organisation, clear lines of reporting and authority were made known'.

The semi-structured interview was piloted in New York over a period of six weeks. From the pilot study it became apparent that there were at least seven distinct phases that evacuees experienced during 9/11, namely: pre-recognition, recognition, response, horizontal evacuation, vertical evacuation, evacuation interruption (where participants chose to interrupt their evacuation, e.g., after the public announcements in WTC2) and exiting the WTC complex. These phases constitute a new model of evacuation behaviours and as such informed the development of the database.

3 Development of HEED Database and Coding Process

The HEED database is developed in Microsoft (MS) Access and is specifically designed to store and retrieve coded HEED WTC evacuation data from interview transcripts. The information stored in the HEED database provides a means to address key research questions relating to human factors issues associated with evacuation from high-rise buildings.

The HEED database was developed from a content analysis of a small subset of participants' interview accounts. The content analysis indicated that participants' evacuations comprised of a variety of complex and detailed experiences ranging from observations and interpretations of events to subsequent feelings and actions. A method was required to systematically identify, categorise and store this experience information into a logical structure for later analysis. From the content analysis, a three level Experience structure was devised in order to systematically categorise participants' rich evacuation experiences into mutually exclusive categories. As further transcripts were anal-

used, new categories were developed and the three level experience structure was expanded. As part of the Experience hierarchy a large number of codes and associated code definitions were developed to uniquely categorise each experience. The Experience hierarchy served as a coding framework enabling the identification of the participants' experiences from interview transcripts and the unambiguous and systematic categorisation of those experiences. The development of the HEED database structure was undertaken in parallel with the development of the three-level Experience hierarchy and associated Experience codes. Data within HEED is stored using the logical arrangement of the three-level Experience hierarchy. In addition to coded Experience information, the HEED database also includes the full transcripts for each interviewed participant and the pre-interview questionnaire responses. The HEED database captures all of the participants' evacuation experiences such as stimuli (e.g., observational cues), cognitions (e.g., incident interpretations) and individual and group behaviours (e.g., actions and reactions) within the three-level Experience hierarchy. Supporting information such as the time of an experience and participant's location are captured by associated contextual information.

The highest level of the hierarchy is the Experience Category or Level 1 experience. There are six core experience categories, namely: Action, Sensory, State, Cognition, Dialogue and Risk Perception. Below the Experience Category is the Experience Type or Level 2 experiences which identify the nature of the experience. The final element in the hierarchy is the actual Experience extracted from the text, also referred to as the Level 3 experience. The hierarchical experience structure can be thought of simply as short cut menus leading to the appropriate Level 3 experience [5].

In addition to coding the Level 3 Experience, 'contextual information' is required to clarify the detail of the experience. For example, the contextual information could be the time at which the experience occurred or an estimation of the crowd density when the experience occurred. As noted earlier, crowd density estimations are provided by the participant during the semi-structured component of the interview using a specially devised Fruin based tool. The time at which an experience occurred is represented within HEED in several ways. It can be actual or estimated times provided explicitly by the participant during the interview or a time interval estimated by the research team based on the evidence provided within the transcript.

The process used in this paper involved defining a total of 17 time sub-intervals around four known event times, namely the impact into WTC1 at 8:47 a.m. (**T1**), the impact into WTC2 at 9:03 a.m. (**T8**), the collapse of WTC2 at 9:59 a.m. (**T15**) and the collapse of WTC1 at 10:28 a.m. (**T21**). As an example of this process, consider the time span between T1 and T8. This was divided into six sub-intervals with **T4** being the sub-interval "Between T1 and T8" i.e. $08:47 < \text{event time} < 09:03$, while sub-interval **T3** is "Closer to T1 than T8" i.e. $08:47 < \text{event time} < 08:55$. The process of estimating the time when an event occurred involved the analyst reading the interview transcript

and from the evidence provided determining which time sub-interval best captured the event time.

Before the experience can be coded into the database it must first be identified. This is achieved by editing the interview transcripts into Behavioural Patterns (BP). BPs are chunks of transcript text which contain experience and corresponding contextual data. Once a BP is identified the relevant experience codes and contextual information relating to the experience are determined and coded into the database, along with the actual BP and its location within the transcript. A BP can have several mutually exclusive experience categories attached.

As part of the data entry, the entire edited transcript of the interview is linked to the database, as is factual information obtained from the pre-interview questionnaire. Names of people and companies are removed from all entries, being replaced with coded IDs, ensuring that the identity of the participant remains confidential. Information within the database can be retrieved by constructing and running queries using MS Access Query. However, this is only for local use and therefore a web based query builder will be developed for accessing the data remotely. This will enable a wider audience to access the information contained within HEED.

4 Preliminary Data Analysis

In total 271 persons who evacuated the WTC on 9/11 were interviewed, 129 from the North Tower (WTC1) and 125 from the South Tower (WTC2), of which 63.6% of the WTC1 population and 59.2% of the WTC2 population were males. The mean age of the populations were 46 and 42.5 years of age for WTC1 and WTC2 respectively. The oldest person interviewed was 68 years of age (in both towers) while the youngest person interviewed was 24 and 22 years of age in WTC1 and WTC2 respectively. Of the population interviewed, 29% and 23% of the WTC1 and WTC2 population respectively had worked in the WTC towers for less than 12 months while 22% and 21% of the WTC1 and WTC2 populations respectively had experienced the 1993 bombing and evacuation.

The majority of people interviewed were located in the upper third of the WTC1 and WTC2 i.e. 42% of the WTC1 sample and 57% of the WTC2 sample were located on floors above the 60th floor (see Fig. 1). Finally, the Body Mass Index (BMI) of the sample was also determined. The BMI is defined as the individual's body weight divided by the square of their height and is used to assess how much an individual's body weight departs from what is normal or desirable for a person of given height. For Western European and North American adults a BMI of: less than 17.5 may indicate anorexia; between 17.5 and 18.5 suggests the person is underweight; between 18.5 and 25 indicates optimal weight; between 25 and 30 suggests the person is overweight; between 30 and 40 the person is obese and over 40, the person is morbidly obese.

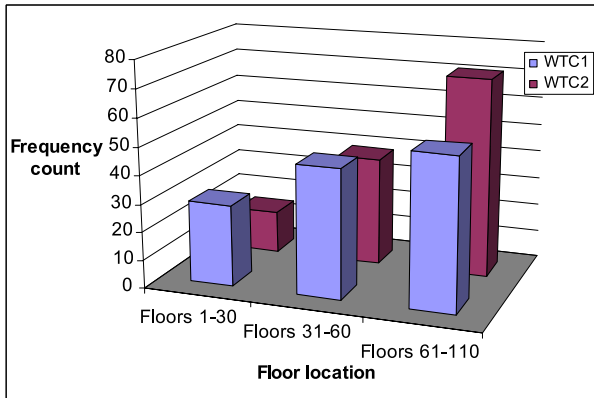


Fig. 1. Floor distribution of survey participants.

For the WTC1 sample, 63% of the population was in the overweight/obese categories with 22% of the population in the morbidly obese category. For WTC2 population, 74% of the population was overweight/obese while 28% of the population was in the morbidly obese category. A total of 68% of the sample population were in the overweight/obese categories.

4.1 Stoppage Data for WTC1

The number of times evacuees stop during their descent is an important parameter as it will impact the average travel speed of the individual. The reason why evacuees stopped is also important as it addresses issues associated with environmental conditions on the stairs and the possible contribution that the population demographic may have on occupant performance on the stairs. Several recent WTC studies [2, 3] have reported lower than expected average stair travel speeds. Unfortunately, due to a lack of data in both these studies, it was not been possible to determine why the travel speeds were so low. There has been considerable discussion in the literature that the growing obesity epidemic [7] may be adversely affecting the ability of building occupants to travel large distances on stairs during building evacuations and may be the cause of the lower than expected average travel speeds found in these studies.

For these reasons stoppage data was extracted from the transcripts of 124 WTC1 participants (those evacuating from above floor 2). The data suggested that 82% of the participants stopped at least once, 30% stopped once and 2.4% reported stopping more than 20 times during their descent. A total of 318 stop incidents were reported by the participants. Congestion was the most frequent cause of stoppages, being reported by 54% of the population and causing 44% of the stoppages. The next most frequent cause of stoppages were caused by ascending fire fighters (17.6% of stoppages) or descending groups of injured people (17.6% of stoppages). In these situations the participants would

Floor region	No stops	Stopped at least once	Total
High: 61–90	10 16%	53 84%	63 100%
Mid: 31–60	5 10%	45 90%	50 100%
Low: 1–30	7 28%	18 72%	25 100%
Total	22 16%	116 84%	138 100%

Table 1. Stoppage frequency for WTC1.

interrupt their descent to allow the fire fighters/injured to pass. These types of incidents were reported by 38% and 31% of the population respectively. The third most common cause of stopping was the need to take a rest, with 9.7% of the reported stoppages due to participants needing to rest. Rest stops were reported by 16% of the population. The fourth most common cause of stoppages was due to environmental conditions. A total of 3.5% of the reported stoppages were caused by environmental conditions such as debris, smoke, heat, water on the stairs, etc. This type of stoppage was reported by 9% of the population.

The stoppage frequency is summarised in Table 1 and includes data from 14 participants who stopped because their companion required a rest stop. We note that 70% of the sample from each of the three floor regions reported stopping at least once however, participants in the High and Mid levels are more likely to stop during descent than those in the Low levels. This information relates to stoppages of all kinds and so does not distinguish between people requiring rest stops and those that stopped due to congestion or other issues.

It is clear from this data that there were frequent interruptions to the steady descent of evacuees which would have contributed to the smaller than expected travel speeds. Also, the higher in the building the evacuee starts the evacuation, the greater the likelihood of stopping due to the greater chance of being subjected to the various stoppage reasons. In addition, 90% of all reported stoppages were caused by reasons other than fatigue. Most participants did not feel the need to take rest stops. This applied even to people located in the upper part of the building and in the Overweight/Obese BMI category. For example, consider the following statement from a participant who started their evacuation from the 73rd floor with a BMI of 27 (Overweight):

WTC1/073/0001, Page 22 L24–37

I: Did you ever get tired yourself and have to stop and rest?

P: Physically, no ... I mean I encountered several people though that were experiencing difficulty getting out ... so

there were people depending on your physical age and condition and whatever that struggled ... I don't mean to make light of ...

I: No, no, it's okay.

P: That it was "a walk in the park" ... but me personally, I never felt physically challenged ...

While this person started their evacuation from the upper third of the tower and was classed as "Overweight", he did not feel the need to take a rest stop. However, this person reported stopping two times due to congestion. Clearly, when participants stop due to congestion, they were also resting. This is demonstrated by another participant who started on the 69th floor and had a BMI of 37 (Obese):

WTC1/069/0001, Page 16 L21–27

I: Did you ever stop to have a break to have a rest?

P: Never no.

I: Nothing like that.

P: Only when I was forced, when it wasn't moving.

I: When it wasn't moving, yes.

P: Then I would sit on the step and I was watching and watching and someone would say okay we are moving now

...

By default, participants forced to stop due to congestion or other external reasons were also resting and recovering. This may mask the effect of BMI in causing the participants to take a rest stop. To put the need to rest into perspective it is worth noting the total travel distances associated with descending from various levels within the WTC buildings. Using Stair C as the egress route and assuming that the central route down the stairs is taken, the total travel distance from 110th floor to the 2nd floor is estimated to be 1,439 m; from the 90th floor, 1,192 m; from the 60th floor 755 m and from the 30th floor, 345 m.

In the following analysis we compare participants who reported stopping to rest with those who reported not stopping. The sample consists of 42 participants, 22 reported not stopping at all and 20 reported the need for a rest stop, of which four were interviewed participants and 16 were participants who reported that their companion (not interviewed) required a rest stop, two of which were disabled and so are not considered (see Table 2) in this analysis. Approximately half the sample in the Mid and High regions required rest stops while less than a third of the sample in the Low region required rest stops. Furthermore, more than a quarter of the sample in the High region required multiple rest stops. Of the interviewed participants requiring a rest stop, two were classified as Obese (BMIs 38, 47) and two were Normal (BMIs 19, 22) according to their BMI. Of the 16 participants reporting companions needing to rest, 14 companions were women and 2 were men. Thus, of

Floor region	No stops	At least 1 rest stop	1 rest stop	2 rest stops	3 rest stops	4 rest stops	Total
High	10	11	5	4	1	1	21
61–90	48%	52%	24%	19%	5%	5%	100%
Mid	5	4	3	0	1	0	9
31–60	54%	44%	33%	0%	11%	0%	100%
Low	7	3	3	0	0	0	10
1–30	70%	30%	30%	0%	0%	0%	100%
Total	22	18	11	4	2	1	40
	55%	45%	28%	10%	5%	3%	100%

Table 2. Rest stop frequency for WTC1.

the 20 people requiring rest stops, 85% were female, 45% were in the Overweight/Obese categories, 45% had medical conditions and 10% were fatigued but not Overweight/Obese.

A total of 16 people requiring a rest stop were not interviewed and so their BMI's were not available. Of these 16, descriptions of six people were provided by their travelling companions (who were interviewed) from which a BMI was estimated. Overall the average BMI for the sample requiring a rest stop (30.4) is similar to average BMI of the sample who did not require a rest stop (29.5)—both bordering on Obese. In the High region (floors 61–90), those requiring rest stops had marginally larger BMI (30.0) than those not requiring rest stops (27.2)—both bordering on Obese. This information suggests that BMI does not appear to be an indicator of whether a person required a rest stop. It should be noted that 60% of the WTC1 population surveyed were in the Overweight/Obese categories and the sample size is small. However, being located high in the building is a reasonable indicator of whether or not a rest stop is required. It is suggested that rather than BMI, the overall level of fitness and the travel distance may be better predictors of whether a person requires a rest stop during a high rise evacuation.

4.2 Stair Travel Speeds

The information presented in this paper relating to stair travel speeds concerns preliminary data analysis derived from Stair C of the North Tower. This stair was 44 inches wide and so was one of the two narrow stairs in the WTC buildings. Several recent WTC studies [2, 3] have reported lower than expected average stair travel speeds. The UK BDAG study [2] first reported lower than expected travel speeds derived from their sample of survivor accounts published in the public domain. Their relatively small sample of usable data suggested a mean speed of 0.24 m/s. The later NIST report [3], based on a larger sample of first hand survivor accounts suggested an even lower mean travel speed of 0.2 m/s.

To put these values into perspective it is worth noting the data reported by Fruin which is often used in engineering analysis [6]. Fruin measured free flow stair travel speeds of 700 males and females of various ages, both descending and ascending stairs. For males aged 30–50 descending stairs, his data produces a mean speed of 0.88 m/s (4.2 floors/min) while for males aged over 50 his data suggest a mean speed of 0.69 m/s (3.3 floors/min) [6]. In recent correspondence between Galea, Pauls and Fruin, it was noted that the free flow stair data measured by Fruin was over only one or two flights of stairs and so does not include the potential impact of fatigue on stair travel speeds [8]. As a result, Galea suggests that this data should be used with care in high-rise building applications. Other data often quoted concerning stair travel speeds is that produced by Pauls derived from observations of high-rise building evacuation drills [9]. This data suggests a mean speed of 0.52 m/s (2.5 floors/min) in optimal flow conditions and 0.22 m/s (1.1 floors/min) in crush conditions [9]. As a reference, it is worth noting that for Stair C of the WTC a speed of 1.0 floors/min is equivalent to 0.21 m/s while 3 floors/min is equivalent to 0.62 m/s. These values were derived using 12.3 m as the average travel distance from floor to floor taking a stair and landing centre line travel path (average value derived for normal and machine floors).

Estimating the stair travel speed from participant transcripts is a difficult and time consuming process. Thus far we have restricted our analysis only to people who used Stair C and who completed their journey from start to finish on Stair C. Analysis is further restricted to individuals for which we have a reasonable estimate of when they entered the stairs and when they left the stair. This is based on the time analysis described in Sect. 3. An individual’s journey between the beginning and end points is reconstructed from information provided in the interview transcript, noting events such as:

- Environmental conditions encountered—where and when?
- Encountering fire fighters—where, when, how long?
- Encountering injured being carried down—where, when, how long?
- Encountering congestion—where, when, how long, Fruin Density?

In reconstructing segments of the journey it is often necessary to make some assumptions concerning aspects of that part of journey e.g.

- Duration of stoppage if not provided,
- Speed in floors/min based on provided Fruin density and description of movement e.g. If Fruin F estimated and participant describes very slow movement, assume approximate speed of 1 floor/min—unless other evidence provided.

Where it is not possible to make reasonable estimates of journey segments, a simple average speed is determined for the journey from beginning to end. The following extract from an account provides an example of where a travel speed is estimated for a journey segment:

WTC1/040/0001, P11 L7–12

I: And, again, you were travelling 40 seconds for each floor? A minute for each floor?

P: At first it was about a minute for each floor and then it gradually picked up. Within a few floors I was moving fairly well. I remember one floor every 30 seconds because I even timed it during my descent for a couple floors so I thought ok we're doing about 2 a minute.

Another example demonstrates an estimation made by the participant of the crowd density (Fruin Density $F = \text{Orange}$) at floor 55, how he travelled very fast down the stairs from floor 60 to 55 and then come to a stop when encountering the Fruin F .

WTC1/060/0001 P11 L24–40

I: Okay, so that's Orange. And so when it got congested, did you say this was because other people were coming into the stairs?

P: Yes, other people were coming in as well as already in the stairwell from whatever floor they had come from.

...

I: And how did that affect the travel speed?

P: It slowed down dramatically.

I: So, were you having to stop at any point?

P: We stopped at 55, right there, because there was obviously a lot more people. I mean we were running down for the first 5 stairs, "Boom, boom, boom, boom, boom", two stairs at a time sometimes. When we got to 55, we couldn't do that because we would plough into people ...

Using this type of information it is possible to construct a "Floor–Time" diagram for the participant. Such diagrams were first used by Pauls to assist in the description of the progress of evacuation drills in multi-floor buildings [10]. The diagram provides a very useful way of visualising the progressive evacuation of a high-rise building. When used forensically in reconstructing an evacuation based on first hand survivor accounts, it also provides a means of corroborating the accounts of the evacuees, checking the consistency of assumptions in reconstructing the path and filling in information gaps in the accounts of some evacuees.

Depicted in Fig. 2 is a Floor–Time diagram for 12 evacuees who used Stair C that meet the criteria described above. The numbers on the curves indicate the participant ID, e.g. 2 refers to participant WTC1/021/0001 (BMI 18.6) who started their evacuation on the 21st floor, while 12 refers to participant WTC1/073/0003 (BMI 33.0) who started their evacuation on the 73rd floor. The slope of the line or line segment represents the speed of the participant in floors/min. For participant 2 we calculate an average travel speed of 2.0 floors/min while for participant 12 we calculate an average travel speed

of 1.2 floors/min. These speeds can be converted to an approximate speed in m/s using the approximate 12.3 m travel distance estimate or a more accurate conversion can be derived using the actual travel distance for the floors covered, including transfer corridors, the later is used here where possible.

There are several innovations to the standard Floor–Time diagram that have been introduced in this project to convey additional information relating to the descent of the individuals. Each line segment is coloured according to the Fruin density that was reported by the individual. Black indicates that no Fruin density was reported, Blue indicates Fruin densities of A ($<0.5 \text{ p/m}^2$) or B ($0.5\text{--}0.7 \text{ p/m}^2$), Green indicates Fruin densities of C ($0.7\text{--}1.1 \text{ p/m}^2$) or D ($1.1\text{--}1.4 \text{ p/m}^2$) and Red indicates Fruin densities of E ($1.4\text{--}2.5 \text{ p/m}^2$) or F ($>2.5 \text{ p/m}^2$). Coloured squares indicate a spot Fruin density only at the specified location. A dashed line indicates that there were complications along the egress route that makes the path unrepresentative of the travel speeds that one would normally expect, even for the level of congestion encountered. For example, participant 2 suffered from a serious pre-incident medical condition which made their travel speed unrepresentative while participant 4 reported stopping 10–20 times during the descent and participant 12 was reluctant to overtake the people in front of him who were carrying a disabled person down the stairs.

Various types of brackets are also shown along some of the journey segments. These are used to represent the presence of factors which may impact the travel speed. A curved bracket indicates that the factor occurred somewhere in the region indicated but a precise location was not provided while a

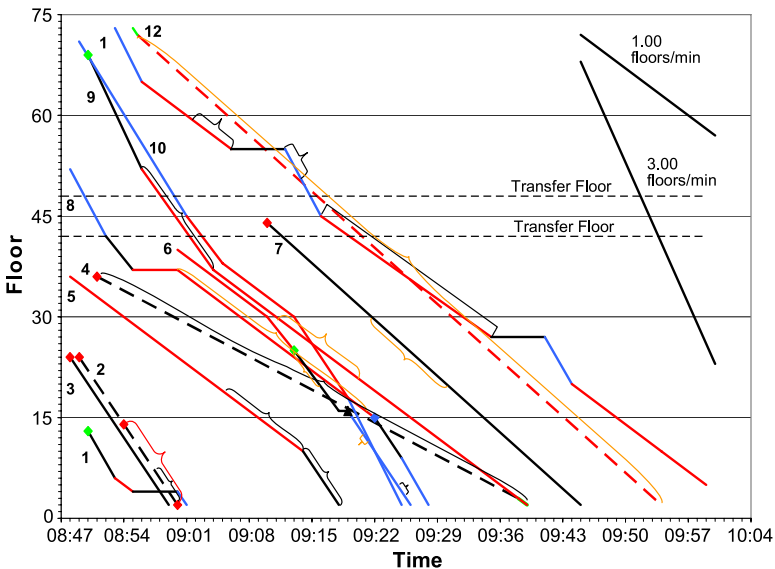


Fig. 2. Floor vs time diagram for 12 evacuees using Stair C.

square bracket indicates that the factor persisted over the entire region indicated. The colour of the bracket also carries some significance. Gold indicates the presence of fire fighters ascending the stair which interfered with the participants downward progress, Red indicates a Fruin density of E or F and Black indicates the presence of environmental factors such as smoke, heat, dust, water or debris which impacted the progress of the participant.

For complicated paths such as 1 or 11 a travel speed can be determined for each segment of the journey and an overall average speed can be determined by simply taking the beginning and end points. For participant 1 the average travel speed for the journey from floor 13 to floor 2 is 1.0 floors/min (0.21 m/s) while for participant 11 the average travel speed from floor 73 is 1.03 floors/min (0.22 m/s). Note that both these participants have periods during their journey where they have passed through high crowd density regions (Fruins E and F) and participant 11 has stopped his journey on two occasions. As can be seen from Fig. 2, when the participant passes through high crowd density regions their travel speed, measured by the slope of the line, is less than when they travel through lower crowd density regions. Using the Floor–Time diagram we thus note that at times participant travel speeds can be considerably higher than suggested by taking the simple average travel speed. Furthermore, we can also measure the impact that the stoppages reported in Sect. 4.1 and high crowd densities can have on the average travel speed. This may begin to explain why the early BDAG [2] and NIST [3] studies found lower than expected travel speeds.

Using the information provided by the interview transcripts it is possible to construct a Fruin Map of the WTC buildings. The Fruin map provides an indication of the crowd densities on the stairs as reported by the survivors. In addition, information relating to the environmental conditions on the stairs and the location and time at which fire fighters were encountered can also be recorded. The Fruin map displays each floor in the tower and indicates the conditions on the stairs in small time slices. Presented in Fig. 3 is an example of a portion of the Fruin Map for Stair C showing floors 25–73 in 6 minute time slices. Each entry in the Fruin Map is derived from a survivor statement. The coloured bars represent the Fruin density as described for Fig. 2. In addition, the coloured bars are numbered so that the particular statement can be found (numbering same as used in Fig. 2) and the coloured bar also carries the actual Fruin density. The coloured entries that cover only a single floor represent the Fruin density estimates provided by the participants on entry into the staircase. As the time slices used in the Fruin map are of finite duration, the crowd density observation provided by the evacuee may not cover the entire duration of the imposed time slice. To reflect this, a fill pattern has been introduced that describes the portion of the time slice that the observation is valid for. A solid fill suggests that the observation is valid for the entire duration of the time slice. A hash fill indicates that the observation starts after, and ends before the time slice. Horizontal bars indicate that the observation ends before the specified time period while diagonal bars

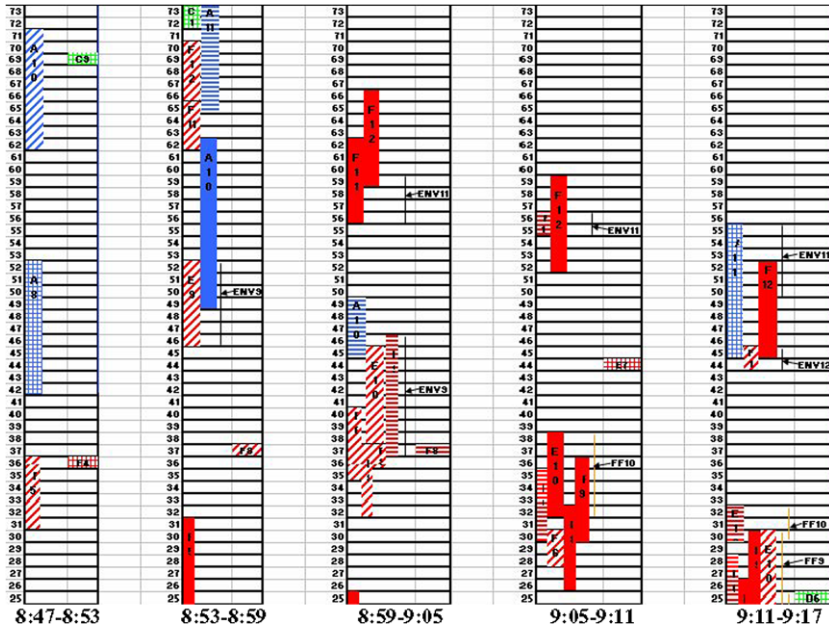


Fig. 3. Fruin map of North Tower Stair C showing floors 25–73 in 6 minute time slices up to 9:17.

indicate that the observation starts after the beginning of the specified time period. Using this system many of the apparent conflicts in crowd density may be explained. In addition, vertical gold lines indicate the presence of fire fighters while vertical black lines indicate adverse environmental conditions were encountered.

The Fruin map can be used in conjunction with the Floor–Time diagram to fill in gaps in the Fruin density information provided by some of the participants. This enables a better understanding of the environment through which the participants travelled. Putting all this information together provides a possible explanation for the apparently low average travel speeds observed. Firstly, the travel speeds of four individuals (1, 6, 8, 11) can be adjusted upwards by taking into account the identified stops. Secondly, two individuals (4, 12) had low travel speeds due to complicating factors i.e. one was travelling behind a group carrying a disabled individual and did not wish to overtake (12), while the other person had pre-existing medical conditions which effectively meant that he had a movement related disability (4). Using this sample of 10 people produces (see Table 3) an average stair speed of 0.33 m/s which is some 65% higher than that reported by the NIST study [3]. While considerably larger than the average reported in the NIST study it is still relatively low.

Further analysis of the travel speed data presented in Table 3 reveals that those individuals with average travel speeds lower than the group mean speed

ID	Graph	BMI	Unknown	Low	High	Original	Average
WTC1	ID		fruits	fruits	fruits	average	adjusted
				(A, B)	(E, F)	speed (m/s)	speed (m/s)
13/0002	1	28	50%	25%	25%	0.21	0.38
21/0001	2	19	87%	–	13%	0.41	0.41
24/0001	3	26	96%	–	4%	0.41	0.41
36/0002	4	28	91%	–	3%	0.15	0.15
36/0003	5	48	23%	–	77%	0.23	0.23
40/0001	6	24	0%	38%	64%	0.30	0.31
44/0002	7	37	98%	–	2%	0.25	0.25
52/0004	8	25	10%	49%	45%	0.27	0.31
69/0001	9	37	0%	24%	75%	0.29	0.29
71/0004	10	32	0%	63%	40%	0.41	0.41
73/0001	11	28	0%	41%	68%	0.22	0.27
73/0003	12	33	96%	–	1%	0.26	0.26

Table 3. Travel speed information and percentage of journey subjected to various crowd densities for the 12 identified individuals who used Stair C.

experienced high crowd densities for more than 45% of their journey, with the lowest average travel speed corresponding to an individual that spent 77% of their journey in high crowd densities. While those with average travel speeds higher than the group mean travel speed spend only short parts of their journey in high crowd densities. This tends to suggest that the lower average stair speed observed for participants using Stair C may simply be due to the relatively high crowd densities encountered during their descent.

4.3 Response Times

Occupant response time data was determined from the transcripts as explained in Sect. 3. The response times for WTC1 evacuees were allocated into one of 10 time bands (measured in minutes from WTC1 impact) based around the four key times, namely: (0–1), (1–4), (1–8), (1–16), (8–16), (12–16), (16–21), (16–26), (16–72), (44–72). A total of 81 response times were derived from the transcripts. Due to small samples within the above time bands, data was collapsed into three broad response time groups i.e. Rapid (<1 min), Moderate (>1 and <8 min) and Long (>8 min) and the vertical spatial distribution of the building was split into three broad categories Low, Mid and High as shown in Table 4.

From Table 4 we note that within each floor group, over half have Moderate response times. In addition, the High region has the smallest Moderate

Region	Rapid <1 min	Moderate 1–8 min	Long >8 min	Total
High: 61–90	25% (8)	56% (18)	19% (6)	32 (40%)
Mid: 31–60	6% (2)	71% (24)	24% (8)	34 (42%)
Low: 1–30	7% (1)	73% (11)	20% (3)	15 (18%)
Total	11 (14%)	53 (65%)	17 (21%)	81

Table 4. Response time distribution for WTC1.

response time group and sizable numbers with Rapid and Long response times. In contrast, the Low and Mid regions while possessing sizable numbers with Long response times has few Rapid responders. The relative high numbers of rapid responders high in the building is thought to be due to the relative proximity to the incident encouraging many of the occupants to respond rapidly. In addition to the time taken to react, the nature of the tasks undertaken during the response phase was examined. Two types of task were considered, **Information Seeking** and **Action** Tasks. The **Information Seeking** tasks involve participants attempting to gather information prior to commencing their evacuation. Examples include; Sought environmental information; sought information from colleagues, authority figures, etc; waited for further info; etc. **Action** tasks involve performing physical actions prior to the commencing horizontal evacuation. Examples include; Collect items; searched office/floor; instructed others to evacuate; shut down computer; secured items (locked safe); changed footwear; etc.

A positive significant relationship was found between total number of tasks completed and response time $\tau = .38$, $p(\text{two tailed}) < 0.01$, i.e. the more tasks completed the longer the response time. In addition, almost a third (30%) of the population undertake two **Action Tasks** while almost half (41%) the population undertake one **Information Seeking Task**. Just over a half (53%) of the population undertake two or less tasks in total prior to starting their evacuation. The two most common **Information Seeking Tasks** were, “Sought environmental information”, reported 52 times and, “Sought information from friends/colleagues”, reported 28 times out of a total of 100 **Information Seeking Tasks** reported by the 81 participants. The two most common **Action Tasks** were, “Collect Items”, reported 36 times and “Instructed Others to evacuate”, reported 24 times out of a total of 139 **Action Tasks** reported. Clearly, participants undertake a number of tasks prior to starting their evacuation. As it was not possible to determine a unique response time for each of the participants the upper end of the response time band associated with each participant was used to represent the maximum likely response time for an individual undertaking a particular set of tasks. Using this information it is possible to estimate the response times associated with undertaking those tasks (see Table 5).

From Table 5 we note that starting the evacuation without undertaking any tasks results in the shortest average maximum response time, requiring

Type of tasks “0 Action and”	Average max response time (mins)	Sample size	Type of tasks “0 Info and”	Average max response time (mins)	Sample size
0 Info	2.7	7	0 Action	2.7	7
1 Info	5.4	9	1 Action	3.5	6
2 Info	11.5	4	2 Action	4.5	8

Table 5. Average maximum response time associated with various task types.

only 2.7 mins. This is an indication of the minimum time required by an individual to start their evacuation in this type of incident. Of great interest is the result that **Information Seeking Tasks** appear to take between $1.5\times$ and $2.6\times$ longer than **Action Tasks**. This highlights the importance of providing a hardened emergency communications system within high-rise buildings. It is suggested that the frequency and number of **Information Seeking Tasks** could be reduced or removed completely if appropriate information could be provided to evacuees via hardened buildings communication systems. Furthermore, it is suggested that the frequency and number of **Action Tasks** could be reduced or removed completely if appropriate training and clear instructions are provided to building occupants.

Finally, the perceived risk (see Sect. 2.2) when the participant decided to evacuate (R2) was compared with their maximum response time. This could be done for 48 participants for which we have a (R2) risk and a maximum response time. Participants with Low Perceived Risk (rating 1, 2) have the highest average maximum response time of 12.4 mins (9 individuals) while those with High Perceived Risk (rating 6, 7) have the shortest average maximum response time of 4.8 mins (13 individuals). Thus those who perceive a high risk respond $2.6\times$ faster than those who perceive a low risk.

5 Concluding Comments

The evacuation of the WTC complex represents one of the largest full-scale building evacuations in modern times. As part of the UK study into the WTC evacuation, 271 WTC survivors have been interviewed in great detail and data from these interviews have been entered into the HEED database. Preliminary analysis of data from WTC1 is shedding light on how people evacuate, the main findings of this preliminary analysis suggests:

Stoppages:

- 82% of sample stopped at least once during descent.
 - 44% stopped due to congestion while 9.7% stopped to rest.
 - 84% of stoppages of all kinds were incurred by those from High and Mid levels.
 - 83% of rest stops were incurred by those from High and Mid levels of which: 85% female, 45% overweight+, 45% disabled, 10% fatigued.

- BMI is not a predictor of whether a person required a rest stop

Stair Travel Speeds:

- Analysis of data for Stair C suggests an average adjusting stair speed of 0.33 m/s (excluding those with disabilities or other reported reasons for travelling slow), some 65% larger than reported in earlier studies.
- This average stair travel speed was negatively affected by the high levels of congestion experienced by sampled participants. If this is taken into consideration, the stair travel speeds appear to be as expected.
- BMI is not a predictor of stair travel speed.

Response Times:

- Over half sample (65%) have moderate response times (1–8 min).
- In the High region (>60th floor) there are sizable numbers with Rapid (<1 min) and Long (>8 min) response times.
- In Low and Mid regions there are sizable numbers with Long response times.
- Just over half the sample undertake up to two tasks prior to evacuating.
- Information Seeking Tasks take between 1.5× and 2.6× as long as Action Tasks.
- Undertaking two Information Seeking Tasks can delay evacuation by as much as 11.5 min.
- Improving emergency communications could greatly reduce evacuation delays by removing the need to perform Information Seeking tasks.
- Improving training could reduce evacuation delays by removing the number of Action tasks prior to evacuation.
- Those with a High Perceived Risk responded 2.6× faster than those with Low Perceived Risk.

An important observation to emerge from this preliminary study is that BMI does not appear to be a predictor of the need to rest or of stair travel speed. Indeed, stair travel speeds derived thus far appear to be consistent with older data. Further analysis is underway and will include fitness as a variable.

Acknowledgements

The authors are deeply indebted to the 9/11 evacuees who gave, and continue to give, so generously of their time. The authors are also indebted to the EPSRC for funding this work (grants GR/S74201/01 and EP/D507790) and to the many supporters of the HEED project without whose assistance the project would have been impossible.

References

1. D. Canter (ed.), *Fires and Human Behaviour*, 2nd edition, David Fulton, London, 1990.

2. E.R. Galea, and S.J. Blake, Collection and Analysis of Data Relating to the Evacuation of the World Trade Centre Buildings on 11 September 2001, Report produced for the UK ODPM, Fire Research Technical Report 6/2005, ODPM Publications, ISBN 1851127658, Dec 2004.
3. J.D. Averill, D.S. Mileti, R.D. Peacock, E.D. Kuligowski, N. Groner, G. Proulx, A.P. Reneke, and H.E. Nelson, Final Report on the Collapse of the World Trade Center Towers, NIST NCSTAR 1-7, Occupant Behaviour, Egress and Emergency Communications. Federal Building and Fire Safety Investigation of the World Trade Center Disaster, Sep 2005.
4. R.R.M. Gershon, P.H.G. Hogan, K.A. Qureshi, and L. Doll, Preliminary Results from the World Trade Center Evacuation Study. Morbidity and Mortality Weekly Report, Vol. 53(35), 2004, pp. 815–817.
5. E.R. Galea, J. Shields, D. Canter, K. Boyce, R. Day, L. Hulse, A. Siddiqui, L. Summerfield, M. Marselle, and P. Greenall, Methodologies Employed in the Collection, Retrieval and Storage of Human Factors Information Derived from First Hand Accounts of Survivors of the WTC Disaster of 11 September 2001, *Journal of Applied Fire Science*, Vol. 15, 2006–2007, pp. 253–276.
6. J.J. Fruin, *Pedestrian Planning Design*, Metropolitan Association of Urban Designers and Environmental Planners Inc., New York, 1971.
7. J. Pauls, Performance of Means of Egress Conducting the Research Needed to Establish Realistic Expectations, to appear in *Proceedings of SFPE 7th Int. Conf. on Performance Based Codes and Fire Safety Design Methods*, April 16–18, 2008, Auckland, New Zealand.
8. J. Pauls, private communication with E.R. Galea, 17 Feb 2008.
9. J. Pauls, Movement of People, in: DiNenno (ed.), *SFPE Handbook of Fire Protection Engineering*, 2nd edition, 1995, pp. 3-263–3-285.
10. J. Pauls, Evacuation Drill Held in the B.C. Hydro Building, 26 June 1969. NRC, Division of Building Research, Tech Note No. 543, 1970.

Evacuation Movement in Photoluminescent Stairwells

Guylène Proulx and Nouredine Bénichou

National Research Council of Canada, Ottawa, Canada

e-mail: guylene.proulx@nrc-cnrc.gc.ca

e-mail: nouredine.benichou@nrc-cnrc.gc.ca

Summary. An experiment was conducted in a 13-storey office building to assess the effectiveness of different installations of photoluminescent material (PLM) in stairwells. For the experiment four identical stairwells were used: three had different PLM installations and one had reduced lighting of an average of 37 lux. Video cameras and a questionnaire were used to gather data on the movement time and behavior of evacuees. Results from the study show that between 65 to 75% of the respondents felt comfortable going down the stairwells with PLM markings, with the visibility assessed as “good or excellent” in the two stairwells with PLM marking across each step. After the sound of the fire alarm, the average time taken by the first occupants to arrive at each stairwell was 1 min 7 s. Overall, the full evacuation lasted about 12 min. The results also indicate that during the busiest moment of the evacuation the mean speed of movement in the stairwells ranged between 0.40 and 0.66 m/s, while the density ranged between 1.56 and 1.60 p/m². Occupants’ judgment of the installations showed the importance of marking across each step of the stairwell.

1 Introduction

Photoluminescent material (PLM) is made of inorganic chemical compounds, referred to as photoluminescent pigment phosphors, encased in flexible or rigid strata or dispersed in a liquid [1]. The photoluminescent pigments consist of crystals of aggregated elements and other agents. The crystals are characterized as being photoluminescent (phosphorescent) due to the excitation they undergo when exposed to a light source and their ability to store light photons, consequently showing luminescence over time. After the crystals have been charged by a light source, they can emit light. In the absence of light, the energy stored will continuously exhaust until its complete depletion. PLM has many applications. In fire safety, the most promising uses are for safety markings such as exit signs, directional signage, door markings, path markings, obstruction identification and other components that compose a safety

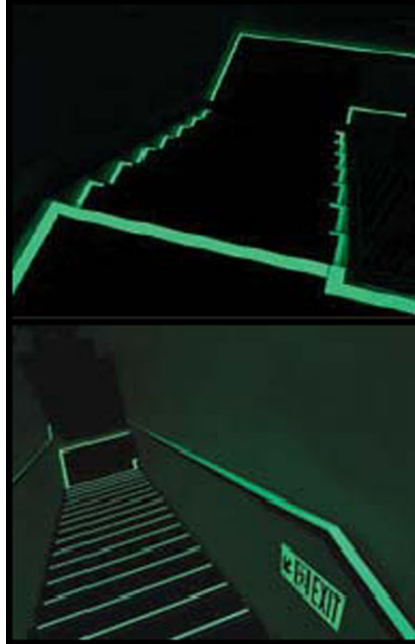


Fig. 1. Examples of PLM safety marking in stairwells [2].

wayguidance system. In blackout situations resulting from power failures or fires, PLM safety markings can aid occupant evacuation, see Fig. 1.

In 2006, the National Research Council of Canada (NRC) prepared a literature review of research studies that have been carried out on the use of PLM as a safety wayguidance system [3]. The review revealed that lessons learned from past tragedies and factual benefits of PLM wayguidance systems have led to the development of requirements, product technical standards and installation guides [4–6]. However, none of these installation standards have ever been tested with human subjects during an evacuation. Also, it is not known if the installations proposed are excessive, and are costing more than is required for safe and effective evacuation. The review of the PLM technology and its applications has led to three recommendations: (1) PLM signage systems have a unique potential for buildings as an effective and sustainable wayguidance system to enhance the security of occupants during building evacuation; (2) further research and field tests are needed to assess the effectiveness of the PLM wayguidance system under evacuation conditions; (3) a methodology for the installation of PLM wayguidance systems should be developed to ensure that the technology is used properly. As a result of these recommendations, a project was developed to address the three objectives:

1. To assess the effectiveness of 3 stairwell installations of a PLM wayguidance system in an office building environment.

2. To compare the effectiveness of PLM wayguidance systems to a stairwell under emergency lighting condition.
3. To develop, based on the research results, an installation guide for a PLM wayguidance system.

Objectives 1 and 2 were pursued through a full building evacuation experiment with human subjects. Some of the findings of this experiment are reported in this paper. The complete results of this study are available in our Research Report #232 published on the NRC website [7].

2 Methodology

To measure people's movement time, ability to find destinations and to obtain people's appreciation of PLM installations, a study of an evacuation drill in an office building was conducted. Several buildings were considered for this study. A set of criteria was established to identify the building most suitable to meet the study objectives. The C.D. Howe building, located in Ottawa, met the study criteria; see Fig. 2. The building was built in 1977 and has 11 floors of office space plus 2 storeys of commercial space, making a total of 13 storeys. Each office floor area is approximately 8000 m², housing around 350 workers.

The building has 6 geometrically identical stairwells among which 4 are windowless (G, C, E, A); these were the stairwells used for the study, see Fig. 3. All stairwells discharge directly to the street. The building has a central fire alarm bell system and is fully sprinklered.

The subjects of this study were the employees working at the C.D. Howe building, although building visitors may have been involved. Around 4,000 employees are expected to be in the building during normal working hours.

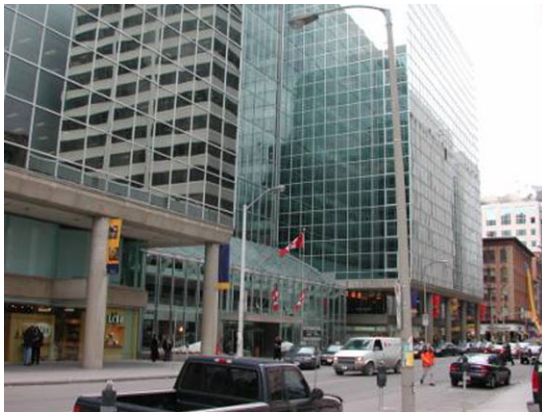


Fig. 2. Picture of the C.D. Howe building.

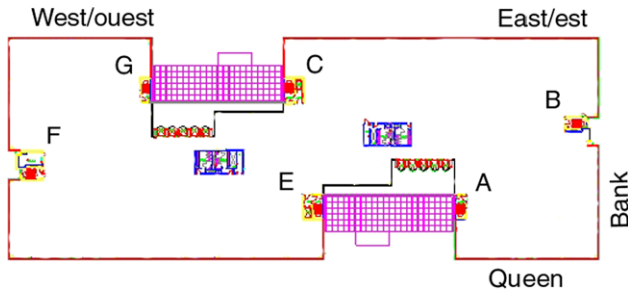


Fig. 3. Stairwells location.

This large number of occupants was of particular interest for this study to allow for measurement of the occupants' speed of movement under crowd conditions. Occupants of the building are typical office workers aged between 18 and 65 years with a mix of men and women. It was expected that some occupants could have limitations preventing them from participating in the evacuation drill. Floor Emergency Officers are trained to assist these occupants in accordance with the Fire Safety Plan.

2.1 Experimental Design

For practical reasons, it was not possible to obtain signed consents from the potential participants to this study. However, an information sheet, detailing the study but not the drill day and time, was sent to all building employees a week prior to the experiment. The drill or experiment was conducted on October 5, 2006 starting at 10:35:23 a.m. In accordance with the emergency procedure for the building, at the sounding of the fire alarm all occupants, supported by the Floor Emergency Officers, started to move toward their designated or the nearest stairwell. At alarm activation, the 3 PLM stairwells (Stairwells A, E and G) were simultaneously put in total darkness. Stairwell C was under emergency lighting (2 out of 3 double-tube fluorescents were removed a day before the drill) providing an average level of lighting of 37 lux [7]. The current code accepts that the emergency lighting be reduced to an average as low as 10 lux [8]. Video cameras, installed on the morning of the drill, were started 30 minutes before the alarm was activated and ran non-stop until after the drill was completed. The cameras were located inside the stairwells to capture the behavior and speed of movement of evacuees, as well as the overall mood and parts of conversations. Upon exiting the studied stairwells, evacuees were handed a questionnaire to fill out. On location were members of the Building Fire Emergency Organization, research team, observers, firefighters, paramedics and police. The evacuation was completed in approximately 12 minutes after which all occupants were allowed to return into the building.

Marking	Stairwell A	Stairwell E	Stairwell G	Stairwell C
Steps	L marker 1"	Marking across each step 1"	Marking across each step 2" plus L marker Anti-slip strip 1"	No marking
Handrail	Continuous 1"	Continuous 1"	Continuous 1"	No marking
Demarcation on landing	Continuous 1"	Continuous 1"	Continuous 2"	No marking
Directional sign "running-man"	On each landing	On each landing	On each landing	No marking
Obstruction	Zebra marking and tag	Zebra marking and tag	Zebra marking and tag	No marking
Final Door	Around door 1" and sign "Final"	Around door 1" and sign "Final"	Around door 2" and sign "Final"	No marking
Lighting	No	No	No	37 lux average

Table 1. Experimental installation of the stairwells.

Three material suppliers, Prolink North America, Jessup Manufacturing Company and Jalite USA, provided and installed the PLM marking and signs for this study. All materials used had received certification in accordance with New York City Standard 6-1 2004 [4]. Three stairwells were equipped with PLM installations. Table 1 summarizes the elements that were installed in the tested stairwells. The 4th stairwell studied, Stairwell C, had no PLM marking but had reduced lighting to an average of 37 lux representing emergency lighting with battery-pack spot-light positioned every second-floor.

Figure 4 shows the 4 studied stairwells as experienced by the evacuees. Installation of the material took place in the two weeks prior to the evacuation drill.

2.2 Data Gathering

The experimental design offered the advantage of comparing the speed of movement and occupant appreciation of the three PLM stairwell installations, which could be compared to a stairwell with emergency lighting. The methodology of using video cameras to record movement and behavior and a questionnaire to obtain feedback were used in this study. The questionnaire contained questions on the participants' characteristics, specific questions on the comfort and safety felt and overall appreciation of the PLM wayguidance emergency evacuation systems in the stairwell used (questionnaire details found in [7]). Twenty-eight video cameras, positioned on floors 11, 9, 7, 5, 3, 1 and B level of the stairwells, were used to gather data on movement time and behavior of evacuees in the stairwells.

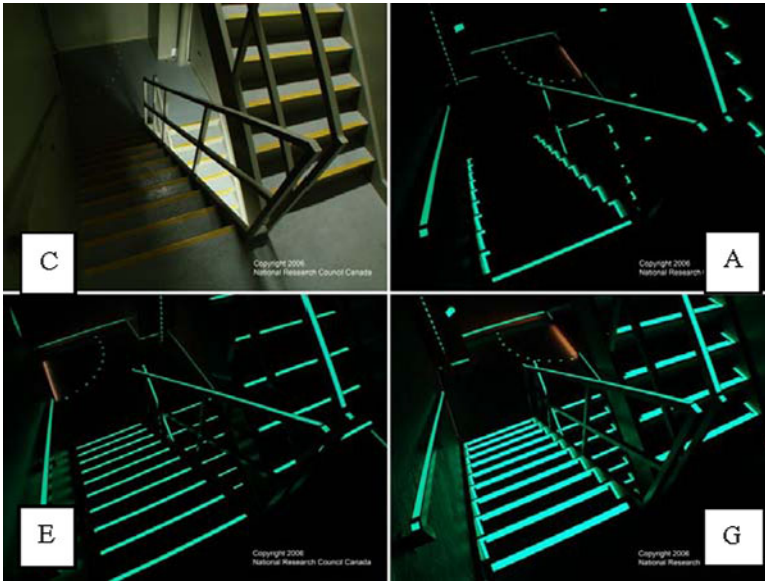


Fig. 4. Four studied stairwell installations.

3 Field Study Results

The evacuation drill unfolded as planned without any unexpected incident to report. Data from the questionnaires and the videos were analyzed and statistical calculations were run using SPSS 13.0.

3.1 Questionnaire Results

In total, 489 questionnaires were returned from the 1191 evacuees observed on the video recordings. Assuming that this sample represents a random selection of the building evacuees, it is calculated that the questionnaire results can be generalized to the entire building population with a 95% confidence level with a potential variation of 3 points. Among the returned questionnaires, 130 or 27% were from respondents who used Stairwell A, 132 or 27% were from Stairwell E, 128 or 26% were from Stairwell G, and 99 or 20% were from Stairwell C. As shown in Table 2, the sample of returned questionnaires represents a return rate of 41%, which is good for this type of study [9]. A statistical analysis on the number of observed evacuees counted shows that there are no statistical differences between the PLM stairwells. Therefore, it is possible to compare tested stairwells with confidence.

Respondent Profile

Among the respondents, 65% were female and 35% were male. The respondents' age distribution demonstrates a rather mature crowd. An important

Stairwell used	Returned questionnaire	Evacuees observed	Return percent
A	130	345	38%
E	132	287	46%
G	128	281	46%
C	99	278	36%
Total	489	1191	41%

Table 2. Returned questionnaires.

Limitations	Frequency	Valid percent
Asthma	12	26%
Overweight	11	23%
Arthritis	8	17%
Heart condition	3	6%
Vision impairment	3	6%
Injury	3	6%
Mobility impairment	3	6%
Hearing impairment	3	6%
Others	2	4%
Total	48	100%

Table 3. Limitation that could impede evacuation.

occupant characteristic that can have an impact on an evacuation is the presence of people with limitations. Among the respondents, 41 individuals or 8% stated that they had a form of limitation that could impede their evacuation from the building. Nevertheless, all these respondents evacuated the building using a stairwell since they filled out a questionnaire. The questionnaire provided 8 categories of limitation to choose from as shown in Table 3 (category “others” refers to hand-written comments; one added claustrophobia and another one pregnancy). Out of the 41 respondents who identified a limitation, 4 had multiple limitations all involving being overweight and other conditions. Among the respondents the most prevalent condition reported was asthma at 26%, followed by being overweight at 23% and arthritis at 17%. It is important mentioning that occupants with a serious mobility limitation who could not use the stairwells to evacuate are not part of this sample. Respondents who reported a disability were well distributed in the 4 different stairwells: 8 used Stairwell A and 11 used each of the other 3 stairwells.

Alarm and Initial Response

Among the respondents, 99% heard the fire alarm at the time of the evacuation. Only 3 respondents stated that they did not hear the alarm in their area. These occupants were located on floors 2, 5 and 6 of the East tower; but somebody rapidly came to warn them. None of them mentioned having a hearing limitation. Of those who commented on the sound level of the alarm,

Action	Frequency	Percent
Get dressed	335	68.5
Gather valuables	265	54.2
Secure files or information	222	45.4
Follow warden's instructions	208	42.5
Return to office	75	15.3
Discuss with a colleague	56	11.5
Seek more information	23	4.7
Continue working	14	2.9

Table 4. Action performed before starting evacuation.

76% found the alarm “loud enough”, however 21% or 102 respondents felt that the alarm was “too loud” and 3% or 14 respondents found the alarm to be “too quiet”. Respondents of both genders provided appreciation of the alarm level in exactly the same proportion so no gender difference was found.

When the alarm sounded, 81% of the questionnaire respondents were at their desks, others were in other locations such as meeting rooms, corridors and washrooms. Respondents were asked if they completed any of a list of 8 actions before starting their evacuation. As shown in Table 4, the most prevalent action before starting evacuation was for 335 or 69% of the respondents to “get dressed”, as the outside temperature was 8°C. The other three most likely actions were to “gather valuables” with 54%, “secure files or information” 45%, and “follow warden’s instructions” 43%. Interestingly, 14 respondents continued working”.

Evacuation Times

Respondents were asked to estimate how much time they spent from the time the evacuation drill started to the time they decided to leave their floor. As presented in Fig. 5, an overall 46% reported starting to leave in less than 1 minute, which is very good. However, some 29% decided to leave between 1 to 2 minutes, 14% decided to leave between 2 to 3 minutes, and 4% decided to leave between 3 to 4 minutes. Over 6% or 31 respondents took more than 4 minutes to start leaving, which is of concern. Among the respondents who took over 4 minutes, 7 returned to their offices after hearing the alarm and completed tasks such as securing files and getting dressed. Another 6 continued working after hearing the fire alarm until they were told to leave. Finally, 6 were Floor Emergency Officers who took time to ensure that their floors were empty before starting their evacuation.

Respondents were also asked to estimate how much time they spent overall to evacuate the building from the time the drill started to the time they reached the outside. Overall, 47% of the respondents estimated that they took less than 5 minutes to evacuate the building. Another 40% indicated that they took from 5 to 10 minutes, and 13% said that they took over 10 minutes to

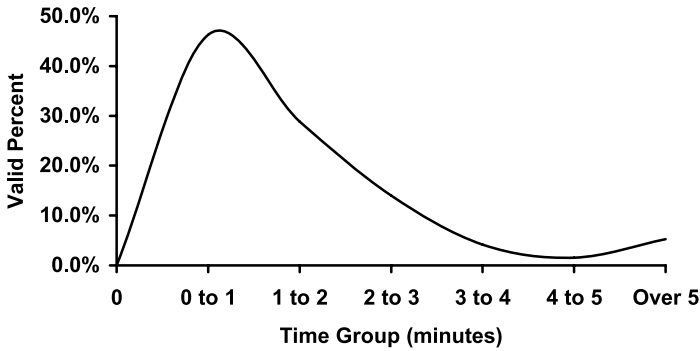


Fig. 5. Distribution of time to start evacuation.

evacuate the building. The analysis of the video recordings provided exact times with which to compare these estimates, which turned out to be pretty accurate.

Stairwell Evacuation

Once occupants decided to evacuate their floor, they moved toward the different stairwells. The questionnaire had several questions for respondents to express their experience descending the studied stairwells. The questionnaire asked the respondents if they encountered any problems as they entered and negotiated the stairwells. No respondent mentioned furniture obstructing the entry to the stairwell. Approximately 22% of the evacuees in the 4 studied stairwells encountered crowding around the entry. Only 2 respondents in Stairwell E and 2 in Stairwell C mentioned difficulty opening the exit stairwell door. Difficulty entering the stairwell because too many people were coming down was felt to be a problem by 23% in Stairwell A, 16% in Stairwell E, 20% in Stairwell G and 21% in Stairwell C. It does not appear that finding the handrail was a problem in the 3 stairwells equipped with PLM marking as well as in the stairwell with reduced lighting. The problem that was the most frequently identified was the difficulty seeing because of poor lighting. This problem was mentioned by 52% of the respondents from Stairwell A and as many in Stairwell E, 50% mentioned this problem in Stairwell G and 45% in Stairwell C. The second problem most frequently mentioned was that the people in front of the descending evacuee were moving too slowly. Counter flow did not seem to be a problem in any of the stairwells studied and most respondents had no difficulty in finding and opening the exit door at the base since the last flight of stairs was fully lit.

Evacuees were asked to judge the visibility in the stairwell they used. Table 5 shows the results when combining the judgments “excellent” and “good” versus “not very good” and “poor”. Stairwells E and G received substantially

Judgment	Percent of answer in stairwell			
	A	C	G	E
Excellent and good	50%	56%	62%	67%
Not very good and poor	50%	44%	38%	33%

Table 5. Judgment of the visibility in the stairwell used.

more judgment that the visibility in these stairwells was good or excellent while Stairwells A and C received less positive judgment.

The evacuees were asked to provide their degree of agreement with 8 specific statements regarding wayguidance attributes that they experienced in the stairwell. Overall, the respondents of the 4 studied stairwells considered the handrail to be easy to find. When asked if the first step to each flight was easy to locate, respondents from the 4 studied stairwells were positive toward this statement with Stairwells E and G respondents providing a larger number of people who strongly agree. It was much easier for evacuees to identify each step in Stairwell E and G, while it was difficult to identify each step in Stairwells A and C. This finding is not surprising as Stairwell A had only the “L” shape marking at the extremity of each step to identify the step and Stairwell C had no marking and reduced lighting which made each step more difficult to identify. Respondents were asked about the easiness to locate the last step of each flight. Over 20% of respondents in each stairwell felt it was difficult to identify the last step of each flight, which suggests that some additional marking should be considered on the last step or on the landing. In terms of sign visibility, Stairwell E scored the best for the visibility of directional signs, although the directional signs were the same in all the PLM stairwells. There was no statistical difference among stairwells for the marking of obstructions, the identification of the crossover floor, or the marking of the final exit. Overall, if we take the stairwell attributes individually and look at the stairwell that received the most favorable appreciations for each feature, Stairwell E is systematically in first place for most attributes with Stairwell G second, see Table 6. Stairwells A and C are in turn at the third and last positions.

Evacuees were questioned on their sense of comfort while going down the stairs during the evacuation. Overall, 65 to 75% of the respondents felt comfortable going down the stairwells with the PLM marking or the reduced lighting. Respondents were asked to judge the density of the crowd in the stairwell they used and Stairwell E was judged the most crowded. This judgment was later confirmed by the videotapes analysis, which showed that 2 evacuees with limitations entered Stairwell E, which stalled the evacuation movement for a while.

From the questionnaire it appears that respondents judged Stairwells A and C similar on several questions while these two stairwells appear less positively evaluated than Stairwell E and G. Stairwell E obtained the best positive evaluation despite the fact that this was also the stairwell that was felt to be the most crowded and that problems such as occupants at the front mov-

Attribute	Rating			
	1st	2nd	3rd	4th
Handrail was easy to find	E	G	C	A
First step of each flight was easy to locate	E	G	A	C
Each step was easy to identify	E	G	C	A
Last step of each flight was easy to find	E	G	C	A
Directional signs were visible	E	G	A	C
Obstructions were well marked	E	G	A	C
Re-entry floors were well identified	G	E	A	C
Final exit was well marked	G	A	E	C

Table 6. Rating of the stairwells for each attribute.

ing too slowly were identified. Stairwell G seems also to have been positively evaluated but somewhat less so than Stairwell E on some of the attributes. The larger 2" stair stripes combined with the "L" shaped marking as well as the 2" demarcation line of Stairwell G did not seem to play a major role in the evaluation of the respondents when compared with Stairwell E. Visibility was judged good to excellent in stairwells E and G and locating each step appeared to be easier with the PLM marking of each step.

3.2 Data from the Video Cameras

Recordings from the 28 video cameras used to survey the evacuation were analyzed. A total of 1191 occupants were observed on the recordings. At 10:35:23, the fire alarm bell sounded to start the evacuation drill. It rang continuously for 11 min 51 s. During this time, as is the procedure for the building, evacuees on all floors moved to the stairwells and began their descent to reach an outside exit.

Time to Start

Due to the building's large surface area and the configuration of the offices and cubicles, it was not possible to record the exact starting time of each occupant upon hearing the fire alarm. It was, however, possible to observe the time of arrival of each person at each exit door leading to the 4 studied stairwells. The overall average time for the first person to reach the exit door after the alarm is 1 min 7 s. It can be estimated that the true time to start or pre-movement time of each occupant was approximately 10–15 s prior to their arrival at the door. As can be seen in Table 7, the time of the first person arriving at the stairwell exit door on six different floors were recorded. It can be seen that the arrival time varies greatly from floor to floor and for different stairwells. This can be explained by the configuration, which varies considerably in the different areas of the building and the type of activity occupants were engaged in at the time of the alarm.

Stairwell	Elapsed time to arrive from alarm			
	Floor	Time min:s	Floor	Time min:s
A	11	1:28	5	0:57
	9	1:40	3	0:22
	7	0:52	1	0:18
E	11	1:06	5	0:35
	9	2:23	3	1:00
	7	1:35	1	0:53
G	11	1:25	5	1:31
	9	1:30	3	0:40
	7	1:19	1	0:31
C	11	0:21	5	1:56
	9	0:42	3	0:43
	7	1:37	1	1:24

Table 7. Time for the first person to arrive at the stairwell exit door.

The average time for the last person to reach the exit door after the alarm is 5 min 29 s. Among the last to enter the stairwells were Floor Emergency Officers, who have as part of their duty to ensure that the area under their responsibility is empty when they leave. Several took the time to visit each office as well as coffee rooms and washrooms before leaving their floor.

Speed of Movement

The speed of movement of each evacuee in each stairwell is important data to be obtained from the video recordings. Speed of movement was calculated in meters per second (m/s) for each evacuee with the exact distance travelled in each stairwell. The speed of movement in Stairwell A ranged from 0.33 m/s to 1.39 m/s. In Stairwell E, the speed ranged from 0.17 m/s to 1.03 m/s, in Stairwell G it ranged from 0.14 m/s to 1.53 m/s and in Stairwell C it ranged from 0.38 m/s to 1.87 m/s. The observed mean speed of movement in all stairwells is presented in Table 8. The slowest mean speed of movement was in Stairwell E, which had a speed of 0.40 m/s. Stairwell G had a mean speed of 0.57 m/s and Stairwells A and C shared the highest mean speed of 0.66 m/s. Table 8 also presents the density of occupants descending which varied slightly for each stairwell. Density of evacuees was calculated in person per meter square (p/m²) during the five busiest minutes of the evacuation from 2 minutes until 6 minutes after the alarm activation. The last column shows the calculated speed of movement, as defined by Pauls [10], which is similar to the observed speed in Stairwells A, G and C. Stairwell E, however, demonstrates a marked difference as its observed mean speed of 0.40 m/s is considerably lower than its calculated speed of 0.62 m/s. When further studying Stairwell E, it was noticed that two individuals with limitations had a major impact on the speed of movement in that stairwell. At 10:37:41, 2 min 18 s after the alarm, entering from floor 7, a heavy person started going down

Stairwell	Number of evacuees	Density (p/m^2) 5 busiest minutes	Observed mean speed (m/s)	Calculated speed (m/s)
A	345	1.56	0.66	0.63
E	287	1.60	0.40	0.62
G	281	1.58	0.57	0.62
C	278	1.60	0.66	0.62

Table 8. Speed of movement in the four stairwells.

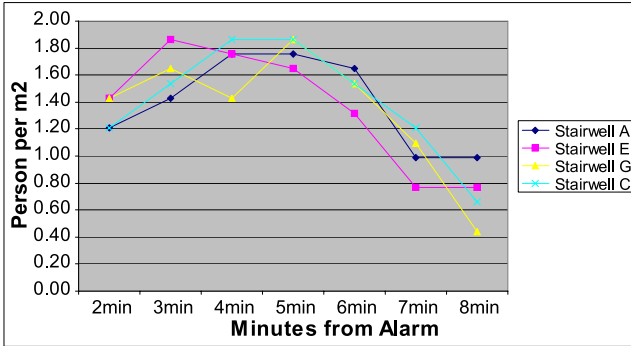


Fig. 6. Density in the 4 stairwells during the 7 busiest minutes.

the stairwell one step at a time, moving sideways to the stairs, holding the handrail with one hand and a jacket and vest with the other. Almost at the same time at 10:37:38, 2 min 15 s after the alarm, another person holding a cane entered from floor 1 with two accompanying occupants who remained behind. Nobody over-took these two evacuees who were slower than the rest of the crowd in the stairwell, and a gap formed in front of them leaving a full flight of stairs empty. The impact on the descending crowd was substantial, stalling the descent for a few minutes.

A closer look at the density in the 4 stairwells is presented in Fig. 6. It can be seen that the density pattern is similar in the 4 stairwells for the 7 busiest minutes of the evacuation, 2 minutes to 8 minutes after the alarm activation. It appears however, that Stairwell E was more crowded earlier in the evacuation than the other stairwells. This could also help explain the lower observed mean speed of evacuation. Having most of the evacuees entering the stairwell at the same time would cause a lot of crowding because of merging from all floors, and therefore reduce the evacuation speed.

The videotapes also showed that the number of people entering on any floor tended to be higher at the beginning of the evacuation, and slowly dropped as the evacuation continued for Stairwells A, C and G. In Stairwell E, however, the number of people who entered peaked on all floors at 2–3 minutes from the alarm, and then fell steeply for the rest of the evacuation. This means that the majority of the evacuees in Stairwell E were all in the stairwell at the same time, causing crowding and congestion.

Floor	Mean speed of movement by stairwell m/s			
	A	E	G	C
11	0.41	0.40	0.43	0.53
9	0.37	0.45	0.45	0.46
7	0.44	0.34	0.48	0.51
5	0.53	0.31	0.43	0.53
3	0.64	0.39	0.49	0.84
2	0.92	0.38	0.79	0.99
1	0.89	0.52	0.93	0.88

Table 9. Mean speed of movement for evacuees entering from different floors of the 4 stairwells.

Evacuees entering a stairwell from an upper floor had typically a lower mean speed of movement, as seen in Table 9. This slower speed is explained by crowding in the stairwell. Due to the simultaneous evacuation of all floors of the building, occupants on higher floors had to merge with an increasing number of people entering at the lower floors. Merging with evacuees entering the stairwell from lower floors appears to be the main factor for slowing down descending occupants. Evacuees entering the stairwell at floor 11 were required to merge with people entering at floors ten to one.

The fastest evacuees were those who entered the stairwell quickly after the alarm from the 1st or 2nd floors. Because the stairwell was empty and they didn't have to merge with evacuees from lower floors, they were able to freely race down to the exit. The slowest evacuees were those who entered the stairwell at a higher floor, more than 2 minutes after the alarm sounded. They were immediately caught in the slowest part of the crowd until the exit. Evacuees of Stairwell E are an exception to this pattern as their mean speed of movement was relatively slow no matter the floor they entered.

Observed Behavior

Observations of the behavior of the evacuees during the evacuation, such as crowding and holding of the handrails, were obtained from the video recordings. There was significant crowding observed in all of the stairwells. The bottom few floors had the largest amount of evacuees, but tended to move along well because there was little merging with lower floors. The middle floors got congested very quickly, and during the busiest few minutes of the evacuation, movement could stop completely for up to 15 s in Stairwells A, C and G, and as long as 1 min 20 s in Stairwell E. This large discrepancy between stairwells is attributable to the two evacuees with limitations who entered Stairwell E and slowed down the evacuation behind them.

Holding of the handrail also contributed to crowding and slowing down movement in the stairwells. Evacuees using the handrails were descending at the sides of the stairwell, tending to favor the inside handrails. This caused them to descend in a single file, which in turn slowed their speed of descent to

the speed of the slowest person ahead of them. Some evacuees not using the handrails were able to pass through the middle of the stairwell. However, there were few attempts at over-taking others possibly due to the limited visibility offered in the stairwells studied and the dense crowd, which prevented such behavior. In some areas, 4–5 evacuees were observed in each stairwell holding on to the handrails on both sides of the 1100 mm wide stairwell, making it difficult for faster occupants to get by. The frequency of people holding the handrail was recorded at some floors. As examples, on floor 9, 88% were holding the handrail in Stairwell A, 81% in Stairwell E, 86% in Stairwell G and 71% in Stairwell C. On floor 5, 84% used the handrail in Stairwell A, 87% in Stairwell E, 80% in Stairwell G and 81% in Stairwell C. On floor B, which was fully lit, 31% used the handrail in Stairwell A, 55% in Stairwell E, 33% in Stairwell G and 61% in Stairwell C. Two possible explanations may be offered for the difference between floor B and the upper floors 5 and 9. The first one is the lighting difference between the floors. Evacuees held on to the handrail more frequently on levels with less lighting. The second explanation is the proximity to the exit. On floor B, evacuees were moving well without much crowding because they were heading directly outside. Because they were so close to the exit, evacuees sped up and stopped using the handrail; many were seen zipping their coat and tightening their scarf on this last flight of stairs.

Density can be represented by showing positions of evacuees in the stairs, as in Fig. 7, which shows density in Stairwell A on floor 3, at 2, 3, 4, 5 and 6 minutes from the alarm. These representations are helpful when analyzing the behavior of the evacuees as they descend. For example, it was very rare to see two people descending the stairs side-by-side during this evacuation. There was not enough room in the 1100 mm stairwell for two to fit comfortably shoulder to shoulder, without one violating the other's personal space. This was usually only seen when two friends were speaking to each other while descending. When the stairwell was relatively empty, evacuees kept to their right. This tendency to stay on the right is explained by the fact that the

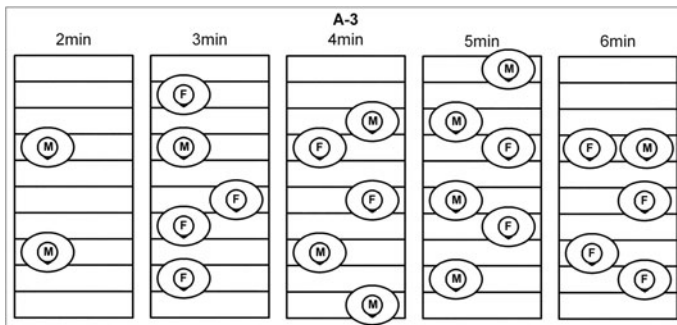


Fig. 7. Representation of density on floor 3 of Stairwell A at different times.

staircase spirals downward to the right; keeping to that side allowed evacuees to descend faster. When the stairwell was more crowded, such as at 5 minutes, the evacuees maintained a scattered pattern to avoid walking too close to each other. The representation at 5 min shows the most crowded time of the evacuation in Stairwell A, with 6–7 evacuees on one flight of stairs, representing 1.98 p/m^2 .

Based on observations from the videotapes, most evacuees were at ease and not alarmed by the PLM marking. Comments such as, “wow” and “this is some lighting” were heard in all three PLM stairwells. One evacuee in Stairwell G commented on the visibility, saying, “you can’t see people, all you can see are the stairs”. Overall, comments about the PLM marking were positive. Most occupants did not overtly react to the material and just followed the evacuation flow.

4 Summary and Conclusions

A field study was conducted to assess the effectiveness of a number of different PLM stairwell installations as a safety wayguidance system to support office occupant evacuation. Following are the major findings and conclusions of this study.

4.1 Evacuees’ Subjective Assessment of PLM Signage

Overall respondents to the questionnaire provided statistically comparable judgments on several attributes of the 4 studied stairwells. There was, however some systematic evaluation that differentiated the stairwells. It appears that respondents judged Stairwells A (L shape marker) and C (reduced lighting) similar on several questions while these two stairwells appear less appreciated than Stairwell E and G (1" and 2" marking, respectively). In Stairwell A, visibility was judged good by half the respondents and not good by the other half. Two important issues for several evacuees of Stairwell A are that each step in the stair, and the last step of each flight, were difficult to locate. The overall evaluation of Stairwell A and C was not as good as for Stairwell E and G. Stairwell E obtained the best appreciation from the respondents.

4.2 Occupant Movement

Video recordings provided a complete account of the movement of occupants. The average time taken by the first occupants to arrive at the exit door leading to a stairwell was 1 min 7 s. Overall, the full evacuation lasted just under 12 min. It seems that the reduced lighting of Stairwell C and the PLM marking without lighting in the other 3 studied stairwells had no impact on the overall time to evacuate that building since the annual evacuation drill takes typically around 14 min.

The results show that speed of movement in the 4 stairwells studied ranged from 0.14 m/s to 1.87 m/s. The mean speed of movement for Stairwell A was 0.66 m/s; 0.40 m/s in Stairwell E; 0.57 m/s in Stairwell G and 0.66 in Stairwell C. The results indicate that Stairwell E had significantly slower speed of movement. Close analysis of the raw data showed that Stairwell E had two individuals with limitations who had a major impact on the evacuation movement. The results also show that occupant density on the stairs was very similar for each stairwell ranging from 1.56 to 1.60 p/m². The driving factor for the speed of movement in the stairwells was not the installation tested but the occupants' density. From the speed of movement it is not possible to conclude which installation is the best.

One interesting observation is the fact that over 80% of the evacuees were holding the handrail in the stairwell during their descent. This fact supports the research team decision to mark the handrail as evacuees seemed to rely considerably on the handrail during movement down as well as during times when the crowd was stopped. It is felt that handrail marking is an essential part of any wayguidance photoluminescent system installation.

4.3 Comparison of PLM Installations

The overall judgment of the respondents favored the installation of Stairwell E with the 1" strip marking across each step. It appears that Stairwell A with the L shaped markers was the less appreciated as it was difficult for evacuees to differentiate each step. Although Stairwell E is the installation that received the best evaluation, its better performance is not based on a faster speed of movement on stairs but essentially on the subjective judgment of respondents.

4.4 Comparison of PLM with Emergency Lighting

Respondents' evaluation of Stairwell C, with reduced lighting, is comparable to Stairwell A, with L shaped markers, although these two stairwells were illuminated differently. Close to half of the respondents who used Stairwell C said that it was difficult to see around because of the poor lighting.

Overall, the conditions experienced in the 4 studied stairwells were judged as fairly difficult by the evacuees as several considered that the lighting was poor, the steps were difficult to identify and it was crowded and slow. However a majority agreed that they would feel comfortable evacuating under such conditions if there was an emergency.

Acknowledgements

This study was a joint research project between the National Research Council Canada (NRC) and Public Works and Government Services Canada

(PWGSC). The authors would like to thank all the participants in the study particularly the occupants of the C.D. Howe building, Brian Kyle and his team, the building management, PLM manufacturers, the Ottawa Fire Service, Ottawa Police, Ottawa Paramedics and NRC-IRC staff.

References

1. Krokeide, G., 1988, An introduction to luminous escape systems, *Safety in the Built Environment*, pp. 134–147.
2. Peckham, G., 2005, Photoluminescent directional egress path marking systems, *Archi-Tech Magazine*, Dec 2005 Issue, Photos used with permission ©Jalite USA.
3. Tonikian, R., Proulx, G., Bénichou, N., Reid, I., 2006, Literature review on photoluminescent material used as a safety wayguidance system, Research report #214, Institute for Research in Construction, NRC Canada, pp. 31.
4. New York City Building Code, RS 6-1 and RS 6-1 A, 2004, Photoluminescent exit path markings, Local Law 26, New York City, USA.
5. ISO 16069, 2004, Graphical symbols—Safety signs—Safety way guidance systems (SWGS).
6. ASTM E 2030-04, 2004, Guide for recommended uses of photoluminescent (phosphorescent) safety markings.
7. Proulx, G., Bénichou, N., Hum, J.K., Restivo, K.N., 2006, Evaluation of the effectiveness of different photoluminescent stairwell installations for the evacuation of office building occupants, RR #232, Institute for Research in Construction, NRC Canada, pp. 72. URL: <http://irc.nrc-cnrc.gc.ca/pubs/rr/rr232/>.
8. COSH, 1994, *Handbook of Occupational Safety and Health*, Fifth Edition, Treasury Board of Canada Secretariat, Human Resources Management Office, Occupational Safety and Health Chapter 3-1, Standard for fire safety planning and fire emergency organization, Ottawa, Canada.
9. Shaughnessy J.J., Zechmeister, B.E., 1994, *Research Methods in Psychology*, Third Edition, McGraw Hill, New York.
10. Pauls, J., 1995, Movement of people, SFPE Handbook of Fire Protection Engineering, Chapter 3-13, SFPE USA, pp. 263–285.

Automatic Extraction of Pedestrian Trajectories from Video Recordings

Maik Boltes¹, Armin Seyfried¹, Bernhard Steffen¹, and
Andreas Schadschneider²

¹ Jülich Supercomputing Centre, Research Centre Jülich, 52425 Jülich, Germany
e-mail: petrack.jsc@fz-juelich.de

² Institute of Theoretical Physics, Cologne University, 50937 Köln, Germany

Summary. To understand and model pedestrian dynamics, reliable empirical data of pedestrian movement are necessary for analysis and verification, but the existing database is small, inaccurate and highly contradictory. For collecting trajectories from extensive experimental series with a large number of persons we are developing a software named **PeTrack** which automatically extracts these trajectories from normal video recordings with high accuracy in space and time.

1 Introduction and Motivation

This paper describes the automatic extraction of highly precise trajectories from normal video recordings, e.g. from observation cameras. The purpose is to obtain a reliable database for the analysis and verification of models of pedestrian movements. A trajectory is the path a moving person follows through space. As described in [1, 2], the available database for collective motion of pedestrians is small, inaccurate and highly contradictory. We performed well-defined experiments to study the movement through corridors and bottlenecks and extract trajectories of individual persons. However, manual procedures for collecting trajectory data are very time-consuming and usually not sufficiently accurate in space and time. Therefore we are developing a free software named **PeTrack** [3] which is able to extract accurate pedestrian trajectories *automatically*. The software package contains all relevant steps, like calibration of the video, recognition, tracking and height detection of the pedestrians. It can deal with normal video recordings, wide angle lenses and a high density of pedestrians. Lens distortion and perspective view are also considered.

With this tool extensive experimental series with a large number of persons can be analyzed. The resulting trajectories of all pedestrians provide data like velocity, flow, density and individual distances at any time and position on a microscopic level. As first step we used markers on the pedestrians' heads

which also indicated their height. For the future, the aim is the extraction of trajectories without using additional markers attached to the persons.

2 Experiments

The first experiments we made to collect highly accurate trajectories that allow to study the dynamics of pedestrian crowds. The experiments included 99 runs distributed over five days with up to 250 test persons. Every run has been filmed with at least 2 cameras which have been mounted at an altitude of 535 cm perpendicular to the floor. The assemblies can be seen in Fig. 1. The setup of the bottleneck experiment with one camera in front of the bottleneck and one camera inside the bottleneck and overlapping fields of vision allows the combination of trajectories from both cameras to connected trajectories. For the fundamental diagram experiments, two cameras recorded the same overall situation and thus twice the amount of data is available.

The industry cameras used have a progressive colour panel, 1024×768 quadratic pixel and a frame rate of 25. To be able to cover a region of more than three by four meters inside a building we used wide angle lenses with a focal length of 0.4 cm for the 1/3" CCD sensor of the cameras. We provided good illumination of the heads to allow a fast shutter speed for sharp images of moving people.

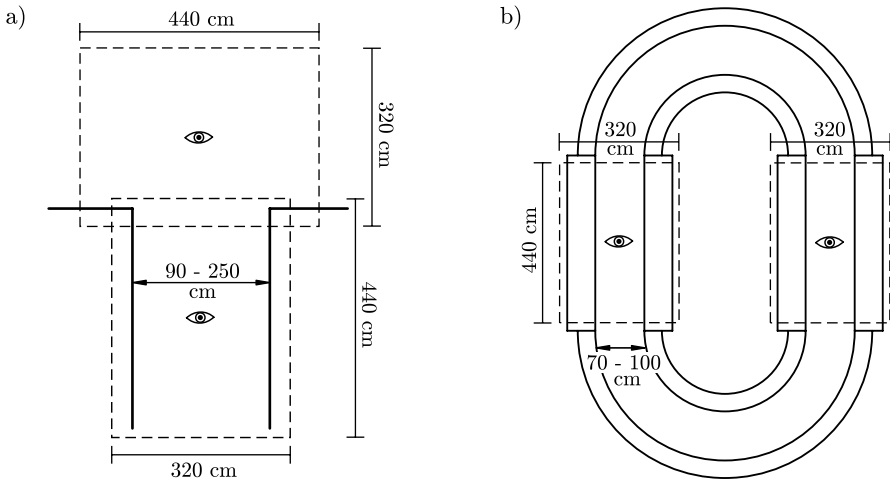


Fig. 1. Experimental setups for the bottleneck (a) and the corridor experiments (b). The cameras are mounted perpendicular to the floor at the position shown by *eyes*. The *dashed lines* indicate the region which are covered by the cameras in the average people's head height of 180 cm.

3 Extraction of Trajectories

To extract highly precise trajectories from video recordings a sequence of procedures has to be performed: undistortion of the video (Sect. 3.1), recognition of persons in a single frame including special markers (Sects. 3.2 and 3.4), and following people over successive frames (Sect. 3.3).

3.1 Calibration

Before extracting metric information the video has to be undistorted. Especially the wide angle lenses generate large distortions at the boundary of the video (Fig. 2a).

To describe the mapping of a homogeneous real world coordinate $\mathbf{x} \in \mathbb{R}^4$ to a homogeneous pixel coordinate $\mathbf{u} \in \mathbb{R}^3$ in the recorded image an ideal model of a pinhole camera with distortion introduced by Brown [4] is adopted. The model uses a camera with the focal length $(f_x f_y)$ and the distortion centre $(c_x c_y)$ as intrinsic parameters and the orientation $\mathbf{R} \in \mathbb{R}^{3 \times 3}$, the position $\mathbf{t} \in \mathbb{R}^3$, the parameters k_1, k_2 of the radial and p_1, p_2 of the tangential distortion up to fourth order as extrinsic parameters. Then the function g describes the mapping of \mathbf{x} to \mathbf{u} :

$$\mathbf{u} = g_{\mathbf{A}, k_1, k_2, p_1, p_2, \mathbf{R}, \mathbf{t}}(\mathbf{x}) = \mathbf{A}d([\mathbf{R}, \mathbf{t}]\mathbf{x}) \quad (1)$$

with

$$\mathbf{A} = \begin{pmatrix} f_x & 0 & c_x \\ 0 & f_y & c_y \\ 0 & 0 & 1 \end{pmatrix} \in \mathbb{R}^{3 \times 3} \quad (2)$$

and

$$d \begin{pmatrix} u \\ v \\ 1 \end{pmatrix} = \begin{pmatrix} u(1 + k_1 r^2 + k_2 r^4) + 2p_1 uv + p_2(r^2 + 2u^2) \\ v(1 + k_1 r^2 + k_2 r^4) + p_1(r^2 + 2v^2) + 2p_2 uv \\ 1 \end{pmatrix}. \quad (3)$$

For the automatic calibration the method of Zhang [5] is used. From a picture sequence of a pattern the parameters are fitted by equating pixel positions with distorted real world positions of characteristic points (Fig. 2b).

For calibration a coordinate system is placed on the floor (Fig. 2c). Because the view is perpendicular to the floor only a 2D coordinate system is needed. Otherwise the image would have to be tilted beforehand. The picture in Fig. 2c is bigger than the picture in Fig. 2a because the undistortion generates larger images to encompass all information of the original image. Thus the printed proportion is equivalent to the proportion of the original image sizes.

With the knowledge of the altitude of the camera above the floor we are able to measure the 3D space seen by the camera. Thus the position of all pedestrians' heads can be calculated if the height of their heads is known. The altitude of the camera can be determined by the parameters from the automatic calculation and the coordinate system on the floor.

The limitations of the model used are described in Sect. 4.5.

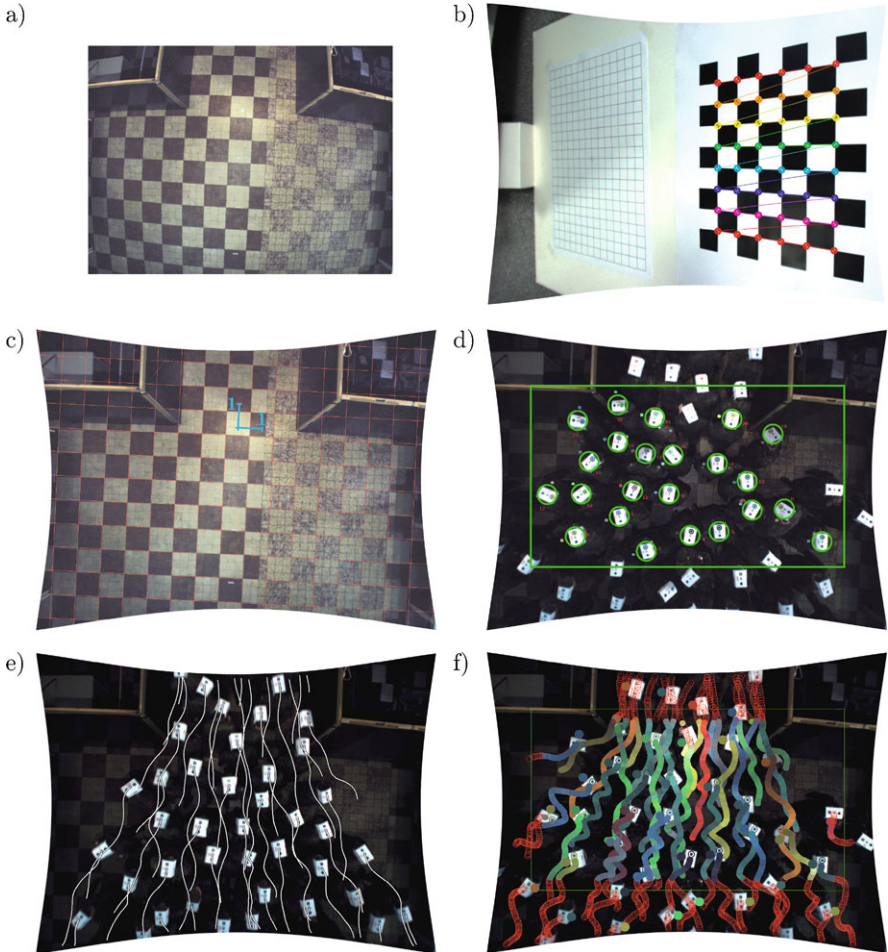


Fig. 2. The picture sequence (a), (c)–(f) represents the successive steps for extracting highly precise trajectories from video recordings. (a) shows an original frame of a video at the beginning of a bottleneck experiment without pedestrians. (b) is an undistorted calibration picture for the automatic calibration and (c) is a result of the automatic calibration of (a). In (d) the individual pedestrians are detected in the *green rectangular* and marked with a *green circle* around their head pasteboard. (e) shows the paths of all head movements in the last two seconds by tracking the recognized heads. (f) displays the colour of the colour markers of pedestrians for some continuous frames.

3.2 Recognition

Because of the experimental conditions we were able to use markers on a pasteboard to detect the centre of the heads and determine trajectories with high accuracy, but the ultimate goal should be the detection of marker-less

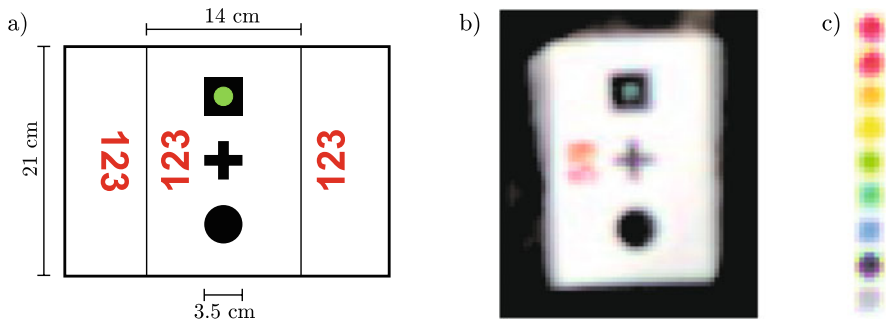


Fig. 3. (a) shows the whole pasteboard and the imprint. After folding the pasteboard at the lines in (a) it was fixed to a hat. The recorded pasteboard looks as shown in (b). (c) shows all possible colours of the top colour marker after recording.

pedestrians without losing the quality of the trajectories. For other markers or marker-less detection only the recognition part described in this section has to be replaced as long as only the intra-frame and not the inter-frame information from the tracking task are used to detect the pedestrians.

We used a pasteboard with high contrast markers and paid attention to constant lighting conditions. The detection is restricted to a modifiable recognition area, which is illustrated as green rectangular in Fig. 2d, where all pedestrians have to go through. The pixel covering is 2.5 pixel/cm in the image centre and 1.9 pixel/cm in the corners. Thus the whole pasteboard covers 35×53 pixel and the colour marker inside the black square covers 4×4 pixel in the image centre.

We are tracking the head and not for example the more stable midpoint of the shoulders because the perspective view would mask some shoulders from the person's head or from nearby persons in dense situations to the boundary of the image.

The pasteboard in Fig. 3a and the recorded result in Fig. 3b has three black markers in a line and red numbers on the top and on both sides of the head after folding the pasteboard at the lines. The numbers have not been used in the extraction process. The head-sized pasteboard has been fixed on a hat.

The middle black cross is the marker which is tracked on sub-pixel accuracy. The line of the three black markers depicts the line of sight. The quadratic black marker coded with different coloured circles indicates the size of the person wearing this pasteboard. The colours shown in Fig. 3c have been used to identify the size of every pedestrian. Section 3.4 describes the height classes and their relevance in detail.

The recognition of the markers is done by detecting directed isolines of the same brightness and subsequent analysis of their shape and colour. For this purpose oriented isolines are calculated for ten brightness values. The

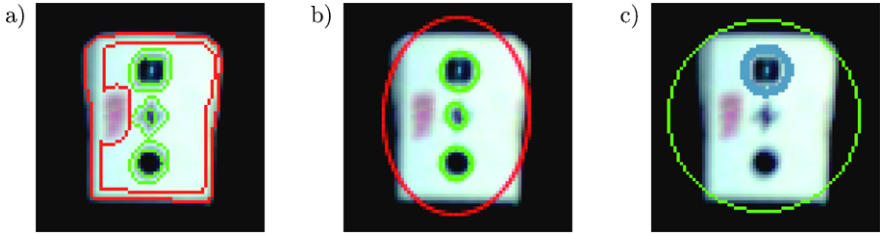


Fig. 4. The recognition first detects directed isolines of the same brightness as can be seen in (a) for two brightness values. The *red lines* corral lighter and *green* darker pixel. (b) All isolines are approximated by ellipses and the right shape matching one are grouped to identify the head and the three markers. (c) The *middle cross marker* as centre of the *green circle* will be tracked and the *circled quadratic outer marker* covers the colour code for the height class.

orientation of the isolines groups them to one which corral lighter pixel and one which corral darker pixel. The first group identifies the complete white pasteboard and is visualized as red lines in Fig. 4a for two brightness values. The second group corral the black markers and is visualized as green lines for the same brightness values.

All isolines are approximated by ellipses with the method of least squares to have easy access to shape data like size, aspect ratio and centre of the region. Ellipses with the right size and aspect ratio are grouped so that at the end one head ellipse and three assigned marker ellipses inside that head ellipse identify and describe the head position (Fig. 4b). We only consider ellipses with the same centre line to exclude ellipses generated by the red numbers. The centre of the middle marker ellipses will then be tracked on sub-pixel accuracy.

The brightest pixel in the centre of the outer marker ellipses defines the colour of the pedestrian wearing the pasteboard. In Fig. 4c the circle with the same colour as the colour marker shows the colour marker detected. Figures 4c and 2d also show a big green circle with the same centre as the middle ellipse from the cross marker, so that centre will be tracked.

To improve the quality of the trajectories, stabilize the colour for height mapping and identify new persons inside the recognition area the recognition is repeated during tracking after some assignable frames.

A quality value is defined for each point of the trajectory to measure improvements. If a head is recognized or the user defines the position by hand the maximum quality of 100 is assigned. When a recognized point is tracked values between 20 and 80 are assigned depending on the calculated tracking error as described in the next section.

The same pedestrian will be handled in a frame again, if an already tracked pedestrian is recognized again or the generation of the trajectories is repeated. The repetition happens if the tracking is also done in the backward direction or with other parameters. Then the one of the double point with the highest

quality is chosen, so that an already tracked point will be replaced by the related recognized one.

3.3 Tracking

After recognizing the pedestrians they have to be tracked. Tracking searches for a point $\mathbf{x}_2 = (x_2 \ y_2) = (x_1 + d_x \ y_1 + d_y)$ in picture \mathbf{B}_2 , which is similar to a point $\mathbf{x}_1 = (x_1 \ y_1)$ in picture \mathbf{B}_1 . Due to mapping errors and robustness the error function $f(d_x, d_y)$ is minimized in a region $[x - w, x + w] \times [y - w, y + w]$:

$$f(d_x, d_y) = \sum_{x=x_1-w}^{x_1+w} \sum_{y=y_1-w}^{y_1+w} (\mathbf{B}_1(x, y) - \mathbf{B}_2(x + d_x, y + d_y))^2. \quad (4)$$

The accurate and robust pyramidal iterative Lucas Kanade feature tracker [6] is used for tracking. The tracker searches with sub-pixel accuracy in regions of same size in recursive Gaussian pyramids

$$\mathbf{B}^L(x, y) = \sum_{i=-1}^1 \sum_{j=-1}^1 2^{-(2+|i|+|j|)} \mathbf{B}^{L-1}(2x - i, 2y - j) \quad (5)$$

with $\mathbf{B}^0 = \mathbf{B}$ and $\mathbf{x}^L = 2^{-L}\mathbf{x}$, starting in \mathbf{B}^{L-1} with $\mathbf{x}^{L-1} = 2\mathbf{x}^L$ and propagates the result to the next higher resolution level as initial guess. The region searched is chosen such that it covers the whole pasteboard in the level \mathbf{B}^{L-1} and only the cross marker in \mathbf{B}^0 . Two successive frames are compared so that the robustness due to the Gaussian pyramids is enhanced by the small differences of the tracked region over the time. Resulting trajectories can be seen in Fig. 2e showing all head movements in the last two seconds.

Recognition is only done in a part of the video, but the tracking produces trajectories also near the border. The tracking paths in front of the recognition region at the bottom of Fig. 2e results from backwards tracking. The tracking ends if the trajectory leaves the picture or the error exceeds a threshold.

3.4 Height Detection

To correct the perspective distortion the knowledge of every persons' height is required. Especially wide angle lenses produce large distortions. A pixel in the image may correspond to different heights at different positions on the ground plane as illustrated in Fig. 7a. Further discussion can be found in Sect. 4.5.

The already mentioned colour markers detected during the recognition process described in Sect. 3.2 classify the height of each person. Ten discrete colours (Fig. 3c) plus the colour white are used to allow 5 cm accuracy.

The colour assigned to a person is the average colour of all colour markers recognized along their trajectories and is visualized as dyed circle in a colour diagram inside the recognition tab as can be seen in Fig. 5. Figure 2f shows

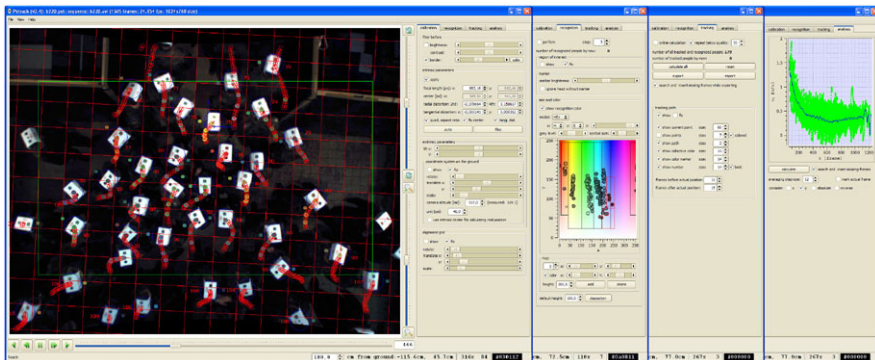


Fig. 5. The software **PeTrack** includes all parts for extracting the trajectories from video recordings. Beside the visualization of the trajectories the tabs shown steer the calibration, the recognition with height detection and the tracking. The last tab allows some direct analysis of the resulting trajectories.

the paths of the colour markers of the pedestrians at some continuous frames where the recognition is performed for every frame inside the recognition area. The hue is stable along the tracking path.

The mapping of colour regions to a height class has to be done manually once with rectangles in a 2D colour space, preferable in the hue-saturation or hue-brightness plane of the HSV colour model as can be seen in Fig. 5 at the recognition tab. Grey scale values are treated separately. Similar hues code similar heights, thus a mismatch would cause only a small additional error. The general error due to the not discriminable people size inside a height class or to the totally unknown height is discussed in Sect. 4.5.

After finishing all tasks for the extraction of the trajectories we are now able to calculate the trajectories in 3D space and the line of sight. For this purpose a coordinate transformation from pixel positions to real positions and an inverse perspective transformation have to be performed.

For future marker-less extraction the most critical part will be the height determination. Probably multiple cameras will be needed for good accuracy.

4 Results

4.1 Implementation

Figure 5 shows a screenshot of the resulting software named **PeTrack** (**P**edestrian **T**racking) [3] with the main tabs corresponding to the steps of the processing pipeline: calibration, recognition, tracking and height detection.

The software can be used interactively or command line oriented for the automatic generation of trajectories for a sequence of video recordings. The

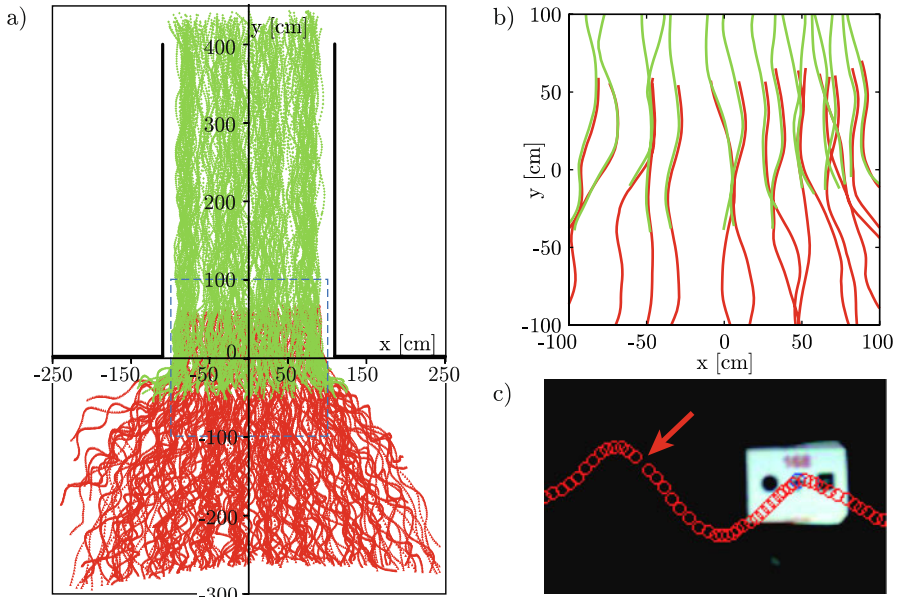


Fig. 6. (a) All trajectories of a bottleneck experiment with a width of 220 cm and 180 pedestrians. The *dashed blue square* is illustrated in (b) with less trajectories. (c) shows every tracked position of a pedestrian; the *arrow* points to a missing one.

im- and export of project files, image sequences, video recordings and trajectories is possible. PeTrack uses the open software libraries Qt, QWT and OpenCV and also is open source and platform independent. The programming language is C++.

4.2 Trajectories

The result of the extraction process are highly precise smooth trajectories of the centre of the head of every pedestrian (Fig. 6a). The time resolution is 0.04 s and with a speed of around 1 m/s the trajectories have a space resolution of 4 cm. That figure shows all trajectories at once so that lane formation can be identified. Figure 6b gives a subset of the trajectories in a quadratic region drawn as dashed blue line in Fig. 6a. The green and red paths result from different cameras. Videos of the trajectory progression can be found at [3].

4.3 Combination of Camera Views

The precision of the trajectories is high, thus overlapping camera views allow a combination of trajectory sets (Fig. 6b). The global offset of 1 cm in x direction of the two sets probably comes from not optimal fitting coordinate systems

placed manually on the floor as described in Sect. 3.1. The other differences result from the increasing error towards the boundary of the camera’s view as explained in Sect. 4.5.

The algorithm which combines the trajectory sets automatically searches for the time where the sets fit best. The combination automatically corrects the global offset and interpolates linear between two matching trajectories, so that the trajectory to the respective boundary has less influence on the resulting behavior of the combined trajectory.

4.4 Missing Frames

Sometimes there have been missing frames while recording the experiments as can be seen in Fig. 6c, where every tracked position in every frame is illustrated by a red circle and an arrow points at a missing one. These missing frames between frame f_n and f_{n-1} can easily be detected by comparing the distance between the tracked positions before $|p_{f_n}^{(i)} - p_{f_{n-1}}^{(i)}|$ and behind $|p_{f_{n+2}}^{(i)} - p_{f_{n+1}}^{(i)}|$ with the possible gap for all v visible pedestrians $i \in \mathbb{N}_v$. The number of missing frames is the rounded g , which can then be calculated by

$$g = \frac{1}{2v} \sum_i \frac{|p_{f_n}^{(i)} - p_{f_{n-1}}^{(i)}| + |p_{f_{n+2}}^{(i)} - p_{f_{n+1}}^{(i)}|}{|p_{f_{n+1}}^{(i)} - p_{f_n}^{(i)}|} - 1. \quad (6)$$

For missing frames ($g \geq 0.5$) the trajectories can be amended by linear interpolation.

4.5 Error

The error in the trajectories depends on the amount of unbalanced lens distortion and the remaining perspective error from the height variations in the height classes. The recognition and tracking with markers gives almost no error.

The calibration is done with the model [4] described in Sect. 3.1. It takes into account the most typical distortion parameters, but it remains a general model, which cannot describe all parts of a real distortion and especially the wide angle lenses used have big distortions to their boundaries.

The error for the lenses used in our experiments can be seen in Fig. 7c. The dashed green line shows the error e'_{dst} due to the lack of undistortion corresponding to the distance to the image centre x on the floor and the solid green line e_{dst} in the persons’ head height. In the centre of the image the error is 0 and increases nearly linearly inside the biggest rectangular which fit into the undistorted image: $e_{\text{dst}}(x) \approx 0.01x$, $\forall x \in [0, 270]$. The light grey region in the diagram marks the outermost corners in the persons’ head height and the dark grey region the outermost corners on the floor, which do not fit to that rectangular. In these corners the error increases up to the maximum error of $e_{\text{dst}}(320) \approx 4$ cm.

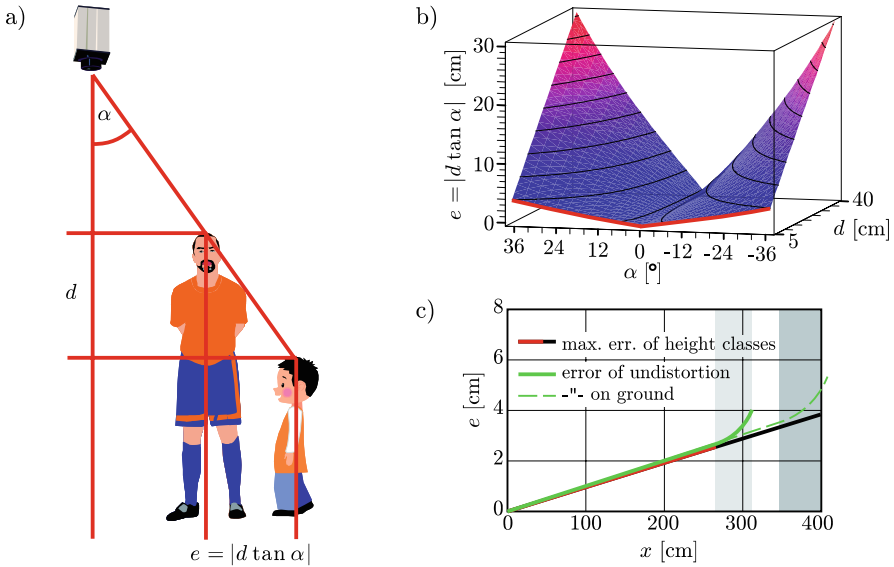


Fig. 7. (a) and (b) illustrates the error e because of the perspective view, if pedestrians have a height difference of d depending on the angle α to the perpendicular of the camera. (c) shows the maximal error e depending on the distance to the image centre x because of the height classes and the imperfect undistortion.

Another error is caused by the perspective view and the not discriminable people size. The reason for the error can be seen in Fig. 7a. The same pixel in the recorded image may correspond to different heights and thus to different positions on the ground plane. With a height difference d of two people and an angle of α to the perpendicular of the camera the error is $|d \tan \alpha|$. For variable height differences and angles the surface in Fig. 7b illustrates the strongly growing error for increasing d and α . With the wide angle lenses used with an aperture angle of 74° and pedestrians heights between 160 and 200 cm the maximal error is 30 cm in the inscribed rectangular described above.

To reduce the error of the perspective distortion the height information is needed. The height classes of 5 cm as described in Sect. 3.4 reduce the maximal error to 3.75 cm. This is illustrated by the red path in front of Fig. 7b and by the red line in Fig. 7c. The continuing black line shows the error for the corners. Also this error is 0 exactly underneath the camera. The maximal error e_{hg} increases linear with the distance x to the image centre: $e_{\text{hg}} = \frac{5}{535}x$.

Inside the rectangular described above the sum of both error types increases with 1.9 cm/m and the maximum error is 5.1 cm and thus the head bearing has a substantially larger influence on the trajectories than the errors.

5 Summary and Outlook

The software **PeTrack** automatically extracts trajectories from normal video recordings with high accuracy and is able to batch-process extensive experimental series with a large number of persons and dense situations. The maximum error is 5.1 cm due to the lack of undistortion and the not discriminable people size. The generated data is reliable to analyze pedestrian crowd characteristics and to verify models on a microscopic level.

The precision of the trajectories could be improved by using more cameras with larger focal lens and a higher altitude. The software will be extended by more analysis features and by automatic local white balance to get better height clusters for easier manual or automatic cluster identification.

For the goal of marker-less extraction to get trajectory data from real situations particularly the way of recognition has to be replaced. This ambitious goal may only be achieved with special hardware or a reduction of precision, but this remains to be studied.

Acknowledgements

PeTrack is developed within a project funded by the German Research Foundation (DFG) KL 1873/1-1 and SE 1789/1-1.

References

1. A. Schadschneider, W. Klingsch, H. Klüpfel, T. Kretz, C. Rogsch, and A. Seyfried. Evacuation dynamics: Empirical results, modeling and applications. In *Encyclopedia of Complexity and System Science*. Springer, Berlin, 2009.
2. A. Seyfried, M. Boltes, J. Kähler, W. Klingsch, A. Portz, T. Rupprecht, A. Schadschneider, B. Steffen, and A. Winkens. Enhanced empirical data for the fundamental diagram and the flow through bottlenecks. In *Pedestrian and Evacuation Dynamics 2008*. Springer, Berlin, 2010.
3. M. Boltes. Software **PeTrack**. Research Centre Jülich, <http://www.fz-juelich.de/jsc/petrack/>.
4. D.C. Brown. Close-range camera calibration. *Photogrammetric Engineering*, 37:855–866, 1971.
5. Z. Zhang. A flexible new technique for camera calibration. *IEEE Transactions on Pattern Analysis and Machine Intelligence*, 22(11):1330–1334, 2000.
6. J.-Y. Bouguet. Pyramidal implementation of the Lucas Kanade feature tracker. *OpenCV Documents*, 1999.

Stairwell Evacuation from Buildings: What We Know We Don't Know

Richard D. Peacock, Jason D. Averill, and Erica D. Kuligowski

National Institute of Standards and Technology, Gaithersburg, MD, USA
e-mail: richard.peacock@nist.gov, jason.averill@nist.gov, erica.kuligowski@nist.gov

Summary. Occupant descent down stairwells during building evacuations is typically described by measurable engineering variables such as stairwell geometry, speed, density, and pre-evacuation delay. In turn, predictive models of building evacuation use these variables to predict the performance of egress systems for building design, emergency planning, or event reconstruction. This paper provides a summary of literature values for movement speeds and compares these to several new fire drill evacuations. Movement speeds in the current study are observed to be quite similar to the range of literature values. Perhaps most importantly though, the typical engineering parameters are seen to explain only a small fraction of the observed variance in occupant movement speeds. This suggests that traditional measures form an incomplete theory of people movement in stairs. Additional research to better understand the physiological and behavioral aspects of the evacuation process and the difference between fire drill evacuations and real fire emergencies are needed.

1 Introduction

Both before and since the World Trade Center tower collapses, there have been numerous events where there was extensive life loss because there was insufficient time for safe evacuation from a threatened building. While much attention has been focused upon the more readily quantifiable input parameters to fire models such as material flammability properties, little effort has focused on the need for a more fundamental understanding of occupant egress. High-profile scenarios such as the World Trade Center collapse routinely lead to public expressions requiring changes to the status quo regarding public safety. While there are dozens of models to simulate the evacuation of occupants from a given building geometry [1], there is limited contemporary data to support the model inputs or assumptions and even less information available to validate the models for actual emergencies. Collection and analysis of basic evacuation data would provide a basis for building code requirements, the practice of egress system design, and ensure robustness for analysis of emerging issues. While some models have had extensive validation efforts by

the developers [2, 3] and others have included uncertainty in the analysis for a few limited data sets [4], there is still a significant need for independent data on evacuation behavior both for further development of the models as well as independent validation efforts.

As a start to provide such data, this paper provides a review of published data for movement speeds on egress stairwells, and an analysis of three recent data sets involving full-building evacuation.

2 Occupant Movement in Building Evacuation

There are many factors and influences that play a role in the evacuation of building occupants. Gwynne et al. discuss these in their article entitled “A Review of the Methodologies Used in the Computer Simulation of Evacuation from the Built Environment” [5] and organizes the factors that influence evacuation into the following categories:

- configuration of the building/enclosure
- procedures within the enclosure
- environmental factors inside the structure
- behavior of the occupants.

Configuration of the building/enclosure involves what is traditionally covered by the codes and standards, such as building layouts, number of exits, exit widths, travel distances, etc. Gwynne proposes that occupants can commit behavioral violations to this factor in a number of ways, for instance exit misuse, because they may be unfamiliar with the building and be without staff guidance to aid in the evacuation. Another main issue that is frequently studied with building configuration is the way people move throughout the different components of the building, including both horizontal and vertical movement. Fruin [6], Nelson and Mowrer [7], Pauls [8], and Proulx [9] have studied this topic to understand movement through building components such as corridors, doorways, and stairways.

Proulx [9] and others have studied the delay from initial notification of a fire event to the beginning of evacuation, often termed pre-evacuation time, but more accurately described as evacuation initiation delay. In three office buildings, Proulx [9] found an average delay of 50 s. Brennan reported delays averaging 150 s in a severe fire in a high rise office building [10]. Lord et al. [4] review a number of sources on evacuation initiation delay. Values reported for office occupancies average $165 \text{ s} \pm 71 \text{ s}$ (uncertainty is expressed as standard deviation).

Stairway geometry, another configuration aspect of the building, also affects movement of the occupants. Overall stairwell effectiveness in building evacuation is impacted by a number of factors including the number and location of stairs in the buildings, the stair geometry, the number of occupants per floor, the number of occupants descending from above a given location,

and any obstacles the occupants may encounter during descent (such as fire responder counterflow). Occupant speed is affected by the number of steps, the angle of the stairway, depth of the tread, height of the riser, and the presence and location of handrails [5]. Proulx [9] found stairway movement involves a complex set of behaviors, such as resting, investigation, and communication. Movement on stairways is also affected by the amount of personal space needed per occupant, whether or not a person is carrying something (such as a child or personal items), and the mobility of the person traveling either up or down a flight of stairs. People sometimes become obstacles in the evacuation process, due to exhaustion or injury.

Literature values are available for movement down stairwells. Proulx [9] and Lord et al. [4] reviewed data on occupant speed, flow, and density. The range of values for occupant speed is shown in Table 1. For occupants with mobility impairments, the literature ranges from 0.16 m/s to 0.76 m/s; for occupants with no impairments, 0.49 m/s to 1.3 m/s (not including Fruin's crush load value).

3 Current Study

As part of a program to better understand occupant behavior during building emergencies, the Building and Fire Research Laboratory at the National Institute of Standards and Technology (NIST) has been collecting stairwell movement data during fire drill evacuations of office buildings. These data collections are intended to provide a better understanding of this principal building egress feature and develop a technical foundation for future codes and standards requirements.

While real emergency data is most desirable and might provide the most realistic predictor of behavior, it is not as readily available as fire drill data. For practical purposes, fire drill data is often used to study emergency behavior. A key assumption, consistent with most of the data presented in Sect. 2 of this paper, is that fire drill data can be used to approximate the response of individuals in an actual emergency [9]. This is, of course, dependent on whether the population is directly exposed to smoke and/or fire cues; meaning that fire drill data may best approximate the reaction and conditions experienced of those who are not close enough to the hazard to identify it as an emergency. In many high-rise evacuations, as is the case in this study, it is conceivable that a significant portion of the population has not been exposed to enough fire cues to be certain if it is an emergency. Information from real emergencies can inform fire drill data collections and provide a check of the validity of fire drill data.

NIST has collected fire drill evacuation data in six high-rise buildings. The data collection has utilized video technology in the stairwells in order to measure individual descent speeds, crowd density, stair entry time (evacuation

Year	Movement speeds (m/s)	Notes	Source
	0.52 ± 0.24^a	18–29 year old	Various ^b , from Lord et al. [4]
	0.52 ± 0.23	30–50 year old	Various ^b , from Lord et al. [4]
	0.49 ± 0.18	> 50 year old	Various ^b , from Lord et al. [4]
	0.16–0.76	Disabled occupant	Various ^b , from Lord et al. [4]
1969	0.58 ± 0.15		Predtechenskii and Milinskii ^c [11]
1972	0.762	Maximum	Fruin [6] from Pauls [8]
1972	0.6096	Moderate	Fruin [6] from Pauls [8]
1972	0.4826	Optimum	Fruin [6] from Pauls [8]
1972	0.2032	Crush	Fruin [6] from Pauls [8]
1988	0.33 ± 0.16	Locomotion disability	Boyce et al. [12]
1988	0.7 ± 0.26		Boyce et al. [12]
1995	1.1	Relatively fit	Proulx [13]
1995	0.5		Proulx [13]
2001	0.2	9/11 WTC towers	Averill et al. [14]
2004	0.76–1.3	Varied walking angle	Fujiyama [15] adapted by Hostikka ^d [16]
2007	0.57 ± 0.23	Photoluminescent stairwell markings	Proulx [17]
2007	0.64		Hostikka [16]

^aUncertainties are expressed as 1σ .

^bIncludes data from Fruin [6], Predtechenskii and Milinskii [11], Boyce [12], Proulx [13], Proulx et al. [18], Fahy and Proulx [19] and Webber [20].

^cIncludes movement speeds for densities the authors define as typical for stairwell evacuation.

^dData converted from horizontal speed to speed along incline with given stair geometry.

Table 1. Occupant movement speeds in stairwells.

delay), and stair entry floor (distance evacuated). The primary video analysis identified the following for each occupant to facilitate these measurements:

- time each person exited the stairwell (or entered the stairwell in the case of firefighters ascending the stairwell),
- times that each person passed each camera in the stairwell,
- density or crowdedness of that stair as indicated by the number of other persons nearby each person as they passed by each camera in the stairwell, and
- floor of entry for each person.

This paper focuses on the first three of these evacuations. The three buildings included in this paper ranged from six to 18 stories in height and were typical office occupancies. Typically 100 to 300 people used a stairway for

	Building 1	Building 2	Building 3
Occupancy	Office	Office / Educational	Office
Floors	6	11	18
Stair width ^a (m)	1.44 / 1.54 ^b	1.22 / 1.22	0.91 / 0.91
Stair riser (mm)	302	186	191
Stair tread (mm)	283	238	254
Exit width (m)	1.83 / 1.73	2.01 / 2.39	0.91 / 0.91
Evacuees	127 / 150	119 / 15	286 / 197
Evacuation time (s)	411	442	1031

^aFull stair width including handrails.

^bStairwell A widened to 1.68 m at the third floor. Stairwell B widened to 2.24 m at the third floor.

Table 2. Buildings included in current study.

evacuation. The stairs in these three buildings varied in width from 0.91 m to 2.24 m wide. A brief description of the three buildings is shown in Table 2.

Six-Story Building. The large office building had with seven wings adjoining and parallel to each other. During the drill, evacuation from two of 14 stairwells was observed. The stairwells (Stairwell A, 1.44 m wide and Stairwell B, 1.54 m wide) were in separate, neighboring wings. The wings observed were mirror images of each other, with the same number of elevators, stairwells, and exterior exit doors. The stairwells in each wing were accessible from all rooms and floors and led occupants into a lobby through double doors. After traveling through the lobby, occupants traveled down a small set of steps to a vestibule. The vestibule then led to the exterior of the building. A total of 277 occupants were observed in the quasi-unannounced drill¹ (127 in Stairwell A and 150 in Stairwell B). In Stairwell B, two groups of three firefighters each traveled up the stairwell at 40 s and 80 s after activation of the building fire alarm to study the impact of firefighter counterflow on the descending occupants. Total evacuation time for this fire drill was 411 s.

Eleven-Story Building. The building was an office occupancy for an educational institution housing faculty offices and research laboratories. Typical of many office buildings, there were two stairwells, both 1.22 m wide, located at opposite corners and accessible from all floors of the building. Both stairwells widened at the lower floors. One of the stairwells was directly adjacent to the building elevators. The stairwells opened directly to the ex-

¹ Occupants were told that a fire drill would take place in the near future, but were not told when the evacuation would take place. Normal alarm procedures were followed for the drill without further notification of the nature of the event.

Building	Pre-evacuation delay time (s)	Speed (m/s)
6-Story, No FF	144 ± 68	0.83 ± 0.18
6-Story, FF	140 ± 53	0.73 ± 0.26
11-Story	89 ± 54	0.62 ± 0.10
18-Story, No FF	220 ± 144	0.40 ± 0.09
18-Story, FF	188 ± 93	0.54 ± 0.18

Table 3. Occupant movement speeds (with standard deviation) in stairwells.

terior of the building. 134 occupants took part in the quasi-unannounced drill, with more than 89% using the stairwell adjacent to the elevators. Total evacuation time was 442 s.

Eighteen-Story Building. The building housed a business occupancy in three wings adjoining a fourth corridor at one end of the wings. Of the twelve 0.91 m stairwells available for egress, visual observations were made in five. Two of these, located in separate wings, were used for this paper. Several of the stairwells exited to the lobby area on the fifth floor through single 0.91 m wide doorways; others continued to the ground floor and exited directly out of the building. The lobby area exited directly to the exterior of the building. 727 occupants participated in the quasi-unannounced fire drill (286 in Stairwell 1 and 197 in Stairwell 12). In Stairwell 12, a total of 17 firefighters traveled up the stairwell in two groups following activation of the building fire alarm. Total evacuation time was 1031 s.

A summary of the pre-evacuation delay times and average stairwell descent speeds is shown in Table 3. Figure 1 shows the range of individual movement speeds for the three fire drills.

For each camera location, the mean speed is shown for occupants who were first observed evacuating at that camera location. (With cameras typically located at every other floor landing, this means entering either at the floor where the camera is located or at one floor above the camera location.) With the possible exception of the first three floors of the 6-story building, the data generally fall within experimental uncertainty of each other for all floors in the three buildings.

The cumulative distribution functions for stairwell movement speeds shown in Fig. 2 provide additional details of the range of speeds in the evacuations. Overall, 19% of the occupants move slower than 0.4 m/s (and these are nearly all in the 18 story building; less than 1% of the occupants in the 6- and 11-story buildings moved slower than 0.4 m/s) and 6% move faster than 1 m/s. Profiles for stairwells with fire fighter counterflow show a broader variation in movement speeds than those without in both the 6- and 18-story buildings. In the six story building, occupants moved slower in the stairwell with firefighters compared to the stairwell without firefighters while they moved faster in the 18-story building. This is likely due to congestion in the 18-story building

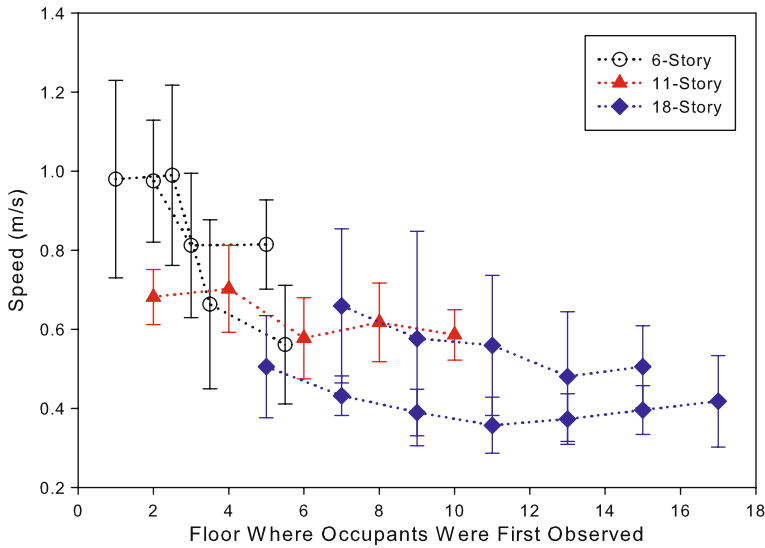


Fig. 1. Occupant movement speeds (with standard deviation) down stairwells in three fire drill evacuations.

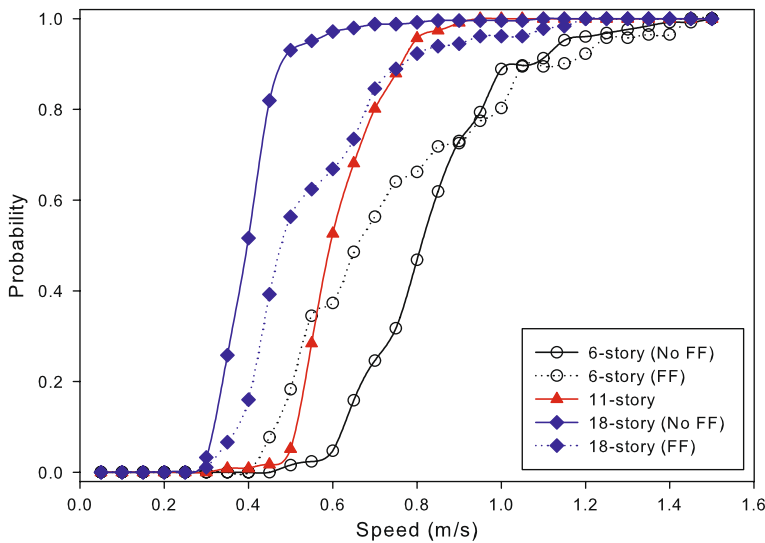


Fig. 2. Cumulative distribution function of movement speeds down stairwells in three fire drill evacuations.

stairwell from the much higher occupant load in the stairwell without fire-fighters. Additional data are needed to understand and verify the differences.

Comparing the recent evacuations to historical data (Fig. 3) shows these data are typically within the range of data in the literature and quite similar

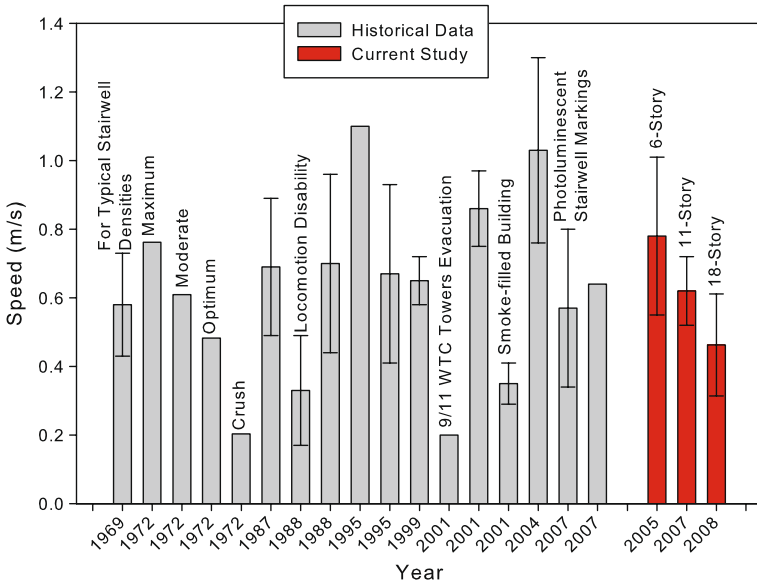


Fig. 3. Comparison of current study stairwell descent speeds with literature values. Where available, data points include standard deviation of average movement speeds.

to the “optimum” or moderate movement speed of Fruin [6]. Values for very dense evacuations (Fruin’s crush load [6], the 9/11 World Trade Center evacuation [14]) are significantly lower than both the current study and average values from the literature. This may be indicative of the difference between fire drill evacuations and real emergency situations or due to higher occupant densities in the slower stairwells. While the current study does not support recent concerns over slowing evacuation speeds resulting from increased obesity rates and lower fitness levels, additional study is needed, particularly to understand the impact of emergency conditions compared to fire drill evacuations.

To investigate the underlying causes for differences in movement speeds, a causal model was constructed to explore the components affecting occupant descent speeds in the stairwells. These included the typical engineering parameters that can be directly measured during the evacuation as follows:

1. Delay in evacuation initiation. Delay evacuation may cause occupants to encounter more or fewer people in the stairwell which may impact their speed. (For evacuation initiation delay, only data from the 6- and 11-story buildings were available. Data from the 18-story building is forthcoming.)
2. Distance traveled during evacuation. Evacuation from higher floors may lead occupants to encounter more congestion in the stairwells or allow

occupants to tire more than those evacuating from lower floors leading to lower movement speeds.

3. Presence or absence of firefighters traveling in flow counter to the descending occupants. Firefighters moving up the stairwell may impede those descending the stairs or may encourage the occupants to move more quickly.
4. Stairwell width. Wider stairwells may allow occupants to descend side by side or allow faster evacuees to pass slower ones. Narrow stairs may lead to congestion.
5. Density of people encountered during the evacuation. The presence additional persons in the stairwells nearby each evacuating occupant that may impede the evacuation of a given building occupant by limiting the maximum attainable speed of the occupant. (For occupant density, only data from the 6- and 11-story buildings were available. Data from the 18-story building is forthcoming.)

Using multivariate linear regression, we can relate these factors to movements speed in a simple regression equation

$$\hat{Y} = \beta_1 X_1 + \beta_2 X_2 + \beta_3 X_3 + \beta_4 X_4 + \beta_5 X_5 + e_{et}, \quad (1)$$

where the β -coefficients, $\beta_1, \beta_2, \dots, \beta_5$ are coefficients of the regression, X_1, X_2, \dots, X_5 are the vectors of the measured engineering parameters above, \hat{Y} is the vector of measured occupant stairwell descent speed, and e_{et} is an added error term that includes all causes not specifically included in the model. The magnitude and sign of the β -coefficients show the relative strength of the relationship between each variable the measured movement speed. That is, how important is the variation in variable X in predicting the variation in speed relative to other variables included in the model? For this simple model, only direct effects of each parameter on movement speed are considered.

Figure 4 shows the results of the causal analysis. Numbers on the connector arrows in Fig. 4 are the β -coefficients of the regression for each variable. Firefighter counterflow, delay, distance traveled, and stair width each had statistically significant impact on occupant movement speed during the evacuation. For example, occupant evacuation speed was inversely related to the distance traveled by the occupant; the higher the starting floor, the slower the overall movement speed. Distance is seen as twice as important as firefighter counterflow or stair width and three times as important as pre-evacuation delay in predicting speed. Stairwell density did not vary sufficiently in the two evacuations included to see a significant impact on evacuation speed.

However, the most notable result of the regression is that all of these easily measurable engineering variables together accounted for only 13% of the variance in occupant speed. Thus, the vast majority of the variance in occupant evacuation speed is not explained by these typical engineering parameters used to describe stairwell flow. Physiological and behavioral factors may be more important in determining occupant speed. While occupant demographics were not available for the current study, NIST [14] has estimated that 6% of the

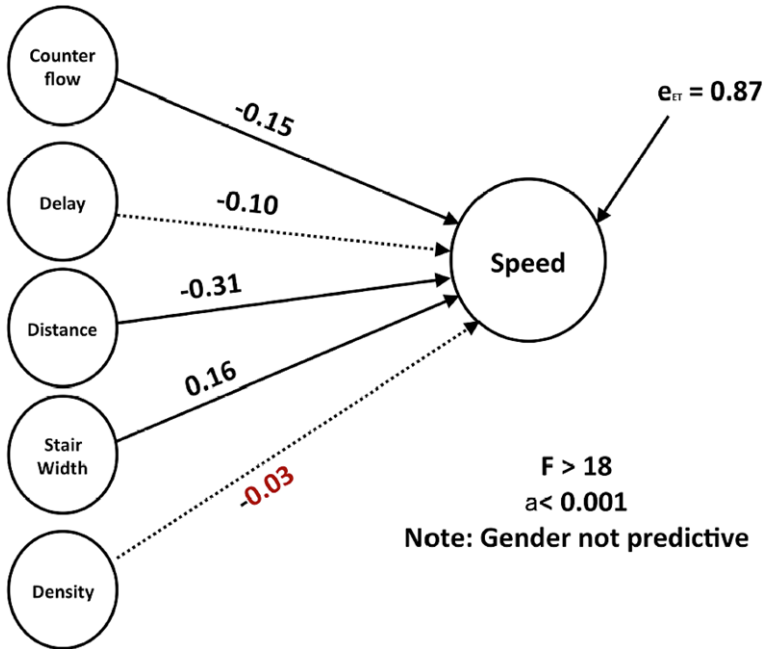


Fig. 4. Model of occupant stairwell descent speed.

occupants who evacuated the World Trade Center towers on September 11, 2001 reported having a mobility impairment that hindered their evacuation. Kuligowski and Gwynne [21] discuss the need to account for human behavior and note that inaccurate results from simplifications about behavior can lead to unsafe building designs and procedures. Clearly there is a need to better understand all the factors that impact the ability of building occupants to take appropriate protective action in the event of a building emergency.

4 Conclusions

This paper has summarized the typical engineering variables used to describe stairwell movement during building evacuations, reviewed literature values for movement speeds, and presented data from three new fire drill evacuations. The following conclusions are evident from the study:

- An “engineering approach” is insufficient to understand variance in occupant stairwell descent speeds. Better understanding of behavioral and physiological factors may improve explained variance across evacuations.
- Firefighter counterflow is a small but significant impact on stairwell movement speeds (in a six story building). The effect in taller buildings is yet to be studied.

- Understanding the context of observed evacuation drills is critically important. For the observed densities in the current study, stairwell width is a minor parameter. At higher occupant densities, literature suggest that stairwell width should be important [7].
- Early evidence does not support the hypothesis that people are moving more slowly, but additional research is needed to understanding movement speeds for a range of buildings and environmental conditions.

References

1. E. D. Kuligowski and R. D. Peacock. Review of Building Evacuation Models. Technical Note 1471, National Institute of Standards and Technology, Gaithersburg, MD, 2005.
2. S. Gwynne, E. R. Owen, and P. Lawrence. Further Validation of the buildingEXODUS Evacuation Model Using the Tsukuba Dataset. Rep. No. 98/IM/31, University of Greenwich, London, 1998.
3. S. Gwynne, E. R. Owen, and P. Lawrence. Validation of the buildingEXODUS Evacuation Model. Rep. No. 98/IM/29, University of Greenwich, London, 1998.
4. J. Lord, B. Meacham, B. Moore, R. Fahy, and G. Proulx. Guide for Evaluating the Predictive Capabilities of Computer Egress Models. GCR 06-886, National Institute of Standards and Technology, Gaithersburg, MD, 2005.
5. S. Gwynne, E. R. Galea, P. J. Lawrence, and L. Filippidis. A Review of Methodologies Used in the Computer Simulation of Evacuation from the Built Environment. *Building and Environment*, 34:741–749, 1999.
6. J. J. Fruin. *Pedestrian Planning and Design*, revised edition. Elevator World, Mobile, AL, 1987.
7. H. E. Nelson and F. W. Mowrer. Emergency Movement. In *The SFPE Handbook of Fire Protection Engineering*, third edition, pp. 3-367–3-380. Society of Fire Protection Engineers, Bethesda, MD, 2002.
8. J. Pauls. Movement of People. In *The SFPE Handbook of Fire Protection Engineering*, second edition, pp. 3-263–3-285. Society of Fire Protection Engineers, Bethesda, MD, 1995.
9. G. Proulx. Movement of People: The Evacuation Timing. In *The SFPE Handbook of Fire Protection Engineering*, third edition, pp. 3-341–3-366. Society of Fire Protection Engineers, Bethesda, MD, 2002.
10. P. Brennan. Timing Human Response in Real Fires. In *Proceedings of the First International Symposium on Human Behavior in Fire*. University of Ulster, Belfast, UK, 1998.
11. V. M. Predtechenskii and A. I. Milinskii. *Planning for Foot Traffic Flow in Buildings*. Amerind, New Delhi, 1978.
12. K. E. Boyce, T. J. Shields, and G. W. H. Silcock. Toward the Characterization of Building Occupants in Fire Safety Engineering: Capabilities of Disabled People Moving Horizontally and on an Incline. *Fire Technology*, 35(1):51–67, 1999.
13. G. Proulx, J. C. Latour, J. W. MacLaurin, J. Pineau, L. E. Hoffman, and C. Laroche. Housing Evacuation of Mixed Abilities Occupants in Highrise Buildings. Internal Report 706, Institute for Research in Construction, National Research Council Canada, Ottawa, ON, 1995.

14. J. D. Averill, D. S. Mileti, R. D. Peacock, E. D. Kuligowski, N. Groner, G. Proulx, P. A. Reneke, and H. E. Nelson. Federal Building and Fire Safety Investigation of the World Trade Center Disaster: Occupant Behavior, Egress, and Emergency Communication. NIST NCSTAR 1-7, National Institute of Standards and Technology, Gaithersburg, MD, 2005.
15. T. Fujiyama and N. Tyler. An Explicit Study on Walking Speeds of Pedestrians on Stairs. In *10th International Conference on Mobility and Transport for Elderly and Disabled People*, Mamamatsu, Japan, 2004.
16. S. Hostikka, T. Paloposki, T. Rine, J. Saari, R. Horhonen, and S. Hellovaara. Evacuation Experiments in Offices and Public Buildings. Technical Report, VTT Technical Research Centre of Finland, Espoo, Finland, 2007.
17. G. Proulx, N. Beónichou, J. K. Hum, and K. N. Restivo. Evaluation of the Effectiveness of Different Photoluminescent Stairwell Installations for the Evacuation of Office Building Occupants. IRC RR-232, Institute for Research in Construction, National Research Council Canada, Ottawa, ON, 2007.
18. G. Proulx. Occupant Response During a Residential High-Rise Fire. *Fire and Materials*, 23(6):317–323, November/December 1999.
19. R. F. Fahy and G. Proulx. Toward Creating a Database on Delay Times to Start Evacuation and Walking Speeds for Use in Evacuation Modelling. In *Human Behavior in Fire, Proceedings of the 2nd International Symposium*. MIT. Interscience Communications, London, 2001.
20. M. S. Wright, G. K. Cook, and G. M. B. Webber. The Effects of Smoke on People's Walking Speeds Using Overhead Lighting and Wayguidance Provision. In *Human Behavior in Fire, Proceedings of the 2nd International Symposium*, MIT. Interscience Communications, London, 2001.
21. E. D. Kuligowski and S. M. V. Gwynne. The Need for Behavioral Theory in Evacuation Modeling. In *Pedestrian and Evacuation Dynamics 2008*. Springer, Berlin, 2010.

Evacuation of a High Floor Metro Train in a Tunnel Situation: Experimental Findings

Monika Oswald, Hubert Kirchberger, and Christian Lebeda

Institute for Building Construction and Technology, Center of Materials and Testing, Fire Safety Science, Vienna University of Technology, Adolf-Blamauergasse 1-3, 1030 Vienna, Austria
e-mail: Monika.Oswald@tuwien.ac.at, Hubert.Kirchberger@tuwien.ac.at, Christian.Lebeda@tuwien.ac.at

Summary. The paper investigates the evacuation of passengers from a metro train in a simulated tunnel situation with a focus on the close geometry of the passage between the metro cars and the tunnel walls. Furthermore trains for underground transportation usually have a high floor which means that people have to overcome a height of 1.0 to 1.2 m to the surrounding ground adopting different types of exiting strategies. In addition people, who try to leave the train through one of the doors onto the escape route, and people who pass this door outside the train at the same time, have to interfere and react to each other in some way. Due to those risks two full-scale evacuation experiments were conducted in a newly released metro train presently used by the Vienna Transport Authorities, in which participants were subjected to the close geometry of a tunnel situation and a high floor evacuation.

1 Introduction

Trains for underground transportation usually have a high floor. This means in case of an evacuation onto the track, that people have to overcome a distance of 1.0 to 1.2 m from the floor level of the train to the level of the surrounding ground. In a tunnel situation the space between the vehicle and the tunnel walls is limited, so the escape route along the train is often very narrow. The distance between exits of the tunnel is sometimes more than 300 m depending on the design rules.

In the worst case the passengers are not able to evacuate to both ends of the train and they have to pass the whole length of the train (inside or outside the train) and interfere with the other people leaving the train.

In the year 2006 experimental studies were performed to evaluate the situation of an evacuation of a metro train in a simulated tunnel situation. The experiment involved more than 440 persons of different age and physical condition.

The scenario was an evacuation of a partially 100% occupied train in a tunnel situation onto the track down to a 0.65 m wide sideway by overcoming a height of 1.2 m [2]. For safety reasons the experiment was performed outside of a tunnel (possibility of rescue attempts from outside), but with the real geometric dimensions (height between sideway and vehicle floor and width of the sideway). Comparing to the tunnel situation an evacuation exercise with the elevated exit level to an open space was also conducted.

The experiments were documented with 10 video and 2 still cameras.

Based on the video footage the behavior of the people can be studied and examined. From this data it is possible to estimate door- and exit-flows for an evacuation to a small sideway and to the open space, both with exit heights of 1.0 to 1.2 m.

The major findings of the experiments were:

- The evacuation is strongly influenced by the interference of people walking on the sideway and people leaving the train trough the doors at the same time.
- The observation of the behavior of the people shows three significant types of ways to leave the train. These three types are classified as: “Jumper”, “Sider” and “Sitter”.
- About 50% of the people leave the train by jumping to the ground, about 30% use the handrail along the tunnel wall and 20% sit down on the train floor level before they slide out of the train.
- The flows on the doors are in the range of 0.25 persons/min m in the tunnel situation.

1.1 Description of the Train

The evacuation experiments were accomplished with a newly established metro car for the new extensions of the metro lines U1, U2 and U3, and as a replacement of existing trains for the underground system of Vienna. The metro trains of the series V-type (V car) are metro vehicles designed on the basis of a modular metro concept, which can run in a four or six car configuration. The four or six car train is basically made up of two different car types (see Fig. 1):

1. The trailer car TR: arranged at each end of the train, equipped with a driver’s cab and non-motorized.
2. The motor cars MC: arranged between the two trailer cars and motorized.

The smallest operable unit is configured as TR + MC + MC + TR, the largest operable unit as TR + MC + MC + MC + MC + TR. Under normal transport conditions the metro train V-type runs as a six car train with a length of approximately 111 m, a width of 2.85 m and a height of 3.50 m. Therefore the evacuation experiments were accomplished with a six car train.

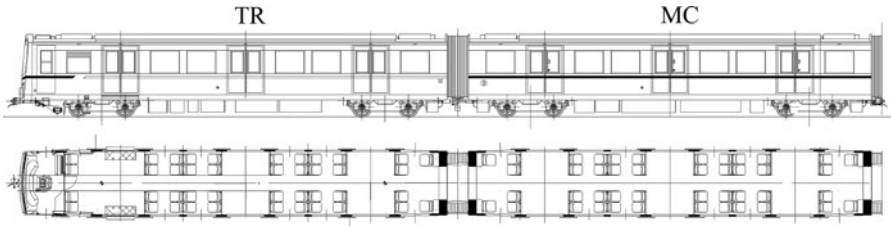


Fig. 1. Trailer car and motor car of metro train of the series V-type [2].

The metro train V-type in the six car configuration is designed for the transport of 878 passengers, of which 260 passengers are seated and 618 persons (4 pers/m^2) are standing. This represents a load factor of 100%. The train has 36 exit doors, of which 18 doors are located on each side of the carriages. The exit doors are double leaf sliding doors of the dimensions 1.30 m by 1.95 m.

1.2 Description of the Environmental Factors

The evacuation trials were conducted on the premises of the Vienna Transport Authorities at the depot Wien Erdberg. Throughout the experiments the train remained stationary to display a high floor evacuation at trial 1 and an evacuation in a tunnel situation at trial 2. The evacuation experiments took place in a metro train consisting of six cars, though only parts of this train were fully occupied (see Sect. 1.3).

For the experiments the participants had to overcome a height of about 1.00 m (trial 1) respectively 1.15 m (trial 2) from the floor level inside the metro train to the surrounding terrain. The evacuation of the carriages took place only on one side of the train. This was a reasonable approach to the evacuation experiments taking into account that the power rail is situated in between the two rail tracks and therefore the evacuation can only be performed on the side away from the other track.

At trial 1 the surrounding terrain at the side of the train, where the evacuation took place, was meant to display open space so that the participants could move away from the hazard area without any obstructions or guiding handrails (see Fig. 2).

At trial 2 the lateral security space had a width of 0.75 m. At a height of about 1.0 m was a handrail that reached about 10 cm into this security space, so that for the sidewalk a clear width of 0.65 m was available (see Fig. 3). The sidewalk was constructed with concrete slabs, so that the participants could move on plain but constricted ground. This situation resembles the close geometry in a metro tunnel accurately (see Figs. 4 and 5), where there



Fig. 2. Exit layout and height at trial 1.



Fig. 3. Exit space and height and positioning of the handrail at trial 2.

is only a narrow space available for the lengthwise evacuation inside the tunnel that allows the occupants to move only as fast as the person in front of them.

1.3 Description of the Participants

Physical Data of the Participants

The volunteers for the experiments were staff of the depot. The physical data of the participants were determined by inquiries concerning general personal information about

- the gender
- the body size
- the body weight and
- the age

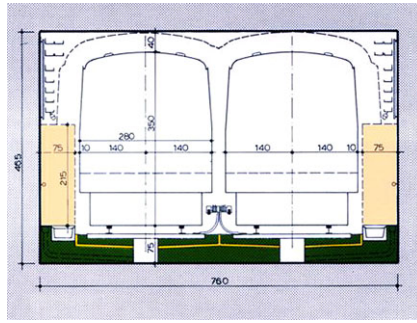


Fig. 4. Profile of the metro tunnel with the lateral security space.



Fig. 5. Position of the side handrail and the stairs leading from the tunnel onto the platform of a station.

Dimension		Value
Gender	Male [1]	404
	Female [1]	46
Body size	Mean value [m]	1.76
	Maximal value [m]	1.97
	Minimal value [m]	1.54
Body weight (Mass)	Mean value [kg]	83.45
	Maximal value [kg]	135.00
	Minimal value [kg]	39.00
Age	Mean value [a]	40
	Maximal value [a]	60
	Minimal value [a]	11

Table 1. Physical data of the participants [2].

Table 1 shows the summarized data of the values mentioned with their maximum, average and minimum.

The evaluation of the physical data of the participants shows that there are clearly more male than female persons taking part at the experiments.

This is due to the fact that all the participants are staff of the depot Wien Erdberg and most of them are male workers. Such a group of passengers is not representable for an average person distribution in a metro train at any rate, but it can resemble special occasions like for example metro trains transporting soccer fans to the stadium in Wien Praterstadion, where mostly there is a clear overhang of male fans.

Distribution of the Participants

Both experiments involved a full occupation of part of the train.

For trial 1 only the trailer car was occupied, that means 141 passengers took part in the first evacuation experiment, of whom 42 persons were seated and 99 were standing (see Table 2).

For trial 2 all seats were occupied and for the aisles 4 persons per m² free standing surface were determined for the trailer car at one end of the train and the following two motor cars. Thus 439 persons took part in the evacuation trial 2, of whom 130 passengers were seated and 309 persons were standing (see Table 3).

Though only parts of the train were occupied by passengers, at both trials a load factor of 100% was achieved for the seats and for the aisles in the examined cars. This represents a regular load factor for the mentioned cars.

Each participant received a starting number, which specified where every single person was located at the beginning of the evacuation trial. For safety reasons inside the train 5 observers were placed at trial 1 and 13 observers at trial 2. They were provided with signal coloured jackets and had the authority to stop the trial at any time there was risk of injury to any of the participants. In the case of non-emergency these observers where instructed not to take part or intervene actively in the evacuation process.

Car	Standing surface [m ²]	Number of seated persons	Number of standing persons	Total number of persons
Trailer Car (TR 1)	24.72	42	99	141
Total number of persons in the train				141

Table 2. Distribution of the participants at trial 1 [2].

Car	Standing surface [m ²]	Number of seated persons	Number of standing persons	Total number of persons
Trailer Car (TR)	24.72	42	99	141
Motor Car 1 (MC 1)	26.55	44	105	149
Motor Car 2 (MC 2)	26.55	44	105	149
Total number of persons in the train				439

Table 3. Distribution of the participants at trial 2 [2].

The participants were loaded from one side of the train, which corresponded to the evacuation side of the trials.

Due to the fact that the experiments would take place in a newly released metro train, which was not yet in operation, most of the participants were completely unfamiliar with the train design and layout. Only some of the workers of the depot Wien Erdberg had some knowledge about the metro train and its layout.

A train operator was placed in the trailer car, which was headed for the direction Simmering. For trial 1 that meant that the driver was situated right in the occupied trailer car and for trial 2 that the driver was seated in the driver's cab, that was positioned furthest away from the occupied cars.

1.4 Documentation and Evaluation of the Experiments

The evacuations were recorded by 10 video cameras and 2 still cameras. Most of the video cameras were positioned outside the metro train right in front of the doors of the cars. One video camera was located on an elevated platform that is part of one of the service buildings next to the tracks.

Furthermore the internal monitoring cameras of the metro train recorded the evacuation experiments and the gained data was used for the evaluation of the flow and behavior of the participants inside the cars.

The physical data of the participants were collected by the Vienna Transport Authorities in the course of the distribution of the starting numbers (see Sect. 1.3).

1.5 Description of the Evacuation Set up

Two full scale evacuation experiments were conducted, in which the basic assumption was the evacuation of a metro train that comes to a standstill someplace on the track at trial 1 and in a tunnel at trial 2. The evacuation in the event of an accident/emergency as for example the derailment, collision or overturning of a car was not considered.

Due to the limited availability of volunteers, the evacuation trials could not be conducted with a fully occupied train consisting of six cars. At trial 1 only the trailer car was occupied with a load factor of 100% and should be evacuated through 3 doors to open space. The main task was to capture the flow rates at the doors and to gain insight into the exit behavior of the participants.

At trial 2 a trailer car and 2 motor cars should be evacuated through 9 doors on to a narrow escape route to simulate a tunnel evacuation; that means half the train was occupied with a load factor of 100%. After leaving the train the participants should move along the sidewalk in a lengthwise evacuation process to a platform which can be reached by overcoming a 5 step stairwell. This approach resembles the geometric situation of a tunnel evacuation onto a

Trial number	Number of participants	Exit height	Evacuation setup
Trial 1	141	1.00 m	Free space
Trial 2	439	1.15 m	Sideway “tunnel” situation with 0.65 m width

Table 4. Overview of the trials 1 and 2 [2].

station platform pretty accurately (see Fig. 5). The number and distribution of persons and the occupancy of the cars are indicated in Sect. 1.3.

Table 4 gives an overview of the conducted experiments and summarizes the facts of the evacuation setup.

2 Observations and Findings

2.1 Trial 1: Flow Rates

In Sect. 2.2 elder data of a commuter train evacuation [1, 3], where the focus of the experiments was also set on the flow rates at the doors, will be compared with the outcomes of the flow rates at the doors of the metro train at trial 1.

At both trials in common were the door width with 1.3 m, the number of persons evacuated through one of the doors with 31 persons, which was a lucky congruence by chance; and the exiting behavior and strategies of the participants.

Different for the two trials were the average age distributions of the participants and the exit heights. At the commuter train experiment the participants were a rather young group of passengers with an average age of 26 years, whereas at the metro train trial the average age of the participants was 40 years. In addition at the commuter train trial the passengers had to overcome a height of 0.65 m from the inside of the carriage to the surrounding ground, and at the metro train trial the passengers had to pass 1.0 m down from the carriage onto the track level (see Table 5).

One of the main outcomes of trial 1 is that at both experiments the passengers adopted similar exit behavior: once the flow of people through the

Matching parameters	Differing parameters
<ul style="list-style-type: none"> • Door width: 1.3 m • Number of persons through the door: 31 • Exit height: staggered strategy to leave the train one by one 	<ul style="list-style-type: none"> • Average age of participants: <ul style="list-style-type: none"> (-) Commuter train: 26 years (-) Metro train: 40 years • Exit behavior: <ul style="list-style-type: none"> (-) Commuter train: 0.65 m (-) Metro train: 1.00 m

Table 5. Comparison of an evacuation trial of a commuter train [1, 3] and the described metro train [2].

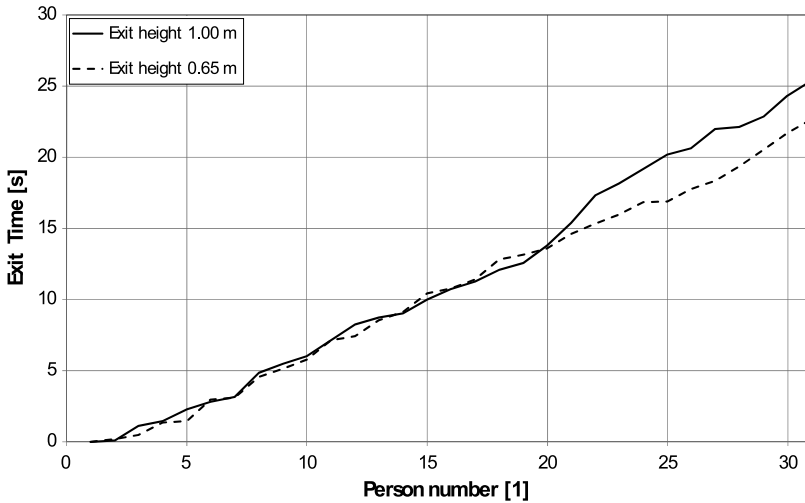


Fig. 6. Comparison of the exit times relating to the exit height for the commuter (exit height 0.65 m) and the metro train (exit height 1.0 m).

doors began only one person at a time exited a door at both trials. The passengers adopted a staggered strategy to leave the train one by one in which one person left the carriage for example through the left side of the door and the next person followed closely at the right side of the door and so forth.

Furthermore the results in Fig. 6 indicate that the exit height doesn't apparently take an influence on the exit times or the flow rates at the doors, though the exit height for the commuter train was 0.65 m whereas the exit height for the metro train was 1.0 m. In our last paper for the PED in the year 2005 [3] was stated that "The rather young group of passengers leads to fast evacuation times and high flow rate capacities, which will definitely be slower respectively lower with an older group of participants considering e.g. the rather high exit height of step down from the carriage onto the track level". The comparison of the exit times for the two different experiments in Fig. 6 shows clearly that those assumptions were wrong. At both trials nearly identical exit times were achieved for completely different exit heights. This result is even more startling under the aspect that the group of passengers at the metro trial was quite older. A possible explanation for this outcome is the gender distribution that is that nearly 90% of the participants at the metro train were male and though the participants were elder at this trial than the passengers of the commuter train, one can't call them old and/or mobility impaired persons.

2.2 Trial 2: Exit Behavior

The major findings of trial 2 are concerned with the exiting strategies and the formation of congestion alongside the train.



Fig. 7. “Jumper”, “Sider” and “Sitter” exiting the train.

The observation of the behavior of the people stepping off the high floor shows three significant types of ways to leave the train. These three types are classified as: Jumper, Sider and Sitter (see Fig. 7).

Jumper: A typical “Jumper” jumps out of the train without the use of the side handrails or the person combines jumping and one-big-step-climbing manoeuvres using the side handrails or the floor of the train for support.

Sider: As a “Sider” a person is categorized that uses the handrails along the sidewalk or the handrails inside the train as well as the handrails along the sidewalk for support to jump out of the train to the surrounding ground.

Sitter: The “Sitter” sits down on the floor level inside the train before he or she slides carefully out of the carriage to the surrounding ground with or without the use of the side handrails.

Visual observations show that the “Jumper” and the “Sider” need the whole width of the space between the car body and the “tunnel wall” (in this case the handrail and a wire mesh fence). It is not possible to pass the door area until the “Jumper or Sider” has left the scene. In a few cases the “Jumper or Sider” uses the back (shoulder) or a helping hand from other participants for support. In case of the sitting manoeuvre it is possible to pass the door even when the “Sitter” is leaving the train at the same time.

A second run of trial 2 was conducted to be able to observe if a training mechanism exists. Figure 8 shows the percentage of the three exiting types for several doors and the average values for all 9 doors for both runs. The results indicate that more persons adopted the jumping strategy and the number of sitters diminished at the second run of trial 2 because the participants were familiar with the surroundings especially the exit height. In general about

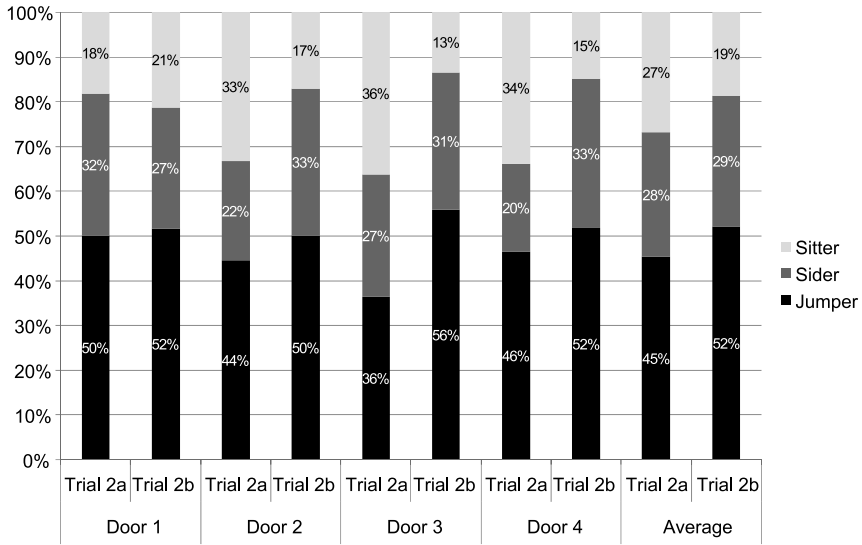


Fig. 8. Comparison of exiting strategies at trial 2.

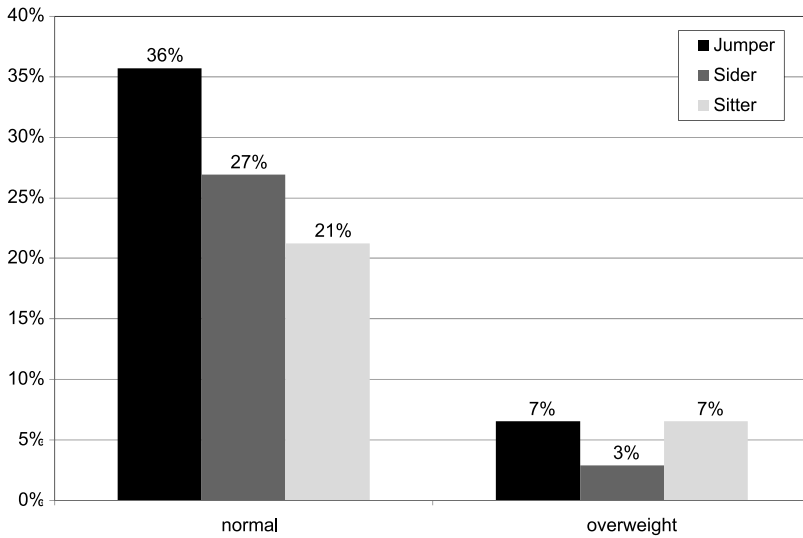


Fig. 9. Comparison of exiting strategies for normal and overweight people.

50% of the passengers adopted the “Jumper” strategy to leave the train, round about 30% used the handrail along the simulated tunnel wall and are therefore categorized as “Sider” and about 20% displayed the “Sitter” strategy that is sitting down on the train floor level before sliding out of the train.

In Fig. 9 the chosen exiting manoeuvres of people with normal weight and overweight passengers are compared. 36% of the passengers adopted the

jumping strategy, 27% tended to use the side handrail and/or the handrails inside the train to exit the carriage and 21% of the participants decided to be cautious and sit down to leave the train. All of them were of normal weight.

Of all the participants round about 17% were overweight. The overweight passengers preferred the “Jumper” (7%) and “Sitter” (7%) manoeuvre in comparison to the “Sider” (3%) strategy, which seems to be one of the more athletic ways of the 3 exiting methods. This outcome is underlined by the fact that just one of the 46 female passengers used the “Sider” strategy to leave the train.

2.3 Trial 2: Formation of Congestions

The formation and dissolving of congestions alongside the train at trial 2 can be divided into 3 stages.

Stage 1: The first stage of the evacuation shows how the participants leave the train through the doors onto the sidewalk adopting the 3 different types of exiting strategy and start moving along the passage way. They walk in one line, one person following the other and do not leave the sidewalk though they could side step into the track bed as soon as they have passed the head of the train.

Stage 2: As soon as the whole sidewalk alongside the train is filled with people from the end of the train to the first door, which is situated at the head of the metro train, the evacuation process along the sidewalk comes to a halt while participants at door 1, 2 and 3 are still leaving the train onto the surrounding ground. Because of the narrow geometry the participants outside the train can't pass the doors where people are still exiting the vehicle, especially when they use the “jumping” or “siding” strategy for exiting. As soon as the doors at the head of the evacuation process are emptied the lengthwise evacuation alongside the train starts moving again till it reaches the next door where passengers are trying to merge into the flow.

Stage 3: At the end of the evacuation experiment most of the participants have already left the train and move along the sidewalk to the platform of the “station”. At the end of the sidewalk there is a stair, consisting of 5 steps that participants have to overcome to reach the platform. The video footage shows clearly that this stairwell causes a minor congestion, that is the evacuation process slows down because it takes some time for the single participant to move up the stairs.

Figure 10 shows the exit times at doors 1 to 6 at trial 2. Because of the congestion at the sidewalk exit times went up, that is people inside the train couldn't merge into the queue building up outside the train on the escape route. And people at doors with higher numbers, which means participants at doors that were further away from the head of the evacuation process, had to wait longer than participants at doors with lower numbers.

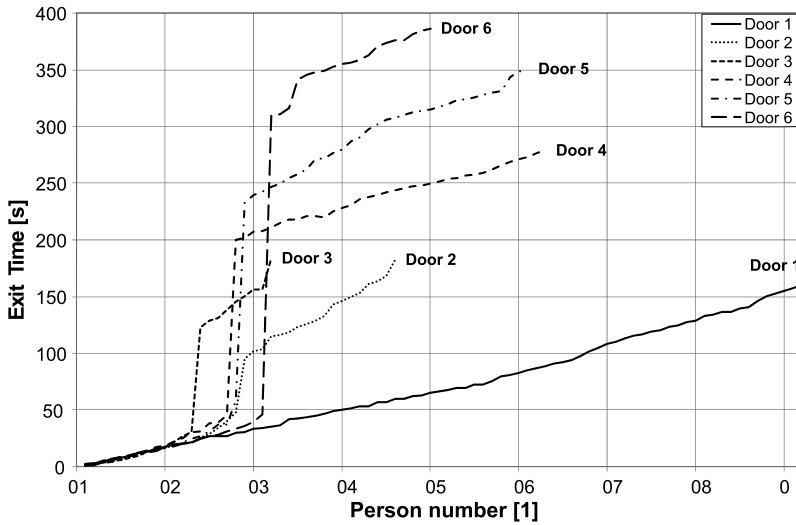


Fig. 10. Exit times at doors 1 to 6 at trial 2.

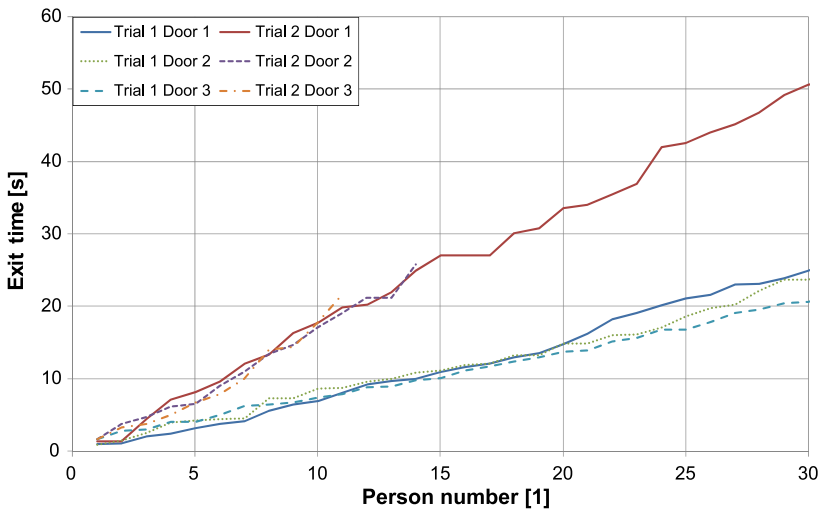


Fig. 11. Exit times at trial 1 and trial 2.

Figure 11 shows a comparison of the exit times at trial 1, where passengers could exit the train to open space, and trial 2, where participants were confronted with a narrow geometry as an exit ground. For trial 2 only those exit times are displayed in the diagram when participants didn't have to merge into the flow of passengers alongside the train, that means it shows only exit times that were observed at the beginning of the trial. The outcome shows

clearly that the flow rates at trial 2 are about half the values of the flow rates at trial 1.

3 Conclusions

As a result of the evacuation trials the following conclusion can be drawn:

- No significant difference was determined for the flow rates at the doors for exit height 0.65 m and 1.0 m.
- The flows at the doors are in the range of 0.25 persons/min m in the tunnel situation.
- The participants displayed 3 different types of exiting the train. These 3 types are classified as “Jumper”, “Sider” and “Sitter”. In average 45% of the passengers adopted a jumping manoeuvre, 28% were “Siders” and 27% exited as “Sitters”.
- Round about 17% of the participants were overweight and 83% of the passengers were of normal weight.
- Overweight passengers preferred the “Jumper” and “Sitter” manoeuvre for exiting the carriage whereas the passengers with normal weight tended to use the jumping manoeuvre prior to the “Sider” strategy to leave the train.
- The limited space along the pathway but also the one-directional evacuation caused flow rates at the doors at trial 2 that were half the values of the flow rates at the doors to open/free space at trial 1.

The findings of the trials have highlighted a number of issues requiring further research covering e.g. more detailed studies of

- the exit times at the doors depending on the exiting strategy
- the influence of the age and gender distribution on the exiting strategy
- the influence of the physical fitness of the participants on the exiting times and strategies
- the influence of the geometric layout on the exiting times and strategies (e.g. exit height, positioning of handrails).

Those issues will be incorporated into future research projects.

References

1. Vienna University of Technology, Institute for Building Construction and Technology, Center of Materials and Testing, Fire Safety Science: Evakuierungsversuch TW 4023, ÖBB “E-Talent” Zug 4023-005. Versuchsbericht. Vienna, July 2004 (unpublished).

2. Vienna University of Technology, Institute for Building Construction and Technology, Center of Materials and Testing, Fire Safety Science: Evakuierungsversuch U-Bahn Wien “V-Wagen”, Serienfahrzeug. Versuchsdokumentation. Vienna, August 2006 (unpublished).
3. Oswald, M., Lebeda, C., Schneider, U., Kirchberger, H.: Full-scale evacuation experiments in a smoke filled rail carriage—a detailed study of passenger behavior under reduced visibility. *Pedestrian and Evacuation Dynamics 2005, Proceedings*, Springer, Berlin, 2007, ISBN: 978-3-540-47062-5, pp. 41–55.

Using Laser Scanner Data to Calibrate Certain Aspects of Microscopic Pedestrian Motion Models

Dietmar Bauer¹ and Kay Kitazawa²

¹ arsenal research, Giefingg. 2, 1210 Wien, Austria
e-mail: Dietmar.Bauer@arsenal.ac.at

² CASA, UCL, 1-19 Torrington Place, London, WC1E 7HB, UK
e-mail: k.kitazawa@ucl.ac.uk

Summary. In this paper an automatic procedure to obtain trajectory data sets for controlled walking experiments based on laser scanner measurements is investigated. The laser range scanners provide raw data consisting of snapshots of scattered points with a frequency of 10 Hertz. A tracking algorithm is applied in order to convert the laser scanner measurements into trajectory data sets. Suitability of the method is demonstrated via the application to walking experiments performed in the London based walking laboratory PAMELA. Beside evaluating the accuracy of the obtained trajectory data the experiments are also used in order to enable data driven modelling of stopping and turning movements within the social force model paradigm. It is shown that via the modelling of a ‘desired velocity’ term inside the models the observed behavior can be modelled with reasonable accuracy.

1 Introduction

Recently a large number of microscopic pedestrian movement models have been reported in the literature. The most prominent ones include cellular-automata models [1–3], variants of the social force models [4, 5] and utility based models [6, 7]. These models have been analyzed with respect to the behavior they are capable of reproducing such as lane formation or trail formation [8]. Only recently, however, research has been directed towards calibrating the models and refinement of the models in accordance with phenomena observed in real scenes. Examples in this respect are [9–12].

There appear to be two main problems for calibration of the models: First and most importantly the calibration of microscopic pedestrian movement models requires the collection of individual trajectory data. The dominant method for obtaining such data sets is trajectory extraction based on recorded video sequences. Manual annotation of such data sets is extremely costly and hence typically sample sizes are small. An exception in this respect is the

pedestrian crossing data set introduced in [13]. The application of automatic tracking procedures currently works reasonably good if it is possible to mark pedestrians, e.g. in laboratory experiments, see e.g. [12, 14]. Typically here top view scenes are chosen in order to eliminate problems with occlusions at the cost of including body sway into the measured trajectories which has to be eliminated subsequently from the obtained trajectories. In real life scenes without marked subjects automatic trajectory extraction is currently subject to severe restrictions. People tracking software exists (e.g. based on the approach of [15]) that is capable of delivering trajectory information in scenarios with very few persons.

The second problem for the calibration of microscopic models lies in the complexity of the models. Typically these models include a number of different effects which all influence the chosen trajectory simultaneously. Hence typical real world or experimental data in real life situations make it hard to isolate the various effects.

As a consequence recently a number of studies [11, 16] are reported using trajectory data sets for relatively simple scenarios, where the data sets are obtained automatically. This is the route followed in this paper. The organization of this paper is as follows: In the next section the experimentation environment is presented. The corresponding data sets are described in Sect. 2 while the tracking algorithm used to obtain the data sets is discussed in Sect. 3. Subsequently the data sets are used in order to investigate stopping and turning movements observed in the experiments as reported upon in Sect. 4. The findings are summarized finally in Sect. 5 which concludes the paper.

2 The Experiments at PAMELA

PAMELA is an abbreviation of Pedestrian Accessibility and Movement Environment Laboratory. It is a research initiative led by Professor Nick Tyler at the Accessibility Research Group, Centre for Transport Studies, University College London. The objective of PAMELA is to research the way people interact with their physical and sensory environment. Using the controlled environment, researchers can simulate and recreate walking environments and can study how people react to changes in the environment. The laboratory [17] is equipped with a re-configurable walking platform, on which controlled pedestrian experiments can be conducted (see Fig. 1). Its surface area is approximately 80 m square, comprising 39 unit modules. Each module is square in shape and 1.2 m in length and width. 6 square tiles and 6 right angle isosceles triangle tiles make up of each unit module. The modules are placed on top of 176 computer controlled hydraulic cylinders that enable positioning the modules at different heights, generating level shifts and various inclinations on the platform. In addition the material of the tiles is also changeable to simulate real world walking surfaces. In our experiments the platform is arranged into a

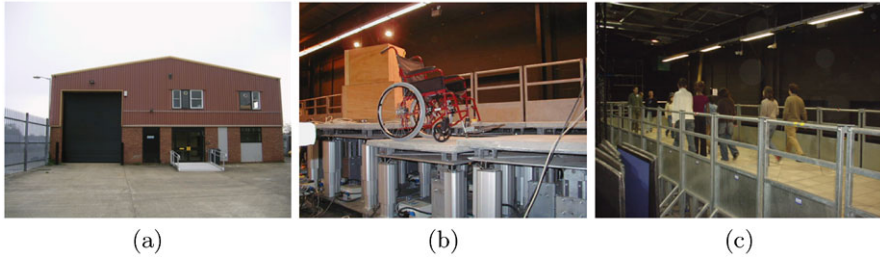
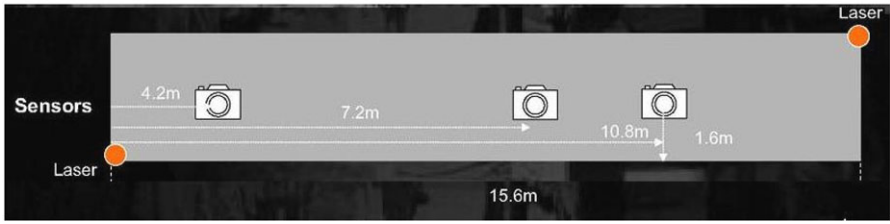


Fig. 1. **a** The PAMELA facility. **b** Hydraulic cylinders underneath the elements. **c** Snapshot of one walking experiment on the platform.

rectangular shape of which dimensions are 3.6 times 15.6 m with a flat surface paved with concrete tiles.

During the experiments two types of measurement systems are used: Three CCD digital cameras, C510R produced by Swann (Victoria, Australia), are placed at three different positions on the ceiling above the platform pointing downward to provide various views of the scene on the platform. Video footage captured in PAL format by each of these cameras is electronically transmitted via cables to camcorders, DCR-TRV30E by Sony (Tokyo, Japan), and recorded onto Mini DV tapes in DV format (360 times 288 pixels, interlaced, 25 fps). A fish-eye lens is attached to one of the cameras to capture the image of whole platform, while the other two cameras record less distorted images of the area directly beneath their respective position. All of the three cameras are placed along the centre line of the platform at the height of 4.1 m. The position and angle of the cameras with a normal lens is arranged in such a way that pedestrian movement around two obstacles (described later) be completely within the coverage of the video footage (Fig. 2(a) indicates the location of the video sensors). Two laser range scanners, LD-A Maker manufactured by IBEO Automobile Sensor GmbH (Hamburg, Germany) are positioned in such a way that they face diagonally across the platform to maximize the coverage of scanning (see Fig. 2(a)). They are mounted on the corner post at approximately 1 m high, which is about waist level as shown in plot (b) of Fig. 2. The laser scanners scan with frequency of ten Hertz on a dense grid in angular domain (1080 equally spaced angles in a 270° wide segment).

The idea of measuring pedestrian movement by laser scanners is similar to one used for obstacle detection radars. Laser beams emitted from scanners horizontally scan the surrounding environment to build up a two-dimensional image that shows the cross-section of the objects in the environment. It searches on a tight grid in the angular frequency for each angle for the first object hit by the laser beam and record its corresponding distance; as the top part of laser range scanner rotates, it emits an infrared laser beam which can travel up to 30 m; when a beam hits a solid surface, it is reflected and received by the scanner; using the time-of-flight concept, the distance and the relative



(a)



(b)



(c)

Fig. 2. a Location of the video sensors and laser scanners on the platform. b Laser scanners. c Laser scanner are mounted on waist level.

angle from the scanner of the object that reflect the beam is calculated. The raw measurement provided by the laser scanners hence consists of a collection of points. The measurement of two scanners are synchronized and combined in a joint coordinate system. An example of such a data set can be seen in Fig. 3(a). As visible there the scanners record a number of points outside of the platform as well as the hand rails on numerous places. Since the dimensions of the platform are known only measurements on the platform are considered leading to an image as provided in Fig. 3(b). In the image the outlines of four pedestrians and two obstacles (plotted in blue; the lower right one is partly occluded) are clearly shown.

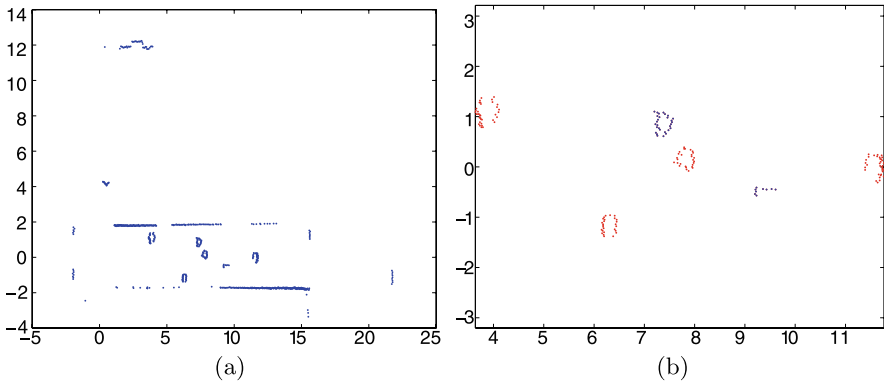


Fig. 3. Snapshot of laser scanner data sets with (a) and without (b) outliers. Scale is in meter.

On this platform a number of experiments have been performed: In the first series of three experiments two pedestrians are instructed to walk from one end of the platform to the other end and to repeat walking back and forth several times. Each of the two pedestrians is told to follow as close as possible the line on the floor separating two modules of the platform. The line is clearly visible to the pedestrians. These experiments will be used in order to evaluate the accuracy of the measurement system, as will be discussed in Sect. 3.

In the second series of experiments up to four pedestrians are told to walk freely from one end to the other for a few minutes. The pedestrians do not interfere with each other. These experiments will be used in Sect. 4 to investigate stopping and turning movements. The participants for both experiments are university graduates in their 20 s and 30 s.

3 The Tracking Algorithm

The raw data produced by the laser range scanners consists of a number of triples (t_i, x_i, y_i) where for each time stamp t a number of points occur for one pedestrian. This number needs not be equal and due to occlusions it might happen that some pedestrians are not represented in one time step at all. This data set is modelled using a hidden Markov model (HMM) [18]. HMMs consist of two quantities: A not directly measurable and hence hidden state vector $x_t \in \mathbb{R}^n$ and observed measurements $y_t \in \mathbb{R}^{p_t}$ of the state. In the current setting the hidden state comprises for each pedestrian five components, x - and y -coordinate of the position, x - and y -components of the velocity vector and the orientation represented as an angle with respect to the x -axis, i.e. the direction the pedestrian is facing (which need not coincide with the direction of heading). Hence given the number m of pedestrians the state vector is

$n = 5m$ dimensional. Pedestrians are represented as an ellipse with fixed ratio of the two axes, where the direction of the longer axis is determined by the orientation. The laser scanner measurements are modelled as noisy observations of points on these ellipses as the laser scanners record points on the surface of the pedestrians. The deviation from the ellipse representing the pedestrian are assumed to be Gaussian with given standard deviation and independent of each other. Thus the HMM is given by the following state equation:

$$x_{t+1} = Ax_t + w_t = \begin{bmatrix} A_1 & & \\ & \ddots & \\ & & A_m \end{bmatrix} \begin{bmatrix} x_{t,1} \\ \vdots \\ x_{t,m} \end{bmatrix}, \quad A_i = \begin{bmatrix} 1 & 0 & dt & 0 & 0 \\ 0 & 1 & 0 & dt & 0 \\ 0 & 0 & 1 & 0 & 0 \\ 0 & 0 & 0 & 1 & 0 \\ 0 & 0 & 0 & 0 & 1 \end{bmatrix}$$

where $dt = 1/10$ seconds denotes the sampling frequency. The state noise $w_t \in \mathbb{R}^5$ is assumed to be multivariate normally distributed with mean zero and variance $\sigma_w^2 I_5$ and is hence proportional to the identity matrix implying independent errors across coordinates.

The observation vector y_t consists of the collection of (x, y) coordinates of the laser scanner observations. For each time stamp the number of data points might be different. Each coordinate pair is modelled as a noisy observation of one of the ellipses, where the distance to the ellipses is normally distributed with variance σ_e^2 . All laser scanner measurements are assumed to be independent. It is assumed that for each laser scanner observation it is known that the observation corresponds to the nearest ellipse.

This completely specifies the probabilistic structure of the HMM. The unknown state is then estimated using particle filtering techniques, see e.g. [19].

The output of the particle filters are for each time instant a number of points (the so called particles) which represent a sample draw from the distribution of the state estimator. A point estimator of the state can be obtained as the sample mean of these points. A snapshot of this can be found in Fig. 4, where the original observations are drawn as blue dots, the location of the particles for this pedestrian are drawn in red and the sample mean as a black star.

Hence the output of the tracker consists of an NTTY data set containing for each time step the estimated coordinates for the center of gravity (projected onto the ground plane) of each of the pedestrians. This trajectory data contains a number of different noise sources originating in inaccuracies of the laser scanner measurements, the approximation error induced by assuming an elliptical shape of the body mid section and finally the estimation error due to representing the state estimation distribution by a finite number of particles. Part of this noise shows in the estimated trajectories as high frequent noise. Thus subsequently the obtained trajectories are smoothed using spline smoothing. The final output then consists of trajectory data containing for each pedestrian a sequence of time stamp and (x, y) coordinates.

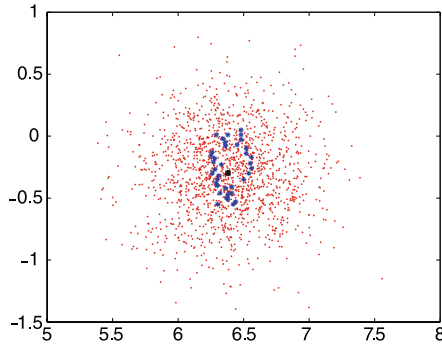


Fig. 4. Snapshot of the observations (*blue dots*) and the filtered particles (*red dots*). Scale is in meters.

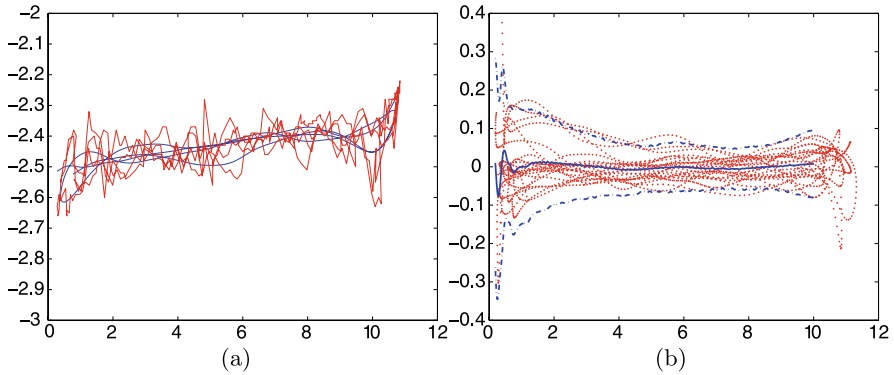


Fig. 5. **a** Raw trajectory and smoothed version. **b** Deviation from prescribed path. Coordinates are measured in meter.

Given measurements of the pedestrian trajectories measures of their accuracy are of interest. The first series of experiments serves this purpose. In this case the ground truth consists of specified trajectories the pedestrians are told to follow. The deviation of the actually measured trajectories from these lines constitutes the estimation error. It has been observed in the evaluation of the estimation error that there is a slight misalignment of the coordinate system imposed by the laser scanners and the actual coordinate system on the ground floor of the PAMELA facility (this can be seen in a slight upward trend in the tracking results in Fig. 5(a)). Accounting for this misalignment the mean of absolute distance of the measured positions from the prescribed path equals 3.8 cm. Restricting the range to x -coordinates between 2 and 10 omitting the ends of the platform (where the turning process most likely leads to deviation from the prescribed path not due to measurements but due to the inability of the pedestrian to follow a kinked path exactly) the mean distance drops to 2.7 cm. Figure 5(b) provides a plot comparing the tracked trajec-

tories with the prescribed paths. Superimposed over the measurements is a kernel estimate of the conditional (on the x -coordinate) mean of the deviation to the prescribed path as well as an estimate of the 2.5% and 97.5% percent percentiles of the conditional distribution indicating a standard deviation of the error of about 3 cm over a broad range of the sample (while at the ends of the platform higher standard errors are noticed).

Hence there is a non negligible error but of limited magnitude. The accuracy of the measurement by laser scanners was also tested through a comparison between the walking trajectories from the laser measurement and ones from manual annotation (labeling of pedestrians' centre of gravity (projected onto the ground plane) in a previously acquired video sequence by a human operator). The results were comparable indicating a mean (over a number of experiments) maximal deviation in position of less than 11 cm (not accounting for misalignment of the laser scanners coordinate system) and a mean maximal deviation of speed measurements of 9.4 cm/s reconfirming that the positional information contains a bias not accounted for properly.

4 Modelling of Stopping and Turning Movements

After dealing with the accuracy of the obtained trajectories a second phase of experiments has been conducted in April 2006. The focus of these experiments was to contribute to an understanding of the social force models advocated by [4]. In real world conditions the motion behavior of pedestrians is influenced by a large number of factors such as the geometry of the infrastructure, the location of obstacles, the position and speed of other pedestrians to name just the most important factors. All these factors are contained in the social force models, which makes identification of the influence of single factors difficult. The advantage of using a controlled experimental environment is that it enables researchers to exclude potential other influential factors so that particular factors can be independently examined.

Here our interest was directed towards the modelling of stopping and turning movements. In each of the walking experiments, up to four people walked on the platform. The data from 26 runs in total was used for our analyzes, which provided us with 58 trajectories in total (including the ones from the first part of the experiment). The number of pedestrians simultaneously on the platform was small such that influences of the location of one pedestrian on the paths taken by others are not to be expected. Also the platform is not bordered by walls but only handrails. Since there is ample space also the influence of the walls is assumed to be negligible. Hence the defining equations for the social force models specifies acceleration a_t of a pedestrian as a function of the desired velocity v_t^d and the actual velocity v_t as follows:

$$a_t = \beta(v_t^d - v_t), \quad \beta > 0. \tag{1}$$

Assuming desired velocity to be a constant one obtains a linear relationship between actual velocity and acceleration.

The trajectory data sets obtained from the walking experiments are used in order to investigate this relation empirically. To this end the trajectories have been partitioned by automatically identifying stopping points (where detection is based on sustained small velocity values) in order to obtain a total of 314 approaching respectively leaving maneuvers. Plots of normalized speed (normalized such that free speed corresponds to one) and acceleration respectively as a function of distance to the stopping points can be seen in Fig. 6. These plots shows a surprisingly small variance of the velocity and acceleration values for given distance to stopping/turning point (neglecting a number of outlying observations due to problems in the automatic detection of stopping/turning points). Also both velocity and acceleration values are very similar for approaching (blue dots) and leaving (red dots) maneuvers.

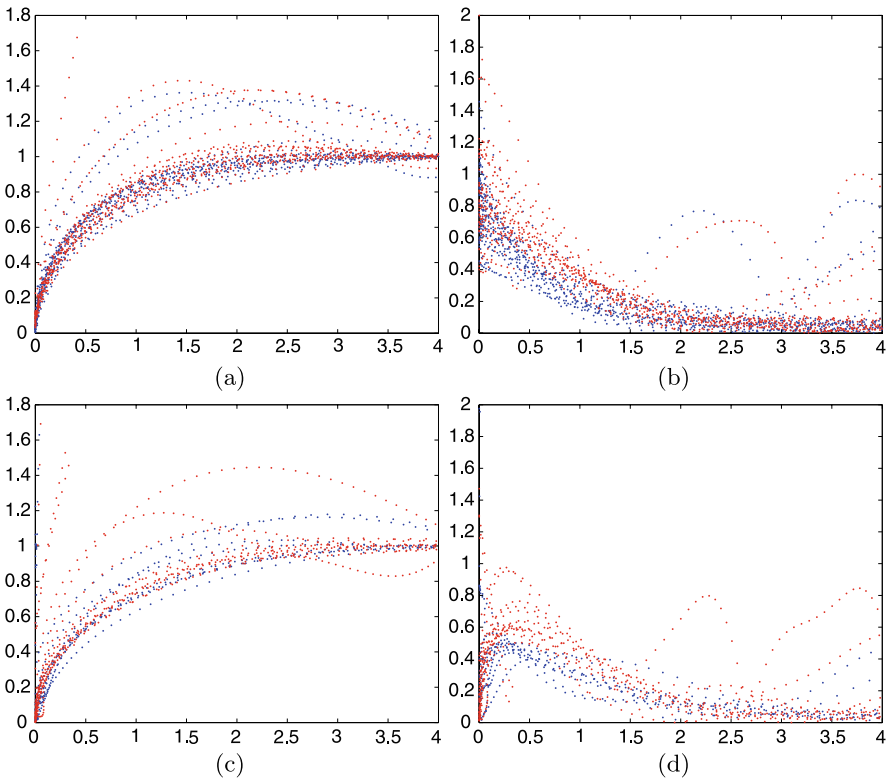


Fig. 6. Velocity [m/s] as a function of distance [m] to stopping (a) and turning point (c), and acceleration [m/s²] as a function of the distance [m] to stopping (b) turning point (d).

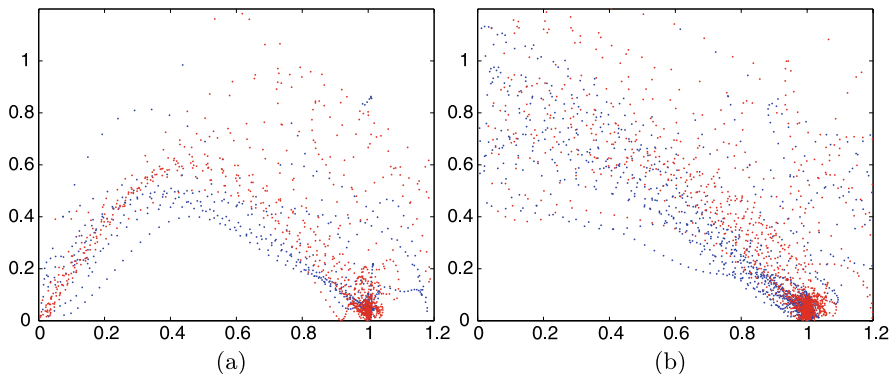


Fig. 7. Acceleration [m/s²] as a function of velocity [m/s] for stopping (a) and turning maneuvers (b).

Moreover, there is a clear distinction between stopping and turning movements: While the drop in velocity is very similar, acceleration values for turning movements do not decrease to zero, for stopping by definition this is the case.

Finally also the implications of the findings for the social force models was examined. Plots of the actual acceleration as a function of actual speed for the data sets considered in this paper (given in Fig. 7) clearly show that at least for the case of stopping acceleration is no linear function of actual velocity. For turning around the evidence of a linear relationship is also weak.

On first thought this might be seen as an indication for rejecting the equations defining the social force models. However, the key concept here is ‘desired speed’. If desired speed is not taken as constant but rather depends on the distance to the stopping point observations and real world data fit together leading to a refinement of the social force model. In this case (1) reads $a_t = \beta(v_t^d(d_t) - v_t)$ where d_t denotes the distance to the stopping/turning point. This can be interpreted as a proportional controller driving the pedestrian towards a prespecified stopping/turning path. The function $v_t^d(d)$ can be estimated as the conditional mean (see Fig. 8). Again the difference between approaching and leaving maneuvers are small. It can be seen that free speed is reached/left approximately at two meters distance. It can be seen that for stopping movements velocity is reduced slightly faster than for turning movements.

5 Conclusions

In this paper walking experiments are used to calibrate social force models to replicate stopping and turning movements. The necessary trajectory data set has been obtained from raw data provided by laser scanner measurements

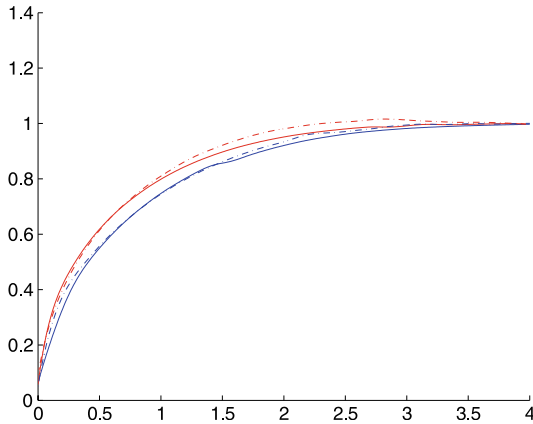


Fig. 8. Velocity [m/s] as a function of the distance [m]. *Blue*: Stopping maneuvers, *red*: turning. *Solid line*: approaching, *broken line*: leaving.

using an HMM tracking algorithm. It has been found that the typical velocity used for turning or stopping movements is surprisingly stable. While stopping and turning movements show significant differences no large differences have been found distinguishing leaving from approaching maneuvers.

The results clearly show that acceleration is no linear function of actual velocity close (closer than 2 meters) to a stopping or turning point. Hence in this case the social force models must be refined using a changed ‘desired velocity’ term in order to produce realistic stopping and turning movements.

Additional data sets have been recorded inside the pedestrian laboratory PAMELA that will be used in the future to model other forces contained in the social force paradigm.

Acknowledgements

The data sets discussed in this paper have been obtained at the London based pedestrian laboratory PAMELA which is gratefully acknowledged.

References

1. V.J. Blue and J.L. Adler. Cellular automata microsimulation of bidirectional pedestrian flows. *Transportation Research Record*, 1678:135–141, 2000.
2. A. Keßel, H. Klüpfel, and M. Schreckenberg. Microscopic simulation of pedestrian crowd motion. In M. Schreckenberg and S.D. Sharma, editors, *Pedestrian and Evacuation Dynamics*. Springer, Berlin, 2001.
3. A. Schadschneider. Cellular automaton approach to pedestrian dynamics—theory. In M. Schreckenberg and S.D. Sharma, editors, *Pedestrian and Evacuation Dynamics*. Springer, Berlin, 2001.

4. D. Helbing and P. Molnar. Social force model for pedestrian dynamics. *Physical Review E*, 51:4282–4286, 1995.
5. D. Helbing, P. Molnar, I.J. Farkas, and K. Bolay. Self-organizing pedestrian movement. *Environment and Planning B: Planning and Design*, 28:361–383, 2001.
6. S.P. Hoogendoorn and P.H.L. Bovy. Pedestrian route-choice and activity scheduling theory and models. *Transportation Research, Part B: Methodological*, 38:169–190, 2004.
7. S. Hoogendoorn and P.H.L. Bovy. Simulation of pedestrian flows by optimal control and differential games. *Optimal Control Applications and Methods*, 24:153–172, 2003.
8. D. Helbing, P. Molnar, and F. Schweitzer. Computer simulations of pedestrian dynamics and trail formation. In *Evolution of Natural Structures*, pages 229–234. Sonderforschungsbereich 230, Stuttgart, 1994.
9. T. Lakoba, D. Kaup, and N. Finkelstein. Modifications of the helbing-molnar-farkas-vicsek social force model for pedestrian evolution. *Simulation*, 81:339–352, 2005.
10. B. Steffen. A modification of the social force model by foresight. In *Pedestrian and Evacuation Dynamics 2008*, Springer, Berlin, 2010.
11. A. Johansson and D. Helbing. Analysis of empirical trajectory data of pedestrians. In *Pedestrian and Evacuation Dynamics 2008*, Springer, Berlin, 2010.
12. S.P. Hoogendoorn and W. Daamen. Microscopic parameter identification of walker models and its implications to pedestrian flow modeling. In *85th Annual Meeting Transportation Research Board*, pages 1–13, 2006.
13. K. Teknomo and G.P. Gerilla. Sensitivity Analysis and Validation of a Multi-Agents Pedestrian Model. *Journal of the Eastern Asia Society for Transportation Studies (EASTS)*, 6:198–213, 2005.
14. M. Boltes, A. Seyfried, B. Steffen, and A. Schadschneider. Automatic extraction of pedestrian trajectories from video recordings. In *Pedestrian and Evacuation Dynamics 2008*, Springer, Berlin, 2010.
15. C. Beleznai, B. Frühstück, and H. Bischof. Human Tracking by Mode Seeking. In *Proc. 4th International Symposium on Image and Signal Processing and Analysis*, 2005.
16. A. Johansson, D. Helbing, and P. Shukla. Specification of the social force pedestrian model by evolutionary adjustment to video tracking data. *Advances in Complex Systems*, 10:271–288, 2007.
17. Pedestrian accessibility and movement environment laboratory (PAMELA). Website see <http://www.cts.ucl.ac.uk/arg/pamela2/>, as of October 2007.
18. R.J. Elliot, L. Aggoun, and J.B. Moore. *Hidden Markov Models: Estimation and Control*. Stochastic Modelling and Applied Probability, 2nd edition. Springer, Berlin, 1997.
19. A. Doucet, J.G. Freitas, and J. Gordon. *Sequential Monte Carlo Methods in Practice*. Springer, New York, 2001.

Pedestrian Vision and Collision Avoidance Behavior: Investigation of the Information Process Space of Pedestrians Using an Eye Tracker

Kay Kitazawa¹ and Taku Fujiyama²

¹ Centre for Advanced Spatial Analysis (CASA), University College London,
1-19 Torrington Place, London WC1E 7HB, UK

e-mail: k.kitazawa@ucl.ac.uk

² Centre for Transport Studies, University College London, Gower Street, London
WC1E 6BT, UK

e-mail: taku@transport.ucl.ac.uk

Summary. This study investigates the Information Process Space (IPS) of pedestrians, which has been widely used in microscopic pedestrian movement simulation models. IPS is a conceptual framework to define the spatial extent within which all objects are considered as potential obstacles for each pedestrian when computing where to move next. Particular foci of our study were on identifying the size and shape of IPS through examining observed gaze patterns of pedestrians. A series of experiments were conducted in a controlled laboratory environment, in which up to 4 participants walked on a platform at their natural speed. Their gaze patterns were recorded by a head-mounted eye tracker and walking paths by laser-range-scanner-based tracking systems at the frequency of 25 Hz. Our findings are three folds: pedestrians pay much more attention to ground surface to detect potential immediate environmental hazards than fixating on obstacles; most their fixations fall within a cone-shape area rather than semicircle; the attention paid to approaching pedestrians is not as high as that to static obstacles. These results led to an insight that the structure of IPS should be re-examined by taking directional characteristics of pedestrians' vision.

1 Background

Following the trend of sustainable development, pedestrian oriented planning has started attracting much attention in several discourses; transport studies, urban planning and architecture. Recent trend in this subject is to develop predictive models of pedestrian movement. When discussing how pedestrian move around, there is a huge variation in its meaning, ranging from migration and commuting movement between cities to how pedestrians manoeuvre

themselves in crowds. This paper puts its focus on the pedestrian movement at the smallest scale, where the individual pedestrian’s movement patterns, more specifically how they avoid bumping into each other or how they avoid obstacles, are analyzed. At this “microscopic” level saw a late surge of studies that utilize disaggregated models designed to forecast the behavior of individual pedestrians to represent their dynamics as a whole [1–10].

Although these models differ in terms of their spatial representation (i.e. discrete space or continuous-space) as well as the techniques used to implement behavior model into computational codes, they share a common element in modelling individual pedestrian’s behavior; Information Process Space. IPS is essentially an approximation of the computational scope limitation in the environment for which modellers assume interactions between any given pedestrian and other pedestrians or obstacles. In a collision avoidance scenario, it corresponds to how far each pedestrian pays an attention when he/she decides where to move next avoiding each other.

IPS is conceptualized in various different ways. Most Cellular Automata (CA)-based pedestrian behavior models represent pedestrians’ walking paths as a chronological transition of the state of cells in a regular 2D space lattice. In CA, the cell states are simultaneously updated in discrete time steps and the change of the state of each cell depends on some local rules defined solely based on its own previous state and that of its neighboring cells. At every step, each of the neighboring cells is examined as a potential next destination in terms of whether it is occupied by other pedestrians or obstacles and thus of if potential collision may occur. Therefore neighborhood is used synonymously here for ISP, and is modelled as an extension of Moore neighborhood in which the number of cells n in the neighborhood of cell x (x included) = $(2r + 1)^2$ as shown in Fig. 1. Pedestrians’ natural walking speed is taken into account for the selection of radius r [8, 11]. This type of ISP allows pedestrians to “perceive” all the information from different directions equally.

Other models use the analogy of human vision field to define the topography of neighborhood. A viewshed or Isovist is an area of continuous space that is visible from a fixed vantage point as shown in Fig. 2(a). Visual neighbor-

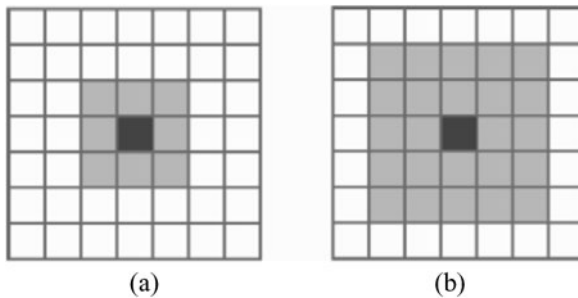


Fig. 1. IPS represented in Cellular Automata-based models; **a** $r = 1$; **b** $r = 2$.

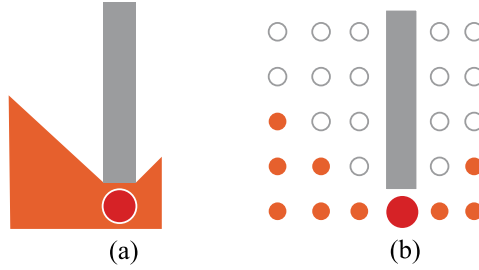


Fig. 2. IPS represented by viewshed (a) and visual neighborhood (b).

hood used by [12] is defined to any given location on the grid-shape graph that represents 2D discrete space as shown in Fig. 2(b). ISP here is a collection of directly visible vertices each of which equally receives pedestrians’ attention regardless of the walking direction in the same way as the neighborhood cells do in CA-based models.

Aforementioned two models assume even distribution of pedestrians’ attention to surrounding environment. There are several models that allow its uneven distribution. Utility-maximization-based models regard pedestrian behavior as an optimization process of the cost functions for each alternative walking path. The model proposed by [5, 13] applies a three-tiered structure for the utility calculation; strategic, tactical and operational levels. The first strategic level concerns the choice of general behavioral and activity area. It sets an activity for a pedestrian to perform, for which he or she needs to make decisions optimizing expected subjective utility. The second level is for way-finding to reach the activity area chosen in the previous process. It is in the third operational level, where a pedestrian computes desired velocity at each time instant and location based on kinematic costs and psychological discomfort, that ISP is implemented. The negative utility (cost) due to walking too close to obstacles and other pedestrians is integrated into the calculation by applying a scaling parameter that describes the proximity discomfort reduction rate as a function of the distance between two objects; in other words, pedestrians and obstacles in the vicinity yield stronger negative proximity cost than those in the distance. The parameters are called *region of influence of obstacle and spatial discount factor*, respectively. These parameter values are further influenced by two *anisotropy factors* [5]. They are the abstract form of the biased pedestrians’ perception to the objects which are located in front of and behind them as shown in Fig. 3, and are provided as the ratio to the perception level for the stimuli coming from their sides, which is given as 1. The “behind” *anisotropy* can be interpreted as how much sensory information other than optical one (e.g. sounds) pedestrians use for negotiating their way in collision avoidance behavior.

Similar parameters are adopted by Social Force models such as [9, 10] to accommodate the difference in pedestrian’s perception of other pedestrians

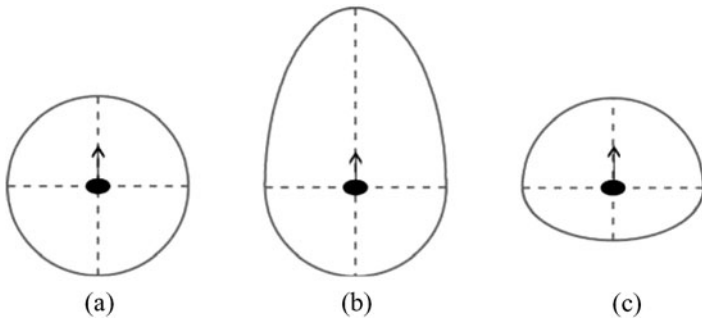


Fig. 3. Even and uneven distribution of pedestrians’ perception represented with three different values for the front and back anisotropy factors; **a** $ff = fb = 1$; **b** $ff = 2, fb = 1$; **c** $ff = 1, fb = 0.5$.

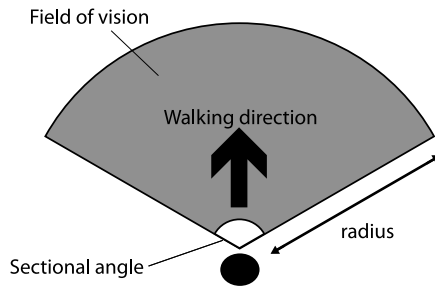


Fig. 4. Field of vision around a pedestrian.

between those approaching front or from behind. Social Force-based models that represent crowd motion by interaction of particles abiding the laws of Newtonian mechanics were first proposed by [14]. The fundamental concept of this type of model is that pedestrians feel and exert *social force*, either repulsive or attractive, each other. The size and the shape of ISP is represented in the form of a parameter called *Fall-Off Length of Social Repulsion Force* weighted by two coefficients that determines which of face-to-face and face-to-back force will be used in the computation of the strength of social force based on the relative angle of their body directions.

The analogy of human vision field for IPS is more explicitly used in other models such as [2, 4] by setting a fan-shaped area around the body of an individual pedestrian. The area is a direct approximation of the field of vision of pedestrians (FOB), which is defined by its sectional angle and radius as shown in Fig. 4. The difference between FOB and aforementioned visual neighborhood lies at the definitive shape of FOB, which is based on the cognitive studies on the physical characteristics human perceptions. Unlike other models, pedestrians’ attention ranges only to the front and partially to the both sides of the body in the FOB-based models.

Despite the fact that IPS forms the core of most microscopic pedestrian's behavior models, neither its validity nor the details of IPS' parameters have been fully examined through the comparison with actual data. Consequently the focus of previous microscopic pedestrian behavior models was on recreating "realistic" movement patterns with a selected number of behavior rules. Its assessment of the behavior rules are solely based on its performance, which is subjectively evaluated from the viewpoint of visual similarity with the reality. This is partly due to the difficulties in obtaining dataset of pedestrian movement at the scale fine enough to analyze the details of IPS.

This study utilizes an automatic tracking system based on laser range scanners to acquire walking trajectories as well as a head mounted eye tracking device to obtain their gaze patterns while walking. The application of such technologies is expected to be useful for the investigation of ISP. Our particular interests are in measuring its size and shape as well as identifying any potential environmental factors that exercise influence on them. Our research questions drawn from them include:

1. What is the distance between a pedestrian and an obstacle, when he or she first pays it an attention?
2. How long does a pedestrian look at the obstacle while avoiding it?
3. Are there any variations in the result of question 1 between when the participant avoids the static obstacles and other pedestrians?
4. Are there any variations in the result of question 2 between when the participant avoids the static obstacles and other pedestrians?

2 Methodologies

The datasets used for this study are taken from two-day observation studies of pedestrian microscopic movement that were conducted at Pedestrian Accessibility and Movement Environment Laboratory (PAMELA) at University College London. The surveys consisted of sets of walking session on the platform (WL: 3.6 m \times 15.6 m) in PAMELA. There were two types of platform setting: with and without two mannequins used as obstacles (WLH: 0.4 m \times 0.4 m \times 1.5 m) placed in the middle of the platform. The number of the pedestrians on the platform also varied from 1 to 4. In each session, the participants were instructed to walk at natural speed from one end of the platform to the other and to repeat until further instruction to stop. Each session took approximately two minutes. Their positions on the platform were observed manually and also recorded by infra-red laser range scanners (LD-A Maker manufactured by IBEO Automobile Sensor, Germany) every 0.1 second. The scanners were pre-installed on the outer wall of the platform as parts of PAMELA facility. The information was sent from the scanners to a computer via Ethernet cable. A piece of custom-made software provided by arsenal research (Austria) was used to extract each pedestrian's walking path on the platform from the time-series laser point dataset.



Fig. 5. An example of the field of view recorded by Eye tracker.

Amongst the participants in each session, one person (three in total for the whole study) wore an eye tracker. The eye tracker used was an iViewX Head Mounted Eye Tracking device (HED) manufactured by SensoMotoric Instruments GmbH (Germany). The device was to measure the gaze position of the participant, which is a point in a person's field of view. It consists of a light-weight helmet, an eye movement tracking camera, and a scene camera that captures the field of view. The gaze position is provided every 0.04 second (25 frames per second) in the form of a cursor inside Bitmap images (see Fig. 5).

The eye movement data and positional data (re-sampled and interpolated at the interval of 0.04 seconds) were then integrated by time-synchronization processes. A continuous gaze at the same point more than 0.08 second was regarded as a fixation. If the gaze point in the next frame falls on the same object and within the range of 3.0 degree (roughly 10 cm) from the axis to the original gaze position, the participant was regarded as gazing at the same point (and thus fixating). The threshold values and other definitions of pedestrians' fixation in this study follow those in a previous study [15]. All the fixations were identified with time information (when it occurred), location (where on the platform it occurred) and the type of object (e.g. other pedestrians, mannequins, etc.).

3 Results

3.1 General Fixation Behavior

During the observation, following points were found:

- Fixation on the static obstacles on the platform was often observed at the beginning of each walking session

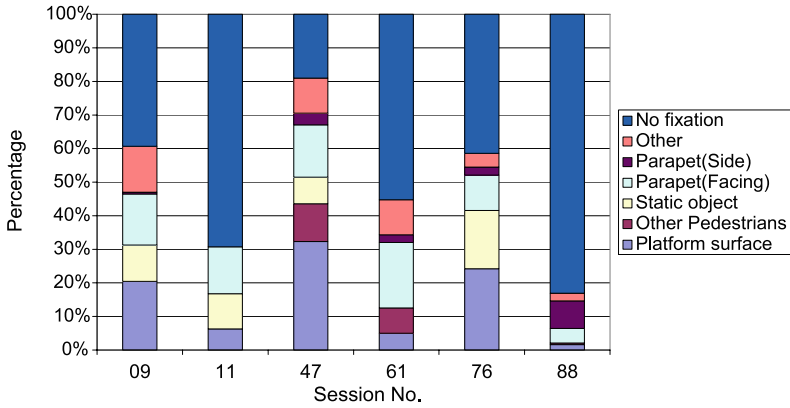


Fig. 6. Observed fixations by object types.

- Fixation on the platform surface was often observed during the walking session
- Fixation on the parapet (hand rail of the platform) placed on the both end of platform at waist level was observed

These results are in contrast to the fact that few pedestrian simulations take account of objects other than fellow pedestrians or boundary walls.

3.2 Fixations by the Object Type

Figure 6 shows observed fixations classified into 7 different categories: other pedestrians in the same walking session, side and facing parapets, platform surface, static objects (mannequins), and other objects such as a building wall, survey staff, and outside of the platform. “No gaze” includes gazes that did not last in two or more frames, which means that its duration was less than our definition of fixation. “No gaze” also includes observations in which the eye tracking system could not analyze where the participant gazed. Figure 6 clearly illustrates that the participants often fixated onto the platform surface as well as other objects on the platform.

3.3 Location of the Observed Fixations

Figure 7 shows the fixation at each point along the walking path of a pedestrian in one of the sessions (session 09). Point (0, 0) in the figure indicates the origin of our coordinate system on the platform. It is located on the one end of the long side of the platform (x axis) and in the middle of its short side (y axis). The figure illustrates that the participant started fixating on a static obstacle (mannequin) when approaching several meters to it.

Figure 8 shows the numbers of observed fixations on a static obstacle by distances between the participant and the obstacle. The data used for this

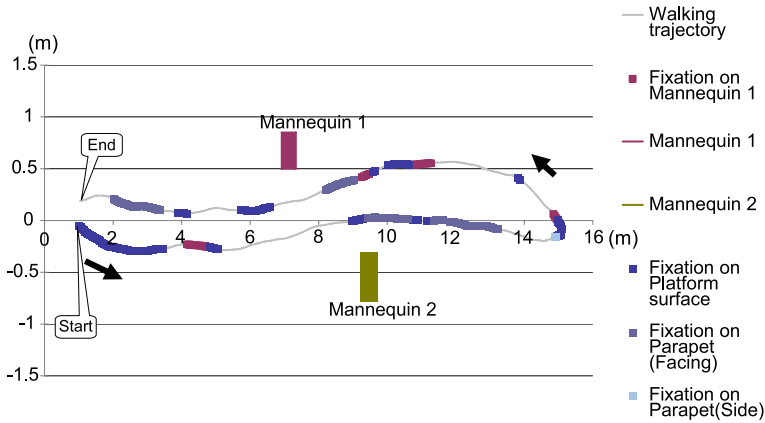


Fig. 7. Trajectory and fixation object in Session 09.

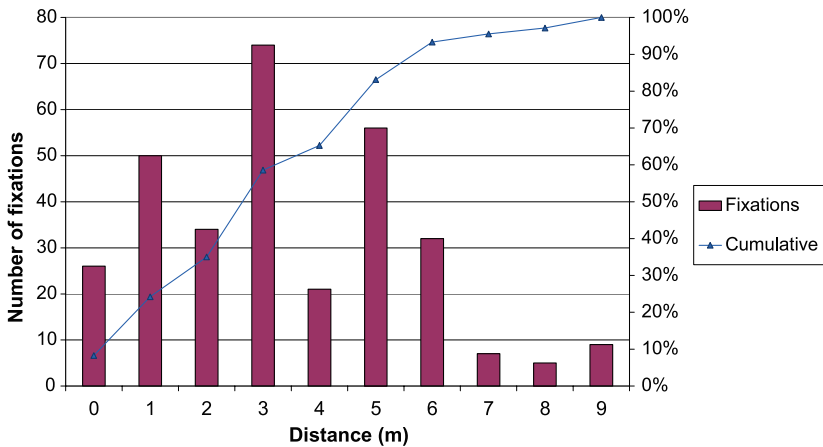


Fig. 8. The number of observed fixations on a static obstacle by distance.

analysis were all the fixations in all the sessions of the experiment. The fixations were aggregated and divided by the distance category. For instance, the category “0” includes the fixations with the distance value between 0.00 to 0.99 (m). On the other hand, Fig. 9 shows the numbers of observed fixations on another participant by distances between the fixated participant and the eye-tracker participant. In this analysis, we did not distinguish coming participants and leading participants, who walked in front of the eye-tracker participant and in the same direction. Comparison between the two figures leads us to notice that distances at which the participant fixated another participant were shorter than that for a static obstacle.

Table 1 shows the average distances when the eye-tracker wearer first fixated on the other pedestrians who walk to the same direction in front (leading

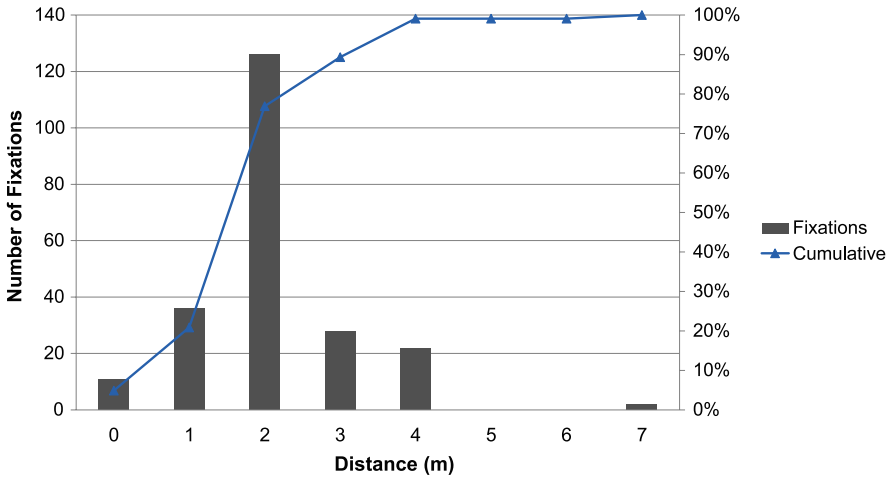


Fig. 9. The number of observed fixations on other pedestrians by distance.

	Leading participants	Approaching participants	Static obstacles
The number of data	24	3	60
Average distance (m)	1.90	3.97	4.58
Standard deviation	0.71	0.54	1.89

Table 1. The number of observed fixations on other pedestrians by distance.

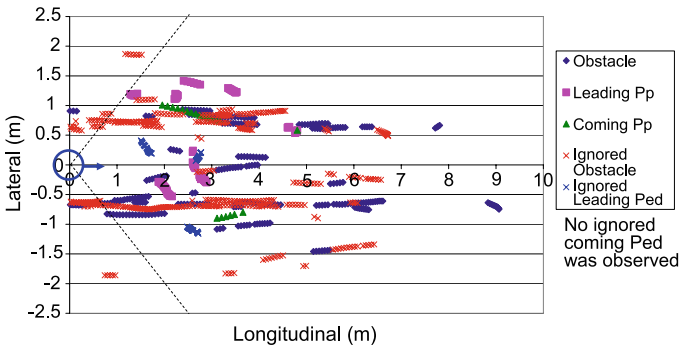


Fig. 10. Relative position of fixated or ignored objects.

participants), on those who approach head-on, and the static obstacles. From all the fixations, the location and time information of the first frame was extracted to calculate the distance between the participant and the object. Table 1 indicates that the participant fixated a static obstacle at the greatest distance, followed by approaching participant and leading participant.

Figure 10 plots the relative position of the fixated object in each observed fixation on another participant or a static obstacle. Positions of objects are

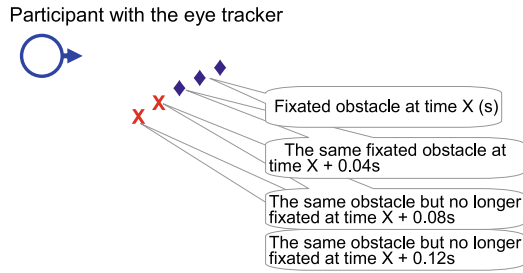


Fig. 11. Schematic representation of transition of an object from “fixated” to “ignored”.

relative to the position of the eye-tracker participant, and therefore the position of the participant is always $(0, 0)$. Also, the walking direction of the participant is set to be toward $(1, 0)$. In the calculation, we assumed that the participant always walked in parallel to the longitudinal direction of the platform as the platform shape is a long rectangular. In the figure, filled-diamonds represent positions of static obstacles, with filled-square leading participants and filled-triangle coming participants. The figure also includes “ignored participant” as well as “ignored obstacle” plotted using cross marks. These are other participants or static obstacles in the sight of the participant but not fixated because the participant fixated another participant or static obstacle. Note that, in some cases in which there were more than one participant or obstacle in the eye tracker participant’s sight, the eye-tracker-participant at first fixated one object (say, an obstacle) for a while and then fixated another participant or obstacle although the obstacle is still in the participant’s sight. In these cases, the first fixated obstacle was plotted as fixated in the figure but later plotted as an “ignored obstacle”, which means that a line of consecutive diamonds marks in the figure becomes a line of consecutive cross marks at a certain point. Figure 11 is a schematic representation for this.

Interestingly, the figure shows that there was few ignored coming participants and obstacles in the area of the exact front of the participant (longitudinal coordinate: 0.0 to around 4.5 m, lateral coordinate: -0.5 m to 0.5 m). Also we can notice that, there was no fixated participant or obstacle in the area with an angle of 45° or more from the walking direction of the participant.

4 Discussion

In this paper, we explored the size and the shape of Information Process Space (IPS), in which a pedestrian takes account of other pedestrians and obstacles for calculating next moves. We conducted an experiment where a participant wore an eye tracker and avoided collision with other participants and obstacles on the platform. The results draw 3 interesting insights on IPS.

Firstly, we expected that the eye-tracker participant frequently fixated static objects or pedestrians. The results show, however, that there were also many fixations on the platform surface or the facing parapet. Interestingly, when the participant first came to platform before starting, it was observed that the participant fixated around objects on the platform. It is speculated that the pedestrian with the eye tracker obtained the basic information of objects on the platform (e.g. the existence and the rough location of other pedestrians and obstacles) before the start of each session, and during the experiment the pedestrian fixated other pedestrians/obstacles when it was really necessary for collision avoidance. On the other hand, the pedestrian often fixated the platform surface because safely walking on the platform surface may be an immediate issue for the pedestrian.

As mentioned in the Introduction section, Hoogendoorn et al. suggested three levels for pedestrians in simulations to decide where to walk: strategic, tactical and operational level [5, 13, 16]. Comparison between our results indicates that there may be one level below the three level; checking environments (e.g. surface) for safe walking. Indeed, this finding makes us recall an important fact: pedestrians take account of not only collision avoidance but also immediate environmental hazards (e.g. gap on the surface). It would be interesting to investigate how these levels interact with each other. Previous studies [17, 18] suggested that pedestrians fixate on “hazard” objects longer than “orientation” objects in low lighting conditions. It is speculated that the more attention a pedestrian pay to hazards object, the less attention may be paid to other pedestrians or obstacles. Pedestrian simulations for evacuation should be able to consider decrease of the visibility (by smoke or low lighting).

Secondly, the results of our experiment give insights of the shape of Information Process Space. Many pedestrian simulations have assumed a semicircle, whereas the results imply that pedestrians are more interested in objects in the exact front to which the relative lateral distance is small. Also, the participants seldom fixated objects to which the angle from walking direction is more than 45 degree. These suggest that Information Process Space can be different from a homogeneous semicircle. It seems that some areas, especially the exact front area, are more prioritized.

It is noteworthy that there was no fixation observed within the immediate vicinity (the area in front of the body within a radius of 1.5 m). Patra and Vickers conducted a series of experiment in which participants were asked to approach and to step over an obstacle, or to step on specific locations [19, 20]. They found that participants fixated on the landing target on average two steps ahead. Two steps can be necessary for the human body to control limb trajectory and then to successfully step over/on a target. On the other hand, collision avoidance requires more movements and more time because a person needs to displace himself/herself against a coming pedestrian or an obstacle. If there is an object in the exact front to which the distance is less

than 1.5 m, it can be too late to fixate another pedestrian or an obstacle and then accordingly avoid collision.

Thirdly, according to our result, durations of first fixations on leading participants were less than those for coming participants. This can be because of a less possibility to collide with a leading participant than a coming participant. On the other hand, first fixations on static obstacles were slightly greater than those for coming participants. This can be because the participants also recognized static obstacles as the object with a greater possibility to collide with. We had expected that first fixations on coming participants took place at an earlier stage than static obstacles because relative velocities to a coming participant were greater than those for static obstacles. However, our results did not match with this hypothesis.

It should be noted that the fixations we observed may mainly be fixations at the collision avoidance or surface-check level. The shape of the information process space at the strategical or tactical level (to find a destination or to understand a rough location of other pedestrians or obstacles) may be different. Also, the presented research is a preliminary research. In order to understand the exact size of Information Process Space, a further investigation is necessary.

5 Conclusions

This research empirically investigated the Information Process Space of pedestrians. Many pedestrian simulations assume a certain area, but little research has empirically investigated this. By analyzing fixation behavior of pedestrians using an eye camera, we examined the Information Process Space of pedestrians in the real world.

As pedestrian simulations become more and more sophisticated and used for various situations, it is necessary to understand how real pedestrians perceive other pedestrians and environments. Such knowledge would help further precise representation of pedestrians in simulations. Especially, as our study pointed out, pedestrians perceive not only other pedestrians or obstacles but also other environmental information, such as hazards on the floor surface. It would be of interest to model such whole environmental recognition systems and to integrate them into pedestrian simulations. In other words, pedestrian simulations can be a platform of knowledge of such human behavior or human perception about environments.

References

1. Bierlaire, M., G. Antonini, and M. Weber. Behavioral dynamics for pedestrians. In 10th International Conference on Travel Behavior Research. 2003. Lucerne.

2. Thompson, A. Developing New Techniques for Modelling Crowd Movement. 1994, University of Edinburgh, Edinburgh, pp. 220.
3. Antonini, G., M. Bierlaire, and M. Weber. Simulation of pedestrian behavior using a discrete choice model calibrated on actual motion data. In Swiss Transport Research Conference—Mobility Session 2004 Conference. 2004.
4. Feurtey, F. Simulating the collision avoidance behavior of pedestrians. In School of Engineering, Department of Electronic Engineering. 2000, The University of Tokyo, Tokyo.
5. Hoogendoorn, S. and P.H.L. Bovy. Simulation of pedestrian flows by optimal control and differential games. *Optimal Control Applications and Methods*, 2003. **24**: pp. 153–172.
6. Yamori, K. Going with the flow: Micro-macro dynamics in the macrobehavioral patterns of pedestrian crowds. *Psychological Review*, 1998. **105**(3): pp. 530–557.
7. Blue, V.J. and J.L. Adler. Cellular automata microsimulation for modeling bi-directional pedestrian walkways. *Transportation Research Part B: Methodological*, 2001. **35**(3): pp. 293–312.
8. Dijkstra, J., A.J. Jessurun, and H.J.P. Timmermans. A multi-agent cellular automata system for visualising simulated pedestrian activity. In *Theoretical and Practical Issues on Cellular Automata, Proceedings of the Fourth International Conference on Cellular Automata for Research and Industry*. 2000, Springer, Karlsruhe.
9. Lakoba, T.L., D.J. Kaup, and N.M. Finkelstein. Exploration of the parameter range of a continuous-space, agent-based model for pedestrian evolution. 2003.
10. Lakoba, T.I., D.J. Kaup, and N.M. Finkelstein. Modifications of the Helbing–Molna’r–Farkas–Vicsek social force model for pedestrian evolution. *Simulation*, 2005. **81**(5): pp. 339–352.
11. Blue, V.J. and J.L. Adler. Flow capacities from cellular automata modelling of proportional splits of pedestrians by directions. In M. Schreckenberg and S.D. Sharma (Eds.) *Pedestrian and Evacuation Dynamics*. 2002, Springer, Berlin, pp. 115–122.
12. Turner, A. and A. Penn. Encoding natural movement as an agent-based system: an investigation into human pedestrian behavior in the built environment. *Environment and Planning B: Planning and Design*, 2002. **29**(4): pp. 473–490.
13. Hoogendoorn, S.P. and P.H.L. Bovy. Pedestrian travel behavior modeling. *Networks and Spatial Economics*, 2005. **5**: pp. 193–216.
14. Helbing, D., I. Farkas, and T. Vicsek. Simulating dynamical features of escape panic. *Nature*, 2000. **407**: pp. 487–490.
15. Suzuki, T. and S. Okazaki. Visual search while climbing or descending the staircases at a subway station. *Journal of Architecture, Planning and Environmental Engineering*, 2002. **558**: pp. 151–158, in Japanese.
16. Hoogendoorn, S., P. Bovy, and W. Daamen. Microscopic pedestrian wayfinding and dynamics modeling. In M. Schreckenberg and S. Sharma (Eds.) *Pedestrian and Evacuation*. 2002, Springer, Berlin, pp. 123–154.
17. Fujiyama, T. Investigating density effects on the “awareness” area of pedestrians using an eye tracker CTS Working Paper 2006/4, Centre for Transport Studies, University College London, London, ISSN 1747-6232. 2006.
18. Fujiyama, T., C.R. Childs, D. Boampong, and N. Tyler. How do elderly pedestrians perceive hazards in the street? An initial investigation towards development of a pedestrian simulation that incorporates reaction of various pedestrians to

- environments. Paper Presented to 11th International Conference on Mobility and Transport for Elderly and Disabled People, Montreal, Canada, June 2007.
19. Patra, A.E. and J.N. Vickers. Where and when do we look as we approach and step over an obstacle in the travel path? *Neuroreport*, 1997. **8**: pp. 3661–3665.
 20. Patra, A.E. and J.N. Vickers. How far ahead do we look when required to step on specific locations in the travel path during locomotion? *Experimental Brain Research*, 2003. **148**: pp. 133–138.

FDS+Evac: An Agent Based Fire Evacuation Model

Timo Korhonen¹, Simo Hostikka¹, Simo Heliövaara², and Harri Ehtamo²

¹ VTT Technical Research Centre of Finland, P.O. Box 1000, 02044 VTT, Espoo, Finland

e-mail: timo.korhonen@vtt.fi

² Systems Analysis Laboratory, Helsinki University of Technology, P.O. Box 1100, 02015 HUT, Espoo, Finland

Summary. In this paper, an evacuation simulation method is presented, which is embedded in a CFD based fire modelling programme. The evacuation programme allows the modelling of high crowd density situations and the interaction between evacuation simulations and state-of-the-art fire simulations. The evacuation process is modelled as a quasi-2D system, where autonomous agents simulating the escaping humans are moving according to equations of motion and decision making processes. The space and time, where the agents are moving, is taken to be continuous, but the building geometry is discretized using fine meshes. The model follows each agent individually and each agent has its own personal properties, like mass, walking velocity, familiar doors, etc. The fire and evacuation calculations interact via the smoke and gas concentrations. A reaction function model is used to select the exit routes. The model is compared to other evacuation simulation models using some test simulations.

1 Introduction

Performance based fire codes allow the use of numerical simulation of fire and evacuation processes to be used to improve fire safety in buildings. However, the usability of many current evacuation models is limited because they do not take into account the individual properties and decision making processes of humans, the dynamics of large crowds, and the interaction between fire and people. This paper presents an evacuation simulation method, which is embedded in a Computational Fluid Dynamics (CFD) based fire modelling programme. The state-of-the-art fire simulation environment of Fire Dynamics Simulator (FDS) [1, 2] is used to calculate the development of fire and the existing Smokeview programme [3] is used to visualise the results of the fire and evacuation simulations. The resulting programme, which is capable of simulating evacuation during a fire, is called as FDS+Evac.

In this paper, the major features of the FDS+Evac method are described and some verification and validation results are shown. The predictions of the model are compared to other evacuation models using some relatively simple test geometries, which represent some typical egress geometries found on many buildings.

The presented computational tool for evacuation modelling, FDS+Evac, is implemented as a part of the Fire Dynamics Simulator (FDS). FDS+Evac is a subprogram of FDS and, thus, the executable and the source code are obtainable from the FDS (version 5) web page at <http://fire.nist.gov/fds/>. The documentation of FDS+Evac is found on the web pages of VTT Technical Research Centre of Finland: <http://www.vtt.fi/fdsevac/>.

2 Method

FDS+Evac follows each person by an equation of motion. This approach allows each person to have his/her own personal properties and escape strategies, i.e., persons are treated as autonomous agents. FDS+Evac allows the modelling of high crowd density situations and the interaction between evacuation simulations and fire simulations. Some social interactions among the agents are introduced in the model and a reaction function model is used to select the exit routes [4].

FDS+Evac treats agents as a combination of three elastic circles moving on a two-dimensional plane. These circles are approximating the elliptical shape of the human body similarly as in the Simulex model [5, 6] and in the MASSEgress model [7], see Fig. 1. Agents experience contact forces and torques as well as psychological and motive forces and torques. The resulting equations of motion for the translational and rotational degrees of freedom are solved using the methods of dissipative particle dynamics [8] on 2D planes representing the floors of a building.

In FDS+Evac method, agents are guided to exit doors by the preferred walking direction vector field, \mathbf{v}_i^0 , and this field is obtained using the flow solver of FDS. This vector field is obtained as an approximate solution to a

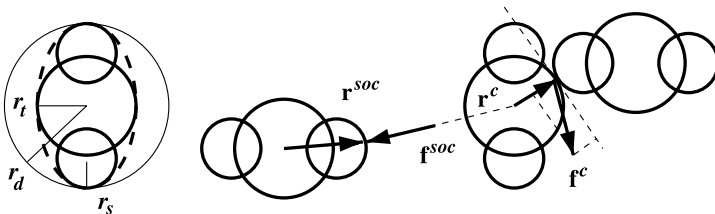


Fig. 1. The shape of a human body is approximated by a combination of three overlapping circles. Shown are also the definitions of the vectors used in the social and contact force calculation.

potential flow problem of a two-dimensional incompressible fluid to the given boundary conditions, where all walls are inert and the chosen exit door acts as a fan, which extracts fluid out of the domain. This method, or rather a trick, produces a nice directional field for egress towards the chosen exit door [4, 9]. A field of this kind will always guide agents to the chosen exit door. This route will not be the shortest one, but usually it is quite close to it.

2.1 Movement Algorithm

The so called social force method introduced by Helbing's group is used as the starting point of the movement algorithm of FDS+Evac. This model is shortly described below. For a longer description, see the papers by Helbing's group [10–13] and references therein. For the modification of the one-circle representation of an agent to a three-circle one, see the papers by Langston et al. [14] and Korhonen et al. [15–17].

The movement algorithm of FDS+Evac has many parameters. Some of these are related to the physical description of the agents, like the body size, the mass, the walking speed, and the moment of inertia. Others are the parameters of the chosen movement model, like the parameters of the social force and the contact force. The effect of the different parameters were carefully analysed and the values of the default parameters were chosen such that the flows through doors and flows in corridors match the experimental findings in the previous papers by the authors [15–17]. Thus, in this paper these default values of the parameters are used in the test simulations.

FDS+Evac uses the laws of mechanics to follow the trajectories of the agents during the calculation. Each agent follows its own equation of motion:

$$m_i \frac{d^2 \mathbf{x}_i(t)}{dt^2} = \mathbf{f}_i(t) + \boldsymbol{\xi}_i(t), \quad (1)$$

where $\mathbf{x}_i(t)$ is the position of the agent i at time t , $\mathbf{f}_i(t)$ is the force exerted on the agent by the surroundings, m_i is the mass, and the last term, $\boldsymbol{\xi}_i(t)$, is a small random fluctuation force. The velocity of the agent, $\mathbf{v}_i(t)$, is given by $d\mathbf{x}_i/dt$.

The force on agent i has many components:

$$\mathbf{f}_i = \frac{m_i}{\tau_i} (\mathbf{v}_i^0 - \mathbf{v}_i) + \sum_{j \neq i} (\mathbf{f}_{ij}^{soc} + \mathbf{f}_{ij}^c) + \sum_w (\mathbf{f}_{iw}^{soc} + \mathbf{f}_{iw}^c), \quad (2)$$

where m_i is the mass of agent i , the first sum describes the agent–agent interactions, the sum over w describes agent–wall interactions, and the first term on the right hand side describes the motive force on the evacuating agent. Each agent tries to walk with its own specific walking speed, $v_i^0 = |\mathbf{v}_i^0|$, towards an exit or some other target, whose direction is given by the direction of the field \mathbf{v}_i^0 . The relaxation time parameter τ_i sets the strength of the motive force, which makes an agent to accelerate towards the preferred walking speed, and

Body type	r_d (m)	r_t/r_d (-)	r_s/r_d (-)	d_s/r_d (-)	Speed (m/s)
Adult	0.255 ± 0.035	0.5882	0.3725	0.6275	1.25 ± 0.30
Male	0.270 ± 0.020	0.5926	0.3704	0.6296	1.35 ± 0.20
Female	0.240 ± 0.020	0.5833	0.3750	0.6250	1.15 ± 0.20
Child	0.210 ± 0.015	0.5714	0.3333	0.6667	0.90 ± 0.30
Elderly	0.250 ± 0.020	0.6000	0.3600	0.6400	0.80 ± 0.30

Table 1. Unimpeded walking velocities and body dimensions in FDS+Evac. The offset of shoulder circles is given by $d_s = r_d - r_s$, for the definition of the other body size variables, r_d , r_t , r_s , see Fig. 1.

m_i is the mass of the agent. The body sizes, preferred walking speeds, and the parameter τ_i are personalised by choosing them from random distributions. A uniform distribution ranging from 0.8 s to 1.2 s is used for τ_i and the uniform distributions used for the body dimensions and for the walking speeds are shown in Table 1. The mass of a default male is 80 kg and for other agents the mass is obtained by scaling by the body size.

The agent-agent interaction force in (2) has two parts. For the social force term, \mathbf{f}_{ij}^{soc} , the anisotropic formula proposed by Helbing et al. [12] is used

$$\mathbf{f}_{ij}^{soc} = A_i e^{-(r_{ij}-d_{ij})/B_i} \left(\lambda_i + (1 - \lambda_i) \frac{1 + \cos \varphi_{ij}}{2} \right) \mathbf{n}_{ij}, \quad (3)$$

where r_{ij} is the distance between the centres of the circles describing the agents, d_{ij} is the sum of the radii of the circles, and the vector \mathbf{n}_{ij} is the unit vector pointing from agent j to agent i . For a three circle representation of the agents, the circles used in (3) are those circles of the two agents, which are closest to each other. The angle φ_{ij} is the angle towards agent j measured from the body of agent i . The parameters A_i and B_i describe the strength and spatial extent of the force, respectively. The parameter λ_i controls the anisotropy of the social force. If $\lambda_i = 1$, then the force is symmetric and if it is $0 < \lambda_i < 1$, the force is larger in front of an agent than behind. The parameters A_i , B_i , and λ_i could be different for each agent but in the present version of FDS+Evac they have same values for each agent and their default values are $A_i = 2000 \text{ Max}(0.5, v_i/v_i^0)$ N, $B_i = 0.08$ m, and $\lambda_i = 0.5$. The psychological wall-agent interaction, \mathbf{f}_{iw}^{soc} , is treated similarly, but values $A_w = 2000$ N, $B_w = 0.04$ m, and $\lambda_w = 0.2$ are used for the force constants.

The physical contact force between agents, \mathbf{f}_{ij}^c , is given by

$$\mathbf{f}_{ij}^c = (k(d_{ij} - r_{ij}) + c_d \Delta v_{ij}^n) \mathbf{n}_{ij} + \kappa(d_{ij} - r_{ij}) \Delta v_{ij}^t \mathbf{t}_{ij}, \quad (4)$$

where Δv_{ij}^t is the difference of the tangential velocities of the circles in contact, Δv_{ij}^n is the difference of their normal velocities, and vector \mathbf{t}_{ij} is the unit tangential vector of the contacting circles. This force applies only when the circles are in contact, i.e., $d_{ij} - r_{ij} \geq 0$. The radial elastic force strength is

given by the force constant k and the strength of the frictional force by the force constant κ . Note, that (4) contains also a physical damping force [14] with a damping parameter c_d , which the original model by Helbing et al. does not have. This parameter reflects the fact that the collision of two agents is not an elastic one. The physical wall-agent interaction, \mathbf{f}_{iw}^c , is treated similarly and same force constants are used. The values $k = 12 \times 10^4 \text{ kg m}^{-2}$, $\kappa = 4 \times 10^4 \text{ kg s}^{-1} \text{ m}^{-1}$, and $c_d = 500 \text{ kg s}^{-1}$ are used both for the agent-agent and for the agent-wall interactions.

Equations (1)–(4) describe the translational degrees of freedom of the evacuating agents. The rotational degrees of freedom are treated similarly, i.e., each agent has its own rotational equation of motion:

$$I_i^z \frac{d^2 \varphi_i(t)}{dt^2} = M_i^z(t) + \eta_i^z(t), \quad (5)$$

where $\varphi_i(t)$ is the angle of the agent i at time t , I_i^z is the moment of inertia, $\eta_i^z(t)$, is a small random fluctuation torque and $M_i^z(t)$ is the total torque exerted on the agent by its surroundings

$$M_i^z = M_i^c + M_i^{soc} + M_i^T, \quad (6)$$

where M_i^c , M_i^{soc} , and M_i^T are the torques of the contact, social and motive forces, respectively. The moment of inertia of a default male agent is $I_i^z = 4.0 \text{ kg m}^2$. For other agents, the moment of inertia are obtained by scaling.

The torque of the contact forces is calculated as

$$\mathbf{M}_i^c = \sum_{j \neq i} (\mathbf{r}_i^c \times \mathbf{f}_{ij}^c), \quad (7)$$

where \mathbf{r}_i^c is the radial vector which points from the centre of the agent i to the point of contact. In FDS+Evac, also the social forces exert torques on agents and these are given by the formula

$$\mathbf{M}_i^{soc} = \sum_{j \neq i} (\mathbf{r}_i^{soc} \times \mathbf{f}_{ij}^{soc}), \quad (8)$$

where only the circles, which are closest to each other, are considered. The vector \mathbf{r}_i^{soc} points from the centre of the agent i to the fictitious contact point of the social force, see Fig. 1.

Analogous to the motive force, the first term on the right hand side of (2), a motive torque is defined as

$$M_i^T = \frac{I_i^z}{\tau_i^z} ((\varphi_i(t) - \varphi_i^0) \omega_i^0 - \omega(t)) = \frac{I_i^z}{\tau_i^z} (\tilde{\omega}_i^0 - \omega(t)), \quad (9)$$

where ω_i^0 is the maximum target angular speed of a turning agent, $\omega(t)$ the current angular velocity, $\varphi_i(t)$ the current body angle, and φ_i^0 is the target

angle, i.e., where the vector \mathbf{v}_i^0 is pointing. The target angular speed, $\tilde{\omega}_i^0$, defined in (9) is larger when the body angle differs much from the desired movement direction. For the angular relaxation time parameter, τ_z , a value of 0.2 s is used. The angular velocity parameter ω_i^0 has a value of $4\pi \text{ s}^{-1}$.

Note that Langston et al. [14] used a different formula for the motive torque, which had a form of a spring force. During this work, it was noticed that a force like that will make agents to rotate around their axis like harmonic oscillators. This is not desired and, thus, some angular velocity dependent torque is used in FDS+Evac to make the rotational motions of the agents to look more realistic.

2.2 Interaction of the Agents and Fire

By using FDS as the platform of the evacuation calculation we have direct and easy access to all local fire related properties, like gas temperature, smoke and gas densities, and radiation levels. Fire influences evacuation conditions; it may incapacitate humans and in extreme cases block major exit routes. On the other hand, humans may influence the fire by opening doors or actuating various fire protection devices. For now, the effect of smoke on the movement speeds of agents and the toxic influence of the smoke are implemented in movement algorithm of FDS+Evac. The exit selection algorithm of the agents uses smoke density to calculate the visibility of the exit doors and to categorise the doors to different preference groups [4].

Smoke reduces the walking speed of humans due to the reduced visibility and its irritating and asphyxiant effects. Recently, Frantzich and Nilsson [18] made experiments on the effect of smoke concentration on the walking speeds of humans. They used larger smoke concentrations than Jin [19] and they fitted the following formula to the experimental values

$$v_i^0(K_s) = \frac{v_i^0}{\alpha}(\alpha + \beta K_s), \quad (10)$$

where K_s is the extinction coefficient ($[K_s] = \text{m}^{-1}$) and the values of the coefficients α and β are 0.706 m s^{-1} and $-0.057 \text{ m}^2 \text{ s}^{-1}$, respectively. The standard deviations are reported to be $\sigma_\alpha = 0.069 \text{ m s}^{-1}$ and $\sigma_\beta = 0.015 \text{ m}^2 \text{ s}^{-1}$, but only the mean values are used in FDS+Evac, i.e., there is no variation between the agents.

The toxic effects of gaseous fire products are treated by using Purser's Fractional Effective Dose (FED) concept [20]. The present version of FDS+Evac uses only the concentrations of the narcotic gases CO, CO₂, and O₂ to calculate the FED value as

$$\text{FED}_{\text{tot}} = \text{FED}_{\text{CO}} \times \text{HV}_{\text{CO}_2} + \text{FED}_{\text{O}_2}. \quad (11)$$

Note, that the above equation does not contain the effect of HCN, which is also narcotic, and the effect of CO₂ is only due to the hyper-ventilation, i.e.,

it is assumed that the concentration of CO_2 is such low that it does not have narcotic effects. Carbon dioxide does not have toxic effects at concentrations of up to 5 percent but it stimulates breathing which increases the rate at which the other fire products are inhaled. The fraction of an incapacitating dose of CO is calculated as

$$\text{FED}_{\text{CO}} = 4.607 \cdot 10^{-7} (C_{\text{CO}})^{1.036} t, \quad (12)$$

where t is time in seconds and C_{CO} is the CO concentration (ppm). The fraction of an incapacitating dose of low O_2 hypoxia is calculated as

$$\text{FED}_{\text{O}_2} = \{60 \exp [8.13 - 0.54(20.9 - C_{\text{O}_2})]\}^{-1} t, \quad (13)$$

where t is time in seconds and C_{O_2} is the O_2 concentration (volume per cent). The carbon dioxide induced hyper-ventilation factor is calculated as

$$\text{HV}_{\text{CO}_2} = 0.141 \exp(0.1930 C_{\text{CO}_2} + 2.0004), \quad (14)$$

where C_{CO_2} is the CO_2 concentration (percent).

An agent is considered to be incapacitated when the FED value exceeds unity. An incapacitated agent is modelled as an agent, which does not experience any social forces from the other agents and whose target movement speed, v_i^0 , is set to zero. The size of an incapacitated agent is not changed, i.e., it remains on its feet. This is a very crude model and it needs to be modified in later versions of FDS+Evac.

3 Results

The presented FDS+Evac method is tested using three different test cases: (A) a large space like a sports hall, (B) a typical open floor office, and (C) a fictitious assembly space. The results of the FDS+Evac simulations are compared to the results of some other evacuation simulation methods. The three test cases are the same ones as was used in the paper by Korhonen et al. [9], where the previous version of the FDS+Evac method was introduced. The previous version used only one circle to represent the shape of the agents and it did not have any rotational degrees of freedom.

3.1 Test Case A

The first test case is a sports hall, whose geometry is shown in Fig. 2. The hall was previously analysed by Paloposki et al. [21]. The sports hall is used to practise different kind of sports. There are no spectator stands in the hall and neither are there any social spaces like showers. People enter the hall through the main entrance (“Door 1”), which is 1.8 m wide. Doors 2 and 3 are 4.0 m wide two-leaf doors and doors 4 and 5 are 0.9 m wide single-leaf

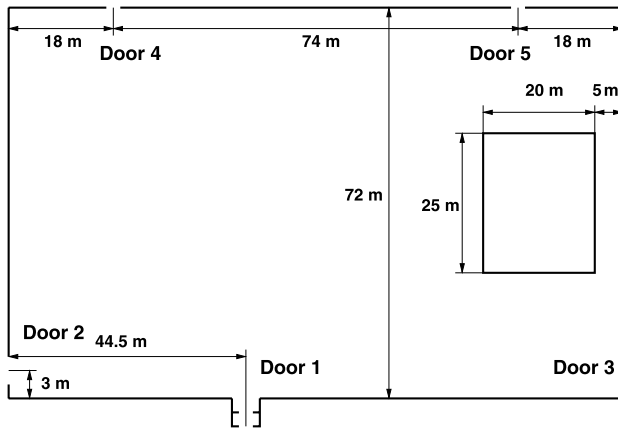


Fig. 2. The geometry of the studied sports hall.

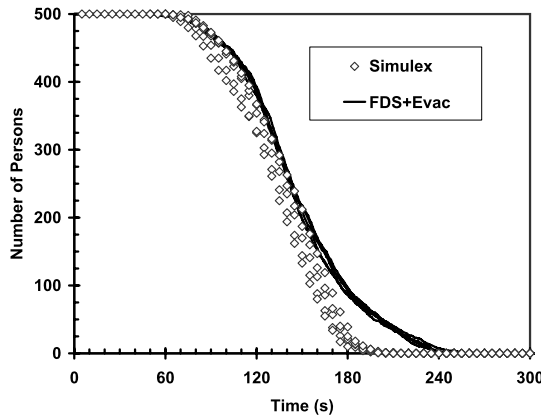


Fig. 3. The comparison of FDS+Evac to Simulex in a sport hall case. Results of five different simulations are shown for each case.

doors. It is assumed that a fire starts close to door 3 so that this door cannot be used for egress. 235 persons use the nearest door (“Door 5”), 130 persons use the main entrance (“Door 1”), 60 persons door 2, and 75 persons use door 4. Persons are initially located at the east end of the hall in an area of $20 \times 25 \text{ m}^2$ (the open rectangle in Fig. 2). The reaction time was modelled by a normal distribution with a standard deviation of 15 s and mean 60 s. The calculations were done also using a much wider distribution for reaction time (log normal) but the results of these calculations are not shown here. This wide reaction time distribution did not produce sizable congestion at the exit doors and, thus, the simulated results merely just reproduced the given input distribution for the reaction time.

The results of the FDS+Evac simulations are compared to Simulex [5, 6] simulations in Fig. 3. Since both FDS+Evac and Simulex are modelling human egress as a stochastic process, the presented results were collected from five different runs per case. The FDS+Evac and Simulex results differ somewhat. The differences arise due to the “Door 5”, which is only 0.9 m wide, but through which 235 persons escape. The flow through this door is larger in Simulex than in FDS+Evac. The specific human flow through this door in the FDS+Evac simulations are 1.65 1/p/m. The other doors are not as crowded and there the capacities of the doors do not show up as much.

3.2 Test Case B

The second test geometry was an open floor office, whose floor plan is shown in Fig. 4. The floor has dimensions of $40 \times 40 \text{ m}^2$ and there are initially 216 persons on this floor. The properties of these agents were assumed to be as the “Office Staff” category in the Simulex model and the reaction times of the agents were assumed to follow a normal distribution with mean of 90 s and standard deviation of 11 s. There are three stairs located at the central core of the building. The widths of the doors opening to the stairs are 1.2 m. In total seven different egress scenarios were simulated, covering the cases where all stairs are in use, one stair is blocked and a case where two stairs are blocked.

The results of FDS+Evac simulations are compared to Simulex simulations in Fig. 4. Only when two exit doors were blocked, queues were formed at the door. For two or three operational doors the main form of the evacuation curves arise from the reaction time distribution. The FDS+Evac and Simulex results are quite similar. It should be mentioned, that in the FDS+Evac sim-

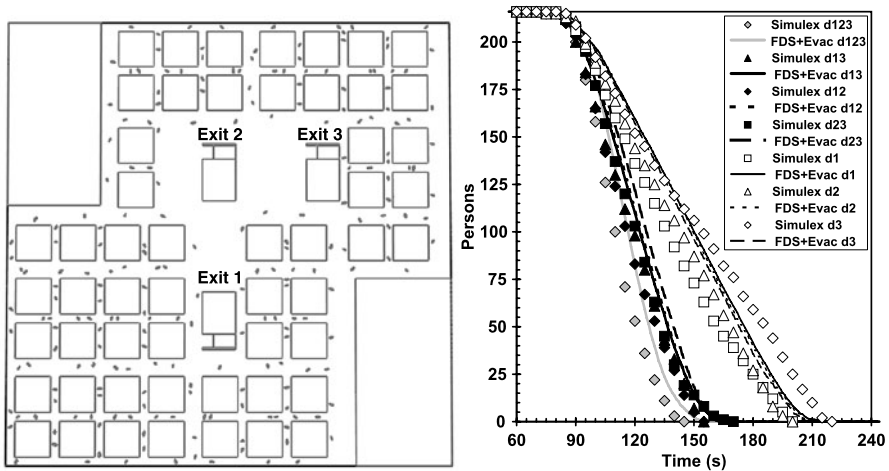


Fig. 4. The geometry of the open floor office test case and the comparison of FDS+Evac to Simulex.

ulations, the initial positions of agents do not change between different door scenarios (see Fig. 4), whereas in Simulex runs the random initial positions are used in each calculation. This explains why the Simulex results have larger scatter.

3.3 Test Case C

The last test case is a large fictitious assembly space having dimensions of $50 \times 60 \text{ m}^2$ and 1000 people initially inside. There is only one 7.2 m wide corridor leading to the exit. The geometry is shown in Fig. 5. The FDS+Evac results are compared to those of Simulex [5, 6] and buildingExodus [22] in Fig. 6. Note, that the FDS+Evac simulations were also done using parameters describing more relaxed egress (labels “FDS+EvacSlow”), where the value of the anisotropy parameter of the social force, λ_i , had a value of 0.3.

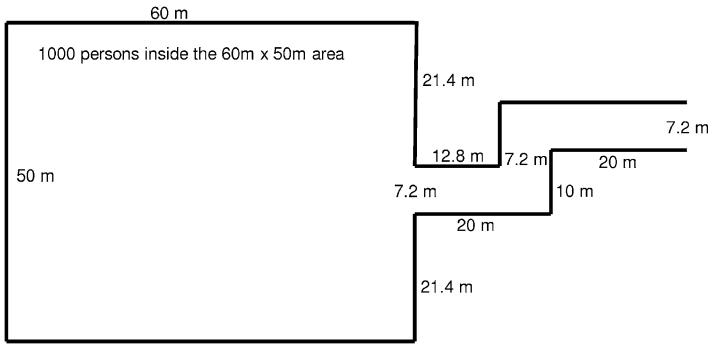


Fig. 5. The geometry of the assembly space test case.

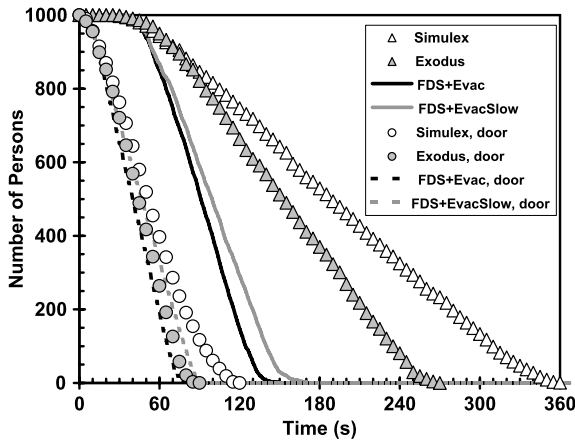


Fig. 6. The comparison of FDS+Evac to buildingExodus and Simulex in an assembly space.

Considerable differences are seen between the results of FDS+Evac and the results of Simulex and buildingExodus codes. These differences can be traced back to the motion of the agents in the corridor. Simulex and buildingExodus are not using the whole width of the corridor efficiently, when the simulations are done using the default values and standard input [9]. (An advanced user of these codes might be able to get different results by using some additional features.)

In Fig. 6 also shown are the results of the simulations for a case, where there is no corridor at all, i.e., there is just one 7.2 m wide exit door located at the wall of the room. In this case, the agreement between the different evacuation programmes is much better. The calculated specific human flows ($1/p/m$) are: Simulex 1.44, Exodus 1.95, FDS+Evac 2.14 ($\lambda_i = 0.5$) and 1.74 ($\lambda_i = 0.3$).

4 Summary

This paper presents a recently developed evacuation modelling programme FDS+Evac that allows the simulation of fire and evacuation at the same time. FDS+Evac was found to run satisfactorily, and fast enough for practical purposes. The comparison of the FDS+Evac simulations with Simulex and buildingExodus, indicated good agreement in two of the test cases (A and B). However, for a congested corridor (case C) considerable differences occurred, where the models perform differently in the bended corridor.

Acknowledgements

The development work of FDS+Evac has been funded by VTT Technical Research Centre of Finland, the Finnish Funding Agency for Technology and Innovation, the Finnish Fire Protection Fund, the Ministry of the Environment, and the Academy of Finland. The Building and Fire Research Laboratory at NIST is acknowledged for cooperation and the hospitality during the visits of one of the authors (T.K.).

References

1. K. McGrattan, S. Hostikka, J. Floyd, H. Baum, and R. Rehm. Fire Dynamics Simulator (version 5) technical reference guide. NIST Special Publication 1018-5, U.S. Government Printing Office, Washington, 2007.
2. K. McGrattan, B. Klein, S. Hostikka, and J. Floyd. Fire Dynamics Simulator (version 5) user's guide. NIST Special Publication 1019-5, U.S. Government Printing Office, Washington, 2007.
3. G.P. Forney. User's guide for Smokeview version 5—A tool for visualizing fire dynamics simulation data. NIST Special Publication 1017-1, U.S. Government Printing Office, Washington, 2007.

4. S. Hostikka, T. Korhonen, T. Paloposki, T. Rinne, K. Matikainen, and S. Heliövaara. Development and validation of FDS+Evac for evacuation simulations: Project summary report. VTT Research Notes 2421, VTT Technical Research Centre of Finland, 2007.
5. P.A. Thompson and E.W. Marchant. *Fire Safety Journal*, 24:131–148, 1995.
6. P.A. Thompson and E.W. Marchant. *Fire Safety Journal*, 24:149–166, 1995.
7. X. Pan. *Computational modeling of human and social behaviors for emergency egress analysis*. Dissertation, Stanford University, Stanford, CA, 2006.
8. I. Vattulainen, M. Karttunen, G. Besold, and J.M. Polson. *Journal of Chemical Physics*, 116:3967–3979, 2002.
9. T. Korhonen, S. Hostikka, and O. Keski-Rahkonen. A proposal for the goals and new techniques of modelling pedestrian evacuation in fires. In *Proceedings of the 8th International Symposium on Fire Safety Science*, pages 557–567. International Association for Fire Safety Science, Beijing, 2005.
10. D. Helbing and P. Molnár. *Physical Review E*, 51:4282–4286, 1995.
11. D. Helbing, I. Farkas, and T. Vicsek. *Nature*, 407:487–490, 2000.
12. D. Helbing, I.J. Farkas, P. Molnár, and T. Vicsek. Simulation of pedestrian crowds in normal and evacuation situations. In M. Schreckenberg, S.D. Sharma (eds.), *Pedestrian and Evacuation Dynamics*, pages 21–58. Springer, Berlin, 2002.
13. T. Werner and D. Helbing. The social force pedestrian model applied to real life scenarios. In *Pedestrian and Evacuation Dynamics—Proceedings of the Second International Conference*, pages 17–26. University of Greenwich, London, 2003.
14. P.A. Langston, R. Masling, and B.N. Asmar. *Safety Science*, 44:395–417, 2006.
15. T. Korhonen, S. Hostikka, S. Heliövaara, H. Ehtamo, and K. Matikainen. Integration of an agent based evacuation simulation and the state-of-the-art fire simulation. In *Proceedings of the 7th Asia–Oceania Symposium on Fire Science & Technology*, 20–22 September 2007, Hong Kong (in print).
16. T. Korhonen, S. Hostikka, S. Heliövaara, H. Ehtamo, and K. Matikainen. FDS+Evac: Evacuation module for Fire Dynamics Simulator. In *Proceedings of the Interflam2007: 11th International Conference on Fire Science and Engineering*, pages 1443–1448. Interscience Communications Limited, London, 2007.
17. T. Korhonen, S. Hostikka, S. Heliövaara, and H. Ehtamo. FDS+Evac: Modelling social interactions in fire evacuation. In *Proceedings of 7th International Conference on Performance-Based Codes and Fire Safety Design Methods*, pages 241–250. Society of Fire Protection Engineers, Boston, MA, 2007.
18. H. Frantzich and D. Nilsson. Utrymning genom tät rök: beteende och förflyttning. Report 3126, Lund University, Lund, Sweden, 2003 (in Swedish).
19. T. Jin. *Journal of Fire & Flammability*, 9:137–147, 1978.
20. D.A. Purser. Toxicity assessment of combustion products. In *SFPE Handbook of Fire Protection Engineering*, 2nd ed., pages 2/28–2/146. National Fire Protection Association, Quincy, MA, 1995.
21. T. Paloposki, J. Myllymäki, and H. Weckman. Application of reliability techniques for calculation of the evacuation safety of a sports hall. VTT Tiedotteita Research Notes 2181, VTT Technical Research Centre of Finland, 2002 (in Finnish).
22. S. Gwynne, E. R. Galea, P. Lawrence, and L. Filippidis. *buildingEXODUS technical manual V4.00*, 2004.

Comparisons of Evacuation Efficiency and Pre-travel Activity Times in Response to a Sounder and Two Different Voice Alarm Messages

David Purser

Hartford Environmental Research, 1 Lowlands, AL9 5DY Hatfield, UK
e-mail: david-purser@ntlworld.com

Summary. Previous studies (Bellamy and Geter, 1990, BRE Report BR 172; Proulx and Sime, 1991, Fire Safety Science, 3rd International Symposium, pp. 843–852; Sime, 1998, Human Behaviour in Fire, Proceedings of the First International Symposium, pp. 299–308; Purser and Bensilum, 2001, Safety Science 38, pp. 157–182) have indicated that recorded voice alarm messages can be more efficient than sounders in motivating occupants to evacuate buildings, and that they produce shorter pre-travel activity (*pre-movement*) times (PTAT), sometimes by a wide margin. More recently, with increased use of voice alarms and other voice announcements, people may have become less responsive. For this study, monitored evacuations using voice alarms were conducted in a shopping centre, a theatre and a large office building (Purser and Bensilum, 2001, Safety Science 38, pp. 157–182). An experimental study was then set up in a university teaching room under hidden video surveillance, in order to examine responsiveness to different alarm systems (including a sounder, long and short voice messages) and provide PTAT data. The findings from both the monitored evacuations and the experimental study were that voice alarms provided more reliable and shorter PTAT response times than sounders, especially in “awake and unfamiliar” behavioural scenarios. Occupants tended to listen to the full voice message and sometimes the first repeat before starting to travel. The short voice message produced a shorter but less reliable PTAT response. Group interactions had a major effect on response behaviours and times.

1 Introduction

Evacuation time, has two major phases: Pre-travel activity time (PTAT; also known as pre-movement time or pre-evacuation time)—the time between that when each occupant becomes aware of an emergency and that when they begin to move towards the exits), and Travel time (the time required for occupants to travel to a place of safety) [1–3]. These are additive for each individual so:

$$\Delta t_{\text{evac}} = \Delta t_{\text{PTAT}} + \Delta t_{\text{trav}}. \quad (1)$$

For occupant populations, PTAT can be expressed in terms of a variable period between the fire alarm and that when the first few occupants begin to travel, followed by a distribution of travel times (approximately log-normal) for the remainder of the population. PTAT and travel distributions interact, as some occupants are in their PTAT phases while others are in their travel phase.

$$\Delta t_{\text{PTAT}} = \Delta t_{\text{PTAT}(\text{first occupants})} + \Delta t_{\text{PTAT}(\text{occupant distribution})}. \quad (2)$$

For each occupant PTAT has two main behavioural components:

- **Recognition**—which starts with the cue or alarm and ends with the first response to the alarm. During this period occupants continue with the activities engaged before the alarm.
- **Response**—which starts with the first behavioural response to the alarm and ends when each occupant begins to travel towards an exit. During this period occupants engage in a range of behaviours such as investigation, warning others, and collecting belongings or family members before entering their travel phase.

During evacuation experiments it is possible to measure the recognition and response times and their distributions.

PTAT is affected by many variables related to individual occupant and group behavioural characteristics, the nature of the occupancy, the building and its systems. Some of the more important include:

- Alertness (sleeping/waking)
- Occupants familiar or unfamiliar with building and systems
- Fire safety management: extent to which trained staff/floor wardens encourage evacuation
- Warnings: sounder, pre-recorded voice alarm or directed Personal Address
- Activities: commitment to ongoing activities
- Training and previous experience
- Group interactions: extent to which evacuation of a group is influenced by individuals (especially staff trained in emergency evacuation procedures)

Two studies reported in 1190 and 1991 [4, 5] demonstrated that recorded voice alarm messages can be more efficient than sounders in motivating occupants to evacuate buildings, and that they produced shorter PTATs. In one study [4] for which subjects attended a London office building and were left to complete a “job application” form, very large time differences were obtained between 10 subjects who were subjected to a voice alarm (triggering evacuation within 0.5 minutes) and a matched group subjected to a fire alarm bell, who took up to 11 minutes to leave the room. In another study in an underground metro station [5], similar differences were obtained between a voice alarm (1.15 minutes response time) and a sounder (9.0 minutes).

The work reported here consists mainly of an experimental study set up in a university teaching room under video surveillance, in order to examine responsiveness to different alarm systems (including a sounder, long and short voice messages) and provide PTAT data. The experimental study design was based on the results of previous monitored evacuation studies, including two cases using voice alarms: in a shopping centre and a large office building [1]. Some of the key findings from the shopping centre, and office building are therefore also presented here, but described in more detail in reference [1].

2 Methods

The two monitored evacuations were unannounced. The shopping centre restaurant contained customers, who were basically unfamiliar with the building and systems, and the restaurant staff. The alarm started with a loud sounder lasting 9 seconds, followed after a 10 second silence by a voice message lasting 13 seconds. The message was as follows:

“Attention please, attention please. This is a public security announcement. Circumstances make it necessary for us to evacuate the building immediately. Please collect your hand-luggage and make your way to the nearest exit and leave the building. Please do not re-enter the building until advised to do so.”

The video record was used to measure the PTAT recognition and response times and travel times to the restaurant exits for each of 11 restaurant customers, and to observe the behaviour and PTAT times of the staff.

The multi-storey office case included video surveillance of a single meeting room on the third floor, containing 12 occupants unfamiliar with the building and its systems. Measurements were made of PTAT recognition and response times, and travel times to the room exit. For this building the alarm consisted of a sounder warning signal lasting 4 seconds followed by the following voice message lasting 13 seconds (total 17 seconds): “Attention please, attention please; this is an emergency, please leave the building by the nearest available exit. Do not use the lifts”.

For the experimental study in the university teaching room, 59 participants mostly unfamiliar with the building and systems were recruited ostensibly to take part in a series of psychological creativity tests for which a £5 fee was offered. They were randomly assigned to seven groups (comprising between 6 and 9 subjects) attending separately to participate in the tests at different times during a single day (and not meeting with other groups). Two groups were exposed to each of three alarms types in a randomised order, consisting of a sounder, long and short voice messages, the seventh (reserve group) was exposed to the short voice message. Tables 1 and 2 show the gender and age distributions of the subjects.

	Male	Female	Total
Sounder	6	11	17
Long message	4	12	16
Short message	5 (9) ¹	11 (17) ¹	16 (26) ¹

¹Includes extra group (Group 6).

Table 1. Gender distribution.

	Under 21	21-30	31-40	41-50
Sounder	4	10	1	2
Long message	4	8	3	0
Short message	9 (15)	7 (11)	0	0
Total	17 (23)	25 (29)	0	0

Table 2. Age distribution.

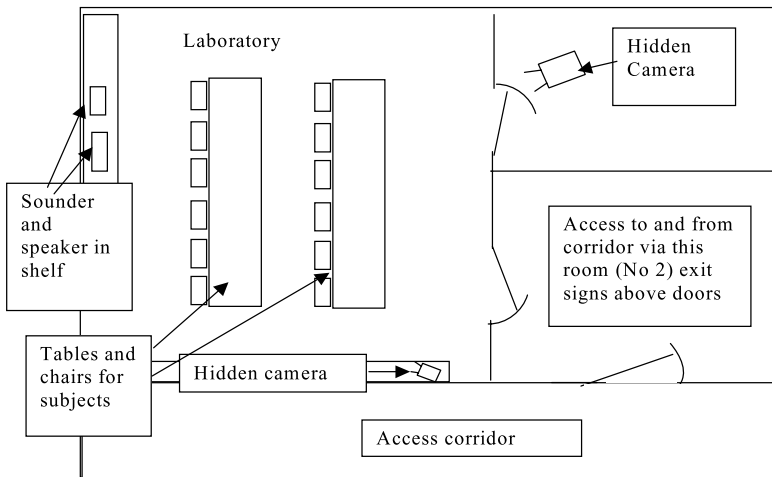


Fig. 1. Layout for alarms response experiments.

The layout of the psychology laboratory is shown in Fig. 1. The main camera was hidden in a darkened (closed) room, with a small subsidiary camera hidden on shelf in the laboratory. Each group of subjects gathered in Room 2, then moved into the laboratory, where the purpose of three (distracter) creativity tests was explained. Papers were then handed out and participants proceeded with the creativity tests. Subjects were asked to keep working through the tests. The experimenter announced that he would return when they had finished and then withdrew into the room containing the main camera. Approximately five minutes into the trials each group was subjected to an alarm. The subsequent behaviours were captured on video. The PTAT recognition and response times, and travel times to the room exit (marked with an exit sign) were recorded. Evacuating subjects were intercepted in the corridor. The

purpose of the experiment was explained and they were requested to fill in a short questionnaire about their experiences.

The three alarms used were as follows:

1. Alarm sounder
2. Long recorded female voice message: “Attention please! Attention please! This is an emergency. Please leave the building by your nearest exit” (total duration 9 seconds)
3. Short recorded female voice message: “This is an emergency! Please leave the building” (total duration 4 seconds)

All alarms were repeated continuously. The questionnaire was used to establish gender, age, previous experience with real life-threatening fire or bomb emergencies and number of fire drills previously involved in. Also, what the subject thought the alarm was for (choice from: fire, bomb, unknown, did not consider what it might be for, other). Further questions scored on a scale of 1–7: how seriously they took the alarm, to what extent they felt they should evacuate the room after hearing the alarm, to what extent they felt they were involved in a real emergency, the extent to which they were motivated by others and by the alarm, the extent to which they attempted to finish their activity before evacuating, their understanding of the voice message and a description of their thoughts and behaviour during the experiment. The “distracter” tasks consisted of a “vividness of visual imagery” questionnaire—rating intensity of mental images, a test making 16 pictures from triangles and twenty interpretations of inkblots.

All statistics were conducted using SPSS and Microsoft Excel. PTAT times could not be obtained from trial 6 (short message) because all occupants remained in the room throughout the test. Trial 6 may therefore have been invalidated so analyses have been carried out with and without trial 6 (which was repeated successfully by trial 7).

3 Results

3.1 Shopping Center Restaurant Evacuation

The results for the shopping centre restaurant evacuation are summarised in Fig. 2. Restaurant customers tended to listen to the alarm signal and the full spoken message while seated at their tables. This resulted in a recognition phase of 28–60 seconds, constituting the longest part of the evacuation time. Only one person started response behaviour before the end of the voice message. The response phase was relatively short, as was the travel phase. One customer waited until the repeat of the voice message before entering their response phase. Once occupants left the restaurant a further 30 seconds of so was required to exit the shopping mall. The staff left soon after the last customer.

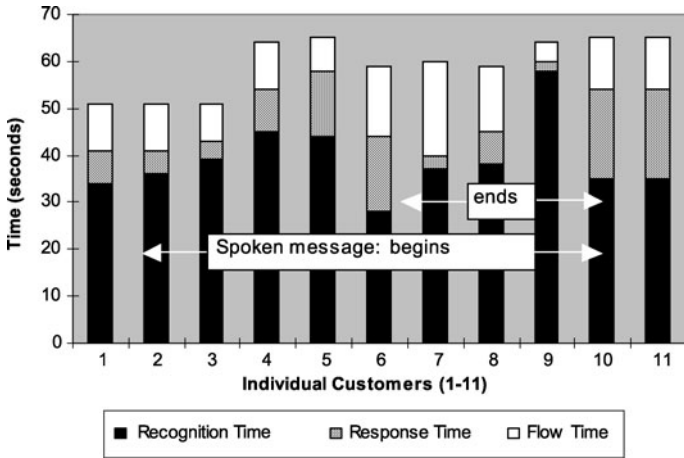


Fig. 2. Evacuation times for each customer leaving a restaurant.

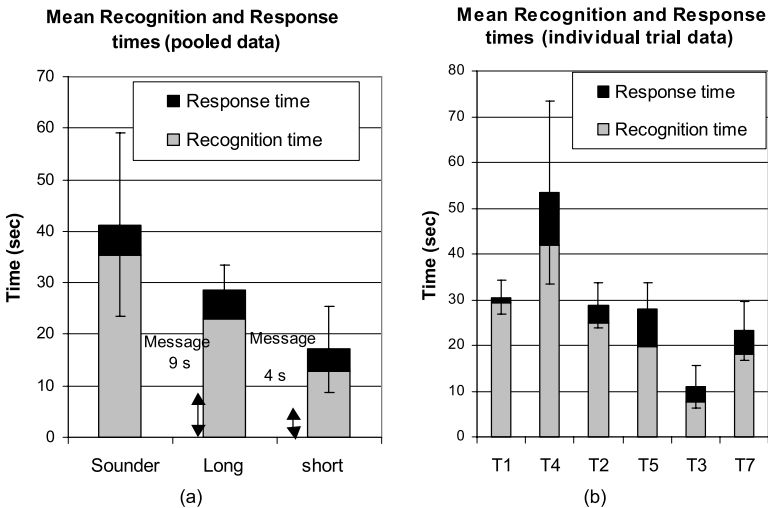


Fig. 3. Mean recognition and response times for Sounder (Trials 1 and 4), Long voice alarm (Trials 2 and 5) and Short voice alarm (Trials 3 and 7) bars show standard deviations.

3.2 Multistory Office Building Meeting Room Evacuation

The behaviour pattern in the office meeting room (Fig. 3) was similar (Table 3) to that in the restaurant. The mean recognition time (17 seconds) was the same as the time taken to deliver the message. All occupants then entered their response phase, getting up and collecting papers and or coats, before travelling to the room exit (one person re-entering to collect a jacket). For this case the response phase was slightly longer than the recognition phase,

Person	Recognition time (s)	Response time (s)	Travel to exit time (s)	Total time (s)
1	16	40	5	61
2	15	17	5	37
3	17	20	2	39
4	20	30	3	53
5	16	30	6	52
6	18	39	5	62
7	?	?	3	67
8	16	30	13	59*
9	?	?	?	55
10	?	?	?	65
11	?	?	2	71
12	?	?	4	51
Mean	17	29	5	56

(Sounder: 4 sec, Message: 13 sec, Total: 17 sec)

Movement to exit: Turned to face exit and leave room.

?—Location out of site of camera, location of occupant guessed.

*Re-enters to collect jacket. Leaves again at 00:01:24

Table 3. Response times of committee meeting room occupants.

and the mean PTAT at 46 seconds was longer than the average travel time of 5 seconds to the room exit (plus 5 seconds to the protected stair).

3.3 University Teaching Laboratory Experiment with Three Alarm Types

From the results of the monitored evacuations, it was considered that the voice alarms were effective, but that the travel phase of evacuation was delayed somewhat as occupants listened to rather long voice messages, in some cases waiting for the message to be repeated before starting to travel.

For this reason the short (4 second) message was included with the sounder and longer (9 second) voice message, which was the same as that used for the office building apart from the reference to the lifts. Also, for the experiments the voice messages were not preceded by a sounder alerting signal. Table 4 shows the individual data for the three alarms, and Table 5 the descriptive statistics. Figures 3, 4 and 5 illustrate key findings. The differences between the six groups for which data were obtained was highly significant (ANOVA $F_{2,47} = 18.66$, $P < 0.001$) and at the 5% level between pairs of alarm types. The results therefore confirmed that the voice messages provided significantly shorter pre-movement recognition times than did the sounder, and that the short message provided significantly shorter PTAT times than did the long message (except on the occasion when no response was obtained to the short message). Observations of the subjects indicated that a level of conformity

Sounder			Long voice message			Short voice message		
Recog. ¹	Rpnse ²	PTAT	Recog.	Rpnse	PTAT	Recog.	Rpnse	PTAT
T1 26	0	26	T2 25	0	25	T3 10	6	16
32	0	32	25	0	25	8	0	8
32	0	32	27	0	27	7	0	7
27	0	27	18	8	26	8	5	13
29	0	29	22	0	22	8	9	17
30	1	31	25	9	34	8	5	13
27	0	27	26	7	33	8	0	8
33	1	34	26	10	36	5	0	5
29	8	37	31	0	31	T7 13	4	17
T2 18	5	23	T5 17	0	17	21	4	25
58	14	72	19	9	28	5	7	12
16	19	35	19	11	30	13	10	23
16	24	40	19	9	28	20	3	23
63	5	68	22	10	32	25	0	25
60	14	74	22	11	33	26	7	33
60	10	70				22	6	28
45	0	45						

¹Recognition time ²Response time

Table 4. Individual recognition, response and PTAT for three alarms.

Alarm type/trial	n	Recognition time (s)				Response time (s)			
		Mean	s.d.	Min	Max	Mean	s.d.	Min	Max
Sounder									
Trial 1	9	29.4	2.51	26	33	1.1	2.62	0	8
Trial 4	8	42	21.69	16	63	11.4	7.96	0	24
Pooled	17	35.4	15.81	16	63	5.9	7.68	0	24
Long message									
Trial 2	9	25	3.54	18	31	3.8	4.55	0	10
Trial 5	6	19.7	1.97	17	22	8.3	4.18	0	11
Pooled	15	22.9	3.98	17	31	5.6	4.84	0	11
Short message									
Trial 3	8	7.8	1.39	5	10	3.1	3.56	0	6
Trial 7	8	18.1	7.18	5	26	5.1	3.04	0	10
Pooled	16	12.9	7.33	5	26	4.22	3.25	0	10

Table 5. Mean PTAT recognition and response times for three alarm types.

and/or group reference was involved in the decision to evacuate and its timing. Subjects looked around and consulted each other before leaving the room. There were often a few key individuals who initiated (or inhibited) the whole group decision to evacuate. The majority of subjects were students but a few older staff members participated. It was notable that on one occasion a female staff subject took a leading role and initiated a timely evacuation. On another

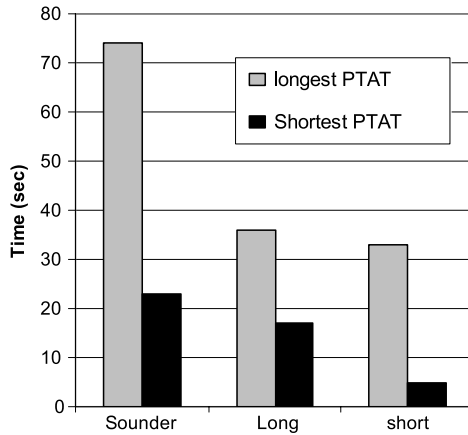


Fig. 4. Shortest and longest PTAT.

occasion a young male suggested that the alarm was not genuine and refused to leave but was left by the group. In trial 6 a few individuals picked up bags as if to leave but put them down when a male subject convinced them the alarm was part of the test, and that they should not respond. It is considered that such group dynamics can be very important in real emergencies and that the results obtained here are somewhat similar to those where subjects fail to respond because they believe an alarm to be a drill.

The basic finding was that the short voice alarm provided the shortest recognition and total PTAT times (Figs. 3 and 4), the long voice message somewhat longer times, and the sounder the longest times. Travel times from this small laboratory were similar to those from the office meeting room at around 5 seconds. As Fig. 3 shows, the sounder produced the most variable PTAT times, with considerable differences between the two trials. The long voice message produced the most reliable and least variable PTAT times, with very similar results for the two trials. The short message produced a more variable response than the long message, with some differences between the two successful trials, and a less reliable response due to the failure of Trial 6. Figure 4 shows the variability in terms of the shortest and longest PTATs for each case.

As with the monitored evacuations, the recognition phase was the longest part of the PTAT response. Once subjects decided to leave the room, they generally stood up, and either started to travel immediately (response time 0 seconds) or collected any belongings and started to travel (within 10 seconds response time for the voice alarms, but longer [within 25 seconds] for the sounder). Occupants tended to listen to the full message and its first repeat before beginning the response and travel phases of their evacuation. Figure 5 shows the PTAT distributions for each trial. The results for each pair of trials are summed to illustrate the distribution of times.

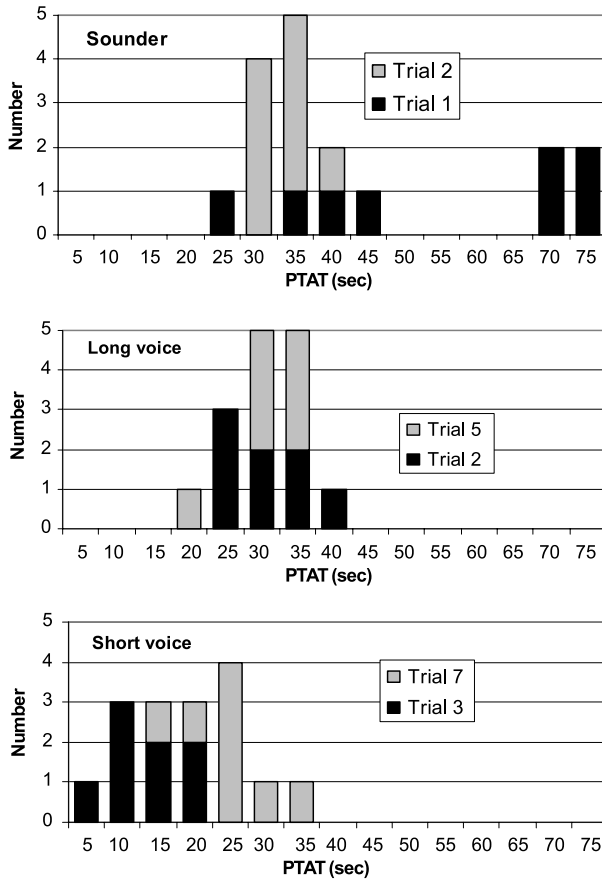


Fig. 5. PTAT distributions.

3.4 Findings from Questionnaire—University Teaching Laboratory Experiment with Three Alarm Types

The response to a multiple choice question about the perceived purpose of the alarm indicated that the majority of subjects interpreted each alarm type as a genuine fire/emergency warning (Table 6), with the exception of the short voice message, which was more likely to be perceived as part of the experiment. This was still the case even when trial 6 was excluded. In all cases where “other” was selected subjects expressed doubt as to the authenticity of the alarm and thought it might be part of the experiment. Subjects were significantly more motivated to leave the room by the long message than by the short message.

Response to the question “To what extent did you attempt to finish the activity you were involved in before leaving the room?” showed some indica-

Answer choice	Sounder	Long message	Short message	Total
Fire/emergency warning	8	6	3	17
Bomb warning	0	3	0	3
Could be either of the above	1	1	3 (4)	5 (6)
Did not know	1	0	1	2
Did not consider purpose	1	2	2 (3)	5 (6)
Other	6	4	7 (15)	7 (25)
Total	17	16	16 (26)	49 (59)

*(Italics: including trial 6)

Table 6. Perceived purpose of alarm from multiple choice question.

	Mean	s.d.	Cases
Sounder	2.53	1.50	17
Long voice	2.00	1.37	16
Short voice	2.13 (3.54)	1.45 (2.45)	16 (26)

*(Italics: including trial 6). s.d. = standard deviation

Table 7. Descriptive statistics for commitment to task and alarm type.

tion of differences between alarm types, which was significant if Trial 6 was included in the analysis ($P < 0.04$) (see Table 7).

There was no significant interaction between alarm types and previous experience with fires or bombs and reaction times, or with perceived seriousness of alarm and reaction times. Of the subjects, 20% had previous experience of a fire incident, 34% a bomb threat incident, and all had previous experience of a number of emergency evacuation drills.

4 Discussion

4.1 Effects of Alarm Type on PTAT Recognition and Response Times

The overall findings of the experimental study were that voice messages produced shorter and more reliable PTAT times than a sounder, which is in agreement with the two previous 1990/1 studies in the London office and underground Metro [4, 5] and other studies [1, 6]. The short message used in the experiment produced the shortest times, but the response was less reliable. The PTAT times for the voice alarms were also similar to those obtained in the earlier studies with mean values of 28 and 17 seconds (maximum 36 and 33 seconds) compared with previously reported maximum values of 30 and 75 seconds [4, 5]. These are also similar to the PTAT times obtained during the monitored office evacuation (maximum 60 seconds) and the shopping centre restaurant (maximum 103 seconds). However the PTAT times obtained using the sounder in the experimental study, although longer than those for the

voice alarms, were also short (mean 41, maximum 74 seconds) with effective evacuations, compared to the 11 and 9 minutes values reported in the earlier studies.

The analysis of both the monitored evacuations and the experimental study showed that the longest component of the evacuation time for both sounder and voice alarms systems was the recognition time. During the period subjects continued with the activities they were engaged in before the alarm sounded, or paused the activities to consider the implications of the alarm. In all three situations reported occupants were all seated at the time the alarm occurred, and all remained seated during the recognition phase. During this period for the sounder (in the experimental study) subjects appeared to be spending some time considering what action to take and tended to look at or consult each other before coming to a decision on a course of action. For the voice alarms they listened to the full voice message (sometimes plus a repeat) before taking action. In this context the use of a shorter voice message definitely reduced the time required to come to a response decision. There were indications that the long voice message was more effective in reducing commitment to the pre-alarm activity.

The office building meeting room and the university experiment both represented relatively simple situations with respect to response period behaviours. The subjects were in small rooms, present as individuals with relatively few commitments or belongings. The response period activities therefore required a relatively short time to complete compared with much more complex behavioural scenarios involved in some fire incidents [1, 7, 8]. The rapid recognition and short response times in the restaurant are of interest, since it has been suggested in actual incidents that occupants can be reluctant to cease eating and leave food (show high commitment) [8].

The questionnaire showed no significant interactions between alarm type, PTAT times and effects of previous experience with fires or fire drills, or bombs. Although it is possible factors such as these may have influenced overall responsiveness to all alarms, the mean scores on these aspects were relatively neutral (i.e. ~ 3 – 4.5 out of 7).

4.2 Perceived Seriousness of the Alarm

An issue with respect to university evacuation experiments was the extent to which subjects took the alarms seriously, since the alarms were not integrated into the building systems. The response to the multiple choice question indicated that the majority of subjects interpreted each alarm type as a genuine fire/emergency warning, with the exception of the short voice message, which was more likely to be perceived as part of the experiment. Some subjects expressed doubt as to the authenticity of the alarm and thought it might be part of the experiment, particularly for the failed short voice message (Trial 6). It is considered that in this regard the experiment findings were similar to those in monitored evacuations and genuine emergencies, in which occupants “often

treat real alarms as false alarms because they cannot see, smell or hear the fire, which may be on another floor” (J. Scanlon [9]).

4.3 Group Interactions

It was evident from observation of the video records that interactions between group members had a strong influence on evacuation behaviour and evacuation times. Subjects looked around and consulted each other before leaving the room, and as described, there were often a few key individuals who initiated (or inhibited) the whole group decision to evacuate (with an older person expediting the group response on one occasion, and younger members either unsuccessfully or successfully preventing evacuation. It is considered that such group dynamics can be very important in real emergencies. The results obtained here with Tral 6 are somewhat similar to those where subjects believe an alarm to be a drill and fail to respond, convincing each other that this is the case. Although differences between alarm types were not significant with respect to “motivation by others to leave the room”, the relatively high mean scores (scale 1–7) for this (sounder 5.0, Long voice 3.9 and short voice 4.8), suggest this may have been a factor, especially for the sounder case.

4.4 Design Behavioural Scenarios

The response of subjects to fire alarms is considered to be influenced by a number of parameters related to their individual characteristics and the building environment, but from previous studies it is considered that PTAT times and distributions are highly dependent upon a small number of key characteristics, which can be classified into a small number of design behavioural scenarios for the collection of data sets and for application to design cases [2, 3, 10]. The scenarios presented here could be classified as “awake and unfamiliar”, in that in all cases the occupants can be considered as largely unfamiliar with the buildings and alarm systems. In such situations voice alarm systems have been found to be particularly appropriate and effective. A further important consideration is the influence of evacuation management by trained staff. It is considered that the restaurant staff encouraged efficient evacuation for the restaurant case and that the scenario was well-managed. For the office meeting room case the building was well-managed and it is believed that a least one of the occupants was familiar with the building systems. The university experiment would not normally be considered to represent a well-managed case, but it is considered that since many of the participants had previous experience of fire drills or other emergency evacuations they behaved as well-trained individuals.

5 Conclusion

Voice alarms are more effective than sounders, providing shorter and more reliable evacuation pre-travel activity response times (PTAT), especially in “Awake and unfamiliar” Design Behavioural Scenarios.

References

1. D.A. Purser and M. Bensilum (2001) *Safety Science* 38, pp. 157–182.
2. D.A. Purser (2003) Behaviour and travel interactions in emergency situations and data needs for engineering design. Proceedings of 2nd International Conference on Pedestrian and Evacuation Dynamics, Greenwich, ed. E. Galea, pp. 355–370. University of Greenwich, London.
3. D.A. Purser (2002) ASET and RSET: addressing some issues in relation to occupant behaviour and tenability. *Fire Safety Science*, Proceedings of the Seventh International Symposium. International Association for Fire Safety Science, 2003, pp. 91–102. Interscience Communications, London.
4. L.L. Bellamy and T.A.W. Geter (1990) Experimental programme to investigate informative fire warning characteristics for motivating fast evacuation. BRE Report BR 172. Building Research Establishment.
5. G. Proulx and J.D. Sime (1991) *Fire Safety Science*, 3rd International Symposium, pp. 843–852. Interscience Communications, London.
6. J.D. Sime (1998) Human Behaviour in Fire, Proceedings of the First International Symposium, pp. 299–308. Fire SERT Centre, University of Ulster, Jordanstown, UK.
7. D.A. Purser and M. Kuipers (2004) Interactions between buildings, fire and occupant behaviour using a relational database created from incident investigations and interviews. Proceedings of 3rd International Symposium on Human Behaviour in Fire. Belfast, 2004, pp. 443–456. Interscience Communications, London.
8. D.A. Purser (2004) Structural fire engineering design: aspects of life safety. BRE Digest 490.
9. J. Scanlon (1979) Human behaviour in a fatal apartment fire. *Fire Journal*, 73, pp. 76–79.
10. D.A. Purser and S. Gwynne (2007) Identifying critical evacuation factors and the applications of egress models. Interflam 2007, Proceedings of 11th International Symposium, pp. 203–214. Interscience Communications, London.

Design of Voice Alarms—the Benefit of Mentioning Fire and the Use of a Synthetic Voice

Daniel Nilsson and Håkan Frantzich

Department of Fire Safety Engineering and Systems Safety, Lund University,
Box 118, 22100 Lund, Sweden
e-mail: Daniel.Nilsson@brand.lth.se

Summary. Preliminary results from a study about voice alarms are presented in this paper. The purpose of the study is to explore both how messages should be worded and how they should be presented. The paper focuses on an introductory questionnaire study at an IKEA store and unannounced evacuation experiments at Lund University. The results of these activities suggest that it is preferable to mention the word ‘fire’ in voice alarms since it makes people remember the content of the message more accurately. No difference could be detected between messages that were read by a human and a synthetic (computer generated) voice.

1 Introduction

In the event of fire it is essential that people respond quickly and without significant delay. Swift response requires that occupants receive information, e.g., that they are exposed to one or more fire cues, at an early stage. A fire cue is a signal that indicates (directly or indirectly) that a fire is in progress and some examples of typical cues are power failures, smoke, flames and fire alarms. In many cases the first cue is some type of fire alarm. Voice alarms have become common in many public buildings in recent years. These alarms are useful since they can inform occupants about the emergency and give them instructions. The use of voice alarms poses an interesting question; How should a message be worded and presented in order to be effective?

As has been pointed out by Sime [1] old building regulations often rest on the assumption that panic may easily occur in the event of fire. It is also sometimes suggested that panic can arise even when the danger caused by fire is minute and that panic may result in fatalities and serious injury [2]. These types of assumptions have in some cases lead to recommendations that information to the public should be restricted in the event of fire [3]. These restrictions are typically based on the belief that too much information about

what has happened, i.e., that there is a fire in the building, will lead to an uncontrolled rush for exits.

The conception of panic as a serious risk in the event of fire has been disputed [4, 5] and Sime [4] has pointed out that the word ‘panic’ is often misused. Research has also shown that clear information about the fire incident and what actions to take seem to promote swift response and effective evacuation [6]. Proulx and Sime [6] have suggested that telling people the truth about what has happened will decrease the risk of panic by making people respond quickly and hence not exposing them to dangerous and highly stressful fire conditions.

There are some additional examples of studies that have focused on the effectiveness of different fire alarms. In a study by Bayer and Rejnö [7] six alarms were tested for a cinema theater setting. The results of the study suggest that the dialect of the person who reads out a fire evacuation message may be important. Bayer and Rejnö found that visitors often believed that the message was part of a practical joke and that it took slightly longer for them to respond if a non-local dialect was used.

Another in-depth study of the effectiveness of fire alarms was conducted by Canter, Powell and Booker [8]. In their study they investigated several aspects of written messages and formulated criteria that must be met to ensure that a fire alarm will be effective. One of the criteria is that the fire alarm must be clearly distinguishable from other alarms, e.g., burglar alarms. Canter, Powell and Booker also suggest that the location of the fire should be mentioned so that the alarm can be authenticated and occupants can better plan their escape.

In order to investigate how voice alarms should be designed a study was initiated at Lund University in 2004. The purpose of the study is to explore both how a message should be worded and how it should be presented. The study focuses mainly on

- (i) the amount of information in the message
- (ii) information about the cause, i.e., mention of the word ‘fire’
- (iii) information about the location of a fire
- (iv) the use of a synthetic voice (computer generated voice)

In this paper preliminary results from the study are presented. The paper focuses on an introductory questionnaire study at an IKEA store and unannounced evacuation experiments at Lund University. These activities are concentrated on investigating how information about the cause and the use of a synthetic voice influence peoples’ interpretation and recall of voice alarms.

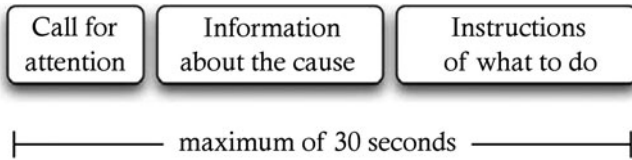


Fig. 1. The tree parts of a message according to Swedish recommendations.

2 Method

2.1 Design of Messages

The first activity of the study was the design of the messages that were going to be tested. In the first step of the design process five messages were formulated based on Swedish recommendations [9], which state that a voice alarms should contain three distinct parts, see Fig. 1. The three parts are a call for attention, information about the cause of the alarm and instructions of what to do. Another restriction in the recommendations is that the message should not exceed 30 seconds, see Fig. 1.

During the formulation process a standard message was first developed. All additional messages were then created by adding or removing sentences. The wording of the standard message was (translated from Swedish)

“Important message, important message! There is a fire in the building. Leave immediately through the closest exit and gather outside the building. Do not use the elevators.”

When the messages had been formulated they were recorded at a local radio station. All the messages were read by four different radio show hosts, namely two men and two women, in a professional studio. Based on an evaluation of the recordings it was decided that one of the male voice was going to be used in the study. The standard message was also recoded with a synthetic voice on a computer with the program Voxit Budgie Pro 1.0 and the Swedish voice called Ingrid [10]. Ingrid is a computer generated voice based on human speech. The voice alarms were finalized by adding the sound of a pulsating siren (4 seconds) in front of the voice recordings and creating sound files.

The design process resulted in six different voice alarms with varying content. For the present paper only three of the messages are relevant, see Table 1. Messages A and B are based on the standard wording, but were recorded with different voices. The wording of message C was identical to the standard message apart from information about the fire. The additional three messages, which are not included in this paper, were two voice alarms that contained the information of the standard message plus one or two less relevant sentences and one voice alarm with information about the location of the fire. All six voice alarms can be downloaded from the web page of the Department of Fire Safety Engineering and Systems Safety, Lund University [11].

Message	Wording	Voice	Length
A	<i>Important message, important message! There is a fire in the building. Leave immediately through the closest exit and gather outside the building. Do not use the elevators.</i>	Human male	21 s
B	<i>Important message, important message! There is a fire in the building. Leave immediately through the closest exit and gather outside the building. Do not use the elevators.</i>	Synthetic female	23 s
C	<i>Important message, important message! Leave immediately through the closest exit and gather outside the building. Do not use the elevators.</i>	Human male	19 s

Table 1. The three messages that are relevant for the present paper.

2.2 Questionnaire Study at IKEA

In order to get a rough estimate of the effectiveness of the different messages an introductory questionnaire study was performed at an IKEA store in Malmö, Sweden. The study was performed 15 and 21 June 2004 and all six messages were evaluated in the questionnaire study.

Participants

The participants consisted of customers who visited the IKEA store. One hundred and twenty-eight participants took part, namely 69 women, 53 men and 6 unknown (people who did not state gender). The average age was 61 years and the standard deviation was 14 years. Participants were given a check when they had completed their participation. The check could be used to purchase food at IKEA.

Procedure

The researchers stood at a location along the marked walking path in the IKEA store and approached customers to enquire if they would like to participate in a study. The information given to participants was that they would take part in a study about messages to customers, that it would take approximately five to ten minutes and that they would receive a check. If a customer agreed to take part he or she was given a pair of cordless headphones and listened to one of the messages, which was played two times. The participant was then interviewed about the message and filled out a questionnaire. The interview and the questionnaire focused on associations, interpretations, recall (memory) and opinion about the message. When the participant had finished he or she was given written information about the study and a check.

2.3 Evacuation Experiments at Lund University

Based on the results from the introductory questionnaire study it was decided that the first part of the study would explore how mention of the word ‘fire’ and the use of a synthetic voice influences the performance of voice alarms. In order to investigate these aspects evacuation experiments were performed at Lund University in 2004 and 2005. Only messages A, B and C were tested in the experiments, see Table 1.

Participants

The participants consisted of mainly first year computer science or electrical engineering students, but a few students from other technical faculties at Lund University also took part. Fifty-one students took part in the experiments, namely 46 men and five women. Their age was between 18 and 30 years and the average age was 20 years.

Procedure

The experiments were performed during tutorials in mathematics at the electrical engineering building, Lund University. A drawing of a typical classroom can be found in Fig. 2.

A total of six experiments were performed and the number of participants per experiment varied between four and 16, see Table 2. All experiments were unannounced, i.e., none of the students had been informed about the alarm beforehand. Before the alarm was activated a researcher, who played the role of a fellow teacher, entered the classroom and asked the teacher if he could spare a minute. Both the researcher and the teacher then exited the room together. After approximately one minute a fire alarm was activated in the classroom. The fire alarm had been installed in the classroom beforehand and

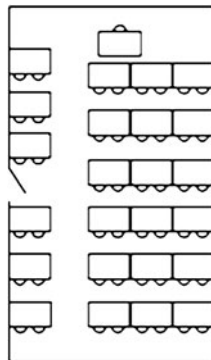


Fig. 2. A drawing of a typical classroom that was used in the evacuation experiments.

Experiment	Year	Message	Number of participants
1	2004	A	9
2	2004	A	5
3	2004	B	8
4	2004	C	16
5	2005	A	9
6	2005	C	4

Table 2. The six evacuation experiments at Lund University.

played one of the voice alarms over and over again until all participants had left the classroom.

The participants were stopped in the corridor outside the classroom and were lead into the classroom again. They were then informed about the study and filled out a questionnaire. The questionnaire contained questions about their interpretation of the alarm and demographic questions. Participants were also asked to try and recall the message and write it down using their own words. All experiments were filmed with a video camera inside the classroom. The video films were used to determine the pre-movement time. The pre-movement time was taken as the time from activation of the alarm until the participants began to move towards the exit.

3 Results

The results of the introductory questionnaire study at IKEA were mainly used to select messages for the evacuation experiments at Lund University. Based on the results it was decided that three out of the six messages that were tested at IKEA were going to be studied more closely, namely messages A, B and C. The reason for this choice was that there seemed to be only limited differences between messages A (human voice) and B (synthetic voice). Since this result was unexpected it was decided to further study the differences between the synthetic and human voice. The questionnaire study also suggested that the use of the word ‘fire’ was beneficial, since participants seemed to associate the alarm with a real emergency more often if fire was mentioned and also specifically mentioned that they wanted more information about the cause of the alarm. It was therefore decided that messages A (with ‘fire’) and C (without ‘fire’) were also going to be included in the experiments at Lund University. A detailed description of the questionnaire study at IKEA can be found in a report by Nilsson [12] and only limited results are presented in this paper. The sections below are based on the evacuation experiments at Lund University. A significance level of five percent has been used in all significance tests.

Number	Statement
1	When I heard the alarm I thought it was a real emergency.
2	When I heard the alarm I thought it was an evacuation drill.
3	When I heard the alarm I thought it was a false alarm.
4	When I heard the alarm I thought it was an evacuation experiment.

Table 3. The four statements in the questionnaire.

3.1 Synthetic Versus Human Voice

The questionnaire that was used in the evacuation experiments at Lund University contained four statements about the participants' beliefs when they heard the fire alarm, see Table 3. Participants were asked to estimate to what degree they agreed with the statements on a seven-point scale from *strongly agree* (1) to *strongly disagree* (7). Based on the four statements a new variable called *association to emergency* was created by taking the value of the answer to statement one minus the values of the answers to statement two, three and four. It is believed that a low value of the variable *association to emergency* corresponds to the belief that the alarm is caused by an emergency. Similarly, a high value would correspond to the opposite belief, i.e., that the alarm is likely caused by a non-emergency situation. The lowest possible value of the variable *association to emergency* is -20 ($1 - 7 - 7 - 7$) and the highest value is 4 ($7 - 1 - 1 - 1$).

A comparison between the experiments with message A (human voice) and B (synthetic voice) indicates that there was only a very small difference between participants' beliefs about the alarm. For message A the average value of the variable *association to emergency* was -7.7 and for message B the value was -8.9 . This result suggests that message B was associated with a real emergency to a greater extent than message A. However, the difference between the messages was not significant.

An interesting result is that none of the participants commented, neither in the questionnaire study at IKEA nor in the evacuation experiments at Lund University, that message B was read by a synthetic voice. The participants were, however, given apt opportunity to give any comments they felt were important. A large proportion of participants also utilized this opportunity. For example, 22 of 51 participants filled in the comment field (free text field) at the end of the questionnaire that was used in the evacuation experiments.

The video films were used to determine the pre-movement time in the experiments, see Table 4. Based on the measured times it was not possible to distinguish any differences between message A and B.

3.2 With Versus Without 'Fire'

A comparison between the experiments with message A (with 'fire') and C (without 'fire') shows that the difference between participants' beliefs about

Experiment	Message	Pre-movement time		Number of participants
		Mean	SD	
1	A	55	9.4	9
2	A	36	3.4	5
3	B	39	8.4	8
4	C	51	16.3	16
5	A	69	11.0	9
6	C	49	5.9	4

Table 4. The pre-movement time in the experiments.

Message	Interpretation	
	Incorrect	Correct
A	1	22
C	6	14

Table 5. The number of participants that gave incorrect and correct content in the questionnaire for message A and C.

the alarm were extremely small. For message A the average value of the variable *association to emergency* was -7.7 and for message C the value was -7.6 . This very small difference between messages was not significant.

In the questionnaire participants were also asked to write down the message using their own words. Based on the participants’ answers it was determined how many participants who stated incorrect content. Incorrect content could be any information that was not part of the message. The most common type of incorrect content was information about the cause of the alarm and information about assembly areas. A comparison between message A (with ‘fire’) and C (without ‘fire’) shows that a much higher proportion of participants gave incorrect information when fire was not mentioned, see Table 5. The Fisher’s exact test of consistency in a 2×2 table shows that the observed difference is significant, $p = .04$.

The pre-movement times from the experiments are shown in Table 4. Based on the observed times it was not possible to distinguish any differences between message A and C.

4 Discussion

The most important finding of the study thus far is that mention of the word ‘fire’ in voice alarms makes people remember the message more correctly. It is believed that accurate recall is an indication that people listen to and understand the information in the message. If a message is not remembered correctly it is possible that people may miss vital information or instructions. Based on the results it is not possible to determine why mention of fire has a positive effect. One possible explanation is that the word ‘fire’ is key word

that makes people focus and listen more carefully. An aim of future research could therefore be to further explore the use of the word 'fire' in voice alarms.

Before the study was initiated the researchers believed that a message read by a human voice would outperform a message read by synthetic voice. However, the results suggest that a synthetic voice may be just as effective as a human voice. Synthetic voices could potentially revolutionize the way voice alarms are used. Today messages are typically recorded in a studio, which means that it is difficult and expensive to create specific messages for a building or parts of a building. If synthetic voices were used a large set of messages could easily be created for a particular building. Messages could therefore be tailored to fit specific building parts or fire scenarios. It should be pointed out that the synthetic voice used in this study sounded almost human. Care must therefore be taken not to use a voice that sounds very artificial, since that type of computer generated voice may not be suitable for voice alarms.

One factor that makes direct comparison between message A (human voice) and B (synthetic voice) difficult is the gender difference. In the study the human voice was male whereas the synthetic voice was female. It can not be ruled out that gender is a factor that influences the performance voice alarms for the tested setting. Even if only female (or only male) voiced were used it would still be difficult to compare messages since other factors, such as age or intonation, may vary. However, the results indicate that there are synthetic voices that may be as effective as a human voice.

The pre-movement time is potentially a good indicator of the performance of voice alarms. If an alarm is effective it should in theory lead to short times, i.e., should make people respond quickly. The pre-movement time was measured in the evacuation experiments, but based on the limited data it was not possible to draw any conclusions about the performance of the messages. When additional data becomes available it may be possible to more adequately compare the performance of the tested voice alarms.

The present paper describes the initial phase of a study about voice alarms. The aim is to perform more similar experiments in the future to further explore how messages should be designed and to test the validity of the preliminary results presented in this paper.

5 Conclusions

The results presented in this paper indicate that mentioning the cause of the alarm, i.e., including the word 'fire', may improve the performance of voice alarms. More specifically mention of fire makes people interpret the message more correctly and leads to fewer misinterpretations. The results also suggest that messages read by a synthetic voice may be as effective as messages read by a human voice.

References

1. Sime, J.D. (1984) *Escape Behaviour in Fires: 'Panic' or Affiliation?* Guilford: Department of Psychology, University of Surrey.
2. Phillips, B.G. (1951) *Escape from Fire—Methods and Requirements*, London: Spon.
3. Home office (1934) *Manual of Safety Requirements in Theatres and Other Places of Public Entertainment*, London: H. M. Stationary Office.
4. Sime, J.D. (1980) The concept of 'Panic', in *Fires and Human Behaviour* (Ed. David Canter), Chichester: Wiley.
5. Keating, J.P. (1982) The myth of panic, *Fire Journal*, 76(3), 57–61, 147.
6. Proulx, G. & Sime, J. (1991) To prevent 'Panic' in an underground emergency: Why not tell people the truth? Paper presented at the Third International Conference on Fire Safety Science, Edinburgh, UK.
7. Bayer, K. & Rejnö, T. (1999) *Evacuation alarm, Optimizing through full-scale experiments (in Swedish)*, Report 5053, Lund: The Department of Fire Safety Engineering, Lund University.
8. Canter, D., Powell, J. & Brooker, K. (1988) *Psychological Aspects of Informative Fire Warning Systems*. Borehamwood: Department of the Environment, Building Research Establishment, Fire Research Station.
9. SBF (2003) *Utrymningslarm 2003* Stockholm: Brandförsvarsförningens Service AB.
10. Voxit (2003) *Voxit Budgie Pro 1.0* [Computer program]. Skellefteå: Voxit AB.
11. Nilsson, D. (2006) *Studie av talade utrymningsmeddelanden*. Retrieved April 30, 2008, from http://www.brand.lth.se/forskning/utrymning/talade_meddelanden/.
12. Nilsson, D. (2006) *Design of pre-recorded fire evacuation messages—experiences gained from a questionnaire study and unannounced evacuation experiments (in Swedish)*, Report 3139, Lund: The Department of Fire Safety Engineering, Lund University.

Enhanced Empirical Data for the Fundamental Diagram and the Flow Through Bottlenecks

Armin Seyfried¹, Maik Boltes¹, Jens Kähler², Wolfram Klingsch²,
Andrea Portz¹, Tobias Rupprecht², Andreas Schadschneider³,
Bernhard Steffen¹, and Andreas Winkens²

¹ Jülich Supercomputing Centre, Forschungszentrum Jülich GmbH, 52425 Jülich, Germany

e-mail: a.seyfried@fz-juelich.de

² Institute for Building Material Technology and Fire Safety Science, Bergische Universität Wuppertal, Pauluskirchstrasse 11, 42285 Wuppertal, Germany

e-mail: klingsch@uni-wuppertal.de

³ Institut für Theoretische Physik, Universität zu Köln, 50937 Köln, Germany

e-mail: as@thp.uni-koeln.de

Summary. In recent years, several approaches for modeling pedestrian dynamics have been proposed and applied e.g. for design of egress routes. However, so far not much attention has been paid to their *quantitative* validation. This unsatisfactory situation belongs amongst others on the uncertain and contradictory experimental data base. The fundamental diagram, i.e. the density-dependence of the flow or velocity, is probably the most important relation as it connects the basic parameter to describe the dynamic of crowds. But specifications in different handbooks as well as experimental measurements differ considerably. The same is true for the bottleneck flow. After a comprehensive review of the experimental data base we give an survey of a research project, including experiments with up to 250 persons performed under well controlled laboratory conditions. The trajectories of each person are measured in high precision to analyze the fundamental diagram and the flow through bottlenecks. The trajectories allow to study how the way of measurement influences the resulting relations. Surprisingly we found large deviation amongst the methods. These may be responsible for the deviation in the literature mentioned above. The results are of particular importance for the comparison of experimental data gained in different contexts and for the validation of models.

1 Introduction

The number of models for pedestrian dynamics has grown in the past years, but the experimental data to test them and to discriminate between these models is still to a large extent uncertain and contradictory (see e.g. [1]). In most models, pedestrians are considered to be autonomous mobile agents,

hopping particles in a cellular automaton or self-driven particles in a continuous space. If the objective is to make quantitative predictions, like evacuation or travel times, the model has to be calibrated with empirical data.

One of the most important characteristics of pedestrian dynamics is the fundamental diagram giving the relation between pedestrian flow and density. Beside its importance for the dimensioning of pedestrian facilities it is associated with every qualitative self-organization phenomenon, like the formation of lanes or the occurrence of congestions. However, specifications of different experimental studies, guidelines and handbooks, all display non negligible differences even for the most relevant characteristics like maximal flow values, the corresponding density and the density where the flow is expected to become zero due to overcrowding. The connection between fundamental diagram and bottleneck flow is important as well and not really understood. In particular the maxima of fundamental diagrams are significantly lower than maximal flow values measured at bottlenecks.

Although a large variety of models for pedestrian dynamics has been proposed, so far there have been only limited attempts to calibrate and validate these approaches. One reason is the unclear situation of the empirical data, as described above. This situation is very unsatisfactory and poses serious limitations on the use of such models e.g. in the area of safety planning. To improve the current state of affairs it is necessary to have more reliable data that can be used as basis for validation and calibration which then would allow to make quantitative predictions based on computer simulations.

In Sect. 2 we give a review of empirical results and discuss their discrepancies by comparing various experimental data and specifications from the literature. To resolve some of the contradictions we initiated a research project including experiments with up to 250 persons under well controlled laboratory conditions, see Sect. 3. Great emphasis was given to the method of data recording by video technique and careful preparation of the experimental setups. This enables the accurate determination of all trajectories providing a microscopic insight into pedestrian dynamics, see [2]. In Sect. 4 we analyze how the measurement method influences the resulting outcomes.

2 Review of Empirical Results

2.1 Fundamental Diagram

The fundamental diagram describes the empirical relation between density ρ and flow J (or specific flow per unit width $J_s = J/w$). The name already indicates its importance and naturally it has been the subject of many investigations. Due to the hydrodynamic relation $J = \rho v w$ there are three equivalent forms: $J_s(\rho)$, $v(\rho)$ and $v(J_s)$. In applications the relation is a basic input for engineering methods developed for the design and dimensioning of pedestrian

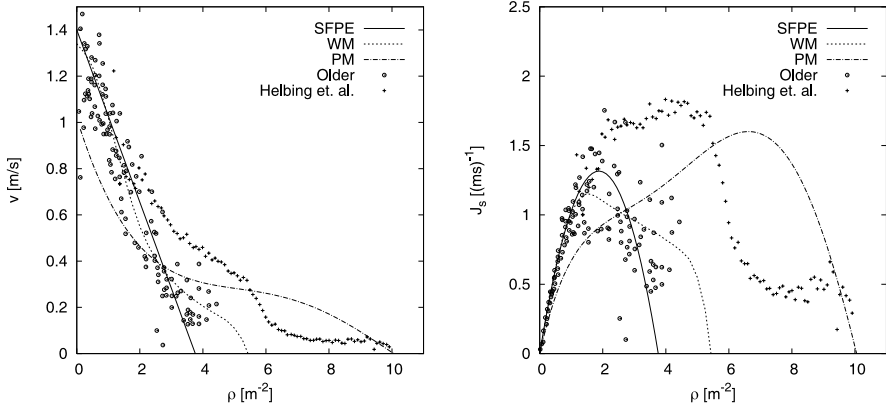


Fig. 1. Fundamental diagrams for pedestrian movement in planar facilities. The lines refer to specifications according to planing guidelines (SFPE Handbook [6], PM: Predtechenskii and Milinskii [3], WM: Weidmann [5]). Data points give the range of experimental measurements [7, 8].

facilities [3–6]. In this section we will concentrate on planar facilities like sidewalks, corridors or halls. For various facilities like floors, stairs or ramps the shape of the diagrams differ, but in general it is assumed that the fundamental diagrams for the same type of facilities but different widths merge into one diagram for the specific flow J_s .

Figure 1 shows various fundamental diagrams used in planing guidelines plus the measurements of two selected empirical studies representing the overall range of the data. The comparison reveals that specifications and measurements disagree considerably. In particular the maximum of the function giving the capacity $J_{s,\max}$ ranges from 1.2 (ms)^{-1} to 1.8 (ms)^{-1} , the density ρ_0 where the velocity approaches zero due to overcrowding ranges from 3.8 m^{-2} to 10 m^{-2} and, most notably, the density value where the maximum flow is reached ρ_c ranges from 1.75 m^{-2} to 7 m^{-2} . Several explanations for these deviations have been suggested, including cultural and population differences [8], differences between uni- and multidirectional flow [9, 10], short-ranged fluctuations [10], influence of psychological factors given by the incentive of the movement [3] and, partially related to the latter, the type of traffic (commuters, shoppers) [11].

The most elaborate fundamental diagram has been given by Weidmann, who collected 25 data sets. An examination of the data which were included in Weidmann’s analysis shows that most measurements with densities larger than $\rho = 1.8 \text{ m}^{-2}$ are performed on multidirectional streams. Weidmann neglected differences between uni- and multidirectional flow in accordance with Fruin, who states in his often cited book [4] that the fundamental diagrams of multidirectional and unidirectional flow differ only slightly. This disagrees with results of Navin and Wheeler [9] who found a reduction of the flow in de-

pendence of directional imbalances. Here lane formation in bidirectional flow has to be considered. Bidirectional pedestrian flow includes unordered streams as well as lane-separated and thus quasi-unidirectional streams in opposite directions. Another explanation is given by Helbing et al. [8] who argue that cultural and population differences are responsible for the deviations between Weidmann and their data. In contrast to this interpretation the data of Hanking and Wright [12] gained by measurements in the London subway (UK) are in good agreement with the data of Mori and Tsukaguchi [13] measured in the central business district of Osaka (Japan), both on strictly uni-directional streams. This brief discussion clearly shows that up to now there is no consensus about the origin of the discrepancies between different fundamental diagrams and how one can explain the shape of the function.

However, all diagrams agree in one characteristic: velocity decreases with increasing density. As the discussion above indicates there are many possible reasons and causes for the velocity reduction. For the movement of pedestrians along a line a linear relation between speed and the inverse of the density was measured in [14]. The speed for walking pedestrians depends also linearly on the step size [5] and the inverse of the density can be regarded as the required length of one pedestrian to move. Thus it seems that smaller step sizes caused by a reduction of the available space with increasing density is, at least for a certain density region, one cause for the decrease of speed. However, this is only a starting point for a more elaborated modeling of the fundamental diagram.

2.2 Bottleneck Flow

One of the most important practical questions is how the capacity of the bottleneck increases with rising width. Studies of this dependence can be traced back to the beginning of the last century [15, 16] and are up to now discussed controversially. At first sight, a stepwise increase of capacity with the width appears to be natural if lanes are formed. For independent lanes, where pedestrians in one lane are not influenced by those in others, capacity increases only if an additional lane can be formed.

In contrast, the study [17] found that the distance of lanes and the speed in a lane increases with the bottleneck width until a new lane is formed, when the lanes come closer together again. This variation of lane distance leads to a very weak dependence of the density and velocity inside the bottleneck on its width. Thus in reference to $J = \rho v w$ the flow does not directly depend on the number of lanes. To find a conclusive judgment whether the capacity grows continuously with the width the results of different laboratory experiments [18–22] are compared in [22].

In the following we discuss the data of flow measurement collected in Fig. 2. The data by Muir et al. [19], who studied the evacuation of airplanes, seem to support the stepwise increase of the flow with the width. They show constant flow values for $w > 0.6$ m. But the flow there does not increase much up to

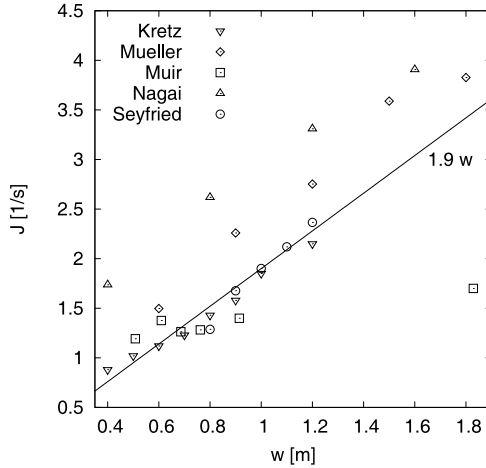


Fig. 2. Influence of the width of a bottleneck on the flow. Experimental data (Müller [18]; Muir et al. [19]; Nagai et al. [20]; Seyfried et al. [22]) of different types of bottlenecks and initial conditions. All data are taken under laboratory conditions where the test persons are advised to move normally.

$w = 1.8$ m, which indicates that in this special setup the flow is limited by some other process, e.g. reaching the corridor. Thus all data collected from flow measurements in Fig. 2 are compatible with a continuous and almost linear increase with the bottleneck width for $w > 0.6$ m. Surprisingly the data in Fig. 2 differ considerably in the values of the bottleneck capacity. In particular the flow values of Nagai [20] and Müller [18] are much higher than the maxima of empirical fundamental diagrams. The comparison of the different experimental setups shows that the exact geometry of the bottleneck is of only minor influence on the flow while a high initial density in front of the bottleneck can increase the resulting flow values. This leads to another interesting question, that is to say how the bottleneck flow is connected to the fundamental diagram. General results for driven diffusive systems [23] show that boundary conditions only *select* between the states of the undisturbed system instead of creating completely different ones. Therefore it is surprising that the measured maximal flow at bottlenecks can exceed the maximum of the empirical fundamental diagram. These questions are related to the common jamming criterion. Generally it is assumed that a jam occurs if the incoming flow exceeds the capacity of the bottleneck. In this case one expects the flow through the bottleneck to continue with the capacity (or lower values). The data presented in [22] show a more complicated picture, we refer to the contribution of A. Winkens and T. Rupprecht in these proceedings. While the density in front of the bottleneck amounts to $\rho \approx 5.0 (\pm 2) \text{ m}^{-2}$, the density inside the bottleneck tunes around $\rho \approx 1.8 \text{ m}^{-2}$.

3 Research Project—Overview

The research project is funded by the DFG and based on cooperation between the Bergische Universität Wuppertal, the Universität zu Köln and Forschungszentrum Jülich GmbH. It covers the execution of large scale experiments, the data collection via automated determination of trajectories with high accuracy, microscopic and macroscopic data analysis and the development of models to describe the dynamic of pedestrians quantitatively. In this section we give an overview of the experiments performed.

As outlined in the previous section, there are a lot of possible influences on the characteristics of pedestrian crowd movement. To reduce as much as possible uncontrollable influences we decided to use a homogeneous group of test persons and to perform the experiments under well controlled laboratory conditions. It is obvious that results performed under special conditions are not suited for design recommendations of e.g. escape routes. However such types of experiments make it possible to study the influence of single parameters, like the bottleneck width, and thus to resolve whether the capacity of a bottleneck increases linearly or step wise. Moreover the determination of the trajectories of all persons with high accuracy allows a microscopic insight into pedestrian dynamics and thus to provide a secure data base for the development and microscopic verification of models. Concerning the determination of trajectories we refer to [2].

The experiments were arranged 2006 in the wardroom of the ‘Bergische Kaserne Düsseldorf’. The group of test persons was composed of soldiers. Fig. 3 (left) shows a sketch of the experimental setup to determine the fundamental diagram. We performed runs for different widths w as well as uni- and bidirectional flows. To scan the whole density regime the number of the pedestrians inside the corridor was changed. The right figure shows the sketch of the experimental setup to analyze the flow through bottlenecks. We performed runs for different bottleneck widths w , corridor widths w_c , bottleneck length l , number of pedestrians N and distances to the entrance d . To ensure an equal initial density for every run, holding areas were marked on the floor (dashed regions). All together 99 runs with up to 250 people distributed over five days were performed.

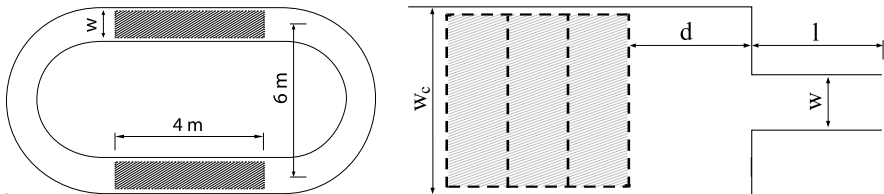


Fig. 3. Sketch of the experimental setup to determine the fundamental diagram (*left*) and to analyze the flow through bottlenecks (*right*).

4 Influence of the Measurement Method

The discussion outlined in Sect. 2 is put into perspective by two observations. First we note that in the majority of cases the data come without fluctuations and error margins and thus, strictly speaking, there is no contradiction. Second it is well known in vehicular traffic that different measurement methods can lead to deviations for the fundamental diagram [24, 25]. In previous experimental studies of pedestrian traffic, different kinds of measurement methods are used, and often a mixture of time and space averages are realized due to cost reasons. But in case of spatial and temporal inhomogeneities it cannot be excluded that the averaging over different degrees of freedom leads to non-comparable results. In this section we analyze how large the deviations due to different measurement methods are. For this purpose we choose the most ordered and controlled system examined in the project, namely the fundamental diagram for the movement of pedestrians along a line under closed boundary conditions during a stationary state. Due to the controlled character of the movement it can be expected that deviations caused by inhomogeneities give a lower bound for deviations in more disordered systems.

In the following we introduce the basic quantities and the flow equation along the measurement methods. The discussion follows the explanation in text books for vehicular traffic [24, 25] and is adapted to pedestrian characteristics. The sketch in Fig. 4 illustrates two principle possibilities to measure the observable like flow, velocity and density.

Method A: local measurement of the observable O at a certain location x averaging over a time interval Δt . We refer to this by $\langle O \rangle_{\Delta t}$. Measurements at a certain location allow a direct determination of the flow J and the velocity v .

$$\langle J \rangle_{\Delta t} = \frac{N}{\Delta t} = \frac{1}{\langle \Delta t_i \rangle_{\Delta t}} \quad \text{and} \quad \langle v \rangle_{\Delta t} = \frac{1}{N} \sum_{i=1}^N v_i. \quad (1)$$

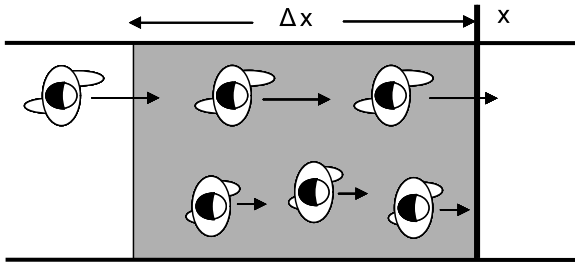


Fig. 4. Illustration of different measurement methods to determine the fundamental diagram. It has to be distinguished between local measurements at cross-section with position x averaged over a time interval Δt and measurements at certain time averaged over space Δx .

The flow is given as the number of persons N passing a specified cross-section at x per unit time. Usually it is taken as a scalar quantity since only the flow normal to the cross-section is considered. To relate the flow with a velocity one measures the individual velocities v_i at location x and calculates the mean value of the velocity $\langle v \rangle_{\Delta t}$ of the N pedestrians. In earlier studies normally the velocity of a single pedestrian was considered and only the number of pedestrians N passing the cross-section in the time interval Δt are counted [3, 12, 26]. In principle it is possible to determine the velocities v_i and crossing times t_i of each pedestrian and to calculate the time gaps $\Delta t_i = t_{i+1} - t_i$ defining the flow as the inverse of the mean value of time gaps over the time interval Δt .

Method B is to average the observable O over space Δx at a specific time t_k which gives $\langle O \rangle_{\Delta x}$. The introduction of an observation area with extend $w\Delta x$ allows to determine directly the density ρ and the velocity v :

$$\langle \rho \rangle_{\Delta x} = \frac{N'}{w\Delta x} \quad \text{and} \quad \langle v \rangle_{\Delta x} = \frac{1}{N'} \sum_{i=1}^{N'} v_i. \quad (2)$$

This method was used in combination with time-lapse photos. Often and due to cost reasons only the velocity of single pedestrians and the mean value of the velocity during the entrance and exit times were considered [7, 9].

Flow equation: To connect these methods and to change between different representations of the fundamental diagram the hydrodynamic flow equation $J = \rho vw$ is used. It is possible to derive the flow equation from the definition of the observables introduced above by using the distance $\Delta \tilde{x} = \Delta t \langle v \rangle_{\Delta t}$. Thus one obtains

$$J = \frac{N}{\Delta t} = \frac{N}{\Delta \tilde{x} w} \frac{\Delta \tilde{x} w}{\Delta t} = \tilde{\rho} \langle v \rangle_x w \quad \text{with} \quad \tilde{\rho} = \frac{N}{\Delta \tilde{x} w}. \quad (3)$$

At this point it is crucial to note that the mean values $\langle v \rangle_x$ and $\langle v \rangle_t$ do not necessarily correspond. This can already be seen by examination of Fig. 4. Thus a density calculated by $\tilde{\rho} = \langle J \rangle_{\Delta t} / \langle v \rangle_{\Delta t}$ may differ from a direct measurement of the density via $\langle \rho \rangle_{\Delta x}$. We come back to this point later.

As already mentioned above we choose the most simple system to get an estimation for the lower bound of deviation resulting from different measurement methods. To measure the fundamental diagram of the movement along a line we performed 12 runs with varying number of pedestrians, $N = 17$ to $N = 70$. Figure 5 shows the projection of the trajectories to the (x, t) -plane for the runs with $N = 45, 56$ and 62 . For the movement along a line we set $w = 1$ in the equations introduced above. We note again that the different measurements shown in the next figures are based on the same set of trajectories determined automatically from video recordings of the measurement area with high accuracy ($x_{\text{err}} \pm 0.02$ m). The data analysis is restricted to the stationary state.

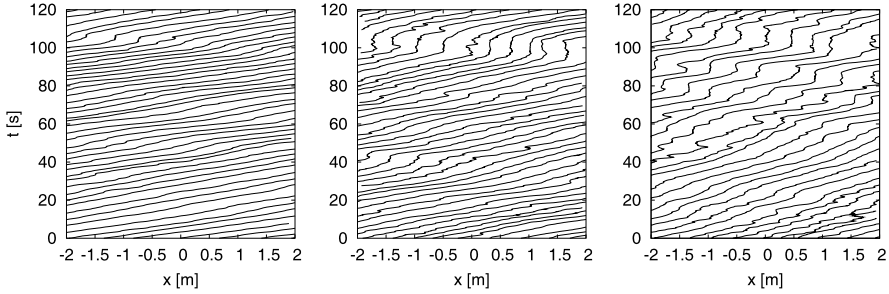


Fig. 5. Projection of the trajectories to the (x, t) -plane of the movement along a line for the runs with $N = 45, 56, 62$ (from left to right). For increasing N the dynamics becomes more unordered and the trajectories show intermittent stopping by a constant x -values in time.

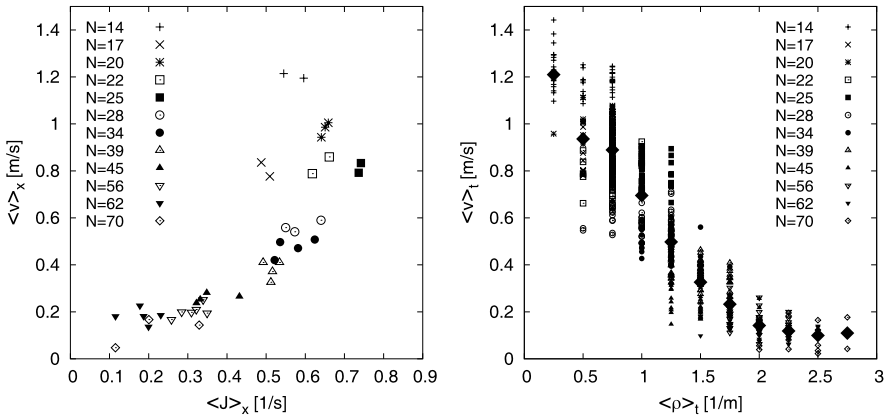


Fig. 6. Fundamental diagrams measured at the same set of trajectories but with different methods. *Left:* Measurement at a certain cross-section averaging over time interval (Method A). *Right:* Measurement at a certain point in time averaging over space (Method B). *Large diamonds* give the over all mean value of the velocity for one density value.

Figure 6 shows the direct measurements according to Methods A and B. For Method A we choose the position of the cross-section $x = 0$ and a time interval of $\Delta t = 30$ s, see Fig. 5. For Method B the area ranges from $x = -2$ m to $x = 2$ m, and we performed the averaging over space each time t_k a pedestrian crossed $x = 0$. For Method B we note that the fixed length of the observation area of 4 m results in discrete density values with distance $\Delta\rho = (4 \text{ m})^{-1}$. For each density value large fluctuations of the velocities $\langle v \rangle_t$ are observed. The large diamonds in the right of Fig. 6 represent the mean values over all velocities $\langle v \rangle_t$ for one density. The flow equation (3) allows to switch the direct measurement of Methods A and B into the most common representation of the fundamental diagram $J(\rho)$.

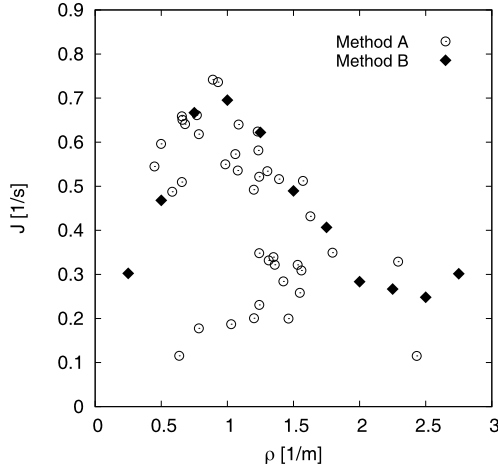


Fig. 7. Fundamental diagram determined by different measurement methods. Method A: Direct measurement of the flow and velocity at a cross-section. The density is calculated via $\rho = \langle J \rangle_{\Delta t} / \langle v \rangle_{\Delta t}$. Method B: Measurement of the density and velocity at a certain time point averaged over space. The flow is given by $J = \rho \langle v \rangle_{\Delta x}$.

Figure 7 shows a comparison of fundamental diagrams using the same set of trajectories but different measurement methods. In particular for high densities, where jam waves are present, the deviations are obvious. This is in agreement with Fig. 1 where almost all curves agree for low densities and disagree for high densities. For the high density regime the trajectories show inhomogeneities in time and space, which do not correspond, see Fig. 5. The averaging over different degrees of freedom, the time Δt for Method A and the space Δx for Method B lead to different distribution of individual velocities. Thus one reason for the deviations is that the mean values of the velocity measured at a certain location by averaging over time do not necessarily conform to mean values measured at a certain time averaged over space. However, the straightforward use of the flow equation neglects these differences. In [24] it was stated that the difference can be canceled out by using the harmonic average for the calculation of the mean velocity for Method A. We test this approach and found that the differences do not cancel out and the data are only in conformance if one takes into account the fluctuations and calculates the mean velocity by the harmonic average. But for states where congestions lead to an intermittent stopping, fluctuations of the density measured with Method A are extremely large and can span over the whole density range observed. This belongs to the fact that in Method A the density is determined indirectly by calculating $\tilde{\rho} = \langle J \rangle_{\Delta t} / \langle v \rangle_{\Delta t}$. In the high density range the flow as well as the velocity have small values causing high fluctuations for the calculated density.

5 Conclusions

This contribution summarizes open questions and differences concerning specifications of the fundamental diagram and bottleneck flow in the literature. In particular for the high density regime of the flow-density relation the discrepancies are not negligible. For the flow through bottlenecks it is an open question, why the maximal flow values through bottleneck exceed significantly the maxima of the fundamental diagrams. To dissolve these discrepancies we performed laboratory experiments with up to 250 people. The trajectories of each pedestrian are determined with high accuracy. As a first step of the analysis we investigated how the way of measurement influence the resulting relations. Surprisingly we found that even for the most regular and simplest system, namely the movement of pedestrians along a line under periodic boundary conditions, large deviations result if different measurement methods are applied. The reason for this is the averaging over different degrees of freedom in a discrete system with large inhomogeneities. Thus it cannot be excluded that the deviations discussed in Sect. 2 result from different measurement methods amongst other causes. This statement is supported by the observation based on Fig. 1, that almost all curves agree for low densities and disagree for high densities. For a systematic study and a meaningful discussion of the influence of culture or the changing population demographics on pedestrian characteristic it is necessary to assure that the studies compared are based on the same measurement approach. This applies accordingly for the validation of model results with experimental data.

Acknowledgements

We would like to thank the German Science Foundation (DFG) for funding this project under DFG-Grant No. KL 1873/1-1 and SE 1789/1-1. A. Seyfried and A. Schadschneider are grateful to the ped-net-group (www.ped-net.org) for intensive and inspiring discussions.

References

1. A. Schadschneider, W. Klingsch, H. Kluepfel, T. Kretz, C. Rogsch, and A. Seyfried. Evacuation dynamics: Empirical results, modeling and applications. In *Encyclopedia of Complexity and System Science*. Springer, Berlin, 2009.
2. M. Boltes, A. Seyfried, B. Steffen, and A. Schadschneider. Automatic extraction of pedestrian trajectories from video recordings. In *Pedestrian and Evacuation Dynamics 2008*. Springer, Berlin, 2010.
3. V. M. Predtechenskii and A. I. Milinskii. *Planning for Foot Traffic Flow in Buildings*. Amerind, New Delhi, 1978.
4. J. J. Fruin. *Pedestrian Planning and Design*. Elevator World, New York, 1971.

5. U. Weidmann. Transporttechnik der Fussgänger. Schriftenreihe des IVT 90, ETH Zürich, 1993.
6. H. E. Nelson and F. W. Mowrer. Emergency movement. In P. J. DiNenno, editor, *SFPE Handbook of Fire Protection Engineering*, National Fire Protection Association, Quincy, MA, 2002.
7. S. J. Older. Movement of pedestrians on footways in shopping streets. *Traffic Engineering and Control*, 10:160–163, 1968.
8. D. Helbing, A. Johansson, and H. Z. Al-Abideen. Dynamics of crowd disasters: An empirical study. *Physical Review E*, 75:046109, 2007.
9. F. D. Navin and R. J. Wheeler. Pedestrian flow characteristics. *Traffic Engineering*, 39:31–36, 1969.
10. B. Pushkarev and J. M. Zupan. Capacity of walkways. *Transportation Research Record*, 538:1–15, 1975.
11. D. Oeding. Verkehrsbelastung und Dimensionierung von Gehwegen und anderen Anlagen des Fußgängerverkehrs. Forschungsbericht 22, Technische Hochschule Braunschweig, 1963.
12. B. D. Hankin and R. A. Wright. Passenger flow in subways. *Operational Research Quarterly*, 9:81–88, 1958.
13. M. Mori and H. Tsukaguchi. A new method for evaluation of level of service in pedestrian facilities. *Transportation Research Part A*, 21(3):223–234, 1987.
14. A. Seyfried, B. Steffen, W. Klingsch, and M. Boltes. The fundamental diagram of pedestrian movement revisited. *J. Stat. Mech.*, page P10002, 2005.
15. D. Dieckmann. *Die Feuersicherheit in Theatern*. Jung München, 1911.
16. H. Fischer. *Über die Leistungsfähigkeit von Türen, Gängen und Treppen bei ruhigem, dichtem Verkehr*. Dissertation, Technische Hochschule Dresden, 1933.
17. A. Seyfried, T. Rupprecht, O. Passon, B. Steffen, W. Klingsch, and M. Boltes. New insights into pedestrian flow through bottlenecks. *Transportation Science* (accepted for publication), 2008. arXiv:[physics/0702004v2](https://arxiv.org/abs/physics/0702004v2).
18. K. Müller. *Zur Gestaltung und Bemessung von Fluchtwegen für die Evakuierung von Personen aus Bauwerken auf der Grundlage von Modellversuchen*. Dissertation, Technische Hochschule Magdeburg, 1981.
19. H. C. Muir, D. M. Bottomley, and C. Marrison. Effects of motivation and cabin configuration on emergency aircraft evacuation behavior and rates of egress. *The International Journal of Aviation Psychology*, 6:57–77, 1996.
20. R. Nagai, M. Fukamachi, and T. Nagatani. Evacuation of crawlers and walkers from corridor through an exit. *Physica A*, 367:449–460, 2006.
21. T. Kretz, A. Grünebohm, and M. Schreckenberg. Experimental study of pedestrian flow through a bottleneck. *J. Stat. Mech.*, page P10014, 2006.
22. A. Seyfried, B. Steffen, A. Winkens, T. Rupprecht, M. Boltes, and W. Klingsch. Empirical data for pedestrian flow through bottlenecks. In *Traffic and Granular Flow 2007*. Springer, Berlin, 2007.
23. V. Popkov and G.M. Schütz. Steady-state selection in driven diffusive systems with open boundaries. *Europhys. Lett.*, 48(3):257–263, 1999.
24. W. Leutzbach. *Introduction to the Theory of Traffic Flow*. Springer, Berlin, 1988.
25. B. S. Kerner. *The Physics of Traffic*. Springer, Berlin, 2004.
26. K. Togawa. Study on fire escapes basing on the observation of multitude currents. Report of the Building Research Institute 14, Ministry of Construction, Japan, 1955.

Parameters of Pedestrian Flow for Modeling Purposes

Valerii V. Kholshchevnikov¹ and Dmitrii A. Samoshin²

¹ State Moscow University of Civil Engineering, Yaroslavskoe Highway 26, 127337 Moscow, Russia

e-mail: reglament2004@mail.ru

² Academy of State Fire Service, B. Galushkin, 4, 129366 Moscow, Russia

e-mail: info@FireEvacuation.ru

Summary. Seventy years of foot traffic flow research in Russia provided unique empirical data base of travel speed values at different flow density, ranging from 0 up to 13–14 persons/m² obtained in approximately 35.000 counts in 100 series of observations and experiments in the different buildings, city territories, route types and experimental settings.

The laws for crossing of boundaries of adjacent sectors of paths, crowding of people, merging, reforming and diffusion of flows were developed. The flow traffic through door openings, cross and contra-flows, movement on a router with “unlimited” width and other special cases were also investigated.

Accumulated empirical database was used to establish valid psychophysiological law describes relation between flow travel speed and flow density considering emotional state of people. This law was expressed as random function.

Established relations were validated against actual observations, experiments and unannounced evacuations which involved able-body and disabled people. Due to high reliability of established laws they were used in all related Russian building codes and also used for flow/evacuation modeling aimed to provide safety of building occupants. Obtained results are presented in the given paper.

1 Introduction

Predtechenskii and Milinskii’s seminal work [1] in relation to pedestrian flows is well known. However, analysis of the experimental results and observations obtained from this series of experimental studies revealed the inherent statistical non-homogeneity of pedestrian flow speeds [2, 3]. As such, the results of these individual experiments cannot be integrated to produce a valid general expression $V = f(D)$ for each type of pedestrian flow path where V is the flow velocity and D is the flow density. In this paper pedestrian flow is treated as a stochastic process, i.e., that which might be observed in a series of experiments as a manifestation of the random function $V = f(D)$. A fundamentally

new random methodology to mathematically describe this function was developed [4]. The high degree of correspondence between observed pedestrian flows and the output from these models has been sufficient for the models to be accepted by statutory authorities and used in building design and regulation in Russia [5–7] for many years.

A shift to performance based design revealed a need for new advanced algorithm, describing movement of each pedestrian in a flow. Together with wide range of analyzed special cases of pedestrian flow (e.g. movement at high density conditions, crossing flows and contra flows, etc.) it makes possible to describe with high preciseness movement of people within a flow.

2 Fundamental Laws of Pedestrian Flow

In 1951 Milinskii established a statistical data base of human flow parameters, comprising field observations of some 3585 counts of travel speed against density of flow, together with 2303 counts of door traffic capacity for doors which ranged from 0.5 m to 2.4 m wide at densities of 1–9 persons/m² [8]. The visual method of observations which was used required the participation of 160 observers. 148 counts of body dimensions were also recorded and presented as f , the horizontal projected area, m², in order to express density of flow (D) in m²/m² as:

$$D = \frac{Nf}{lb} \quad (1)$$

where N —number of people, l —length of the pathway (m), and b —width of pathway (m).

For the first time, in cooperation with Prof. Predtechenskii fundamental laws of pedestrian flow relating to:

- changes of flow characteristics at the interface of route sectors with different widths or route types (j);
- merging and branching of flows;
- dynamics of crowding and bottlenecking at the interface of a sector with insufficient traffic capacity; and
- convergence and divergence of a flow were determined.

The results of this work have been presented in [1, 9–12], and the most important outcomes of this work are briefly summarized below.

Changes of flow characteristics (V and D) at the interface of a sector of width b_i to a sector with width b_{i+1} is determined by changes of intensity of flow from q_i to q_{i+1} :

$$q_{i+1,j} = \frac{q_{i,j}b_i}{b_{i+1}}. \quad (2)$$

The intensity of flow $q = VD$ person/(m/min) or m²/(m/min) is the product of flow velocity and density of flow.

In the case of the merging of several flows, the intensity of flow can be described as

$$q_{i+1,j} = \frac{\sum q_{i,j} b_i}{b_{i+1}}. \quad (3)$$

Delay of a flow at the interface of the next sector occurs because of its inherent traffic capacity, i.e. if the sector cannot accommodate all the people approaching it. Denoting the number of people coming from the previous sector as $P_{i,j} = q_{i,j} b_i$, and the traffic capacity of the adjacent sector as $Q_{i+1,j} = q_{\max,j} b_{i+1}$ then, if $Q_{i+1,j} \geq \sum P_{i,j}$ the flow is unimpeded. Alternatively, if $Q_{i+1,j} < \sum P_{i,j}$ at the interface with the adjacent sector $i + 1$, movement delay develops with the duration

$$\Delta t = \sum N_i \left(\frac{1}{Q_{i+1,j}} - \frac{1}{\sum P_{i,j}} \right). \quad (4)$$

The condition $q_{i+1,j} > q_{\max,j}$ used in the calculations is indicative of imminent movement delay.

The speed (V_1) of movement at the interface between two parts of a flow of different densities, so called reforming or converging, is given by

$$V_1 = \frac{q_1 - q_2}{D_1 - D_2} \quad (5)$$

where:

- D_1 and q_1 are the density of the first part of the flow and intensity of its movement, and
- D_2 and q_2 are the density of the second part of the flow and intensity of its movement.

The graphical method used in the analysis, which clearly illustrates flow movement, was developed in the fifties based on the above expressions and the linear relation $l = Vt$ [1]. Given the lack of available computing power at the time, this was the method of calculation developed to describe human flow movement along egress routes, and flow formations towards building exits.

It is clear that, for such calculations, a mathematical relationship between V and D was required [13].

The results of series of experiments and observations were used in statistical analysis. Series for horizontal route are given on Fig. 1. However, examination of the data sets indicated their non-homogeneity [2, 3]. This can also be said for the datasets describing horizontal pedestrian flows [1]. Whilst a relationship between pedestrian flow, speed and density existed, the fundamentals underpinning this relationship $V = f(D)$ had not yet been addressed.

The widespread use and acceptance of empiricism and mechanistic approximations re travel speed and flow density continues. However, the fundamental theory is lacking. Building design decisions, whether forced by compliance

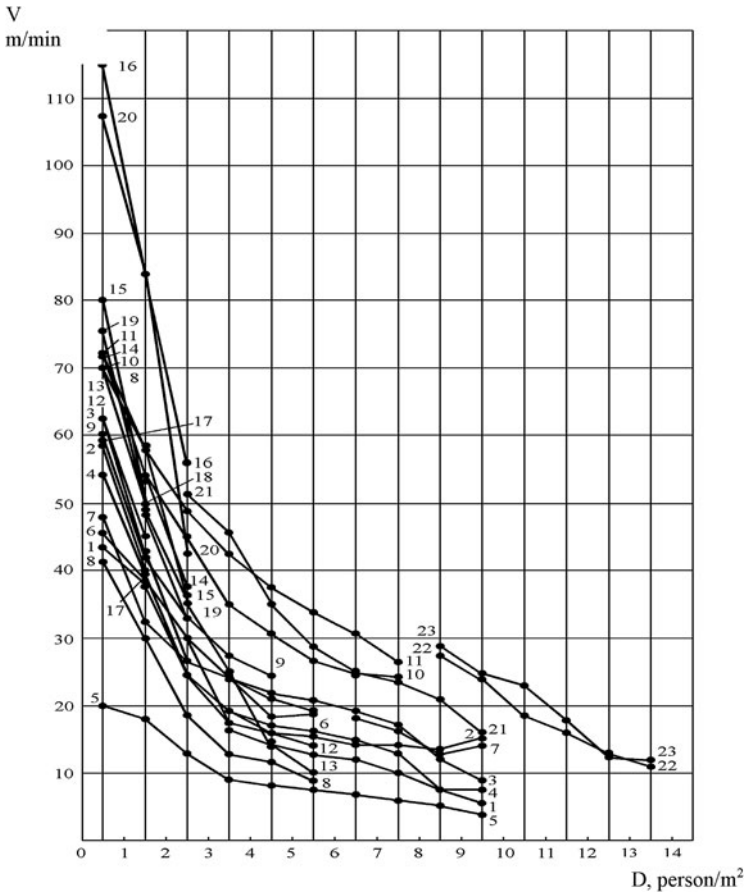


Fig. 1. Empirical relations between travel speed and density of pedestrian flow. Horizontal ways (No. of the series):
Buildings: theaters, cinemas 1, 5; universities 2; industrial 3; transport structures 4, 13, 14; sports 6; other 7; trade 8; schools: senior group 9, middle 10, young 11;
Streets: shopping center 12; transport junction 15, 16, 18;
Industrial unit: 19;
Underground stations: 20, 21;
Experiment: 22, 23.

with prescriptive codes or as a part of performance based design, should be based on fundamentals, not mechanistic approximations derived from one off, seldom if ever to be repeated, experiments. In the following paragraphs the potential impact of emotional state on travel speed is introduced and a theory of pedestrian movement which relates speed of movement to flow density, nature of pathway traversed and emotional state is developed.

3 The Theory for Emotional State, Density of Flow and Travel Speed Law

Two concepts determinate the new methodology development for emotional state, density of flow and travel speed relation [2, 3]. The first is the foot traffic flow is a random process and that travel speed fluctuation is consequence of that random function. The second is that travel speed is a behavioral indicator, i.e. an indicator of motional activity, that is the result of human body's system intercooperation [14]. The general law described by a random function, was base on 24 thousand measures obtained from a series of 69 field observations and experiments (the series for horizontal paths are given on a Fig. 1), i.e.:

$$V_{D,j}^E = V_{0,j}^E \left(1 - a_j \cdot \ln \frac{D_i}{D_{0,j}} \right) \quad \text{if } D_i > D_{0,j}, \quad (6)$$

$$V_{D,j}^E = V_{0,j}^E \quad \text{if } D_i \leq D_{0,j} \quad (7)$$

where $a_j \cdot \ln(D_i/D_{0,j})$ is general psychophysiological law in its particular case—Weber–Fekhnner law [15]. $V_{D,j}^E$ —random magnitude of pedestrian flow speed at the density D_i at the movement on route type j at emotional state E , m/min; $D_{0,j}$ —is a threshold value of flow density on the j route type. As soon as the threshold density is exceeded it influences flow speed. $V_{0,j}^E$ —random magnitude pedestrians' travel speed on a route j without the influence of density. D_i is the current density of the flow; a_j —is an empirical dimensionless coefficient, depends on route type.

The conception of motion activity indicators and emotional state levels might be obtained from the data [16] used in emotional states modeling. The sample extremities law [17] and double mean exceeding law [20] were used. The law was validated by actual observations. The values of a_j and $D_{0,j}$ are given in Table 1. The values of travels speed ranges dependent on the emotional states of people are given in Table 2.

The developed type of law describes the relation between parameters with high degrees of correlation (for all types of path they exceed 0.98).

Route type	a_j	$D_{0,j}$ person/m ²
Horizontal outdoors	0.407	0.69
Horizontal indoors	0.295	0.51
Door aperture	0.295	0.65
Stair downwards	0.400	0.89
Stair upwards	0.305	0.67

Table 1. Values of a_j and $D_{0,j}$ for each route type.

Categories of movement	Emotional state level	Free travel speed, m/s	
		Horizontal way, door aperture, stairs downward	Stairs upward
Comfortable	0.00	<0.82	<0.45
Quiet	0.45	0.82–1.10	0.45–0.63
Active	0.68	1.10–1.50	0.63–0.92
Of increased activity	0.70	1.50–2.00	0.92–1.25

Table 2. Categories of movement, emotional state and free travel speed.

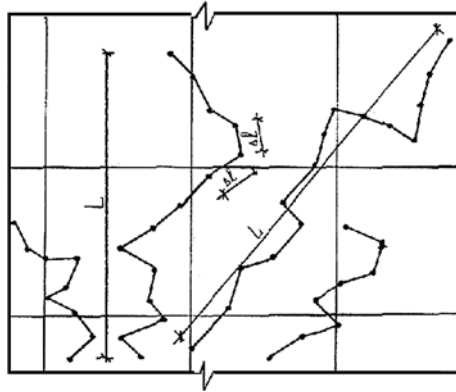


Fig. 2. Pedestrians’ trajectory in a flow.

4 Special Cases of Foot Traffic Flows

In general, its travel speed of people in a flow depends on their physical abilities and its density of crowd. In the main part of a flow, “displacement of people . . . is always nonuniform and often random. The distance between moving people constantly changes, with local increases in densities which are resolve only to reoccur” [9, pp. 24–25]. The trajectory of person movement in a flow is given on Fig. 2.

The maximum observed density is often 9 person/m [1]. The density 13–14 person/m² was obtained during the special experiment [18]. Maximum density taken for evacuation computation in Russian building codes is 9 m²/m² (i.e. 9 person with the square of horizontal projection equal 0.1 m²). Predtechenskii and Milinskii distinguish foot traffic flows as shown in Table 3.

At the low density (up to 1–1.5 person/m²) pedestrians’ “dynamic size” might be observed. This is the area (considered as a rectangle), which pedestrians try to keep clear for maneuvering. Average size is 0.8 × 2.0 m [19].

It is of interest to note, how precisely density affects travel speed. Travel speed depends on two factors: length of the step and a frequency of steps. Density of flow, from this point of view, limits the length of a step. But if we analyze the inter-person distance, it might be seen, that at a density of

Flow density D , m^2/m^2	Category	
0–0.05	FREE (UNIMPEDED)	
0.05–1.15	STREAMLINED UNIMPEDED	
0.15–0.40	Without contact interferences	CONSTRAINED
0.40–0.75	With contact interferences	
0.75–0.92	Conjoint	CONSTRAINED, WITH FORCE IMPACT
0.92–1.0	With shape changing	
1.0–0.15	With compressing	

Table 3. Description pedestrian movement in a flow.

2–2.5 person/ m^2 the area for full-step movement (average step is equal 0.7 m) is available, but travel speed is less than free speed (i.e. at the range where density does not affect travel speed, approximately up to 0.6 person/ m^2). It means, that the density of flow affect also influenced by limiting the space for maneuvering, which also cause the flow speed to decrease. But if overtaking is possible, the person estimates distance up to a person or several person ahead (not just next person) and travel speed might not be reduced.

4.1 Cross Flows

Cross flows create if inflows and outflows (flow gravity points) are in the same location [20, 21]. The maximum density is in areas, called conflict points. The maximum density at which flows can cross is 0.4 m^2/m^2 . At flow densities approaching 0.4 m^2/m^2 , the flow expands, because people deviate from the shortest route between inflow and outflow. People take a bigger trajectory around its conflict point. The flow density value, that pedestrians tolerate around themselves is around 0.2 m^2/m^2 or at average square of horizontal projection equal 0.15 m^2 in underground stations—1.5 persons/ m^2 . In general, travel speed is much higher at the cross point because people try to overcome the uncomfortable zone quicker.

4.2 Contra Flows

The study [22] showed, that in case of contrary flows the intensity (and consequently travel speed) of people in a boundary area between flows is lower, that at same condition for one-way flow. Pedestrians moving along the boundary of flows are afraid of collisions, and they keep their speed lower. Field observations establish of the speed-reducing coefficient for entire flow—0.85. Possibly, in case of wide communications routes, the travel speed deceleration spreads only for pedestrians of boundary layer of both contraries flows. So, the travel

speed reduction might be accepted for outer lane pedestrians only. The study showed the cross and contrary flows should be strictly avoided during evacuation.

4.3 Movement on Routs with Unlimited Width

If a flow exits on a route with unlimited width (e.g. foyer of vestibule), it does not spread themselves in width infinitely and its density is stills higher then at $D_{0,j}$. Apparently, density of the flow is a kind of compromise between high travel speed and traffic along the remote route, and low travel speed and traffic along the direct route. The flow is a cigar-shape: at the entering the sector, it spreads at 30° angle, and at exiting the sector, it converges at 45° angle. The average flow density is 1.5 persons/ m^2 . The width of a flow (b) depends on a number of people within and length of the route (l): $b = 4$ m, if $N < 100$ and $l \leq 6$ m, and $b = 6$ m in all the rest cases [23].

4.4 Movement Through Door Aperture

This type of movement is the most crucial during the evacuation movement, because their insufficient traffic capacity is often the reason for fatalities. In general, travel speed is somewhat higher, because pedestrians try to overcome potentially dangerous door aperture quicker. In the study [18] the adjustment coefficient, applying if density of flow is higher 0.5 m^2/m^2 , considering phenomenon called “false aperture” was established:

$$m = 1.25 - 0.5D. \quad (8)$$

The “false aperture” phenomenon is that if density of flow is higher 0.5 m^2/m^2 , than the people passing an aperture on the edge of flow are driven against the door surrounds by the dense flow. So, they try to push themselves away from the exit surrounds to the center of the aperture, decreasing its width.

At the maximum density 0.9 m^2/m^2 the intensity of flow movement (q) through door of different width is taken by the formula, based on minimum values of q :

$$q = 2.5 + 3.75b. \quad (9)$$

5 Modeling of Pedestrians Movement in a Flow

For realization of theoretical and practical research the stochastic models were developed [3, 24]: ADLPV (analysis of foot traffic flows, probability) and SDLP (free foot traffic flows). The models for complicated cases of movement were also developed: contrary and crossing flows, movement on unlimited width routes [25–28]. The results of different situations modeling show the high models’ reliability (Fig. 3).

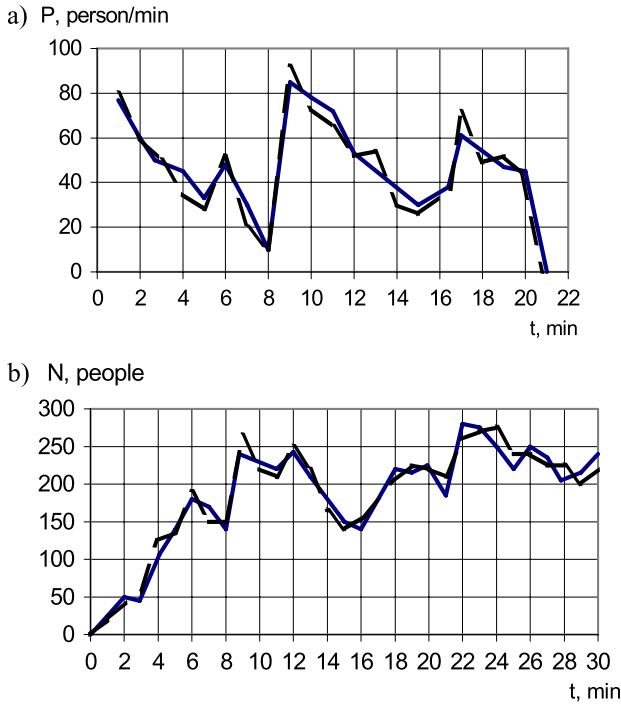


Fig. 3. The comparison of field observation (—) and modeling (----): **a** model SDLP—plant territory; **b** model ADLPV—communication route of Moscow’s underground system.

Nowadays, capability of computers allows modeling each pedestrian in a flow. To do it, we need:

- The law of flow density influence to pedestrians’ travel speed.
- Travel speed values for people with different emotional state, for people with different age and gender.

1. As it has been shown above, the density of flow affects by limiting the space for movement. The most simple and quite reliable criteria for modeling is inter-person distance. That is why this approach is widely spread today, for example [29]. The most important issue here is a choice of correct relations.

Taking the formulae, connecting the density of flow in person/m² with linear density in m/person [30], the formula for inter-person distance and density of flow might be derived. In their turn, formula for inter-person distance and travel speed might be obtained:

$$V_{D,j}^E = V_{0,j}^E \left(1 - a_j \cdot \ln \frac{l_0}{l_D} \right), \tag{10}$$

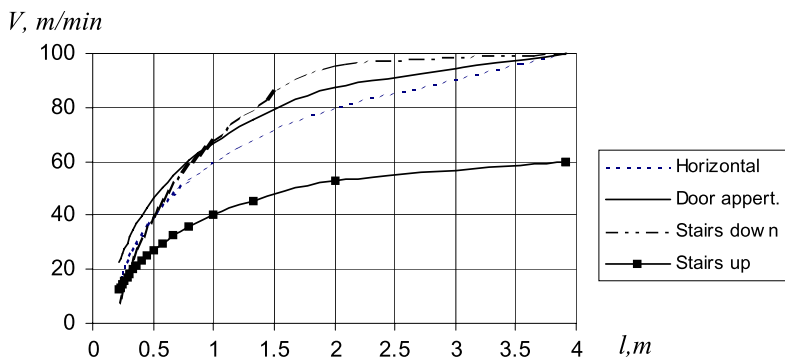


Fig. 4. Graph of travel speed (at mean value of unimpeded pedestrians’ speed (V_0) at high active emotional state equal $V_0 = 60$ m/min for stairs up and $V_0 = 100$ m/min for the rest types of routes) against distance between geometrical centers of person l

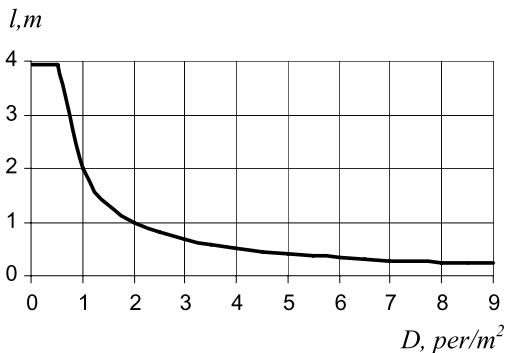


Fig. 5. Graph of inter-person distance and flow density.

where $l_D = 1/(c \cdot D_i)$ is inter-person distance at D_i , m; $l_0 = 1/(c \cdot D_0)$ is inter-person distance at D_0 , m; and c is average body width (taken 0.5 m).

Graphical relation between travel speed and inter-person distance, and inter-person distance and density of flow is given in Figs. 4 and 5. At that it should be realized, that the l is a distance between geometrical body centers. That is why, at high density of flow, where the physical compression takes place [18], the distance is 20 cm only. Moreover, relatively high values of distance l_0 is because it is the distance for ahead person, because just ahead person is not an obstruction, so as he might be overtaken easily. The overtake possibility is restricted by a density of flow equal 0.15–0.20 m²/m². If overtake is impossible, l should be considered as a distance to the closest person ahead (Fig. 6).

2. Pedestrians in a flow, does not go as a machine with a constant travel speed (at all other condition being equal) they sometimes either decel-

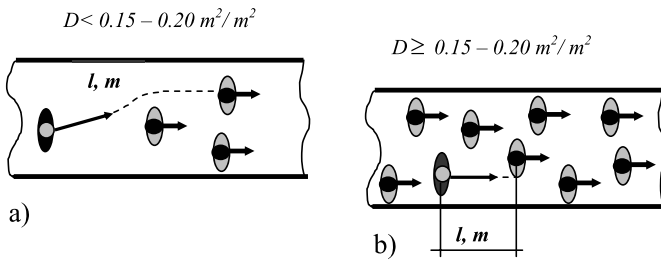


Fig. 6. Inter-person distance and density of a flow. **a** Overtake is possible; **b** overtake is impossible.

erate speed to avoid collisions or accelerate for overtaking. That is why assigning the certain labels for people of different age or gender is very provisional.

Analysis of field observation data allows to conclude, that for evacuation computations, the category “of increased activity” should be used. The free travel speed range for the interval is from 1.5 m/s to 2.0 m/s. The values 1.66 m/s (100 m/min) is accepted as an average value for evacuation computation in Russian Buildings Codes. If we turn to Table 4, which is used in for forensic road accidents analysis [31], we can see, that average travel speed of almost all people from the category “walk with hurried steps” fit the range “of increased activity” providing required integration for gender and age. For people who walk with hurried steps with a speed lower than 1.5 m/s, their travel speed should be taken 1.5 m/s anyway, because they would apply more efforts (run) to keep themselves in a flow. Hence, for individual pedestrian modeling in a flow, the value $V_{0,j}^E$ for formulae (10) could be taken from Table 4. But evacuation is a casual process, so all computations (modeling) should be done many times to collect all require statistic for egress time and other parameters. In that case, individual travel speed might be taken randomly from a provided range (Table 4).

For foot traffic modeling in other emotional states, the reducing coefficient should be use, equal ratio of average travel speed of considered emotional state to average travel speed “of increased activity” category (105 m/min).

6 Conclusions

Intense foot traffic flow research facilitated to gathering of valuable empirical data, to find general laws, to work out and validate the theory, that has been use in fire prevention buildings codes for 20 years [6, 32]. On the base of studies conducted, algorithms, each pedestrian in a flow base on age, gender, emotional state, type of egress route and density of flow (expressed as inter-person distance) have been developed. For more precise modeling, the cases that have special characteristics are considered in more detail.

Age group, years	Gender	Number of counts	Walk with hurried steps, m/s	Average speed, m/s	Number of counts	Calm running, m/s	Average speed, m/s
7–8	M	23	1.50–1.81	1.63	28	2.00–2.89	2.36
	F	29	1.39–1.72	1.47	31	1.94–2.78	2.22
8–10	M	56	1.56–1.86	1.67	62	2.06–2.97	2.47
	F	54	1.44–1.78	1.53	53	2.00–2.86	2.33
10–12	M	43	1.58–1.92	1.72	46	2.11–3.08	2.58
	F	48	1.50–1.83	1.61	48	2.06–2.97	2.47
12–15	M	76	1.64–1.97	1.81	118	2.17–3.25	2.78
	F	78	1.56–1.89	1.69	75	2.14–3.11	2.64
15–20	M	38	1.67–2.17	1.89	12	2.99–3.61	2.86
	F	20	1.58–1.92	1.75	11	2.25–3.50	2.78
20–30	M	57	1.75–2.17	1.92	25	2.44–3.61	3.06
	F	72	1.67–2.06	1.83	47	2.36–3.56	2.94
30–40	M	51	1.75–2.17	1.89	29	2.28–3.33	2.94
	F	53	1.64–2.00	1.81	45	2.25–3.22	2.72
40–50	M	55	1.67–2.00	1.86	25	2.11–3.08	2.67
	F	74	1.53–2.00	1.69	41	2.11–2.94	2.47
50–60	M	46	1.50–1.89	1.67	15	1.94–2.78	2.39
	F	50	1.44–1.81	1.56	24	1.92–2.50	2.19
60–70	M	33	1.25–1.67	1.42	8	1.72–2.11	1.94
	F	42	1.25–1.56	1.36	17	1.72–2.08	1.89
Over 70	M	19	1.00–1.39	1.17	20	1.42–1.81	1.56
	F	71	1.00–1.33	1.14	26	1.36–1.72	1.53
Amputees	M	10	1.11–1.47	1.25	4	1.53–1.86	1.67
Drank	M	19	1.39–1.78	1.5	22	1.94–2.39	2.28
Child led by adult by hand	F	28	1.31–1.53	1.44	16	1.61–2.31	1.92
Adult carrying a child	M	6	1.39–1.53	1.47	2	1.72–2.00	1.86
	F	18	1.33–1.56	1.42	3	2.36–2.78	2.50
With large package	M	9	1.5–1.75	1.61	–	–	–
	F	4	1.47–1.67	1.53	8	1.92–2.61	2.31
With baby carriage	F	5	1.31–1.58	1.44	2	1.83–2.00	1.92
Walking hand in hand	–	22	1.53–1.86	1.67	9	2.08–3.14	2.5

Table 4. Pedestrians' travel speed depend on pace.

References

1. Predtechenskii V.M., Milinskii A.I. Planning for Foot Traffic Flow in Buildings. Stroizdat, Moscow, 1969.
2. Kholshchevnikov V.V. The Study of Human Flows and Methodology of Evacuation Standardisation. MIFS, Moscow, 1999.
3. Kholshchevnikov V.V. Human flows in buildings, structures and on their adjoining territories. Doctor of Science Thesis. MISI, Moscow, 1983.
4. Kholshchevnikov V.V., Shields T.J., Boyce K.E., Samoshin D.A. Recent development in pedestrian flow theory and research in Russia. Fire Safety Journal, vol. 43, 2008, pp. 108–118.
5. Building Regulations. Fire Safety of Buildings and Structures. SNiP II-2-80. Stroizdat, Moscow, 1981.
6. State Standard 12.1.0004-91 (GOST). Fire Safety. General Requirements. Moscow, 1992.
7. Building Regulations. Building Accessibility for Disabled People. SNiP 35-01-2000. Stroizdat, Moscow, 2000.
8. Milinskii A.I. The study of egress processes from public buildings of mass use. Ph.D. Thesis, Moscow Civil Engineering Institute, 1951.
9. Predtechenskii V.M., Milinskii A.I. Planning for Foot Traffic Flow in Buildings. Amerind, New Delhi, 1978.
10. Predtechenskii V.M., Milinskii A.I. Personenströme in Gebäuden. Berechnungsmethoden für die Projektierung. Köln Braunsfeld, 1971.
11. Predtechenskii V.M., Milinskii A.I. Evakuace Osobz Budov. Ceskoslovensky Svaz Pozarni Ochrany, Praha, 1972.
12. Predtechenskii V.M., Milinskii A.I. Planning for Foot Traffic Flow in Buildings. Revised and updated edition. Stroizdat, Moscow, 1979.
13. The State Council of Ministers of USSR Act. 14th of January 1971.
14. Volgin A.N. The Principles of Coordinated Optimum. Sovetskoye Radio, Moscow, 1977.
15. Zabrodin J.M., Lebedev A.T. Psychophysiology and Psychophysics. Nauka, Moscow, 1977.
16. Volkov P.P., Oksen V.H. Informational Modeling of Emotional States. Moscow, 1978.
17. Gumbel E.I. Statistical Theory of Extreme Values and Some Practical Applications. National Bureau of Standards, Washington, 1954.
18. Kopylov V.A. The study of people' motion parameters under forced egress situations. Ph.D. Thesis, Moscow Civil Engineering Institute, 1974.
19. Piir R.L. Pedestrian traffic flow study on city's main streets. Ph.D. Thesis, Leningrad, 1971.
20. Gvozdyakov V.S. Regularity of human flow movement in traffic structures. Ph.D. Thesis, Moscow Civil Engineering Institute, 1977.
21. Isaevich I.I. Working out the basics of multi-variation analysis of planning design solution of subway stations and transfer knots on modeling relationships of people' foot traffic flow' basic. Ph.D. Thesis, MISI, Moscow, 1990.
22. Grigorjanc R.G. The study of permanent human flows. Ph.D. Thesis, Moscow Civil Engineering Institute, 1971.
23. Ovsyannikov A.N. The regularity of communication routes design in covered stadiums. Ph.D. Thesis, MISI, Moscow, 1981.

24. Kholshevnikov V.V. Foot traffic flow modeling. In: Fire and Explosions Modeling (eds. Brushlinskii N.N., Korolchenko A.Y.), Pozhnauka, Moscow, 2000.
25. Kholshevnikov V.V., Isaevitch I.I. Modeling of contrary flows. Deposited in VNIINTPI Gosstroï USSR, No. 9428, Moscow, 1988.
26. Kholshevnikov V.V., Isaevitch I.I. Modeling of crossing flows. Deposited in VNIINTPI Gosstroï USSR, No. 9429, Moscow, 1988.
27. Kholshevnikov V.V., Isaevitch, I.I. Modeling of pedestrians flows on platforms of underground stations. Deposited in VNIINTPI Gosstroï USSR, No. 9430, Moscow, 1988.
28. Kholshevnikov V.V., Isaevitch, I.I. Pedestrian flow modeling on unlimited routs width. Deposited in VNIINTPI Gosstroï USSR, No. 9427, Moscow, 1988.
29. Thompson P.A. Simulex: Development new computer modeling techniques for evacuation. Proceedings of the Fourth International Symposium on Fire Safety Science, 1994, pp. 613–624.
30. Belyaev S.V. Public Building Evacuation. All-Russian Academy of the Architectures Publisher, Moscow, 1938.
31. Bekasov V.A., Bograd G.Y., Zotov B.L., Indichenko G.G. Autotechnical Expertise. Yuridicheskaya Literatura, Moscow, 1967.
32. Building Regulations. SNiP II-2-80. Fire Regulations for Buildings' and Structures' Design. Stroizdat, Moscow, 1981.

Emergency Preparedness in the Case of a Tsunami—Evacuation Analysis and Traffic Optimization for the Indonesian City of Padang

Gregor Lämmel¹, Marcel Rieser¹, Kai Nagel¹, Hannes Taubenböck², Günter Strunz², Nils Goseberg³, Thorsten Schlurmann³, Hubert Klüpfel⁴, Neysa Setiadi⁵, and Jörn Birkmann⁵

¹ Transport Systems Planning and Transport Telematics, TU Berlin, Salzufer 17-19, 10587 Berlin, Germany
e-mail: laemmel@vsp.tu-berlin.de

² German Remote Sensing Data Center (DFD), German Aerospace Center (DLR), Münchner Straße 20, 82234 Wessling, Germany

³ Franzius Institut for Hydraulic, Waterways and Coastal Engineering, Leibniz University of Hannover, Nienburger Str. 4, 30167 Hannover, Germany

⁴ TraffGo HT GmbH, Bismarckstraße 142a, 47057 Duisburg, Germany

⁵ Institute for Environment and Human Security, United Nations University, Hermann-Ehlers-Str. 10, 53113 Bonn, Germany

Summary. The “Last-Mile Evacuation” research project develops a numerical last mile tsunami early warning and evacuation information system on the basis of detailed earth observation data and techniques as well as unsteady, hydraulic numerical modeling of small-scale flooding and inundation dynamics of the tsunami including evacuation simulations in the urban coastal hinterland for the city of Padang, West Sumatra, Indonesia. It is well documented that Sumatra’s third largest city with almost one million inhabitants is located directly on the coast and partially sited beneath the sea level, and thus, is located in a zone of extreme risk due to severe earthquakes and potential triggered tsunamis. “Last-Mile” takes the inundation dynamics into account and additionally assesses the physical-technical susceptibility and the socio-economic vulnerability of the population with the objective to mitigate human and material losses due to possible tsunamis. By means of discrete multi-agent techniques risk-based, time- and site-dependent forecasts of the evacuation behavior of the population and the flow of traffic in large parts of the road system in the urban coastal strip are simulated and concurrently linked with the other components.

1 Introduction

Seventeen out of twenty of the most disastrous natural hazards, since 1950, have occurred in the last 10 years. Extreme environmental events grow in frequency and magnitude. Hence, the number of human losses since the 1950's has now reached 1.7 million; and the economic damage is exceeding USD 1.4 billion [1]. Most of the hazards affect more than just one region, the most prominent example being the devastating tsunami of 26 December 2004 in the Indian Ocean. This, according to the current estimates, killed more than 220,000, made more than 1 million people homeless, and left many thousands without any basis of existence. This clearly indicates that the aftermath of the seaquake to the west of Sumatra also consists of certain unforeseen dimensions. Therefore a significant shift in risk perception of an extreme event must follow. The aftermath of the tsunami, with all its consequences has already affected the development politics and the international, multi-sectoral research communities. The overarching goal of these initiatives is to improve disaster prevention by preparedness methodologies, including public and political awareness of the residual risk and addressing the global hazard resilience. The current multi-disciplinary project "Last-Mile" attempts to incorporate all of these guiding principles and jointly develops with local partners a numerical last mile tsunami early warning and evacuation information system on the basis of detailed earth observation data and techniques as well as unsteady, hydraulic numerical modeling of small-scale flooding and inundation dynamics of the tsunami including evacuation simulations in the urban coastal hinterland for the city of Padang, West Sumatra, Indonesia. It is well-documented that Sumatra's third largest city with one million inhabitants is located directly on the coast and partially sited beneath the sea level, and thus, is located in a zone of extreme risk due to severe earthquakes and tentatively triggered tsunamis.

An important aspect is the amount of time that is needed for the evacuation. Since the advance warning time before the tsunami wave reaches the coast line is only 20–40 minutes, the evacuation must be as quick as possible. Even if not all of the estimated 1,000,000 inhabitants need to be evacuated, the number of evacuees could be hundreds of thousands. Therefore a detailed analysis of aspects that could influence the evacuation process is necessary. With this analysis it should be possible to:

- Give an estimate of the evacuation time.
- Detect bottlenecks that could for example emerge at bridges.
- Detect highly endangered areas, where a vertical evacuation⁶ seems the only way.

Because of the complexity of the system, an analytic solution to this problem seems to be hard. Therefore a microscopic multi-agent simulation for the city

⁶ Vertical evacuation means that it is planned to build quake and tsunami proof shelters, where the evacuees can flee to.

with all its inhabitants will be developed. With this simulation it should be possible to get an estimate of the evacuation process. To develop a realistic evacuation simulation, a wide range of different input information is needed. The needed input information covers almost all aspects of the project. In this paper we will give an overview about basic input data, show some preliminary simulation results, discuss some problems and open questions and finally we will give a conclusion and outlook. Since the focus of this paper is on evacuation simulation, we will not introduce the “Last-Mile Evacuation” project in detail. However, the interested reader is referred to [2] for detailed information about the project, project partners and their particular work packages.

2 Related Work

“Last Mile” is based upon some of the information and evaluations that are developed or generated in GITEWS (German Indonesian Tsunami Early Warning System—www.gitews.org). Certain work packages of GITEWS are directly related to “Last Mile” since the tsunami risk assessment studies in GITEWS are being conducted for the whole Indonesian coastal stretches (approximately 4000 km) bordering the Indian Ocean (Sumatra, Java, Bali, etc.). However, the hydro-dynamical models used in former studies do neither incorporate local infrastructures nor do they consider street networks or urban waterways in the respective cities. Instead, those simulations make use of constant coastal slopes representing the near shore region and the urban hinterland without determining infrastructures. In addition, neither are numerical evacuation simulations envisaged in those research projects on tsunami preparedness nor is information produced that relies on detailed, time-dependent inundation dynamics and evacuation recommendations. Thus, it can be argued that “Last-Mile” erects its scientific basis upon previous scientific studies, but goes far beyond them by providing these much more microscopic aspects.

3 Input Data

The evacuation simulation depends on several input sources, which could be divided into three parts:

- Geographical information derived from remote sensing data (street network, safe places, surface conditions . . .)
- Inundation scenarios
- Socio-economic data (e.g. population distribution as a function of time)

All this input data has to be compiled to a simulation framework which makes it possible to simulate different inundation scenarios at any desired time of day. Below we will discuss the different input sources, the data that has been obtained so far and the pending issues as well.

3.1 Geographical Information Derived from Remote Sensing

The geographical information mainly depends on remote sensing data. For the “Last-Mile” project, we draw on high resolution satellite imagery made by the Ikonos satellite. Ikonos data features four spectral bands (blue, green, red, NIR) and a geometric quality of 1 m for the panchromatic band, 4 m multispectral, and 1 m pan-sharpened. The most important geographical input is the information about the street network and all the other walkable area like open spaces or meadows. Using an object-oriented hierarchical classification approach in combination with manual enhancement an area-wide and up-to-date land-cover classification has been derived [3].

In a first step the street network has been extracted from the satellite data. This is shown in Fig. 1 a). However, to make the street network usable for the physical evacuation simulation it had to be converted into a graph. This has been done by converting streets to links and crossings to nodes. A graph representation of the street network is show in Fig. 1 b). The original length and width of the street segments has been appended as additional attributes to the links. An accurate model of the street network is all the geographic information that is needed for a basic simulation setup. However, it is planned to integrate much more detailed data from the satellite imagery. One example are shapes of all the buildings in the city, with a classification according to there vulnerability. A clipping of such a floor plan is shown in Fig. 1 c). The colors red, yellow and green are indicating the vulnerability (in descending order) and the blue colored buildings are suitable for vertical evacuation. However, the classification of the buildings is still work in progress and has to be verified by on-site examination. A detailed description of this work is given in [4, 5].

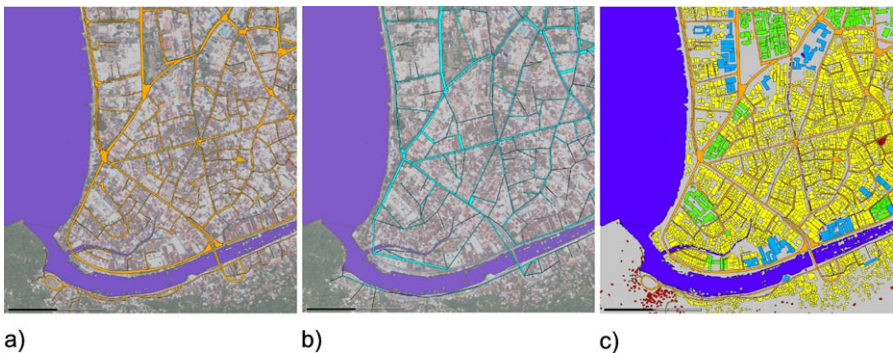


Fig. 1. Geographical information extracted from Ikonos imagery.

3.2 Inundation Scenarios

The city of Padang has been hit by tsunamis in the past. The most well documented tsunamis are the ones from 1797 and 1833 [6]. Both tsunamis inundated large parts of the city. However, these past Tsunami events are hardly comparable with the current local situation due to major changes in land use pattern. What is more, population figures have risen strongly. Today the city has approx. 1,000,000 inhabitants and the most densely populated parts of the city are located directly at the shore line. The risk of future tsunami originating off the Sunda megathrust stipulates the need for applied research leading to a greater insight into tsunami run-up and inundation mechanisms. The city of Padang is located in a zone of extreme risk due to severe earthquakes and tentatively triggered tsunamis. Inundation dynamics of long-wave run-up in urban areas is basically conditioned by wave amplitude and period, coastal geometry and shape as well as characteristics of the incoming wave train. As a first consequence some parts of the city have to be evacuated faster than others. By means of small-scale inundation simulation information about temporal distribution of flow height and velocity on a building-specific level becomes available. Models with less accurate spatial resolution for Padang have been accomplished by Borrero [7] on a 200 m grid basing on a coarse underlying datasets. Venturato et al. [8] clearly outlines the importance of high-quality geo datasets for proper modeling of onshore inundation pattern. Therefore we achieved a highly resolved spatial database by extensive multi-beam echo sounder surveys in the shallow waters in front of the coast and airborne topographical field data surveys in the hinterland. To obtain a final digital elevation model (DEM) as basis for the simulations these data were merged with manually taken DGPS data of relevant boundaries and infrastructures as well as cross section data of flood water canals and rivers.

In the applied numerical model the shallow-water equations are solved by a finite-volume technique [9]. The flexible mesh capabilities and a robust wetting and drying algorithm allow modeling run-up, overtopping and inundation as well as wave-structure interaction.

Numerical studies of credible tsunami run-up and inundation scenarios in urban agglomerations confirm that the impact of a tsunami and the extent of inundation areas generally depend on the roughness parameters, but if buildings and structures are explicitly considered in the numerical grid the situation changes (Fig. 2). In this case flow velocities between structures get remarkably higher and near shore water levels at the Padang sea wall rise while areas onshore are less inundated. This additional information is essential for adequate evacuation planning in the city of Padang and can further be employed into an upcoming decision support system (DSS).

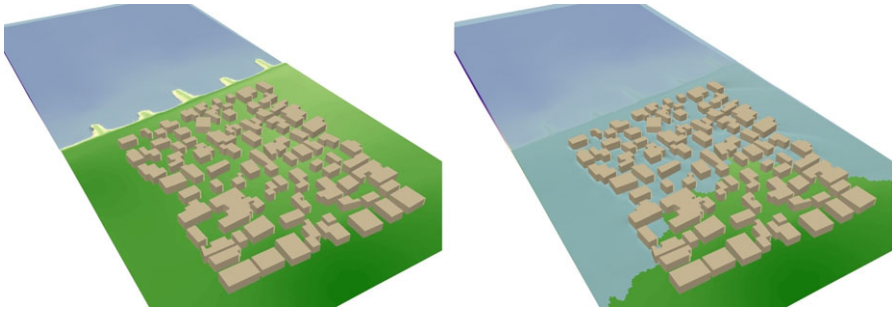


Fig. 2. Flow around structures and buildings due to a hypothetical earthquake of $M_w = 8.5$ southwest of Padang.

3.3 Socio-Economic Data

The socio-economic profile of the city has a major impact on the evacuation itself and is therefore an important input for the simulation framework. Moreover, a detailed knowledge on the socio-economic vulnerability of the population will also help to give recommendations of preparedness strategies for potential tsunami events. In the scope of this project, a detailed assessment of socio-economic vulnerability components according to the tsunami early warning chain is carried out. It focuses, among others, on dynamic exposure based on performed daily activities in the different tsunami hazard zones, predicted evacuation, behavior and evacuation capability of different social groups. To obtain the needed input data different data sources will be used. Information about land use or the detection of critical infrastructures like hospitals or schools will be detected by remote sensing techniques, complementary to data of infrastructure distribution per village obtained from the official statistical office [10].

There are potential data sources from the official statistical bureau (BPS), which are collected regularly at residential district and village level and may contain relevant socio-economic data, such as Population Census [11] and Sub-district in Figures [12]. These data sources provide information on population density, sex and age composition of the population at the village level, which describe to some extent the static distribution of the population (assuming that all people are at home the whole time) and physical capability to perform an evacuation.

As far as it has been assessed by the project, more detailed information with regards to work places or daily activities, from which it is possible to reconstruct the distribution of the population during day time, is not available. There are available data on travel pattern in the city for different transportation zones (a transportation zone covers more than one village) obtained from the Transportation Agency [13]. As a preliminary approximation, data on travels from and to different transportation zones by various travel purposes (working, going to school, etc.) may also be used to weight the population dis-

tribution at daytime. In addition to data from different agencies, it is planned to undertake a household survey with a sample of 1000 households selected based on their socio-economic characteristics and the physical structure of their homes. The developed questionnaire also includes questions about the daily activities of the households. The survey results will allow derivation of the distribution of the population as a function of time. This is important since we want to develop evacuation scenarios for different times of the day. The preparation, implementation of the survey as well as analysis of the results will take several months. In the mean time a population distribution based on census data—assuming that all people are at home—is used for the evacuation simulation.

Figure 3 shows the population figure for Padang’s residential districts. This data rests upon the census for 2005 and was provided by the statistical bureau of Padang [12]. The initial population for the evacuation simulation framework is based on this data. Moreover, other parameters that will be derived from the socio-economic vulnerability survey, such as lagging time due to performing other activities before evacuating, non-participating evacuation rate, and other social-related difficulties during evacuation are interesting factors to be integrated or taken into consideration in the simulation in the later phase of this project.



Fig. 3. Population figures of Padang’s subdistricts.

4 Simulation Framework

The evacuation simulation is based on the MATSim (multi-agent traffic simulation www.matsim.org) framework, where each evacuee is modeled as an individual agent. The agents make independent decisions about escape routes or when to start with the evacuation (i.e. they decide about their response time). Consequently, the evacuation for every single agent has to be modeled separately and will be stored in a so-called plan containing the starting time and the evacuation route. All agents' plans are simultaneously executed in the simulation of the physical system. The underlying flow model simulates the traffic based on a simple queue model [14, 15] where only free speed and bottleneck capacities are taken into account. The queue simulation, albeit simple, captures the most important aspects of evacuations such as the congestion effects of bottlenecks and the time needed to evacuate the endangered area.

After a simulation run is finished, every agent will be selected with a probability of 10% for re-routing. These agents generate new plans with new evacuation routes based on the information of the experienced travel times from the last run. For every agent that has not been chosen for re-routing, a probabilistic discrete-choice model selects a plan out of its memory, where the probabilities of the plans increase with decreasing evacuation time. After this a new simulation run with these new plans will be started. Repeating this iteration cycle of learning, the agents' behavior will move towards a Nash equilibrium. If the system were deterministic, then a state where every agent uses a plan that is a best response to the last iteration would be a fixed point of the iterative dynamics, and at the same time a Nash Equilibrium since no agent would have an incentive to unilaterally deviate. Since, however, the system is stochastic, this statement does not hold, and instead we look heuristically at projections of the system. From experience it is more than enough to run 100 iterations until the iterative dynamics has reached a steady state. In most (but not all) evacuation situations, the Nash equilibrium leads to a shorter overall evacuation time than when everybody moves to the geographically nearest evacuation point. On the other hand, a Nash equilibrium means that nobody has an incentive to deviate. The Nash equilibrium in an evacuation situation can therefore be considered as a solution that could be reached by appropriate training.

Clearly, a Nash equilibrium can only be considered as benchmark solution. In evacuation situations, people tend to be irrational and to display herd behavior [16, 17]. Still, if even the Nash equilibrium solution does not leave enough time, then this would be a strong indicator that major measures would need to be taken to rectify the situation.

Because of the limited amount of space and the more general character of this paper we could only give this brief description of the simulation framework. However, a more detailed and more technical description of the framework is given in [18, 19].

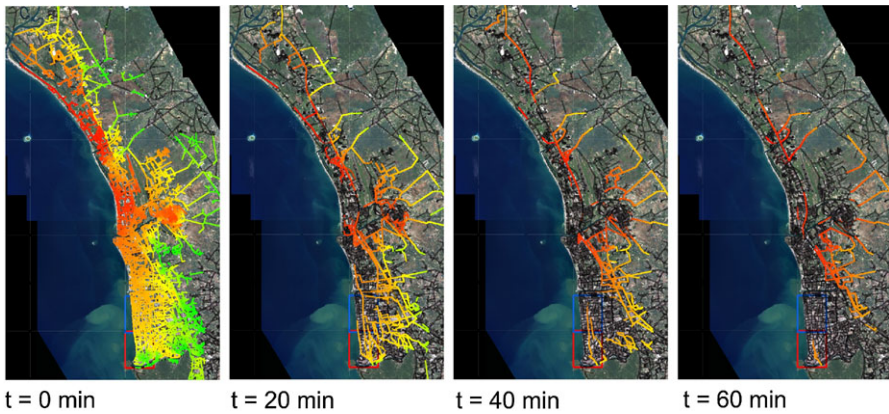


Fig. 4. Visualizer snapshots of the evacuation simulation.

5 Results

As discussed earlier not all of the proposed attributes (i.e. a detailed socio-economic profile of the city, spatially highly resolved inundation scenarios, etc.) are yet available. For that reason a simpler scenario has been chosen to test the simulation framework. In this scenario it is assumed that all people are at home. And instead of an inundation based on simulations, it is assumed that the entire area with an elevation below 10 m has to be evacuated. A software agent has been created for every person that lives within this area. In the end, there were about 450,000 agents. With this setup a simulation run of 100 learning iterations has been executed. Some snapshots of the last iteration of the simulation run are shown in Fig. 4. After these 100 iterations of learning the evacuation of the endangered area took about 2 hours. However, these results are preliminary and an inundation of the entire area below 10 m seems to be unrealistic and so it is expected that this results will change with the integration of better inundation scenarios or other population distributions.

6 Existing Problems

There are some problems and open questions that have to be addressed. First there are many streets with a median. This causes problems by the automatic extraction of the street network from satellite imagery. The extraction algorithm classifies streets based on the surface conditions and will consequently produce two parallel streets if there is a median. This issue is depicted in Fig. 5 a). If an evacuee wants to flee from *origin* to *destination* she has to make a detour along the red colored path. However, there is no simple solution for this problem, since it is not possible to detect obstacles (e.g. fences) on the median and so it is not clear if the median is traversable by pedestrians.

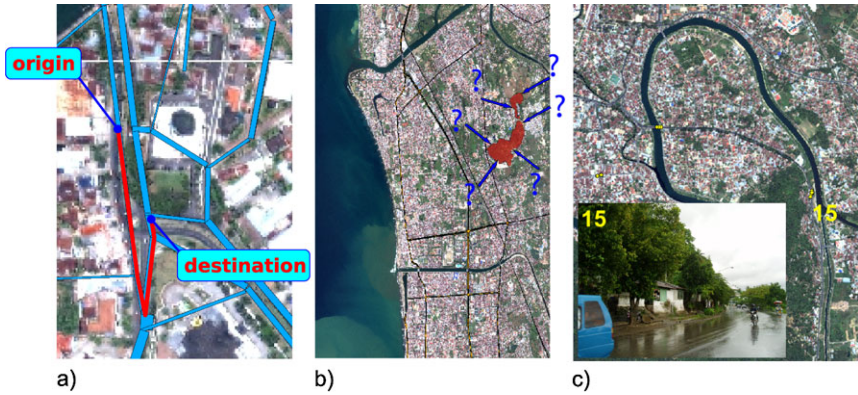


Fig. 5. Problems and open questions.

Another issue is the lack of information about the accessibility of safe places. For example there are some hills in the city that could be used as evacuation places (see Fig. 5 b)). About 80,000 agents escape to these hills in the current simulation results. But from the available information we could neither determine if there is enough space nor if there are sufficient access possibilities. A reasonable solution to these problems would be to examine the hills, streets with median etc. on site. This could be done by taking GPS tagged photos of those places for a manual correction of accessibility parameters. This has already been done for some parts of the city (as shown in Fig. 5 c)), but with other simulations there will emerge other (potential) bottlenecks that need to be examined in detail.

7 Conclusion

We introduced the “Last-Mile Evacuation” research project with a focus on a microscopic large-scale evacuation simulation based on the MATSim framework. It is implemented as Multi Agent Simulation, where every agent tries to optimize its individual evacuation plan in an iterative way. We discussed the needed input data for such an evacuation simulation, showed preliminary simulation results and discussed some open problems.

As discussed, the objective is to develop a toolbox, which gives the option to simulate different inundation scenarios at different times of day. The results will be an estimation of the occurrence of bottlenecks and of the overall evacuation time. A major determinant for the overall evacuation time will be the number and place of shelters and places of refuge. In the simulation, these are modeled as sinks. Different to the natural places of refuge like hills, the number and place of shelters (including buildings used as shelters like concrete multi-storey buildings) can be influenced by the administration (and

potentially the city's inhabitants and especially owners of buildings). Therefore, a second strategy within "Last-mile" (next to providing information and guidance on evacuation strategies) is to provide recommendations on the number and place of shelters and to identify buildings and recommend their use as shelters.

But before we could use the simulation results to formulate concrete recommendations, the validity and reliability of those results have to be ensured. Therefore, it is planned, besides the integration of inundation scenarios and a more detailed model of the socio-economic profile of the city, to validate the results of the physical simulation. Since there is no real world data to validate the evacuation simulation, we could fall back on other simulation models that are known to be realistic (e.g. models based on Cellular Automata (CA) [20, 21]). However, such models are geared towards smaller problems (cf. [18]). But even if a standard CA-based approach is not applicable here, one could validate the physical simulation based on a clipping of the street network. The improvement of the behavioral model (e.g. herd behavior [16] modified for large-scale scenarios [22]) could also be a topic of future work.

Acknowledgements

This project was funded in part by the German Ministry for Education and Research (BMBF), under grants numbers 03G0666E ("last mile") and 03NAPI4 ("Advest").

References

1. UDNP. *Reducing Disaster Risk: A Challenge for Development*. United Nations Development Programme, Bureau for Crisis Prevention and Recovery, New York, 2004.
2. J. Birkmann et al. Numerical last-mile tsunami early warning and evacuation information system. In L. Stroink, editor, *GEOTECHNOLOGIEN Science Report No. 10: "Early Warning Systems in Earth Management"*, Technical University Karlsruhe, October 2007. Die Deutsche Bibliothek.
3. H. Taubenböck and A. Roth. A transferable and stable classification approach in various urban areas and various high resolution sensors. In *Urban Remote Sensing Joint Event*, Paris, 2007.
4. H. Taubenböck et al. Risk and vulnerability assessment to tsunami hazard using very high resolution satellite data. In C. Jürgens, editor, *Remote Sensing—New Challenges of High Resolution*. European Association of Remote Sensing Laboratories, Bochum, 2008.
5. S. Kass et al. Automated assessment of building vulnerability with high resolution Ikonos data for Padang, Indonesia. In *The International Symposium on Disaster in Indonesia: Problems and Solutions*, Padang, July 2007.

6. D.H. Natawidjaja et al. Source parameters of the great Sumatran megathrust earthquakes of 1797 and 1833 inferred from coral microatolls. *Journal of Geophysical Research*, 111:B06403, 2006.
7. J.C. Borrero, K. Sieh, M. Chlieh, and C.E. Synolakis. Tsunami inundation modeling for western Sumatra. *Proceedings of the National Academy of Sciences of the United States of America*, 103:19673–19677, 2006.
8. A.J. Venturato, D. Arcas, and U. Kânoğlu, *Modeling tsunami inundation from a Cascadia subduction zone earthquake for Long Beach and Ocean Shores*. NOAA Technical Memorandum OAR PMEL-137. Pacific Marine Environmental Laboratory, Seattle, 2007.
9. O. Nielsen et al. Hydrodynamic modelling of coastal inundation. In *Int. Congress on Modelling and Simulation*, pages 518–523, 2005.
10. BPS. *Village Potential—PODES 2006*. Statistical bureau (BPS) Kota Padang, Padang, 2000.
11. BPS. *Population Census 2000*. Statistical bureau (BPS) Kota Padang, Padang, 2000.
12. BPS. *Kecamatan Dalam Angka—Subdistricts in Numbers*. Statistical bureau (BPS) Kota Padang, Padang, 2005.
13. *Final Report of Transportation Master Plan the City of Padang*. Dinas Perhubungan Kota Padang (Transportation Agency of the city of Padang), Padang, 2006.
14. C. Gawron. An iterative algorithm to determine the dynamic user equilibrium in a traffic simulation model. In D.E. Wolf and M. Schreckenberg, editors, *Traffic and Granular Flow'97*, pages 469–474. Springer, Berlin, 1998.
15. P.M. Simon, J. Esser, and K. Nagel. Simple queueing model applied to the city of Portland. *Journal of Modern Physics C*, 10(5):941–960, 1999.
16. D. Helbing, I. Farkas, and T. Vicsek. Simulating dynamical features of escape panic. *Nature*, 407:487–490, 2000.
17. C. Lieberman et al. Conceptual framework for simulating the pedestrian evacuation behavior from buildings. Paper 05-2297, Transportation Research Board Annual Meeting, Washington, D.C., 2005.
18. G. Lämmel, M. Rieser, and K. Nagel. Bottlenecks and congestion in evacuation scenarios: A microscopic evacuation simulation for large-scale disasters. In *Proc. of 7th Int. Conf. on Autonomous Agents and Multiagent Systems (AAMAS 2008)*, Estoril, Portugal, May 2008.
19. G. Lämmel, M. Rieser, and K. Nagel. Large scale microscopic evacuation simulation. In *Pedestrian and Evacuation Dynamics 2008*. Springer, Berlin, 2010.
20. K. Nagel and M. Schreckenberg. A cellular automaton model for freeway traffic. *Journal de Physique I France*, 2:2221–2229, 1992.
21. K. Nishinari, A. Kirchner, A. Nazami, and A. Schadschneider. Extended floor field CA model for evacuation dynamics. *IEICE Transactions on Information and Systems*, E84-D:726, 2001.
22. C. Gloor, P. Stucki, and K. Nagel. Hybrid techniques for pedestrian simulations. In *Lecture Notes in Computer Science*, volume 3305, pages 581–590. Springer, Berlin, 2004.

Case Studies on Evacuation Behaviour in a Hotel Building in BART and in Real Life

Margrethe Kobes, Nancy Oberijé, and Martina Duyvis

Netherlands Institute for Safety (NIFV), PO Box 7010, 6801 HA Arnhem,
The Netherlands
e-mail: margrethe.kobes@nifv.nl

Summary. BART is the Behavioural Assessment and Research Tool. BART makes use of an interactive, real-time, physics-based virtual environment with realistic 3D visuals and audio. In BART it is possible to face people with the phenomenon fire in a safe way, without being exposed to the extreme health risk of a real fire. The primary objective of the tool in virtual reality (VR) is to generate the information that fire safety engineers have need of for the design of a safe building that complies with actual human behaviour in fires. For the development of the innovative tool first a trial version of BART is developed, which consists of the visualisation of an existing Dutch hotel building. In this paper some case studies on evacuation behaviour in a real hotel building, as well as in a virtual hotel building in *BARTtrial*, are described. Furthermore some key findings of the earliest trials of behavioural assessment in VR are given.

1 Evacuation Behaviour

In the beginning of the 20th century the research on evacuation behaviour started [1–3]. The main focus was on the movement of people in corridors, on stairs and through doors. Several researchers, in particular Pauls, Fruin, Predtetschenski, Milinski, Habicht and Braaksma [4–6] have collected detailed information about occupant density and travel speed. This information has been of large influence on the approach of fire safety in building regulations worldwide. For the fire safety in buildings, the required measures are technology based. And more seriously, the real evacuation behaviour of people in case of fire seems to be neglected.

Evacuation is the process in which the people present in a building notice a fire and whereupon they experience several mental processes and carry out several actions before and/or during the movement to a safe place in or outside the building [6]. The evacuation process is characterised by three certain basic activities [1, 4, 7]:

- Awareness of danger by external stimuli (cue validation)

- Validation of and response to danger indicators (decision-making)
- Movement to / refuge in a safe place (movement / refuge).

Theoretically the basic activities can be converted into phases of the evacuation process, namely the cue validation period, the decision-making period and the movement / refuge period. The last mentioned period is also referred as the movement phase. The cue validation period and the decision-making period together is referred as the pre-movement phase. The processes in the pre-movement phase are believed to be more decisive on survival [2, 8] than the actual movement speed.

Way finding covers the way how people orientate themselves within a building [9]. People need to have spatial knowledge and various cognitive abilities to succeed in way finding. Two aspects are crucial in the way finding performance, namely cues and choices. The way finding performance is determined by the perception and prior knowledge of persons who has to find their way within a building. Furthermore, there are four classes of environmental variables that influence way finding performance [9]:

- Visual access
- The degree of architectural differentiation
- The use of signs and room numbers to provide identification or directional information
- Plan configuration.

Way finding is believed to be more dependent on the lay-out of the building and seems to be barely dependent on (escape) route signs [9]. Incident evaluations indicate that evacuees are hardly aware of the presence of escape route signs at ceiling level or at least their route choice is not based upon it [10, 11]. Route choice depends upon the familiarity of the occupants with the building, the availability of exits, the accessibility of the route towards exits and upon the lay-out complexity [1, 6]. Occupants normally evacuate by using familiar routes, mostly the main exit which is normally the entrance of a building [12, 13]. Not the actual length but the perception of the length determines the route choice [12–14]. For example, corridors with several bends and unfamiliar routes are experienced to be longer than straight and familiar routes [15]. Fire exits which are not regularly used tend to have a negative association [16].

According to the Dutch Building Regulation buildings should be designed in such a way that occupants can escape by themselves in case of fire. However, case studies show that occupants often are found to be incapable to escape in time. Moreover, incident evaluations indicate that the major fatalities occur in evacuations with a long pre-movement time, especially in hotels and apartment buildings [7]. It is also found that occupants behave frequently in contradiction to the assumptions in the regulations. Therefore, it is better to let the fire safety of buildings be based on actual human behaviour in fire, instead of to assume that human's behaviour will comply with technology based safety measures [17].

2 Research Method

2.1 Research Aim, Focus and Selected Object

The primary aim of our behavioural research in virtual reality is the validation of a research instrument in VR. The additional aim of the research is (1) obtaining insight in human behaviour in fires, particularly in the intentions on which the route choice of evacuees are based upon; (2) appointing lay-out measures or design options which create optimum preconditions for people present in buildings so that they choose the safest escape route; and (3) determining the effectiveness of the appointed measures and design options (the degree in which the behaviour of occupants is affected by the appointed measures and design options). Subsequent to the validation of the research instrument in VR the instrument will be used to generate the information that fire safety engineers have need of for the design of a safe building that complies with actual human behaviour in fires.

The focus of the research is on way finding. There are three main reasons for the focus on way finding. First of all, the way in which persons find the safest escape route, and how this process can be supported with lay-out and design measures has been hardly examined [18, 19]. Thus, there is need for insight in the decision-making processes which evacuees pass through. Secondly, way finding itself can pre-eminently be studied in a virtual surrounding, since building modifications, for example design alterations of the escape route, are easily made within VR. Thirdly, building specifications are expected to influence evacuation behaviour.

The selected object is a hotel building. Evaluations of fatal fires reveal that (in The Netherlands) the major fatal fires have mostly occurred at night in residential buildings and in public buildings [17]. Furthermore, it appears that particularly hotel accommodations have a high risk profile. In the Netherlands some thousands of this type of buildings are present and millions of individuals make use of hotel accommodations annually. Therefore a hotel building is selected as the object for closer research on human behaviour in fires. Nevertheless, it must be noticed that the other types of buildings mentioned in this paper are also interesting as a research object. But with regard to the scope of this research, that is the validation of a VR research instrument, a less complex building is preferred wherein persons are present who are mobile and capable of evacuating without the help from others.

2.2 Test Scenario

In public buildings, for example in hotels, a manager is responsible for the safety of the people present. Such buildings have the possibility for the simultaneous presence of dozens of persons and with that the potential to a fire with many casualties and subsequently high media and political attention. However, incident evaluations have revealed that in most of the fatal fires a

trained Building Evacuation Team (BET) was not present [17]. Consequently, people tend to fall back on their own capabilities and performances in case of an emergency. Therefore all the way finding tests are individually.

For the first scenario there is no fire or smoke simulated in the (virtual) hotel. The tests are conducted between 03:00–06:30 a.m. while the test persons are sleeping in their hotel room. The test persons are waked up by a telephone call. In the real hotel the message is: “*This is the reception speaking. There is a mention of fire on your floor. Leave the hotel as quickly as possible. The other guests are alarmed by us. I repeat: This is the reception speaking. There is a mention of fire on your floor. Leave the hotel as quickly as possible. The other guests are alarmed by us.*” In the tests in *BARTtrial* the test person is asked to come to the test room as soon as possible. A researcher is waiting in the corridor in front of the hotel room and guides the test person to the test room. When the test person is in the test room and stands in front of the projection screen the researcher speaks out the message that is also given to the test persons in the real hotel.

2.3 Participants

The participants are invited by colleagues, by a flyer or by an invitation on the webpage of NIFV. The participants fill in a questionnaire with questions about their health. Based on the information in the health questionnaire the participant is (or is not) invited to conduct the test. In the evening, before the tests, the participant signs a informer consent. In the form is taken down that the tests are on fire safety and that the tests are not dangerous. Furthermore it is taken down that the test person is allowed to stop the test at every moment and that the test will be taped on video.

In the tests in *BARTtrial* the fee of the participants consists of a free dinner, a free hotel room in the NIFV training facility, the compensation of the travel expenses and a coupon of € 25. The fee of the participants in the real hotel consists of a free dinner, a free hotel room in the (four stars) Hotel Mercure Amersfoort and the compensation of the travel expenses.

Eight persons in the age of 22 to 56 years conducted the test in *BARTtrial*, of which five men and three women. Two young women were excluded for the test in *BARTtrial* because of cyber sickness after the tests in the evening. Nine persons in the age of 25 to 48 years conducted the test in the real hotel, of which three men and six women (see Table 1).

Environment	Number of participants			Age		
	Male	Female	Total	Mean	Min	Max
BARTtrial	5	3	8	42.9	22	56
Real hotel	3	6	9	33.9	25	48

Table 1. Participants.

Personality test	Real hotel			BARTtrial		
	Mean	Min	Max	Mean	Min	Max
BIS total	19	16	20	19	16	22
BAS total	28	23	29	29	25	32
BAS reward	11	8	13	11	9	12
BAS drive	9	7	12	10	8	11
BAS fun	9	4	13	8	6	11
ACS total	54	40	79	50	35	64
ACS focus	25	20	34	24	21	31
ACS switch	29	20	45	26	13	38
CERQ short	43	25	54	44	36	54

Table 2. Personality of participants.

The test persons have to fill in three different personality questionnaires. The two questionnaires which are taken before the tests are the ‘Behavioural Inhibition System and Behavioural Approach System’ (BIS/BAS score) developed by Carver and White (1994) [20] and the ‘Attention Control Scale’ (ACS score) developed by Derryberry and Reed (2002) [21]. The questionnaire which is taken after the test is the ‘short Cognitive Emotion Regulation Questionnaire’ (CERQ score) developed by Garnefski and Kraaij (2006) [22]. The personalities of the test persons in the real hotel are comparable with the personalities of the test persons in BARTtrial (see Table 2).

2.4 Observations

The observations in both the virtual and the real hotel are taped on video. The observations are (1) a pre-test personality questionnaire and health measurement, (2) a VR training session in the evening with a time measurement test, (3) a risk perception test in a virtual environment, (4a) an unannounced evacuation test at night in real life, or (4b) an unannounced evacuation test at night in *BARTtrial*, (5) a post-test health measurement, (6) an open interview, partly during watching the video tape of the taken actions in the evacuation test, and (7) a post test personality questionnaire.

In the VR training sessions the observations have focus on the opinion of the test persons with regard to the reality level of the visualised hotel building, the most attractive projection device, the most attractive controlling device and on the needed training time for getting familiar with the controlling device. The unannounced evacuation tests, together with the open interview and the health measurements, have focus on way finding in the virtual hotel building, the motives of the route choices the test person makes, the feelings and thoughts during the (virtual) evacuation drill and on the (by the test person) experienced and (by the researcher) measured stress level. The stress level is measured by the blood pressure and the heart rate, which is taken in the health measurements before and after the test.

The test at night is the real test. The VR training session questionnaires, the time measurement test and the risk perception test during the evening are fake tests. After the evening session the test persons are given some first results of the tests they conducted in the evening. Furthermore they are told by the research team that the experiment session is over. The evening session ends with a social event in the pub of the test accommodation (hotel facility NIFV Arnhem or Hotel Mercure Amersfoort). The research team participates in this social event.

2.5 BARTtrial

To obtain insight in the evacuation behaviour and in the effect of the building design on that evacuation behaviour (way finding) a Behavioural Assessment and Research Tool (BART) has been developed [23]. BART is based upon a well tried and tested simulation platform that is used by emergency training organisations all over the world for years now, that is the Advanced Disaster Management Simulator (ADMSTM). ADMSTM is an interactive, real-time, physics-based virtual environment with realistic 3D visuals and audio. In BART it is possible to face people with the phenomenon fire in a safe way, without being exposed to the extreme health risk of a real fire. For the development of the innovative tool first a trial version of BART is developed, which consists of the visualisation of an existing Dutch hotel building, namely Hotel Mercure Amersfoort. In Fig. 1 the degree of similarity between the real hotel and the virtual hotel is shown.

The movement of the virtual test person in *BARTtrial* is controlled by using a joystick, a game pad or a keyboard and mouse. In the training session the test person tries all three of the controlling devices and selects the most attractive device. In the real test at night the test person controls *BARTtrial* with the selected device. The projection takes place by means of a beamer on a 2 by 2 meter sized flat projection screen. Differences between ADMSTM-BART and BARTtrial are shown in Table 3.



Fig. 1. Degree of similarity between the real hotel and the virtual hotel.

Functionality	BARTtrial	ADMS TM BART
Walking in hotel	X	X
Fire and smoke		X
People present		X
Sounds		X
Health indicator		X

Table 3. Difference between ADMSTM-BART and BARTtrial.

3 Case Studies

3.1 BARTtrial

BARTtrial participant 7082903

The participant is a 29 years old woman. She has no prior experience of an evacuation and has had training or education in fire safety. She did not expect to be awaked during the night for an evacuation test. She slept in room 112 and was waked up at 05:10 a.m. It took 173 seconds before she opened the hotel room door of the NIFV training facility. After hearing the emergency message and opening the hotel room door in *BARTtrial*, the first walking direction was to the left, heading in opposite to the reception. She took exit E06 towards the staircase. In the staircase she took the door to the corridor towards the reception. Then she turned back to the staircase and took the emergency exit to the outside. She was not familiar with the route she took. The nearest exit was exit E11 with a distance of 15.8 meters to the hotel room door. She walked 49.3 meters in 100 seconds, with an average speed of 0.49 m/s. She classified herself as not skilled with computer games. After the VR training session she gave herself a score of 8 (1 is low and 10 is high). The chosen exit was not the nearest exit and she walked not in a straight line towards it. The difference between the chosen and the shortest route is 33.5 meters. She passed 2 other exits. The score in the self evaluation, in which the score of 1 is low and 10 is high, for the feeling of time pressure is 7, for the feeling of a real emergency situation is 7 and for the feeling of a good result of the test is 7. The score for the perception of the ease of way finding is 6 and for the ease to recognise the exit is 7.

BARTtrial participant 7082904

The participant is a 54 years old man. He has no prior experience of an evacuation and has had no training or education in fire safety. He did expect to be awaked during the night for an evacuation test. He slept in room 121 and was waked up at 06:05 a.m. It took 337 seconds before he opened the hotel room door of the NIFV training facility. After hearing the emergency message and opening the hotel room door in *BARTtrial*, the first walking direction was to the right, heading in opposite to the reception. He took the emergency

exit E11 towards the outside. He was not familiar with the route he took. The nearest exit was exit E11 with a distance of 14 meters to the hotel room door. He walked 14 meters in 62 seconds, with an average speed of 0.23 m/s. He classified himself as not skilled with computer games. After the VR training session he gave himself a score of 3 (1 is low and 10 is high). The chosen exit was the nearest exit and he walked in a straight line towards it. The score in the self evaluation, in which the score of 1 is low and 10 is high, for the feeling of time pressure is 4, for the feeling of a real emergency situation is 3 and for the feeling of a good result of the test is 9.5. The score for the perception of the ease of way finding is 10 and for the ease to recognise the exit is 10.

BARTtrial participant 7082905

The participant is a 22 years old man. He has no prior experience of an evacuation and has had no training or education in fire safety. He did not expect to be awaked during the night for an evacuation test. He slept in room 119 and was waked up at 04:30 a.m. It took 270 seconds before he opened the hotel room door of the NIFV training facility. After hearing the emergency message and opening the hotel room door in *BARTtrial*, the first walking direction was to the right, heading in opposite to the reception. He took the emergency exit E11 towards the outside. He was not familiar with the route he took. The nearest exit was exit E11 with a distance of 19.5 meters to the hotel room door. He walked 19.5 meters in 48 seconds, with an average speed of 0.41 m/s. He classified himself as skilled with computer games. After the VR training session he gave himself a score of 9 (1 is low and 10 is high). The chosen exit was the nearest exit and he walked in a straight line towards it. The score in the self evaluation, in which the score of 1 is low and 10 is high, for the feeling of time pressure is 1, for the feeling of a real emergency situation is 1 and for the feeling of a good result of the test is 10. The score for the perception of the ease of way finding is 10 and for the ease to recognise the exit is 10.

BARTtrial participant 7120401

The participant is a 48 years old man. He has no prior experience of an evacuation and has had no training or education in fire safety. He did expect to be awaked during the night for an evacuation test. He slept in room 110 and was waked up at 03:18 a.m. It took 89 seconds before he opened the hotel room door of the NIFV training facility. After hearing the emergency message and opening the hotel room door in *BARTtrial*, the first walking direction was to the left, heading in opposite to the reception. He took the emergency exit E11 towards the outside. He was familiar with the route he took. In the VR training session he looked for the emergency exit. The nearest exit was exit E11 with a distance of 17.9 meters to the hotel room door. He walked 17.9 meters in 30 seconds, with an average speed of 0.6 m/s. He classified

himself as not skilled with computer games. After the VR training session he gave himself a score of 8 (1 is low and 10 is high). The chosen exit was the nearest exit and he walked in a straight line towards it. The score in the self evaluation, in which the score of 1 is low and 10 is high, for the feeling of time pressure is 2, for the feeling of a real emergency situation is 1 and for the feeling of a good result of the test is 9. The score for the perception of the ease of way finding is 9 and for the ease to recognise the exit is 7.

BARTtrial participant 7120402

The participant is a 56 years old man. He has no prior experience of an evacuation and has had no training or education in fire safety. He did not expect to be awaked during the night for an evacuation test. He slept in room 119 and was waked up at 03:50 a.m. It took 84 seconds before he opened the hotel room door of the NIFV training facility. After hearing the emergency message and opening the hotel room door in *BARTtrial*, the first walking direction was to the left, heading towards the reception. He took exit E01 towards the reception. He was familiar with the route he took and that was the reason for taking this route. The nearest exit was exit E11 with a distance of 19.5 meters to the hotel room door. He walked 74.3 meters in 79 seconds, with an average speed of 0.94 m/s. He classified himself as not skilled with computer games. After the VR training session he gave himself a score of 8.5 (1 is low and 10 is high). The chosen exit was not the nearest exit and he walked in a straight line towards it. The difference between the chosen and the shortest route is 54.8 meters. The score in the self evaluation, in which the score of 1 is low and 10 is high, for the feeling of time pressure is 9, for the feeling of a real emergency situation is 7 and for the feeling of a good result of the test is 8.5. The score for the perception of the ease of way finding is 8 and for the ease to recognise the exit is 9.

BARTtrial participant 7120403

The participant is a 51 years old woman. She has no prior experience of an evacuation and has had no training or education in fire safety. She did expect to be awaked during the night for an evacuation test. She slept in room 110 and was waked up at 04:25 a.m. It took 102 seconds before she opened the hotel room door of the NIFV training facility. After hearing the emergency message and opening the hotel room door in *BARTtrial*, the first walking direction was to the right, heading towards the reception. At the intersection she turned and took the emergency exit E11 towards the outside. She was not familiar with the route she took. She chose this exit because of the green exit signs and because it seems to be the shortest route. The nearest exit was exit E11 with a distance of 17.9 meters to the hotel room door. She walked 33.1 meters in 50 seconds, with an average speed of 0.66 m/s. She classified herself as not skilled with computer games. After the VR training session she

gave herself a score of 3 (1 is low and 10 is high). The chosen exit was the nearest exit and she walked not in a straight line towards it. The difference between the chosen and the shortest route is 15.2 meters. The score in the self evaluation, in which the score of 1 is low and 10 is high, for the feeling of time pressure is 6, for the feeling of a real emergency situation is 4 and for the feeling of a good result of the test is 8. The score for the perception of the ease of way finding is 8 and for the ease to recognise the exit is 8.

BARTtrial participant 7120404

The participant is a 45 years old man. He has no prior experience of an evacuation and has had no training or education in fire safety. He did expect to be awaked during the night for an evacuation test. He slept in room 112 and was waked up at 05:10 a.m. It took 95 seconds before he opened the hotel room door of the NIFV training facility. After hearing the emergency message and opening the hotel room door in *BARTtrial*, the first walking direction was to the left, heading in opposite to the reception. He walked towards the staircase but after passing the door in the corridor he turned and took the emergency exit E11 towards the outside. He was familiar with the route he took. In the VR training session he looked for the emergency exit. The nearest exit was exit E11 with a distance of 15.8 meters to the hotel room door. He walked 19 meters in 21 seconds, with an average speed of 0.91 m/s. He classified himself as skilled with computer games. After the VR training session he gave himself a score of 6.5 (1 is low and 10 is high). The chosen exit was the nearest exit and he walked not in a straight line towards it. The difference between the chosen and the shortest route is 3.2 meters. The score in the self evaluation, in which the score of 1 is low and 10 is high, for the feeling of time pressure is 7, for the feeling of a real emergency situation is 6 and for the feeling of a good result of the test is 8. The score for the perception of the ease of way finding is 7 and for the ease to recognise the exit is 8.

BARTtrial participant 7120405

The participant is a 38 years old woman. She has no prior experience of an evacuation and has had training or education in fire safety. She did expect to be awaked during the night for an evacuation test. She slept in room 119 and was waked up at 05:40 a.m. It took 89 seconds before she opened the hotel room door of the NIFV training facility. After hearing the emergency message and opening the hotel room door in *BARTtrial*, the first walking direction was to the right, heading in opposite to the reception. She took the emergency exit E11 towards the outside. She was not familiar with the route she took. She chose this exit because of the green exit signs. The nearest exit was exit E11 with a distance of 19.5 meters to the hotel room door. She walked 19.5 meters in 22 seconds, with an average speed of 0.89 m/s. She classified herself as not skilled with computer games. After the VR training session she gave herself a

score of 8 (1 is low and 10 is high). The chosen exit was the nearest exit and she walked in a straight line towards it. The score in the self evaluation, in which the score of 1 is low and 10 is high, for the feeling of time pressure is 4, for the feeling of a real emergency situation is 3 and for the feeling of a good result of the test is 8. The score for the perception of the ease of way finding is 8 and for the ease to recognise the exit is 7.

3.2 Real Hotel

Real hotel participant 7101901

The participant is a 39 years old woman. She has no prior experience of an evacuation and has had no training or education in fire safety. She did not expect to be awaked during the night for an evacuation test. She slept in room 108 and was waked up at 04:25 a.m. It took 109 seconds before she opened the hotel room door. She was fully dressed and had her handbag with her. After opening the hotel room door, the first walking direction was to the right, heading towards the reception. She took exit E01 towards the reception. She was familiar with the route she took. The nearest exit was exit E11 with a distance of 23.4 meters to the hotel room door. She walked 70.7 meters in 64 seconds, with an average speed of 1.11 m/s. The chosen exit was not the nearest exit and she walked in a straight line towards it. The difference between the chosen and the shortest route is 47.3 meters. The score in the self evaluation, in which the score of 1 is low and 10 is high, for the feeling of time pressure is 7, for the feeling of a real emergency situation is 7 and for the feeling of a good result of the test is 7. The score for the perception of the ease of way finding is 7 and for the ease to recognise the exit is 7.

Real hotel participant 7101902

The participant is a 38 years old woman. She has no prior experience of an evacuation and has had no training or education in fire safety. She did not expect to be awaked during the night for an evacuation test. She slept in room 114 and was waked up at 04:50 a.m. It took 330 seconds before she opened the hotel room door. She was dressed in pyjamas and a bathrobe. After opening the hotel room door, the first walking direction was to the right, heading towards the reception. She took exit E01 towards the reception. She was familiar with the route she took. The nearest exit was exit E11 with a distance of 10.2 meters to the hotel room door. She walked 83.2 meters in 60 seconds, with an average speed of 1.39 m/s. The chosen exit was not the nearest exit and she walked in a straight line towards it. The difference between the chosen and the shortest route is 73 meters. The score in the self evaluation, in which the score of 1 is low and 10 is high, for the feeling of time pressure is 5, for the feeling of a real emergency situation is 3 and for the feeling of a good result of the test is 2. The score for the perception of the ease of way finding is 8 and for the ease to recognise the exit is 7.

Real hotel participant 7101903

The participant is a 27 years old woman. She has no prior experience of an evacuation and has had training or education in fire safety. She did expect to be awaked during the night for an evacuation test. She slept in room 110 and was waked up at 03:05 a.m. It took 66 seconds before she opened the hotel room door. She was dressed in pyjamas and a bathrobe and had her handbag with her. After opening the hotel room door, the first walking direction was to the left, heading in opposite to the reception. She took the emergency exit E11 towards the outside. She was not familiar with the route she took. The nearest exit was exit E11 with a distance of 17.9 meters to the hotel room door. She walked 17.9 meters in 17 seconds, with an average speed of 1.05 m/s. The chosen exit was the nearest exit and she walked in a straight line towards it. The score in the self evaluation, in which the score of 1 is low and 10 is high, for the feeling of time pressure is 4, for the feeling of a real emergency situation is 4 and for the feeling of a good result of the test is 7. The score for the perception of the ease of way finding is 8 and for the ease to recognise the exit is 9.

Real hotel participant 7101904

The participant is a 25 years old man. He has no prior experience of an evacuation and has had no training or education in fire safety. He did expect to be awaked during the night for an evacuation test. He slept in room 112 and was waked up at 03:40 a.m. It took 85 seconds before he opened the hotel room door. He was dressed in trousers and a bathrobe. After opening the hotel room door, the first walking direction was to the left, heading in opposite to the reception. He took the emergency exit E11 towards the outside. He was not familiar with the route he took. The nearest exit was exit E11 with a distance of 15.8 meters to the hotel room door. He walked 15.8 meters in 15 seconds, with an average speed of 1.05 m/s. The chosen exit was the nearest exit and he walked in a straight line towards it. The score in the self evaluation, in which the score of 1 is low and 10 is high, for the feeling of time pressure is 1, for the feeling of a real emergency situation is 0 and for the feeling of a good result of the test is 9. The score for the perception of the ease of way finding is 9 and for the ease to recognise the exit is 7.

Real hotel participant 7101905

The participant is a 48 years old woman. She has no prior experience of an evacuation and has had no training or education in fire safety. She did not expect to be awaked during the night for an evacuation test. She slept in room 121 and was waked up at 05:10 a.m. It took 125 seconds before she opened the hotel room door. She was dressed in pyjamas and a bathrobe and was barefooted. Before the evacuation she went to the toilet. After opening the hotel room door, the first walking direction was to the left, heading towards

the reception. She took exit E01 towards the reception. She was familiar with the route she took. The nearest exit was exit E11 with a distance of 14 meters to the hotel room door. She walked 79.8 meters in 55 seconds, with an average speed of 1.45 m/s. The chosen exit was not the nearest exit and she walked in a straight line towards it. The difference between the chosen and the shortest route is 65.8 meters. The score in the self evaluation, in which the score of 1 is low and 10 is high, for the feeling of time pressure is 8, for the feeling of a real emergency situation is 3 and for the feeling of a good result of the test is 8. The score for the perception of the ease of way finding is 7 and for the ease to recognise the exit is 9.

Real hotel participant 7101906

The participant is a 28 years old woman. She has no prior experience of an evacuation and has had no training or education in fire safety. She did expect to be awaked during the night for an evacuation test. She slept in room 117 and was waked up at 03:25 a.m. It took 67 seconds before she opened the hotel room door. She was dressed in pyjamas and a bathrobe and had her handbag with her. After opening the hotel room door, the first walking direction was to the right, heading in opposite to the reception. She took the emergency exit E11 towards the outside. She was not familiar with the route she took. The nearest exit was exit E11 with a distance of 21.5 meters to the hotel room door. She walked 21.5 meters in 17 seconds, with an average speed of 1.27 m/s. The chosen exit was the nearest exit and she walked in a straight line towards it. The score in the self evaluation, in which the score of 1 is low and 10 is high, for the feeling of time pressure is 5, for the feeling of a real emergency situation is 4 and for the feeling of a good result of the test is 8.5. The score for the perception of the ease of way finding is 9 and for the ease to recognise the exit is 9.

Real hotel participant 7101907

The participant is a 30 years old woman. She has prior experience of an evacuation and has had training or education in fire safety. Actually she was member of a junior fire brigade. She did expect to be awaked during the night for an evacuation test. She slept in room 119 and was waked up at 04:05 a.m. It took 85 seconds before she opened the hotel room door. She was dressed in pyjamas and a bathrobe. After opening the hotel room door, the first walking direction was to the right, heading in opposite to the reception. She took exit E06 towards the staircase. In the staircase she took the emergency exit to the outside. She was not familiar with the route she took. The nearest exit was exit E11 with a distance of 19.5 meters to the hotel room door. She walked 46.4 meters in 50 seconds, with an average speed of 0.93 m/s. The chosen exit was not the nearest exit and she walked in a straight line towards it. The difference between the chosen and the shortest route is 26.9 meters. She passed 1 other exit. The score in the self evaluation, in which the score of 1

is low and 10 is high, for the feeling of time pressure is 3, for the feeling of a real emergency situation is 0 and for the feeling of a good result of the test is 7. The score for the perception of the ease of way finding is 7 and for the ease to recognise the exit is 7.

Real hotel participant 7101908

The participant is a 38 years old man. He has prior experience of an evacuation and has had training or education in fire safety. Actually he is a fireman. He did expect to be awaked during the night for an evacuation test. He slept in room 115 and was waked up at 05:25 a.m. It took 98 seconds before he opened the hotel room door. He was fully dressed. After opening the hotel room door, the first walking direction was to the left, heading towards the reception. Then he stopped and looked on the flight plan in the corridor. He turned and took the emergency exit W11 towards the outside, which is actually a window with a collapsible ladder. Then he went round the building to the entrance of the hotel (reception). He was not familiar with the route he took. The window was with a very small indication mentioned on the flight plan as the nearest fire exit. The nearest exit (door, as mentioned on the flight plan) was exit E11 with a distance of 26.9 meters to the hotel room door. He walked 13.5 meters towards the window and about 80 meters towards the entrance. The walking time was not measured. The chosen exit was the nearest exit (but not the safest) and he walked not in a straight line towards it. The score in the self evaluation, in which the score of 1 is low and 10 is high, for the feeling of time pressure is 6, for the feeling of a real emergency situation is 3 and for the feeling of a good result of the test is 9. The score for the perception of the ease of way finding is 10 and for the ease to recognise the exit is 5.

Real hotel participant 7102004

The participant is a 32 years old man. He has prior experience of an evacuation and has had training or education in fire safety. Actually he is a fireman. He did expect to be awaked during the night for an evacuation test. He slept in room 114 and was waked up at 05:30 a.m. It took 170 seconds before he opened the hotel room door. He was fully dressed. After opening the hotel room door, the first walking direction was to the left, heading towards the reception. He took exit E01 towards the reception. He was familiar with the route he took. Afterwards he told that he took that route to please the research team, but possibly it was an excuse to justify his action. The nearest exit was exit E11 with a distance of 10.2 meters to the hotel room door. He walked 83.2 meters in 57 seconds, with an average speed of 1.46 m/s. The chosen exit was not the nearest exit and he walked in a straight line towards it. The difference between the chosen and the shortest route is 73 meters. The score in the self evaluation, in which the score of 1 is low and 10 is high, for the feeling of time pressure is 7, for the feeling of a real emergency situation is 1 and for the feeling of a good result of the test is 10. The score for the perception of the ease of way finding is 10 and for the ease to recognise the exit is 10.

4 Comparison of Case Studies in BARTtrial and in Real Hotel

The mean reaction time of the participants who were sleeping in the NIFV training facility is 154.9 seconds. The mean reaction time of the participants who were in Hotel Mercure Amersfoort is a little bit faster with 126.1 seconds. The chosen routes are visualised in Figs. 2 and 3.

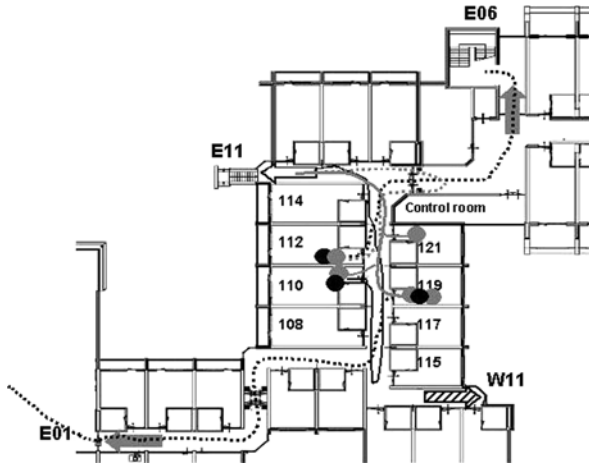


Fig. 2. Chosen routes in *BARTtrial*.

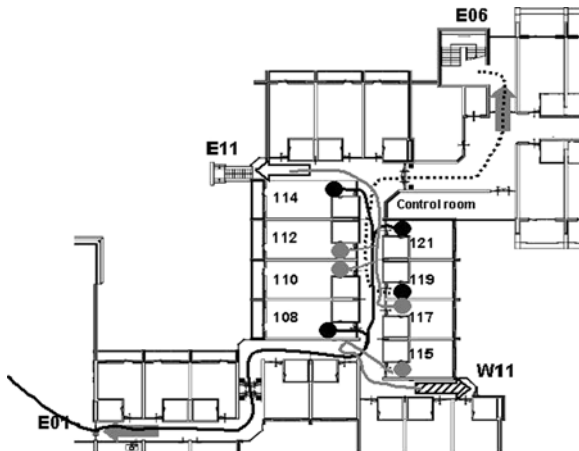


Fig. 3. Chosen routes in real hotel.

	Distance chosen			Distance nearest			Speed (m/s)		
	exit (m)			exit (m)					
Environment	Mean	Min	Max	Mean	Min	Max	Mean	Min	Max
BARTtrial	30.8	14.0	74.3	17.5	14.0	19.5	0.67	0.23	0.94
Real hotel	48.8	13.5	83.2	17.7	10.2	26.9	1.03	0.93	1.46

Table 4. Walking distances and walking speed.

Item	Scores* in BARTtrial			Scores* in real hotel		
	Mean	Min	Max	Mean	Min	Max
Ease of way finding	8.3	6	10	8.5	7	10
Feeling alert	7.5	6	9	7.6	3	10
Feeling of emergency	4.0	1	7	2.3	0	7
Feeling of time pressure	5.0	1	9	4.9	1	8
Feeling of control of situation	8.0	7	9	7.4	3	10
Feeling of good result	8.5	7	10	7.6	2	10

*Scale 1 (low) to 10 (high), scale 0 means that the feeling is not present at all

Table 5. Scores for self evaluation and for ease of way finding.

Three of the eight participants in the tests in *BARTtrial* did not expect to be awaked during the night for an evacuation test. Two of them did not choose the shortest route. In addition, two of the five participants who did expect to be awaked during the night for an evacuation test did not walk the shortest route. The other four test persons did walk towards the nearest exit. In the real hotel tests three of the nine participants did not expect to be awaked during the night for an evacuation test. All of them did not walk the shortest route. Also two of the six participants who expected to be awaked during the night did not took the nearest exit. The other four test persons chose the nearest exit. In total five of the six persons who did not expect to be in an evacuation during the night, and four of the eleven persons who did expect it, did not walk the shortest route.

After the test the participants had to give a self evaluation and give a score for the ease of way finding in the hotel. The results of the self evaluation and the score for the ease of way finding in *BARTtrial* are comparable to the results in the real hotel. The results are given in Tables 4 and 5.

Before the test the body mass index (BMI), the blood pressure (RR, rest) and the heart rate (HR, rest) is measured. After the test the blood pressure (RR, action) and the heart rate (HR, action) is measured again for obtaining insight in the level of stress. The results of the measurements are given in Tables 6 and 7. The results seems to indicate that there was no appearance of stress, or at least it is not measured.

Age	M/F	BMI	RR, rest	HR, rest	RR, action	HR, action
22	M	15.9	104/61	76	114/69	70
51	F	21.0	142/78	68	125/70	74
29	F	24.3	130/83	63	135/83	75
56	M	24.9	173/102	60	162/64	104
48	M	27.5	129/78	78	130/79	78
54	M	28.9	156/90	85	143/88	77
38	F	32.4	135/94	72	157/81	112
45	M	34.4	126/78	78	129/71	80

Table 6. Health measurements in tests in BARTtrial.

Age	M/F	BMI	RR, rest	HR, rest	RR, action	HR, action
48	F	19.6	117/97	108	131/88	110
39	F	20.7	124/67	64	122/58	64
28	F	22.6	121/69	66	140/77	79
27	F	23.2	135/81	70	127/78	87
38	F	23.7	130/85	54	135/91	50
25	M	23.7	149/87	61	144/100	70
38	M	23.8	138/85	62	131/92	81
32	M	27.5	159/76	63	125/85	101
30	F	28.3	142/96	82	143/90	101

Table 7. Health measurements in tests in real hotel.

5 Conclusions and Further Work

The quantity of the first case studies ($n = 8$ and $n = 9$) is too low for a validation of BARTtrial. For the validation of the final version of BART there will be about 30 tests per scenario conducted in BART and in the real hotel (in total 60 participants per scenario). There will be three or four scenarios conducted with the final version of BART. Although the quantity is low, the results of the first tests indicate that way finding tests in BART will give corresponding results with the same tests in the real hotel. In BARTtrial as well in the real hotel about half of the participants did not walk the shortest route. There are also no major differences in the scores of the self evaluation. A point of attention is the relative low score of the feeling of an emergency, both in BARTtrial (score of 4) and the real hotel (score of 2.3). A explanation for the low score is possibly that there were no signs of fire (smoke) in the corridors. In the following scenarios there will a simulated fire in a hotel room and smoke will seep out of the room into the corridor.

Acknowledgements

The authors would like to thank Eric Dideren, trainer/consultant of NIFV, and Marco van Wijngaarden, president of ETC Simulation, for their expert

involvement in the development of the research instrument for fire safety engineering. The authors also give thanks to the members of the NIFV research team, in particular to Karin Groenewegen-Ter Morsche, Theo Uffink and Martin Veldhuis.

The research is made possible by financial support of the Dutch ministry of the Interior and Kingdom Relations. The experiments in real life are conducted in a Mercure hotel of Accor Hotels The Netherlands. ADMSTM-BART is developed by ETC Simulation, Orlando, Florida and the visualisation of the Mercure hotel is made by Danny Kroonen, consultant of Movares, Utrecht, The Netherlands.

References

1. D.J. O'Connor. Integrating Human Behaviour Factors into Design. *Fire Protection Engineering* 28, 2005, pp. 8–20.
2. J.L. Bryan. A Selected Historical Review of Human Behavior in Fire. *Fire Protection Engineering* 16, 2002, pp. 4–10.
3. D. Tong, D. Canter. The Decision to Evacuate: A Study of the Motivations which Contribute to Evacuation in the Event of Fire. *Fire Safety Journal* 9, 1985, pp. 257–265.
4. H. Frantzich. *A Model for Performance-Based Design of Escape Routes*. Lund, 1994. Lund University.
5. R.F. Fahy, G. Proulx. Toward Creating a Database on Delay Times to Start Evacuation and Walking Speeds for Use in Evacuation Modelling. *Proceedings of the 2nd International Symposium on Human Behaviour in Fire*, Boston, 2001, pp. 175–183.
6. *Engineering Guide to Human Behaviour in Fire: Review Draft*. 2002. SFPE.
7. D.A. Purser, M. Bensilum. Quantification of Behaviour for Engineering Design Standards and Escape Time Calculations. *Safety Science* 38, 2001, pp. 157–182.
8. G. Proulx. Occupant Behaviour and Evacuation. *Proceedings of the 9th International Fire Protection Symposium*. Munich, 2001, pp. 219–232.
9. M. Raubal, M.J. Egenhofer. Comparing the Complexity of Wayfinding Tasks in Built Environments. *Environment and Planning B* 25 (6), 1998, pp. 895–913.
10. C.W. Johnson. Lessons from the Evacuation of the World Trade Centre, 9/11 2001 for the Development of Computer-Based Simulations. *Cognition, Technology and Work* 7, 2005, pp. 214–240.
11. M.J. Ouellette. Visibility of Exit Signs. *Progressive Architecture* 74, 1993, pp. 39–42.
12. T.L. Graham, D.J. Roberts. Qualitative Overview of Some Important Factors Affecting the Egress of People in Hotel Fires. *Hospitality Management* 19, 2000, pp. 79–87.
13. A. Sandberg. Unannounced Evacuation of Large Retail-Stores. An Evaluation of Human Behaviour and the Computermodel Simulex. Lund, 1997. Lund University.
14. S. Gwynne, E.R. Galea, P.J. Lawrence, L. Filippidis. Modelling Occupant Interaction with Fire Conditions Using the BuildingExodus Evacuation Model. *Fire Safety Journal* 36, 2001, pp. 327–357.

15. G.G. Løvås. Models of Wayfinding in Emergency Evacuations. Theory and Methodology. *European Journal of Operational Research* 105, 1998, pp. 371–389.
16. L. Benthorn, H. Frantzich. *Fire Alarm in a Public Building: How Do People Evaluate Information and Choose Evacuation Exit*. Lund, 1996. Lund University.
17. M. Kobes. *Zelfredzaamheid bij Brand. Kritische Factoren voor het Veilig Vluchten uit Gebouwen*. Den Haag, 2008. Boom Juridische uitgevers. (In Dutch).
18. J.D. Sime. An Occupant Response Shelter Escape Time (ORSET) Model. *Safety Science* 38, 2001, pp. 109–125.
19. N.E. Groner. Intentional Systems Representations Are Useful Alternatives to Physical Systems Representations of Fire-Related Human Behaviour. *Safety Science* 38, 2001, pp. 85–94.
20. C.S. Carver, T.L. White. Behavioural Inhibition, Behavioural Activation and Affective Responses to Impending Reward and Punishment: the BIS/BAS Scales. *Journal of Personality and Social Psychology* 67, 1994, pp. 319–333.
21. D. Derryberry, M.A. Reed. Anxiety-Related Attentional Biases and their Regulation by Attentional Control. *Journal of Abnormal Psychology* 111, 2002, pp. 225–236.
22. N. Garnefski, V. Kraaij. Cognitive Emotion Regulation Questionnaire: Development of a Short 18-Item Version (CERQ-Short). *Personality and Individual Differences* 41, 2006, pp. 1045–1053.
23. M. Kobes, I. Helsloot, B. de Vries, N. Oberijé, N. Rosmuller. Fire Response Performance in a Hotel. *Behavioural Research. Conference Proceedings Interflam 2007. 11th International Fire Science and Engineering Conference*. Vol. 2, pp. 1429–1434.

Analysis of Empirical Trajectory Data of Pedestrians

Anders Johansson¹ and Dirk Helbing^{1,2}

¹ Department of Humanities and Social Sciences, ETH Zurich, UNO D 11
Universitätstrasse 41, 8092 Zurich, Switzerland
e-mail: andersj@ethz.ch

² Collegium Budapest, Institute for Advanced Study, Szentháromság u. 2,
1014 Budapest, Hungary
e-mail: dhelbing@ethz.ch

Summary. We investigate how the characteristics and dynamics of a crowd is changing when the crowd density is increased from a few pedestrians only, up to extremely high crowd densities. Video analysis of the crowd disaster in Mina, Kingdom of Saudi-Arabia, in 2006 gives an empirical base for further analysis which reveals two transitions of the flow; one transition from laminar flow to stop-and-go flow and a second transition to turbulent flow. Finally, an improved specification of the social-force model is suggested in order to explain some of the phenomena occurring in dense crowds.

1 Introduction

For any attempt to simulate pedestrians, one first needs to look at the empirical data, in order to find out how pedestrians are interacting. This has successfully been done for low and medium crowd densities, which has resulted in a variety of fundamental diagrams, i.e. density vs. flow, for pedestrian streams.

For higher densities, however, the crowd enters a dynamic regime, which can not be explained only with the static fundamental diagram. In this contribution we will make a journey starting from a few pedestrians interacting with each other and then observe how the behaviors and characteristics will change by an increasing crowd density.

2 Low Density

It has been assumed that pedestrians,

- adapt their walking velocity with an acceleration decaying exponentially with the distance to the fellow pedestrians, being avoided [1],

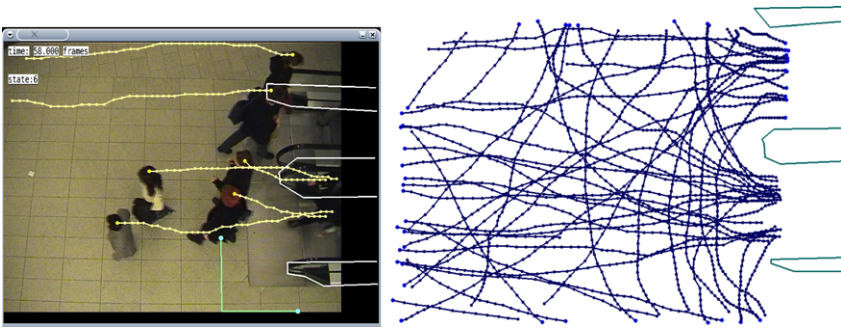


Fig. 1. Extraction of pedestrian trajectories from videos. *Left:* Tracking procedure. *Right:* Resulting trajectories, after projection on the floor.

- react stronger to what happens in front of them compared to what happens behind them [1].

To test these hypotheses, one first needs an empirical foundation. Therefore, we extract pedestrian trajectories from video recordings. See Ref. [2] and Fig. 1 for details. Extracting trajectories of pedestrians from videos has become a popular way of obtaining empirical data of pedestrian movement [3, 4].

We use a semi-automatic software where the user has to click the heads of the pedestrians, as they appear in the video. For successive frames, the software will track the heads. The tracking is performed by a local search in a small neighborhood, by using a kernel with a size corresponding to the size of a head. By doing so, the velocity $\vec{v}_\alpha t$, at time t for pedestrian α is found as the offset between two successive frames, giving the minimum difference when comparing the kernels.

To evaluate the characteristics of the pedestrians, we couple a simulation with the social-force model [1, 5, 6] to the dataset of trajectories obtained from the videos. We make the following assumptions:

- the desired walking speed of each person in the video corresponds to the maximum walking speed during the time the persons was tracked,
- the interaction of a pedestrian α with pedestrian β at locations $\vec{r}_\alpha(t)$ and $\vec{r}_\beta(t)$ can be described by one distance-dependent function and one angular-dependent function, and
- the resulting interaction force can be defined by a product of the two parts.

2.1 Hybrid Approach

Some fundamental quantities such as walking speed, density and time headway can be directly extracted from the trajectory datasets. More complex quantities, such as the interaction and avoidance behaviors can not be directly

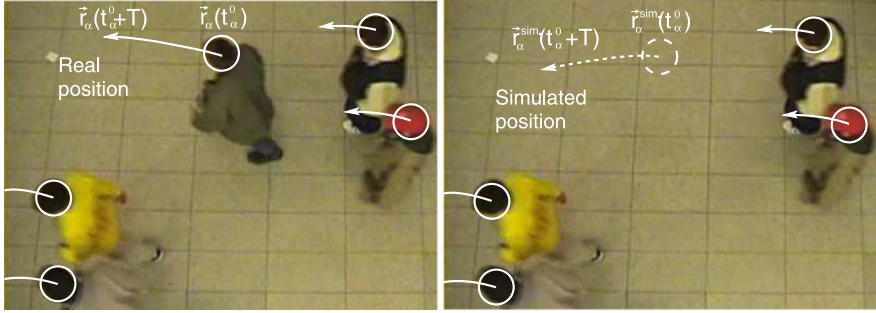


Fig. 2. Illustration of the hybrid approach, used for fusing empirical trajectory data with microscopic simulations. *Left:* All pedestrians (*solid circles*) follow the empirical trajectories. *Right:* For each pedestrian α (*dashed circle*) and for different starting times t_α^0 , a simulation is run during T seconds. One can then obtain a fitness value of the simulation by comparing the actual position to the simulated position.

extracted from the data though. Therefore we propose a hybrid method, fusing empirical trajectory data and microscopic simulation data of pedestrian movement.

To each tracked pedestrian, we assign a virtual pedestrian in the simulation domain and then start a simulation for $T = 1.5$ seconds, in which one pedestrian α is moved according to a simulation with the social-force model, while the others are moved according to the trajectories extracted from the videos.

The reason why we choose $T = 1.5$ seconds, is that for a low forecasting time, $T < 1.0$, any combination of low A or B values, gives a reasonable goodness of fit. This is interpreted as: For a very short forecasting time, a zero-acceleration model gives realistic results, where for larger forecasting times, $T > 1.0$, a more sophisticated model is needed in order to fit the trajectories. See Fig. 3 for the goodness-of-fit surface, spanned by the parameters A and B , for four different values of T .

Anyhow, the forecasting procedure is repeated for every pedestrian α and for several different starting times, t^o , using a fixed parameter set for the social-force model.

Each simulation run is performed according to the following scheme:

1. Define a starting point and calculate the state (position \vec{r}_α , velocity \vec{v}_α , and acceleration $\vec{a}_\alpha = d\vec{v}_\alpha/dt$) for each pedestrian α .
2. Assign a desired speed v_α^0 to each pedestrian. In our simulations, we specify the desired speed as the maximum speed $v_\alpha(t) = \|\vec{v}_\alpha(t)\|$ during the pedestrian's tracking time, which is sufficiently accurate if the overall pedestrian density is not too high and the desired speed is constant in time.
3. Assign a desired target location for each pedestrian. We assume that it corresponds to the point at the end of the trajectory.

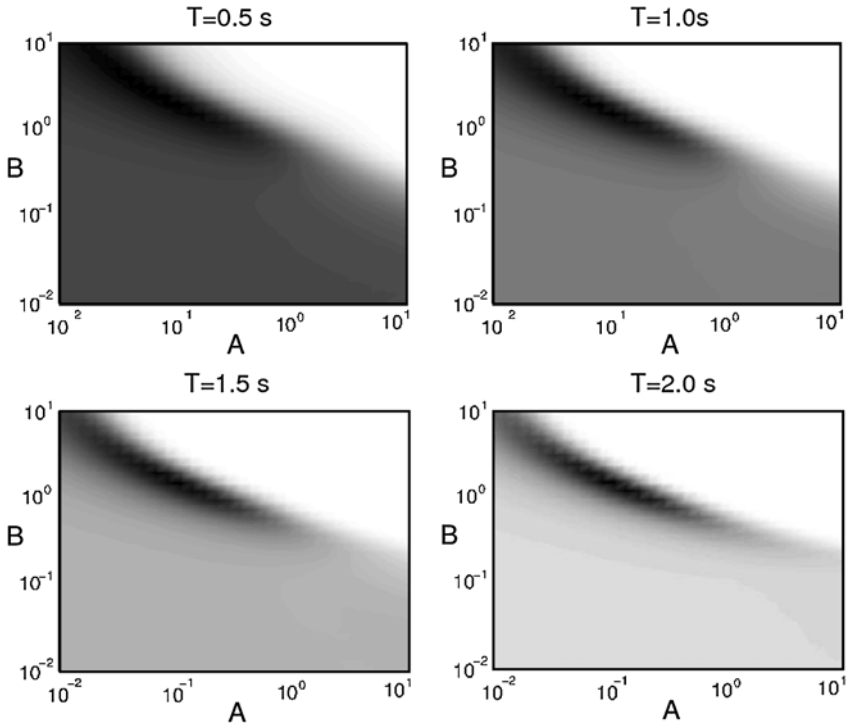


Fig. 3. The goodness-of-fit surface, spanned by the parameters, A and B , for different values of the forecasting time, T . The *darker shades* corresponds to the best goodness-of-fit values. For low values of the forecasting time, T , any combination of low A or B values, gives a fairly good goodness of fit. For this reason, we choose the value $T = 1.5$ for our further analysis.

4. Given the tracked motion of the surrounding pedestrians $\beta (\neq \alpha)$, simulate the trajectory of pedestrian α based on the social-force model during T seconds of time, starting at the actual location $\vec{r}_\alpha(t)$.

After each run, we determine the relative distance error,

$$\frac{\|\vec{r}_\alpha^{\text{simulated}}(t^o + T) - \vec{r}_\alpha^{\text{tracked}}(t^o + T)\|}{\|\vec{r}_\alpha^{\text{tracked}}(t^o + T) - \vec{r}_\alpha^{\text{tracked}}(t^o)\|}. \tag{1}$$

A batch of microscopic simulations are ran and a Genetic Algorithm is adapting the angular-dependent and the distance-dependent functions, until the trajectories of the simulated pedestrians match with the trajectories extracted from the video. See Ref. [2] for details.

The resulting optimized functions are seen in Fig. 4. It turns out that the angular dependence can successfully be approximated by a half-circle in front of the pedestrian. The distance dependence on the other hand turns out to have an exponential decaying function.

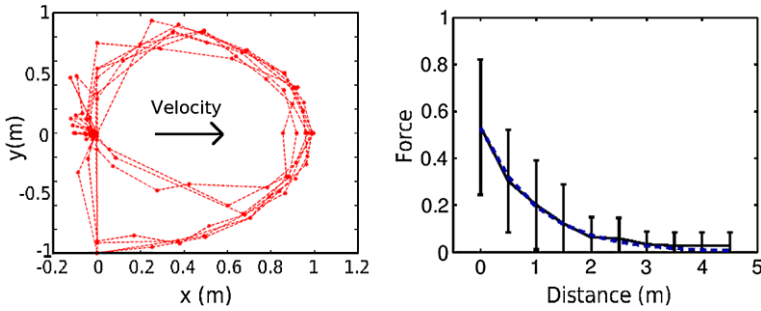


Fig. 4. The interaction strengths depending on angle of interaction and the distance between two pedestrians, has been found by fitting two polygons to the trajectory data. *Left:* Angular-dependent interactions. *Right:* Distance-dependent interactions. The *error bars* show the standard deviation, which is high due to cultural differences from the different datasets as well as different personalities between different persons within the same dataset.

3 Medium-to-High Density

It has been suggested that pedestrians will always follow the smooth flow-density relationship called *fundamental diagram*. For pedestrians, it is assumed to look like the one in Ref. [7].

$$V(\rho) = 1.34 \text{ ms}^{-1} \left\{ 1 - \exp \left[-1.913 \text{ m}^{-2} \left(\frac{1}{\rho} - \frac{1}{5.4 \text{ m}^2} \right) \right] \right\} \quad (2)$$

where V is the walking velocity with unit m/s and ρ is the crowd density with unit $1/m^2$. Fundamental diagrams from different studies agree fairly well in the low density region, while for high crowd densities they look very different from each other (see Fig. 5). An explanation for this is that the body-size distributions differ for different populations. Much higher flow rates and densities have been measured in Asian countries compared to western countries [3, 12].

While the different scales can be explained by varying body sizes, a recent study of the crowd disaster in Mina, Kingdom of Saudi-Arabia, in 2006 [12], suggests that the shape of the fundamental diagram for very high densities looks different from what has been previously suggested. In fact, pedestrian velocities will not decay to zero and stay there as soon as the crowd density is high enough. Rather, the average velocity will stay finite. Note however that it is the *average* velocity which stays constant. In the high-density region, the crowd is entering a dynamic regime, therefore the static fundamental diagram fails to grasp the movement of the crowd.

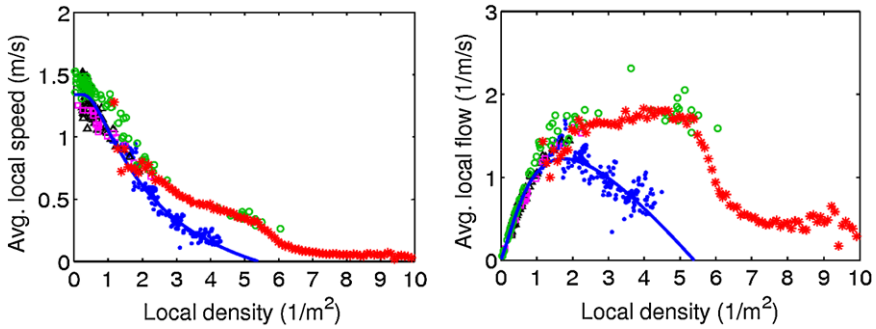


Fig. 5. Fundamental Diagrams. Our data from the crowd disaster in Mina, 2006 is shown as *red stars*. Other symbols correspond to: *black triangles* (Fruin, 1971) [8], *green circles* (Mori and Tsukaguchi, 1987) [9], *purple squares* (Polus et al., 1983) [10], and *blue dots* (Seyfried et al., 2005) [11]. The *solid curve* is from (Weidmann, 1993) [7].

4 High Density

We have analyzed videos from the crowd disaster in Mina, Kingdom of Saudi-Arabia in 2006 where the crowd density was increasing more and more until a crowd disaster occurred. From this analysis we have seen: when the crowd density is building up, the average walking velocity in the crowd will decrease until it reaches zero and stay there for a while, but then the crowd will suddenly start moving again—not in a smooth, laminar way, but rather in a dynamic way. There is a transition from laminar flow to stop-and-go waves. Later on, there is a second transition to turbulent flow. See Fig. 6 for three representative trajectories, one from each phase.

The stop-and-go waves are characterized by a dynamic motion where persons alternate between total stand-still and sudden forward movement. Figure 7 shows how the crowd density is changing in time and space. The tilted lines correspond to the stop-and-go waves propagating backwards, against the walking direction.

After more than 20 minutes with stop-and-go waves, there is a second transition to a chaotic motion, which turns out to have some similarities with turbulence. Both the structure function as well as the histogram of velocity increments correspond well to fluid turbulence [12].

5 Social-Force Model

The social-force model [1, 5, 6] assumes that each individual α is trying to move in a desired direction \vec{e}_α with a desired speed v_α^0 , and that it adapts the actual velocity \vec{v}_α to the desired one, $\vec{v}_\alpha^0 = v_\alpha^0 \vec{e}_\alpha$ within a certain relaxation

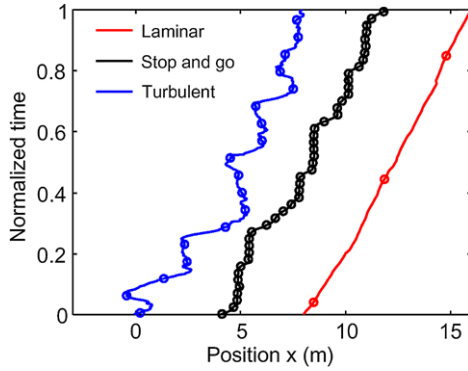


Fig. 6. Representative pedestrian trajectories from each of the three phases; laminar flow, stop-and-go waves and turbulent flow. There is a *marker* every 5 seconds and the time has been normalized to allow intuitive comparison of trajectories from the different phases.

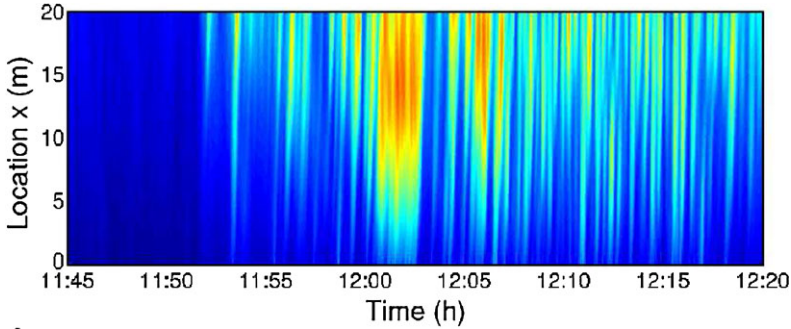


Fig. 7. The crowd density as a function of time and space reveals the stop-and-go waves, which are seen as *tilted lines*.

time τ_α . The velocity $v_\alpha(t) = d\vec{r}_\alpha/dt$, i.e. the temporal change of the location $r_\alpha(t)$, is itself assumed to change according to the acceleration equation

$$\frac{d\vec{v}_\alpha(t)}{dt} = \vec{f}_\alpha(t) + \vec{\xi}_\alpha(t), \quad (3)$$

where $\vec{\xi}_\alpha(t)$ is a fluctuation term and $\vec{f}_\alpha(t)$ the systematic part of the acceleration force of pedestrian α given by

$$\vec{f}_\alpha(t) = \frac{1}{\tau_\alpha}(v_\alpha^0 \vec{e}_\alpha - \vec{v}_\alpha) + \sum_{\beta(\neq\alpha)} \vec{f}_{\alpha\beta}(t) + \sum_i \vec{f}_{\alpha i}(t). \quad (4)$$

The terms $\vec{f}_{\alpha\beta}(t)$, $\vec{f}_{\alpha i}(t)$ denote the repulsive forces describing the attempts to keep a certain safety distance to other pedestrians β and obstacles i . The

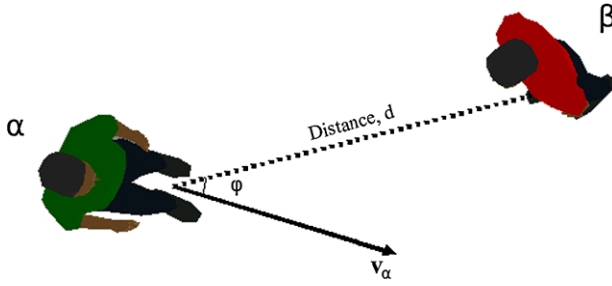


Fig. 8. A simplified interaction force is assumed, which has one angular-dependent part and one distance-dependent part.

fluctuation term $\vec{\xi}_\alpha(t)$ reflects random behavioral variations arising from deliberate or accidental deviations from the average way of motion. The above equation can be solved numerically using Euler’s method. In very crowded situations, additional physical contact forces come into play [6, 13].

There is a suggested improvement of the social-force model [13] which takes into account peoples’ increased propulsive forces in very dense crowds. This model can be used in order to explain the turbulent motion.

For the time being, we will assume a simplified interaction force, consisting of one angular-dependent part and one distance-dependent part (see Fig. 8). of the form

$$\vec{f}_{\alpha\beta}(t) = w(\varphi_{\alpha\beta}(t))\vec{g}(d_{\alpha\beta}(t)), \tag{5}$$

where $\vec{d}_{\alpha\beta} = \vec{r}_\alpha - \vec{r}_\beta$ is the distance vector pointing from pedestrian β to α and $\varphi_{\alpha\beta}$ the angle between the normalized distance vector $\hat{d}_{\alpha\beta} = \vec{d}_{\alpha\beta}/\|\vec{d}_{\alpha\beta}\|$ and the direction \vec{e}_α of motion of pedestrian α , i.e. $\cos(\varphi_{\alpha\beta}) = \vec{e}_\alpha \cdot \hat{d}_{\alpha\beta}$. It has, for example, been suggested to reflect by the function

$$w(\varphi_{\alpha\beta}(t)) = \left(\lambda_\alpha + (1 - \lambda_\alpha) \frac{1 + \cos(\varphi_{\alpha\beta})}{2} \right) \tag{6}$$

that the reaction of pedestrians to what happens in front of them is much stronger than to what happens behind them. Here, λ_α with $0 \leq \lambda_\alpha \leq 1$ is a parameter which grows with the strength of interactions from behind. Later on, we will try to determine this angular dependence from video-tracking data. The distance dependence $g(d_{\alpha\beta}(t))$ has been specified in different ways. We will start with the *circular specification* of the interaction force,

$$\vec{g}(d_{\alpha\beta}) = A_\alpha e^{(R_\alpha + R_\beta - d_{\alpha\beta})/B_\alpha} \hat{d}_{\alpha\beta}, \tag{7}$$

where R_α and R_β denote something like the radii of pedestrians α and β , while A_α and B_α are parameters. A_α reflects the strength of interaction, while B_α corresponds to the interaction range. While the dependence on α explicitly allows for a dependence of these parameters on the single individual, we will

assume $A_\alpha = A$ and $B_\alpha = B$ in the following. Otherwise, it would be hard to collect enough data for parameter calibration.

5.1 Improved Specifications of the Social-Force Model

Pedestrian interactions are more complicated than suggested above. For example, it is known that the angle $\phi_{\alpha\beta}$ matters, at which two pedestrians α and β approach each other (see Fig. 8). Apart from this, the step sizes and, therefore, the speeds matter as well. In the following, we will shortly discuss two anisotropic models of pedestrian interactions:

Elliptical specification I: In Ref. [1], a generalization of (7) was formulated, which assumed that the repulsive potential

$$V_{\alpha\beta}(b) = AB e^{-b_{\alpha\beta}/B} \quad (8)$$

is an exponentially decreasing function of b with equipotential lines having the form of an ellipse directed into the direction of motion. The semi-minor axis $b_{\alpha\beta}$ is determined by

$$2b_{\alpha\beta} = \sqrt{(\|\vec{d}_{\alpha\beta}\| + \|\vec{d}_{\alpha\beta} - v_\beta \Delta t \vec{e}_\beta\|)^2 - (v_\beta \Delta t)^2} \quad (9)$$

in order to take into account the length $v_\beta \Delta t$ of the step size of pedestrian β , where $v_\beta = \|\vec{v}_\beta\|$. The reason for this specification is that pedestrians require space for movement, which is taken into account by other pedestrians.

The repulsive force is related to the repulsive potential via

$$\vec{g}_{\alpha\beta}(\vec{d}_{\alpha\beta}) = -\vec{\nabla}_{\vec{d}_{\alpha\beta}} V_{\alpha\beta}(b_{\alpha\beta}) = -\frac{dV_{\alpha\beta}(b_{\alpha\beta})}{db_{\alpha\beta}} \vec{\nabla}_{\vec{d}_{\alpha\beta}} b_{\alpha\beta}(\vec{d}_{\alpha\beta}). \quad (10)$$

Considering the chain rule, $\|\vec{z}\| = \sqrt{\vec{z}^2}$, and $\vec{\nabla}_{\vec{z}} \|\vec{z}\| = \vec{z}/\sqrt{\vec{z}^2} = \hat{\vec{z}}$, this leads to the explicit formula

$$\vec{g}_{\alpha\beta}(\vec{d}_{\alpha\beta}) = A e^{-b_{\alpha\beta}/B} \cdot \frac{\|\vec{d}_{\alpha\beta}\| + \|\vec{d}_{\alpha\beta} - \vec{y}_{\alpha\beta}\|}{2b_{\alpha\beta}} \cdot \frac{1}{2} \left(\frac{\vec{d}_{\alpha\beta}}{\|\vec{d}_{\alpha\beta}\|} + \frac{\vec{d}_{\alpha\beta} - \vec{y}_{\alpha\beta}}{\|\vec{d}_{\alpha\beta} - \vec{y}_{\alpha\beta}\|} \right) \quad (11)$$

with $\vec{y}_{\alpha\beta} = v_\beta \Delta t \vec{e}_\beta$. For $\Delta t = 0$, we regain the expression of (7).

Elliptical specification II: Recently, a variant of this approach has been proposed [14], assuming

$$2b := \sqrt{(\|\vec{d}_{\alpha\beta}\| + \|\vec{d}_{\alpha\beta} - (\vec{v}_\beta - \vec{v}_\alpha) \Delta t\|)^2 - \|(\vec{v}_\beta - \vec{v}_\alpha) \Delta t\|^2}. \quad (12)$$

In order to illustrate the effect of introducing velocity dependence in the social-force model, Fig. 9 depicts the resulting force fields when pedestrian

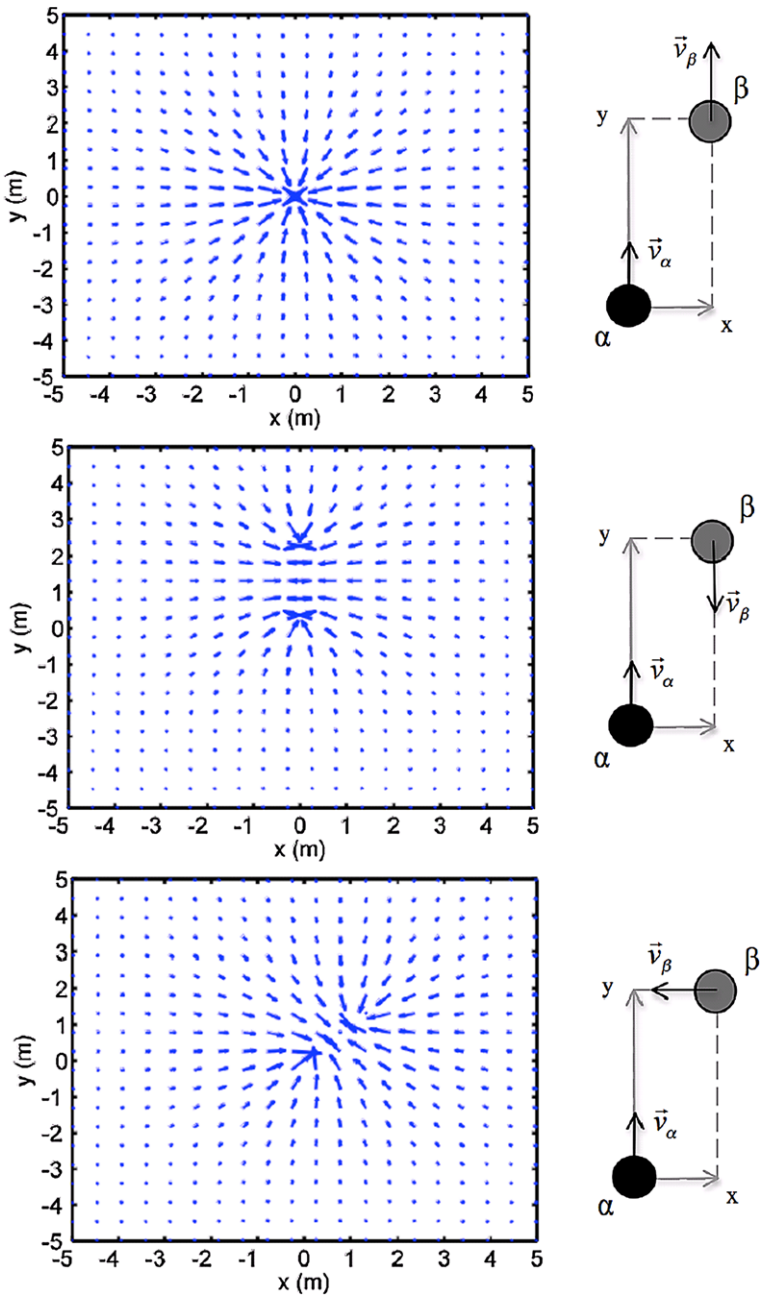


Fig. 9. The force fields resulting from the *Elliptical II* specification of the social-force model. The force fields shows how pedestrian α (located in the origin) is influenced of the fellow pedestrian β . Note that, in the top most figure, when $\vec{v}_\alpha = \vec{v}_\beta$, the Elliptical II specification is reduced to the Circular specification.

α reacts to pedestrian β , for different velocities, \vec{v}_β , of pedestrian β . If the velocity of the two persons are equal, the Elliptical II specification of the social-force model, is reduced to the original circular social-force model. However, when there is a difference in velocities, the force fields becomes stronger into the direction of the velocity difference.

6 Summary

The dynamics of how pedestrians interact has been discussed for varying degrees of crowd density. Starting by investigating the interaction between a few number of pedestrians, we find that the angular-dependence of interaction can be approximated by a half-circle in front of the pedestrian. The distance-dependence of the interactions, on the other hand, can be approximated by an exponential decay. When the crowd density is building up, the flow makes a transition from smooth flow to stop-and-go flow, and when the density is increasing even more, there is a second transition to crowd turbulence. These two transitions were identified while analyzing videos from the crowd disaster in Mina, Kingdom of Saudi-Arabia, in 2006.

Finally, a modification of the social-force model is discussed, which takes into account, not only distances and angles, but velocity differences as well.

Acknowledgements

The authors want to thank Salim Al-Bosta and HE Habib Al-Abideen for providing the high-density data from the pilgrimage to Makkah. Furthermore, they want to acknowledge their cooperation with Pradyumn Shukla, for working out the improved social-force-model specification.

References

1. D. Helbing and P. Molnár, Social force model for pedestrian dynamics, *Physical Review E* **51**, 4282–4286 (1995).
2. A. Johansson, D. Helbing, and P. K. Shukla, Specification of a microscopic pedestrian model by evolutionary adjustment to video tracking data, *Advances in Complex Systems*, **10**, 271–288 (2007).
3. K. Teknomo, Microscopic pedestrian flow characteristics: development of an image processing data collection and simulation model, Ph.D. Dissertation, Japan (2002).
4. S. P. Hoogendoorn, W. Daamen, and P. H. L. Bovy, Extracting microscopic pedestrian characteristics from video data, in: *Annual Meeting Transportation Res. Board Pre-print CD-Rom*, Mira Digital Publishing, Washington, DC (2003).

5. D. Helbing, L. Buzna, A. Johansson, and T. Werner, Self-organized pedestrian crowd dynamics: Experiments, simulations, and design solutions, *Transportation Science* **39**, 1–24 (2005).
6. D. Helbing, I. Farkas, and T. Vicsek, Simulating dynamical features of escape panic, *Nature* **407**, 487–490 (2000).
7. U. Weidmann, *Transporttechnik der Fußgänger* (Schriftenreihe des Institut für Verkehrsplanung, Transporttechnik, Straßen- und Eisenbahnbau **90**, ETH Zürich, 1993).
8. J. J. Fruin, Designing for pedestrians: A level-of-service concept, *Highway Research Record* **355**, 1–15 (1971).
9. M. Mori and H. Tsukaguchi, A new method for evaluation of level of service in pedestrian facilities, *Transportation Research A* **21**(3), 223–234 (1987).
10. A. Polus, J. L. Schofer, and A. Ushpiz, Pedestrian flow and level of service, *Journal of Transportation Engineering* **109**, 46–56 (1983).
11. A. Seyfried, B. Steffen, W. Klingsch, and M. Boltes, The fundamental diagram of pedestrian movement revisited, *J. Stat. Mech.*, P10002 (2005).
12. D. Helbing, A. Johansson, and H. Z. Al-Abideen, The dynamics of crowd disasters: an empirical study, *Physical Review E* **75**, 046109 (2007).
13. W. Yu and A. Johansson, Modeling crowd turbulence by many-particle simulations, *Physical Review E* **76**, 046105 (2007).
14. P. K. Shukla, Modeling and simulation of pedestrians, Diploma Thesis (2005).

Model-Based Real-Time Estimation of Building Occupancy During Emergency Egress

Robert Tomastik¹, Satish Narayanan², Andrzej Banaszuk², and Sean Meyn³

¹ Pratt & Whitney, 400 Main St., East Hartford, CT, USA

e-mail: robert.tomastik@pw.utc.com

² United Technologies Research Center, 411 Silver Lane, East Hartford, CT, USA

e-mail: NarayaS@utrc.utc.com, BanaszA@utrc.utc.com

³ University of Illinois at Urbana-Champaign, 1308 W. Main Street, Urbana, IL, USA

e-mail: meyn@uiuc.edu

Summary. This paper provides a viable and practical solution to the challenge of real-time estimation of the number of people in areas of a building, during an emergency egress situation. Such estimates would be extremely valuable to first responders to aid in egress management, search-and-rescue, and other emergency response tactics. The approach of this paper uses an extended Kalman filter, which combines sensor readings and a dynamic stochastic model of people movement. The approach is demonstrated using two types of sensors: video with real-time signal processing to detect number of people moving in each direction across a threshold such as an entrance/exit, and passive infra-red motion sensors that detect people occupancy within its field of view. The people movement model uses the key idea that each room has a “high-density” and “low-density” area, where high-density corresponds to a queue of people at a bottleneck exit doorway, and low-density represents unconstrained flow of people. Another key feature of the approach is that constraints on occupancy levels and people flow rates are used to improve the estimation accuracy. The approach is tested using a stochastic discrete-time simulation model of a 1500 square meter office building with occupancy up to 100 people, having a video camera at each of the three exits, and motion sensors in each of the 42 office rooms. The simulation includes stochastic models of video sensors having a probability of detection of 98%, and motion sensors with probability of detection of 80%. Averaged over 100 simulation runs and averaged over the evacuation time, the sensor-only approach produced a mean estimation error per room of 0.35 people, the Kalman filter with cameras only had a mean error of 0.14 people, and the Kalman filter with all sensors produced a mean error of 0.09 people. These results show that an effective combination of models and sensors greatly improves estimation accuracy compared to the state-of-the-art practice of using sensors only.

1 Introduction

This paper addresses the challenge of real-time estimation of occupancy in buildings or other critical infrastructure (such as subway stations, airports, and industrial facilities) during emergencies such as fire, hazardous gas releases, or chemical spills. Real-time estimates of occupancy can be provided to first responders (such as fire fighters and facility personnel) to accelerate search and rescue, for egress management, and to determine emergency response tactics (such as prioritization of resources for threat mitigation and suppression, and search). State-of-the-art agent-based models (ABM), which model and simulate individual occupant trajectories, are computationally expensive and unsuitable for real-time use. A reduced-order representation of the ABM is developed here and combined with building sensor data to provide fast and accurate estimates of occupancy during evacuation.

The occupancy estimation problem is to determine the number of people in different areas of a building (in each room, zone, floor, etc.) along with an estimation variance to establish a confidence level. The information that can be provided at various spatial scales will be required for decisions made by an incident commander (located outside the facility or en route), or a responder in the facility. The mean and variance of the estimate must be provided in real-time, with a short delay and fast update rate (e.g. 5 seconds or less). The occupancy estimator can utilize all types of sensing devices in a building, including video cameras, motion sensors, and access control. For video cameras, signal processing algorithms are available to detect the number of people moving in each direction across a threshold such as an entrance/exit to a floor or room.

The challenges of this problem are many. First, there are diverse modes of sensing available within a building, providing different types of measurement; for example, a video camera can detect the number of people in a room, whereas a passive infra-red motion sensor can only provide coarse occupancy information. Each sensor has a certain reliability and accuracy, where accuracy is typically specified by detection and false alarm rate. Second, not only are there diverse types of sensors, but the number of sensors in a building is large—typically 100's to 1000's. Thus, the volume of data to be processed in real-time is high. Third, despite the large number of sensors, there are many parts of a building which are not covered by sensors, making it difficult to measure occupancy in those areas. Finally, redundancy and distributed processing are highly desirable to ensure reliable estimation during a dynamically evolving emergency such as a fire.

The approach here uses an extended Kalman filter to provide real-time occupancy estimates and is novel in the combination of sensor measurements and a model of how people move during emergency egress, resulting in vastly improved estimation accuracy when compared to sensors-only approach. The approach draws on previous work [1], and extends it along several dimensions including occupancy estimation at the room level, an improved model

of people movement capturing the dynamic of people queuing at an exit, and inclusion of states for flow of people between rooms, allowing direct incorporation of flow sensing into the Kalman filter framework. Also, a projection of the filter-generated estimates is performed to create an estimate that falls within the constraints of non-negative occupancy and people flow. Lastly, an improved approach for propagation of estimation variance is presented which takes into account the nonlinearity arising from state space constraints (bounds on flow through doorways and occupancy).

2 Problem Definition

For clarity of presentation, we describe the estimation problem of a particular building, although the approach is generally applicable. The building has two floors, where we address the second floor. The floor plan is shown in Fig. 1. During an emergency egress, occupants typically use the nearest stairs to reach the first floor, where they then exit the building. Occupants do not use the elevator for emergency egress. The floor has area of 1,500 square meters, and has up to 100 occupants during normal business hours.

The end-users of the occupancy estimates desire to view occupancy at various spatial scales. For a building of this size, the spatial scales are: floor-level, zone-level, and room-level. Figure 2 shows the zone definitions that comprise the zone-level spatial scale.

The building has a look-down digital video camera above each of the three stairwell exits to the first floor. The cameras provide live video to a real-time digital signal processing software, which counts the flow of people moving in each direction through each exit. These cameras provide a probability of detection of 98% and a false alarm rate of once every four hours. Also, each of the offices and conference rooms have a passive infra-red motion sensor. This Boolean-output sensor can detect if the room is occupied with 80% accuracy.

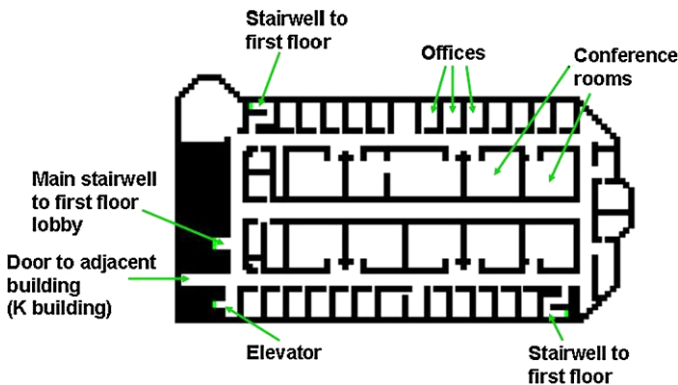


Fig. 1. Floor layout of example building.

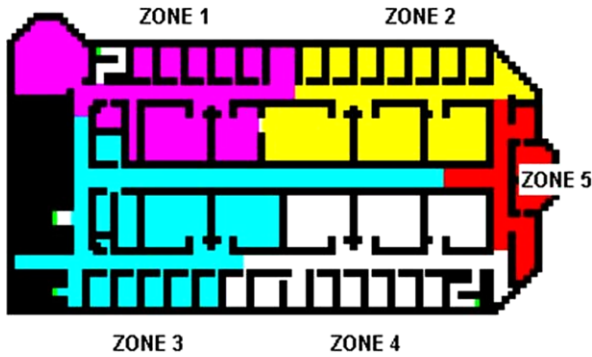


Fig. 2. Floor layout showing zone definitions.

The occupancy estimation problem is to determine the number of people in each room, each zone, and the total on the floor. Also, the estimate must have an estimation variance to establish a confidence level. The mean and variance of the estimate must be provided in real-time, with a short delay and fast update rate (e.g. 5 seconds or less). The occupancy estimator should utilize all sensing devices in the building.

3 Sensor-Only Estimator

To assess the benefit of our combined model-sensor estimator, we developed a sensor-only estimator, and compare test results of both approaches.

Commercial state-of-the-art products for estimating occupancy use video cameras mounted above (and pointing down) each exit/entry point to the building areas for which occupancy estimates are desired. These video cameras use digital signal processing to perform real-time count of people moving in each direction through each exit/entry. A running count is used for each area of the building, based on readings from the cameras that are at each entry/exit to each area.

We use this approach, but extend it to include use of motion sensors, and to estimate occupancy in each room (and thus each zone). The heuristic algorithm consists of three basic steps that are performed at each time sample. These steps are:

- (1) The 3 people-flow cameras at the exits are used to track total occupancy on the floor, by simply adding/subtracting camera readings from a running total.
- (2) Room level occupancy estimates for rooms where motion sensors are reading “unoccupied” are set to zero.
- (3) For other rooms, the running total for the building is divided equally among the number of these rooms.

4 Model-Based Estimator for Building Egress Mode

The estimation problem of this paper lends itself extremely well to using the extended Kalman filter (EKF) [2], which is a well-known and well-tested estimation method for combining sensor data with a model of dynamics (people movement, in this case). In this general approach, the dynamic model is represented as a non-linear dynamic stochastic state-space model:

$$x(t+1) = f(t, x(t)) + v(t), \quad (1)$$

where x is the vector of state variables (people occupancy and flow, to be described later), f is some non-linear function of time t and states $x(t)$, and $v(t)$ is process noise, representing the uncertainty in how people move in a building. The form of f for people traffic during emergency egress is presented later in this section.

The extended Kalman filter also requires a sensor model:

$$z(t) = h(t, x(t)) + w(t), \quad (2)$$

where z is the vector of sensor outputs, h is some function of t and state vector x , and w is sensor noise.

In this paper, we extend our previous approach [1] in several significant ways:

- An improved people-movement model that captures the dynamics of people queuing at bottleneck doorways, using the results of [3]
- Use of multiple types of sensors, specifically video cameras plus passive infra-red motion sensors, and
- Improved handling of state-space constraints in the estimation algorithm.

Each of the following sub-sections describe the above improvements.

4.1 People Movement Model

The need for real-time estimation requires a people movement model that is computational efficient, and of course is as accurate as possible. The “kinetic model” of [3] fulfills these key requirements, and is used here. The key idea of the kinetic model is to model the “high-density” and “low-density” area of each room, where high-density corresponds to a queue of people at a door, and low-density represents unconstrained flow of people. In the Kalman filter, we model as states for each room: the number of people in the high-density area of the room, the number of people in low-density area of the room, and the number of people moving into and out of each of these areas. Figure 3 shows a simple two-room example, where the states are thus defined as:

x_1 : No. of people in Area 1

x_2 : No. of people moving from Area 1 to Area 2

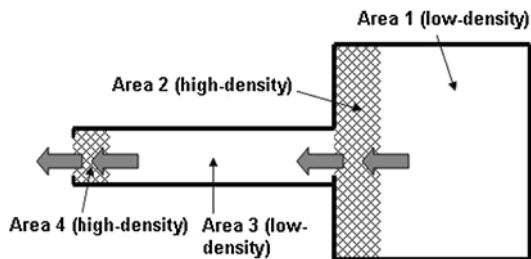


Fig. 3. Two-room example used to explain state variables.

x_3 : No. of people in Area 2

x_4 : No. of people moving from Area 2 to Area 3

x_5 : No. of people in Area 3

x_6 : No. of people moving from Area 3 to Area 4

x_7 : No. of people in Area 4

x_8 : No. of people exiting Area 4

The state-space model $f(x, t)$ for this simple example is:

$$x_1(t+1) = x_1(t) - x_2(t), \quad (3)$$

$$x_2(t+1) = \alpha_1 x_1(t), \quad (4)$$

$$x_3(t+1) = x_3(t) + x_2(t) - x_4(t), \quad (5)$$

$$x_4(t+1) = \min(C_1, \alpha_2 x_3(t), A - (x_4(t) + x_5(t) + x_7(t) - x_8(t))), \quad (6)$$

$$x_5(t+1) = x_5(t) + x_4(t) - x_6(t), \quad (7)$$

$$x_6(t+1) = \alpha_3 x_5(t), \quad (8)$$

$$x_7(t+1) = x_7(t) + x_6(t) - x_8(t), \quad (9)$$

$$x_8(t+1) = \min(C_2, \alpha_4 x_7(t)). \quad (10)$$

The parameters α_i represent the rate of flow of people, and can be dependent on time and states (please see [3] for details). The parameters C_i represent the maximum number of people that can move through each door at each time step. The parameter A is the maximum occupancy of the left-most room (areas 3 and 4), and the term $A - (x_4(t) + x_5(t) + x_7(t) - x_8(t))$ expresses the available space in the left-most room.

The state space model also includes a noise term $v(t)$. The Kalman filter algorithm uses a covariance matrix of this noise, where the dimension of the matrix corresponds to the number of states, and the matrix is diagonal. In the case of the people movement model, this covariance matrix represents the uncertainty in how people move from area to area. For states that represent occupancy levels (for example, in the two-room model, these are states 1, 3, 5, and 7), the diagonal term of the covariance matrix is zero since there is no uncertainty in these state space equations. For flow states, the diagonal term represents the uncertainty in flow. Specifically for flow states, using $x_2 =$

$\alpha_1 x_1(t)$ as an example, the term α_1 represents the rate at which the $x_1(t)$ number of people want to move to the area 2. We use the interpretation that α_i is the probability that each person will move to the next area. As a result, the probability distribution function of $\alpha_1 x_1(t)$ is a Poisson process with variance $x_1(t)\alpha_1(1 - \alpha_1)$. The variance is adjusted to account for constraints, as occur in the equations for x_4 and x_8 . In the implementation of this approach, the Kalman filter uses the state estimate of x_1 in place of the actual state, which is unknown.

4.2 Sensor Models

As described earlier in the problem statement, our estimation approach uses video cameras that count people flow, and uses motion detectors. The Kalman filter model $h(x(t), t)$ is described in this sub-section, using the two-room example.

For video cameras, assume that there are two video cameras—one at each exit of each room. This video camera thus measures states x_4 and x_8 directly, with noise term based on the probability of detection and probability of false alarm. Thus:

$$z_1(t) = x_4(t), \quad (11)$$

$$z_2(t) = x_8(t). \quad (12)$$

For motion sensors, assume that there is a motion sensor in each room. Thus, motion sensor 1 measures whether $x_1 + x_3 \geq 1$ and motion sensor 2 measure whether $x_5 + x_7 \geq 1$:

$$z_3(t) = \begin{cases} P_1 & \text{if } x_1 + x_3 \geq 1 \\ 0 & \text{if } x_1 + x_3 < 1, \end{cases} \quad (13)$$

$$z_4(t) = \begin{cases} P_2 & \text{if } x_5 + x_7 \geq 1 \\ 0 & \text{if } x_5 + x_7 < 1 \end{cases} \quad (14)$$

where P_1 is a parameter whose value is the typical number of people occupying the first room (and P_2 is likewise). The variance for the terms in $w(t)$ for these motion sensors are based on the reading of the sensor. If the sensor is reading “unoccupied,” then the sensor is considered reliability in its value of $z_i = 0$, and thus the variance term is based on the sensor probability of detection. If the sensor is reading “occupied,” then the value of its reading is considered very noisy because the sensor is not able to count the number of people in its range of detection; thus, the noise covariance is set very high (such as to the maximum flow).

4.3 Accounting for Constraints in the Estimate

The Kalman filter can be interpreted as a recursive algorithm to compute the conditional mean (and in fact the entire conditional distribution) of occupancy based on sensor measurements. The filter is not designed to take into

account hard constraints such as non-negativity of occupancy, upper bounds on occupancy, and bounds on the rate of occupancy flow.

Let \mathcal{R} denote a convex region to which the state process $x(t)$ is known to evolve. At each time step, the Kalman filter computes estimation covariance matrix P (see [2] for details). For any vector x we define,

$$[x]_{\mathcal{R}} = \arg \min_{y \in \mathcal{R}} \{(y - x)^T P^{-1} (y - x)\}. \quad (15)$$

This is the projection of x onto \mathcal{R} in the weighted Euclidean norm, with weighting matrix specified by the inverse of the covariance matrix P .

The new estimate is then determined by taking the Kalman filter-produced (unconstrained) estimate and projecting it onto \mathcal{R} using the above equation. The reason for the non-standard projection is to ensure stability of the filter. In particular, in the ideal setting in which there is no state noise and $x(t)$ is known to evolve in \mathcal{R} for each time t , it can be shown that these estimates strictly out-perform those of the unmodified Kalman filter with respect to the weighted norm. This then establishes consistency of the algorithm [4].

4.4 Accounting for Constraints in the Covariance Estimate

As can be seen in the state space equations, the flow states can be constrained. These constraints can be factored into the predicted covariance calculated by the Kalman filter. These constraints have the effect of reducing uncertainty in the estimate, because the constraints act as an upper bound on the possible values of the estimates of the flow state variables, as shown in Fig. 4.

Figures 4a and 4b illustrate how the probability distribution function (PDF), which is generated based on the predicted mean estimate for a state variable and the covariance associated with the state variable, is modified based on flow constraint values. The covariance estimate for each flow state is modified to be the variance of the modified PDF, as in Fig. 4b.

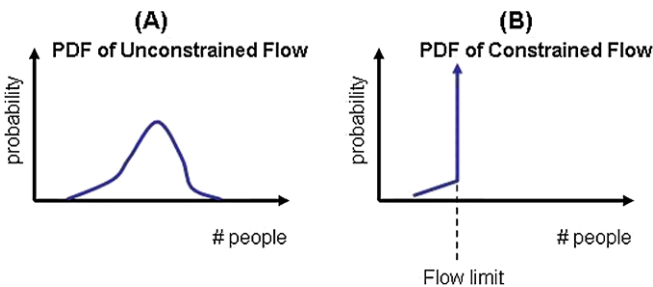


Fig. 4. Modification of PDF due to flow constraints.

5 Simulation Test Results

The extended Kalman filter is tested using a stochastic discrete-time simulation model of people movement during egress, including stochastic simulation of sensor performance. The model is of the building shown in Fig. 1, and has average occupancy of 1.4 people per room at the start of the evacuation, which lasts about 100 seconds. The building has a video camera at each of the three exits, and each video camera can detect number of people crossing the exit in each direction. The accuracy of this measurement is 98%. Each of the 42 rooms has a motion sensor that detects if the room is occupied at 80% accuracy. The simulation was run for three different estimators: a sensor-only estimator, the extended Kalman filter using only the three cameras, and the extended Kalman filter using all cameras and motion sensors.

Averaged over 100 simulation runs and averaged over the evacuation time, the sensor-only approach produced a mean estimation error per room of 0.35 people, the Kalman filter with cameras only had a mean error of 0.14 people, and the Kalman filter with all sensors produced a mean error of 0.09 people. Figure 5 shows a comparison between the actual occupancy in a building zone (comprising several rooms) and that from the model-based estimator, where all video cameras and motion sensors are used. Figure 6 shows a room-level result, and shows the impact of using motion sensors.

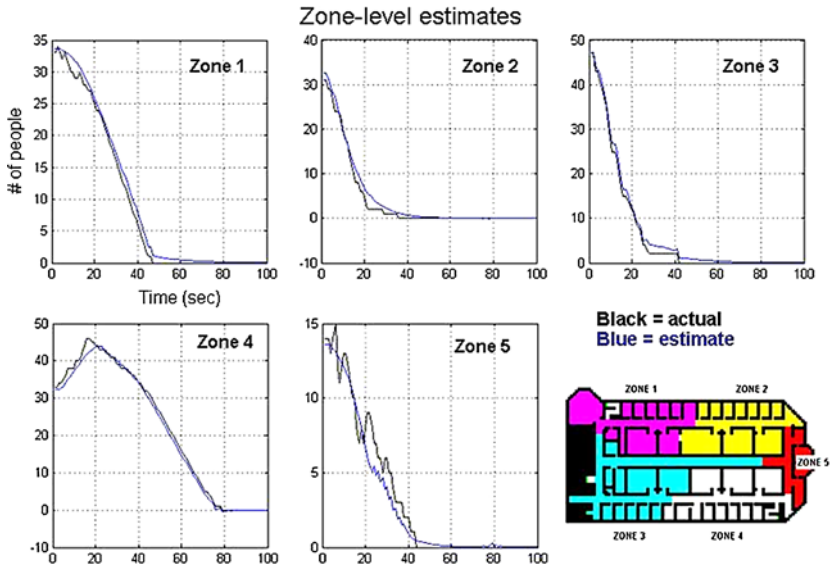


Fig. 5. Simulation test results showing zone-level occupancy estimates and actuals.

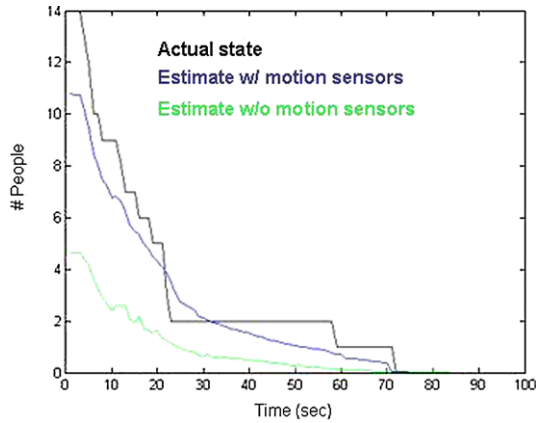


Fig. 6. Simulation test results showing conference room occupancy estimates and actuals.

6 Conclusion

In summary, the model-based estimation approach reduces error by an average of 74% compared to using sensors only. Another valuable conclusion is that even though motion sensors indicate only whether a room is occupied, use of such information can still be of value, reducing estimation error by 36%. The computational requirements of the extended Kalman filter are such that the update rate of 5 seconds or less is easily met.

References

1. R. Tomastik, Y. Lin, and A. Banaszuk. Video-based estimation of building occupancy during emergency egress. In *Proceedings of the American Control Conference*, pp. 894–901, IEEE, Seattle, 2008.
2. Y. Bar-Shalom, X. Rong Li, and T. Kirubarajan. *Estimation with Applications to Tracking and Navigation*, Wiley-Interscience, New York, 2001.
3. S. Burlatsky, V. Atrazhev, N. Erikhman, and S. Narayanan. A novel kinetic model to simulate evacuation dynamics. In these proceedings.
4. T.-L. Chia. *Parameter identification and state estimation of constrained systems*. PhD thesis, Case Western Reserve University, 1985.

Experiments on Evacuation Dynamics for Different Classes of Situations

Jarosław Was

Institute of Automatics, AGH University of Science and Technology,
al. Mickiewicza 30, 30-059 Kraków, Poland
e-mail: jarek@agh.edu.pl

Summary. The article presents experiments on pedestrian evacuation in different situations. The presented experiments involved evacuation of a lecture room. A group of 31 students took part in four evacuation experiments. The experiments are devoted for three classes of situations: normal conditions, controlled evacuation (noncompetitive evacuation) and panic (competitive evacuation).

1 Introduction

Pedestrian dynamics modeling is an important issue in multidisciplinary fields of science (architecture, sociology, psychology and computer science etc.). The knowledge of phenomena connected with pedestrian movement is very important in the process of developing public facilities.

Two methods of computer simulation seem to be particularly popular: the first is Social Forces Method [1] based on Molecular Dynamics and the second Cellular Automata, in the broad meaning of the term ([2–5] etc.).

The transmission for of new issues into practical solutions connected with safety is a very significant aspect of research in this field. Thus, there is a need for realistic and efficient computer simulations and, at the same time, a need for data for validation and verification of proposed models.

The paper presents experiments in pedestrians evacuation for modeling a situation of a room evacuation by a group of pedestrians in normal conditions, in a situation of controlled evacuation and in panic. Some models and computer simulations were described in the previous works of the author [6–11].

Figure 1 presents exemplary view of application PIESI. The application is dedicated for pedestrians evacuation in different conditions [6, 8]. The model is based on CA algorithms SPA (Strategical Pedestrian Abilities) and SPA-BNE (BottleNeck Effect) presented in [7].

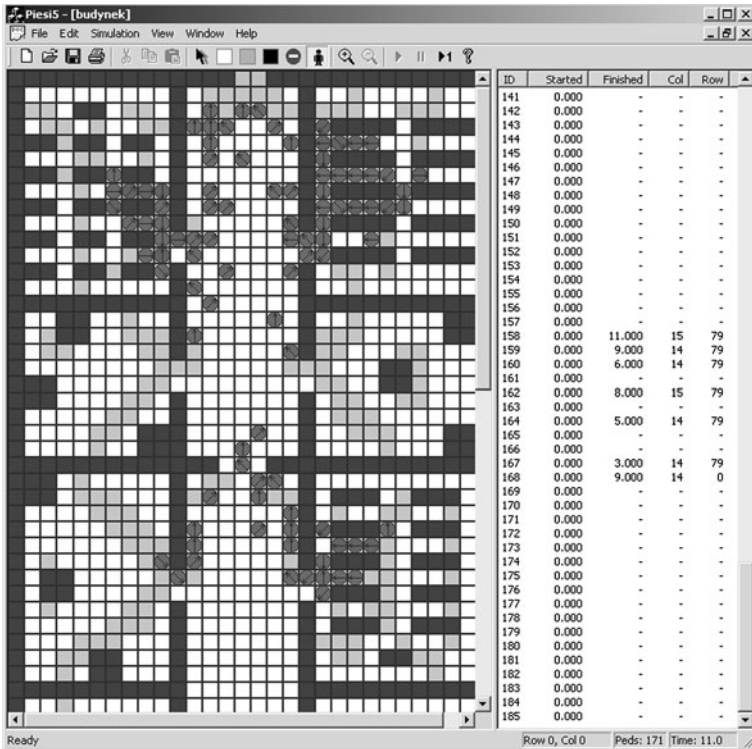


Fig. 1. Exemplary screen shot of building evacuation—application PIESI presented in [6, 7].

2 Experiments

2.1 Description

The presented experiments involved evacuation of a lecture room. A group of 31 students took part in four evacuation experiments during which, and they were supposed to simulate different situations: panic (two experiments), controlled evacuation, and normal conditions. All participants were identified by number (the same for all experiments) and they all started evacuation in the same place. Figure 2 shows the topology of the lecture room and the situation plan. As we can see in Fig. 2 the lecture room had two accessible exits: rear exit (number 1) in the top left-hand corner of the picture and front exit (number 2) in the bottom. We can also see three video cameras which were installed for record all of the experiments (K1, K2, K3 on the Fig. 2). Timing lines (check points) were situated at the front and the rear door (dash lines in the front of K1 and K2).

Before the experiments all the participants were informed about the assumptions and tasks for the current experiment:

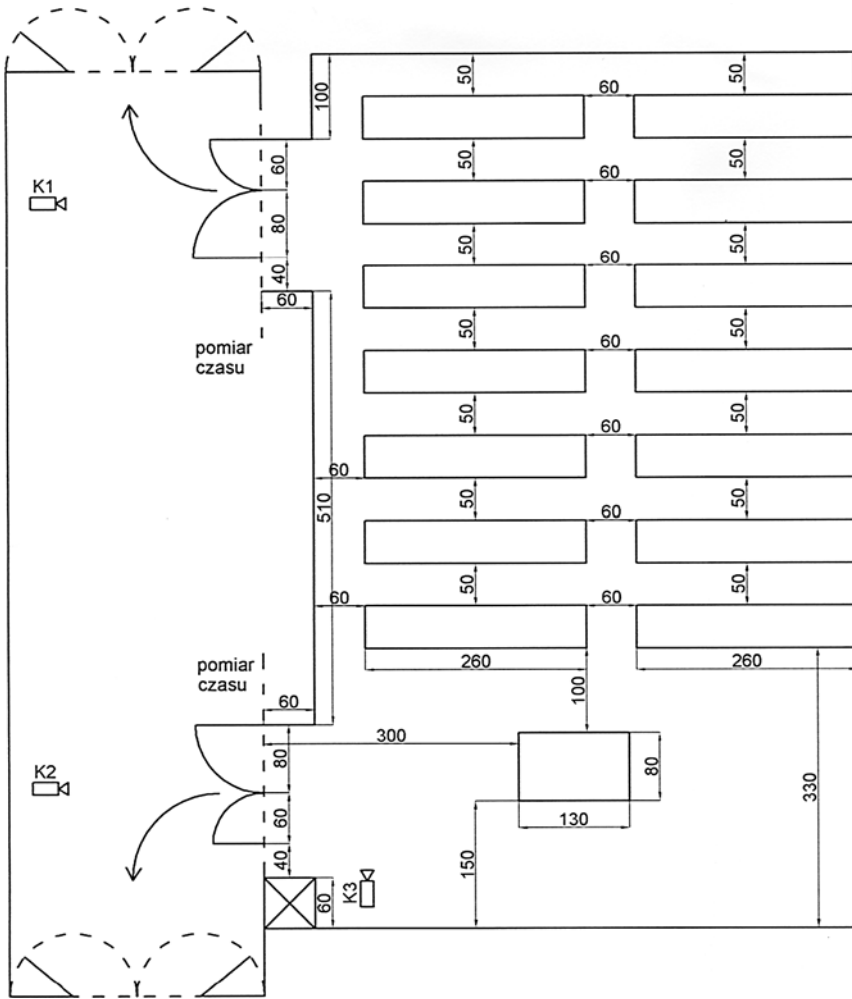


Fig. 2. Topology of the lecture room and layout of the experiment.

- Panic simulation (experiments 1 and 2)—the aim for each participant is to gain possibly the best *individual evacuation time*.
- Controlled evacuation—the aim for each participant is to gain possible the best *evacuation time of all participants*.
- Normal condition—the aim for each participant is to leave the room in normal conditions (timing is not important).

During all the experiments the rear exit (double door) was fully open, while the front exit (also double door) has been fully open only for the 1st experiment, for experiments 2, 3 and 4 only one wing of the front exit was open.

After experiments 1, 3 and 4 each participant filled in a short questionnaire regarding the criteria for choosing the particular exit: the distance to exits, crowd density in the exits neighborhood, following the others, exit throughput etc.

2.2 Results

Figures 3 and 4 presents the results of the panic simulation (experiments 1 and 2). The initial participants allocation is shown, in accordance to the topology presented in Fig. 2. The pedestrian ID is presented at the top part of each square, while the evacuation time is shown at the bottom. If the time score is underlined it means that this participant chose the front door. If time score is not marked, the rear exit was chosen.

Figure 5 presents the results of controlled evacuation. In the figure egress times distribution in experiment 3 is presented.

Figure 6 presents pedestrian timing results in normal conditions.

During the first and the second experiments (panic) we could observe strong rivalry among pedestrians (collisions, blocking others etc.). Whilst experiments number 3 and number 4 were characterized by a high degree of cooperation between participants.

Table 1 presents evacuation times for each exit. The last column of the table presents the time ratio for the front and rear exit. This factor could be understood as “equability” of evacuation.

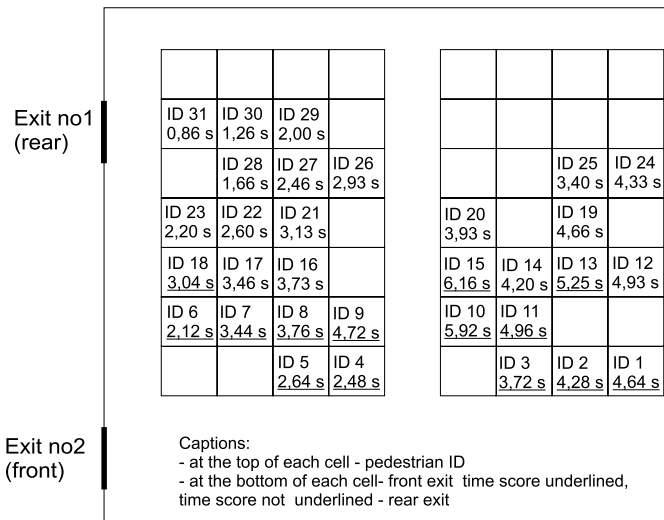


Fig. 3. The initial allocation of pedestrians in the lecture room. Evacuation times for all participants for two experiments devoted for the situation of panic. The table presents experiment 1.

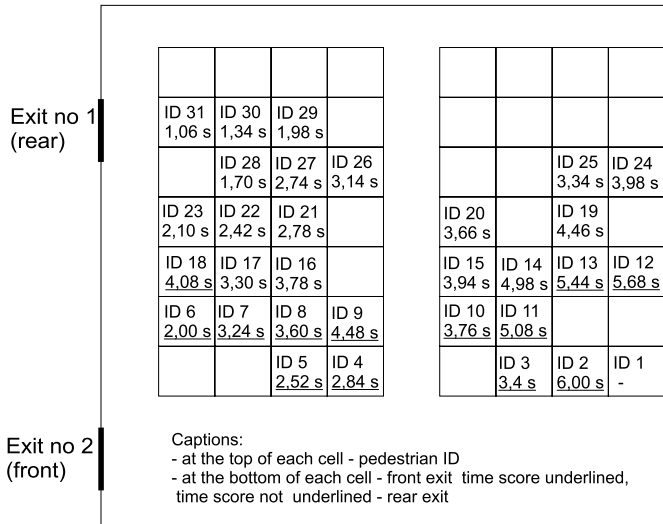


Fig. 4. The initial allocation of pedestrians in the lecture room. Evacuation times for all participants for two experiments devoted for the situation of panic. The table presents experiment 2.

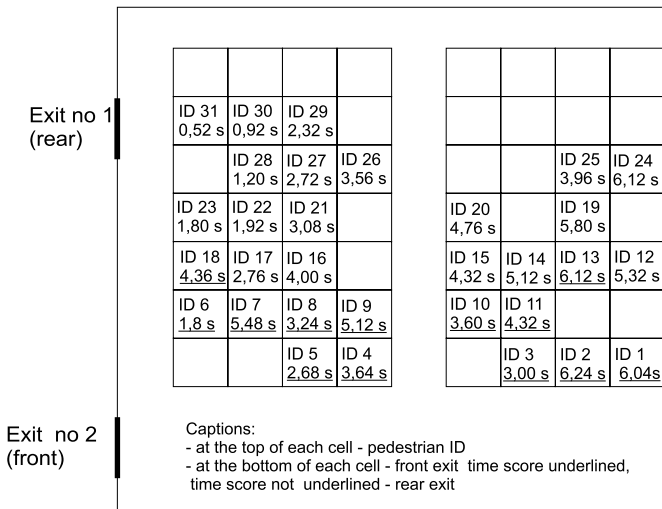


Fig. 5. The initial allocation of pedestrians in the lecture room. Evacuation times for all participants for controlled evacuation are presented in the table—experiment 3.

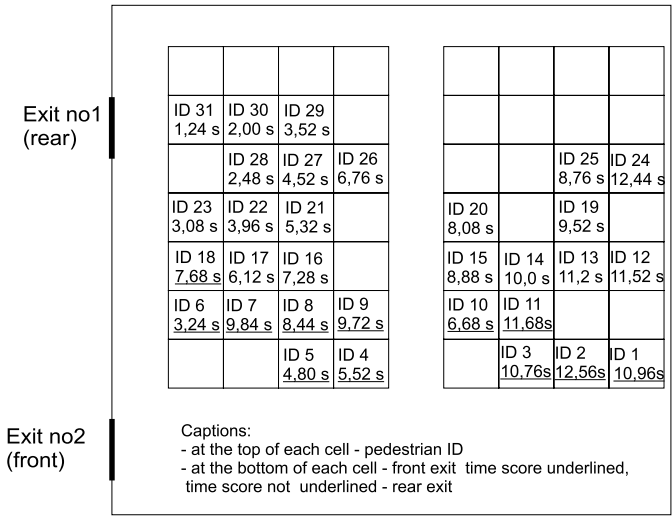


Fig. 6. The initial allocation of pedestrians in the lecture room. Evacuation times for all participants for normal conditions in the table—experiment 4.

Experiment number	Evacuation time		Time ratio front/rear
	front exit	rear exit	
1	6.16 s	4.93 s	80.03%
2	6.00 s	4.98 s	83.00%
3	6.24 s	6.12 s	98.08%
4	12.56 s	12.44 s	99.04%

Table 1. Evacuation time for particular exits.

As we can notice in Table 1 the total evacuation time was the shortest for the second experiment, similar for the first and the third experiment and about two times as low for the last experiment. It is very characteristic that times for each exit in a given evacuation experiments are equalized.

Table 2 presents the factors which had influenced the decision making process during the evacuation. The question a participant had to answer was: Which exit should I head towards, to minimize evacuation time? Each participant could point more than one answer in the questionnaire. We could notice that the most important criterion of choosing the exit during evacuation is *distance*. The second criterion crowd density in exit has a maximum value for controlled evacuation, while for normal condition it becomes the lowest. For normal condition, the criterion of following the others has the highest value.

	Distance	Crowd density in exit neighborhood	Following others	Exit throughput
Panic simulation	90.32%	29.03%	3.23%	25.81%
Controlled evacuation	87.10%	41.94%	12.90%	16.13%
Normal condition	73.33%	23.33%	26.67%	23.33%

Table 2. Criteria of choosing a particular exit—data from the questionnaire.

3 Conclusions

The carried out experiments constituted an attempt at modeling different classes of situations.

The tasks for participants for the situation of panic and controlled evacuation caused two different types of behavior: competitive and cooperative. During the two panic experiments with the situation of panic strong rivalry could be observed (collisions, pushing, forcing the way etc.). On the other hand controlled evacuation induces cooperation among participants (collision avoiding, enabling others to pass by, etc.). Similar cooperative behavior could be observed during the experiments with normal conditions.

Total evacuation times are similar for panic and controlled evacuation simulations. In the author's opinion, this could be due to two main reasons: a relatively small group of participants and they determination which does not have high level as for real panic.

In the questionnaire the participants pointed out distance from an exit as the main reason for choosing the particular evacuation exit but other reasons were also pointed out (Table 2).

There are some interesting questions and problems connected with the experiments. The first is a pedestrian motivation. Generally, no problems with participant motivation and experiment organization occurred during the presented experiments, but if a group of people were larger these problems could occur.

The next question is, whether a group of people could be the same for all of the experiments? On the one hand, the answer is yes, because we can observe the reaction of *the same group in different situations*. On the other hand, the answer is no, because we can expect that chosen route and reaction of a participants would *be the same in a new situation as for the previous one*.

An interesting added value of experiments carried out with the same group of people is equalizing the evacuation times for each exit. This effect of pedestrian *learning* was explicitly noticeable and it proves purposefulness of evacuation exercises.

References

1. D. Helbing, P. Molnar: A Social Force Model for Pedestrian Dynamic, *Phys. Rev. E* 51 (1995) 4284–4286.
2. C. Burstedde, K. Klauck, A. Schadschneider, J. Zittartz: Simulation of Pedestrian Dynamics Using a 2-Dimensional Cellular Automaton, *Physica A* 295 (2001) 507–525.
3. J. Dijkstra, A.J. Jessurun, H. Timmermans: A Multi-Agent Cellular Automata System for Visualising Simulated Pedestrian Activity, *Proceedings of ACRI*, (2000) 29–36.
4. C. Gloor, P. Stucki, K. Nagel: Hybrid Techniques for Pedestrian Simulations, *Proceedings of 6th ACRI*, *Lecture Notes in Computer Science* 3305, Springer, Berlin (2004) 581–590.
5. H. Klüpfel: Cellular Automaton Model for Crowd Movement and Egress Simulation, PhD thesis, Duisburg-Essen (2003).
6. J. Was, B. Gudowski: Simulation of Strategical Abilities in Pedestrian Movement Using Cellular Automata, *Proceedings of 24th IASTED MIC Conference*, Innsbruck (2005) 549–553.
7. J. Was: Intelligent Behaviour Modelling Algorithms in Pedestrian Dynamics Issues Using Nonhomogeneous Cellular Automata, PhD thesis, AGH University of Science and Technology (2006).
8. J. Was: Cellular Automata Model of Pedestrian Dynamics for Normal and Evacuation Conditions, *Proceedings of Intelligent Systems Design and Applications*, Wroclaw, IEEE CS, Washington (2005) 154–159.
9. E. Dudek–Dyduch, J. Was: Knowledge Representation of Pedestrian Dynamics in Crowd. Formalism of Cellular Automata, *Proceedings of ICAISC*, *Lecture Notes in Artificial Intelligence* 4029 (2006), Springer, Berlin 1101–1110.
10. J. Was, B. Gudowski, P.J. Matuszyk: Social Distances Model of Pedestrian Dynamics, *International Conference on Cellular Automata for Research and Industry*, Perpignan, France, *Lecture Notes in Computer Science* 4173, Springer, Berlin (2006).
11. B. Gudowski, J. Was: Modeling of People Flow in Public Transport Vehicles, *Proceedings of PPAM*, *Lecture Notes in Computer Science* 3911, Springer, Berlin (2005) 333–339.

Prediction and Mitigation of Crush Conditions in Emergency Evacuations

Peter J. Harding¹, Martyn Amos¹, and Steve Gwynne²

¹ Manchester Metropolitan University, Manchester, UK

e-mail: m.amos@mmu.ac.uk

² Hughes Associates, Inc, Boulder, CO, USA

e-mail: sgwynne@haifire.com

Summary. Several simulation environments exist for the simulation of large-scale evacuations of buildings, ships, or other enclosed spaces. These offer sophisticated tools for the study of human behaviour, the recreation of environmental factors such as fire or smoke, and the inclusion of architectural or structural features, such as elevators, pillars and exits. Although such simulation environments can provide insights into crowd behaviour, they lack the ability to examine potentially dangerous forces building up *within* a crowd. These are commonly referred to as *crush conditions*, and are a common cause of death in emergency evacuations.

In this paper, we describe a methodology for the prediction and mitigation of crush conditions. The paper is organised as follows. We first establish the need for such a model, defining the main factors that lead to crush conditions, and describing several exemplar case studies. We then examine current methods for studying crush, and describe their limitations. From this, we develop a three-stage hybrid approach, using a combination of techniques. We conclude with a brief discussion of the potential benefits of our approach.

1 Introduction

The events of 9/11 were widely seen and examined in the safety community and beyond. The catastrophic outcome and the minutiae of the evacuation have been examined by numerous official agencies, research organisations, media outlets, as well as Hollywood. Given this, the events of the day are incredibly well known; possibly more so than any other recent event.

Tall buildings are designed based on the assumption that an evacuation is managed, i.e. that the evacuation will take place in stages, if required, with only certain sections of the population evacuating at any one time. The evacuation will usually take place from those floors closest to the incident, then occur from more distant floors. This assumption is key to the successful evacuation of these tall structures; the stair capacity is calculated based on the assumption that the majority of the population follow the evacuation

procedure. This means that the stair capacity within the structure will not be sufficient for the simultaneous evacuation of the entire population.

After 9/11 the assumption that tall buildings can be evacuated in a phased and controlled manner is being questioned. Instead, it is often suggested that evacuees will be reluctant to remain behind in a structure, fearful of a failure in structural integrity similar to that experienced in the twin towers. Given the nature of the incident on 9/11 and the possible consequences of remaining within the building (either by choice or through compulsion), it is now suggested that residents may choose to ignore the instructions of a staged procedure and instead move to the stairwells. This may then overload the available staircase capacity.

Given this is the case, the consequences of failure should be examined. If there is a failure in the acceptance of procedure then either the failure should be made as graceful as possible, or measures should be taken to resolve the issue; in either case, an understanding of the consequences of failure is vital.

It should be noted that during these scenarios it is not assumed that the conditions are dependent upon the existence of panic, which is difficult to predict and rarely the dominant evacuee behaviour [1]. In reality, it has been found that panic and irrational behaviour are a direct effect of the deteriorating conditions, rather than the cause of the deterioration itself. Here we are assuming that crush conditions may develop simply because of the overloading of a route and may therefore be influenced by architectural, procedural, or behavioural factors.

One of the consequences of a full evacuation from a tall structure, that was originally designed for phased evacuation, is the overloading of an escape route in a relatively short period of time. One of the most dangerous consequences of such an incident is that the exits, such as those at the base of stairways, would become overloaded, leading to many evacuees arriving at a bottleneck; i.e. the exit component is used above and beyond its design capacity. This may then lead to conditions similar to those observed at the Rhode Island [2] and Gothenburg [3] incidents, where crush incidents and falls were evident and lead to blocked egress routes and injuries. It is therefore critical for the safety of tall structures to develop an understanding of: (1) Exactly when these conditions may develop? (2) What factors need to be present in order for crush conditions to occur? (3) When do these conditions become critical? (4) How can we establish the possible consequences of this type of incident and design against them?

Here, we outline a program of work that will enable the assessment of architectural and procedural designs in order to establish whether they are prone to crush conditions developing in certain scenarios, what the consequences of this might be, and how we might best mitigate against this event. The development of a similar tool is mentioned in the recommendations within the 9/11 report [4]:

NIST recommends that tall buildings be designed to accommodate timely full building evacuation of occupants when required in building-specific or large-scale emergencies such as widespread power outages, major earthquakes, tornadoes, hurricanes without sufficient advanced warning, fires, explosions, and terrorist attacks. Building size, population, function, and iconic status should be taken into account in designing the egress system. Stairwell capacity and stair discharge door width should be adequate to accommodate counter-flow due to emergency access by responders.

Improved egress analysis models, design methodologies, and supporting data should be developed to achieve target evacuation performance for the building population by considering the building and egress system designs and human factors such as occupant size, mobility status, stairwell tenability conditions, visibility, and congestion.

Although numerous egress models exist that are able to simulate general movement, none are able to simulate all of the conditions highlighted in NIST recommendations, along with a comprehensive crush model. Developing such a model, that is publicly available and that can be embedded into existing egress tools, meets an identified need and will allow for a broad and vital examination of these situations.

2 Definition of Crush Conditions

There are many factors that play a part in the initial formation of crush conditions during an evacuation, these can be classified under the broad headings of spatial, temporal, perceptual, procedural, and cognitive components.

2.1 Spatial

The spatial components of crush conditions are the simplest to quantify. They relate to the ratio of space available for egress to the number of persons that are expected to use the escape routes. Fruin defined this metric as the “level of service” [5], and highlighted the level at which the population density has the potential to facilitate the formation of crush as “Level of Service F”, which is the density at which a single individual would have, on average, less than 0.46 m² of space available to them. It should also be noted that the International Maritime Organisation (IMO) considers an evacuation to be unsafe if, for 10% of the overall evacuation time, the density of the evacuees reaches 4 persons per square metre [6]. This is due to the fact that, even at relatively low levels of force, prolonged exposure to “light” crush conditions may still cause serious injury or death.

2.2 Temporal

Temporal factors of egress vary, and depend heavily upon the rate at which conditions change. The RSET (Required Safe Egress Time), defined as the elapsed time between the initialisation of an evacuation and the final evacuee reaching safety [7], i.e. the time required for a complete evacuation under ideal circumstances. The ASET (Available Safe Egress Time), defined as the total time *available* for evacuation [7], is a far more specific metric, as it will vary depending on the catalyst for evacuation (i.e. the nature of the emergency). Traditionally, the RSET and ASET metrics have been used to determine whether or not the occupants of a building could evacuate under specific conditions. Generally, a structure could be considered safe if the ASET value exceeds that of the RSET, i.e. there is more time available for an evacuation than would be required. The rate at which conditions change can compound time constraints, as the ASET calculation will change dynamically with the changing conditions. The Rhode Island nightclub fire (see Sect. 3.1), is a good example of this, and shows how the rapidity with which an incident escalates can place severe time constraints on the evacuating population.

2.3 Perceptual and Cognitive Factors

Perceptual and cognitive factors that lead to the formation of crush conditions are intrinsically linked, as an individual must rely on their perception of events in order to decide upon a course of action. The individuals' perceived level of threat plays a large part in this, as it has the most direct effect on the decision making process. Whilst the perception of threat plays a great part in the decision making process, the relationship between these two factors is highly complex, and can result in individuals displaying a wide range of behaviour, from the altruistic at one end of the scale, right through to highly competitive egress behaviour, e.g. running, pushing, etc.

The perception of information also plays a key part in the formation of crush. During emergency situations, it is often found that information relating to the current conditions is slow to propagate throughout a crowd of people, e.g. the evacuees that are placed further back in a crowd may not be aware of the conditions further ahead. This has been found in many situations, such as the Hillsborough disaster (see Sect. 3.4), where the people attempting to enter a structure were unaware of the already dangerously overcrowded conditions that existed inside. In these cases the persons at the rear of a crowd can compound the situation by producing additional force that will propagate forward through the crowd, and also by limiting the extent to which the pressure could be alleviated by inadvertently blocking the most immediate exit routes.

2.4 Procedural

The procedural components of crush were already alluded to (see Sect. 1), and centre around the inability, or unwillingness, of evacuees to follow strict evacuation plans in emergency situations. This type of problem is extremely common in public buildings, where a great number of the occupants will be unfamiliar with the structure and have little, or no, knowledge of the evacuation plans, e.g. hospitals, town halls, museums, stadiums, etc. When an evacuation takes place under these circumstances the crowd will often attempt to leave by the most familiar route, generally the route by which they entered, even though there may be exits in closer proximity. An example of this type of behaviour can be found in the Rhode Island nightclub incident (see Sect. 3.1), where the majority of the crowd converged at just one point of escape, even though there were numerous other exits available.

2.5 Summary

The formation of crush conditions within crowds is a highly complex, emergent phenomena, and the causes of this cannot be explained by simply attributing it to the presence of panic within the crowd, which is widely regarded as being somewhat of a fallacy. We suggest that crush conditions can only be reliably defined as a combination of all the factors mentioned above, which culminate in the individuals' inability to fully control their direction and speed of movement, thus leading to an increase in the physical forces that they are subject to.

3 Case Studies

Here we present case studies representing situations where the formation of crush conditions have led to both serious injuries and fatalities. Each case study also represents some failure within a system (e.g. failure to limit the capacity of a structure to safe levels, failure to adhere to official guidelines or fire laws, failure to follow crowd control policies, etc.). These types of failure are often observed in cases where the evacuation of a building leads to the death or injury of many people. Failures of this kind are common, and we believe that they should be expected, and be considered during the design of buildings, the creation of evacuation plans, and especially in simulated evacuation exercises.

3.1 Rhode Island Nightclub

The Station Nightclub, Rhode Island, was the scene of a tragedy when, on February 20th 2003, a fire during a rock concert caused 100 fatalities and significant injuries [2]. The fire started when the band's pyrotechnics ignited

the flammable soundproofing foam that surrounded the stage, and quickly filled the club with dense, choking smoke. The fire spread from the stage, igniting a large portion of the ceiling, and within five minutes of the initial ignition those outside the club observed flames breaking through a portion of the roof.

Despite the existence of four possible exits, the majority of the crowd headed for the most familiar exit; the entrance to the club. This exit point was soon overwhelmed, and people began to trip or fall during their escape. The official time-line of the fire (compiled by NIST [2]) states that just 1 minute and 42 seconds after the start of the fire, there existed a “pile” of people, blocking the main exit and making further egress through that route impossible.

3.2 Gothenburg Dancehall

When fire broke out in a dancehall in Gothenburg, Sweden, on October 28th 1998, it claimed the lives of 63 people and injured over 180 others. The first floor venue in question was packed to over double its 150 capacity, with officials estimating that there may have been over 400 people in attendance. Eyewitness accounts of the incident state that population density prior to the start of the fire was already at dangerously high levels, with a number of the occupants observing that there were so many people present that they were unable to dance [3]. Shortly before midnight, a fire was discovered in one of the two stairways leading out of the first floor dancehall, and those near to the affected area began to evacuate. No announcement was made to the remaining occupants, and some survivors who had been at the far end of the hall when the fire was initially discovered stated that they smelled smoke but had initially believed it to be cigarette smoke and felt no need to evacuate. As the full evacuation began, the one remaining exit to the building quickly became overwhelmed, and the mass of evacuees began to trip or fall over others, further diminishing the capacity of the exit.

3.3 E2 Nightclub Incident

In Chicago’s E2 nightclub on Feb 17th 2003, the security guards’ use of pepper spray, to intervene during an altercation, became the catalyst for an evacuation that claimed the lives of 21 patrons [8]. When the security guards released the pepper spray in an enclosed space, the effects of the chemical compound on the surrounding crowd were significant. Those close to the attack began to rush toward the exit in an attempt to escape the pepper spray, which by this point was already spreading around the club. As the initial wave of evacuees made their way through the club, those who had not witnessed the incident began to fear for their safety, especially as it became obvious that some form of chemical agent was present.

Within seconds the entire crowd, consisting of over 1500 people, rushed towards the main exit. The door to the street opened inwards, whilst the door leading to the dance floor opened outwards. As people rushed from the club, the upper door flew outwards, pushing those on the upper landing down the steep flight of stairs. As more people attempted to exit, they were forced on top of the fallen evacuees, and the bodies began to “stack up” and block the exit. It was the tremendous pressure placed upon the fallen evacuees that caused the 21 deaths during this incident. The most common cause of death was asphyxiation.

3.4 Hillsborough

The Hillsborough disaster [9] (Sheffield, UK), claimed the lives of 96 people and caused the hospitalisation of a further 300. Due to the heightened public interest in the incident (the match had been transmitted live on English television), and also because of the multiple perceived failures on the part of the authorities, the Hillsborough disaster has become one of the most thoroughly investigated crowd disasters in living memory.

The tragedy at Hillsborough stadium occurred when police stewarding the match made the decision to open an extra set of gates, intended as an exit, in order to relieve the extreme levels of congestion that were forming as the crowds tried to enter the stadium through the turnstiles at the Lepping’s Lane end of the ground. These gates did not have turnstiles, and the result was an influx of up to 5,000 fans through the narrow corridor that lead into the standing terrace. The sudden arrival of so many additional fans pushed the capacity of the central pens far above their legal maximum, and soon a dangerous crush formed at the front of the stands. Those fans still entering the stadium were unaware of this, and continued to attempt to enter the stand as the people inside were slowly crushed against the crowd barriers and fences at the front of the stands. The conditions at the front of the terrace became so bad that most of the 96 victims died from asphyxiation, or other crush related injuries, within five minutes of the game starting.

4 Previous Work in the Field

In general, each crush detection method that has been used to date can be classified into one of two generic groups; explicit methods and implicit methods. These two generic methodologies are outlined below, along with a brief discussion of their relative strengths and weaknesses.

4.1 Implicit

The implicit methodology is the original crush detection approach, and is still highly popular, being used in a large number of simulation models [10]. This

methodology relies on the expert analysis of factors such as population density (see Sect. 2.1), behavioural analysis, and environmental considerations. The analysis of conditions within these models, therefore, is left to the engineer, who interprets the output of the simulation to determine whether crush conditions have occurred.

Implicit modelling does not take into account the possibility that evacuees may exhibit any competitive egress behaviours (e.g. pushing), as there is no accurate method for simulating these behaviours without the inclusion of force calculations. This makes it ideally suited for general evacuation simulations; i.e. timely evacuations under “ideal” conditions.

As the exact force being exerted upon individuals is never calculated, the precise physical danger that may exist in the evacuation can never be quantified. The only assertion that can be made, based on an implicit analysis, is that crush conditions *may* form during the evacuation in question. The benefit of this approach is that, as the physical force calculation are not performed, it requires far less processing power than other methods.

There are too many implementations of the implicit methodology to list here but a popular, well documented example is Simulex [11], from Crowd Dynamics Ltd.

4.2 Explicit

The explicit modelling of crush conditions incorporates an assessment of crush into the model itself, and therefore requires less user analysis than the implicit approach. Often based on the calculation of Newtonian force values, and generally operating in 2-dimensional space, explicit methodologies may be used to detect the presence of crush conditions much more precisely than would be possible with implicit modelling techniques. By simulating the exact forces being exerted by each individual, and enabling the propagation of forces throughout a crowd, the explicit methodology can be used to measure the exact amount of force that any individual is subject to. This, therefore, offers the possibility of *quantifying* the dangers that individuals may face, which is not possible using the implicit modelling techniques.

Whilst the explicit methodologies offer an accurate measure of the forces acting within a crowd, the calculations needed to measure force require much more processing power than an implicit implementation, so there exists a definite trade-off between the two techniques.

The most well-known implementation of this methodology is the Social Forces Model [12], which combines the force equations mentioned above with the modelling of the social forces acting within crowds. Although the original Social Forces Model was created as a learning tool, rather than an full-featured simulation environment, the model has recently been incorporated into the FDS+Evac Simulation environment [13].

5 Our Proposed Approach

We propose a three stage approach to this problem, consisting of separate processes for the *identification*, *qualification*, and *quantification* of crush conditions. By employing different methods for all three stages of the analysis, we believe that the entire process may be completed at relatively low computational expense. We hope to implement these techniques as part of a suite of applications, that would offer existing egress simulations the possibility of including either full or partial crush analyses, depending on the level of accuracy required.

Two of the three techniques that we propose are still relatively novel and untested, so will require validation before they would be suitable for integration into existing environments. Each methodology will be fully tested as stand-alone applications, but a full validation will be required before the concepts are proven. At present, the team intends to attempt to integrate the applications into the open source simulation environment FDS+Evac, to enable full validation of the models, including historical data validation and peer validation [14].

5.1 Identification

In order to first identify crush conditions, we propose treating their formation as a simple phase transition, similar to those found in many social and biological systems [15]. In many of these systems a point is reached at which a change (often an abrupt change) can be observed, this change is characterised as a movement away from one general rule of system behaviour to another, different set of observable behaviours that dictate the state of the system as a whole.

In egress situations, a crowd will usually head towards the most familiar exit, often forming groups either before or during this action. The evacuees that make up these groups will have similar trajectories to their closest neighbours and will be travelling at a similar speed (i.e the flow, within each group, can be considered laminar). This would form the general rule for the ordered state of this system (see Fig. 1A). If the evacuees are impeded in any way during their exit (e.g. they come across an obstacle in their path, or reach a congested area), they will reduce their speed and be forced to change their directions of movement, or forced to remain stationary (i.e. the flow becomes non-laminar, or turbulent). This would form the general rule for the disordered state of this system (see Fig. 1B).

Buckingham's *II* Theorem [16] is a key theorem in dimensional analysis, and can be used to create a set of dimensionless variables that allow the analysis of an unfamiliar system, i.e. a system for which the equations governing its behaviour are either partially or wholly unknown. We will apply this theorem to the agent data within an egress model, to reduce the system to a number of dimensionless quantities, which can then be analysed to ascertain the state of

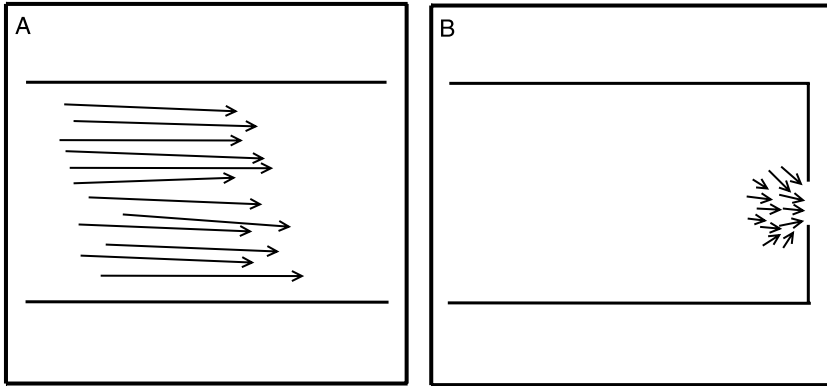


Fig. 1. *Slide A* shows an example of the movement vectors of evacuees during the ordered state of the system, with all vectors showing a good deal of similarity. *Slide B* shows example vectors during the disordered state, with the vectors varying a great deal more in both direction and magnitude.

the system at any one time. The advantage of this approach is that both the agent’s physical variables (e.g. speed, direction, mass) and their decision making variables (e.g. perceived level of threat, tendency toward competition) are considered, which will provide a more comprehensive analysis of crush than could be achieved by movement variables alone.

Further analysis is achieved by the use of Mutual Information (MI) [17], a technique that has been used to quantify the similarity of two signals. This methodology was first used by Wicks et al. [18] to detect phase transitions within a well-known flocking model [19], and was found to accurately identify the point of phase transition even when only a subset of the agents’ data were analysed. We will employ a similar methodology to detect the formation of crush conditions within localised groups of agents, using the MI method to quantify the extent to which our “idealised” (ordered) agent-state (see Fig. 1), differs to that of the current state. We will dynamically restructure agents into groups, based on their current locale, and treat each group as a system within its own right, tracking a subset of each “sub-system” to identify the earliest stages of crush formation without the need to track *every* agent throughout the *entire* evacuation.

5.2 Qualification

To qualify the presence of crush conditions within the crowd, we intend to use a time-series, neural network classifier [20] to analyse the agent variables and movement patterns. This will give an indication of the amount of pressure that is likely being exerted on the individual in the crowd. The classifier acts as a statistical data analysis tool, and is configured to recognise the conditional similarities shared by individuals affected by the onset of crush conditions.

The neural network approach has been selected for two main reasons. Firstly, after the initial training program, the neural network approach requires far less computational power to make its classification than other statistical analysis techniques, reducing the classification during normal running conditions to little more than matrix arithmetic. The reduction in computation, in relation to other techniques, will free up system resources for utilisation by other tasks. Secondly, the method of classification used in a neural network is highly robust, as it does not rely on any “system specific” variables, which makes the deployment of this technique possible across a wide range of existing egress simulations, without the need for extensive configuration.

By employing a time-series, neural network [21] (i.e. a neural network that accepts input in the form of sequential data representing changes over time), we also hope to identify the qualitative similarities of individuals exhibiting competitive egress behaviour. It will enable us to analyse growing behavioural trends, rather than just classify an agent’s behaviour at one precise moment in time.

To train the network, we will collect time-series agent data from a “full-force” simulation, i.e. a simulation in which a physical force model is running, which should enable the network to recognise the qualitative similarities that individuals affected by crush share. We hope that training the network using this type of data will allow the network to associate the existence of a variety of conditions to the presence of crush, therefore negating the need to engage a physics engine for all subsequent simulation runs.

5.3 Quantification

To fully quantify the effects of force propagating through a crowd, a physical force model is employed, based on the explicit crush detection method mentioned previously (see Sect. 4.2). We currently plan to implement this physical force model as a rigid body dynamics engine [22], with representations of such variables as mass, velocity, friction, and force propagation, modelled according to the laws of Newtonian mechanics. The engine will solve simplified physical equations in two dimensional space, resulting in good approximations [23] of force calculations that can be completed in as little time as possible.

The possibility of modelling this phenomena as a soft body dynamical system will be investigated, as recent research has highlighted the need to incorporate calculations for the compression forces acting within crowds [24], but our initial research into the feasibility of this approach leads us to believe that the calculations involved would be prohibitively computationally expensive at this time.

5.4 Hybrid Approach

The methodologies outlined above may each be employed individually, to add differing degrees of crush analysis to a simulation, but we also propose a conceptual framework, within which all three methodologies could be combined

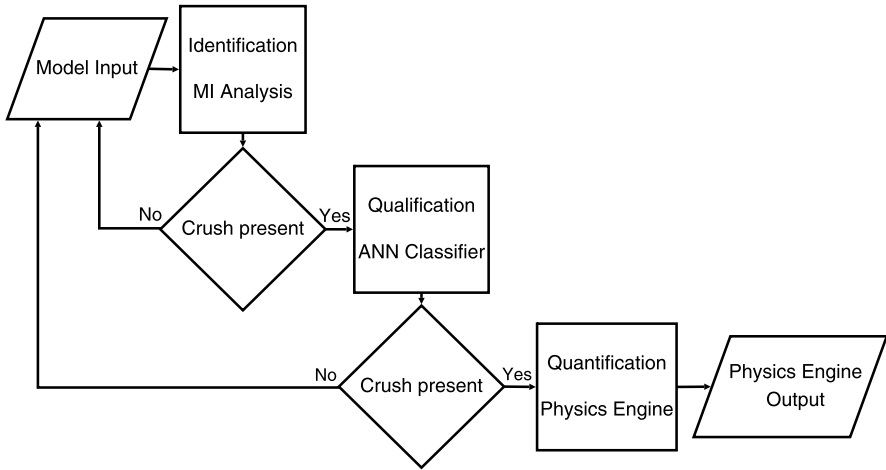


Fig. 2. Process flow diagram depicting the interactions between the three application, according to the suggested framework.

to create an analytical tool that applies crush calculations intelligently. This approach will allow us to retain the accuracy of force calculations whilst reducing the computational expense associated with it.

The proposed approach requires the analysis of conditions based on locale, i.e. analysing conditions in different locations as if they were separate systems, and the escalation of analytical accuracy upon confirmation of crush. Figure 2 shows the flow of control across the three applications.

By applying the more accurate analyses *only* once crush has been confirmed by the previous method, the most computationally expensive techniques will only be applied to affected areas, rather than across the entire behaviour space. This leaves us with the possibility of having different analyses being applied simultaneously, within the same simulation, but in different geographical locales, e.g. the identification method is running on a corridor where the flow of pedestrians is laminar, whilst at the exit of a stairwell, where a crowd has formed, the analysis would be carried out by the quantification method. The advantage of engaging each application in this way is that it will ensure that the most serious effects of crush, the build up of forces within a crowd, are measured precisely, without calculating force for all agents within the simulation.

6 Benefits of Our Approach

This approach to crush analysis will provide a new tool, suitable for integration into existing simulation environments, that will allow engineers the ability to incorporate different levels of analysis for each specific simulation. The

inclusion of such analytical methods will add a further dimension to traditional models, and further the realism of current simulation tools.

The addition of crush analysis techniques into models will allow engineers to better test the robustness of evacuation procedures, carry out more realistic recreations of historical incidents, and more comprehensively investigate the safety of architectural designs. It is the aim of this project to supply further tools to the evacuation sciences community that will allow this to happen, and act as a further weapon in the armoury of the engineers, technicians, and analysts that operate in this field.

7 Conclusion

The need for further crush analysis techniques has been clearly stated, and the phenomena that we wish to simulate precisely defined. We have presented three methodologies for the detection, confirmation, and measurement of crush conditions within a simulation environment, and a theoretical framework within which they could operate in unison, reducing computational expense without a reduction in accuracy.

The short-term goal of this research is simply to prove the suitability of these concepts for use in the analysis of crush, by the creation of a prototype implementation that may be used for experimentation. In the long-term we are looking to integrate this prototype into a larger simulation environment, to prove its feasibility as an “off the shelf” component to an evacuation model.

Acknowledgements

This work is partially supported by the Dalton Research Institute, Manchester Metropolitan University.

References

1. J. Sime. Escape behaviour in fires and evacuations. In *Design Against Fire*, Chapman & Hall, London, 1994.
2. W. Grosshandler, N. Bryner, D. Madrzykowski, and K. Kuntz. Report of the technical investigation of the station nightclub fire. Technical report, NIST, 2005.
3. E. Comeau and R.F. Duval. Dance hall fire Gothenburg, Sweden, October 28, 1998. Technical report, National Fire Protection Association, 2000.
4. Final report on the collapse of the World Trade Center towers. Technical report, NIST, 2005.
5. J. Fruin. *Pedestrian Planning and Design*. Metropolitan Association of Urban Designers and Environmental Planners, Alabama, 1971.

6. IMO. Interim guidelines for evacuation analyses for new and existing passenger ships. Technical report, International Maritime Organisation, 2002.
7. J. Sime. An occupant responses escape time (ORET) model. In *Proceedings of the First International Symposium*, 1998.
8. J. Wilgoren. 21 die in stampede of 1,500 at Chicago nightclub. *New York Times*, 18.02.2003.
9. The Hillsborough stadium disaster: final report. Technical report, U.K. Home Office, 1989.
10. E. Kuligowski. Review of 28 egress models. In *Workshop on Building Occupant Movement During Fire Emergencies*, 2004.
11. P.A. Thompson and E.W. Marchant. A computer model for the evacuation of large building populations. *Fire Saf. J.*, 24:131–148, 1995.
12. D. Helbing, I. Farkas, and T. Vicsek. Simulating dynamical features of escape panic. *Nature*, 407:487–490, 2000.
13. J.-M. Kuusinen. Group behavior in FDS+evac evacuation simulations. Published online, August 2007.
14. J. Kleijnen and R. Sargent. A methodology for fitting and validating metamodels in simulation. *Eur. J. Oper. Res.*, 120:14–29, 2000.
15. M. Beekman, D.J.T. Sumpter, and F.L.W. Ratnieks. Phase transition between disordered and ordered foraging in Pharaoh’s ants. *Proc. Natl. Acad. Sci. USA*, 98(17):9703–9706, 2001.
16. M. Longair. *Theoretical Concepts in Physics: An Alternative View of Theoretical Reasoning in Physics*, 2 edition. Cambridge Univ. Press, Cambridge, 2003.
17. A. Kraskov, H. Stogbauer, and P. Grassberger. Estimating mutual information. *Phys. Rev. E*, 69, 2004.
18. R. Wicks, S. Chapman, and R. Dendy. Mutual information as a tool for identifying phase transitions in dynamical complex systems with limited data. *Phys. Rev. E*, 75(5), 2007.
19. T. Vicsek, E. Ben-Jacob, A. Czirok, I. Cohen, and O. Shochet. Novel type of phase transition in a system of self-driven particles. *Phys. Rev. Lett.*, 75:1226, 1995.
20. M.H. Hassoun. *Fundamentals of Artificial Neural Networks*. MIT Press, Cambridge, 1995.
21. A. Kehagias and V. Petridis. Predictive modular neural networks for time series classification. *Neural Netw.*, 10(1):31–49, 1997.
22. J. Wittenburg. *Dynamics of Multibody Systems: Dynamics of Systems of Rigid Bodies*. Springer, Berlin, 2007.
23. R. van Zon and J. Schofield. Numerical implementation of the exact dynamics of free rigid bodies. *J. Comput. Phys.*, 225:145–164, 2007.
24. L.U. Chunxia. Analysis of compressed force in crowds. *J. Transp. Eng. Inf.*, 7(2):98–103, 2007.

Start Waves and Pedestrian Movement— An Experimental Study

Christian Rogsch

Institute for Building Material Technology and Fire Safety Science,
University of Wuppertal, Pauluskirchstr. 11, 42285 Wuppertal, Germany
e-mail: christian@rogsch.de

Summary. Pedestrian movement has different quantities, e.g. densities and walking velocities. But these quantities can only be measured during a dynamic process of movement, thus they are depending on each other. But an important point is: How do people start walking? In this contribution it will be shown how fast people start walking and how this process is influenced by the initial density. Furthermore the velocity of the start wave moving through the group of pedestrians is determined.

1 Introduction and Experimental Setup

The experiment has taken place at the 4th PED Conference in Wuppertal, Germany. The location was a parking area in front of the conference building, so that the markers for the parking space could be used for measurements. Participants of these experiments were conference delegates from all over the world. It should be noticed that all of these participants are familiar with the field of pedestrian and evacuation dynamics. In total, six different runs with different participants were performed.

At the start of each experiment, all participants were positioned along a 22.5 m long line. The initial density (initial numbers of pedestrians) is varied during the six runs. After the start signal (a count-down: 3-2-1-start) all pedestrians start walking in normal fashion along the line without overtaking, thus the movement is only one-dimensional. The experimental setup is shown in Fig. 1. The experiment was recorded by using video camcorders. Videos can be obtained from the author by email inquiry.

2 Results and Discussion

At high densities (ca. 2.09–2.27 peds/m) a start wave from left to right can clearly be recognized. The speed of this start wave is ca. 1.07 m/s. A higher start density was not possible, this can be seen on the video recordings. At

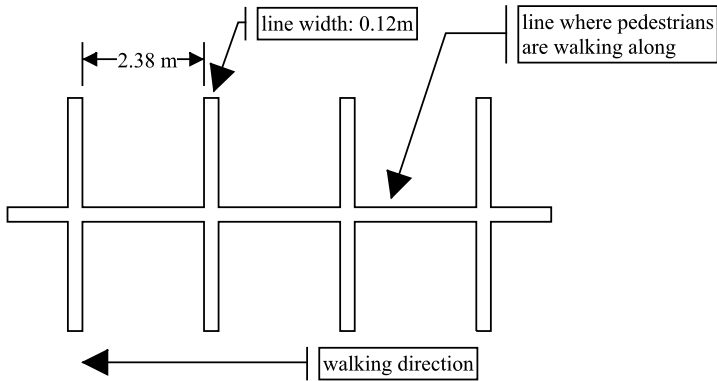


Fig. 1. Experimental setup. Pedestrians are placed on the middle line and start walking from right to left.

Run #	# of pedestrians	Density (peds/m)	Time until last pedestrian reaches start position (s)	Time until last pedestrian starts (s)	Start wave velocity (m/s)
1	51	2.27	40	21	1.07
2	47	2.09	38	21	1.07
3	25	1.11	23	1	no start-wave
4	29	1.29	23	1	no start-wave
5	19	0.84	17	0	no start-wave
6	16	0.71	15	0	no start-wave

Table 1. Quantitative results of the experiments.

lower start densities (ca. 1.11–1.29 peds/m) the start wave does not exist because of the low density. Pedestrians are able to start walking at the signal, but during the walking process a stop-start wave can be observed. Very low densities (ca. 0.84–0.71 peds/m) do not show any start or stop wave. At the lowest density (0.71 peds/m) the median walking velocity of the last pedestrian is 1.5 m/s, at a density of 0.84 peds/m it is 1.33 m/s thus it could be assumed that free walking velocity could be reached at this initial density. All measurements and calculations of the experiment are shown in Table 1.

Acknowledgements

The author would like to thank all participants of the experiment. Furthermore he would like to acknowledge the conference organizers for their support.

Clearance Time for Pedestrian Crossing

Craig R. Childs, Taku Fujiyama, and Nick Tyler

Department of Civil, Environmental, and Geomatic Engineering, University
College London, Gower Street, London, UK
e-mail: pamela@transport.ucl.ac.uk

Summary. Analysis of free flow pedestrian dynamics is not sufficient when considering pedestrian crossings. In addition, there is no current evidence of how pedestrian flows are affected by the inclusion of additional items like prams or trolley style luggage. This paper presents work that starts to consider the complex dynamics related to pedestrian crossings.

1 Purpose of the Study

It is impossible to design a pedestrian environment without physical restrictions; pedestrians will have to encounter restrictions at some point on almost every journey. An example of this is a pedestrian crossing where there is guard railing or comparable restriction at both sides of the crossing (often the case when there is a central reservation to break crossing one road into two actions). These barriers can cause problems when people are trying to leave the road for the relative safety of the footpath, but their path is blocked by people waiting to cross at the next pedestrian phase or are crossing in the opposite direction. In addition, it is of interest to see if there is a difference in how people cross when they are unencumbered, and when they have an additional item, for example, are pushing a pram, or pulling trolley type luggage behind them. If pedestrians are often left on the crossing after the pedestrian crossing phase because there are difficulties getting people onto the footpath, it is likely that the more vulnerable pedestrians will stop using such areas. With more information on how people cope with such barriers at pedestrian crossings, simulations incorporating different layouts could help redesign pedestrian environments; making the crossing appear to be safer, and thus potentially increasing its use, whilst minimizing the additional time required for pedestrian crossing phases. To facilitate these simulations, we need a better understanding of how people cope with barriers in pedestrian crossing situations. Free flow walking speeds are particularly useful when pedestrians can be considered as a relatively homogenous group with a single purpose, for ex-

ample evacuation. For most everyday activities, pedestrians are certainly not homogenous and they rarely have a single purpose. Thus we need to test for situations where there are different barriers to progress. The results may also be useful for how people with additional items (for example trolley luggage or a pram) negotiate other path constrictions where there is pedestrian flow in more than one direction. Knoblauch et al. [1] were not unusual in their intentional exclusion of pedestrians pushing strollers, prams, wheelchairs, or with suitcases/luggage from their research. However, we need more information on how such people use pedestrian environments.

As Tyler [2] discussed, to achieve improved access for disadvantaged people, it is better to assess performance based, rather than dimension based criteria. In this context, from an individual perspective, most people would be able to get through the gap between the barriers. However, with more people crossing the performance will suffer, slowing crossing times and potentially increasing stress levels for leaving the crossing. With recent disability based requirements such as the DDA [3] in the UK and the ADA [4] in the United States of America, we should be trying to include rather than exclude more disadvantaged people. The concept of performance based measures was further discussed in Shi et al.'s [5] evaluation of pedestrian environments. In particular, they noted that crossing zones are important areas, where there is no steady state flow of pedestrians and their direction is open.

2 Methodology

The Pedestrian Accessibility and Mobility Environment Laboratory (PAMELa [6]) provides a safe location where environmental factors can be controlled and people monitored whilst carrying out required tasks. In this work, the PAMELa facility was arranged as a section of road approximating a signal controlled pedestrian crossing. The road crossing approximated one lane (Short Cross: 3.6 m) and two lanes wide (Long Cross: 7.2 m). Barriers were located on either side of the 'road' representing space (2.4 m) between street furniture (for example guard railing). The road surface was dry 400 mm × 400 mm chamfered concrete slab. Ambient lighting was approximately 300 lux.

There were 16 participants, mostly students with 3 people representing people with limited mobility; a slow walker, someone pushing a pram, and someone with luggage. For comparison, some tests were completed with the same people, but without the pram or luggage.

The participants were asked to "cross the road" when the light signal changed to green. The numbers crossing from one side to the other were controlled: in some tests people crossed unopposed, in others some participants crossed in the opposite direction. We recorded video from 4 CCTV cameras situated around the laboratory. Each barrier was covered by its own camera view and there were two camera views covering the whole platform. Using Noldus Observer 5.0 [7] software we noted the time between "green light on";

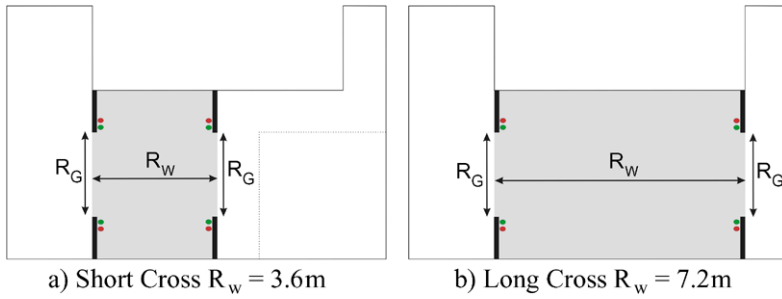


Fig. 1. Platform layout. The gap widths between barriers ($R_G = 2.4\text{ m}$) were the same on each side of the ‘road’ for each crossing width tested (R_w). The space on the other side of the barrier was for people waiting to cross, or clear the road area; the equivalence of the footway section of the street.



Fig. 2. CCTV cameras were set up monitoring each barrier, with two further cameras giving platform overviews.

when the last participant passed the first barrier; and when the last participant passed the second barrier. These times were recorded for people travelling in each direction. The time was noted when an approximation of the centre of body of the participant crossed the line between the barriers.

Start up times are defined here as time from green light on, to when the person passes the first barrier. This is the equivalent of leaving the footpath and entering the road section of a real pedestrian crossing. People were asked only to cross when the green light was on. For the larger groups, this time sometimes reached the full 6 seconds that the green light was on, thus not everyone managed to cross every time.

3 Results

It was noted that participant behaviors corresponded to the characterization noted by Fugger et al. [8], where approximately half of the participants looked

ahead, approximately a quarter anticipated the light change, and the other quarter looked distracted. As the definition of start up time in this experiment was different to that used by Knoblauch et al. [1], the time taken for the last person to cross the first barrier was longer, often around 6 s when there were greater than 10 people waiting to cross.

The following results consider the trials where equivalent numbers were crossing in each direction for the two lengths of crossing: a small number of people (5) opposing a larger number (11). It was difficult to get the same number of tests for each crossing distance and gap width without losing people who couldn't cross within the 'green' period; hence, for the Long Cross with luggage and pram, the groups had 4 and 12 people, rather than 5 and 11.

As may be expected the time taken to clear the starting area increased as the number of people crossing increased.

Including people pushing a pram and pulling trolley luggage increases the time taken to cross for both the Long and Short Cross widths (Table 1). The difference in time taken between with and without extras is not statistically significant for the Short Cross for the smaller group, but is for the larger group ($t\ 0.01$). This result is repeated for the Long Cross, where the larger group takes significantly longer when the pram and luggage are included ($t\ 0.04$). The larger group takes longer to cross both the Short and Long Cross widths than the smaller group.

Table 1 only included values from repeated tests comparing groups of 4/5 and 11/12 people. Table 2 shows a summary of the additional time taken for the last person to pass the second barrier, ignoring the group's size, and only considering whether or not the pram, luggage, or both were included in the test group. The Long Cross did not take twice as long as the Short Cross even though the Short Cross was half the Long Cross distance. This is partly due

Road width	SG; no P/L	SG; with P/L	LG; no P/L	LG; with P/L
Short Cross	9.6 ± 0.82	10.3 ± 1.07	9.8 ± 0.33	11.3 ± 1.44
Long Cross	12.3 ± 2.08	12.1 ± 2.15 ^a	13.8 ± 1.03	15.7 ± 1.85 ^b

SG—small group of 5 people; LG—large group of 11 people; no P/L—there were no additional items; with P/L—the pram and trolley luggage were used; ^agroup size reduced to 4 people; ^bgroup size increased to 12 people

Table 1. Time taken to pass the second barrier with and without additional items, for each group size (mean time to cross in seconds ± one sd).

	Short Cross	Long Cross
Groups without pram or luggage	11.06	13.15
Mean additional time required		
Luggage only	0.64	1.26
Pram only	1.66	2.09
Both pram and luggage	1.61	2.84

Table 2. Mean time (s) to pass second barrier for all group sizes.

to the time taken for people to acknowledge the start signal and partly due to the manoeuvring required to get through the gap between the barriers. For the Short Cross, there were occasions when some people from the opposite side were trying to get through the barrier before some people had left their side of the crossing. The inclusion of the pram caused greater delays than including just the person with the luggage or having neither in the group.

3.1 Experiment Examples

The examples shown in Fig. 3 include the pram and the luggage in each of the Short and Long Cross tests. The ‘lane formation’ as described by Daamen and Hogendoorn [9] was a common feature of the tests. Example 1 shows how the first people from the small group (blue) have arrived at their second barrier before the last person from the large group has passed their first barrier. Due to the direction of the lane of people passing the upper first barrier, the upper lane of the smaller group (blue) had to wait until the last (red) person had passed the barrier before they could leave the road part of the crossing. With the additional distance in the Long Cross people were less likely to be blocked by the lane passing round the barrier onto the road (Example 2).

If there were people in front, the person pushing the pram would drift out into clear space. This is indicated in Example 1, where this person approached the footpath at an angle. It is likely that this reduced the risk of the person pushing the pram into the back of someone as they approached the far side of the crossing; giving themselves more clear space to manoeuvre. However, it was noted that on some occasions, the person had difficulty manoeuvring the pram round the tight corner of the barrier. This caused the longer delays for getting people off the crossing. As Older [10] discussed, external factors such as gradient and surface condition can affect pedestrian movement, but the presence of additional pedestrians is one of the most important. This may be the case for most ambulant pedestrians; however, the person had some difficulty manoeuvring the pram round the barrier, which was further com-

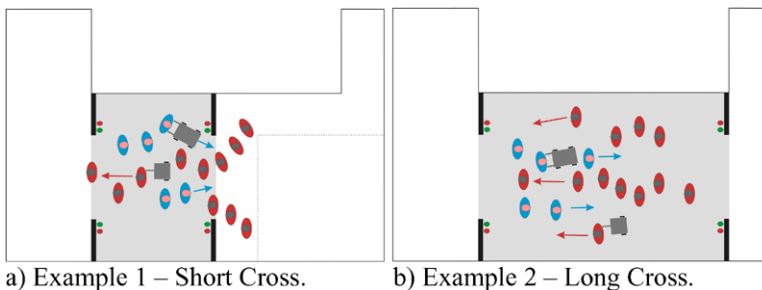


Fig. 3. Representations of people during a crossing test. The *blue* people are moving from left to right and the *red* people from right to left, the *arrows* indicating the direction.

plicated by the wheels catching on irregularities in the surface. In Example 2, the person pushing the pram is behind a slower walker. As has been described, there is an attempt to move out from behind this slow walker into clear space, but this is blocked by the lane of people coming in the opposite direction. Under these circumstances, the person pushing the pram stays in the lane and does not adversely affect the crossing times of the group. The person with the trolley luggage made fewer attempts to leave the lane they were crossing with. This is likely to be because they had the trolley luggage behind them, giving them a clearer view of the person in front and thus the distance to that person.

4 Conclusions

Inclusion of pram or luggage affects clearance times, with prams having a greater effect than luggage. This is dependent on the nature of the person travelling with the item in question, and the type of person they are surrounded by. If the person with the item approaches the barrier at an acute angle, the action of manoeuvring round the barrier adds to the clearance time; most likely causing some distress to the person pushing the pram as they will be left on the crossing after vehicular traffic phase commences.

The action of manoeuvring the item round the barrier is facilitated by the state of the surface material at the barrier: if smooth, it is more likely that the item's wheels will run in the required line, however, surface imperfections jolt the wheels off line, consequently making the item more difficult to manoeuvre at a potentially crucial stage in the crossing task. If the footpath the person is trying to get onto is full of people who have missed the previous phase and are waiting for the next phase, this action is additionally complicated.

Following people closely whilst pushing something in front, like a pram, reduces the visual information regarding the activity of the person in front making it more difficult to react to any changes in direction or speed. It may appear that this is the same as for people not with prams, but the additional turning action combined with uneven surfaces makes it more difficult to manoeuvre the pram. The length of the pram means that the pusher is still exposed on the crossing if slowly following the person in front. It would be interesting to see if there is an increase in stress for people crossing roads with prams or other additional items compared to crossing the same roads without such items.

To make road crossing infrastructure and comparable spaces with multiple barriers more inclusive, designers need to consider the effects described in this paper of including pedestrians with prams in the group of people crossing the road, not just unencumbered pedestrians. Otherwise, if people do not feel able to clear a crossing safely they will avoid the area and thus be excluded.

References

1. Knoblauch RL, Pietrucha MT, Nitzburg M (1996) Field studies of pedestrian walking speed and start-up time, *Transportation Research Record*, 1538, p 27–38.
2. Tyler NA (2002) *Accessibility and the bus system: from concepts to practice* (Ed).
3. www.direct.gov.uk/en/DisabledPeople/RightsAndObligations/DisabilityRights/DG_4001068.
4. www.ada.gov/.
5. Shi J, Chen Y, Rong J, Ren F (2005) Research on pedestrian crowd characteristics and behaviors in peak time on Chinese campus, *Proceedings of the 3rd International Conference on Pedestrian and Evacuation Dynamics*, Vienna, Austria, p 79–90.
6. Childs C, Fujiyama T, Tyler NA (2007) A laboratory for the assessment of pedestrian capabilities, *Proc. of Eleventh International Conference on Mobility and Transport for Elderly and Disabled People*, Montreal, Canada.
7. www.noldus.nl.
8. Fugger TF, Randles BC, Stein AC, Whiting WC, Gallagher B (2000) Analysis of pedestrian gait and perception-reaction at signal-controlled crosswalk intersections, *Transportation Research Record*, 1705, p 20–25.
9. Daamen W, Hoogendoorn SP (2003) Qualitative results from pedestrian laboratory experiments, *Proceedings of the 2nd International Conference on Pedestrian and Evacuation Dynamics*, Greenwich, UK, p 21–132.
10. Older SJ (1968) Movement of pedestrians on footways in shopping streets, *Traffic Engineering and Control*, 10(4), p 160–163.

Ship Evacuation—Guidelines, Simulation, Validation, and Acceptance Criteria

Hubert Klüpfel

TraffGo HT GmbH, Bismarckstraße 142, 47057 Duisburg, Germany
e-mail: kluepfel@traffgo-ht.com

Summary. This paper deals with various aspects of ship evacuation: Guidelines, Simulation, Validation, and Acceptance Criteria. The first section addresses general aspects of ship evacuation, like environmental influences, ship motion, the special evacuation procedure on board ships, and guidelines. The second section covers the simulation of ship evacuation. Section 3 focuses on calibration, validation, and acceptance criteria. Finally, some information resources are presented together with a summary and an outlook towards the concept of “safe return to port”.

1 Ship Evacuation: History and Guidelines

1.1 Historical Background

Developments in the evacuation of passenger ships have often been triggered by accidents: most prominently the sinking of the Titanic and the Estonia. In the aftermath of the Titanic tragedy, the International Convention for Safety of Life at Sea was developed and was the initial trigger of further regulatory developments which also led to the foundation of the International Maritime Organization (IMO). In the aftermath of the Estonia tragedy in 1994, the IMO established “Guidelines on Evacuation Analyses for Ro-Ro passenger ships”. Further information on the subject and the IMO itself can be found at the IMO’s website www.imo.org.

1.2 Guidelines for Ship Evacuation

The International Maritime Organization is the sub-organization of the United Nations specifically concerned with (among other areas) safety of ships (not only passenger vessels). In 2002, an extended version of the guidelines [1] was adopted, which contained two methods for performing an evacuation analysis: the simplified method based on a hydraulic or flow model (already present in MSC/Circ.909 [2]) and a so called advanced method based on computer simulations. Both methods are used to determine the RSET.

Concerning the topic of this paper—evacuation analysis for passenger ships—the decisive steps were taken in the aftermath of the sinking of the Ro-Ro-ferry Estonia in the Baltic sea in 1994, which cost the lives of nearly 900 people. Prior to the development of “performance based evacuation analyses”, the layout of a ship’s escape routes, evacuation systems, and procedures was evaluated based on the lengths of escape paths, the width of corridors and stairways.¹

One major criterion for evacuation safety is the time it takes to evacuate a ship compared to the time available, though. In case of ships—different from buildings—the possible sinking of the vessel provides an upper limit for the available safe evacuation time (ASET). When talking about evacuation of a ship, this comprises the assembly of the passengers, the embarkation of the life boats or life rafts, and their launching.

Starting with MSC/Circ.909 [2] the IMO issued a number of regulations dealing with the performance based analysis of a ship’s evacuation procedures, layout of escape routes, and evacuation systems. This approach is based on a comparison of the available safe egress time (ASET) based on a calculation or simulation and the required safe egress time (RSET), based on fire safety standards applicable to the vessel:

$$RSET \leq ASET. \tag{1}$$

The ASET was set to 60 minutes in the first version of the guidelines [2] for Ro-Ro passenger ships, based on fire resistance considerations.

2 Simulation of Evacuation Processes on Passenger Ships

2.1 Influences on Ship Evacuation

The following Fig. 1 summarizes the external factors on the movement of persons onboard a ship in case of an evacuation. Those influences have to be taken into account (either explicitly or implicitly) when determining the evacuation safety of a ship’s layout.

MSC.1/Circ.1238 [3] lists the following categories of parameters (Fig. 1):

- geometrical,
- population,
- environmental, and
- procedural.

2.2 The Procedure: Assembly and Embarkation Phase

Put into an equation, the different phases of evacuation as outlined above provide the parts of the total time, in its simplest form, the detection and

¹ This is actually the fact for most building codes up to now.

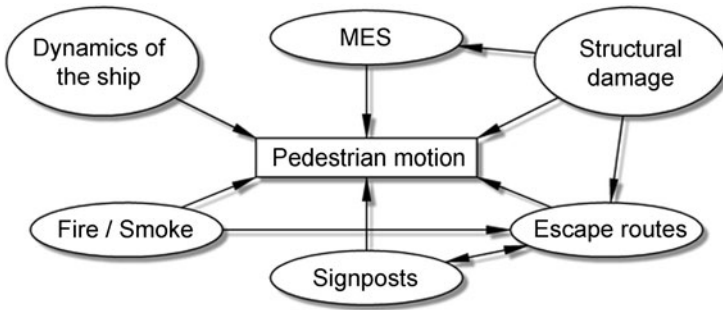


Fig. 1. The different influences on ship evacuation. MES is short for Marine Evacuation System.

response (awareness time a), the travel time (to the assembly stations and further to the life boats or MES²), the embarkation time E and launching time L :

$$T = a + t + 2/3(E + L) \leq 60 \text{ minutes.} \quad (2)$$

T is the required safe egress time RSET determined at an early stage of design (as part of a design acceptance criterion). The 60 minutes are based on fire resistance. The factor of $2/3$ is chosen to take into account the fact that assembly and embarkation and launching might proceed in parallel. For the time being, this is an arbitrary factor and not backed up by empirical evidence. This approach for determining RSET is a design criterion for approval of a ship's layout.

2.3 ASET in the Case of a Ship

The determination of the available safe egress time in the case of a ship has already been briefly addressed before. It has to be compared to the required safe egress time (2). One approach is to determine the ASET based on fire resistance, i.e. if a fire resistance of 60 minutes is assumed and required by the regulations, then this time is taken. A more elaborate approach is to determine the ASET based on a hazard identification (HAZID) and risk analysis. The simulation of fire and smoke is part of such an analysis and can be used to determine the ASET.

3 Calibration, Validation, and Verification

3.1 Calibration of Evacuation Models for Ships

Calibration in statistics is a reverse process to regression. The calibration problem is the use of known data on the observed relationship between a

² Marine Evacuation Systems.

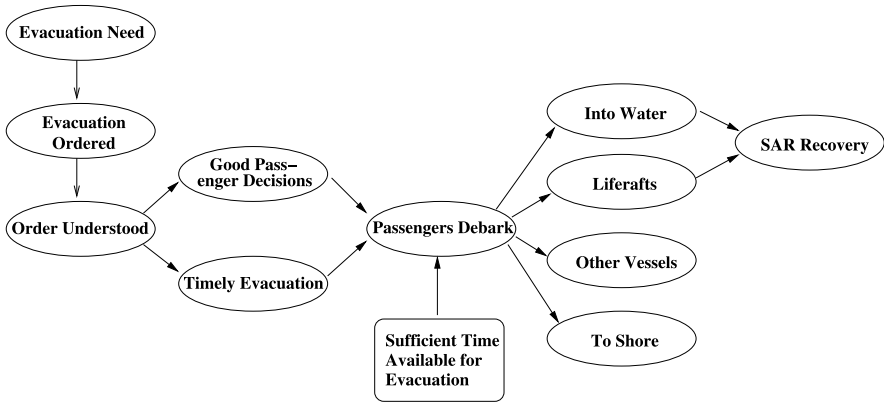


Fig. 2. Sequence of events in an evacuation (adapted from the US Coast Guard Evacuation Analysis Plan, see www.uscg.mil/hq/g-m/nmc/evacuation/nfpapers.htm).

dependent variable and an independent variable to estimate other values of the independent variable from new observations of the dependent variable. In the context of evacuation simulation, this would mean to calibrate model parameters according to empirical data, i.e. a model for simulating the evacuation time based on actual evacuation times. Since there are many different influences (Figs. 1 and 2), the calibration is usually restricted to the assembly phase, i.e. the movement of the passengers to the assembly stations. The embarkation and launching times are at the moment either determined on the basis of mock-up tests by the manufacturers (e.g., for type approval) are just assumed to be 30 minutes ($E + L = 30$ minutes).

When using a simulation software to determine the overall evacuation time, resp. assembly time (2), it is not sufficient to use a calibrated model. The simulation (i.e. the implementation of the model) have also to be verified (low-level or static testing) and validated (high-level or dynamic testing).

3.2 Implementation and Verification

In software project management, software testing, and software engineering:

- *Verification and Validation* (V&V) is the process of checking that a software system meets specifications and that it fulfills its intended purpose.
- *Verification* ensures that the final product satisfies or matches the original design (low-level checking), i.e., you built the product right. This is done through static testing.
- *Validation* checks that the product design satisfies or fits the intended usage (high-level checking), i.e., you built the right product. This is done through dynamic testing and other forms of review.

(all quoted from www.wikipedia.org)

It is important to keep in mind that verification is a matter of checking the correct implementation of a specified design. It does not check whether the design is fit for the intended purpose. Validation is the second step. In order to be able to validate the product design (i.e. the model and its implementation) it has to be verified first. The results of a verified implementation of a model can be used to validate the model itself.

3.3 Validation of a Model Based on Simulation Results

Validation will be used here in the same way as in the previous section. Therefore, verification refers to the implementation and validation refers to the results obtained from the simulation. Simulation is used in two different ways (which is not unambiguous but reflects the generally accepted use): (1) as the implementation of the model, i.e. *simulation program* or computer program and (2) the activity of performing a simulation, i.e. applying the computer program. This loose terminology has the disadvantage of meaning different things (software/activity), but has the advantage of being intuitively understood by the majority of people in the field and being generally accepted.

When speaking of validation of simulation results, this comprises dynamic testing and other forms of review. Test cases are in that sense not part of the validation process but rather a means of verification. If the results are judged by an expert in the field, though, validation is the appropriate term. Just comparing a specified input and output in forms of numbers is not. There are therefore at least three forms of validation:

1. running simple test scenarios (plausibility checks or component testing), i.e., simulation of test cases like those provided in the Guidelines [3],
2. comparison of empirical phenomena for crowd movement with simulated phenomena (qualitative verification), and
3. comparison of evacuation exercises with simulation results (quantitative/validation).

3.4 Acceptance Criteria

As mentioned earlier, one acceptance criterion is the overall evacuation time. This criterion has been formulated in (1) as comparison of the required safe egress time as determined by the calculation or simulation and the available safe egress time specified in the guidelines (60 minutes for Ro-Ro passenger ships and other passenger ships having less or equal than three main vertical zones and 80 minutes for passenger ships other than Ro-Ro passenger ships having more than three main vertical zones).

4 Conclusions and Outlook

4.1 Safe Return to Port

We have presented recent developments in the area of ship evacuation and its simulation. Additionally, the regulatory regime was addressed. Concerning the expected future developments, the safe return to port approach (*The ship is its own best lifeboat*) is expected to have considerable impact on the evacuation procedures of (especially large) passenger ships. The most recent ships under construction are certified to carry up to 6,000 persons. Ships with up to 10,000 persons on board might be built within the next decade. One aspect that has not yet been addressed in this paper is Search and Rescue (SaR), which is one major reason why the safe return to port approach has been adopted by the IMO. SaR for that many people is a very difficult task. Bringing several thousand persons from lifeboats and life rafts back to other ships and finally back to shore might exceed the SaR capacities currently available.

4.2 Information Resources

For the sake of easy reference, here is a list of information resources:

- www.imo.org: The International Maritime Organizations website
- www.traffgo-ht.com/en/pedestrians/downloads/index.html: contains a list of publications (most of the author's papers are available) and a free demo-version of the software AENEAS for simulating ship evacuation
- www.ped-net.org: The pedestrian and evacuation dynamics network
- www.evacmod.net: The evacuation modeling network

Acknowledgements

I like to thank T. Kretz, C. Rogsch, A. Schadschneider, and A. Seyfried (aka ped-net) for valuable discussions and continuing cooperation.

References

1. MSC-Circ.1033. Interim guidelines for evacuation analyses for new and existing passenger ships. Technical report, International Maritime Organization, Marine Safety Committee, London, June 6, 2002. MSC/Circ. 1033.
2. MSC-Circ.909. Interim guidelines for a simplified evacuation analysis on ro-ro passenger ships. Technical report, International Maritime Organization, 1999. MSC/Circ. 909 (replaced by MSC/Circ. 1033).
3. MSC.1-Circ.1238. Guidelines for evacuation analyses for new and existing passenger ships. Technical report, International Maritime Organization, Marine Safety Committee, London, June 6, 2008. MSC/Circ. 1033.

Empirical Study of Pedestrians' Characteristics at Bottlenecks

Andreas Winkens¹, Tobias Rupprecht¹, Armin Seyfried², and
Wolfram Klingsch¹

¹ Institute for Building Material Technology and Fire Safety Science,
University of Wuppertal, Pauluskirchstrasse 11, 42285 Wuppertal, Germany
e-mail: winkens@uni-wuppertal.de

² Jülich Supercomputing Centre, Forschungszentrum Jülich GmbH, 52425 Jülich,
Germany
e-mail: a.seyfried@fz-juelich.de

Summary. The design procedures of Nelson and Mowrer in the SFPE Handbook of Fire Protection Engineering (Society of Fire Protection Engineers, Bethesda, MD, 2002) and Predtetchenskii and Milinskii (PM) in Planning for Foot Traffic Flow in Buildings (Amerind, New Dehli, 1969) are frequently used for capacity analysis of pedestrian facilities, e.g. egress routes. Both agree that congestion occurs in front of a bottleneck, if the incoming flow exceeds the capacity. However, in case of a present congestion in front of a bottleneck, their approaches differ considerably. Nelson assumes that in this case the flow inside a bottleneck is determined by the bottleneck capacity. PM instead expect that the density in front of the entrance to the bottleneck is significant higher than the density, which is attributed to the capacity, and thus the flow inside is lower than the capacity. Furthermore PM assume that the density inside is generally significant lower than the density in front of the bottleneck.

To resolve these discrepancies we studied the pedestrian flow through a bottleneck (Rupprecht, Diploma thesis, University of Wuppertal, 2006) as well as the density and the jam occurrence in front of a bottleneck (Winkens, Diploma thesis, University of Wuppertal, 2007) by an experiment performed under laboratory conditions. The aim was to get reliable data concerning the density directly in front of and inside the bottleneck and thereby to check the assumptions of Nelson and Mowrer and Predtetchenskii and Milinskii.

We found that during the stationary state the density in front of the bottleneck does not depend on the bottleneck width b for $0.8 \text{ m} \leq b \leq 1.2 \text{ m}$. In conformance with PM the density inside is significantly lower than in front of the bottleneck. In reference to the continuity equation these results cast doubts on the assumption of Nelson that the flow through a bottleneck maintains the value of the capacity if a congestion appears in front of the bottleneck.

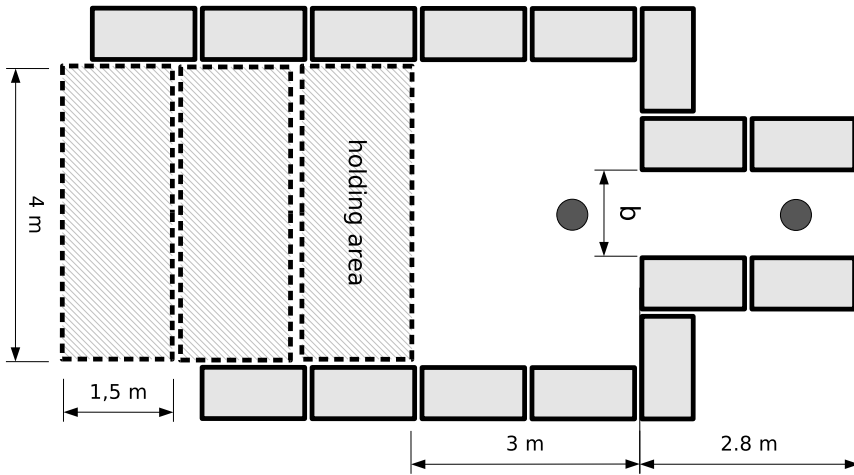


Fig. 1. Experimental setup. The holding areas are *hatched*. The *circles* mark the camera positions, which were geared to the centers of the measurement areas, which were used.

1 Experimental Setup

The whole setup was arranged from desks and tables. The configuration is shown in Fig. 1. Test persons were a group composed of students and staff of Forschungszentrum Jülich GmbH. A constant width from the hips to the shoulders of the test persons was assured by the height of the bottleneck (approx. 1.80 m) and the fixing of tables and desks. The length of the bottleneck amounted to $l_{\text{bck}} = 2.8$ m. Three holding areas in front of the bottleneck ensured an equal initial density of the pedestrian bulk for runs with different numbers of people N . The straight distance from the first holding area to the entrance of the bottleneck was three meters.

All together 18 runs were performed to analyze the effect of the width of bottleneck, b , and the number of pedestrians, N . The width of bottleneck was increased from the minimum value of $b = 0.8$ m in steps of 0.1 m to a maximum value of $b = 1.2$ m. At the beginning of each run $N = 60$ test persons were placed in the holding areas with a density of $\rho_{\text{ini}} = 3.3 \text{ m}^{-2}$ (i.e. 20 persons per holding area). We also measured the flow for $N = 20$ and $N = 40$ but for this study we just focus on the tests with $N = 60$. The test persons were advised to move through the bottleneck without haste but purposeful. It was emphasized not to push and to walk with normal velocity. The test persons started to move after an acoustic signal. The whole cycle of each run was filmed and photographed by two cameras, one situated above the center of the bottleneck and the other above the entrance of the bottleneck (indicated by the circles in Fig. 1). Furthermore there was one camera which filmed a side view of the bottleneck.

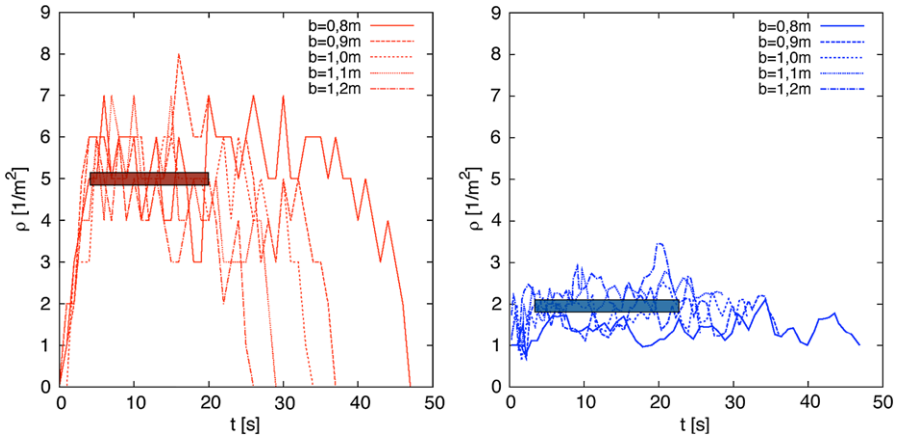


Fig. 2. Time dependence of density for all widths **in front of** (left figure) and **inside** the bottleneck (right figure). The horizontal bars indicate the mean value of the density during the stationary state (see also Fig. 3).

2 Results

2.1 Density in Front of the Bottleneck

Three different phases can be observed in front of the bottleneck. The first phase, which lasts up to eight seconds, shows the increase of density, when people enter the measurement area.

During the second phase the density is more or less stationary with steady states. As one can see on the left diagram in Fig. 2 there are large fluctuations at each run. However it is obvious, that these fluctuations oscillate between maximum and minimum values ($3 \text{ m}^{-2} \leq \rho \leq 8 \text{ m}^{-2}$) around a constant value for every width and during the several runs. Some part of the fluctuations is due to the small measurement area of 1 m^2 , which was needed to avoid boundary effects. The density measurements using small areas will be subject of further research.

In the third phase during the approx. last ten seconds of every run the density decreases when the last pedestrians leave the measurement area.

2.2 Density Inside the Bottleneck

Inside the bottleneck the time development of the density shows two phases. During the first phase there occurs a transient effect due to the optimization of required space.

Phase two is stationary just like in front of the bottleneck. Here also fluctuations appear, but not as large as in front (see Fig. 2). This refers to fixed

boundaries inside the bottleneck: in front of the bottleneck persons can enter the measurement area from three directions, inside it is limited to one direction.

As one can see in Fig. 2 the averaged density inside the bottleneck ($\rho_{\text{inside}} \approx 1.7 \text{ m}^{-2}$) is clearly lower than in front ($\rho_{\text{front}} \approx 5.0 \text{ m}^{-2}$). This result is confirmed qualitatively for non-steady states by Daamen [1].

Unlike in front of the bottleneck the density inside rises slightly with increasing width of the bottleneck caused by decreasing fringe effects in combination with the zipper effect. The zipper effect at bottlenecks was described first by Hoogendoorn and Daamen [2] and further studied in [3]. It is a self-organization phenomenon of pedestrians leading to an optimization of the available space and the velocity inside the bottleneck. The zipper effect appears for bottleneck widths $b > 0.8 \text{ m}$ and leads to lane separation inside the bottleneck. In [3] it was shown that the distances between the lanes are growing continuously with the width leading to a continuous increase of the flow due to an almost width independent density and velocity. For a detailed documentation of the trajectories, time evolution of the flow and velocities inside the bottleneck we refer to [3, 4].

3 Conclusions and Outlook

By means of an experiment performed under laboratory conditions we studied the pedestrian density in front and inside a bottleneck during the steady states of density.

The main result is that the density in front amounts $\rho_{\text{front}} = 5.0 \text{ m}^{-2}$ and is significantly higher than inside the bottleneck $\rho_{\text{inside}} = 1.7 \text{ m}^{-2}$. This cast doubts on the design procedure of Nelson acting on the assumption that the flow will maintain the value of the capacity if a congestion in front of the bottleneck occurs.

With our study we could obtain new information about the density and flow of a pedestrian stream moving through a bottleneck. We just looked at the steady states, thus our results can be compared with the fundamental diagrams of Nelson and Mowrer [5] and Predtetchenskii and Milinskii [6].

The time series of the density shows that during the stationary state of density in front of the bottleneck the density reaches a value of $5.0 (\pm 2.0) \text{ m}^{-2}$ while inside the bottleneck the density is about $1.7 (\pm 0.6) \text{ m}^{-2}$. In reference to the continuity equation these two states of the density must belong to one flow value. Based on the fact that the fundamental diagram has only one maximum either this maximum range at least from 2 m^{-2} to 5 m^{-2} or the flow through the bottleneck is lower than the capacity when a congestion in front of the bottleneck occurs.

Furthermore we want to point out that the density in front of a bottleneck does not depend on the bottleneck width for $0.8 \text{ m} \leq b \leq 1.2 \text{ m}$. Moreover

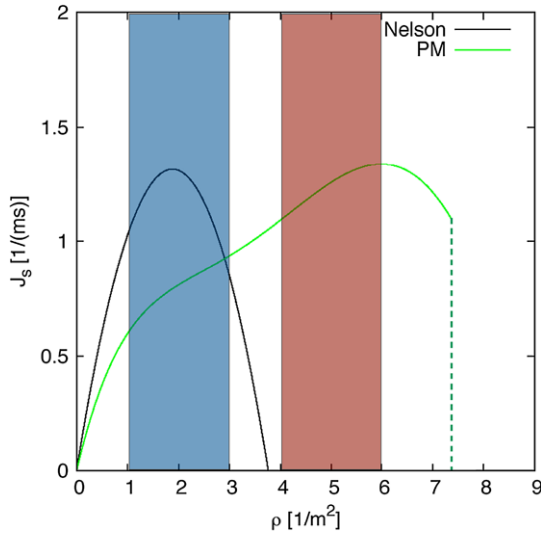


Fig. 3. The flow–density-relationship diagram of Nelson and Mowrer [5] and PM [6]. The *red* and *blue* colored areas mark the ranges of our measurements.

the flow does not become 0 for values of $\rho > 3.8 \text{ m}^{-2}$ as it is given by the fundamental diagram of Nelson and Mowrer (see Fig. 3).

In summary these results support the method of PM and cast doubts on the oversimplified assumptions of the procedure suggested by Nelson and Mowrer.

We will continue our studies. Just recently we made another experiment with up to 250 test persons. In this experiment we also had laboratory conditions but more parameters could be varied. Thus we want to confirm our previous results with more details.

Furthermore we want to enhance the data base for fundamental diagrams in general as well as for bottlenecks in particular. Details concerning the experimental setups and measurement techniques of these experiments can be found in the contributions of M. Boltes and A. Seyfried in these proceedings.

Acknowledgements

The financial support by the DFG (German Research Foundation) is grateful acknowledged (Grant No. KL 1873/1-1 and SE 1789/1-1).

References

1. W. Daamen and S.P. Hoogendoorn. Flow–density relations for pedestrian traffic. In A. Schadschneider, T. Pöschel, R. Kühne, M. Schreckenberg, and D.E. Wolf, editors, *Traffic and Granular Flow 2005*, pages 315–322. Springer, Berlin, 2007.
2. S.P. Hoogendoorn and W. Daamen. Pedestrian behaviour at bottlenecks. *Transportation Science*, 39(2), pages 147–159, 2005.
3. A. Seyfried, O. Passon, B. Steffen, M. Boltès, T. Rupprecht, and W. Klingsch. New insights into pedestrian flow through bottlenecks. *Transportation Science*, 43(3), pages 395–406, 2009.
4. T. Rupprecht. *Untersuchung zur Erfassung der Basisdaten von Personenströmen*. Diploma thesis. Universität Wuppertal, Wuppertal, 2006.
5. H.E. Nelson, and F.W. Mowrer. Emergency movement. In P.J. DiNenno, editor, *The SFPE Handbook of Fire Protection Engineering*, pages 3-367–3-380. Society of Fire Protection Engineers, Bethesda, MD, third edition, 2002.
6. V.M. Predtetchenskii and A.I. Milinskii. *Planning for Foot Traffic Flow in Buildings*. Amerind, New Dehli, 1969.
7. A. Winkens. *Analyse der lokalen Dichte in Fußgängerströmen vor Engstellen*. Diploma thesis. Universität Wuppertal, Wuppertal, 2007.

RFID Technology Applied for Validation of an Office Simulation Model

Vincent Tabak, Bauke de Vries, and Jan Dijkstra

Design Systems Group, Faculty of Architecture, Building, and Planning,
Eindhoven University of Technology, PO Box 513, 5600 MB Eindhoven,
The Netherlands
e-mail: V.Tabak@bwk.tue.nl

Summary. This paper presents the validation of an office utilisation model for the research project called “User Simulation of Space Utilisation (USSU)”. The result of this research is a system that can be used for analysing and evaluating the space utilisation of a building for any given organisation. A system for building usage simulation that produces data about activities of members of an organisation can substantially improve the relevance and performance of building simulation tools. This is relevant for engineering domains as well as for architects to evaluate the performance of a building design. For a thorough evaluation of the system an experiment was executed for assessing its predictive quality in the context of a real building, organisation and actual human behaviour; this experiment was executed using RFID technology. The result of the experiment was observed data about the space utilisation of the selected organisation. This data set was compared with the space utilisation predicted by the USSU system to evaluate the simulation model. The validation of USSU showed that there were no significant differences between the predicated and observed activity behaviour. As a consequence, the output of USSU is considered to be valid.

1 Introduction

Activity and location schedules are input for office utilisation simulations. These schedules however, are often assumptions rather than based on measured observations and resulting descriptive and predicting models. Thus, the results of such simulation systems are tentative at best and may often be misleading. Therefore, a more advanced scheduling method is needed that adequately represents real-life complexity of human activity and location schedules. The main objective of the research project User Simulation of Space Utilisation (USSU) was to develop a system that can be applied for analysing and evaluating the space utilisation of a building for any given organisation. The system generates activity schedules that provide a representation of human activities that are executed in building spaces. An activity schedule not

only describes which activities are performed and at which location, but also the route that is followed between the locations of these activities. These activity schedules are a source of dynamic input data for building usage simulation tools. Reliable data on human movement is scarce. It is valuable input for several research areas. For instance, the relevance and performance of building simulation tools like indoor climate simulations or working conditions assessments will substantially improve when realistic input data is applied. If reliable human movement models can be created, then these models can not only be used to analyse existing situations, but also to simulate new building designs taking the digital design as input. This is also relevant for architects to evaluate the performance of a building design.

USSU models the scheduling behaviour of employees following their heuristics. The proposed scheduling method is not producing schedules for planning purposes based on an optimisation method. Neither, does the scheduling method try to find the optimum activity schedule for instance with regard to the priority of its activities. The goal of the scheduling method is to mimic the behaviour of real human beings when scheduling activities [1].

USSU serves as a pre-processor for other simulation systems that need real-life data about the location of persons at a specific time, such as indoor climate calculations, evacuation simulations and working condition assessment simulations. The underlying model integrates activity modelling and workflow modelling constrained by spatial conditions of a building [2]. The combination of these two methods provides a solid basis that ensures process consistency, inclusion of individual (re)scheduling behaviour and allows execution in compressed time intervals. With this model, space utilisation can be simulated at a high level of realism instead of make assumptions as usual in many building simulation systems. This is possible through the incorporation of human activities as they are executed in real life, split up into skeleton activities (i.e. workflow dependent activities) and intermediate activities (i.e. social and/or physiological activities). Scheduling of activities is executed under bounded rationality. Persons are only aware of their own agenda which evolves in compressed time.

The scheduling method can accommodate real-life complex organisational structures and maintains consistency between the activity schedules. Most existing approaches to model activity schedules assume an individual-based decision making process. These models do not take into account the interaction between individuals. A special feature of the USSU system is the incorporation of interactions between activities (e.g. meetings). The interaction between activities contributes significantly to the realism of the activity schedules.

The final step in this project was to validate the system. For a thorough evaluation of the system an experiment was performed using RFID technology. The goal of this experiment was to collect data for assessing the predictive quality of USSU in the context of a real building, organisation and actual human behaviour. The experiment resulted in observed data about the actual space utilisation of a chosen organisation. The observed data was compared

with the space utilisation predicted by USSU to evaluate its predictive quality. This paper focuses on the validation approach and observation method selected with regard to the validation of USSU.

2 Validation Approach

For the validation of USSU a specific existing organisation and a building was used, namely two chairs in our Faculty which are located on the same floor. The validity of USSU was determined by comparing predicted space utilisation with observed space utilisation. Activity schedules predicted by the USSU prototype were compared with activity schedules observed in the real world. To assess the validity of the system the predicted space utilisation was compared with the observed space utilisation on a set of performance indicators, so-called criterion variables. These criterion variables (e.g. the usage of facilities or movement behaviour of employees) specify the aspects on which the comparison of the observed and predicted activity schedules was performed. The values of the criterion variables were derived from both the predicted and observed activity behaviour of all employees. The following criterion variables were chosen:

- Zone utilisation.
- Mean walking distance of employees.

These criterion variables are discussed below.

2.1 Criterion Variables

The first criterion variable relates to the amount of time a zone on the test floor is used during a working day, either observed in the real world or simulated using USSU. The zone utilisation is a proportion of the total simulated or observed time. It is calculated by dividing the total time a zone is used by the total simulated or observed time. In formula:

$$P_x = \frac{T_x^{\text{zone}}}{T_s}, \quad (1)$$

$$T_x^{\text{zone}} = \sum_{i=1}^{n_x} \Delta T_{a_{x,i}} \quad (2)$$

where:

- P_x is utilisation of zone x for an average working day
- T_x^{zone} is total time zone x is used during simulation/observation
- T_s is total simulated or observed time
- $a_{x,i}$ is activity a_i using zone x
- $\Delta T_{a_{x,i}}$ is duration of activity $a_{x,i}$
- n_x is total number of activities using zone x

The second criterion variable examines the movement behaviour of employees. The activity schedule of an employee reveals the required movement behaviour as a result of its activities. First the total walking distance for all simulated or observed days is calculated as follows:

$$W_e^{\text{total}} = \sum_{i=1}^m W_e^{\text{day}}, \tag{3}$$

$$W_e^{\text{day}} = \sum_{i=1}^{n-1} L_{[a_{e,i}, a_{e,i+1}]} \tag{4}$$

where:

- W_e^{total} is total walking distance of employee e for all work days
- W_e^{day} is total walking distance of employee e for one work day
- m is total number of simulated or observed working days
- $L_{[a_{e,i}, a_{e,i+1}]}$ is length of route between location of activity $a_{e,i}$ and location of activity $a_{e,i+1}$
- n is number of activities in the activity schedule for a work day

Next, the mean walking distance of an employee on a work day is calculated:

$$W_e^{\text{mean}} = \frac{W_e^{\text{total}}}{m} \tag{5}$$

where:

- W_e^{mean} is mean walking distance of employee e for a working day

2.2 Goodness-of-Fit

The goodness-of-fit was measured using a combination of the following two tests, namely:

- Student’s t -test for paired samples combined with a correlation coefficient determination.
- Variability test.

Although, the variability test is not a standard statistical test it gives further insight in the differences between the observed and predicted sets of data. The smaller the variability is (i.e. the closer it gets to zero) the better the match between the two data sets, e.g. the observed and predicted activity behaviour. The variability can be calculated using the following formula:

$$\nu^2 = \frac{\sum_{i=1}^n (s_{c,i} - o_{c,i})^2}{n} \tag{6}$$

where:

- ν^2 is variability
- $s_{c,i}$ is predicted value i of the criterion variable c
- $o_{c,i}$ is observed value i of the criterion variable c
- n is the number of observations

3 Observation Method—RFID

A relative new technology called RFID (Radio Frequency Identification) could be the key for a non obtrusive way of collecting data about human movement and activity behaviour. Using this system, participants only have to carry a small device and the RFID system automatically registers their movements. During the observation period participants themselves do not have to perform any additional actions besides performing their normal activity behaviour. Due to the passive nature of this system the behaviour of people is only influenced in a limited manner and probably only the most in the beginning of the experiment. This system results in observed data about the daily movement behaviour with a relative high degree of precision.

An RFID system consists of readers and tags. An RFID tag is a device which can be remotely accessed to retrieve data stored in its chip. Each tag is equipped with an antenna to receive and respond to radio-frequency queries from an RFID reader. There are two types of RFID tags: passive and active tags. Passive tags do not have an internal power supply; the power required to transmit a response is induced through the incoming radio-frequency signal. These tags can only be read out from short distances (up to several meters). However the active tags can have a read distance of up to several hundreds of meters. Therefore these tags are equipped with an internal power source. An active RFID tag will send out a signal for example every 1.5 seconds. The battery of these tags last up to 5 years. In this experiment the active tags were applied in combination with a number of readers. Currently, RFID technology is used by some Dutch organisations for access control and as a means of working hours registration, but up to now never on the detailed level as it was used in this experiment.

All employees working on the test floor were asked to participate in the RFID experiment. Roughly 50 employees are officially located on this floor. In the end 37 persons accepted the request. Each person was asked to wear a RFID tag for a period of 3 months. On the office floor 16 receivers were installed. The placement of readers was such that the real movement behaviour of the employees could be tracked throughout the whole floor.

In 46 days the RFID system recorded about 360,000 events; each event relates to one of the 37 participants entering or leaving one of the RFID zones. These events had a total duration of more than 32,000 hour.

When the data collected in the RFID experiment was compared with the predicted space utilisation attention had to be paid to the way in which the activity behaviour is collected. Although the USSU system predicts space utilisation on the level of (parts of) building spaces, in the RFID experiment the space utilisation was observed on level of sets of spaces, called zones. The main reason for this was that it proved to be too costly to equip each space with an RFID reader. To be able to compare the observed space utilisation with the predicted space utilisation, the predicted data had to be aggregated to allow for comparison and hence model validation.

4 Validation Results

This section discusses the results of the validation. First the results of the validation with regard to the zone utilisation criterion variable are discussed. Then, the validation results related to the second criterion variable (i.e. movement behaviour of employees) are treated.

4.1 Zone Utilisation

Table 1 indicates a strong correlation between the predicted usage of zones (USSU) and the observed usage of zones (RFID); this result is significant at 0.05 level. As a consequence, it was allowed to perform a paired samples *t*-test. The paired samples *t*-test for the zone utilisation shows a powerful outcome (Table 1). Consequently, the null hypothesis could not be rejected. In other words, there were no significant differences between the predicted (USSU) and observed (RFID) usage of zones. This rather strong outcome of the *t*-test was further emphasised by the variability test. The results of this test also indicate negligible differences between the USSU and RFID data sets with regard to the utilisation of zones.

4.2 Employees

Not only did the RFID tracking system store the amount of time an individual was in a certain zone, it also stored the routes which were followed between the RFID zones. This meant that the data collected in the RFID experiment could also be used to validate USSU on the level of human movement behaviour, in particular the mean walking distance per employee.

Table 2 shows the correlation coefficient between the USSU and RFID data sets in relation to the mean walking distance. The correlation coefficient was significant and indicated a strong link between the two data sets. The results of the paired samples *t*-test for the mean walking distance were significant

Criterion variable	Correlation coefficient		Paired-samples <i>t</i> -test		Variability	
	<i>r</i> -value	<i>P</i>	<i>t</i> -value	<i>P</i>	value	std. dev.
Zone utilisation	0.77	0.01	0.00	1.00	0.00	0.00

Table 1. Validation results for the usage of zones.

Criterion variable	Correlation coefficient		Paired-samples <i>t</i> -test		Variability	
	<i>r</i> -value	<i>P</i>	<i>t</i> -value	<i>P</i>	value	std. dev.
Time percentage	0.70	0.04	1.62	0.14	0.05	0.08

Table 2. Validation results for movement behaviour of employees.

(Table 2). This meant that for this criterion variable the null hypothesis could not be rejected. With regard to the mean walking distance there were no significant differences between the two data sets. Finally, the variability test also suggests only minor differences between the two data sets with regard to movement behaviour (Table 2).

5 Discussion

The validation of USSU showed that there were no significant differences between the predicted and observed activity behaviour. This is further emphasised by that fact that all statistical tests (i.e. Student's *t*-test, correlation coefficient and variability test) supported each other and pointed in the same direction. As a consequence, the output of USSU is considered to be valid. In other words, USSU can be used to accurately predict the space utilisation of an organisation (at least when applied within the limitations set for this project).

RFID technology allows for a non obtrusive way of collecting data about human movement. Participants of the experiment only had to carry a small RFID tag, for instance in their wallet, and the RFID system automatically registered their movements using a number of strategically placed readers. The RFID system made it possible to track the movements of all participants across the floor and thereby collecting data about the real movement behaviour of the participants.

References

1. V. Tabak, B. de Vries, J. Dijkstra and A.J. Jessurun. Interaction in activity location scheduling. In Proceedings of the 11th International Conference on Travel Behavior Research, Kyoto, Japan, 2006. CD-ROM.
2. V. Tabak, B. de Vries and J. Dijkstra. User behaviour modelling—applied in the context of space utilisation. In J.P. van Leeuwen and H.J.P. Timmermans, editors, Developments in Design & Decision Support Systems in Architecture and Urban Planning, Eindhoven University of Technology, Eindhoven, Netherlands, 2004.

Study on Crowd Flow Outside a Hall via Considering Velocity Distribution of Pedestrians

Xiang Shu Liu¹, Jia Xiu Pan¹, Liang Yujuan^{1,2}, and Yu Xue^{1,3}

¹ Institute of Physical Science and Engineering, Guangxi University, Nanning, 530004, China

² Department of Physics, Hechi College, Guangxi, 546300, China

³ Shanghai Institute of Applied Mathematics and Mechanics, Shanghai University, Shanghai, 200072, China

e-mail: yuxuegxu@gxu.edu.cn

Summary. The dynamical behaviors of pedestrians outside a hall is investigated by using the extended lattice-gas model with different maximum velocities. A numerical simulation illustrates that fast and slow pedestrians will affect some dynamical characteristic from the choking flow to the decaying flow. In the choking-flow region, the scaling relation of crowd flow rate and the evacuation time are obtained, respectively. The slow pedestrians, initial density of walkers and the location of the exit influence the evacuation time.

1 Introduction

In recent years, pedestrian flow dynamics have attracted the interest of a community of physicist [1–5], because of many interesting physical phenomena such as self-organization phenomena, noise-induced ordering, and collective phenomena with “freezing by heating” in panic situations, the “faster-is-slow effect”, and herding behavior [6, 12]. Many models have been proposed for modeling the pedestrian flow, these models include the social force model [6], artificial intelligence-based model [7], lattice-gas model [8], and cellular automaton model [9], etc. Muramatsu et al. have studied the counter flow of pedestrian within an underpass by using the lattice-gas model of biased-random walkers. It is shown that the dynamical jamming transition occurs at a critical density [8]. Yusuke Tajima and Takashi Nagatani have used the similar lattice-gas model to investigated crowd flow going outside a hall [10]. They have found a dynamical phase transition and obtained a scaling relationship between the crowd flow rate J and W (the size of the door). More recently, Rui Jiang et al. have introduced the lattice-gas model with the ve-

locity distribution to study the pedestrian traffic and obtained some results in accordance with the real pedestrian flow [11].

In this paper, we study the dynamical behavior of crowd flow outside the hall via considering the velocity distribution of pedestrians. In Sect. 2, the pedestrian model with mixing different pedestrians outside a hall is proposed and define the transition probability for all possible configurations of a walker. In Sect. 3, we conduct the simulation and analysis for the different situation outside a hall. Finally, the conclusion is obtained.

2 Model

In reality, a pedestrian consist of a walker with different velocity. Thus, the velocity between 1 and $v_{\max} > 1$ of pedestrians is introduced in the lattice-gas model [11]. Slow pedestrians have the maximum velocity $v_{\max 1}$ and fast pedestrian $v_{\max 2}$. We mimic the crowd flow outside a hall using the pedestrian flow model. The system is made up of the hall with $L(\text{length}) \times L(\text{width})$, the exit of width of W , and the space $L/2(\text{length}) \times L(\text{width})$ linking to the exit. The schematic illustration of the crowd flow outside the hall through the exit can be found in [10]. The model is defined on the square lattice of $L \times L$ sites to represent the hall. Each pedestrian is a biased-random walker and move toward the exit outside a hall. The excluded-volume effect is taken into account. A single walker only occupied a site. Overlapping on the site is prohibited. When the walker arrives at the wall of channel, it is reflected by the wall and never goes out through the wall.

Each walker moves in a preferential direction with no back step. The preferential direction of walkers is toward the exit. A bias (drift) is applied to the preferential direction for random walkers. The strength of drift for a walker depends on the position of a walker since the preferential direction to the exit varies with the position of a walker. Accordingly, as a walker moves toward the exit, the drift direction changes from position to another.

Initially N pedestrians are randomly distributed inside the hall. From time step t to $t + 1$, a pedestrian is chosen randomly, and a sign s is given as $s = v_{\max}$. This means that in one time step, the pedestrian can walk at most s cells away. The walking is fulfilled through s sub-steps. In each sub-step, the pedestrian follows the rules of walk in [10] and [11]. When a walker goes out of the exit and far from the exit, the walker is removed from the system.

3 Simulation and Results

Initially, walkers are distributed randomly inside the hall at an occupation probability c . All walkers are numbered randomly from 1 to N , where N is the number of walkers existing within the system, including the walkers out of the exit. Following the rule in [10], the numbered walkers are updated in

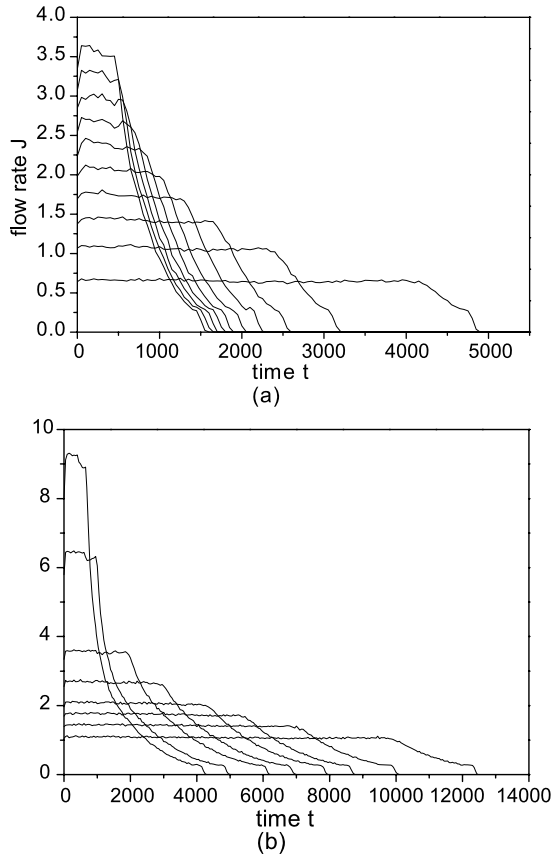


Fig. 1. Plots of mean flow rate J against t for $v_{\max 1} = 1$, $v_{\max 2} = 2$, $R = 0.5$. **a** $L = 100$ from bottom to top $W = 1 \rightarrow 10$, **b** $L = 200$ from the bottom to the top $W = 2, 3, 4, 5, 7, 10, 20, 30$.

order. If the walkers go out of the system, they are removed from the system. After the above procedure is carried out, one time step is completed, thus the above procedure is repeated.

Figures 1(a) and (b) show the time t dependence of the mean flow rate J for various values of door size W , where the maximum velocity of pedestrian is $v_{\max 1} = 1$, $v_{\max 2} = 2$, $R = 0.5$. The flow-rate increases rapidly with time. When the choking occurs, only a few walkers go outside the hall with a constant value of mean flow-rate. It exhibits that a dynamical phase transition occurs from the choking flow to the decaying flow. Contrary to the maximum velocity $v_{\max} = 1$ of identical pedestrians, it shows that the mean flow rate J of the mixing pedestrian is larger under the same door size W . Due to the maximum velocity of pedestrian $v_{\max} > 1$, more walkers can go through the exit per time step in the choking state and the evacuation time is smaller. For

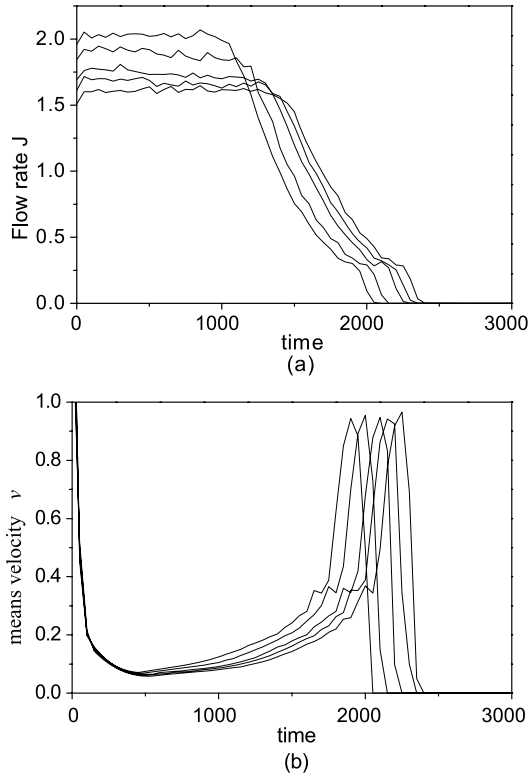


Fig. 2. Plot of mean flow rate J (a) and means velocity v (b) against t for different R (the ratio of the number of the slow pedestrians to the number of all pedestrians), from bottom to top $R = 1, 0.7, 0.5, 0.2, 0$ ($L = 100$, $W = 4$).

example, under the same door $W = 4$ and the hall length $L = 100$, the evacuation time with the maximum velocity $v_{\max} > 1$ is 2300 time steps, which is smaller than one with the maximum velocity $v_{\max} = 1$.

The effect of the mixing ratio R (the ratio of the number of the slow pedestrians to the number of all pedestrians) on the evacuation time t_e and pedestrian flow rate is investigated. Figure 2(a) shows the plots of mean flow rate J against time t for different R under the hall length $L = 100$ and door size $W = 4$. Results indicate that the mean flow rate J decreases and the evacuation time t_e increases with the increase of R . It seems that more pedestrians reduce their velocity to induce the whole evacuation to slow down. Figure 2(b) is the plot of mean velocity v against t for different R .

By simulation, the scaling relation between evacuation time t_e and door size W is shown in Fig. 3 for different length of the hall ($L = 60, 80, 100$). The evacuation time t_e scales as

$$t_e = W^{-0.51 \pm 0.02}. \tag{1}$$

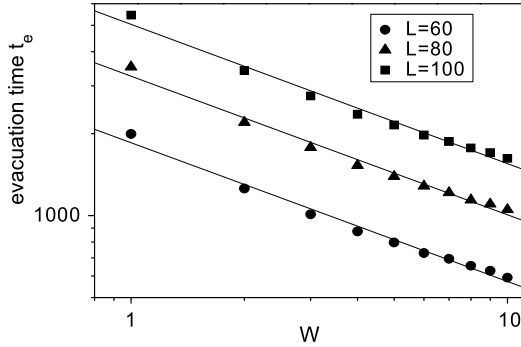


Fig. 3. log–log plot of evacuation time t_e against door size W where the *circular*, *triangular* and *square points* indicate the simulation data for $L = 60, 80$ and 100 , respectively.

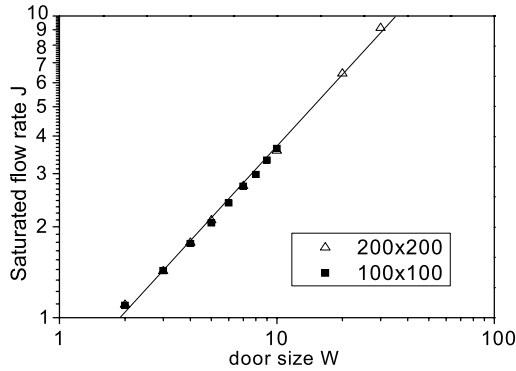


Fig. 4. The log–log plot of the saturated flow rate J against door size W . The *square* and *triangular points* indicate the simulation data for $L = 100$ and 200 , respectively.

The evacuation time depends on the hall length L . The scaling exponent does not depend on L , which has not been found in the granular flow.

The scaling behavior of the mean flow rate J in a choking-flow region is also studied. Figure 4 shows the log–log plot of the saturated flow rate J against door size W . The saturated flow rate J scales as follows

$$J = W^{0.79 \pm 0.01}. \tag{2}$$

The initial distribution of walkers also affects the evacuation time. Figure 5 shows the evacuation time t_e under the initial density of walkers c from 0.1 to 0.9. From Fig. 5, one can see that the evacuation time t_e increases linearly with the increase of the initial density of walkers.

Figure 6 reveals the evacuation time t_e against x , where x represents the coordinate of the center of the exit. It confirms that when the exit is in the

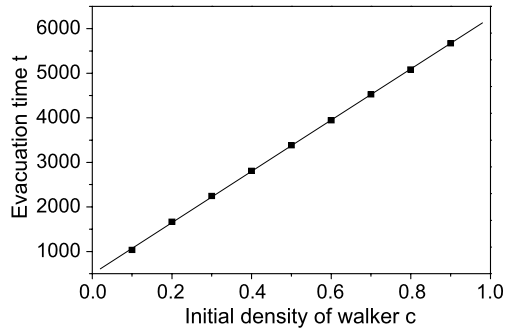


Fig. 5. Plot of the evacuation time t_e against the initial density of walkers c ($L = 100, W = 4$).

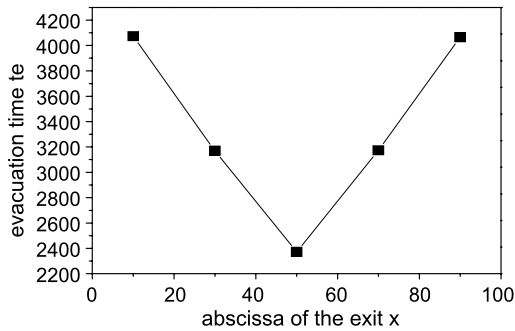


Fig. 6. The evacuation time t_e against the abscissa of the exit x ($L = 100, W = 4$).

center, the evacuation time is smaller, thus the best location of the exit is the center of the hall.

4 Conclusion

The dynamical behaviors of pedestrians outside a hall is investigated by using the extended lattice-gas model with different maximum velocities. A numerical simulation illustrates that fast and slow pedestrians will affect some dynamical characteristic from the choking flow to the decaying flow. In the choking-flow region, the crowd flow rate J scales as $J = W^{0.79 \pm 0.01}$ and the evacuation time t_e scales as $t_e = W^{-0.51 \pm 0.02}$, where W is the width of the exit. The fast pedestrians reduce the evacuation time t_e and increase the flow rate J . The initial state of walkers and the location of the exit have some effects on the evacuation time.

Acknowledgements

Project supported by the National Basic Research Program of China (No. 2006CB705500), the National Natural Science Foundation of China (Grant No. 10662002 and 10532060), the Natural Science Foundation of Guangxi Zhuang Autonomous Region, China (Grant No. 0640003) and the Special Foundation for the New Century Talents Program of Guangxi Zhuang Autonomous Region, China (Grant No. 2005205).

References

1. M. Schreckenberg, S.D. Sharma (Eds.), *Pedestrian and Evacuation Dynamics*, Springer, Berlin, 2001.
2. E.R. Galea (Ed.), *Pedestrian and Evacuation Dynamics*, 2003, CMS Press, London, 2004.
3. D. Helbing, *Rev. Mod. Phys.* 73 (2001) 1067.
4. T. Nagatani, *Rep. Prog. Phys.* 65 (2002) 1331.
5. S.P. Hoogendoorn, P.H.L. Bovy, M. Schreckenberg, D.E. Wolf (Eds.), *Traffic and Granular Flow'03*, Springer, Heidelberg, 2005.
6. D. Helbing, I.J. Farkas, T. Vicsek, *Nature* 407 (2000) 487.
7. J. Dijkstra, J. Jessurun, H. Timmermans, in: M. Schreckenberg, S.D. Sharma (Eds.), *Pedestrian and Evacuation Dynamics*, Springer, Berlin, 2001, p. 173.
8. M. Muramatsu, T. Irie, T. Nagatani, *Physica A* 267 (1999) 487.
9. V.J. Blue, J.L. Adler, *Transp. Res. B* 35 (2001) 507.
10. J.Y. Tajima, T. Nagatani, *Physica A* 292 (2001) 545.
11. J.R. Jiang, Q.S. Wu, *Physica A* 373 (2007) 683.
12. D. Helbing, I.J. Farkas, T. Vicsek, *Phys. Rev. Lett.* 84 (2000) 1240.

Analysis on the Propagation Speed of Pedestrian Reaction: Velocity of Starting Wave and Stopping Wave

Akiyasu Tomoeda¹, Daichi Yanagisawa^{1,2}, and Katsuhiro Nishinari^{1,3}

¹ Department of Aeronautics and Astronautics, Graduate School of Engineering, The University of Tokyo, 7-3-1 Hongo, Bunkyo-ku, Tokyo, 113-8656, Japan
e-mail: tt67055@mail.ecc.u-tokyo.ac.jp

² Japan Society for the Promotion of Science, 1.8, Chiyoda-ku, Tokyo, 102-8472, Japan

³ PRESTO, Japan Science and Technology Corporation, 7-3-1 Hongo, Bunkyo-ku, Tokyo, 113-8656, Japan

Summary. We investigate the reaction speed of a pedestrian to the predecessor in a queue which significantly affects the flow inside the queue. This is one of the most essential points for studying the dynamics of pedestrians. We have performed experiments of pedestrians' walk in a queue on a flat road, upslope and downslope to measure the propagation speed of the starting wave and stopping wave. We have found that the propagation speed of stopping wave is faster than starting wave on a flat road, whereas the speed of stopping wave is slower than starting wave on the other cases. This reverse result has been studied by using stochastic cellular automaton model in which a perspective of predecessors and the inertial effect are introduced. Moreover, in the case of starting wave we can estimate the elapsed time of the last pedestrian in a queue to move after the leader starts by using mean field analysis.

1 Introduction

We always create an action such as walking and driving as applied to the situation we have. If many pedestrians are slow to react to the changing situation, they can not move smoothly and some congested areas are created. By contraries, if all pedestrians are very sensitive, jam is obviously vanished away in the world.

Now, how fast is the propagation speed of pedestrian reaction? This question is very meaningful for studying not only self-driven many-particles systems [1, 2], e.g. pedestrian dynamics and traffic flow, but also the sonic wave in the aerodynamic theory since the dynamics of pedestrians are considered as the supersonic flow.

The main aim of this paper is to measure and investigate the two types of wave velocity (*starting wave* and *stopping wave*) in three situations (*flat road*, *upslope* and *downslope*) by *experiments*, *numerical simulations* and *analytical calculations*. Note that, *starting wave* means the propagation wave when pedestrians start to walk, on the other hand, *stopping wave* means the propagation wave when pedestrians stop walking.

This paper is organized as follows, in Sect. 2 we describe two experiments concerning pedestrians' walk. In Sect. 3 we show several simulation results by using stochastic cellular automaton model and the results of analytical calculations are shown in Sect. 4. Section 5 is devoted to conclusions and discussions.

2 Experiments

In this section, we explain two experiments concerning one-dimensional pedestrians' walk in a queue in detail.

2.1 Forthright Walking

In this experiment, we have measured the propagation speed of starting wave and stopping wave under three situations i.e. flat road, upslope and downslope.

In the case of starting wave, the initial condition is that ten pedestrians line up behind each other. After we measure the length of initial queue, the leader of queue starts to walk and then we measure the elapsed time until the last pedestrian starts to walk. Whereas, in the case of stopping wave, ten pedestrians are walking as an initial condition and then the leader suddenly stops. We measure the length of final queue and the elapsed time until the last pedestrian stops walking.

In general, it is a good guess that the stopping wave is faster than the starting wave, since pedestrians avoid dangers involuntarily, which means that pedestrians feel more dangerous when they stop walking than when they start to walk. However, the result of these experiments (Fig. 1(a)) shows that the starting wave is faster than the stopping wave except in the case of a flat road. Furthermore, in the case of upslope this phenomenon is observed prominently and both wave velocities are considerably low compared to other two cases.

We suppose that perspectives of predecessors and the inertial effect cause this phenomenon, since this result is dependent on the configuration of roads. In order to investigate this phenomenon, we need to obtain the optimal velocity function.

2.2 Circular Walking

From this experiment, we have obtained the fundamental diagram, which shows the relation between the pedestrian density and the pedestrian flow.

Then, from the fundamental diagram, we decide the optimal velocity function $V_{\text{opt}}(h)$, where h corresponds to the headway distance [3].

In this experiment we set a circular path with the internal radius 1.8 meters and external radius 2.3 meters. The length of the circuit L is 12.88 meters. The parameter of this experiment, which we varied, is the number of people m . The number density of people is defined by $\rho = m/L$. Thus we measure the lap time for the parameters $m = 4, 6, 8, 9, 11, 13, 15, 20$.

Figure 1(b) shows the fundamental diagram for these parameters. The solid line corresponds to the experimental data and the dashed line corresponds to the approximate data by using least-squares method. Since the dynamics of self-driven particles intersect at a origin coordinate, the quadric curve $Q(\rho)$ based on the least-squares method is given by

$$Q(\rho) = -\rho^2 + 1.984\rho. \quad (1)$$

By using an transformation $\rho = 1/(h + 0.5)$ and basic relation $Q = \rho V_{\text{opt}}(h)$ in (1), we obtain the optimal velocity function,

$$V_{\text{opt}}(h) = -\frac{1}{h + 0.5} + 1.984. \quad (2)$$

It is useful for cellular automaton simulations to transform the headway distance from meters into cells as 1 cell corresponds to 0.5 meters. Thus, we obtain the optimal velocity function expressed in cells at a flat road. Since at a upslope (downslope) the gait velocity is slower (faster) than at a flat road, the optimal velocity function is accordingly scaled. In this regard, if the value of the optimal velocity function is larger than 1, we define the value as $V_{\text{opt}}(h) = 1.0$. If the headway distance is larger than 6 cells, we also define the value as $V_{\text{opt}}(h) = 1.0$ ($h > 6$).

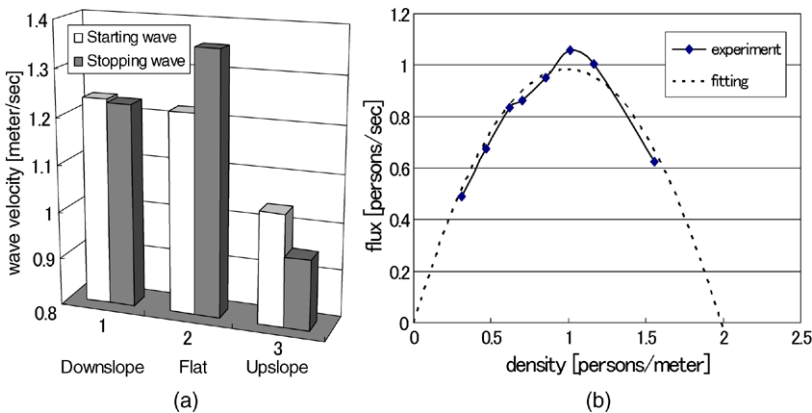


Fig. 1. a Propagation speed by experimental data. b Fundamental diagram of pedestrians' walk.

3 Cellular Automaton Simulations

In this section by using stochastic optimal velocity (SOV) model [4] we simulate one-dimensional walking model of pedestrians. This SOV model is expressed as the cellular automaton model and updated in parallel by following two relational expressions:

$$v_i^{t+1} = (1 - a)v_i^t + aV_{\text{opt}}(x_{i+1}^t - x_i^t), \quad v_i^t, V_{\text{opt}}, a \in [0, 1], \quad (3)$$

$$x_i^{t+1} = x_i^t + v_i^{t+1}. \quad (4)$$

In these expressions, v_i^t and x_i^t correspond to the velocity and position of i th vehicle at time t respectively. a is a parameter of sensitivity and $V_{\text{opt}}(h)$ is previously obtained the optimal velocity function. The first expression (3) is “Decision of the velocity” and the second expression (4) is “Movement”.

In the simulations of starting wave, we set the initial condition as all pedestrians are closely-apposed and their velocities equal to 0. While on the other hand, in the case of stopping wave the initial condition is set as all pedestrians are apposed every one cell except the upslope. In the case of upslope, all pedestrians are apposed every two cells, since pedestrians have few perspectives of predecessors compared to other cases and the length of queue becomes longer in the steady state. In the all case of stopping wave, the velocity of all pedestrians equal to 1 as an initial condition. Furthermore, in order to take into account the effect of a perspective of predecessors, in the simulation of upslope we set the sensitivity parameter $a = 0.9$ and in other simulations we set $a = 1.0$.

As the results of simulations, some conspicuous results are obtained (see Figs. 2 and 3). Typical space-time plots of each situation are given in Fig. 2(a).

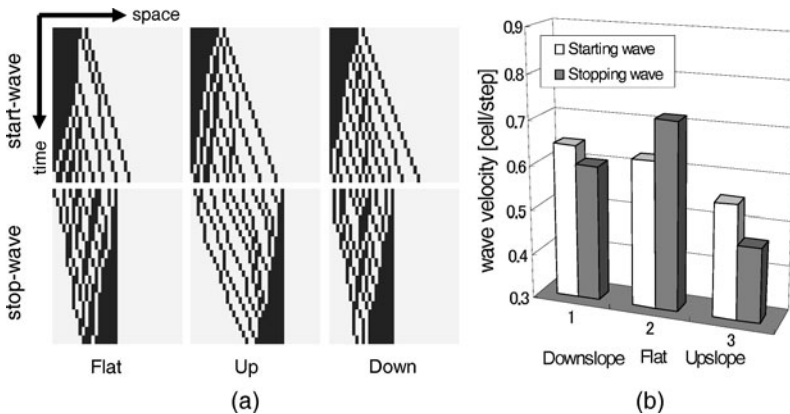


Fig. 2. **a** Time–space plots of each situation. *Upper figures* correspond to the case of starting wave and *lower figures* correspond to the case of stopping wave. **b** Propagation speed by cellular automaton simulations.

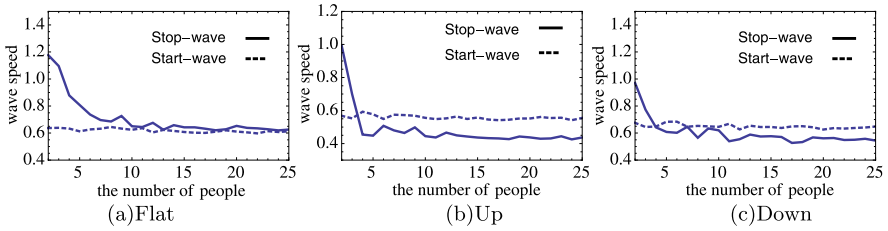


Fig. 3. Propagations speed of starting wave and stopping wave is plotted against the density in each situation.

There is no difference of the propagation speed on the flat road and on the downslope. However, in the case of upslope, the propagation speed is slower than in other two cases. Note that, though all cases of starting wave are all the same initial condition, only the initial condition of stopping wave of upslope is longer than the other cases. Figure 2(b) shows the propagation speed obtained from numerical simulations. From this result, we have found that the reverse result is occurred as we observed in the experiment.

Furthermore, the propagation speed against the number of pedestrians is plotted in Fig. 3. The reverse result is surely occurred on the downslope and upslope as the number of pedestrians increases.

4 Mean Field Analysis

In order to estimate the elapsed time analytically, we assume that pedestrians never stop after they once start to walk. Under this assumption, the required time T_m before a last pedestrian starts to walk is given by

$$T_m = (m - 1) \times \left\{ v^t(1) \times 1 + \sum_{j=2}^{\infty} \left[\left(\prod_{t=1}^{j-1} (1 - v^t(t)) \right) v^j(j) \times j \right] \right\}, \quad (5)$$

where m is the number of pedestrians and $v^t(t)$ is the hopping probability at t steps later. The second term on the right hand side of (5) is the average time per one pedestrian before starting to walk. Note that, when the headway distance is larger than 6 cells, all the hopping probability correspond to 1. Therefore, by using infinite series in (5) we have obtained the analytical results in Table 1. This table shows the comparative table of starting wave among experimental data, numerical simulations and analytical calculations. In the case of flat road and downslope, we have found that both numerical simulations and analytical calculations are good agreement with the experimental data. However, only in the case of upslope, the analytical result is prominently different from other cases though the result of numerical simulations agrees with the experimental data. When the dynamics are influenced by correlations, our mean field analysis is broken down, since our analytical calculations are based on the assumption that pedestrians never stop.

Configuration	Experiment [sec]	Simulation [step]	Mean Field Analysis [step]
Upslope	4.34	16.31	19.88
Flat road	3.69	14.36	13.75
Downslope	3.68	13.98	13.23

Table 1. The comparative table of starting wave among experimental data, numerical simulations and analytical calculations (1 sec \sim 3.4 step).

5 Conclusion

In this study, first of all we perform the experiments in three situations, which are flat road, upslope and downslope, in order to measure the propagation speed of starting wave and stopping wave of pedestrians. As the results of this experiment, we have observed the reverse result, that is, the starting wave is faster than the stopping wave except the flat road.

By introducing a perspective of predecessors and the inertial effect into the cellular automaton model, the numerical simulations give the correspondent results with the experiment. Furthermore, in the case of starting wave we have also estimated the elapsed time by analytical calculations, which are good agreement with the experimental data except the upslope. Only in the situation of upslope, the mean field analysis is broken down, since our assumption does not hold true due to a correlation of successive pedestrians.

In future work, we intend to perform experiments without the effect of perspectives, and calculate the elapsed time analytically taking into account correlations.

Acknowledgements

The author (AT) was supported through the 21st Century COE Program, ‘Mechanical Systems Innovation’, by the Ministry of Education, Culture, Sports, Science and Technology.

References

1. D. Chowdhury, L. Santen, and A. Schadschneider. *Phys. Rep.*, 329:199, 2000.
2. D. Helbing. *Rev. Mod. Phys.*, 73:1067, 2001.
3. M. Bando, K. Hasebe, A. Nakayama, A. Shibata, and Y. Sugiyama. *Phys. Rev. E*, 51:1035, 1995.
4. M. Kanai, K. Nishinari, and T. Tokihiro. *Phys. Rev. E*, 72:035102, 2005.

Simulation and Modeling

Toward Smooth Movement of Crowds

Katsuhiko Nishinari^{1,3}, Yushi Suma¹, Daichi Yanagisawa^{1,2},
Akiyasu Tomoeda¹, Ayako Kimura¹, and Ryouyusuke Nishi¹

¹ Faculty of Engineering, The University of Tokyo, Hongo 7-3-1, Tokyo 113-8656,
Japan

² Japan Society for the Promotion of Science, 1.8, Chiyoda-ku, Tokyo 102-8472,
Japan

³ PRESTO, Japan Science and Technology Corporation, 7-3-1 Hongo, Bunkyo-ku,
Tokyo 113-8656, Japan

e-mail: tknishi@mail.ecc.u-tokyo.ac.jp

Summary. “Jamology” is an interdisciplinary research of all sorts of jams, e.g. those of vehicles, pedestrians, ants, etc. Our model of pedestrians, called the floor field model, is based on this study, and it is a two-dimensional generalization of an ant trail model. It is a rule-based cellular automaton model, and efficient in computations since the long-range interaction between pedestrians is imitated by the memory of the floor of only neighboring cells. Recently several generalizations of this model are proposed to make the model more realistic. We use an extended model to study how to make crowd movement smooth. Not only computer simulations but also experiments are shown in this paper. Introduction of pedestrians’ anticipation into the model affects the crowd movement significantly, and leads the counterflow smooth. Moreover it is clearly shown experimentally that evacuation dynamics near a bottleneck becomes smooth if we put an obstacle at a suitable place.

1 What is Jamology?

Jamming phenomena are seen not only at a motorway, but also at a concert hall and an Internet network. That is, vehicles, pedestrians, and data packets similarly suffer from traffic congestion in their transporting processes. Moreover, there are traffic jams inside our body which cause various diseases, e.g., malfunction of protein transportation in a neural network can lead the Alzheimer’s disease [1]. In a production network, we also have a similar jam of inventories which should be reduced for efficient management. The Toyota production system is known as one of the famous method for reducing jams of inventories, and this can be also modeled by a similar technique as that of vehicle traffic [2].

We now come to an important point that there is universality of jam formation among various sorts of flows as shown above. This is one of the

central topics of physics of complex systems for the last few decades [3, 4]. We have been studying so far various transportation phenomena including cars, buses, ants, molecular motors and pedestrians, which are all considered as “self-driven particles” [5, 6].

We recently call this interdisciplinary research on jamming of self-driven particles as “jamology”. It is noted that, of course, in each field there are specialists who have been studying why congestion occurs and how we should avoid it. However, we sometimes need fresh ideas from other fields outside one’s own community in order to solve traffic problems which are now a tough and complicated issue in modern society. It is difficult for specialists in a single field, say, vehicle traffic engineers to propose a fundamental solution of this problem since it is nowadays related to economics, psychology, sociology, biology, etc. Also one needs statistical and physical background in order to analyze the jamming phenomena accurately and trustworthily. Therefore we believe it is very important for researchers to have knowledge of various fields in their own brain as well as to collaborate with researchers in different fields. Unfortunately there are few interactions between, e.g., vehicle traffic engineers and biologists, or architects and physicists, etc. Thus we have recently started a new type of interdisciplinary study called jamology in order to consider fundamental solutions for all sorts of jamming issues. Researchers who are interested in jamming phenomena gather and discuss new ideas for jam solution, or new ways for analysis regardless of what research field they belong to. Through these discussions we have found, for example, a similarity among pedestrians, ant trails and public conveyance of buses and trains [7–9].

Recently we are particularly interested in engineering applications of the results we have obtained through this interdisciplinary study. We consider it is valuable to keep the balance between engineering applications and basic studies such as mathematics and physics. Sometimes researchers easily go to one of the two extremes. Thus we have done so far many experiments and observations on vehicles and pedestrians, etc., as well as theoretical analysis.

In this paper we focus on jamming phenomena of pedestrians, and show a new modeling and experiments in order to study how to make pedestrian flow smooth. Several ideas for attaining smooth movement is studied and presented in this paper. It is shown that introduction of pedestrians’ anticipation into the model leads the counterflow at a corridor smooth. Our experiments also clearly show that, if an obstacle is put at a suitable place, then evacuation dynamics near a bottleneck becomes smooth.

2 Modeling Crowds

2.1 Different Type of Models

Crowd modeling has been one of the recent growing studies of physics of complex systems and social sciences [10, 11]. From 1990s the number of research

papers published in physical journals has been rapidly increasing. There are roughly two ways for describing the dynamics of pedestrians: i.e., using coupled differential equation of motions by assuming interaction forces between pedestrians, and rule-based approaches. The former model is a molecular dynamics approach similar to the study of granular matter. Pedestrian interactions are modeled via long-ranged repulsive forces that reflect interpersonal psychological relation. An example is the social force model proposed in [12]. This model is also derived by using the variational principle in which a cost function of pedestrians is minimized [13].

In the latter type of models, cellular automaton(CA) is usually used as a method to represent the rules of pedestrian's behaviors. CA is a fully discrete model of time and space, hence it is computational efficient. Multi-agent models are also used as the rule-based models [14], which are usually a continuous type model and have more complex rules than CA approaches. Our model presented in this paper, called the floor field (FF) model, is one of the CA models [15, 16]. In this model two kinds of FFs, i.e., a static and a dynamic one, are introduced to translate a long-ranged spatial interaction into an attractive local interaction, but with memory, similar to the phenomenon of chemotaxis in biology [5]. The reasons to use this model are that the rules are not so complex and computational efficient, and it is sometimes possible to treat theoretically [17]. Moreover this model is able to reproduce various fundamental phenomena, such as lane formation in a corridor, herding and oscillation at a bottleneck [15, 16], and the so-called faster-is-slower effect [12]. These are indispensable properties for any reliable models of pedestrian dynamics, especially for discussing safety issues.

2.2 Floor Field Model and its Extensions

Here let us summarize the original FF model, then several extensions of it proposed so far are discussed. The model is implemented as a CA where pedestrians correspond to particles that move on a two-dimensional lattice of cells. The size of cells is usually taken as 50 cm \times 50 cm, and each cell can be occupied by at most one particle. This reflects the fact that the interactions between them are repulsive for short distances.

Each pedestrian can move to one of the unoccupied next-neighbor cells (i, j) , or stay at the present cell at each discrete time step $t \rightarrow t + 1$ according to certain transition probabilities p_{ij} (Fig. 1).

The probabilities p_{ij} are determined by three factors: (1) the desired direction of motion, (2) interactions with other pedestrians, and (3) interactions with the infrastructures (walls, exits, etc.). First of all, transition probabilities are determined by the desired walking direction and speed of each individual in the form of a matrix of preferences M . The entries of this matrix can be related to the preferred velocity vector and its longitudinal and transversal standard deviations [15].

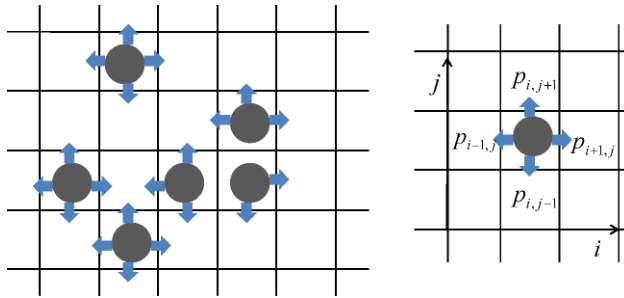


Fig. 1. Target cells for pedestrians at the next time step. The Neumann neighborhood is used for simplicity.

Next two kinds of interactions between pedestrians are taken into account, i.e., the short-range repulsion and the long-range interaction. In CA models the short-range repulsion is naturally incorporated by the exclusion principle of cells. The long-range interaction becomes both attractive and repulsive depending on situations. When walking in a crowded area, it becomes often attractive since it is usually advantageous to follow directly behind the predecessor. Also it is known that in a panic people shows herding behavior to others due to a deteriorating of the ability of thinking and judgment [12]. This is implemented by virtual chemotaxis. Moving particles create a “pheromone” at the cell which they leave, thus creating a kind of trace. So apart from the occupation number, each cell carries an additional field similar to the pheromone field in the ant trail model [7]. It is called the dynamic FF since it has its own dynamics given by diffusion and decay [15] which leads to a dilution and finally the vanishing of the trace after some time.

For interaction with infrastructures, another floor field, called the static FF is introduced, which describes the shortest distance to a destination, e.g., an exit. In each cell the distance is stored which never changes during the simulations, hence it is static. It is noted that the static FF can sometimes be used to incorporate the information usually contained in the matrix of preference. Therefore in the followings we omit the matrix of preference M for simplicity.

Basic Update Rules

First we calculate the static FF by the Dijkstra method which is described later, then store the distance from the cell (i, j) to the destination as S_{ij} in each cell. At $t = 0$ for all sites (i, j) of the lattice the dynamic FF is zero, i.e., $D_{ij} = 0$. The update rules of our CA have the following structure:

1. In each time step of the simulation the whole D_{ij} decays with probability δ and diffuses with probability α to one of its neighboring cells.

2. For each pedestrian, the transition probabilities p_{ij} for a move to an unoccupied neighbor cell (i, j) are determined by the two FFs, inertia p_I and the wall potential p_W [18]. The values of the two FFs are weighted with two sensitivity parameters k_D and k_S as

$$p_{ij} = N \exp(k_D D_{ij}) \exp(-k_S S_{ij}) p_I p_W, \quad (1)$$

with the normalization N . Here p_I represents the inertia effect given by $p_I(i, j) = \exp(k_I)$ for the direction of one's motion in the previous time step, and $p_I(i, j) = 1$ for other cells, where k_I is a parameter. Thus the probability of choosing the direction of one's velocity vector is enhanced by this inertia term. p_W is the wall potential which is given by $p_W = \exp(k_W \min(D_{\max}, d))$, where d is the minimum distance to the nearest wall, and k_W is a parameter. The range of the wall effect is restricted up to the distance D_{\max} from the wall. This term represents that people tend to avoid walking close to walls and obstacles. In (1) we do not take into account the obstacle cells (walls, etc.) as well as occupied cells. An example of a modification of the treatment of occupied cells is seen in [19].

3. Each pedestrian chooses randomly a target cell based on the transition probabilities p_{ij} determined by (1).
4. The pedestrians who are allowed to move perform their motion to the target cell chosen in step 3. Whenever a particle jumps from site (i, j) to one of the neighboring cells, D at the origin cell is increased by one, $D_{ij} \rightarrow D_{ij} + 1$, i.e. D can take any non-negative integer value.

The above rules are applied to all pedestrians at the same time, i.e., parallel update.

Resolution of Conflicts

Due to the use of parallel dynamics it is possible that two or more particles choose the same destination cell in the update procedure. Such situation is called *conflicts*. A friction parameter $\mu \in [0, 1]$ is introduced in order to describe conflicts between the pedestrians [20]. Whenever two or more pedestrians try to attempt to move to the same target cell, the movement of *all* involved particles is denied with the probability μ , i.e. all pedestrians remain at their site. This means that with probability $1 - \mu$ one of the individuals moves to the desired cell. Which particle actually moves is then determined randomly for simplicity (see Fig. 2).

Calculation of the Static Field in Arbitrary Geometries

The static FF is calculated by a combination of the visibility graph and Dijkstra's algorithm [18]. This method enables us to determine the minimum Euclidean (L^2) distance of any cell to a door with arbitrary obstacles between them.

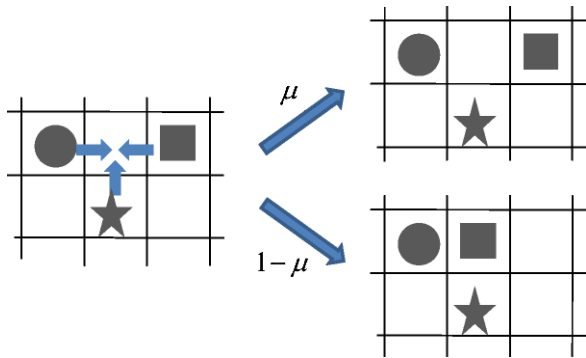


Fig. 2. The friction parameter μ and the illustration of its rule.

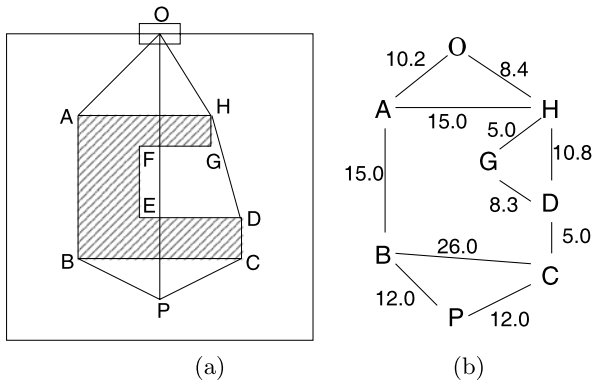


Fig. 3. An example for the calculation of the static FF using the Dijkstra method. **a** A room with one obstacle. The door is at O and the obstacle is represented by lines $A - H$. **b** The visibility graph for this room. Each node connected by a bond is “visible”, i.e., there are no obstacles between them. The real number on each bond represents the distance between them.

Let us explain the idea of this method by using the configuration given in Fig. 3(a) where there is an obstacle in the middle of the room. We will calculate the minimum distance between a cell P and the door O by making a detour around the obstacle. We see there are two candidates for the minimum path, i.e., lines $PBAO$ and $PCDHO$. The shorter one finally gives the minimum distance between P and O . We first introduce the concept of the *visibility graph* in which only the nodes that are visible to each other are bonded. The set of nodes consists of a cell point P , a door O and all the nodes in the room. Each bond has its own weight which corresponds to the Euclidean distance between them. Once we have the visibility graph, we can calculate the distance between P and O by tracing and adding the weight of the bonds between them. The path with minimum total weight represents the shortest route between them. The optimization task is easily performed by using the

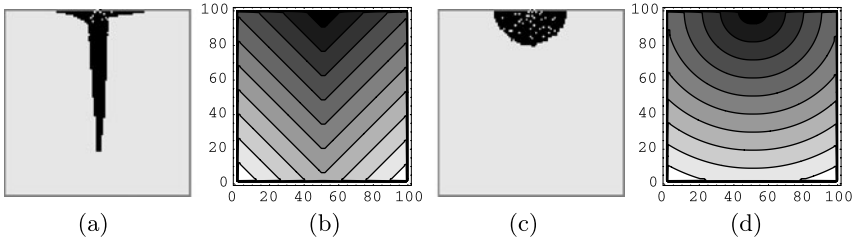


Fig. 4. Comparison of typical snapshots of pedestrians’ motion in the case of the Manhattan (a) and Dijkstra (c) metric for the static FF. We see a queue formation in front of the door in (a). This comes from the triangular shape of the contour of the Manhattan metric as seen in (b), while the Dijkstra metric gives a semicircular static FF from the door (d). Parameters are $k_S = 3.0$, $k_D = 1.0$, $k_I = 0.2$, $\mu = 0.2$ and the initial density is $\rho = 0.04$.

Dijkstra method which enables us to obtain the minimum path on a weighted graph. Performing this procedure for each cell in the room, the method allows us to determine the static floor field for arbitrary geometries.

Next, we compare the Dijkstra metric with the simpler Manhattan metric [16]. Figure 4 shows the comparison of typical configurations during an evacuation from a simple room with no obstacles. We see that pedestrians form a queue in front of the door if the Manhattan metric is used, whereas for the Dijkstra metric we see a symmetric gathering of the semicircular shape. It is noted that, in Tokyo we usually see a queue-like gathering in front of the exit, but in some other area in Japan or countries people shows a more competitive behavior which leads a semicircular gathering.

Contraction at a Wide Exit

If the width of an exit becomes large, a more careful treatment is needed in the calculation of the static FF. People usually tend to rush to the center of the exit to avoid the walls. Thus one should introduce an effective width of the exit by neglecting certain cells from its each end. We call this effect *contraction*, whose terminology comes from hydrodynamics where fluid runs through a orifice with a smaller diameter than that of the orifice immediately after the fluid goes out of it. The shortest distance from a cell in the room to one of the exit cells is calculated by using the Dijkstra metric, but only those exit cells near the center of the door are taken into account owing to the contraction. Then we take the minimum of those shortest distances among them and use it as the value of the static floor field at the cell. Here we define the ratio of contraction of an exit as $c = W'/W$, where W is the true width of the exit and W' is the effective width. If $c = 1$, i.e., there is no contraction, and we see the artifact of two crowds near the edges of the exit (Fig. 5(a)). Introducing the contraction makes the evacuation behavior more realistic (Fig. 5(b)).

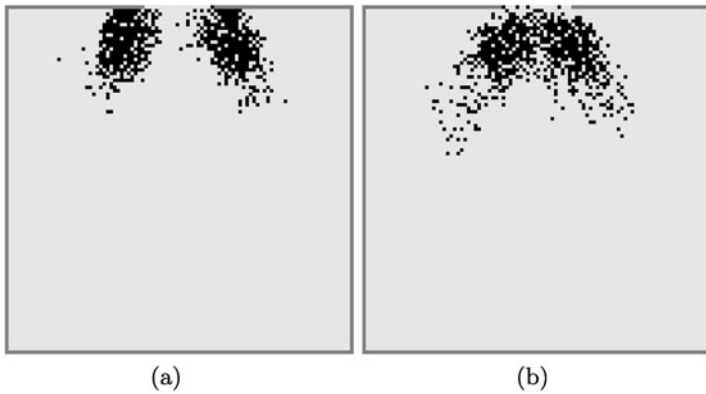


Fig. 5. Contraction of flow through a wide exit. The width of the exit is set as 20 cells. In (a) we set the ratio of contraction as 1, while in (b) it is 0.3. In (a) we see the artifact of the crowd at both ends of the exit even if they can easily evacuate through the center of the exit. Parameters are $\rho = 0.05$, $k_I = 1.0$, $k_S = 2.0$, $k_D = 1.0$, $k_W = 0.3$ and $\mu = 0.2$.

Parameters and Their Physical Relevance

There are several parameters in the FF model, and the important ones are listed below with their physical meaning which is helpful in understanding the collective behaviors in the simulations.

1. $k_S \in [0, \infty) \dots$ The coupling to the static field characterizes the knowledge of the shortest path to the doors, or the tendency to minimize the costs due to deviation from a planned route.
2. $k_D \in [0, \infty) \dots$ The coupling to the dynamic field characterizes the tendency to follow other people, i.e., herding behavior. The ratio k_D/k_S can be interpreted as the degree of emergency since people try to follow others particularly in emergency situations.
3. $k_I \in [0, \infty) \dots$ This parameter determines the strength of inertia which suppresses quick changes of the direction of motion. It also reflects the tendency to minimize the costs due to deviation from one's desired route and acceleration.
4. $\mu \in [0, 1] \dots$ The friction parameter might be interpreted as the effect of a moment of hesitation: Pedestrians in conflict situations slow down or hesitate for a short moment when trying to resolve the conflict. This reduces on average the velocities of all involved particles. It also works as a kind of local pressure between the pedestrians. If μ is high, the pedestrians handicap each other trying to reach their desired target sites.
5. $\alpha, \delta \in [0, 1] \dots$ These constants control diffusion and decay of the dynamic floor field. It reflects the randomness of people's random movement and the visible range of a person, respectively. If the room is full of smoke, then δ takes large value due to the reduced visibility.

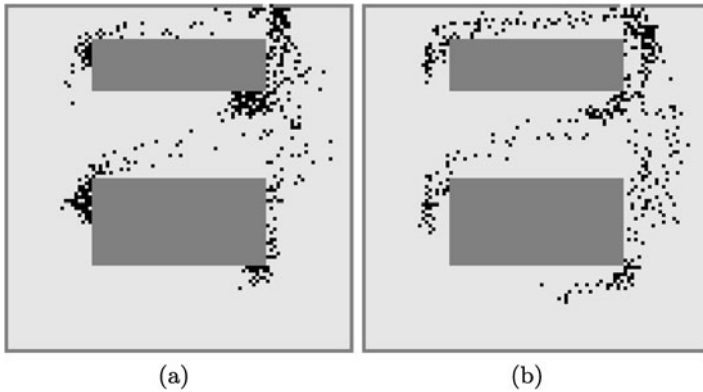


Fig. 6. Snapshot of evacuation **a** without ($k_W = 0$) and **b** with ($k_W = 0.5$) wall potential. We can clearly see the artifact of jamming at every corner without the wall potential. Parameters are $D_{\max} = 10$, $k_S = 2.0$, $k_D = 1.0$, $k_I = 0.2$, $\mu = 0.2$ and the initial density is $\rho = 0.03$.

6. $k_W \in [0, \infty)$. . . Pedestrians tend to avoid walking close to walls and obstacles. k_W is the sensitivity to the walls, and the ratio k_W/k_S reflects to which degree deviations from the shortest route are accepted to avoid the walls. Figure 6 shows an example for an evacuation from a room with obstacles using the wall potential. Without wall potentials ($k_W = 0$), jamming areas near every corner can be observed, because everybody tries to evacuate along the same path of minimum length. For $k_W \neq 0$ these areas are clearly suppressed. Thus the introduction of this additional potential improves the realism of the model.

Force Field

Recently a new force field is introduced in the FF model in order to simulate the movement of pedestrians under extremely high density [19]. In such a situation, the motion of each pedestrian is not always determined by the transition probability p_{ij} , but sometimes it is bypassed and he/she has to move according to the contact force applied to him/her. The contact force is accumulated through the contact network in a crowd. If the strength of the force becomes larger than a certain threshold, then we use the force vector to move a pedestrian instead of using p_{ij} . In this paper we focus on the situation that pedestrians can determine the direction of motion by their own will, and not consider the force field in the FF model.

3 Smooth Movement

In this section let us study how we can make the pedestrian flow smooth by using computer simulations and experimental observations. For this purpose we study the following four ideas for making the crowd movement smooth.

3.1 Inertia Effect

First we study the total evacuation time from a room without any obstacles, which is shown as function of k_D in the cases $k_I = 0$ and $k_I = 3$ in Fig. 7. It is monotonously increasing in the case $k_I = 0$, because perturbation from other people becomes large if k_D increases, which causes the deviation from the minimum route. Introduction of inertia effects, however, changes this property qualitatively as seen in Fig. 7. The *minimum* time appears around $k_D = 1$ in the case $k_I = 3$. The smooth movement of crowd in this case is well explained by taking into account the physical meanings of k_I and k_D . If k_I becomes large, people become less flexible and all of them try to keep their own direction of motion regardless of congestion. By increasing k_D , one begins to feel the disturbance from other people through the dynamic floor field. This perturbation makes one flexible and hence contributes to avoid congestion. Large k_D again works as strong perturbation as in the case of $k_I = 0$, which diverts people from the shortest route largely. Thus we have the minimum time at a certain magnitude of k_D , which depends on the value of k_S and k_I .

3.2 Anticipation

Introduction of one’s ability of anticipation of other pedestrians’ behaviors into the FF model has not been studied up to now. In reality pedestrians try to avoid collision among others prior to their close meeting by looking far around

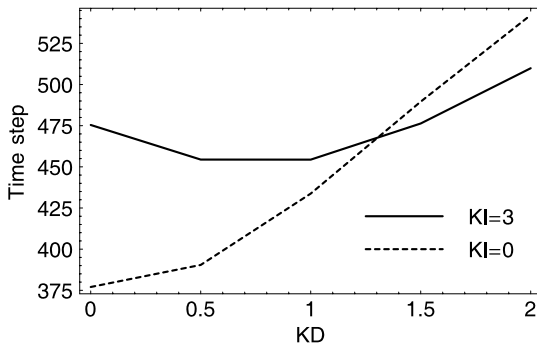


Fig. 7. Total evacuation time vs. coupling k_D to the dynamic floor field in dependence of k_I . The room is a simple square without obstacles and 50 simulations are averaged for each data point. Parameters are $\rho = 0.03$, $k_S = 2$, $k_W = 0.3$ and $\mu = 0$.

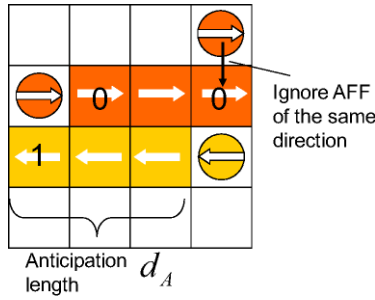


Fig. 8. The rules of the anticipation FF in the counterflow case.

and anticipating who possibly collide. If one judges that he will collide with someone, then he slightly changes his velocity or walking direction in advance in order to deviate the collision path. Taking into account this behavior, we newly introduce the anticipation FF (AFF) in our model. Pedestrians have their preferred direction while walking, and do not want to deviate the path in order to minimize the effort to reach their destinations. Thus we set a string of anticipation cells in front of each pedestrian which represent one’s preferred path as described in Fig. 8. The anticipation cells are considered to be reserved cells for each pedestrian, and they try to avoid other’s reserved cells in choosing the next target cell. These cells are taken along the gradient of the static FF, and the number of cells d_A depends on how far the pedestrians predict other’s walking path. For simplicity we restrict ourselves to the case of counterflow in a corridor in the following. Then it is shown that this new rule helps pedestrians to avoid the artifact of freezing of the counterflow even at low density [21], and makes the model more realistic.

The transition probability is then modified as

$$p_{ij} = N \exp(-k_a A_{ij}) \exp(k_D D_{ij}) \exp(-k_S S_{ij}) p_{IPW}, \tag{2}$$

where A_{ij} is the AFF and k_a is its sensitivity parameter. The AFF is set as follows. At each time step the string of cells of length d_A is set in front of each pedestrian. An integer value A_{ij} represents the number of pedestrians who have their anticipation cells at (i, j) . Then A_{ij} is stored in each cell as the AFF, and updated at every time step. However, a pedestrian do care only the AFF that is generated by those who are moving to the opposite direction. Since we consider counterflow where there are only two groups of pedestrians, i.e., moving from left to right and *vice versa*, we neglect the AFF of the same group in (2) as illustrated in Fig. 8.

Results of the simulations using the AFF are given in Fig. 9. Pedestrians are generated at each end of a corridor with the probability 0.035. The length and width of the corridor is 100 and 20, respectively. The average travel time steps from one end to the other is obtained by averaging the numerical data. We change the strength of the weight of the AFF from $k_a = 0$ to $k_a = 6$,

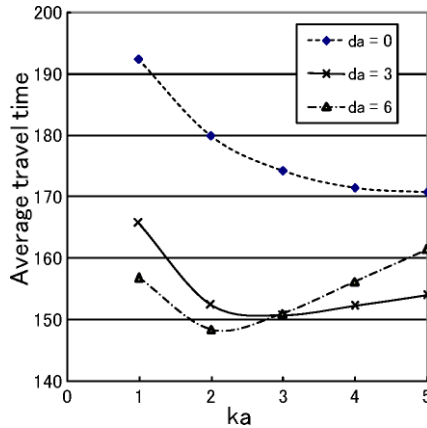


Fig. 9. Average travel steps from one end to the other in the corridor in terms of the change of k_A from 0 to 6. Parameters are $k_S = 3$ and $k_D = 2$.

and found that there is a *minimum* at $k_a = 3$ as shown in Fig. 9. The reason is follows: When the anticipation is weak, then the pedestrians are likely to collide in counterflow, which decreases the travel time in the corridor. As increasing the strength, the flow becomes smooth since pedestrians avoid the collisions in advance and the total number of collisions decreases. However further increase of the anticipation leads to the frequent collisions between pedestrians in the same group due to the overreaction to the counterflow.

3.3 Obstacles

It has been known that putting an obstacle near the exit will sometimes help the crowd evacuation be smoother. However, this is sometimes just a rumor, or comes from the naive analogy with granular flow from a bin where putting a toothpick at the opening will lead smooth flow of the contents. Since we do not find any quantitative and theoretical researches of the phenomena, we have done both experiments and theoretical analysis in order to find the suitable position and the shape of the obstacles. Of course if we put the obstacle at a wrong place or with a wrong size, then the evacuation time becomes much worse. Thus it is important to know the mechanism why we have the reduction of evacuation time if we put the appropriate obstacle near the exit.

Experimental settings are follows. There are 40 adult persons in front of an exit of 50 cm width in a square room. They are motivated to evacuate through the exit, but strong interaction among others, e.g., pushing others, is prohibited. The obstacle is a column with 20 cm diameter and is set at 75 cm north and 25 cm east from the center of the exit as seen in Fig. 10. We have done the experiment six times for the case with and without the obstacle. The total evacuation time without the obstacle is 35.73 sec in average and the standard deviation is 0.45. On the other hand, when the obstacle is set, the



Fig. 10. A snapshot of the experiment of evacuation from a small square room with one exit of 50 cm width. (Left) Evacuation without the obstacle. (Right) A column is put near the exit.

average evacuation time becomes 33.70 sec and the standard deviation is 0.61. From this result we have succeeded to show that this obstacle has made the pedestrian outflow from a bottleneck smooth. This is well explained by the fact that the obstacle will reduce the conflicts near the exit. The theoretical analysis is presented in the separate paper in this proceedings [22].

3.4 Deterministic Evacuation

From the previous experiment of putting an obstacle, it is seen that conflicts among pedestrians will significantly reduce the evacuation time. In order to test this, we have compared the two kinds of evacuating process experimentally. One is a normal evacuation where pedestrians move to an exit simultaneously in a competitive way, and hence conflicts occur in front of the exit, as seen in Fig. 10(left). Since the width of the exit is 50 cm, it is too narrow to escape with more than one person simultaneously. Then the order of the pedestrians escaping from the door is not determined *a priori*, but is the result of competition near the exit. We call this case as stochastic evacuation. On the other hand, we have done deterministic evacuation by forming queues in front of the exit, as seen in Fig. 11. In this case, the order of evacuation is completely determined *a priori*, then there is no conflict among pedestrians throughout the evacuation process.

Pedestrians walk with their normal speed in the latter case and there is no jam in front of the exit. The total evacuation time become 30.55 sec in average and the standard deviation is 0.6, which is even faster than the case with an obstacle. From the experiment we have got a lesson that keeping the order of pedestrians without competition is quite important for smooth movement of crowd, since this reduces the conflicts which is a cause of the delay and jams.

Finally we point out that the evacuation flow from an exit is not always symmetric. An example is shown in Fig. 12, which is depicted by the above experiment of stochastic evacuation without obstacles. We observe both symmetric and asymmetric flow from the exit alternatively in the middle stage of evacuation. In the asymmetric case, only the people on the right or left hand



Fig. 11. Deterministic evacuation from a bottleneck. 40 pedestrians initially form queues (*left*), then from the leftmost queue pedestrians walk through the exit in order (*right*).

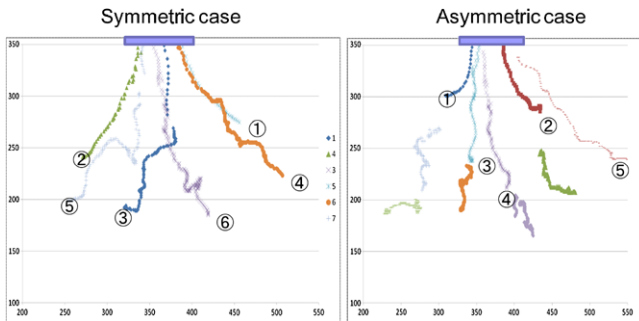


Fig. 12. Symmetric (*left*) and asymmetric (*right*) outflow from an exit of 50 cm width which is located at the center of the top edge. From the video of the experiment we depict the track of some pedestrians. The numbers are the leaving order of pedestrians from the exit.

side can evacuate smoothly. This is like the granular flow from a hopper [23]. If the flow is symmetric, then it is possible to study the outflow theoretically [24]. However it is not easy to study this asymmetric flow, and this is one of the challenging problems in crowd evacuation.

4 Concluding Discussions

In this paper we have stressed on the importance of the interdisciplinary research on jamming phenomena, which we call jamology. Modeling pedestrians is not an exact science like mechanics in physics since psychological aspects of pedestrians significantly affect the results. However, it is important to study the crowd dynamics as precise as possible since it is sometimes related to our lives, e.g., in the case of emergency studies. Our model of pedestrians, called the floor field model, is a rule-based CA model, and several generalizations of it have been proposed so far to make the model more realistic. We have shown

that the introduction of pedestrians' anticipation affects the crowd movement significantly and leads the counterflow smooth. It is also clearly shown experimentally that evacuation dynamics near a bottleneck becomes smooth if we put an obstacle at a suitable place. Further investigation of this effect of obstacles will appear elsewhere.

Acknowledgements

We thank the NHK TV program "Science ZERO" for their assistance of the crowd experiments. We also thank the Kozo Keikaku Inc. for their software "ProTrack" in analyzing the pedestrian tracks from videos. This work is partially supported by a Grant-in-Aid for Scientific Research from Japan Society for the Promotion of Science.

References

1. K. Nishinari, Y. Okada, A. Schadschneider, and D. Chowdhury. Intracellular transport of single-headed molecular motors KIF1A. *Phys. Rev. Lett.*, 95:118101, 2005.
2. D. Helbing, S. Lämmer, U. Witt, and T. Brenner. Network-induced oscillatory behavior in material flow networks and irregular business cycles. *Phys. Rev. E*, 70(5):56118, 2004.
3. D. Chowdhury, L. Santen, and A. Schadschneider. Statistical physics of vehicular traffic and some related systems. *Phys. Rep.*, 329:199, 2000.
4. D. Helbing. Traffic and related self-driven many-particle systems. *Rev. Mod. Phys.*, 73:1067, 2001.
5. D. Chowdhury, K. Nishinari, and A. Schadschneider. Self-organized patterns and traffic flow in colonies of organisms: from bacteria and social insects to vertebrates. *Phase Transit.*, 77(5):601–624, 2004.
6. D. Chowdhury, A. Schadschneider, and K. Nishinari. Physics of transport and traffic phenomena in biology: from molecular motors and cells to organisms. *Phys. Life Rev.*, 2(4):318–352, 2005.
7. D. Chowdhury, V. Guttal, K. Nishinari, and A. Schadschneider. A cellular-automata model of flow in ant trails: non-monotonic variation of speed with density. *J. Phys. A, Math. Gen.*, 35:L573–L577, 2002.
8. A. Kunwar, A. John, K. Nishinari, A. Schadschneider, and D. Chowdhury. Collective traffic-like movement of ants on a trail: Dynamical phases and phase transitions. *J. Phys. Soc. Jpn.*, 73:2979–2985, 2004.
9. A. Tomoeda, K. Nishinari, D. Chowdhury, and A. Schadschneider. An information-based traffic control in a public conveyance system: Reduced clustering and enhanced efficiency. *Physica A*, 384:600–612, 2007.
10. D.E. Wolf, M. Schreckenberg, and A. Bachem (Eds.). *Traffic and Granular Flow*. World Scientific, Singapore, 1996.
11. M. Schreckenberg and S.D. Sharma (Eds.). *Pedestrian and Evacuation Dynamics*. Springer, Berlin, 2001.

12. D. Helbing, I. Farkas, and T. Vicsek. Simulating dynamical features of escape panic. *Nature*, 407:487–490, 2000.
13. S.P. Hoogendoorn and P.H.L. Bovy. Pedestrian route-choice and activity scheduling theory and models. *Transp. Res. B*, 38:169–190, 2004.
14. G. Antonini, M. Bierlaire, and M. Weber. Discrete choice models of pedestrian walking behavior. *Transp. Res. B*, 40:667–687, 2006.
15. C. Burstedde, K. Klauck, A. Schadschneider, and J. Zittartz. Simulation of pedestrian dynamics using a two-dimensional cellular automaton. *Physica A*, 295:507–525, 2001.
16. A. Kirchner and A. Schadschneider. Simulation of evacuation processes using a bionics-inspired cellular automaton model for pedestrian dynamics. *Physica A*, 312:260–276, 2002.
17. D. Yanagisawa and K. Nishinari. Mean-field theory for pedestrian outflow through an exit. *Phys. Rev. E*, 76:061117, 2007.
18. K. Nishinari, A. Kirchner, A. Namazi, and A. Schadschneider. Extended floor field CA model for evacuation dynamics. *IEICE Trans. Inf. Syst.*, E87-D:726–732, 2004.
19. C.M. Henein and T. White. Macroscopic effects of microscopic forces between agents in crowd models. *Physica A*, 373:694–712, 2007.
20. A. Kirchner, K. Nishinari, and A. Schadschneider. Friction effects and clogging in a cellular automaton model for pedestrian dynamics. *Phys. Rev. E*, 67:056122, 2003.
21. Li Jian, Yang Lizhong, and Zhao Daoliang. Simulation of bi-direction pedestrian movement in corridor. *Physica A*, 354:619–628, 2005.
22. D. Yanagisawa, A. Tomoeda, and K. Nishinari. Conflicts at an exit in pedestrian dynamics. In *Pedestrian and Evacuation Dynamics 2008*. Springer, Berlin, 2010.
23. J. Biarez and M. Gourves (Eds.). *Powders and Grains: Proceedings of the International Conference on Micromechanics of Granular*. Balkema, Rotterdam, 1990.
24. D. Helbing, A. Johansson, J. Mathiesen, M.H. Jensen, and A. Hansen. Analytical approach to continuous and intermittent bottleneck flows. *Phys. Rev. Lett.*, 97:168001, 2006.

Modeling Evacuees' Exit Selection with Best Response Dynamics

Harri Ehtamo¹, Simo Heliövaara¹, Simo Hostikka², and Timo Korhonen²

¹ Systems Analysis Laboratory, Helsinki University of Technology, P.O. Box 1100, 02015 HUT Espoo, Finland

e-mail: simo.heliovaara@tkk.fi

² VTT Technical Research Centre of Finland, P.O. Box 1000, 02044 VTT Espoo, Finland

Summary. We present a model for occupants' exit selection in emergency evacuations. The model is based on the game theoretic concept of best response dynamics, where each player updates his strategy periodically according to other players' strategies. A fixed point of the system of all players' best response functions defines a Nash equilibrium of the game. In the model the players are the occupants and the strategies are the possible target exits. We present a mathematical formulation for the model and analyze its properties with simple test simulations.

1 Introduction

Selection of the exit route is one of the most important decisions that occupants will face in an emergency evacuation. This decision is influenced by many factors, such as personal characteristics, building geometry, and observations concerning the dynamic evacuation situation. It is natural that one of the evacuees' main goals is to get out of the building as fast as possible. On the other hand, evacuees tend to prefer familiar alternatives, because they feel that unknown alternatives increase the threat [1]. The visibility of exits also influences the decisions of occupants, since the information of population and conditions at an exit are limited if the exit is not visible [2]. In fire evacuations, occupants will naturally avoid the routes that are smoky or in flames. After all, the ultimate goal of evacuees is to get out of the building alive and the above mentioned tendencies are just means of achieving this goal.

The decisions that occupants make on their exit routes will affect the outcome of the evacuation. Therefore, it is important to take these decisions into account in evacuation simulation models. Some evacuation models make the assumption that all evacuees will head straight to the nearest exit at the start of evacuation. Also many prescriptive fire codes implicitly assume that the total exit width of buildings is used in evacuation. Experience and studies

have shown that this assumption is unrealistic in many occasions [1, 3]. Let us briefly recall some previous studies in the field of exit selection modeling. The exit selection model of buildingEXODUS [2] uses an adaptive decision making model, where the evacuees are allowed to change their target exit a few times during the evacuation. This model considers several factors that influence the decision, e.g., occupants' familiarity with the exits, visibility of exits and the lengths of queues at the exits. In a subsequent article also the effect of fire conditions on exit selection have been considered [4]. The buildingEXODUS model uses a heuristic approach, and specific formulas and parameters of the model have not been published. Lo et al. [5] presented a game theoretic approach for exit selection. The model simplifies the exit selection situation to a two player zero sum game, where the crowd is considered to play a "virtual entity".

In this article, we present a game theoretic model for evacuees' exit selection. The model is based on the game theoretic concept of players' best response functions. A fixed point of the system of these functions defines a *Nash equilibrium* of the game. In our game theoretic model, we interpret evacuees' updating of their best response actions as an adaptive dynamical model. The model has two stages: on one hand the evacuees try to select the fastest exit route. On the other hand, there are also other factors affecting the decision making, like smokiness, familiarity, and visibility of exits. These factors are taken into account by adding constraints to the evacuation time minimization problem.

It is quite obvious that factors like distances to the exits, queue length, and the visibility of the exits need to be taken into account in an exit selection model. These things are considered in our model as well as in some previous approaches. The key contribution of this article is to formulate and analyze the model in a game theoretic framework. We present a mathematical formulation for the reaction function model. We also analyze the emerging phenomena, such as convergence to a Nash equilibrium, using numerical simulations.

2 The Model and a Game Theoretic Formulation

In this chapter we present a game theoretic model for exit selection. In the model, the occupants update their decisions based on their best response functions. A fixed point of the system of these functions is a Nash equilibrium of the game. Best response dynamics have been successfully used in many fields of science, e.g., in telecommunications networks [6, 7] and various road traffic situations [8].

To formulate our exit selection model as an *N-player game* in a normal form, we begin by defining the concepts of best response and Nash equilibrium. For thorough explanations of the concepts, see [9].

2.1 An N -Player Game

In a *normal form static game*, each of the N players, or *agents*, playing the game selects a strategy s_i , where i refers to agent i . Let S_i be the set of all strategies for agent i , so that $s_i \in S_i$. The payoff of the game for agent i is a function of the strategies of all players. This function is called *payoff function* and it is denoted by $u_i(s_1, \dots, s_n)$. The objective of each player is to select the strategy, which maximizes his own payoff, given that also other players maximize their payoffs. In an implementation of this one-stage game the players act according to their maximizing strategies.

A *Nash equilibrium* (NE) of the game is a profile of strategies (s_1^*, \dots, s_n^*) such that each player's strategy is an optimal response to the other players' optimal strategies. Hence, a strategy profile $s^* = (s_1^*, \dots, s_n^*)$ is a NE if s_i^* solves

$$s_i^* = \arg \max_{s_i \in S_i} u_i(s_1^*, \dots, s_{i-1}^*, s_i, s_{i+1}^*, \dots, s_n^*) \quad (1)$$

for all i . This means that no player can profit by deviating from NE if the others play the NE strategies. When the sets S_i are finite, a game may not have a Nash equilibrium in *pure strategies*, but in *mixed strategies*, i.e., when the strategies are distributions over the sets of pure strategies S_i , any game has at least one equilibrium. This result was shown by John Nash in his seminal paper in 1950 [10].

The *best response function* of player i is defined by

$$s_i := BR_i(s_{-i}) := \arg \max_{s'_i \in S_i} u_i(s'_i, s_{-i}), \quad (2)$$

where $s_{-i} := (s_1, \dots, s_{i-1}, s_{i+1}, \dots, s_n)$. This function defines the strategy s_i that is the *best response* of player i to the other players' strategies, s_{-i} , i.e., the strategy that maximizes the payoff of player i when the others play s_{-i} .

The best response function is also called *best response correspondence*, since $BR(s_{-i})$ can be a set. It is easy to show that if a strategy profile $\bar{s} = (\bar{s}_1, \dots, \bar{s}_n)$ satisfies the equation

$$\bar{s}_i = BR_i(\bar{s}_{-i}), \quad \text{for all } i, \quad (3)$$

then \bar{s} is a NE of the game. Mathematically, note that \bar{s} is a *fixed point* of the system of all players' best response correspondences.

Under suitable assumptions, an iterative process, where players update their strategies according to their best response correspondences, will converge to a Nash equilibrium [11]. In this paper we shall consider a familiar fixed point iteration to define the NE and interpret it as an adaptive process for the exit selection dynamics.

2.2 Exit Selection Model

In the exit selection model we assume that the occupants tend to select the exit route through which the evacuation is the fastest. However, there are also

other factors influencing the decision. We will include three other factors in this model: familiarity and visibility of the exits and the fire related conditions at the exits.

To calculate an estimate for an agent’s evacuation time through an exit, one needs to consider two things, the distance to the exit and the queue length in front of the exit. Thus, the *estimated evacuation time* of an agent is calculated as the sum of *estimated moving time* and *estimated queuing time*. The moving time is estimated simply by dividing the distance to the exit by the walking speed of the agent.

The queuing time of an agent at an exit depends on the width of the exit and on the number of the other agents that are heading to that exit and are closer to it than the agent itself. Adding the queue length into the model in a fashion where the queuing time of an agent depends not only on the locations of other agents but also on their target exits, makes the decision of an agent dependent on the decisions of the others. This makes this model a game model.

During an evacuation, the fastest exit may change. In these situations the agents should be able to react to the new situation and change their target exits. This is modeled by updating the best response functions of each agent in certain periods of time.

The familiarity, visibility, and conditions at the exit are taken into account by constraining the set of feasible exits according to these factors. These factors divide the exits into six groups that have a preference order. Each agent will select an exit from the nonempty group that has the highest preference. If there are several exits in this group, the selection is made by minimizing the evacuation time as presented above.

2.3 Mathematical Formulation of the Model

We refer to the agents with indices i and j , where $i, j \in \mathcal{N} = \{1, 2, \dots, N\}$. The strategies of the agents are the exits e_k , $k \in \mathcal{K} = \{1, 2, \dots, K\}$. We shall also use the notation $s_i \in \{e_1, \dots, e_K\} = S_i$, $i \in \mathcal{N}$ for strategies and strategy sets. We denote the profile of all agents’ strategies by

$$s := (s_1, \dots, s_N) \in S_1 \times \dots \times S_N = S, \tag{4}$$

and will also use notation $s_{-i} := (s_1, \dots, s_{i-1}, s_{i+1}, \dots, s_N) \in S_{-i}$ for the strategies of all other agents but agent i , and notation (s_i, s_{-i}) for the whole strategy sequence s .

Let us denote the positions of agent i and exit e_k by \mathbf{r}_i and \mathbf{b}_k , respectively, and let $\mathbf{r} := (\mathbf{r}_1, \dots, \mathbf{r}_N)$. Agent i ’s distance from exit e_k is

$$d(e_k; \mathbf{r}_i) = \|\mathbf{r}_i - \mathbf{b}_k\|. \tag{5}$$

Now, the payoff function of agent i is the estimated time of evacuation, $T_i(s_i, s_{-i}; \mathbf{r})$, which he attempts to minimize. It is the sum of estimated queuing time and estimated moving time. When agent i chooses strategy $s_i = e_k$,

T_i is evaluated as

$$T_i(e_k, s_{-i}; \mathbf{r}) = \beta_k \lambda_i(e_k, s_{-i}; \mathbf{r}) + \tau_i(e_k; \mathbf{r}_i), \quad (6)$$

where β_k is a scalar describing the capacity of exit e_k , $\lambda_i(e_k, s_{-i}; \mathbf{r})$ is the number of other agents that are heading to the same exit e_k as agent i and are closer to it, and $\tau_i(e_k; \mathbf{r}_i)$ is the estimated moving time of agent i to exit e_k . The function λ_i is defined by $\lambda_i(e_k, s_{-i}; \mathbf{r}) = |A_i(e_k, s_{-i}; \mathbf{r})|$, where

$$A_i(e_k, s_{-i}; \mathbf{r}) = \{j \neq i | s_j = e_k, d(e_k; \mathbf{r}_j) \leq d(e_k; \mathbf{r}_i)\}, \quad (7)$$

and $|\cdot|$ denotes the number of elements in a subset of \mathbb{N} .

The estimated moving time to an exit is calculated by

$$\tau_i(e_k; \mathbf{r}_i) = \frac{1}{v_i^0} d(e_k; \mathbf{r}_i), \quad (8)$$

where v_i^0 is the moving speed of agent i . The strategy of agent i is the best response to the other agents' strategies:

$$s_i = BR_i(s_{-i}; \mathbf{r}) = \arg \min_{s'_i \in S_i} T_i(s'_i, s_{-i}; \mathbf{r}). \quad (9)$$

A Nash equilibrium of the game satisfies $s_i^* = BR_i(s_{-i}^*; \mathbf{r})$ for all i .

The effects of *familiarity*, *visibility* and *fire related conditions* are taken into account by defining three binary variables

$$fam_i(e_k), vis(e_k; \mathbf{r}_i), con(e_k; \mathbf{r}_i), \quad \forall i \in \mathcal{N}, k \in K,$$

where

$$\begin{aligned} fam_i(e_k) &= \begin{cases} 1 & \text{if exit } e_k \text{ is familiar to agent } i, \\ 0 & \text{if exit } e_k \text{ is not familiar to agent } i, \end{cases} \\ vis(e_k; \mathbf{r}_i) &= \begin{cases} 1 & \text{if exit } e_k \text{ is visible to agent } i, \\ 0 & \text{if exit } e_k \text{ is not visible to agent } i, \end{cases} \\ con(e_k; \mathbf{r}_i) &= \begin{cases} 1 & \text{if conditions are tolerable at exit } e_k \text{ for agent } i, \\ 0 & \text{if conditions are intolerable at exit } e_k \text{ for agent } i. \end{cases} \end{aligned}$$

Now the exits can be divided into groups that have preference numbers from one to six according to the values of these binary variables. The smaller the preference number is, the more preferable the exit. Definitions for these numbers are presented in Table 1. The familiarity of an exit is considered to be more important to the agents than the visibility. This is based on social psychological findings, according to which evacuees prefer familiar routes even if there were faster unfamiliar routes available [1, 3].

Hence, the complete exit selection model can be presented for each agent $i \in \mathcal{N}$ as follows:

Preference number	Exit group	$vis(e_k, \mathbf{r}_i)$	$fam_i(e_k)$	$con(e_k, \mathbf{r}_i)$
1	$E_i(1)$	1	1	1
2	$E_i(2)$	0	1	1
3	$E_i(3)$	1	0	1
4	$E_i(4)$	1	1	0
5	$E_i(5)$	0	1	0
6	$E_i(6)$	1	0	0
	No preference	0	0	1
	No preference	0	0	0

Table 1. The preference numbers of exit groups used in our model. The smaller the preference number is, the more preferable the exit. The combinations of the last two rows have no preference. This is because the evacuees are unaware of the exits that are unfamiliar and invisible, and thus cannot choose these exits.

$$\begin{aligned}
 s_i = BR_i(s_{-i}; \mathbf{r}) &= \arg \min_{s'_i \in S_i} T_i(s'_i, s_{-i}; \mathbf{r}), \\
 \text{s.t. } s'_i &\in E_i(\bar{z}), \tag{10}
 \end{aligned}$$

where $E_i(\bar{z})$ is the non-empty exit group with the best preference number \bar{z} for agent i .

2.4 Additional Features of the Model

There are some other matters that need to be taken into account in the exit selection model but are not included in the basic formulation above.

Sometimes an alternative exit is only slightly faster than the current target exit. We assume that an agent may not always notice the small difference, or may not react to them. This is why a *patience parameter* is added to the model. The parameter describes how much faster an alternative exit needs to be in order for an agent to change its target exit. This behavior can be taken into account by subtracting the patience parameter from the evacuation time through the current target exit. Another possibility would be to define the patience parameter as a proportion of the estimated evacuation time, instead of absolute seconds. In this case the estimated evacuation time of the current exit is multiplied by the parameter, which can have values between zero and one.

In some situations, an agent may not be able to estimate the queue length in front of an exit. This is especially the case in situations where the agent cannot see the exit. In these cases the estimated evacuation time should not depend on the queuing time, and thus, (6) should be replaced by

$$T_i(e_k, s_{-i}; \mathbf{r}) = \beta_k \lambda_i(e_k, s_{-i}; \mathbf{r}) + vis(e_k, \mathbf{r}_i) \tau_i(e_k; \mathbf{r}_i). \tag{11}$$

This makes the estimated evacuation times shorter for the invisible exits. However, this does not affect the functioning of the model, because the estimated evacuation times are only compared between exits in the same exit group.

3 Computational Results

The presented exit selection model has been implemented to the FDS+Evac software [12, 13], which enables the use of fire related data in the model. However, in this article we study its computational properties using a simple cellular automata based program. The focus of our analysis is on the convergence properties of the iterative model. We shall use fixed point iteration to simulate the convergence of best response dynamics to a Nash equilibrium. The iterative process can be presented with an equation as follows:

$$s_i^{t+1} = BR_i(s_{-i}^t; \mathbf{r}), \quad \forall i \in \mathcal{N}, t \geq 1. \quad (12)$$

Thus, in every iteration round the strategy of agent i is his best response to the other players strategies in the previous round. Basically, this means that all agents are considered to update their strategies simultaneously. This *parallel update algorithm* is not the only possible method for updating a best response algorithm. For descriptions of other possible approaches, see [6].

In the following examples, we present numerical results on the convergence of the model in a situation, where the agents do not move during the iteration. The agents just update their target exits at each iteration as best responses to the other agents' decisions. Basically, these iterations could be interpreted as situations where, at each iteration round, all agents tell each other the exit they are heading to. Then, in the next round, they all update their target exits as best responses to the strategy profile of the previous round. It turns out that in fairly large agent populations, the iteration converges to a NE with a quite small number of iterations. The fast convergence is a little bit astonishing, since fixed point iterations do not always converge very well for games with pure strategies [9].

Figure 1 shows how the iteration converges to a NE in a simple test geometry. Total of 100 agents are located randomly into a square 40 m \times 40 m room with two exits. Both of the exits are on the same wall and they are represented in the figures with large circles. The circles representing the left-hand and right-hand exits are white and black, respectively. The white exit is twice as wide as the black exit. The smaller white and black circles represent the agents and their target exits. In the initial position, the target exit of each agent is picked randomly. At each iteration, the agents update their target exits as a best responses to the current situation. In this example, the iteration converged into a NE in five iterations. In the equilibrium, a small majority of the agents are heading to the wider white exit. The widths of the exits are not very significant in this simulation, because the population density is quite small, and thus, the estimated queuing times are small relative to the estimated moving times. As population density increases, the queuing times increase relative to the moving times and the exit width becomes more important. As a result, a larger proportion will select the wider exit as population density increases. This can be seen in Fig. 2, which shows Nash equilibria for the same geometry with 300 and 500 agents.

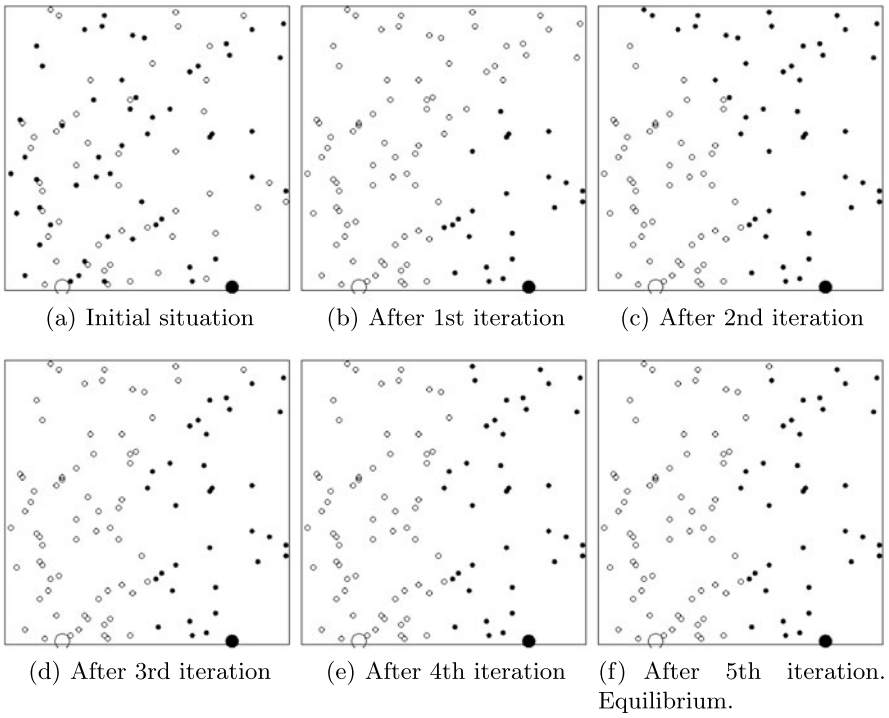


Fig. 1. An example of the convergence of the iteration.

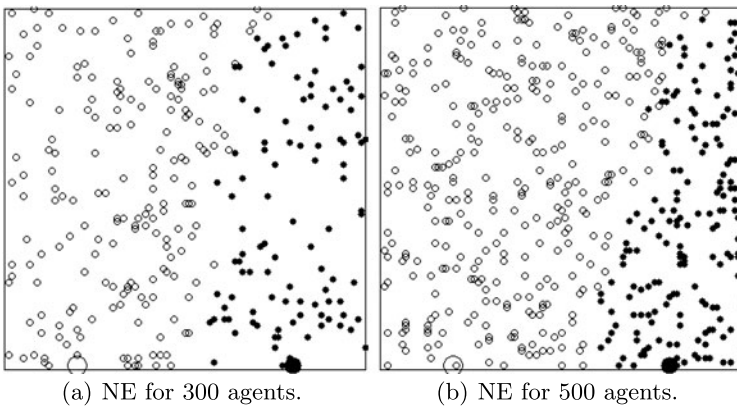


Fig. 2. Nash equilibria for simulations with 300 and 500 agents.

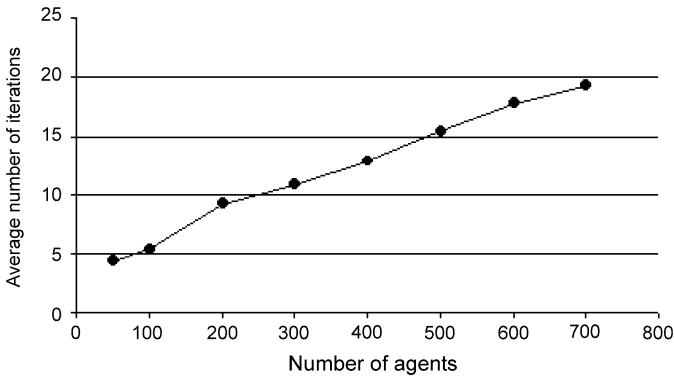


Fig. 3. The average number of iterations to NE versus the number of the agents. In these simulations the patience parameter is set to zero.

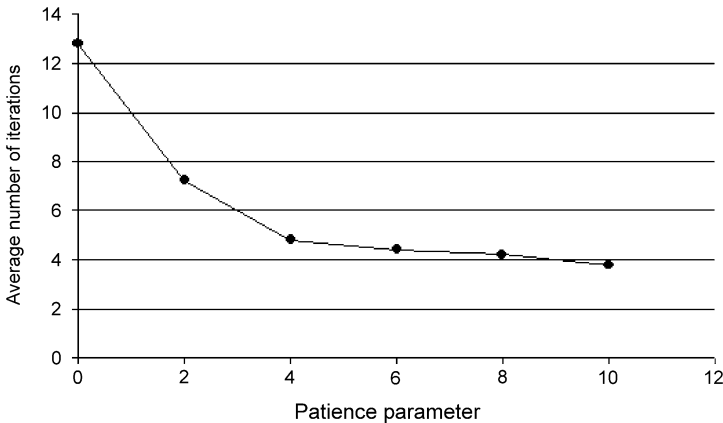


Fig. 4. The average number of iterations to NE for 400 agents versus the patience parameter. A unit measure of the patience parameter is one second.

The graph in Fig. 3 describes the dependence between the number of agents and the average number of iterations needed to achieve the equilibrium. The number of iterations seems to increase linearly and even in large crowds the amount is very reasonable.

It is quite obvious that the value of the patience parameter affects the number of iterations needed to achieve a NE. This is because as the parameter value increases, some strategy profiles that were not equilibria with a smaller patience parameter become equilibria. Figure 4 shows the dependence between the patience parameter and required iterations in the simple test geometry. The number of iterations rapidly decreases as the value of the parameter is increased from zero. As a consequence the equilibrium becomes really fast to compute when the parameter has nonzero values.

4 Discussion

We introduced a game theoretic reaction function model for evacuees' exit selection. The model considers several factors influencing the decision maker, such as distances to the exits, amount of crowd in front of the exits, and familiarity and visibility of the exits. The effects of these factors have been discussed in some previous articles [2, 4], however our approach is somewhat different as we formulate and analyze the model in a game theoretic framework. In the model, we interpret the exit selection of agents as an adaptive dynamical process, where agents update their decisions according to their best response functions and take an action accordingly. A Nash equilibrium of the game is a fixed point of the system of all agents' best response functions.

We also presented simple test simulations to analyze the properties of the model. It was found out that an iterative implementation of the model produces a Nash equilibrium with a reasonable number of iterations. When the patience parameter was added to the model the number of required iterations reduced rapidly as the parameter value was increased from zero. The effect of the parameter is natural, because as the value of the parameter is increased, some strategy profiles that were not equilibria with smaller parameter values become equilibria. Fixed point iterations do not always converge for games with pure strategies, and thus, analysis of the convergence properties of our model is a interesting topic for future research.

Acknowledgements

The research is funded by The Academy of Finland, The Finnish Funding Agency for Technology and Innovation, The Finnish Fire Protection Fund, The Ministry of the Environment, and VTT Technical Research Centre of Finland.

We would also like to acknowledge Katri Matikainen for her work on the social psychological aspects of evacuation.

References

1. G. Proulx. *Journal of Environmental Psychology*, 13:137–147, 1993.
2. S. Gwynne, E. Galea, P. Lawrence, M. Owen, and L. Filippidis. In *Proceedings of the Sixth IAFSS Symposium*, pages 1041–1052, 2000.
3. X. Pan. *Computational Modeling of Human and Social Behaviors for Emergency Egress Analysis*. Dissertation, Stanford University, Palo Alto, CA, 2006.
4. S. Gwynne, E. Galea, P. Lawrence, M. Owen, and L. Filippidis. *Fire Safety Journal*, 36:327–357, 2001.
5. S. M. Lo, H. C. Huang, P. Wang, and K. K. Yuen. *Fire Safety Journal*, 41(5):364–369, 2006.

6. E. Altman and T. Basar. *IEEE Transactions on Communications*, 46:940–949, 1998.
7. Y. Korilis and A. Lazar. *Journal of the ACM*, 42(3):584–613, 1995.
8. E. Altman, T. Basar, T. Jimenez, and N. Shimkin. *IEEE Transactions on Automatic Control*, 47:92–96, 2002.
9. D. Fudenberg and J. Tirole. *Game Theory*. MIT Press, Cambridge, MA, 1991.
10. J. Nash. Equilibrium points in n -person games. *Proceedings of the National Academy of Sciences*, 36(1):48–49, 1950.
11. D. Fudenberg and D. K. Levine. *The Theory of Learning in Games*. MIT Press, Cambridge, MA, 1998.
12. T. Korhonen, S. Hostikka, S. Heliövaara, H. Ehtamo, and K. Matikainen. FDS+Evac: Evacuation module for fire dynamics simulator. In *Proceedings of the Interflam2007: 11th International Conference on Fire Science and Engineering*, 2007.
13. S. Hostikka, T. Korhonen, T. Paloposki, T. Rinne, K. Matikainen, and S. Heliövaara. Development and validation of FDS+Evac for evacuation simulations, project summary report. VTT Research Notes 2421, VTT Technical Research Centre of Finland, 2007. ISBN 978-951-38-6981-6; 978-951-38-6982-3.

Front-to-Back Communication in a Microscopic Crowd Model

Colin Marc Henein and Tony White

Institute of Cognitive Science, Carleton University, 1125 Colonel By Drive,
Ottawa, Canada
e-mail: cmh@ccs.carleton.ca

Summary. Failures in front-to-back communication (F2BC) in crowd disasters are commonly cited, but mechanisms and effects of F2BC have not been studied. We develop a plausible characterization and model of F2BC and evaluate it in a simple scenario. To study F2BC in a naturalistic context we then reconstruct a consistent geometry for the Who concert disaster, explore the mechanisms for that disaster, and introduce F2BC. Our qualitative analysis suggests that F2BC can reduce injuries at the cost of lower exit rates.

1 Introduction

Crowd disasters frequently involve high pressures that cause crushing injuries and death by compressive asphyxia [1]. These pressures directly originate with crowd members as people within the crowd apply force through pushing and leaning; forces of over 4500 N have been observed in crowd disasters [1]. One might ask why these forces are applied, given their disastrous effects. Crowd research suggests that failures in front-to-back communication (F2BC) are common in crowd disasters (e.g. [1, 2]). These failures occur when those applying force at the rear of a crowd do not know of important conditions (e.g. blocked exits, fallen people) at the front of a crowd. As forces become large, those at the rear also do not know that their actions are injuring those at the front.

A good example of a failure of F2BC occurred at the Who concert disaster at Riverside Coliseum on December 3, 1979, in Cincinnati, Ohio. Eleven people died during ingress for unreserved seating before the concert. Johnson's analysis of the event suggests that people pushing at the rear of the crowd were unaware of problems at the front [3]. When the crowd surged forward to access the stadium, about 25 people fell to the ground a short distance from an entrance. Despite the efforts of those around them to assist (or at least avoid) the fallen and to protect them from further assault, additional ranks of crowd members fell on top of them or were forced over them; the pile grew

to 3–5 people deep at its worst, was 10–12 feet in diameter, and some people were lying on concrete for as long as 30 minutes. Those farther back (just 10 feet back according to one interviewee) were unaware of the situation and continued to push to gain access to the stadium [3, 4]. Although the media described the event as a stampede driven by mob psychology, Johnson found the opposite, that helping behaviors were widespread, even between strangers.

Although F2BC failures have long been suspected as a significant factor in the unfolding of a crowd disaster (e.g. [1, 2]), we have not found in the literature a systematic investigation of F2BC in crowds, neither its benefits nor model proposals. This means that although we hypothesize that increased F2BC would be helpful, we do not know the circumstances under which F2BC is possible or what benefit could be practically expected from employing it. We do not know whether situation-specific factors affect F2BC. The purpose of this paper is to begin to investigate some of these issues within the context of a microscopic crowd model. The principal contributions of this paper are the development of a F2BC model and its evaluation in both simple and realistic crowd situations.

The organization of the paper proceeds as follows. To begin we develop a characterization of F2BC itself, as it has not previously been formally described. We then turn to the details of our implementation of this characterization. We use the resulting simulation model to explore F2BC in a simple laboratory-like scenario. Wishing to consider how a more realistic scenario affects F2BC, we reconstruct the Who concert disaster in the model, making plausible observations concerning mechanisms of this disaster, and looking at those mechanisms when F2BC is added. We close with some preliminary conclusions on the nature of F2BC in crowds and proposals for further research work.

2 Characterizing Front-to-Back Communication

We are not aware of a study of F2BC in the literature—either a formal review of case studies or a theoretical discussion about how F2BC works within a crowd. In order to implement and study this phenomenon within a model, we need to specify a plausible mechanism for F2BC. Our mechanism is derived from the following premises, which underlie our hypotheses and understanding of F2BC in crowds.

1. **Initiation:** A person consciously initiates F2BC, based on stimuli that are cognitively available in the local environment. This occurs in response to a perceived threat to safety from an experienced strong force (e.g. resulting from external restriction of action). In other words, we suppose that people use the force they are experiencing in the crowd as a source of information, and use this information as the basis to initiate F2BC.

2. **Retransmission by dyads:** We take F2BC to be a distributed process of communication that involves direct personal interactions. Our supposition is informed, in this regard, by reports that yelling over a distance of 10 feet was impossible due to the noise at Riverside Coliseum [3]. As in other confusing or noisy environments, successful communication requires 2 things: first, obtaining the attention of another individual, and second, directly communicating a simple message to them. Propagation of F2BC through the crowd depends on consecutive dyads repeating the information over time.
3. **Local information:** People in large crowds do not have an overall view of an unfolding crowd situation and may not know their exact position. They cannot be expected to know why others push or move in particular directions. Multiple points of attraction further confuse interpretation of movement and forces. Accordingly, we presume that, when we speak of front-to-back communication, ‘*back*’ is not a global concept, and can only be determined locally. Each individual deduces this direction by considering the direction of incoming forces. Two people, even in close proximity, may conclude that the back of the crowd lies in different directions.
4. **Action:** People were powerless to avoid the fallen at Riverside Coliseum [3]. Individual control can be lost in tightly packed crowds [1]. Given these constraints, we assume that people who are capable of voluntarily pushing can cease to do so, although their involuntary leaning forces cannot be controlled. Johnson reported a willingness to help [3], and we presume that this would be expressed by reducing determination to move to goal locations.
5. **Decay:** We suppose that people who are motivated to achieve a goal will co-operate with the actions described, but that people will not co-operate indefinitely. They will eventually return to normal individual behavior, such as pursuing personal goals and including sensitivity to new incoming force and/or communication that would restart the F2BC cycle.

We acknowledge that in reality people would probably use several cognitive strategies to trigger initiation or decay of F2BC behaviors, likely including visual, auditory, movement and force cues. These cues could be noisy, uninformative, or could be valid only locally, being inappropriate judgments from a global perspective. Our model does not have facilities for these cues and judgments, but in keeping with the principles of microscopic human factors [5] we provide for an abstract representation of them.

By specifying our F2BC mechanism in the absence of data from real crowds, we leave open the possibility that these rules may not completely capture the behavior of F2BC. However, our goal is a qualitative investigation (a quantitative model would require model parameters for which experimental measures have yet to be forthcoming). We believe that these premises are plausible for the purpose of evaluating the potential benefits of F2BC as well as the viability of person-to-person directed communication within a crowd.

3 Modeling Front-to-Back Communication

It is our continuing view that microscopic crowd models can help to shed light on the workings of crowds by examining how interactions at the level of the individual (microscopic level) combine to create emergent crowd effects (macroscopic level). In a microscopic crowd model, behavior is modeled from the point of view of individual crowd members. In principle, each modeled individual (agent) in the crowd can draw on its own experience and local observations, applying its rules of behavior to determine desired actions. This individual modeling paradigm is well suited to studying the movement of information in a crowd. Agents can in principle have internal memory, a sense of their immediate surroundings, and the ability to communicate with each other. Particular models imbue agents with the particular capacities required to implement the social behaviors required. In a simple microscopic model, we can establish a causal connection between emergent global level behaviors and the rules and capacities of individual agents.

The floor field model (FFM) [6] is a cellular automaton and microscopic crowd model of individuals on a 2 dimensional grid. Agents interact according to a neighborhood defined by the cardinal compass directions and move according to local rules, balancing their movement decisions between reducing their distance from desired goals on a mental map of the environment and following other nearby agents. FFM as originally specified does not provide for individual cognition beyond the interaction of the 2 perceptions just described, or for physical force between and upon agents. We view it as an ideal starting point for a multi-agent system that can easily include additional agent capabilities such as memory, direct communication and reflection before action, all required by our characterization of F2BC. We have previously extended the model to include force and injuries [7], required to model crowd safety in crush conditions and to provide the motivation for F2BC. We have also extended the model to study direct agent communication in milling [8] and that communication model has also contributed to this work.

3.1 The Floor Field Model

In FFM, agents have a single action: they move. They are initially distributed at random on a grid that provides a co-ordinate system both for movement and for maps of information available to agents called *fields*. Fields are so-named due to their analogy with physical fields, carrying information accessible to agents based on their position on the grid, used in making movement decisions. The model provides for two fields: the *static* field and the *dynamic* field. The static field—in an in/egress scenario—encodes the distance from the agent to the nearest entrance/exit. This definition can be fulfilled according to several different metrics, with different simulation dynamics resulting [9, 10]. Agents consult the values of the static field in cells neighboring their current location in order to follow a gradient towards the exit. A second, *dynamic*, field provides

a mechanism for agents to become aware of the movement of other agents by analogy with ant pheromone chemotaxis. Each agent leaving a cell drops *dynamic bosons*, which have a dynamics by which they diffuse to neighboring cells and decay with a certain probability each time step. Agents can consult the values of the dynamic field in cells neighboring their current location in order to follow “paths” left by previous agents.

In reality people do not have perfect information concerning the movement of others, and the location of points of interest. The model provides for sensitivity parameters that agents multiply with the values of the static and dynamic fields to obtain a measure of the desirability of a cell:

$$\text{desirability} = \exp(k_D D_{ij}) \exp(k_S S_{ij})(1 - n_{ij})\xi_{ij}. \quad (1)$$

Here, k_S and k_D are the sensitivity parameters for the static field, S , and the dynamic field, D . By providing for a high k_S relative to k_D , an agent values movement to the exit more than following others—perhaps simulating a knowledgeable agent with a definite goal. With a low k_S relative to k_D , the agent will tend to follow others more than aim for an exit—perhaps like a visitor to an unfamiliar space with poor lighting. When k_S and k_D are both low, the agent tends not to prefer one cell to another. The value n_{ij} is 1 (0 for occupied cells), and the value ξ_{ij} is 1 (0 for walls). When making a movement decision, the agent considers the desirability of each neighboring cell; the probability of selecting a neighbor is proportional to its desirability.

Agent movement is synchronous. Only one agent may occupy a cell at a time; conflicts in the original FFM are resolved randomly. Of course, it is also possible that a cell occupied by a stationary agent will be selected, in which case an agent desiring that cell must remain stationary as well.

3.2 The Swarm Force Model

Our swarm force model (SFM) is an agent-based derivative of FFM. In this model agents are provided with a further action, that of pushing. Force in SFM is represented by a third floor field. Agents that attempt to move to a cell and find it blocked will perform *voluntary pushing* in which they deposit onto their cell *force bosons*: vector particles with unit magnitude and having the same direction as the agent intended to move. Like the dynamic field, the force field also evolves with time. Between time steps, the force field propagates: the vector sum of bosons on each cell is calculated, the force direction is quantized toward one of the four neighbors, and then deposited on that neighboring cell. Empty cells, wall cells and cells with injured agents (see below) absorb force and do not re-propagate it.

Force carries two consequences. First, agents that experience force above a particular threshold, f_{nochoice} , lose control over their choice of cells. These agents are required to select cells in the direction of the force. (If the required cell is not available at movement time, the agent will push. The mechanism

for this is identical to voluntary pushing, but in this case the pushing is termed *involuntary*, and is intended to represent a leaning force.) Second, agents that experience force above a higher threshold, f_{crush} , become injured. These agents stop moving, do not participate in any form of communication, and are essentially treated as new wall cells. It should be noted that both of these force thresholds are measured against the scalar force on the agent's cell rather than the vector force that is calculated during field propagation.

3.3 Front-to-Back Communication in the Swarm Force Model

The four key processes of initiation, action, retransmission and decay are implemented as follows in our F2BC simulation.

1. **Initiation:** Initiation of F2BC occurs when the local scalar force rises above the f_{nochoice} threshold.¹ Similarly to communication in our swarm information model [8], a direct agent-to-agent communication is used. Agents deliver a simple signal toward the back. In accordance with the *local information* premise, this is defined locally as the direction opposite to the quantized vector sum of force bosons present. The receiving agent, if any, accepts the communication with probability p_{receive} . Otherwise the agent is deemed not to have heard the communication, or to have heard it but to have decided not to comply. Agents who initiate F2BC and continue to experience force above the threshold may initiate again on the next time step.
2. **Action:** An agent initiating or accepting F2BC will take action in two ways. First, a new factor multiplying k_S in (1) changes from 1 to 0. This m_S factor dynamically eliminates the receiving agent's desire to move toward exits by decreasing the static field's importance, consequently reducing pressure on the originating agent. Second, the agent refrains from voluntary pushing. Involuntary pushing continues as normal, as does normal propagation of existing force. This yields a new desirability equation (SFM replaces n_{ij} with ϕ_{ij} : 1, except 0.5 for occupied ij ; see [7] for a discussion of this point):

$$\text{desirability} = \exp(k_D D_{ij}) \exp(m_S k_S S_{ij}) (1 - \phi_{ij}) \xi_{ij}. \quad (2)$$

3. **Retransmission:** An agent that receives one or more F2BC signals in a particular time step will consider, with probability p_{retrans} , retransmitting one signal to another agent on the subsequent time step only. Retransmission only occurs if the scalar force present on the retransmitting agent's cell exceeds its pushing force. In accordance with the *local information*

¹ The initiation threshold was formerly $f_{\text{crush}}/2$. This value, well beyond agents' loss of movement control, conflicted with our premise that agents cognitively decide to initiate based on feeling unsafe, and promoted very late initiation of F2BC. We now base initiation on loss of control.

premise, a retransmitting agent reverses the force vector on its own cell to determine which way appears ‘back’. Communication then occurs identically to initiation.

4. **Decay:** Agents acting upon F2BC signals have a probability, p_{decay} , in each time step of returning to normal behavior. Normal behavior involves a resumption of voluntary pushing, and cell selection with $m_S = 1$.

4 Laboratory Scenario

We have evaluated the proposed F2BC model using two different scenarios, a simple laboratory-type scenario and a realistic scenario. The laboratory scenario utilizes parameters used by previous investigations into FFM and SFM [6, 7]. The space consists of a grid of 61×61 cells encircled by wall cells—excepting one exit cell located in the middle of the front wall. The space is filled 30% full with agents distributed randomly. Additional fixed parameters: α and δ (dynamic boson diffusion and decay probabilities) 0.3, agent pushing force ρ drawn from a normal distribution with $\bar{\rho} = 5$, $\sigma = 1$. $f_{\text{nochoice}} = 3\rho$. In these trials p_{receive} and p_{retrans} are set to 1, while $p_{\text{decay}} = 0.1$.

We used the three combinations of k_S and k_D values used in the egress analysis of FFM [11], and also varied the threshold for agent injury, f_{crush} , from a very low threshold (easy to become injured) to a very high threshold (difficult to become injured). We counted the number of agents exiting the space and the number of agents injured in 350 time steps of the model, repeating each trial 50 times, averaged results shown in Fig. 1.

The injury results, shown in Fig. 1a, demonstrate that introduction of F2BC into a laboratory-type scenario does reduce injuries, regardless of whether agents are motivated to exit quickly, to follow others, or to strike a balance between the two options.

An important question that arises from these results is how exit rates are affected by the reduction in injury rates. Figure 1b indicates that F2BC does affect the exit rate. When $k_S = 0.4$ and $k_D = 10$ agents are primarily guided by the movement of others. In this case the drive to exit and crowd density remain low [7], injuries are not a significant factor, and F2BC further slows what is already a non-urgent exit from the space. When $k_S = 1$ and $k_D = 4$ again the dominant factor is other-agent movement, although movement toward the exit is much facilitated by the increasing ratio $k_S : k_D$. Crowd density and drive to the exit are moderate [7]. Introducing F2BC improves the exit rate when agents are easily crushed, largely due to a postponement in injuries that allows more agents through the exit before it becomes clogged with injuries. When agents are more robust, numbers of injuries drop, revealing that—in the absence of injuries—the tendency of F2BC to produce a more patient crowd results in lower exit rates. The third case, in which $k_S \gg k_D$, tends to produce fast movement toward the exit, high crowd densities, and large

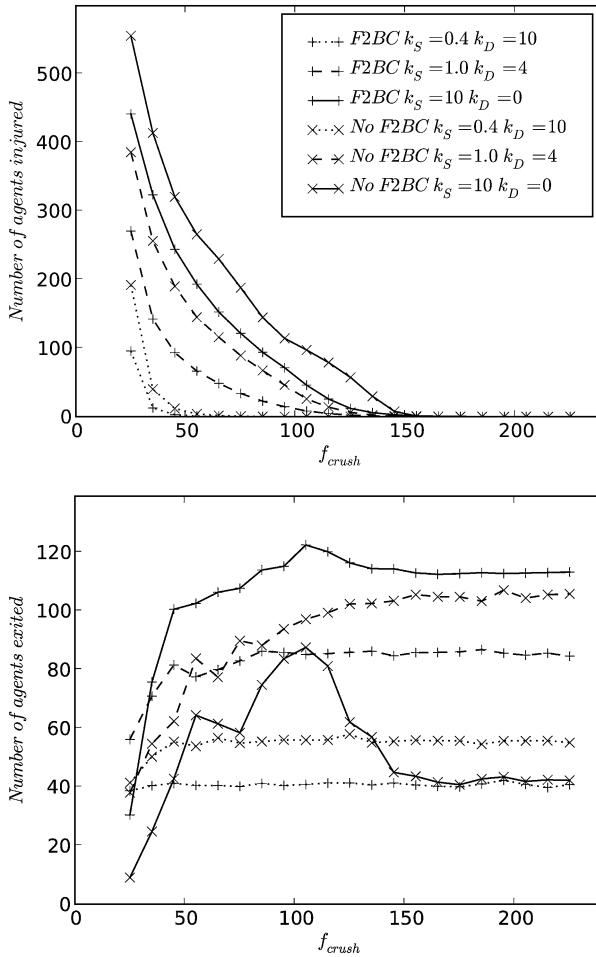


Fig. 1. a Agents injured vs. f_{crush} . **b** Agents exiting vs. f_{crush} (same legend).

forces [7]. In this case F2BC both reduced injuries and also resulted in a faster exit.

This third case, in which the exit rate is facilitated, is quite interesting in the context of earlier work on this scenario. In the original examination of SFM [7] we found that high pressures in the crowd led to a formation called the aisle—a region centred on the door extending from the front to the back of the crowd in which agents are able to exit even under high pressure (Fig. 2a). By contrast, agents adjacent to the aisle are not able to choose a lateral step into the aisle because the forward pressure upon them exceeds $f_{nochoice}$ and they are pinned in place. A stable configuration of this sort greatly decreases the exit rate. When injuries were introduced into the model an interaction emerged between f_{crush} and the exit rate in which moderate f_{crush} values

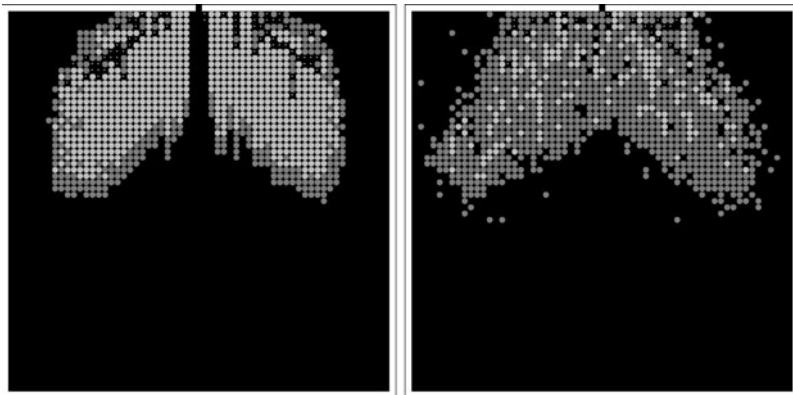


Fig. 2. Disappearance of aisle region. *Light grey* agents exceed f_{nochoice} threshold, *small dots* indicate injured agents. **a** No F2BC, **b** with F2BC. (Both with $k_S = 10$, $k_D = 0$, $f_{\text{crush}} = 105$, time step = 127.)

(circa 100 in Fig. 1b) provoke moderate numbers of injuries. These injuries provide force-breaks within the crowd, resulting in the best exit rates. Just forward of these breaks agents are free to choose their own cells, and can step into the aisle. This breaks the stable configuration and allows more agents to exit. When f_{crush} is low, too many agents become injured, hampering the exit rate. With high f_{crush} , no force breaks form and the aisle pattern remains.

When we introduce F2BC into the model the aisle pattern disappears. The results of Fig. 1b, along with observations we have made of the model, suggest that F2BC is an alternative to force breaks in facilitating exits in high-pressure egress. When F2BC occurs within the crowd, agents effectively communicate with those behind them, reducing the pressure below their f_{nochoice} threshold. This prevents aisle creation as agents control the force upon them sufficiently to allow the lateral steps that they would otherwise be prevented from making. With no force breaks required, high f_{crush} values (when injuries drop to zero) do not impede the exit rate and the aisle is not formed (see Fig. 2b). Low f_{crush} values continue to produce high numbers of injuries and a consequent decrease in exit rate through clogging of the exit area by injuries.

5 Who Concert Disaster Scenario

In order to provide further support for the hypothesis that F2BC can improve crowd dynamics, we wanted to evaluate the effect that F2BC could have in a non-laboratory situation. We chose to simulate the Riverside stadium concert disaster because of an encouraging and detailed account of communication and social behavior [3], and the good descriptions of the physical surroundings and events [3, 4].

5.1 Reconstructing the Plaza at Riverside Coliseum

The plaza of the stadium has been altered since the time of the disaster, however we attempted to reconstruct its physical dimensions based on three sources: a news photo taken the night of the disaster [12], an aerial photo of the original plaza and building [13] and Fig. 3. (Hereinafter, all reference marks are to Fig. 3.) Despite perspective effects, we were able to produce a consistent plaza geometry.

Photo [12] of location *A* shows a bank of 8 doors. We supposed these doors were full size (914 mm) establishing our scale. Photo [12] also shows a large squarish column (~ 4 doors wide) at *i*, and a smaller column (~ 1 door wide) at the building-lobby junction near *A* (call this *BLJ*). These estimates fix the length of wall *A* at 11.8 m. The view of the doors at *B* in [12] is partially obstructed, but we suppose that there were 8 identical doors there, flanked by column *i* and an identical column, setting wall *B* at 14.6 m long. The wall measures set the scale for Fig. 3 (used for all front-to-back estimations, scale set from length of *A*) and photo [14] (used for all side-to-side estimations, scale set from the doors at *B*). The model's *x*-axis is parallel to wall *B*; the model's *y*-axis is parallel to wall *A*.

The lookout at the right of the plaza is an isosceles trapezoid with height 3.9 m, whose parallel sides measure 37.1 m and 44.6 m. Remaining side-to-side dimensions (all projected onto the *x* axis) are: *BLJ* to *E* 17.7 m, *E* to *ii* 4.9 m, ramp width 15.6 m. Remaining front-to-back dimensions (all projected onto the *y* axis) are: *ii* to *F* 17.8 m, *BLJ* to *iii* 47.5 m, *E* to *BLJ* 10.9 m, the wall of *C* opposite *A* is 5.9 m.

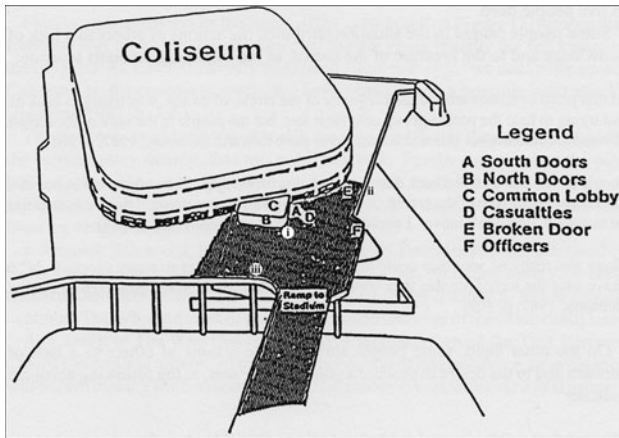


Fig. 3. Plaza at Riverside Coliseum. Lower-case reference marks ours. (Used by permission of NR. Johnson and University of California Press, from [3]; permission conveyed through Copyright Clearance Center, Inc.)

Although units of space, time and pressure in SFM are not calibrated to real-world units, we needed to set the size of a grid cell. We chose 56 cm, the commonly cited (if dated) reference human body width [14]. The above estimates were quite consistent, only requiring minor adjustments of ± 1 cell to make the various structures line up correctly. The 56 cm cell implies approximately 13 cells per bank of 8 doors. We interpreted remarks that insufficient doors were open by supposing that half of the doors were open, so we have included 6 exit cells in the centre of each bank.

Although a police officer inside the coliseum reported “there must be 8000 people standing on the outside trying to get in,” [3] we feel from the description of the officer’s circumstances that this was conjecture rather than a reliable estimation. Given our estimates and our square grid cells, 5000 agents provided a very high density sufficient for our purposes. We distributed agents randomly within the shaded (high density) area of Fig. 3.

5.2 Analysis of the Disaster

We ran the simulation using the same settings used in the laboratory experiments, except that we fixed k_S and k_D at 1.0 and 0.5 respectively. We sampled a range of f_{crush} values from 100 to 300, with and without the F2BC simulation active, for the first 350 time steps of model execution.

First we consider the coliseum scenario without F2BC enabled. We found that forces were high and the scenario was prone to producing injuries. In such a large scenario injury thresholds have a strong effect on injury distribution. This is because, at low values of f_{crush} , agents rapidly become injured throughout the crowd due to relatively small numbers of other agents required to inflict damage (see Fig. 4a). In SFM injured agents throughout the crowd prevent force from propagating over long distances. When the f_{crush} parameter is higher, injuries are more focused because many ranks of agents are required to generate the cumulative forces required to cause injuries.

In observing the simulation, we noted that injuries tend to appear first at certain force hotspots, particularly when the geometry and lack of intermediate force breaks allowed many ranks of agents to generate large cumulative forces over significant distances. An additional facilitating factor for injury involves a scenario where force can move in two directions. While conscious of the fact that our model is only a qualitative simulation and reconstruction from secondary sources, our observations of the simulation suggest that the area around D (where injuries occurred in the real disaster) is particularly prone to being a site for injuries once long range forces can build up (Fig. 4b). This occurs because pushing and leaning forces originating from those exiting the ramp can proceed unimpeded to D , with many ranks pushing in this direction. In the simulation, agents near the ramp pushing forward quickly overwhelmed the free choice of agents in front of them on the plaza, forcing them to add their pushing and leaning forces toward D rather than allowing

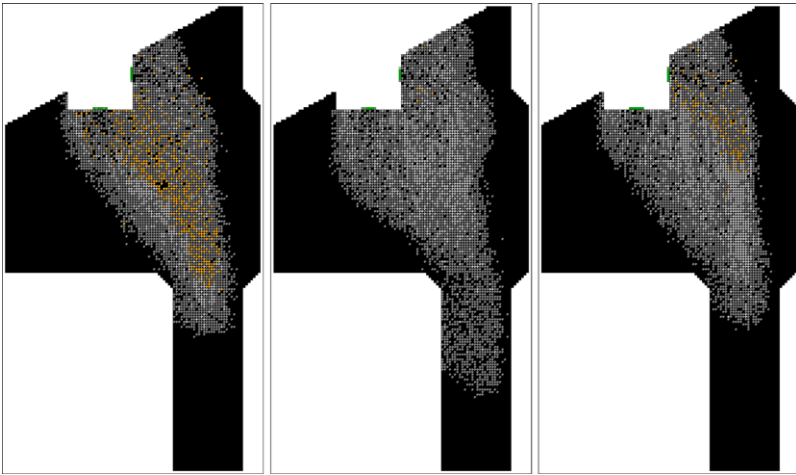


Fig. 4. Riverside Coliseum scenario. Exits cells are *green*, agents are *grey*, agents beyond f_{nochoice} are *light grey*, injured agents are *yellow*. **a** $f_{\text{crush}} = 100 \times 350$; **b** $f_{\text{crush}} = 210 \times 161$; **c** $f_{\text{crush}} = 210 \times 350$.

some to aim for B . Compounding this, agents near the coliseum end of the lookout generate additional perpendicular forces toward D .

When these forces continue to be applied at a high level, our model shows injuries continuing to propagate from the area around D onto the plaza, toward the ramp (Fig. 4c). This continuing propagation onto the plaza was not reported in the disaster. We note here three possible reasons for this discrepancy. First, SFM does not distinguish between fatal and non-fatal injuries; non-fatal injuries in the crowd at this event are poorly documented and there may indeed have been high forces propagating to these locations. Second, other non-modeled factors in the scenario (e.g. the sudden increase in drive toward the exits brought on by the band's warm up) may be relevant in limiting peak injuring forces to particular time periods. Third, it may simply be that SFM, a fairly abstract force model, lacks the fidelity to model additional dissipative factors that prevented injury in these locations despite continuous pushing.

We then enabled the F2BC simulation in the Riverside Coliseum scenario. We carried out 50 runs per data point, and the averaged results, both for exits and injuries, are shown in Fig. 5.

We found that, as with the laboratory scenario, agents were able to control forces over a long distance, substantially reducing the number of injuries. As the lobby was the movement goal for agents, it is not surprising that at high values of f_{crush} (when injuries are low) remaining injuries occur in this area. Observations of the model suggest injuries were more distributed, with hotspots for injuries near i , near the exits and between A and E .

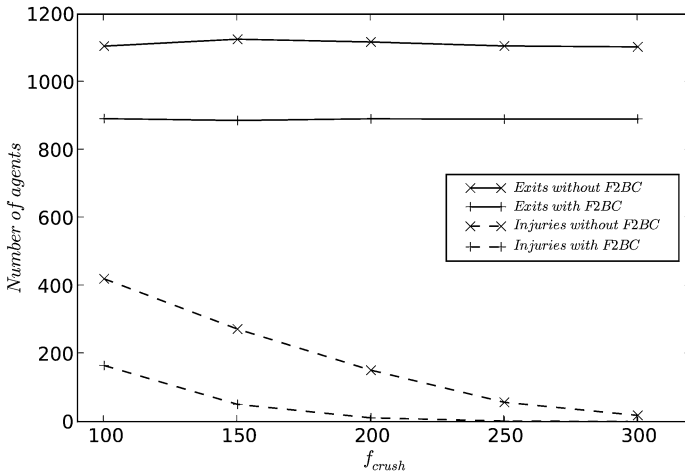


Fig. 5. Agents exited and injured in the Riverside Coliseum scenario.

We found that injuries within the model did not have an impact on egress rate. As f_{crush} increased, making agents less susceptible to injuries, exit rates remained constant. Introducing F2BC into the model resulted in a more patient, less forceful crowd. This had a consequent effect to decrease the exit rate, which was also unaffected by numbers of injuries.

6 Conclusion

Noting that failures of front-to-back communication are commonly cited as important factors in crowd disasters, our goal was to study this phenomenon within a microscopic model to determine what potential benefits F2BC may provide, and the effect of introducing F2BC into a crowd situation. We have proposed a model of F2BC that includes: initiation based on a loss of individual movement control, retransmission through successive dyads, behavior modification for parties to the communication in the form of reduced voluntary pushing and movement drive, and a time-based method of decay of this behavior modification. We implemented this conception of F2BC by extending SFM [7], itself a variant of FFM [6]. Our results suggest that F2BC does have the potential to reduce damaging forces in a laboratory scenario, at the cost of reducing the exit rate due to increased patience.

To evaluate F2BC in the context of a more realistic scenario, we reconstructed the geometry of the plaza at Riverside Coliseum in Cincinnati, Ohio that witnessed the Who concert disaster of December 1979. We based our approximation of this space on secondary sources such as published diagrams and photos available on the Internet, and obtained a consistent conformation. Although our simulation is designed to obtain qualitative results relating to

the introduction of F2BC we found that our model predicted a force hotspot, with subsequent agent injuries, in the same area that saw real injuries in 1979. The results suggest that forces built up over a long distance from the plaza ramp toward the coliseum, and were compounded by perpendicular forces from the plaza lookout. When we added F2BC the number of injuries decreased substantially, as did the exit rate. These results suggest that F2BC may be protective in crowd situations.

Although the model contains parameters that can tune the degree to which agents co-operate in F2BC, the present work has not considered changes to these parameters, instead supposing full compliance with the protocol. In future work we plan to establish the degree of compliance required for benefits to occur, and whether benefits degrade smoothly with a decrease in compliance. We also note that unlike at the Who concert tragedy, many crowd venues now have voice communication systems and overview facilities for trained crowd management personnel. We would like to consider the interactions that global information and communication may have with F2BC in a crowd situation.

References

1. J. Fruin (1993) The causes and prevention of crowd disasters. In R.A. Smith and J.F. Dickie (eds.) *Engineering for Crowd Safety*. Elsevier, Amsterdam.
2. J. Pauls (1984) *Fire Technol.* 20, 27–47.
3. N.R. Johnson (1987) *Soc. Probl.* 34, 362–373.
4. J.M. Chertkoff and R.H. Kushigian (1999) *Don't Panic*. Praeger, Westport, CT.
5. C.M. Henein and T. White (2010) The microscopic model and the panicking ball-bearing. In *Pedestrian and Evacuation Dynamics 2008*. Springer, Berlin.
6. C. Burstedde, K. Klauack, A. Schadschneider, and J. Zittartz (2001) *Physica A* 295, 507–525.
7. C.M. Henein and T. White (2007) *Physica A* 373, 694–712.
8. C.M. Henein and T. White (2006) Information in crowds: The swarm information model. In *Lecture Notes in Computer Science* 4173, 703–706. Springer, Berlin.
9. K. Nishinari, A. Kirchner, A. Namazi, and A. Schadschneider (2004) *IEICE Trans. Inf. Syst.* E87-D, 726–732.
10. T. Kretz, C. Bönisch, and P. Vortisch (2010) Comparison of various methods for the calculation of the distance potential field. In *Pedestrian and Evacuation Dynamics 2008*. Springer, Berlin.
11. A. Kirchner and A. Schadschneider (2002) *Physica A* 312, 260–276.
12. Cincinnati Enquirer (1999-12-03) Concert industry learned from Who tragedy. http://www.enquirer.com/editions/1999/12/03/loc_concert_industry.html (retrieved 2008-01-31).
13. Photo of Riverside Coliseum. <http://www.biwa.ne.jp/~presley/concert/river.jpg> (retrieved 2008-01-31).
14. J.L. Pauls, J.J. Fruin and J.M. Zupan (2007) Minimum stair width for evacuation, overtaking movement and counterflow. In Waldau, Gatterman, Knoflacher and Schreckenberg (eds.) *Pedestrian and Evacuation Dynamics 2005*. Springer, Berlin.

Comparison of Various Methods for the Calculation of the Distance Potential Field

Tobias Kretz, Cornelia Bönisch, and Peter Vortisch

PTV AG, Stumpfstraße 1, 76131 Karlsruhe, Germany

e-mail: tobias.kretz@ptv.de, cornelia.boenisch@ptv.de, peter.vortisch@ptv.de

Summary. The distance from a given position toward one or more destinations, exits, and way points is an important input variable in most models of pedestrian dynamics. Except for special cases without obstacles in a concave scenario—i.e. each position is visible from any other—the calculation of these distances is a non-trivial task. This is not a big problem as long as the model only demands the distances to be stored in a *Static Floor Field* (or *Potential Field*), which never changes throughout the whole simulation. Then a pre-calculation once before the simulation starts is sufficient. But if one wants to allow changes of the geometry during a simulation run—imagine doors or the blocking of a corridor due to some hazard—in the *Distance Potential Field*, calculation time matters strongly. We give an overview over existing and new exact and approximate methods to calculate a potential field, analytical investigations for their exactness, and tests of their computation speed. The advantages and drawbacks of the methods are discussed.

1 Introduction

The will to move through space is the will to reach some kind of destination. On a smaller time scale this is the will to reduce the distance toward some kind of destination. Therefore it appears to be natural to use the gradient of the distance toward a destination in some kind of measure as primary input and impetus for motion in the simulation of the movement of pedestrians.

Note that the potential discussed in this contribution has the meaning and is used in the way as in the simulation of pedestrian dynamics [1–7] and not robotics [8, 9]. The difference is that in robotics it is usually assumed that an autonomous robot knows about his destination coordinate but has no knowledge of the position of obstacles except for those which it “sees”. For pedestrians typically the opposite is assumed. This has consequences for the calculation and use of the potential.

It is assumed that it is always sufficient to have a discrete distance potential field, either because the model itself is formulated in a discrete manner,

or because some finite—yet arbitrarily large—exactness of the distance potential field is sufficient. Although potential fields are by no means confined to rectangular grids [10], only rectangular grids are investigated.

2 Methods for the Calculation of a Distance Potential Field

Short Mathematical Parenthesis: Vector Norms

In two dimensions the so-called *p-norms* are defined as

$$\|\mathbf{x}\|_p := (|\Delta x|^p + |\Delta y|^p)^{\frac{1}{p}}, \quad \text{with } p \in \mathbb{R}_+ \quad (1)$$

of these $p = 2$ is the well known *Euclidean Metric* (Pythagorean Theorem). So, for $p = 2$ the norm has the everyday life meaning of the word “distance”. At first two other well known norms, which are relevant here, will be discussed: the ones with $p = 1$ and the limit $p \rightarrow \infty$. In principle the problem can be stated this way: only the metrics for $p = 1$ and $p \rightarrow \infty$ can be calculated by a flood fill, what one wants, however, is the metric with $p = 2$ for which no equally fast and simple calculation method exists.

In this paper the following notation is used: the distance D from a certain point to the exit on the shortest path for a method X is called D^X . It is composed of a sum of distances d_i^X of (straight) line segments of the visibility graph [11], i.e. they connect consequently the exit, corners of obstacles, and the coordinate under consideration. Note that for the flood fill methods the visibility graph does not have to be known explicitly for the calculations.

2.1 Flood Fill Methods

In *Flood Fill* (sometimes also called *Wavefront*) methods the distance is calculated by consequently moving cell to closest neighbor cell and by that summing up the distances.

Manhattan Metric

For $p = 1$ one has the famous *Manhattan Metric*—also called *Taxicab Metric* or *Manhattan Distance*. It was introduced by Hermann Minkowski—but note that the name “Minkowski Metric” is reserved for the elementary metric of special relativity. Just as a taxi driver in Manhattan needs to sum up the number of Streets and the number of Avenues which he has to cross during the drive to get an estimation of the distance, the distance D^M according to the Manhattan metric simply is the sum of the absolute values of the differences in x - and y -coordinate. Flood Fill therefore only acts within the

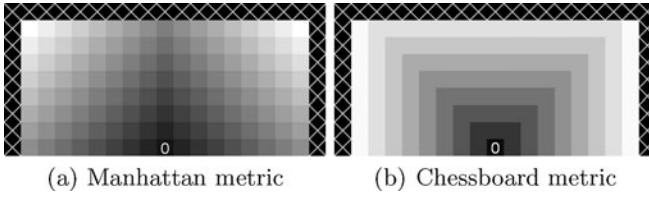


Fig. 1. Manhattan and Chessboard metric.

von Neumann Neighborhood, i.e. grid cells need to be connected via a common edge (see Fig. 1(a)).

$$\Delta x = \sum_i |\delta x_i| \quad \text{and} \quad \Delta y = \sum_i |\delta y_i|, \tag{2}$$

$$D^M = \sum_i d_i^M = \Delta x + \Delta y. \tag{3}$$

Chessboard Metric

For the limit $p \rightarrow \infty$ one arrives at the *Maximum Norm*—also called *Chebyshev Distance* D^C or *Chessboard Metric*. It was introduced by Pafnuty Chebyshev and got its alternative names from the way the king in chess is allowed to move, respectively the fact that the distance measured with this norm is the maximum of the differences in x - or y -coordinate. In other words: flood fill acts within the *Moore Neighborhood* and the added value is the same (typically 1) whether grid cells are connected via an edge or a corner (see Fig. 1(b)).

$$d_i^C = \max(|\delta x_i|, |\delta y_i|), \tag{4}$$

$$D^C = \sum_i d_i^C. \tag{5}$$

The advantage of Manhattan and Chessboard metric is the fact that the typically very fast flood fill procedure can be applied. For $2 < p < \infty$ it is in general not possible to calculate the correct distance (i.e. the Euclidean distance) between two arbitrary grid cells with a flood fill with local rules. The major drawback of course is that aside from Manhattan, Mannheim, or chess there are only few occasions where one of the two norms gives an exact result. However, there are possibilities to stick with the flood fill method and gain exactness. Some of these will be discussed in the following.

Variante 1: Combination of Manhattan and Chessboard

There is a method which uses flood fill and which is exact in the Euclidean sense for all positions which are visible from the destination. Since Manhattan metric gives $d_{i=1}^M = |\delta x_{i=1}| + |\delta y_{i=1}|$ and Chessboard metric results in

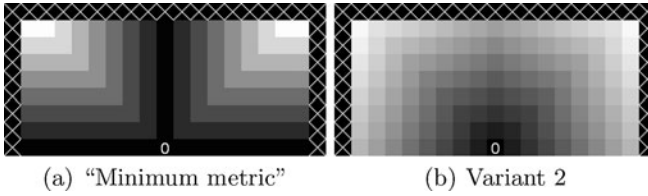


Fig. 2. “Minimum metric” and metric for variant 2.

$d_{i=1}^C = \max(|\delta x_{i=1}|, |\delta y_{i=1}|)$, one can simply calculate $d_{i=1}^m = d_{i=1}^M - d_{i=1}^C = \min(|\delta x_{i=1}|, |\delta y_{i=1}|)$. This “Minimum Norm” (see Fig. 2(a)) is of no use in itself, but $(d_{i=1}^m)^2 + (d_{i=1}^C)^2$ must equal $(\delta x_{i=1})^2 + (\delta y_{i=1})^2$, as one of the two δ s as trivially as necessarily needs to be the maximum and the other one the minimum. And $(\delta x_{i=1})^2 + (\delta y_{i=1})^2$ is the square of the exact Euclidean distance ($p = 2$) between the exit and a coordinate which is directly visible from the exit. If one generalizes this for line segments which are not directly visible from the exit ($i > 1$) one makes an error, since one can only calculate the square root of the sum of squared line segment (Euclidean) distances, while the exact result would be the sum of the square roots of squared line segment (Euclidean) distances:

$$\sqrt{\sum_i (d_i^E)^2} \neq \sum_i \sqrt{(d_i^E)^2}. \tag{6}$$

Regardless of this problem, equations (7)–(9) can be motivated by the initial observation that the calculation of distances is exact “to the point of the next corner”. This is achieved at the expense of making two flood fills—the final value of D^{V_1} can not be calculated by a single flood fill—and having to calculate a square root for each cell in the end.

$$d_i^m = d_i^M - d_i^C = \min(|\delta x_i|, |\delta y_i|), \tag{7}$$

$$D^m = \sum_i d_i^m = D^M - D^C, \tag{8}$$

$$(D^{V_1})^2 = (D^C)^2 + (D^m)^2. \tag{9}$$

Variant 2: $\sqrt{2}$ over Corners

Another simple modification is a Chessboard flood fill where flooding across corners adds a $\sqrt{2}$ instead of 1. If one does so, not only distances parallel to the discretization axis will be exact, but also distances deviating by exactly 45° from that. A version of such a modification, which additionally includes a smoothing mechanism, is introduced in [12]. Since the number of diagonal steps is $\min(\delta x_i, \delta y_i)$ and the number of horizontal or vertical steps is $\max(\delta x_i, \delta y_i) - \min(\delta x_i, \delta y_i)$ one can write

$$d_i^{V_2} = \sqrt{2}d_i^m + (d_i^C - d_i^m), \quad (10)$$

$$D^{V_2} = \sum_i d_i^{V_2} = (\sqrt{2} - 1)D^m + D^C. \quad (11)$$

Variant 3: Larger Neighborhoods

A modification which gains computation speed on the cost of exactness is to increase the neighborhood further, so cells with a distance of two or three or even more are included. As one only has to continue the calculation with the border cells as new center cells, the recursion depth or stack size is reduced, but one runs the risk of overlooking small obstacles. This method is not investigated further here.

2.2 Dijkstra's Algorithm on a Visibility Graph

Another method is to try to find a subset of grid cells which form a *Visibility Graph* [5, 11, 13]. These grid cells are all grid cells which are necessary as navigation cell for at least one arbitrary cell if a pedestrian wants to move from that arbitrary grid cell around the obstacles to the destination. Two nodes of the visibility graph are connected if and only if they are mutually visible. Once one has created such a visibility graph, one can calculate the distance toward the destination for all grid cells which are part of the visibility graph using *Dijkstra's Algorithm* [14]. After having done that one can calculate the distance from all other grid cells toward the destination by using the visibility graph and the distance information now contained within it. Note that strictly spoken the method used to measure the computation time is the one from [13] and not from [5, 11], where the latter one is probably more efficient.

2.3 Ray Casting

Another very intuitive method is an iterated *Ray Casting*. In detail, the following algorithm is applied:

1. Calculate the distance toward the destination for all grid cells which are visible from the destination.
2. If possible, find that grid cell X_0 , which is the closest to the destination of all those grid cells which have been assigned a distance, but which have at least one neighbor which is neither an obstacle, nor has been assigned a distance toward the destination, or has been assigned a distance, but a distance which is too large.
3. Calculate the distance toward the destination of all cells which are visible from X_0 . If there are cells which are visible to X_0 and which have already been assigned a distance toward the destination, this distance is only overwritten, if the newly calculated distance is smaller.
4. Repeat steps 2 and 3 until step 2 does not find any grid cell anymore.

It is important for the calculation time how the check for visibility is done. For the ray tracing part one can use the *Bresenham Line Drawing Algorithm* [15]. But it is important that this algorithm is not used to draw a line (cast a ray) each time one wants to calculate the visibility of a grid cell. It is better to draw a rectangle around the whole scenario (“border”) and cast rays from the cell in focus to each of those border cells. All cells before the first obstacle are then marked as visible, all behind as “not visible”. Because of the discreteness, it might occur that the ray casting toward neighbored border cells gives different results for the visibility of some cell (when a cell is part of multiple casts). In that case, the cell needs to be marked as visible, because otherwise in scenarios with narrow spaces “blind spots” can appear, of which the algorithm would claim that they are not accessible at all. With this strategy the number of lines, one has to draw, only grows as the border size instead of as the area.

2.4 Other Methods of Error Reduction

One has to distinguish the *distance error* in the distance potential field from the *speed error* in a model. If the pedestrians move on a discrete lattice as well, the lattice structure can lead to errors in the speed, just as it leads to errors in the distance. Speed errors can be compensated for by making pedestrians suspend certain moves depending on the ratio of corner versus edge steps they did in recent moves. Such strategies are proposed for example in [12, 16].

3 Analytical Considerations

3.1 Errors for Manhattan and Chessboard Metric

The maximal errors of the two simple metrics are both: well known and trivial to calculate, nevertheless for the sake of completeness, they are given in the following. The absolute error compared to the Euclidean distance d_i^E of a single straight line element of some path using the Manhattan metric is

$$e_i^M = d_i^M - d_i^E \quad (12)$$

$$= d_i^E (|\cos \varphi_i| + |\sin \varphi_i| - 1) \quad (13)$$

$$\text{with } d_i^E = \sqrt{|\delta x_i|^2 + |\delta y_i|^2} \quad (14)$$

with φ_i being the angle between the connecting line of the two points and the x -axis. This simply sums up to a total error of

$$E^M = \sum_i d_i^E (|\cos \varphi_i| + |\sin \varphi_i| - 1) \quad (15)$$

which always lies between the boundaries

$$0 \leq E^M \leq (\sqrt{2} - 1)D^E \quad (16)$$

$$\text{with } D^E = \sum_i d_i^E \quad (\text{exact total Euclidean distance}). \quad (17)$$

The maximal error arises from diagonal motion.

The corresponding values for the Chessboard metric are

$$e_i^C = d_i^C - d_i^E \quad (18)$$

$$= d_i^E (\max(|\cos \varphi_i|, |\sin \varphi_i|) - 1), \quad (19)$$

$$E^C = \sum_i d_i^E (\max(|\cos \varphi_i|, |\sin \varphi_i|) - 1) \quad (20)$$

with the latter one always satisfying the relation

$$(\sqrt{0.5} - 1)D^E \leq E^C \leq 0. \quad (21)$$

Here as well the extreme value is reached for diagonal motion.

3.2 Error for Variant 1 (Combination)

To calculate the (extremal) errors, one has to deal with in variant 1, is a bit more complicated than it is for the two basic metrics above. The error is

$$E^{V_1} = D^{V_1} - D^E \quad (22)$$

$$= \sqrt{\left(\sum_i \max(|\delta x_i|, |\delta y_i|)\right)^2 + \left(\sum_i \min(|\delta x_i|, |\delta y_i|)\right)^2} - \sum_i \sqrt{|\delta x_i|^2 + |\delta y_i|^2}. \quad (23)$$

Remember that

$$|\delta x_i| = d_i^E |\cos(\varphi_i)| \quad \text{and} \quad |\delta y_i| = d_i^E |\sin(\varphi_i)| \quad (24)$$

and use as abbreviation

$$M_i = \max(|\cos(\varphi_i)|, |\sin(\varphi_i)|), \quad (25)$$

$$m_i = \min(|\cos(\varphi_i)|, |\sin(\varphi_i)|) \quad (26)$$

in (23).

$$E^{V_1} = \sqrt{\sum_i \sum_j d_i^E d_j^E (M_i M_j + m_i m_j)} - \sum_i d_i^E \quad (27)$$

$$= \sqrt{\sum_i (d_i^E)^2 + \sum_i \sum_{j \neq i} d_i^E d_j^E (M_i M_j + m_i m_j)} - \sum_i d_i^E \quad (28)$$

$$= \sqrt{\left(\sum_i d_i^E\right)^2 + \sum_i \sum_{j \neq i} d_i^E d_j^E (M_i M_j + m_i m_j - 1)} - \sum_i d_i^E \quad (29)$$

$$= D^E \left(\sqrt{1 + \frac{\sum_i \sum_{j \neq i} d_i^E d_j^E (M_i M_j + m_i m_j - 1)}{(\sum_i d_i^E)^2}} - 1 \right). \quad (30)$$

With the relations

$$0 \leq m_i \leq \sqrt{0.5} \leq M_i \leq 1, \quad (31)$$

$$\sqrt{0.5} \leq m_i m_j + M_i M_j \leq 1 \quad (32)$$

one gets for the error

$$D^E \left(\sqrt{1 + (\sqrt{0.5} - 1) \frac{\sum_i \sum_{j \neq i} d_i^E d_j^E}{(\sum_i d_i^E)^2}} - 1 \right) \leq E^{V_1} \leq 0 \quad (33)$$

which is extremal for direction changes from horizontal/vertical to diagonal or vice versa. No error at all arises, when the new direction can be generated from the old by a reflection at one of the axis or diagonals. The left part will take the most extreme value, if all of the d_i^E are equal. With N as the number of single straight line elements one gets

$$D^E \left(\sqrt{1 + (\sqrt{0.5} - 1) \frac{N-1}{N}} - 1 \right) \leq E^{V_1} \leq 0. \quad (34)$$

This confirms the initial observation that there is no error for $N = 1$. However, the error in this variant depends on the number of line elements and therefore the number of obstacles in—respectively the complexity of—the scenario. In the limit $N \rightarrow \infty$ the error can in the worst case (denoted by the hat) be

$$\hat{E}^{V_1} = D^E(0.5^{0.25} - 1) \approx -0.159D^E. \quad (35)$$

3.3 Error for Variant 2 ($\sqrt{2}$ over Corners)

For variant 2 the error is

$$E^{V_2} = ((\sqrt{2} - 1)D^m + D^C) - D^E \quad (36)$$

$$= \sum_i ((\sqrt{2} - 1) \min(|\delta x_i|, |\delta y_i|) + \max(|\delta x_i|, |\delta y_i|) - d_i^E). \quad (37)$$

With (25) and (26) this is

$$E^{V_2} = \sum_i d_i^E \left((\sqrt{2} - 1)m_i + \sqrt{1 - m_i^2} - 1 \right) \quad (38)$$

bearing in mind that $0 \leq m_i \leq \sqrt{0.5}$ one finds the maximum of each summand at

$$\hat{m}_i = \frac{\sqrt{2 - \sqrt{2}}}{2} \quad (39)$$

which corresponds to an angle of exactly $\hat{\phi} = \pi/8 = 22.5^\circ$ and any corresponding angle in the other seven octants. The maximum error then is

$$\hat{E}^{V_2} = \left(\sqrt{4 - 2\sqrt{2}} - 1 \right) D^E \quad (40)$$

$$\approx 0.082 D^E, \quad (41)$$

which is slightly better than the maximum error $\hat{E}_2^{V_1} \approx 0.099$ for variant 1 for $N = 2$. With this method there can never be a negative error. If one wants the error to vanish on the average of all angles, one can add the values

$$s_{hv} = \frac{\hat{\phi}}{\alpha} = \frac{\pi}{8(\sqrt{2} - 1)} \approx 0.948, \quad (42)$$

$$s_d = \sqrt{2} \frac{\hat{\phi}}{\alpha} = \sqrt{2} \frac{\pi}{8(\sqrt{2} - 1)} \approx 1.341 \quad (43)$$

when flooding horizontally or vertically respectively diagonally. I.e. there is a global factor of ≈ 0.948 multiplied to any distance, as $s_d/s_{hv} = \sqrt{2}$. In this case the directions $\varphi_{1,2}$ (of the first octant) with exact measurements are at

$$\sin \varphi_{1,2} = \frac{4 - 2\sqrt{2}}{\pi} \pm \sqrt{\frac{1}{4 - 2\sqrt{2}} - \frac{8}{\pi^2}} \quad (44)$$

which is approximately $\varphi_1 \approx 9.55^\circ$ and $\varphi_2 \approx 35.45^\circ$. In the range between these two angles distances are measured too large, outside of this range too small.

4 Computation Times

4.1 Geometries

The test geometries were a ‘‘typical’’ room, a maze with 200×200 grid cells, a circle shaped room with a diameter of 996 grid cells, a square shaped room with a side length of 3998 grid cells, a room with a large column in the middle, and a ring, the latter two with the same size as the circle (Fig. 3).

4.2 Results

Table 1 gives the results for computation time (standard PC) and the largest distance from the exit that was found by the method. Among the flood fill

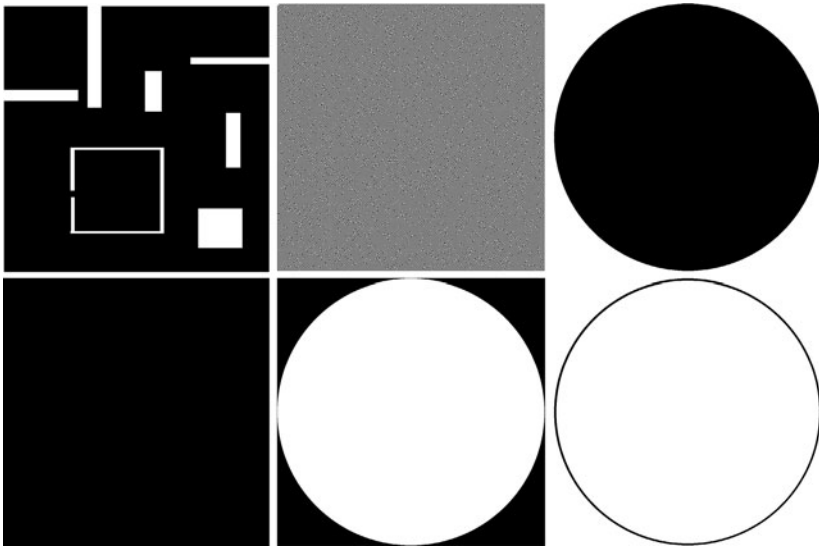


Fig. 3. Test geometries. Walkable areas are colored *black*, walls *white*. Note that the scenarios were largely different in size and just scaled differently to fit the page (compare description in the text).

based methods variant 2 is different from all other flood fill methods regarding the fact that taking a square root for each grid cell is a necessary part of the calculation. For square roots and other elements of the calculation the calculation time not only depends on the algorithm but also on the details of the implementation.

In the visibility graph method, the visibilities were calculated via the area method. This led to the comparatively large calculation times. Though most of the time they were smaller than those of the ray casting method with visibility calculation by the area method. The only exception was the circle scenario. The reason for this is that the node generating method presented in [13] generates many unnecessary nodes, as the bending of the circle's border was so small that many local neighborhoods might also have been part of a convex corner, although the inner border of a circle is entirely concave. If the circle had been given as geometric object this could have been avoided.

The ray casting method which uses the border method for visibility calculations was pleasingly fast, although never as fast as the Manhattan flood fill, and probably not yet fast enough to be applied each time step for many destinations.

Geometry: Typical	Calc.	Maximal	Maze	Calc.	Maximal
Method	time [s]	distance		time [s]	distance
Manhattan	0.04	1246.00		0.00	7507.00
Chessboard	0.06	960.00		0.01	7198.00
Variant 1 (comb.)	0.12	1001.70		0.02	7204.63
Variant 2 ($\sqrt{2}$)	0.08	1091.35		0.01	7325.97
Ray casting (edge)	1.18	1052.85		72.72	7361.20
Visibility graph	11.00	1052.16		386.2	7325.97
Ray casting (area)	51.00	1053.72		1156	7507.00
Geometry: Circle			Square		
Manhattan	0.06	1202.00		2.44	7994.00
Chessboard	0.10	996.00		2.69	3997.00
Variant 1 (comb.)	0.18	996.24		5.52	5652.61
Variant 2 ($\sqrt{2}$)	0.10	1037.52		2.68	5652.55
Ray casting (edge)	0.34	996.24		4.29	5652.61
Visibility graph	100.80	996.24		628.00	5652.61
Ray casting (area)	19.00	996.24		1606.00	5652.61
Geometry: Column			Ring		
Manhattan	0.02	1993.00		0.01	1971.00
Chessboard	0.03	1408.00		0.01	1386.00
Variant 1 (comb.)	0.06	1524.69		0.02	1504.40
Variant 2 ($\sqrt{2}$)	0.03	1650.30		0.01	1628.30
Ray casting (edge)	8.89	1565.08		7.36	1542.24
Visibility graph	47.80	1564.94		7.00	1542.09
Ray casting (area)	163.00	1565.26		22.00	1542.39

Table 1. Computation time and maximal distance for the geometries of Fig. 3.

5 Conclusions

In this contribution various methods for the calculation of distances in an obstacle filled space were investigated for their deviation from the true Euclidean distance and the time consumption for their calculation. Starting with the two well-known metrics—Manhattan and Chessboard—variants of such flood fill methods were reviewed respectively introduced. Following that a visibility graph and a ray casting method were discussed. It was found that compared to the standard metrics it is possible to significantly reduce the error while sticking to the flood fill method by making subtle changes to or using combinations of the standard metrics. The errors that remain balance with the fact that their calculation is significantly quicker than the calculation of the two other methods which are—in principle—error-free.

Acknowledgements

For valuable discussion and hints we thank U. Hanebeck, S. Hengst, A. Pohlmann, and L. Spannehl.

References

1. C. Burstedde, K. Klauck, A. Schadschneider, and J. Zittarz. Simulation of pedestrian dynamics using a 2-dimensional cellular automaton. *Physica A*, 295:507, 2001.
2. A. Schadschneider, Bionics-inspired cellular automaton model for pedestrian dynamics. In M. Fukui, Y. Sugiyama, M. Schreckenberg, and D.E. Wolf (eds), *Traffic and Granular Flow '01*, page 499. Springer, Berlin, 2003.
3. A. Kirchner and A. Schadschneider. Simulation of evacuation processes using a bionics-inspired cellular automaton model for pedestrian dynamics. *Physica A*, 312(1–2):260–276, 2002.
4. A. Kirchner. *Modellierung und statistische Physik biologischer und sozialer Systeme*. PhD thesis, Universität zu Köln, 2002.
5. K. Nishinari, A. Kirchner, A. Namazi, and A. Schadschneider. Extended floor field CA model for evacuation dynamics. *IEICE Transactions on Information and Systems*, E87-D:726–732, 2004.
6. T. Kretz and M. Schreckenberg. The F.A.S.T.-model. In S. El Yacoubi, B. Chopard, and S. Bandini (eds), *Cellular Automata—7th International Conference on Cellular Automata for Research and Industry, ACRI 2006, Proceedings*, page 712. Springer, Berlin, 2006.
7. A. Schadschneider, W. Klingsch, H. Klüpfel, T. Kretz, C. Rogsch, and A. Seyfried. Evacuation dynamics: empirical results, modeling and applications. In R.A. Meyers (ed), *Encyclopedia of Complexity and System Science*. Springer, Berlin, 2009.
8. O. Khatib. The potential field approach and operational space formulation in robot control. In K.S. Narendra (ed), *Adaptive and Learning Systems—Theory and Application*, page 367. Plenum, New York, 1986.
9. J.-C. Latombe. *Robot Motion Planning*. Kluwer Academic, Dordrecht, 1991.
10. J. Meister. Simulation of crowd dynamics with special focus on building evacuations. Master's thesis, Fachhochschule Wedel, 2007.
11. M. de Berg, M. van Kreveld, M. Overmars, and O. Schwarzkopf. *Computational Geometry*. Springer, Berlin, 1997.
12. H. Klüpfel. *A Cellular Automaton Model for Crowd Movement and Egress Simulation*. PhD thesis, Universität Duisburg-Essen, 2003.
13. T. Kretz. *Pedestrian Traffic—Simulation and Experiments*. PhD thesis, Universität Duisburg-Essen, 2007.
14. E.W. Dijkstra. A note on two problems in connexion with graphs. *Numerische Mathematik*, 1:269–271, 1959.
15. J.E. Bresenham. Algorithm for computer control of a digital plotter. *IBM Systems Journal*, 4:25–30, 1965.
16. M. Schultz, S. Lehmann, and H. Fricks. A discrete microscopic model for pedestrian dynamics to manage emergency situations in airport terminals. In N. Waldau, P. Gattermann, H. Knoflacher, and M. Schreckenberg (eds), *Pedestrian and Evacuation Dynamics 2005*, page 369. Springer, Berlin, 2006.

Agent-Based Simulation of Evacuation: An Office Building Case Study

Yiqing Lin¹, Igor Fedchenia¹, Bob LaBarre¹, and Robert Tomastik²

¹ United Technologies Research Center, 411 Silver Lane, East Hartford, CT 06108, USA

e-mail: liny@utrc.utc.com, fedcheii@utrc.utc.com, labarre@utrc.utc.com,

² Pratt & Whitney, 400 Main Street, East Hartford, CT 06108, USA

e-mail: Robert.tomastik@pw.utc.com

Summary. Understanding people behavior and movement characteristics during building evacuation is valuable in evaluating building designs and the effectiveness of evacuation policies. Simulation can be a powerful tool since real data on building evacuation are rarely available and costly to obtain. On the other hand, state-of-the-art in evacuation modeling is the use of agent-based simulations, which are computationally expensive for simulating evacuation in very large buildings. In this paper, we present an agent-based simulation model developed for a 2-story office building verified using the evacuation data collected using video cameras during fire drills in the building. Following model parameter calibration to reflect the actual building traffic characteristics, it is shown that the agent-based simulation model is able to match the real data with high accuracy in terms of the cumulative number of people exiting the building during the evacuation. The paper also presents a graph-based complexity reduction approach that can reduce computation requirements and thus be used for large-scale applications.

1 Introduction

Studies have been conducted to understand people behavior and movement characteristics during building evacuation, since it is valuable in evaluating building designs and the effectiveness of evacuation policies [1, 2]. Based on the studies, various models for people movement have been developed such as cellular automaton [3], the social force model [4] and the gas-kinetic model [5]. Among those models, agent-based simulation has received increasing attention due to their capability of modeling complex interaction between pedestrians. Many of the simulation models have been shown to be capable of reproduce some known collective behavior in pedestrian dynamics, mostly for normal situations [4, 6]. On the other hand, model validation using real evacuation data is rare due to the fact that those data are generally rarely available

and costly to analyze. Some efforts on evacuation data collection and model validation based on real data include [7, 8].

In this paper, the results from the analysis of a fire drill data collected in a 2-storey office building are reported. The analysis confirms certain types of people behavior found in other studies of evacuation such as flocking and leader-following phenomenon. It also shows the velocity pattern with respect to density that is similar to those discovered in highway traffic [9]. In addition, an agent-based simulation model is presented which has been validated against the fire drill data set. Following model parameter calibration, it is shown that the model is able to match the real data with high accuracy in terms of the cumulative number of people exiting the building during the evacuation.

Although agent-based simulation can be a powerful tool on evaluating building safety and evacuation efficiency, it can be computationally expensive for simulating evacuation in very large buildings. Therefore, a graph-based complexity reduction approach has been proposed that is able to reduce computation requirements and thus be used for large-scale applications.

The paper is organized as follows. Section 2 describes the details of the fire drill data analysis. In Sect. 3, the agent-based simulation model is presented followed by its calibration results using the real data. Next in Sect. 4, the graph decomposition approach is given in details. Section 5 concludes the paper.

2 Evacuation Data Analysis

2.1 Evacuation Description

The office building under study is a 2-storey building with two normal and two emergency exits. One of the normal exits is considered as the main exit and is used by most people during normal time. The building is about 32,000 square feet with typical occupancy of around 100 people. There are 48 video cameras in the building that were used to record the egress event. The set of cameras were arranged in a way that each person can be tracked in any part of the corridors. Figure 1 shows the floor plan and the camera locations of the first floor of the building.

In order to gain understanding of people movement in the building under study, the evacuation data from an unannounced fire drill was collected and analyzed. The recorded video was manually processed to find out each person's initial position, delay before starting to evacuation and his/her trajectory to an exit. Since there is no camera inside any office, the initial position is defined as the first time the person appears in the field of view of any camera. The delay before starting to evacuation is defined as the time difference between when the fire drill starts and when the person appears in his initial position.

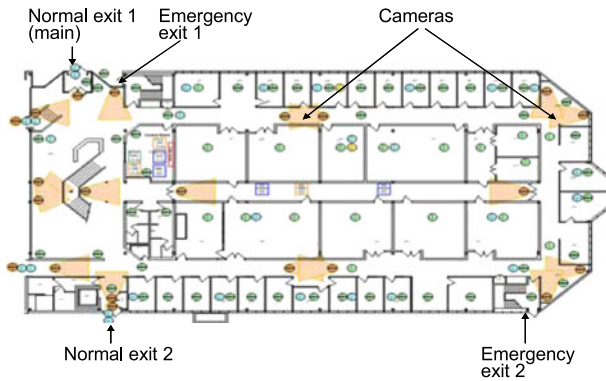


Fig. 1. Floor plan and camera locations.

2.2 Analysis Results

Velocity vs. Density

From the data, the velocity distributions in un-obstructed areas as well as in the exit areas were calculated. The velocity characteristics have been found to be similar to those found in highway traffic. It has been found in studies of traffic jams on high-speed roads that vehicle traveling velocities depend on the density of traffic [9]. Traffic models have indicated cross-over from free un-obstructed motion at a speed close to the maximal to a slower motion limited by conditions at the boundary such as exit and entrance points with some transient region in between where flow with both velocities can be observed. The theoretical predictions have been confirmed in many field measurements e.g., [10].

Here we report the results from the analysis of the fire drill data where the same effects of bimodal velocity distribution have been clearly observed and attributed to the dependency on the people density.

During the fire drill of the building shown in Fig. 1, people flow has been recorded by the set of cameras arranged in such a way that each person could be tracked in all parts of the corridors and in the exit areas. The area of the main exit shown in Fig. 2 has been monitored by three cameras that allow detailed and accurate measurement of individual velocity. Blue circles marks the reference point of 10 feet distance from the exit point where the individual speed has been evaluated.

Four streams of people—from two stair cases and from two corridors—converged to the main entrance creating a slowly moving queue of more or less round shape in the vicinity of the doorway. The exit velocity of each person is calculated based on the time difference between the first time the person crossed the 10-foot circle marked in blue in Fig. 2 and the time he crossed the exit door line.

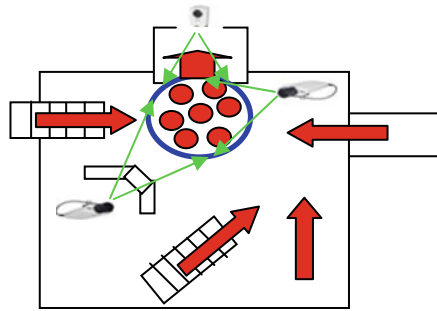


Fig. 2. People flow streams in the main exit area.

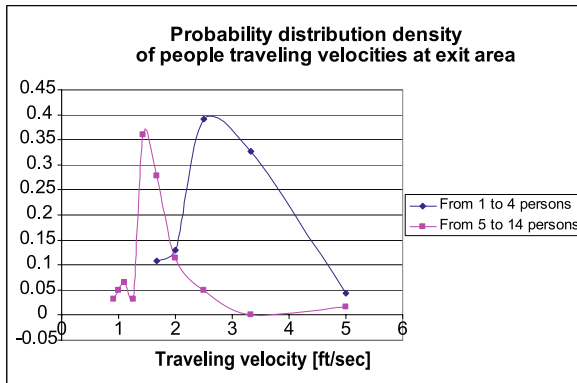


Fig. 3. Probability distribution of individual velocity in two groups in the exit area.

The measurements of individual exit velocity in the door area aggregated in two groups reveal pronounced dependency on the density of people as shown in Fig. 3. The blue line plots the velocity distribution when there are 1 to 4 people in the 10-foot circle shown in Fig. 2, and the red line plots the velocity distribution when there are 5 to 14 people in the circle. The size of the groups has been chosen to achieve the best peak separation.

The observed bimodal velocity distribution is analogous to the findings for traffic flow in linear highways represented by a two-phase model in which the phase transition is made as the traffic density increases.

Additional interesting observation that can be drawn from Fig. 3 is that two phases of slow and fast movement coexist over a range of densities. This is clearly observable from the egress footage when some individuals in the high density group managed to move to the exit with nearly the same speed as those in the low density group taking advantaged of free space randomly emerging in the crowd. Coexistence of slow and fast phases has been observed in the modeling results of [9, 11] and traffic measurement [10].

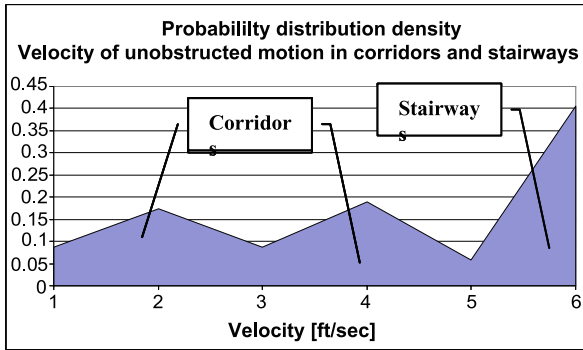


Fig. 4. Probability distribution density of individual velocities for people moving in different conditions.

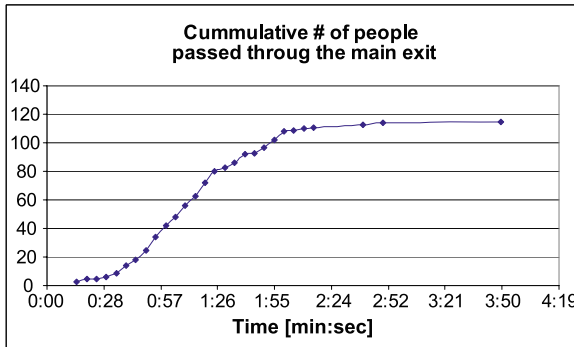


Fig. 5. Cumulative number of people leaving the building from the beginning of the evacuation.

Figure 4 shows individual velocity distribution measured in different corridors and stairways. The multi-peak character of the distribution reflects different moving conditions for people participating in the fire drill.

Cumulative Characteristics of Egress

Cumulative dynamics of egress is shown in Fig. 5 and the evacuation rate is shown in Fig. 6. The red line in Fig. 6 is the sliding average of the blue line using 5 neighboring points. The largest queue before main exit has been observed between 1:15 and 1:45 minutes counted from the egress start.

It is interesting to see the dynamics of evacuation rate calculated from the dependency of Fig. 5. The rate has reached its maximum approximately at the time of the largest queue at the main exit area. It drops after that because people flux started to recede. The multi-peak shape is due to compact arrivals from the distant parts of the building.

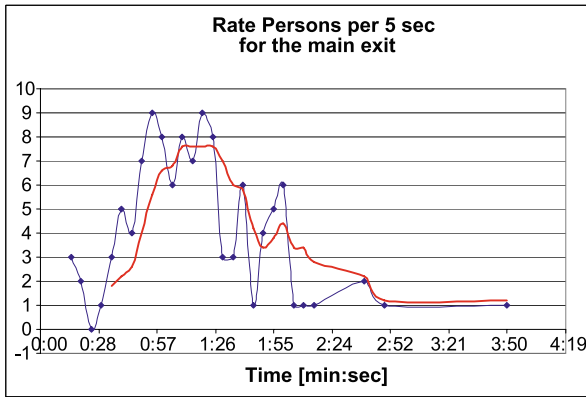


Fig. 6. Evacuation rate during the egress.



Fig. 7. Snapshot of fire drill video.

People Behavior

The analysis also confirmed certain types of people behaviors found in other studies of evacuation including:

- Flocking: occupants originating from the same room stayed together
- Leader-follower: some occupants would follow others, even to a non-nearest exit
- Choice of an exit that is most familiar: only 63% of occupants used the nearest exit
- Delay in beginning to egress: occupants waited an average of 32 seconds to begin egress, with maximum wait time of 1.5 minutes.

Figure 7 is a snapshot from the fire drill video illustrating the leader-follower phenomenon. Due to familiarity, most people moved toward the main exit in the direction shown by the solid arrow, while there is a much closer exit shown in the direction of the dotted arrow.

3 Simulation Model

An agent-based simulation model is developed and then calibrated using the fire drill data. The model is discrete-space, discrete-time, and has the basic features found in most commercial tools. Specifically, the building is divided into cells of the size of two feet by two feet. Each cell can only be occupied by one agent at a time. The position of each agent is updated at each fixed time step. At each time step, each agent either stays at the current cell or moves to one of the adjacent cells. It is assumed in the current version that all agents move with a constant speed. The only exception is at the main exit, where agents may be slowed down due to congestion. It is assumed that the flow rate at the exit is a function of the people density in the vicinity of the exit. Depending on the speed defined, the time unit used in the simulation model may correspond to different real time in seconds. For example, if the speed is defined to be 4 feet per second, then each time unit corresponds to 0.5 second, since the distance between adjacent cells is 2 feet.

The model is able to simulate people movement in both normal operation and evacuation mode. In the evacuation mode, the simulation starts with agents at their initial positions. People movements towards exits are then modeled. Each cell is pre-assigned an exit based on some pre-determined evacuation strategy, for example, the nearest exit strategy. A shortest path from each cell to its assigned exit is pre-calculated before any simulation run. When an agent is in a cell, he tries to move towards the cell's pre-assigned exit using the cell's shortest path to the exit. An agent may deviate from the exit and path assigned to his initial cell due to congestion and randomness in the model. Specifically, the choice of the next cell is probabilistic based on the occupancy of the adjacent cells as well as their distance to their assigned exits. The shorter the distance is to its assigned exit, the higher the probability is for an unoccupied cell to be chosen. An agent will never choose an occupied cell or a cell that moves him further away from any exit.

Then the simulation model was calibrated using the fire drill data. The calibration was to match the cumulative number of people exiting through the main exit during the evacuation process. Only the main exit data was used for calibration because the majority of the people (90%) used the main exit which created congestion, while there was no congestion at the other three exits. The input data used for the calibration included

- The initial position of each person on the first floor of the building
- The number of people entering the floor through stairways and adjacent buildings every five seconds
- The exit each person used as well as the velocity distributions in both congested and non-congested area.

The model parameters that were calibrated included the walking speed, exit assignment and the flow rate in the main exit area. Through calibration, the walking speed in the un-congested area is set to 4 feet per second, and the

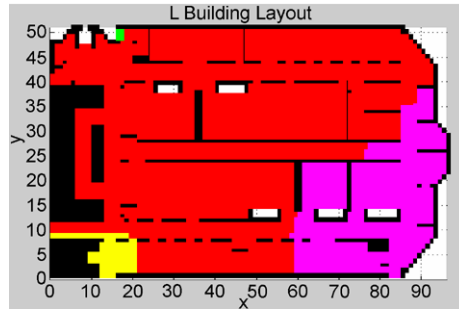


Fig. 8. Exit usage based on fire drill data.

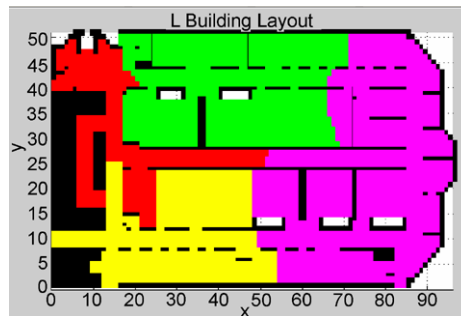


Fig. 9. Exit usage based on shortest paths.

exit assignment is based on the actual exit usage, which is quite different from the original nearest exit assumption. Figures 8 and 9 show the comparison of exit assignments based on shortest paths and the drill data. In both figures, the floor is divided into different-color regions, and each region corresponds to the same exit assignment.

It has been found that the flow rate at the main exit is the key parameter in achieving good correlation between the simulation output and actual data. Figure 10 shows the comparison between the actual data and the results of the 20 simulation runs on the number of people exiting the main exit.

4 Graph Decomposition

The computational speed of agent-based simulations satisfies the typical use case, which is to evaluate a particular scenario in an off-line mode. For other important uses, speed can be insufficient. For example, when used in optimization of design of building layout (egress paths, location of stairwells, smoke containment features such as doors/windows/etc.), typically the designer would need to run hundreds or thousands of scenarios to evaluate various threat situations and design options, and would need the simulation runs

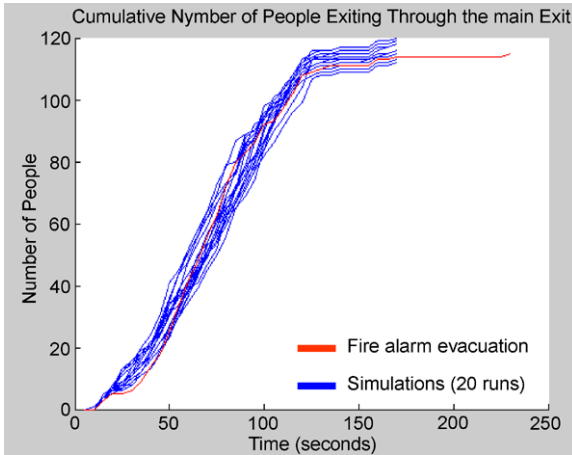


Fig. 10. Comparison between fire drill and simulation result.

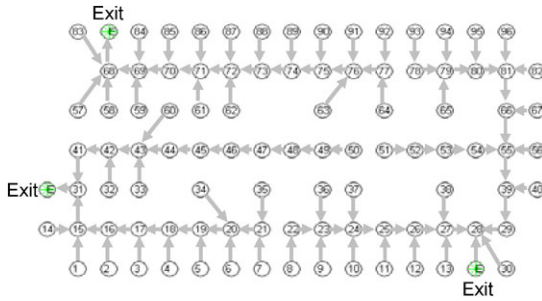


Fig. 11. Graph representation of the building layout.

to complete in hours. Another example is the use of simulations for decision support during an actual emergency; in this case, computational speed is essential for timely decision-making.

A promising approach for computational speed-up of simulations is network decomposition. The key idea is to treat people movement as dynamics on a loosely-connected graph, and then exploit the weak graph connections to decompose the problem into sub-systems to enable distributed computation. In this section, we present a decomposition technique and demonstrate it on the building in Fig. 1. We refer the reader to [12] for further research on how the decomposition can be exploited using computational techniques.

The first step in decomposition is to represent people movement as dynamics on a graph. Using the building layout in Fig. 1 to demonstrate, the layout is divided into rooms (and room-sized sections of the hallway), where each room is a node on a graph, as shown in Fig. 11. The connections between nodes represent the shortest path that a person would use to exit the building. Each connection has a parameter associated with it, and this parameter

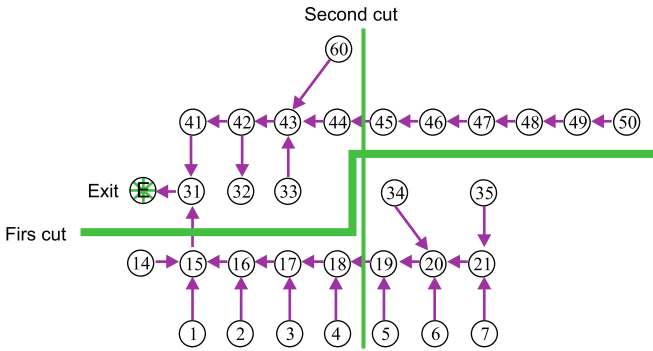


Fig. 12. Graph decomposition.

represents the rate or probability that a person moves along that connection at each time step. This graph model can be thought of as a Markov chain.

The other step is to perform the decomposition, where we use the approach of [13]. In this approach, the graph is treated as a Markov chain, and the graph Laplacian is computed based on the Markov chain’s transition matrix. The eigenvalues of the Laplacian provide the decomposition information. The eigenvector corresponding to the smallest eigenvalue shows the first split of the graph where the weakest connections exist. The signs of the elements of the eigenvector indicate how the graph is split. In Fig. 12, for example, we show a subset of the building graph, and show the first cut of this graph. The second cut of the graph is found similarly, using the second-smallest eigenvalue. Based on the graph decomposition, distributed computation is then made possible.

5 Conclusion

In summary, an agent-based simulation and analysis study of a commercial building is presented. Based on the analysis of an unannounced fire drill data, some typical people behavior during evacuation have been confirmed, and a bimodal velocity distribution has been observed that is similar to those found in highway traffic studies. Based on the analysis, the agent-based simulation model was validated and can be used to evaluate alternative evacuation policies for the building. Finally, a novel graph decomposition approach is proposed to reduce the complexity of the agent-based model and its computation for large-scale applications.

Acknowledgements

The authors acknowledge the funding support by United Technologies Research Center and guidance from Dr. Andrzej Banaszuk for model reduction techniques.

References

1. J. Bryan. Human behavior and fire, in A. Cote (Ed.), *Fire Protection Handbook*, 19th Edition, Vol. 1, National Fire Protection Association, Quincy, MA, 2003.
2. X. Pan. Computational modeling of human and social behaviours for emergency egress analysis. Ph.D. thesis, Stanford University, 2006.
3. A. Schadschneider. Cellular automaton approach to pedestrian dynamics—theory, in M. Schreckenberg and S. Sharma (Eds.), *Pedestrian and Evacuation Dynamics*, Springer, Berlin, 2002.
4. D. Helbing and P. Molnar. Social force model for pedestrian dynamics, *Physical Review E* 51:4282–4287, 1995.
5. S. Hoogendoorn and P. Bovy. Gas-kinetic modeling and simulation of pedestrian flows, *Transportation Research Record* 1710:28–36, 2000.
6. C. Burstedde, A. Kirchner, K. Klauck, A. Schadschneider, and J. Zittartz. Cellular automaton approach to pedestrian dynamics—application, in M. Schreckenberg and S. Sharma (Eds.), *Pedestrian and Evacuation Dynamics*, Springer, Berlin, 2002.
7. J. Pauls and B. Jones. Building evacuation: Research methods and case studies, in D. Canter (Ed.), *Fires and Human Behaviour*, Wiley, New York, 1980.
8. S. Gwynne, E.R. Galea, M. Owen, L. Lawrence, and L. Filippidis. A systematic comparison of building EXODUS predictions with experimental data from the Stapelfeldt trials and the Milburn House evacuation, *Applied Mathematical Modelling* 29:818–851, 2005.
9. D.W. Huang. Dynamics of the congestion triggered by boundary, *Physica A* 387:587–598, 2008.
10. G. Wei and H. Shuyan. Statistical features and phase identification of traffic flow on urban freeway. *Journal of Transportation Systems Engineering and Information Technology* 7:42–50, 2007.
11. J. Dominic and K. Nagel. Traffic jam dynamics in traffic flow models, in 3rd Swiss Transport Research Conference, Monte Verita/Ascona, March, 2003.
12. M. Huzmezan and T. Kalmar-Nagy. Propagation of uncertain inputs through networks of nonlinear components, in *Proc. of the IEEE CDC*, Bahamas, 2004.
13. S. Varigonda, T. Kalmar-Nagy, B. LaBarre, and I. Mezic. Graph decomposition methods for uncertainty propagation in complex, nonlinear interconnected dynamical systems, in *Proceedings of the 43rd CDC*, 2004.

A Genetic Algorithm Module for Spatial Optimization in Pedestrian Simulation

Lukas Kellenberger and Ruedi Müller

Institute of 4D Technologies, University of Applied Sciences Northwestern Switzerland, Steinackerstrasse 5, 5210 Windisch, Switzerland,
e-mail: lukas.kellenberger@fhnw.ch, ruedi.mueller@fhnw.ch

Summary. Regarding pedestrian simulation applications, technologies to optimize the built-up environment apart from pure analysis of pedestrian flows, and based on simulation results, are of crucial importance for the wider acceptance of pedestrian simulation. Apart from conventional pedestrian analysis measures such as density maps, flow rates and travel times, optimization of spatial configurations, leading to congestion or travel time reduction, promises an additional benefit for users of the simulation. Spatial optimization therefore delivers specific solutions for the application of pedestrian simulation in general.

Here we present a genetic algorithm optimizer module, a prototype created for the pedestrian simulation software SimWalk. Based on CAD plans, the module allows optimizing plans and objects (walls, obstacles, etc.) automatically. The user defines and marks a plan section for optimization where, for example, pedestrian density problems occur. Additionally, the user defines which changes of the built-up environment are allowed, based on boundary conditions predefined by his or her architectural or engineering knowledge. After having defined these boundary conditions, the evolutionary process performed by the genetic algorithm gets started, and a first generation of plans and predefined populations is generated. Every succeeding plan shows random variations of the selected obstacles. To evaluate the fitness of each generation, density maps and travel times generated by the software are used to optimize the selected environment. The ultimate goal consists in finding plan configurations with low densities and shorter travel times. If the first generation is established, the best plans can be identified. Based on “elite selection” (“survival of the fittest”), the next generation then gets started, using various GA operators like random generators, selectors, recombination and mutation to generate new plan variations. Every generation, in optimal cases, results in a better plan configuration. A main topic of the research project consisted in mapping the scalability of plan obstacles to the chromosomes of an already existing GA framework of the research institute. To get trend information during the software development, it was necessary to develop a graphical user interface (GUI). It made it possible to edit and prepare plans for optimization, and additionally to select interim solutions for simulation with different parameters, boundary values, population sizes and operators. Statistical tests have shown that with the existing operator set and favorably chosen parameters, after a few generations a significantly improved plan can be achieved.

With this prototype, a first result for the optimization of spatial environments in pedestrian simulation regarding congestion and travel times has been accomplished.

Further research will include an extended operator framework to find better results in a shorter time. Additionally, the application workflow will be improved for more intuitive work.

1 Introduction

With the increase of pedestrian flows more and more people are commuting into and out of main traffic junctions. Railway stations get crowded during peak hours with seemingly inevitable jams in front of entrances, gates, staircases and lifts. Masses moving in different directions tend to block the traffic flow. This takes place in stadiums, shopping malls, airports and harbor terminals in problem zones which repeatedly lead to undesirably high pedestrian concentrations.

The difficulty with the planning of buildings and grounds consists in avoiding such problem areas. A major challenge is the planning of escape and rescue routes as the behavior of individuals in exceptional situations is hard to predict.

Pedestrian bottlenecks caused by a faulty architectural design have devastating effects if in case of an evacuation a few seconds are crucial to avoid casualties. For building projects it is therefore desirable to have a tool at hand which incorporates the testing and the assessing of different pedestrian solution scenarios in an early planning stage. Problem areas should be recognized and tackled as soon as possible thus allowing for a better composition of “architectural” obstacles.

1.1 Initial Situation

The Institute of 4D Technologies¹ has been conducting research in the field of optimization since its existence. Within the scope of a research project with the industry partner Savannah Simulations,² an agent based simulation software is available which models each pedestrian as an individual. By means of SimWalk’s agent technology it is possible to simulate pedestrian flows both in a realistic and flexible way. Besides modeling pedestrian’s everyday behavior the software features simulations of panic and evacuation situations. The software quickly reveals high pedestrian densities in building plans.

Currently it is possible to directly import CAD data modeling buildings and topology. The goal is to subject the CAD plans to an automated optimization to obtain results which guarantee as safe and smooth a pedestrian flow as possible. Adding a software plug-in to the existing application allows

¹ Institute of 4D Technologies, FHNW, www.i4ds.ch.

² Savanna Simulations, www.savannah-simulations.com.

users benefit from a software which supports planning in the early phases or which helps improve existing plans with subsequent optimization [1, 2].

1.2 Objectives

This project is about the development of an optimization module in order to enhance SimWalk—a software to simulate pedestrian flows. The economical goal is geared towards achieving a competitive advantage. Optimization is an important step towards an improved and all-embracing pedestrian simulation. It adds solutions to the aforementioned addressed problems beyond interactions among pedestrians and their environment. None of the currently (2006) available software products has tackled this problem yet.

The scientific and technical goal is aimed at the development of an optimization module which automatically changes CAD building plans leading to improvements regarding optimal pedestrian flows. Ideally the modules would plug into the existing software and would deliver suggestions for solutions of how the design and the layout of buildings could be changed for the better. In addition, users (architects, engineers, etc.) should be equipped with tools which would make it easy to change, adapt and prepare plans as well as review them at a later point in time. Propositions of how a workflow could look should also be made.

1.3 Requirements

Solutions must be found within an drastically reduced period of time. Consequently, plan optimization has to be reduced to a subarea, preferably to a (suspected) problem zone. Computational cost of the simulation can be drastically reduced if an inclusion is limited to just the essential objects and agents.

The spatial, i.e. the multi-level, compatibility must be preserved as problem zones may easily extend over several floors, e.g. with stairs etc.

In this project, genetic algorithms (GA) are used. GA often lead to good solutions in an acceptable period of time. Know-how concerning the use of GA have been accumulated at the institute i4Ds in past and recent years. As a matter of fact several projects in different fields take advantage of GA and yield good results.

During the development of the prototype, existing program code should be left untouched as much as possible, even if a few exceptions regarding the adaptation for the plug-in interface cannot be avoided. The implementation is to be carried out with the programming language *C++* including additional libraries such as the Standard Template Library (*stl*) and *boost*.

The realization of the graphical user interface (GUI) will be conducted with Microsoft's Foundation Classes (*MFC*).

2 Genetic Algorithms (GA)

2.1 General Definitions

Genetic Algorithms (GA) denote heuristic searching methods which are based on Darwin's theory of evolution. To sum up Darwin's theory: Two individuals (parents) exchange their genetic material to reproduce progeny who are well adapted to their environment, possibly even better than their parents. For generations a natural selection of the fitter young occurs thus favoring more improved solutions.

In a similar way, GA choose from a number of individuals by means of fitness functions to determine how well these individuals solve a given problem. Probabilistic mechanisms such as selection, recombination and mutation are imposed on individuals, thereby exposing them to a kind of artificial evolution. The goal is to create a generation who hopefully emerges to be fitter, i.e. to solve the given problem even better.

For our optimization this means that floor layout plans with good fitness results in their generation being preserved and propagated into a next iteration, whereas layouts with poor results are eliminated. The remaining number of solutions are used to create a new generation of individuals applying the mentioned evolutionary mechanisms.

2.2 The Evolutionary Model

Starting with a first population consisting of randomly generated individuals the evolutionary model depicted in Fig. 1 is repeatedly applied. From each generation a newer (possibly) fitter generation comes into being.

A certain percentage of the new generation consists of cloned best individuals of the old generation (which is known as elite selection) which assures that results from generation to generation do not deteriorate. Some individuals who are randomly chosen from all parents undergo a direct mutation: successors with randomly mutated chromosomes become part of the new generation. Also offspring are created by reproducing (recombining) old population individuals. In addition, this model allows the creation of new individuals applying both recombination and mutation in just one interaction. Finally, old individuals chosen at random (RG) can be transferred into the new generation. This measure helps to check for non-local optima [3, 4].

2.3 Use of GA Framework

The evolutionary model shown in Fig. 1 has been implemented in a GA framework at the institute i4Ds. The framework can be characterized by its good parameterization (by choosing the population size, by choosing and arbitrarily combining random generators) and is extendable due to its operator concept. Operators, i.e. selectors, mutators, and recombinators can be added in a pool,

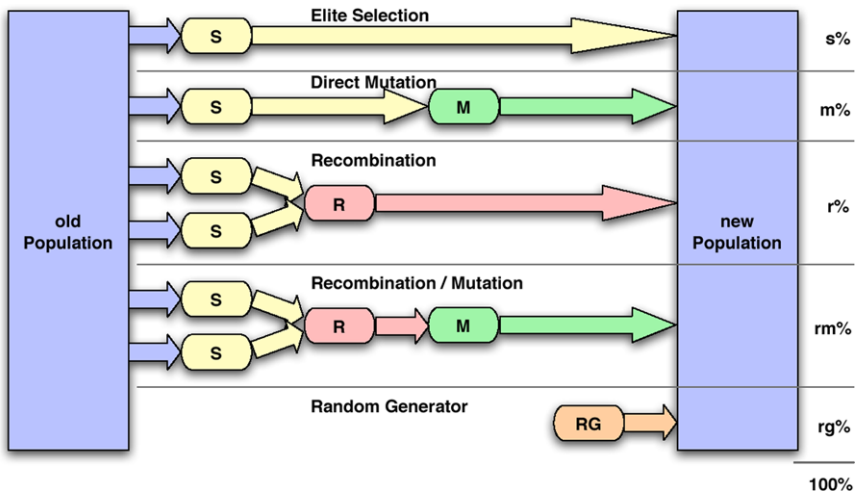


Fig. 1. In the Darwinian model the old population is transformed into the new one applying selection (S), mutation (M), and recombination (R).

where they can be picked from whenever required. The same is true for fitness functions which are flexibly integrated into the framework [5].

3 Realization of the Optimization Module

3.1 Data Structure

SimWalk allows users to open and analyze CAD plan files. Plans comprising several floors are split up into individual levels thereby reducing building elements in simple geometrical elements. These in turn are packed into an all-embracing object. This means that walls are interpreted as lines, closed rectangular rooms as rectangles, and curves as line sections which are stored in what is called a shape. Unfortunately valuable information about geometrical relationship is lost during this process.

A crucial point when developing the optimization module is the modeling of an extended data structure. This structure must satisfy requirements of the SimWalk main application on the one hand and meet needs of the plug-in with its GA on the other hand. To keep changes with the main application as small as possible, an abstraction layer of interfaces has been introduced. The benefit is the availability of an unchanged basic structure and its functionality enhanced with additional elements for the plan optimization at relatively low costs.

The existing structure consisting of plan, level, shape, node, agent and density objects is augmented with objects like groups, obstacles and a set of obstacle behavior. By means of the obstacle and group objects the lost

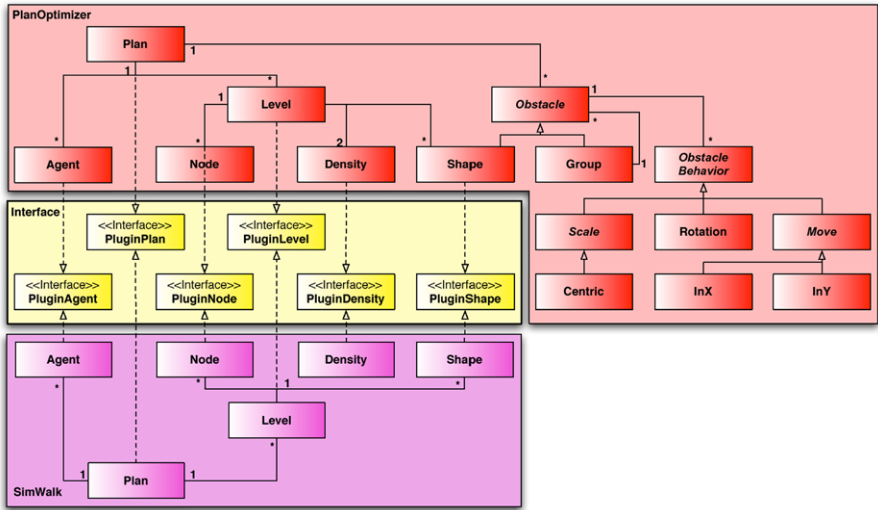


Fig. 2. The introduction of an abstraction layer (interfaces) between SimWalk and the plug-in helps ease data exchange. The existing data structure is extended adding extra functionality needed for plan optimization with the GA framework.

information on how the objects are interrelated can be restored and it is even possible to define new hierarchical groups of elements.

Hence it is feasible to select a single wall or a whole ensemble of grouped objects and match them with behavior, like the permission to be rotated by the GA to give a simple example. Furthermore, a single obstacle within a group or several obstacles collected in a subgroup can be equipped with additional behavior, e.g. the permission to be translated within certain constraints. Therefore whole data trees can be built from which new variants of plans can be generated.

3.2 Mapping

A challenge with this project consists of transforming the building plan (the phenotype) into an individual (genotype) to obtain good results. The above mentioned data structure is a prerequisite for our solution using the GA framework.

The transformation takes several steps. Firstly a tree with obstacles and user defined behavior must be set up. In doing so the obstacles represent the leaves and the group the nodes of the tree—comparable to an operating system with its file system defined by folders and subfolders as nodes and documents as leaves.

Secondly, a table is created which is filled row by row in *pre-order* using the obstacle tree. The filling starts with the leaves whereupon the related node is added, etc. The columns of the table show the possible behavior of the

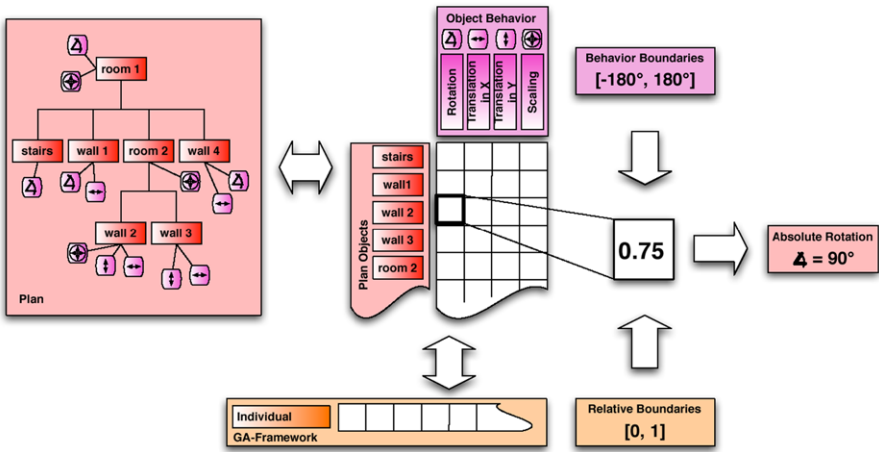


Fig. 3. The introduction of an abstraction layer (interfaces) between SimWalk and the plug-in helps ease data exchange. The existing data structure is extended adding extra functionality needed for plan optimization with the GA framework.

obstacles. The filled-in value gives a measure of how strong obstacle behavior should take effect on the obstacle. Empty fields symbolize a non-existent behavior and are ignored by the algorithm. To be independent of the underlying semantics the field numbers are normalized to values between 0 and 1. Therefore absolute boundaries are needed to normalize the numbers. A value of 0.75 will be interpreted as a rotation of 90° for *wall 2* as shown in Fig. 3. The rotation constraints are set to -180° and +180° in this example.

Finally the values are transferred in an array representing a building plan. In other words: single and grouped obstacles are coded into an individual’s chromosome and are now ready to be used by the GA.

In order to retrieve the plan with the changed obstacles—this corresponds to a retransformation from genotype to phenotype—the decoding has to be executed in reversed order. The modified plans are then readable and can be interpreted by humans [6].

3.3 Assessment Criteria

A retrieved plan is now to be assessed. To this end a pedestrian flow simulation is carried out with each newly generated plan. The quality factors in the form of fitness functions to determine the plan’s fitness are applied. The results are assessed in various respects:

Density field Heavily frequented areas show higher values than the ones which are less frequented. One goal is to achieve a plan with a well balanced density. The fitness (with higher values showing better plans) is expressed by the following formula:

$$fitness_{density} = \sum_y^m \sum_x^n density_{xy}^2. \tag{1}$$

Agents' tracks The tracks of the agents are examined. The shorter a track the better it is assessed. The criterion which path an agent chooses to be his rescue route is of utmost importance in overall performance.

$$Trace_{Agent_j} = \sum_i^{Trace} \sqrt{\Delta x_i^2 + \Delta y_i^2}, \tag{2}$$

$$fitness_{trace} = \sum_j^{Agents} Trace_{Agent_j}. \tag{3}$$

Run-time An additional criterion for the quality of a plan is how long it takes the agents to reach their destination. Reformulated: The fitness of a plan 1 is higher than the fitness of plan 2, if the simulation time of plan 1 is completed earlier:

$$fitness_{runtime} = time_{simulation}. \tag{4}$$

Agent validity Under certain simulation conditions not all of the agents reach their destination. An explanation for this can be found with repositioned and/or resized obstacles which block escape routes, in worst case in the form of cul de sacs. To prevent such solutions from taking part in the evolutionary process they are heavily penalized.

$$fitness_{penalty} = \sum_j^{Agents} a_j \quad \text{where} \tag{5}$$

$$a_j = \begin{cases} 0 & \text{if target reached,} \\ penalty & \text{if target not reached.} \end{cases}$$

The overall fitness can now be calculated by adding the introduced formulae. Chosen parts can be favored over others in setting a weight factor as shown below:

$$fitness_{total} = \sum_i^{Criteria} fitness_i \cdot w_i. \tag{6}$$

3.4 Graphical User Interface (GUI)

Visualization

In parallel with the development of the optimization module a graphical user interface is implemented. The need arises to test the plans before and after

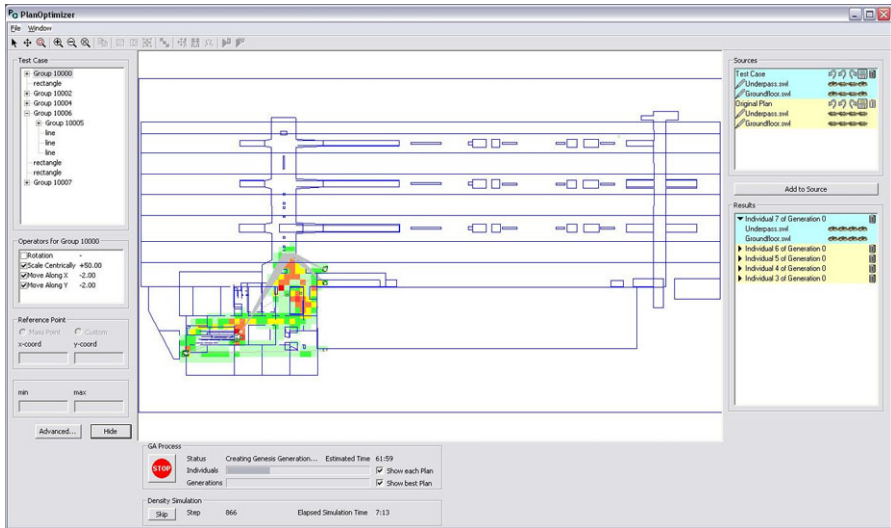


Fig. 4. The plans are prepared for a simulation with a number of tools. After each simulation, the status, the original plans, and result plans are shown together with parameters characterizing object behavior.

their retransformation, to test editing functionalities, and to roughly assess results.

The plans are separated into single floors which can optionally be layered in any combination. This simplifies the analyzing and handling of problem areas. The density fields of a simulation are painted on a plan in different colors (with dark red depicting high density to a light green showing low density), but can also be hidden, e.g. if several floors are shown. Agent tracks for each floor can be shown or hidden individually. This flexibility supports testing and provides users with tools to check whether a solution seems plausible (or not).

Interaction

A plan can be modified with tools from the toolbox—analogue to popular drawing programs. Objects can be selected or deselected, starting points and destination points for pedestrians can be defined, subareas for optimization can be indicated and object behavior can be set and parameterized.

Managing Plans

The managing of building plans is an important factor as the number of plans with performing simulations often grows rapidly. In order not to lose track of the starting points after having modified plans or results of modified plans the GUI is organized accordingly: In one list all original plans are kept. Plans

have to be enabled for modification. Simulations can only perform with this kind of plan, unlike result plans, which are managed in a second list. The latter cannot be modified unless they are copied to the original plan list. All plans can be named and renamed. This feature eases manual backtracking considerably [7].

3.5 Performance

During an optimization several dozens of density field simulations are performed in order to calculate the quality of plans. The better part of the time during an optimization is required by these density field simulations. The following measures are taken to reduce simulation time:

Reduction of area to be optimized The duration of a density field simulation is dependent on the size of a plan and especially on the number of objects contained therein. Moreover, the number of agents, with their starting and destination points, play an important role. For this reason the optimization should be reduced to the subarea of interest. Unnecessary floors should not be included. With the chosen subarea, all starting and destination points are recalculated. Agents which are not included in the reduced area are ignored. Significant time savings can be realized this way.

GUI feedback During a simulation or an optimization the GUI constantly updates the graphical user interface. Due to the updating of plans, which involves retransformation and drawing, performance suffers especially on one-core computer systems. Performance can be greatly improved by switching off feeding data back to the GUI. As it is possible to switch back on updating dynamically (i.e. during a simulation) this should not be too much of a disadvantage.

3.6 Tests

Concerning the GA optimization different tests are carried out:

Population size In a first test series the population size is varied with all other parameters left unchanged. The results show that a medium population size is a good compromise between simulation run-time and quality of the result. Obviously larger population sizes cause longer run-times whereas smaller ones yield large/r standard deviations.

Number of generations In a second test series the number of generations comes under scrutiny. Good results are obtained after 20 generations or so. Again, this is a compromise between run-time and quality of the plan.

Effectiveness of operators used Further tests are carried out with various GA operators. The findings show that in general best results are obtained if the combined recombination and mutation operators are favored over single operators, although all operators are involved to some extent.

Weighting of fitness functions Fitness functions influence plans in many respects. Results show that the density functions are of more importance than the time used to complete a simulation. This is weighted accordingly. Weighing the functions so that each of them contributes equally to the result tends to yield poorer plans. On the other hand all fitness functions have a share in the final result as suppressing a function does not pay off either.

4 Results

PlanOptimizer is a powerful, user-oriented plug-in integrated into the SimWalk software. It supports architects and planning personnel during their design phase of complex building projects with respect to the fitness assessment of pedestrian flows. The plug-in allows for the simulation of escape route scenarios, for the testing of safety aspects and for optimized options.

With the modeling of a dedicated data structure for CAD plans the available GA framework can be used in the first place. Optimized plans can be obtained due to efficient operators (selectors, predominantly recombinators paired with mutators). In the future possibly better operators can be integrated into the framework with little effort—if need even be for new optimization goals.

The graphical user interface is a contribution to how a user workflow can look, an interactive interface which is meant to improve the finding of solution variants.

5 Outlook

There is no development which cannot be refined and improved in the course of new transitions and iterations. We do not claim to have found the best operators. The same is certainly true for the chromosome modeling. More investigating is needed.

Additional research with combining operators, adding more dedicated ones and combining those in turn, could bear fruit.

Interactivity and intuitive workflow for this kind of software support represent a starting point. More usability tests would be beneficial and user feedback could help to take easy operability some steps further.

Acknowledgements

We would like to express our gratitude to the following people: Prof. Dr. Manfred Vogel (head of the institute, i4Ds), Alexander Schmid (project partner, Savannah Simulations), Stefan Müller (software developer, i4Ds), and Marco Rietmann (software developer, i4Ds).

References

1. Pascal Stucki, *Obstacles in Pedestrian Simulations*, Master Thesis, ETH Zurich, 2003.
2. Björn Walther and Mike Widmer, *Semesterarbeit II SS05*, Windisch, 2005.
3. Ingrid Gerdes, Frank Klawonn, and Rudolf Kruse, *Evolutionäre Algorithmen*, Vieweg/Teubner, Wiesbaden, 2004.
4. Karsten Weicker, *Evolutionäre Algorithmen*, Teubner, Stuttgart, 2002.
5. Fabian Märki, Marc Suter, Manfred Vogel, and Manfred Breit, Optimization of 4D process planing using genetic algorithms. In *Proceedings of the Xth International Conference on Computing in Civil and Building Engineering*, Weimar, 2004, pages 1–12.
6. Lukas Kellenberger, *PlanOptimizer—Plug-in: Dokumentation*, Windisch, 2007.
7. Lukas Kellenberger, *PlanOptimizer—Plug-in: Handbuch*, Windisch, 2008.

Opinion Formation and Propagation Induced by Pedestrian Flow

Yu Xue^{1,2}, Yan-fang Wei², Huan-huan Tian¹, and Li-juan Liang^{1,3}

¹ School of Physics and Engineering, Guangxi University, Daxue Rd. 100#, Nanning, Guangxi, China,
e-mail: yuxuegxu@gxu.edu.cn

² Shanghai Institute of Applied Mathematics and Mechanics, Shanghai University, Yuechang Rd. 149#, Shanghai, China,
e-mail: yanfangwei2007@shu.edu.cn

³ Department of Physics and Electronics, Hechi College, Yizhou, Guangxi, China

Summary. In this paper, we extend a rule on two-way and four-way traffic to study the formation and propagation of opinions in virtue of the mobility of pedestrian. The results show that formation and propagation of opinion is generated by occurrence of phase transition. Collective behavior of pedestrians is in favor of opinion formation and propagation. When pedestrian density and initial density of opinion are below their critical value, there is no formation of the consistent opinion. Even though pedestrian traffic has congested, if initial density of opinion is below its critical value, it is very difficult to give rise to consensus, else, it must undergo great fluctuation to generate a stable opinion.

1 Introduction

Nowadays information can spread rapidly through various media like Internet, etc., and play a more important role in an economic society. Everyone will be influenced by information more or less. Sometimes, his neighbor's or friend's opinions frequently force him to change his viewpoint. In recent years, there are some new developments in opinion dynamics. Since Axelrod proposed a model for the dissemination of culture to explain how different cultural islands could be generated from a local tendency to convergence [1], a number of simple agent-based models, such as Sznajd model [2], Deffuant model [3, 4] and KH model [5], etc., have been proposed.

The Sznajd model is a very simple cellular automata model in opinion dynamics [2]. It is to apply an Ising model to simulate the problem of opinion formation. The model is restricted to the two-state opinion problem, because many questions have only two possible answers (yes or no). So the simple Ising spin system with the two possible states (spin up or down) is suitable in modeling such systems. The Sznajd model is constructed as flows. Consider

a chain of spins S_i , $i = 1, 2, 3, \dots, L$, that are either up (+1) or down (-1). Assume that each pair of adjacent spins can affect the state of their nearest neighbors using the following updating rule:

$$\begin{cases} \text{if } S_i S_{i+1} = +1 & \text{then } S_{i-1} = S_{i+2} = S_i; \\ \text{if } S_i S_{i+1} = -1 & \text{then } S_{i-1} = S_{i+1}; S_{i+2} = S_i. \end{cases} \quad (1)$$

This updating rule is the principle “united we stand, divided we fall” in a computerized form. Starting with half of the spins randomly up and the other half down, where at each time step the site i is selected randomly, the chain always reaches a fixed point after which spins no longer flipped. In about half of the cases, it becomes ordered antiferromagnetically, in the other half, all spins become parallel (either all up or all down). That is to say simulation for long time, finally, one of the three fixed points: $\uparrow\uparrow\uparrow, \dots, \downarrow\downarrow\downarrow, \dots, \uparrow\downarrow\uparrow\downarrow$, with probability 0.25, 0.25, 0.5 are obtained respectively. The time-dependent autocorrelation function of the magnetization decays roughly exponentially if averaged over many samples [2]. Also, it is used to explain the distribution of votes among candidates in the Brazilian local elections. Stauffer et al. generalized this Sznajd model to the square lattice and worked out six different rules: Ia, Ib, IIa, IIb, IIc, II [6]. They have found that in all cases except rule IIb, the system reached the same fixed points as in one dimension after typically a few thousand sweeps through the lattice (this time increases with increasing size). It indicates that each site in the Sznajd model on the usual square lattice reaches an opinion which is either “spin up” or “spin down” by phase transition. Later, Moreira et al. have studied this phase transition between these two fixed points, if the usual square lattice is replaced by a disordered square lattice, in order to find a more realistic description of society [7]. However, the above investigations just consider the opinion formation of individual in the static state without taking mobility of individuals into account. In fact, people do not rest on a site of a square lattice connected to their nearest neighbors. They move from one place to another. We now want to search for this phase transition between these two fixed points, when individual migrates or moves to lead to the usual square lattice replaced by a disordered square lattice, trying to find a more realistic description of society. Considering the effect of the mobility of pedestrian on the opinion formation and propagation is analogous to the transportation of media in fluid.

In more recent years, pedestrian flow dynamics have also attracted considerable attention of scientists because of the observed non-equilibrium phase transitions and many interesting physical phenomena, such as self-organization phenomena, noise-induced ordering, and collective phenomena with “freezing by heating” in panic situations, the “faster-is-slow effect”, and herding behavior [8, 9], in the process of crowd congestion and evacuation. And pedestrian dynamics is a kind of many-body system of interacting individuals. Many modeling and simulation methods for traffic flow can be applied to the pedestrian flow. Moreover, many models have been proposed to

mimic the pedestrian flow dynamics. These models include the hydrodynamic models, the social force model, micro-simulation models, cellular automaton models, lattice gas model, emergency and evacuation models, and artificial-intelligence-based models, etc. Ever since Muramatsu et al. have first proposed the lattice-gas model with biased random walker to simulate the pedestrian counter flow in the channel of the sub-way [10], the lattice-gas model has attracted the interest of researchers. The two-dimensional pedestrian traffic under the periodic and open boundary condition is studied by using the lattice-gas model of biased-random walkers [11, 12]. It has been found that the dynamical jamming transition occurs at a critical density [11, 12]. Later on, the evacuative behaviors [13, 14], pedestrian flow induced by a bottleneck [15], the effects of following the front pedestrians with the same direction [16], etc., are studied by lattice-gas model (LG model).

In this paper, we will consider the effect of the mobility of pedestrian on the opinion formation and propagation via studying phase transition from a fixed point to another. In Sect. 2, a opinion model will be constructed on two-way and four way pedestrian traffic of lattice gas model. The simulation and analysis is conducted in Sect. 3. Finally, the conclusion will be obtained.

2 Model

Stauffer et al. first generalized the Sznajd model to the square lattice and worked out six different rules *Ia*, *Ib*, *IIa*, *IIb*, *IIc*, *III* as follows [6].

- I. A 2×2 plaquette of four neighbors, if not all four center spins are parallel, leaves its eight neighbors unchanged. Otherwise, we investigated two rules:
 - Ia*. The neighbors follow the plaquette orientation.
 - Ib*. The neighbors become oriented opposite to the plaquette orientation.
- II. A neighboring pair persuades its six neighbors to follow the pair orientation if and only if the two pair spins are parallel; otherwise, three different rules were studied (formulated for a horizontal pair; the vertical case is analogous):
 - IIa*. The neighbors remain unchanged.
 - IIb*. The left three neighbors follow the orientation of the left part of the pair, the right 3 neighbors follow the right part of the pair.
 - IIc*. The left three neighbors follow the orientation of the right part of the pair, the right three neighbors follow the left part of the pair.
- III. The above one-dimensional rule of [2] is applied for each of the four chains of four spins each, centered about the two horizontal and the two vertical pairs of a 2×2 plaquette.

The simulation have been conducted typically averaged over 10^4 samples of size $L \times L$ with $L = 101$ where again every spin can be up or down with random sequential updating [5]. Moreira et al. have extended the above rule to

study phase transition between these two fixed points on a disordered square lattice [7]. The Moreira's rule is that all k ($1 \leq k \leq 4$) spins with same opinion in one randomly selected plaquette convince all existing spins on the their neighbor sites (for $k = 0$, nobody is convinced). We must take mobility of pedestrians on two-way and four-way traffic into account to generate formation of opinion and propagation via extending Moreira's rule to a real opinion model.

The model is defined on the square lattice of $W \times W$ sites where W is the system size. Generally, pedestrians at the crossing go to the right or left and go up and down, i.e. two-way or four-way traffic [10, 11]. For the two-way traffic, a pedestrian at the crossing go to the right or up. Each site contains only a single walker. The walker is inhibited from overlapping on the site via considering the excluded-volume effect. The transition probability of a walker depends on eight configurations. In literature [7], Muramatsu et al. yielded the transition probabilities $p_{t,x}, p_{t,y}, p_{t,-y}$ of the right walker corresponding to each configuration as follows:

1. $p_{t,x} = D + (1 - D)/3; p_{t,y} = (1 - D)/3; p_{t,-y} = (1 - D)/3$ for configuration (a);
2. $p_{t,x} = D + (1 - D)/2; p_{t,-y} = (1 - D)/2$ for configuration (b);
3. $p_{t,x} = D + (1 - D)/2; p_{t,y} = (1 - D)/2$ for configuration (c);
4. $p_{t,y} = 1/2; p_{t,-y} = 1/2$ for configuration (d);
5. $p_{t,x} = 1$ for configuration (e);
6. $p_{t,y} = 1$ for configuration (f);
7. $p_{t,-y} = 1$ for configuration (g);
8. $p_{t,x} = p_{t,y} = p_{t,-y} = 0$ for configuration (h),

where D indicates the strength of the drift. Similarly, the transition probabilities $p_{t,y}, p_{t,x}, p_{t,-x}$ of the up walker going to the up are given by replacing x with y . The densities p_x , and p_y of the right and up walkers are set by constant values.

Initially, the N pedestrians are randomly endowed up (+1) or down (-1) with probability p and $1 - p$, respectively. It represents the different opinion with "agree" or "oppose". Accordingly, N_1 pedestrians go to the left, N_2 pedestrians to the right in the horizontal direction, N_3 pedestrians go up and N_4 pedestrians go down in the vertical direction. For simplicity, it is assumed that pedestrians along their directions are equal. In each time step, each walker in one randomly selected site follows their transition probability to move and their viewpoint will change in term of Moreira's rule. That is to say if one walker randomly selected goes to a new site, a box of his four nearest neighbors with the same opinion (spin) in Fig. 1 will convince its eight or six neighbor spins around to the box opinion; if the four spins are divided in their opinion, they convince nobody. If his nearest-neighbor is empty, nobody is convinced.

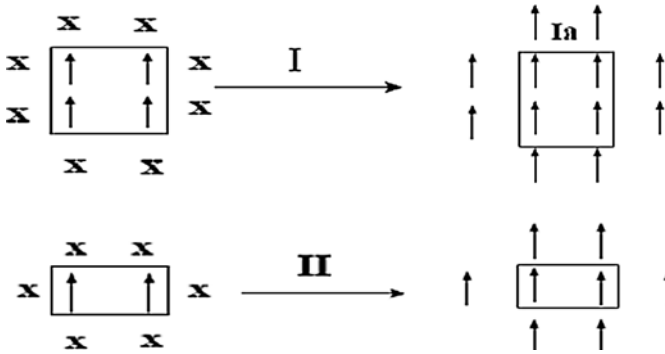


Fig. 1. Schematic presentation of the extended rule I and II, where “X” may be a empty or up spin or down spin.

3 Simulation and Analysis

In all of simulation, Stauffer et al. [6] took initially half of the spins up and half down. If the initial density of opinions is changed away from 1/2, then, for rule I, a phase transition will be observed: densities below 1/2 lead to all down and densities above 1/2 lead to all up for large enough systems. Similarly, in our simulation, we choose the initial density of opinions below 1/2 in order to find the existence of phase transition from mostly spin down to mostly spin up under the different density of pedestrians. All of simulation are carried out on the square lattice with the different size $W \times W$ and employ the periodic boundary condition. The drift D is chosen as 0.0.

Figure 2 shows the formation of the same opinion near initial density $p \approx 0.594$ of opinion on two-way pedestrian traffic under the fixed density of pedestrian $q = 0.8$ and 1000 samples. It indicates that individuals have respective viewpoints as opinion density is small. With the increase of opinion density, some individuals will trend to the same viewpoint and a opinion in contrast to disorder opinion will form via phase transition.

Figure 3 also shows the formation of the same opinion via a phase transition near initial density $p \approx 0.647$ on four-way pedestrian traffic under the fixed density of pedestrian $q = 0.8$. The above curves for the fraction of samples with a fixed point “up” give a transition from mostly spin down on the left to mostly spin up on the right. The transition on four-way traffic is more sharper than one on two-way traffic. Moreira et al. found the transition is near initial density $P = 0.592746$ [7], which is less than our values. It illustrate the mobility of pedestrian will difficultly give rise to consensus. Pattern of spins in Figs. 4(a) and (b) show respectively initial distribution of pedestrians and corresponding opinions on four-way traffic, where density of pedestrians is 0.8 and initial density of opinions is 0.6 on the square lattice 100×100 . From Fig. 4(c), it is found that the existence of just a single spin implies the formation and propagation of the same opinion in final state. Figure 4(d) exhibits

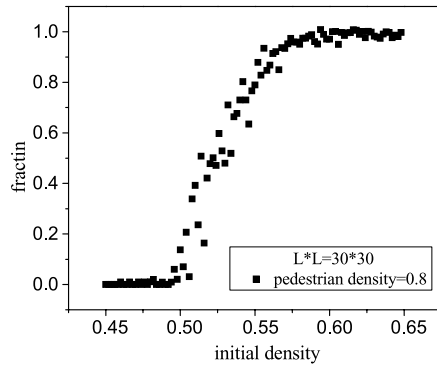


Fig. 2. There is a formation of the same opinion near initial density $q \approx 0.594$ on two-way pedestrian traffic.

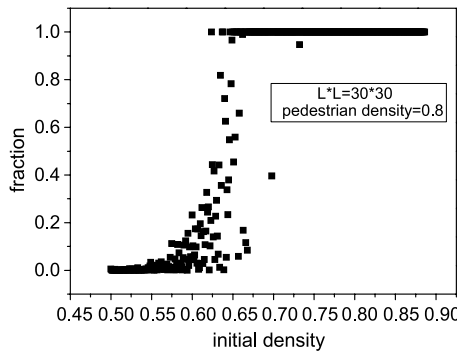


Fig. 3. There is a formation of the same opinion near initial density $q \approx 0.647$ on four-way pedestrian traffic.

the collective behavior of pedestrian on four-way traffic in final state. It is different from those of Sznajd model in the formation of opinions. It is this collective behavior to lead to the attractive effect between four nearest neighbors with same viewpoint and force their neighbors to change opinions in terms of the generalized rule I and II.

Next, we try to study whether the congestion of pedestrian affects the formation and propagation of the same opinion. Figure 5(a) shows the formation of the same opinions on two-way traffic before the velocity will drop for large initial density while no opinion forms in Fig. 5(c) due to small initial density. Figure 6 is the variation of velocity and fraction with the pedestrian density on four-way traffic. Figure 6(a) shows the curve of opinions must heavily oscillate to arise a stable opinion while the collective behavior of pedestrian will enable to reach consensus for large initial density. Conversely, If initial density of opinion is small as Fig. 6(b), it must undergo great fluctuation to obtain a stable opinion even though pedestrian traffic have congested.

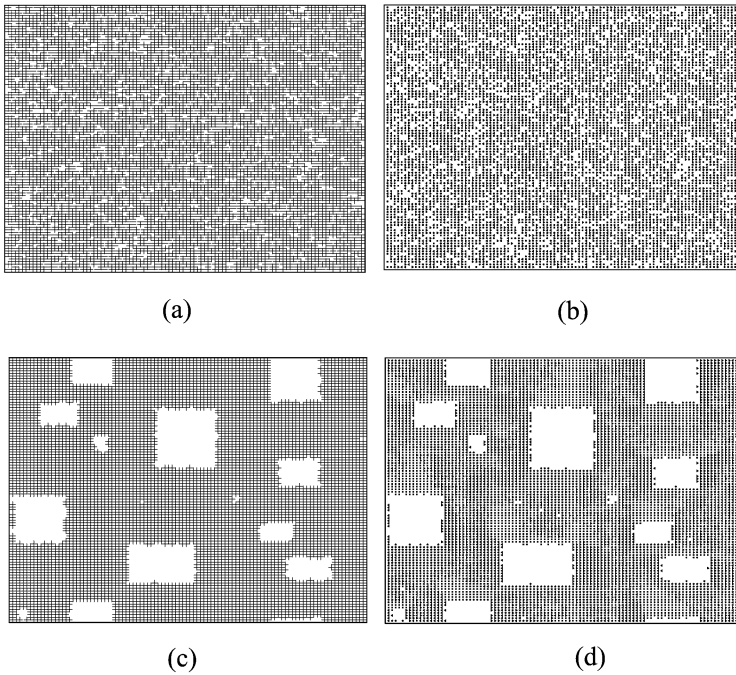


Fig. 4. Pattern of spins in initial (a, b) and final (c, d) distribution of pedestrians and corresponding opinions on four-way traffic, respectively.

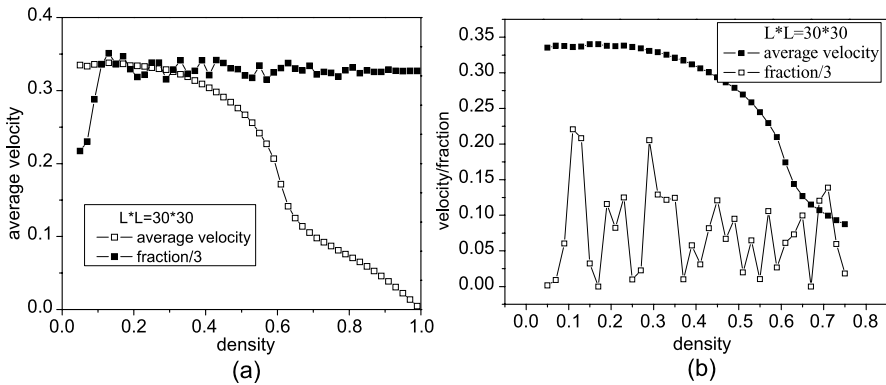


Fig. 5. Relation of velocity and fraction in the congestion of pedestrians. **a** Initial density is 0.8, **b** initial density is 0.2.

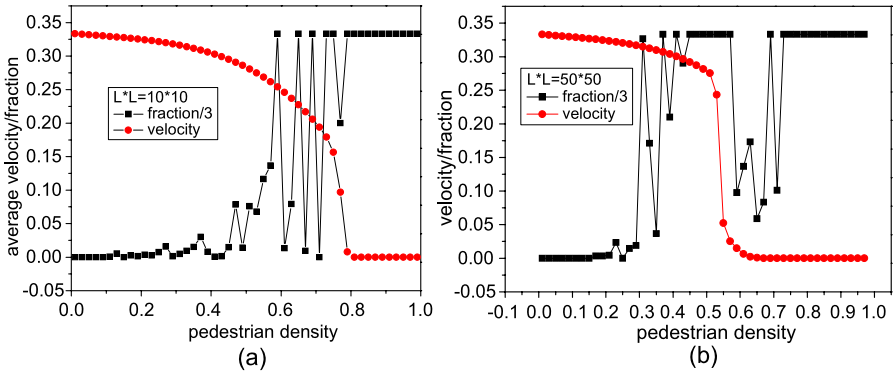


Fig. 6. Relation of velocity and fraction in the congestion of pedestrians on four-way traffic. **a** Initial density is 0.8, **b** initial density is 0.65.

4 Conclusion

In this paper, we have studied the formation and propagation of opinions via employing the extended rule on two-way and four-way pedestrian traffic and obtained conclusions as follows.

1. The collective behavior of pedestrian is in favor of the formation and propagation of opinion.
2. The formation and propagation of opinion is generated by occurrence of phase transition.
3. When pedestrian density and initial density of opinion are below their critical value, there is no formation of the consistent opinion. Even though pedestrian traffic has congested, it must undergo great fluctuation to generate a stable opinion. However, if initial density of opinion is below its critical value, it is very difficult to give rise to consensus in virtue of the mobility of pedestrian.
4. The rule of evolution has a great effect on the formation of opinion. It is a key of opinion formation to make out a rule to reflect real society.

Acknowledgements

This work was supported by the National Basic Research Program of China (No. 2006CB705500), and the National Natural Science Foundation of China (Grant Nos. 10362001, 10532060), and the Special Foundation for the New Century Talents Program of Guangxi Zhuang Autonomous Region, China (Grant No. 2005205), and the Natural Science Foundation of Guangxi (Grant No. 0640003).

References

1. R. Axelrod, *J. Confl. Resolut.* 41 (1997) 203.
2. K. Sznajd-Weron, J. Sznajd, *Int. J. Mod. Phys. C* 11 (2000) 1157.
3. G. Deffuant, D. Neau, F. Amblard, G. Weisbuch, *Adv. Complex Syst.* 3 (2000) 87.
4. G. Weisbuch, *Eur. Phys. J. B* 38 (2004) 339.
5. R. Hegselmann, U. Krause, *J. Artif. Soc. Soc. Simul.* 5(3) (2002) Paper 2.
6. D. Stauffer, A. O. Sousa, S. M. De Oliveira, *Int. J. Mod. Phys. C* 11 (2000) 1239.
7. A. A. Moreira, J. S. Andrade Jr., D. Stauffer, *Int. J. Mod. Phys. C* 12 (2001) 39–42.
8. D. Helbing, I.J. Farkas, T. Vicsek, *Nature* 407 (2000) 487.
9. D. Helbing, I.J. Farkas, T. Vicsek, *Phys. Rev. Lett.* 84 (2000) 1240.
10. M. Muramatsu, T. Irie, T. Nagatani, *Physica A* 267 (1999) 487–498.
11. M. Muramatsu, T. Nagatani, *Physica A* 275 (2000) 281–291.
12. M. Muramatsu, T. Nagatani, *Physica A* 286 (2000) 377.
13. D. Helbing, M. Isobe, T. Nagatani, et al., *Phys. Rev. E* 67 (2003) 067101.
14. T. Nagatani, R. Nagai, *Physica A* 341 (2004) 638.
15. Y. Tajima, K. Takimoto, T. Nagatani, *Physica A* 294 (2001) 257.
16. M. Isobe, T. Adachi, T. Nagatani, *Physica A* 336 (2004) 638.

Passenger Dynamics at Airport Terminal Environment

Michael Schultz, Christian Schulz, and Hartmut Fricke

Air Transport Technology and Logistics, Technische Universität Dresden, Hettner Strasse 1-3, 01069 Dresden, Germany
e-mail: schultz@ifl.tu-dresden.de, schulz@ifl.tu-dresden.de, fricke@ifl.tu-dresden.de

Summary. We report on a specific calibration for an individual-based simulation environment. For this purpose field data of traveling people inside an airport terminal was recorded. The advantage of using video surveillance system is the granting unbiased gathering of person behavior. The presented results are derived from an observed area of 10×30 m area between the check-in facilities and the security control at the Dresden International Airport. By means of statistical analyses a significant difference in behavior between business and leisure related passenger groups was resolved. The influence of carry-on baggage after the check-in procedure is very small and remaining trolley bags do not affect the maximum speed of passengers. In contrast, the size of a passenger group has a significant influence on walking speed, whereas large groups tend to diverge into smaller groups with 2–3 members.

1 Introduction

Airports possess a complex infrastructure and represent a central component of the traffic system as intermodal traffic junctions. They have to fulfill several tasks. From the passenger point of view, the building is primarily designed for dispatch (arrival/departure) procedures. These procedures possess different environmental demands, which result from security/safety and legal requirements. On the other hand, the airport revenues are increasingly dependent on the non-aviation sector (retail revenues). To ensure an optimal combination of the frequently conflictive requirements the airport operator has to balance the demands of passengers, and those of the airlines, being sometimes even co-owner of the infrastructure.

1.1 Trends and Challenges at Airports

Studies of pedestrian dynamics focused on emergency cases [1–3], on mass events [4] or on common person behavior [5–10]. Our research area is related to the airport environment. Previous projects dealt with common modeling

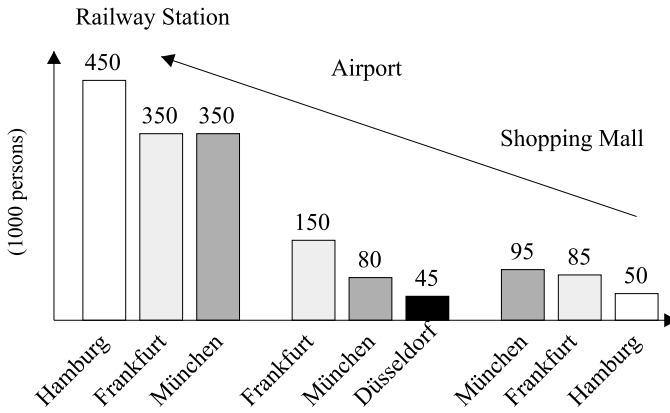


Fig. 1. Passenger/Pedestrian densities per transportation node [15].

approaches of passenger behavior [11, 12], emergency cases at terminals [13] and the development of active guidance systems [14]. In this report, we investigate into tracking passenger behavior at airports, extract motion trajectories and analyze the influencing factors on passengers speed. From the airport point of view the safety and security of processes are a major issue, while the passengers expect adequate service and comfort levels. Compared to other transportation nodes or shopping environments, the airport is also an important location for business activities. In Fig. 1 the daily amount of persons gathering at railway station, airport and shopping mall is shown.

From the economic (revenue) point of view, airports are not only service providers to handle aircrafts and to manage the dispatch procedures. In addition to the aviation related revenue part, the non-aviation segment could reach up to 50% of the airport revenue. So, airports are aiming at providing additional services to passengers, attendants and visitors. For selected airports, the revenue per passenger is shown in Fig. 2.

Considering the non-aviation revenue share and the total revenue per passenger, the Munich Airport is one of the leading European airports. The portfolio of e.g. Frankfurt/Main Airport non-aviation segment over the last years (Table 1) clearly indicates that the airports recognize the importance of non-aviation revenues as well. This trend will further be supported by the new, constraining regulation for airport handling fees EC 2007/0013, getting compulsory by the end of 2008. In 2004, Frankfurt/Main Airport therefore completed the terminal reconstruction to provide additional area for concessionaires. As expected, the revenues increased significantly from 68.8 Mio. Euro in 2004 up to 85.1 Mio. Euro in 2007. The airport operator has to find a corresponding target concept for the airport facilities according to the several tasks of the terminal building evolving from the primary dispatch facilities (e.g. check-in or security controls), the business conditions of the concession-

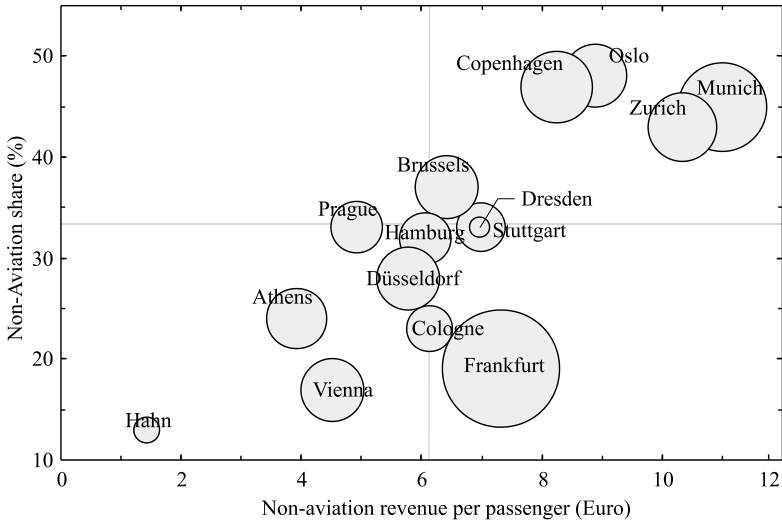


Fig. 2. Revenue share of non-aviation business according to passengers [15].

	2002	2003	2004	2005	2006	2007
Shop	70.5	69.9	68.8	70.9	76.8	85.1
Advertise	16.6	17.1	20.4	20.6	31.0	25.5
Services	22.8	20.5	24.1	26.4	27.3	35.2
Sum	109.9	107.5	113.3	117.9	135.1	145.8
Percentage of revenue (%)	6.6	5.4	6.8	7.4	8.0	8.3
Per passenger	2.27	2.22	2.22	2.26	2.56	2.69

Table 1. Development of non-aviation business at Frankfurt Airport (in Mio. Euro).

aires [16] and the passenger service requirements (e.g. comfort and service level [17, 18] or guidance information [19]).

In a previous research project we developed an airport simulation environment to allow for investigating the effect of passenger behavior on terminal processes [13, 14, 20]. This environment is expanded to evaluate different terminal concepts with diverse objectives. Besides the objectives of safety and security, the effect on the non-aviation sector will be taken into consideration as well. To provide a reliable database of passenger behavior and potential influence factors, this study will point out the findings from video-based surveillance of passenger motion behavior.

1.2 Status Quo of Passenger Behavior

The behavior of airport passengers (pax) differs from the behavior under normal conditions, e.g. shopping in a mall or crossing a traffic intersection. The pax have to fulfill several tasks to get on board of the airplane. When the pax

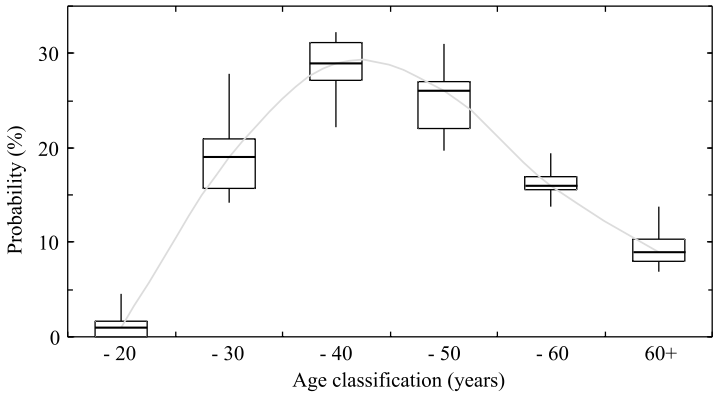


Fig. 3. Age structure at airports.

Age (years)	≤ 20	21-30	31-40	41-50	51-60	≥ 60
Percentage (%)	1.3	19.4	28.3	25.1	16.4	9.5

Table 2. Percentage of pax per age category.

arrive at the airport, they have to figure out the correct check-in counter at the airport information panel. If they have already checked in, by means of web check-in at home or late night check-in the day before, they may proceed directly to the security control area. Due to the complex structure of some huge terminal buildings, their behavior (“movement strategy”) is directly coupled to their experience with airports. Therefore, frequent (business) travelers often manage orientation tasks along their way through the terminal, while leisure pax have to search for orientation and direction information. These differences influence passenger behavior in terms of walking speed and direction. The amount of baggage before and after the check-in (carry-on baggage) could influence the motion behavior as well. A straight forward approach is to determine the expected pax speed according to the age structure of airport passengers (see Fig. 3).

For the average age distribution at terminals, data from German airports Frankfurt (2005), Berlin-Tegel (2006), Berlin-Schönefeld (2006), Hamburg (2006), Munich (2007), Hannover (2007), Dresden (2006), statistical data from German Airports Association (2003) and airline data from SWISS (2006) are considered. The average percentages derived for each age category are shown in Table 2.

Together with the speed-age distribution (Fig. 4) taken from [21], the expected pax travel speed at airports is around $\bar{v} = 1.4$ m/s. The expected speed values will range between the speed of pedestrian with leisure purpose ($\bar{v} = 1.1$ m/s) and the speed of pedestrian with travel purpose ($\bar{v} = 2$ m/s).

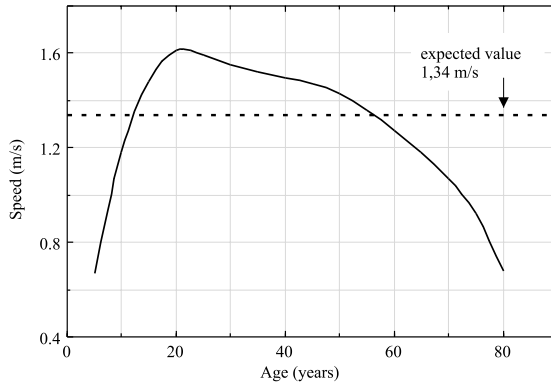


Fig. 4. Speed-age distribution [21].

Due to the fact that the age of the average passenger will globally increase over the next decades (the aging society), effects on speed in particular and mobility in general will have to be considered carefully. For the design of terminal structures it is important to have more detailed information on passenger’s motion behavior. Beside age, speed is also affected by gender, group size (to which the individual temporarily belongs), the amount of baggage, and the travel purpose. Generally, these external parameters can be measured by visual observation without any additional information, except the travel purpose. In the forthcoming investigations the travel purpose is derived from the flight destination [22]. The visual observation is an adequate option to collect data, because the motion behavior of the passenger is not affected and effort to install a monitoring system is at an appropriate level. Therefore, an investigation with a video surveillance system at Dresden International Airport is performed to figure out all influences of parameters influencing passenger travel speed.

2 Airport Environment

Dresden International Airport (Fig. 5) features a suitable environment to track the passenger motion behavior. There are three major areas for passenger movement at the terminal and nine potential video surveillance positions. Passengers reach departure level through different entry points (E1–E3), either via skywalk (E2, linking the terminal with the parking deck), a central escalators or elevator (E1) and staircases left and right hand (E3). Basically, the passengers prefer the center entrance area (E1).

At the entrance to the departure level (area I) the flight information panel is located. Arriving passengers and passengers gathering information about their flights are observed in area I. After the check-in procedure in area II or III, the pax walk to the security control into the direction of the camera

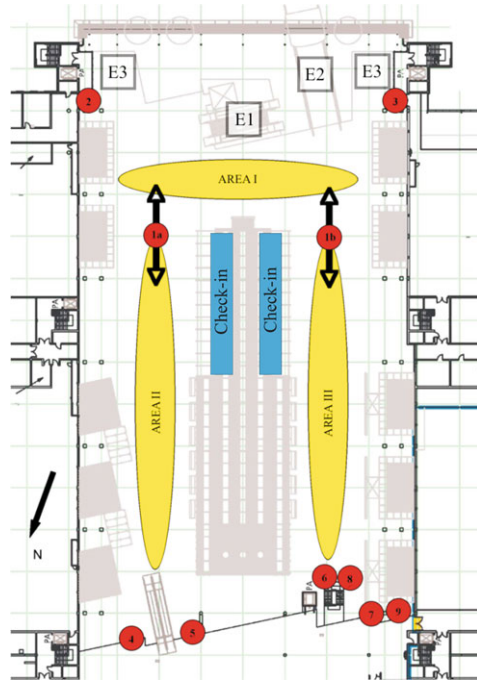


Fig. 5. Dresden International Airport, overview of terminal area.

positions. On their way, they can visit additional service facilities in area II (e.g. shops, restaurant or toilet). According to the flight plan, in the morning (until 9 a.m.) business and city break pax use the left side of the check-in area. After 9 a.m. the first leisure pax enter the terminal and walk to the right side of the check-in area (III), because the associated flights are handled on these counters.

This pre-selection ensures a pretty good separation of the business and leisure groups. The fact, that not the entire group members are business (or leisure) related passengers will be neglected. The observations suggest homogeneous groups, because all passengers of the specific area have a comparable motion behavior which differs significantly from the other area. Furthermore, visual comparison points out the obvious differences between business and leisure clothes. The positions of the observed areas are highlighted in Fig. 6, whereas the area II and III will be important for the following motion analysis. The area II is observed by two cameras (position 4 and 5) and the area III by cameras at the position 6 and 9. Due to the use of two cameras for one observation area, a passenger tracking environment (see section III) can process the different views to increase the accuracy of the determination of pax position.

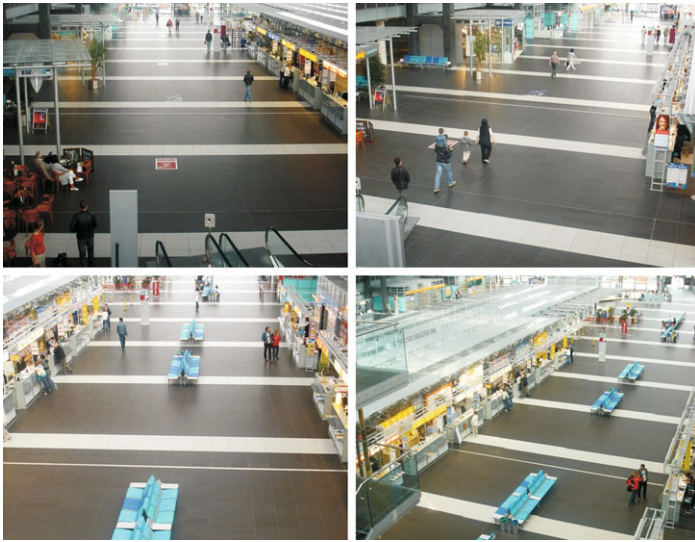


Fig. 6. Final camera positions at departure level of Dresden International.

First tests with the tracking environment point out, that the difference between the camera positions (observing one area) should be as high as possible to reach a significantly increased accuracy in position determination. Therefore, camera position 7 and 8 are not considered. The effort for a ceiling mounted camera (position 1 and 2) is too high, so that these positions are disregarded as well. Pictures from the final camera positions are shown in Fig. 6.

3 Passenger Tracking Tool

First tests with normal camcorders clearly show that the resolution is not sufficient to monitor the complete observation area. Comparing the standard camera resolution (PAL, 720×576 pixel) to the HD resolution (1440×1080 pixel) allows for tracking an additional tracking area of 150 m^2 , equivalent to an extra distance of 15 m (40 m total) and a doubled resolution in transverse direction. A manual tracking is realized without major difficulties, but the developed automatic software solution *Passenger Tracking Tool* (PTT [23]) performed much better using high-definition recording hardware. The manual tracking of person is very time consuming (8 hours per 30 min observed video) and allows for tracking only one person over the time. In contrast, the semi-autonomous PTT environment offers the ability to track several moving objects simultaneously. The manual corrections to the extracted trajectories are less time-consuming. The general methodology and algorithms for pattern

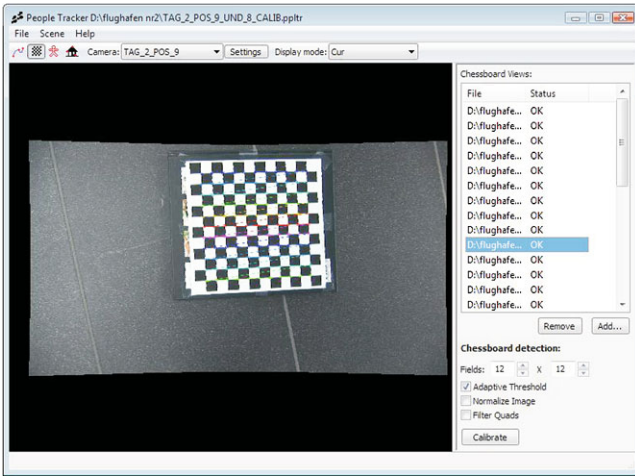


Fig. 7. Camera calibration in PTT environment.

recognition and robust tracking of moving objects which were applied for that software can be found in [23–25].

The tracking takes place on the so called image plane (perpendicular to the axis of the camera lens). To determine the position of the pax regarding to the terminal floor level, intrinsic and extrinsic transformations must be performed. Intrinsic parameters are camera related, e.g. focal length and distortion, whereas extrinsic parameters define the transformation of the camera coordinate system into the terminal level related coordinate system (e.g. height above floor level or rotation of view). A common technique to calibrate the camera is to use a checkerboard pattern. The identification of the correct shape of the board and adjustment of the intrinsic parameters lead to a calibrated picture. The effect of distortion correction is shown in Fig. 7.

Once calibrated, the tracking software performed without major difficulties even at slightly crowded areas. However, with increasing passenger density, the occlusion probability naturally increases and the tracking algorithm has to rely on statistical assumptions. Due to these assumptions (variations) the accuracy of the extracted trajectories decreases. These decreasing effects are partly compensated by the information coming from the second camera. Due to a manual intervention trajectories are corrected afterwards and disconnected trajectories are linked finally. The result of the tracking process is shown in screen shot of the PTT environment (see Fig. 8).

After the (semi-manual) tracking process the trajectories are located at the image plane. Using the scaled representation of the Dresden International Airport departure level (see Fig. 9) the trajectories can finally handled in the context of terminal processes.

The transformation of the trajectories to the terminal coordinate system allows for investigating passenger speed changes according to their conditions.

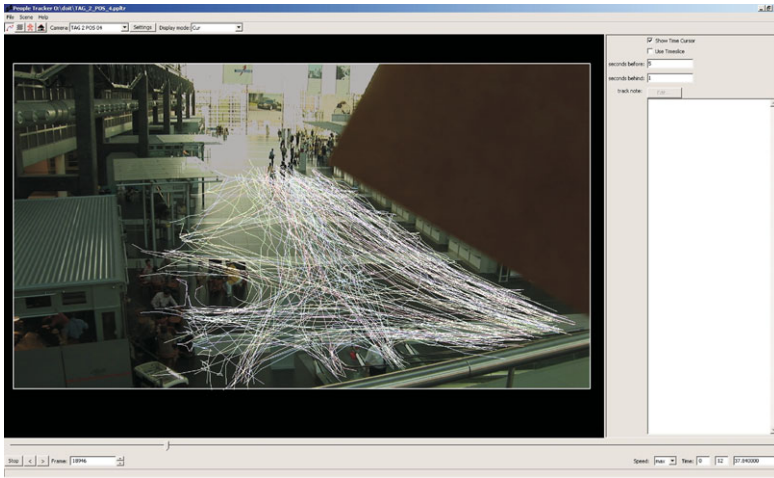


Fig. 8. Trajectories at PTT environment.

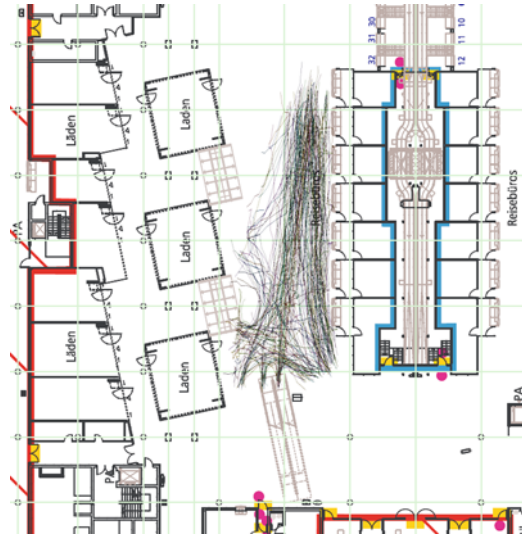


Fig. 9. Transformed trajectories at terminal level.

By means of the visual surveillance four different dependent relationships are observed, which are analyzed in detail in the following result section.

4 Results

The presented results base on the measurement of 595 passengers, parted into 330 business and 265 leisure pax. To analyze the differences in speed the

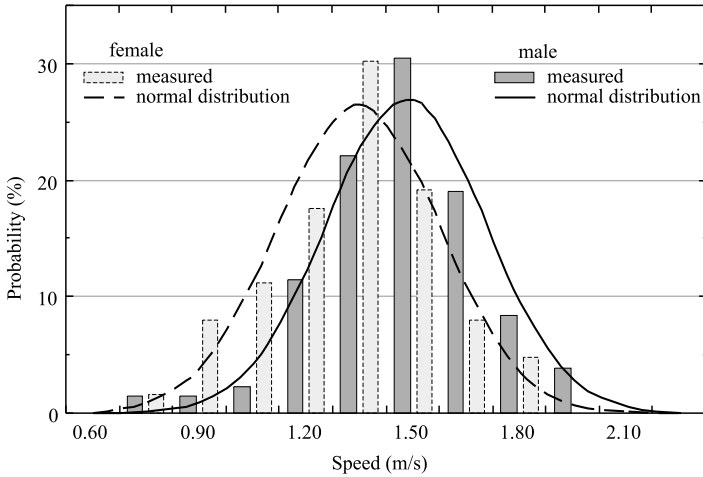


Fig. 10. Speed–gender interdependencies.

influences of the parameters gender, travel purpose (business/leisure), group size, and the amount/type of carry-on baggage are investigated. In addition to the extracted trajectories information about gender, groups and baggage have to be collected manually.

4.1 Gender

According to [21] the difference of the average speed between male and female is of the order of 10%. The measured group included 52% of men, 44% of women, and 4% children. The characteristics of the speed distribution according to the gender are shown in Fig. 10. While the standard deviations of the different groups are of the same magnitude of $\sigma = 0.22$ m/s, the average speed of male pax is $v_M = 1.4$ m/s and of female pax is $v_F = 1.27$ m/s, respectively. In compliance to the expected speed difference of 10%, the measured value is at level 9.3%.

4.2 Travel Purpose—Business vs. Leisure

Generally, the travel purpose of the pax is an internal parameter and is identified by passenger surveys. Based on the findings of [22] and the separation of the check-in area into typical business and leisure destinations at Dresden International Airport, the travel purpose is derived from the chosen check-in. The speed characteristics in Fig. 11 evidence that the average speed difference between business and leisure pax is about 24% ($v_B = 1.36$ m/s, $v_L = 1.0$ m/s) with a smaller standard deviation for business pax ($\sigma_B = 0.22$ m/s, $\sigma_L = 0.23$ m/s).

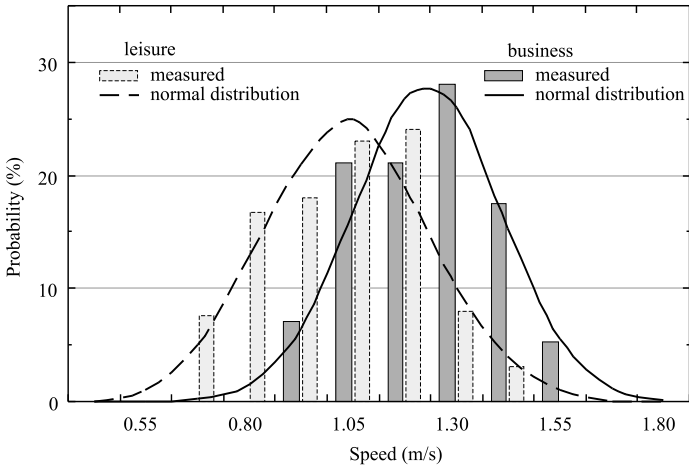


Fig. 11. Travel purpose interdependencies regarding to speed.

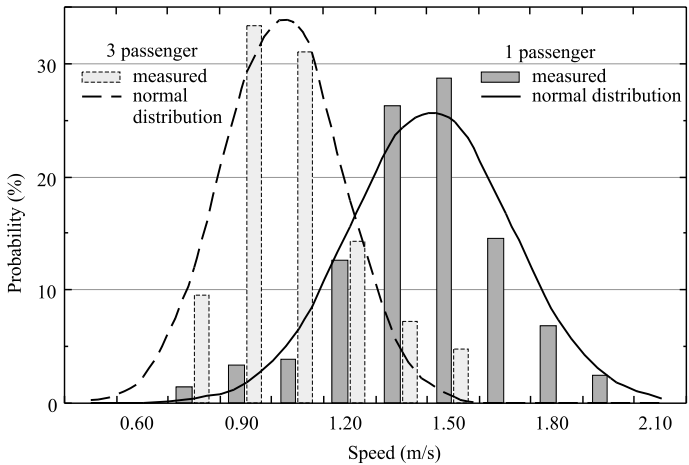


Fig. 12. Group size interdependencies regarding to speed.

4.3 Groups

The number of group members is expected to influence the speed of the individual, because intra group coordination (speed and direction adjustments) yields additional friction effects. In fact, measurements of three different group configurations confirm these assumptions. In Fig. 12 the differences between groups with one and with three members are shown. The observation clearly points out the significant influence of group size regarding to pax speed. In the monitored areas, group sizes up to 5 pax are observed, whereas groups with 4 or more members tend to diverge into smaller groups with 2 or 3

Group size (members)	1	2	3
v (m/s)	1.36	1.06	0.96
σ (m/s)	0.23	0.21	0.19

Table 3. Speed and standard deviation of different groups.

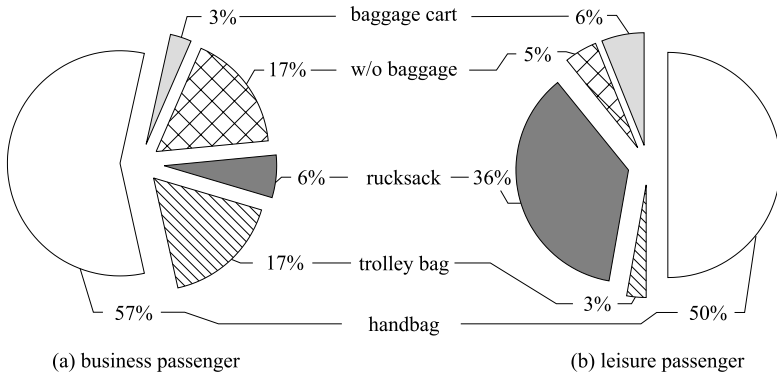


Fig. 13. Baggage distribution of business and leisure passengers.

members. This effect is amplified by increasing pax density, whereas acting in smaller groups avoids collisions. The results of the speed change according to the number of group members are shown in Table 3.

Pax walking alone are 22% faster than a group of pax with 2 members and 30% faster than a group with 3 members. In contrast, the standard deviation for single pax is slightly higher than for a group with 3 members.

4.4 Baggage

To determine the influence of the carry-on baggage on pax speed, the amount and type of carry-on baggage is counted manually. Finally, the trajectory data are merged with baggage data to allow for analyzing the dependency in detail. The type of carry-on baggage is parted into 5 categories: no bags, baggage cart, rucksack, trolley bag, and handbags. The distribution of carry-on baggage is shown in Fig. 13.

Due to the fact that many business pax do not check in their baggage, the amount of trolley bags is significantly higher within this group. In contrast, most of the leisure pax prefer to carry a rucksack or have no baggage at all. To compare the pax from the different categories of baggage types, only pax with one piece of baggage are considered in the investigation. In Table 4 the results are presented. As a baseline the pax group preferring rucksack is chosen ($\Delta v = 0$).

Investigations on the speed influences due to different baggage type point out, that the usage of a trolley bag does not decrease the pax speed. The

	Business			Leisure		
	v (m/s)	σ (m/s)	Δv (%)	v (m/s)	σ (m/s)	Δv (%)
Trolley bag	1.42	0.2	7.6	1.19	0.19	11.2
Handbag	1.33	0.22	0.8	1.07	0.22	0.0
Rucksack	1.32	0.25	0.0	1.07	0.21	0.0
Bag cart	1.27	0.24	-3.8	1.04	0.20	-2.8

Table 4. Baggage interdependencies regarding to speed.

results show a significant higher speed of trolley bag users (7.6% and 11.2%), which is obviously not directly correlated with the type of carry-on baggage. Pax using carry-on baggages only (no baggage check-in necessary, trolley bag as carry-on baggage) are often frequent travelers, which are very familiar with the airport environment. These pax often minimize the airport dwell time and they tend to arrive at the terminal latest [9, 22]. Due to the close time distance to the scheduled time of departure they are moving faster than the other pax.

The use of a trolley cart for the baggage has a decreasing speed effect of about 3%, which seems to be very low. Two additional facts have to be considered. First, only a few trolley cart users are observed after the check in process, because the pax try to park the baggage cart at the check-in area. Second, if they using the cart until the security control, the carts will be empty and easy to control. Therefore, the interdependencies of baggage carts regarding to pax speed have to be investigated in detail separately.

5 Conclusion

The investigations at Dresden Airport points out that the pax speed is significantly influenced by the gender, travel purpose (business/leisure), group size, and the amount/type of carry on baggage. The PTT environment allows for efficient tracking in less-crowded areas. With increased number of pax, the automatic tracking mode has to be supported by data from the second camera and manual corrections. Enhancements of the PTT performance are necessary to further investigate short-range interactions of passengers to avoid collisions. The effect of gender and travel purpose to pax speed was at the expected level. The group size is an important factor for the major terminal processes (e.g. significant influences on check in procedures). The decreasing speed effects coming from group size are higher than estimated. This is also very important for the determination of passenger flow at terminals, because approximately 50% of the measured pax are walking in groups. After the check-in process the pax only carry small baggage, which seemed to have a small influence on pax speed. The trolley bag has no disadvantageous effect on the pax speed. The behavior in crowded areas was not being investigated, but it is important for predicting pax behavior at peak hours. The influence of baggage carts after the check-in procedure is very small.

6 Outlook

The results of the data collection at Dresden airport will be integrated into the terminal simulation environment developed at Dresden University of Technology [12–14]. This allows for increasing the reliability of the simulation results and the transfer of the results into real terminal environments, so terminal processes at Dresden International Airport will be analyzed in detail. The results of our investigation point out, that the motion behavior of passengers are directly coupled on several factors (e.g. gender, travel purpose or group size). The gathered trajectories of real passengers are very important for modeling the passenger itself. Due to the fact, that passenger tend to walk in small groups, their behavior is comparable to a granular flow. Consequences to the common microscopic (individual based) and macroscopic (flow based) modeling approaches are inevitable.

Using an animation environment (screen shot see Fig. 14), data taken from video recordings can be displayed without any privacy concerns [20]. So, further studies and the exchange of non-personalized trajectory data could sustainable improve scientific research. The semi-automatic analysis of passenger motion behavior at airport environment points out the capabilities of video surveillance system without privacy concerns. Further investigations should be focused on affecting and controlling passengers motion intention. The airport is interested to provide efficient terminal facilities and controlled passenger flows will ease the workload prediction. Furthermore, affecting passenger behavior could increase the non-aviation revenues due to adequate guidance systems and could result in saver terminal environment.

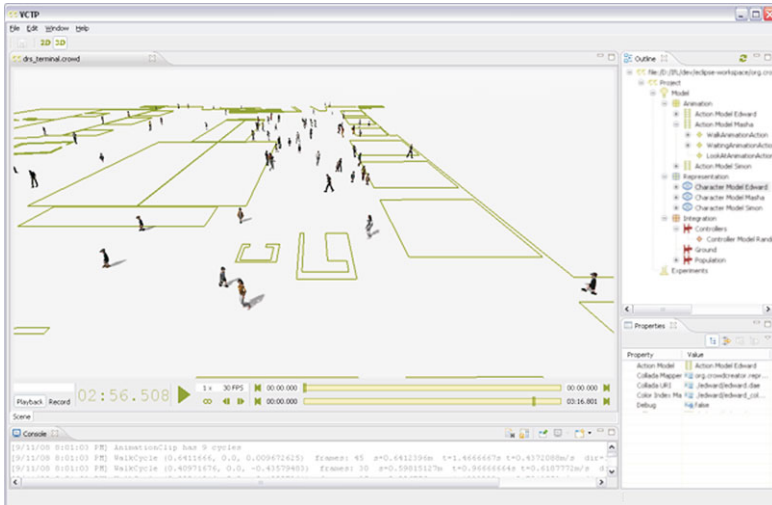


Fig. 14. Passenger simulation on visual computing tools platform [20].

Acknowledgements

The authors like to thank Dresden Airport for the authorization to collect data and for supporting this research fundamentally. Thanks go to Tilman Blumhagen for developing the tracking software and to Bernd Oreschko for data acquisition.

References

1. H. Klüpfel and T. Meyer-König. Modelle für die Berechnung von Personenströmen und Evakuierungssimulationen. VdS-Fachtagung Evakuierung und Räumung von Gebäuden, 2005.
2. A. Kirchner, H. Klüpfel, K. Nishinari, A. Schadschneider, and M. Schreckenberg. Simulation of competitive egress behavior. *Physica A*, 324:689–697, 2002.
3. D. Helbing, I. Farkas, and T. Viscek. Simulating dynamical features of escape panic. *Nature*, 407:487–490, 2000.
4. H. Klüpfel. The simulation of crowds at very large events. A. Schadschneider, R. Kühne, T. Pöschel, M. Schreckenberg, and D.E. Wolf, editors, *Traffic and Granular Flow '05*, 2006.
5. J.J. Fruin. *Pedestrian Planning and Design*. Metropolitan Association of Urban Designers and Environmental Planners, New York, 1971.
6. D. Helbing. A mathematical model for the behavior of pedestrians. *Behavioral Science*, 36:298–310, 1991.
7. D. Helbing, L. Buzna, A. Johansson, and T. Werner. Self-organized pedestrian crowd dynamics: Experiments, simulations, and design solutions. *Transportation Science*, 39:1–24, 2005.
8. D. Helbing and P. Molnar. Social force model for pedestrian dynamics. *Physical Review E*, 51:4282–4287, 1995.
9. N. Ashford, N. Hawkins, M. O’Leary, D. Bennetts, and P.M. Ginity. Passenger behavior and the design of airport terminals. Transportation Research Board Record, No. 588, 1976.
10. S.P. Hoogendoorn and P.H.L. Bovy. Pedestrian route-choice and activity scheduling theory and models. Transportation Research Board, 2003.
11. S. Theiss. Passagierflusssimulationssysteme—Bestandsaufnahme im Hinblick auf innovative Abfertigungskonzepte und Notfallmanagement. Technische Universität Dresden, 2003.
12. M. Schultz, S. Lehmann, and H. Fricke. Development of a computer-aided model for reliable terminal evacuation simulation—a statistical approach to handle unpredictable passenger behavior. *ICRAT*, Zilina, 2004.
13. M. Schultz, S. Lehmann, and H. Fricke. A discrete microscopic model for pedestrian dynamics to manage emergency situations in airport terminals. *Pedestrian and Evacuation Dynamics 2005*, Wien, 2005.
14. M. Schultz, A. Wachtel, and H. Fricke. Standardized concept for passenger guidance systems at aerodromes. *CEAS*, Berlin, 2007.
15. A.T. Kearney. Airport cities—Marktplätze des 21. Jahrhunderts, 2006.
16. C.I. Hsu and C.C. Chao. Space allocation for commercial activities at international passenger terminals. *Transportation Research E*, 41:29–51, 2005.

17. N. Martel and P.N. Seneviratne. Analysis of factors influencing quality of service in passenger terminal buildings. *Transportation Research* (No. 1273): Airport Terminal and Landside Design and Operation, Publication of the Transportation Research Board, Washington, DC, 1990.
18. A.R. Correia and C. Wirasinghe. Development of level of service standards for airport facilities. *Journal of Air Transport Management*, 2006.
19. P. Wenzel. Fußgänger-Leitsysteme—Planung von Leitsystemen in Fußgänger-Verkehrsanlagen am Beispiel von Fluggastempfangsgebäuden. PhD Thesis, Stuttgart, 1999.
20. C. Schulz. Entwicklung eines Eclipse-basierten Animations-Werkzeugs für virtuelle Menschengruppen. Hochschule für Technik und Wirtschaft Dresden, 2008.
21. U. Weidmann. Transporttechnik der Fußgänger. Zurich, 1992.
22. S. Spranger. Problemorientierte Analyse des Check-In-Prozesses am Beispiel des Flughafens Stuttgart. Technische Universität Dresden, 2008.
23. T. Blumhagen. Implementierung eines Systems zur video-gestützten Personenverfolgung. Hochschule für Technik und Wirtschaft Dresden, 2008.
24. *10th IEEE International Workshop on Performance Evaluation of Tracking and Surveillance*. University of Reading, 2007.
25. M. Andriluka, S. Roth, and B. Schiele. People-tracking-by-detection and people-detection-by-tracking. Technische Universität Darmstadt, 2008.

Application Modes of Egress Simulation

Steve M.V. Gwynne¹ and Erica D. Kuligowski²

¹ Hughes Associates, Inc., 3515 28th st #307, 80301 Boulder, USA
e-mail: sgwynne@haifire.com

² National Institute of Standards and Technology, 100 Bureau Drive, Stop 8664,
20899-8664 Gaithersburg, USA
e-mail: erica.kuligowski@nist.gov

Summary. Egress models are being used more frequently to simulate people movement; i.e. how people enter, use and leave a building. However, little has been written on the different aspects of people movement that can be examined and how these models may achieve this. This paper outlines six modes in which an egress model can be applied: *Naïve*; *Operational*; *Predictive*; *Engineered*; *Real-Time*; and *Interactive*. The paper outlines what is needed to enable these application modes, in terms of data, expertise and model functionality, and the benefits of doing so. This is intended to highlight the challenges faced by egress models and the complexities of the subject matter being examined: people movement under emergency and non-emergency scenarios. Currently, no model includes all of the six modes identified. The authors hope that this discussion will identify the importance of these modes, the need for them to be addressed within the same model and the clear benefits of doing so.

1 Introduction

Computational egress models have grown more sophisticated and are now frequently used as part of a performance-based assessment. This development has followed an increase in our understanding of human behavior in fire and a modest increase in the supporting empirical data available. The model developments have responded to this increased understanding, albeit in an imperfect, delayed and inconsistent manner. This has allowed computational egress models to be applied to new and more complex application areas. This has both increased the overall application of egress models and prompted a more rigorous examination of the functionality of the models in question. In addition, this increased breadth and depth of application requires a greater degree of expertise from the user and more comprehensive and reliable supporting data.

The expansion of the modeling capability poses questions regarding new application opportunities. This paper describes the different application modes

of egress models; i.e. what the modes require of the computational models, the user, the data and the applications that they enable. This will provide a clearer understanding of the capabilities and limitations of the models, the expertise required of the user and the increasing demand for new, more comprehensive and more detailed data to the development and application of these models.

2 People Movement System (ICE)

A building can be seen as a people movement system that operates at different states [1]. This system is formed from three phases of people movement (ICE): ingress; circulation; and egress. These phases of movement can exist under emergency and non-emergency conditions. Each of these phases will have informal or formal procedures to manage their effectiveness; e.g. security, emergency evacuation, etc. All forms of movement in relation to the structure (i.e. procedural responses), will fall into one of the six combinations, as shown in Table 1.

Models can be applied to assess the effectiveness of these procedures. Each combination of phase and scenario requires a different set of assumptions and modeling capabilities.

Also, an incident does not occur independently of previous events: the prior use of a structure will influence the current event [1, 2]. Therefore, in addition to the procedural efforts to manage people movement, these other historical factors will also have an impact on occupant behavior. Procedural and historical influences will therefore coexist. The history of the structure’s use will be stored in occupant recollections (see Fig. 1). These occupants will have a base knowledge and level of experience reflecting their previous use of the building and related training. They will also be provided with new information during any event. *Procedural and historical factors will influence their activities during any of the phases of movement highlighted.*

These procedural and historical factors are highly coupled: coexisting procedures can influence each other; an individual’s experience will influence their

ICE		Scenario	
		Emergency	Non-Emergency
Phase of movement	Ingress (I)	Crowd management, Fire Department arrival	Security, ticketed access
	Circulation (C)	Ensuring initiation of response, disengagement of population from activities	Providing information on facilities and services
	Egress (E)	Managing emergency evacuation	Leaving the building, crowd management

Table 1. Examples of the procedures employed given the phase of movement and the scenario [1].

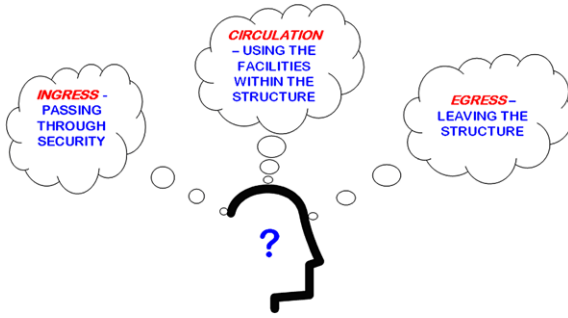


Fig. 1. The individual brings their history with them to the evacuation.

behavior and their response to a procedure [1, 2]. The application of one procedure (e.g. managing security) may influence the effectiveness of another (e.g. evacuation). This may occur directly (e.g. congestion produced by security delays evacuation movement) or indirectly (e.g. where an individual's prior restricted access due to security inhibits their use of certain exits). This can have an enormous influence over the performance of the people movement system. This performance, and our assessment of it, is critical, especially when making design decisions for emergency scenarios.

Computational models are increasingly employed to examine the people movement system. Given the highly coupled nature of the procedural and historical factors, it is contended that for an egress model to accurately represent any phase of movement, that it should ideally be able to represent all of them. This would then allow the model to capture the indirect and direct influences of these factors upon the results produced. If this is not possible then the results produced by a model may be quantitatively inaccurate (e.g. the evacuation times produced are too optimistic) and qualitatively inaccurate (e.g. congestion is not produced, exit use is unrealistic, etc.). This may lead to flawed and potentially unsafe design.

Sophisticated models are therefore required. These models will need to cope with the range of influences, situations and applications highlighted above. In the next sections, six different application modes are described. Each of these provides a means to estimate a different set of results or assess a different phase of people movement. It is contended that each of these modes provides an invaluable insight into the people movement system; it is also contended that to gain reliable insight into any single phase of people movement, that all of these modes should be available in the same computational model.

3 Six Degrees of Simulation

In the following sections, six simulation modes are characterized: *Naïve*; *Operational*; *Predictive*; *Engineered*; *Real-Time*; and *Interactive*. Each is described

in detail outlining the nature of each mode, the different demands placed on the user, the assessments made possible by each mode, and the data required to support the use of the mode.

3.1 Naïve Mode

Naïve mode establishes movement patterns within a structure prior to the population's experience and knowledge levels developing; i.e. before the building design is put into practice. The model achieves this by simulating the movement of naïve occupants who gain experience and knowledge of the building by exposure to information as they move around the space. This movement could be biased or managed through the insertion of facilities, egress routes, signage, etc. In order for this mode to be possible within a simulation model, occupants start with no information or knowledge regarding the layout of the building. They initially move towards route elements that can be detected from their current position, or learn about the existence of such routes. General rules are used to govern the naïve movement of the individuals, although this movement evolves as more information becomes available to them. As this population becomes more informed, so their movement depends more on the routes available, their familiarity with these routes, and their typical use of these routes. This movement can be compiled and an understanding of the critical and most frequently used paths attained.

This mode can be used prior to the construction of a building or where the building has yet to be occupied. For instance, an engineer/architect/authority having jurisdiction (AHJ) may be interested in understanding how a shopping mall is used, given the positioning of certain facilities, signs and exits. The engineer can then modify the position of these facilities in order to improve the efficiency of the use of the space. This may have an impact on comfort levels, usage and on commercial viability.

The user would need to provide information on the location of the facilities, amenities, routes, information available, the structure, and the population characteristics. For each of the physical and informational components, the user would need to establish their relative impact on the knowledge levels of the population. The user would then need to understand the relationship between these physical and informational components, and the behavioral response of the population. The user would also need to identify critical events (e.g. congestion) and key components (e.g. exits, signs, etc.) that have an important impact on the use of the space. The results would require a high degree of interpretation; i.e. current engineering assessment criteria do not provide explicit guidance on this mode of application.

For a model to include this mode, it would need to represent the population at the individual level. The information levels available to each individual would need to be simulated; this information would need to be dynamic; and sensitive to the surrounding conditions. The structure would need to be represented in detail, including amenities and other elements that influence the

individual's understanding of the structure. Behavioral algorithms would need to represent the impact of these amenities and elements upon the individual. The results produced would need to reflect the usage of certain elements, the information levels of the population, and the level of influence exerted by amenities and elements. This type of mode is currently available. The EVAS Pedestrian Modeling Software [3] produced by the University College London has a *Naïve* mode.³

3.2 Operational Mode

Operational mode establishes the impact of 'normal' circulatory movement within a structure; i.e. how people routinely use the structure. This may be informed by the results produced in *Naïve* mode; i.e. that the initial conditions of *Operational* mode will be the results from *Naïve* mode. These results will influence the familiarity levels that people have with the space and with their preferred access routes. In the absence of these results, dedicated empirical data can be collected or engineering judgment regarding the use of the existing structure.

The model is applied in *Operational* mode by distributing the population about the space according to its use and then using the space as expected. In this case, the population will have a pre-determined understanding of the space and a set of actions that they would normally complete as part of their daily routine within the building. For instance, people's movement about an office-tower can be assessed given their office location, the location of the dinner hall, meeting rooms, etc. The movement patterns around the structure can then be simulated and areas of high use identified. This mode might be used to improve the efficiency of the usage of the building and also to improve the non-emergency management of the structure. It can also be used to understand the population's familiarity of the structure and also where the population might be at any one time. Both of these factors will directly influence the results produced during an emergency scenario.

Operational mode can be used after the structure's construction has been completed and when the building is in operation. It would allow further insight into the current use of the structure and into the impact of procedural and structural changes upon this use.

In order for *Operational* mode to function, it requires the initial distribution of the population (either from empirical data or from *Naïve* mode), the routes used during non-emergency movement, and the locations of key components within the structure. These requirements are similar to those of the

³ Certain commercial entities, equipment, or materials may be identified in this document in order to describe an experimental procedure or concept adequately. Such identification is not intended to imply recommendation or endorsement by the National Institute of Standards and Technology, nor is it intended to imply that the entities, materials, or equipment are necessarily the best available for the purpose.

Naïve mode except that the population is credited with having a previously established familiarity with the space.

In order to apply *Operational* mode, the user requires an understanding of how people make use of the structure in question, an understanding of non-emergency behavior in general in order to identify anomalous behaviors and the ability to interpret the results produced. This mode will require a high degree of interaction between the user and the model in order to configure the model for simulation and then to interpret the results produced.

A simulation model would need to represent a population as individuals and associate pre-defined, non-emergency tasks to them; e.g. visit cafeteria, go to bathroom, attend meeting, etc. These tasks might implicitly or explicitly be associated with the typical operations within the structure; e.g. the tasks can be specifically defined, or alternatively the time delay associated with the task can be represented. The simulated population would need to be sensitive to a range of influences upon their behavior. The model would need to simulate actions as well as movement, cope with a range of different procedures, and possibly generate people during simulation; e.g. the arrival of people at a rail station.

A number of models are currently available that include this type of functionality: one example being the EXODUS model [4], which is able to simulate non-emergency activities that can then develop into an emergency scenario. The population can be given pre-determined activities as part of a non-emergency event. These activities are followed until an emergency arises, when these activities can potentially be ignored.

3.3 Predictive Mode

Predictive mode allows the user to investigate the impact of local evacuee decision-making on egress performance; i.e. to examine the outcome of an evacuation from the bottom-up rather than imposing a behavioral response. Rather than these behaviors being entirely pre-determined by the user, they instead occur through an adaptive process: low-level behaviors (e.g. delay, move, redirect, etc.) produce emergent high-level conditions (evacuate, seek refuge, etc.). The mode represents an attempt to genuinely predict the behavioral response, given the conditions faced, rather than simply to investigate the consequences of an entirely imposed response to an event.

The ‘intelligence’ is built into the model rather than residing in the engineer. For instance, instead of the engineer prescribing the response of the evacuating population (e.g. they respond between times X and Y and use exit Z), the behaviors are instead dependent upon local conditions, the actions of the surrounding population, the information available to the individual and their abilities. This reliance on the model’s capabilities produces significant (and often warranted) levels of skepticism. The value of this approach is therefore highly sensitive to the sophistication of the behavioral model employed. However, the benefits of this approach do not necessarily rely on the location of

the expertise (although the inconsistent understanding of human behavior in the field of engineering is certainly an issue). It instead relies on the ability to *generate* evacuee responses, rather than having them prescribed.

This mode can inform further scenario design for assessment; for instance, in a performance-based analysis the *Predictive* mode can be used to identify additional scenarios of interest. In typical engineering applications, a set of scenarios (questions) is posed, the model is set up to address these scenarios and then results are produced. The engineer configures and constrains the model to answer the questions posed; however, this does not ensure that the correct questions are being posed. By definition, the engineer prescribes the behaviors that can be performed during the simulation in order to focus on the questions being investigated; e.g. a set of pre-evacuation times, response to the presence of smoke or congestion, etc. that relate to these questions.

The use of the *Predictive* mode, where the simulated population is allowed to adapt to the scenario, may generate new questions, allow new worst-case scenarios to be developed (although given the limited time available the term ‘worse-case’ is more appropriate), and highlight new previously unforeseen conditions. These are made possible by the adaptive response of the evacuees; e.g. the pre-evacuation times might be generated by the presence of a type of alarm, the presence of smoke, the actions of others, etc., rather than being imposed by the engineer. These emergency conditions may allow the identification of informed worse-case scenarios, rather than those produced beforehand by the engineer. It can also be used to determine the underlying causes of observations: it allows a genuinely investigative process to take place. If the user predetermines evacuee responses then only these responses can be tested.

The *Predictive* mode requires the initial conditions to be provided in great detail, as these conditions will influence the behavioral response of the evacuees. These include the initial distribution of the population, the nature of the population, the scenario conditions, etc. These could be provided by the collection of empirical data or from earlier model calculations; e.g. the data provided by *Operational* mode. Critically, it also requires a comprehensive behavioral model that is sufficiently developed to provide the range of behaviors needed. This model will need to be based on an adaptive approach rather than a purely deterministic approach; i.e. it will need to be sensitive to the emergent qualities necessary for the *Predictive* mode. This will require the individually simulated evacuees assessing the surrounding conditions and then selecting their response accordingly. This adaptive process will represent the connection between external events and the actions performed by the individual.

The primary expertise required to employ this mode is in the configuration of the scenario, determining that the simulated behavioral responses are reasonable, and in the analysis of the results produced. The key behavioral decisions (i.e. the appropriateness and selection of a behavioral response to certain conditions) are taken *within* the model itself. As mentioned previously,

the expertise required is embedded in the model itself by the model developers. This does not imply that the engineer is exempt from expertise in egress behavior, as this is critical when configuring the model; only that this expertise is not employed in selecting evacuee behaviors. However, a great deal of expertise is required in examining the results and extracting the underlying factors and behaviors that influenced them. This is more complex as it is not always apparent that a direct relationship exists between a particular behavior and an outcome. This requires an understanding of the simulated conditions, the methods employed and the subject matter being simulated.

Currently, there are no fully predictive egress models. There are some models that include adaptive behaviors (such as the MASSEgress model [5]), but these are primarily research-based. Where these models are commercially available (see [4, 6]), the adaptive capabilities tend, by default, to be disabled given that most applications require that the evacuee behavioral response is constrained; i.e. that the behavioral responses are controlled by the engineer. The absence of a fully predictive model is due to a number of reasons:

- the difficulty in producing such models; e.g. they are computationally expensive, and technically complex.
- the difficult in supporting their development with appropriate data; e.g. most data represents high-level behavioral responses, rather than the constituent components required for this mode to function.
- the skepticism that such predictive modes face, given their emergent nature; e.g. it is more likely that an AHJ would trust an engineer that can explain his/her assumption regarding a scenario than rely on the documented theoretical assumptions in support of complex behavioral algorithms.
- and the nature of the current performance-based regulations; i.e. that they are relatively immature.

3.4 Engineered Mode

Engineered mode allows the user to pre-determine emergency scenarios and then impose them and the subsequent behavioral response upon an evacuating population; i.e. to examine the outcome of an evacuation from the top-down. This is the mode typically used by engineers to assess design performance. It allows specific questions to be posed and variables to be controlled within the simulation process to allow specific answers to be produced. This control allows the engineer to prescribe the behavioral response, reducing the number of confounding variables; e.g. evacuees respond between X and Y seconds and use exit Z. This is very useful given the current performance-based regulations [7].

Engineered mode requires data-sets that address specific egress components, rather than those that support a comprehensive, behavioral model. Indeed, one of the key benefits of this mode is that it allows, to some degree, the engineer to account for the current limitations in the data available. The data

employed will be model-specific, but will generally relate to the key egress components: the pre-evacuation time; the relationship between population density and flow; the movement rates for different sections of the population and different structural components; simple evacuee behaviors, such as route usage; and possibly the impact of certain impairments. This will then allow the model to simulate the required evacuee responses given the pre-determined questions posed by the engineer.

The engineer will need to provide a description of the initial conditions: population, structure, procedure and environment. These may be informed by *Operational* mode. The scenarios examined may be informed by the results produced in the *Predictive* mode, where new ‘worse-case’ scenarios had previously been identified. The engineer is responsible for posing the correct questions and then configuring the model such that it can answer these questions. Given that the pre-determined questions are being addressed, the results produced can be examined to assess the outcome. Although some interpretation is required, it is certainly less than that required in the *Predictive* mode, and clearer guidance exists on what results need to be examined. However, expertise is still required. It is often the case that the results produced by simple models are presented as definitive, whereas they are, at best, suggestive [8].

To enable *Engineered* mode, a model must represent the required scenario conditions and allow the questions to be posed; i.e. allow the user to have control over the behavioral response and the scenario conditions. For instance, the engineer may need to have people respond instantaneously or according to a representative distribution; have them use their nearest exits or use exits according to familiarity; and include an unimpaired population and then a population that includes a section that has an impairment. A number of models are available to do such analysis (one example is Simulex [9]). In terms of fire safety engineering, this represents the most common form of analysis and the most commercially viable.

3.5 Interactive Mode

Interactive mode allows the engineer to modify aspects of the incident and/or the evacuee response *during* the simulation. It achieves this by allowing the engineer to interact with the simulation as it is running: to modify conditions and then have the model react to these changes. The engineer may act as a simulated evacuee (i.e. allowing them to take decisions for an evacuee) or as an ‘overseer’ (i.e. changing the scenario conditions to which the simulated evacuees are exposed and forced to react). The simulated conditions and/or evacuee responses are then modified by the engineer during the simulation. This mode allows the engineer to gain first-hand insight into the evacuation conditions, into the effectiveness of different evacuee responses, investigate worse-case scenarios, and/or be of value as a training/demonstration tool.

The engineer will have to initially configure the scenario conditions, as he/she would have in *Engineered* mode. However, additional data may have

to be provided given the evolution of the scenario in response to the engineer's intervention. The engineer will also need to know how to use such a mode responsibly; e.g. to respond reasonably when controlling a simulated evacuee, and making scenario changes that address real concerns and scenarios of interest when acting as an overseer. This mode will require a high-degree of interpretation of the results produced and, by definition, of user interaction.

The data requirements fall somewhere between the *Predictive* and *Engineered* modes, depending on the exact nature of the simulation and the scope of the engineer interaction. The model will have to respond to the changes in the scenario conditions and have sufficient data to do this. The current scarcity of data may limit the scope of the interaction between the model and the user. A model will need to simulate the evacuees as individuals, accept user input during the simulation and allow evacuees to respond accordingly; i.e. have a sufficiently developed behavioral model to allow the simulated evacuees to do this. Models currently exist that are able to do this (e.g. EVI [10]). EVI is often used as a training tool, enabling trainees to directly interact with the evacuation scenario and more clearly see the effect of their actions.

3.6 Real-Time Mode

Real-Time mode allows the user to gain feedback from a model during an actual situation, be it emergency or non-emergency; i.e. to direct the real-life procedure employed as the situation evolves. This requires a direct feed from the observed real-life conditions to the conditions simulated within the egress model. This might be through a CCTV (closed-circuit television) system/sensor system/manual observation that monitor real-life events and then provide this information directly to the egress model. The model then simulates how the situation evolves. The operator would then be able to play the current situation forward allowing them to estimate how the current situation may develop given different procedural responses. This would need a link between the observed and simulated conditions and the model run-time to be significantly faster than real-time in order to allow the results to be produced and processed in time.

In some occupancies, *Real-Time* mode would be used in the normal operation of the building to assess current behavior and performance. Feedback could then be provided on the movement of people around the space and procedural modifications made if required. For instance, in high occupancy spaces, such as stadiums, the comfort levels of people can be managed using *Real-Time* analysis. Procedures can be employed to maintain or improve comfort levels. These procedures would be better informed and tested through the use of *Real-Time* mode. In addition, *Real-Time* mode can be used to prevent the normal operations within stadiums developing into emergency situations. In other occupancies, this type of use may not be warranted; e.g. in an office building. However, there may be value in assessing the response of the evacuating population and determining whether this can be improved in response

to the evolving scenario. This could be of value to the evacuees, the building managers, and also to the first responders.

In *Real-Time* mode, the initial scenario conditions are determined by external sources. Where there are omissions, data can be provided from empirical data, from the use of *Operational* mode, or from the engineer. Otherwise, the configuration of the mode would be similar to those of *Engineered* mode: allowing key procedural changes to be assessed in faster than real-time. Currently, it is not feasible for the intensive analysis required by *Predictive* mode to be conducted under such time constraints.

In *Real-Time* mode, the engineer will be responsible for setting up the initial conditions and interpreting the results produced. It is critical that the engineer understands the model accuracy sacrificed to cater for real-time application: the results are generally indicative and may be further compromised due to time constraints. The engineer may also be under the same time constraints. The results provided may need to be analyzed quickly in order to provide feedback to the procedures implemented. This will require an intuitive understanding of the results and of the procedures available. *Real-Time* mode may be accompanied by analytical tools that assist the engineer in this process.

Several models are currently available that can run faster than real-time (one example is EVACNET [11]), although many of these do not have the sophistication to provide the necessary detailed feedback to the engineer. In addition, models exist that are designed specifically to operate in the manner described above (e.g. the model being produced by UTRC [12]), although there is currently little information on their capabilities.

4 Discussion

Each of these modes provides an opportunity to examine different phases of people movement; i.e. one of the six combinations identified in Table 1. Currently, an engineer would require several simulation models in order to employ all of these modes. However, in reality, these modes are highly coupled; i.e. the results from one will affect the conditions in another. Therefore, it would be highly beneficial if the modes were included in a single model that allowed information to migrate between the modes directly. Although it would be possible to port information between models, it is more prone to error; it is more likely that data will be lost in the translation; and it will invoke the cost of purchasing/training for several models.

An integrated model (i.e. one that includes all six modes and allows information to propagate between them) may be used in the following manner. An airport design is presented to an engineer prior to construction along with information on the use of the space; e.g. expected movement around an airport. The engineer employs *Naiïve* mode in order to investigate how the airport configuration influences people movement. Issues and recommendations are

passed on to the architects. Once the design is confirmed the engineer is asked to assess egress performance as part of a performance-based design (PBD). The engineer first employs *Predictive* mode to identify key scenario conditions. This is based on the calculations in *Naïve* mode and on the limited empirical data available. *Engineered* mode is then employed to conduct the standard PBD assessment, where specific scenario questions are answered by the simulation model. Guidance may also be provided on the procedural design. Once the design has been accepted then the model can be used in *Operational* mode to optimize the non-emergency procedures employed; e.g. checking in, security issues, etc. This will be influenced by the results produced by *Naïve* mode. This will identify critical egress components, exit familiarity and also how the population is distributed. In order to improve (non-)emergency preparedness, the model can be employed in *Interactive* mode. As part of their training staff may engage with the model on an individual or global level giving them first-hand insight into the scenario and the procedural response. Once the building is operational, the model could be running in *Real-Time* mode, with information from CCTV cameras, providing safety managers with some indication as the effectiveness of different procedures. If an incident does occur, the model can be employed in *Engineered* and *Predictive* modes to investigate the behavioral/procedural response and recommend improvements to it.

Although it is improving, the application of computational egress models is still relatively immature, especially in comparison with comparable approaches such as the use of computational fluid dynamics (CFD) models. This may produce problems, especially given the broader range of application types and the increased level of expertise required. It is often assumed that expertise from the traditional hydraulic calculations can be translated directly into the computational arena. Although experience in the application of hydraulic models may be necessary for applying egress models, it is certainly not sufficient. This becomes all the more evident as the project applications become more complex and require a greater understanding of human behavior in fire.

5 Conclusion

Six modes of application have been presented. These broadly reflect the different approaches that are available to simulation models when examining people movement. These require different levels of model development, data, and user expertise. Although this is not an exhaustive list of modes, it does demonstrate the variability in the use of the simulation models and the impact on the user and on the data required. It also demonstrates the interdependence of these modes, given their highly coupled nature.

All of these modes have great value; however, currently no model can address all of them. This will inevitably require the engineer to make a greater number of assumptions. Incorporating all of these modes into a single model would produce a number of benefits. The engineer would be able to represent

the impact of occupant experience, the different phases of people movement and the interaction between the procedures given a situation. This should be a future goal, given the need for this integrated approach and the increasing interrelatedness of incident scenarios. It would also implicitly encourage the view of the building as a highly coupled people movement system rather than as a set of distinct situations that can be examined in isolation.

References

1. Boswell, D., Gwynne, S.M.V., Air, fire and ICE: fire & security challenges unique to airports, *Fire and Security Today*, August 2007, pp. 30–37.
2. Sime, J., Escape behaviour in fire: ‘panic’ or affiliation?, PhD Thesis, Department of Psychology, University of Surrey, 1984.
3. Turner, A., Penn, A., Encoding natural movement as an agent-based system: an investigation into human pedestrian behavior in the built environment, *Environment and Planning B: Planning and Design* 29(4):473–490, 2002.
4. Xie, H., Filippidis, L., Galea, E.R., Gwynne, S., Blackshields, D., Experimental study and theoretical analysis of signage legibility distances as a function of observation angle, Proc. Pedestrian and Evacuation Dynamics 2005, eds. Waldau, N., Gattermann, P., Knoflach, H., Schreckenberg, M., Springer, Berlin, 2007, ISBN 878-3-540-47062-5, pp. 131–143.
5. Pan, X., Computational modeling of human and social behaviors for emergency egress analysis, PhD Dissertation, Dept. Civil and Environmental Engineering, Stanford University, 2006.
6. Paulsen, T., Soma, H., Schneider, V., Wiklund, J., Lovas, G., Evaluation of simulation models of evacuation from complex spaces, SINTEF Report, STF75 A95020, ISBN 82-595-8583-9, June 1995.
7. Meacham, B.J., Custer, R.L.P., Performance-based fire safety engineering: an introduction of basic concepts, *Journal of Fire Protection Engineering* 7(2):35–53, 1995.
8. Kuligowski, E.D., Gwynne S.M.V., What a user should know about selecting an evacuation model, *Fire Protection Engineering Magazine*, Human Behaviour in Fire Issue, Fall, 2005.
9. Thompson, P., Marchant, E., A computer model for the evacuation of large building populations, *Fire Safety Journal* 24:131–148, 1995.
10. Vassalos, D., Kim, H., Christiansen, G., Majumder, J., A mesoscopic model for passenger evacuation in a virtual ship-sea environment and performance-based evaluation, Proceedings of Pedestrian and Evacuation Dynamics, eds. Schreckenberg, M., Sharma, S.D., Springer, Berlin, 2001, ISBN 978-3-540-42690-6, pp. 369–391.
11. Kisko, T.M., Francis, R.L., Evacnet+: a computer program to determine optimal evacuation plans, *Fire Safety Journal* 9:211–220, 1985.
12. Presented by UTRC at Pedestrian Evacuation Dynamics 2008.

Investigating the Impact of Aircraft Exit Availability on Egress Time Using Computer Simulation

Edwin R. Galea, Madeleine Togher, and Peter Lawrence

Fire Safety Engineering Group, University of Greenwich, London, UK
e-mail: E.R.Galea@gre.ac.uk

Summary. This paper examines the influence of exit availability on evacuation time for narrow body aircraft under certification trial conditions using computer simulation. A narrow body aircraft which has previously passed the certification trial is used as the test configuration. While maintaining the certification requirement of 50% of the available exits, six different exit configurations are examined. These include the standard certification configuration and five other exit configurations based on commonly occurring exit combinations found in accidents. These configurations are based on data derived from the AASK database and the evacuation simulations are performed using the airEXODUS evacuation software. The results show that the certification practise of using half of the available exits predominately down one side of the aircraft is neither statistically relevant nor challenging. For the aircraft cabin layout examined, the exit configuration used in certification trial produces the shortest egress times. Furthermore, three of the six exit combinations investigated result in predicted egress times in excess of 90 seconds, suggesting that the aircraft would not satisfy the certification requirement under these conditions.

1 Introduction

The evacuation certification trial (see FAR 25.803 [1]) is the aviation industry benchmark of aircraft evacuation performance, and rightly or wrongly, is considered by the travelling public and safety professionals alike as the ultimate kite-mark of evacuation safety. However, for the benchmark to be effective it should serve as an indicator of safety, and to do so the benchmark should be both as representative of reality and challenging as practical. While it is acknowledged that in the interests of safety it is not desirable or possible to make the evacuation certification trial closely resemble real accident situations, it is possible and indeed essential that the exit availability resemble as closely as possible challenging exit configurations likely to be found in real accidents. Furthermore, while it is true that no two accidents are alike, it is possible to investigate statistical data and identify frequently occurring exit

combinations and from these select the most challenging exit combinations to use in evacuation certification analysis.

In the evacuation certification trial half the exits are usually made inoperative and usually all or the majority of the serviceable exits are on one side of the aircraft. It is a commonly held (and not unreasonable) belief by safety professionals that this exit configuration is selected because it is most frequently found in survivable accident situations or that it is the most challenging evacuation exit configuration. While the origins of this particular part of the evacuation certification demonstration are not clear, it possibly stems from the belief that in a crash/emergency situation fire is most likely to occur on one side of the aircraft (e.g. due to ruptured fuel lines/wing tank) and so it would be reasonable to assume that the exits on that side of the aircraft would be unavailable. Furthermore, the regulatory community would (rightly) argue that the evacuation demonstration is not intended to represent a real situation, but is intended to be a benchmark examination of evacuation performance allowing both absolute (i.e. better than 90 seconds) and relative (i.e. one aircraft configuration against another) performance. While it is understood that the evacuation certification trial is intended to benchmark aircraft evacuation performance, this does not mean that the selected benchmark evacuation scenario should be both unrepresentative of real incidents and unchallenging in terms of required evacuation performance. For the benchmark to be effective it should serve as an indicator of safety, and to do so the benchmark should be as representative of reality as practical, taking into account relevant and challenging scenarios based on accident data.

In this paper we use the AASK database [2, 3] to suggest likely exit combinations found in aviation accidents and then using the airEXODUS [4, 5] evacuation model, identify the most challenging exit combinations.

2 The AASK Database

The Aircraft Accident Statistics and Knowledge (AASK) database is a repository of survivor accounts from aviation accidents conducted by investigative organisations such as the U.S. National Transportation Safety Board (NTSB) and the U.K. Air Accident Investigation Branch (AAIB). Its main purpose is to store observational and anecdotal data from the actual interviews of the occupants involved in aircraft accidents. The quality and quantity of this data is variable ranging from short summary reports of the accident to transcripts from most of the surviving passengers and crew involved in the accident. The database has wide application to aviation safety analysis, being a source of factual data regarding the evacuation process.

Work started on developing the AASK database in 1997 with support from the UK Engineering and Physical Sciences Research Council (EPSRC) and the UK Civil Aviation Authority (CAA). The most recent version of the database, AASK V4.0 contains accounts from over 2000 survivors of aviation

accidents [2, 3]. The database consists of four main components which address; the nature of the accident (105 accidents), accounts from surviving passengers (1917 passengers), accounts from surviving cabin crew (155 cabin crew) and information relating to fatalities (338 fatalities) [2, 3] AASK V4.0 contains information from 105 accidents and detailed data from 1917 passengers and 155 cabin crew, with information relating to some 338 fatalities. The accidents included in AASK V4.0 cover the period 04/04/77–23/09/99. Access to the database is available on-line at <http://fseg.gre.ac.uk/aask/index.html>. The database has a powerful query engine allowing investigators to mine the data.

3 The airEXODUS Evacuation Model

The airEXODUS aircraft evacuation model is part of a suite of software tools designed to simulate the evacuation of large numbers of people from a variety of complex enclosures. Development of the EXODUS concept began in 1989 and today, the family of models consists of buildingEXODUS, maritimeEXODUS and airEXODUS for the built, maritime and aviation environments respectively. airEXODUS is designed for use in aircraft design, compliance with 90-second certification requirements, crew training, development of crew procedures, resolution of operational issues and accident investigation [4, 5].

The EXODUS software takes into consideration people-people, people-fire and people-structure interactions. It comprises five core interacting sub-models: the **Passenger**, **Movement**, **Behaviour**, **Toxicity** and **Hazard** sub-models. The software describing these submodels is rule-based, the progressive motion and behaviour of each individual being determined by a set of heuristics or rules. These submodels operate on a region of space defined by the **GEOMETRY** of the enclosure. The model tracks the trajectory of each individual as they make their way out through the geometry, or are overcome by fire hazards such as heat, smoke and toxic gases. The basis of the model has frequently been described in other publications [4, 5] and so only specialist components of the model will be described briefly here.

The **PASSENGER SUBMODEL** describes an individual as a collection of defining attributes and variables such as gender, age, maximum unhindered fast walking speed, maximum unhindered walking speed, response time, agility, etc. Each passenger can be defined as a unique individual with their own set of defining parameters. Cabin crew members can also be represented and require an additional set of attributes such as, range of effectiveness of vocal commands, assertiveness when physically handling passengers and their visual access within certain regions of the cabin. Some of the attributes are fixed throughout the simulation while others are dynamic, changing as a result of inputs from the other submodels. Passengers with disabilities may be represented by limiting these attributes.

The **BEHAVIOUR SUBMODEL** determines an individual's response to the current prevailing situation on the basis of his or her personal at-

tributes, and passes its decision on to the movement submodel. The behaviour submodel functions on two levels, global and local. The local behaviour determines an individual's response to the local situation e.g. jump over seats, wait in queue, etc while the global behaviour represents the overall strategy employed by the individual. This may include such behaviour as, exit via the nearest serviceable exit, exit via most familiar exit or exit via their allocated exit. The local behaviour of the passenger may also be affected through the intervention of cabin crew. As certain behaviour rules e.g. conflict resolution and model parameters e.g. passenger exit hesitation times, are probabilistic in nature, the model will not produce identical results if a simulation is repeated. In studying a particular evacuation scenario, it is necessary to repeat the simulation a number of times in order to produce a distribution of results.

4 Exit Availability Analysis Conducted Using AASK

A full account of the analysis of exit availability in aircraft accidents presented in this section may be found in [3]. Here we present a summary of the analysis and the main conclusions. As part of this analysis it is essential to define what is meant by an available exit. In this analysis an exit is considered to be 'available' when the exit and its evacuation assist means are physically and fully/safely functional, and passengers are permitted to use it by the crew. In addition, exits which may not meet the specified criteria, but which were actually used by at least one passenger are also considered to be 'available'. Furthermore, here we consider exit availability as a function of the total number of exits on board the aircraft, irrespective of the exit position (e.g. forward, aft, left, right) or whether exits are associated with exit pairs or are single exits. Incidents within the database which are classed as precautionary evacuations or post-incident deplaning are not included in this analysis. Here the results for aircraft with three exit zones are presented however, an analysis involving aircraft with four exit zones may also be found in [3].

Within AASK V4.0, 42 accidents were found to meet the criteria, 31 accidents involving aircraft with three exit zones and 11 accidents involving aircraft with four exit zones. In contrast to the evacuation certification requirements, the AASK V4.0 study suggests that a third (33%) of the emergency evacuations examined involve aircraft in which less than 50% of the exits are available. In addition, the data suggests that the available exit distribution for small (i.e. aircraft with three exit zones) and large aircraft (i.e. aircraft with four exit zones) is different with smaller aircraft having a greater tendency than larger aircraft to have less than 50% of their exits available during an emergency evacuation. Furthermore, the accident analysis suggests that over half (55%) of the accidents investigated involve a cabin section in which no exits were available [3].

However, the statistics suggest that approximately 67% of the accidents investigated involve an exit availability of 50% or more. Thus, as the most

frequently occurring exit availability involves more than 50% of the exits, it would not be unreasonable to require 50% exit availability in certification evacuation scenarios. Indeed, if frequency were the sole driver for selecting exit number in certification trials, taking 50% of the available exits would be considered conservative. This line of argument ignores the fact that a significant minority (33%) of the accidents investigated had less than 50% exit availability, resulting in a significantly more challenging evacuation scenario. In addition, based on the data, there would be a strong argument to assume a configuration in which at least one exit zone had no available exits.

In the previous analysis, exit availability was considered from a global perspective i.e. as a function of the total number of exits on board. Here we consider the availability of exits within exit pairs. The accidents used in this analysis ignore all those where the aircraft ended up in water or where substantial damage occurred to the aircraft fuselage, i.e. cases where there were significant breaks in the fuselage, and include only those accidents where information is known about all the exits. Unless passengers actually used an exit, the exit is only considered to be ‘available’ when the exit and its evacuation assist means are physically and fully/safely functional, and passengers are permitted to use it by cabin crew. Using this definition, 12 accidents were considered suitable for analysis, each one involving an aircraft with three pairs of exits. All cases included here have a strict arrangement of exit pairs in forward, mid and aft positions.

From these accidents it was concluded that at the FWD generalised location, two exits are available in the majority of cases (50%), with a single exit available being the next most likely (42%) [3]. In the case of MID positioned exits, the results suggest that in most cases (59% of the time) both exits are available while 33% of the time one exit is available. In both the FWD and MID generalised location, it is very unlikely for there to be no exits available (8% of the cases). Finally, the AFT positioned exits again show that having two exits available is most likely (42%) and having one exit available is next most likely (33%). However in a significant number of cases, (25%) there are no AFT exits available [3].

As part of the evacuation certification exercise, the trial criteria stipulate that only half of the exits can be used. Without exception, where aircraft have exit pairs, only one exit of each pair is selected. For aircraft with three exit zones, this data suggests that it is quite rare to have a situation in which no exits are available in the FWD or MID sections, but one in four cases involved no exits being available in the AFT section of the aircraft. Having one or two exits available in the AFT section is almost equally likely [3].

Based on this data, a suite of more representative exit combinations for aircraft with three exit pairs—while maintaining the certification required 50% availability condition—has been suggested [3]. These involve both exits in one of the locations and a single exit available in one other location. Suitable combinations of exits based on the frequency data identified, in decreasing order of likelihood include [3]:

- (i) A single forward exit, both over-wing exits and no exits in the aft section available.
- (ii) Both forward exits, a single over-wing exit and no exits in the aft section available.
- (iii) Both forward exits, no exits in the over-wing section and a single aft exit available.
- (iv) A single forward exit, no exits in the over-wing section and both aft exits available.
- (v) No exits in the forward section, a single over-wing exit and both aft exits available.

In the next section we use computer evacuation simulation to explore which of these exit combinations is the most challenging.

5 Evacuation Modelling Analysis

Here we use the airEXODUS evacuation model to explore each of the exit combinations identified in Sect. 4. A common evacuation scenario, based on the industry standard certification trial is used to investigate each of the exit combinations.

5.1 The Geometry, Model Parameters and Scenarios

The aircraft geometry used in this analysis is that of a narrow body aircraft with three exit pairs seating 149 passengers with three cabin crew. This configuration represents an actual aircraft which successfully passed the evacuation certification test. Three exits were used in the certification trial, all on the right side of the aircraft, consisting of two Type C exits (R1 and R3) and the over-wing Type III exit (R2). The L1 and L3 exits were Type B. The over-wing exits are not placed in the middle of the aircraft as determined by the passenger distribution. There are 10 seat rows between the front and over-wing exits and 14 seat rows between the over-wing and aft exits.

In the simulations presented in this paper, the default generalised passenger exit hesitation time distribution (assuming assertive crew) appropriate for the various exit types were used with default exit ready times of 8.2 s for the R1 and R3 exits, 12.0 s for the passenger operated R2 and L2 exits and 9.4 s for the L1 and L3 exits. Passenger attributes are set from the default certification parameter set. The airEXODUS parameter “Off-Time distribution” (i.e. the time required to descend the slide or wing) was also assumed to follow the default distribution appropriate for the various exit types. Other model parameters are set to achieve optimal distributions of passengers between exits with non competitive behaviour e.g. seat jumping is not permitted. Each scenario was run 1000 times using 10 different populations which fitted the scenario description (i.e. each population was run 100 times). Six

exit combinations were examined including the base case which represents the standard certification scenario. The five additional cases represent each of the exit combinations identified in Sect. 3. Scenario 1 represents the most likely exit configuration based on data from the AASK database and Scenario 5 represents the least likely of the 5 cases.

5.2 Evacuation Simulation Results

The first scenario examined is the base case or actual evacuation certification scenario. As can be seen in Fig. 1, airEXODUS predicts that under strict evacuation certification conditions this aircraft is likely to produce on-ground times of between 67.0 s and 76.8 s with a mean of 71.2 s and a 95th percentile time of 73.8 s. The time achieved by this aircraft in the actual certification trial falls on the predicted curve and is between the minimum and mean predicted times. This result suggests that the airEXODUS model is capable of predicting the likely outcome of evacuation certification trials.

We also note from this analysis that the passengers and crew travel an average distance of 6.5 m and require an average of 39.6 s to exit the aircraft. In addition, on average, the passengers spend 24.7 s caught in congestion (Cumulative Wait Time or CWT). This suggests that on average a passenger wasted 62% of their PET (Personal Evacuation Time) in unproductive congestion. Furthermore, unlike the certification process which only requires a single trial, these simulations suggest that the outcome of all 1000 optimal evacuation simulations were sub-90 seconds and so this aircraft with 154 passengers and crew and all the exits on the right hand side available comfortably satisfies the “intent” of the evacuation certification trial. However, the certification pass-fail criterion clearly does not take into account the possibility of multiple trial executions. In an attempt to address this point and in anticipation of the eventual use of evacuation simulation tools to assess aircraft evacuation performance for certification, Galea [6] has suggested a procedure for the use of evacuation simulation models as part of the evacuation certification process. As part of this process he suggests that the 95th percentile result from a distribution of simulated evacuation times should satisfy the 90 second criteria.

Having established the certification performance of the aircraft we now turn our attention to the performance of the aircraft under certification conditions but with exit combinations as indicated in Sect. 3. The results from these five scenarios are summarised in Table 1 with the distribution of evacuation times produced for each scenario displayed in Fig. 1. The results for Scenario 1 suggest the aircraft can produce on-ground times of between 79.5 s and 99.6 s with a mean of 87.7 s and a 95th percentile time of 92.4 s. In this case we note that the mean on-ground time has increased by 23% when compared to the base case. We also note that passengers travelled an average of 8.5 m representing an increase of 2 m compared to the certification scenario. The average PET increases to 46.6 s, while the average CWT is 29.3 s. Using

Scenario		On-ground time (s)	Av. PET (s)	Av. CWT (s)	Av. DIST (m)
1	Mean	87.7	46.6	29.3	8.5
(R1-R2-L2)	95th %ile	92.4	48.4	30.9	8.7
2	Mean	98.1	49.8	31.0	10.2
(R1-L1-R2)	95th %ile	105.4	52.3	33.4	10.4
3	Mean	77.7	41.9	25.5	8.3
(R1-L1-R3)	95th %ile	81.4	43.7	27.3	8.3
4	Mean	76.5	41.7	25.1	8.5
(R1-R3-L3)	95th %ile	80.5	43.6	26.9	8.5
5	Mean	91.1	48.3	29.9	9.9
(R2-R3-L3)	95th %ile	97.8	50.8	32.4	10.3

Table 1. airEXODUS optimal predicted results.

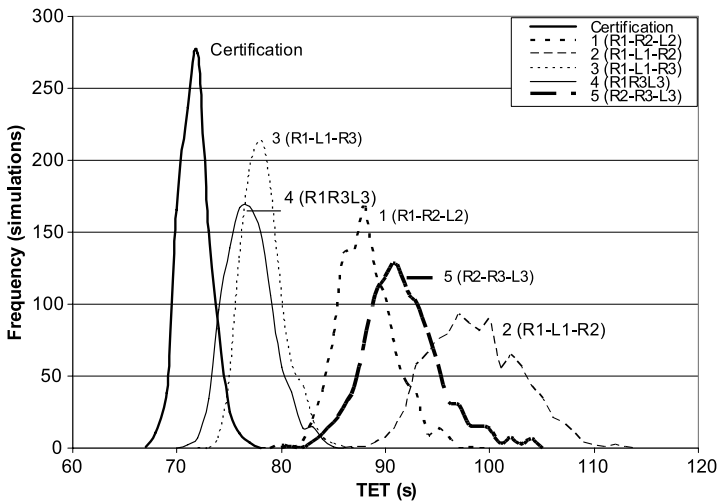


Fig. 1. Frequency distribution for TET (on-ground times) for all scenarios.

the 95 percentile pass/fail criterion, the aircraft with available exits configured as indicated in Scenario 1 just fails the evacuation certification trial (see Fig. 1).

The results for Scenario 2 suggest the aircraft can produce on-ground times of between 86.7 s and 112.3 s with a mean of 98.1 s and a 95th percentile time of 105.4 s. In this case we note that the mean on-ground time has increased by 38% when compared to the base case. We also note that passengers travelled an average of 10.2 m representing an increase of 3.7 m compared to the certification scenario. The average PET increases to 49.8 s, while the average CWT is 31.0 s. Once again we find on average 62% of the

PET is wasted in congestion which is the same as in the certification case. Using the 95 percentile pass/fail criterion, the aircraft with exits configured as indicated in Scenario 2 clearly fails the evacuation certification trial (see Fig. 1).

The results for Scenario 3 suggest the aircraft can produce on-ground times of between 73.5 s and 85.3 s with a mean of 77.7 s and a 95th percentile time of 81.4 s. In this case we note that the mean on-ground time has increased by 9% when compared to the base case. We also note that passengers travelled an average of 8.3 m representing an increase of 1.8 m compared to the certification scenario. The average PET for a passenger was 41.9 s, while the average CWT is 25.5 s. Therefore approximately 61% of the PET is wasted in congestion which represents a reduction by 1% when compared to the certification scenario. Using the 95th percentile pass/fail criterion, the aircraft with available exits configured as indicated in Scenario 3 comfortably passes the evacuation certification trial, albeit with a smaller margin than the base case (see Fig. 1)

The results for Scenario 4 suggest the aircraft can produce on-ground times between 70.8 s and 84.5 s with a mean of 76.5 s and a 95th percentile time of 80.5 s. These results are very similar to Scenario 3. In this case we note that the mean on-ground time has increased by 7% when compared to the base case. We also note that passengers travelled an average of 8.5 m representing an increase of 2.0 m compared to the certification scenario. Using the 95 percentile pass/fail criterion, the aircraft with available exits configured as indicated in Scenario 4 comfortably passes the evacuation certification trial, albeit with a smaller margin than the base case (see Fig. 1).

The results for Scenario 5 suggest the aircraft can produce on-ground times of between 80.7 s and 103.7 s with a mean of 91.1 s and a 95th percentile time of 97.8 s. While the configuration is similar to Scenario 2, with the two forward exits in Scenario 2 replaced by two aft exits in Scenario 5, the results are considerably quicker than those produced by Scenario 2. In this case we note that the mean on-ground time has increased by 28% when compared to the base case. We also note that passengers travelled an average of 9.9 m representing an increase of 3.4 m compared to the certification scenario. The average PET for a passenger was 48.3 s, while the average CWT is 29.9 s. Thus in this case approximately 62% of the PET is wasted in congestion which is identical to the certification scenario.

Using the 95 percentile pass/fail criterion, the aircraft with available exits configured as indicated in Scenario 5 convincingly fails the evacuation certification trial (see Fig. 1). Furthermore, we note from Fig. 1 the wide distribution in evacuation times produced by the various exit combinations. This figure emphasises the significant difference in egress times that can result from taking different combinations of 50% of the available exits. It also strongly emphasises that the certification combination of exits is the least challenging of the exit combinations.

From these results we note a number of interesting outcomes:

- The certification exit configuration produces the quickest on-ground times and is therefore the least challenging of the six configurations.
- The worst performing exit configuration which also fails to meet the certification criterion is the second most likely exit configuration i.e. Scenario 2.
- Three exit configurations produce on-ground times that actually fail to meet the certification criterion.
- The two most frequently occurring exit configurations i.e. Scenarios 1 and 2, fail to meet the certification criterion.
- Two of the exit configurations that fail the certification criterion have the same exit capacity as the certification case.
- Scenarios with greater exit capacity than the base case i.e. Scenarios 3 and 4 produce slower on-ground times albeit satisfying the certification requirement.
- Two scenarios with similar exit configurations i.e. Scenario 2 (two forward and one over-wing exit) and Scenario 5 (two aft and one over-wing exit) and hence similar exit capacities produce very different on-ground times.

The results are summarised in Table 2 where the 95th percentile on-ground times are presented along with the average total exit flow rates for the six scenarios ranked from the fastest to the slowest evacuations.

If a single exit from an exit pair is functioning, the flow rate achieved through the exit will be optimal. This is because a single cabin aisle cannot provide sufficient supply of passengers to maintain maximal flows through both exits in an exit pair. As a result, flows achieved through exit pairs are predicted to be on average 30% lower per exit for Type C exits and 10% less on average for Type III exits. Thus for a narrow body aircraft with three exit pairs consisting of Type B/C/I exits in the forward and aft and a pair of Type III exits in the over-wing position, if only 50% of the exits are available, selecting a single exit from each exit pair is likely to produce the greatest overall exit flow rate. In addition, this distribution of exits will produce the smallest average travel distance for the passengers as it results in the most number of passengers being close to an exit. These two factors combine to produce the shortest total egress times.

Other combinations of two Type B/C/I exits and a Type III exit (i.e. Scenarios 2 and 5) will produce significantly slower egress times due to the 30% reduction in exit efficiency for the paired Type B/C/I exits. For the particular aircraft examined, the combination involving the forward and over-wing configuration (i.e. Scenario 2) is likely to produce slower egress times due to the proximity of the Type III exit to the forward exit creating a greater need for exit by-pass in order to keep the forward exits working.

Combinations of three Type B/C/I exits (i.e. Scenarios 3 and 4) will produce better egress times than paired Type B/C/I exits and a single Type III exit (i.e. Scenarios 2 and 5) due to the greater flow rate achieved by the single


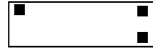
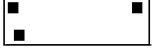

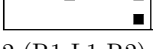
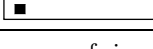
Rank	Scenario	95th percentile on-ground time (s)	Av. dist. (m)	Av. total exit flow rate (ppm)
Base case	(R1-R2-R3) 	73.8	6.5	156.9
1	4 (R1-R3-L3) 	80.5	8.5	140.8
2	3 (R1-L1-R3) 	81.4	8.3	138.2
3	1 (R1-R2-L2) 	92.4	8.5	125.4
4	5 (R2-R3-L3) 	97.8	9.9	120.4
5	2 (R1-L1-R2) 	105.4	10.2	108.7

Table 2. Summary of simulation results for the various configurations ranked from the fastest to the slowest.

Type B/C/I compared to the single Type III. There should be little difference between having the pair located in the front or the rear. However, in this particular case, the exit off-set in the front of the cabin made this case (Scenario 3) slightly less efficient than the case with the pair in the rear of the cabin (Scenario 4).

The configuration with a pair of Type III exits is more difficult to place (Scenario 1). The pair of Type III exits will only suffer 10% degradation in performance due to being paired. However, this will produce a performance for the pair of Type IIIs which is less than that for a pair of Type B/C/I exits. Thus we would expect the performance of this configuration to be slower than that for the case with three Type B/C/I exits (i.e. Scenarios 3 and 4). While the pair of Type III exits will produce a slower flow rate than a pair of Type B/C/I exits, the single Type B/C/I exit (Scenario 1) will produce a much better flow rate than the single Type III exit (Scenarios 2 and 5). We could therefore expect the configuration with a pair of Type III exits and single Type B/C/I (Scenario 1) exit to outperform the configurations with a pair of Type B/C/I exits and a single Type III exit (Scenarios 2 and 5). However, this result may not be generally true as it is affected by the particular configuration of exits found in this study i.e. none centrally located Type III exit and off set forward exits.

It should be remembered in viewing these results that they are all based on model simulations and not actual experiments. To the best knowledge

of the authors, full scale experiments have not been conducted (or at least reported in the academic or professional press) to substantiate the findings from these simulations. However, while the precise timings produced by these simulations may be questioned and as a result the precise resultant ranking of the scenarios, it is likely that the main conclusion that the exit configuration used in the current evacuation certification trial is neither representative of likely real accident scenarios nor particularly challenging is valid.

The findings of this work have implications as to the appropriateness of the current evacuation certification trial as a relevant and informative benchmark of egress performance and safety. Galea [6] has suggested that it would be more appropriate to investigate several exit combinations as part of the certification process using computer egress simulation. Furthermore, if 90 seconds is considered to be a real and valid measure of the required evacuation performance of aircraft in the event of a fire, these results convey even more significance. This point will be explored in another paper presented by the authors at this conference.

6 Conclusions

This work has shown—through computer based evacuation simulation—that the certification practise of using half the available exits predominately down one side of the aircraft is neither statistically relevant nor challenging—at least for aircraft with three exit pairs. Indeed, for the aircraft cabin layout examined, of the six exit combinations investigated involving 50% of the available exits, the exit configuration used in certification trials produced the shortest egress times. Furthermore, three of the six exit combinations investigated resulted in (95th percentile) egress times of greater than 90 seconds, suggesting that the aircraft would not satisfy the certification requirement under these conditions.

These results draw into question the appropriateness of the current evacuation certification trial as a relevant and informative benchmark of egress safety. Demonstrating that the aircraft can be evacuated in 90 seconds using the current exit certification combination says little about how the aircraft is likely to perform in more realistic and challenging exit combinations. By addressing issues associated with the certification and acceptance of aircraft configurations, we may achieve the goal of producing safer aircraft, which the industry claim they desire and the travelling public certainly deserve.

Acknowledgements

Professor Galea is indebted to the UK CAA for their financial support of his personal chair in Mathematical Modelling at the University of Greenwich. Ms Togher gratefully acknowledges the financial support of FSEG in providing her with a bursary under its Doctoral Programme.

References

1. FAR Part 25.807 Airworthiness Standards. Transport Category Airplanes. Including amendment 25-67 as published in the Federal Register on June 16th, 1989, Washington DC, USA, 1989.
2. E.R. Galea, K.M. Finney, A.J.P. Dixon, A. Siddiqui, and D.P. Cooney, The AASK DATABASE V4.0: Aircraft Accident Statistics and Knowledge. A Database to Record Human Experience of Evacuation in Aviation Accidents. Report for CAA Project 560/SRG/R+AD, Dec 2003.
3. E.R. Galea, K.M. Finney, A.J.P. Dixon, A. Siddiqui, and D.P. Cooney, “An analysis of exit availability, exit usage and passenger exit selection behaviour exhibited during actual aviation accidents”. The Aeronautical Journal of the Royal Aeronautical Society, Vol 110, Number 1106, pp 239–248, 2006.
4. S. Blake, E.R. Galea, S. Gwynne, P. Lawrence, and L. Filippidis, “Examining the effect of exit separation on aircraft evacuation performance during 90-second certification trials using evacuation modelling techniques”. The Aeronautical Journal of the Royal Aeronautical Society, Vol 106, pp 1–16, 2002.
5. E.R. Galea, S. Blake, S. Gwynne, and P. Lawrence, “The use of evacuation modelling techniques in the design of very large transport aircraft and blended wing body aircraft”. The Aeronautical Journal, Vol 107, Number 1070, pp 207–218, 2003.
6. E.R. Galea, “Proposed methodology for the use of computer simulation to enhance aircraft evacuation certification”. AIAA Journal of Aircraft, Vol 43, Number 5, pp 1405–1413, 2006.

Bounded Rationality Choice Model Incorporating Attribute Threshold, Mental Effort, and Risk Attitude: Illustration to Pedestrian Walking Direction Choice Decision in Shopping Streets

Wei Zhu and Harry Timmermans

Urban Planning Group, Eindhoven University of Technology, Postbus 513,
Den Dolech 2, 5600 MB Eindhoven, The Netherlands
e-mail: w.zhu@tue.nl, h.j.p.timmermans@tue.nl

Summary. Discrete choice models have been widely used in modeling individual choice behavior. By assuming that people are rational and utility-maximizers, these models are effective in capturing underlying preferences and choice outcomes. However, these models are not explicitly developed to represent decision processes. On the other hand, models of bounded rationality, for the majority based on decision heuristics, are meant to be more realistic representations of decision processes based on the assumption that people have limited mental capacity for making a decision.

People may apply different heuristics for a decision. To reflect this idea, we first introduce a conceptual framework which articulates (i) that individuals use attribute thresholds to map external continuous factors into discrete internal representations, (ii) information search costs effort which is considered important for individual selecting heuristics, and (iii) individual's risk attitude towards heuristics, reflecting expected outcome diversity implied in a heuristic decision. The framework is general enough to identify several typical heuristics, including conjunctive, disjunctive and lexicographic rules. A decision can be modeled as a two-stage process, first choosing a heuristic, and then applied it to reach a decision.

To illustrate this approach, it is applied to a dataset about pedestrians choosing walking directions in a shopping street in Shanghai, China. Results about parameter estimates and estimated probabilities of applying different heuristics are presented. Implications of the model results are discussed.

1 Introduction

Models of pedestrian choice behavior (and other types of activity choices) have predominantly been based on theories of rational choice. This concept suggests that individuals invariably take into account the set of factors influencing their choice behavior, attach some value judgment (utility, attitude,

satisfaction) to each choice option and choose the option that maximizes their value judgment. For example, in the context of pedestrian store or shopping center choice behavior, pedestrian's utility of alternatives are commonly defined as the summation of weighted (evaluation of) physical factors like store floorspace, store type and variety, distance, and traffic conditions [1–3]. Pedestrians are assumed to choose the store bringing them maximum utility. Hoogendoorn and Bovy [4] developed an extensive framework based on expected utility maximization to model not only pedestrian route choice but also optimal activity schedule, trajectory and speed. In terms of microscopic movement, Antonini and Bierlaire [5] used a multinomial logit model to represent how pedestrians choose local walking directions which are divided as discrete surrounding radial regions. A potential limitation of these models is that they do not explicitly represent decision processes, such as cognition and information search. Pedestrians are assumed to have very good knowledge about the environment and the ability to take into account all relevant factors influencing decisions, which could be highly unrealistic especially in emergent situations when pedestrians may concentrate on very few factors.

In contrast to these models of rational choice behavior, models of bounded rationality assume that decisions are made on subsets of factors and do not necessarily result in optimal choices. These models often use non-compensatory rules, or say decision heuristics, to indicate that decisions may be made on an attribute-by-attribute basis as opposed to a compensatory decision process [6–8]. However, the state-of-the-art in heuristic modeling indicates some shortcomings. Firstly, the models are limited in the sense that they focus on the non-compensatory nature of the decision rule. The process that leads to the selection of factors entering the decision process is usually not modeled. Secondly, the choice of heuristics to be investigated largely depends on the researcher's individual experiences and intuition. A general approach will be helpful to overcome the arbitrariness involved in this selection process. Thirdly, a particular heuristic model is assumed to apply to all individuals. In reality, however, it is unlikely that different individuals will use the same choice rules. Even for the same individual, decision strategies may be context-dependent. An approach that accounts for heuristic heterogeneity would thus enhance models of bounded rationality.

This paper proposes a modeling approach that overcomes the limitations discussed above and requires no more information as required by conventional discrete choice models, while it is based on richer behavioral assumption, including: (i) Attribute cutoffs are incorporated in the utility function and estimated as cognitive thresholds; (ii) Heterogeneous decision heuristics can be exactly identified; (iii) Mental effort and risk attitude of heuristics are defined and their influences on heuristic choice are estimated. In the following of this paper, we will elaborate the theoretical framework underlying the approach. Next, the approach will be applied to direction choice decisions of pedestrians in East Nanjing Road, the city center of Shanghai, China. This will be followed

by a discussion of the main findings of the model calibration. The paper is completed with a conclusion.

2 Conceptual framework

2.1 Preference Structure

Let $X = \{x_j; j = 1, 2, \dots, J\}$ represent the set of attributes or factors influencing the decision of interest. We assume that individuals do not necessarily take all these factors into account, but rather solve a decision problem by mentally (re)constructing the problem and selecting a subset of the factors. This *filtering* process is not invariant, but will depend on the decision problem, and more importantly on the activation level of the individual. Thus, we assume that decision makers will construct a mental representation of the decision problem. Let $\Delta_j = \{\delta_{j1} < \delta_{jn} < \delta_{jN}; n = 1, 2, \dots, N\}$ be a set of successively increasing activation thresholds for x_j , corresponding to stricter judgment standards. (Note that N can be factor-dependent, so it should be N_j . For representation simplicity, subscript is ignored.) A factor may then meet one or more of these increasingly stricter activation thresholds and hence becomes more informative. Mathematically, this can be expressed as:

$$s_{jn} = \begin{cases} 0 & \text{if } x_j < \delta_{jn}, \\ 1 & \text{if } x_j \geq \delta_{jn}, \end{cases} \tag{1}$$

$$X' = \{x_j | s_{jn} = 1\} \quad \forall x_j \in X, \forall n$$

where s_{jn} is the state of the factor against the threshold δ_j , X' is the set of factors that are considered in the decision. Thus, filtering and factor representation transforms categorical and continuous external factors into a set of activated and non-activated internal (mental) factor states.

Then the decision maker attaches judgment values, w_{jn} , to factor states, which implies that the state is judged in light of the decision goal. Let $u_{jn} = w_{jn}s_{jn}$ denote the value judgment (utility) of state n of factor x_j . All states that are incorporated in the decision making process need to be combined according to some integration rule to arrive at an overall value judgment for each choice alternative. Various rules can be used. Thus, if an additive integration rule is assumed, the overall value judgment of choice alternative i equals:

$$v_i = \sum_j \sum_n u_{jn}. \tag{2}$$

In the final step, we assume that the overall values are also categorized and mapped by checking them against a set of successively increasing overall thresholds $\Lambda = \{\lambda_1 < \lambda_m < \lambda_M; m = 1, 2, \dots, M\}$, resulting in the overall states, p_{im} . This can be expressed as:

$$p_{im} = \begin{cases} 0 & \text{if } v_i < \lambda_m, \\ 1 & \text{if } v_i \geq \lambda_m. \end{cases} \tag{3}$$

In case this mapping only involves two preference orders (reject or accept), only one λ is needed and $p_{i1} = 0$ defines rejecting the alternative, whereas $p_{i1} = 1$ implies accepting it. For representation simplicity, in the remainder of this paper, we will assume that only two orders exist.

Define a state value set for each factor,

$$V_j = \left\{ v_{j1} = 0, v_{j2} = w_{j1}, v_{j3} = w_{j1} + w_{j2}, \dots, v_{jN+1} = \sum_{n=1}^N w_{jn} \right\} \tag{4}$$

which includes all possible value judgments related to the factor. Let \bar{v}_k represent any factorial combination from value judgments in the sets and construct the value set of all possible overall value judgments,

$$\bar{V} = \left\{ \bar{v}_1 < \bar{v}_k < \bar{v}_K; k = 1, 2, \dots, K; K = \prod_j (N_j + 1) \right\}. \tag{5}$$

Checking these overall value judgments against the overall threshold λ , results in a unique pattern of relationships with some value judgments above the threshold, and some below the threshold. Thus, the set of overall value judgments \bar{V} can be divided into a subset \bar{V}_0 of rejected overall value judgments and a set \bar{V}_1 of accepted ones. This pattern can be viewed as a discrete preference structure, Φ , that is used to classify overall value judgments of alternatives into an ordered set of preferences (in this case reject or accept). Mathematically,

$$\Phi = \left\{ \begin{array}{l} \bar{v}_k \in \bar{V}_0 | \bar{v}_k < \lambda \\ \bar{v}_k \in \bar{V}_1 | \bar{v}_k \geq \lambda \end{array} \right\}. \tag{6}$$

2.2 Decision Heuristics

We assume that in every choice context, individuals will consciously or unconsciously define a set of threshold values and apply choice heuristics which are logically consistent with the preference structure. Because for different individuals or in different contexts preference structures may differ in terms of the pattern of the sets of accepted and rejected values, this implies that our cognitive process model automatically generates *heterogeneous choice heuristics*. On extreme is the strictest preference structure in the sense that no single value (judgment) combination survives the overall threshold,

$$\Phi = \{ \bar{v}_k \in \bar{V}_0 | \bar{v}_k < \lambda \}. \tag{7}$$

That means that regardless of the states of the factors, the choice alternative under consideration will be rejected. In this case, no choice heuristics are

implied (or the heuristic of “no action” since the individual has no need to consider any information). Relaxing λ a little leads to the preference structure where only the value combination of factor states with the highest threshold values is accepted,

$$\Phi = \left\{ \begin{array}{l} \bar{v}_k \in \bar{V}_0 | \bar{v}_k < \lambda \\ \bar{v}_k \in \bar{V}_1 | \bar{v}_k \geq \lambda, \bar{v}_k = \sum_j v_{jN+1} \end{array} \right\}. \quad (8)$$

This preference structure implies conjunctive heuristics in the sense that an alternative will be accepted only when all factors are in their highest states. During the decision process, any single factor being unsatisfactory will cause the decision process to stop, regardless of the states of the other factors. At the opposite end is the most relaxed preference structure, represented the case that all factor combinations will be accepted,

$$\Phi = \{ \bar{v}_k \in \bar{V}_1 | \bar{v}_k \geq \lambda \}. \quad (9)$$

This preference structure implies the other “no action” heuristic since factors being in whatever state will lead to the alternative being accepted. A little less tolerance for λ may result in a preference structure where all but the value combinations of non-activated factor states are accepted,

$$\Phi = \left\{ \begin{array}{l} \bar{v}_k \in \bar{V}_0 | \bar{v}_k < \lambda, \bar{v}_k = \sum_j v_{j1} \\ \bar{v}_k \in \bar{V}_1 | \bar{v}_k \geq \lambda \end{array} \right\}. \quad (10)$$

Disjunctive heuristics can be inferred from this preference structure since any factor state (except the non-activated state) being satisfactory will cause the decision process to stop and accept the choice alternative, regardless of the state of the other factors. Within the spectrum, various other preference structures and heuristics can be identified. For example, the lexicographic heuristic is implied in a preference structure,

$$\Phi = \left\{ \begin{array}{l} \bar{v}_k \in \bar{V}_0 | \bar{v}_k < \lambda, \sum_k \sum_{t=1}^n s_{jt|k} = 0 \\ \bar{v}_k \in \bar{V}_1 | \bar{v}_k \geq \lambda, \prod_k \prod_{t=n'}^N s_{jt|k} = 1 \end{array} \right\}, \quad n < n'. \quad (11)$$

According to this preference structure, there exists at least one factor j . When some states of this factor are not activated, the decision process will stop and reject the alternative. When some states are activated, the decision process will stop at accepting the alternative. In-between are those states whose status cannot determine accepting or rejecting the alternative and further consideration on other factors is needed.

2.3 Choice of Heuristics

We assume that individuals in different contexts may apply different preference structures and corresponding choice heuristics to solve problems. That is, individuals will have a context-dependent repertoire of preference structures and corresponding heuristics. Although we should always try to specify the context as much as possible, there will always remain some stochastic element from the viewpoint of the analyst. Such randomness can be mathematically included into the overall threshold, so that we get $\lambda \sim D$, where D is a probability distribution. Because \bar{V} is a discrete set, between consecutive pairs of \bar{v}_k , there is a range of λ , satisfying $\bar{v}_{k-1} < \lambda_k \leq \bar{v}_k$. It represents the range of an invariant preference structure. The probability of this preference structure Φ_{k+1} being applied, p_{k+1} , equals the probability of λ being in this range:

$$p_{k+1} = \int_{\bar{v}_k}^{\bar{v}_{k+1}} D dt. \quad (12)$$

So any single decision may be a two-stage process, choosing an appropriate preference structure and applying this structure to the choice task, forming preference among alternatives and making the choice. For the preference structure actually applied by the decision maker is usually unknown, the final probability of choosing an alternative can be modeled as the expected result of choice aggregated from all possible choice outcomes under these latent preference structures, mathematically,

$$p_i = \sum_{k=1}^{K+1} p_k p_{i|k}. \quad (13)$$

$p_{i|k}$ is the probability that alternative i is chosen when preference structure k is applied. But since within an invariant range, the value of λ does not affect choice outcome, λ does not have to be identified. Instead, \bar{V} is enough as critical values for overall thresholds.

Although the process of selecting preference structure itself may be susceptible to bounded rationality, here we only care about the outcome of this process. Assuming the distribution of preference structures to be multinomial logit distribution will be a convenient approximation. So the probability of a preference structure being applied can be modeled as

$$p_k = \frac{\exp(u_k)}{\sum_{k=1}^{K+1} \exp(u_k)} \quad (14)$$

where u_k is the observable/definable utility that the individual expects from applying preference k . In fact, it is heuristic that is implied in a preference structure is selected. But since within certain preference structure applying different heuristics does not affect the choice outcome, (14) can also be formulated as the aggregation of probabilities that heuristics within the preference are chosen,

$$p_k = \sum_{h=1}^{J!} p_{kh} = \frac{\sum_{h=1}^{J!} \exp(u_{kh})}{\sum_{k'=1}^{K+1} \sum_{h'=1}^{J!} \exp(u_{k'h'})} \quad (15)$$

where u_{kh} is the utility of heuristic h within preference structure k . We define the utility of each heuristic, following the idea of effort-diversity trade-off, to be composed of mental effort, e_{kh} , which is inflicted in considering the factors, representing their states and attaching values, and risk attitude, r_{kh} , which represents accuracy of applying a heuristic. The meaning of mental effort is straightforward while risk attitude may need more explanation. Preference structures with either very strict thresholds or very relaxed thresholds are risky because most information about factors falls into respectively the non-activated states or the activated states. This will make the decision of rejecting or accepting alternatives very certain, but at the same time increases the potential risk of false rejection respectively false acceptance. Risk attitude therefore can be inversely measured by outcome diversity. We assume that the utility of a decision heuristic equals some weighted linear trade-off between mental effort and risk attitude,

$$u_{kh} = \beta_e e_{kh} + \beta_r r_{kh}. \quad (16)$$

A complicating factor is that individuals cannot be sure about the amount of mental effort that will be involved in a decision ahead. They can only subjectively estimate it based on their beliefs p_{jn} that the activated factors occupy states that make any further consideration of subsequent factors useless. To illustrate, let three factors x_1 , x_2 and x_3 have A , B , and C states respectively. Assume that the heuristic under consideration implies search sequence $x_1 \rightarrow x_2 \rightarrow x_3$. Let e_1 , e_2 and e_3 denote the amount of mental effort inflicted when considering factors x_1 , x_2 and x_3 respectively, and let p_a , p_b and p_c represent the individual's beliefs that factors are in states s_a , s_b and s_c respectively, such that $\sum_a p_a = 1$, $\sum_b p_b = 1$, $\sum_c p_c = 1$. The expected amount of mental effort is then defined as

$$e_h = e_1 + \sum_a \left(p_a e_2 I_{ab} + \sum_b p_a p_b e_3 I_{abc} \right), \quad (17)$$

$$I_{ab} = \begin{cases} 0 & \text{if } v_{abc} < \lambda \vee v_{abc} \geq \lambda \forall b, \forall c, \\ 1 & \text{otherwise,} \end{cases} \quad (18)$$

$$I_{abc} = \begin{cases} 0 & \text{if } v_{abc} < \lambda \vee v_{abc} \geq \lambda \forall c, \\ 1 & \text{otherwise.} \end{cases} \quad (19)$$

Equation (17) reflects the fact that e_1 is inevitably expected to be fully inflicted since x_1 is considered first. For each possible state of x_1 , expected efforts are derived from two terms. First, the effort of considering x_2 is weighted by the probability of x_1 being in a particular state and I_{ab} , an identity function defined by (18). I_{ab} represents a judgment process, according to which

an individual checks whether all subsequent value combinations $v_{abc}|a$, are inactivated against given λ , or all value combinations are activated. If all value combinations are inactivated, the corresponding factor is not considered and no additional mental effort is involved. If all factors are activated, it means that the same decision or preference applies to all instances of that factor and hence considering the factor will not have any effect on the preference ordering or decision. In these cases, $I_{ab} = 0$. In contrast, $I_{ab} = 1$, and x_2 needs to be considered. According to the same logic, the second term relates to considering x_3 when at a state of x_2 . e_3 is weighted by $p_a p_b$, the joint probability of being in the previous two factor states, and I_{abc} is another identity function judging whether the simultaneous conditions $v_{abc}|a, b$ against λ are satisfied or not. By this definition, due to that efforts for considering factors may differ and different factor values may cause earlier or later termination of the decision process when the expected overall values are homogeneously against the overall threshold, the expected efforts of consideration sequences may differ also.

Risk attitude, is defined in terms of Shannon’s Information Entropy measure since entropy measure is exactly designed for representing uncertainty (diversity). Let \bar{p}_k , corresponding to \bar{v}_k , be the joint product of the probabilities of factor states across factors. The probability of a positive, r_{kh}^+ , respectively negative, r_{kh}^- , outcome equals

$$r_{kh}^+ = \sum_k \bar{p}_k | \bar{v}_k \geq \lambda \quad \forall k, \tag{20}$$

$$r_{kh}^- = 1 - r_{kh}^+.$$

From here we can see the risk attitude for heuristics within the same preference structure is the same because different information search sequences do not change the choice outcome. For simplicity, subscript h can be omitted from r . Then, the risk attitude of a preference structure is

$$r_k = -r_k^+ \log_2(r_k^+) - r_k^- \log_2(r_k^-). \tag{21}$$

3 Illustration

3.1 Data

A dataset about pedestrian shopping diary was collected in May 2007 in East Nanjing Road (ENR), the city center of Shanghai, China. The street is about 1,600 meters long, and 1,000 meters of this is pedestrianized. People’s Square, a multifunctional place for gathering, leisure, shopping, and museums, is located in the western end of the street. The eastern end locates the Bund, an internationally famous tourism site featured for buildings of the early 20th century. Most of the stores are located along both sides of the street, which

is largely shaped as a linear shopping space. Twenty undergraduate students from Tongji University administrated the survey by randomly inviting pedestrians in the street to complete a questionnaire. It took about 20 min for a respondent to answer two types of questions, their socio-demographics and shopping activities, such as which stores they visited, what they bought and expenditure, which had been conducted up to the moment they were being interviewed. In total, 811 valid responses were collected. For this particular analysis about walking direction choice, because we did not observe for every pedestrian where the decisions were made, we assumed that they happened after each store was visited. In addition, we recorded those locations that were reported by respondents as turning points. The total number of decision cases is 2268.

3.2 Operationalization

Based on pedestrian's location where the decision was (assumed to be) made and the next stop, we may infer the outcome of the decision, that is, the chosen walking direction. There may be up to four directions for each decision (e.g., east, south, west, north), depending on specific locations in ENR. Assume that there are four factors influencing pedestrian's evaluation on a direction:

- (i) x^A (Area), the total retail floor space in the direction. Although pedestrians do not really know the exact amount of floorspace, this variable serves as an approximation of pedestrian's feeling about the intensity of retail activities.
- (ii) x^P (Pdst), the length of the section in the direction that is only dedicated to pedestrians, which represents the attractiveness of walking conditions.
- (iii) x^B (Bund), a 0/1 variable represents whether the Bund is located in the direction. Because there is considerable number of tourists in ENR, the Bund could be a landmark guiding their movement.
- (iv) x^F (From), a 0/1 variable indicating whether the direction is the one where the pedestrian came from. Usually pedestrians do not tend to turn back to previous direction, so we may assume negative influence from this factor.

Let i be the index for each direction and v_i be the overall value judgment (utility) that the pedestrian evaluates on the direction,

$$v_i = I(x^A \geq \Delta^A) \mathbf{W}^A + I(x^P \geq \Delta^P) \mathbf{W}^P + x^B w^B + x^F w^F \quad (22)$$

where $I(\zeta)$ is an element-wise identity function assigning 1 when the relation ζ is true, and assigning 0 when ζ is false; $\Delta^A = [\delta_1^A \dots \delta_m^A \dots \delta_M^A]$, the value thresholds for x^A , is a row vector with M elements; $\Delta^P = [\delta_1^P \dots \delta_n^P \dots \delta_N^P]$, the value thresholds for x^P , is a row vector with N elements; $\mathbf{W}^A = [w_1^A \dots w_m^A \dots w_M^A]^T$ and $\mathbf{W}^P = [w_1^P \dots w_n^P \dots w_N^P]^T$ are column vectors for corresponding state values; w^B and w^F are scalars.

Assume that the pedestrian makes the decision by sequentially comparing alternatives and choosing the one with maximum utility. The difference from conventional utility-based approach is that we assume it is the utility rank that is compared. Based on (3), the probability that alternative i is better than alternative j is,

$$\begin{aligned}
 p_{ij}^R &= \begin{cases} 0 & \text{if } v_{ij}^R < \lambda, \\ 1 & \text{if } v_{ij}^R \geq \lambda, \end{cases} & 1 \leq \lambda \leq K, \\
 v_{ij}^R &= v_i^R - v_j^R
 \end{aligned} \tag{23}$$

v_i^R is the rank of alternative value within the overall value set \bar{V} . v_{ij}^R is the rank difference (RD) between alternative i and j . So the number of rank differences as well λ is limited to K , the maximum number of overall values. Equation (23) implies that individual sets a discriminant threshold to judge whether an alternative has enough advantage over the other. Note that p_{ij}^R is not equivalent to the probability that alternative i will be chosen over alternative j , which is defined as

$$p_{ij} = \begin{cases} 1 & \text{if } p_{ij}^R = 1, \\ 0 & \text{if } p_{ji}^R = 1, \\ 0.5 & \text{if } p_{ij}^R = 0 \wedge p_{ji}^R = 0. \end{cases} \tag{24}$$

That means alternative i is chosen when it has enough rank advantage over j . Moreover, we assume a uniform random choice is applied when neither alternative is better enough than the counterpart. According to (13), the expected choice probability considering latent preference structures turns out to be

$$\bar{p}_{ij} = \sum_{k=1}^K p_k p_{ij|k}. \tag{25}$$

3.3 Model Estimation

With the probability of choice, the model was estimated based on a likelihood estimator. A hybrid algorithm combined of a genetic algorithm and a BFGS algorithm was applied to estimate the parameters which maximize the estimator. Bayesian Information Criterion (BIC) was used to identify the appropriate model with enough goodness-of-fit and parsimony, because the numbers of thresholds, M and N , also have to be estimated.

Table 1 shows the results of model calibration. The retail floorspace seems to be cognized as two states [$<107948, \geq 107948$), divided by one threshold. The length of pedestrian street has three states [$<110, 110-341, \geq 341$), divided by two thresholds. The parameter for the location of the Bund is positive, suggesting that it is a kind of attraction for direction guidance. The parameter for previous direction is negative, confirming the hypothesis that

Parameter	Estimate
δ_1^A : threshold 1 for x^A	107948 m ²
$[w_1^A]$: value 1 for x^A	1
δ_1^P : threshold 1 for x^P	110 m
δ_2^P : threshold 2 for x^P	341 m
w_1^P : value 1 for x^P	5.9794
w_2^P : value 2 for x^P	4.8806
w^B : value for x^B	1.0176
w^F : value for x^F	-5.9489
β_e : effort	-4.0839
β_r : risk attitude	11.4721
Number of cases	2268
Number of free parameters	9
Log-likelihood	-1006
BIC	2081

Note: [] means the parameter value is set

Table 1. Results of model calibration

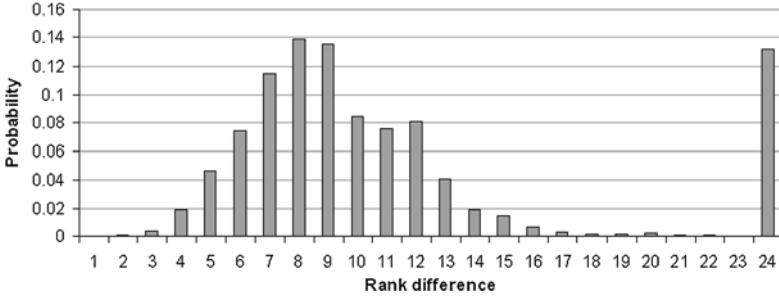


Fig. 1. Probabilities of rank differences.

pedestrians tend not to turn back. The parameter for effort is negative because it is specified as a kind of cost. The positive parameter for risk attitude suggests that pedestrians are risk averse (prefer diversity) with other conditions equal.

The most important advantage of this approach is that we may derive the distributions of strategy usage and information search. Figure 1 portrays the estimated probabilities of rank differences that could have been applied by pedestrians to differentiate alternative directions. It indicates that the distribution concentrates around 8, relatively small RDs. From this point, when RDs become smaller, the probabilities drop, suggesting that pedestrians tend to avoid using extremely low judgment standards which could make an alternative preferable to another even with nuisance advantages, although the decision tends to be quick. When the RDs become larger, the probabilities also drop due to the fact that fewer alternatives can be differentiated under such high standards and random choice has to be made, which gives the pedestri-

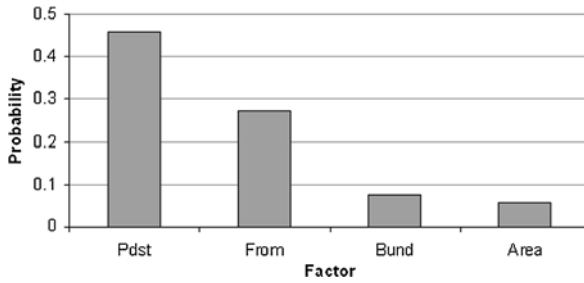


Fig. 2. Probabilities of factors being considered first.

ans the feeling of loosing control. The exception is that the probability of the largest RD 24 is very high, even though pedestrians make random choices all the time without considering any information, because this strategy is almost effortless. In general, pedestrians are risk averse and prefer information search in this particular decision problem. Their way of decision making approaches rational mechanisms.

Figure 2 shows the estimated probabilities of factors being considered first. For each factor, the probability is aggregated from all the probabilities with the factor considered first because the sequences are complete permutations among factors which are too many for the limited space here. The general information search pattern is that walking condition (represented by the length of pedestrian street) is the most important factor for consideration. It has the strongest impact on the decision outcome. The previous direction is the second most important factor. This relationship explains the fact that there were many pedestrians who stopped following their current walking direction into the non-pedestrianized section and turned back at the end of the pedestrian section. The location of the Bund and floorspace are considered relatively late in decisions.

4 Conclusion

We suggested an alternative approach to modeling decision processes of pedestrians, based on the notion of bounded rationality, and illustrates the approach to direction choice decisions. The approach incorporates factor thresholds as the basic mechanism for factor selection as well internal problem representation. It has the generality to show to what extent a decision process approaches heuristic rules or rational choice in the sense that all factors are considered. Besides its ability as conventional choice models to model individual preferences and choice outcomes, a lower level mechanism—the choice of decision strategies is also incorporated. A decision outcome is modeled in the form of latent class structure, as the expectation of all potential decision outcomes under different overall judgment standards. This submodel captures the het-

erogeneity of decision processes and represents the fact that individuals think differently and decisions are context-dependent.

The illustrated application showed reasonable results, which can be seen as evidence of face validity of the approach. In this particular case, pedestrians seem to be risk-averse and prefer extensive information search for their direction choice decision. Knowing the distributions of information processing strategies, we may design better environments which provide information in ways that can be more easily cognized and processed by individuals, and as a result may induce higher overall system efficiency.

References

1. Borgers A, Timmermans H J P, 1986, "A Model of Pedestrian Route Choice and Demand for Retail Facilities Within Inner-City Shopping Areas", *Geographical Analysis* **18** (2) 115–128.
2. Saito S, Ishibashi K, 1992, "A Markov Chain Model with Covariates to Forecast Consumer's Shopping Trip Chain Within a Central Commercial District", presented at Fourth World Congress of Regional Science Association International, Marloca.
3. Oppewal H, Timmermans H J P, 1997, "Modelling the Effects of Shopping Centre Size and Store Variety on Consumer Choice Behavior", *Environment and Planning A* **29** (6) 1073–1090.
4. Hoogendoorn S P, Bovy P H L, 2003, "Pedestrian Travel Behavior Modeling" in *Moving Through Nets: The Physical and Social Dimensions of Travel*, Axhausen K (Ed.), 1–33, 10th International Conference on Travel Behavior Research, Lucerne.
5. Antonini G, Bierlaire M, 2007, "A Discrete Choice Framework for Acceleration and Direction Change Behaviors in Walking Pedestrians", in *Pedestrian and Evacuation Dynamics 2005*, Waldau N, Gattermann P, Knoflacher H, Schrechenberg M (Eds.), 155–166.
6. Tversky A, 1972, "Elimination by Aspects", *Psychological Review* **79** (4) 281–299.
7. Payne J W, Bettman J R, 1988, "Adaptive Strategy Selection in Decision Making", *Journal of Experimental Psychology: Learning, Memory and Cognition* **14** (3) 534–552.
8. Gigerenzer G, Todd P M, ABC Research Group, 1999, *Simple Heuristics that Make Us Smart*, Oxford University Press, Oxford, New York.

A SCA-Based Model for Open Crowd Aggregation

Stefania Bandini¹, Mizar Luca Federici², Sara Manzoni¹, and Stefano Redaelli¹

¹ CSAI—Complex Systems & Artificial Intelligence Research Centre, University of Milano, Bicocca, Italy
e-mail: bandini@disco.unimib.it, manzoni@disco.unimib.it,
redaelli@disco.unimib.it

² MVA Consultancy Ltd., London, UK
e-mail: gopal@oddrecords.com

Summary. This paper proposes a SCA-based model for crowd dynamics phenomena. SCA (Situated Cellular Agents) is a modeling and simulation approach based on Multi Agent Systems principles that is characterized by the representation of an explicit spatial structure. This paper is focused on the crowd aggregation phenomenon described by Elias Canetti. This work will provide a methodology example of translation of a social theory into a SCA-based computational model.

1 Introduction

In this paper we apply Situated Cellular Agents (SCA), a modeling and simulation approach based on Multi-Agent Systems (MAS) and Cellular Automata (CA) principles, to formally represent and simulate *aggregation phenomenon in open crowds*. The latter is one of the main representative phenomenon in the context of *crowd dynamics*, that is the study of how and where crowds form and move [1].

Within MAS-based modeling approaches [2], SCA defines spatially situated agents in an environment endowed with an explicit structure that qualifies their perceptions, interactions and action abilities. The structure of SCA environment influences agents' actions and perception abilities giving a wide set of instruments to model and represents the elements of the theory. SCA has been presented also as an extension of Cellular Agents [3] in relation to the discrete representation of space and time, but it inherits the MAS dynamism and flexibility to represent situations characterized by heterogeneous behavioral rules at an individual scale. In the crowd context SCA has been already experimented in several situations of pedestrian dynamics among which the modeling of groups of pedestrians where phenomenon as Freezing by Heating

and Lane Formation were reproduced [4]. In this paper we present how SCA can be adopted to model crowds' aggregation phenomenon, the formation of an "Open Crowd", as described in the work of Elias Canetti [5]. This work can also provide a representative methodological example of how a social theory of crowds can be experimented through the translation into SCA computational framework.

The paper is structured as follows. Section 2 presents an overview on related works and computational approaches for modeling and simulating crowds. Section 3 introduces SCA approach, and in Sect. 4 an example of application of SCA approach to model a Open crowds aggregation phenomenon is described. Conclusions and future works end the paper.

2 Related Works

Several modeling and computational approaches have been proposed to tackle the complexity of *crowding phenomena* that is, phenomena that can emerge from the dynamic interaction of groups of moving entities (i.e. persons, in the case of human crowds) that share a limited space. Computational models for pedestrian dynamics can be classified into three main classes: force-based models, models based on Cellular Automata (CA) and models based on Multi Agent Systems (MAS). Following a brief introduction to the three approaches:

2.1 Force-Based Models

Models where the dynamics of spatial features is studied through spatial occupancy of individuals, represented as moving particles subjected to forces: each pedestrian is attracted by its goal and repelled by obstacles. One of the most successful approach is Helbing's Social Force Model [6, 7]. Similar approaches are the one of Hoogendoorn [8] that exploits gas-kinetic metaphor.

This approach reports some analogies of crowds with gasses, fluids and granular media. Foot prints in snow, for example, look similar to steamlines of fluids while at border lines between opposite direction of walking one can observe "viscous fingering". The analogies are also the emergence of pedestrian streams through standing crowds that seem analogous to the formation of river beds etc. Helbing underlines that Fluid dynamics analogies work better in normal situations while granular aspects become important in panic situations [9].

Helbing states that for each component (agent position, goal position, position of obstacles, position of other pedestrians) it is associated a force that pushes the agent towards a specific direction, and the resultant of these forces will decide the final direction:

$$\begin{aligned} \text{NewPosition} = & \text{OldPosition} + \text{DesiredPosition} + \text{GeometricRepulsion} \\ & + \text{SocialRepulsion} + \text{SocialAttraction} + a \text{ constant.} \end{aligned}$$

One of the problem of this approach is that in order to produce a reasonable behavior, weights of the forces must be accurately balanced. Another problem is the solution of limit situations as a pedestrian subjected to two opposite forces of the same intensity.

2.2 CA-Based Models

Peculiarities of CA-based models is the explicit representation as a regular grid of the modeled environment [10–12], where the size of each cell is the minimal space occupied by a pedestrian (e.g. 40×40 cm). The state of the cell includes the representation of the presence of individuals, of environmental obstacles and the direction of pedestrian's goals, through static and dynamic potential fields. The cell local interaction involved in CA state transition function, therefore, represents also pedestrian movement by cell state change (e.g. an occupied cell becomes empty and, synchronously, an adjacent empty cell becomes occupied).

Into the context of pedestrian and crowd dynamics, approaches based on Cellular Automata are demonstrated to be particularly adequate [13]. The success of CA-based approaches derives mainly from the fact that are simpler to understand and to use by experts of several application contexts.

However they suffer the limitation of considering individuals as homogeneous entities and generally do not provide a support to dynamism and flexibility of represented situations, while sometimes it is preferred to introduce some behavioral rules at individual scale. It has to be also underlined that movement in CA models is just an apparent movement, as it is just an effect of state transitions of cells on a grid. Another problem of this approach is the representation of heterogeneous goals influencing pedestrian movements; for this reason usually CA-approach is applied to evacuation scenarios, where all pedestrians are heading toward the exits (examples of evacuation dynamics works from public spaces are: classrooms evacuation [14], metro stations [15], an example of a more general modeling approaches able to reproduce several phenomena and situations is [4]).

2.3 MAS-Based Models

The third class is the MAS approach (e.g. see [16, 17]). In an agent-based simulation pedestrian are represented by autonomous entities, with the ability to perceive information from the environment and to interact each other. Recently MAS approach to pedestrian (and crowd) modeling have been largely applied and experimented [18, 19], since a MAS can represent a potentially heterogeneous system of agents in a partially known environment. The concept of a pedestrian as an adaptive, self-contained, autonomous entity situated in its environment allows to separate pedestrian behavior from the particular spatial layout. This is one of the most important advantages of the MAS approach, because modifications of the layout and environmental changes can

be done without manipulations in the pedestrian model. Therefore, layout changes are rather cheap in modeling cost. Another important advantage is the possibility to integrate into pedestrian agents higher-level cognitive information to obtain a more complex and heterogeneous behavior (e.g. cognitive mental maps, path planning and orientation).

3 SCA Approach to Pedestrian Dynamics

According to SCA modeling approach, human crowds are described as system of autonomous, situated agents that act and interact in a spatially structured environment. Situated agents are defined as reactive agents that, as effect of the perception of environmental signals and local interaction with neighboring agents, can change either their internal state or their position on the structured environment. Agent autonomy is preserved by an action-selection mechanism that characterizes each agent, and heterogeneous MAS can be represented through the specification of agents with several behavioral types through L*MASS formal language (an execution for SCA agents is provided by SCA platform [20]). Interaction between agents can occur either locally, causing the synchronous change of state of a set of adjacent agents, and at-a-distance, when a signal emitted by an agent propagates throughout the spatial structure of the environment and is perceived by other situated agents (heterogeneous perception abilities can be specified for SCA agents).

SCA model is rooted on basic principles of CA: it intrinsically includes the notions of state and explicitly represents the spatial structure of agents' environment; it takes into account the heterogeneity of modeled entities and provides original extensions to CA (e.g. at-a-distance interaction).

According to SCA framework, the spatial abstraction in which the simulated entities are situated (i.e. *Space*) is an undirected graph of *sites* (i.e. $p \in P$), where graph nodes represent available space locations for pedestrians and graph edges define the adjacency relations among them (and agents' suitable movement directions). Each $p \in P$ is defined by $\langle a_p, F_p, P_p \rangle$, where $a_p \in A \cup \{\perp\}$ is the agent situated in p , $F_p \subset F$ is the set of fields active in p and $P_p \subset P$ is the set of sites adjacent to p .

Pedestrians and relevant elements of their environment that may interact with them and influence their movement (i.e. *active elements of the environment*) are represented by different types of SCA agents. An agent *type* $\tau = \langle \Sigma_\tau, Perception_\tau, Action_\tau \rangle$ is defined by:

- Σ_τ : the set of states that agents of type τ can assume;
- $Perception_\tau : \Sigma_\tau \rightarrow W_F \times W_F$ **function** for agents of type τ : it associates each agent state to a pair (i.e. *receptiveness coefficient* and *sensitivity threshold*) for each field in F ;
- $Action_\tau$: the behavioral specification for agents of type τ in terms of L*MASS language [21].

A SCA-agent is defined by a type τ , its current state ($s \in \Sigma_\tau$) and position in *Space* (*Space* is the undirected graph of sites $p \in P$, where P is the set of available positions for situated agents).

4 Aggregation in Open Crowds

As a representative example of translation methodology from a social theory to a SCA-based computational model, this paper presents the SCA model of a specific aggregation phenomenon: the formation of an “Open Crowd”, described in the work of Elias Canetti. Canetti published in 1960 the results of a 40-years study on crowds behavior [5]. His analysis comprehends a very specific classification of crowds and is rich of considerations from many perspectives, from the psychological to the anthropological point of view. His work has been chosen because it has been evaluated as the more detailed and clearly conceptualized between the ones taken into consideration (see for example [22–25]). Moreover, it presents a clear semantics and explicit reference to concepts of loss of individuality, crowd uniformity and spatio-temporal dynamics that could be fruitfully represented by modeling approaches like SCA.

Elias Canetti’s definition of “*crowd*” can be:

... a unic entity dominated by uniform moods and feelings; it is characterized by the spontaneous will of growing and aggregating other pedestrians, and has a target, that is identified as a location of the environment or an object that all the individuals aggregated into the crowd desire. The *aggregation* phenomenon describes the growing effect that starts from an aggregative psychological impulse called the “*discharge*”. The “*discharge*” occurs spontaneously in people and overcomes the natural social repulsive behavior of the “*fear to be touched*”. On the other side, crowd disgregation is the result of an other psychological impulse called “*panic*”, rising as the result of “*individualistic impulses*”.

According to Canetti’s definition, an Open Crowd is the most general kind of crowd, not constrained by obstacles and not limited into a spatial area.

Before translating the theory into the computational model we need a further step. In fact crowd dynamics phenomena are usually expressed only by complex sociological theories, and also Canetti’s definitions lack in the quantification of aggregation and disgregation mechanism. As the challenge of this work is to translate these theoretical described phenomena into a formal model, we decided to adopt a paradigm coming from physics to interpret the Open Crowd aggregation phenomenon before translating it into SCA. This passage helps us in the difficult step of describing and modeling phenomena according to individuals’ behavioral rules and inter-mechanisms. Aggregating behavior of molecular meso-structures are described by the London Van der

Waals interactions, that has been chosen as physical paradigm to analytically describe attractive–repulsive interactions within crowds.

This paradigm describes the aggregation of matter through the behavior of single molecules and the laws that govern the establishing of bonds between molecular meso-structures. It has been chosen because includes the model of a behavioral change of molecules that can be easily adapted to our aims: molecules, normally neutral, ignore each other (i.e. *repulsive behavior*); the movement of electrons can occasionally transforms a molecules in a dipole for a very short time (*spontaneous possible discharge genesis*), but if another molecule moves near a transient dipole, it is induced to became a dipole too. The bond established between the two dipoles is described by the London Van der Waals forces, and can be extended to other proximal molecules by electrical induction *aggregative behavior*. Moreover, Van del Waals function has been already translated into CA rules in [26]. Finally, it opens to further representation of phenomena involving Open Crowds (i.e. the disaggregation phenomenon).

According to these considerations we defined a set A of pedestrian agents (i.e. $\forall a \in A, a = \langle s, p, \mathbf{ped} \rangle$) where

$$\mathbf{ped} = \langle \Sigma_{\text{ped}}, \text{Perception}_{\text{ped}}, \text{Action}_{\text{ped}} \rangle$$

and $\Sigma_{\text{ped}} = \{\mathbf{normal}, \mathbf{dipole}, \mathbf{excited}\}$.

Agent behavior is defined as the reactive response to external signal perceived by agents.

In the proposed model fields represent at-a-distance indirect interactions between agents through the emission and perception of signals. In our experiments we have identified three different field types: $F = \{F_{\text{rep}}, F_{\text{dis}}, F_{\text{att}}\}$:

- F_{rep} (**repulsive** field): agents in **normal** state emit a repulsive field and move within the space avoiding sites with higher values of other **repulsive** fields (*fear to be touched* principle).
- F_{att} (**attractive** field): agents in **excited** state follow **attractive** fields and emit themselves **attractive** field.
- F_{dis} (**discharge** field): when an agent is reached by a **discharge** field, it changes its internal state into **excited**.

All field types defined for the experiments have additivity property, therefore in the SCA-based model fields can compose each other by addition of their values (the *attraction power of a crowd* can be represented as the resultant of all the fields emitted by crowd components). Let f_g^p indicate the unique value of a given field type F_g at a specific site p ,

$$f_g^p = \sum_{i=1}^{|F_g|} f_i^p.$$

If p_0 is the site in which a field $f_g \in F_g$ has been emitted and $f_g^{p_0}$ indicates the emission intensity value in p_0 , the diffusion function of the field is defined

as follows:

$$\forall p \in P, \quad Diffusion_g(p_0, f_g^{p_0}, p) = \begin{cases} \frac{f_g^{p_0}}{1+dist(p_0, p)^6}, & f_g^p > thr, \\ 0 & \text{otherwise} \end{cases}$$

where thr is a threshold value set to filter lower values of fields that cannot be physically perceived by agents. This function describe a cusp-shaped field with the maximum value in the middle and a uniform distribution of the field value in the space according to a decreasing gradient. The expression $1/dist(p_0, p)^6$ represents the decreasing of the field intensity. In our experiments it has been set equal to $1/r^6$ for the London Van der Waals forces, in a discrete space.

In a SCA-based model, each pedestrian has been represented as an agent that ignores other agents in **normal** state, while when it is in **excited** state, as effect of a discharge event, it can influence eventual proximal agents with an aggregation desire. Since the London Van der Waals forces are very short forces, and the SCA-based model imposes a spatial discrete representation, agents can influence only other agents laying in the neighbor places. If an agent is proximal to an agent in a dipole state it becomes excited, and it begins establishing bonds with near agents inducing the state excited. In this way excited agents start to aggregate each other.

Following is described the behavior of **ped** agents and sketched the formal specification of $Action_{ped}$ according to L*MASS language.

The agent behavior in **normal** state is described by the following rules:

- if state is **normal**:
 1. emit field: **repulsive**
 2. draw a random number r from 0 to 0.99 and if $0.98 \leq r \leq 0.99 \rightarrow$ change the state in **dipole**
 3. if perceive **repulsive** fields \rightarrow move according to the negative gradient
 4. if perceive a **discharge** or an **attractive** field \rightarrow assume **excited** state

In M*MASS these rules are expressed in actions that agents of type τ can perform. $Action_\tau$ specifies whether and how agents change their state and/or position, how they interact with other agents, and how neighboring and at-a-distance agents can influence them. Specifically, the basic action primitives are:

- $emit(s, p, f)$ allows an agent to *start the diffusion of field f on p* , that is the site it is placed on;
- $react(s, a_{p_1}, a_{p_2}, \dots, a_{p_n}, s')$ is the primitive that allows the specification of a *coordinated change of state* among adjacent agents;
- $transport(p, f, q)$ allows to *define agent movement* from site p to site q following the information perceived by the field f ;
- $trigger(s, f, s')$ specifies that an agent must *change its state* when it perceives the field f .

Below we expressed the rules describing the behavior in **normal** state in the M*MASS formal language:

action: $emit(\mathbf{normal}, p, f_{rep})$
 condit: $a = \langle \mathbf{normal}, p, \mathbf{ped} \rangle$
 effect: $added(f_{rep}, p)$

action: $randomstatechange(\mathbf{normal}, \mathbf{dipole}, r)$
 condit: $a = \langle \mathbf{normal}, p, \mathbf{ped} \rangle, 0.98 \leq random(r) \leq 0.99$
 effect: $a = \langle \mathbf{dipole}, p, \mathbf{ped} \rangle$

where $randomstatechange(s, s', r)$ specifies that an agent must *change its state* according to the value of the random variable r .

action: $transport(p, f_{rep}, q)$
 condit: $a = \langle \mathbf{normal}, p, \mathbf{ped} \rangle, A_q = empty(q), q \in P_p, perceive(f_{rep}), lessworst(q, f_{rep})$
 effect: $a = \langle \mathbf{normal}, q, \mathbf{ped} \rangle, A_p = empty(q)$

where $lessworst(q, f_q)$ is verified if

$$\nexists r \neq q, r \in P_p \mid Compare(f_g^q, f_g^r) = true \wedge a_q = empty(q)$$

In other words this action specifies that the agent a , upon perception of a field f_g must move towards the adjacent vacant site which presents the lowest value for this field.

action: $trigger(\mathbf{normal}, f, \mathbf{excited})$
 condit: $a = \langle \mathbf{normal}, p, \mathbf{ped} \rangle, perceive(f), f \in F_{att} \vee f \in F_{dis}$
 effect: $a = \langle \mathbf{excited}, p, \mathbf{ped} \rangle$

The agent behavior in **dipole** state is:

- if state is **dipole**:
 1. emit field: **discharge**
 2. if perceive an **attractive** field \rightarrow assume **excited** state
 3. if not perceive an **attractive** field \rightarrow assume **normal** state

That expressed in the formal language of MMass is:

action: $emit(\mathbf{dipole}, p, f_{dis})$
 condit: $a = \langle \mathbf{dipole}, p, \mathbf{ped} \rangle$
 effect: $added(f_{dis}, p)$

action: $trigger(\mathbf{dipole}, f_{att}, \mathbf{excited})$
 condit: $a = \langle \mathbf{dipole}, p, \mathbf{ped} \rangle, perceive(f_{att})$
 effect: $a = \langle \mathbf{excited}, p, \mathbf{ped} \rangle$

action: $statechange(\mathbf{dipole}, \mathbf{normal})$
 condit: $a = \langle \mathbf{dipole}, p, \mathbf{ped} \rangle$
 effect: $a = \langle \mathbf{normal}, p, \mathbf{ped} \rangle$

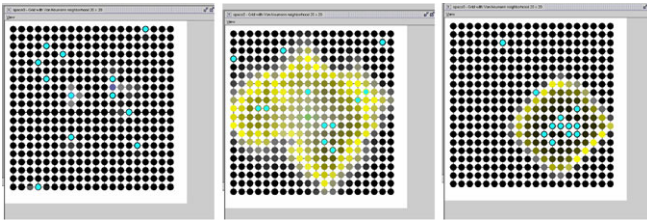


Fig. 1. Screenshots of the aggregation model. From the left to the right: agents in normal state avoiding each other; the discharge field attracts the agents; agents are aggregated in a group.

where $statechange(s, s')$ specifies that an agent must *change its state* from s to s' .

The agent behavior in **excited** state is:

- if state is **excited**:
 1. move according to positive gradient of **attractive** fields
 2. emit field: **attractive**

That in the MMASS formal language is:

```

action: transport(p, f_att, q)
condit: a = ⟨excited, p, ped⟩, A_q = empty(q), q ∈ P_p, perceive(f_att),
best(q, f_att)
effect: a = ⟨excited, q, ped⟩, A_p = empty(q)
    
```

where $best(q, f_g)$ is verified if

$$\nexists r \neq q, r \in P_p \mid Compare(f_g^r, f_g^q) = true \wedge a_q = empty(q)$$

In other words this action specifies that the agent a , upon perception of a field f_g must move towards the adjacent vacant site which presents the highest value for this field.

```

action: emit(excited, p, f_att)
condit: a = ⟨excited, p, ped⟩
effect: added(f_att, p)
    
```

Figure 1 shows some screenshots of the aggregation phenomenon.

5 Conclusion and Future Works

The resulted simulation model can give its contribution to the interpretation of very complex sociological theories and adds a further step to proof of the

expressive capability of the SCA-based approach. After this phase of theoretical application we will start a campaign of experiments. Into this context we intend to develop a more specific software platform for crowd simulation in order to make easier the experimentation process and to make simulations accessible also to not experts in MAS and SCA-based modeling.

References

1. K. Still. *Crowd Dynamics*. PhD thesis, Dept. of Mathematics, University of Warwick, 2000.
2. J. Ferber. *Multi-Agent Systems*, Addison-Wesley, Reading, 1999.
3. S. Bandini, S. Manzoni, and C. Simone. Enhancing cellular spaces by multilayered multi agent situated systems. In *Cellular Automata, Proceedings of 5th International Conference on Cellular Automata for Research and Industry (ACRI 2002), Geneva (Switzerland), October 9–11, 2002, Volume 2493 of Lecture Notes in Computer Science*, Springer, Berlin, 2002.
4. S. Bandini, M.L. Federici, S. Manzoni, and G. Vizzari. Pedestrian and crowd dynamics simulation: Testing SCA on paradigmatic cases of emerging coordination in negative interaction conditions. In *Proc. of PACT07*, 2007.
5. E. Canetti. *Crowds and Power*, Farrar, Straus and Giroux, New York, 1984.
6. D. Helbing and P. Molnar. Social force model for pedestrian dynamics. *Phys. Rev. E* 51:4282–4287, 1995.
7. D. Helbing, J. Keltsch, and P. Molnar. Modelling the evolution of human trail systems. *Nature*, 338:47–50, 1997.
8. S. Hoogendoorn and P.H.L. Bovy. Gas-kinetic modeling and simulation of pedestrian flows. *Transportation Research Record*, 1710:28–36, 2000.
9. D. Helbing, I. Farkas, and T. Vicsek. Simulating dynamical features of escape panic. *Nature*, 407:487–490, 2000.
10. A. Schadschneider. Cellular automaton approach to pedestrian dynamics—theory. In *Pedestrian and Evacuation Dynamics*, eds. M. Schreckenberg and S. Sharma, pages 75–85. Springer, Berlin, 2002.
11. A. Burstedde, A. Kirchner, K. Klauck, A. Schadschneider, and J. Zittartz. Cellular automaton approach to pedestrian dynamics—applications. In *Pedestrian and Evacuation Dynamics*, eds. M. Schreckenberg, S. Sharma, pages 87–97. Springer, Berlin, 2002.
12. M. Schreckenberg and S. Sharma (eds.). *Pedestrian and Evacuation Dynamics*, Springer, Berlin, 2002.
13. V.J. Blue and J. Adler. Cellular automata microsimulation for modeling bidirectional pedestrian walkways. *Transportation Research Part B*, 35:293–312, 2001.
14. H. Klüpfel. *A Cellular Automaton Model for Crowd Movement and Egress Simulation*. PhD thesis, Universität Duisburg-Essen, 2003.
15. S. Morishita and T. Shiraiishi. Evaluation of billboards based on pedestrian flow in the concourse of the station. In *Proc. of 7th International Conference on Cellular Automata (ACRI 2006)*, pages 716–719, 2006.
16. M.C. Toyama, A.L.C. Bazzan, and R. da Silva. An agent-based simulation of pedestrian dynamics: from lane formation to auditorium evacuation. In *Proc. of AAMAS 06*, pages 108–110, 2006.

17. F. Klugl and G. Rindsfuser. Large-scale agent-based pedestrian simulation. In *Multiagent System Technologies*, pages 145–156, 2007.
18. P. Torrens. Cellular automata and multi-agent systems as planning support tools. In *Planning Support Systems in Practice*, pages 205–222, 2002.
19. M. Batty, H. Couclelis, and M. Eichen. Urban systems as cellular automata. *Environment and Planning B*, 24:159–164, 1997.
20. S. Bandini, S. Manzoni, and G. Vizzari. Towards a platform for M*ASS-based simulations: focusing on field diffusion. *Applied Artificial Intelligence*, 20:327–351, 2006.
21. S. Bandini, S. Manzoni, G. Pavesi, and C. Simone. L*MASS: A language for situated multi-agent systems. In *Proc. of the 7th Congress of the Italian Association for Artificial Intelligence (AI*IA 2001)*, Volume 2175, 2001.
22. H. Blumer. *Collective Behavior*, Irvington Publishers, New York, 1993. 1st edition 1951.
23. G. Le Bon. *The Crowd: a Study of the Popular Mind*, Dover, New York, 2002. 1st edition 1895.
24. L.H. Turner and L.M. Killian. *Collective Behavior*, Prentice-Hall, New York, 1987.
25. L. Levy. A study of sports crowd behavior: The case of the great pumpkin incident. *Journal of Sport and Social Issues*, 13:69–91, 1989.
26. S. Bandini and M. Magagnini. Pattern control in the generation of artificial percolation beds: a cellular automata approach. In *ACRI2000*, pages 1–10, 2000.

Hardware Implementation of a Crowd Evacuation Model Based on Cellular Automata

Ioakeim G. Georgoudas, Georgios C. Sirakoulis, and Ioannis T. Andreadis

Laboratory of Electronics, Department of Electrical and Computer Engineering,
Democritus University of Thrace, 67100 Xanthi, Greece
e-mail: igeorg@ee.duth.gr, gsirak@ee.duth.gr, iandread@ee.duth.gr

Summary. Cellular Automata (CA) can sufficiently represent phenomena of arbitrary complexity and at the same time they can be precisely simulated by digital computers, because of their intrinsic discreteness. A two-dimensional (2-D) CA dynamic system has been proposed to efficiently model crowd behaviour inside bounded areas to contribute to the upgrade of public facilities. This paper examines the on-chip realisation of the proposed model. The hardware implementation of the CA model is based on FPGA logic. CA cells obtain discrete values, thus indicating their status; either free or occupied. Significant parameters of the local CA rule, such as the number and the allocation of the exits or the obstacles are inputs of the dedicated processor. Initial data is loaded to the dedicated processor in a semi-parallel way, i.e. all rows of the CA grid are loaded simultaneously while data propagates in a serial way from one cell of column j to the other cell of its successive column, $j + 1$. The automatic response of the processor provides the signals that guide the crowd in correspondence to its density around exits. In collaboration with smart cameras, the proposed FPGA processor could be incorporated in an efficient, real-time, decision-support system that would be able to guide the crowd in cases of emergency, using sound and optical signals.

1 Introduction

Thorough research in panic crowd movements [1, 2] indicates that individuals under panic develop herding behaviour and clogging, thus becoming unable to effectively use all means of emergent evacuation. Crowd safety and comfort not only depend on the design and the operation of the place, but also on the behaviour of each crowd individual. The traditional approach of motion prediction applied to large crowds of pedestrians was based on the modelling of the crowd as a continuous homogeneous mass that behaves like a fluid flowing along corridors [3]. Recent approaches, enhanced by modern computer power, suggest that the crowd consists of discrete individuals able to react with their surroundings [1].

Computational intelligent techniques such as CA were introduced in order to model more efficiently crowd behaviour [4]. CA can sufficiently represent phenomena of arbitrary complexity and at the same time can be simulated exactly by digital computers, because of their intrinsic discreteness [5]. Regarding simulation of pedestrian dynamics, 2-D CA models have been reported in literature [6, 7], some treating pedestrians as particles subject to long-range forces [7] others using walkers leaving a trace by modifying the underground on their paths [6] etc.

Furthermore, evacuation process is inherently complex, meaning that is a system multi-parameterised and its response cannot be easily estimated. There are interactions among occupants, buildings and environment and there are also socio-psychological parameters that should be taken under consideration [8, 9]. Evacuation could be defined as a non linear problem with many factors affecting it. A system of Partial Differential Equations (PDEs) could effectively approach it. But this would lead to a system of PDEs very difficult to handle, which would also be demanding in terms of computer power and computation time. On the other hand, CA can act as an alternative to PDEs [10–12]. These equations contain much more info than it is usually needed, because variables may take an infinite number of values in a continuous space and PDEs are used to compute values of physical quantities at points in continuous time. But the values of physical quantities are usually measured over finite volumes at discrete time steps. CA are used to compute values of physical quantities over finite areas (CA cells) at discrete time steps.

A CA model which simulates the movement of the crowd in cases of room evacuation has been developed [13]. Empirical studies of the international bibliography have been taken into account as well as studies of the social psychology that describe and model crowds in state of panic [8, 9]. This computational model is properly parameterised in order to be equipped with the ability of receiving and properly processing data from a camera-based multiple people detecting system. This paper examines the on-chip realisation of the presented model. The hardware implementation of the CA model is based on FPGA logic. CA cells obtain discrete values, thus indicating their status; either free or occupied. Significant parameters of the local CA rule, such as the number and the allocation of the exits or the obstacles are inputs of the dedicated processor. During each time step, an individual moves towards the closest exit trying to occupy one of the eight possible states of its closest neighbourhood, i.e. incorporating a multi-directed motion. In Sect. 2 the theoretical background of CA is presented while in Sect. 3 a short description of the model and its architecture is given. Section 4 presents the principles of the design of the dedicated processor and Sect. 5 includes simulation results. Finally, the conclusions drawn are presented in Sect. 6.

2 Cellular Automata

CA are models of physical systems, where space and time are discrete and interactions are local. In this section a formal definition of a CA will be presented [14]. In general, a CA requires:

- (1) a regular lattice of cells covering a portion of a d -dimensional space;
- (2) a set $\mathbf{C}(\vec{r}, t) = \{C_1(\vec{r}, t), C_2(\vec{r}, t), \dots, C_m(\vec{r}, t)\}$ of variables attached to each site \vec{r} of the lattice giving the local state of each cell at the time $t = 0, 1, 2, \dots$;
- (3) a rule $R = \{R_1, R_2, \dots, R_m\}$ which specifies the time evolution of the states $\mathbf{C}(\vec{r}, t)$ in the following way: $C_j(\vec{r}, t+1) = R_j(\mathbf{C}(\vec{r}, t), \dots, \mathbf{C}(\vec{r} + \vec{\delta}_q, t))$, where $\vec{r} + \vec{\delta}_k$ designate the cells belonging to a given neighbourhood of cell \vec{r} .

In the above definition, the rule R is identical for all sites and it is applied simultaneously to each of them. However, spatial (or even temporal) inhomogeneities can be introduced. Furthermore, in the above definition, the new state at time $t + 1$ is only a function of the previous state at time t . It is sometimes necessary to have a longer memory and introduce a dependence on the states at times $t - 1, t - 2, \dots, t - k$. The neighbourhood of cell \vec{r} is the spatial region in which a cell needs to search in its vicinity. For 2-D CA, two neighbourhoods are usually considered: The von Neumann neighbourhood, which consists of a central cell (the one which is to be updated) and its four geographical neighbours north, west, south and east. The Moore neighbourhood contains, in addition, second nearest neighbours northeast, northwest, southeast and southwest that is a total of nine cells.

The local rules of CA define an emulation of actual macroscopical behaviour. CA are very effective in simulating physical systems and solving scientific problems, because they can capture the essential features of systems where global behaviour arises from the collective effect of simple components which interact locally [15]. The CA approach is consistent with the modern notion of unified space–time. In computer science, space corresponds to memory and time to processing unit. In CA, memory (CA cell state) and processing unit (CA local rule) are inseparably related to a CA cell [16]. In addition, models based on CA lead to algorithms, which are fast because they exploit the inherent parallelism of the CA structure [17–19].

3 Basic Characteristics of the Evacuation Model

The computational model is based on a 2-D CA and simulates the movement of the crowd in cases of emergency (e.g. fire). The grid of the 2-D CA is considered as homogeneous and isotropic, while the CA cells are able to exist in two possible states; either free or occupied by exactly one particle. During each time step, an individual chooses to move in one of the eight possible

<i>i=1</i>	NW	N	NE	W	reference cell	E	SW	S	SE
.
.
<i>i=n</i>	NW	N	NE	W	reference cell	E	SW	S	SE

Fig. 1. The $n \times 9$ matrix.

directions of its closest vicinity, thus incorporating a multi-directed motion. Each particle moves towards the direction which is closest to an exit. The key of the evacuation is an $n \times 9$ matrix, which is calculated for each occupied cell. Each of its elements represents a possible updated spatial and temporal state of the occupied cell (Fig. 1).

Variable n , the number of the matrix rows, indicates the number of the escape points, which is user-defined. Moreover, each element of the i th row ($i = 1, \dots, 9$) indicates the distance of the occupied cell and each of its eight neighbours from the i th exit. The distance is defined as the minimum number of cells that a pedestrian has to pass in order to reach the exit, moving strictly either vertically or horizontally.

As depicted in Fig. 1, the occupied cell is always represented by the fifth cell of each row, while all other cells represent the eight closest neighbours, i.e. the north-west (NW), north (N), north-east (NE), west (W), east (E), south-west (SW), south (S) and south-east (SE) neighbour, respectively. As soon as all possible routes are detected, i.e. as soon as each of the $n \times 9$ elements of the matrix are evaluated, the shortest prevails. Hence, both the destination exit, represented by the row of the minimum value element and the next step direction, indicated by the column of this element, are defined.

In case that two pedestrians target the same cell, then are prevented from colliding following a simple rule that provides priority to the occupant that fronts the exit. The rule stands on the idea that moving forward is simpler than any other action that would require enhanced physical effort. Prohibited pedestrians do not stay fixed but attain a parallel, slightly different route towards the chosen destination.

As depicted in Fig. 2, prominent features of evacuation process such as blockings in front of exits, collective behaviour and random to coherent motion are successfully encountered by the model, thus qualitatively strengthening its validation. In particular, regarding the latter characteristic, it has been proven that in a system of self-propelled particles as the amount of noise decreases a phase transition from a disordered to an ordered state—from random to coherent motion takes place [20].

Finally, a graphical user interface (GUI) based on Matlab[®] has been developed (Fig. 2). The user is able to predefine distinguished features of the

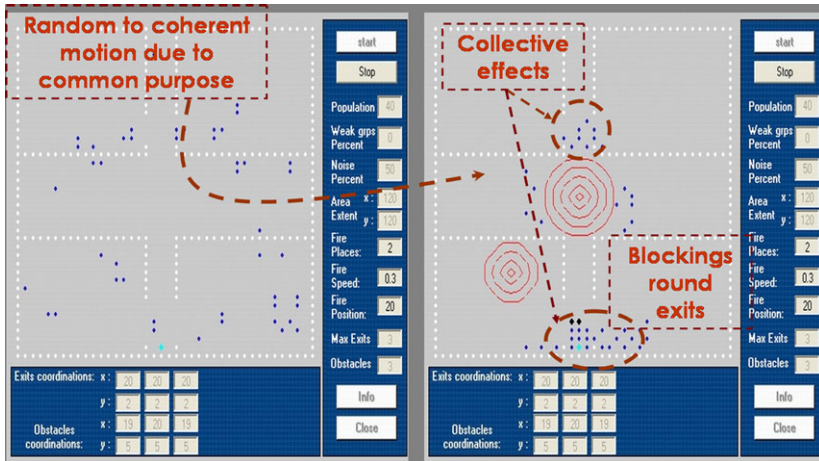


Fig. 2. Distinct features of evacuation process.

evacuated area, incorporating both topological-oriented parameters and parameters that describe crowd formation. In Fig. 2, the evacuation process takes place in four separated rooms, divided by two corridors crossed at the middle of the floor. People attempt to evacuate the building from the unique exit, which is located at the end of the vertical corridor. Simulation displays that, due to fire spread, people, coloured in light blue, try first to reach the exit of the rooms they are in and then they move towards the exit of the building. Corridors are white coloured, while obstacles, coloured black, appear suddenly further hindering exit approach. The existence of several, user-defined parameters enhance the surveillance perspectives of a certain area, since various hypotheses can be investigated.

4 Implementation of the CA Model

Modern computers offer sufficient processing power to handle most of the analysis that several complex phenomena require. Though, the application of a general-purpose computer in some cases may not be desirable, or it is even impossible, due to high power consumption and significant size. Portable, embedded general-purpose processors may however be unable to handle more complex computational tasks. One of the methods to achieve the speed-up execution of the algorithm in such embedded systems is to use the potential of available FPGA-devices. They enable parallel processing of data using custom digital structures. Besides, CA circuit design reduces to the design of a single, relatively simple cell and layout is uniform. The whole mask for a large CA array (the cells with their internal connections as well as the interconnection between cells) can be generated by a repetitive procedure so no silicon area is

wasted on long interconnection lines and because of the locality of processing, the length of critical paths is minimal and independent of the number of cells [21]. Halbach and Hoffman [22] have implemented CA on FPGAs and reported a speed-up of 3 times for a medium complexity rule and a speed up of 22 times for a high complexity rule concluding that the implementation of CA is significantly faster in FPGA hardware than in optimised software.

The hardware implementation of the CA model is based on FPGA logic. The device that has been used for the realisation of the model is the Stratix EP1S80B956C6 that belongs to the ALTERA family. The CA grid consists of two types of cells; external and internal cells. Every cell covers an extent of approximately $40 \times 40 \text{ cm}^2$, including even the situation of a dense crowd [6]. The number and the allocation of the exits or the obstacles are inputs of the dedicated processor. As already referred, during each time step, an individual moves towards the closest exit trying to occupy one of the eight possible states of its closest neighbourhood. The design of each CA cell follows sequential logic. This means that each cell is separated into two parts; the combinational one, which mainly includes all computations taking place into cells and the memory part that passes the combinational results to the adjacent cells during the next time step. In practise, the implementation is more complicated in order delay matters to be confronted.

As depicted in Fig. 3, the combinational part consists of three structures that are connected the one right after the other: (1) the closest exit identification circuit, (2) the closest neighbourhood coordinates calculation circuit, and (3) the shortest route tracking circuit. As soon as the initialisation process has finished and a cell is occupied, the first circuit identifies the closest exit for the given cell. In the meanwhile, the second circuit has already calculated the coordinates of the Moore neighbourhood and the third circuit is able to start searching for the closest neighbour to the closest exit.

Figure 4 is an insight look to the design of the closest exit tracker. It realises the following simple relation between the occupied cell (element) and the user defined exits:

$$D_{\min} = \min\{|x_{\text{element}} - x_{\text{exit}_i}| + |y_{\text{element}} - y_{\text{exit}_i}|\}, \quad (1)$$

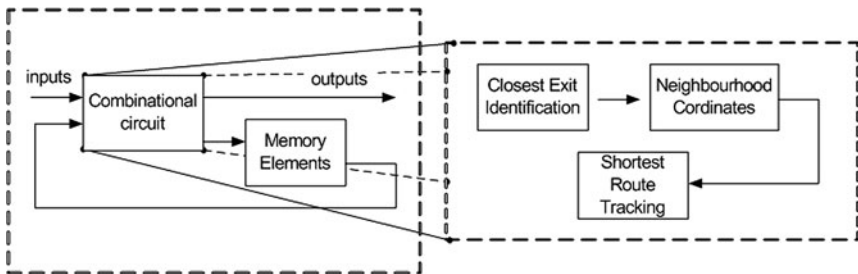


Fig. 3. Combinational part of a CA cell.

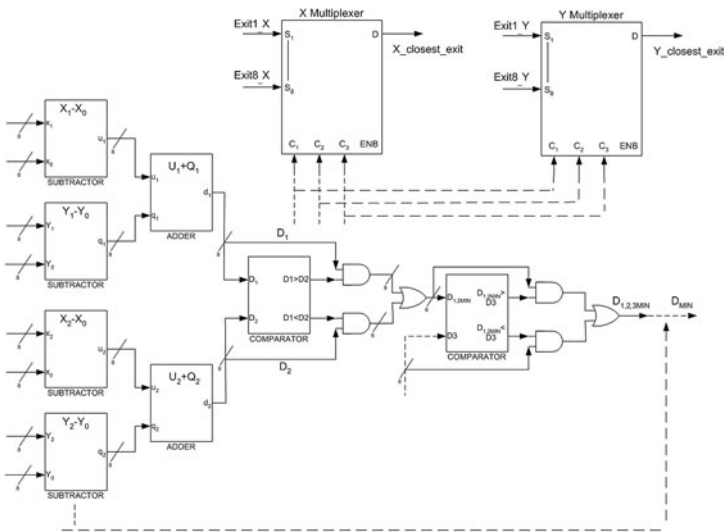


Fig. 4. The design of the closest exit tracker.

where D corresponds to the distance of element with coordinates $(x_{element}, y_{element})$ from the exit i with coordinates (x_{exit_i}, y_{exit_i}) .

The exit coordinates are loaded to two multiplexers and the control input defines each time which is the closest exit. The control input is driven by a sub-circuit of adders, subtractors and comparators, properly connected. In fact, the minimum Euclidean distance is found between the occupied cell and the exits.

The second and third structural parts of the combinational circuit of each CA cell are illustrated together in Fig. 5. The left part of this figure depicts the circuit that implements the computation of the coordinates of the eight closest neighbours of the occupied cell. The right part shows the corresponding hardware realisation of the aforementioned closest to the chosen exit neighbour tracker for one of the nine elements of the $n \times 9$ matrix. The same implementation is repeated (indicated by the dashed line) for the rest of the matrix elements. These parts combined with the previous one (depicted in Fig. 4) realise in hardware the shortest route tracking methodology, i.e. the operation of the $n \times 9$ matrix. For reasons of better understanding, Fig. 6 visualises the transformation of the $n \times 9$ matrix to its 3×3 formation, in the case of unique exit, i.e. $n = 1$. The distance is defined as the minimum number of steps in order a pedestrian to reach the chosen exit moving strictly vertically or horizontally.

The outputs of the eight adjacent cells are single one-bit inputs for a single cell. *Initial State* and *Obstacle* are also one-bit inputs. The former defines whether the cell is occupied or not, thus enabling or disabling the aforementioned circuits (closest exit to the cell, neighbours coordinates and

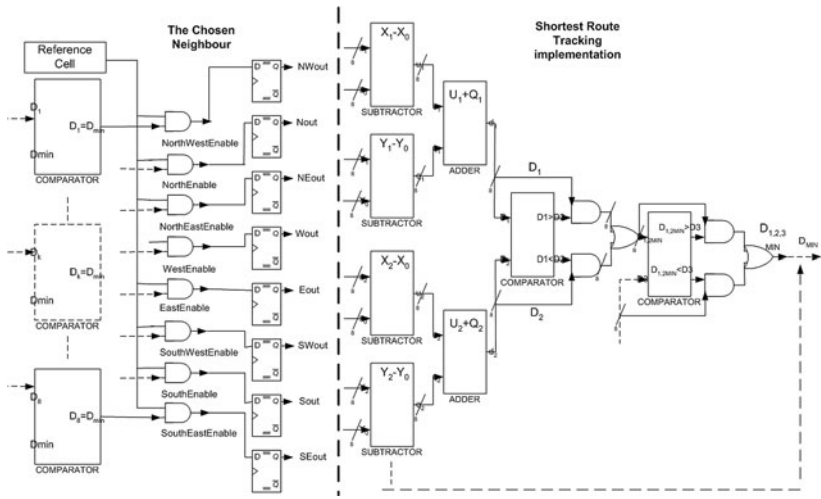


Fig. 5. Neighbours coordinates computation circuit (*left*) and closest-to the chosen exit-neighbour tracker (*right*).

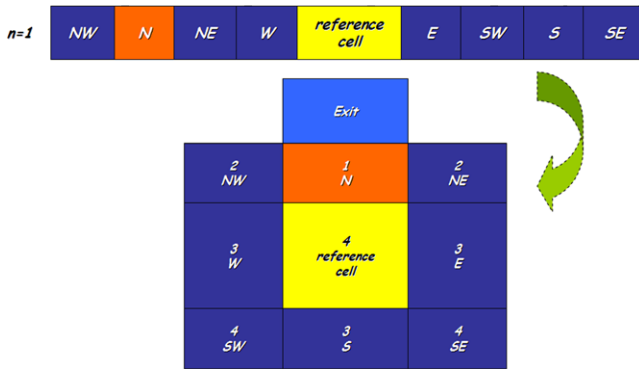


Fig. 6. The 3×3 visualisation of the $n \times 9$ matrix, for $n = 1$.

shortest route tracker). The latter defines whether a cell or a group of cells should be identified as obstacles or not. *Itenable* is an enabling input that is on during the initialisation process. The other four inputs are multi-bit ones and define the coordinates of the cell and the exits. There are eight single-bit outputs to the eight adjacent cells. Only one of them is equal to one at each time step. *Feeder* output is activated during the initialisation process and provides the cell with the appropriate initial data. There are also parallel to serial converters that drive parallel outputs to serial inputs in order to minimise the number of pins of the processor and serial to parallel converters inside the block that modify the serial routes to parallel.

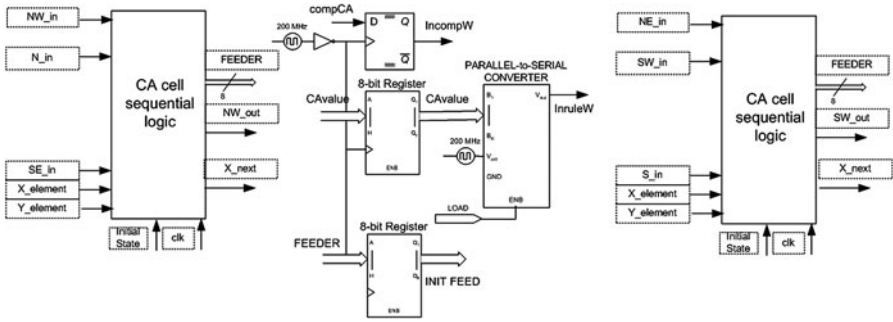


Fig. 7. Interconnection between cells.

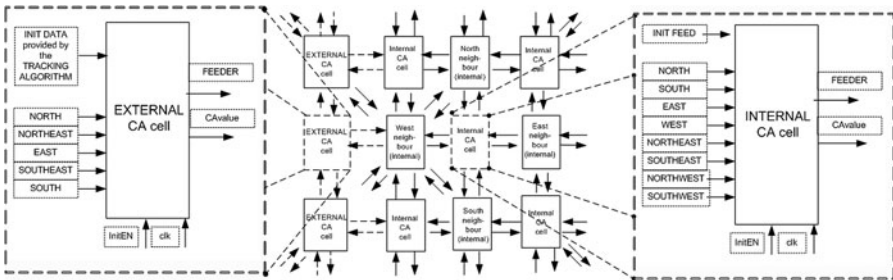


Fig. 8. External and internal cells.

Figure 7 displays a typical interconnection between cells. Apart from the parallel-to-serial converter, supplementary memory components are used in order to balance delays during signal propagation. Moreover, main structural devices pipeline the function they represent, incorporating a latency of some clock-cycles. The essence of pipelining is to break up a long process into smaller parts, and then to have each part to accomplish its mission and pass the result to the next part. Pipelined circuits contain registers in-between the logic blocks that break up the circuit into smaller pipeline stages. Applying this technique, the addition of eight-bit registers in-between structural devices is also essential for reasons of synchronisation, further increasing latency. Nevertheless, the appearance of a result at a constant period is reassured, hence the throughput and/or the frequency of the entire circuit increases.

A distinct feature of the design is the existence of different kind of cells in the CA grid; namely external and internal cells (Fig. 8). Their existence forms a solution for the initialisation of all cells. In fact, the difference is that external cells have a serial data port, *Initdata* that supplies initial data to the grid, while internal cells have a parallel port, *Initfeed* that forwards initial data to internal grid. As far as the initialisation process concerns; initial data (e.g.

coordinates) are serially provided to the processor through external cells. They are provided, though, simultaneously (that is in parallel) to all cells located at the left part of the CA grid. Inside the grid, data propagates through parallel channels, from one internal cell to the other. During initialisation, *Initenable* input, driven by an auxiliary circuit keeps all other inputs inactive.

Furthermore, a detecting algorithm is incorporated, capable to estimate the number and the distribution of the pedestrians in front of exits, in real time, using instant images provided by video technology and sensor networks. This information is elaborated by the processor in order to guide the crowd. In particular, if the number of people gathering in front of exits overcomes a predefined threshold, then audio-visual signals are activated to rearrange crowd and to prevent clogging. The selected detecting algorithm is based on a background subtraction algorithm, which isolates foreground information from background images. It continues with the segmentation of the foreground pixels, which aims at the moving objects clarification. Foreground pixels are detected using luminance contrast and grouped into blobs. Detection of the moving objects is finally succeeded by comparing consecutive frames, i.e. boxes from two consecutive frames are matched. The matching process uses the information of overlapping boxes, colour histogram back projection or different blob features (colour or distance between blobs). The implemented algorithm combines the required resolution along with the execution rate succeeding real-time, display and image processing.

5 Simulation Results

In this section a simple example of how the dedicated processor evaluates the closest neighbour to the closest exit is presented. For the given data, which regards the coordinates of the occupied cell and all possible exits, the results prove the validation of the design. Actually, for an occupied cell at point (3,3), the closest exit, compared to the given ones, is the exit (5,3) and the closest neighbour to that exit is the East one.

Output results prove the validation of the operation of the processor. As depicted in Fig. 10, among all exits, the one with coordinates (5,3) was chosen, which is actually the closest exit to the pedestrian located at cell (3,3). Furthermore, as also visualised to the embedded matrix, the closest neighbour of the reference cell to that exit is its east neighbour, i.e. the one located at (4,3). Indeed, E_{out} output is the only one among all single-bit outputs of the cell that is equal to 1, thus indicating the direction that the pedestrian should follow at the next time step.

In case that X_{next} and Y_{next} outputs of two different pedestrians (A and B) are the same, that means that two cells target the same cell for the coming time step. As already referred, in such a case, priority is given to the pedestrian (B) that fronts the exit. In fact, this derives from the fact that the Euclidean distance from cell A to target cell T is greater than that of cell B

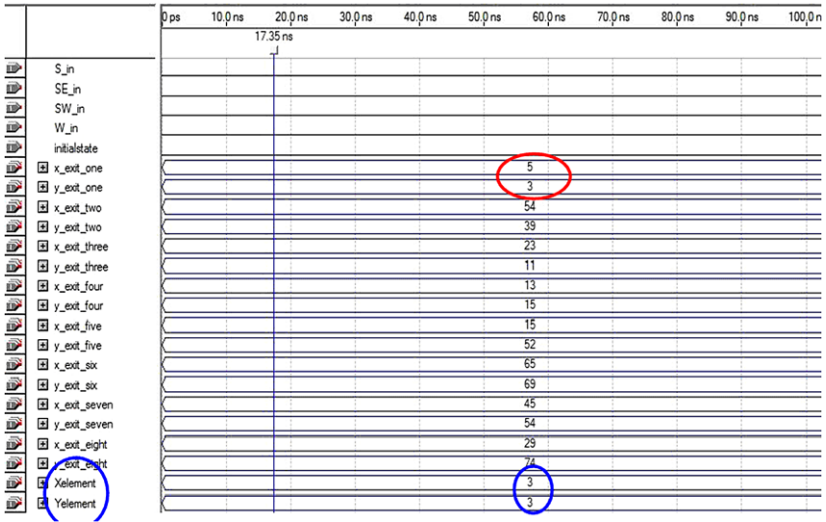


Fig. 9. Input data; the coordinates of the occupant (3,3) (in blue circle) and the coordinates of all exits (in red circle the coordinates of the closest exit).

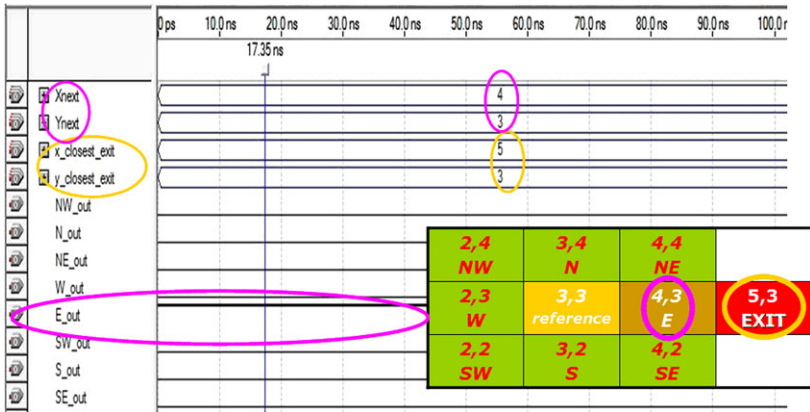


Fig. 10. Output data; the coordinates of the closest exit (in yellow circle), the coordinates of the closest neighbour to that exit (in purple circle).

from target cell (Fig. 11). Hence, less physical effort is required for pedestrian B to reach the target cell T. The hardware implementation should carry out this relationship (equation (2)). A circuit similar to the one that realises closest exit identification also realises the distance comparison in case of common target. The equation that is implemented in the latter case is the following:

$$E_{\min} = \min\{(|x_A - x_T| + |y_A - y_T|), (|x_B - x_T| + |y_B - y_T|)\}. \quad (2)$$

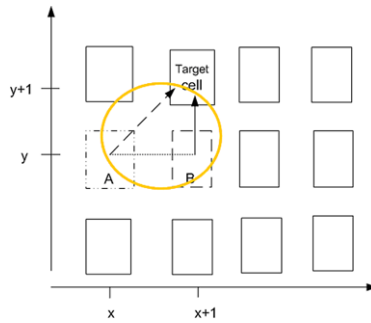


Fig. 11. Common target cell.

6 Conclusions

The proposed model successfully encounters distinct attributes of crowd behaviour, such as collective effects, collisions and delaying factors. In terms of circuit design and layout, silicon-area utilisation and maximisation of clock speed, CA are efficient computational structures for hardware realisation. The implementation of the proposed CA model is straightforward with no silicon overhead. Secondary circuits have been designed to operate as bit converters in order to avoid multiple-pins input driving as well as to preserve the functionality of the design. Furthermore, the pipelining technique has also been used to enhance the throughput of the system.

The resulting CA implementation is advantageous in terms of compactness, portability, high-speed, low-power consumption, low cost. The next step is the collaboration with modern smart cameras that detect the crowd density in front of exits. In case of high density around escaping points, the processor would produce signals of increasing intensity that would redirect pedestrians to different routes in order to prevent exits from clogging. That would lead to an efficient surveillance system that could succeed real-time active guidance of crowd during evacuation.

References

1. D. Helbing, I. Farkas, and T. Vicsek. *Nature* 407, 487–490 (2000).
2. K. Hirai and K. Tarui. A simulation of the behavior of a crowd in panic. *Systems and Control, Japan*, 1977.
3. D. Low. *Nature* 407, 465–466 (2000).
4. S. Wolfram. *Theory and Applications of Cellular Automata*. World Scientific, Singapore, 1986.
5. A. Adamatzky, *Identification of Cellular Automata*. Taylor & Francis, London, 1995.
6. C. Burstedde, K. Klauck, A. Schadschneider, and J. Zittartz. *Physica A* 295, 507–525 (2001).

7. F. Aubé and R. Shield. Modeling the effect of leadership on crowd flow dynamics, in: *Lecture Notes in Computer Science*, vol. 3305. Springer, Berlin, 2004, 601–611.
8. L.Z. Yang, D. L. Zhao, J. Li, and T. Y. Fang. *Building and Environment* 40, 411–415 (2005).
9. H. H. Kelley and J.W. Thibaut. In G. Lindzey and E. Aronson, editors, *The Handbook of Social Psychology*, vol. 4. Addison-Wesley, Reading, MA, 1969.
10. I. Karafyllidis and A. Thanailakis. *Ecological Modelling* 99, 87–97 (1997).
11. T. Toffoli. *Physica D* 10, 1–2, 117–127 (1984).
12. I. Bialynicki-Birula. *Physical Review D* 49, 6920–6927 (1994).
13. I. G. Georgoudas, G. Ch. Sirakoulis, and I. Andreadis. A simulation tool for modelling pedestrian dynamics during evacuation of large areas, in: *IFIP Artificial Intelligence Applications and Innovations*, vol. 204. Springer, Boston, 2006, 618–626.
14. B. Chopard and M. Droz. *Cellular Automata Modeling of Physical System*. Cambridge University Press, Cambridge, 1998.
15. R.P. Feynman. *International Journal of Theoretical Physics* 21, 467–488 (1982).
16. G.Ch. Sirakoulis, I. Karafyllidis, and A. Thanailakis. *Microprocessors and Microsystems* 27, 8, 381–396 (2003).
17. I. Karafyllidis, I. Andreadis, P. Tzionas, Ph. Tsalides, and A. Thanailakis. *Pattern Recognition* 29, 689–699 (1996).
18. I. Andreadis, I. Karafyllidis, P. Tzionas, A. Thanailakis, and Ph. Tsalides. *Journal of Intelligent and Robotic Systems* 16, 89–102 (1996).
19. G.Ch. Sirakoulis. *Integration, The VLSI Journal* 37, 1, 63–81 (2004).
20. T. Vicsek, A. Czirok, E. Ben-Jacob, I. Cohen, O. Shochet. *Physical Review Letters* 75, 1226–1229 (1995).
21. T. Toffoli. *Physica D* 10, 1–2, 195–204 (1984).
22. M. Halbach and R. Hoffmann. Implementing cellular automata in FPGA logic, in: *18th International Parallel and Distributed Processing Symposium, IPDPS 2004*. Santa Fe, NM, 2004, 3531–3535.

Applying a Discrete Event System Approach to Problems of Collective Motion in Emergency Situations

Paolo Lino¹ and Guido Maione²

¹ DEE, Politecnico di Bari, Via E. Orabona, 4, 70125, Bari, Italy
e-mail: lino@deemail.poliba.it

² DIASS, Politecnico di Bari, Viale del Turismo, 8, 74100, Taranto, Italy
e-mail: gmaione@poliba.it

Summary. A proper management of evacuation of crowds in panic situations requires the adaption of strategies and escape routes, depending on information collected from the real scenario. To design an effective supervisory controller, a model representing the main aspects of the evacuation dynamics and based on data coming from a distributed sensors network is necessary. To this aim, a Discrete Event System model is developed here to describe the sequence of events occurring in escape procedures. In particular, a systematic approach consisting of few steps allows to define a modular Petri Net representing flows of individuals during egress. A simple case study shows the feasibility of the proposed method.

1 Introduction

Models for evacuation dynamics in emergency situations are employed for building design, improvement of safeness criteria, better staff training, and accident analysis. In particular, hypothesis are formulated concerning the crowd distribution and characteristics, and their possible behavior in case of emergencies. The main drawback of this approach is the difficulty in managing the variability of crowd dynamics and distribution, occurrence of random events (e.g. interruption of escape routes, overcrowding of specific areas or ways out), different reaction to alarms, individual decision-making and adaptation. Moreover, the evacuation strategy should be adjusted according to the specific circumstances. This work proposes a modeling approach based on Discrete Event Systems theory. It is part of a broader research project of Technical University of Bari. The aim is to explore the feasibility of coordination and control of telecommunication systems and wireless sensor networks for managing evacuation from buildings during emergencies.

The project integrates knowledge coming from computer science, control systems engineering, telecommunications and electronics. The first problem

is data acquisition by wireless sensor networks. A flexible telecommunication framework integrating different technologies and adapting to different monitoring and intervention scenarios is under development. Information comes from different sensors, measuring environmental parameters and revealing the presence of toxicant, and from RFID (Radio Frequency Identification) devices and cameras. The control system aim is to drive and influence escape routes in real-time in order to reduce the evacuation time. This process involves signs modification, use of sound signals, instructions addressed to staff or individuals equipped with PDAs or Palmtop computers. The control law is based on feedback from the real scenario about deadlock situations, overcrowding of specific areas causing reduction of transit speeds, hold-ups due to fire/smoke/collapses. The first step in the supervisory control design is the development of an appropriate model describing the evacuation dynamics. Existing models can be roughly classified in two main categories, i.e. macroscopic and microscopic models [1, 2]. The former category includes models which are based on the building topology; the latter contemplates models detailing individual characteristics and dynamics. Macroscopic models are suitable for planning escape routes, usually achieved by solving a static optimization problem (e.g. “quickest flow” or “maximum flow” problems). The real-time adaptation of escape routes depending on feedback from the real scenario is not considered. Microscopic models are not expressly developed for real-time management of emergency situations. They can accurately represent evacuation dynamics, but the real-time optimization could require high computational effort and large simulation time for analyzing different alternatives. Finally, a proper set-up of the simulation environment could require a set of real data not easily collectible. Control design requires a trade-off between accuracy in representing the most significant variables and the need of reducing the complexity of the design process. Hence, to represent the crowd behavior, a macroscopic level of description seems to be adequate.

Then, the control system elaborates the characteristics of available data to undertake a proper action. Feedback information typically consist of discrete data, which are generated by sensors displaced within the emergency area. On this basis, a control law, consisting of discrete events and using discrete collected data, can be easily derived from a Discrete Event System (DES) model of the evacuation dynamics. DES are dynamic systems characterized by the asynchronous occurrence of instantaneous events (message, start/end of process, accident, fault, etc.) and by the discrete nature of some variables. Events change the system state according to transition mechanisms and need to be observed, traced, coordinated and controlled to guarantee a correct operation. DES are used in many applications (e.g. manufacturing, communications and traffic networks, logistics) and for control supervisors.

In this paper, a DES model suitable for a controller design and based on Petri Nets (PN) is developed. PN provide a formalism for modeling and analysis of DES, and their use for evacuation dynamics is justified by the following peculiarities: an easy graphical representation of precedence relations, syn-

chronization, parallelism, mutual exclusion in systems with shared resources; a strong mathematical foundation; modularity; suitability for simulation, performance evaluation, design and control.

This paper is organized as follows. Section 2 describes the main characteristics of DES and PN, briefly introducing their mathematical foundation. Section 3 proposes the PN approach to model crowd flows inside buildings, clearly showing how to represent each component. To assess the feasibility of the approach, a simple case study is considered in Sect. 4. Finally, Sect. 5 gives some conclusions.

2 Discrete Event Systems Modeling with Petri Nets

An approach inspired by the existing DES formalisms [3, 4] is followed to model the dynamical processes occurring in emergency situations. Namely, each individual in a collective motion can be considered as an entity receiving/sending events from/to other individuals or the environment. He/she is subject to discrete events coming from the environment or messages from other individuals, and at the same time he/she may trigger events causing a state change in the environment or messages. Then, events can be randomly generated (interruption of escape routes, blocking of doors and ways out, overcrowding of specific areas, etc.), associated to individual reaction to emergency conditions (panic, saving relatives), caused by expert agents in routing people towards emergency exit or by distributed actuators controlled by an evacuation policy. Both information detected by sensors and control actions can be adapted to the DES framework.

2.1 DES Basic Principles

A discrete event system dynamics is usually modeled with a language generator [3], i.e. the 5-tuple $\mathbf{G} = (\Sigma, Q, \delta, \mathbf{q}_0, Q_f)$, where: Σ is the set of events; Q is the set of states; the transition function $\delta : \Sigma \times Q \rightarrow Q$ is a partial function defined at each $\mathbf{q} \in Q$ for a subset $\Sigma(\mathbf{q}) \subseteq \Sigma$; $\mathbf{q}_0 \in Q$ is the initial state; $Q_f \subseteq Q$ indicates the subset of final states. Any event $\sigma \in \Sigma$ represents a state transition from \mathbf{q} to \mathbf{q}' , where $\delta(\sigma, \mathbf{q}) = \mathbf{q}'$. Moreover, if Σ^* denotes the set of all the finite strings of elements of Σ , including the empty string \emptyset , the definition of δ can be extended as follows: $\delta : \Sigma^* \times Q \rightarrow Q$, with $\delta(\emptyset, \mathbf{q}) = \mathbf{q}$ and $\delta(s\sigma, \mathbf{q}) = \delta(\sigma, \delta(s, \mathbf{q}))$. In the previous notation, $s\sigma \in \Sigma^*$ is the string obtained by concatenation of string $s \in \Sigma^*$ and event label $\sigma \in \Sigma$.

The DES model describing how individuals are evacuated is based on static information on egress sequences of resources and on a transition mechanism showing how the system state is dynamically updated. Namely, an apartment, a building, a facility, etc., can be viewed as a system of \bar{R} reusable *resources* (rooms, room spaces, room doors, exit/entrance doors, etc.) that individuals

successively acquire, use exclusively and release. Each resource r_i is characterized by a *capacity* $C(r_i)$, i.e. the maximum number of identical resource-units available for r_i , for $i = 1, \dots, \bar{R}$. Resource units can dynamically become inaccessible or disabled (a fired space, a blocked door, elevator disabled by an actuator after sensing a fire, etc.), in which case the capacity is decreased by the number of units that cannot be used.

People to be evacuated are grouped in a set I . Advancing in its way to the exit, each person follows a sequence of planned moves and operations. Then, an *egress procedure* corresponds to each initial position where the individual is at the beginning of the evacuation. The procedure consists of a sequence $\mathbf{e} = [r_{i1}, r_{i2}, \dots, r_{iL}]$ of L resources, necessary to execute all the operations (e.g., cross a room, open the door, go through a corridor, use stairs, exit). In the sequel, $E = \{\mathbf{e}_k : k = 1, 2, \dots, \bar{E}\}$ denotes the set of all egress procedures.

The Discrete Event Dynamical System (DEDS) model is associated to the flow of people among resources, which is ruled by asynchronous occurrence of discrete *events*, which determine the evolution of the system state. Typically, the state variables are only permitted to jump at discrete points in time from one discrete value to another. At a given instant of time, it is possible to define the state $\mathbf{q} \in Q$ containing information on: the resources available; the set $I_{\mathbf{q}}$ of people still to be evacuated; the egress procedure, $\mathbf{e}_{\mathbf{q}}(i)$, assigned to each individual $i \in I_{\mathbf{q}}$; the resource $HR_{\mathbf{q}}(i)$ currently held by each $i \in I_{\mathbf{q}}$; the next resource $NR_{\mathbf{q}}(i)$ to be acquired by each $i \in I_{\mathbf{q}}$; and, finally, the subsequent residual procedure of resources to complete the evacuation of each $i \in I_{\mathbf{q}}$.

By assumption, each individual detains a single unit of resource at a time, and releases the unit only if acquiring a new resource. The initial state \mathbf{q}_0 is detected by distributed sensors and depends on the location of people and the available resources at that time: each person $i \in I_{\mathbf{q}_0}$ has an associated egress procedure $\mathbf{e}_{\mathbf{q}}(i) \in E$, which may be suggested by external supervisors, or directed by local expert agents, or even chosen by his/her own decisions or (panic) feelings. The final desired state is when no one is left in the evacuated space. Last, we assume that an event occurs when a person acquires and/or releases a resource. Then, events in Σ may be classified as follows: a person entering or exiting from the evacuated environment; a person releasing a resource r_i to acquire resource r_m .

2.2 Fundamental Notations of Petri Nets

PN [5] can be used as a powerful graphical tool for modeling, analyzing, designing and controlling DES. PN are often considered as the most appropriate DES modeling tool to describe the interactions between entities competing and/or concurring to use shared and limited resources. The processes associated with the flow of entities are typically asynchronous, parallel, and mutually exclusive. In emergency/panic contexts, an entity can be a general person, a leader, an emergency operator or can even represent a group of individuals with similar characteristics or behaviors. PN are easily built as

bi-partitioned directed graphs connecting two classes of nodes, namely places and transitions, through oriented edges, also called arcs.

Places usually represent conditions, executions of activities or resource availability. *Transitions* represent events changing conditions and the available resource units. *Tokens* are entities marking places to represent where individuals are or the number of currently available resource units. Connection *arcs* represent how tokens flow through the net, then the flows of individuals in the system and how resource units are allocated and freed. Formalization of PN is as follows.

Definition. A marked PN is the 5-tuple $\mathbf{PN} = \langle P, T, F_I, F_O, M_0 \rangle$, where:

- $P = \{p_1, p_2, \dots, p_n\}$ and $T = \{t_1, t_2, \dots, t_m\}$ are finite, nonempty and disjoint sets of places and transitions, respectively. In graphical representations places are drawn as circles and transitions as bars.
- $F_I : P \times T \rightarrow \{0, 1, 2, \dots\}$ is an input function that defines directed arcs from places to transitions. $F_I(p_i, t_j)$ gives how many tokens flow through the input arc when t_j is executed, i.e. the weight which labels the input arc. In graphical representations arcs are drawn as arrows if $F_I(p_i, t_j) > 0$, and weight is not shown if unitary.
- $F_O : T \times P \rightarrow \{0, 1, 2, \dots\}$ is an output function that defines directed arcs from transitions to places. $F_O(t_j, p_i)$ gives how many tokens flow through the output arc when t_j is executed, i.e. the weight of the output arc. Arcs with $F_O(t_j, p_i) = 0$ are not shown. If $F_O(t_j, p_i) = 1$ the label is not shown.
- $M_0 : P \rightarrow \{0, 1, 2, \dots\}$ is the initial marking (state), which assigns to each place a non-negative integer. A generic marking is denoted by a vector M , with as many entries as the total number of places. Moreover, $M(p_i)$ gives the value of the entry of M corresponding to p_i . If $M(p_i) = k$, then p_i is marked with k tokens. Pictorially, we put k black dots in place p_i . An unmarked place p_i does not contain tokens: $M(p_i) = 0$.

The subsequent markings of PN, i.e. the distribution of tokens in the net, represent the successive states of the people involved in the egress procedures. The state changes describe the behavior of the crowd. The markings change according to the following rules.

- **Enabling rule:** A transition is enabled if each of its input places is marked by a number of tokens at least equal to the weight of the input arc. An enabled transition may or may not fire, depending on whether or not the event actually takes place.
- **Firing rule:** A firing of an enabled transition consumes as many tokens from each input place as the weight of the input arc, and produces as many tokens into each output place as the weight of the output arc. We assume that only one transition fires at a time. If more than one transition is enabled, then the transition to be fired is usually selected at random or by specific rules.

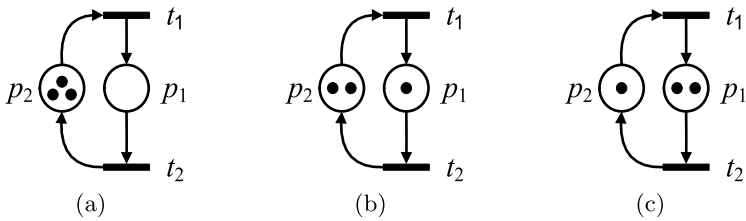


Fig. 1. PN modeling the occupation/release of a space: **a** no person in space; **b** one person occupies space; **c** two persons occupy space.

A sequence of firings results in a sequence of markings. A marking M_f is reachable from the initial marking M_0 if a sequence of N firings, namely $s = [t_{k1}, t_{k2}, \dots, t_{kN}]$, transforms M_0 to M_f . In this paper, we assume that the initial marking is established by the initial distribution of individuals in the spaces of the considered environment, and by the consequent occupation of all the resources: $M_0(p_i) = x_i$ (or 0), for every p_i denoting a resource r_i initially available in x_i units (not available), and $M_0(p_i) = C(r_i) - x_i$ (or $C(r_i)$), for every p_i denoting the individuals using r_i (filling r_i at full capacity). For example, consider the case in which a space has a capacity to hold three individuals. The PN in Fig. 1 models acquisition of space by t_1 and release by t_2 ; p_1 represents the persons occupying space units, p_2 the units still available. Initially, three space-units are available and no one is inside them (state M_0 in Fig. 1(a), t_1 is enabled). Then, event t_1 occurs, one space is occupied by one person, and two units are left available (state M_1 in Fig. 1(b), t_1 and t_2 are both enabled). If event t_1 occurs again, one more space is occupied by one person, and only one unit is left available (state M_2 in Fig. 1(c), t_1 and t_2 are enabled). If event t_2 occurs, one space is freed, and two units are available again (state M_1 in Fig. 1(b)). Finally, if t_2 is executed again, one more space is freed, and all three units become available (state M_0 in Fig. 1(a)). One can verify that each state is invariant with the total number of tokens in places p_1 and p_2 , i.e. the space maximum capacity.

3 Petri Net Application to Egress Dynamics

In this section we give the systematic procedure to define a PN model for the crowd flows or egress procedures from an environment. The model integrates standard modules, each modeling a different part of the environment. Basically, we define two modules: one used for rooms; one valid for doors, windows, exits, entrances, lifters and gateways.

3.1 PN Modules for Rooms and Gateways

The PN module in Fig. 1 is defined to represent how people enter or exit from a room. The room space is divided in more units. Successive states are shown

by different markings but the PN module structure is the same. Place p_1 represents the resource-units occupied, p_2 the units currently available in the room. Tokens in p_1 represent the number of individuals currently in the room, tokens in p_2 are the remaining spaces for other persons. The room capacity, i.e. the maximum number of individuals allowed in the room, is always given by $M(p_1) + M(p_2)$. Transition t_1 represents a person entering the room and occupying a space, transition t_2 a person exiting the room and releasing the occupied space.

The PN module given to represent people passing through a gateway (door, window, exit, entrance, etc.) is depicted in Fig. 2. Successive states are shown by different markings but the PN module structure is the same. Place p_1 represents the entrance point, p_2 the door availability, i.e. the number of resource units still available, p_3 the door occupancy, p_4 the exit point. Tokens in p_1 are the number of individuals ready and waiting to pass, tokens in p_2 are the number of available units, tokens in p_3 are the number of individuals using the door, tokens in p_4 are the individuals passed through. The door capacity, i.e. the maximum number of individuals that can contemporaneously pass through it, is given by $M(p_2) + M(p_3)$. Transition t_1 represents a person acquiring the door, transition t_2 defines a person releasing this resource. Then, Fig. 2(a) indicates 3 persons at the entrance before an available door, which allows only one of them to pass at a time. After event t_1 , Fig. 2(b) shows that one person is using the door (not available for the other two). After event t_2 , Fig. 2(c) shows that one person passed and that the door is now available for the other two.

This basic structure can be generalized to allow bidirectional flows through the doors. Namely, two more transitions and the consequent connecting arcs can be added to the net, as in Fig. 3: t_{1F} and t_{2F} are executed for a forward flow, while t_{1R} and t_{2R} for a return flow. Starting from the marking in Fig. 3(a) (3 persons waiting in the entrance point), t_{1F} may be executed taking to state in Fig. 3(b) (2 persons in the entrance point, 1 person using the door). Then,

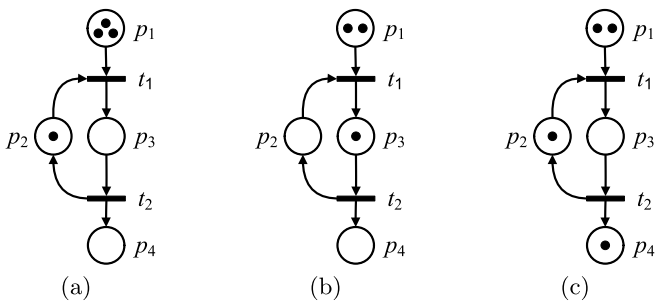


Fig. 2. PN modeling the occupation/release of a gateway: **a** 3 persons at entrance, gateway available; **b** 1 person is passing, 2 waiting, gateway not available; **c** 1 person passed, 2 waiting, gateway available.

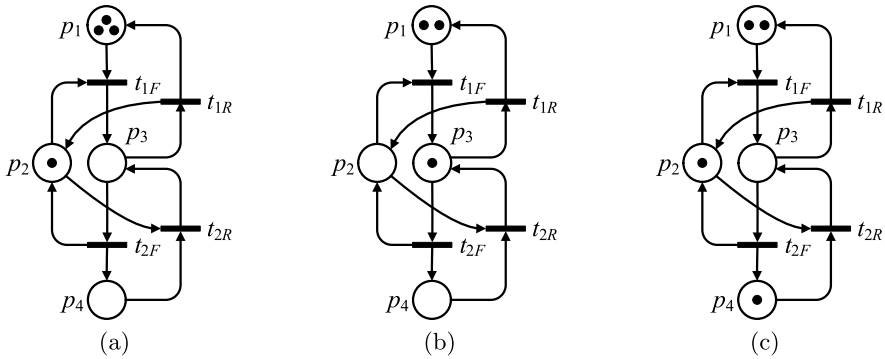


Fig. 3. PN modeling the occupation/release of a bidirectional gateway: **a** 3 persons at entrance, gateway available; **b** 1 person is passing, 2 waiting, gateway not available; **c** 1 person passed, 2 waiting, gateway available.

state in Fig. 3(c) is reached if t_{2F} is fired (2 persons in the entrance point, 1 person at the exit point). Now, both t_{1F} and t_{2R} are enabled: if t_{2R} is fired, state in Fig. 3(b) is reached again; consequently, if t_{1R} is fired, the finale state is again as in Fig. 3(a). The firing of t_{2R} and t_{1R} describes the reversed flow of a person from exit to entrance point of the gateway. To simplify, one could merge t_{1F} and t_{1R} in t_1 , and t_{2F} and t_{2R} in t_2 . Moreover, all the arcs connecting merged transitions and places would become bidirectional.

If rooms or spaces are considered as the entrance and exit points of a gateway (places p_1 and p_4 in Fig. 3), we may establish the connection between the PN modules for rooms and gateways. Each door module is connected to two room modules. The transit of an individual from one room to another is by passing through a door according to the allowed direction. For example, t_{1F} and t_{2F} are sequentially executed to go from room-place p_1 to room-place p_4 ; instead, t_{2R} and t_{1R} are sequentially executed to go from room-place p_4 to room-place p_1 . In few words, we build the complete net as follows.

We consider two places for each of the ordered resources required in every egress procedure e_k : an occupancy place and a residual capacity place. Then, for every occupancy place, we add a first input transition (acquisition event) with an output arc directed to the place, and a second output transition (release event) receiving an input arc from the place. The second transition for one resource is the same as the first transition for the next one in e_k . In this way, each transition gives the event determining the transfer of a person from a resource to the next one. Now, we consider the residual capacity place. An arc stems from it to the first transition for the occupancy place. In addition, an arc joins the second transition and the residual capacity place.

Modularity allows us to represent complex buildings by connecting several instances of the introduced elementary PN modules. Each instance will represent a different resource. Buildings constituted of different floors can be

represented. Namely, each floor is represented by a sub-net integrating several PN elementary modules, and each connecting lifter is represented by a module with the same structure as in Fig. 1: the two places represent the lifter occupancy and the residual capacity, the two transitions represent acquisition and release of the lifter.

3.2 Remarks About PN Generalization and Timing

If the PN modeling the considered system becomes too complex, then some abstractions make the PN more amenable. For example, hierarchical models can be defined, or colors can be associated to tokens, places and transitions.

Firstly, hierarchical decomposition allows to model complex and large systems by using a number of sub-modules, each being a PN. A main PN recalls several sub-nets, each representing a part of the system.

Secondly, *Colored Petri Nets* use colors as attributes of tokens to represent different behaviors or performance of (groups of) individuals, according to their sex, age, physical condition and psychological attitude, training to extreme conditions, etc. In this way, tokens are different each other.

Moreover, the previously introduced elementary PN modules consider untimed transitions, to easily represent the logical sequence of all the events in egress flows. The developed untimed model can be used for monitoring purpose, if each marking is mapped to a visualization of individuals in the considered environment. Thus, a simple control mechanism could be based on the monitored states. But timing can be introduced for the time necessary to exit from a room, to cross a corridor, even to pass through a gateway. Then, the time needed to evacuate a set of individuals can be estimated. This allows us to obtain a dynamical representation of successive states, to analyze the performance of the egress procedures, to simulate different scenarios, and to propose alternative control strategies.

Randomly distributed transition times take into account randomness of some processes and uncertainty of individual behaviors. To this aim, *Generalized Stochastic Petri Nets* are mostly used for performance modeling and evaluation. These nets consider both *immediate transitions* with zero firing time for instantaneous state changes, and *timed exponential transitions* for the amount of time needed to use resources. A *firing function* is defined for exponential transitions: the firing time is a continuous random variable with exponential distribution. A further generalization is with *Extended Stochastic Petri Nets*, that consider a general distribution for timed transitions.

Another remark is about availability of resources. Namely, spaces or gateways may become unavailable, because of particular events or phenomena in emergency conditions (fire, smoke, gas, blocked doors, lifters out of service, etc.). A properly designed supervisor may change the capacity of the resources in the PN based on sensor detection. Moreover, the supervisor blocks dangerous events (opening a door to a room which is firing): then, the associated

enabled transitions in the PN are inhibited by an empty input place; this place will be marked by the controller only if the event is permitted.

Finally, the mathematical foundation of PN makes it possible to analyze performance parameters and properties that must be guaranteed for the modeled system. Both formal analysis methods and simulation techniques exist. If a PN is live, then tokens may proceed, so that the flow of people through the exit is assured. If a PN is bounded, there is no token overflow, so that congestion and accumulation of people in certain locations is avoided. Furthermore, given the initial conditions of the evacuated environment, one can simulate a PN to observe and record behaviors, delays, throughput, the minimum/average/maximum number of evacuated people in a certain amount of time, the minimum time required to evacuate a given initial number and distribution of people.

4 The Case Study

In this section, we show how a PN models the evacuation from a structured building. In this context, simplifying assumptions concerning the building occupants and their behavior are made.

We consider a simple single floor building, consisting of four rooms and one corridor (Fig. 4). The main exit is at the end of corridor, and two secondary exits are in rooms 1 and 4. The corridor is accessible from each room. For sake of simplicity, only doors 6 and 8 allow bi-directional transits, whereas doors 7, 9, 10, 11 and 12 only allow flows toward the outside. Modules described in Sect. 3 are suitably combined by following the proposed approach to define the PN model of the building, which is depicted in Fig. 5. Table 1 describes the meaning of constitutive places and transitions. Figure 5 represents the initial state. In particular, rooms $\{s_2, s_5\}$ hold the maximum number of 3 tokens, so that their reception capacities are saturated (c_2 and c_5 empty). Corridor is initially empty (no tokens in s_3) and its capacity is given by tokens in c_3 . It is accessible from rooms $\{s_1, s_2, s_4, s_5\}$ through doors $\{p_6, p_7, p_8, p_9\}$, which are characterized by residual capacities $\{c_6, c_7, c_8, c_6\}$, respectively. Rooms s_1 and

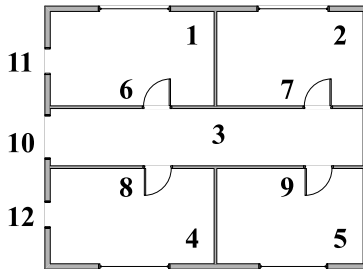


Fig. 4. Building layout for the case-study.

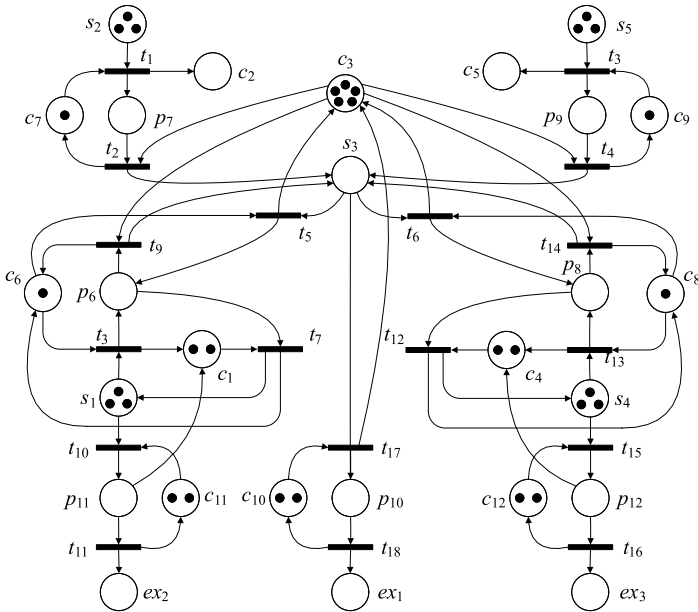


Fig. 5. Petri net for the case-study.

Symbol	Description
s_i, p_i	Occupancy places of room i and door i
c_i	Residual capacity place of room/door i
ex_i	Place for exit i
$t_1, t_3, t_8, t_{10}, t_{13}, t_{15}$	From rooms $\{2, 5, 1, 1, 4, 4\}$ to doors $\{7, 9, 6, 11, 8, 12\}$
t_5, t_6, t_{17}	From corridor to doors $\{6, 8, 10\}$
t_7, t_{12}	From doors $\{6, 8\}$ to rooms $\{1, 4\}$
t_2, t_4, t_9, t_{14}	From doors $\{7, 9, 6, 8\}$ to corridor
t_{11}, t_{16}, t_{18}	From doors $\{11, 12, 10\}$ to exits $\{ex_2, ex_3, ex_1\}$

Table 1. Symbols associated to places and transitions in the PN of the case study.

s_4 are not completely filled and can accommodate more individuals according to the number of tokens in c_1 and c_4 , respectively. All doors are considered initially clear, and external doors are characterized by a double capacity than internal ones.

Let us analyze transitions which allow system evolution. As far as internal ways are concerned, transitions $\{t_1, t_3, t_8, t_{13}\}$ represent acquisition of doors $\{p_7, p_9, p_6, p_8\}$ from individuals in rooms $\{s_2, s_5, s_1, s_4\}$, respectively. Each transition is enabled only if an individual, i.e. a token in the room place, wants to cross an available door (one token in the capacity place). Firing each transition determines the doors occupancy, so that the corresponding capacity is reduced. Transitions $\{t_2, t_4, t_9, t_{14}\}$ get enabled provided that the corridor

has enough space. Analogous remarks hold true for p_{10} , p_{11} and p_{12} , and for the corresponding transitions $\{t_{17}, t_{10}, t_{15}\}$ and $\{t_{18}, t_{11}, t_{16}\}$. Note that doors p_6 and p_8 allow reverse flows if transitions $\{t_7, t_{12}\}$ are enabled.

By analyzing the PN topology, it is possible to identify 15 main escape paths not considering complex trajectories (e.g. an individual going back to collect personal belongings, exploring different rooms, etc.). A sequence of resources defines each path. Starting from Room 1: $\{1, 11\}$, $\{1, 6, 3, 10\}$, $\{1, 6, 3, 8, 4, 12\}$; from Room 2: $\{2, 7, 3, 10\}$, $\{2, 7, 3, 6, 1, 11\}$, $\{2, 7, 3, 8, 4, 12\}$; from Room 3: $\{3, 10\}$, $\{3, 6, 1, 11\}$, $\{3, 8, 4, 12\}$; from Room 4: $\{4, 12\}$, $\{4, 8, 3, 10\}$, $\{4, 8, 3, 6, 1, 11\}$; from Room 5: $\{5, 9, 3, 10\}$, $\{5, 9, 3, 6, 1, 11\}$, $\{5, 9, 3, 8, 4, 12\}$.

5 Conclusion and Future Developments

We developed a systematic procedure to build PN models of egress procedures. These were used to derive the logic and possible trace of events in the simulated case-study. But they can also be used for monitor and control purposes. Namely, distributed sensors give information about locations of individuals, thus giving the PN token distribution, i.e. the current system state. Then, critical conditions can be checked (congestion, queues, doors blocked, etc.) and feedback of system state can be used to design control actions (inhibition of spaces, corridors, doors, signals for alternative escape routes, etc.). To this aim, the PN can be used to identify all escape routes and the minimal time/length one. In future works, the PN models could be timed, generalized and extended to analyze performance in different scenarios, to simulate random events and behaviors, and to allow definition of control supervisors.

Acknowledgements

This work is part of the Research Project “Infrastrutture di telecomunicazione e reti wireless di sensori nella gestione di situazioni di emergenza” funded by Regione Puglia.

References

1. M. Schreckenberg, S.D. Sharma, editors. *Pedestrian and Evacuation Dynamics*, Springer, Berlin, 2003.
2. N. Waldau, P. Gatterman, H. Knoflachner, M. Schreckenberg, editors. *Pedestrian and Evacuation Dynamics 2005*, Springer, Berlin, 2007.

3. P.J. Ramadge and W.M. Wonham. Supervisory control of a class of discrete event processes. *SIAM Journal on Control and Optimization*, 25(1):206–230, 1987.
4. B.P. Zeigler, H. Praehofer, and T.G. Kim. *Theory of Modelling and Simulation*, second edition, Academic Press, San Diego, 2000.
5. T. Murata. Petri nets: Properties, analysis and applications. *Proceedings of IEEE*, 77(4):541–580, 1989.

SIMULEM: Introducing Goal Oriented Behaviours in Crowd Simulation

Sébastien Paris¹, Delphine Lefebvre², and Stéphane Donikian²

¹ Cognitive Science Lab., Dep. of Computer Science and Software Engineering,
Laval University, Pavillon Pouliot, 1065 rue de la Médecine, G1K 7P4 Quebec,
QC, Canada
e-mail: parissebastien@free.fr

² Bunraku project-team, INRIA, Campus de Beaulieu, 35042 Rennes cedex, France
e-mail: dlefebvr@irisa.fr, donikian@irisa.fr

Summary. Simulating human activity is a research field with multiple applications, especially regarding the validation of public buildings. Early work in this area focused on security considerations, especially for evacuation scenarios. However, recent needs have emerged to validate a public building considering its normal operation in order to provide the best quality of service. This problem is addressed here by proposing a simulation tool for crowds of autonomous pedestrians, where individual behaviours take into account medium term goals. We propose an agent’s model with embodied and situated decision abilities which determine its movements inside the environment as well as its interactions with equipments. This model is applied in a tool called *SIMULEM*, which supports all the simulation phases from the environment’s specification to the results analysis. Finally, this tool is operated on real cases for the simulation of train stations by our industrial partners (*AREP* and *SNCF*).

1 Introduction

Architectural domain needs for crowd simulation in order to validate the design of buildings that can host a large number of users, such as train stations, bus stations, or airports. Some simulation tools already exist to study flows of people inside constrained areas (such as Legion [1] or Myriad [10] in Fig. 1), but they only address the most visible behaviour of human beings: *navigation*. Then, the environment is only considered as a set of obstacles to avoid, and the objectives of the simulated pedestrians are only a set of predefined destinations in the environment. This approach is generally used for evacuation scenarios, where the individuals only need low decisional abilities. Models already exist for realistic navigation in very populated environments, such as

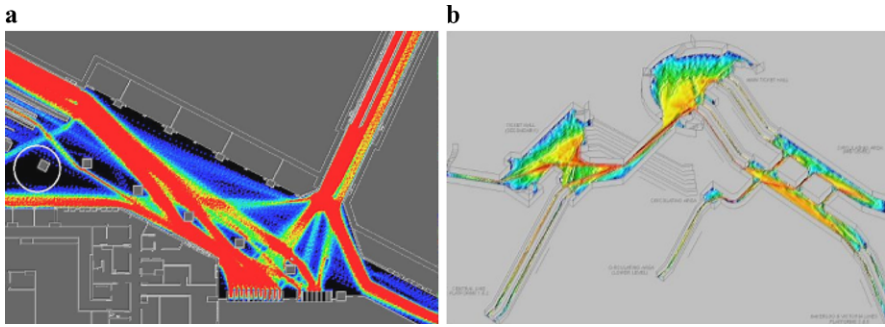


Fig. 1. Examples of the output of two commercial crowd simulation tools. **a** *Legion* from *Legion Limited* (www.legion.com). **b** *Myriad* from *Crowd Dynamics* (www.crowddynamics.com).

the particle based models [3] which are demonstrated for high densities of people [2].

However, real humans achieve higher level goals usually related to the interactions they must accomplish within their environment, such as in a train station: buying a ticket, consulting the departure board, etc. These interactions have a strong impact on the navigation tasks because they define a set of emergent destinations for a simulated pedestrian, and also provoke waiting queue formations. Thus, a goal oriented behaviour based on interactions with equipments should be placed at the heart of a simulation tool in order to study the everyday usage of public buildings.

We propose in this paper a new crowd simulation architecture which manages these kinds of high level behaviours for virtual humans. Our approach combines two main components. First, a realistic environment description represents exactly the geometry and topology of a public building. This environment is informed with interactive objects which situate the interaction opportunities, allowing to include them in the decision mechanism of a virtual human. Second, our virtual human is able to perform some interactions in the informed environment with regard to its goal oriented behaviours. Thus, the decision process of our virtual human takes into account its final goal, including all the necessary interactions to reach this goal and their impact on the navigation.

This paper is organised as follows. First, Sect. 2 describes our agents' goal oriented behavioural model. Then, we present in Sect. 3 an overview of our simulation architecture, with the different phases of a simulation. Finally, we demonstrate our approach over examples in Sect. 4. We conclude by presenting our perspectives in Sect. 5.

2 Goal Oriented Behavioural Model

2.1 Model Overview

We have based our behavioural model on a cognitive approach by adopting the well known *perception–decision–action* loop. In fact, the decision process of our autonomous agent is based on a multilayered model, which can easily be compared to A. Newell’s pyramid [5] (Fig. 2(a)). Each layer in this pyramid is independent from the others, only requiring a set of identified data to work. The upper layer of the pyramid, concerning the social behaviours, is not represented in our model and not addressed by this work.

Let us introduce the other layers of the pyramid, and the way they communicate (Fig. 2(b)):

- **Rational:** this layer is in charge of the **logical decisions** of the autonomous agent. These decisions are based on un-embodied notions describing the goals and sub-goals of the agent at a conceptual level. This layer also organises these goals to find the feasible actions independently of their location. Finally, this layer performs a pre-selection over the agent’s goals, to reduce their number for the next phase.
- **Cognitive:** this layer is in charge of the **situated decision** of the autonomous agent. This decision refines the pre-selection made at a rational level by taking into account the place where actions can be performed. Thereby, the impact of the actions on the agent’s necessary movements is considered. Finally, this layer elects one primary goal to perform, and a set of secondary goals. The remaining goals, if any, are temporarily ignored by the agent. The primary goal is managed by a behaviour which has a full control over the agent’s reactive abilities, such as the navigation. The secondary goals are managed by concurrent behaviours, which only have a limited control over the agent’s reactive abilities, in order to influence them. A typical control is to divert the agent from an optimal trajectory towards its primary goal in order to perform a secondary goal while walking. For example, an agent can read a sign while going to a cash dispenser, and so slow down to have enough time to fulfil the interaction.

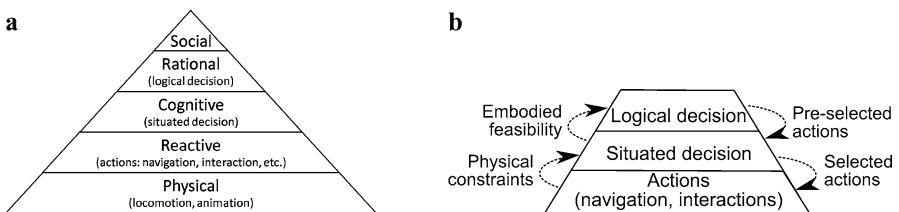


Fig. 2. Our multilayered model of decision in the same way as Newell’s pyramid. **a** Overview of the decision mechanisms of an agent. **b** Communication between the three central layers of the pyramid.

- **Reactive:** this layer is designated for the management of the finally selected **actions**. The short term decisions made at this stage only manage physical behaviours, like the navigation [9] or the perception [8] of the autonomous agent, but also the actions on objects. Finally, this layer directly control the lower layer of the pyramid by producing low level actions.
- **Physical:** this layer is in charge of the agent's **physiological** management. In our case, this management is limited to the locomotion and optionally the animation of the agent. Both of these tasks are directly managed by the *MKM* model [4] developed in our team.

We must emphasise that this goal oriented decision management needs an informed environment description to resolve the goals selection. Indeed, the rational layer must manipulate a conceptual representation of the environment in order to perform the pre-selection, and then the cognitive part requires to situate these concepts in order to spatially refine the selection. That is why we propose an architecture to describe and situate the interaction concepts.

2.2 Interaction Concepts

We propose a generic architecture defining the way interaction concepts operate together: *BIIO* [7] for *Behavioural Interactive and Introspective Objects*. Indeed, *BIIO* proposes an operational framework, which can be extended by specialising or unifying the proposed high level concepts. These concepts are mainly oriented towards interaction, which is certainly the kind of behaviours which have the most impact on the environment, and so on the results of a crowd simulation. We define an interaction to be any action between an autonomous agent and another embodied element situated in the environment, such as another autonomous agent or an equipment. The set of concepts we introduce are defined in Fig. 3.

- **Physical Object:** this concept describes a situated object, i.e. an object whose location is identified inside the environment. This concept is specialised in two other concepts:
 - **Effector:** this concept represents something which sustains an interaction, i.e. which participates to an interaction without having initiated it. For example, an equipment like a computer is an effector.
 - **Interactor:** this concept represents an autonomous agent which can realise an interaction. An interactor is able to manage two concepts representing its behaviours: the *affordance* and the *cognitive task*.
- **Affordance:** this concept describes an interaction between an interactor and an effector, and so a behaviour of the interactor which is directly observable. These interactions are defined globally in the virtual environment, allowing to easily add new affordances without having to modify the effectors nor the interactors. An affordance represents a goal for the interactor. Thereby, the rational and cognitive layers of the interactor choose

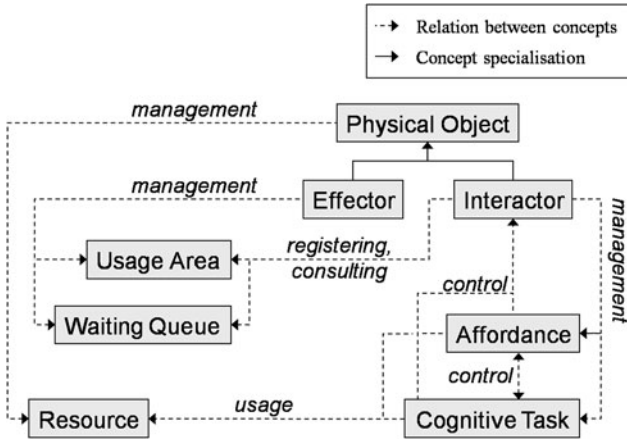


Fig. 3. Predefined set of concepts introduced with *BIIO*.

between a set of affordances required by the interactor. Moreover, the effectors also manage the affordances they are compatible with, for example concerning the waiting queue and the usage area managements.

- **Cognitive Task:** this concept describes an internal behaviour of the interactor, which is not directly observable. It allows to extend the internal behaviours of the agents to manage specific cases, such as simulating an agent with advanced perception abilities. Some cognitive tasks are also provided for all the agent, for example to manage the primary and secondary goals in the cognitive decision layer.
- **Resource:** this concept symbolises an internal property of a physical object, such as electricity for an equipment or the ability to move for an autonomous agent. A resource can be transitory or permanent, and can have multiple internal properties which might evolve. Both behavioural concepts (affordance and cognitive task) use resources to define their run, as for example to manage their competition. We propose four kinds of resources: *basic*, which can only be tested to be present or not (typically for a knowledge representation); *exclusive*, which can be reserved by only one process at the same time (like a member of an organism); *shared*, which can be reserved by several processes at the same time (like the perception ability of a human being); *dynamic*, which is a specialisation of the shared resource, whose parameter grows automatically (like the hunger).
- **Usage Area:** this concept describes the positioning of an interactor in order to use an effector. There are two kinds of usage areas: *single user*, if the interaction with the effector is only possible for one interactor at the same time, such as getting money at a cash dispenser; *multiple users*, if the interaction can be performed by many interactors at the same time, such as looking at a bulletin board. Usage areas are managed by the effectors

for any of their compatible affordances, and used by interactors to get informations about the way to interact.

- **Waiting Queue:** this concept describes the way interactors must socially organise in order to wait for a specific interaction with an effector. Three kinds of waiting queues are proposed: *none*, which means that the interaction cannot be waited for; *first in/first out*, which means that the first interactor which is waiting for the interaction will be the next user; *nearest*, which means that the closest interactor to the effector will be the next user. Waiting queues are managed on the same way as usage areas.

3 Simulation Architecture

We propose a novel crowd simulation software called *SIMULEM* which integrates our agent’s model. The architecture of *SIMULEM* is divided into four phases (Fig. 4), which are detailed in the following sections.

3.1 Simulation Software Upgrades

In order to easily improve the simulation tool, we propose a way to upgrade and extend its internal components thanks to external plugins. These extensions are allowed by *BIIO*, the interaction description and management framework, which allows to specialise the concepts it proposes. Additionally, some specific user interfaces can be added to the simulation software on the same principle. We will not detail these points here because they are out of the scope of this paper. One can all the same notice that this first phase is optional and is only available to computer science professionals, because of its high technical aspect. Finally, this first step produces plugins that are natively managed by the simulation software. These plugins can be used during the current simulation, and reused for any future simulation.

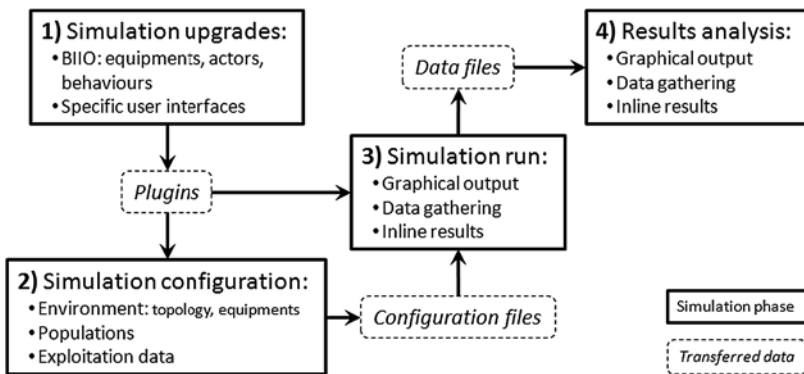


Fig. 4. The four phases of the *SIMULEM*’s simulation architecture.

3.2 Simulation Configuration

The simulation configuration phase allows a user to define information required to run a simulation. These information can be saved in an *XML* format, and so can be reused to run the same simulation or to configure a new simulation.

First, the user can define the environment of simulation by importing an external *AutoCAD* file (Fig. 5(a)). This file format is commonly used by architects to describe the plans of buildings. We have defined modelling standards for the *AutoCAD* tool allowing one to indicate the topology of multi floors buildings, and to position the available equipments at the same time. Then, the simulation tool is able to automatically extract all of these data from the *AutoCAD* file, and to store them in the *XML* file. From these data, the simulation tool produces an internal representation of the simulation environment thanks to a topological abstraction [6] which entirely preserves geometrical data (Fig. 5(b)). Then, the found equipments are automatically generated inside the virtual environment and configured.

When the virtual environment is defined, more specific configurations can be done for the populations, the trains, and the exploitation data. These configurations are directly done inside the simulation tool thanks to dedicated user interfaces. For the populations, some archetypes are first defined which corresponds to statistical distributions over the internal parameters of the simulated agents, such as speed, age, gender, size, etc. Then, populations are

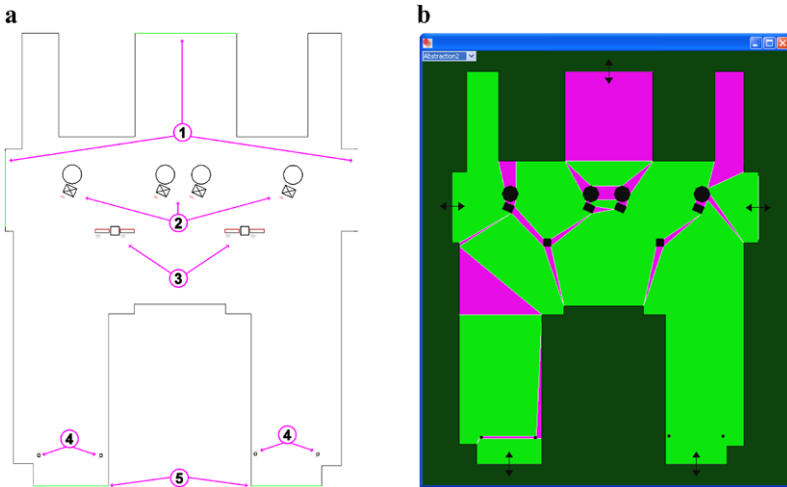


Fig. 5. Environment configuration with *SIMULEM*. **a** Initial *AutoCAD* definition. **b** Environment abstraction. The numbers on the *left picture* represent semantical information extracted from the *AutoCAD* file: (1) standard accesses of the train station, (2) ticket vending machines, (3) departure boards, (4) ticket punchers, and (5) train accesses.

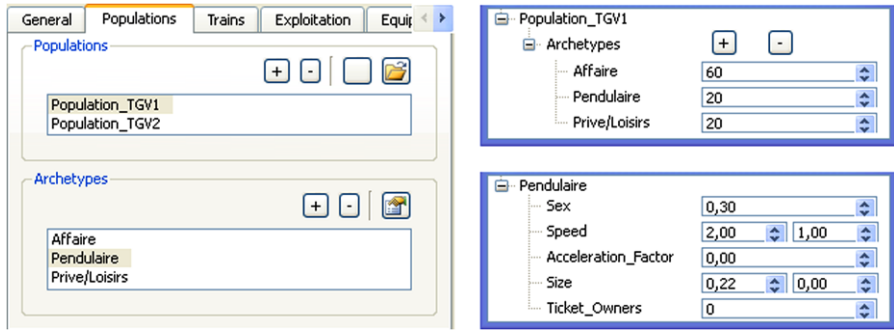


Fig. 6. Populations configuration with *SIMULEM*. A simulated entity belongs to a population class (*top right*), which is a statistical distribution over archetypes (*bottom right*), which are each defined by a statistical distribution over the internal parameters of a humanoid.

	Number	Departure Time	Arrival Time	From	To	Quality	Material	Population	Platform	engers in	engers out
1	5360	10:56	10:54	MARSEILLE ST CHARLES	RENNES	QualiteTGV_1	TGV_type1	Population_TGV1	Voie_1	100	100
2	5214	11:18	11:15	LILLE EUROPE	RENNES	QualiteTGV_1	TGV_type1	Population_TGV1	Voie_2	100	100
3	5326	10:56	10:51	PARIS	RENNES	QualiteTGV_1	TGV_type1	Population_TGV1	Voie_1	100	100
4	5128	10:57	10:52	BREST	PARIS	QualiteTGV_1	TGV_type1	Population_TGV1	Voie_2	100	100
5	5264	10:58	10:53	TOULOUSE MATABIAU	LILLE EUROPE	QualiteTGV_1	TGV_type1	Population_TGV1	Voie_1	100	100
6	5213	11:18	10:56	LILLE EUROPE	NANTES	QualiteTGV_1	TGV_type1	Population_TGV1	Voie_2	100	100
7	5318	12:00	11:27	RENNES	MARSEILLE ST CHARLES	QualiteTGV_1	TGV_type1	Population_TGV1	Voie_1	100	100
8	5224	12:21	12:18	LILLE EUROPE	RENNES	QualiteTGV_1	TGV_type1	Population_TGV1	Voie_2	100	100
9	5227	12:21	12:18	LILLE EUROPE	NANTES	QualiteTGV_1	TGV_type1	Population_TGV1	Voie_1	100	100
10	5218	12:30	12:28	LILLE EUROPE	TOULOUSE MATABIAU	QualiteTGV_1	TGV_type1	Population_TGV1	Voie_2	100	100
11	5368	12:48	12:45	MARSEILLE ST CHARLES	NANTES	QualiteTGV_1	TGV_type1	Population_TGV1	Voie_1	100	100

Fig. 7. Exploitation data configuration with *SIMULEM*. The exploitation data concerns the trains dynamics inside the station during the simulation, with all the information related to time, space, material, and involved population.

defined by a statistical distribution over some archetypes. For example, on Fig. 6 the population *Population_TGV1* is a distribution over the archetypes *Affaire* (people coming for *business* purpose), *Pendulaire* (people who just *pass by* the station), and *Prive/Loisir* (people coming for *leisure* purpose).

Finally, the exploitation data inside a train station concern the dynamics of trains. First, a user interface allows to define some train models: the number of rail cars, their capacity, the location of the doors, etc. Then, another interface contains all the data concerning the trains for the simulation (Fig. 7): their unique identifier, the departure and arrival times, the destination, the involved population, etc. Additionally, an arrival time distribution is specified for each train, which defines the amount of people who enters in the environment at relative times before the train arrival. All of these exploitation data are then automatically used by the simulator in order to generate and configure the

actors of the simulation, i.e. to create them through time, at a given location, and with a given goal.

3.3 Simulation Run

The third phase of the software architecture consists in running the simulation. Videos and pictures can be extracted from the simulation. A data file is also produced, which can be saved for the fourth phase.

The simulation can be done automatically by the tool in order to only retrieve some results for the next phase, or allows a user to interact with the tool for two purposes. First, one can change the simulation conditions on-line to check the impact of some events on the results. For example, a ticket vending machine could be turned off while the simulation runs, or the direction of an escalator can be changed. Second, one can extract on-line results to check the evolution of the simulation. These on-line results are various:

- the 3D animation of the simulation environment, with diverse camera options allowing to view all the scene (Fig. 8);
- 2D maps which summarise relevant data through time: local densities of people, trajectories, or instant speeds;
- graphics which present more quantitative data: input and output flows at the accesses of the station, or the total number of people inside the environment.

Finally, a user can control the simulation run with a remote control. This user interface allows the standard operations: start, stop, or pause the simulation. The user can also choose the acceleration factor of the simulation time compared to real time, with a maximal value limited by the hardware, and a special *free run* value without time constraint. This tool also presents the time information to the user: the simulation time, and the currently reached acceleration factor.

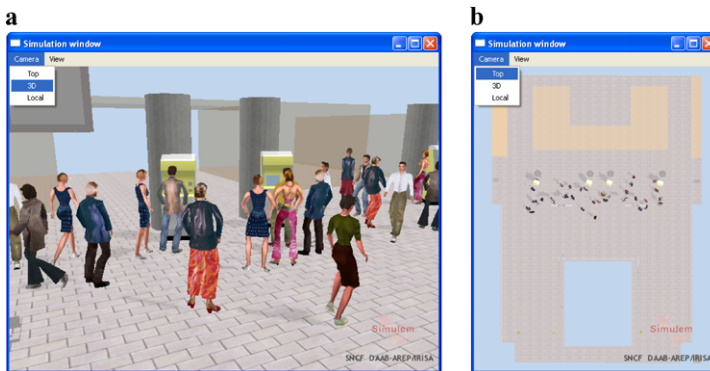


Fig. 8. Simulation 3D output with *SIMULEM*. **a** Free view. **b** Top view.

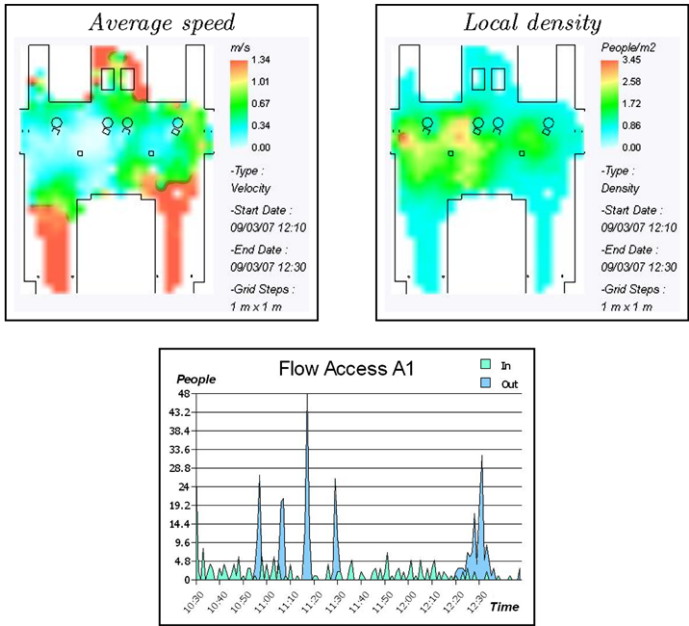


Fig. 9. Examples of the results output of *SIMULEM*. 2D maps: the average speeds (*left*) and local densities of people (*right*) for a given time interval in the environment. *Bottom graph*: incoming and outgoing flows of people for one access of the environment through time.

3.4 Results Analysis

The fourth and last phase of the simulation consists in the off-line analysis of the results of simulation runs. The analysis uses the data saved by the previous phase, which are mainly individual positions recorded over time for every simulated entities. These data can be presented to the user with graphical outputs and 2D maps, on the same way than the online results (maps and graphics are illustrated on Fig. 9). Moreover, the user can freely navigate through time to show the results of different instants. Finally, the user can select a time interval to either show instantaneous results, or average ones over a period.

4 Results

The *SIMULEM* architecture is industrially operated by our partners, *AREP* and *SNCF*, for the validation of exchange areas, and principally train stations (Fig. 10). The simulation performances are very good, allowing to fully simulate approximately 2,000 agents with full behavioural abilities in real time (without graphical output which divides the performances by two). Such high



Fig. 10. Crowd simulation of a real case: *Gare de Lyon in Paris*. All agents are fully autonomous with individual behaviours.

results allow to perform simulations of large environments with very high populations in a reasonable time, while maintaining a good behavioural realism.

5 Conclusion and Future Work

We have proposed in this paper a novel crowd simulation architecture. This architecture is easily upgradable to manage new simulation cases, either concerning the environment and equipments, or the actors of the simulation. Moreover, this architecture handles all the stages of the simulation, from the environment's description, to the simulation run, the results extraction, and finally their analysis. The simulation kernel is based on the most recent approaches of cognitive agent models, integrating an embodied and situated goal oriented behavioural mechanism. Thereby, *SIMULEM* does not only simulate people navigation, like actual evacuation simulators, but allows to perform a new kind of simulation where the goals of people are taken into account.

Our future work is divided in two parts. First, we plan on upgrading the agent's model with a social layer, allowing to manage groups of people. These groups will represent static social structures, like a family, or emergent structures, like the gathering of people with a similar attitude. Second, we plan on upgrading the simulation application for many purposes. We could upgrade the set of proposed *BIIO* concepts in order to simulate new kinds of environments, by proposing new effectors and affordances. This perspective will also require new user interfaces depending on the kind of exploitation data of the new environments. We have recently proposed a virtual reality application where a user can be immersed in the simulation by taking control of an agent. This possibility allows new validation perspectives, e.g. to check the visibility of signs depending on the density of people. Another possible application of this improvement is to cure psychological sickness, like agoraphobia.

Acknowledgements

We wish to thank our industrial partners of *AREP* and *SNCF* for their implication in this project. We also want to thank the *ANR* institution to have partially funded the *SIMULEM* project (reference *ANR05RNTL02501*). Finally, we want to thank the members of our team who have provided the *MKM* [4] animation module.

References

1. J. L. Berrou, J. Beecham, P. Quaglia, M. A. Kagarlis, and A. Gerodimos. Calibration and validation of the Legion simulation model using empirical data. In *Pedestrian and Evacuation Dynamics 2005*, pages 167–181. Springer, Berlin, 2007.
2. D. Helbing, L. Buzna, A. Johansson, and T. Werner. Self-organised pedestrian crowd dynamics: Experiments, simulations, and design solutions. *Transportation Science*, 39(1):1–24, 2005.
3. D. Helbing, I. Farkas, and T. Vicsek. Simulating dynamical features of escape panic. *Nature*, 407:487–490, 2000.
4. R. Kulpa, F. Multon, and B. Arnaldi. Specific representation of motions for interactive animation with several characters. *Computer Graphics Forum*, 24(3):343–352, 2005.
5. A. Newell. *Unified Theories of Cognition*. Harvard University Press, Cambridge, MA, 1990.
6. S. Paris, S. Donikian, and N. Bonvalet. Towards more realistic and efficient virtual environment description and usage. In *First International Workshop on Crowd Simulation (V-Crowds'05)*. VRlab, EPFL, Nov 2005.
7. S. Paris, S. Donikian, and N. Bonvalet. Behavioural interactive and introspective objects for crowd simulation. In *ACM SIGGRAPH / Eurographics Symposium on Computer Animation (poster session)*, Sep 2006.
8. S. Paris, S. Donikian, and N. Bonvalet. Environmental abstraction and path planning techniques for realistic crowd simulation. *Computer Animation and Virtual Worlds*, 17:325–335, 2006.
9. S. Paris, J. Pettré, and S. Donikian. Pedestrian reactive navigation for crowd simulation: a predictive approach. In *Computer Graphics Forum, Eurographics'07*, 2007.
10. G. K. Still. *Crowd Dynamics*. PhD thesis, University of Warwick, Department of Mathematics, Aug 2000.

Conflicts at an Exit in Pedestrian Dynamics

Daichi Yanagisawa^{1,2}, Akiyasu Tomoeda¹, and Katsuhiro Nishinari^{1,3}

¹ Department of Aeronautics and Astronautics, School of Engineering,
The University of Tokyo, 7-3-1, Hongo, Bunkyo-ku, Tokyo 113-8656, Japan

² Japan Society for the Promotion of Science, 1.8, Chiyoda-ku, Tokyo
102-8472, Japan

³ PRESTO, Japan Science and Technology Corporation, 7-3-1 Hongo, Bunkyo-ku,
Tokyo 113-8656, Japan
e-mail: tt087068@mail.ecc.u-tokyo.ac.jp

Summary. In this paper, we have detailedly studied the effect of conflicts on the pedestrian outflow through an exit. Pedestrians conflict each other at the exit, which is a bottle neck, when they evacuate from a room. The pedestrian outflow decreases when there are many conflicts. In the floor field model, which is a pedestrian model using cellular automata, the conflicts are taken into account by the *friction parameter*. However, the friction parameter is a constant and does not depends on the number of the pedestrians conflicting at the same time. We have extended the friction parameter to the *friction function*, which is a function of the number of the pedestrians involved in the conflict. The results of theoretical analysis using the friction function agree with the experimental results much better than using the friction parameter. We have also found that putting an obstacle in front of the exit increase the pedestrian outflow from our experiments. The friction function clearly explains the mechanism of the effect of the obstacle, i.e., the obstacle blocks a pedestrian moving to the exit and decrease the average number of pedestrians involved in the conflicts.

1 Introduction

Pedestrian Dynamics has been studied vigorously over last decades [1, 2]. Many microscopic models are developed such as the floor field (FF) model [3–6], the social force model [7], and the lattice gas model [8], to simulate the crowd of the pedestrians movement realistically. In addition to the simulations, there are also many pedestrian experiments [9, 10] to study collective behaviors of pedestrians.

The pedestrian behavior around a bottleneck and an exit is focused on by many researchers since it greatly affect total evacuation time in an emergency situation [4, 6, 9, 10]. One of the major phenomenon observed at an exit is a conflict, which occurs when more than one pedestrian move to the same place at the same time. When many conflicts occur, the pedestrian outflow, which is a number of pedestrians go through an exit per unit time, decreases.

In the floor field model, which is a pedestrian dynamics model using cellular automaton, conflicts are taken into account by *friction parameter* $\mu \in [0, 1]$. It describes clogging and sticking effects between pedestrians, and in a conflict situation, the movement of all involved pedestrians is denied with probability μ . Since μ is a constant parameter, the strength of clogging and sticking does not depend on the number of pedestrians involved in the conflict. In reality, however, it is more difficult to avoid a conflict when three pedestrians move to the same place at the same time than two pedestrians move to the same place at the same time. Therefore, we newly introduced the *friction function*, which is a function of the number of pedestrians involved in the conflict. This extension of the floor field model makes it possible to describe the pedestrian behavior around an exit more precisely and realistically, and the outflow obtained by the extended model agrees with the experimental data well.

We have also found that we can increase the pedestrian outflow by putting an obstacle in front of the exit from our experiments. The mechanism of the effect of the obstacle is difficult to explain by friction parameter, however, we have successfully explained it by the friction function.

This paper is organized as follows. In Sect. 2 we briefly review the FF model, and the friction function is introduced in Sect. 3. In Sect. 4 we show the conditions of our experiments, and compare the results of the experiments and the theoretical analysis using friction function in Sect. 5. In Sect. 6 the mechanism of increasing pedestrian outflow by obstacle is studied. Section 7 is devoted to summary and discussion.

2 Floor Field Model

2.1 Floor Field

We consider a situation that every pedestrian in a room moves to the same exit. The room is divided into cells as given in Fig. 1(a). Man shaped silhouettes represent pedestrians, an alphabet **E** and alphabets **O** represent the exit cell and obstacle cells, respectively. Each cell contains only a single pedestrian at most. Every time step pedestrians choose which cell to move from 5 cells: a cell which the pedestrian stands now $((i, j) = (0, 0))$ and the Neumann neighboring cells $((i, j) = (0, 1), (0, -1), (1, 0), (-1, 0))$ (Fig. 1(b)). Two kinds of FFs determine the probability of which direction to move, i.e., Static FF S_{ij} , which is the shortest distance to the exit cell, and Dynamic FF D_{ij} , which is a number of footprints left by the pedestrians [5]. The transition probability p_{ij} for a move to a neighbor cell (i, j) is determined by the following expression,

$$p_{ij} = N\xi_{ij} \exp(-k_s S_{ij} + k_d D_{ij}). \quad (1)$$

Here the values of the FFs S_{ij} and D_{ij} at each cell (i, j) are weighted by two sensitivity parameters k_s and k_d with the normalization N . There is a minus sign before k_s since pedestrian move to a cell which Static FF decreases.

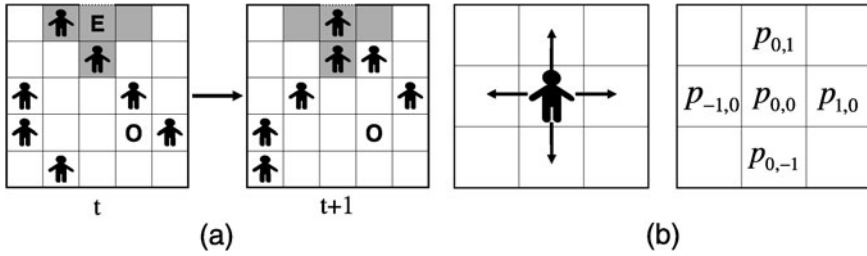


Fig. 1. a A schematic view of an evacuation simulation by the FF model. Pedestrians proceed to the exit by one cell at most by one time step. **b** Target cells for a pedestrian at the next time step. The motion is restricted to the Neumann neighborhood in this model.

ξ_{ij} returns 0 for an obstacle or a wall cell and returns 1 for other kinds of cells. Note that in our paper a cell occupied by a pedestrian is not regarded as an obstacle cell, thus it affects the normalization N . In the following, we consider only the effect of Static FF, i.e., $k_d = 0$.

When the bottleneck parameter $\beta \in [0, 1]$, which was introduced in [6], is considered, the transition probability of pedestrians who occupy one of the Neumann neighboring cells of the exit cell is described as follows:

$$\begin{cases} p_{ij} = \beta \bar{N} \xi_{ij} \exp(-k_s S_{ij} + k_d D_{ij}), & (i, j) \neq (0, 0), \\ p_{0,0} = (1 - \beta) + \beta \bar{N} \exp(-k_s S_{0,0} + k_d D_{0,0}), \end{cases} \quad (2)$$

where \bar{N} is the term necessary for normalization [6]. β controls the velocity of the pedestrians who are at the neighboring cells of the exit. When k_s is large, the transition probabilities of pedestrians at neighboring cells of the exit are approximated by using β [6]. This simplification enables us to analyze the pedestrian behavior theoretically.

2.2 Conflict Resolution and Friction

Due to the use of parallel dynamics it happens that two or more pedestrians choose the same target cell in the update procedure. Such situations are called conflicts in this paper. To describe the dynamics of a conflict in a quantitative way, *friction parameter* $\mu \in [0, 1]$ was introduced in [3, 4]. This parameter describes clogging and sticking effects between the pedestrians. In a conflict the movement of *all* involved pedestrians is denied with probability μ , i.e., all pedestrians remain at their cell. Therefore, the conflict is solved with probability $1 - \mu$, and one of the pedestrians is allowed to move to the desired cell (Fig. 2(a)). The pedestrian which actually moves is then chosen randomly with equal probability. In a situation with large μ pedestrians are competitive and do not give way to others. Thus they hardly move due to the conflict between them. Contrary in a situation with small μ they give way and cooperate each other.

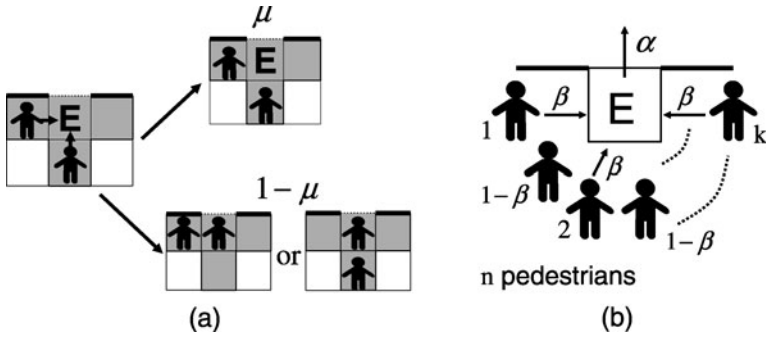


Fig. 2. **a** The way of solving conflicts. In a conflict situation, movement of all involved pedestrians remain at their cell with probability μ . One of them is randomly allowed to move to the desired cell with probability $1 - \mu$. **b** Transition probabilities of pedestrians around the exit cell **E**. α is the probability of getting out from the exit cell, and β is a bottleneck parameter, which is the probability of moving to the exit cell from the neighboring cells of it. k pedestrians are moving to the exit cell and $n - k$ pedestrians are staying at the neighboring cells in the figure.

3 Friction Function

3.1 Introduction of the Friction Function

The friction parameter, which represents the strength of clogging and sticking between pedestrians, is a constant and does not take the difference of the number of the pedestrians involved in the conflict into account. However, the clogging effect is stronger when three pedestrians conflict each other than when two pedestrians conflict each other. Therefore, we newly introduce the friction function μ_1 and μ_2 , which are functions of the number of pedestrians involved in the conflict, which is described as $k \in \mathbf{N}$. μ_1 and μ_2 are described as follows:

$$\begin{aligned} \mu_1(\zeta_1, k) &= 1 - \exp[-\zeta_1(k - 1)], \\ \mu_2(\zeta_2, k) &= 1 - (1 - \zeta_2)^k - k\zeta_2(1 - \zeta_2)^{k-1}, \end{aligned} \tag{3}$$

and both μ_1 and μ_2 satisfy the conditions of friction functions: $\mu_i(\zeta_i, 1) = 0$, $\mu_i(\zeta_i, \infty) = 1$ ($i = 1, 2$). The former equations mean that there is no conflict when only one pedestrian move to the exit cell, and the latter means that no one can move to the exit cell when greatly many pedestrians move to there at the same time.

μ_1 is one of the simplest form of friction functions, which satisfies the conditions of them. We decide to use an exponential function since it is used in the transition probability (1) in the FF model. An exponential function is also easy to analyze theoretically. $\zeta_1 \in [0, \infty)$ is friction coefficient, which represent the strength of the clogging irrelevant to k . When ζ_1 increases, μ_1 increases.

We define μ_2 by considering the psychological effect of pedestrians. $\zeta_2 \in [0, 1]$ is a probability of not giving way to others when more than one pedestrian move to the exit cell at the same time. The second term in the expression of μ_2 in (3) is the probability that every pedestrians involved in the conflict try to give way to others. The third term is the probability that only one pedestrian does not give way to others while the others do. By subtracting the two terms, which are the probabilities of resolving a conflict, we obtain the friction function μ_2 . When ζ_2 increases, μ_2 increases.

To deal in the friction parameter in the same way as the friction functions, we describe friction parameter as μ_0 in the following. The explicit form of friction parameter μ_0 is described as follows by using k , which is the number of pedestrians involved in the conflict.

$$\mu_0 = \begin{cases} 0 & (k = 1), \\ \zeta_0 & (k \geq 2). \end{cases} \tag{4}$$

ζ_0 is a value of friction parameter, when a conflict occurs.

Figures 3(a0), (a1), and (a2) are the plots of μ_0 , μ_1 , and μ_2 as a function of k , respectively. μ_0 is constant in $k \geq 2$, while μ_1 and μ_2 gradually increase as k increases and reflect the difference of the strength of clogging against k . ζ_1 and ζ_2 used in the figures are decided by the following equation:

$$\frac{\mu_i(\zeta_i, 2) + \mu_i(\zeta_i, 3)}{2} = \mu_0(\zeta_0, 2) \quad (i = 1, 2). \tag{5}$$

For example, the value of ζ_1 for the dashed line in Fig. 3(a1), i.e., 0.071, is decided by solving $(\mu_1(\zeta_1, 2) + \mu_1(\zeta_1, 3))/2 = \mu_0(0.1, 2) = 0.1$.

3.2 Average Pedestrian Outflow Through an Exit

In this subsection, the average pedestrian outflows through an exit using friction function are calculated. We extend the FF model around an exit and consider a situation that n pedestrians are at the neighboring cells of the exit cell **E** (Fig. 2(b)). The case $n = 3$ and $n = 5$ corresponds to the FF model using the Neumann neighborhood and Moore neighborhood, respectively. We consider the case that all pedestrians know the position of the exit and are going to there in the shortest way, i.e., $k_s \rightarrow \infty$ in the following. Then the probability of moving to the exit cell **E** is represented as β , and the probability of staying the neighboring cells is represented as $1 - \beta$. α is the probability of getting out from the exit cell, which is set as 1 throughout this paper. The probability of k pedestrians trying to move the exit cell is

$$b_k(\beta) = \binom{n}{k} \beta^k (1 - \beta)^{n-k}. \tag{6}$$

By using (6), the probability of one pedestrian succeeds to move to the exit cell is described as follows:

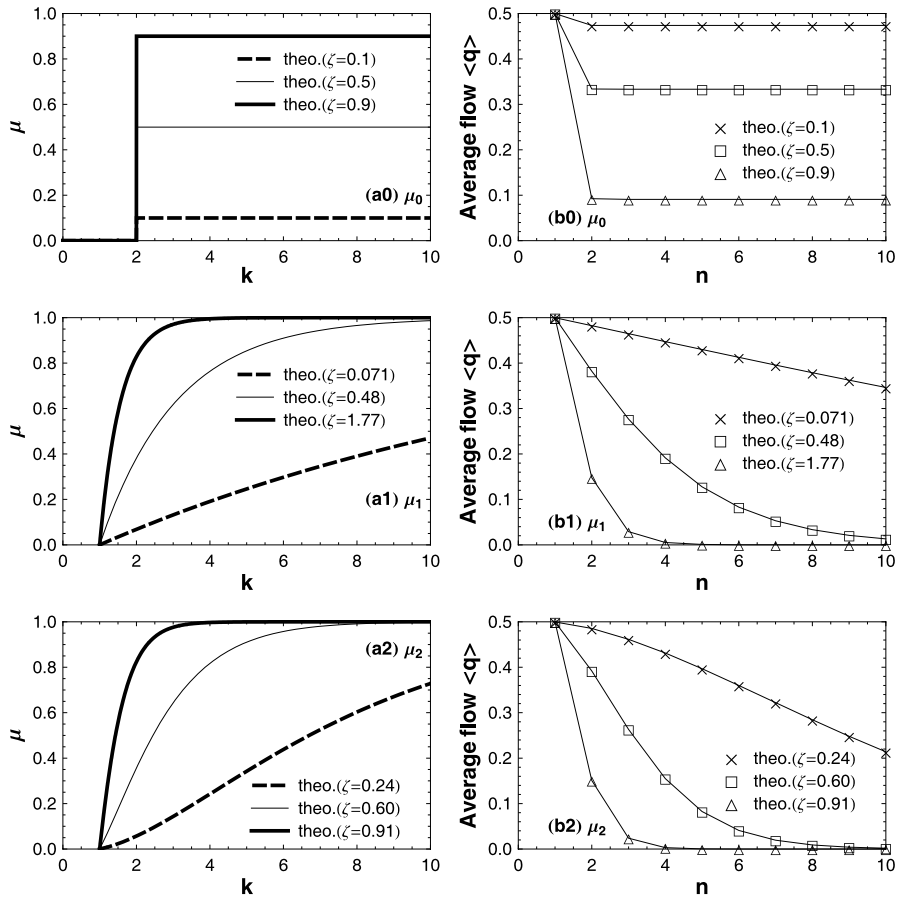


Fig. 3. **a** Values of the friction parameter and the friction functions against k , which is a number of pedestrians who move to the exit cell at the same. **a0** Friction Parameter $\mu_0(\zeta_0, k)$. **a1** Friction Function $\mu_1(\zeta_1, k)$. **a2** Friction Function $\mu_2(\zeta_2, k)$. We see that μ_0 is constant in $k \geq 2$, while μ_1 and μ_2 increase gradually. The values of ζ_1 and ζ_2 are calculated by (5). **b** Average pedestrian outflow against n , which is a number of pedestrians at the neighboring cells of the exit cell in the case $\beta = 1$. **b0** In the case using $\mu_0(\zeta_0, k)$. **b1** In the case using $\mu_1(\zeta_1, k)$. **b2** In the case using $\mu_2(\zeta_2, k)$. The average pedestrian outflows are constant in **b0**, however, decrease gradually in **b1** and **b2**.

$$r(\beta, \zeta_i, n) = \sum_{k=1}^n [(1 - \mu_i(\zeta_i, k))b_k(\beta)] \quad (i = 0, 1, 2). \tag{7}$$

We define $p_t(0)$ as the probability that a pedestrian is not at the exit cell at time step t and $p_t(1)$ as the probability that a pedestrian is at the exit cell at time step t . If greatly many pedestrians are gathering around the exit, i.e., there are always $n \in \mathbb{N}$ pedestrians at the neighboring cells of the exit cell,

the master equation is described as follows:

$$\begin{bmatrix} p_{t+1}(0) \\ p_{t+1}(1) \end{bmatrix} = \begin{bmatrix} 1 - r(\beta, \zeta_i, n) & \alpha \\ r(\beta, \zeta_i, n) & 1 - \alpha \end{bmatrix} \begin{bmatrix} p_t(0) \\ p_t(1) \end{bmatrix} \quad (i = 0, 1, 2). \quad (8)$$

By using (7) and (8) with the normalization condition $p_t(0) + p_t(1) = 1$, we obtain the average pedestrian outflow through an exit as

$$\langle q(\beta, \alpha, \zeta_i, n) \rangle = \alpha p_\infty(1) = \frac{\alpha r(\beta, \zeta_i, n)}{\alpha + r(\beta, \zeta_i, n)} \quad (i = 0, 1, 2). \quad (9)$$

The expression for the pedestrian outflow using μ_0 , i.e., friction parameter, was obtained in [6], which can be recovered using $\langle q(\beta, \alpha, \zeta_0, n) \rangle$. Thus (9) is a generalization of the previous result.

Figures 3(b0), (b1), and (b2) show the theoretical results of the average pedestrian outflow as a function of n , which is the number of pedestrians at the neighboring cells of the exit, in the case μ_0 , μ_1 , and μ_2 , respectively. Since the bottleneck parameter $\beta = 1$ in the figures, pedestrians are rushing into the exit cell. Thus, when n increases, the probability of conflicts increases, and the pedestrian outflows decrease in Figs. 3(b1) and (b2). However, in Fig. 3(b0), the pedestrian outflows are constant in $k \geq 2$. Therefore, the influence of the number of the pedestrians involved in a conflict on the pedestrian outflow in the case $\beta = 1$ is observed for the first time by introducing the friction functions.

4 Experiments

We did the evacuation experiment to verify the relation between the number of pedestrians at the neighboring cells of the exit cell n and the pedestrian outflow $\langle q \rangle$. The schematic view of the room is described in Fig. 4(a). The width of the exit is as wide as the breadth of the participants' shoulders, i.e., 50 cm. There are 18 participants of the experiment, who are all men.

The experiments started when we clapped our hands and finished when the all participants evacuated from the room. Six kinds of initial conditions are put into practice (Fig. 4(b)). In the case (E) and (F) pedestrians could move as they want after the evacuation started, however, in the case (A), (B), (C), and (D) pedestrians had to follow the former pedestrian, i.e., they were prohibited from putting the queues into disorder.

The results of the experiments are described in Table 1. There are three remarkable points in this table. First, we see that the pedestrian outflow decreases in $n \geq 2$. This indicates that when the number of pedestrians at the neighboring cells of the exit increases, the outflow decreases. Second, the maximum outflow is attained at $n = 2$. See Fig. 5(a), which is a snapshot of the experiment (B). We see that pedestrians in the left queue and the right queue go through the exit one after the other. This phenomenon is called

Case	(A)	(B)	(C)	(D)	(E)	(F)	(E&F)
n	1	2	3	4	–	–	–
Pedestrian outflow $\langle q \rangle$ [person/(m · s)]	2.65	2.94	2.68	2.47	2.44	2.52	2.48
Number of experiments	3	3	2	2	2	3	–

Table 1. The results of the experiments. “Case” in the table is corresponding to the case in Fig. 4(b) and n is the number of pedestrians at the neighboring cells of the exit cell. The pedestrian outflows in the table are the average of the several experiments. The numbers of the experiments are described in the last line of the table. The pedestrian outflow in the case (E&F) represents the average pedestrian outflow of the case (E) and (F).

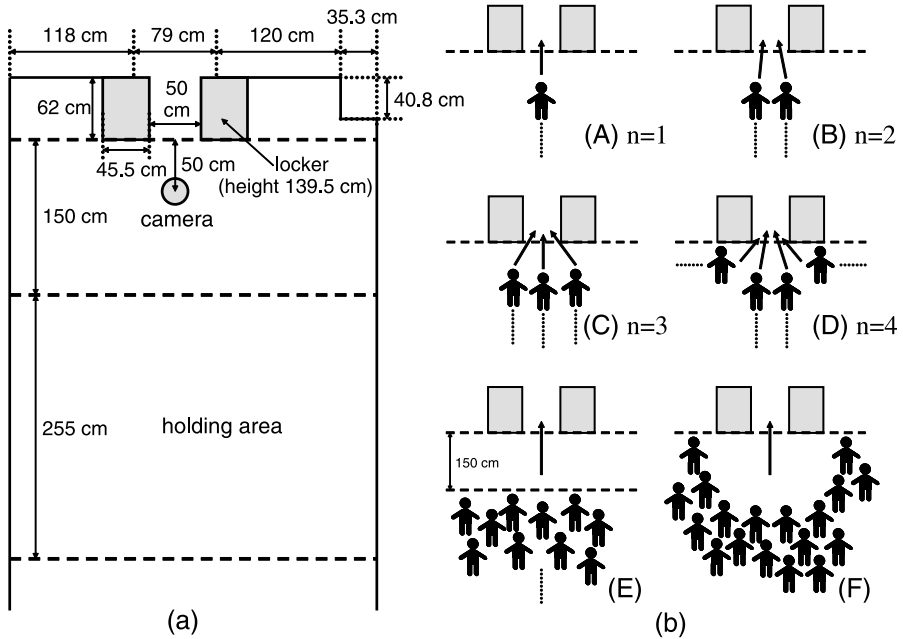


Fig. 4. **a** Schematic view of the room used in the experiments. The width of the door is 79 cm, thus we adjusted it to 50 cm by putting lockers in front of the door. The dashed lines in the figure are drawn for the explanation. They were not drawn in the experiment-room. **b** Schematic views of six initial conditions of the experiments.

zipper effect [10], when it occurs, the outflow increases since the number of conflicts between pedestrians decrease dramatically. Pedestrians are intelligent enough to avoid conflicts by their selves. Third, the pedestrian outflow in the case (D) ($n = 4$) and the average of pedestrian outflow in the case (E) and (F) (Table 1 (E&F)) are similar. This indicates that there are approximately four pedestrians at the exit in the normal evacuation situation when the width of the exit is 50 cm.

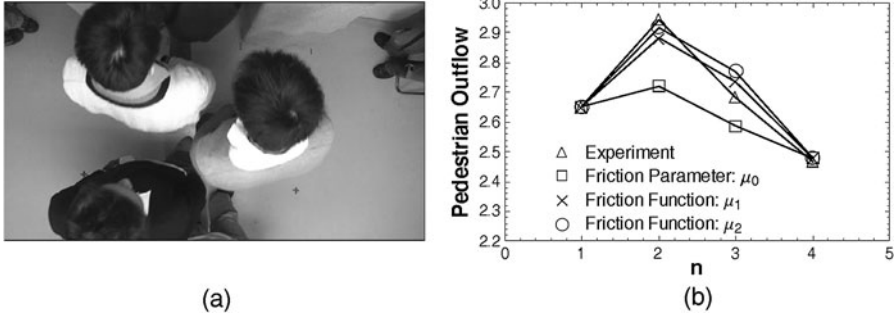


Fig. 5. **a** Snapshot of the experiment (B) ($n = 2$). The pedestrians in the left queue and the right queue go through the exit one after the other. **b** Pedestrian outflows of the experiment, the friction parameter μ_0 , and the friction functions μ_1 and μ_2 .

5 Comparison Between the Experiment and the Theory

In this section, we compare the pedestrian outflows from the experiment and the theoretical analysis using friction function. We calculate the parameter in the following way. First, we decide the β from the equation as follows by using the result of the experiment (A), and defining the cell size as $50 \times 50 \text{ cm}^2$ and 1 time step as 0.3 sec.

$$\langle q(\beta, 1, 0, 1) \rangle = 2.65 \times 0.5 \times 0.3 \quad (i = 0, 1, 2) \quad \rightarrow \quad \beta = 0.66. \quad (10)$$

In the experiment (A) there is no conflict, thus we obtain the value of β independent from the kinds of the friction functions. Next we calculate the friction coefficient ζ_i ($i = 0, 1, 2$) by using the value of (E&F) in Table 1. The experiments (A) to (D) are far from the real evacuation since the participants are forbidden from putting the queues into disorder; however, (E) and (F) are normal evacuation. Thus, we use the data of (E&F) to obtain the ζ_i in the normal evacuation situation. In Sect. 4 we found that there are approximately four pedestrians at the exit in the normal evacuation situation. Therefore, we decide $n = 4$. We obtain the value of ζ_i ($i = 0, 1, 2$) by solving the following equation:

$$\begin{aligned} \langle q(0.66, 1, \zeta_i, 4) \rangle &= 2.48 \times 0.5 \times 0.3 \quad (i = 0, 1, 2), \\ \zeta_0 &= 0.447, \quad \zeta_1 = 0.332, \quad \zeta_2 = 0.494. \end{aligned} \quad (11)$$

Figure 5(b) shows the pedestrian outflows of the experiment, the friction parameter, and the friction functions as a function of n , which is the number of pedestrians at the neighboring cells of the exit cell. We see that the results of the friction functions agree with that of the experiment very well, however, the results of the friction parameter does not. The value of the friction parameter is constant in $k \geq 2$. Thus, the friction parameter, which is decided by using the experimental result in the normal evacuation situation, i.e., $n = 4$, is large

for the case $n = 2$ and $n = 3$. The pedestrian outflow of the friction parameter is small for this reason. Since the friction functions consider the difference of n , they reproduce the value of the experiment.

6 The Effect of an Obstacle

We study the effect of the obstacle put in front of the exit in this section. We did the evacuation experiment at the NHK TV studio in Japan. Two large walls were set up in the studio, and we could adjust the width of the exit by moving them (Fig. 6(a)). We decided it as 50 cm. The participants of the experiment were fifty women, who were their thirties and forties. We did three kinds of experiments in Fig. 6. The experiment (a) (Fig. 6(a)) was the evacuation in a line, which was the same as the experiment (A) in Fig. 4(b)-(A). The experiment (b) (Fig. 6(b)) was the normal evacuation, whose initial condition was the same as the experiment (F) in Fig. 4(b)-(F). The initial condition and the way of the evacuation in the experiment (c) (Fig. 6(c)) was the same as the experiment (b), however, the column, whose diameter was 20 cm, was put in front of the exit.

Table 2 shows the pedestrian outflow of the three cases. The outflow in the experiment (a) is the largest, since there was no conflict. Comparing the

Experiment	Pedestrian outflow $\langle q \rangle$ [person/(m·s)]
(a) Going through the exit in a line	3.20
(b) Normal evacuation	2.75
(c) Putting an obstacle in front of the exit	2.93

Table 2. The result of the experiments. We did (a) three times, and (b) and (c) six times. The values are the average of the each experiment.

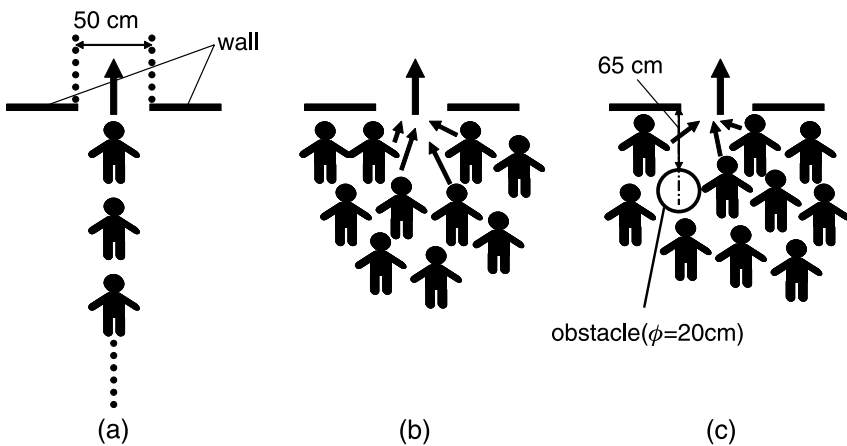


Fig. 6. Schematic views of the three kinds of experiments.

Kind of μ	ζ_i	Pedestrian outflow $\langle q \rangle$ [person/(m·s)]
μ_0	0.300	2.75
μ_1	0.133	2.94
μ_2	0.294	3.00

Table 3. Analytical calculation in the case experiment (c).

result of the experiment (b) and (c), we surprisingly find that the out flow of the experiment (c), i.e., the experiment putting an obstacle in front of the exit, is larger than the experiment (b), which is a normal evacuation.

Looking the video of the experiment, we see that the obstacle blocks the participant moving to the exit. In Sect. 4, we found that in the normal evacuation there are approximately four pedestrians at the exit, i.e., $n = 4$ (Fig. 6(b)). When the obstacle is put in front of the exit, there are approximately three pedestrians at the exit, since it blocks one pedestrian moving to the exit. Therefore, we consider that $n = 3$ in the experiment (c) (Fig. 6(c)). We decide β from the experiment (a) and ζ_i ($i = 0, 1, 2$) from the experiment (b) in the same way as in Sect. 5. Then we calculate the pedestrian outflow in the case experiment (c), i.e., $\langle q(n = 3) \rangle$. We obtain $\beta = 0.924$, and ζ_i ($i = 0, 1, 2$) and the pedestrian outflows as in Table 3.

We see that the pedestrian outflows of the friction functions μ_1 and μ_2 in Table 3 agree with that of the experiment(c) in Table 2 well again, while the pedestrian outflow of the friction parameter is much smaller. This result justifies our assumption that the obstacle increase the pedestrian outflow since it decreases n , which is the number of pedestrians at the neighboring cells of the exit cell.

7 Conclusion

In this paper we introduce the *friction function*, which changes its value against the number of pedestrians involved in a conflict. By using the friction functions, we obtained the more realistic figure of the pedestrian outflow through an exit, which corresponds to the result of the experiments very well. The pedestrian outflow using friction parameter does not agree with the experimental result well, therefore, the introduction of the friction function is necessary.

We also discovered that the pedestrian outflow increases by putting an obstacle in front of the exit in the experiment. Our assumption that the pedestrian outflow increases since the obstacle decreases the conflicts at the exit by blocking the pedestrians' movement is verified by theoretical calculation using friction functions.

The strength of a conflict is also affected by the pedestrians' walking velocities and the angle of the pedestrians' walking direction. Our future work is to obtain the friction function, which takes account of those effects.

Acknowledgements

This work is supported by Japan Society for the Promotion of Science. The experiment, which is described in Sect. 6, was supported by the NHK TV program *Science Zero* in Japan.

References

1. D. Chowdhury, L. Santen, and A. Schadschneider. *Phys. Rep.* 329, 199, 2000.
2. D. Helbing. *Rev. Mod. Phys.* 73, 1067, 2001.
3. A. Kirchner, H. Klüpfel, A. Schadschneider, K. Nishinari, and M. Schreckenberg. *Physica A* 324, 689, 2003.
4. A. Kirchner, K. Nishinari, and A. Schadschneider. *Phys. Rev. E* 67, 056122, 2003.
5. K. Nishinari, A. Kirchner, A. Namazi, and A. Schadschneider. *IEICE Trans. Inf. Syst.* E87-D, 726, 2004.
6. D. Yanagisawa and K. Nishinari. *Phys. Rev. E* 76, 061117, 2007.
7. D. Helbing and P. Molnar. *Phys. Rev. E* 51, 4282, 1995.
8. W. Song, X. Xu, B.H. Wang, and S. Ni. *Physica A* 363, 492, 2006.
9. T. Kretz, A. Grünebohm, and M. Schreckenberg. *J. Stat. Mech.* 10014, 2006.
10. A. Seyfried, T. Rupprecht, O. Passon, B. Steffen, W. Klingsch, and M. Boltes. [arXiv:physics/0702004](https://arxiv.org/abs/physics/0702004), 2007.

Improving Pedestrian Dynamics Modeling Using Fuzzy Logic

Phillip Tomé¹, François Bonzon¹, Bertrand Merminod¹, and Kamiar Aminian²

¹ Geodetic Engineering Lab (TOPO), EPFL, Station 18, 1015 Lausanne, Switzerland

e-mail: bertrand.merminod@epfl.ch

² Laboratory of Movement Analysis and Measurement, EPFL, Station 11, 1015 Lausanne, Switzerland

e-mail: kamiar.aminian@epfl.ch

Summary. The complementary nature of MEMS based pedestrian dead-reckoning (PDR) navigation and GNSS (Global Navigation Satellite System) has long been recognized. The advantages are quite clear for those applications requiring indoor positioning and that, for one reason or another, cannot rely on short-range infrastructure-based positioning systems (e.g. WiFi, UWB) to cope with the lack of availability of GNSS indoors. One such example of application is firemen coordination during emergency interventions.

Classification of human displacement using signal pattern recognition techniques often rely on an estimation model or statistical data to compute the step length or horizontal speed information. In general, an initial calibration phase is needed which can constrain the ability to follow the quasi-erratic behavior of a pedestrian in real time. Moreover, existing state-of-the-art PDR solutions enable only the reconstruction of the 2D trajectory.

This paper introduces a different approach to PDR navigation, in which pattern recognition is correlated to biomechanical principles and combined with fuzzy logic for detection and classification of a broader range of walking behaviors in 3D. Furthermore, to avoid the aforementioned limitations of stride length estimation, the step length is effectively computed by a simple inverse segment model during a specific phase of the gait cycle.

Besides a description of the algorithm, this paper includes results of a real-time implementation capable of detecting/classifying four different types of steps: forward walk, stair climbing, stair descent forward and stair descent backward. This development has been conducted in the framework of the European project LIAISON [Renaudin et al., Technical Reports D046 (2006) and D077 (2007), LIAISON Consortium Deliverable] funded by the Sixth Framework Program to specifically address one of its test case scenarios, the coordination of a fire brigade intervention.

1 Introduction

The first applications using inertial systems were developed for the marine and aviation fields. Nowadays, every ship, aircraft and spacecraft is equipped with some form of inertial system. The inertial systems used in pedestrian navigation are made of Micro Electromechanical Systems (MEMS). Sensors are placed somewhere on the walker and recorded signals are processed to derive changes in position. One of the main advantages of this approach is that the MEMS based positioning method is an independent and autonomous process that, contrary to other current position-tracking technologies, does not require any instrumented, marked or pre-mapped environment.

1.1 Conventional vs Pattern Recognition PDR Navigation

Two approaches are commonly used in PDR navigation: conventional inertial navigation using zero velocity updates or classification of human displacement using signal pattern recognition techniques. Usually, the former approach consists of a classical double integration of the accelerometer signals, that allows the computation of the traveled distance. However, this distance is affected by sensors noise and drift when sampling over a long period of time. While this method is appropriate when using high-grade sensors, it performs poorly when using low-cost sensors such as MEMS [3, 4].

The second approach, being less sensitive to the quality of the sensors, has to deal with the complexities of the human movement. Body motion induces inertial acceleration and a variable gravitational component due to the change of segment inclination with respect to the vertical axis. So, by attaching a MEMS sensors box to the walker's body, usually at the hip level, it is possible to associate the recorded data with signals signatures that enable to identify and quantify body displacements.

1.2 State of the Art Solutions in Gait Analysis

The Laboratory of Measurement and Movement Analysis (LMAM) of EPFL has developed monitoring devices (Physilog® and ASUR) and methods using MEMS sensors attached to body sites in the context of several bioengineering research programs. A patented method [5] has been introduced for monitoring physical activity based on identification of postural transition. In addition, an original and patented algorithm was proposed which computes the values of spatio-temporal gait parameters from angular velocity of the lower limbs [6] (Fig. 1).

The state of the art solutions in PDR navigation compute the step length thanks to estimation models or statistical data [7], and do not deal with vertical displacement in 3D. We introduce a method to effectively compute

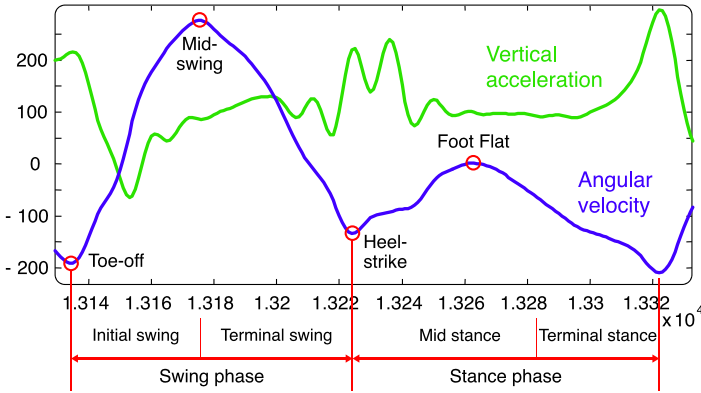


Fig. 1. Signals from a shank MEMS sensor during a full gait cycle, showing the main gait events and phases.

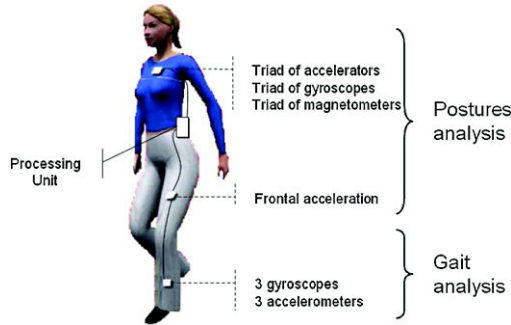


Fig. 2. Distributed MEMS sensors architecture.

the stride length using a simple inverse pendulum model, and a classification of a broader range of walking behaviors in 3D using fuzzy logic.

2 Gait Analysis

In the framework of the LIAISON project, we intend to develop a novel approach to pedestrian navigation. By placing the MEMS sensors in specific body parts, one may be able to infer specific movements for navigation purposes. Based on EPFL’s past research activities, three main placements were identified: the trunk, the thigh and the shank, as illustrated in Fig. 2. The top part of the body is essentially useful for postures detection and pedestrian orientation determination, while the lower part of the body offers great possibilities for gait analysis. Sensors mounted on the legs allow the computation of traveled displacement in the horizontal direction but also in the vertical dimension, for example when climbing stair.

3 Step Type Classification

The interviews of fire-fighters have allowed to focus the research effort only on basic and recurring movements. A new approach was developed on the classification of four classes of activity: flat forward walk (FW), stair ascent (SA), stair descent forward (SDF) and stair descent backward (SDB). The backward descent is a specific requirement of the fire brigade because it is safer and easier than descending in the usual forward direction. In fact, with backward descent, a fall tends to be less dangerous.

To classify the detected step into a class, an original Mamdani fuzzy classification system was used (see Fig. 3). Based on the periods of the activities so far, the whole period of monitoring was divided into a list of several smaller periods and parameters. Each of these smaller periods or parameters was a fuzzy input variable and was passed to the fuzzy classifier to decide the type of activity:

- **FFV** The value of the shank velocity at the Foot Flat time. Determined as the maximum peak of the shank velocity between the Heel-Strike and the Toe-Off of the next step.
- **DAP** Difference Anterior Posterior. The difference of the velocity between the Mid-Swing and the Toe-Off.
- **DPA** Difference Posterior Anterior. The difference of the velocity between the Heel-Strike and the Mid-Swing.
- **APV** Acceleration Peak value. Determined as the minimum peak of the shank acceleration between the Toe-Off and the Mid-Swing.
- **APT** Time of the APV, relative to Toe-off to Mid-Swing period.
- **A_amp** Absolute amplitude of acceleration signal during the entire cycle.
- **LastState** The activity immediately before the current activity.
- **MSM** Mid-Stance Mean. The mean of the velocity during a small period of the mid-stance.
- **Nb_succ** The number of SA, SDF or SDB performed consecutively.

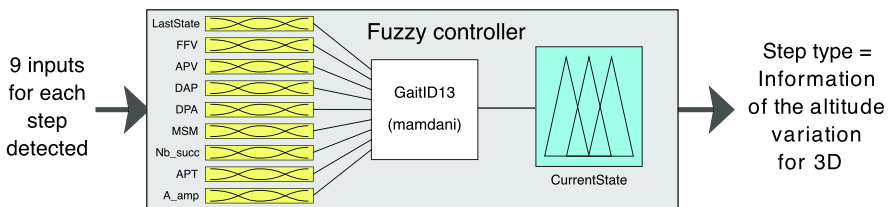


Fig. 3. The use of a fuzzy logic allows the handling of the diversity of walking patterns among different subjects, or for the same subject under different conditions.

4 Stride Length Computation

During the mid-stance and the terminal phase, the leg can be modeled as a simple inverse pendulum (see Fig. 4). The distance d is obtained from the angular velocity of the shank. By considering α the angular rotation of the shank during this phase, it is calculated from the trigonometric relation

$$d = L \cdot \sqrt{2 \cdot [1 - \cos(\alpha)]} \tag{1}$$

where the angle α is computed by integrating the angular rate rotation of the shank during this phase. The length of the leg L is estimated by the assumption that $L = 0.54 \cdot \text{height of user}$. The mean walking velocity is then given by

$$V = \frac{d}{T2 - T1} \tag{2}$$

where $T2$ is the end of the terminal stance and $T1$ is the beginning of the mid-stance. Finally, the mean stride length corresponds to

$$ST = V \cdot GCT \tag{3}$$

where GCT is the gait cycle time.

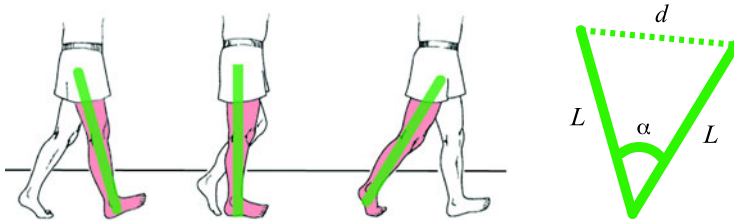


Fig. 4. Rotation of the leg during mid-stance and terminal stance.

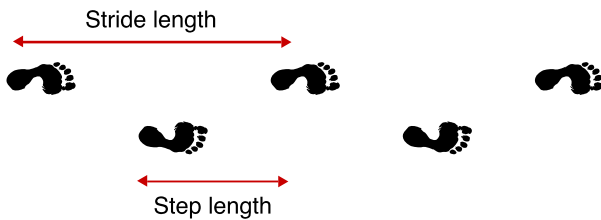


Fig. 5. The stride length is double, and not to confuse with, the step length.

	Sensitivity	Specificity
Forward Walk (FW)	98.1 ± 0.6	97.8 ± 0.8
Stair Ascent (SA)	93.5 ± 1.7	98.9 ± 1.5
Stair Descent Forward (SDF)	95 ± 3.1	99.1 ± 3.2
Stair Descent Backward (SDB)	96.1 ± 1.2	98.5 ± 1.8

Table 1. Performance of the system in detecting basic walking.

5 Tests and Results

To evaluate the performance of the classification algorithms, two statistics were calculated: sensitivity and specificity. The sensitivity parameter is defined as the capacity of the algorithm to correctly identify the walking type, and the specificity as the ability not to provide false identification. Table 1 shows the performance of the proposed method in the detection of basic activities during a specific experiment. The test was performed by a group of 5 healthy adults with average age of 28 years and they consisted of 5 consecutive trials for SA, SFD, SDB and FW. Except for FW, all trials were performed on the stairs of a building composed of 66 steps and a foot flat at each 11 steps.

6 Conclusion

An original fuzzy logic classifier has been developed to improve the detection and the identification of the gait. The type of activity detected was restricted in order to focus on the basic and recurring movements of the users. Based on the results obtained, this new algorithm appears especially promising.

References

1. V. Renaudin, O. Yalak, P. Tomé, B. Merminod, B. Najafi, and K. Aminian. D046, EPFL contribution on MEMS based positioning. Technical report, LIAISON Consortium Deliverable, 2006.
2. V. Renaudin, O. Yalak, P. Tomé, B. Merminod, and K. Aminian. D077, EPFL contribution on MEMS-AGPS hybridisation. Technical report, LIAISON Consortium Deliverable, 2007.
3. R.G. Stirling. Development of a pedestrian navigation system using shoe mounted sensors. Master's thesis, University of Alberta, 2004.
4. E. Foxlin. Pedestrian tracking with shoe-mounted inertial sensors. *IEEE Computer Graphics and Applications*, 2005.
5. B. Najafi and K. Aminian. Body movement monitoring system and method. Patent EP 00810 920.9, October 2000.
6. K. Aminian, C. Bula, P.-F. Leyvraz, and Ph. Robert. Spatio-temporal parameters of gait measured by an ambulatory system using miniature gyroscopes. *Biomech*, 35:689-699, 2002.
7. Q. Ladetto. *Capteurs et algorithmes pour la localisation autonome en mode pédestre*. PhD thesis, Ecole Polytechnique Fédérale de Lausanne, 2002.

Modeling the Link Volume Counts as a Function of Temporally Dependent OD-Flows

Dietmar Bauer

arsenal research, Giefingg. 2, 1210 Wien, Austria
e-mail: Dietmar.Bauer@arsenal.ac.at

Summary. This paper proposes a model for parameterizing time dependent origin-destination (OD) matrices. This model builds the basis for the exploitation of high frequent count data for the estimation of OD-matrices. Such data sets become increasingly available due to recent advances in automatic pedestrian counting technology paired with a business interest to analyze the number as well as the fluctuation of the number of customers for shopping centres or passengers for junctions of mass transport. OD-matrices are needed for simulation, monitoring of the demand and (depending on the location of the counting sensors) for the evaluation of the attractiveness of parts of the building. The model contains a full specification of the data set including a stochastic model for the measurement errors which directly suggests a method for the estimation of the parameters.

1 Introduction

Despite the fact that OD-flows are a main input to pedestrian simulation models, there are not many options for measuring them for a given pedestrian infrastructure such as e.g. a subway station or a shopping centre. Shadowing has been the primary observation method but is only able to provide data for a very small sample over a limited time span. Therefore in particular information on the dependence on time for the OD-flows cannot be extracted from this data source. Also a quantification of the estimation accuracy is hard if not impossible to obtain. These disadvantages are shared by all survey based methods.

Recently automatic pedestrian counting techniques (based on video or infrared technology) have been marketed and incorporated in some public infrastructures such as airports, subway stations and supermarkets. These methods allow to obtain high frequent count data covering all entries and exits of a particular counting region to measure bidirectional pedestrian flows. In most cases it is not possible to infer OD-flows directly from the link volume counts. This paper provides a model linking specific link volume counts to

OD-flows and thus provides the basis for the estimation of OD-matrices from this data source.

The outline of the paper is as follows: In the next section the structure of the data sets needed is described. Section 3 presents the proposed model and in Sect. 4 the implications of the model are discussed.

2 Data Sets

In this paper we consider a situation where for a public infrastructure pedestrian counting sensors are located at every entry/exit delivering for a large number of intervals per day the bidirectional (entering and leaving) pedestrian flow data. The interval length offered by commercially available systems ranges between 30 seconds and 15 minutes. Assuming that there are I entries and J exits the measurements are denoted as $In_{t,i}$ and $Out_{t,j}$, $t = 1, \dots, T$, $i = 1, \dots, I$ and $j = 1, \dots, J$ where t indexes the time interval and i and j respectively index the entries/exits.

For the model to be presented below it is vital that all relevant entries and exits are covered by the measurement. OD-flows can only be reconstructed in areas where all in- and outgoing flows are counted (except possibly for doors where it is known that only negligible quantities occur that are of the same magnitude as typical measurement noise). The measurement technology on the other hand is not of importance for the applicability of the proposed model (while of course the measurement accuracy strongly affects the achievable results) and hence e.g. video based counting systems can be mixed with infrared based counts.

Every measurement is subject to measurement errors. Empirically the measurement error of the used people counting system can be evaluated. In several cases¹ it was found that the measurement errors typically involve a heteroskedastic component of increasing variances for increasing number of persons to be counted. Also it was found that counts based on a small observation interval such as 120 seconds tend to be unreliable, while fifteen minute counts provide good information in terms of signal/noise ratio. For 120 seconds a signal to noise ratio as low as approximately 3 has been observed for an infrared based counting system (corresponding to a deviation of ± 3 persons for 10 persons), while also uncorrelatedness over time is observed such that the signal/noise ratio roughly triples for the fifteen minutes counts. For video based systems similar accuracies have been observed.

¹ Experiments performed at arsenal research within the projects ‘OD-Metrics’ and ‘RAVE’ support this claim, see [1].

3 The Proposed Model

The proposed model extends the models used for explaining turning fractions in individual vehicular traffic (see e.g. [2–5]) and builds on the intuitive assumption that everybody entering the infrastructure has to leave it in a later interval. Hence for each entry i the number $In_{t,i}$ of pedestrians entering the infrastructure in the t -th time interval of the observation period is distributed on the J exits and the subsequent $L + 1$ time intervals which is characterized by providing the fractions $\beta_{t,i,j,l}$, $j = 1, \dots, J$, $l = 0, \dots, L$ such that

$$0 \leq \beta_{t,i,j,l} \leq 1 \quad (j = 1, \dots, J, l = 0, \dots, L),$$

$$\sum_{j=1}^J \sum_{l=0}^L \beta_{t,i,j,l} = 1 \quad (i = 1, \dots, I, t = 1, \dots, T).$$

This leads to the model equation

$$Out_{t,j} = \sum_{i=1}^I \sum_{l=0}^L \beta_{t-l,i,j,l} In_{t-l,i} + u_{t,j} \quad (t = L + 1, \dots, T, j = 1, \dots, J). \quad (1)$$

Here $u_{t,j}$ denotes the residuals summarizing a number of different effects:

- measurement errors in the outgoing counts,
- effects of measurement errors in the ingoing counts,
- model errors due to quantization effects or choice probabilities.

Here $\beta_{t,i,j,l}$ denotes the expected fraction of pedestrians entering the infrastructure in the time interval t via entry i and leaving the infrastructure l time periods later via exit j . The actual fraction of people making this choice need not coincide with the expected fraction. For fixed i and t the coefficients $\beta_{t,i,j,l}$ ($j = 1, \dots, J$, $l = 0, \dots, L$) specify a multinomial distribution. If each person independently makes a decision based on this distribution, then the expected fractions coincide with $\beta_{t,i,j,l}$ providing an interpretation of the coefficients.

The parameters in the model according to (1) are restricted which can be avoided using the logistic function:

$$\beta_{t,i,j,l} = \frac{\exp(\gamma_{t,i,j,l})}{\sum_{a=1}^J \sum_{b=0}^L \exp(\gamma_{t,i,a,b})}.$$

The parameters $\gamma_{t,i,j,l}$ have the advantage that they are unrestricted. For every possible choice the resulting parameters $0 < \beta_{t,i,j,l} < 1$ are the probabilities of a discrete random variable. Moreover, for each combination of t, i one parameter $\gamma_{t,i,j,l}$ can be set to zero in order to eliminate nonidentifiability of the model. The restrictions $\beta_{t,i,j,l} = 0$ can be imposed further reducing the number of parameters.

Clearly this model is not estimable since it contains too many parameters since only ITJ measurements are available but $IT(J(L + 1) - 1)$ parameters

must be supplied. Here in particular the dependence on time introduces many parameters.

Thus in this paper it is proposed to model explicitly the dependence on time using a flexible model structure. Thus let $\gamma_{t,i,j,l} = f(t; \theta_{i,j,l})$ where $f(x; \theta)$ denotes a function of time depending on the parameter $\theta \in \mathbb{R}^d$. This reduces the number of parameters needed significantly if $d \ll T$. In this paper neural networks based on radial basis functions are used in order to parameterize a flexible class of univariate functions $f(\tilde{t}; \theta)$ where \tilde{t} denotes the time of the day. Of course this specification is somewhat arbitrary. Instead of modeling the dependence on the time of the day analogously also the dependence on other factors could be modeled such as e.g. a temporal drift or seasonal changes.

Neural networks achieve flexibility by linearly combining a number of components (typically called nodes) such that

$$f(\tilde{t}; \theta) = \sum_{m=1}^k \theta_{m,1} \varphi(\theta_{m,3}(\tilde{t} - \theta_{m,2})^2) + \theta_0$$

for some function $\varphi : \mathbb{R} \rightarrow \mathbb{R}$. Typical choices for φ include the Gaussian bell curve and the logistic function $\varphi(x) = (1 + \exp(-x))^{-1}$ (see Fig. 1). According to [6] this class of functions has the property to be able to approximate each continuous function arbitrarily well (in a certain sense) for a wide range of functions φ (essentially only linear functions are excluded) for k large enough. However, depending on the function to be approximated different choices of φ might lead to different required values of k in order to provide a reasonable approximation accuracy.

For k nodes these models hence require the specification of $3k + 1$ parameters. Summing up the elements given above we obtain the model

$$\beta_{t,i,j,l} = \frac{\exp(\gamma_{t,i,j,l})}{\sum_{a=1}^J \sum_{b=0}^L \exp(\gamma_{t,i,a,b})}$$

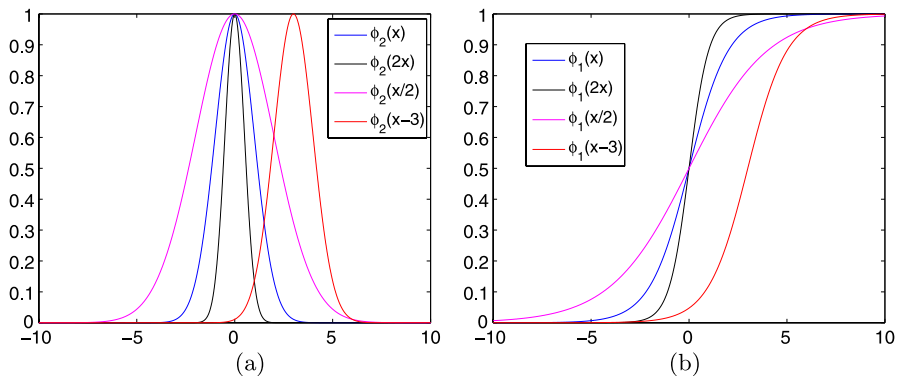


Fig. 1. **a** Gaussian bell curve and **b** logistic function, for different values of θ_2, θ_3 .

$$\gamma_{t,i,j,l} = \sum_{m=1}^k \theta_{m,1}^{(i,j,l)} \varphi(\theta_{m,3}^{(i,j,l)} (\tilde{t} - \theta_{m,2}^{(i,j,l)})^2) + \theta_0^{(i,j,l)}$$

or $\beta_{t,i,j,l} = 0$ for the restricted entries.

4 Discussion of the Model

There are two **assumptions** underlying this model: First the existence of a maximal duration of L time periods. This seems to be a mild assumption, as in most infrastructures the time spent inside the infrastructure is rather limited for the overwhelming majority of visitors. For subway stations it seems to be fair to assume that most passengers will not stay longer than half an hour, for shopping centers two hours seems an appropriate length of stay.

Second and more important the model is based on the assumption that for every day the pedestrians entering at a specific time interval via a given door are distributed across durations of stay and exits using a fixed and constant (i.e. not changing for different days) discrete distribution specified by providing the expected fractions. This does not imply that the actual fractions are constant but that they deviate from their mean value only by chance. This will be unrealistic for many infrastructures where also a weekly periodicity is expected. In this case separate models for each day of the week need to be specified. Other than that the assumption appears to be reasonable. Moreover, within a statistical framework this assumption can also be tested for.

There are two important **implications** that can be derived from the model: The coefficients $\beta_{t,i,j,l}$ determine the expected OD-flows and the expected durations of stay as a function of the door where pedestrians enter as well as of the time of the day. Summing the number of exiting pedestrians specified via the fractions $\beta_{t,i,j,l}$ one obtains the expected OD-flows:

$$OD_{t,i,j} = \sum_{l=0}^L \beta_{t-l,i,j,l} In_{t-l,i} \quad (t = L + 1, \dots, T, i = 1, \dots, I, j = 1, \dots, J). \quad (2)$$

Secondly the expected duration of stay can be calculated:

$$D_{\tilde{t},i} = \sum_{l=0}^L l \left(\sum_{j=1}^J \beta_{\tilde{t},i,j,l} \right) \quad (\tilde{t} = 1, \dots, \tilde{T}, i = 1, \dots, I). \quad (3)$$

This information potentially is valuable for the infrastructure management, if the length of the stay is related to the activity inside the infrastructure (e.g. for cinemas, restaurants and cafes).

Using this model estimation methods can be proposed which can be used in order to continuously estimate actual OD-flows: Note that (1) provides a parametric model giving the residuals $u_{t,j}(\theta)$ as a function of the in- and outgoing counts. Automatic pedestrian counting systems provide large databases

which can be used in order to improve the model accuracy by including more parameters as more observations are available. Here it is important to take the characteristics of the data set into account. Since the ingoing counts (acting as regressors in the equations) are observed only subject to measurement errors, conventional least squares estimation is prone to estimation biases. As an alternative instrumental variables or their generalizations, i.e. generalized methods of moment (GMM) estimators (see [7]) can be used. More details on the estimation procedure are contained in [8].

This provides a method for the estimation of OD-flows which does not show the same limitations as shadowing and survey based methods since it is able to provide a complete picture of the temporal dependence of the OD-flows on seasonal, weekly or daily patterns. Moreover, since a completely specified stochastic model is used it is possible to provide estimates of the achieved accuracy for the estimated models.

The major challenge for the approach lies in the typically huge dimension of the parameter set. If no coefficients are restricted to equal zero the number of parameters to be estimated equals (if for each component the same number k of nodes is used) $I(J(L+1)-1)(3k+1)$ and hence e.g. for $I=J=3$, $L=3$, $k=4$ the parameter space is of dimension 429. This poses challenges in terms of model selection as well as initialization for the nonlinear search procedures typically used to obtain the parameter estimate.

Acknowledgements

The presented results originated in the project “OD-Metrics” that was co-funded by the Austrian Ministry of Transport, Innovation and Technology (BMVIT) which is gratefully acknowledged.

References

1. S. Seer, N. Brändle, and D. Bauer. Design of decision rules for crowd controlling using macroscopic pedestrian flow simulation. In *Pedestrian and Evacuation Dynamics 2008*. Springer, Berlin, 2010.
2. M. Bell. The estimation of origin-destination matrices by constrained generalized least squares. *Transp. Res.*, 25B:13–22, 1991.
3. M. Cremer and H. Keller. A new class of dynamic methods for the identification of origin-destination flows. *Transp. Res.*, 21B(2):117–132, 1987.
4. M. Maher. Inferences on trip matrices from observations on link volumes: A Bayesian statistical approach. *Transp. Res.*, 17B:435–447, 1983.
5. E. Cascetta and S. Nguyen. A unified framework for estimating or updating origin/destination matrices from traffic counts. *Transp. Res.*, 22B:437–455, 1988.
6. K. Hornik, M. Stinchcombe, and H. White. Universal approximation of an unknown function and its derivatives using multilayer feedforward networks. *Neural Networks*, 3:551–560, 1990.

7. W. Newey and D. McFadden Large sample estimation and hypothesis testing. In R.F. Engle and D.L. McFadden, editors, *Handbook of Econometrics*, pages 2111–2245. Elsevier, Amsterdam, 1994.
8. D. Bauer. Estimating OD-matrices based on high frequent link volume counts. Technical report, Arsenal Research, 2008.

Effect of Subconscious Behavior on Pedestrian Counterflow in a Lattice Gas Model Under Open Boundary Conditions

Kuang Hua^{1,2}, Song Tao¹, Li Xingli^{1,3}, and Dai Shiqiang¹

¹ Shanghai Institute of Applied Mathematics and Mechanics, Shanghai University, No. 149, Yanchang Road, Shanghai 200072, China

e-mail: khphy@hotmail.com; tsong@shu.edu.cn; sqdai@shu.edu.cn

² College of Physics and Electronic Engineering, Guangxi Normal University, No. 15, Yucai Road, Guilin 541004, China

e-mail: khphy@shu.edu.cn

³ School of Applied Science, Taiyuan University of Science and Technology, No. 66, Waliu Road, Taiyuan 030024, China

e-mail: lx1326@163.com

Summary. In this paper, human subconscious behavior in pedestrian counterflow is investigated under open boundary conditions by using an extended lattice gas model with different maximum velocities. Four types of walkers are distinguished in the model and their dynamical characteristics are discussed. The simulation results show that the model can capture some essential features of pedestrian counterflows, such as lane formation, segregation effects and phase separation at higher densities. By analyzing the obtained phase diagram it is found that subconscious behavior plays a key role in reducing the occurrence of jam clusters in comparison to the case of un-subconscious behavior.

1 Introduction

Recently, pedestrian flow has attracted considerable attention in the field of physical science and engineering [1–5]. As a typical pedestrian flow phenomenon counterflow has been extensively studied in different scenarios [6–20], such as a T-shape channel [6], with the effects of following the front pedestrians in the same direction [7], sidling through the crowd [8], exchanging positions between face-to-face pedestrians [9], different velocities [10] and mixed drift coefficients [11, 12], and different sizes of slender particles [13, 14]. The pedestrian characteristics with people going on all fours have also been investigated [15].

However, until now, in the existing lattice gas models the maximum velocity of pedestrians was mostly supposed to be $V_{\max} = 1$ and the related

work with larger maximum velocity $V_{\max} > 1$ is very scarce [10]. This is not in accordance with the real situation, where different pedestrians might have different walking speeds. In addition, pedestrians generally have some subconscious behavior in counterflow where they are accustomed to overtaking the preceding walkers in the same direction from one side (e.g., from the left side in China and from the right side in Japan or UK), avoiding colliding with others in the opposite direction and walking along a certain side of the road (e.g., the right-hand side in China or the left-hand side in Japan; hereafter we only consider the scenarios in China). How do these factors affect the pedestrian dynamics in counterflow? This is an interesting but still open problem. The floor field CA model has been extended to $V_{\max} > 1$ in [16], and the effects of different maximum velocities and the right-moving preference of pedestrians on the counterflows have been considered respectively in [17–19].

In a recent work [20], we have proposed an extended lattice gas model to investigate the effect of subconscious behavior and different maximum velocities on pedestrian counterflow under periodic boundary conditions. Here we further study crowd counterflow under open boundary conditions.

2 Outline of Model

The model is defined on a square lattice of $W \times L$ sites, where W and L are respectively the width and length of the channel, as shown in Fig. 1. There are four classes of pedestrians: faster or slower walkers going to the right and faster or slower walkers to the left. Each site contains only a single walker and each walker moves to the preferential direction with no back step. Walkers are inhibited from overlapping on the site. The excluded-volume effect is taken into account. When a walker arrives at the wall of channel, he/she will be reflected by the wall. The left and right boundaries are open. The entrance density P_l of the right walkers from the lower half of the left boundary is set to be a constant. The entrance density P_r of the left walkers from the upper half of the right boundary is set to be different constant. The right (left) walker goes into the channel from the lower (upper) half of the left (right) boundary, proceeds through the channel and goes out of the right (left) boundary. When the right (left) walker arrives at the right (left) boundary, he/she is removed from the channel.

Figure 1 shows the pedestrian counterflow within a channel. The top and bottom sides of the channel are walls. The faster (slower) walkers going towards the right and to the left are indicated, respectively, by right triangle (circle) and left triangle (square). Arrows indicate the possible moving directions of the four groups. The bold arrow indicates the moving direction of walkers with subconscious behavior, i.e., different kinds of pedestrians would subconsciously cross different partition lines, e.g., the faster (or slower) right walkers may walk toward the right-hand side and cross the central partition line (or partition line CD) of the channel. In this study, we assume that the

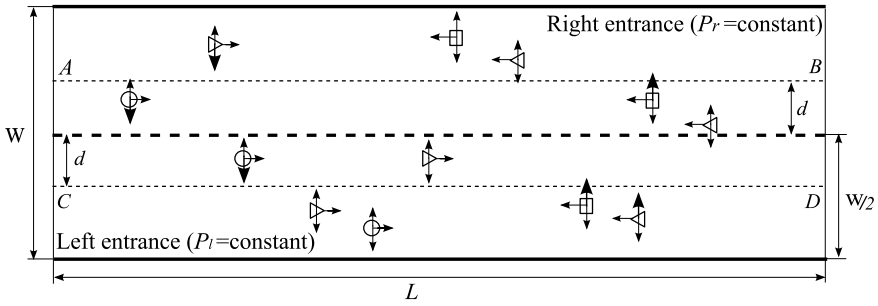


Fig. 1. Sketch of pedestrian counterflow.

walkers have the tendency to walk towards the right-hand side. In other words, this subconscious behavior means the convention of sideways direction preference during their movement in a crowd. The parameter d represents the distance between the partition line CD and the central one, which reflects the fact that the slower walkers prefer to move along the right-hand side of the walkway. Similarly, the faster (slower) left walkers have the same situations.

Each walker moves to the unoccupied nearest neighbors. The possible configurations and the corresponding transition probabilities for one walker are given in [20]. The updating rules are the same as those used in [20]. Here note that D_1 indicates the strength of the drift pointing to the exits (right or left), and D_2 represents the strength of the preferential direction of subconscious behavior.

3 Simulation Results and Discussions

In the simulations, the parameters are taken as $W = 20$, $L = 100$, $d = 5$, $V_{\max,1} = 3$, $V_{\max,2} = 1$, $P_{fl} = P_{fr} = 0.5$, $D_1 = 0.6$ and $D_2 = 0.9$ unless otherwise mentioned. Here P_{fl} (P_{fr}) is the entrance density of the faster right (left) walker.

The mean velocity $\langle V \rangle$ in one update time step is defined as the sum of the velocities of walkers moving forward divided by the total number of walkers in the channel. The mean occupancy ρ of pedestrian is defined as the total number of walkers in the channel divided by the channel area ($W \times L$). For each simulation, 10000 time steps were run, and the value of $\langle V \rangle$ and ρ were computed using the last 4000 time steps averaged over 20 runs.

The phase diagrams with un-subconscious behavior ($D_2 = 0$) and subconscious behavior ($D_2 = 0.9$) are shown in Figs. 2(a) and (b), respectively. The freely moving and the jamming regions are divided by the critical density curve (solid line). Obviously, the freely moving region in Fig. 2(a) is smaller and the jamming region is larger compared with those in Fig. 2(b). We have also found that the freely moving region A and region B are almost symmetric

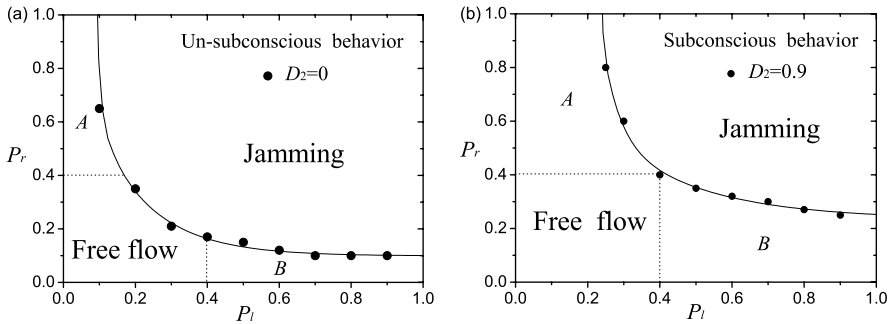


Fig. 2. Comparisons of phase diagrams between **a** the case without subconscious behavior and **b** the case with subconscious behavior, where the *solid line* is the fitting curve, i.e., the critical density curve.

for $P_l > 0.4$ and $P_r > 0.4$. Actually, the sizes of the different P_r regions depend considerably on D_2 and the increase of D_2 will lead to the expansion (shrink-age) of the freely moving (the jamming) region. From these observations we can conclude that the subconscious behavior has an important influence on the pedestrian flow. It could effectively decrease the occurrence of jam cluster.

In order to gain a deeper insight into the phase transition, we study the variation of the mean occupancy ρ . Figure 3 shows the 3D plot of the mean occupancy ρ against the entrance densities P_l and P_r with the un-subconscious behavior (see Fig. 3(a), $D_2 = 0$) and subconscious behavior (see Fig. 3(b), $D_2 = 0.9$), respectively. From Fig. 3, it can be clearly seen that the phase transition from freely moving phase to completely jamming phase happens. Compared with Fig. 3(a), Fig. 3(b) corresponds to a larger (smaller) region of the freely moving (the jamming) state. In other words, subconscious behavior, to some extent, could retard the occurrence of the jam. This conclusion is in agreement with the results shown in Fig. 3. We have also found some concavities at higher occupancy ρ , which correspond to the different cases. In some regions, the density is high but does not attain 1, which means the channel is not completely occupied by the walkers. At this time, the completely jammed phases appear in different regions. However, in other regions, where the density is equal 1, the channel is fully occupied by pedestrians. As a result, the completely jammed phases occur in the whole channel. These situations are the combined consequence of the initial distribution as well as the walkers' subconscious behavior and interactions.

We also investigate the flow patterns at the free moving phase and observe the jamming transition evolution. These patterns show that our model can capture some essential features of pedestrian counter flows, such as the lane formation, segregation effect and phase separation at higher densities. Especially, an interesting feature for counterflow is that the faster walkers overtake the slower ones and then form a narrow-sparse walkway can be observed in

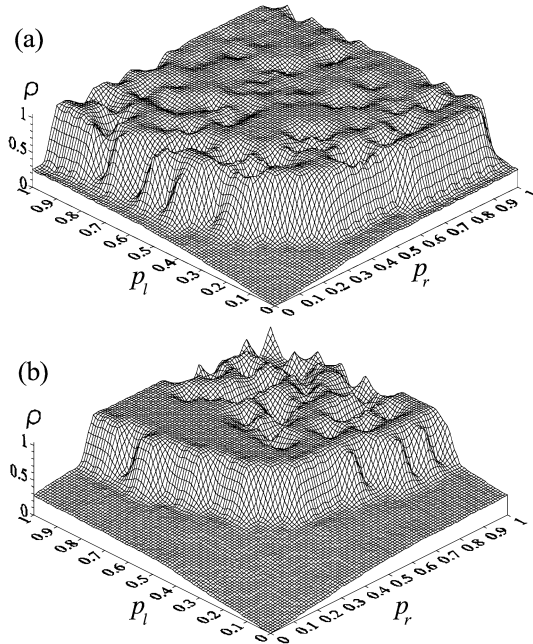


Fig. 3. Comparisons of 3D plots for the case **a** with un-subconscious behavior and **b** with subconscious behavior.

the region near central partition line. These results are consistent with what we have found for periodic boundary conditions in [20].

4 Conclusions

In this paper, an extended lattice gas model is proposed to investigate pedestrian counterflow under open boundary conditions by considering the human subconscious behavior and different maximum velocities, which can lead to appropriate responses in complex situations. The simulation results show that the presented model can reproduce such essential features of pedestrian counterflows as the lane formation, segregation effect and phase separation. Especially, an interesting feature for counterflow is that faster walkers overtake slower ones and then form a narrow-sparse walkway in the region near central partition line. Through the phase diagram analysis we find that the subconscious behavior plays a key role for pedestrian dynamics, where the freely moving region is larger and the jamming region is smaller compared with the case of un-subconscious behavior. In future work this model will be extended to more complex situations, such as the effect of different partition lines, the combination of different entrance densities on pedestrian dynamics, etc.

Acknowledgements

The authors would like to thank Prof. Y. Xue, Dr. L.Y. Dong, Ms. Y.F. Wei and Mr. J.P. Meng for helpful discussions and suggestions. This work was supported by the National Basic Research Program of China (Grant No. 2006CB705500), the National Natural Science Foundation of China (Grant Nos. 10532060 and 10562001) and the Shanghai Leading Academic Discipline Project (Grant No. Y0103).

References

1. M. Schreckenberg and S.D. Sharma, editors, *Pedestrian and Evacuation Dynamics*, Springer, Berlin, 2002.
2. E.R. Galea, editor, *Pedestrian and Evacuation Dynamics 2003*, CMS Press, Greenwich, 2003.
3. S.P. Hoogendoorn, S. Luding, P.H.L. Bovy, M. Schreckenberg, and D.E. Wolf, editors, *Traffic and Granular Flow'03*, Springer, Berlin, 2005.
4. D. Helbing, *Rev. Mod. Phys.* 73 (2001) 1067.
5. T. Nagatani, *Rep. Prog. Phys.* 65 (2002) 1331.
6. Y. Tajima and T. Nagatani, *Physica A* 303 (2002) 239.
7. M. Isobe, T. Adachi, and T. Nagatani, *Physica A* 336 (2004) 638.
8. M. Fukamachi and T. Nagatani, *Physica A* 377 (2007) 269.
9. J. Li, L.H. Yang, and D.L. Zhao, *Physica A* 354 (2005) 619.
10. R. Jiang and Q.S. Wu, *Physica A* 373 (2007) 683.
11. M. Fukamachi, R. Kuwajima, Y. Imanishi, and T. Nagatani, *Physica A* 383 (2007) 425.
12. Y. Imanishi, R. Kuwajima, and T. Nagatani, *Physica A* 387 (2008) 2337.
13. R. Nagai and T. Nagatani, *Physica A* 366 (2006) 503.
14. S. Ito, T. Nagatani, and T. Saegusa, *Physica A* 373 (2007) 672.
15. R. Nagai, M. Fukamachi, and T. Nagatani, *Physica A* 358 (2005) 516.
16. A. Kirchner, H. Klüpfel, K. Nishinari, A. Schadschneider, and M. Schreckenberg, *J. Stat. Mech.: Theory Exp.* (2004) P10011.
17. W.G. Weng, T. Chen, H.Y. Yuan, and W.C. Fan, *Phys. Rev. E* 74 (2006) 036102.
18. W.G. Weng, S.F. Shen, H.Y. Yuan, and W.C. Fan, *Physica A* 375 (2007) 668.
19. L.Z. Yang, J. Li, and S.B. Liu, *Physica A* 387 (2008) 3281.
20. H. Kuang, T. Song, X.L. Li, and S.Q. Dai, *Chin. Phys. Lett.* 25 (2008) 1498.

Hand-Calculation Methods for Evacuation Calculation—Last Chance for an Old-Fashioned Approach or a Real Alternative to Microscopic Simulation Tools?

Christian Rogsch, Henning Weigel, and Wolfram Klingsch

Institute for Building Material Technology and Fire Safety Science,
University of Wuppertal, Pauluskirchstr. 11, 42285 Wuppertal, Germany
e-mail: christian@rogsch.de; klingsch@uni-wuppertal.de

Summary. Evaluation and optimization of emergency systems can be done by means of several engineering methods, which are entirely different: macroscopic hydraulic models, which can be calculated by hand (the so called “Hand-calculation Methods”), and microscopic computer simulation methods. Both allow forecasting of evacuation-times for various settings. The authors compare results of four commercial software tools (ASERI, buildingEXODUS, PedGo, Simulex) and some macroscopic hydraulic models with real evacuation trials in high-rise buildings. Furthermore a theoretical research of a school building is shown.

1 Analysis of a High-Rise Building with Microscopic and Macroscopic Models

The real evacuation-trial which we compare with results of commercial software tools was performed [1] in the middle of the 1970 at the Mannesmann-Building, which was built in 1959 in Germany. It consists of three basements, one ground floor, one mezzanine floor and 22 top floors. During the evacuation trial one staircase was closed, thus all people had to use the same staircase. In total, 427 people stayed in the top floors and were evacuated by using the evaluated staircase. A floor plan with measurements is shown in Fig. 1, a detailed overview about walking velocity and distribution of people inside the building can be found in [2]. As pre-movement time we choose $50 \text{ sec} \pm 20 \text{ sec}$, this time based upon the original study [1].

1.1 Results of Commercial Software Tools

The results show, that commercial software are able to predict a total evacuation time for a high-rise building (see Table 1). If one takes a closer look at

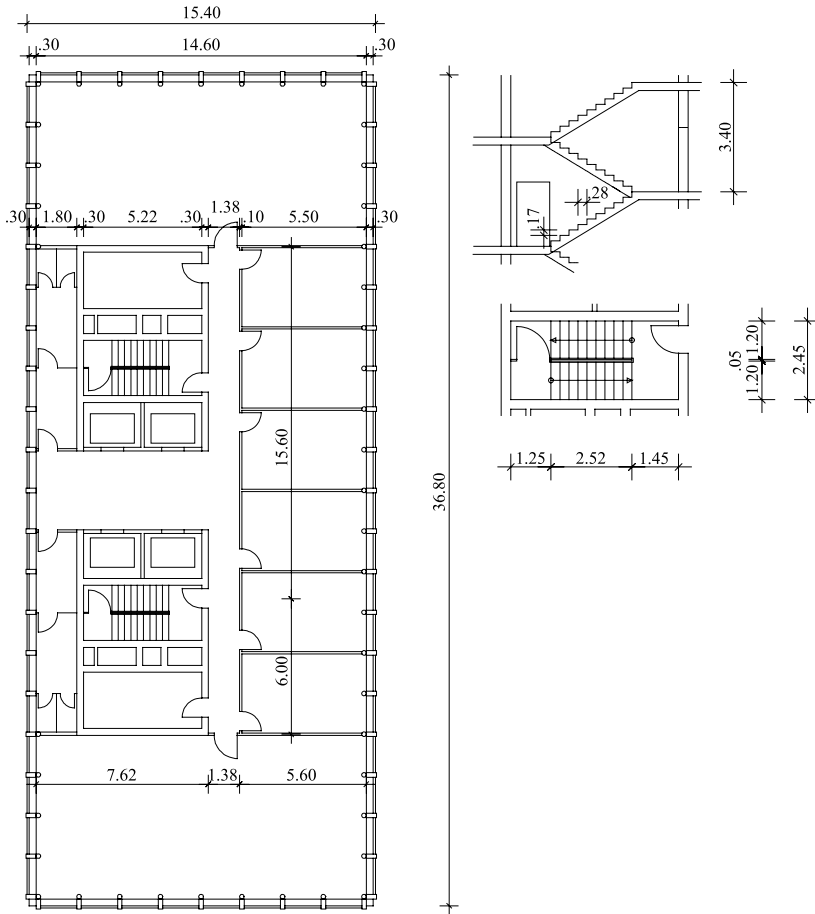


Fig. 1. Floor plan of the Mannesmann Building [1].

the calculated evacuation times for selected floors, it appears that they differ considerably from the real times (see Table 1). Because of this results we calculate this high-rise building with different macroscopic hand-calculation methods. These methods should also be able to predict total evacuation times for a high-rise building.

1.2 Results of Macroscopic Hand-Calculation Methods

The results shown in this section (see Table 2) based upon calculations of ten different macroscopic hand-calculation methods. As we can see, some of these hand-calculation methods are able to predict “correct” evacuation times for a total building, the average value of all hand-calculation methods agrees in a good way with measured and simulated times.

	Evacuation trail	ASERI	buildingEXODUS	PedGo	Simulex
Total building	8.78 min	ca. 9 min	ca. 8.5 min	ca. 8 min	ca. 8 min
2nd floor	50–149 s	40–82 s	38–74 s	44–94 s	44–82 s
4th floor	45–75 s	35–86 s	49–73 s	50–82 s	41–86 s
5th floor	61–101 s	36–87 s	35–83 s	42–89 s	42–90 s
6th floor	31–102 s	42–82 s	35–78 s	41–95 s	42–85 s
7th floor	67–132 s	43–96 s	37–77 s	39–96 s	43–95 s
10th floor	51–102 s	33–117 s	41–83 s	39–92 s	43–90 s
15th floor	48–155 s	38–83 s	38–81 s	45–88 s	42–80 s

Table 1. Comparison of calculated evacuation times with a real evacuation trial. At selected floors the table shows the first and last person moving into the staircase.

Macroscopic hand-calculation method	427 people (19 in each floor) with 0.8 min response time
Predtechenskii and Milinskii, standard method [3]	9.10 min
Predtechenskii and Milinskii, simplified method [4]	9.15 min
SFPE/NFPA Handbook [5]	14.78 min
Method of W. Müller [6–9]	14.58 min
Method of K. Togawa [10]	5.65 min
Method of M. Galbreath [11]	6.52 min
Effective-width model by J. Pauls [12]	7.84 min
Method of Melinek and Booth [13]	7.67 min
Method of E. Kendik [14]	7.98 min
Method of Seeger and John [1]	8.83 min
Average of 10 methods	9.21 min
Real evacuation trial [1]	8.78 min (without 0.8 min response time: 7.98 min)

Table 2. Comparison of calculated evacuation times by macroscopic hand-calculation methods with a real evacuation trial.

2 Analysis of a Theoretical School Building with Microscopic and Macroscopic Models

The School Building is based upon a theoretical building from the book of Roitman [15]. Thus the building is symmetric, only one half of the building is shown and calculated. It consists of one ground floor and 3 top floors. Each classroom consists of 40 pupils. In the ground floor 2 classrooms are located and in each top floor 3 classrooms are located. In total, 880 pupils are calculated. A floor plan with measurements is shown in Fig. 2.

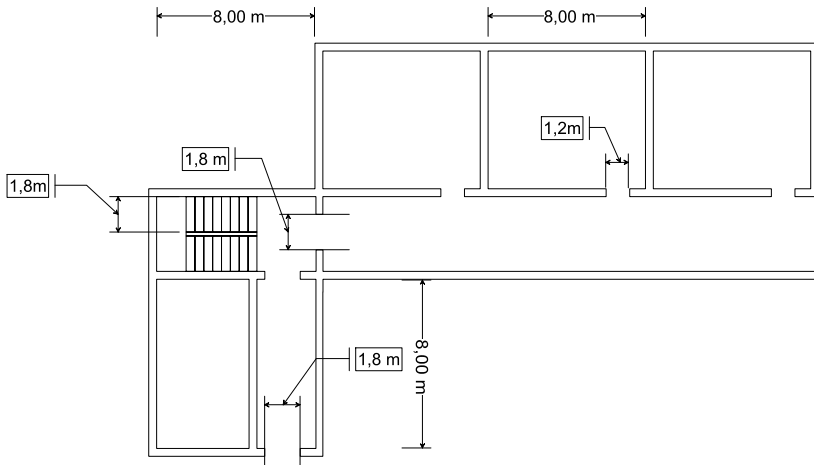


Fig. 2. Floor plan of the School Building [15].

	PedGo	Simulex
Pupils ($0.9 \text{ m/s} \pm 0.3 \text{ m/s}$)	ca. 8.17 min	ca. 8.00 min
Men ($1.35 \text{ m/s} \pm 0.2 \text{ m/s}$)	ca. 7.00 min	ca. 6.00 min

Table 3. Calculated evacuation times by microscopic software tools for a theoretical school building.

2.1 Results of Commercial Software Tools

The results (see Table 3) show, that the two chosen commercial software tools predict similar results for the selected building. The two different settings (pupils and men) show, that the group of men with higher free walking velocity ($1.35 \text{ m/s} \pm 0.2 \text{ m/s}$) is faster evacuated than the slower group of pupils with a slower free walking velocity ($0.9 \text{ m/s} \pm 0.3 \text{ m/s}$). This result shows, that both software tools calculate results in an expected way.

2.2 Results of Macroscopic Hand-Calculation Methods

The results shown in this section (see Table 4) based upon calculations of seven different macroscopic hand-calculation methods. As shown in Sect. 1.2, in this case some of the used hand-calculation methods predict similar evacuation times than commercial software tools, too. Thus it is not possible in most of the hand-calculation methods to choose free walking velocities like in software tools, the results may be express the results for a “optimal” setting for adults. Because of the large differences of the calculated values it is recommended to use an average of all values, because the mean value of all seven hand-calculation methods agrees in a acceptable way with the results calculated by the software tools for “Men”.

Macroscopic hand-calculation method	880 people in total with no response time
Predtechenskii and Milinskii, standard method [3]	9.00 min
Predtechenskii and Milinskii, simplified method [4]	9.07 min
SFPE/NFPA Handbook [5]	4.76 min
Method of W. Müller [6–9]	5.33 min
Method of Roitman [15]	5.88 min
Method of NFPA 130 [16]	4.34 min
Method of Weidmann [17]	5.63 min
Average of 7 methods	6.30 min

Table 4. Calculated evacuation times by macroscopic hand-calculation methods for a theoretical school building.

3 Conclusion

The analysis shows that chosen software tools are able to predict total evacuation times for such kind of buildings. However by taking a closer look at evacuation times for selected floors, calculated results by software tools differ from the results of the trials. Hand-calculation methods are able to predict total evacuation times for the chosen building, but mostly they are not able to predict evacuation times for selected floors, like the software tools. With hand-calculation methods it is also possible to calculate evacuation times in a very fast way. But different hand-calculation methods calculate different evacuation times, thus the user has to know what he/she does and if the results may be correct.

To ensure that the results of different hand-calculation methods are comparable to calculated results by software tools, it is recommended to calculate an average value of the results calculated by different hand-calculation methods. The user has to ensure, that he/she uses sufficient hand-calculation methods, thus the outliers of some methods do not be of consequence. The mean values of seven or ten different hand-calculation methods agree in a good way with the calculated values of software tools, so this is a good approach to calculate evacuation times of total buildings in a relatively fast way.

Acknowledgements

The authors thank all software companies who provided their evacuation software free of charge. Furthermore we thank BPK GmbH for using their buildingEXODUS software and IES Ltd. for their student offer of Simulex. Last but not least the authors want to thank the group of ped-net.org for very useful discussions.

References

1. P. G. Seeger and R. John. Untersuchung der Räumungsabläufe in Gebäuden als Grundlage für die Ausbildung von Rettungswegen, Teil III: Reale Räumungsversuche. Technical Report T395, Forschungsstelle für Brandschutztechnik an der Universität Karlsruhe (TH), 1978.
2. C. Rogsch, W. Klingsch, A. Seyfried, and H. Weigel. How reliable are commercial software-tools for evacuation calculation? In *Interflam 2007, Conference Proceedings*, pages 235–245, 2007.
3. W. M. Predtetschenski and A. I. Milinski. *Personenströme in Gebäuden, Berechnungsmethoden für die Modellierung*. Müller, Köln–Braunsfeld, 1971.
4. W. M. Predtetschenski, W. W. Cholstschewnikow, and H. Völkel. Vereinfachte Berechnung der Umformung von Personenströmen auf Wegabschnitten mit begrenzter Länge. *Unser Brandschutz, wissenschaftlich-technische Beilage*, 6:90–94, 1972.
5. H. E. Nelson and F. W. Mowrer. Emergency movement. In P. J. DiNenno, editor, *SFPE Handbook of Fire Protection Engineering*, page 367. National Fire Protection Association, Quincy, MA, 3rd edition, 2002.
6. W. Müller. Untersuchung über zulässige Räumungszeiten und die Bemessung von Rückzugswegen in Gebäuden, 1970.
7. W. Müller. Die Beurteilung von Treppen als Rückzugsweg in mehrgeschossigen Gebäuden. *Unser Brandschutz, wissenschaftlich-technische Beilage*, 3:65–70, 1966. To be continued in 4/1966.
8. W. Müller. Die Beurteilung von Treppen als Rückzugsweg in mehrgeschossigen Gebäuden. *Unser Brandschutz, wissenschaftlich-technische Beilage*, 4:93–96, 1966. Continuation from 3/1966.
9. W. Müller. Die Überschneidung der Verkehrsströme bei dem Berechnen der Räumungszeit von Gebäuden. *Unser Brandschutz, wissenschaftlich-technische Beilage*, 4:87–92, 1968.
10. K. Togawa. Study on fire escapes basing on the observation of multitude currents. Report of the building research institute, Ministry of Construction, Japan, 1955. In Japanese.
11. M. Galbreath. Time of evacuation by stairs in high buildings. Fire Research Note 8, NRCC, May 1969.
12. J. L. Pauls. Movement of people. In P. J. DiNenno, editor, *SFPE Handbook of Fire Protection Engineering*, page 263. National Fire Protection Association, Quincy, MA, 2nd edition, 1995.
13. S. J. Melinek and S. Booth. An analysis of evacuation times and the movement of crowds in buildings. Technical Report CP 96/75, BRE, 1975.
14. E. Kendik. *Die Berechnung der Personenströme als Grundlage für die Bemessung von Gehwegen in Gebäuden und um Gebäude*. PhD thesis, TU Wien, May 1984.
15. M. J. Roitman. *Die Evakuierung von Menschen aus Bauwerken*. Staatsverlag der Deutschen Demokratischen Republik, Berlin, 1966.
16. NFPA. *NFPA 130: Standard for Fixed Guideway Transit and Passenger Rail Systems*. NFPA.
17. U. Weidmann. Transporttechnik der Fußgänger, Transporttechnische Eigenschaften des Fußgängerverkehrs (Literaturauswertung). Schriftenreihe des IVT 90, ETH Zürich, 1993. 2nd edition, in German.

Adding Higher Intelligent Functions to Pedestrian Agent Model

Toshiyuki Kaneda¹, Takumi Yoshida¹, Yanfeng He¹, Masaki Tamada², and Yasuhiro Kitakami²

¹ Nagoya Institute of Technology, Gokiso, Showa, Nagoya, Japan
e-mail: kaneda@nitech.ac.jp, sinsei_1384@hotmail.co.jp

² Kozo Keikaku Engineering Co. Ltd, Nakano, Nakano, Tokyo, Japan
e-mail: tamada@kke.co.jp, kitakami@kke.co.jp

Summary. Pedestrian dynamics studies have brought the potential for application to a wide variety of urban planning field, not only crowd accident risk analysis but also simulation-oriented spatial design. Our up-versioned ASPF (Agent Simulator of Pedestrian Flows) ver.4 has newly introduced higher function such as a target maintaining (Helmsman) function, a route-choice function etc. into a pedestrian agent. In an example case of patio-shaped shopping mall, Asunal Kanayama, we have verified that pedestrian agents can walk autonomously along way points to destination points in a complicated space, and that ASPFver.4 can be a useful tool for ordinary commerce space design. We also refer to the ASSA (Agent Simulator of Shop Around) project for implementing much higher functions.

1 Introduction

Pedestrian dynamics studies have brought the potential for application to a wide variety of urban planning field, not only crowd accident risk analysis but also simulation-oriented spatial design in corporation with the progress of agent technology. Our ongoing project ASPF (Agent Simulator of Pedestrian Flows) that derived from Cellular Automata model has been up-versioned step by step. In a previous paper, ASPFver.2 had demonstrated a crowding process on a L-shaped corridor, as a model of the Asagiri overpass accident of 2001 [1].

By using a flexible agent modeling platform artisoc (former KKMAS), ASPFver.3 adopted a hybrid style of discrete (cell space)-based behavioral rules on continuous (xy-coordinates) space, so each agent can walk in any direction across the restriction of grid [2]. However, in this version, a pedestrian agent still merely walks straight ahead and simply avoids other agents, and it was impossible to analyze crowd flows on a large-scale space with a complicated shape. Therefore, in ASPFver.4, some higher functions are required such

as Helmsman and route-choice functions, etc. These functions were suggested by an existing research.

Following this context, this paper first explains *artisoc* briefly that supplies a pedestrian modeling platform, next it explains the features of ASPFver.4 that simulates Multipurpose MultiStop (MPMS) trip behavior of shopping visitors in an example case of a patio-shaped shopping mall. We also refer to a new project ASSA (Agent-Simulator of Shopping-Around behavior) to deal with much higher functions of shopping visitor agent.

2 Pedestrian Modeling Platform for Hybrid Space Representation System

In ASPFver.3 or later, the relative coordinate system is used for space representation. In this system, each agent has his/her own cell space based on walking direction and applies a cell-based behavioral rule. As the random sequential update is adopted, they all interact on the real one continuous space without conflict. This system is a hybrid representation of discrete (cell) and continuous (real) 2D space, thus each agent is allowed to move in any direction of 360 degree. This is a useful feature comparing against only four direction moves in a pure CA-derived models (Fig. 1). In this section, we address an agent modeling platform *artisoc* (former KKMAS) that realizes this system easily.

2.1 Introducing *Artisoc*

Artisoc is an agent based simulator which is designed for applications in mainly social science fields [3]. The key features of *artisoc* are an ease of model complex building and modeling capability and an ability to link with other applications. *artisoc* simplifies the modeling processes; the user interface is designed in a way that allows intuitive adding and editing of agents. Also, the behavior rules for agents are written in BASIC language thus behaviors of agents can be easily described. In addition, the mapping outputs and chronological graphs of the simulation results can be easily defined in only a few steps. In order to initiate complex modeling, *artisoc* is designed with a capability to define freely multiple spaces, agents and variables.

When linking with other applications, *artisoc* is designed with a network link function which corrects information from a web servers while running a simulation, and with a database link function which acquires values from databases, too. When building large scale models, *artisoc* has a distributed execution function which enables rapid modeling by linking multiple PC's. It also has log function which saves calculation results in a database and can execute a high-speed playback.

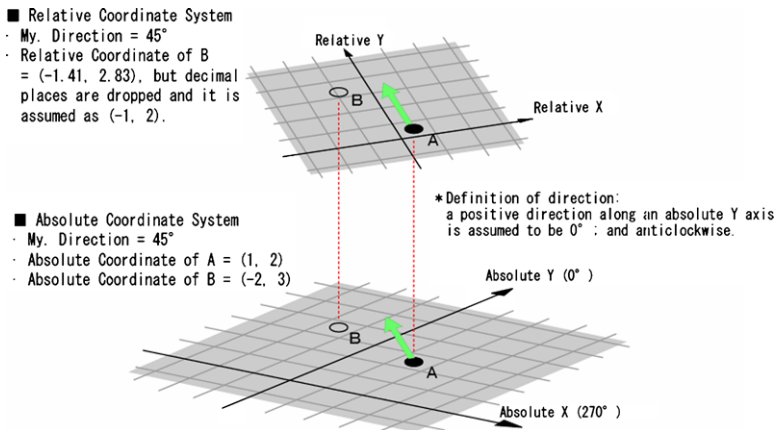


Fig. 1. Hybrid space representation of ASPFver.4.

3 ASPF(Agent Simulator of Pedestrian Flow) ver.4—Implementation of Autonomous Pedestrian Agent

ASPFver.4 has inherited the basic design of the previous version. The spatial scale is represented by 40 square cm cell and the time scale is set at one step per 0.5 seconds. The pedestrian agent’s ‘cell-to-cell’ conditional behavior rules are also taken from the previous version, 6 basic behavior rules, 8 slow-down rules, 4 avoidance rules, 3 high density flow rules and 1 following rule. In addition, 14 wall avoidance rules were newly designed to avoid a wall. The relative coordinate system in that each agent behaves on his/her own cell space based on walking direction and the interaction on the real continuous space is also inherited. This is called ‘Mover’ function, but a pedestrian agent still merely walks straight ahead and simply avoids other agents and obstacles.

Thus, the second basic function, the Helmsman (target maintaining) function is introduced. This function refers to a function that firstly determines the direction of movement towards a given (visible) target and secondly by regularly reconfirming the location of the target correcting any difference of directions between movement and target; such differences may occur because of behavior to avoid other pedestrians and walls while moving towards the target.

In addition, in a large-scale and complicated shaped space, there is no guarantee that a destination can be always confirmed visually; in this case, a list of way points which satisfy the visual confirmation conditions from the starting point to the destination is given in advance and a pedestrian agent walks along the list of the way points. The target mentioned above is either the final target destination or a way point. Update of the target means that agents regularly confirm whether they are closing on their target and when

they arrive in the neighborhood of the target, they update their target to the next one.

In ASPFver.4, the following parameters were set: confirmation to maintain a target was carried out every 10 steps, target update was confirmed every 2 steps by checking whether they were located within the 2 cells from a way point.

In order to simulate pedestrians' shop-around behavior in a complicated shape shopping mall, we need to find the route to move from a shop to another shop. This is called 'Route chooser' function. In ASPFver.4, on a given visible way point network, each agent has to search the shortest route by Dijkstra method. It implies all agent have knowledge on shop location, etc. [4].

We had studied the actual mall, Asnal Kanayama, as a case. Firstly, by using data of visitors' behavior research which was conducted in the previous year, we created a list of shop-around facilities from research data by attributes. Then, this time, as an expedient, we aggregate a 'between-shops' Origin-Destination (OD) matrix, and form the OD transition probability matrix. Visitor Agents decide the next destination probabilistically. This is also 'Planner' function as an expedient.

In ASPFver.4, pedestrian agent behaves in the following order: (1) decide the next destination; (2) set a route; (3) maintain the target; (4) apply behavior rules; and (5) update the target. Table 3 shows each feature of Mover, Helmsman, Route chooser, and Planner functions comparing to a functional layer suggested in the STREETS project [5, 6] (Table 3).

Here, the target maintaining function was demonstrated. In a cross-shaped space, 40 cells in road width, opposing flows with a flow coefficient of 0.5 person/m · sec were generated from both sides (right and left), and after the number of pedestrians had become steady, three crossing pedestrians were generated from the lower part and the locations of these pedestrians were examined (Fig. 2). Target maintaining behavior by agents crossing a pedestrian flow from two different directions was confirmed. We can see that the agents kept holding their target destination by correcting their direction though he/she had drifted by the flows. Moreover, in this study simulations were tested in

Layered-modules proposed by STREETS project	Implementations in ASPFver.4
Higher (5) Planner	Choice of the next destination by given transition probability matrix
(4) Route Chooser	Optimization by Dijkstra method (rational model)
(3) Navigator	Not implemented (necessary in dark/panic cases)
(2) Helmsman	A way point-check and direction modification each ten steps
Basic (1) Mover	Existing functions of ASPFver.3 (hybrid space representation, 22 rules and proper speed)

Table 1. Functional features of ASPFver.4 in comparison with STREETS project.

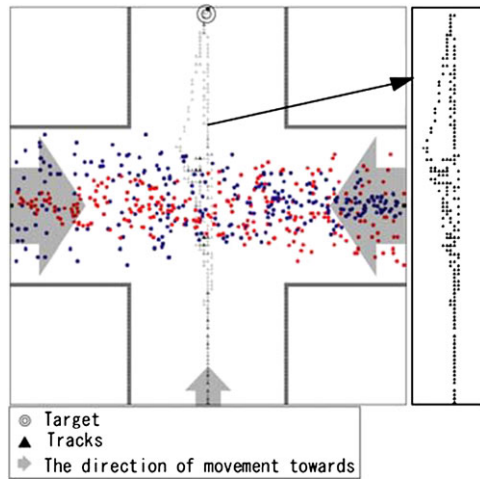


Fig. 2. Performance of Helmsman function, ASPF ver.4.



Fig. 3. Snapshot of pedestrian flows in patio-shaped shopping mall.

case of relationship between density and speed with a straight movement flow and in an L-shaped corridor. The same results as in the previous version were confirmed.

Figure 3 shows a snapshot of a pedestrian flow simulation on Asunal Kanayama. Based on measurements of crowd densities of four different simu-

lation cases ((1) weekday case, (2) weekday double case, (3) holiday case, and (4) at time of a music event in holiday case) the performance of ASPFver4 was also verified. Due to a series of these version-ups, we can conclude that ASPF is now available for analyzing crowd flows and density in space with complicated shapes.

4 Concluding Remarks—ASSA Project as Further Study

ASPFver.4 has newly introduced a target maintaining (Helmsman) function, a concept of way point (target), and a route-choice function for searching a route (list of way points) to visible/invisible destinations by using a Dijkstra method. So, ASPFver.4 enables each agent to walk along a list of visible target ‘way points’ towards a destination by keeping directions to each of the targets against the crowd flows. Moreover, MultiPurpose MultiStop (MPMS) shopping behaviors are expressed by Origin–Destination (OD) transition probability matrix, a still simple planner function. In comparing with the functions that had suggested by the STREETS project, (1) Mover, (2) Helmsman, (4) Route-Chooser, and (5) Planner functions are implemented, thus it is enough to be a useful tool for ordinary commerce space design.

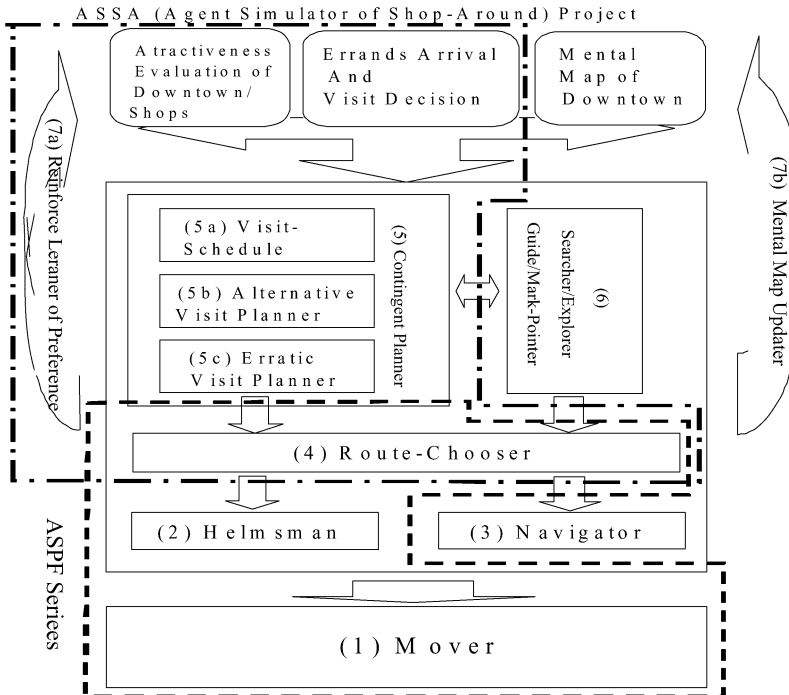


Fig. 4. Diagram of ‘adaptive’ pedestrian agent model.

We have also illustrated an example case of patio-shaped shopping mall, Asunal Kanayama, 150 m \times 100 m scale, 11 entrances/exits, 19 shops on ground floor, 105 way points and 7,656 sets of the route. An OD transition matrix is based on an actual survey on the visitors' Shop-Around behaviors. In this case, we have verified that pedestrian agents can walk autonomously along way points to destination points in a complicated space by setting way points in appropriate locations and a fixed OD transition matrix.

From the viewpoint of real shopping visitors, fixed OD transition probability is a too strong assumption, because they have neither historical memory, schedule planning nor ad-lib behaviors. So, the authors have started a new agent development project, ASSA (Agent Simulator of Shop Around). Features of ASSA are to implement schedule planning function, contingent re-scheduling function, and adaptive learning function on shop-preference etc. Our further research includes an integration of ASPF and ASSA (Fig. 4).

References

1. T. Kaneda. Developing a Pedestrian Agent Model for Analyzing an Overpass Accident. In N. Waldau et al., editors, *Pedestrian and Evacuation Dynamics 2005*, Springer, Berlin, 2007.
2. T. Kaneda, and D. Okayama. A Pedestrian Agent Model Using Relative Coordinate Systems. In T. Terano et al., editors, *Agent-Based Approaches in Economic and Social Complex Systems*, Springer, Tokyo, 2007.
3. Kozo Keikaku Engineering Inc.: <http://mas.kke.co.jp/en.html>.
4. Y. He, and T. Kaneda. Modeling and Development of an Autonomous Pedestrian Agent—As a Simulation Tool for Crowd Analysis for Spatial Design. In T. Terano et al., editors, *The Fifth International Workshop on Agent-Based Approaches in Economic and Social Complex Systems (AESCS'07)*, Tokyo, 2007.
5. T. Schelhorn, et al. *STREETS: An Agent-Based Pedestrian Model*, Working Paper 9, Centre for Advanced Spatial Analysis, University College London, 1999.
6. M. Haklay, and M. Thurstain-Goodwin, D. O'Sullivan and T. Schelhorn. "So Go Downtown": Simulating Pedestrian Movement in Town Centres, *Environment and Planning B* 28, 343–359, 2001.

“FlowTech” and “EvaTech”: Two Computer-Simulation Methods for Evacuation Calculation

Ilya Karkin¹, Vladimir Grachev², Andrey Skochilov¹, and Vladimir Zverev¹

¹ SITIS Ltd, Dolores Ibarruri 2, Ekaterinburg, Russia
e-mail: ilya@sitis.ru

² Ural State Technical University, Mira 19, Ekaterinburg, Russia
e-mail: vladimir.grachev@gppb.ru

Summary. FlowTech and EvaTech are software tools for evacuation simulation, representing two different approaches: macroscopic and microscopic. FlowTech was developed due to the need that arose in Russia in a software tool for evacuation calculation which would correspond to methods and correlations enlisted in the present Russian State Standard of evacuation calculation “GOST 12.1.004-91*. Fire Safety. General Requirements” (IPK Standards, Moscow, 1996), based on the work of V.M. Predtechenskii and A.I. Milinskii (“Planning for Foot Traffic Flow in Buildings” (Amerind, New Delhi, 1978). FlowTech supports now different “hand-calculation” methods of evacuation calculation such as “GOST 12.1.004-91*”, the Moscow city standard “Moscow City Construction Regulations” (MGSN 4.19-2005, Moscow Government, Moscow, 2005) and the method recommended by the Society of Fire Protection Engineers (SFPE) (Nelson and Mowrer in The SFPE Handbook of Fire Protection Engineering, SFPE, Bethesda, MD, 2002). FlowTech approaches modeling of flow movement as a representation of evacuation process which consists of formation, movement and merging of flows. Since separate persons are not singled out from the flow, this approach is called a macroscopic approach. In spite of its simplicity it allows to predict evacuation times and congestion points in buildings quite accurately and can be widely used as a fast means of evacuation calculation with little effort of a building model construction. For cases when a representation of individuals is needed (e.g. in case of evacuation from a room with a complex planning, or when human behavior is an important factor which will affect the simulation) the software tool EvaTech is under development.

1 “FlowTech”. Flow Movement Modeling

FlowTech (see Table 1) is a software tool for calculation of evacuation times of large populations from multi-storey buildings, based on modeling of people flow movement.

Availability to public	The model is available for public
Modeling method	Movement model
Purpose	Simulation of any type of building with high population density
Grid/Structure	Coarse network
Perspective of the model/occupant	Global/Individual
Behavior	No behavior
Movement	Density correlation/User's choice
Fire data	No (under development)
CAD	No (under development)
Visual	2-D (3-D under development)
Validation	The model uses "handcalculation" methods for evacuation calculation, validated by their authors. The model was validated against hand-calculated results to assure that the implementation of the methods is correct.
Defining groups	Yes
Delays/pre-movement times	Yes
Elevator use	No (under development)
Toxicity of the occupants	No (under development)
Route choice of the occupants	User-defined route with limitations

Table 1. FlowTech evacuation model features.³

In FlowTech a floor plan is divided into nodes: rooms, corridors, stairs. Links between the nodes are either created by the program (corridor links) or specified by the user (doors, exits). All occupants from one room follow the same route specified by user. The user-defined routes include stairs and exits, and path between a room and stairs or an exit is the shortest path calculated by the program. The coarse network constructed in such a way and the flow modeling have their advantages. Occupants cannot get "stuck" in small elements of CAD drawings or building bottlenecks.

Although many evacuation models employ *fine network* and import of CAD drawings, the refining of imported building topology with trials and errors to make the model work with it may take too much time and negate the advantage of reusing of CAD drawing.

1.1 Workflow with FlowTech

FlowTech was designed to thoroughly support the "life-cycle" of evacuation analysis project: from import of initial data to output reports, using just one project file. That makes an update of results take least efforts after entering changes to the initial data.

³ Used categorization from [5].

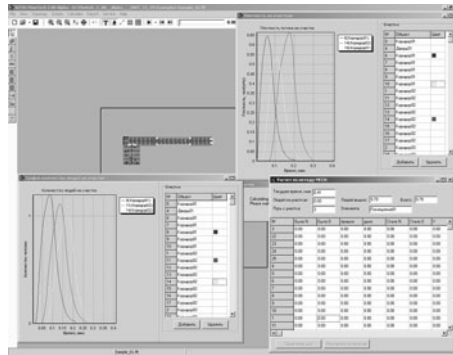


Fig. 1. Analysis of results.

1. **Scene topology creation.** It is possible to import a floor plan as a file in graphic format (*.jpg, *.bmp) for using it as a guide while creating topology. The editor supports such convenient features as snapping and copying.
2. **Scenarios creation.** A *scenario* defines the number of people in each building element, their characteristics and the paths they will take to exit the building (i.e. which stairs and exits they will use). One can create and save any number of scenarios in the same project to investigate different occupant loads, different building uses and “what-if” cases. It is possible to copy scenarios and drag and drop their elements.
3. **Calculation and analysis of results.** Calculation results can be viewed as tables or graphs (see Fig. 1). Information about egress is available in detail for each building element.
4. **Reporting.** FlowTech allows to form report and save it as RTF text. Every time a report is created report options are saved as well, so the user can work out his own template for a routine reporting and use it over and over. Report can contain initial data, egress paths, times, congestion points and other.
5. **Report features**
 A report generated by the program can contain various information depending on the user settings. For every scenario it may consist of:
 1. Initial data: occupant loads, their characteristics, room properties etc. That serves to control input data of the model.
 2. Total evacuation times as well as times for every building element.
 3. Scheme of evacuation, paths taken by occupants.
 4. Tessellations by rectangular sections used for calculation method.
 5. Building elements where congestion was observed. Detailed tables with wait times.

Evacuation model	Evacuation initiation delay input	Evacuation time (min): 19,800 occupants	Evacuation time (min): 25,500 occupants
EXODUS	0–10 minute delay no delay	112 110	142 141
EXIT89	0–10 minute delay No delay	92–113 97–117	119–139 114–140
FLOWTECH(GOST)	No delay	92	128

Table 2. Evacuation time.

1.2 Evacuation Simulation Example: WTC1

Data for evacuation times for Exodus and EXIT89 is from “Table D-5” (Scenario 2 and 3) in [6]. Results of the WTC1 simulation are shown in Table 2.

1.3 Future Work

The future development of the program will include taking into account hazards of fire (including blocking of exits with smoke), a 3-D visualization of the building and animation of flow movement in a 3-D viewing mode, graphical representation of flow density on the floor plan, support of ramps, escalators and lifts. Besides that an option of batch running of calculation with a random variation of parameters will be made possible.

2 “EvaTech”. Individual Movement Modeling

EvaTech (see Table 3) is an agent based software designed for simulation of evacuation process in multi-storey buildings and other environments.

Pedestrian movement towards exits is not the only part of evacuation process. Occupant behavior during an emergency situation may include such actions as firefighting, looking for other occupants and others. Modeling of every occupant as an agent with his/her own goals and behavior allows us to involve more detailed mechanisms in prediction of situation development.

For specification of a place while modeling behavior of persons in *EvaTech* one can use object “location”. Location is a user-defined rectangular area in the scene which can serve as a destination if it is specified in behavior of the occupants. But this is only one of various uses of this object. If specified so the occupants will move along a route, where each way point will be a location. Therefore there are no “exits” in *EvaTech*. A location can act as an exit, if it is defined as a final destination for occupants.

When a location is used as a destination for the occupants a path map is generated for it. The algorithm of path map construction is a modified Dijkstra’s algorithm [7] on a regular grid, which produces rectified paths. A path map allows to get quickly the shortest path to a location from any point of the scene.

Availability to public	The model is under development. The model will be available to public after its validation
Modeling method	Behavioral model
Purpose	Simulation of any type of building (currently supports only one storey)
Grid/structure	Continuous space for movement/fine network for distance mapping and navigation
Perspective of the model/occupant	Individual
Behavior	AI (under development)
Movement	Density correlation/User’s choice
Fire data	No (under development)
CAD	Yes
Visual	2-D/3-D
Validation	The model is still under validation
Counterflow	Yes (currently at low densities only)
Fire conditions affect behavior	No (under development)
Defining groups	Yes
Disabilities/slow occupant groups	Yes
Delays/pre-movement times	Yes
Elevator use	No (under development)
Toxicity of the occupants	No (under development)
Route choice of the occupants	Shortest route/User-defined route

Table 3. EvaTech evacuation model features.

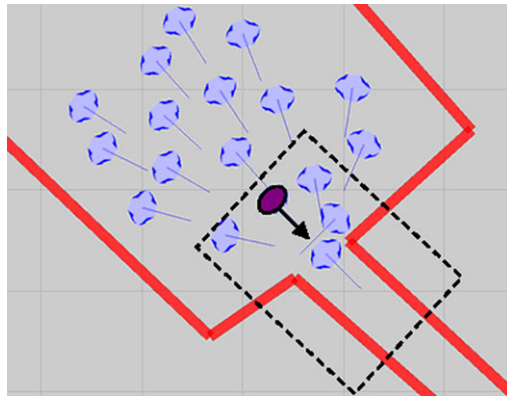


Fig. 2. Density definition.

For defining of a person’s velocity reduction in the flow it is used a velocity-density correlation of the State Standard (GOST 12.1.004-91*) or other correlations, including a user-defined correlation in the form of a table.

A rectangular section which is used for density calculation for an occupant is centered at the occupant and aligned with the movement direction of the occupant (see Fig. 2). Density is calculated as a sum of projection areas of occupants situated inside the section divided by overall area of the section.

Only area that is available for person from his/her position is taken into account for calculation. This approach gives good qualitative results. If during quantitative verification of the model using this approach satisfactory result cannot be achieved, then other approaches will be tried, such as “social forces model” or “inter-person distance”.

2.1 Pedestrian Movement

It is important to identify the main patterns of flow movement because an inaccurate simulation may produce imperfect results, e.g. mistakes in identifications of bottlenecks of the building. One of the stages of validation of EvaTech is comparison of calculation results with evacuation trials carried out in different schemes of topology of a building. Comparison of the results of real evacuation trials with the results of simulations in other evacuation models shows that even well-known commercial software tools for evacuation calculation in some cases appear to be inaccurate in modeling of people movement.

For example, wrong movement algorithm leads to formation of a congestion at the acute angles of route. At the bottleneck the steady flow is observed and the width of the bottleneck doesn't influence evacuation results (Fig. 3, left). More realistic situation is achieved by improving of the movement algorithm. Now the width of the bottleneck controls the flow movement (Fig. 3, right).

2.2 Human Behavior

Modeling of human behavior is in its early stages of development. An occupant, modeled as an agent, plans his/her actions depending on the current goals and data available from the environment and observe the environment for events which he is concerned with (see Fig. 4). The environment includes building elements, objects to interact with (e.g. elevator call buttons) and other occupants.

The user defines the goals of the occupant in a script. The goals can vary in their level and complexity. There are low-level goals (e.g. “go to location”)

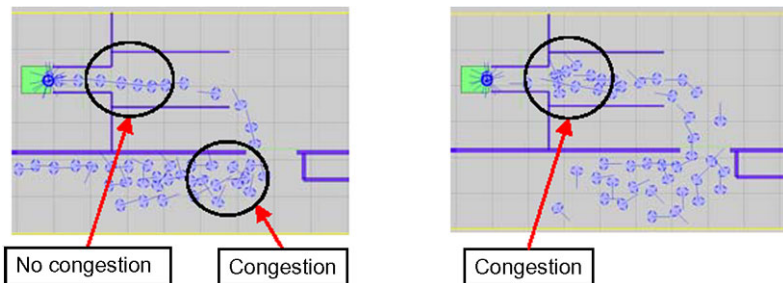


Fig. 3. Movement around corner.

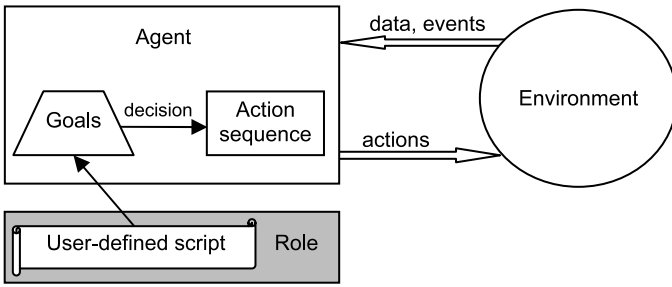


Fig. 4. Model of behavior.

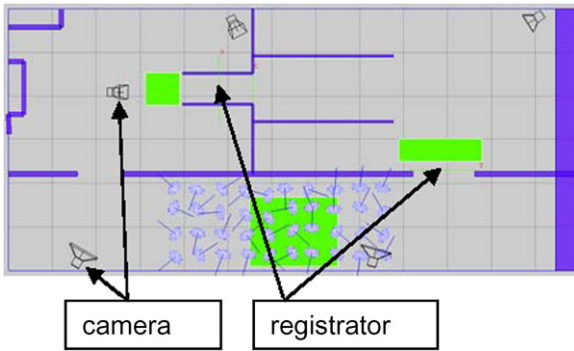


Fig. 5. Camera and registrator objects in EvaTech.

and high-level goals (e.g. “fight fire”, “evacuate from building”). When an occupant starts to achieve a goal, the goal is decomposed by the planning algorithm to a number of low-level goals and finally to a sequence of actions, simulating human-like decisions. The actions of an occupant can be “go to point”, “open door”, “take fire extinguisher” etc. It is intended to keep the planning algorithms absolutely clear and controllable by the user.

2.3 EvaTech Model Validation

A number of movement trials were executed by SITIS Ltd. The process of the trials was recorded on video- and thermo cameras (see Figs. 6 and 7).

For validation against trials EvaTech was instrumented with special objects: *camera* and *registrator* (see Fig. 5), which are intended to imitate a video camera and a thermo camera respectively. *Camera* is just a user-defined view of scene, which is saved in the project. A registrator is an object in the form of a line that allows to count persons and collect such data as flow capacity.

The output of these objects is compared with the output of their analogues. This approach is malleable to automation, and since the evacuation is a stochastic process demanding multiple trials on the same scheme, this is a useful advantage.

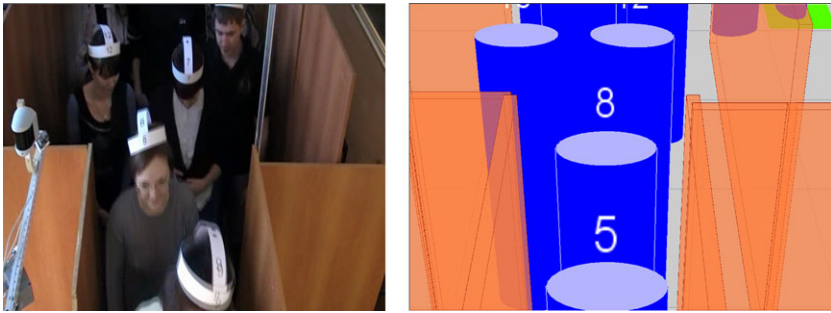


Fig. 6. View from real video camera and camera object in EvaTech.

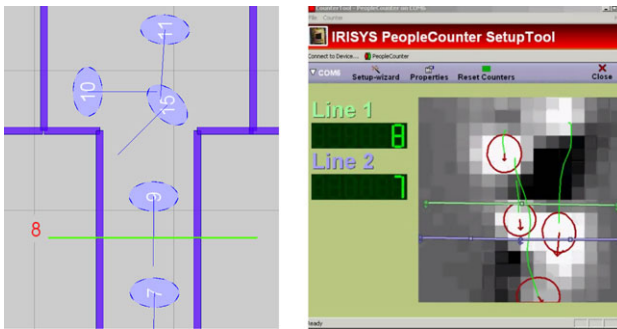


Fig. 7. Object registrator in EvaTech, showing number of occupants that passed the check line (*left*) and a view of the output of a thermo camera “IRISYS IRC1004” in the “IRISYS PeopleCounter SetupTool” (*right*).

2.4 Future Work

While continuing to develop the model of human behavior and implementing of people-people interactions today, EvaTech will be able to model lifts and escalators and will be integrated with FDS in the future, allowing fire and smoke to affect the process of evacuation and vice versa.

References

1. GOST 12.1.004-91*. Fire Safety. General Requirements. IPK Standards, Moscow, 1996.
2. V.M. Predtechenskii, A.I. Milinskii. Planning for Foot Traffic Flow in Buildings. Amerind, New Delhi, 1978.
3. MGSN 4.19-2005. Short Term Design Code of Multifunctional High-Rise Buildings and Buildings-Complexes in Moscow city. Moscow government, Moscow, 2005.

4. H.E. Nelson, F.W. Mowrer. Emergency movement. In P.J. DiNenno, W.D. Walton et al., editors, *The SFPE Handbook of Fire Protection Engineering* (Third ed.), Society of Fire Protection Engineers, Bethesda, MD, 2002.
5. E.D. Kuligowski, R.D. Peacock. *A Review of Building Evacuation Models*. National Institute of Standards and Technology, Washington, 2005.
6. J.D. Averill, D.S. Mileti, R.D. Peacock, E.D. Kuligowski, N. Groner, G. Proulx, P.A. Reneke, H.E. Nelson. *Occupant Behavior, Egress and Emergency Communications. Federal Building and Fire Safety Investigation of the World Trade Center Disaster*. National Institute of Standards and Technology, Washington, 2005.
7. E.W. Dijkstra. A note on two problems in connexion with graphs. *Numerische Mathematik*, 1, 269–271, 1959.

Large Scale Microscopic Evacuation Simulation

Gregor Lämmel¹, Marcel Rieser^{1,2}, and Kai Nagel¹

¹ Transport Systems Planning and Transport Telematics, TU Berlin,
Salzufer 17-19, 10587 Berlin, Germany
e-mail: laemmel@vsp.tu-berlin.de

² Institute for Transport Planning and Systems, ETH Zurich, 8093 Zurich,
Switzerland

Summary. The evacuation of whole cities or even regions is an important problem, as demonstrated by recent events such as evacuation of Houston in the case of Hurricane Rita or the evacuation of coastal cities in the case of Tsunamis. A robust and flexible simulation framework for such large-scale disasters helps to predict the evacuation process. Existing methods are either geared towards smaller problems (e.g. Cellular Automata techniques or methods based on differential equations) or are not microscopic (e.g. methods based on dynamic traffic assignment). This paper presents a technique that is both microscopic and capable to process large problems.

1 Introduction

Disaster and evacuation planning has become an important topic in science and politics. In principle there are two different situations: evacuation of buildings, ships and airplanes or the like on the one hand, or evacuation of whole cities or even regions on the other hand. The former involves normally the evacuation of pedestrians, whereas the latter is often associated with the evacuation by car. Corresponding to the two different types of problems, there are two different basic approaches for simulating the traffic flow:

- (1) Methods of dynamic traffic assignment (DTA) have been applied to evacuation simulation on the city or regional scale (e.g. MITSIM [1] or DYNAMSMART [2]). The DTA approach is based on the analogy between traffic and hydrodynamic characteristics of fluids. That means DTA is a macroscopic approach and reduces the problem of evacuation dynamics to a well known physical problem. However, in DTA it is not straightforward to deal with the inhomogeneity of a population. For this, a microscopic simulation is needed, where all people are simulated as individuals.
- (2) Microscopic simulations are often based on Cellular Automata (CA) [3, 4]. In CA models each evacuee is designed as an individual; therefore it is possible to simulate also population structures where people have different

speeds or ranges, or more complex behavior. The modeling of complex behavior in evacuation simulation has become important in recent years. People could for example ignore warnings or might not choose the nearest emergency exit, furthermore people tend to follow others (herd behavior) [5, 6]. Agent oriented research groups have modeled such behavior [7, 8]. In general it is expected that complex behavior leads to longer evacuation times, consequently a simulation that ignores such behavior patterns is probably optimistic.

One possible approach to deal with large-scale scenarios (hundreds of thousands of persons) but to retain persons as individual agents is based up on a modified queuing model [9, 10]. The queuing model simplifies streets to edges and crossings to nodes. This graph-oriented model is defined by lengths/widths, free speed and flow capacity of the edges. This simplification leads to a major speedup of the simulation while keeping results realistic.³

2 Simulation Framework

The evacuation simulation is based on the MATSim framework (www.matsim.org), which is constructed around the notion of agents that make independent decisions about their actions. Each evacuee is modeled as an individual agent that optimizes its personal evacuation route. The objective is a Nash equilibrium, where every agent attempts to find a route that is optimal for the agent. In reality this might be achieved by appropriate training or guidance while maintaining acceptability in the sense that no person could gain by deviating from this solution. The results from the simulation give an estimate of the time it could take to evacuate the endangered area.

The escape routes are encoded in so-called *plans*. Besides the escape route a *plan* also contains the departure time. That means it would also be possible to model an arbitrary variance in the evacuees' response time. However, in the work presented here, it is assumed that all evacuees start to evacuate at the same time. The traffic flow simulation is implemented as a queue simulation, where each street (link) is represented as a FIFO (first-in first-out) queue with three restrictions [9]. First, each agent has to remain for a certain time on the link, corresponding to the free speed travel time. Second, a link flow capacity is defined which limits the outflow from the link. If, in any given time step, that capacity is used up, no more agents can leave the link. Finally, a link storage capacity is defined which limits the number of agents on the link. If it is filled up, no more agents can enter this link. The difference to standard queueing theory is that agents (particles) are not dropped but spill back, causing congestion. An illustration of the queue model is shown in Fig. 1. The

³ For example, the simulation of the whole (motor) traffic of Switzerland (approx. 5 million trips) takes less then 5 minutes for 24 h real time [11].

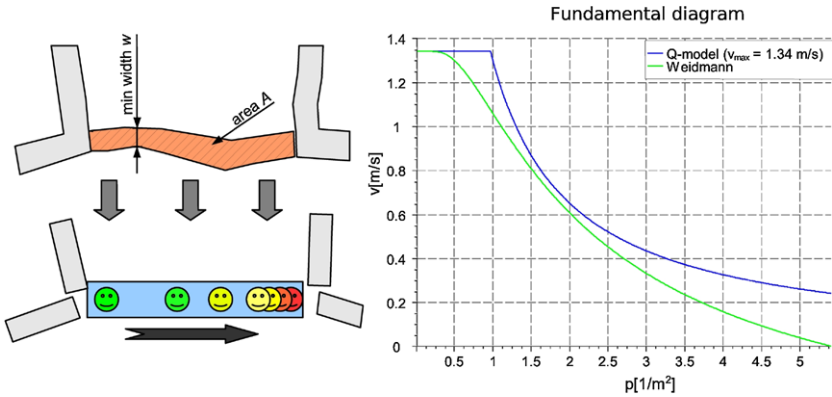


Fig. 1. Illustration of the queue model.

free parameters (i.e. flow capacity, storage capacity and free speed) are chosen to approximate Weidmann’s fundamental diagram [12].⁴

The initial escape routes are generated by applying (a time-dependent) Dijkstra’s shortest path algorithm [14] assuming free speed is possible on all links. Dijkstra’s algorithm is designed to deal with single-destination problems, but in the case of an evacuation there are many different safe places possible. The standard approach (e.g. [15]) is to transform this multi-destination problem into a single-destination problem by creating a new node as super-sink. All links which lead out of the evacuation area are connected, using virtual zero cost links, to that super-sink (see Fig. 2a). Doing so, Dijkstra’s algorithm will find the shortest route from any node inside the evacuation area to this super-sink.

The outcome of the traffic flow simulation (e.g. congestion) depends on the planning decisions made by agents. It is obvious that simulating the initial escape routes only will not provide a good or realistic solution for the evacuation problem and the results will be far away from Nash equilibrium. To find the Nash equilibrium, the simulation framework runs learning iterations: At the end of each iteration, every agent scores the performed plan. In this study the scoring function is simply the negative of the travel time. This score is then memorized for the plan. After the agents have updated their score, each of them decides with a certain probability to revise its plan. In the re-planning procedure, the Dijkstra router is again applied to find the fastest escape route for each agent. The difference to the initial routing is that the weights for the links are no longer based on free speed travel times but on the experienced travel times from the last iteration. For every agent that has not been chosen for re-planning, a probabilistic discrete-choice model selects a plan out of its memory, where the probabilities of the plans increase with the achieved score.

⁴ Newer studies [13] imply other fundamental diagrams than those from Weidmann. An adaptation of these values could, in consequence, become necessary in future.

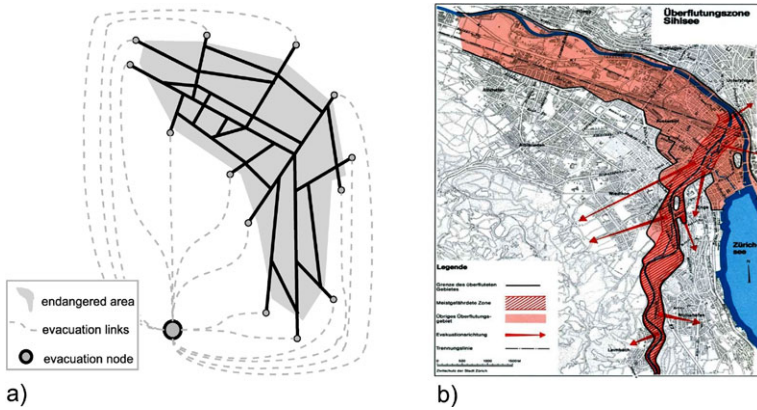


Fig. 2. Inundation map and evacuation network.

Repeating this iteration cycle, the agent behavior will move towards a Nash equilibrium.

3 Results

A hypothetical event of a dam-break of the Sihlsee dam was chosen as a scenario. This would lead to an inundation of parts of the city of Zurich. According to the civil defense office there will be an advance warning time of about 110 minutes until the inundation will reach the city center. The civil defense office also provides an instruction sheet with an inundation map of the area at risk (Fig. 2b). A NAVTEQ network (www.navteq.com) for Switzerland was chosen as evacuation network and adapted for pedestrian simulation. The affected part of the city of Zurich consists of 3037 nodes and 6120 links. The synthetic population embraces 165571 agents and was extracted from census data and contains all people with their work place within the evacuation area.

The simulation run was performed on a dual core CPU at 2.33 GHz with 2 GB of RAM. The computer runs JAVA jdk1.5_012 on Linux. The evacuation simulation has been stopped after 100 re-planning cycles. The overall runtime was 3 hours and 24 minutes. The simulation consumed up to 1393 MB of RAM. As expected, the evacuation time decreases significantly with the iterations and levels out at approximately 45 minutes (see Fig. 3a). Using a visualizer, some bottlenecks could be detected. This is shown in Fig. 3b. These bottlenecks mainly occur at bridges. The snapshot was taken after 100 iterations of learning, consequently there seems to be no better solution for the individual agent than to queue up on these bridges.⁵

⁵ For those who know the area: Since this preliminary study is based on a vehicular traffic network, it ignores links which can be used by pedestrians only. This could be corrected by using different network data.

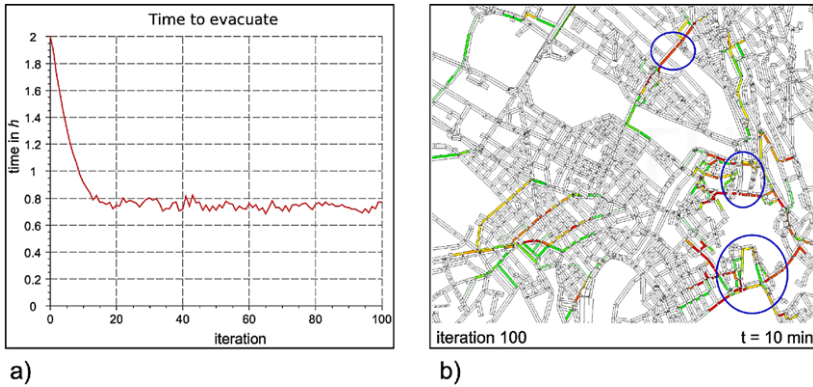


Fig. 3. Results of the simulation.

4 Conclusions

We introduced a microscopic pedestrian simulation framework for large-scale evacuations. It is implemented as a Multi Agent Simulation, where every agent tries to optimize its individual evacuation plan in an iterative way. The simulation framework is demonstrated through a case study based on a hypothetical dam-break of the Sihlsee dam near Zurich. Despite the underlying behavioral model being quite simple, the simulation gives plausible results regarding the predicted evacuation time and bottlenecks. The runtime performance shows that this approach is well suited for large scale scenarios. With state of the art hardware it is no problem to simulate much larger scenarios with over one million agents. In future work it is planned to apply this framework to an evacuation simulation in the case of a Tsunami warning for the Indonesian city of Padang. The improvement of the behavioral model (e.g. herd behavior [5] modified for large-scale scenarios [16]) could also be a topic of future work.

Acknowledgements

We thank *Schutz & Rettung Zürich* for the permission to reprint the inundation map shown in Fig. 2b. This project was funded in part by the German Ministry for Education and Research (BMBF), under grants numbers 03G0666E (“last mile”) and 03NAPI4 (“Advest”). A similar but more extended paper has appeared under the title “Bottlenecks and Congestion in Evacuation Scenarios: A Microscopic Evacuation Simulation for Large-Scale Disasters” in [17].

References

1. M. Jha, K. Moore, and B. Pashaie. Emergency evacuation planning with microscopic traffic simulation. Paper 04-2414, Transportation Research Board Annual Meeting, Washington, DC, 2004.
2. E. Kwon and S. Pitt. Evaluation of emergency evacuation strategies for downtown event traffic using a dynamic network model. Paper 05-2164, Transportation Research Board Annual Meeting, Washington, DC, 2005.
3. K. Nagel and M. Schreckenberg. A cellular automaton model for freeway traffic. *J. Phys. I*, 2:2221–2229, 1992.
4. K. Nishinari, A. Kirchner, A. Nazami, and A. Schadschneider. Extended floor field CA model for evacuation dynamics. *IEICE Trans. Inf. Syst.*, E87-D:726, 2004.
5. D. Helbing, I. Farkas, and T. Vicsek. Simulating dynamical features of escape panic. *Nature*, 407:487–490, 2000.
6. C. Lieberman, D. Kurowski, M.R. Avila, L. Ricci, N. Thomas, C. Collyer, and B. Aguirre. Conceptual framework for simulating the pedestrian evacuation behavior from buildings. Paper 05-2297, Transportation Research Board Annual Meeting, Washington, DC, 2005.
7. Y. Murakami, T. Ishida, T. Kawasoe, and R. Hishiyama. Scenario description for multi-agent simulation. In *Autonomous Agents and Multiagent Systems (AAMAS'03)*, Melbourne, Australia, July 2003.
8. X. Pan, C.S. Han, K. Dauber, and K.H. Law. A multi-agent based framework for the simulation of human and social behavior during emergency evacuations. *Artif. Intell. Soc.*, 22(2):113–132, 2007.
9. C. Gawron. An iterative algorithm to determine the dynamic user equilibrium in a traffic simulation model. In D.E. Wolf and M. Schreckenberg, editors, *Traffic and Granular Flow'97*, pages 469–474. Springer, Berlin, 1998.
10. P.M. Simon, J. Esser, and K. Nagel. Simple queueing model applied to the city of Portland. *Int. J. Mod. Phys. C*, 10(5):941–960, 1999.
11. B. Raney, N. Cetin, A. Völlmy, M. Vrtic, K. Axhausen, and K. Nagel. An agent-based microsimulation model of Swiss travel: First results. *Netw. Spat. Econ.*, 3(1):23–41, 2003.
12. U. Weidmann. *Transporttechnik der Fussgänger*, volume 90 of *Schriftenreihe des IVT*. Institute for Transport Planning and Systems ETH Zürich, Zürich, 2nd edition, 1993. In German.
13. A. Schadschneider, W. Klingsch, H. Klüpfel, T. Kretz, C. Rogsch, and A. Seyfried. Evacuation dynamics: Empirical results, modelling and applications. In B. Meyers, editor, *Encyclopedia of Complexity and System Science*. Springer, Berlin, 2009.
14. E. Dijkstra. A note on two problems in connexion with graphs. *Numer. Math.*, 1:269–271, 1959.
15. Q. Lu, B. George, and S. Shekhar. Capacity constrained routing algorithms for evacuation planning: a summary of results. In *Lecture Notes in Computer Science*, volume 3633, pages 291–307. Springer, Berlin, 2005.
16. C. Gloor, P. Stucki, and K. Nagel. Hybrid techniques for pedestrian simulations. In *Lecture Notes in Computer Science*, volume 3305, pages 581–590. Springer, Berlin, 2004.

17. G. Lämmel, M. Rieser, and K. Nagel. Bottlenecks and congestion in evacuation scenarios: A microscopic evacuation simulation for large-scale disasters. In *Proc. of 7th Int. Conf. on Autonomous Agents and Multiagent Systems (AAMAS 2008)*, Estoril, Portugal, 2008.

Numerical Optimisation Techniques Applied to Evacuation Analysis

Rodrigo Machado Tavares and Edwin R. Galea

Fire Safety Engineering Group, University of Greenwich, London, UK

e-mail: E.R.Galea@gre.ac.uk

Summary. A common problem faced by fire safety engineers in the field of evacuation analysis concerns the optimal design of an arbitrarily complex structure in order to minimise evacuation times. How does the engineer determine the best solution? In this study we introduce the concept of numerical optimisation techniques to address this problem. The study makes use of the buildingEXODUS evacuation model coupled with classical optimisation theory including Design of Experiments (DoE) and Response Surface Models (RSM). We demonstrate the technique using a relatively simple problem of determining the optimal location for a single exit in a square room.

1 Introduction

In attempting to find the optimal design which minimises egress time for an arbitrarily complex structure the engineer typically identifies several design variables and associated constraints which may be adjusted to modify the egress time. In practise the engineer would select several scenarios covering the allowable range of the design variables, run the simulations and select the scenario which produces the shortest evacuation time. But how does the engineer know that the solution is optimal or near optimal? The more cases the engineer runs the more likely they will be to have identified the optimal solution however, the more cases that are run, the longer the design time. Indeed, to be certain of finding a near optimal solution many hundreds of scenarios may need to be run and analysed to ensure that the entire design space is covered.

To address this problem we propose to use classical optimisation theory including Design of Experiments (DoE) and Response Surface Models (RSM) coupled to evacuation simulation using the buildingEXODUS evacuation software [1, 2].

2 The Methodology

The methodology uses four main steps:

- **STEP 1: Identify the Objective Function (OF)**

The OF is the function that is to be optimised, in these problems the OF is the Total Evacuation Time (ET). The main objective is to minimise ET.

- **STEP 2: Define Design Variables (DV) and constraints**

For an OF there may be many DV (DV1, DV2, DV3, ...) e.g. number of exits, exit location, exit width, shape of the enclosure, number of occupants, etc. Thus the OF may be multi-dimensional.

- **STEP 3: Construct Response Surface (RS) describing OF**

The RS is a multi-dimensional surface in DV space. Each point on the RS is determined by running the evacuation software for each unique set of DV. This requires many hundreds of evacuation scenarios to be simulated ensuring that the entire design space is covered. As this is impractical, an approximation to the RS is developed by running only a handful of scenarios for selected KEY values of the DV. The KEY values for the DV required to produce a “reasonable” approximation to the RS are determined using DoE techniques. These techniques identify strategic combinations of DV which provide a good coverage of the design space and which hopefully will produce a reasonable approximation to the RS. Examples of DoE techniques are the *Latin Hypercube* and *Central Composite Design* (CCD) [3, 4]. DoE techniques can only be used in unconstrained problems. In constrained problems, random selection procedures must be used.

Each strategic combination of DV identified by the DoE technique defines a scenario which is then run using the evacuation model. The RSM is determined by fitting a mathematical function to the surface of points (ET, DV1, DV2, ...) in the design space. Examples of RSM which were used in this study are the *full-quadratic* and *high order polynomial* approximations [5].

- **STEP 4: Determine the minimum of the RSM**

Numerical optimisation techniques are used to find the minimum of the multi-dimensional RSM. There are many optimisation algorithms [6] which can broadly be categorised into two families, the classical gradient-based methods and the stochastic-based methods. Examples of optimisation techniques include: *Fletcher–Reeves*—a gradient method and *Particle Swarm Optimisation (PSO)*—a stochastic method [6].

The Fletcher–Reeves method can be used for constrained and unconstrained problems and its algorithm is based on the first derivatives of the OF and is considered to be very robust [6]. The technique does not use information obtained from matrix operations which also makes it numerically efficient. The main advantages of this method are: the gradient is linearly independent of all previous direction vectors; the searching process makes good progress because it is based on gradients and the formula to

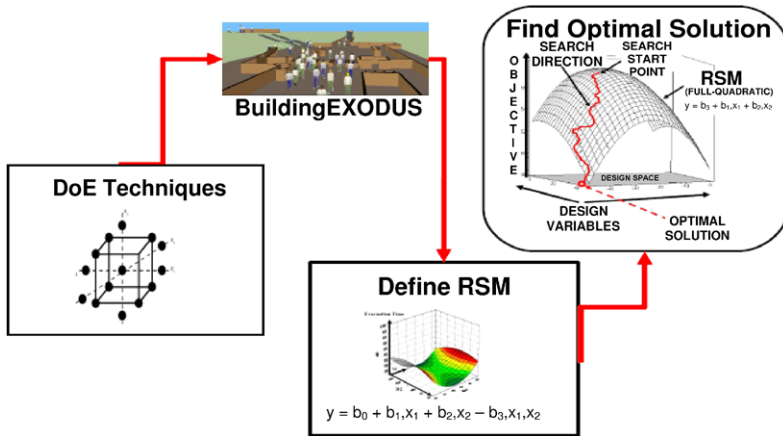


Fig. 1. The proposed optimisation methodology.

determine the new direction is simple. The Particle Swarm Optimisation (PSO), is based on a simplified social model that is closely tied to swarming theory [7]. It was developed by Dr. Eberhart and Dr. Kennedy in 1995 and it is inspired by social behaviour of bird flocking or fish schooling [8, 9]. The principle is that the design variables are understood as particles with associated velocities. The method is analogous to the Fletcher–Reeves, however instead of using the gradients of the objective function to insert the searching algorithm, the vectors are represented by uniform random numbers between 0 and 1.

In the work presented in this paper both these techniques were used. Once the minimum of the RSM is found it represents the set of DV required to produce the OPTIMAL solution. The proposed methodology is summarised in Fig. 1.

3 Demonstration Problem

The problem to be investigated can be stated very simply as follows, for a room of given size, containing an arbitrarily large population and a single exit, is there an optimal location for the exit that will minimise egress times? The square room used in the analysis has an area of 100 m² and an exit of width 1.0 m is considered. The population of the room consists of 200 people producing a population density of 2 people/m².

Our specific problem involves the determination of the optimal location of a single exit in a square room that results in the minimum evacuation time for the room. Here the Evacuation Time (ET) is the Objective Function (OF) and the exit location, measured from an arbitrary point on the perimeter is

the single Design Variable (DV). As the exit can be placed anywhere on the perimeter of the room, the problem is considered unconstrained.

4 The Solution

The approach adopted involves the use of the buildingEXODUS evacuation software to simulate the evacuation of the compartment for each relevant exit configuration. The egress simulations were conducted assuming ideal conditions of zero response times and population behaviour such that occupants would move to their nearest exits. Both assumptions are made to simplify the analysis and to focus on issues associated with exit location. The population was randomly generated with a maximum travel speed varying between 1.2 m/s and 1.5 m/s. The unit flow rate of the exit was capped to a maximum value of 1.33 occupants/m/sec. The simulations were repeated a total of 600 times for each scenario. Thus all the numerical predictions represent an average over 600 simulations. For each repeat simulation the starting location of the population was also randomised. This ensured that the population was distributed throughout the confines of the geometry with little bias resulting from population starting position contributing significantly to the overall results.

4.1 The Design Variables

The geometry is defined by a $10\text{ m} \times 10\text{ m}$ room with a single 1 m wide exit. The DV is the exit position (EP) which is measured from the bottom left corner of the room to the leading edge of the door. Given the symmetry of the room, the domain of the DV is $0 \leq \text{EP} \leq 4.5$. For instance, when $\text{EP} = 0$ the exit is located in the bottom left corner while when $\text{EP} = 4.5$ the exit is located 4.5 m from the left corner and is located within the centre of the wall.

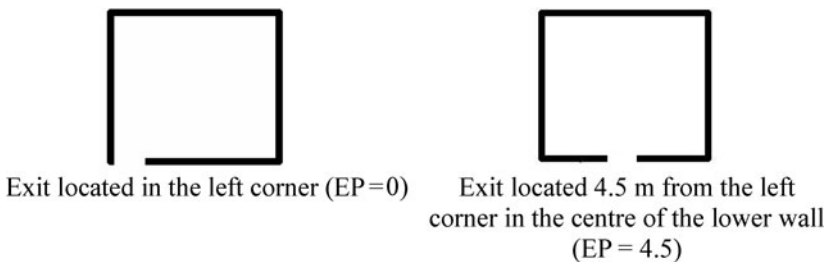


Fig. 2. Exit locations for single exit cases with 1.0 m wide door.

4.2 Results and Discussion

The solution to this problem was determined by “brute force” by defining seven unique exit locations and performing 4,200 simulations using building EXODUS [10]. The seven exit locations were selected by attempting to cover as many unique locations in the DV domain as was thought to be practical. The results of this “brute force” approach (or traditional approach) suggested that an exit located in the corner of the room would produce a minimum evacuation time of 165.4 sec as shown in Fig. 3.

The problem was also solved using the Optimisation Method described in this paper. Two different approaches were used. In the first case all seven design points were used to define the RSM while in the second case a DoE technique was used to define the number and location of the DV. The solution found based on the seven different values of the DV used a forth order polynomial function to define the RSM and two optimisation techniques, Fletcher–Reeves and PSO. The forth order polynomial function defined the RSM with an R^2 of 0.95 producing a good fit. Using the optimisation techniques and the RSM defined using seven values of the DV the same optimal solution was found as using the brute force technique i.e. (0; 165.4). This suggests that if a sufficiently accurate RSM is used, these optimisation techniques are capable of accurately determining the optimal solution. However, we have gained little advantage as we have used as many design points as was used in the brute force method to locate the optimal solution.

For the second approach DoE techniques were used to identify the number and value for the DV. The Latin Hypercube DoE technique suggests that six design points must be used resulting in 3,600 simulations. Using the CCD DoE technique only three design points are required resulting in 1,800 simulations. In both cases a Full-Quadratic polynomial was used to define the RSM, pro-



Fig. 3. Average ET for the single exit cases.

ducing a R^2 of 0.99. In both cases, both optimisation techniques were again used and in all four cases the correct optimal solution was obtained.

Thus using the DoE techniques combined with optimisation methods we have been able to identify the optimal egress solution using considerably less computational effort, and hence time than the brute force method.

5 Concluding Comments

In this paper we have presented a method to reduce the effort involved in determining optimal design to minimise evacuation time. The method is based on classical DoE, RSM and Numerical Optimisation techniques. The technique was demonstrated using a simple square room with a single exit. The optimisation method correctly identified the location of the exit that results in producing the minimum evacuation time for the structure.

Using the CCD DoE technique to identify three unique values of the DV, the Full Quadratic Smooth technique to define the RSM and two optimisation techniques, a gradient-based technique, the Fletcher–Reeves and a stochastic technique, the PSO, the correct solution was found and, most importantly, required 57% less effort than the brute force method of finding the optimal solution.

While the example application is considered quite simply, the authors have also successfully applied the technique to more complex problems involving rooms with two exits. In this case the problem is constrained as the location of the exits cannot overlap and non-square shaped rooms. In all these cases the technique is capable of identifying reasonable solutions to these problems. Further testing of the method continues to determine its robustness.

Acknowledgements

Mr. Rodrigo Machado Tavares gratefully acknowledges the financial support he received from the Programme Alban (Alban Code: E03D05378BR) and also the University of Greenwich from their bursary scheme.

References

1. J. Park, S. Gwynne, E.R. Galea, P. Lawrence, Validating the building EXODUS evacuation model using data from an unannounced trial evacuation. Proc. of 2nd Int. Pedestrian and Evacuation Dynamics Conference, Ed. E.R. Galea, CMS Press, Greenwich, UK, 2003, pp. 295–306. ISBN 1904521088.
2. L. Filippidis, E.R. Galea, S. Gwynne, P. Lawrence, Representing the influence of signage on evacuation behaviour within an evacuation model, Journal of Fire Protection Engineering, Vol 16, No 1, pages 37–73, 2006. DOI: [10.1177/1042391506054298](https://doi.org/10.1177/1042391506054298).

3. D.C. Montgomery, *Design and Analysis of Experiments* (6th edition), Wiley, New York, 2005. ISBN 0-471-48735-X, www.wiley.com/college/montgomery.
4. G.E.P. Box, W.G. Hunter, J.S. Hunter, *Statistics for Experiments: An Introduction to Design, Data Analysis, and Model Building*, Wiley-Interscience, New York, 1978. ISBN 0-471-09315-7.
5. G.E.P. Box, N.R. Draper, *Empirical Model-Building and Response Surfaces*, Wiley, New York, 1987.
6. L.R. Foulds, *Optimization Techniques: An Introduction*, UTM (Undergraduate Texts in Mathematics), 1948. ISBN 0-387-90586-3.
7. VisualDOC Design Optimization Software, Version 1.0 Reference Manual, Vanderplaats Research and Development, Inc., Colorado Springs, CO, 1998.
8. L. Xu, T. Reinikainen, W. Ren, A simulation-based multi-objective design optimization of electronic packaging under thermal cycling and bend loading. Proc. of EuroSimE 2003, IEEE Press, New York, 2003.
9. G. Venter, J. Sobieszczanski-Sobieski, Multidisciplinary optimization of a transport aircraft wing using particle swarm optimization, *Structural and Multidisciplinary Optimization*, Vol 26, pages 121–131, 2004.
10. R. Machado Tavares, E.R. Galea, Optimal positioning of exits to minimise egress time for a square room with one or two exits of equal size, submitted to *Journal of Fire Protection Engineering*, 2008.

A Multi-Method Approach to the Interpretation of Pedestrian Spatio-Temporal Behaviour

Alexandra Millonig^{1,2} and Georg Gartner¹

¹ Department of Geoinformation and Cartography, Vienna University
of Technology, Gusshausstr. 27–29, 1040 Vienna, Austria
e-mail: millonig@cartography.tuwien.ac.at; ggartner@mail.tuwien.ac.at

² Human Centered Mobility Technology, arsenal research, Giefingg. 2,
1210 Vienna, Austria
e-mail: alexandra.millonig@arsenal.ac.at

Summary. The development of mobile spatial-information technologies requires a profound understanding of pedestrian spatio-temporal behaviour. In a currently ongoing project we use several empirical methods following the concept of “across-method” triangulation to comprehensively study human spatial behaviour. In this contribution we will introduce a multi-method approach including a combination of localisation and tracking techniques (GPS, Bluetooth, unobtrusive observation) as well as enquiries concerning intentions, lifestyle attributes, socio-demographic characteristics, route quality preferences, and preferred way-finding strategies. The combination of qualitative-interpretative and quantitative-statistical data will lead to the determination of a typology of lifestyle-based pedestrian mobility styles, which can serve as a basis to customise navigational and environmental information to individual needs, and to create pedestrian interest profiles in ubiquitous environments. We present experimental results of the first of two consecutive empirical phases based on a data set containing of more than 100 trajectories of people observed by path following in an indoor and outdoor environment.

1 Introduction

In recent years, ubiquitous computing technologies have made it possible for individuals to gain ubiquitous access to information services. Especially in urban areas, people routinely rely on mobile phones, smart phones and Internet-enabled personal digital assistants (PDAs) to coordinate their activities. Mobile tools for way-finding combined with location based information now offer the possibility to obtain practical information concerning optimal routes and useful facilities in the vicinity. However, the consideration of “optimal routes” or “useful information” differs from person to person. Several studies indicate that human route decision processes and information preferences depend on

various different parameters (physical, emotional, cognitive, or lifestyle related factors) [1–3].

The complexity of human walking behaviour and route decision processes calls for the employment of a combination of different empirical techniques in order to unveil observable motion behaviour as well as an individual’s intentions and personal characteristics. In a currently ongoing project we use an “across-method” triangulation approach combining several empirical methods to investigate and thoroughly comprehend human walking behaviour. As a result, we aim at the determination of a pedestrian typology based on qualitative-interpretative and quantitative- statistical data. Types will be described according to characteristic attributes identified in their route choice behaviour, walking patterns and interest foci. Possible types of behaviour may for example include the “broadly interested flaneur” (low velocity, frequent turns, various interests), or the “goal-oriented, efficient go-getter” (high velocity, shortest routes between stops, specific interests). This typology of lifestyle-based pedestrian mobility styles can subsequently serve as a basis to create pedestrian interest profiles in ubiquitous environments and to customise navigational and environmental information to individual needs.

In this contribution we give an introduction to the design of the currently ongoing study, focusing on the methods and initial results form the first of two consecutive empirical phases.

2 Methodology

In order to gain a comprehensive insight to human spatio-temporal behaviour, we employ two consecutive phases of empirical data collection, followed by hypothesis testing and the development of a model of pedestrian mobility styles. Figure 1 shows the study design including the empirical methods we use in each phase of the study.

For the current project we decided to follow the concept of “across-method” triangulation [4] recommending a combination of at least two different methods to overcome methodological drawbacks and to maximise the benefits of different techniques. Techniques being used in this study include:

- *Unobtrusive Observation*: Observation of the “natural”, unswayed spatio-temporal behaviour of pedestrians; only visible behaviour, no insight to intentions and motives.
- *Non-disguised Observation*: Continuous observation over a long period in combination with standardised interviews (data from both the structural and the agent-centred perspective); observer effects possible.
- *Enquiry*: Motivations, self-assessments of individual motion patterns; responses can be incorrect and constructed ex post.

The first heuristic phase is to hypothesise and identify basic types of pedestrian route choice behaviour and movement patterns. In Sect. 3, the data col-

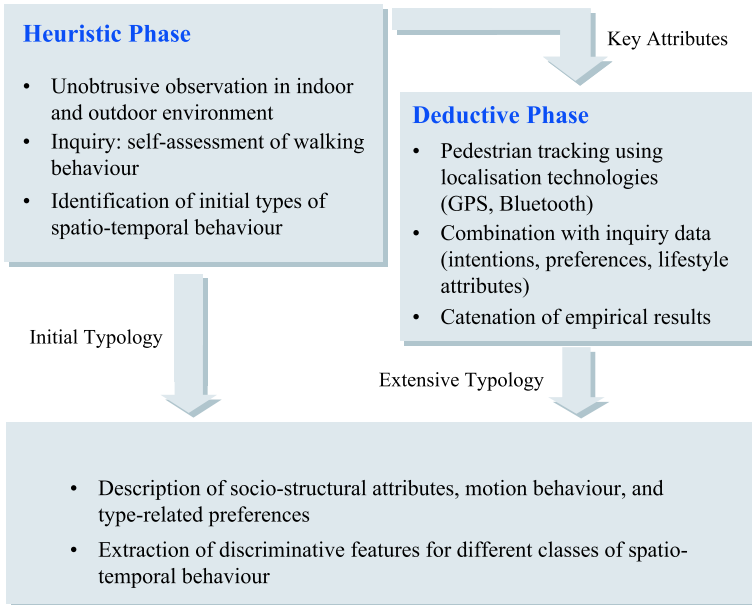


Fig. 1. Methodology.

lection methods and analysis procedures of this already completed phase are described in more detail.

In the consecutive following deductive phase the initial typology is tested using a combination of localisation technologies (outdoor: GPS; indoor: Bluetooth) and detailed semi-standardised interviews. Results of both empirical phases are subsequently related to each other in order to identify specific spatial behavioural styles for the provisional categories. This leads to the development of a model of pedestrian mobility styles including multiple aspects of each detected type (basic parameters of velocities, stops, and turns; behavioural characteristics; preferences; socio-demographic and lifestyle attributes). Discriminative features are determined and extracted, which can be used to provide customised information to specific types of pedestrians using an implemented way-finding system.

3 Heuristic Phase

The first phase of the empirical study has been conducted in Vienna in 2007. As investigation fields a shopping centre for the indoor observations and two major shopping streets for monitoring outdoor behaviour have been chosen in order to avoid the occurrence of behavioural differences caused by different context situations. In this phase the empirical methods used for data collection

consist of unobtrusive observation (also known as “tracking” or “shadowing” [5]) and standardised interviews.

Observation procedures started with a random selection of unaccompanied walking pedestrians and following the individual as long as possible while mapping her or his path on a digital map, recording the specific point in time and the coordinates within the map for each point of the path. After completing an observation (e.g. when the subject left the observation area or the observer lost sight of the subject), additional notes concerning visible attributes of the subjects were taken (gender, age, appearance).

After the observation period an enquiry in the form of face-to-face interviews was conducted in each investigation area. The questionnaire included standardised questions concerning socio-demographic attributes, questions related to the current goals and tasks, and questions referring to individual walking preferences (e.g. slow or fast, exploring or goal oriented).

The analysis procedures performed on the collected data included qualitative-interpretative methods and multivariate analysis methods (factor analysis, cluster analysis). Data have been analysed according to three aspects:

- *Motion data*: Observed trajectories were analysed with respect to velocities (variations in velocity, velocity histograms), stops (frequency, duration, and position of stops), and significant changes in direction.
- *Self-assessment profiles*: Interview data referring to individual walking preferences were analysed in order to derive classes of subjective behaviour.
- *Lifestyle attributes*: Lifestyle related features have been extracted according to the visual appearance of observed individuals and the categories of visited shops or facilities.

In the following section example results derived from the analysis of motion data are presented.

4 Initial Results

In total, 111 individuals with a balanced gender and age ratio have been observed; 57 trajectories have been collected in the outside investigation area, 54 observations have been completed in the indoor environment. Outdoor observations had an average length of 12 minutes (maximum: 62 minutes), in the indoor area the observed individuals have been tracked for an average of 16.5 minutes (maximum: 57 minutes). The enquiry provides data collected from 130 interviews (30 outdoor; 100 indoor).

4.1 Example Results Based on Motion Data

The collected trajectories have been analysed according to the velocity computed between each marked point in the observed path, additionally locations and durations of stops within the trajectories have been detected (cf. Fig. 2).

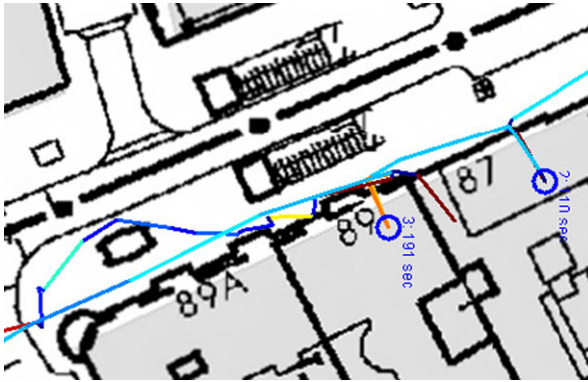


Fig. 2. Velocities (*colour-coded*) and stops of a typical trajectory.

Subsequently, histograms of each trajectory have been compiled, showing the proportional amount of time an individual walked at a velocity within a specific speed interval. A comparison of all histograms indicates differences in spatio-temporal behaviour in indoor and outdoor observations. Results show that subjects observed in the indoor environment spend significantly more time stopping e.g. in front or inside a shop and walk in general at lower speed than subjects observed in the outdoor area.

Clustering analysis performed on both datasets from outdoor and indoor observations produced rather diverse results. While the analysis of the outdoor data showed eight discriminative clusters, the analysis of indoor observations resulted in only three homogeneous clusters of motion behaviour. This difference might be explained by the greater diversity of potential goals (other than shopping) pedestrians might be pursuing in the outdoor environment.

As an example the results of the indoor analysis are now explained in more detail, as the context situation (shopping) can be assumed to be more homogeneous than outdoors. In total datasets of 54 observations have been classified. The three clusters of motion behaviour can be interpreted as “swift shoppers”, “convenient shoppers”, and “passionate shoppers”.

- *Swift shoppers:* This group consists of 60% male and 40% female participants who are relatively young compared to the other groups. They walk at comparably high speed (1.2 m/s on average) and stop rarely and for a very short time (7 sec on average, up to a maximum duration of 1 min).
- *Convenient shoppers:* Almost two thirds of this group are male shoppers (64%; 36% female). The average age lies between 35 and 40 years and is higher than in the comparison groups. They stop more frequently (on average 1.4 times per observation) and hence show a lower average speed (0.6 m/s). Stops last approximately 2.5 min (up to 8 min).
- *Passionate shoppers:* Two thirds of this group are females (67%; 33% male), aged around 30 to 35 years. They stop very frequently (about 3.6 times per

person) and for a comparatively long time (4.7 min on average, maximum 17 min). This results in a very low average speed of 0.2 m/s.

5 Conclusion

Preliminary results of the first empirical phase indicate that a number of homogeneous behaviour patterns can be observed, especially in consistent context situations. Currently ongoing investigations using a non-disguised form of observation combined with detailed interviews include and test basic findings of the first analyses. Further empirical analyses of more data during the currently ongoing second empirical phase as well as a careful examination of the results in different context situations during the final stage of the study are expected to lead to a comprehensive interpretation of pedestrian spatio-temporal behaviour. This can on the one hand be used in future mobile navigation services to provide customised route suggestions and location based information, and on the other hand serve as a basis for determining parameters for pedestrian simulation models.

Acknowledgements

This work is part of the UCPNavi project which is a cooperation project with arsenal research, Vienna. The project is supported by the Austrian Funds for Scientific Research (FWF). Special thanks go to M. Ray (arsenal research) for providing the tracking tool used in this survey; furthermore the authors would especially like to thank N. Brändle (arsenal research) for his help and advice concerning data analysis.

References

1. A. Millonig and K. Schechtner. Decision loads and route qualities for pedestrians key requirements for the design of pedestrian navigation services. In *Pedestrian and Evacuation Dynamics 2005*, pages 109–118. Springer, Berlin, 2007.
2. W. Daamen and S. Hoogendoorn. Research on pedestrian traffic flows in the Netherlands. In *Proceedings Walk 21 IV*, Portland, Oregon, United States, pages 101–117, 2003.
3. D. Helbing, P. Molnar, I.J. Farkas, and K. Bolay. Self-organizing pedestrian movement. *Environment and Planning B: Planning and Design*, 28:361, 2001.
4. A. Jakob. Möglichkeiten und Grenzen der Triangulation quantitativer und qualitativer Daten am Beispiel der (Re-) Konstruktion einer Typologie erwerbsbiographischer Sicherheitskonzepte. *Forum: Qualitative Social Research*, 2(1):online, 2001.
5. A. Keul and A. Kühberger. Tracking the Salzburg tourist. *Annals of Tourism Research*, 24:1008–1024, 1997.

The Microscopic Model and the Panicking Ball-Bearing

Colin Marc Henein and Tony White

Institute of Cognitive Science, Carleton University, 1125 Colonel By Drive,
Ottawa, Canada
e-mail: cmh@ccs.carleton.ca

Summary. Prominent microscopic models simulate panic (which has been described as a myth) allowing unwarranted simplifying assumptions that people are irrational, non-deliberative and interchangeable. While these assumptions can be remedied by increasing the behavioral repertoire of modelled individuals, large cognitive architectures would stifle a model's power to explain emergent crowd effects. We propose the microscopic human factor (MHF) approach that increases behavioral repertoire without compromise to the elegant simplicity from which the models derive their explanatory power.

1 Introduction

Jonathan Sime once admonished building designers for creating *ball-bearing designs* that treat people “as if they are nonthinking objects rather like the elements of a building structure” [1]. He argued that such designs neglect the important interactions between people and spaces. Sime also touched on evacuation simulations, suggesting that human cognition, decision making and social behaviors were excluded from models for practical reasons of modelling difficulty [2].

Since that time microscopic models have been developed. These models can, in principle, incorporate individuality. Yet, because of a continued focus on irrational “panic” behaviors, these models largely simulate homogenous crowds and ignore human factors. They still model ball-bearings.

The purpose of this paper is to argue that microscopic models must leave panic behind by modelling people rather than ball-bearings, and furthermore that this improvement is both possible and practical. In aid of this position, we begin by briefly reviewing the case against panic in crowds. We then turn to a consideration of two prominent microscopic models, their foundations in panic as a description of human behavior and the problems introduced by the panic assumption. We will then describe our *microscopic human factor* (MHF) approach that moves a microscopic model away from panic by

increasing behavioral repertoire—without jettisoning the benefits of microscopic modelling in the process. Finally, as a demonstration of the utility of the MHF approach, we will discuss our experience in using MHF techniques to expand the repertoire of the floor field model [3].

2 Panic

People are generally familiar with the concept of panic. Informed only by attention-seeking media reports and the emotionally-appealing images of Hollywood action blockbusters, it is easy to believe that people in large crowds are prone to mindless flight and irrational behavior on the one hand, and deliberate violence and uncontrolled aggression on the other. Dictionary definitions of panic support this populist view, emphasizing uncontrolled flight with an accompanying state of emotional arousal and unreasoned behavior [4]. Johnson’s sociological investigation found that the concept of panic includes “selfish competition uncontrolled by social and cultural constraints” [5]. In our view, the hallmark of panic, then, is irrational and asocial or anti-social behavior.

The question is: do people really panic in crowd situations? The academic view opposes the pop-psychological irrationalist view just described. It is the academic perspective that the behavior of people in emergency situations (such as fire and crowd disasters) is not irrational—rather, making sense in the context of the information available at the time [2, 6]. Additionally, sociologists tell us that social norms continue to be important in these situations and that incidences of injuries in crowds are seldom deliberate acts by violent people [5, 7]. Although competitive evacuations do occur, irrational panic (despite its media-driven allure) is at best non-explanatory and is at worst seen as a myth [8].

3 Panic in Microscopic Models

Panic is such a compelling concept, however, that it continues to crop up in non-behavioral disciplines modelling crowd behavior, particularly in microscopic models (see below). Although these disciplines may be less familiar with the evidence from the social sciences against panic, there is another reason why panic is compelling for crowd modellers. Because panicked individuals are assumed to exhibit behavior that is irrational and free of social constraints the modeller is relieved of the responsibility to simulate cognitive/psychological/behavioral factors in crowd dynamics. The result is agents (modelled individuals) that are non-cognitive; specifically they are non-rational (taking actions that do not make sense), non-deliberative (containing no mental state or processing) and interchangeable. This in turn reduces the complexity of the model, and encourages techniques used traditionally to model inanimate objects.

Although the panic assumption may be convenient in that it reduces complexity, it means that the behavior modelled is at odds with our concept of human behavior. This opens the model to the criticism that its results cannot be meaningfully applied to people because it is not a model of people. Let us consider the human behavior simulation in two prominent microscopic models that use different modelling approaches.

The social force model is explicitly presented as a model for investigating panic [9]. This explains why its agents are reactive rather than deliberative, and why they have homogenous behavior; its agents are interchangeable, operating on the same information to the same ends. This sets the stage for a particle-dynamics-based numerical simulation. We note that this model incorporates a simulation of personal space within the numerical simulation (the social force). Although this is a positive aspect of the model, it is overshadowed by the continued focus on panic as a predictor of behavior.

The floor field model [3], born from a vehicular cellular automaton, has been used to study several different pedestrian phenomena (notably bottlenecks at an exit during evacuation [10]). The authors, while unfortunately following [9] in identifying panic as a likely outcome of some situations, take the positive step of modelling “normal” conditions as well. The normal conditions in the model, however, still resonate with Sime’s ball-bearing metaphor. The agents lack facilities for the heterogeneity that comes from human cognition and behavior—the authors state their desire to keep the model simple by avoiding agent intelligence.

Although we are concerned about the applicability of these models to general human behavior, we do not wish to imply that these models have no value. The great value of microscopic models, in our view, is that they simulate emergent macro-level crowd effects through simple local rules evaluated from the perspective of each agent. By analyzing these micro-level rules it is possible to determine the conditions under which the macro-level effects will be produced, enhanced or moderated. Notwithstanding this, we argue that there is an opportunity to improve the microscopic explanatory power of the models by moving away from the unwarranted assumption of panic.

4 Microscopic Human Factors

The way to improve these microscopic models, in short, is to make the agents behave more like people. Currently, for example, the agents have one fixed goal, they do not change their goals based on information obtained from the environment, they do not communicate information amongst themselves, they queue indefinitely at bottlenecks, they do not intentionally originate any forces, etc. Humans, by contrast, are cognitive with a rich behavioral repertoire available for deployment. Ultimately it is this behavioral repertoire that is denied by the panic assumption and which is therefore not represented in the microscopic models. It is the lack of these behaviors—even more than the

precise cognitive process that underlies them—that calls into question these models’ applicability to human crowds.

The question we are left with, then, is how to (a) improve microscopic models’ treatment of human behavior without (b) losing the benefits of these models. One approach to (a) is to import large-scale cognitive architectures such as ACT-R [11], which aim to simulate complex cognitive processes including perception, memory, attention, planning, etc. Although this approach may improve relevance to people, it negates one of the key benefits of microscopic models: the establishment of causal connections between emergent macro-level crowd effects and their origins in individual behavior. Simple agent rules give way to a complex cognitive simulation that tends to be analytically opaque (as cognitive architectures are emergent systems themselves). The microscopic model becomes little more than an arena, simulating the physics and movement of agents, but divorced from the real action unfolding within the cognitive simulators. This disconnection breaks the causal chain and it becomes difficult to explain the macro-level crowd effects by reference to processes within the individual.

The key to maintaining the benefits inherent in microscopic models is to respect the simplicity and elegance that is their nature. Any model is, by definition, an abstraction that discards detail through simplification in favor of explanatory power. We can simplify and abstract behavioral characteristics in order to bring them within the framework of the microscopic model. Our approach is to simulate cognitive behavior and structures at the same level of abstraction at which the microscopic models currently simulate movement behaviors. We can then increase behavioral repertoire by expressing human characteristics as simple local rules, fusing them with the simple local rules of the microscopic model. We call these simple local rules *microscopic human factors* (MHFs). This technique ensures that the causal connection between emergent crowd behaviors and the local agent rules is not broken.

5 Microscopic Human Factors in the Floor Field Model

In order to demonstrate the potential of the MHF technique, we now turn to an example: a discovery and communication simulation [12]. This is one of several extensions we have made to the floor field model. (For other examples, see the voluntary pushing in our force model [13] and our model of front-to-back communication [14].)

We have found the floor field model to be particularly amenable to extension because its simple cellular automaton rules are both defined and evaluated from the perspective of the individual. These rules are easily expressed within the context of a multi-agent system (MAS), our preferred tool for modelling emergent effects and studying collective behavior. In a MAS, agents are considered to be autonomous, with internal rules and the possibility for internal state; this allows for the possibility that agents with different sets of rules

can be simulated together, for agent memory and consequently for behaviors that unfold over time. By implementing the rules of the floor field model in a multi-agent system we gain the opportunity to specify more internal behavior for the agents.

We have noted above that the agents in the floor field model are homogeneous with respect to their movement goals. Case studies of fire events (e.g. [15]) indicate that people can be reasonably expected to have different experience, goals and behaviors in a fire, that not everyone will move to the same exit and that communication (e.g. of exit locations) can change people's goals. Our goal in introducing this MHF was to reduce agent homogeneity through discovery and communication of exit locations in the physical environment. We will proceed by outlining the relevant parts of the floor field model, summarizing our changes to the basic model, and discussing our results.

In the classic floor field model (see [3] for complete details) an agent's behavior is driven by two floor fields. These fields are like maps in that they store information in the context of its location; when making movement decisions, agents make reference only to their immediate surroundings. The *static field*, S , provides, for each location, a distance to points of interest (e.g. the closest exit). The *dynamic field*, D , provides, for each location, a measure of the number of agents that have recently moved through. Agents' use of these fields is further altered by the use of sensitivity parameters that can decrease sensitivity to a field (e.g. decreased sensitivity to the static field implies poor knowledge of the space) or increase sensitivity to a field (e.g. increased sensitivity to the dynamic field promotes following behaviors). In our model, an agent considers movement from its current cell to the four cardinal neighbors rating each neighboring cell according to the following (slightly simplified) formula in which k_D and k_S are the sensitivity parameters and i and j identify the cell being rated.

$$\text{desirability} = \exp(k_D D_{ij}) \exp(k_S S_{ij}). \quad (1)$$

Each neighbor cell is evaluated for desirability according to this formula, and a probabilistic decision is made in which better-rated neighbor cells are more likely to be selected as a desired destination. Each agent undertakes this desirability calculation at the same time. Movement is then done in parallel, and agents may or may not get to complete their movement depending on whether they collide with or are blocked by others.

We used the MHF approach to add evolving goals by introducing additional static fields into the floor field model. As static fields underlie an agent's navigational ability—representing knowledge of the space—replacing an agent's static field with a more elaborated one is analogous to the agent integrating new information into its mental map. We fused this new behavioral concept with the model done microscopically at the level of the desirability calculation (1). The agent now considers one of a set of static fields by changing the S_{ij} term to $S_{n_{ij}}$, n indicating the index into the set. We also added two ways that an agent's static field change can be triggered: discovery and

communication. The discovery method involves the addition of a new floor field, the *discovery field*.¹ This field simply encodes a number on each cell indicating the static field that should be consulted. If the agent moves to a cell with a higher number, it is assumed to gain the information available there, and switches to the corresponding static field. Regarding communication, if an agent is blocked in movement (because another agent is occupying its desired cell) then the blocked agent communicates its static field number. The blocking agent, hearing a (higher-numbered) static field, incorporates this information by switching to the indicated static field.

Let us consider an application of these changes to the model. Consider an egress scenario in which there are two well-known exits from a space, but one is blocked. In a real life we expect that people who approach a blocked exit change their goal, moving to an alternate exit. The classic floor field model cannot simulate this because agent goals are determined by the modeller at the outset and are fixed. Our discovery and communication MHF handles the scenario using two static fields: the first, in which there are two exits, and the second, in which the blocked exit does not appear. At the outset, all agents use the first static field. The discovery field causes agents who approach the blocked exit to change to the second static field. These agents can communicate news of the blocked exits to others.

There are two patterns of agent behavior when the model is run. Some of the agents use the good exit directly, never learning of the exit blockage. Others move to the blocked exit, discover the new information, change their mental map, and start moving toward the good exit, potentially alerting naïve agents along the way.

Because this is a microscopic model with very simple rules, the MHF approach allows us to study the emergent effects of communication and information. For example, if communication is prevented, large numbers of naïve agents trying to reach the blocked exit can pin knowledgeable agents in place, preventing them from reaching the open exit and creating an impasse (see Fig. 1).

6 Conclusion

While behavioral researchers have exposed the myth of panic, microscopic models continue to be panic-based. By leaving panic behind we can begin, as Sime suggested, to model people rather than ball-bearings. The Microscopic Human Factors (MHF) approach can improve the behavioral repertoire of microscopic models, and hence reduce their focus on irrational, homogenous, interchangeable agents. This approach simulates cognitive behavior and structures at the same level of abstraction at which the microscopic models currently simulate movement behavior. This allows behavioral rules to be fused

¹ We originally called this the *information field* but this name was confusing because all fields carry information. We have renamed it the *discovery field*.

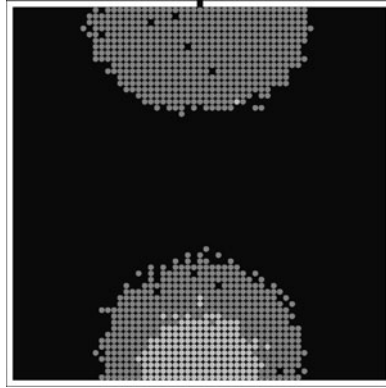


Fig. 1. Knowledgeable agents (*light gray*) know the lower exit is blocked, but are pinned in place by naïve agents (*dark gray*).

with existing model rules and preserves the causal connection between agent rules and emergent crowd-level effects—ultimately allowing for a study of the emergent consequences of human behavior in agents. The MHF approach helps to distance microscopic models from panic simulation by increasing the models’ relevance to human crowds—without compromise to the simplicity from which the models derive their explanatory power.

References

1. J. Sime (1985) *Des. Stud.* 6, 163–168.
2. J. Sime (1995) *Saf. Sci.* 21, 1–14.
3. C. Burstedde, K. Klauck, A. Schadschneider, and J. Zittartz (2001) *Physica A* 295, 507–525.
4. Oxford English Dictionary Online (retrieved 2008-02-13) Panic, adj. & n. #2.
5. N.R. Johnson (1987) *Soc. Prob.* 34, 362–373.
6. G. Proulx (2002) *Fire Prot. Eng.* 16, 23–25.
7. E. Quarantelli (1957) *Sociol. Soc. Res.* 41, 187–194.
8. L. Clarke (2002) *Contexts* 1, 21–26.
9. D. Helbing, I. Farkas, and T. Vicsek (2000) *Nature* 407, 487–490.
10. A. Kirchner and A. Schadschneider (2002) *Physica A*, 312, 260–276.
11. J.R. Anderson and C. Lebiere (1998) *The Atomic Components of Thought*. Erlbaum, Hillsdale.
12. C.M. Henein and T. White (2006) Information in crowds: The swarm information model. In *Lecture Notes in Computer Science* 4173, 703–706. Springer, Berlin.
13. C.M. Henein and T. White (2007) *Physica A* 373, 694–712.
14. C.M. Henein and T. White (2010) Front-to-back communication in a microscopic crowd model. In *Pedestrian and Evacuation Dynamics 2008*. Springer, Berlin.
15. J.M. Chertkoff and R.H. Kushigian (1999) *Don't Panic*. Praeger, New York.

Design of Decision Rules for Crowd Controlling Using Macroscopic Pedestrian Flow Simulation

Stefan Seer, Norbert Brändle, and Dietmar Bauer

arsenal research, Giefinggasse 2, 1210 Vienna, Austria

e-mail: stefan.seer@arsenal.ac.at

Summary. Crowd control mechanisms such as temporary access restrictions allow affecting pedestrian flows in public transport facilities in order to avoid overcrowding. Such access restrictions can be based on decision rules depending on measured pedestrian density. In order to design these decision rules, simulations of pedestrian flows are a valuable tool. In this paper we describe the design of decision rules for a real case study constituted by a subway station next to the main soccer stadium in Vienna. The simulations use a macroscopic model which (1) includes dynamic elements (like e.g. arriving and departing trains) and (2) integrates the implementation of decision rules based on real time measurements of real people flows. The model also takes into account measurement errors. We discuss the simulation results for the case study with the resulting decision rules in place.

1 Introduction

After large public events (e.g. soccer games or pop concerts) pedestrian flows in public transport facilities may occur which largely exceed typical everyday quantities. In order to avoid potentially dangerous dense crowds on the platforms, temporary access restrictions at the entrances of the facility allow affecting pedestrian flows (e.g. via closing of doors). Given the possibility to



Fig. 1. Subway station close to the main soccer stadium in Vienna. (©Wiener Linien)

restrict access to the infrastructure, the question arises how to design decision rules governing the decisions when to restrict or to allow access. Such decision rules should be based on real-time observations of pedestrian densities in critical areas such as the platforms. Since real world experiments with different strategies cannot be performed due to security and ethical reasons, simulations must be used to design decision rules for access restrictions.

In this contribution we describe the definition of decision rules for entry restrictions based on real world flow measurements for a particular case study. The development is based on a macroscopic pedestrian flow simulation model. In contrast to other simulation approaches, the model allows to incorporate dynamic elements (such as open or closed doors), where the corresponding state depends on dynamic elements determined from the simulation itself. This feature is necessary to implement the decision rules within the simulations. The proposed model also takes into account the uncertainty in measured real world people flows which are always subject to measurement errors.

The paper is organized as follows. Section 2 describes the concept for crowd controlling applied in this paper. Section 3 presents the main ideas underlying the macroscopic simulation model. The results of experiments for the evaluation of the accuracy of automatic people counting system are outlined in Sect. 4. Section 5 proposes the design of decision rules and shows results from a case study in a Viennese subway station.

2 Control Concept

Figure 2 depicts the main concept used for controlling the passenger inflow in a subway station: The controlled system covers passenger movement inside the subway station from the entrance of the station to the departing trains. The variable to be controlled is the number of passengers \hat{y}_t on the platform which needs to remain below the available train capacity given by $r - w_t$. Under this condition all passengers on the platform can be transported with the next train which is necessary in order to avoid accumulation of measurement errors.

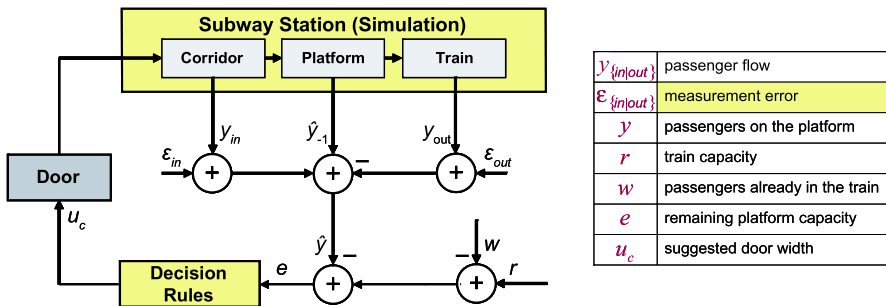


Fig. 2. Closed-loop circuit for crowd controlling in a subway station.

The simulation model allows to represent the time evolution of this variable depending on the inflow of passengers $y_{in,t}$ and the outflow of passengers $y_{out,t}$. Passenger inflow is automatically measured in real time as $\hat{y}_{in,t} = y_{in,t} + \varepsilon_{in,t}$ and outflow is measured as $\hat{y}_{out,t} = y_{out,t} + \varepsilon_{out,t}$ at certain locations inside the station, resulting in an estimate $\hat{y}_t = \hat{y}_{t-1} + \hat{y}_{in,t} - \hat{y}_{out,t}$. It is important to include the measurements' particular error characteristic $\varepsilon_{\{in|out\},t}$ in the simulation model. The remaining estimated capacity of the platform $e_t = r - w_t - \hat{y}_t$ is used as the input signal for the decision rule. Access restriction to a certain number of walking lanes (collected in the signal u_c) is suggested according to the decision rules, thereby influencing $y_{in,t}$.

3 Macroscopic Simulation Model

The simulation model represents pedestrian motion in discrete time and discrete space on a macroscopic level [1]. Figure 3 shows a snapshot of a simulation of the case study in a Viennese subway station. The accessible area is partitioned into a number of regions (shown as rectangles in Fig. 3). Regions on the edges of the platform are defined as sink regions (upper part of Fig. 3). A weighted network graph encodes neighborhood relations as well as distances between region centers. This network graph is used to derive shortest paths towards the sink regions for navigation purposes. The dynamic equations model the evolution of pedestrian density in the regions by equating in- and outflow of the regions as a function of the pedestrian velocities in the regions, the pedestrian density in the region, the densities in the neighboring regions and the width of the connection between adjacent regions. Pedestrian velocities are determined according to fundamental diagrams relating velocity

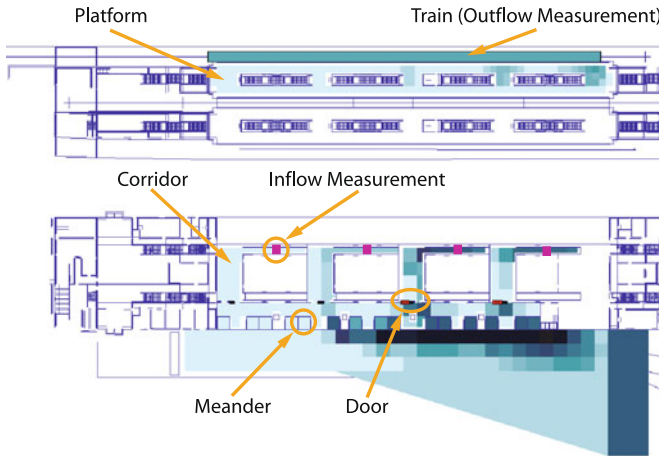


Fig. 3. Snapshot of the simulation results at the Viennese subway station.

and density depending on the type of region, i.e. open space, upward leading stairs etc., see [2]. In Fig. 3 region densities are color-coded, with darker regions representing higher pedestrian densities.

Access restrictions can be realized by modeling doors as borders between adjacent regions (plotted as red rectangles in Fig. 3) and resetting the corresponding width of the connection to a fraction depending on the number of walking lanes available determined by u_c . A width of zero corresponds to a closed door with no pedestrian flow.

Pedestrian inflow is measured on the stairs (see Fig. 3) and outflow is measured inside the trains. To the quantities measurement errors are added having the same characteristic as real measurement errors (see Sect. 4).

4 Measurement Error Characteristics

Pedestrian flow estimation requires adequate measurement techniques for automatic people counting in real time, since the overall quality of the controller crucially depends on the achievable counting accuracy. However, for most commercially available people counting systems detailed information about realtime counting accuracy is not available. We have therefore collected real world data at a staircase in a subway station (located next to the second largest soccer stadium in Vienna) in order to evaluate the counting accuracy of two video- and one infrared-based technology with respect to a manually annotated ground truth. The empirical data set comprises observation periods of one hour periods captured in the aftermath of four different games in the soccer stadium.

The video footage of a PAL camera mounted in top-view position above the staircase (see Fig. 4a) was analyzed offline with the software Vis-à-pix (see www.visapix.de). The system in Fig. 4b delivered automatic people counts in real time, where the video data was captured from a FireWire (IEEE 1394) camera and analyzed online with a software based on [3]. The infrared-based counting system IRMA from Iris GmbH (see www.irisgmbh.de) consists of several active infrared sensors which have been installed above the lower end of the stairs as shown in Fig. 4c. An IP-camera captured video footage for

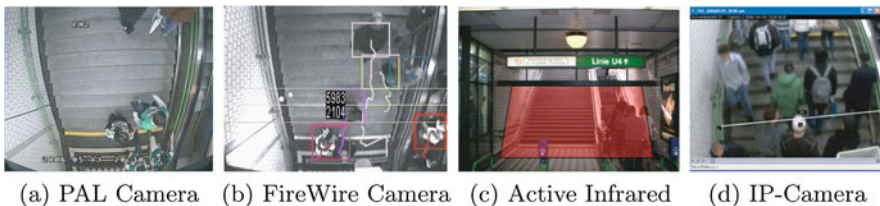


Fig. 4. Experiments with people counting systems.

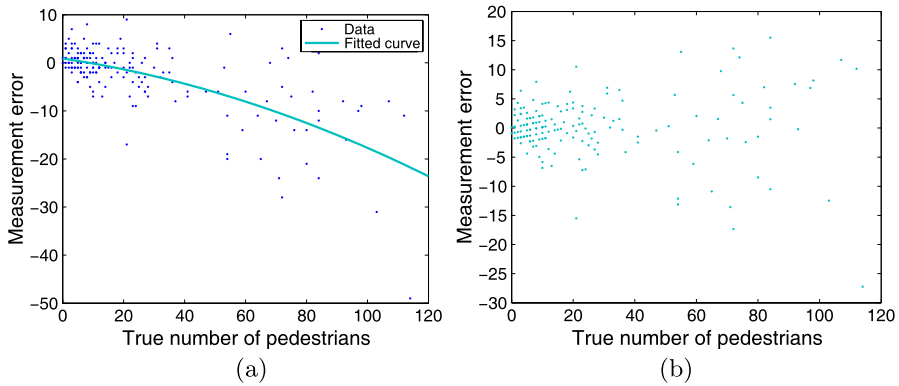


Fig. 5. Evaluation results for the infrared based system: **a** measurement errors and **b** true counts versus residuals compensated for systematic bias.

which manual ground truth counts at superimposed cross-sections have been obtained (see Fig. 4d).

The observation period was partitioned into one minute intervals and the corresponding automatic counts have been compared to the manual counts. Figure 5 provides a scatter plot of the true manual counts versus the measurement errors for the infrared-based counting system. In addition to a systematic bias, one can also observe heteroskedasticity (measurement error variances increasing with the true number of people). While the systematic error can be compensated for by calibration, the variation in the measurements errors is unavoidable. Figure 5b provides the measurement error after compensating for the systematic bias.

5 Design of Decision Rules

The simulation model was used for experimentally determining the parameters for a PID-controller used for deriving the decision rules. In the setup we assumed that each train will arrive empty in the station and the number of passengers on the platform must be kept below 750 persons due to safety reasons. The number of allowed walking lanes for each of the four doors ranges from zero to five and are provided by quantizing the output signal of the PID-controller to an integer in the range $\{0, 1, \dots, 5\}$.

The simulation results using the developed decision rules are shown in Fig. 6. Using the number of pedestrians for one of four corridors in the station (hence the maximum equals $750/4 = 187.5$) given by the macroscopic simulation model in Fig. 6a, the developed decision rules suggested the number of walking lanes presented in Fig. 6b. The plots show a time delay between completely closing the door after approximately 90 seconds and a constant number of passengers on the platform after approximately 125 seconds, since

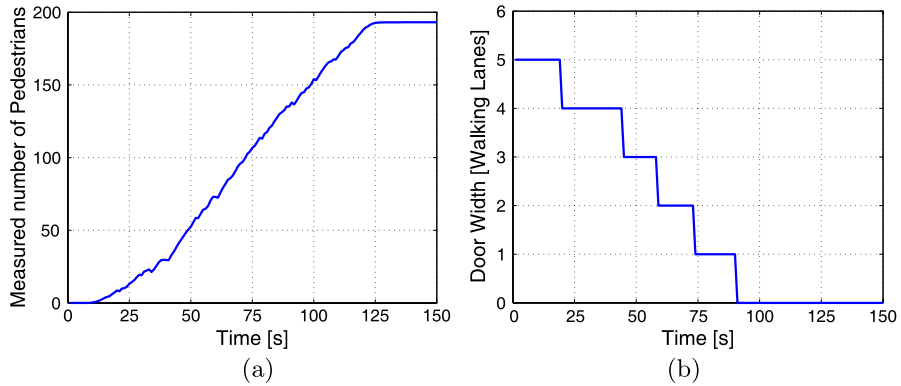


Fig. 6. Simulation results for one corridor of the subway station: **a** pedestrian inflow and **b** door width in walking lanes.

the passengers need to walk up the stairs. Also the reduction in inflow due to narrower passage is clearly seen in the slopes of the number of passengers on the platform as given in Fig. 6a.

6 Conclusion

In this paper we have discussed the design of decision rules for access control to a subway station in Vienna. The underlying macroscopic model is relatively simple and hence leaves ample space for improvements. In contrast to other models, however, the model incorporates the effects of uncertainty in real-time measurements which are vital in a situation where safety standards need to be guaranteed by the controller setting. Future work will be directed towards a thorough calibration of the model against real world data which is to be gathered at future soccer events in the stadium.

Acknowledgements

This work has been supported by the Austrian Ministry for Traffic, Innovation, and Technology (BMVIT). The authors thank ‘Wiener Linien’ for supporting us with their expertise.

References

1. D. Bauer, S. Seer, and N. Brändle. Macroscopic Pedestrian Flow Simulation for Designing Crowd Control Measures in Public Transport after Special Events. In *Proceedings of the 2007 SCSC Conference*, 2007.

2. W.M. Predtetschenski and A.I. Milinski. *Personenströme in Gebäuden—Berechnungsmethoden für die Projektierung*. Verlagsgesellschaft Rudolf Müller, Köln–Braunsfeld, 1971.
3. C. Beleznai, B. Frühstück, and H. Bischof. Human Tracking by Mode Seeking. In *Proc. 4th International Symposium on Image and Signal Processing and Analysis*, 2005.

3-Tier Architecture for Pedestrian Agent in Crowd Simulation

Gao Peng and Xu Ruihua

School of Traffic and Transportation Engineering, TongJi University, CaoAn Road 4800#, Campus JiaDing, Shanghai 201804, China
e-mail: blue.silver@hotmail.com

Summary. After extensive investigations and in-depth studies of crowd dynamics with Chinese characteristics, especially in stations of Urban Mass Transit, we proposed a new architecture for agent oriented pedestrian simulation. It's designed to simulate the movement of thousands of individual pedestrians through large, geometrically complex 2D space.

Our PSS (Pedestrian Simulation System for Urban Mass Transit Station) based on this architecture has been developed. The results of the case studies show that the architecture is feasible and effective in simulating intelligent human behaviors. Characteristic by openness and scalability, it can be easily applied to other situations, such as Olympics and Expo, etc.

1 Introduction

Construction of railway transit station requires a significant amount of human, material and financial resources. Besides, it's very expensive or impossible to make any alteration after the blueprints turn into realities. The issue of security, convenience and coziness for passengers, and the facility utilization, operation costs for operators largely depend on the size, space structure and equipments layout of railway station. Moreover, how to deal with emergencies and how to evacuate passengers timely in the case of fire, explosion and poison gas is a formidable problem.

Computer simulation is a feasible and effective way to test and evaluate optional designs and emergency strategies of railway stations. However, existing pedestrian simulation systems usually are:

1. Based on CA (Cellular Automata) theory, thus movement of pedestrians seems a little "mechanical", because velocity is discrete and it's hard to take acceleration into consideration.
2. Inadequate for intelligent real-time path planning, especially simulating large number of pedestrians. Users often have to add certain kinds of navigations by hand.

Aiming at simulating accurately and effectively, the movement of thousands of pedestrians through large, geometrically complex 2D space, a 3-tier architecture is presented in this paper, which combines many algorithms and models to deal with problems such as “mechanical movement”, intelligent real-time path planning and so on.

2 How the Issue Raised

In the field of Game Programming and Artificial Intelligence, there are many studies on multi-agent movement. Programmers are usually confronted with several common problems, e.g. “conflicts in path planning”, “realistic movement” and “long-distance path finding”.

2.1 Conflicts in Path Planning

In a multi-agent system, one agent may easily collide with others when moving along the path that previously planned, because the map for search algorithm is changing with time (other agents as obstacles are moving).

One strategy to solve this problem is “Waiting until others go away”. With this strategy, a queuing effect can be observed sometimes. Unfortunately, it may lead to “dead lock” when two agents are waiting for each other. After that, more and more agents get together stupidly. Another strategy is “re-plan the path when conflicts occur” (e.g. “Local Repair A*”, which describes a family of algorithms widely used in the video-games industry). Although it can solve the conflicts sometimes, often incur substantial computational overhead.

In order to avoid game characters huddle together stupidly, many algorithms have been developed, e.g. David Silver [1] and Alborz Geramifard [2] (Department of Computing Science, University of Alberta, Canada) proposed “Cooperative Pathfinding”. This algorithm add time dimension into search space, which is originally 2D. With full information about the routes of others, agents could find non-colliding routes to separate destinations.

After some experiments we found out that there are still some problems if applying “Cooperative Pathfinding” to a pedestrian simulation:

1. Agents can’t achieve acceleration variable, curvilinear movement, or it’s too complex to search non-collide path.
2. Hard to keep efficiency when the number of agents is too large (10,000 for example).

Thus we strike out in another direction: do not try to solve these problems within pathfinding, while separate the tasks and set a tier to take charge of them. The paths by search algorithm are only used as rough navigation. In this way, the agents not only could achieve acceleration variable, curvilinear movement, but also avoid each other smoothly.

2.2 Realistic Movement

Since the output paths by basic search algorithm seem too stiff and often have “zigzag effect”, many methods have been proposed to make the movement of game characters more realistic and visually interesting.

For example: Marco Pinter [3], expert of game design and development, from California, suggests that we can add some realistic curved turns for agents, so that they don’t appear to change direction abruptly (see Fig. 1).

While after some tests we found that: comparing with calculating curved turns in geometric way, better performance and less calculation costs can be achieved when turning to consider the physical parameters of the agents. (Force exerted by other objects, acceleration, speed, etc.) It seems a simpler, more natural way to achieve smooth and realistic movement.

2.3 Long-Distance Pathfinding

Generally speaking, a map with 10,000 nodes can be called “large scale”. Since the computational cost increases rapidly with size of search space, pathfinding on large maps can result in serious performance bottlenecks.

R.C. Holte (Computer Science Dept., University of Ottawa, Canada) [4] presents a hierarchical approach for reducing problem complexity. This technique abstracts a map into linked local clusters (as Fig. 2), Small clusters are grouped together to form larger clusters. At the global level, clusters are traversed in a single big step. In this way, large number of meaningless nodes (e.g. the nodes in cluster 1 and 4, Fig. 2) can be avoided. A hierarchy can be extended to more than two levels.

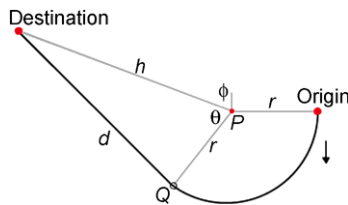


Fig. 1. Adding realistic turns.

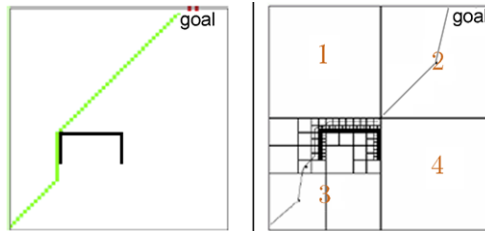


Fig. 2. Hierarchical Pathfinding.

Based on “Hierarchical Pathfinding”, this paper abstracts the behavior of agents into a series of “events”, then separates the task of “big-step search” and set a tier to manage these events. The events also can be organized in hierarchical structure, thus similar results can be obtained with more flexibility. From the above analysis we can conclude that it is usually very hard to solve these difficulties in pedestrian simulation within one level. Thus we decoupled the task and proposed an architecture, which combined many algorithms in different levels. Based on the architecture, a computer program is clearly structured, explicit in division of responsibility, and easy to implement.

3 Structure of the Architecture

Comparing with automobile, a pedestrian is more free and flexible, his behavior is complex and is easily affected by other pedestrians or the environment, thus we can hardly describe the nature of crowd with one set of formulas or simulate pedestrian behaviors with one kind of model. In this paper, pedestrian’s complex behaviors are decoupled into 3 tiers, which are from macroscopic to microscopic (see Fig. 3).

3.1 Event Flow Control Tier

The first tier called “Event Flow Control”, which is responsible for event flow management (such as walking, queuing, buying tickets, etc.) and event motivation (such as detour, overtaking, etc.). For the sake of convenience, the paper will take the passengers who enter the subway station as an example, to demonstrate how the architecture works over the simulation process.

In general, the behavior of agents in a simulation system is composed of a series of events. To passengers who enter the subway station, it might be such a flow: “enter–buy tickets–check in–through staircases–waiting train–boarding”. Each event can be divided into many sub-events, e.g. “buy tickets” may contain: “choose a tickets area–walk to the area–choose a tickets device–queuing–buy tickets”. Each sub-event also can be divided into even smaller events, e.g. “walk to tickets area” can be made up of “route choice”, “speed up/down”, “make a detour”, etc.

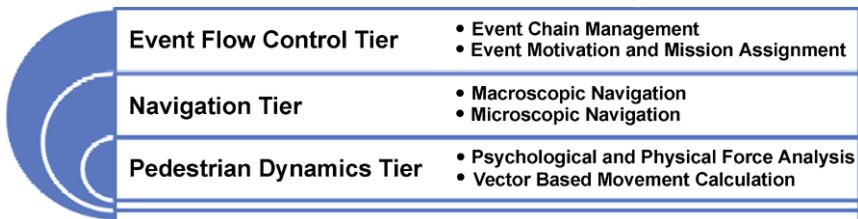


Fig. 3. Structure of the architecture.

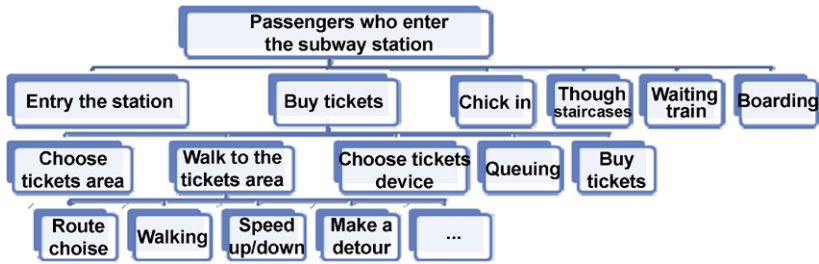


Fig. 4. Tree-like diagram of agent status.

Therefore, events are divided into 3 categories in this paper: “macro-events”, “meso-events”, and “micro-events”. Proper data structures (classes) have been designed for each category and an enumerable variable has been set to identify the status of the agent. Combining events of different levels, we can get a tree-like diagram of status (due to the limitation of space, there are only the events mentioned above), see Fig. 4.

The flow of macro-events can be specified by users; otherwise, some search algorithm (such as Ants Colony) also can be used if you like the agent smarter. Relevant floor, facilities and flow of meso-events can be stored in the data structure of the macro-event. Since the motivation of micro-events is relatively random (they can’t be managed in the way of flow), so we set an engine to invoke micro-events on certain condition. By the way of changing the status variables, tiers can communicate with each other.

In brief, events at all levels are managed in a hierarchical way. To different situations (such as Olympics and Expo, etc.), corresponding event control tier can be designed to meet specific needs. Furthermore, some complex social behavior model can be integrated into the architecture, served as the first tier.

3.2 Navigation Tier

After the “Event Flow Control Tier” makes sure the status of a agent, it may assign some missions and transmit parameters to lower tiers, depending on the characteristics of current status diagram (is it leisure or in hurry, walking on passageway or staircase and so on). Among all missions, the most common one is “move”, so navigation is crucial.

In real life, pathfinding of pedestrians is usually not completed at one time. On the contrary, they would like to divide the whole journey into many small parts, and set many local targets (e.g. a guidance, a corner, etc.), and then find a comfortable local path.

Hence, the “Navigation Tier” is divided into 2 levels:

1. Macro-navigation: refers to identify a rough route from the source to the destination;

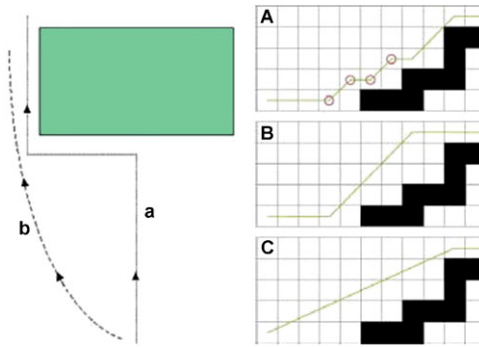


Fig. 5. Problems of basic A*.

2. Micro-navigation: is responsible for real time path planning (depending on density, geometry, etc.).

For effective pathfinding, we adopt A* algorithm, which is a typical heuristic search algorithm and is widely used in Game Programming, Artificial Intelligence and robotics. Heuristic search means estimating the cost of every location in the search space, and choosing the lowest one for next step, so tremendous unnecessary searching can be avoided and high efficiency can be obtained.

However, basic A* algorithm is inadequate for pedestrian simulation:

- To large-scale pedestrian simulation system, there can be thousands of agents require real-time pathfinding, and that may easily incur computational overhead. So we need to optimize A*.
- A* is grid-based, the output path usually gets “zigzag effect” (see Fig. 5 left), while nobody would like to walk in that way in real life.
- The output paths by basic A* seems “clinging to obstacles” too much, but pedestrian would like to make a detour earlier before the obstacle in real life (see Fig. 5 right).

To solve the problems mentioned above, many modifications have been done:

- Special data structure is designed for the implementation of A*, thus it can achieve high performance and meets the pathfinding needs of numerous agents.
- The problem of the output path “clinging to obstacle” of the basic A* has been solved by imposing penalty on nodes near obstacles in map preprocessing.
- A “Trimming Algorithm” is developed, which could reduce the “zigzag effect” and achieve smooth straight-line movement.
- Several heuristic functions are compared and improved. A* has an ability of vary its behavior based on the heuristic functions; we take advantage

of the ability to embody pedestrian’s route preference. For more details, please refer to “A Modified Heuristic Search Algorithm for Pedestrian Simulation” [5].

3.3 Pedestrian Dynamics Tier

After the problem of Navigation, the next question is how the agents move and how to avoid each others. One of the simple ways is using a CA (Cellular Automata): the movement of agents based on grid and they move one square for each step. Although this approach is easy to implement with less computational costs, it’s hard to embody complex interaction between agents.

In this paper, we introduce the “Social Force Model” into Pedestrian Dynamics Tier, which is responsible for psychological and physical force analysis, and for vector based movement calculation (see Fig. 6).

Social Force Model is presented by Dirk Helbing et al. [6] in 1998. “Social force” represents the effect of the environment (e.g. other pedestrians or borders) on the behavior of the described pedestrian.

The equation in Fig. 6 can be interpreted as the “social force” that imposes on a pedestrian at a time and can be decomposed into 5 forces:

1. Driving Force: the motivation of getting to its destination.
2. Interactions: the motion of a pedestrian is influenced by other pedestrians.
3. Repulsions: repulsive force exerted by obstacles, fire and so on.
4. Attractions: something interesting attracts the pedestrian.
5. Fluctuations: some stochastic fluctuations.

Among the 5 forces, “Interactions” also can be decomposed into 3 forces:

1. Psychological repulsions: Pedestrians like to keep certain distance from each other.
2. Physical interactions: physical force exerted by others with body contact.
3. Attractions: attractions between people, e.g. friends and relatives.

$$\begin{aligned}
 m_i \underbrace{\frac{d\vec{v}_i(t)}{dt}}_{\text{Acceleration}} &= \underbrace{\frac{m_i}{\tau_i} (\vec{v}_i^0 \vec{e}_i(t) - \vec{v}_i(t))}_{\text{Driving Force}} + \underbrace{\sum_{j(\neq i)} \vec{F}_{ij}^{ww}(t)}_{\text{Interactions}} + \underbrace{\vec{F}_i^b(t)}_{\text{Borders, Fire}} + \underbrace{\sum_k F_{ik}^{att}(t)}_{\text{Attractions}} + \underbrace{\vec{\xi}_i(t)}_{\text{Fluctuations}} \\
 &\quad \downarrow \\
 \vec{F}_{ij}^{ww}(t) &= \underbrace{\vec{F}_{ij}^{psy}(t)}_{\text{Psychological Repulsion}} + \underbrace{\vec{F}_{ij}^{ph}(t)}_{\text{Physical Interactions}} + \underbrace{\vec{F}_{ij}^{att}(t)}_{\text{Attractions between People}}
 \end{aligned}$$

Fig. 6. Basic equations of the Social Force Model.

The Social Force Model can simulate acceleration and deceleration of pedestrians accurately, so we can gain experimental data to support facility comfort evaluation. Besides, it can solve the problem of path conflicts and achieve agents avoiding each other smoothly. The series of points by micro-navigation algorithm can serve as local targets for the Social Force Model. One thing needed to be emphasized is that the distances between each two points need some more considerations: If the distances are too large, then the agents are constrained on the path and the Social Force Model could not work well. Contrary to this, if the distances are too small, then the agents may easily get lost.

Although the Social Fore Model could simulate some behaviors in the perspective of pedestrian dynamics, it also has two shortcomings: first, it has no ability for path planning; second, computational cost is high. To the first question, we combine navigation algorithm with the Social Force Model, then we solved the problem. To the second question, we add an inter-medium (called “info space”) into the Social Force Model, then the agents exchange information through “info space” other than communicating directly, so large amount of nonsensical communications are voided.

4 Computer Experiments

In order to collect human and social behavioral data to specify parameters of models in the architecture, and validating consistency and reliability of our system, we made many on-spot investigations in Shanghai, such as transfer station “People Square”, intersection of Middle Xizhang Road–West Nanjin Road etc. The results of the case studies show that the architecture is feasible and effective in simulating intelligent human behaviors.

4.1 Finger Effect

In high density crowds, especially bidirectional flows, pedestrians usually follow others to reduce resistance. Then the two opposing flows self-organize into long chains of people passing each other, like conga lines at a party. This is a phenomenon unique to interactive systems but not to fluid systems: the so called “Finger Effect”.

“Finger Effect” can be obviously observed in real life (Fig. 7 left), as well as in the animation of our simulation system (Fig. 7 right).

4.2 Edge Effect

According to study of G. Keith Still (University Warwick of London [7]): in a unidirectional high density flow, pedestrians at the edge can move faster than whom at the center. By the “density map”, which is calculated by our simulation system automatically, we also witnessed this phenomenon clearly.

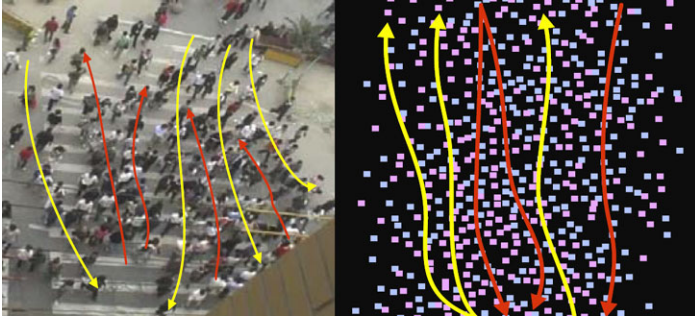


Fig. 7. “Finger Effect” in real life and in our simulation system.

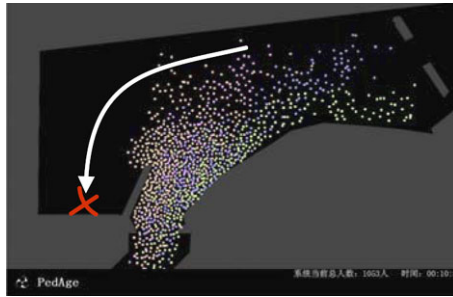


Fig. 8. Case study with “dead end”.

4.3 Case Study with “Dead End”

As Fig. 8 shows, in this case there are large numbers of pedestrians enter from the right-top corner of the map and exit at the left-bottom corner. There is a “dead end” in the middle of their journey, which they can see clearly before the entry. Generally speaking, pedestrians would never walk deeply into the dead end in real life, since they can see it. But in a simulation system, it’s not very easy to do this without incurring computational overhead.

Since the architecture proposed in this paper has the ability of real time path planning, agents would never “been trapped”, and the simulation result is consistent with reality.

5 Conclusions

In the field of Game Programming and Artificial Intelligence, there are many studies on multi-agent movement. A number of approaches have been proposed to solve some common problems, such as “conflicts in path planning”, “realistic movement” and “long-distance path finding”. Being confronted with similar problems in pedestrian simulation, we designed a new architecture to

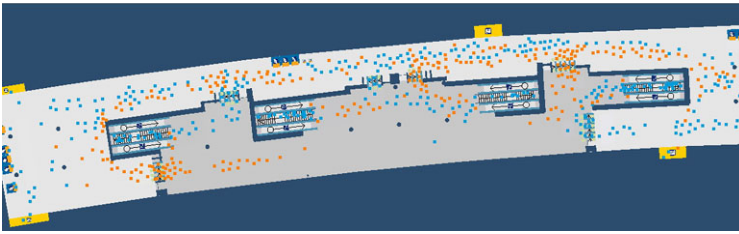


Fig. 9. Simulation snapshot of transfer station “Zhongshan Park” in Shanghai.

combine many algorithms to handle them, other than trying to do this within one tier. The advantages are:

- With clear structure and explicit components responsibility, the architecture is flexible and scalable;
- The 3 tiers is from macroscopic to microscopic, which is consistent with behavioral processes of pedestrians in real life;
- Pedestrian agents based on this architecture have ability of real time path planning. Comparing with simulation systems that require from the user to add navigation objects manually, our system can obtain more real and objective results with much less efforts;
- Due to Social Force model being integrated, the movement of agents is more realistic than Cellular Automata, so our system can provide experimental data support for comfort evaluation. Besides, the problem of “conflicts in path planning” is solved.

Our PSS (Pedestrian Simulation System for Urban Mass Transit Station) based on the architecture has been developed in C#. It’s a self-contained system characteristic by “AutoCAD Drawing Processing Technology”, “Image Analysis Technology”, and Agent oriented Simulation.

The feature of real-time path planning in our system can significantly reduce the workload of creating simulation projects (no longer requires user to add navigation objects manually). Besides, it reduces the impact of human factors (users) on simulation results. Figure 9 shows a Simulation snapshot of the transfer station “Zhongshan Park” located in Shanghai.

Since the tiers are independent, you can design a new “Event Flow Control Tier” or integrate a more complex “social behavior/decision model” instead to meet specific needs. In a word, the architecture is open and scalable, and can be easily applied to other situations, such as Olympics and Expo, etc.

References

1. D. Silver. Cooperative pathfinding. In R.M. Young, J.E. Laird (Eds.): Proceedings of the First Artificial Intelligence and Interactive Digital Entertainment Conference, June 1–5, 2005, Marina del Rey, CA. AAAI Press, Menlo Park, CA, 2005.

2. A. Geramifard and P. Chubak. Efficient cooperative path-planning, Computing Science Department, University of Alberta. October, 2005.
3. M. Pinter. Toward more realistic pathfinding. *Game Developer*, 2001, 3.
4. R.C. Holte et al. Hierarchical A*: searching abstraction hierarchies efficiently. University of Ottawa Science Technical Report, TR-95-18, 1995.
5. G. Peng, X. Ruihua, and Z. Xiaolei. A modified heuristic search algorithm for pedestrian simulation. In *Proceedings of the 7th International Conference of Chinese Transportation Professionals*. Shanghai, China: ASCE, 2007.9.
6. D. Helbing. Traffic jams, pedestrian streams, escape panics, and supply chains. *Reviews of Modern Physics*, 73(4), 1067–1141 (2001).
7. G.K. Still. *Crowd Dynamics*. London: University of Warwick, BSc Physical Sciences (Robert Gordon's Institute of Technology, Aberdeen 1981), 2000.

Optimising Vessel Layout Using Human Factors Simulation

Steven J. Deere, Edwin R. Galea, and Peter J. Lawrence

Fire Safety Engineering Group, University of Greenwich, London, UK
e-mail: e.r.galea@gre.ac.uk

Summary. Evaluating ship layout for human factors (HF) issues using simulation software such as maritimeEXODUS can be a long and complex process. The analysis requires the identification of relevant evaluation scenarios; encompassing evacuation and normal operations; the development of appropriate measures which can be used to gauge the performance of crew and vessel and finally; the interpretation of considerable simulation data. In this paper we present a systematic and transparent methodology for assessing the HF performance of ship design which is both discriminating and diagnostic.

1 Introduction

When modifying the internal configuration of a ship, it is important to determine what, if any, HF benefits or disbenefits may result. How these aspects can be assessed is less well defined. In this paper we present a novel mathematical procedure, based on computer simulation of evacuation and normal operations (NOP), for assessing the overall HF performance of ship design.

Making modifications to the internal layout of a ship or its operating procedures will have HF implications for crew and passengers, which in turn will have an impact on overall levels of safety under emergency conditions and efficiency of operation in normal conditions. For naval vessels, the location and distribution of compartments may have an impact on the time required by crew to go from one state to another, it may also have an impact on the minimum number of crew required to safely and efficiently operate the vessel under a variety of different conditions. These factors will have an impact on the vessels overall operating efficiency, ability to fulfil the assigned mission and lifetime costs associated with crewing requirements.

Advanced ship evacuation models such as maritimeEXODUS can be used to determine the performance of personnel under emergency conditions for both passenger and naval vessels as well as the normal circulation of personnel for both passenger and naval vessels [1, 2]. These models produce a

wide variety of simulation outputs, such as time to assemble and the levels of congestion experienced. As the number of different scenarios investigated increases, so does the volume of output data. It therefore becomes increasingly difficult to consistently assess changes in HF performance associated with changes in vessel configuration across a wide range of scenarios and performance requirements.

In this paper we explore a methodology to assess changes in HF performance resulting from changes to vessel configuration and/or crew procedures. The approach is intended to be both diagnostic and discriminating. The identified methodology is being developed as part of a collaborative project between the authors and the Design Research Centre (DRC) of University College London, funded by the UK EPSRC with support from MoD.

2 Methodology for Assessing Human Factors Performance

In order to gauge the HF performance of the vessel it is essential to define a range of relevant Evaluation Scenarios (ES) against which the vessel will be tested. These scenarios are intended to define the scope of the challenges the vessel will be subjected to. In order to gauge vessel performance across a range of criteria, the ES are made up of both evacuation and NOP scenarios.

Relevant evacuation scenarios may include those required by MSC Circular 1238 [3] and include the IMO night and day scenarios or their naval equivalent [4]. In addition to defining the ES, a range of Performance Measures (PM) must be defined that measure various aspects of personnel performance in undertaking the tasks associated with the ES. PM for passenger ship evacuation scenarios may include the time required to complete the assembly process while for a naval vessel NOP scenario, the total number of water tight doors (WTD) opened and closed may be relevant. The suitability of the vessel layout will be evaluated for fitness of purpose through some combination of the PM resulting from the execution of the ES.

Collectively the particular combination of ES and PM that results in a meaningful measure of the performance of the crew and vessel are described as the Human Performance Metric (HPM). The HPM works by systematically evaluating one layout design against another, whether this is two variants of the same design or two completely different designs. In this paper we will focus on applications involving naval vessels and in particular frigate type surface combatants.

3 The Components of the Human Performance Metric

To demonstrate the concept of the HPM we define the key components of the HPM for a naval surface combatant (i.e. a frigate class vessel).

3.1 Evaluation Scenarios

NOP scenarios represent situations where the ships crew move around the vessel carrying out specific tasks. An example of a NOP scenario for a naval vessel is the 'State 1 preps'. This scenario disregards the normal non essential tasks and brings the organisation of personnel, equipment, machinery and water tight (WT) integrity to the highest state of preparedness and readiness to deal with any emergency that might occur.

3.2 Functional Groups

As members of the ships complement may be involved in undertaking different tasks during a particular ES, the ships complement is divided into subgroups. Membership of each subgroup is determined by the nature of the tasks undertaken by the individuals in the particular ES, with each subgroup being made up of people undertaking a common set of tasks. These subgroups are labelled Functional Groups (FG). An example of a FG is the 'damage control and fire fighting' (DCFF) group which is a prime example of a FG used in circulation ES. In addition to the FGs defined by specific sub-populations, a special FG, identified as Ships Company, is included in all ES. This paper will make use of the FG; 'Entire Ships Company' and 'Damage control and fire fighting'.

3.3 Performance Measures

To assess the performance of each FG in each ES, a set of Performance Measures (PM) have been defined, each of which uniquely assesses a particular aspect of the scenario. Each of the PMs returns a value determined from the computer simulation of the ES which is then used in part to complete the HPM. The higher the value of the PM, the poorer the performance of the FG in the ES. Some 31 PM have been defined which assess many aspects of crew performance for a frigate.

4 Defining the Human Performance Metric

The HPM is used to compare the human performance capabilities of competing vessel designs. These alternative designs may simply be different design iterations of a particular vessel or competing design options. To assess the performance of the vessels, a set of evaluation scenarios are selected which are relevant to the intended operation of the vessel. The design alternatives are then crewed with the required number of personnel and the crew assigned to their functional groups. The number and type of FG may differ between design alternatives for each ES. Finally, each functional group has a set of performance measures defining the performance of the FG.

Each PM extracts its value from maritime EXODUS simulation software. The PM are then normalised in order to carry out a direct comparison between designs. The weighted sum of the normalised PM values produces the FG score. The weighted sum of the FG scores produce the ES score and the weighted sum of the ES scores produce the overall vessel performance (VP) score. The overall Vessel Performance (VP) for design X can then be compared against the VP score for all other designs to determine which design produced the best overall performance. The matrix is also diagnostic in that it allows the identification of which measures contributed to the poor performance of a failed vessel design, or which PM could be improved in a winning design.

5 Demonstration Application of the HPM

The use of the HPM concept in evaluating the relative performance of two designs of a hypothetical naval vessel will be demonstrated in this section. To do this, seven ESs are considered, three evacuation scenarios and four NOP. The aim of this analysis is to determine which design variant is the most efficient in terms of its HF performance and whether any improvements to the winning design can be identified.

5.1 The Geometry

The baseline vessel design (Variant 1) consists of 453 compartments spread over eight decks. Decks No. 1 and No. 2 (deck 4 and 5 respectively) have a single central passageway connecting the aft to forward section of the deck. The second variant design (Variant 2) consists of the 445 compartments spread over eight decks as in Variant 1. The key difference between the two designs is that Variant 2 has two passageways running in parallel from the aft to the forward end of the vessel on both decks.

5.2 The Scenarios

Each vessel has a complement of 262. The crew are initially located in the location they would be expected to be at the start of each scenario as determined by the “state” of the vessel. Crew members not on watch are located in their cabin. The seven ES used to assess the performance of each vessel are; ‘normal day cruising A’, ‘normal day cruising B’, ‘Action Station evacuation’, ‘State 1 Preps’, ‘Blanket Search’, ‘Family Day A’ and ‘Family Day B’ scenarios. It must be noted that the scenarios used in this demonstration are not intended to accurately represent actual naval operations, but are used simply to demonstrate the HPM concept.

5.3 The Simulation Software

The ship evacuation model maritimeEXODUS [1, 2] produced by FSEG was used to perform the personnel simulations presented in this paper. The software has a number of unique features such as the capability to represent the performance of both naval personnel and civilians in the operation of watertight doors, vertical ladders, hatches and 60 degree stairs. Another feature of the software is the ability to assign passengers and crew a list of tasks to perform. In addition, a separate utility program has been developed (the Human Performance Metric Analyser) which automatically constructs the matrix of human performance scores from maritimeEXODUS output that are used in the evaluation of the vessel design.

5.4 Results and Analysis

The seven ES were each run 50 times and representative simulation result files were selected for each scenario to construct the HPM for each variant. The PMs for each variant were then determined and the final HPM constructed for each variant as shown in Table 1.

As can be seen from Table 1, Variant 1 produces an overall Vessel Performance (VP) score of 523.7 while Variant 2 produces a VP score of 531.2. Thus we note that the overall performance of both variants is broadly similar, with Variant 1 producing a marginally better (1.4%) overall human factors performance according to the measures we have identified. Furthermore, we note that Variant 2 outperformed Variant 1 in most of the scenarios, however Variant 1 significantly outperformed Variant 2 in two NOPS and the worst performing scenario for Variant 1 is the ‘Action Stations Evacuation’. As Variant 1 produces the better overall performance and produces significantly better NOPS performance it would be consider the design of choice. However, its performance may be improved by investigating why it did poorly in its worst performing ES.

It must be emphasised that this conclusion is based on the particular Evaluation Scenarios, Performance Measures and Weights that have been used

Evaluative scenario	Scenario weight	Variant 1	Variant 2	% difference between Variant 1 and Variant 2
Normal day cruising A	1	46.14	44.33	3.93%
Normal day cruising B	1	50.81	46.79	7.92%
Action stations evacuation	1	51.45	46.70	9.23%
State 1 preps	1.5	67.46	75.47	-11.87%
Blanket search	1.5	78.04	84.29	-8.01%
Family day A	1.5	48.65	47.20	2.99%
Family day B	1.5	56.03	55.32	1.26%
Overall performance of design		523.7	531.2	

Table 1. Scenario Scores for Variant 1 and Variant 2.

FG ₁ —Entire Ships Company	Weight	Variant 1		Variant 2	
		raw	norm	raw	norm
C1—number of locations in which pop density exceeds 4 p/m ² for more than 10% of overall scenario time	8	4	1	4	1
C2—the max time the pop density exceeded the regulatory max 4 p/m ² for 10% of sim time	3	75.40	1	42.14	0.56
G1—average time required to complete operations	4	256.7	1	193.54	0.75
G2—average time spent in transition	3	36.61	0.80	45.76	1
G3—time to reach final state	8	666.7	0.22	594.50	0.20
G4—average time spent in congestion	3	150.6	1	74.93	0.50
G5—average distance travelled	4	47.11	0.94	50.11	1
M1—the number of WTD used during scenario	2	24	0.89	27	1
M8—the number of times the FG moved between decks	2	373	1	322	0.86
M16—average number of doors used/person	3	1.59	0.82	1.94	1
M17—average number of WT doors/person	3	1.46	1	1.19	0.82
M18—average number of hatches used	3	0.27	1	0.23	0.83

Table 2. Variant 1 and Variant 2 PM results for FG₁ in ES₃.

in the analysis. To better understand why Variant 2 out performed Variant 1 in the ‘Action Stations Evacuation’ scenario and to identify potential areas in which Variant 1 can be further improved it is necessary to delve into the sub-components of the HPM. Presented in Table 2 are the PM scores for Variants 1 and 2 for this scenario.

We note that for Variant 2, the overall average time spent in congestion (as measured by G4) was some 50% less than in Variant 1. This significant reduction in congestion results in Variant 2 being able to complete the scenario 11% quicker than Variant 1 (as measured by G3). Indeed, we note that while both vessels easily satisfy the international set evacuation time requirements (as measured by G3) the levels of congestion experienced exceed the international set limits in four locations (as measured by C1) and Variant 1 experiences the most severe congestion (as measured by C2). To address this issue and to improve the overall performance of Variant 1, further investigation is required to uncover the causes of the severe congestion. Exploring the areas of congestion in Variant 1 suggested that a single additional ladder connecting 01 Deck with No. 1 Deck between two of the severe congestion regions

may alleviate some of the congestion by providing an additional means of vertical movement. With this modification in place the HPM was re-evaluated for the Modified Variant 1. The Modified Variant 1 now outperforms the original Variant 1 in each scenario and produces an overall VP which is 6% more efficient than the original Variant 1 and 8% more efficient than the Variant 2 design. We also find that the Modified Variant 1 design outperforms the Variant 2 design in all but the 'Normal day cruising A' evacuation scenario.

6 Concluding Comments

This paper has described and demonstrated a general methodology, the Human Performance Metric (HPM), for evaluating HF performance of competing ship designs. The approach is both systematic and transparent allowing user priorities to be clearly stated as part of the methodology. The user priorities can be identified through the selection of appropriate evaluation scenarios and the weights assigned to the various components of the HPM. The methodology is intended to be used as a comparative tool, where the performance of one variant is compared with the performance of an alternative variant.

Acknowledgements

The authors gratefully acknowledge the support of the UK EPSRC under grant GR/T22100/01 and the Directorate of Sea Systems, Defence Equipment and Support organisation of the UK MoD (DES-SESea) and our partner organisation DRC of UCL.

References

1. S.J. Deere, E.R. Galea, P.J. Lawrence, and S. Gwynne. The impact of passenger response time distribution on ship evacuation performance. *The Transactions of The Royal Institution of Naval Architects, Part A1 (Journal of Maritime Engineering)*. Vol. 148, 2006, pp. 35–44.
2. P. Boxall, S. Gwynne, L. Filippidis, E.R. Galea, and D. Cooney. Advanced evacuation simulation software and its use in warships. *Proc. of the Human Factors in Ship Design, Safety and Operation*, London, UK, 23–24 Feb 2005. The Royal Institute of Naval Architects, London, 2005, pp. 49–56.
3. International Maritime Organisation. *Guidelines for Evacuation Analysis for New and Existing Passenger Ships*, IMO MSC.1/Circ. 1238, 2007.
4. NATO Naval Armaments Group, Maritime Capability Group 6. *Chapter VII Escape Evacuation and Rescue*, Allied Naval Engineering Publication ANEP-77, Naval Ship CoDE, 2006.

Agent-Based Animated Simulation of Mass Egress Following an Improvised Explosive Device (IED) Attack

Douglas A. Samuelson¹, Matthew Parker², Austin Zimmerman³, Stephen Guerin⁴, Joshua Thorp⁴, and Owen Densmore⁴

¹ Serco—North America, 1818 Library Street, Reston, VA, USA
e-mail: samuelsondoug@yahoo.com

² ANSER, 2900 S. Quincy Street, Arlington, VA, USA
e-mail: mprk@cox.com

³ Homeland Security Institute, 2900 S. Quincy Street, Arlington, VA, USA

⁴ Redfish Group, 624 Agua Fria St., Santa Fe, NM, USA
<http://www.redfish.com>
e-mail: stephen.guerin@redfish.com

Summary. We achieved a new degree of scale and realism in developing agent-based simulation models of mass egress from large facilities, following one or more detonations of improvised explosive devices (IED), to evaluate some proposed ways to facilitate evacuation and reduce casualties. We modeled two venues: a sports stadium and a subway station. Our models offer ease of input and animated realism of output that make them much more suitable than traditional discrete-event models as aids to decision-makers. The development and analysis completed to date, while far from exhaustive, suffice to demonstrate the utility of models such as these for evaluating proposed countermeasures, for indicating policy and technology issues that should be analyzed further, and for response planning.

1 Venues Modeled and Software Used

Our team carried out this work for the Science and Technology Directorate (S&T) of the Department of Homeland Security (DHS), as part of a study of how to assess the benefits of technologies to prevent or mitigate IED attacks. We chose to focus on modeling mass egress following one or more attacks because that was one of the most challenging issues, and one identified as critical by bomb squad commanders.

The stadium model represents PNC Park, the major-league baseball stadium in Pittsburgh, Pennsylvania. Redfish Group, of Santa Fe, New Mexico, designed this model under subcontract to HSI, primarily in Processing. Anti-IED countermeasures modeled include guidance to exits, egress onto the play-

ing field, and shock- and shrapnel-absorbing baffles inside the spiral stairways that provide the largest-volume routes of egress.

The subway model represents one level of the Metro Center subway station, in Washington, D.C. Redfish Group trained HSI's analysts to design this model and continued to provide guidance as needed throughout the modeling process. This model was developed primarily in NetLogo. Countermeasures represented in the subway model include guidance to exits, versus the expected less orderly actions people would typically take, and the presence or absence of baffles on the platform to absorb shock and shrapnel.

2 Models' Features

The stadium model handles up to 70,000 people and produces real-time movie-like output and files that can be rendered into more realistic movies, playable at higher speeds than real time. Crowd movement patterns appear realistic to subject matter experts.

The subway model incorporates representations of explosions that offer realism unprecedented in agent-based simulations. Shock and shrapnel are both represented by swarms of agents, whose behavior conforms to physics equations and includes interactions with barriers, reflecting surfaces, and other elements of the environment. We benchmarked the explosion effects against BlastX, a more detailed, highly precise model often used by the U.S. military to estimate effects of explosions. This approach, while not intended to rival well-known models constructed specifically to assess explosion effects, does offer considerably more realism than previous models of crowd dynamics following explosions.

The subway model also incorporates the new "Continuum Crowds" algorithm, first published in August 2006 [1], offering unprecedented similarity to reported observed phenomena.

The movie-like output shows crowd movements in a way that non-technical users can readily assess and contrast, without substantial training or analytical support.

3 Model Results

Model runs indicate strongly that improved guidance to exits would greatly expedite evacuation. In the stadium, allowing people to exit via the playing field generates lesser but still substantial similar benefit. It is not clear, however, that improved guidance to exits would reduce trampling or crushing. This issue is highly sensitive to assumptions about how improved guidance and additional exit routes will affect people's perceptions of urgency

and threat. Prior studies of crowd behavior in disasters indicate that subtle differences in the way the incident is managed critically affect these perceptions [2], so our uncertainty reflects current understanding of such situations.

Additional implications include:

1. While previous analyzes have focused almost exclusively on detection, prevention and defeat of IEDs, DHS or other authorities could also generate substantial benefits to the public by improving mitigation, especially management of mass egress and other aspects of crowd control after one or more explosions.
2. For situations on land, in relatively safe structures, getting everyone out of the facility quickly is *not* synonymous with preventing death and injury; in fact, these goals often compete. Trampling can easily cause many more casualties than the precipitating explosion(s). Enhancing and encouraging shelter-in-place appears likely to be preferable to needlessly accelerating egress.
3. Careful consideration of how to model selected scenarios, including discussion with subject matter experts, yields useful questions and insights by itself, even prior to or aside from model development.

We reached additional policy conclusions that S&T/DHS decided to mark “For Official Use Only”. We can state that the model results were interesting, not necessarily obvious, and—clearly, from S&T’s decision—relevant to current policy issues of some importance.

4 Models’ Advantages and Limitations

From our analysis to date, we identified a number of advantages and limitations of these models and others like them. These include:

1. Advantages:
 - 1.1. Agent-based simulation modeling is useful for evaluating the effects of proposed countermeasures. The balance of realism and ease of use enables decision-makers to gain useful insights.
 - 1.2. The visual, movie output enables facility operators, emergency planners, and other decision-makers with little statistical or modeling background to see patterns of activity, to assess quickly whether the model’s predictions conform to experience, and to grasp new questions the model highlights.
 - 1.3. This approach should offer substantial value in planning and readiness exercises as well, as it greatly facilitates “what-if” studies.
 - 1.4. Agent-based models can handle much larger numbers of people, more types of interactions, and more realistic representations of precipitating events than other approaches to analyzing crowd dynamics.

2. Limitations:

- 2.1. Agent-based modeling is highly realistic; therefore, it is also highly sensitive to modeling assumptions. This sensitivity highlights the need for better understanding of likely crowd behaviors and influences on those behaviors in order for modeling to be accurate. This is not a deficiency of the modeling, but a natural consequence of the (fortunate) scarcity of data from actual events, making empirical validation difficult, if not impossible. Notional validation, based on verifying input rules, is the best method applicable.
- 2.2. The sensitivity of the models to unverifiable assumptions indicates that models such as these, without better data about actual behavior, cannot give sufficiently definitive predictions to be dependable for real-time incident management.
- 2.3. Traditional statistical validation methods have limited applicability to these models. Statistical significance tests are based on the assumption that only random variation—essentially sampling error—and the effect being modeled contribute to total variation. In this analysis, there are many more or less arbitrary assumptions about behavior and materials, and changing those assumptions would most likely cause substantial changes in the results. Hence uncritical application of standard estimation procedures to a limited variety of model runs would yield spurious precision. On the other hand, we can conceive of few rigorous validation experiments, of sufficient scope to address these concerns, that we would want or expect a human subjects committee to approve.
- 2.4. Given the scarcity of data on real events of this nature, validation must focus mostly on accuracy of small-scale behaviors within the larger activity. This is a limitation of the data, not the model. The ability to model such phenomena and the validation questions such modeling raises lead to interesting questions about validation in general: building a case and assessing overall logic and the quality of supporting evidence, as a lawyer would do, seems likely to supplant traditional prediction-focused methods.
- 2.5. The models are highly sensitive to factors about which real-life data are scarce, and the available data are insufficient to support precise estimates of effects. In particular, there are few if any sets of high-quality real-event data about how the nature and urgency of a threat affects people's behavior. Therefore, the models are useful for raising questions and suggesting likely advantages of some mitigating measures, both in assessing technologies and in incident planning, but not for real-time prediction and incident management.

5 Conclusions

Our agent-based simulation models of a stadium and a subway station provided useful and interesting insights into how one or more explosions would affect mass egress and the eventual number injured or killed. Our analysis supports the conclusions that this modeling approach is valuable for assessing the likely benefits of proposed mitigation technologies, and that such models would also be useful for assessing the costs and inconvenience other technologies, such as screening, would impose. From this study, agent-based simulation appears to provide greater realism, adaptability, ease of use and ease of interpretation than traditional simulation methods. It also uses a visual, intuitive interface and produces movie-like output, making these models much easier to use, even by non-modelers, to conduct “what-if” analyzes. Therefore, such models appear valuable for pre-incident planning and exercises, as well as the technology assessment purpose for which they were designed.

We strongly recommend agent-based modeling as a way to assess benefits of proposed technologies and to assess the likely impacts of policy options. In addition, with current methodology and software, the modeling is itself one of the technologies of interest, especially for planning and exercises. We therefore also strongly recommend further investigation of the uses of simulation in preparedness for incident management.

The models are available, in open source form, in a CD from HSI or the lead author, or, for the stadium model, on Redfish Group’s Web site, <http://www.redfish.com>.

References

1. A. Treuille, S. Cooper, Z. Popovi, Continuum crowds, *ACM Transactions on Graphics* 25(3), 1160–1168 (2006). <http://www.washington.edu/projects/crowd-flows/>.
2. J.M. Chertkoff, R.H. Kushigian, *Don’t Panic: the Psychology of Emergency Egress and Ingress*, Praeger, New York, 1999.

A Novel Kinetic Model to Simulate Evacuation Dynamics

Sergei Burlatsky¹, Vladim Atrazhev², Nikolay Erikhman², and Satish Narayanan¹

¹ United Technologies Research Center, 411 Silver Lane, East Hartford, CT 06108, USA

e-mail: BurlatS@utrc.utc.com, Narayas@utrc.utc.com

² Institute of Biochemical Physics, Russian Academy of Science, Kosygina 4, Moscow, Russia

Summary. We present the Kinetic Model (KM) as an alternative to combat the computational barrier posed by state-of-the-art evacuation modeling and simulation approaches. Instead of tracing individual agents, the KM simulates a coarse measure, namely the local occupant density. The two-phased approach tracks two distinct kinds of traffic, namely individual motion in “rarefied” (i.e. non-congested) regions and vacancies left by individual motion in “dense” (i.e. congested) regions. The dynamics of the phase boundary is governed by the balance of individuals moving from the “rarefied” region and vacancies moving from the “dense” regions across the boundary, making the approach intrinsically computationally efficient. The paper presents the theoretical formulation of the KM and comparisons of the model predictions of occupancy during evacuation with that from higher fidelity ABM. The KM computations are nearly 3 orders of magnitude faster than the ABM simulations with minimal degradation of prediction accuracy.

1 Introduction

There have been substantial efforts to model and simulate the dynamics of people movement during evacuation [1–4] and evaluated in buildings, subway stations, stadiums, ships and aircraft, since it is valuable in evaluating layout designs and the effectiveness of evacuation policies. State-of-the-art in accurate modeling of evacuation is agent-based modeling (ABM) which simulates the complex interaction between people [5]. These models, however, are complex when scaled to large buildings and unsuitable for real-time implementation in applications such as “active guidance systems” to optimize the evacuation time and paths, or for the purposes of augmenting information at the fire detection and alarm panel used by first responders [6]. In this paper, a new model for evacuation is presented—the Kinetic Model (KM). Simulations in an office building are used to evaluate the model and comparisons with

ABM simulations are used to show that, although adopting coarse measures, the KM does not sacrifice prediction accuracy significantly and substantially reduces computational expense.

2 Evacuation Dynamics Model

Evacuation traffic exhibits gaseous (*low density*) and dense (*queue*) phases, and agent motion in these phases are distinct. The fundamental premise of the Kinetic Model (KM) proposed here is to simulate agents in the gaseous phase and vacancies (i.e. space left by agents moving from one location to another) in the dense phase (illustrated in Fig. 1).

2.1 Problem and Model Formulation Description

In Fig. 2a, an example floor map for the evacuation model formulation is presented. For computations, the interconnected floor illustrated above is split into low level objects, namely segments. In Fig. 2b, segments are denoted by multiple rectangular blocks. Sometimes more than one segment is needed to represent a single room, due to room geometry. The other object is a door to connect two segments. Each door i is characterized by its width w_i .

In current model, equations of agent motion are the same for each segment, with differences in geometric parameters of the segment and its topology. The parameters and equations described below are for the example of a single

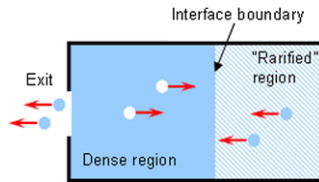


Fig. 1. Schematic of two-phase evacuation dynamics illustrating vacancies in dense regions and agents in the “rarefied” region.

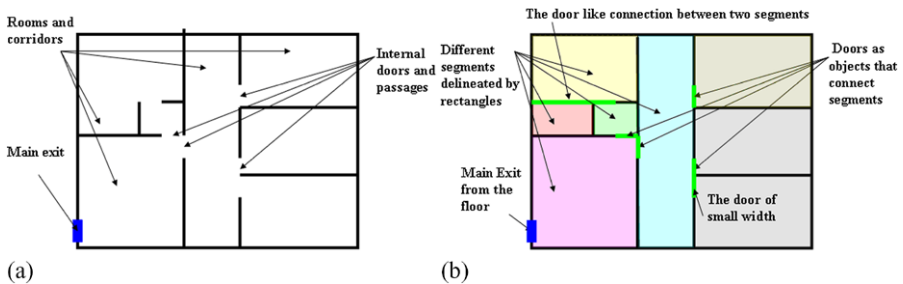


Fig. 2. Evacuation model formulation geometry description.

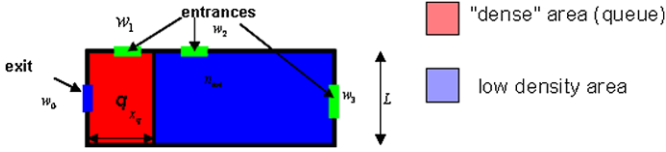


Fig. 3. Building segment schematic illustrating evacuation model parameters.

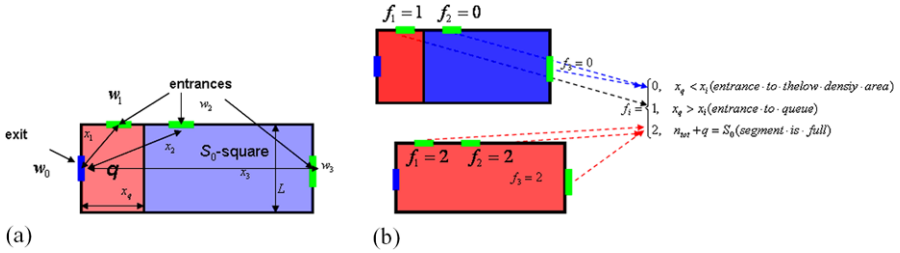


Fig. 4. Building segment model and queuing parameters.

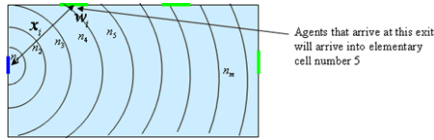


Fig. 5. Schematic illustrating agent motion from segment entrance to exit.

segment (as illustrated in Fig. 3). Each segment is described by: Area S_0 ; Segment length x_0 ; Segment width L ; Number of entrances N_E (may be zero); Coordinates of entrances and entrances width (w_i is the width of exit i); Distance from the entrance i to the exit x_i ; Transversal time from i th entrance to exit (V_0 is agent velocity) $\tau_i = x_i/V_0$; Coordinates of exit and exit width w_0 . The segment area $S (\equiv x_0 \times L)$ is expressed via geometric width L and length x_0 . The agent distribution includes regions of high density near the exit (queue) and low density. The coordinate of the queue end x_q is given by $x_q = q/L$, where q is the number of agents in queue. The number of agents in the low density area is n_{tot} . If the number of agents in the queue is small, the whole queue leaves the segment in one time step, the low density limit.

Each entrance i is characterized by the distance between location of this entrance and that of the exit from segment x_i (see Fig. 4a). The state of each entrance i is described by the flag f_i (see Fig. 4b).

Each segment is divided into elementary cells. The cell number k is equal to the number of time steps required to reach the nearest exit. Schematically (see Fig. 5) this can be regarded as radial segments with the center located at the exit. Via entrance i , agents arrive into the cell k , defined by the condition $k - 1 < \tau_i < k$. The area of the elementary cell s_k , is computed as follows. The segment on the elementary are split into unit squares and coordinates of the

center of each square are computed. A number of squares, with centers laying at the distance $[k - 1, k]$ from the exit are then computed. The distance from the center of square to the closest point of exit is measured. For example, the interval $[0, 1]$ for the first elementary cell $k = 1$, $[1, 2]$ for the second cell $k = 2$. The total number of elementary cells is $m = x_0/V_0$.

The initial number of agents in the cells is proportional to the area. The state of the segment is described by the number of agents in the queue and in each elementary cell $\{q, n_1, n_2, \dots, n_m\}$. The number of agents in the low density area is $n_{tot} = \sum_{k=1}^m n_k$. The probability to enter a low density area is multiplied by the factor $(1 - n_{t+\tau_i}/L)$. For this study, a rectangular segment shape approximation is used. This is needed to account for multiple entrances, a common feature of corridors. The segment width L is substantially smaller than the length, and therefore elementary cells are rectangular of length V_0 (distance is $\Delta t \times V_0$ for time step $\Delta t = 1$). The location of the end of the queue, comprising q agents, is $x_q = q/L$. The transversal time is defined as the time that would be required to exit from the end of the queue x_q in an empty building: $\tau_q = x_q/V_0$. All elementary cells with the number k , $k < \tau_i$ are occupied by the queue, and agents from the elementary cell $k + 1$ join the queue in one time step.

2.2 Theoretical Model Formulation: The Kinetic Model of Evacuation

The equations for agent density dynamics are now presented. The flux from the entrance i is a function of the entrance state. Agents arrive via entrance i from the adjacent segment queue and denoted by q_i (as illustrated in Fig. 6). The number of agents $r_i(t, k)$, that arrive through the entrance i to the segment k at time t is given by (1).

$$r_i(t, k) = \begin{cases} V_0 w_i \left(1 - \frac{n_{ki}(t)}{L}\right) [\chi(q_i(t) - w_i V_0) + \frac{q_i(t)}{w_i V_0} (1 - \chi(q_i - w_i V_0))], & f_i = 0, \\ P_i V_0 w_0 [\chi(q_i(t) - P_i w_0 V_0) + \frac{q_i(t)}{P_i w_0 V_0} (1 - \chi(q_i(t) - P_i w_0 V_0))], & f_i = 1, \\ 0, & f_i = 2. \end{cases} \tag{1}$$

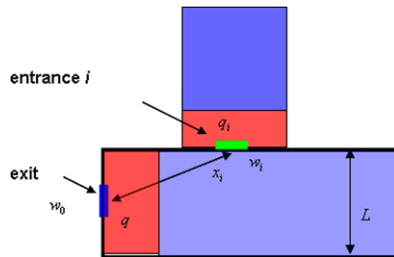


Fig. 6. Schematic of traffic dynamics between building segments.

Here,

$$\delta(j) = \begin{cases} 1, & j = 0, \\ 0, & j \neq 0 \end{cases}$$

is the Dirac delta-function,

$$\chi(x) = \begin{cases} 1, & x > 0, \\ 0, & x \leq 0 \end{cases}$$

is the Heavyside step function, and $n_k(t)$ is the number of agents in the elementary cell k , where entrance i is located. For numerical solution, a discrete time step $\Delta t = 1$ is used, therefore the time $t = 1, 2, 3, 4, \dots$. The last line in (1) implies that if the segment is full, no entrance is possible. The first line describes the entrance to the low density area. Thus, if the queue q_i in the adjacent segment is small, it arrives at this segment in one time step. If the queue is large, the number of entering agents is proportional to the entrance width w_i , velocity of agents V_0 and density factor for appropriate segment $(1 - n_{\tau_i}/L)$. The second line corresponds to the entrance to the queue. In this case, the entrance probability is calculated using vacancies dynamics. The probability of a vacancy reaching the k th entrance is given by

$$P_k = \left[\prod_{j=1}^{k-1} \left(1 - \frac{p_j}{L} \chi(x_q - x_j) \right) \right] \cdot \frac{p_k}{L} \chi(x_q - x_j) \tag{2}$$

where the probability that the vacancy turns to an exit k of the width w is $p_k = 1 - (1/2)^{w_k}$. The products in (2) reflect the probabilities of the vacancy to escape from the queue to one of the exits that are located between the vacancy entrance point and the exit k . The evolution of agent number in elementary cell k is given by:

$$n_k(t + 1) = n_{k+1}(t) + \sum_i r_i(t, k),$$

where the sum is taken over all entrances corresponding to the elementary cell k . The dynamics of the agent number in the queue is described

$$q(t + 1) = q(t) + n_{\tau_q+1} - I(t) + \sum_j r_j(t, k),$$

where $I(t)$ is the agent flux from the queue through the exit. Since the segment exit under consideration is the entrance for an adjacent segment, $I(t)$ is calculated using the above algorithm to the corresponding adjacent segment, closing the numerical algorithm.

3 Model Simulation Studies and Comparison Results

The well-known ABM is used to evaluate the KM. In ABM the area under consideration is split on elementary squares of fixed geometric size. Each square may be empty or occupied (by one person). The motion of individuals is organized as successive jumps from one cell to an adjacent cell. Each jump is directed to an exit, with a probabilistic random choice. ABM requires relatively large computational time for large scale geometry, and can scale as poorly as N^2 (where N is the number of agents). More details on ABM are provided separately [5]. The KM predictions were compared with those from ABM for the same building for various initial people densities. The office building under study is a 2-storey building with two normal and two emergency exits [5]. The building is about 32,000 square feet with typical occupancy of 50–150 people. For KM, initial people density is uniform and the total initial amount of people equals the initial density multiplied by total area. For ABM, initial density is the probability of each elementary cell to be occupied. For ABM, results are averaged over 200 independent runs.

Figure 7 displays the layout of the office building second floor denoting the exits and the three regions where predictions of the occupant number as a function of time is compared for the ABM and the KM. For low initial occupant densities ($p = 0.03, 0.05$), the two models exhibit nearly indistinguishable predictions. This demonstrates good KM prediction fidelity.

Figure 8 displays a second set of ABM and KM predictions and comparisons for higher initial occupant densities ($p = 0.37, 0.1$). While the two models exhibit similar predictions, quantitative differences can be observed. For instance, over-prediction of occupancy in region 3 from KM in the midst of evacuation, where congestion is expected to be the highest (due to proximity to adjacent exit). The difference (particularly over-prediction by KM) is believed to be because of differences in the motion rules for ABM (where the occupant density in a queued region is lower than the limiting density) and KM (where the density of people in a queue is equal to the limiting density).

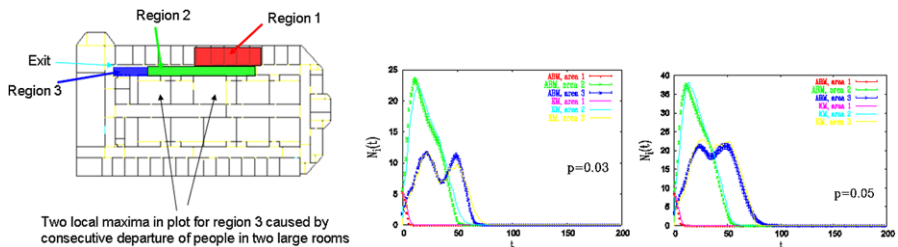


Fig. 7. Comparisons of KM prediction of occupant count during evacuation with those from agent-based model for different building regions.

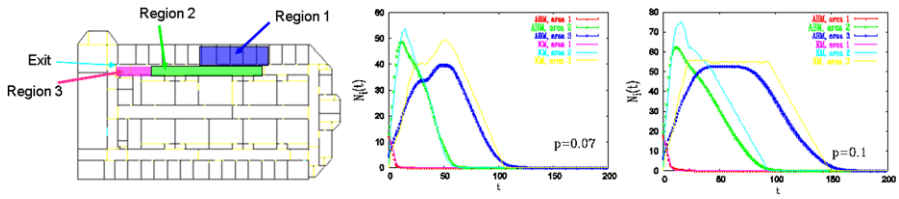


Fig. 8. Comparisons of KM prediction of occupant count during evacuation with those from agent-based model for different building regions.

4 Conclusion

A new Kinetic Model (KM) for simulating the dynamics of evacuation is presented. Instead of tracing individual agent trajectories, the model simulates a coarse measure, namely the local occupant density. For small initial density, the evacuation process is governed by the low density regime. For the high density regions queues are formed, the location and size of which depend on the building geometry and initial density distribution. Consequently, the evacuation time is defined by motion in bottle-necks. Statistical physics methods developed for condensed matter during phase transition are used to describe motion in high density regions. Comparisons of the KM predictions of occupancy during evacuation with that from high fidelity agent-based models (ABM) shows that the KM predictions are in quantitatively good agreement. ABM computations can be accurate but are computationally expensive. This makes them unsuitable for design or optimization studies in large-scale buildings and for real-time use, such as a fire safety warning or first responder decision support system. The KM computations are nearly 3 orders of magnitude faster than the ABM simulations. A companion paper [6] describes and demonstrates the use of the KM for real-time estimation of occupancy during evacuation in buildings.

Acknowledgements

The authors are grateful to United Technologies Research Center for financial support extended to this project and research team.

References

1. M. Owen, E.R. Galea, and P.J. Lawrence. The exodus evacuation model applied to building evacuation scenarios. *Journal of Fire Protection Engineering*, Vol. 8, No. 2, pp. 65–84, 1996.
2. A. Schadschneider. Cellular automaton approach to pedestrian dynamics—theory, in M. Schreckenberg and S. Sharma (Eds.), *Pedestrian and Evacuation Dynamics*. Springer, Berlin, 2002.

3. D. Helbing and P. Molnar. Social force model for pedestrian dynamics, *Physics Review E*, Vol. 51, pp. 4282–4287, 1995.
4. S. Hoogendoorn and P. Bovy. Gas-kinetic modeling and simulation of pedestrian flows, *Transportation Research Record*, Vol. 1710, pp. 28–36, 2000.
5. Y. Lin, I. Fedchenia, R. LaBarre, and R. Tomastik. Agent-based simulation of evacuation: an office building case study, in *Pedestrian and Evacuation Dynamics 2008*. Springer, Berlin, 2010.
6. R. Tomastik, S. Narayanan, A. Banaszuk, and S. Meyn. Model-based real-time estimation of building occupancy during emergency egress, in *Pedestrian and Evacuation Dynamics 2008*. Springer, Berlin, 2010.

Egress Route Choice Modelling—Concepts and Applications

Volker Schneider and Rainer Könnecke

I.S.T. Integrierte Sicherheits-Technik GmbH, Feuerbachstr. 19, Frankfurt am Main, Germany
e-mail: v.schneider@ist-net.de

Summary. Most microscopic evacuation models offer the possibility to determine the individual egress route based on a shortest path criteria. This option has the advantage that the egress route is only depending on the building structure and can thus be calculated in advance. Yet there has to be the possibility for individual and dynamic adjustments depending on egress route load (avoid congestions), attractiveness of route alternatives or external influences like smoke spread if appropriate. However, care has to be taken that these adjustments do not lead to unrealistic counter flows or artificial blocking effects. Human egress behavior is triggered by a very complex interaction of perception, anticipation and fine-tuning of movement that can up to now only be modelled in a very approximative way on a large scale. The basic concepts of egress route choice modelling implemented in the microscopic evacuation model ASERI are presented together with case studies demonstrating the effect of certain egress route choice options on evacuation efficiency and calculated egress time. Emphasis is put on the mechanisms modelling avoidance strategies in case of congestion or in the presence of equivalent egress route options. Some of these mechanisms are dynamic, based on local occupant load and the local building environment and may involve non-deterministic rules.

1 Introduction

Egress route choice by individuals or groups is one of the major factors effecting evacuation efficiency and egress time. The attractiveness of specific egress routes is depending on a multitude of attributes including complexity and use of the building environment, clarity of egress route courses, familiarity and training of the occupants, degree of perceived danger, alarm and information system, safety management and—in case of a fire—smoke and heat spread. Since high attractiveness does not necessarily correspond to high effectivity, this may result in unbalanced exit use and merging or splitting of flows that can considerably increase individual egress time and cause congestion. These effects are best described on an individual basis applying the concepts of microscopic evacuation modelling.

A standard criterion implemented in most microscopic evacuation models is the determination of the individual egress route based on the shortest path available. This can be the shortest local path out of a room or a certain building section or the shortest global path from initial position to one the building exits or a safe place defined as a possible goal of the egress movement. This option has the advantage that the egress route is only depending on the building structure and can thus be calculated in advance. Yet there is the necessity to consider dynamic effects like occupant load and occupant density, congestion and external impact like heat or smoke if appropriate. Technically, the models are faced with the challenge of crossings, counter-flow or blocking effects that have to be described in realistic manner. The basic concepts of egress route choice modelling implemented in the microscopic evacuation model ASERI are presented together with one simplified sample calculation and two real-case applications demonstrating the effect of certain egress route choice options on evacuation efficiency.

2 Egress Route Choice Mechanisms Implemented in ASERI

The ASERI egress route mechanism can be subsumed into the categories:

- optimization with respect to (local or global) path length,
- prescriptive egress route choice,
- avoidance strategies in case of congestion,
- selection criteria in case of equivalent route sections,
- modelling activities other than egress movement,
- effect of smoke or heat on egress route choice.

Egress along the shortest global path takes place from initial location to any one of the available safe place areas. These safe place areas are the ultimate goal of the occupants and may be located inside or outside the building. This option is the ASERI default for individual egress movement. However, local egress route criteria assigned to specific rooms or building sections (e.g. shortest path to an available exit) have priority over the shortest global egress route criterion. This feature thus describes occupants choosing familiar with the building layout or a path marked by egress route signs and is thus usually a reasonable choice to start an analysis based on numerical simulations. There is of course the possibility that the shortest path criteria will result in an unbalanced egress route choice, possibly causing the occurrence of congestion. Figure 1 exemplifies this problem for a schematic assembly set-up. In this case, almost all occupants inside the assembly hall (Saal) will use the main entrance via the Foyer, ignoring the additional exits at the side and back.

There are several mechanisms included in ASERI to model avoidance strategies in case of congestion or balancing the choice in the presence of

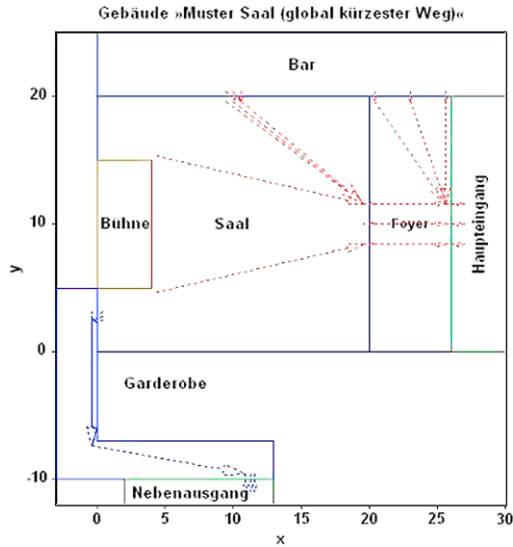


Fig. 1. Shortest global egress route in sample assembly configuration.

equivalent egress route options. These mechanisms are dynamic, based on local occupant load and the local building environment. For the special case of large assemblies with high initial occupant density there is an additional option based on a static distribution principle. The maximum possible occupant flow for each exit is estimated based on standard (e.g. empirical derived formula) methods. Then the number of occupants to be assigned to each exit is determined in proportionality to the respective maximum exit flow. Each person is then assigned to one of the available exits by selecting the occupant with the shortest distance to the respective exit—always one occupant for each exit in turn, until each exit has reached its assigned total occupant number. This simple procedure yields realistic results as can be seen from the superposition of individual egress paths shown in Fig. 2. This method especially includes the possibility that occupants avoid congestions at nearby exits by travelling a longer distance to larger and less crowded exits. This mechanism also reduces the probability of crossings or counter-flow.

Dynamic avoidance strategies implemented in ASERI include the “Balance” and “Dynamic Exit Choice” options. “Balance” is a more general and dynamic version of the balanced exit use mechanism described above. It can be applied throughout the entire individual egress process. The method is based on an in advance estimation of occupant flow and related congestion time at exits and bottlenecks in order to optimize local egress time. It also includes probabilistic weight parameters. “Dynamic Exit Choice” on the other hand does not use estimated flow values at exit or bottlenecks but rather information on local occupant density. This information has to be available (“visible”) for a person that is about to decide which egress route alternative to choose. If

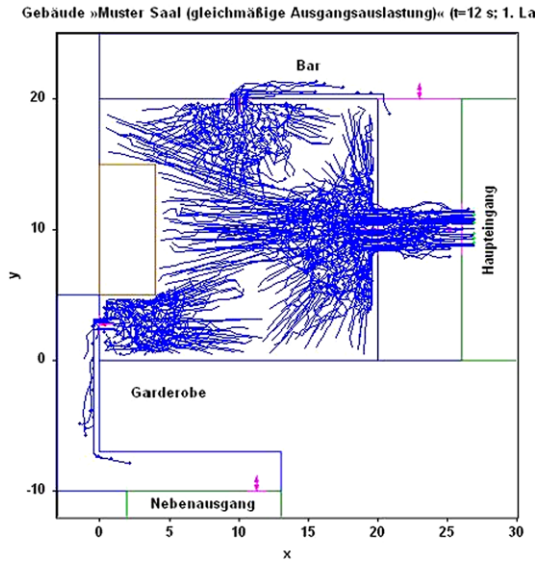


Fig. 2. Balanced exit use in assembly configuration.

a certain tolerance limit of occupant density is exceeded, a less occupied route is chosen if available. This is in principle a deterministic procedure, but its effects are in practice similar to those obtained using probabilistic concepts if large crowds are involved. It has the advantage that it is not only effective in avoiding congestions but also in distributing occupants in a reasonable way to equivalent routes (e.g. splitting of an egress route). Figure 3 shows the effect of “Dynamic Exit Choice” for the assembly sample. The pattern is similar to Fig. 2 but somewhat less regular. Occupants tend to move towards the initially desired (according to the local or global shortest egress route) exits first and then—after realizing the onset of congestion—some of them change direction towards less crowded exits.

All dynamic egress route choice mechanisms require a free line of sight from the individual occupant location to the respective exits. This is a conservative but reasonable approach since it can not be assumed for sure that all occupants are familiar with the building layout.

In the case of prescriptive egress routes occupants starting egress movement in certain regions of the building are assigned a specific destination (safe place area). Additionally it is possible to demand or exclude certain units (building sections) along the individual egress path. This method has the advantage that the user has complete control on the balance of the egress routes. It requires however a detailed sensitivity analysis if there is no comprehensible unique way of prescribing the distribution of occupants to the destinations available. Figure 4 illustrates this type of behavior.

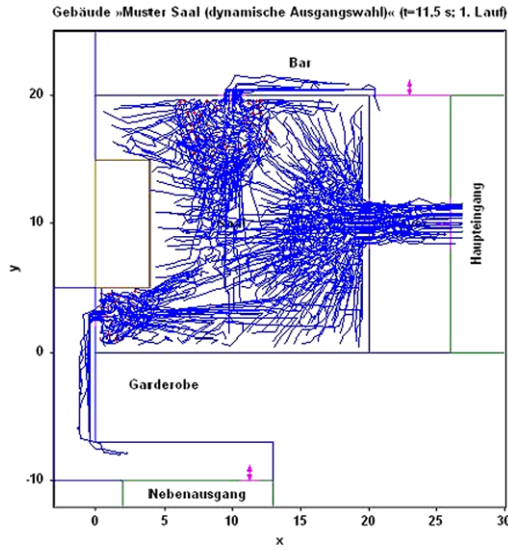


Fig. 3. Dynamic congestion avoidance strategies in assembly configuration.

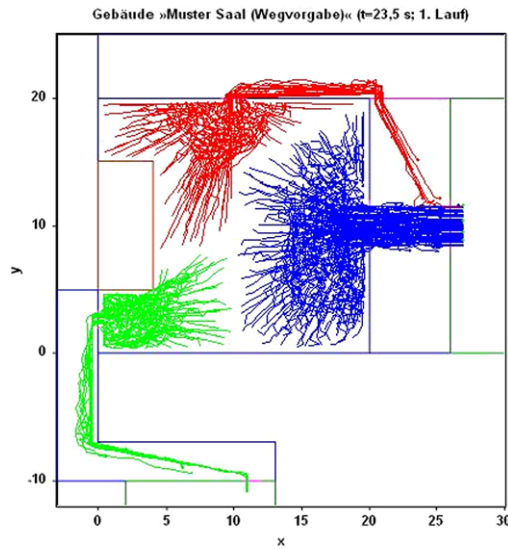


Fig. 4. Prescribed egress route choice in assembly configuration.

Smoke spread can effect the individual mobility (reduced walking speed, incapacitation) and occupant can get lost in case of reduced visibility. Furthermore, the reluctance to enter smoke laden atmospheres will have a strong influence on egress route choice. The implementation of these effects in ASERI is discussed in more detail in [1].

3 Applications

Two applications are demonstrated in Figs. 5 and 6. Figure 5 presents the floor layout of a multi-storey office building. Due to periodical fire-drills—most of them in co-operation with the local fire brigades—the staff is well trained, thus using the local shortest egress path to the emergency exits, as

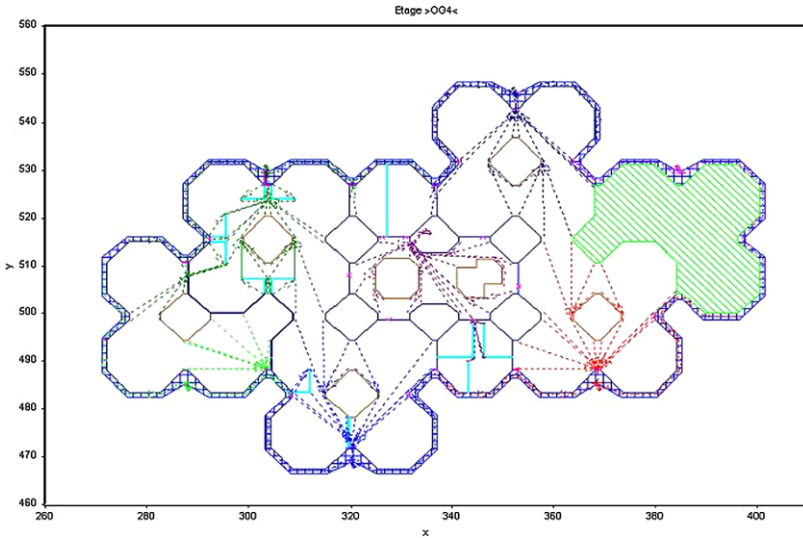


Fig. 5. Egress routes inside the floor of a multi-storey office building.

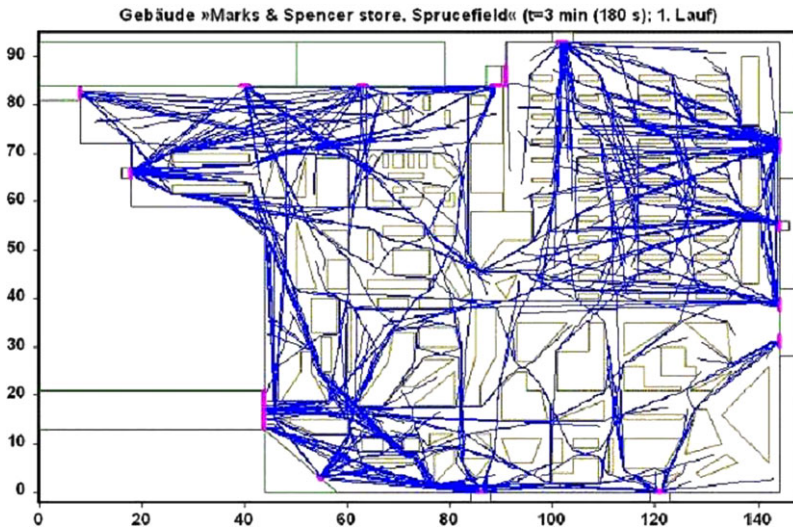


Fig. 6. Individual egress routes inside a store.

shown in Fig. 5. Figure 6 shows the reconstruction of a fire drill in a Marks & Spencer store [2]. Each of the 14 exits available is assigned the number of persons known from the documentation of the fire drill. Also the initial location of the occupants is roughly known. Due to the advice of the staff most persons use one of the nearby emergency exits. Only a few occupants show considerably longer egress routes. Nevertheless the calculated and observed egress time of about 3 minutes (a good result when compared to other drills in warehouses) could be reduced by about one minute (assuming the same response time distribution as applied for the drill case) if all occupants would use the shortest local egress path.

Both examples demonstrate the importance of training and good fire safety management in order to achieve a high evacuation efficiency by reducing the individual response time and optimizing the individual egress route choice.

References

1. V. Schneider, R. Könnecke: Simulation der Personenevakuierung unter Berücksichtigung individueller Einflußfaktoren und der Ausbreitung von Rauch, *VFDB-Zeitschrift* 3 (1996) 98.
2. A. Sandberg: Unannounced Evacuation of Large Retail-Stores, Department of Fire Safety Engineering Lund Institute of Technology, Lund University, Lund, 1997.

Architectural Cue Model in Evacuation Simulation for Underground Space

Chengyu Sun¹, Bauke de Vries², and Qi Zhao³

¹ College of Architecture and Urban Planning, Tongji University, Si Ping Road No. 1239, Shanghai, China

e-mail: ibund@126.com

² Architecture, Building and Planning, Eindhoven University of Technology, P.O. Box 513, 5600 MB, Eindhoven, The Netherlands

e-mail: b.d.vries@tue.nl

³ Underground Space Design Institute, Shanghai Municipal Engineering Design General Institute, Zhong Shang Bei Er Road No. 901, Shanghai, China

e-mail: zhao.q.dxzx@smedi.com

Summary. In this paper, a CAVE-based experiment for measuring the evacuees' preference on architectural cues is introduced. The research method has proven that a paired cue evacuation decision model can be constructed through the Conjoint Analysis method. According to the preference function the nearest exit assumption in other evacuation models is questionable in some circumstances. Moreover, a set of architectural cue attributes and their quantitative utilities on the preference are discovered.

1 Introduction

Under the pressure of the endless land demand, the underground development is inevitable in the mega cities. The developing underground spaces have been joined into each other as a complex underground network with multi functions. To evaluate its performance in emergency, the authority relies on the performance-based evaluation methods, which depend heavily on the composite evacuation models. Such models predict the available safe egress time (ASET) and the required safe egress time (RSET) to be sure that the former is longer than the latter [1]. ASET is predicted by a set of models on fire and smoke dynamics. RSET is predicted by a set of models on human egress behavior. As the starting point of RSET calculation, the predicted evacuees' routes to exit are the most basic and crucial part.

As argued by both Arthur and Passini, the evacuation is a kind of wayfinding, in which evacuees use so-called cues that all the information available in the environment are used to find the route to exit. The cues include the verbal (from information desk, staffs, etc.), the graphic (signage, map, etc.), the

architectural (entrance, corridor, stair, etc.), and the spatial (how things relates to each other) [2, 3]. Additionally, the information derived from other evacuees' movement is also regarded as a useful cue to find the way out [4–7].

There are a few models trying to explain and predict how the evacuees make use of the architectural cues to look for the route to exit. In general, according to methods of computing the route to exit, existing evacuation models can be classified into the non-architectural cue based model and the subjective architectural cue based model [8–10]. At public underground space the visitors are mostly unfamiliar with the global layout and have no exterior building form to understand the circulation system, which lead to the lack of spatial information and the heavier reliance on the sequential architectural information. In contrast with the spatial information, the architectural information from the attractive architectural elements works at a local level. Consequently all the global information based models (ALLSAFE; ESCAPE; Egress Complex Model; EgressPro; EXIT89; GridFlow; MagneticModel; PedGo; Simulex; VEgAS; EVACNET4; PEDROUTE; TIMTEXT; WAYOUT; ASERI; SimWALK; FDS+Evac; BFIRE-2; buildingEXODUS; CRISP3; EGRESS; EvacSim; EXITT; E-SCAPE; F.A.S.T; Fluid Model; FPETool; Legion; Myriad; PathFinder; STEPS) are non-architectural. Another model (PEDroute) capable of signage following belongs to the non-architectural, too. In the category of the subjective architectural based models, BGRAF demands the operator to designate the importance for every part of the space according to his personal judgement on the architectural attractiveness. Another model (MASSegress) drives the agent to search the exit randomly and to approach the nearest visible exit with the familiarity designated by the operators. Obviously none of the above models makes the use of the architectural information properly in the route-to-exit searching.

In this research an agent-based evacuation simulation model is developed to predict how the evacuees will use the architectural cues to find their route to exit, which can be used to evaluate the space design independently in the initial stage and be integrated into the existing compositive evacuation models to provide supports on architectural information. Other information sources such as the signage, cognitive map, crowd and threatening situation are not considered in this model. The core of the model is a preference function to predict the evacuees' choice among the architectural cues, which is set as the goal of the next step. With the assumption that "If a setting works well under normal conditions, it will have a better chance of working well in emergency conditions" [11], a set of CAVE-based experiments are implemented to collect about one hundred subjects' choices on the five kinds of architectural cue pairs. Then the preference function is built from these data by conjoint analysis method.

The outline of the paper is as follows: First we will describe the list of architectural cues and the framework of the whole model. Next the focus is put on the research how to measure the evacuees' preference including the

method, the experiment design and the data analysis. We will finish with conclusions and outlooks.

2 Architectural Cue Model for Underground Space Evacuation

From previous research [12] a list of recognizable architectural cues was deduced from questionnaires, namely Outdoors, Exits, Stairs, Slopes, Escalator, Raised Ceilings, Columns and Doorways. Three main cues: Doorway, Stair/Slope/Escalator, and Exit are selected from the list to be the elementary architectural cues of the model in this stage according to Tubbs' Egress Design Checklist [1].

The model assumes that from the architectural cues in sight and memory, the evacuee selects the architectural cue with the highest preference and approach to it. If he passed an Exit cue or a Stair cue to the ground level, the evacuation terminates. Otherwise, he will see, choose and move step by step (Fig. 1).

To simulate this process, the agent uses its artificial vision to perceive the environment and recognize the three kinds of elementary cues in the 3-dimensional space to support the decision making during the evacuation

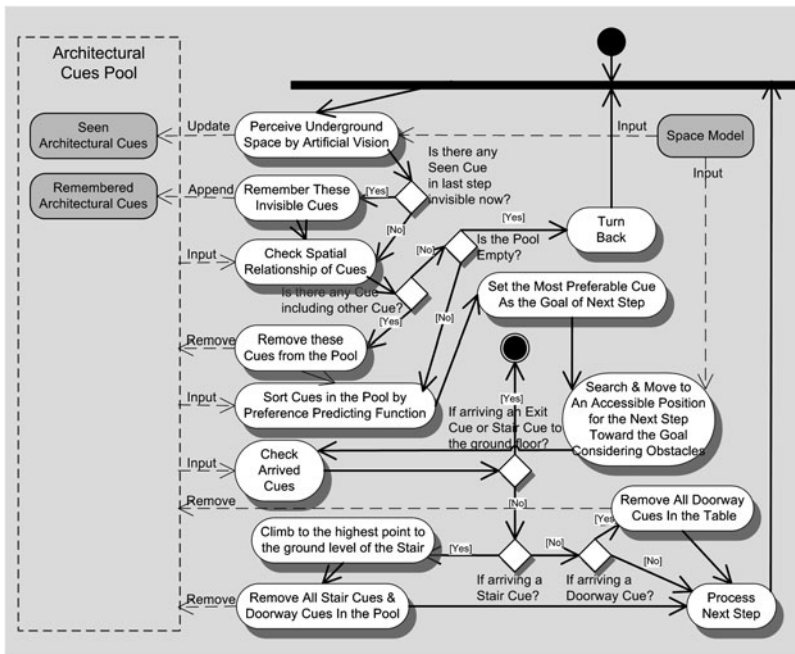


Fig. 1. The framework of architectural cue model.

simulation. The pixel-based recognition algorithm of the cues in the agent's vision will be presented in another publication. In the following section the research is described to measure the evacuees' preference on the architectural cues to build the crucial preference function in this model.

3 Research Method

To observe the evacuees' preference only on the architectural cue, the authors used the experimental psychology research method with controlled stimulant to the subjects in a CAVE-based virtual drill. The subjects' choices between the cue pairs as the responses to the stimulants are regressed into evacuees' preference by the Conjoint Analysis approach.

3.1 CAVE-Based Conjoint Analysis

Concerning the risk of the real environment evacuation based observation [11] and the interferences from the other non-architectural information, the authors regarded the laboratory experiment based observation as the suitable solution for the research.

The experimental psychology develops its research methods from paper-and-pencil technique to visual aided techniques and simulations [13]. Recently, the virtual reality technology was argued as a better solution for the space related research. It features [14]:

- the avoidance from the risks in real environment;
- the sense of time and space;
- the interaction between the subject and the environment;
- the complete control of stimulants;
- the built-in technique to record the subjects' response.

Among the virtual reality techniques, CAVE system is the only one that is capable to provide the similar view field as human beings and the sense of scale and distance [15], which is necessary for the virtual drill. Consequently, a CAVE system was built for the research.

Similar to the other CAVE-based preference researches e.g. ICARUS [16], the preference function is surveyed according to the Conjoint Analysis approach, in which the architectural cues are presented as paired evacuation directions to the subjects in a set of scenes designed carefully. The subjects are asked to evacuate in this virtual scene by choosing one of the two cues as the egress direction. The recorded choices are collected and used to estimate the parameters of the evacuees' preference function

$$p(c_i) = \frac{e^{z_i}}{e^{z_i} + e^0} \quad (1)$$

where

$p(c_i)$ is the probability of cue i being chosen in the cue pair;
 $z_i = \beta_{\text{type}} + \beta_{\text{side}} + \beta_{A1} + \beta_{A2} + \beta_d + \beta_w + \beta_h + \beta_0$;
 β_0 is the intercept; and β_i is the B value related to the variable level.

3.2 Attributes of the Architectural Cues

The variables of the above function map to the attributes of the architectural cues, which are defined as follows (Figs. 2, 3 and 4):

- The cue type is defined as TYPE.
- The side of the cue in a cue pair is defined as LR.

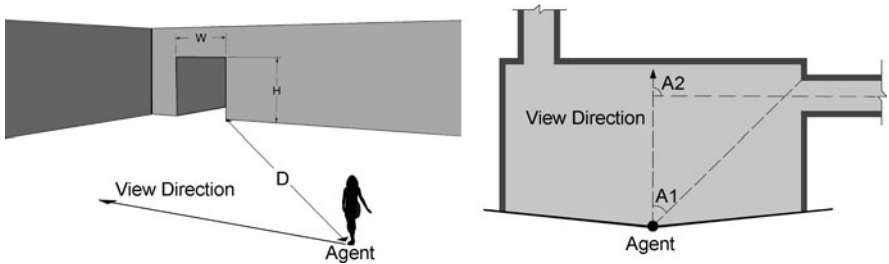


Fig. 2. Variables of Doorway.

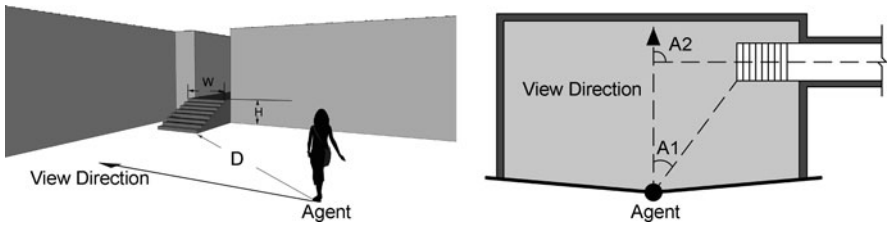


Fig. 3. Variables of Stair/Slope/Escalator.

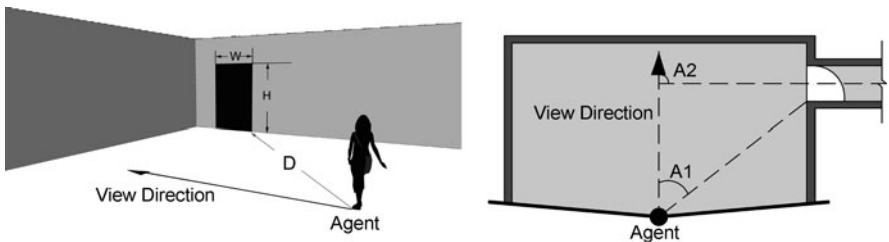


Fig. 4. Variables of Exit.

Scene type	Levels of the variables							Number of scenes by fractional factorial design
	Type	LR	A1	A2	D	H	W	
Doorway– Doorway	n/a	2	7	7	7	5	7	49
Stair–Stair	n/a	2	7	7	7	5	7	49
Exit–Exit	n/a	2	7	7	7	5	7	49
Doorway–Stair	2	2	7	9	7	5	7	81
Exit–Stair	2	2	7	9	7	5	7	81

Table 1. Design of the variable level and scene profile.

- The distance from the cue to observation point, defined as D.
- The width of the cue is defined as W.
- The height of the cue is defined as H.
- The angle between the direction of the view direction and the cue is defined as A1.
- The angle between the direction of the view direction and the cue direction is defined as A2.

3.3 The Design of Scenes with Paired Cues

The three elementary cues are combined into five kinds of cue pairs each related with a set of scenes with the attributes at different levels. The Doorway–Exit pair is not included in the experiment because of the obvious evacuation preference on them.

According to the practical values used in the underground design and the size of the subjects, the levels and the corresponding profiles of the five scene sets are designed as in Table 1.

3.4 Encoding and Decoding

Every scene is generated into a set of variable levels by fractional factorial design. For an example, the generated scene No. 39 in Stair–Exit set is indicated in Table 2.

Next, the levels are decoded into attribute values of the two cues in one scene. The level of variable “Type” maps to Doorway, Stair, or Exit. The level of variable “LR” maps to the Left or Right side the cue is on to the other. The level of the variable “A1” maps to the ratio between the two A1 attribute values of the both sides. The level mapping of the other variables “A2”, “D”, “H”, “W” is the same as A1. When the pair contains only one kind of cue, the ratio is the value of the left cue to the value of the right. When the pair contains two different kinds of cues, the ratio is the value of the stair to the

ID	Left cue type level	Ratio level				
		A1	A2	D	W	H
39	2	1	7	5	7	4

Table 2. Designed levels of scene No. 39 in Stair–Exit set.

ID	Left type	Right type	lA1–rA1 (degree)	lA2–rA2 (degree)	lD–rD (meter)	lW–rW (meter)	lH–rH (meter)
39	Exit	Stair	60 : 7.5	5 : 40	10 : 20	1 : 7.2	2.5 : 5.0

Table 3. Practical dimensions of scene No. 39 in Stair–Exit set.

Chosen	Cue type	Side	A1	A2	D	W	H
1	1	1	1	7	5	7	4
0	0	0	14	12	10	8	7

Table 4. Recorded data of scene No. 39 in Stair–Exit set.

value of the other cue. The exact values of the both sides of a pair are assigned by the ratio and the underground design practise. Scene No. 39 is decoded in Table 3.

When the subject makes a choice between the two cues, the choice will be recorded into two rows of variables with the levels encoded again. In the cue pair with the same cue type, the first row is encoded from the left cue. The second is for the right. In the cue pair with the different cue types, the first row is encoded from the cue of Stair. The second is for the other cue. If the cue is picked, the variable “Chosen” is set to 1, otherwise 0. If the cue is a Stair, variable “Cue type” is set to 1, otherwise 0. If the cue is on the right side to the other, the variable “Side” is set to 1, otherwise 0. To achieve a high resolution capable to distinguish the ratio of the left to the right from the ratio of the right to the left, or the ratio of the stair to the other from the ratio of the other to the stair, the number of levels in the scene generation (Table 1) is doubled. Scene No. 39 is taken as an example in Table 4.

With these rows, the parameters of the evacuees’ preference function can be estimated by the Multinomial Logistic Regression module in SPSS.

4 Experiment

The CAVE-based virtual drill was executed in October 1–7, 2007 at College of Architecture and Urban Planning, Tongji University. The first group of subjects are 96 undergraduate students from grade 1 to 4. They did the drill for scene sets of Doorway–Doorway, Stair–Stair and Stair–Doorway. The second group of subjects are 91 undergraduate students from grade 1 to 4. They did the drill for scene sets of Exit–Exit, Stair–Exit and one extra scene of Doorway–Doorway. One subject’s record of a Stair–Exit scene missed.

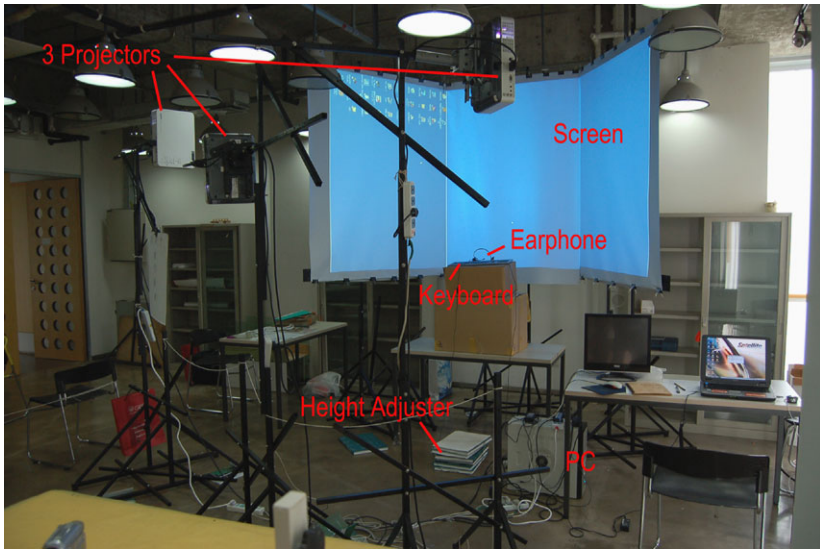


Fig. 5. The CAVE for the experiment.

4.1 The Experiment Facilities

A special CAVE system is designed and built for this experiment, which provides all the observers a same observing height by the “height adjuster” and a wide view field (180 degree in horizontal and 70 degree in vertical). Such a special design moves the eyes of the observer to 1.75 m above the ground and enables them to see an object 7.5 m above the ground at a distance of 5 m (Fig. 5).

To impose some stress on the subjects, they are asked to complete the evacuation choices as soon as possible for a higher score. Moreover they hear a noisy alarming sound during the experiment. And they can notice a counting down timer in the view. All these strategies make the subjects strained through the experiment.

To avoid the operational preferences of the mouse or the arrow keys by one hand, the subjects are asked to use the both hands, the left one on key Z to run toward the left side and the right hand on key M to run toward the right side.

The evacuating choices of all the subjects are composed of the side of choice, the cue type and the geometric features at every key stroke, which is recorded by a Visual Basic program.

4.2 The Experiment Procedure

Every subject is asked to hear a recorded direction first, in which they are told that they are staying in a set of underground spaces. There is an alarming



Fig. 6. A subject is making choice between two stairs.

sound urging all the persons to evacuate as soon as possible for some emergent situation. Most persons have evacuated successfully. He is the only person in this space. He or she can press Key Z to run toward the left architectural cue in the scene or Key M toward the right to evacuate to the most likely safe direction by their instinct. All the scenes that they explore are separated and not related to each other in space.

Then the experiment assistant tunes up the height adjustor to set the observer's eyes on a proper height. After he practices choosing between the left and right cues in the virtual environment, the virtual evacuation choice sampling starts. The subjects can notice a counting down timer on the screen during their decision making. And they are told that the time of the choices is used for scoring. With such a kind of pressure all the choices of the scenes are recorded for further estimation (Fig. 6).

To keep the subjects fresh in mind, the time period of the experiment for one subject is designed within 10 minutes. The average time of the first group on the 49 scenes of Doorway–Doorway, the 49 scenes of Stair–Stair and the 81 scenes of Stair–Doorway is about 6 minutes. The average time of the second group on the 49 scenes of Exit–Exit and the 81 scenes of Stair–Exit is about half and 4 minutes.

5 Analyzes

After the experiment, the subjects' choices on the five kinds of cue pairs were collected. They are 4795 choices on Doorway–Doorway, 4704 choices on Stair–Stair, 4459 choices on Exit–Exit, 7776 choices on Stair–Doorway, and 7370 choices on Stair–Exit.

5.1 The Model Performance

The five sets of parameters of (1) were estimated from the corresponding choices by Multinomial Logistic Regression module in SPSS. The five sets of parameters are ranked from low to high by the McFadden R square and the overall predicted correction percentage, which indicates the good-of-fitness and the prediction performance of the model (Table 5).

It is obvious that to make choice between Stair and Doorway is much easier and with more confidence than to make choice between two Doorways for an evacuee in the underground. Thus, the performance disparity between the five kinds of cue pairs corresponds to the uncertainty of the choice itself naturally.

5.2 The Attributes of Architectural Cues

In Figs. 7–11 the estimated parameters also indicate the relationship between the weight and the ratio. To illustrate the symmetry of the ratio, it is pre-processed by a logarithm function. The trend of these curves indicates that reducing Distance, or increasing Width, or increasing Height can all raise the preference of a cue being chosen. In contrast, increasing Distance, or reducing Width, or reducing Height can make the preference to decline.

Cue pair type	McFadden R square	Overall predicted correction percentage
Doorway–Doorway	0.105	65.1%
Stair–Exit	0.149	69.2%
Stair–Stair	0.209	71.8%
Exit–Exit	0.220	73.5%
Stair–Doorway	0.314	79.7%

Table 5. The performance of the model.

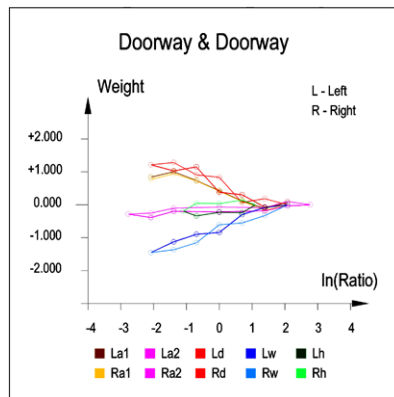


Fig. 7. Curves of Doorway–Doorway.

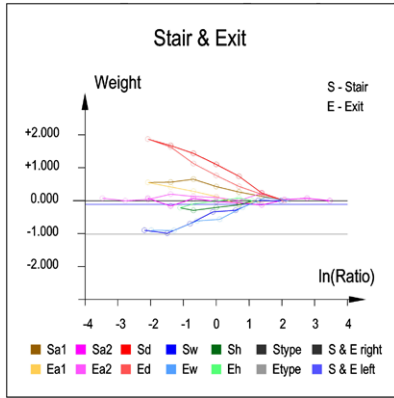


Fig. 8. Curves of Stair-Exit.

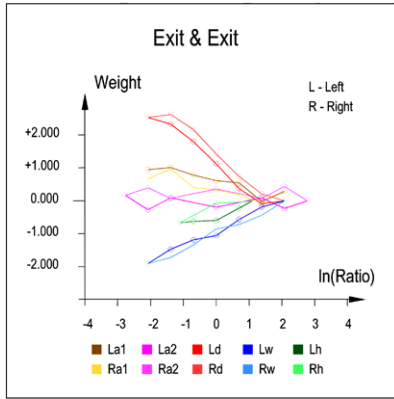


Fig. 9. Curves of Stair-Stair.

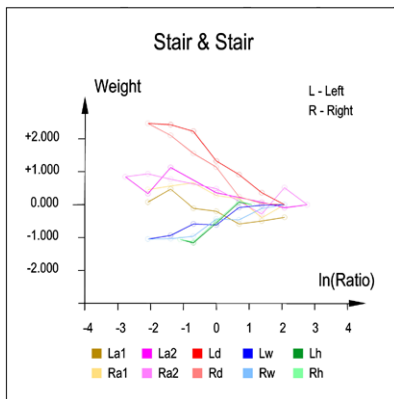


Fig. 10. Curves of Exit-Exit.

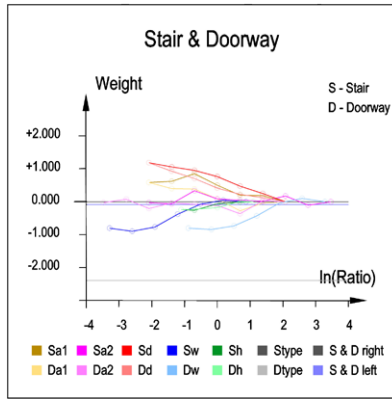


Fig. 11. Curves of Stair–Doorway.

Cue pair type	Ability to influence the preference (range of B value from (1))
Doorway–Doorway	Width > Distance > Height (1.449 > 1.352 > 0.474)
Stair–Exit	Distance > Width ≈ Cue type > Height (1.875 > 1.08 ≈ 1.009 > 0.373)
Stair–Stair	Distance > Height > Width (2.473 > 1.267 > 1.043)
Exit–Exit	Distance > Width > Height (2.713 > 1.909 > 0.663)
Stair–Doorway	Cue type > Distance > Width > Height 2.392 > 1.184 > 0.997 > 0.271

Table 6. The variable utility on the preference.

From these curves it is also clear that the variable Distance usually has a larger weight value range than the other variables, except for the variable Width in Doorway–Doorway pair. Such an observation may be an ostensible evidence to support the assumption used by some evacuation models that the evacuees always run to the closest exit or staircase. However, it is indeed all the variables that influence the preference of the cue being chosen in concert.

The variable utility on the preference is different for sure according to the weight value range of each variable. From the view of an architect, some variables can be configured in the design process such as the variable Cue type, D, W and H. The others are varying dynamically according to the evacuee’s orientation such as the variable A1, A2 and LR, which are out of their control. Then the variable Cue type, D, W and H are observed for their utilities on the preference. The abilities of the variable to influence the cue choice are indicated in Table 6, which is related to the weight value ranges.

5.3 Preference Between Stair and Exit

There is an obvious and interesting evidence indicating subjects have a propensity to choose a stair rather than an exit sometimes. The weight value range of variable type is 1.009, which can have a great impact on the over all preference function comparing to the weight value ranges of the other variables (D: 1.875, W: 1.08, H: 0.373). With several interviews after the experiment, the authors realized that the preference between Stair and Exit is greatly affects by the tons of reports about the death caused by the blocked exits on TV and Radio in Shanghai. So the local social background does have an impact on the evacuees' preference.

6 Conclusions

The measured evacuees' preference function on architectural cues can predict their choices at different levels of correction according to the ease or difficulty of the choice itself. Ranked from the highest correction choice pair to the lowest they are: Stair–Doorway, Exit–Exit, Stair–Exit, Stair–Stair, Doorway–Doorway. This result is very natural when we recall how easy we making choice between Stair and Doorway, and how difficult we searching a way out in a labyrinth only with doorways.

The preference function indicates that all the attributes effect the choice on the architectural cues, not only distance but also width, height and the directions. Consequently the assumption that evacuees always go to the exit with shortest distance is incorrect. The other variables should be also considered simultaneously. For example, it might be possible that a further doorway but much wider is more attractive than a closer one but much narrower, which was also observed in a previous experiment [17]. However, the impact of the variable on the preference is different indicated by its weight value range. The Distance is the most powerful attribute in the four kinds of cue pairs, except for Doorway–Doorway pair, in which the Width is the most powerful one and it is always a competitor to Distance in the other cue pairs. Moreover, Height becomes the second powerful attribute in Stair–Stair pair naturally.

The preference to Stair rather than Exit indicates the local social effect on searching the route to exit. This observation is an evidence for the argument of social effect on human behavior in built environment [18].

7 Outlook

The next step in this research project is to validate the architectural cue model supported by this preference function. Finally the model will be integrated into a CAD system to support architects in evaluating their underground designs and enhance the other compositive evacuation models.

References

1. J.S. Tubbs and B.J. Meancham. *Egress Design Solutions: A Guide to Evacuation and Crowd Management Planning*. New York, 2007. Wiley.
2. P. Arthur and P. Passini. *1-2-3 Evaluation and Design Guide to Wayfinding*. Ottawa, 1990. Architectural and Engineering Services.
3. R. Passini. *Wayfinding in Architecture*. New York, 1984. Van Nostrand-Reinhold.
4. D. Helbing, I. Farkas, and T. Vicsek. Simulating dynamical features of escape panic. *Nature* 407 (2000), 487–490.
5. Y. Murakami, K. Minami, T. Kawasoe, and T. Ishida. Multi-Agent Simulation for Crisis Management. Paper presented at the Proceedings of the IEEE Workshop on Knowledge Media Networking (KMN 02), 2002.
6. J. Was, B. Gudowski, and P.J. Matuszyk. Social Distances Model of Pedestrian Dynamics. Paper presented at the ACRI, 2006.
7. A. Schadschneider. Cellular Automaton Approach to Pedestrian Dynamics—Theory. Paper presented at the Pedestrian and Evacuation Dynamics, Duisburg, 2001.
8. S. Hostikka, T. Korhonen, T. Paloposki, T. Rinne, K. Matikainen, and S. Heliovaara. Development and Validation of FDS+Evac for Evacuation Simulations: Project Summary Report (Research Notes 2421). Helsinki, 2007. Julkaisija-Utgivare.
9. E.D. Kuligowski and R.D. Peacock. A Review of Building Evacuation Models (Technical Note No. 1471). Gaithersburg, 2005. National Institute of Standards and Technology.
10. X. Pan. Computational Modeling of Human and Social Behaviors for Emergency Egress Analysis. Unpublished Doctor of Philosophy, Stanford University, 2006.
11. P. Arthur and R. Passini. *Wayfinding: People, Signs, and Architecture*. New York, 1992. McGraw-Hill.
12. C. Sun and B. de Vries. An architecture-based model for underground space evacuation, in W. Borutzky, A. Orsoni, and R. Zobel (eds), *Proceedings of the 20th European Conference on Modelling and Simulation ECMS 2006*. Bonn, 2006. ECMS, pp. 578–583.
13. P.H.L. Bovy and E. Stern. *Route Choice: Wayfinding in Transport Networks*. London, 1990. Kluwer Academic.
14. A.A.W. Tan. The Reliability and Validity of Interactive Virtual Reality Computer Experiments. Unpublished Doctor of Philosophy, Technische Universiteit Eindhoven, Eindhoven, 2003.
15. A. Friedman. *Frames of Reference and Direct Manipulation Based Navigation*. Delft, 2005. Technische Universiteit Delft.
16. J. Dijkstra, H.J.P. Timmermans, and W.A.H. Roelen. *Conjoint Analysis and Virtual Reality (No. 1999/1)*. Eindhoven, 1999. Eindhoven University of Technology.
17. C. Sun, B. de Vries, and J. Dijkstra. Measuring Human Behavior Using Head-Cave, in *Computer Aided Architectural Design Futures—Proceedings of the 12th International Conference on Computer Aided Architectural Design Futures, Sydney (Australia)*. Dordrecht, 2007. Springer, pp. 501–511.
18. E.T. Hall. *The Hidden Dimension*. Garden City, New York, 1966. Doubleday.

Integrating Strategies in Numerical Modelling of Crowd Motion

Juliette Venel

Laboratoire de Mathématiques, Université Paris-Sud XI, 15 rue Georges Clémenceau, 91405 Orsay Cedex, France
e-mail: juliette.venel@math.u-psud.fr

Summary. We propose here to integrate sophisticated strategies in the model of crowd motion presented by Maury and Venel (Proceedings of Traffic and Granular Flow 2007, Springer, 2009). This model is based on two different velocities: a spontaneous (or desired) velocity and an actual velocity taking congestion into account. In this paper, we propose several strategies to define the spontaneous velocity: follow the shortest path, adapt its own velocity to the one of his neighbors, or avoid jams. Finally, we present numerical results.

1 Introduction

Since designers are interested in the pedestrians' safety in their buildings, planes or ships, simulations of pedestrian traffic flow in an emergency case are frequently requested. Such situations are often characterized by high densities and many contacts.

The cellular automata models [1–3] as well as queuing models [4, 5] are usually employed to simulate emergency situations because they are computationally efficient. Other models that don't handle intrinsically the contacts have been proposed (see for example the social force model [6, 7]).

In this paper, we use the model proposed in [8], allowing collisions and taking into account simultaneously all the contacts during a time interval (see Sect. 2). We focus here on the fact that people can have different strategies to reach the exit. We propose a way to integrate these strategies in the model. We describe three choices in Sect. 3: follow the shortest path, adapt its own velocity to the one of his neighbors, or avoid jams. We present numerical results in Sect. 4.

2 From Spontaneous to Actual Velocity

We briefly describe the model proposed in [8], where the reader will find the mathematical framework and the associated numerical scheme.

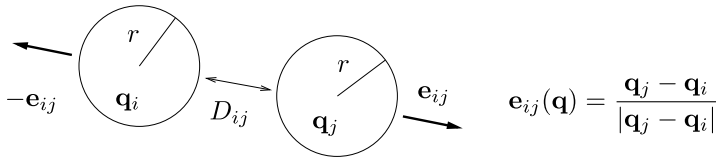


Fig. 1. Notations.

2.1 Notations

We consider N persons identified with rigid disks. For the sake of simplicity, the disks are supposed to have the same radius r . The centre of the i th disk is denoted by \mathbf{q}_i . As overlapping is strictly forbidden, the vector of positions $\mathbf{q} = (\mathbf{q}_1, \dots, \mathbf{q}_N) \in \mathbb{R}^{2N}$ must belong to the set of feasible configurations:

$$Q_0 = \{ \mathbf{q} \in \mathbb{R}^{2N}, \forall i, j : i \neq j, D_{ij}(\mathbf{q}) = |\mathbf{q}_i - \mathbf{q}_j| - 2r \geq 0 \}.$$

The spontaneous velocity of the N persons will be written as

$$\mathbf{U}(\mathbf{q}) = (\mathbf{U}_1(\mathbf{q}), \dots, \mathbf{U}_N(\mathbf{q})) \in \mathbb{R}^{2N},$$

where \mathbf{U}_i represents the velocity person i would like to have if he were alone.

In Sect. 3, different choices will be proposed. Let us now proceed with the description of the actual velocity.

2.2 Handling of Contacts

Owing to the non-overlapping constraint, most of the people can't move with their spontaneous velocity. In fact, the distance between two persons in contact can only increase. That's why the set of feasible velocities is introduced:

$$\begin{aligned} \mathcal{C}_{\mathbf{q}} &= \{ \mathbf{v} \in \mathbb{R}^{2N}, \forall i < j, D_{ij}(\mathbf{q}) = 0 \Rightarrow \mathbf{G}_{ij}(\mathbf{q}) \cdot \mathbf{v} \geq 0 \}, \quad \text{with} \\ \mathbf{G}_{ij}(\mathbf{q}) &= \nabla D_{ij}(\mathbf{q}) = (0, \dots, 0, -\mathbf{e}_{ij}, 0, \dots, 0, \mathbf{e}_{ij}, 0, \dots, 0) \in \mathbb{R}^{2N}. \end{aligned}$$

The actual velocity field is the feasible field which is the closest to \mathbf{U} for the Euclidean distance, which writes

$$\frac{d\mathbf{q}}{dt} = P_{\mathcal{C}_{\mathbf{q}}} \mathbf{U}(\mathbf{q}),$$

where $P_{\mathcal{C}_{\mathbf{q}}}$ denotes the euclidean projection onto the closed convex cone $\mathcal{C}_{\mathbf{q}}$.

3 Examples of Spontaneous Velocity

3.1 Shortest Path

We consider here the simplest choice for the spontaneous velocity. All the individuals have the same behavior: they want to reach the exit by following the shortest path. Then, the spontaneous velocity's expression can be specified:

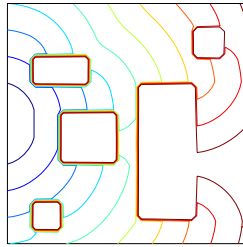


Fig. 2. Contour levels of the geodesic distance \mathcal{D} to the exit situated to the left.

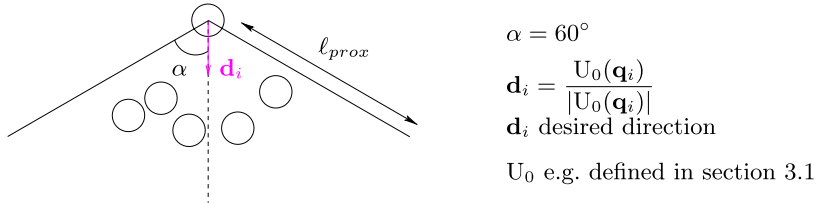


Fig. 3. Illustration of the set N_i .

$$\mathbf{U}(\mathbf{q}) = (\mathbf{U}_0(\mathbf{q}_1), \dots, \mathbf{U}_0(\mathbf{q}_N)) \quad \text{with } \mathbf{U}_0(\mathbf{x}) = -s \nabla \mathcal{D}(\mathbf{x}),$$

where $\mathcal{D}(\mathbf{x})$ represents the geodesic distance between the position \mathbf{x} and an exit. Since $|\nabla \mathcal{D}(\mathbf{x})| = 1$ by definition, s is a nonnegative scalar that denotes the speed, i.e. the norm of the vector $\mathbf{U}_0(\mathbf{x})$. So this spontaneous velocity takes only the room’s geometry into account (see isovalues of \mathcal{D} in Fig. 2).

In order to compute \mathcal{D} , we have used the fast marching method introduced by Kimmel and Sethian in [9]. In this method, the value of \mathcal{D} is computed at each point of a grid. The value at the exit’s nodes is set to zero. Then, the values of the distance at the other points is computed step by step so that a discrete version of $|\nabla \mathcal{D}| = 1$ is satisfied. Moreover, the distance at the nodes situated in the obstacles is fixed to a large value, which prevents the shortest path from going across them.

3.2 Individual Strategies

We consider now that people can elaborate complex strategies to escape. For example, in case of congestion, they may decelerate or try to avoid the jam, instead of keeping pushing inefficiently. The velocity of one person becomes dependent upon the position of people he can see in front of him. More precisely, we define the set N_i (see Fig. 3) containing persons who are near and visible to the individual i :

$$N_i = \{j, |\mathbf{q}_i - \mathbf{q}_j| < 2r + \ell_{prox}, \mathbf{d}_i \cdot \mathbf{e}_{ij} \geq \cos \alpha\}.$$

Two choices are possible for the individual i if his neighbors (belonging to N_i) walk slower than him.

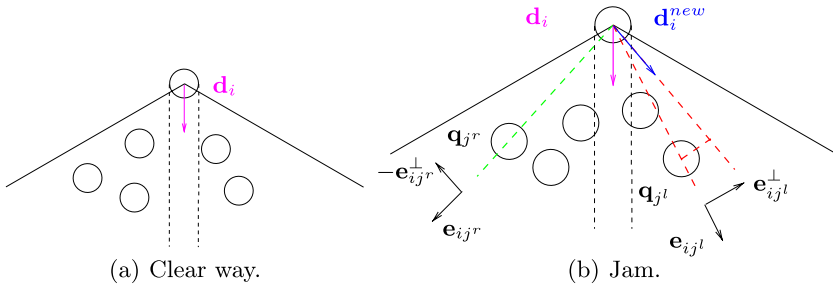


Fig. 4. Possibilities in a hurry.

1. He can decelerate instead of going through the crowd. In this case, his speed s_i^n (i.e. his velocity's norm) at time t^n is made dependant upon his neighbors' behavior at time t^{n-1} . More precisely, it is computed as a barycenter of his neighbors' speeds, weighted by their relative positions:

$$s_i^n = \frac{\sum_{j \in N_i} w_j s_j^{n-1}}{\sum_{j \in N_i} w_j} \quad \text{with}$$

$$w_j = w_j^\theta w_j^d, \quad w_j^\theta = \frac{\mathbf{d}_i \cdot \mathbf{e}_{ij} - \cos \alpha}{1 - \cos \alpha} \quad \text{and} \quad w_j^d = \frac{\ell_{\text{prox}} - D_{ij}}{\ell_{\text{prox}} - 2r}.$$

2. He can also be in a hurry and prefer changing his way instead of slowing down. In that case, if the way in front of individual i is free (see Fig. 4(a)), he will go straight ahead. If there exists another clear way through the set N_i , he follows it while keeping his desired speed, or else he will go round the group N_i . Among all directions allowing him to do so, he chooses $\mathbf{d}_i^{\text{new}}$ the closest to the one he wanted (see Fig. 4(b)).

$$\mathbf{d}_i^{\text{new}} = \frac{(D_{ij_0} + 2r)\mathbf{e}_{ij_0} \pm 2r\mathbf{e}_{ij_0}^\perp}{|(D_{ij_0} + 2r)\mathbf{e}_{ij_0} \pm 2r\mathbf{e}_{ij_0}^\perp|} \quad \text{with } j_0 = \text{argmax}(\mathbf{d}_i \cdot \mathbf{e}_{ij^l}, \mathbf{d}_i \cdot \mathbf{e}_{ij^r}),$$

where \mathbf{q}_{j^r} (\mathbf{q}_{j^l}) represents the extremal right (left) neighbor of individual i (see Fig. 4(b)).

4 Numerical Results

In this section, we want to illustrate the different models proposed for the spontaneous velocity. These results were obtained by integrating the previously described strategies in the numerical algorithm detailed in [8].

In order to understand the strategy of avoiding (see Sect. 3, case 2), we run a test with one person willing to exit a room where 1000 other people are still. In Fig. 5, we plot his trajectories in both cases: with and without strategy.

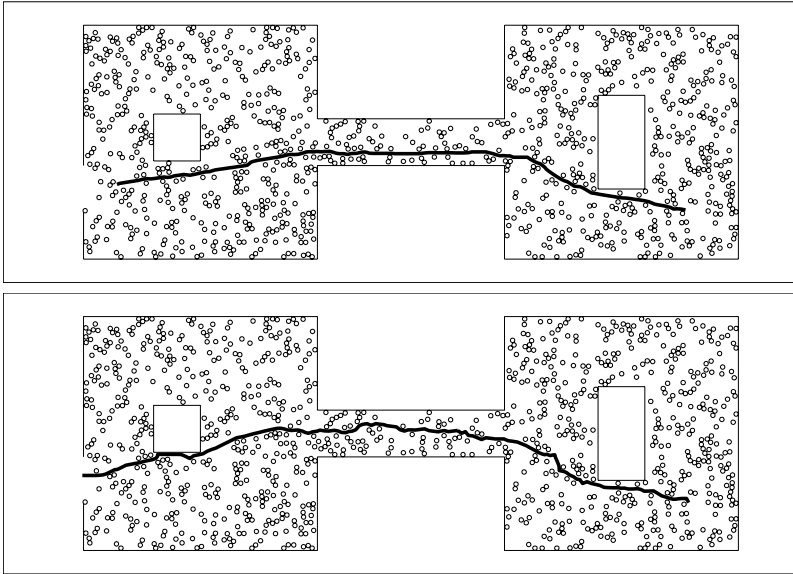


Fig. 5. Comparison of trajectories without (*top*) or with (*bottom*) the strategy of avoiding.

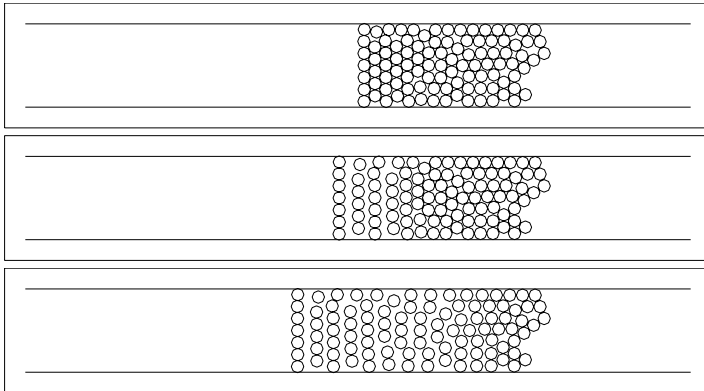


Fig. 6. Rarefaction wave.

We observe that with strategy he escapes faster even if he takes a longer way. That is due to the fact that without strategy he has to push people on his way which slows him down.

Now we illustrate the tendency to decelerate (see Sect. 3, case 1). For that purpose, we consider 100 people initially jammed who want to go to the left at $t = 0$. In Fig. 6, we plot different time steps and observe a rarefaction wave: the individuals begin to move one after the other.

Acknowledgements

The author would like to thank Prof. B. Maury for helpful suggestions and numerous discussions about this subject. The author is also grateful to A. Lefebvre for valuable comments.

References

1. D. Helbing, M. Isobe, T. Nagatani, and K. Takimoto. Lattice gas simulation of experimentally studied evacuation dynamics. *Phys. Rev. E*, 67:067101, 2003.
2. A. Kirchner and A. Schadschneider. Simulation of evacuation processes using a bionics-inspired cellular automaton model for pedestrians dynamics. *Physica A*, 312:260–276, 2002.
3. T. Meyer-König, H. Klüpfel, and M. Schreckenberg. Assessment and analysis of evacuation processes on passenger ships by microscopic simulation. In M. Schreckenberg and S.D. Sharma, editors, *Pedestrian and Evacuation Dynamics*, Springer, Berlin, 2002.
4. G.G. Løvås. Modelling and simulation of pedestrian traffic flow. *Transp. Res. B*, 28:429–443, 1994.
5. S.J. Yuhaski and J.M. Macgregor Smith. Modelling circulation systems in buildings using state dependent queueing models. *Queueing Syst.*, 4:319–338, 1989.
6. D. Helbing and P. Molnár. Social force model for pedestrians dynamics. *Phys. Rev. E*, 51:4282–4286, 1995.
7. D. Helbing, I.J. Farkas, and T. Vicsek. Simulating dynamical features of escape panic. *Nature*, 407:487, 2000.
8. B. Maury and J. Venel. Handling of contacts in crowd motion simulations. In *Traffic and Granular Flow 2007*, Springer, Berlin, 2009.
9. R. Kimmel and J. Sethian. Fast marching methods for computing distance maps and shortest paths. Technical Report 669, CPAM, Univ. of California, Berkeley, 1996.

Small-Grid Analysis of Evacuation Processes with a Lattice Gas Model for Mixed Pedestrian Dynamics

Yan-fang Wei^{1,3}, Yu Xue^{2,1}, and Shi-qiang Dai¹

¹ Shanghai Institute of Applied Mathematics and Mechanics, Shanghai University, Shanghai 200072, China

e-mail: yanfangwei2007@hotmail.com, sqdai@shu.edu.cn

² Institute of Physical Science and Engineering, Guangxi University, Nanning 530004, China

³ Department of Physics and Information Science, Yulin Normal University, Yulin 537000, China

Summary. Pedestrian flow out of a hall is investigated by using a small-grid lattice gas (LG) model with different maximum velocities. Some dynamical characteristics of the transition from choking flow to decaying flow are found. In the choking-flow region, the flow rate increases with the increase of the fraction of faster pedestrians and the door width. The evacuation time decreases with increasing fraction of faster pedestrians and door width. In addition, the dependence of the average velocity on the mixture fraction and door width is discussed. Finally, the relationship of evacuation time with mixture fraction and door width are obtained.

1 Introduction

The understanding of the dynamical features of pedestrian and evacuation dynamics has been the aim of many investigations over the last few years [1–6]. Three kinds of methods are usually used to study the pedestrian flows. The first is to set up macroscopic equations of pedestrian flows based on the theory of hydrodynamics [7–9]. With this kind of methods, macroscopic characteristics of pedestrian flows are successfully elucidated, but it cannot explain the self-organization behavior of the pedestrian flows. The second is to set up microscopic equations of pedestrian flows based on the characteristics of the pedestrian’s movements [1, 2, 10]. With this kind of methods, the self-organization behaviors can be successfully described, but they are difficult to generalize and the equations are too complex to be solved. The third is to construct a model based on “rules” on a set of lattice sites, and simulate the evolution of pedestrian flows by computer [11–19]. By establishing sets of simple rules, the movements of pedestrians under different circumstances can be

realistically simulated. The self-organization behaviors and critical phenomena can also be reproduced with this approach. Since the models can easily be simulated and generalized, this method is widely used in the studies on the pedestrian flows.

The main models of the third method are cellular automata and lattice gas (LG) models. By applying the classic LG model, Tajima and Nagatani [11] found that a dynamical phase transition occurs from the choking flow to the decaying flow at a critical phase transition time and obtained a power-law relation between the crowd flow rate, the transition time and the width of door. Fukamachi et al. [16] studied the LG model which consists of two types of walkers with different biases (drift coefficients) and found that the mean velocity of slow particles in the binary mixture is enhanced higher than that in lattice-gas consisting of only slow particles. Jiang and Wu [17] extended the LG model to larger maximum velocity $v_{\max} > 1$ and studied the counter flow of mixed pedestrians with different velocities.

However, coarse grid partition was used in the traditional lattice gas models which leads to the collective phenomena, such as the arching and clogging behavior, etc., could not be reproduced well. So a fine grid partition lattice gas model is proposed in [18, 19]. Here we employ the small-grid LG model to study the evacuation process with different speeds from a hall with only one door via numerical simulation. The next section describes simulation and results, followed by the conclusions.

2 Simulation and Results

In our simulation, the usual occupied space of a walker, say, a square of $40 \times 40 \text{ cm}^2$ is divided into smaller grids of $10 \times 10 \text{ cm}^2$ and a walker can move one or many small grids (1–4 grids) at a time step. The scenario of simulation is some pedestrians attempting to leave a one-door square room. There are two kinds of pedestrians: the faster ones, who have the maximum velocity of 6 small grids at a time step, and the slower ones, who have the maximum velocity of 3 small grids at a time step. The room size is $20 \times 20 \text{ m}^2$ and the exit door size is W . Initially, pedestrians are distributed randomly in the room. In simulation, sequential update is chosen. At each time step, the walkers are numbered randomly from 1 to N , where N is the total number of walkers in the hall, and then each walker is updated once in the sequential order from 1 to N . After all the walkers are updated, if the walkers go out of the system, they are removed from the system. After the above procedure has been carried out, one time step is completed. The above procedure is repeated.

We present the simulation results obtained from the above procedure, in which the occupation probability and the drift are set as 0.3 and 0.5, respectively. We use R to denote the fraction of faster pedestrians. The process of evacuation is simulated 500 times by computer.

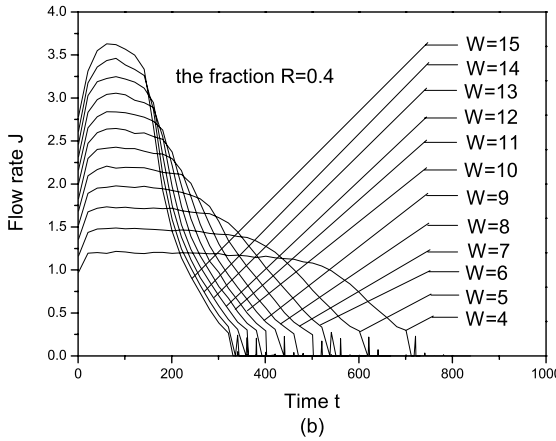
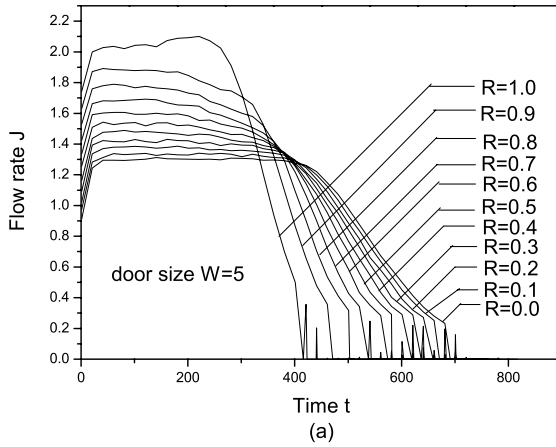


Fig. 1. Curves of flow rate against time for **a** door size $W = 5$ and **b** the fraction $R = 0.4$.

Figure 1 gives the relationship between flow rate and time. The flow rate is averaged over 20 time steps for 500 samples. At the beginning, the flow rate increases linearly, which means the pedestrians move out of the exit without clogging. After some time, it reaches its maximum and remains constant over a long period. Because more and more pedestrians move toward the door, the pedestrians are clogged in front of the door and can not move out of the exit. When most pedestrians have left the room, the flow rate decreases quickly. Figure 1(a) indicates that the flow rate increases with increasing fraction of faster pedestrians for a door size of 5 coarse grids. Because faster pedestrians can leave the room more quickly, the flow rate is enhanced and the evacuation time is reduced. From Fig. 1(b), it is obvious that the flow rate increases when the door size changes from 4 to 15 coarse grids with $R = 0.4$. The pedestrians

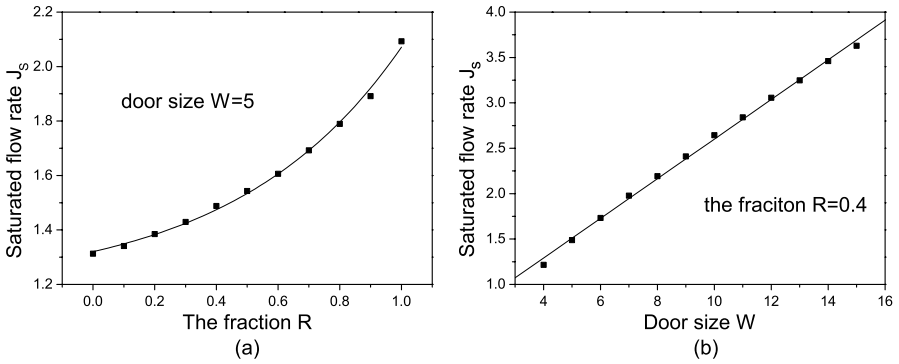


Fig. 2. Saturated flow rate against fraction and door size for **a** door size $W = 5$ and **b** fraction $R = 0.4$. The *solid lines* are fitting results.

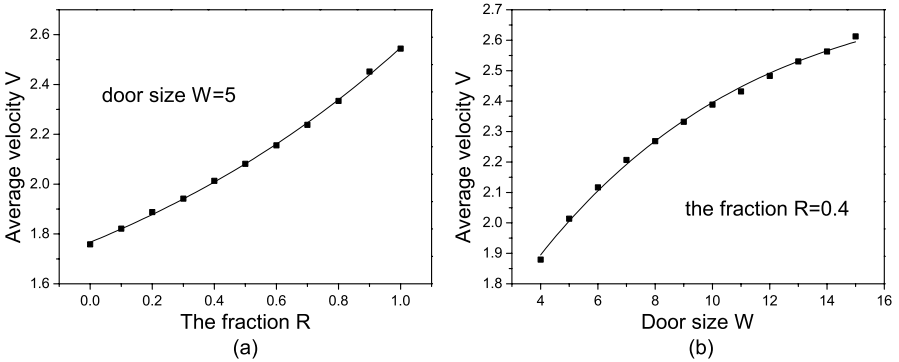


Fig. 3. Average velocity against fraction and door size for **a** door size $W = 5$ and **b** fraction $R = 0.4$. The *solid lines* are fitting results.

move out of the exit smoothly when the door is larger and that is the reason of the enhancement of flow rate and the reduction of evacuation time.

Figure 2 shows the saturated flow rate J_s for different values of the fraction R and the door size W . For fixed door size i the saturated flow rate increases exponentially with the fraction of the faster pedestrians. The relationship is given as $J_s \sim \exp(R/0.54)$. The saturated flow rate increases linearly as the door size is increased for $R = 0.4$. One can obtain the relationship of $J_s \sim (0.22 \pm 0.003)W$.

Figure 3 shows the curves of average velocity against the fraction of the faster pedestrians and the door size. The average velocity increases exponentially with the increase of the fraction of the faster pedestrians and the door size. When the door size is 5 coarse grids, the relationship between average velocity and the fraction is $V \sim \exp(R/1.28)$.

Figure 4 shows the evacuation time as function of the fraction of faster pedestrians and door size. For fixed door size the evacuation time decreases

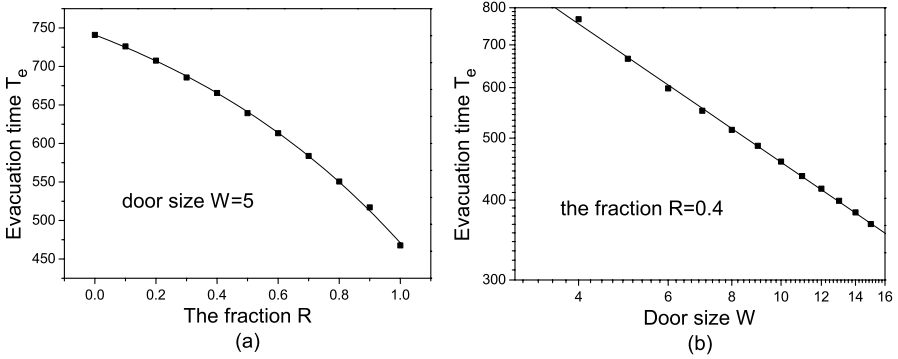


Fig. 4. Evacuation time against fraction and door size for **a** door size $W = 5$ and **b** fraction $R = 0.4$. The *solid lines* are fitting results.

exponentially with the increase of the faster pedestrians because faster pedestrians can leave the room more quickly than the slower pedestrians. For fixed fraction of faster pedestrians one finds that the evacuation time T_e scales as

$$T_e \propto W^{-0.54 \pm 0.005}.$$

3 Conclusions

We have investigated the dynamical behavior of pedestrians escaping out of a hall via a small-grid LG model with different maximum velocities of pedestrians. In the choking-flow region, the flow rate J increases with increasing fraction of faster pedestrians as the door width is fixed. As the fraction of faster pedestrians is kept unchanged, the flow rate J also increases with the increase of the door width. The saturated flow rate J_s increases exponentially with the increase of the fraction of faster pedestrians and increases linearly with the increase of the door width. The average velocity V increases exponentially as the fraction of faster pedestrians and the door width increase. The escape time decreases exponentially with the increase of the faster pedestrians for fixed door width. For fixed fraction of faster pedestrians is fixed, the evacuation time T_e scales as $T_e \propto W^{-0.54 \pm 0.005}$.

Acknowledgements

This work was supported by the National Basic Research Program of China (Grant No. 2006CB705500), the National Natural Science Foundation of China (Grant Nos. 10532060, 10662002 and 10762005) and the Shanghai Leading Academic Discipline Project (Grant No. Y0103).

References

1. D. Helbing. *Phys. Rev. E*, 51:4282, 1995.
2. D. Helbing, I. J. Farkas, and T. Vicsek. *Nature*, 407:487, 2000.
3. D. Helbing. *Rev. Mod. Phys.*, 73:1067, 2001.
4. T. Nagatani. *Rep. Prog. Phys.*, 65:1331, 2002.
5. M. Schreckenberg and S. D. Sharma, editors. *Pedestrian and Evacuation Dynamics*. Springer, Berlin, 2001.
6. S. P. Hoogendoorn and P. H. L. Bovy. Normative pedestrian behavior theory and modeling. In M. A. P. Taylor, editor, *Transportation and Traffic Theory in the 21st Century*, pp. 219–245. Pergamon, Elmsford, NY, 2002.
7. L. F. Henderson. *Nature*, 229:381, 1971.
8. L. F. Henderson. *Nature*, 240:353, 1972.
9. L. F. Henderson. *Transpn. Res.*, 8:509, 1974.
10. W. J. Yu, R. Chen, L. Y. Dong, and S. Q. Dai. *Phys. Rev. E*, 72:026112, 2005.
11. Y. Tajima and T. Nagatani. *Physica A*, 292:545, 2001.
12. T. Itoh and T. Nagatani. *Physica A*, 313:695, 2002.
13. A. Kirchner and A. Schadschneider. *Physica A*, 312:260, 2002.
14. C. Burstedde, K. Klauck, A. Schadschneider, and J. Zittartz. *Physica A*, 295:507, 2001.
15. V. J. Blue and J. L. Adler. Modelling four directional pedestrian movements. In *Proceedings of 79th Transportation Research Board*, Washington, DC, 2000.
16. M. Fukamachi, R. Kuwajima, Y. Imanishi, and T. Nagatani. *Physica A*, 383:424, 2007.
17. R. Jiang and Q. S. Wu. *Physica A*, 373:683, 2007.
18. W. G. Song, X. Xu, B. H. Wang, and S. J. Ni. *Physica A*, 363:492, 2006.
19. W. G. Weng, L. L. Pan, S. F. Shen, and H. Y. Yuan. *Physica A*, 374:821, 2007.

Evacuation Simulation and Human Behaviour Models in Tall Buildings

Marja-Liisa Siikonen and Janne S. Sorsa

KONE Elevators Ltd., Keilasatama 3, Espoo, Finland
e-mail: marja-liisa.siikonen@kone.com, janne.sorsa@kone.com

Summary. In tall buildings, staircases are usually the only means for evacuation. It can take more than two hours for an occupant to reach a refuge floor by the stairs owing to congestion and long travel distance. In a non-fire situation, elevators also could be used in evacuation. Where there are several alternative transport devices available for egress, occupants need to decide which one to use. This decision is based on the occupant's knowledge of the egress routes in the building. Evacuation models consider human behaviour mostly for horizontal movement and low buildings, without considering elevators as a means of egress. In this article, we describe vertical transportation and agent-based human behaviour models of the Building Traffic Simulator. The evacuation of the World Trade Centre is simulated and the results are compared with published data.

1 Introduction

According to current practise, staircases are the only way out of a building during emergency evacuation. Typically, there are two or three stairwells running through a tall building with more than 30 floors. The number of staircases correlates to the occupancy of only one floor, but not to the total population or the number of floors in the building. Elevators for office buildings are planned according to a criterion that the building can be filled in less than 40 minutes and emptied in less than 30 minutes. In contrast, the evacuation of a tall office building can last hours if using only staircases. Using both staircases and elevators for evacuation is the fastest way to empty the building [1].

In addition to the normal passenger elevators, there can be service and goods elevators, firefighters' elevators and dedicated elevators, e.g., for bed transportation. Passenger elevators are gathered in elevator groups, typically consisting of 4 to 8 elevators, to improve efficiency. During emergency, only firefighters' elevators are available for firemen to bring up their equipment while passenger elevators are taken out of service. If the building is not damaged normal passenger elevators could be used for evacuation.

In 1986, the Advanced Lift Traffic Simulator, ALTS, was developed for testing elevator group control systems [2]. ALTS was capable of simulating only one elevator group at a time. Later on, ALTS was taken into elevator planning use after implementation of building parameters. At the end of the 1990s, a successor to ALTS, the Building Traffic Simulator, BTS, was designed [3]. BTS is capable of simulating multiple elevator groups, escalators, autowalks and staircases simultaneously. Choosing the best one among multiple transportation devices requires the development of passenger behaviour models [4].

2 Building Traffic Simulator

2.1 Passenger Model

The passenger arrival process in buildings follows a Poisson distribution [5]. In BTS, the arrival process is defined by the arrival rate and components of vertical traffic for time intervals of any length. The traffic components are incoming traffic to the building, outgoing traffic as in evacuation, and inter-floor traffic. During a day, portions of the components as well as the arrival rate vary. In BTS, measured and published traffic profiles can be used for hotels, offices, and residential buildings.

For a building with multiple tenants, each tenant can have their individual traffic profiles. In addition, each tenant is divided into passenger groups such as adults, children, elderly people, disabled people and persons with baby carriages or shopping trolleys [4]. The passenger groups have their own physical characteristics such as horizontal movement speed, descending speed in stairs, physical space occupation, and transfer times through the elevator doors, see Table 1. They also have behavioural characteristics to determine which transportation device they prefer under the prevailing circumstances [6].

2.2 Staircase Model

In BTS, people descending in staircases are simulated using the flow model [8]. Passengers enter the staircases on each floor in the beginning of an emergency. In the case of congestion in the stairs, full flow with a descending speed of

Passenger group	Portion of tenant (%)	Space occupation (persons)	Movement speed (m/s)	Descending speed (free flow) (m/s)	Transfer time (s)
Adult	80	1	1.2	0.9	1
Elderly people	19	1	0.6	0.4	2
Wheelchair	1	4	0.4	N/A	4

Table 1. Typical characteristics of passenger groups [7] in BTS.

0.6 m/s and density of two persons per square meter [9] is assumed and occupants already in the stairwell block others from entering on intermediate floors. If the flow is less than full flow, also other occupants are allowed to enter in the stairwell.

2.3 Elevator Model

The elevator parameters modelled in BTS are the number of elevators in the group, car capacity, door times, and kinematics. Speed ranges from 0.6 m/s up to 16 m/s depending on the building height. Nominal travel time $t = s/v$, where s is elevator travel and v is its nominal speed, is a rough measure for selecting the speed of an elevator. Nominal travel time should be about 30 seconds. In simulation, the speed of the elevator is determined at each moment from kinematics equations using nominal speed, acceleration and jerk of the elevator [2].

Door operation consists of opening, closing and photocell signal. Passengers can enter or exit the elevator if the doors are about 800 mm open. In offices, car capacities normally vary from 13 persons to 24 persons with a minimum of 1100 mm-wide doors. The door opening and closing times are about 1.5 and 3 seconds, respectively. The photocell delay after the last passenger transfer through the door opening before the doors start to close is about one second.

Passengers give the landing calls in the elevator lobbies. The elevator group control system dispatches the elevators to the active landing calls. In evacuation with elevators, the most efficient way to empty the floors is to use automatic down collective control without attendant. In full collective control, elevators pick people up in sequential order according to the travel direction of the elevator.

3 Human Behaviour Model for Vertical Movement

Passenger movement in the building is represented by an agent model. The model has a macroscopic level with information of all paths in the building, and a microscopic level with the passenger reacting to local conditions. Passengers decide their routes by taking into account both levels of information. The route decision is revised during the journey when new information becomes available, e.g., when entering a floor.

3.1 Macroscopic Routing Model

The locations of transportation devices in the building and connections between them are defined by a directed graph $G = (\mathcal{N}, \mathcal{A})$. Each transportation device has its own entry and exit node in the set \mathcal{N} . Agents start and end

their journey at special locations, entry and exit nodes of the building on each floor.

The set of arcs, \mathcal{A} , determines the paths the agents are able to use. Nodes are connected by arcs linking transport devices to the building entry and exit nodes. Each arc $(i, j) \in \mathcal{A}$ has a travel time a_{ij} associated with it. The travel time of a path (i_1, i_2, \dots, i_k) is the sum of the travel times of its arcs [10]

$$T(i_1, i_k) = \sum_{n=1}^{k-1} a_{i_n i_{n+1}}. \tag{1}$$

Agents decide the route they will start to follow from their current node $i \in \mathcal{N}$ to the destination node $k \in \mathcal{N}$, i.e., building exit node on the destination floor. Let nodes j_1, j_2, \dots, j_J represent the nodes adjacent to node i , i.e., \mathcal{A} contains all arcs $(i, j_1), (i, j_2), \dots, (i, j_J)$. From a set \mathcal{R} of all possible paths from i to k , a subset \mathcal{R}_a containing J shortest paths $(j_1, \dots, k), (j_2, \dots, k), \dots, (j_J, \dots, k)$ with respect to travel time T , is selected.

A probability $\Pr[X = r]$ is assigned for each path $r \in \mathcal{R}_a$, describing its preference with respect to other paths in \mathcal{R}_a . Behavioural reaction models, \mathcal{B} , are used to evaluate each path. $\Pr[X = r]$ is a combined probability of normalised reaction model probabilities $p_{b,r}$

$$\Pr[X = r] = \prod_{b \in \mathcal{B}} \left(p_{b,r} / \sum_{r \in \mathcal{R}_a} p_{b,r} \right)^{w_b}, \quad \forall r \in \mathcal{R}_a, \tag{2}$$

where w_b is the weight of reaction model $b \in \mathcal{B}$. The probabilities $\Pr[X = r]$ are normalised, and the final route decision of the agent is drawn from discrete probability distribution

$$f(r) = \Pr[X = r] / \sum_{r \in \mathcal{R}_a} \Pr[X = r], \quad \forall r \in \mathcal{R}_a. \tag{3}$$

3.2 Microscopic Reaction Models

In the following, some examples of the microscopic reaction models are introduced. The probabilities given by the reaction models transformed by a scale invariant power law using c as the exponent. Let us denote by i the current node, by j_r the node adjacent to i on route r , and by k the destination node of an agent.

Route cost. The routing network is initialised in the beginning of the simulation and is regarded as static knowledge. Agents are more likely to select a fast route than a slow one according to the cost of the shortest paths $r \in \mathcal{R}_a$

$$p_{b,r} = T(j_r, k)^{-c}, \quad r \in \mathcal{R}_a. \tag{4}$$

Queue length. Agents are assumed to see the queues in front of the transport devices that they can enter next. The probability of selecting a

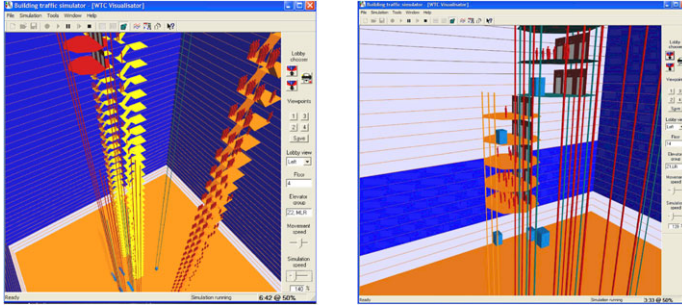


Fig. 1. BTS simulation with stairs (left) and elevators (right).

route $r \in \mathcal{R}_a$ with queue of length q_{j_r} in front of the first transport device, is

$$p_{b,r} = q_{j_r}^{-c}. \quad (5)$$

Transport type. The agent prefers to select the transport type with higher probability than other types. For example, elderly people may avoid stairs. The probability of selecting a particular transport type is

$$p_{b,r} = w_t^c, \quad r \in \mathcal{R}_a, \quad (6)$$

where $w_t \in [0, 1]$ is a weight of transport type t at node j_r .

4 World Trade Centre Evacuation

The evacuation of the World Trade Centre is simulated by BTS with normal adult occupants. The simulation results along with published data are summarised in Table 2. The location of stairwells and elevators as well as simulation scenarios were obtained from WTC report [11]. Occupants start to evacuate either immediately or with 0–10 minutes' delay. Scenarios 1–4 without damage to the building were simulated:

Simulator	Transport means	Evacuation delay (min)	Evacuation time (min)			
			Scenario 1	Scenario 2	Scenario 3	Scenario 4
EXODUS	Stairs	0–10	11	112	142	55
		No delay	4	110	141	52
BTS	Stairs	0–10	11	111	138	53
		No delay	4	109	137	51
	Stairs and shuttles	No delay	4	53	67	26
		Elevators	No delay	14	53	66

Table 2. Summary of WTC egress simulation results.

1. Phased evacuation of occupants from the emergency floor and floors above and below it travel three floors below the fire (600 persons)
2. Full capacity tower without visitors (19,800 persons)
3. Full capacity tower with visitors (25,500 persons)
4. September 11th capacity tower (8800 persons)

Transport means available for egress in simulation scenarios:

1. Staircases only
2. Descend to skylobbies by stairs, then express down with shuttle elevators
3. Elevators only

Evacuation times with BTS are nearly the same as with EXODUS [12] when only the stairs are used. If stairs and shuttle elevators are used, the evacuation takes about half of the time compared to stairs. Full evacuation with all elevators takes as long as with stairs and shuttle elevators. For phased evacuation of some floors only, stairs are still the fastest way to rescue level.

References

1. H. Hakonen, T. Susi, and M.-L. Siikonen. Evacuation of tall buildings. In F. Shafii et al., editors, *Proceedings of the CIB-CTBUH Conference on Tall Buildings*, pp. 219–226, Malaysia, 2003. CIB.
2. M.-L. Siikonen. Elevator traffic simulation. *Simulation*, 61(4):257–267, 1993.
3. R. Leinonen. Building traffic simulator. Master’s thesis, Helsinki University of Technology, Finland, 1999.
4. T. Susi, J. Sorsa, and M.-L. Siikonen. Passenger behavior in elevator simulation. *Elevatori*, 34(5):28–37, 2005.
5. N.A. Alexandris. Statistical models in lift systems. Ph.D. thesis, Victoria University of Manchester, UK, 1977.
6. J. Sorsa, H. Hakonen, T. Susi, and M.-L. Siikonen. Study of human factors in vertical evacuation. In *Proceedings of International Symposium on Elevator Evacuation During High-Rise Fires*, Shanghai, China, 2–3 November 2007.
7. R.F. Fahy and G. Proulx. Toward creating a database on delay times to start evacuation and walking speeds for use in evacuation modeling. Technical Report NRCC-44758, NRCC, 2001.
8. S.J. Melinek and S. Booth. An analysis of evacuation times and the movement of crowds in buildings. Building Research Establishment, FRS CP 96/75, 1975.
9. J. Pauls. Calculating evacuation times for tall buildings. *Fire Safety Journal*, 12(3):237–245, 1987.
10. D.P. Bertsekas. *Network Optimization: Continuous and Discrete Models*. Athena Scientific, Belmont, MA, 1998.
11. J.D. Averill et al. Occupant behavior, egress, and emergency communications. Technical Report NCSTAR 1-7, NIST, 2005.
12. E.R. Galea. Simulating evacuation and circulation in planes, trains, buildings and ships using the exodus software. In M. Schreckenberg and S.D. Sharma, editors, *Pedestrian and Evacuation Dynamics*, pp. 203–226. Springer, Berlin, 2002.

Proof of Evacuation Routes and Safety Exits: Time Data as the Main Criteria for the Evaluation of Escape Routes and Safety Exits?

Nathalie Waldau¹, Marita Kersken-Bradley², and Thilo Hoffmann²

¹ WALDAU Engineering, Hackhofergasse 5/11, 1190 Vienna, Austria
e-mail: office@ibw-wien.at

² Kersken + Kirchner GmbH, Consulting Engineers VBI, Pernerkrepe 11, 81925
Munich, Germany
e-mail: office@kk-fire.com

Summary. Building codes specify means of egress mainly in terms of requirements concerning the arrangement of means of egress, egress capacities and maximum travel distances, derived on an empirical basis. Alternative solutions are increasingly substantiated by egress simulations and resulting evacuation times. Indicative values for the appraisal of calculated times are available, however, they refer to flow times only and no systematic evaluation of evacuation times for means of egress complying with code requirements has yet been performed.

Within this project evacuation times are calculated for examples complying with German building code requirements. The intention was to investigate, whether current code specifications render reasonable results when they are translated into the time domain and whether specified evacuation times may be used as superior criteria for a performance based design of means of egress.

1 Settings

1.1 Evacuation Times

Only evacuation times are calculated. Evacuation time is considered to be the elapsed time from the beginning of the evacuation until the last person has left the room. Alarm and reaction times are not included. Statistically the mean average of multiple cases is calculated.

The population has the following characteristics:

- the walking speed: 0.80–1.60 m/s
- reaction time: 0 seconds

1.2 Investigated Study Cases

Examples studied herein mainly involve assembly halls, i.e. large indoor and outdoor spaces with high occupancy loads. Calculations are confined to the evacuation of the actual assembly seating.

The following facilities are examined (see Fig. 1):

1. facilities with standing rooms and variable arrangement of exits
2. facilities with seats arranged in rows
3. facilities with chairs arranged around tables

All rooms are considered high-occupancy.

Exit widths are in accordance with MVStättV guide lines:

- 100 persons per 0.6 m indoor
- 300 persons per 0.6 m outdoor

The examples represent situations that frequently experience bottle necks at exits.

1.3 Simulation Models

Due to the basic differences in simulation methods for such microscopic models, three different programs were utilized: ASERI 3.3 and 4.0g, buildingEXO-DUS V4.0, Level 2, and PedGo version 2.2.4. In order to exclude program vari-

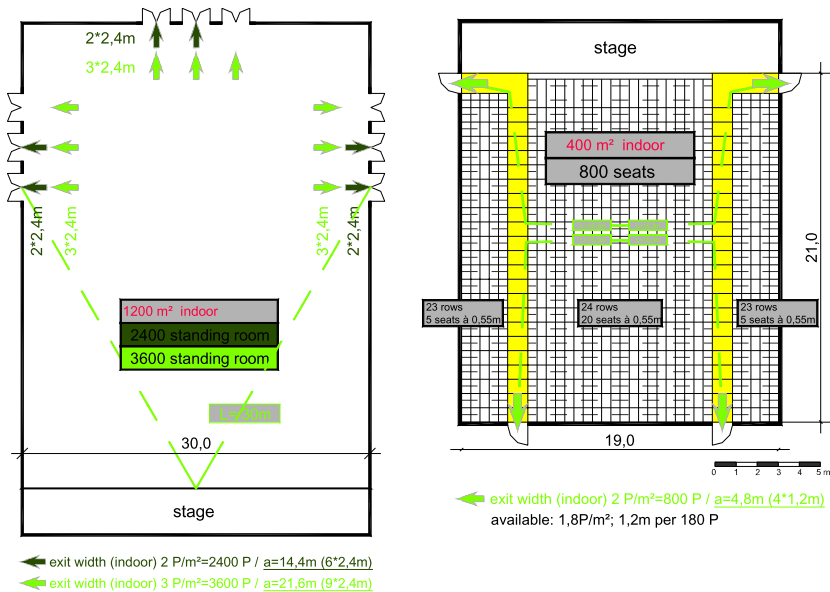


Fig. 1. Standing room with 2,400 to 3,600 persons and seated room with 800 persons.

ances when modeling reactions of persons, functions of modeling are mostly excluded.

The programs utilize varying cell sizes or shoulder widths:

- PedGo: 40 cm cells
- ASERI: 52.5/31.5 cm shoulder/chest widths
- BuildingEXODUS: 50 cm cells

For comparison reasons ASERI utilizes a variation that has been adjusted for PedGo:

- ASERI: 40/40 cm shoulder/chest widths

Initial calculations were scaled to the required width per VStättV, namely an exit width of 2.4 m (PedGo), which equals ASERI 40/40 cm, and 4 cells with buildingEXODUS.

Subsequently evacuation times are longer than with a starting point of 6 or 5 cells—roughly by a factor of 1.26 (PedGo) and 1.13 (buildingEXODUS). Upon closer examination it was determined that adjustments to scale were not absolutely required.

2 Outcomes

2.1 Evacuation Times

It is possible to identify a limiting value for indoor occupancies in the order of 3.5 minutes, however, computed evacuation times differ considerably for the various computer models with an increasing tendency for outdoor occupancies with low egress capacity. Results are shown in Fig. 2. User options in the programs, the choice of which is up to personal appraisal, render additional variations.

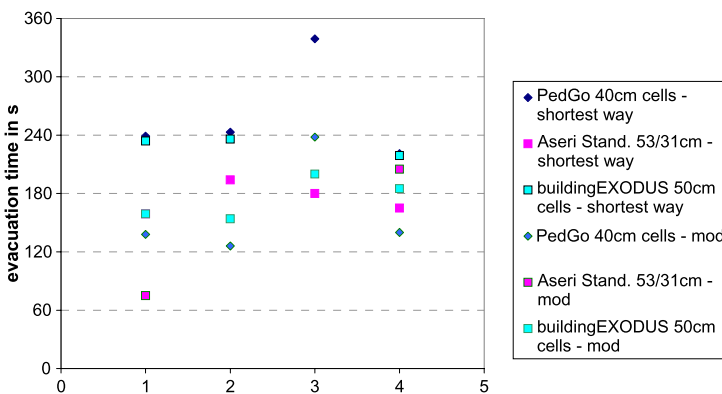


Fig. 2. Evacuation times for examples with standing rooms.

2.2 Exit Width

The effect of exit widths for outdoor facilities were examined indoors. Results are shown in Fig. 3.

In case of approximate uniform distribution of persons at exits (variation “mod”) an increase of exit widths generally results in reduced evacuation times. For example, an increase of exits by a factor of 1.5, the evacuation time is reduced by a factor of approximately 1.5 ($t_E \sim 1/a$).

2.3 Path Length

The travel distance only plays a minor role in cases where bottle necks at the exits are primarily responsible for evacuation times.

It is feasible that distances to exits can be considerably longer than regulations permit. Especially in the case of meeting facilities accommodating a

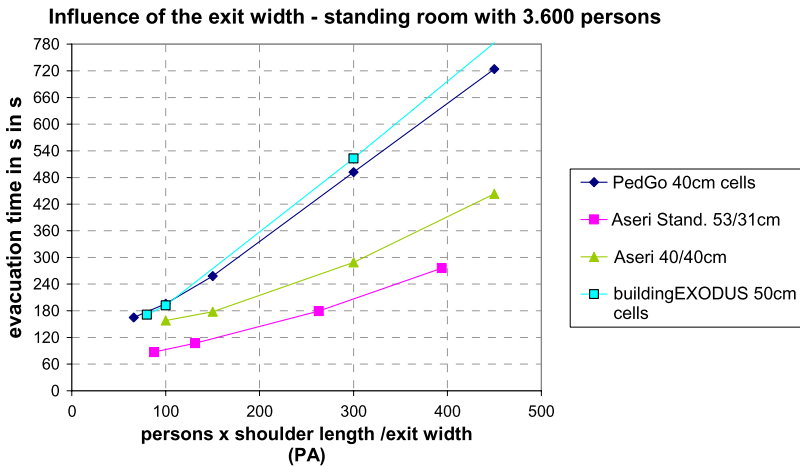


Fig. 3. Influence of exit width with approximate uniform distribution of persons per exit (3,600 persons), shown with index PA , where—depending on the model—shoulder widths equal actual shoulder widths, or cell width, with all calculations.

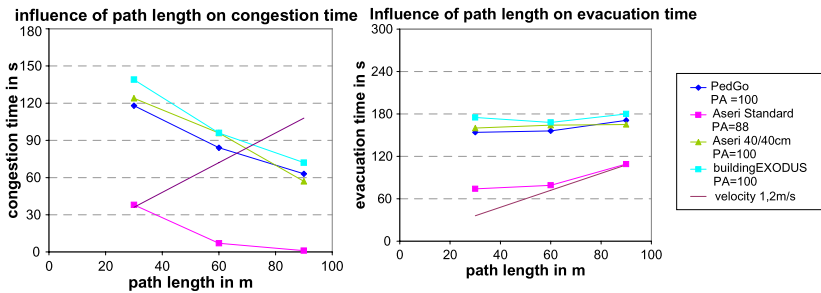


Fig. 4. Influence of path length on congestion time and evacuation time.

large number of people the delays at the exits significantly effect total evacuation time; alternatively, low traffic densities would eliminate delays at the exits, and only the time required to traverse the distance of the evacuation route is of importance. Calculated results are shown in Fig. 4.

3 Conclusions

It is possible to identify a limiting upper value for indoor occupancies under certain conditions, however, computed evacuation times differ considerably for the various computer models with an increasing tendency for outdoor occupancies with low egress capacity. User options in the programs, the choice of which is up to personal appraisal, render additional variations.

For limiting model and user related differences it is essential to establish a set of guidelines and benchmarks. Only when these are established and implemented into computer models, specified evacuation times present sound criteria for performance-based design.

Presently, computer models for egress calculations may nevertheless be regarded as useful tools for supporting alternative solutions on a comparative basis: Comparing evacuation times obtained when adhering to code requirements with times obtained for deviating conditions. E.g.: What is the effect of increased travel distances? Can longer evacuation times be compensated by increasing egress capacities?

The main application of computer-based egress calculations is for optimizing rescue routes and for investigating the arrangement of means of egress in terms of identifying and avoiding crowd congestions, not only for individual rooms but for an entire building. Since these tools are available, it is reasonable and appropriate to use them, at least for large premises where crowd safety is relevant.

References

1. ARGEBAU, Fachkommission Bauaufsicht: Musterverordnung über den Bau und Betrieb von Versammlungsstätten (Muster-Versammlungsstättenverordnung—MVStättV), June 2005.
2. ARGEBAU, Fachkommission Bauaufsicht: Begründung und Erläuterung zur Musterverordnung über den Bau und Betrieb von Versammlungsstätten (Muster-Versammlungsstättenverordnung—MVStättV), May 2002.
3. Department of Building and Housing: Compliance Document for New Zealand Building Code. Clauses C1, C2, C3, C4. Fire Safety, 2005.
4. Europäisches Komitee für Normung (CEN): EN 13200-1: 2003, Zuschaueranlagen—Teil 1: Kriterien für die räumliche Anordnung von Zuschauerplätzen—Anforderungen, December 2003.
5. H. Frantzich. A model for performance-based design of escape routes, Report 1011 of Lund Institute of Technology, Lund University, 1994.

6. J. Fruin. *Pedestrian Planning and Design*, Metropolitan Association of Urban Designers and Environmental Planners, New York, 1971.
7. E.R. Galea. *buildingEXODUS V4.00*, User guide and technical manual *buildingEXODUS V4.0*, Fire Safety Engineering Group, University Greenwich, Revision 1.0, March 2004.
8. E.R. Galea (Ed.). *Pedestrian and Evacuation Dynamics 2003*, CMS Press, London, 2003.
9. D. Helbing, I.J. Farkas, P. Molnár, T. Vicsek. Simulation of pedestrian crowds in normal and evacuation situations, in: M. Schreckenberg, S.D. Sharma (Eds.). *Pedestrian and Evacuation Dynamics*, Springer, Berlin, 2002, pp. 21–58.
10. D. Helbing, I.J. Farkas, T. Vicsek. Simulating dynamical features of escape panic, *Nature* 407, 2000, pp. 487–490.
11. IMO. *Interim Guidelines for Evacuation Analyses for New and Existing Passenger Ships*. IMO. MSC/Circ. 1033, 2002.
12. H. Klüpfel. *A Cellular Automaton Model for Crowd Movement and Egress Simulation*, University Duisburg-Essen, Dissertation, 2003.
13. E.D. Kuligowski, R.D. Peacock. *A Review of Building Evacuation Models*, Technical Note 1471, National Institute of Standards and Technology, 2005.
14. T.L. Lakoba, D.J. Kaup, N.M. Finkelstein. Modifications of the Helbing–Molnár–Farkas–Vicsek social force model for pedestrian evolution, *Simulation*, 81, 2005, pp. 339–352.
15. H.E. Nelson, H.A. MacLennan. Emergency movement, in: P. DiNenno (Ed.). *The SFPE Handbook of Fire Protection Engineering*, 2nd Edition, National Fire Protection Association, Quincy, 1995, pp. 3-286–3-295.
16. H.E. Nelson, H.A. MacLennan. Emergency movement, in: P. DiNenno (Ed.). *The SFPE Handbook of Fire Protection Engineering*, 3rd Edition, National Fire Protection Association, Quincy, 2002, pp. 3-367–3-380.
17. *New Zealand Building Code*, Part C1, C2, C3 and C4, 2001.
18. NFPA 101. *Code for Safety to Life from Fire in Buildings and Structures*, National Fire Protection Association, Quincy, 1981.
19. NFPA 101. *Code for Safety to Life from Fire in Buildings and Structures*, National Fire Protection Association, Quincy, 2003.
20. NFPA 101. *Code for Safety to Life from Fire in Buildings and Structures*, National Fire Protection Association, Quincy, 1994.
21. NFPA 130. *Standard for Fixed Guideway Transit Systems*, National Fire Protection Association, Quincy, 1986.
22. NFPA 130. *Standard for Fixed Guideway Transit and Passenger Rail Systems*, National Fire Protection Association, Quincy, 2003.
23. J. Pauls. Movement of people, in: P. DiNenno (Ed.). *The SFPE Handbook of Fire Protection Engineering*, 2nd Edition, National Fire Protection Association, Quincy, 1995, pp. 3-263–3-285.
24. D.A. Purser. Behaviour and travel interactions in emergency situations and data needs for engineering design, in: E.R. Galea (Ed.). *Pedestrian and Evacuation Dynamics 2003*, Greenwich, CMS Press, London, 2003, pp. 355–369.
25. W.M. Predtetschenski, A.I. Milinski. *Personenströme in Gebäuden. Berechnungsverfahren für die Projektierung*, Verlagsgesellschaft Rudolf Müller, Köln–Braunsfeld, 1971.
26. G. Proulx. Movement of people. The evacuation timing, in: P. DiNenno (Ed.). *The SFPE Handbook of Fire Protection Engineering*, 3rd Edition, National Fire Protection Association, Quincy, 2002, pp. 3-263–3-285.

27. Manual ASERI, Frankfurt/Main: Integrierte Sicherheits-Technik GmbH, 1999.
28. Manual ASERI-Update Version 4.0, Frankfurt/Main: Integrierte Sicherheits-Technik GmbH, September 2005.
29. Manual PedGo 2 und PedGo Editor 2. Version 2.1.0, TraffGo HT GmbH, 2005.
30. C. Rogsch. Vergleichende Untersuchungen zur dynamischen Simulation von Personenströmen, University of Wuppertal, Master-Thesis, 2005, <http://hdl.handle.net/2128/483>.
31. V. Schneider. Personenstromanalyse mit rechnerischen Nachweisverfahren, in: D. Hossler (Ed.). Leitfaden Ingenieurmethoden des Brandschutzes, VFDB-Referat 4, Braunschweig, June 2005.
32. M. Schreckenberg, S.D. Sharma (Eds.). Pedestrian and Evacuation Dynamics, Springer, Berlin, 2002.
33. P. Thompson. Simulex: simulated people have needs too, in: Workshop on Building Occupant Movement During Fire Emergencies, National Institute of Standards and Technology, 2004.
34. UK-Building Regulations, Approved Document B, Part B1, 2000.
35. N. Waldau, P. Gattermann, H. Knoflacher, M. Schreckenberg (Eds.). Pedestrian and Evacuation Dynamics, Springer, Berlin, 2007.
36. H. Weckman, S. Lehtimäki, S. Männikkö. Evacuation of a theatre. Exercise vs calculation, Fire and Materials 23, 1999, pp. 357–361.
37. U. Weidmann. Transporttechnik der Fußgänger. Transporttechnische Eigenschaften des Fußgängerverkehrs. Literaturauswertung, Schriftenreihe des Instituts für Verkehrsplanung, Zürich, 1992.

Dependence of Modelled Evacuation Times on Key Parameters and Interactions

David Purser

Hartford Environmental Research, 1 Lowlands, AL9/5DY Hatfield, UK
e-mail: david-purser@ntlworld.com

Summary. Times and patterns of buildings evacuations involve interactions between many behavioural parameters reflected in the increasing complexity of computer simulations. A combination of detailed GridFlow computer evacuations simulations, calculation models and experimental evacuations have been used to determine the extent to which evacuation patterns and times are largely dependent upon a small number of key parameters and interactions. Cases investigated included a single retail enclosure and multi-enclosure, multi-storey office buildings designed following UK prescriptive guidance. It is concluded that evacuation times are very dependent upon a small number of critical factors (including PTAT distributions, exit choice ratios, maximum flow rates, merge ratios, and densities of stationary and moving groups), and that even the most sophisticated computer simulations can give misleading results if these factors are not adequately represented. It is considered that simple calculation methods can provide a useful first estimate of evacuation times for designers, and a useful check on the performance of more complex simulation models.

1 Introduction

Evacuation from buildings comprises two main phases:

- Pre Travel Activity Time (PTAT)—time from alarm until occupants begin to move toward the exits
- Travel Time—time for occupants to move to exits and through escape routes.

Both involve complex interactions between many different behavioural and movement parameters, increasingly being incorporated into more complex computer simulations [1–3].

From previous studies of monitored evacuations and computer simulations [1–4], evacuation times appear to depend on a small number of key variables and their interactions, while other variables may have little effect on outcomes.

If so, simple calculations can provide a useful first estimate of evacuation times and a validation check on computer simulations—which can provide valid results only if the key variables are adequately represented in the models.

For the work reported here a combination of monitored evacuation experiments, detailed computer modelling, and simple calculations were used to investigate the effects of key parameters on evacuation times for:

- A single retail enclosure
- A multistorey office building

2 Methods

2.1 Evacuation of a Single Rectangular Retail Enclosure (2000 m²)

The modelled enclosure (Fig. 1), following UK prescriptive guidance, consisting of a simple generic square retail space (sides 42.4 m, direct travel distance 30 m) with 4 available exits [1.125 m width]), divided with rectangular racking as in a supermarket and a 900 max design population.

Estimation of evacuation times for different populations using three methods:

1. **Detailed computer simulation** using (GridFlow) [1] with all individual occupant locations and other parameters randomly assigned from defined distributions (see Fig. 2 for PTAT distribution) for each of 10 runs, for 9 different populations
2. **Spread-sheet calculation** using the full PTAT, travel speed and travel distance distributions and maximum exit flow capacities. Evacuation time was calculated as the time to queue formation plus the total exit flow time for the population

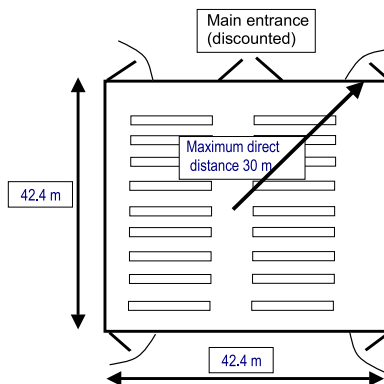


Fig. 1. Generic retail enclosure.

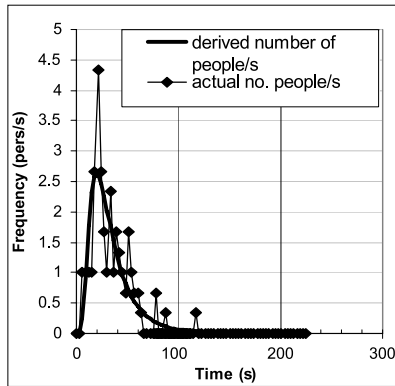


Fig. 2. Measured and derived PTAT distribution from a monitored evacuation of a retail enclosure used as input to evacuation modelling.

3. **Simple calculation** using the 1st and 99th percentile PTAT times, average travel speed and travel distance, and maximum exit flow capacities using the following expressions:

- *For a crowded case:* Evacuation time for an enclosure (Δt_{evac}) given by:

$$\Delta t_{\text{evac}} = \Delta t_{\text{pre(1st percentile)}} + \Delta t_{\text{trav(walking)}} + \Delta t_{\text{trav(flow)}} \quad \text{where}$$

$$\Delta t_{\text{pre(1st percentile)}} = \text{time from alarm to movement of first few occupants,}$$

$$\Delta t_{\text{trav(walking)}} = \text{walking time (unimpeded average walking speed } \times \text{ average travel distance to exits),}$$

$$\Delta t_{\text{trav(flow)}} = \text{exit flow time of total occupant population.} \quad (1)$$

- *For a sparsely occupied case:* Evacuation time from an enclosure is then given by:

$$\Delta t_{\text{evac}} = \Delta t_{\text{pre(99th percentile)}} + \Delta t_{\text{trav(walking)}} \quad (2)$$

where $\Delta t_{\text{pre(99th percentile)}}$ = time from alarm to movement to time of movement of last few occupants (= time to 1st percentile plus time from 1st to 99th percentile).

Each occupant was assumed to leave by their nearest exit, although effects of exit choice variations could be accounted for simply for each method.

2.2 Multi-Enclosure Building (up to 10-Storeys Served Office)

Used Gridflow simulations for clearance times from each floor into the protected stairs (PTAT times set to zero) or generic 4 to 10-storeys served rectangular floor plan office buildings with two lobby-protected stairs at each end (open plan floor area 1440 m² [53.7 × 26.9 m] and a maximum direct travel distance of 30 m. Occupants evacuated to their nearest stair, so modelling

was restricted to a single stair and the “half” floor it served (except for fire floor where entire population on that floor used one exit and stair). Evacuation was simultaneous for the whole building: storey exit width 1.05 m, stair width 1.3 m.

The populations evacuated were: (non-fire floors) from 102/floor for 4 storeys served to 71/floor for 10 storeys served (maxima according to UK prescriptive guidance). Maximum density on stair was set to either 2 or 4 persons/m².

Maximum flow rates through exits were capped at 80 persons/minute/metre effective width (60 persons/minute/metre effective width for stairs).

Validation data on maximum exit and stair flow rates, occupant densities on stairs and merge ratios at storey exits were obtained from a series of monitored unannounced evacuations in four buildings with different stair layouts in London and in Ulster (by D. Purser and K. Boyce).

3 Results

3.1 Retail Enclosure Evacuations

Method 1: GridFlow simulation results (Figs. 3 and 4).

The horizontal broken lines in Fig. 3 show the 95th and 99th percentile PTAT and 99th percentile presentation times of 95, 114 and 128 seconds (Presentation time = the time each individual presents themselves at the exit ready to walk through (assuming infinite exit flow capacity), which is given by their PTAT + walking time). The three lines with symbols show the times required for 95%, 99% and last out from full computer simulations (average of 10 simulations for each.). N&M = minimum flow time at 80 persons/min/metre effective width) [5]. At high occupant densities the evacuation time is limited by the physical exit dimensions, plus the time required for queues to form. The

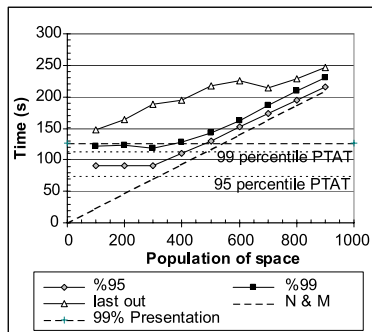


Fig. 3. Phases of evacuation times for different populations in a square retail enclosure with an area of 18,000 m² using GridFlow simulations and the measured PTAT distribution.

separation between the N&M time and the actual 99% evacuation time gives time to queue formation (20 seconds), represented by the presentation time at the exits of the first few occupants. The PTAT and walking times of the rest of the population after the first 20 seconds have no effect on the evacuation time of 99% of occupants. For low occupant numbers of $\sim 1/3$ of the design number, evacuation time depends on the PTAT of the last occupants to start to leave, and so approaches the 95 and 99 percentile PTAT times plus a small constant representing the average walking time to the exits (14 seconds), giving an exit presentation time of approximately 128 seconds, representing the minimum time required to evacuate assuming unimpeded movement. Figure 4 shows the effect of extending the PTAT distribution. The 99th percentile evacuation time is unaffected until the PTAT distribution is extended by a factor of two.

Method 2: No computer simulation, but individual PTAT and walking time distributions (Fig. 5) used to calculate time at which the rate of arrival

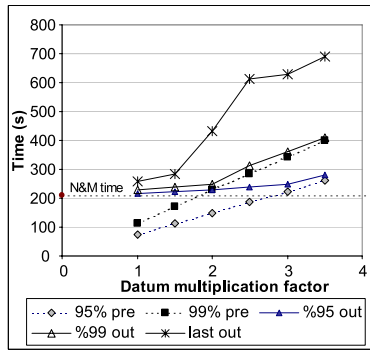


Fig. 4. Effect of extending the PTAT distribution by different multiples to simulate the effect of a less well-managed evacuation.

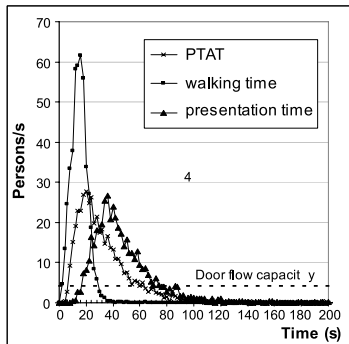


Fig. 5. Calculated distributions of individual unrestricted walking times to an exit, PTAT distribution and presentation time. Individual walking time \times individual PTAT = individual exit presentation time.

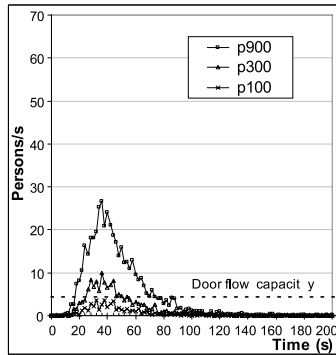


Fig. 6. Presentation time distributions for three populations. Queue formation occurs when presentation rate > door flow capacity. Time to of queue formation is slightly longer and of shorter duration for smaller populations, and is never achieved for a population of 100–200 persons.

Numbers of occupants	Full computer simulation	Spreadsheet distributions	Simple calculation
900	230, s.d. = 4.4	229	232
200	123, s.d. = 17.7	126	128

Table 1. 99th percentile evacuation time predictions using three methods.

of occupants at the exits (presentation time—Figs. 5 and 6)) exceeds the exit flow capacity (= time to queue formation). 99th percentile evacuation time is time to queue formation plus the minimum exit flow time for the occupant population. Where queue formation is predicted not to occur, 99th percentile evacuation time = 99th percentile presentation time.

Method 3: The simple calculation method is similar to Method 2, but uses average data instead of individual data as input to (1) and (2) for application to the crowded or sparsely occupied limiting cases.

The calculated 99th percentile evacuation times for both high and low populations using spread-sheet and simple calculation methods are very similar to those obtained using the full computer simulation and within the standard deviations for 10 computer runs.

3.2 Results: Multi-Storey Evacuation Simulations and Experiments Simulations

Figure 7 shows simulation results in terms of time for evacuation into a protected stair for each floor of two-stair buildings, for 4–10 storeys served, assuming a maximum density on the stair of 4 persons/m². Floor evacuation time increases with floor level, often exceeding the prescriptive design clearance time of 2.5 minutes. Figure 8 shows that decreasing the assumed maximum density on the stair to 2 person/m² considerably increases floor clearance

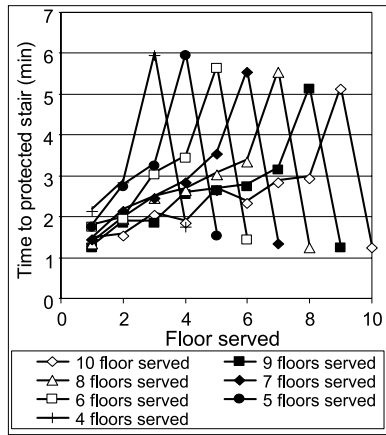


Fig. 7. Floor clearance times for 4–10 storeys served.

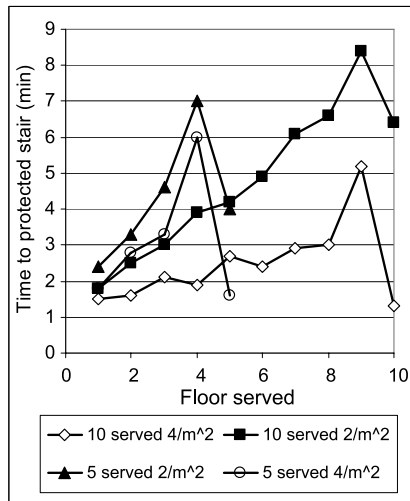


Fig. 8. Floor clearance times for 5 and 10 storeys served at densities on stair of 2 or 4 persons/m².

times. Gridflow provides a merge ratio of approximately 50:50 as occupants descending from the floor above slow at the turn on the storey exit landing to take the shortest line near the central handrail—enabling occupants from the storey exit to merge in and take the outside line. This results in the lower floors clearing first. Floor and building clearance rates are sensitive to the assumed maximum specific flow rates through exits and on stairs.

Validation—Unannounced Evacuation Experiments

Exit and stair flow rates were 86.7 p/min/m effective width (57.8 p/min/m full width) for exits and 60.1 p/min/m effective width (45.6 p/min/m full

width) for stairs (stair widths 0.85–1.3 metres in different buildings), but under optimised “drill” conditions, higher rates obtained at 99.4 p/min/m effective width (61.1 p/min/m full width) for exits and 72.9 p/min/m effective width (55.4 p/min/m full width) for 1.25 metre stairs. Maximum densities on stairs under near static flow conditions averaged 2.1 persons/m². Merge ratios averaged close to a 50:50 (average for four building 50.6:49.4 stairs-storey exit), irrespective of stair layout.

4 Conclusions

4.1 Conclusions from Single Enclosure Evacuations

For simple enclosures, evacuation times can be calculated accurately using simple constants for PTAT and walking time, calculated from average travel distance and unimpeded walking speed.

Only minor errors are introduced by not to using detailed computer models that take into account the full distributions of variables for individual occupants. Key determinants are the PTAT of the first and last occupants, estimated from available data for similar scenarios [1, 2], average walking time and maximum flow capacity of the exits.

4.2 Conclusions from Multi-Storey Building Evacuations

Times required to clear each floor of a multi-storey building, and the patterns of floor clearance, are likely to be highly dependent upon:

- assumed maximum specific exit and stair flow rates
- merge-ratios at the storey exits—(so adequate representation of stair layout in simulations important)
- standing capacities on the stairs (in turn dependent upon occupants densities on the stairs during crowded evacuation conditions).

References

1. Purser, D.A. and Bensilum, M., *Safety Science* 38:157–182 (2001).
2. Purser, D.A. ASET and RSET: addressing some issues in relation to occupant behaviour and tenability. *Fire Safety Science—Proceedings of the Seventh International Symposium*, International Association for Fire Safety Science, 2003, pp. 91–102.
3. Purser, D.A. and Gwynne, S.M.V. Identifying critical evacuation factors and the application of egress models. *Interflam 2007 Conference Proceedings*, pp. 203–214.

4. Bensilum, M. and Purser, D.A. GridFlow: an object-oriented building evacuation model combining pre-movement and movement behaviours for performance-based design. *Proceedings of 7th International Symposium on Fire Safety Science*, June 2002, pp. 941–952.
5. Nelson, H.E. and Mowrer, F.W. Emergency movement. *The SFPE Handbook of Fire Protection Engineering* (3rd edn.), DiNenno, P.J. (ed.), National Fire Protection Association, Quincy, MA, 2002, pp. 3/367–380.

A Modification of the Social Force Model by Foresight

Bernhard Steffen

Juelich Institute for Supercomputing, Forschungszentrum Jülich GmbH,
52425 Jülich, Germany
e-mail: b.steffen@fz-juelich.de

Summary. The motion of pedestrian crowds (e.g. for simulation of an evacuation situation) can be modeled as a multi-body system of self driven particles with repulsive interaction. We use a few simple situations to determine the simplest allowed functional form of the force function. More complexity may be necessary to model more complex situations. There are many unknown parameters to such models, which have to be adjusted correctly to give proper predictions of evacuation times, local densities and forces on rails or obstacles.

The parameters of the social force model can be related to quantities that can be measured independently, like step length and frequency. The microscopic behavior is, however, only poorly reproduced in many situations, a person approaching a standing or slow obstacle will e.g. show oscillations in position, and the trajectories of two persons meeting in a corridor in opposite direction will be far from realistic and somewhat erratic.

One of the reasons why these models are not realistic is the assumption of instantaneous reaction on the momentary situation. Obviously, persons react with a small time lag, while on the other hand they will anticipate changing situations for at least a short time. Thus basing the repulsive interaction not on the momentary situation but on a (linear) extrapolation over a short time (e.g. 1 s) eliminates the oscillations at slowing down and smoothes the patterns of giving way to others to a more realistic behavior. The exact extrapolation time is of little importance, but a combination of long time with linear extrapolation may get unstable. One second anticipation seems reasonable, and while the actual anticipation in peoples mind will most likely not be based on linear extrapolation, the differences will be small.

A second reason is the additive combination of binary interactions. It is shown that combining only a few relevant interactions gives better model performance.

1 Introduction

The motion of pedestrians can be modeled as self driven particles. This requires the definition of an accelerating (or decelerating) force depending on the situation—parameters of the pedestrian (walking speed, fitness, motivation),

the next (intermediate) goal (door etc.), the restrictions placed by obstacles, and position and movement of other persons in the neighborhood. The best known such model is the social force model [1–4] which assumes an accelerating force proportional to the difference between the desired speed and the present speed, and an influence of other people given by the sum of binary person-person interactions which are derived from an exponential potential. The simplest form depends on the distance only:

$$F_i = F_{i,\text{acc}} + \sum_{i \neq j} F_{i,j} \quad \text{with} \quad (1)$$

$$F_{i,\text{acc}} = C_1(v_{i,\text{des}} - v_i); \quad (2)$$

$$F_{i,j} = C_2 \exp^{\lambda \|x_i - x_j\|}. \quad (3)$$

Forms including the direction of motion have been developed and are more realistic. The obstacles are modeled similar to rows of standing people. While there is little debate on F_{acc} , which can easily be tested for free movement, the binary interaction is not clear at all, and it is not plausible that the combination of binary interactions is additive. To clarify this issue, we will consider a few simple but extreme setups.

2 Single Lane Walking

The simplest possible situation is that of people walking along a lane, and the two extreme cases are a line of people following each other with identical speed and two people meeting head on in a narrow channel.

People following each other is the case of the 1D fundamental diagram (FD) [4, 5]. This is related to the 2D FD [6, 7] via the width of people, modified by the zipper effect. This width is speed dependant and not well known, so a factor of 1.5 to 3 between pers/s in 1D and pers/(s·m) in 2D (smaller factors for higher speeds) is reasonable. With this, the 1D fundamental diagram [4] is compatible with the 2D diagrams given. Accuracy cannot be obtained and is not needed here. It is clear that the minimal distance obtainable is about 30 cm (with cultural differences), while at about 2 m distance the full speed will be attained so the force should be near zero. The exponential decay of the force in (3) is an approximation to this if C_2 and λ are appropriate.

The first, almost trivial, conclusion to be drawn here is that the force f_{ij} cannot be symmetric, otherwise the forces from people in front and behind would cancel out and the speed would not be density dependant. Until physical contact occurs, persons behind have negligible influence. A further conclusion is that the combination of the binary interactions is not additive. Actually, assuming F_{acc} given, for a situation with identical persons following each other at constant speed and distance we have $F_{i,\text{acc}} = -\sum_{i \neq j} F_{i,j}$. Regardless of which fundamental diagram we take—there is considerable disagreement between different measurements—the resulting binary interaction is not plausible.

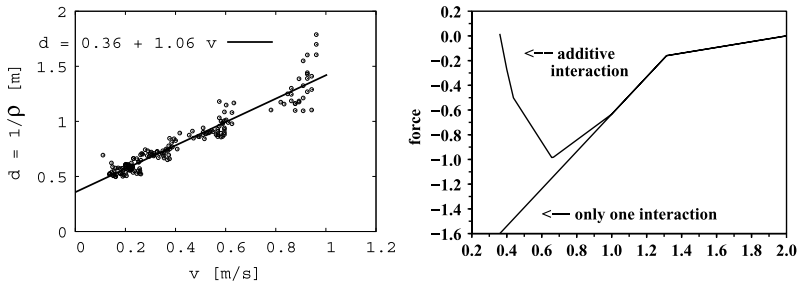


Fig. 1. Left: Distance versus speed, right: Interaction force calculated from FD.

2.1 Binary Interactions from Single Lane Following

Keeping in mind that $F_{i,j} = 0$ (full speed) for inter-person distances beyond 2 m, we can directly calculate $F_{i,j}(\Delta x) = -F_{acc}$ for $1\text{ m} < x < 2\text{ m}$, as there is only one nonzero binary interaction, and the speed corresponding to Δx and such F_{acc} is known from the FD.

For $2/3\text{ m} < x < 1\text{ m}$ we have $F_{i,j}(\Delta x) = -F_{acc} - F_{i,j}(2\Delta x)$, and so on till $F_{i,j}(\Delta x) = -F_{acc} - \sum_{k=2}^7 F_{i,j}(k\Delta x)$ for $29\text{ cm} < x < 33\text{ cm}$.

In a 1D experiment with low motivation (therefore not relevant for evacuation), we have measured the following relation between velocity and distance:

$$v = \begin{cases} -0.34 + 0.945d & \text{for } 0.36 < d < 1.314, \\ 0.71 + 0.146d & \text{for } 1.314 < d < 2, \\ 1 & \text{for } d > 2. \end{cases}$$

Under the additivity assumption, the linear relation fitting the measurements gives even attractive binary forces for short distances. Therefore it is reasonable to assume that in this situation there is interaction only with the person immediately in front, which gives a reasonable binary interaction. This results in the force equation

$$F_{i,j} = -2.14 + 1.51\Delta x, \quad 0.3 < \Delta x < 1.315, \tag{4}$$

$$F_{i,j} = -0.47 + 0.23\Delta x, \quad 1.315 < \Delta x < 2. \tag{5}$$

For more complicated situations, more than one interaction will be relevant, but certainly not many. For the 1D following, taking only the strongest binary interaction is sufficient. More complicated situations may (and do) ask for combining interactions, but this combination will in general not be additive.

2.2 Single Lane Head-on Collisions

Another situation accessible to analytic calculations is the head-on collision of two persons. In this situation, the force must be strong enough to stop both

at a reasonable distance from each other. Further, the speed should come to zero smoothly, especially not show any oscillations. Neither the standard social force model nor any force extracted from a fundamental diagram by the method described above will fulfill these requirements. Further, it is easy to estimate that any interaction function depending on Δx only will either be too strong to give a reasonable speed for walking in file at $\Delta x = 1.5$ m, or too weak to handle a head-on collision. Adding a dependence on v alone does not help, because any such dependence will be compensated by a corresponding change of the dependence on Δx . The most simple functional form possible will therefore depend on Δx and on Δv . A simple and reasonable assumption is that a person does not react on the momentary situation, but has some foresight and therefore reacts on the extrapolation of the momentary situation. More realistic, but more complicated, would be an extrapolation out of the recent past to allow for reaction times. Hoogendoorn et al. [8] have shown a finite reaction time to be essential, but this can be taken care of here by shortening the foresight. With foresight of 1 s, both the binary force from (1)–(3) and the force calculated from the FD give reasonable smooth stopping of two persons meeting head-on in a narrow corridor.

The case of groups in head-on collisions shows that the repulsive force is not always given by the closest interaction, and more than a single person must be taken into account. The second or third person in a group has the closest interaction with somebody going in the same direction, while the most relevant interaction is with the first person walking in opposite direction. However, the persons in between do not simply disappear, so they have to be allotted sufficient space. A reasonable procedure is: For each person in front calculate the extrapolated distance, reduce it by the space needed by the persons in between, and calculate the resulting binary force. The repulsive force then is the maximum of the binary forces. It should be noted that the space needed by persons in between depends on the speed of the person to

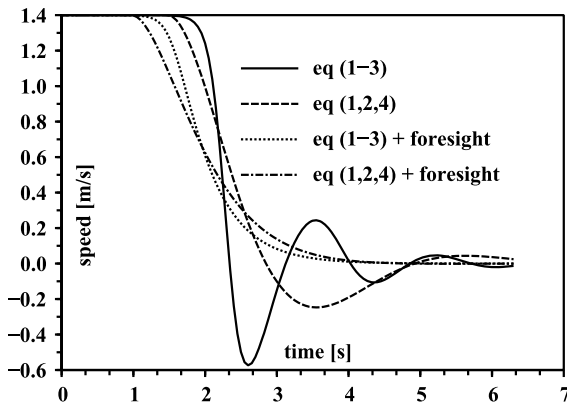


Fig. 2. Stopping with and without foresight—speed versus time.

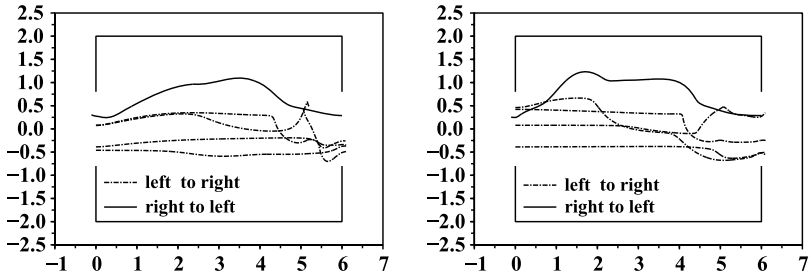


Fig. 3. Passing a corridor, *left*: without foresight, *right*: with foresight.

which the binary interaction is calculated. For a person walking in the same direction, this is bigger than for a person with opposite direction, and it increases with speed.

3 2D Walking

The situation has some added complications relative to the 1D situation. One is the possibility of partial interference without totally blocking the path. These ask e.g. for twisting the upper body, which gives some delay but no stopping. There is however no data available on how much delay this would give. The second complication is that people can change directions rapidly. Again, exact data is not available, but it is easy to test that a single 60° turn can be done within one step without much slowing down. Because of this possibility, foresight is very restricted in a medium or even high density situation where people have reasons to change directions. Only in low density situations, where the avoidance behavior involves only a small number of people, a simple foresight model like 1 s extrapolation will be beneficial, and more realistic models require knowledge on human perception and decision processes that is not available at the moment.

Still a limited amount of foresight can be helpful. In Fig. 3 we compare the paths of people passing through a 6×4 m corridor with 1.4 m doors at each side. The walking with foresight is somewhat smoother, and the last person out takes 2 s less. The difference is small, but enough to look deeper into this subject.

4 Conclusions

Simple distance-based repulsive forces are not capable of adequately describing microscopic pedestrian behavior. For 1D head-on collision, the inclusion of a 1 s foresight resolves this deficiency. In the more interesting low density 2D situation of meeting in a corridor, the foresight makes the simulation a little

bit more realistic, but the collision avoidance still produces unrealistic sharp bends and unnecessary slowdowns.

References

1. D. Helbing and P. Molnár, Social force model for pedestrian dynamics, *Phys. Rev. E* 51, 4282–4286 (1995).
2. D. Helbing, I. Farkas, and T. Vicsek, Simulating dynamical features of escape panic, *Nature* 407, 487–490 (2000).
3. T. Werner and D. Helbing, The social force pedestrian model applied to real life scenarios, in E.R. Galea (ed.), *Pedestrian and Evacuation Dynamics*, CMS Press, London (2003).
4. A. Seyfried, B. Steffen, W. Klingsch, and M. Boltes, The fundamental diagram of pedestrian movement revisited, *J. Stat. Mech.*, P10002, 2005.
5. A. Seyfried, B. Steffen, and Th. Lippert, Basics of modelling the pedestrian flow, *Physica A*, 368 (2006), 1, 232–238.
6. W.M. Predtetschenski and A.I. Milinski, *Personenströme in Gebäuden—Berechnungsmethoden für die Projektierung*, Verlagsgesellschaft Rudolf Müller, Köln–Braunsfeld (1971).
7. U. Weidmann, *Transporttechnik der Fußgänger*, Schriftenreihe des IVT Nr. 90, 2nd edition, ETH Zürich (1993).
8. S.P. Hoogendoorn, W. Daamen, and R. Landman, Microscopic calibration and validation of pedestrian models—cross-comparison of models using experimental data, in N. Waldau, G. Gattermann, H. Knopflacher, and M. Schreckenberg (eds.), *Pedestrian and Evacuation Dynamics*, Springer, Berlin (2005).

Models for Crowd Movement and Egress Simulation

Hubert Klüpfel

TraffGo HT GmbH, Bismarckstraße 142, 47057 Duisburg, Germany
e-mail: kluepfel@traffgo-ht.com

Summary. This paper lists models currently available for the simulation of crowd movement and egress simulation. The number of models that have been developed in the last decades are numerous and it is therefore neither possible nor useful to describe all the models in detail in a paper. This is even more the case since new models will be developed and existing models will be changed continuously. Therefore, the more appropriate approach for detailed model description is an open and editable website (wiki) which has already been put up: www.gratis-wiki.com/ped-bib.

The outline of this paper is as follows: The first section contains some general remarks on models.

1 Some General Remarks

Before going into the details of model classification, two clarifications shall be made. The first addresses the connection between theory, modeling, and simulation. This is depicted in Fig. 1.

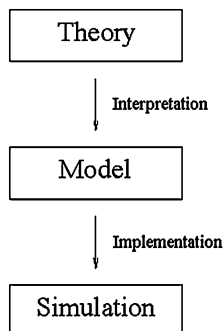


Fig. 1. Connection between theory, model, and implementation (simulation).

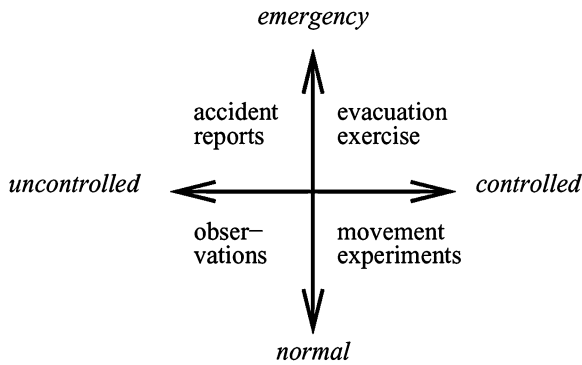


Fig. 2. Classification of data.

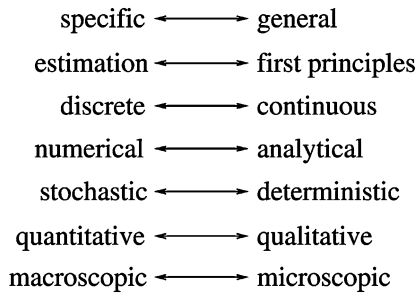


Fig. 3. Modeling criteria.

The second aspect is connected to the classification of data in general. This comprises empirical data as well as simulation results and is illustrated in Fig. 2.

One might argue that this distinction between controlled and uncontrolled on the one hand and normal and emergency is present in the application range of a model, too. Of course, the general aim is to develop a model (and implement it correctly, which is an ambitious task in itself) that has a general range of application. We will get back to that topic in the next section.

2 Model Classification

Models can be classified on the basis of various schemas. Further details concerning model classification can be found in the review article [3].

As already mentioned in the previous section, the general aim is to develop a general model in the sense that is able to cover all different scenarios (i.e., emergency as well as normal situations, reproduce uncontrolled/observed as well as experimental data). The further modeling criteria shown in Fig. 3 are rather self-explaining. One criterion that might be added is high fidelity

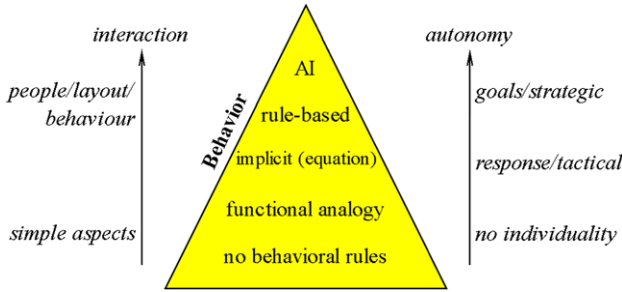


Fig. 4. Different levels of detail when representing decision making.

Name	Person	Comm.	Organization	Links
Aseri	Schneider	yes	I.T.S	www.ist-net.de
Exodus	Galea	yes	FSEG	www.fseg.gre.ac.uk
PedGo (AENEAS)	Meyer-König	yes	TraffGo (with GL)	www.traffgo-ht.com
Simulex	Thompson	yes	IES4D	www.ies4d.co.uk
Simwalk	Stucki	yes	Savannah	www.simwalk.ch

Table 1. List of Models investigated in [2, 4].

(many parameters) versus low fidelity (few parameters). The last distinction is more controversial than the ones shown in the figure, though.

Another way of classifying models is concerning the population (i.e. the individuals—if there are any—in the model). This is shown in Fig. 4.

3 List of Models

Table 1 contains a list of models for crowd movement and egress simulation that are commercially available.

This list is completely biased and only for the sake of illustration. For a less biased and more complete list, please visit www.gratis-wiki.com/ped-bib. We have tried to include all the models that have come to our knowledge. It is clear from the beginning, though, that this list cannot be complete. Therefore, an interactive internet-site (wiki) has been put up. It can be reached at www.gratis-wiki.com/ped-bib (see Fig. 6).

Figure 5 shows a combination of the basic ideas. The models there are ordered by the representation of space (geometry). On the second level, the ordering is according to the persons’s perspective.

4 Existing Model Reviews

In order to avoid reinventing the wheel, this paper rather aims at being a meta-review in the sense of listing review articles on models (and some empirical data and theory). Therefore, we list a few reviews.

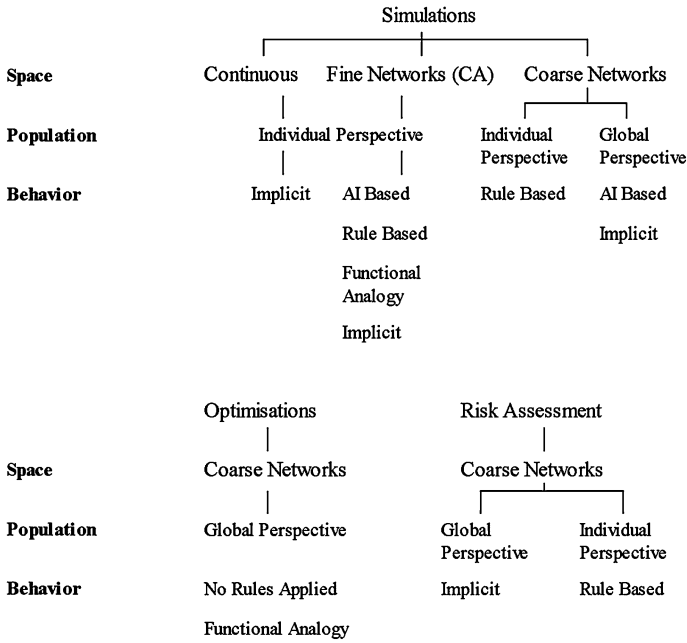


Fig. 5. Model overview.

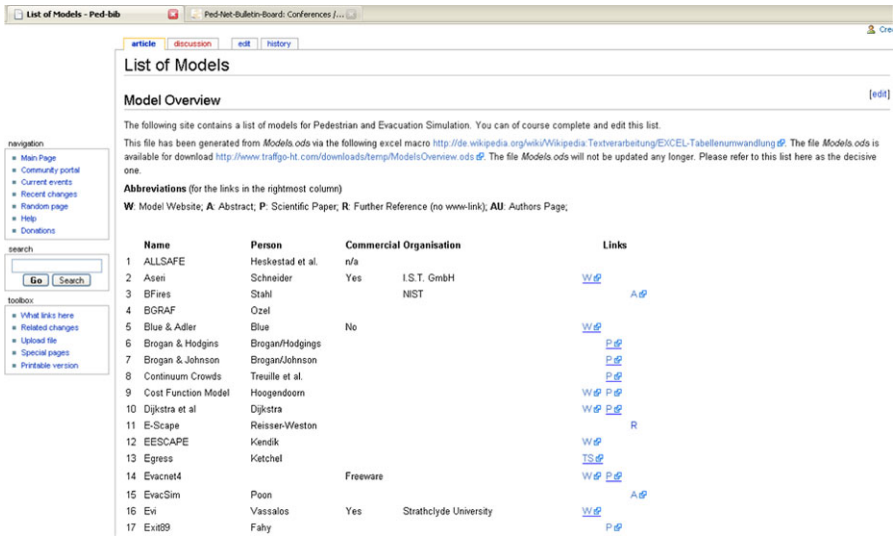


Fig. 6. A screenshot of the model wiki at www.gratis-wiki.com/ped-bib.

- Firemodelsurvey www.firemodelsurvey.com—has also a section on evacuation models
- Kuligowski Review—The review of 28 models is available at the NIST website. The book by Tubbs contains an appendix with an updated version [3, 7]
- Santos Review [5]
- Guidelines for Software Assessment [1]

This list is again non intended to be complete but rather a starting point.

5 The Wiki Approach

As has already been mentioned, the best choice to overcome all the problems of incompleteness and new models being developed is an interactive website where all model developers and those interested can contribute their knowledge.

6 Internet Resources

With respect to the rapidly growing number of models for crowd dynamics and the continuous updating and extension of existing models and simulation programmes, a complete and final list of models or description of a single model is hardly possible. This is an advantage and disadvantage at the same time. Especially when evacuation simulations are used to address safety issues, a well-defined version of the simulation or program is desirable and it is essential to be able to reproduce the results. Therefore, changes in the model must be documented in detail and explained with respect to their consequences for measurable quantities like flow rates, overall evacuation times, etc.

For covering the currently available models, the contribution of the model developers is pivotal. Otherwise, the list of models will always be limited by the knowledge and time of the author. Therefore, we have set up (within the framework of ped-net.org) an wiki site, where everyone can contribute his knowledge.

- The site www.ped-net.org is an internet bulletin board and discussion forum. Its strength is probably the discussion group with nearly 200 members (April 2008).
- The site www.evacmod.net is a similar project with a strong focus on a literature database where everyone can upload articles. Furthermore, there is a monthly newsletter containing information about new literature and recent events.
- Finally, www.safetylit.org is an internet site sponsored by the WHO that extracts literature information from numerous journals. It has an extensive search function which provides an excellent starting point for a literature search.

A recently published article provides a comprehensive overview over the theoretical and empirical foundations of pedestrian traffic [6].

Acknowledgements

I would like to thank Tobias Kretz, Christian Rogsch, Andreas Schadschneider, and Armin Seyfried (aka ped-net) for valuable discussions and continuing cooperation.

References

1. C.J.E. Castle. Guidelines for assessing pedestrian evacuation software applications. Technical report, University College London, 2007.
2. S. Hebben. Leitfaden für die Erstellung von Evakuierungsgutachten auf der Grundlage von Personenstromsimulationen und deren Bewertung durch die Genehmigungsbehörde. Master's thesis, Universität Duisburg-Essen, April 2008.
3. E. Kuligowski and S. Gwynne. What a user should know when choosing an evacuation model. *Fire Protection*, 3:30–40, 2005.
4. C. Rogsch, A. Seyfried, and W. Klingsch. Comparative investigations of the dynamical simulation of foot traffic flow. In *Pedestrian and Evacuation Dynamics 2005*. Springer, Berlin, 2007.
5. G. Santos and B.E. Aguirre. A critical review of emergency evacuation simulation models. <http://www.fire.nist.gov/bfrlpubs/fire05/art012.html>, June 2004.
6. A. Schadschneider, W. Klingsch, H. Klüpfel, T. Kretz, C. Rogsch, and A. Seyfried. Evacuation dynamics: Empirical results, modeling and applications. In B. Meyers, editor, *Encyclopedia of Complexity and System Science*. Springer, Berlin, 2009.
7. J. Tubbs. *Egress Design Solutions*. Wiley, New York, 1st edition, 2007.

Modelling Pedestrian Escalator Behaviour

Michael J. Kinsey, Edwin R. Galea, Peter J. Lawrence, Darren Blackshields, Lynn Hulse, Rachel Day, and Gary Sharp

Fire Safety Engineering Group, University of Greenwich, London, UK
e-mail: m.j.kinsey@gre.ac.uk, e.r.galea@gre.ac.uk

Summary. This paper presents an escalator model for use in circulation and evacuation analysis. As part of the model development, human factors data was collected from a Spanish underground station. The collected data relates to: escalator/stair choice, rider/walker preference, rider side preference, walker travel speeds and escalator flow rates. The dataset provides insight into pedestrian behaviour in utilising escalators and is a useful resource for both circulation and evacuation models. Based on insight derived from the dataset a detailed microscopic escalator model which incorporates person-person interactions has been developed. A range of demonstration evacuation scenarios are presented using the newly developed microscopic escalator model.

1 Introduction

Escalators provide a means for pedestrians to traverse a small number of vertical levels (typically 1–5 floors) in a relatively short period of time, providing greater comfort and requiring less physical exertion compared with equivalent stairways. Consequently it is common to find escalators as the primary form of vertical transport in underground/subway stations. They provide a more attractive and efficient alternative to long stairs in both circulatory and evacuation situations. However, in the event of an emergency evacuation, escalators are typically turned off, in some cases they may be closed, preventing occupants from even using them as a stair and in other cases escalators may be used only if staff are present to supervise [1].

There are many reasons for the restricted use of escalators in emergency situations, most notably the possibility that the moving escalator may be carrying people to, rather than away from danger. Regardless of these concerns, escalators have been used both in the “off” and “on” condition to good effect in some evacuation situations. In the 9/11 World Trade Center evacuation escalators were used as a means of evacuation in both the North and South towers to move people from the Mezzanine to the lobby [2]. In both towers escalators were used as stationary stairs [2] while in the South Tower survivors

reported using moving escalators during the “unofficial” evacuation prior to the South Tower being hit [2]. It is clear that escalators are used for evacuation purposes and so there is a need to represent escalators within both evacuation and pedestrian dynamics circulation models. As a result there is a need to understand and quantify pedestrian behaviour associated with the use of escalators. Despite this, at present, there is little data pertaining to micro-level pedestrian dynamics on and around escalators and a subsequent lack of understanding.

2 Data Collection

As part of the EU FP6 project AVATARS, human factors data associated with escalator usage in underground stations was collected. The data was collected within the Provença station, Barcelona Spain using CCTV (Closed Circuit Television) video footage. Data was collected in both rush-hour and non rush-hour conditions. Two escalators were studied, an escalator moving in an upwards direction and an escalator moving in a downwards direction. Analysis of the video footage allowed the formation of a human factors dataset containing information pertaining to: escalator/stair choice, boarding/alighting behaviour, escalator side preference, proportion of walkers to riders, walker speeds and entry/boarding and exit/alighting flow-rates. In total some 7,206 data points were collected from the video footage relating to 1,283 people. The rush-hour data was collected from 895 people while the non rush-hour data was collected from 388 people.

3 Escalator Model

The core software used in this paper is the buildingEXODUS V4.0 evacuation model [3]. The basis of the model has frequently been described in other publications and so will not be described here. Here we describe the extension of the model to include escalators for both evacuation and circulation. The microscopic escalator model requires the identification and quantification of appropriate agent behaviour associated with the use of escalators and the development of appropriate behaviour rules to represent the behaviour.

3.1 Microscopic Escalator Model

The behaviour rules incorporated in the prototype microscopic escalator model are based on the study of the AVATARS data and include: escalator/stair choice model, proportion of riders/walkers, side preference for riders and walker speeds. In addition to the behaviours identified from the data analysis, additional behaviours associated with the existing stair model, such as inter-person spacing (staggering/packing behaviour [3]) are also included

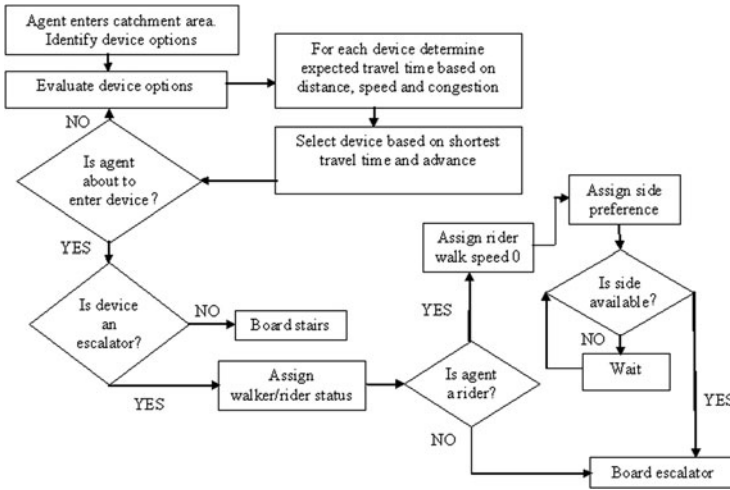


Fig. 1. Microscopic escalator model logic.

within the escalator model. The logic of the microscopic escalator model is summarised in Fig. 1.

When an escalator and stair or indeed any type of vertical transfer device is closely co-located, pedestrians approaching the device are required make a point-of-choice decision as to which device they will adopt. There are a number of factors which influence the selection decision including; personal preference, levels of energy expenditure required, level of urgency felt. In circulation situations all of these factors may exert an influence on the decision making process while in evacuation situations the desire to minimise ones egress time may become the overriding factor. This later factor is incorporated into the current device selection model.

4 Escalator Model Evacuation Demonstration

A simple demonstration case was developed to demonstrate the application of the microscopic escalator model in an evacuation scenario. The geometry consisted of two levels connected via two stairs and an escalator. The vertical drop was 6 m and the width of the stairs and escalator was 1.2 m. The horizontal speed of the escalator was 0.5 m/s with a horizontal length of 10 m. A total of 400 people are used in the simulation. A total of eight different scenarios were examined. Each case was run five times and all the results presented below represent the average for five simulations.

4.1 Evacuation Results

The results for the various scenarios are summarised in Table 1, it should be noted that in these scenarios, stair 2 is immediately adjacent to the escalator. Very early in the evacuation crowds develop at the head of the stairs/escalator and persist until near the end of the evacuation. In all scenarios the shortest travel time device selection algorithm ensures that “reasonable” use is made of the devices throughout the simulation. Without the device selection algorithm, agents would either use their nearest or their assigned device rather than use an alternative nearby device irrespective of local conditions such as queue length/congestion levels, possibly resulting in unrealistic longer than required evacuation times. In all other cases where the escalator is operating, the escalator takes the greater number of users due to the expected greater speed of transit afforded by the escalator.

Table 1. Summary results for escalator evacuation demonstration scenarios.

Scenario	Av. TET (s)	Av. CWT (s)	Av. max density (p/m ²)	Escalator usage	Stair 2 usage	Stair 1 usage
Scenario 1: Two stairs	302	61.0	4.0	0	203	197
Scenario 2: Two stairs + stopped esc	229	27.0	3.9	127	137	136
Scenario 3: Two stairs + escalator 0% riders	196	16.5	2.6	193	115	92
Scenario 4: Two stairs + esc 100% riders, 50% left, 50% right	210	16.9	3.1	198	101	101
Scenario 5: Two stairs + esc 100% riders, 100% right	221	20.7	3.6	169	117	114
Scenario 6: Two stairs + esc 50% riders, 100% right	210	18.0	3.1	197	101	102
Scenario 7: Two stairs + esc 50% riders, 50% left, 50% right	212	19.7	3.1	197	103	101
Scenario 8: Two stairs + esc 76% riders, 28% left, 72% right	211	18.5	3.1	193	104	103

With just two stairs in operation the average Total Evacuation Time (TET) is 302 s (see Scenario 1), when the stopped escalator is made available the average TET reduces to 229 s (see Scenario 2), a reduction of some 26%. Clearly, even a stopped escalator can provide considerable advantage however, it should be noted that these simulations do not attempt to represent the likelihood of trips or falls on the escalator (or stairs). When the escalator is functioning (Scenario 3) and we assume that 100% of the population will walk down the escalator the average TET reduces to 196 s, some 35% better than having two stairs only and 14% better than the case with the stopped escalator available. We also note that in Scenario 3 almost 50% of the population utilise the escalator and that the average maximum density at the entrance to the stairs/escalator and the average CWT attain their minimum values for this scenario. The evacuation time achieved in this scenario is the quickest of all the scenarios and indicates the advantage a moving escalator can have during an evacuation. Also, by reducing the average density at the entrance to the stair/escalator, the use of the escalator can be argued to reduce the possibility of adverse crowd related incidents occurring.

If we now assume that 100% of the escalator users will ride the escalator and they will equally utilise the left and right location on the escalator tread (Scenario 4) we find that the TET has increased slightly to 210 s. At first glance, this modest 7% increase in evacuation time compared to Scenario 3 does not appear to be logical however, when it is recalled that escalator walkers attempt to keep two treads between them and the person ahead the difference becomes more understandable. When full of walkers, the escalator has a reduced capacity compared with the situation in which it is full of riders. Thus in Scenario 4 the increased apparent capacity of the escalator partially compensates for the reduced travel speed produced by the stationary riders. Thus from a global perspective, in evacuations in which there is expected to be heavy use of escalator/stair combinations, there is little to be gained by having the escalator users walk down the moving escalator. Indeed, there may be advantages in reducing the chances of injury resulting from trips or miss steps by preventing the escalator users from walking. However this conclusion is derived from taking a global perspective, from an individual person's perspective, their personal evacuation time will be reduced by walking down the escalator and so this type of behaviour may be difficult to enforce.

If we consider the extreme of inefficient escalator usage and assume that 100% of the people will ride the escalator and 100% will utilise the right side (Scenario 5)—effectively halving the capacity of the escalator we note that the evacuation time increases to 221 s, a 5% increase over Scenario 4 and a 13% increase over Scenario 3. At first sight this modest increase in the total evacuation time is surprising however, it should be noted that the number of escalator users has decreased by some 15%. Thus the device algorithm has allowed the agents to make use of under utilised capacity on the neighbouring stairs. Had the escalator been the only device linking the two levels, we would have expected to incur a significantly greater increase in evacuation time.

With 50% the escalator users walking down the escalator and all the riders utilising the right side of the escalator (Scenario 6) the average total evacuation time is 210 s, which is 7% slower than the case with 100% walkers (Scenario 3) and equal to the case with 100% riders with an equal usage of both sides of the escalator tread (Scenario 4). This is a complex case with competing trends resulting from increased capacity and decreased speed due to the riders (all to one side) and decreased capacity and increased speed due to the walkers. These effects almost cancel each other however, we also note that the average Cumulative Wait Time (CWT) for Scenario 6 is larger than that for Scenario 3 in which there are 100% walkers. This increase in CWT is consistent with only a single lane being available for the walkers, thus if a walker is caught behind a slower walker, there is no chance for them to overtake and hence they will be forced to travel at the slower speed, hence increasing their personal CWT. We note that for Scenario 7, in which 50% of the escalator users are walkers—as in Scenario 6—but in which the riders occupy both the left and right lanes, the total evacuation time has increased slightly to 212 s, with a further increase in the average CWT. This is due to the walkers now being impeded in both lanes by riders, making it more difficult for them to pass without increasing their personal CWT.

The final scenario consists of the same distribution of riders with the same distribution of left/right usage as found in the AVATARS data (Scenario 8) i.e. 76% riders with 28% of riders occupying the left lane. Thus the break down of walkers to riders and left/right usage is the same as may be expected in a non-emergency circulation example. Here we find the total evacuation time is 211 s and is consistent with other cases involving 100% riders (Scenario 4) producing a total evacuation time of 210 s and 50% riders (Scenarios 6 and 7) producing evacuation times of 210 s and 212 s. This suggests that virtually any situation with more than 50% riders will produce similar total evacuation times.

5 Concluding Comments

This paper has presented a summarised analysis of human factors data relating to pedestrian escalator behaviour within a Spanish underground station. The dataset provides insight into pedestrian behaviour in utilising escalators and is a useful resource for both evacuation and circulation model developers.

A range of demonstration evacuation scenarios were performed using the newly developed model. The results suggest that under evacuation conditions, in which the simulated agents are assumed to select the device which is expected to produce the minimum total transit time, the best evacuation times can be obtained if all the escalator users walk down the escalator. However, if we assume that all the escalator users ride down the escalator, and that they display an equal preference for the left and right lanes on the escalator there is only a marginal increase in the total evacuation times. These results

suggest that from a global perspective, there is little to be gained by walking down the escalator, indeed, under crowded emergency conditions suggesting that escalator users ride the escalator may be a better strategy as it reduces the risk of injuries arising from miss steps. However this conclusion is derived from taking a global perspective, from an individual person's perspective, their personal evacuation time will be reduced by walking down the escalator and so this type of behaviour may be difficult to enforce. In addition, it must also be considered that this analysis is based on a single escalator/stairway group, and any difference between scenarios is expected to be magnified with the addition of other escalators/stairways groups in the geometry.

Acknowledgements

The authors are indebted to the EU Framework 6 programme for funding a portion of this work through project AVATARS (TST4-CT-2005.012462), their AVATARS partners (BMT, FGC, ATM, University of Salford and Buro Happold) for their co-operation and to the UK EPSRC for funding a portion of this work through project HEED (GR/S74201/01 and EP/D507790).

References

1. BS5588-12, Fire precautions in the design, construction and use of buildings, Part 12: Managing Fire Safety. 2004.
2. E.R. Galea, J. Shields, D. Canter, K. Boyce, R. Day, L. Hulse, A. Siddiqui, L. Summerfield, M. Marselle, and P.V. Greenall. The UK WTC 9/11 evacuation study: methodologies used in the elicitation and storage of human factors data. *Interflam 2007*, Vol. 1, pp. 169–181, 2007.
3. S. Gwynne, E.R. Galea, P.J. Lawrence, and L. Filippidis. Modelling occupant interaction with fire conditions using the buildingEXODUS evacuation model. *Fire Safety Journal*, Vol. 36, Issue 4, pp. 327–357, 2001.

Introducing a Coupled Model for Simulating Crowd Behaviour

Alicia Guadalupe Ortega Camarena and Dominik Jürgens

Institute of Scientific Computing, Technische Universität Braunschweig, 38106
Braunschweig, Germany
e-mail: alicia.ortega@tu-bs.de, d.juergens@tu-bs.de

Summary. The simulation of human behaviour is a complex and unsolved problem. In the simulation of crowd behaviour due to evacuations, many different approaches are present, which in most cases incidently consider psychological aspects of this phenomenon. We assume human behaviour in crowds to be the result of coupled individual processes. The introduced *perceiving–acting model* follows this assumption and integrates perceiving, thinking and acting as primary factors in the individual human behaviour. The model focuses on evacuation scenarios and therefore some of the intrinsic complexity of the human and its acting can be neglected.

1 Context of Our Model

Human behaviour is complex and unpredictable by nature, moreover the response to a stimulus may vary from individual to individual, and from time to time. Several studies concerning this complexity have been done, and different pedestrian phenomena distinguish normal and panic behaviour [1]. Up to now several models describing pedestrian phenomena in crowds have been developed [2]. The two main scopes used for the development of models are engineering- and psychological-based. In the present paper it is assumed that human response depends strongly on the surrounding environment and the information that the observed individual will obtain from it [3]. Therefore a model considering psychological aspects of human response results to be necessary.

2 Perceiving–Acting Model

In any situation a big amount of *data* is present in our surrounding environment, but just a part of it will be perceived and processed in our brain. This process transforms the available data into information and derives it into

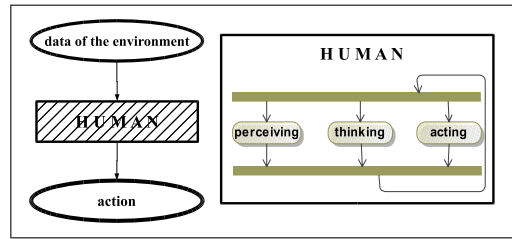


Fig. 1. The *left-hand* figure shows the basic idea of our model. We understand the human as a black-box which collects data from its surrounding environment. Inside this blackbox an integrating process *decides* for goals to be achieved and translates this decisions into actions. The *right-hand* figure shows the involved parallel process in an abstract way.

our actions, as illustrated in Fig. 1. How and which surrounding data takes part in the implicit situation processing is strongly dependent on influences which can not be mathematically formalised in a direct way; as for example experience.

Figure 1 shows the central idea of the *perceiving–acting model* which assumes that human behaviour is mainly based on parallel processes of perceiving, thinking and acting. In the case of an evacuation, *special* activities are involved in this processes. The assumed connection between these activities is shown in Fig. 2 as an abstract process of human thinking in evacuation scenarios—*evacuation-thinking* process (ETP).

The ETP (in Fig. 2) can be summarised as a coupling of several sub-processes, where perceiving and planning happens in parallel but not independently. During the perception process an identification of the surrounding environment takes place together with a classification of the observed objects with respect to their relevance. In the planning process the previously classified information is used to derive decisions. These decisions are modelled through targets which are to be achieved and obstacles which are to be avoided. The global target—to succeed the evacuation—can be thereby divided into strongly dependent subgoals.

As it occurs in reality, not all the available information is capted by the human. Therefore the perceiving model strongly influences the planning process. Achieving a more realistic simulation of evacuation scenarios, intrinsic processes like the use and collection of memory and experience as well as stress sensing and future extrapolation are also to be considered. In the proposed model they are present as independent sub-processes which affect the human decision taking. The taken decisions can be transformed into actions which may (or may not) help to achieve the intended goals.

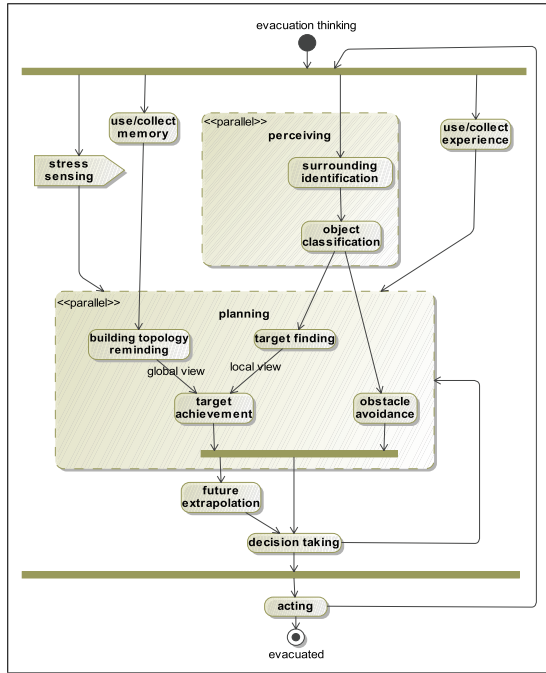


Fig. 2. The process chart of the thinking in evacuation scenarios shows the assumed connection between relevant brain activities. The connection between these activities is ordered in a way which assumes the brain to be a causal parallel system. Causality implies that a response to an input can only be measured after its occurrence.

3 The Model Process

3.1 A Perception Model

The last section describes the different processes involved in the perceiving-acting model and the computational implementation still remains. In this section, we discuss the computational strategies and tools which can be used to implement our model.

In general human perception can be considered as the transmission of sensory data through specific organs [4]. The human senses are seeing, hearing, touching, smelling and tasting. Therefore eyes, ears, skin, nose and tongue are the typical receptors of the surrounding environment of the human. The brain acts as the central organ capable to select, organise and transform these data into information. A model integrating all these senses may result to be too complex to implement. What a person is able to see is here assumed to be the most important part of human perception. The visual perception of humans can be modelled with different methods depending on the scenario. Two of

these methods are *geometric filtering* and—as a more sophisticated one—*ray tracing*.

Geometric filtering is a simple technique, where the field of vision is modelled by a geometric shape; objects which are geometrically inside this shape are *selected* to be perceivable while all others are ignored. It is a very simple technique gaining unrealistic results, since also hidden objects can be perceived and a far-field vision is impossible unless the geometry is chosen to be very large.

Ray tracing is a more sophisticated and realistic technique from computer-graphics [5]. It is a mathematical model to simulate an eye-like visual sensor, making this method the ideal choice for a visual perception model. It models vision by tracing the broadening of a number of randomly emitted rays. If one of those rays strikes an object, this object is defined to be perceivable. The ray-tracing procedure must be executed for every simulated individual, making this approach computationally very expensive. For complex scenarios with a large number of simulated individuals, this technique needs to be simplified and combined with other techniques.

3.2 A Planning Model

Another part of the human perceiving–acting model is the planning of routes. Obtaining an adequate evacuation route is eminently more difficult in geometrically complex (concave) rooms. An example of a decomposition of a given concave domain into a number of convex sub-domains is shown in Fig. 3. This

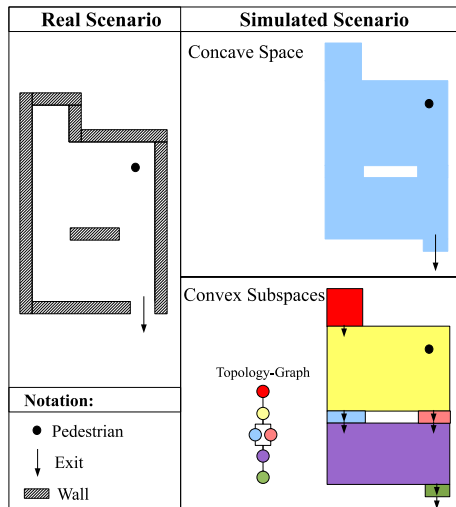


Fig. 3. In a concave scenario a global route planning is used. Therefore a decomposition of the domain into convex subspaces has to be achieved.

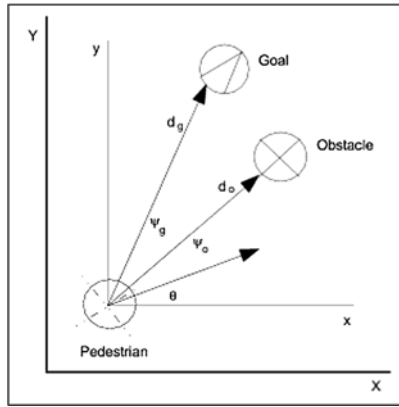


Fig. 4. The figure shows the model parameters involved in the local navigation model.

decomposition derives convex subspaces and the calculation of a route is therefore divided into two steps. A concave space can thereby be represented with a topology-graph like indicated in the figure; here a node represents a convex subspace and the edges are the connections between them. This graph can be used to compute a global evacuation route, while the local route planning inside a convex subspace is reduced to the solution of an obstacle avoidance (Fig. 4).

Target-Achievement and Obstacle-Avoidance as Local Navigation Model

A *local navigation model* is used to simulate the movement of a pedestrian in a considered convex subspace. This navigation model was first presented in [6] as a semi-empirical model for describing the trajectories of pedestrians trying to reach a certain point of interest (*attractor*) and avoiding certain obstacles (*repellers*) present in its surrounding. The moving direction of the pedestrian (θ) is the behavioural state-variable of the model, and it changes according to the relative position of the attractor and the repellers, respectively, as shown in Fig. 4. The speed of the pedestrian in the original model is a constant. The ODE describing this model is the following:

$$\frac{d^2\theta}{dt^2} = -f_d \left(\frac{d\theta}{dt} \right) - f_g(\theta - \Psi_g, d_g) + \sum_{i=1}^N f_o(\theta - \Psi_{o_i}, d_{o_i}). \quad (1)$$

Equation (1) consists of three main terms; a so-called *damping term* (f_d) which *smooths* the change of pedestrian direction. The other terms give a goal (f_g) and n-obstacle contributions (f_o) as functions of their relative offset (Ψ_g, Ψ_{o_i}) and the distance (d_g, d_{o_i}) to them respectively.

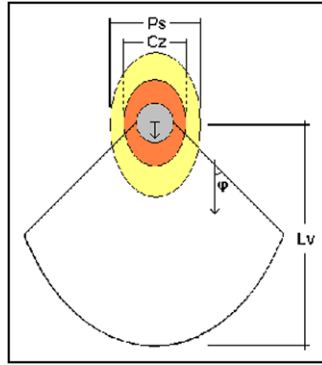


Fig. 5. Schema of the sensing-parameters of a pedestrian.

3.3 Stress-Sensing Model

Pedestrian behaviour varies from individual to individual in the same situation, therefore individual parameters are needed. We introduce personal space (P_s), a critical zone (C_z), length and angle of vision (L_v , φ) as individual sensing-parameters for each pedestrian as shown in Fig. 5. By means of these sensing-parameters an *objective* measure of stress induced by the surrounding environment can be mapped into individual stress parameters. This new information correlates the degree of stress induced by the scenario with the level of stress the person experiences (i.e., an increase of stress may start by a sudden decrease of available *personal space*).

We can also use this mapping to identify zones in a building, where a high level of stress is most likely. Once these zones are identified, corresponding changes in the design of the building can be considered. This can help to assure the possibility to evacuate a building in its design-phase. This provides a novel tool for the identification of dangerous zones for pedestrians in a building and a new way for understanding crowd dynamics during evacuations.

4 Conclusions and Outlook

This article introduces the *perceiving-acting model* to describe human behaviour in building evacuations. It incorporates the processes of perceiving, thinking and acting. The model takes into account the strong dependency between human behaviour and its environment. Therefore a spacious local coupling (perceiving) between the individual and its surrounding as well as a global planning activity (thinking) are considered. The simulation of the pedestrian trajectories (acting) is done by a *local-navigation model*. A stress-sensing model allows us to measure the degree of stress that a person may experience in a given situation, and therefore to locate the zones and levels of stress present during a simulated evacuation.

Future Work

The numerical results of the model explained here, will be presented in following papers. The major goal we follow is the improvement of our model with respect to psychological aspects rather than algorithmical.

Validation is a basic problem in the development of numerical models. In the simulation of building evacuations, validation is needed but difficult to achieve due to a lack of available measurements. A further goal in our work is the validation of our model under the psychological view. A comparison of our results with descriptions of crowd phenomena provided by psychologists is therefore important.

Acknowledgements

The authors would like to thank to Prof. H.G. Matthies and Dr. R. Niekamp, for their support and constructive comments on this topic.

References

1. M. Schreckenberg and S.D. Sharma, editors. *Pedestrian and Evacuation Dynamics*. Springer, Berlin, 2002.
2. A.G. Ortega Camarena. Numerical Simulation of Building Evacuation in Emergency Conditions. *Proc. Appl. Math. Mech.*, 7:2140007–214008, 2007.
3. P.A. Bell, J.D. Fisher, and R.J. Loomis. *Environmental Psychology*. Saunders, Philadelphia, 1987.
4. D. Roberts, editor. *Signals and Perception: The Fundamentals of Human Sensation*. Palgrave MacMillan, Basingstoke, UK, 2002.
5. G.H. Spencer and M.V. Murty. General Ray-Tracing Procedure. *J. Opt. Soc. Am.*, 52:672–678, 1962.
6. B.R. Fajen, W.H. Warren, S. Temizer, and L.P. Kaelbling. A Dynamical Model of Visually-Guided Steering, Obstacle Avoidance, and Route Selection. *Int. J. Comput. Vis.*, 54(1/2/3):13–34, 2003.

Evacuation Modelling of Fire Scenarios in Passenger Trains

Jorge Capote, Daniel Alvear, Orlando Abreu, Mariano Lázaro, and Arturo Cuesta

GIDAI—Fire Safety-Research & Technology, University of Cantabria,
Ave. Los Castros s/n, 39005 Santander, Spain
e-mail: capotej@unican.es

Summary. Fire incidents inside passenger trains constitute a significant risk factor for life safety. Therefore, it is necessary to count on a suitable evacuation strategy, during the instants previous to the rail vehicle halt and the subsequently evacuation. In this paper, the evacuation of passengers from different fire scenarios and several evacuation conditions were investigated. The analysis was divided into two stages of the evacuation process considering two different high speed trains: (1) the movement and behaviour of passengers in fire scenarios inside the vehicle before the train stopped, and (2) the analysis of train evacuation under different conditions. The results, obtained by means of the egress model STEPS (see MacDonald, STEPS Simulation of Transient and Pedestrian Movements User Manual), allowed to determine the influence of the limitations of the different train geometries under different evacuation conditions, give an estimation of the evacuation times and analyse the impact of human parameters considered in the evacuation process.

1 Introduction

The evacuation of trains depends on the design of the train, the decisions regarding fire control or the train halt as previous activities before initiating the evacuation process, and finally, it depends on the movement and behaviour of passengers. A significant number of people converge in high speed trains. In case of fire emergency, the number of available exits can be reduced, causing congestion. In these narrow spaces, people decision has a relevant influence on the evacuation process. If a passenger does not perceive the menace before evacuating, he may take the time to pick up the baggage and personal items thus blocking the aisle and risking the safety of the rest of the passengers. To avoid this inappropriate behaviour, the strategies for improving the managing of an emergency are focused on an adequate training of the crew and direct and verbal messages. The imminent conclusion is that to avoid these situations people need more and better information [2]. On the other hand, panic or uncontrolled behaviours in fire situation, even under extreme conditions, only

represent a minimum percentage. Generally, people show a cooperative human behaviour [3]. In an emergency situation, immediate people reaction is not common; rather it takes them a while to begin the evacuation movements.

In the train there might be many passengers who are sleeping, listening to music in earphones or reading. The delay time corresponds to the time needed to take the decision of evacuating and the activities prior to evacuation. When passenger evacuation is realised inside a tunnel, there is a need to ensure that crew procedures are adequate to allow the safe egress of passengers under variety conditions. The visibility conditions inside the tunnel can be a decisive factor in the evacuation process. Based on studies of evacuation under low visibility conditions [4–7], it is possible to conclude that people: reduce their walking speed, tend to take known routes, search for walls trying to maintain a contact and using them as a guide during their movements as well as trying to maintain physical contact with the people in front of them, and go towards lighted zones.

2 Evacuation Cases

For the present study two high speed trains were selected. The first train (train A) has an overall length of 200 m, two locomotives and 12 passenger coaches and carries 318 passengers. The second train (Train B) has an overall length of 200 m, 8 passenger coaches and carries 404 passengers. The evacuation cases proposed in this study correspond to the following fire scenarios:

- **Scenario 1:** fire inside passenger area at the end front passenger coach
- **Scenario 2:** fire inside passenger area at the rear end passenger coach
- **Scenario 3:** external fire in the middle section of train
- **Scenario 4:** external fire at the rear end of the train

In a train with a fire onboard there is no possibility of evacuating towards the exterior, the strategy consists in moving away from the fire inside the trains. The first situation analysed was the study of movement and the passengers' response when detecting a fire inside the train. The location of the fire have influence on the route chosen by passengers when evacuating. It is assumed the passengers inside the affected coach and the adjacent coach moved towards a third coach considered as a safe place. Fire scenarios 1 and 2 are considered for both trains. On the other hand, in order to analyse the evacuation conditions in high speed trains, three different cases were selected based on the fire scenarios previously described.

- **Case 1** (Scenarios 1 and 2): due to the immediate stop of the train, the passengers have to evacuate down to the railway embankment [8] through one or two emergency ladders.
- **Case 2** (Scenarios 1 and 2): once the fire is detected, the train should be possible to operate during 15 min until reaches a suitable zone (platform)

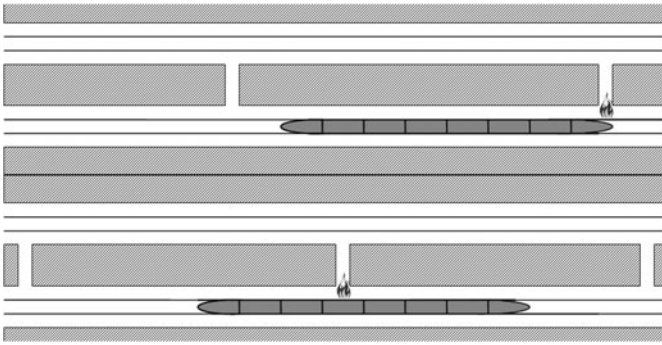


Fig. 1. Position of train and location of fire in case 3.

for evacuation [9, 10]. In this case it is assumed that the evacuation is only on one side of the train and the fire exposed and adjacent passenger coaches were empty.

- **Case 3** (Scenarios 3 and 4): the analysis was focused on train B which stopped inside a twin bore tunnel due to the external fire event. The passengers have to leave the affected tunnel through cross-passages between 250 m to reach a safety parallel tunnel. The position of train and fire scenarios considered for this case are shown in Fig. 1.

3 Input Data

It was considered that the aisle of the passenger coaches as well as the exits of both trains had a capacity of one person per unit of time. A full occupancy (100%) was considered taking into account the available seats. To reproduce the behaviour of passengers when detecting a fire inside the train, different walking speed and response times were introduced in the model. In the first simulations the parameters were assigned in a deterministic way with an unimpeded walking speed for all passengers of 0.628 m/s and a minimum response time of 30 s for passengers close to fire source and the response time for the rest of passengers was assumed to have a “domino effect” thus, increasing the response time depending on the distance from fire. In addition to these simulations, additional simulations were performed using a random delay time by uniform distribution between 30–60 s for passengers in fire exposed coach and 75–105 s for passengers in adjacent coach and individual walking speeds for passengers range from 0.80–1.35 m/s. In case 1 and case 2 all the passengers in queue waiting to be evacuated were assumed to have a collective behaviour. No delay time and the same walking speed (0.628 m/s) for all passengers were considered. Additionally, for case 2 premovement times were considered (uniform distribution) with minimum value of 15 s and maximum value of 45 s assuming that passengers were warned about the emergency when the train

Visibility	INPUT data
Normal	Horizontal walking speed: from 0.8 to 1.35 m/s Evacuation platform capacity 2 person/t
Low	Horizontal walking speed: 0.628 m/s Evacuation platform capacity 2 person/t
Limited	Horizontal walking speed: 0.628 m/s. Evacuation platform capacity 1 person/t
Scarce	Horizontal walking speed: 0.314 m/s. Evacuation platform capacity 1 person/t

Table 1. Inputs under different visibility conditions inside the tunnel.

stopped. In case 3 the delay time uniform distribution was assigned with a minimum value of 45 s and maximum of 75 s. To reproduce the low visibility conditions inside the tunnel, the walking speed and the width of the evacuation platform were modified. Table 1 outlines the inputs chosen to model the different visibility conditions inside the tunnel.

4 Evacuation Results

Attained results allowed to have an approach of to the total times required for passengers evacuation in both trains and also valued the safety conditions in which this evacuation conditions were performed.

4.1 Movement Inside the Train

In train A Scenario 1, the results of the model indicated that the travelling time required for passengers to reach a safe place was between 1 min and 58 s and 2 min. In this scenario the last passenger was exposed to the harmful effects of fire between 67 and 75 s from the start of the fire. In Scenario 2 the number of passengers involved was higher than the results above but the time required to evacuate the fire exposed passenger coach and the adjacent coach was not much higher (between 2 min and 10 s and 2 m and 21 s). In train B Scenario 1, the fire exposed passenger coach was fully evacuated between 92 and 107 s. In Scenario 2, passengers needed between 3 min and 32 s and 3 min and 41 s in their movement towards a safe place. In this Scenario the last person to evacuate remained exposed to the harmful effects of fire for 99 s. The results showed that the individual evacuation inside the train depend on the interior configuration of passenger coach and the density levels. The initial passengers travelling in aisles move at their maximum fast walk rate but later the movement depends on the density of occupancy. The passengers, provided from the fire passenger coach, increased the density of people in the adjacent passenger coach. The passengers seated in the adjacent coach, could not enter the aisle, occupied by other persons. The movement time of passengers was determined for the high-density levels between 1.5 and 3.5 persons/m².

Train	Fire scenario	Evacuation times (mm:ss)	
		1 emergency ladder	2 emergency ladders
Train A	Scenario 1	5:25	2:59
	Scenario 2	5:26	3:11
Train B	Scenario 1	6:37	4:16
	Scenario 2	6:34	4:28

Table 2. Evacuation times for case 1.

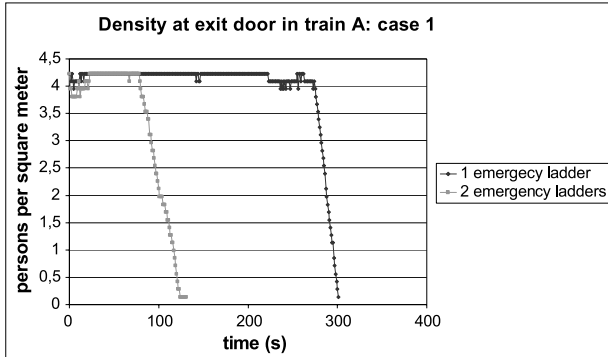


Fig. 2. Density of persons at exit door in train A.

4.2 Evacuation of the Trains

The results of case 1 are exposed in Table 2 showing an important reduction in the evacuation times with the introduction of an additional exit ladder. In train A, Scenario 1 the evacuation time was reduced approximately by a half (45.8%); the Scenario 2 also showed a significant reduction (41.4%).

The passengers moved along the interior of the train to access the exits, thus increasing the time inside the passenger coaches when getting close to the exits. Inside train A, with one emergency ladder, a situation of permanent crowding occurred during 5 minutes approx. thus, reaching values higher than 4 persons/m² as it is shown in the curve of the graph in Fig. 2. When considering two exits doors, the density levels were the same but the passengers were under these conditions for lower time (1.5 minutes).

The time reported in Table 3 is the one it takes the passengers to exit the train once the doors are opened for case 2. The results showed the need to warn passengers before the train stop. In this situation all passengers in queue waiting to be evacuated were assumed and the evacuation well-organised was more effective.

In case 3 total evacuation times obtained inside the tunnel under different visibility conditions for Scenario 4 oscillated between 9 min 04 s and 22 min 55 s. Under limited and low visibility conditions in which the passengers maintained contact to the tunnel walls, the movements were organised and evacuation times were not significantly higher than those obtained under normal

Train	Number of passengers	Scenarios	Last passenger leaves the train (sec)	
			No delay	Delay (15-45 sec)
A	318	Scenario 1	50	81
		Scenario 2	51	84
B	404	Scenario 1	93	118
		Scenario 2	74	109

Table 3. Evacuation times for case 2.

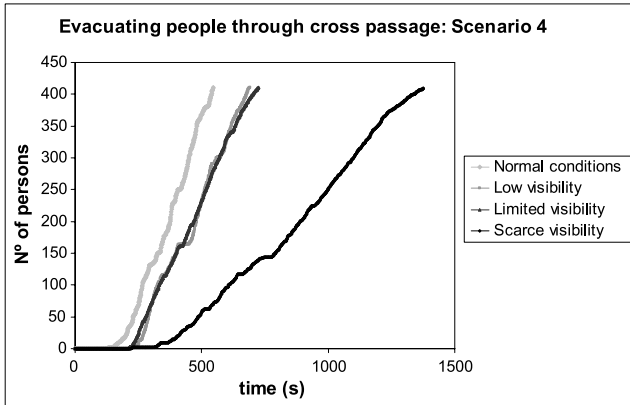


Fig. 3. Evacuating people through cross passage: Scenario 4.

conditions where there was more available space and passengers evacuated in an uncontrolled way as it can be observed in the Fig. 3.

5 Conclusions

Diverse evacuation cases of four fire scenarios were considered. In a train with a fire onboard and when there was no possibility of evacuating towards the exterior, results were very similar despite of having considered different response times of passengers to fire and a relative short time of passengers exposure to fire were obtained. In case 1 the use of two emergency ladders reduced the evacuation times and minimised the risks for passengers. In this case a proper training of the crew to manage different emergency situations is essential as well as an appropriate management of flows of people in order to reduce congestions and overcrowd when the passengers try to reach an exit. In case 2, the time in which the train continues operating during the fire as well as the pre-movement time of passengers are crucial for passengers safety. In case 3, the time spent by passengers to leave the contaminated tube inside the tunnel is crucial for the people safety. The disposition of train respect to the cross passages and the location of fire respect to the rail vehicle were decisive factors in the evacuation process. For this case of study pre-movement

times and different visibility conditions were simulated. The results showed the advantages of evacuation under controlled conditions or handled by the crew compared to a self-rescue strategy in emergency situations with reduced visibility conditions to prevent passenger risks.

References

1. M. MacDonald, STEPS Simulation of Transient and Pedestrian Movements User Manual, unpublished, available with egress model from Mott MacDonald.
2. J.L. Bryan, Behavioral response to fire and smoke, *The SFPE Handbook of Fire Protection Engineering*, Third Edition. Society of Fire Protection Engineers, Bethesda, 2002. Chapter 12.
3. E.R. Galea and S. Gwynne, Evacuation an overturned smoke filled rail carriage. *Fire and Materials*, vol. 24, Issue 6, 2000, pp. 291–302.
4. T.J. Shields and K. Boyce, Towards developing an understanding of human behaviour in fire tunnels, 3rd International Symposium on Human Behaviour in Fire, Belfast, 2004.
5. J.H. Park et al., Development of an agent-based behaviour module for evacuation models-focused on the behaviours in the dark, *Pedestrian and Evacuation Dynamics 2005*, Vienna, 2005.
6. S. Gwynne, E.R. Galea, P.J. Lawrence, and L. Filippidis, Modelling occupant interaction with fire conditions using the building EXODUS evacuation model. *Fire Safety Journal*, vol. 36, Issue 4, 2001, pp. 327–357.
7. H. Frantzich and D. Nilsson, Evacuation experiments in smoke filled tunnel, 3rd International Symposium of Human Behaviour in Fire, Belfast, 2004.
8. P. Kagendal and D. Nilson, Fire safety on intercity and interregional multiple unit trains, Sweden, 2002. Department of Fire Safety Engineering, Lund University.
9. Commission Decision concerning the technical specification for interoperability relating to the rolling stock subsystem of trans-European high speed rail system referred to in Article 6 (1) of Directive 96/48/EC', 2002. Official Journal of The European Community, L 245/402.
10. EN 45545, Fire resistance requirements for fire barriers and partitions. Fire protection on railway vehicles. Brussels, 2004. European Committee for Standardisation—CEN, Part 3.

Pedestrian Dynamics with Event-Driven Simulation

Mohcine Chraibi¹ and Armin Seyfried²

¹ Technical University Hamburg-Harburg, 21071 Hamburg, Germany

e-mail: mohcine.chraibi@tu-harburg.de

² Central Institute for Applied Mathematics, Research Centre Jülich, 52425 Jülich, Germany

e-mail: a.seyfried@fz-juelich.de

Summary. The social-force model is systematically modified to achieve a satisfying agreement with the fundamental diagram. Furthermore, our modification allows an efficient computation of the simulation. Finally, different simulation-results will be compared to empirical data.

1 Introduction

Microscopic models are state of the art for computer simulation of pedestrian dynamics. The modeling of the individual movement of pedestrians is used to design a description of macroscopic pedestrian flow which allows e.g. the evaluation of escape routes, the design of pedestrian facilities and the study of more theoretical questions. For a first overview see [1–3]. One primary test, whether a model is appropriate for a quantitative description of pedestrian flow, is the comparison with the fundamental diagram [4–7].

2 Social-Force Models

2.1 General Considerations

The social-force model was introduced in [8]. It is expressed by the equation of motion

$$m_i \frac{d^2 x_i}{dt^2} = m_i \frac{dv_i}{dt} = F_i = F_i^{\text{drv}} + F_i^{\text{rep}} + \text{fluctuations}, \quad (1)$$

where x_i is the position of the i th pedestrian, v_i its velocity and m_i its mass.

$$F_i^{\text{rep}} = \sum_{j \neq i}^n F_{ij}^{\text{rep}}(x_j, x_i, v_i), \quad n \in \mathbb{N} \quad (2)$$

is the force due to interaction with other pedestrians. In the original model the introduction of the repulsive force F_i^{rep} between pedestrians is motivated by the observation that pedestrians try to keep distance to others to secure their ‘private sphere’. This behavior is also observed for the environment, i.e. pedestrians do not walk too close to walls and stairs. F_i^{drv} is a driving term that makes the pedestrians attempt to move with their intended velocity.

The term *fluctuations* is added to take into account random variations of the behavior of pedestrians. Additionally *fluctuations* arise from deviations from the usual rules of motion. This term becomes important in high density situations [8].

2.2 Simplified One-Dimensional Realization

For the modeling of pedestrian dynamics the pedestrians are represented by one-dimensional ‘circles’ with velocity dependent length d_i and position (of the center of mass) x_i moving in a continuous space.

An important aspect is the dependency between the current velocity and the required space of pedestrians [9]. As mentioned in [10] it is possible, on basis of empirical results, to determine the required length d_i for the i th pedestrian, that moves in a single file with a velocity v_i , with $0.1 \text{ m/s} < v_i < 1.0 \text{ m/s}$:

$$d_i = a + bv_i \quad \text{with } a = 0.36 \text{ m and } b = 1.06 \text{ s.} \tag{3}$$

One fundamental quantity in the model is the distance between the i th pedestrian and the j th pedestrian which is defined as:

$$\text{dist}_{i,j}(t) = \Delta(x_{i,j}) - \frac{d_i + d_j}{2} \tag{4}$$

with $\Delta(x_{i,j}) = |x_i - x_j|$ the distance between the center of mass of the i th pedestrian and the j th pedestrian. $|\cdot|$ denotes the absolute value in \mathbb{R} .

The velocity v_i and the centre of mass x_i are calculated by integrating (1) once and twice, respectively.

For simplicity *fluctuations* in (1) are neglected and thus the forces are reduced to a driving and a repulsive term $F_i = F_i^{\text{drv}} + F_i^{\text{rep}}$. It is assumed

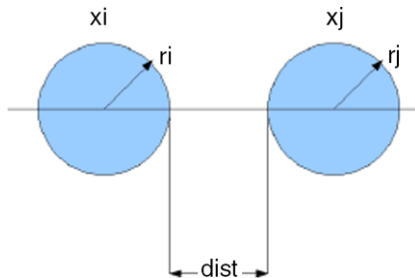


Fig. 1. Illustration of two pedestrians.

that in the one-dimensional case a pedestrian only interacts with the man directly in front. Consequently (2) reduces to

$$F_i^{\text{rep}} = F_{i,i+1}^{\text{rep}}(x_{i+1}, x_i, v_i). \tag{5}$$

According to [8] we choose the driving term

$$F_i^{\text{drv}} = m_i \frac{v_i^0 - v_i}{\tau}, \tag{6}$$

where v_i^0 is the intended velocity of the i th pedestrian and τ is the acceleration time. For simplicity we set $v_i^0 > 0$, $x_{i+1} > x_i$ and $m_i = 1$. The repulsive force is modeled as:

$$F_i^{\text{rep}}(t) = \begin{cases} -\frac{v_i(t)}{\tau} & \text{if } (dist_{i,i+1}(t) \leq \alpha \wedge \frac{d(dist_{i,i+1})}{dt} < 0) \\ & \vee (dist_{i,i+1}(t) > \beta \wedge \frac{d(dist_{i,i+1})}{dt} > 0), \\ 0 & \text{otherwise.} \end{cases} \tag{7}$$

The quantities α and β are chosen such that $\alpha < \beta$. To avoid the case where two pedestrians pass each other, we assume that the i th pedestrian stops once she/he is in contact with the pedestrian in front, i.e. $dist_{i,i+1} = 0$.

3 Motivation for Event-Driven Simulation

An event is a single occurrence of a change in the forces acting on a pedestrian e.g. when the i th pedestrian comes ‘too close’ to the pedestrian in front, the force F_i changes at a special time— t_{event} —from F_i^{drv} to $F_i^{\text{drv}} + F_i^{\text{rep}}$. The search for eventually occurring events is performed stepwise with a time bound Δt . It should not be so small as to make the simulation run too long, nor should it be so large as to make the number of events unmanageable. Since the forces acting on the pedestrians do not change between two events (event1 and event2), one can integrate (1) from t_{event1} to t_{event2} to calculate the velocity and the position of the pedestrians in the interval $[t_{\text{event1}} \ t_{\text{event2}}]$. This approach uses a list of events that occur at various times, and handles them in order of increasing time. The simulation makes time ‘jump’ to the time of the next event. The simulation proceeds event-by-event rather than step-by-step.

4 Event-Driven Simulation with Velocity-Adaptation

The pedestrians shall adjust their actual velocity in such a way that they keep a minimum distance to the pedestrian in front. Again the forces are only influenced by actions in front of a pedestrian. At the moment where the distance between the i th pedestrian and the pedestrian in front reaches

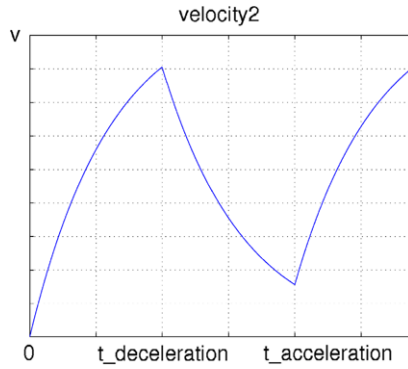


Fig. 2. The variation of the velocity of a pedestrian.

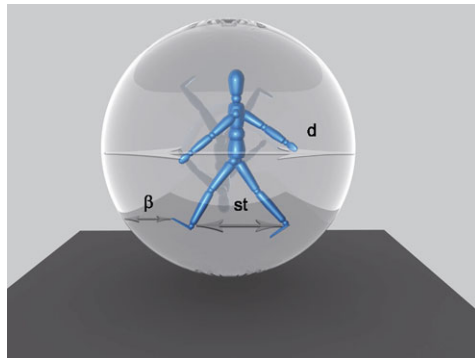


Fig. 3. Illustration of α , β and d .

decreasingly α , the i th pedestrian is subject to the repulsive force (7). This leads to a reduction in the velocity v_i . Once the distance between the i th pedestrian and the pedestrian in front reaches increasingly β the action of (7) vanishes. The velocity of the i th pedestrian increases again.

As the required length d is modeled as a linear function of the velocity, the quantities α and β are chosen to be linearly velocity-dependent. β is defined as the difference between the required length d_i and the step-length $st_i(t)$ of the i th pedestrian and α as $\frac{\beta}{2}$. See Fig. 3.

Because of

$$st_i = st_a + st_b v_i \quad \text{with } st_a = 0.235 \text{ m and } st_b = 0.302 \text{ s} \quad (8)$$

according to [11] and (3) one gets the complete definition of $\beta = \beta_a + \beta_b v$ ($\beta_a = 0.125 \text{ m}$, $\beta_b = 0.758 \text{ s}$) and thus of $\alpha = \alpha_a + \alpha_b v$ ($\alpha_a = 0.0625 \text{ m}$, $\alpha_b = 0.392 \text{ s}$).

From the definition of the repulsive force (7) one recognizes that times, at which the distance between two pedestrians is 0, α or β , are times where

events occur, i.e. at those times force-variations happen. To calculate those events, one solves the equation:

$$dist_i(t) = \zeta, \quad \zeta \in \{0, \alpha, \beta\}. \tag{9}$$

5 Results

To compare the model result with the empirical fundamental diagram of the single-file movement [10], a periodic passageway of length $L = 17.3$ m is selected. The values for the intended velocity v_i^0 is distributed according to a normal-distribution with a mean value of $\mu = 1.24$ m/s and $\sigma = 0.05$ m/s. According to Helbing [8], $\tau = 0.61$ s is a reliable value.

For every run at $t = 0$ all velocities are set to zero and the pedestrians are uniformly distributed. After 300 s relaxation, measurement are performed 300 s long. The determination of velocity mean value over all pedestrians is done after every event-evaluation.

Figure 4 presents the dependency between mean velocity and density for different approaches to the velocity function (with and without adaptation). To demonstrate the influence of the velocity dependence of the required length different values for the parameter b were selected. With $b = 1.06$ s and the repulsive force (7) a good agreement at low densities between the velocity-density relation predicted by the model and the empirical fundamental diagram is obtained. However at high densities the velocity-density relation predicted by the model is inaccurate.

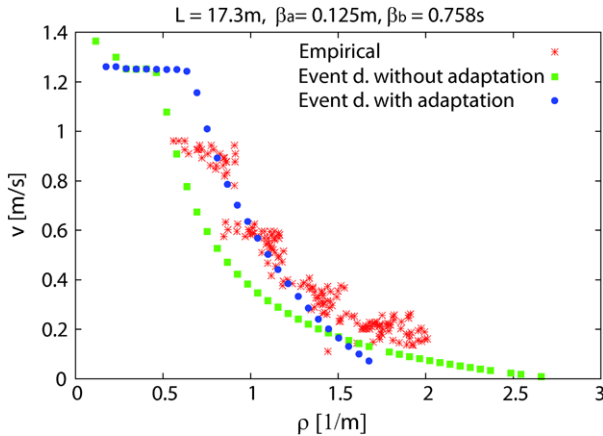


Fig. 4. Results: The fundamental diagram.

6 Discussion and Summary

From the empirical fundamental diagram one determines $b = 1.06$ s and $a = 0.36$ m [10]. The parameters for the step-length st are also empirically known [11]. Thus the only free parameter of the model is α . The concept of velocity adaptation and the empirically known parameters lead to a good agreement with the fundamental diagram at low densities if one chooses $\alpha = \frac{\beta}{2}$.

However at high densities one observes a discrepancy between the obtained results and the fundamental diagram. This can be explained by the fact, that at high densities the reaction-time and the behavior of pedestrians becomes more random so that the deterministic character of the model does not reflect the stochastic behavior of the pedestrians anymore. An improvement of the model should include a stochasticity in the reaction-time of pedestrians and determining an appropriate ratio of α to β (here it was set to $\frac{1}{2}$).

References

1. M. Schreckenberg and S. D. Sharma, (Editors). *Pedestrian and Evacuation Dynamics*. Springer, Berlin, 2001.
2. E. R. Galea, (Editor). *Pedestrian and Evacuation Dynamics 2003*. CMS Press, London, 2003.
3. N. Waldau, P. Gattermann, H. Knoflacher, and M. Schreckenberg (Editors). *Pedestrian and Evacuation Dynamics 2005*. Springer, Berlin, 2006.
4. T. Meyer-König, H. Klüpfel, and M. Schreckenberg. Assessment and analysis of evacuation processes on passenger ships by microscopic simulation. In E. R. Galea (Editor). *Pedestrian and Evacuation Dynamics 2003*, CMS Press, London, 2003, p. 297.
5. A. Kirchner, H. Klüpfel, K. Nishinari, A. Schadschneider, and M. Schreckenberg. Discretization effects and the influence of walking speed in cellular automata models for pedestrian dynamics. *J. Stat. Mech.*, paper P10011, 2004.
6. S. P. Hoogendoorn and P. H. L. Bovy. Nonlocal continuous-space microscopic simulation of pedestrian flows with local choice behavior. *Transp. Res. Rec.*, 1776:201–210, 2001.
7. RIMEA-Richtlinie für Mikroskopische Entfluchtungs-Analysen. www.rimea.de.
8. D. Helbing and P. Molnar. Social force model for pedestrian dynamics. *Phys. Rev. E*, 51:4282–4286, 1995.
9. A. Seyfried, B. Steffen and Th. Lippert. Basics of modelling the pedestrian flow. *Physica A*, 368(1):232–238, 2006.
10. A. Seyfried, B. Steffen, W. Klingsch, and M. Boltes. The fundamental diagram of pedestrian movement revisited. *J. Stat. Mech.*, paper P10002, 2005.
11. U. Weidmann. *Transporttechnik der Fussgänger*. Schriftenreihe des IVT 90, ETH Zürich, 1993.

Part III

Psychology

The Need for Behavioral Theory in Evacuation Modeling

Erica D. Kuligowski¹ and Steve M.V. Gwynne²

¹ National Institute of Standards and Technology, 100 Bureau Drive, Stop 8664, 20899-8664 Gaithersburg, USA

e-mail: erica.kuligowski@nist.gov

² Hughes Associates, Inc., 3515 28th st # 307, 80301 Boulder, USA

e-mail: sgwynne@haifire.com

Summary. This paper posits the need for a complete, comprehensive conceptual model about human behavior in fire evacuations. This would be of intrinsic value to improve training, education, and future data collection efforts, but would also allow for a complete behavioral representation to be embedded within simulation tools. This paper begins by discussing the current, separate theories or “behavioral facts” extracted from research on evacuations from building fires. Then, the paper discusses the methods used by current computer evacuation models to simulate these “behavioral facts” and the limitations of these methods. Last, the paper argues for the inclusion of a comprehensive behavioral conceptual model in computer evacuation models, specifically by highlighting the benefits of behavioral theory for evacuation models and providing examples of social theories used to predict whether people will evacuate from disasters in communities.

1 Introduction

The rapid increase in computer capability and decrease in monetary cost has expanded the use of computer models in all fields of engineering. This is particularly true for evacuation models. Developers are consistently creating and updating evacuation models to simulate and visualize larger and more complex structures. These models are based on movement and behavioral data in order to simulate how occupants evacuate from buildings on fire. However, there is one particular aspect that is continually missing from computer evacuation models: the ability to *accurately* and *comprehensively* simulate human behavior in fire [1]. To do this would require a complete behavioral conceptual model to be embedded within the simulation tool.

It is suggested here that instead of simulation tools being based on the piece-meal inclusion of “behavioral facts” or theories, as they are currently, they should instead be based on a comprehensive conceptual model of how people move and behave during building fires. Evacuation models currently

include comprehensive theory on how people *move* during evacuations [2–6], including equations from this type of data [7], graphical representations of speed and flow with density [4, 7], and even data that accounts for occupants with disabilities [8] or other impairments. However, there is an absence of a comprehensive theory on how people behave during fires.

This paper posits the need for a complete conceptual model of human behavior in fire evacuations. These would be of intrinsic value to improve training, education, and future data collection efforts, but would also allow for a complete behavioral representation to be embedded within simulation tools for use in performance-based design. Without this conceptual model, evacuation models rely on user assumptions and model simplifications about occupant behavior that are unrealistic and can produce inaccurate results, as will be explained in this paper. In cases where assumptions lead to the unrealistic *reduction* in evacuation results, buildings or procedures are designed according to an unrealistic calculation of the required egress time which can lead to insufficient egress routes and fire protection systems in the building, inadequate notification systems, and/or unsafe procedures; putting lives at risk. In other cases, where assumptions in evacuation models lead to the use of an unnecessarily large safety factor, buildings may be designed with a higher-than-needed level of safety and an overly expensive cost to the building owner.

This paper begins by discussing the “behavioral facts” extracted from research on evacuations from building fires. Then, the paper discusses the methods used by current computer evacuation models to simulate these “behavioral facts” and the limitations of these methods. Last, the paper argues for the inclusion of a comprehensive behavioral conceptual model in computer evacuation models, specifically by highlighting the benefits of behavioral theory for evacuation models and providing examples of social theories used to predict whether people will evacuate from disasters in communities.

2 “Behavioral Facts”

Currently, in the field of human behavior in fire, “behavioral facts” have been obtained from a variety of incidents about what people do in fires [9]. These “facts” represent key points that explain separate behaviors in fire evacuation. However, there has been little attempt to connect all of these “behavioral facts” and develop an overarching, complete conceptual model for human behavior in fire. These “facts” therefore remain as isolated key statements used in current egress analysis, rather than a coherent behavioral framework. When/if these statements are embedded within egress models and simulated in isolation, the results generated contain significant gaps in the simulated evacuee response.

There are specific “behavioral facts” that have been gleaned from research into evacuation from building fires and community disasters. First, when a fire

event occurs in a building, people's initial response is to believe that they are safe [10, 11]. The phenomenon, known as normalcy bias, states that people in any type of crisis tend to initially interpret their situation as safe and secure [12]. When occupants are faced with ambiguous and/or inconsistent cues (i.e. cues that are difficult to understand or interpret), normalcy bias is likely to extend for longer periods of time while the occupants remain inside the building. *Behavioral fact #1: People's first instinct is to feel safe in their environment.*

When presented with ambiguous cues, people in building fires and other emergencies consistently attempt to gain additional information about what is going on [2, 9, 13–15]. People are likely to engage in information seeking activities, such as asking others, forming groups to discuss the situation (i.e. milling), investigating the building for the source of the event, and searching for information from media or Internet sources. In emergencies, people are “information hungry” and will make efforts to gain additional information, especially in situations that are unclear and/or confusing. *Behavioral fact #2: People will engage in information seeking actions, especially when cues are ambiguous and/or inconsistent.*

Generally, people in building fires act rationally and altruistically rather than being panic-stricken [9, 16]. Previous building fire and community disaster events have shown that people help others during evacuations, including looking for others inside the building, rescuing people from situations where they are trapped or injured, and assisting occupants out of the building and out of danger (e.g., carrying them down several flights of stairs). Also, people have shown that they will remain on their floor and fight the fire before the fire department arrives to save property and/or others from harm [15, 17, 18]. *Behavioral fact #3: People act rationally and altruistically during building fires.*

In addition to information seeking and helping others, occupants will also perform preparation activities before moving to the stair [2, 19]. These activities can include dressing or putting on their coat, gathering personal items, securing their office or residence, and obtaining items for longer stair travel (e.g., a change of shoes, a flashlight, and other supplies). *Behavioral fact #4: People are likely to engage in preparation activities before beginning their evacuation response (e.g., stair travel, elevator travel, etc.).*

Once people have decided to evacuate, they are likely to move to the familiar [20, 21]. Occupants are likely to traverse familiar routes in the building and move toward familiar exits (e.g., the elevator lobby) in a building fire or other emergency. *Behavioral fact #5: Once they begin evacuation movement, people move to the familiar.*

All of these actions and tendencies are likely to delay people from reaching safety and take certain periods of time to complete [2, 15, 22, 23]. All of these “behavioral facts” show that people are more likely to delay in a building fire rather than immediately and efficiently move to a position of safety outside (or even inside) of the building. Therefore, the “behavioral facts” provide

fire researchers with important information about what behaviors can occur during a building evacuation and that these behaviors result in significant delay times for occupants.

However, there is little or no understanding of why these behaviors occur. The evacuation modeling field is then left with only piece-meal “facts” or theories to use when incorporating the simulation of behaviors in a computer evacuation model. Without a complete behavioral conceptual model, evacuation model developers rely on the user to (or not to) include these separate, piecemeal “behavioral facts,” leading to the piecemeal simulation of disconnected behaviors, as discussed in the following section.

3 Building Evacuation Models³

Currently, there are over 40 different evacuation models [24, 25] available to users interested in simulating evacuations under a variety of circumstances (e.g., building configurations, evacuation procedures, and environmental conditions). Generally, these models simplify behavior during evacuations, if behavior is included at all. This section provides an overview of the three primary methods in which evacuation models simulate human behavior, includes examples from evacuation models and demonstrates potential problems with each method. The three methods are the following: (1) behavior is defined entirely by the user, (2) behavior is simulated based on a specific condition (if-then statements), and (3) behavior is simulated based on multiple conditions.

3.1 Behavioral Technique 1: The Behavior Is Defined Entirely by the User

The first way that behavior can be included in evacuation models is based entirely on user input. In this technique, the user defines the behavior before the simulation begins for an individual or a group in the building. The user assumes that the behavior is likely to occur (or even that it will definitely occur) at some point during the simulation. Through this technique the evacuation model is being used to specifically assess the consequence of a particular action rather than predicting whether the action will occur at all.

There are many examples of how a user defines behavior (both spatial and/or implicit⁴ behavior) from the models that currently exist. Examples of

³ All references for this section can be found in [24].

⁴ Spatial behavior is a behavior performed by the occupant that utilizes movement over some distance/area of the floor plan in the building (e.g., physically moving from one space on the floor plan to another) and implicit behavior [25] is behavior that is not overtly performed by the occupant, but accounted for by other means (e.g., simulating that all occupants wait at a location for a set period of time to account for actions that could be performed).

defined spatial behavior are: (1) the user can assign⁵ certain individuals or groups a lower unimpeded movement speed (e.g., EXIT89⁶, STEPS, ASERI) to simulate slower people, (2) the user can assign certain individuals or groups a route from point “A” to point “B” in the building to simulate route choice on their floor and/or through the building (e.g., Simulex, GridFlow, EXIT89), and (3) the user can assign a specific itinerary (a sequence of actions) or a specific action to an individual or group (e.g., CRISP, buildingEXODUS). The user can also define implicit behavior [25], i.e., accounting for actions that are not “physically” performed by the simulated occupants. Examples of defined implicit behavior are: (1) the user assigns time periods of delay/waiting (e.g., an actual time period of delay, a distribution of delay times, etc.) to individuals or groups to account for any actions that they might perform during the pre-evacuation or evacuation periods of a building fire (e.g., Simulex, EXIT89, GridFlow), and (2) the user defines a specific area of the stair that is blocked for a time period to simulate counterflow of individuals and fire fighters (e.g., EXIT89).

There are problems associated with this behavioral technique. No behavior is simulated without input from the user. The behavior simulated in the scenario is actually prescribed by the user rather than predicted by the model. Therefore, the user is required to have sufficient expertise to define the different actions that would take place in the scenario, as well as being required to assume that these actions take place even before understanding the other dynamics of the scenario that occur while the simulation is running (e.g., the fire spread, what other occupants are doing in the building, what the staff is doing, etc.). The user is required to be both an expert and a psychic; both of which cannot and should not be expected.

3.2 Behavioral Technique 2: The Behavior Is Simulated Based on a Specific Condition (if-then)

The second way that behavior can be included by evacuation models is to simulate a known behavior when the occupant encounters a specific condition. This technique is based on “if, then” statements; meaning that if an occupant encounters X, then s/he or the group will do Y. Even when using this technique, the user is still involved in enabling the capability of the “if, then” statements or even identifying the condition that may (probabilistically) or will (deterministically) prompt the action to occur. In this technique, both the evacuation model and the user play a role in simulating behavior.

⁵ The user can assign by manual (providing an actual value) or through probabilistic (providing a distribution or a probability) means.

⁶ Certain commercial entities, equipment, or materials may be identified in this document in order to describe an experimental procedure or concept adequately. Such identification is not intended to imply recommendation or endorsement by the National Institute of Standards and Technology, nor is it intended to imply that the entities, materials, or equipment are necessarily the best available for the purpose.

There are many examples of conditional behavior in current evacuation models. In this technique, there are simulated actions influenced by the building, environmental cues (i.e. smoke density and layer height), and/or the actions of other simulated individuals/groups. First, an example of an action influenced by the building includes: if an exit route is simple to traverse and/or if the route is memorable, then the occupant is likely to traverse this route to safety (e.g., BGRAF), in comparison with the other routes in the building. Examples of actions influenced by environmental cues include: (1) if the occupant is exposed to smoke that reaches an optical density of a certain level, s/he will redirect to another route (e.g., BGRAF, EXITT, CRISP), (2) if the occupant is exposed to smoke that reaches an optical density of a certain level, then s/he will stop “investigating” (e.g., EXITT), (3) if an occupant is exposed to specific levels of gases within the smoke layer, then s/he will slow his/her walking speed and may even become incapacitated (e.g., GridFlow, buildingEXODUS), and (4) if the occupant is exposed to smoke that reaches a certain extinction coefficient and/or smoke layer height, then s/he will crawl (e.g., buildingEXODUS).

Last, there are examples of actions that are influenced by other occupants in the building. These examples include the following: (1) if there is a specific threshold of people waiting at a current exit, then an occupant will redirect to another exit route (e.g., BGRAF, EXITT), (2) if an occupant is identified as sleeping or disabled (by the user), s/he will follow the movements made by able-bodied individuals (e.g., EXITT), and (3) if the “target” occupant in the current room has already been warned (or rescued), then the occupant will warn the rest of the household (destination equals room with most senior occupant) (e.g., CRISP offers several other conditions and actions to select for each scenario).

As with Technique 1, there are problems associated with the conditional simulation of behavior. As mentioned earlier, model users are required to either enable the capability of the “if, then” statement(s) or identify the conditions that will prompt these actions to occur, meaning that behavior is not predicted by the model, but again prescribed by the user. This requires a high level of expertise from the user. Also, this technique does not account for all possible actions that could occur in a building evacuation but rather only those are specified as conditional.

3.3 Behavioral Technique 3: The Behavior Is Simulated Based on Multiple Factors of Influence

Behavior can also be simulated based on multiple influential factors. Although the simulated actions are similar to those in Behavioral Technique 2 (e.g., choosing a route, turning back, helping others, and closing doors), these actions are individually chosen for occupants based on a series of factors throughout the evacuation. Factors can include information that the occupant knows

prior to the fire, what information is gathered during the event, and what others know in the building. The user's role in this technique involves providing occupant threshold values for many of the factors, such as crowding factors, initial knowledge of the best exits (e.g., BFIRES), smoke tolerance, and preference levels, such as preference to wait, crowding, etc. (e.g., BGRAF).

There are examples of behavior that is influenced by multiple factors. Exit route choice, for example, can be established by consensus of the occupants within a certain space in the building (e.g., BFIRES). Exit choice of the featured occupant is influenced by whether any occupants co-occupy the space with him/her, whether any other occupants have information that this occupant is not aware of (e.g., the best way out of the building), whether others in the space are injured or in need of help, and whether all occupants in the space agree on an exit route. Also, an occupant can choose an exit route choice (e.g., buildingEXODUS) based on a variety of different influences, including whether other occupants are nearby, the nature of the information about an exit provided by other occupants, the identity or the role of the occupant sharing information, and whether the exit provides an advantage (e.g., distance, environmental conditions); and will redirect to another exit based on the extinction coefficient of the smoke at the current exit, the occupant's knowledge of other exits, the known distance to other exits, and the likelihood of redirecting (from empirical fire data [17, 18]).

In Technique 3, behavior is included in the model based on multiple factors. Whereas some actions are simulated as a result of a multi-stage process model, others are simulated as a result of a variety of prioritized influences that prompt actions taken. Fire studies have shown that realistic behavior is the result of multiple factors rather than binary relationships [19, 26]. As with the other techniques, however, the user is required to provide threshold values for influential factors and/or enable the behavioral algorithm to run during the simulation, which limits prediction capabilities.

3.4 Summary

As shown by the three techniques, the current computer models attempt to simulate behavior during building fire scenarios. Evacuation models can simulate actions such as route choice, crawling, rerouting, moving at a slower speed, delay of response or stopping action, any kind of itinerary (spatial sequence of movement from one point to another), and even group sharing of information to make decisions on movement. These types of actions are likely to occur in building fire evacuations; however, the current models are essentially simulating separate "behavioral facts" rather than attempting to represent behavior based on a complete behavioral conceptual model.

There are significant consequences that result from a lack of a conceptual model of human behavior in fire for users, evacuation models, and those who judge evacuation results (i.e. the authority having jurisdiction). Currently,

without a conceptual model embedded within egress models, computer models are limited in how evacuation is simulated; often requiring users to provide a large amount of input data on occupant behaviors. In addition, users' understanding of human behavior in fire is also limited by the lack of theory, prompting greater emphasis on the simulation of isolated key statements and/or the use of default values provided by the evacuation model. Default values available to users, such as behavior on stairs (e.g., staggered stair movement in building EXODUS), behavioral patterns for specific occupant types (e.g., fire fighters in Simulex), and familiarity with the building (e.g., movement to the closest exit in Evacnet4), may encourage a more passive role on the part of the user and reduce the current, necessary preparation and analysis required by the user to run the simulation responsibly.

4 Benefits of Behavioral Theory

There are many benefits to the development of a comprehensive conceptual model for the field of human behavior in building fires. The inclusion of a conceptual model into computer evacuation tools will enable a comprehensive model that can actually *predict* occupant behavior in a building fire based only on initial input. A computer model that incorporates a complete behavioral conceptual model would be able to predict situations rather than engineer an outcome based heavily on user input. A conceptual model will reduce the burden placed on users of evacuation models and rely on the model to simulate behavior during an event. Additionally, a comprehensive behavioral model of building evacuations illustrates where more data needs to be collected in order to truly understand human behavior in future fire evacuations.

Researchers in the field of disasters have been developing conceptual models for human behavior in response to community-wide disaster events for decades [14, 27, 28]. These can provide a roadmap to the development of conceptual models for occupant evacuation from building fires. Disaster researchers have developed theories to predict whether a member of a community will evacuate in response to a (or several) community-wide warnings. Data, collected (e.g., survey techniques) and analyzed (e.g., regression models) via quantitative methods, are used to identify those factors that influence certain stages of warning response, including whether a person believes the warning message, whether he/she feels at risk in the face of the incoming disaster, whether he/she confirms the warning by asking or seeking additional information about what is going on, and eventually whether the person evacuates his/her home or business based on the warning message. From a comprehensive understanding of human behavior, as shown in Fig. 1, quantitative computer models can then be developed to predict whether a person evacuates the community when warned to do so.

In addition to creating more improved evacuation models, conceptual models similar to Fig. 1, can help to improve evacuation response in the event

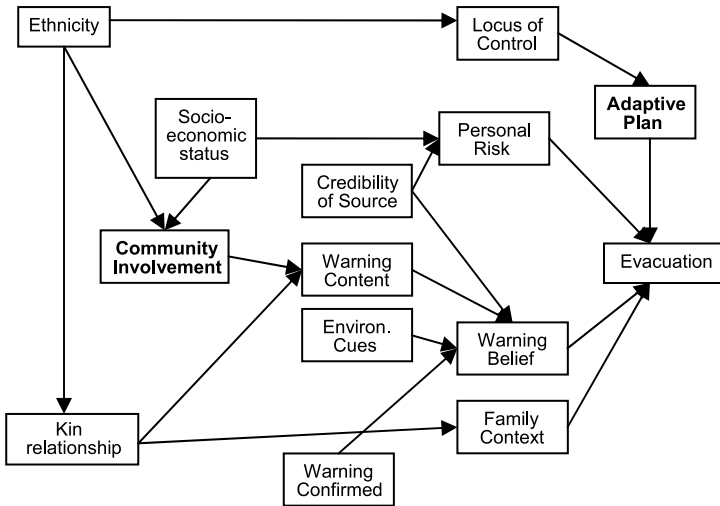


Fig. 1. Conceptual model for predicting whether a member of a community will evacuate or not [29].

of future disasters. By understanding which factors influence evacuation response, steps can be taken to improve community (or building-wide) disaster readiness before any type of event occurs. For example, emergency officials can stress the importance of having an evacuation (adaptive) plan for disasters at home or for the office. Also, emergency officials, by understanding that community involvement influences effective warning response, can plan community-wide (or building-wide) social events so that members of a community (or building) can meet one another. These factors, bolded in Fig. 1, can be implemented beforehand and may help to elicit an effective evacuation response when a disaster actually does hit a community.

Once a disaster occurs, steps can also be taken at the community-level to positively influence evacuation behavior. For instance, emergency managers in charge of developing the warning message can positively influence evacuation by crafting the message content in a certain way and providing a credible person or group (e.g., the fire department) to deliver the message to the community. These factors, in addition to allowing for the creation of an improved evacuation model, can inform local and community officials on how to better their community evacuation in response to future events.

5 Conclusion

There is a need in the field of computer evacuation modeling for a comprehensive conceptual model of human behavior in fire to more completely simulate behavior during building evacuation scenarios. Currently, separate,

“behavioral facts” on human behavior in fire exist and are used to simulate behavior in computer evacuation models. Without a conceptual model, simulated behaviors will be partial and susceptible to inexpert judgments made on the part of the user. Evacuation models rely on user assumptions and model simplifications about occupant behavior that are unrealistic and can produce inaccurate results. These inaccurate results can lead to unsafe building designs and procedures (in the event that evacuation times are underestimated) and/or to the assignment of inappropriate and unfounded safety factors which can unnecessarily increase the cost of buildings.

Finally, the paper investigates the theories from social science (e.g. the sociology of disasters) to demonstrate the construction of a conceptual model of human behavior in fire during building evacuations. This paper lays the foundation for a more comprehensive behavioral model that could then be directly implemented within a simulation model. A comprehensive (and predictive) model would then be less susceptible to significant behaviors being omitted and more sensitive to a range of influential factors, which in turn provides more accurate results for understanding occupant and building performance during a fire evacuation. Not only can a conceptual behavioral model serve as a blueprint for the development of a more comprehensive and accurate computer evacuation model, but can also provide guidance for future data collection efforts in the field of evacuation from building fires.

References

1. Santos, G. and Aguirre, B. E. (2004). A Critical Review of Emergency Evacuation Simulation Models. In *NIST Workshop on Building Occupant Movement During Fire Emergencies* (pp. 25–50). Gaithersburg, MD: NIST.
2. Proulx, G. (2002). Movement of People: The Evacuation Timing. In P. J. DiNenno and W. D. Walton (Eds.), *The SFPE Handbook of Fire Protection Engineering* (Third ed., pp. 3-341–3-366). Bethesda, MD: Society of Fire Protection Engineers.
3. Fahy, R. F. and Proulx, G. (2001). Toward Creating a Database on Delay Times to Start Evacuation and Walking Speeds for Use in Evacuation Modeling. In *2nd Int. Symp. on Human Behaviour in Fire* (pp. 175–183). London, UK: Interscience.
4. Pauls, J. (1995). Movement of People: The Evacuation Timing. In P. J. DiNenno and W. D. Walton (Eds.), *The SFPE Handbook of Fire Protection Engineering* (Third ed., pp. 3-263–3-285). Bethesda, MD: SFPE.
5. Fruin, J. J. (1987). *Pedestrian Planning and Design*. Mobile, AL: Elevator World. (Revised ed.)
6. Predtechenskii, V. M. and Milinskii, A. I. (1978). *Planning for Foot Traffic in Buildings*. New Delhi: Amerind.
7. Nelson, H. E. and Mowrer, F. W. (2002). Emergency Movement. In P. J. Denno and W. D. Walton (Eds.), *The SFPE Handbook of Fire Protection Engineering* (Third ed., pp. 3-367–3-380). Bethesda, MD: SFPE.

8. Boyce, K. E., Shields, T. J., and Silcock, G. W. H. (1999). Toward the Characterization of Building Occupancies for Fire Safety Engineering: Capability of Disabled People Moving Horizontally and On and Incline. *Fire Technology*, 35, 51–67.
9. Bryan, J. L. (2002). Behavioral Response to Fire and Smoke. In P. J. DiNenno and W. D. Walton (Eds.), *The SFPE Handbook of Fire Protection Engineering* (Third ed., pp. 3-315–3-340). Bethesda, MD: SFPE.
10. Aguirre, B. E. (2005). Emergency Evacuations, Panic, and Social Psychology: Commentary on ‘Understanding Mass Panic and Other Collective Responses to Threat and Disaster.’ *Article #402*. Newark, DE: University of Delaware, Disaster Research Center.
11. Quarantelli, E. L. (1991). Radiation Disasters: Similarities to and Differences from Other Disasters. *Preliminary Paper No. 153*. Newark, DE: University of Delaware Disaster Research Center.
12. Okabe, K. and Mikami, S. (1982). A Study on the Socio-Psychological Effect of a False Warning of the Tokai Earthquake in Japan. A Paper presented at the Tenth World Congress of Sociology, Mexico City, Mexico, August.
13. Fahy, R. F. and Proulx, G. (1997). Human Behavior in the World Trade Center Evacuation. In Y. Hasemi (Ed.), *5th Fire Safety Science* (pp. 713–724). London: Interscience Communications.
14. Mileti, D. S. and Sorensen, J. H. (1990). *Communication of Emergency Public Warnings: A Social Science Perspective and State-of-the-Art Assessment*. Oak Ridge, TN: Oak Ridge National Laboratory, U.S. Department of Energy.
15. Canter, D., Breaux, J., and Sime, J. (1980). Domestic, Multiple Occupancy and Hospital Fires. In D. Canter (Ed.), *Fires and Human Behaviour* (pp. 117–136). New York: Wiley.
16. Sime, J. D. (1980). The Concept of Panic. In D. Canter (Ed.), *Fires and Human Behaviour* (First ed., pp. 63–81). London: Wiley.
17. Bryan, J. L. (1977). Smoke as a Determinant of Human Behavior in Fire Situations (Project People). *Rep. No. NBS-GCR-77-94*. Washington, DC: National Bureau of Standards.
18. Wood, P. G. (1972). *Fire Research Note 953*. Borehamwood, UK: Building Research Establishment.
19. Averill, J. D., Mileti, D. S., Peacock, R. D., Kuligowski, E. D., Groner, N., Proulx, G., Reneke, P. A., and Nelson, H. E. (2005). Federal Building and Fire Safety Investigation of the World Trade Center Disaster: Occupant Behavior, Egress, and Emergency Communications. *Report NCSTAR 1-7*. Gaithersburg, MD: NIST. <http://wtc.nist.gov/NISTNCSTAR1-7.pdf>.
20. Sime, J. D. (1983). Affiliative Behaviour During Escaping to Building Exits, *Journal of Environmental Psychology*, 3, 21–42.
21. Gwynne, S., Galea, E. R., Owen, M., and Lawrence, P. (1999a). Escape as a Social Response. Report Published by the Society of Fire Protection Engineers.
22. Proulx, G. and Fahy, R. F. (1997). Time Delay to Start Evacuation: Review of Five Case Studies. In *5th Fire Safety Science* (pp. 783–806). London: Interscience Communications.
23. Proulx, G. (1995). Evacuation Time and Movement in Apartment Buildings. *Fire Safety Journal* 24:229–246.
24. Kuligowski, E. D. and Peacock, R. D. (2005). Review of Building Evacuation Models. *Report NIST TN 1471*. Gaithersburg, MD: NIST.

25. Gwynne, S., Galea, E. R., Lawrence, P. J., Owen, M., and L. Filippidis (1999b). A Review of the Methodologies Used in the Computer Simulation of Evacuation from the Built Environment. *Building and Environment* 34:741–749.
26. Proulx, G., Reid, I. M. A., and Cavan, N. R. (2004). *Human Behavior Study, Cook County Administration Building Fire, October 17, 2003, Chicago, IL*. Ottawa, Canada: National Research Council of Canada.
27. Perry, R. W., Lindell, M. K., and Greene, M. R. (1981). *Evacuation Planning in Emergency Management*. Lexington, MA: Lexington Books.
28. Perry, R. W. (1979). Evacuation Decision-Making in Natural Disasters. *Mass Emergencies* 4:25–38.
29. Perry, R. W. and Mushkatel, A. (1984). *Disaster Management: Warning Response and Community Relocation*. Westport, CT: Quorum Books. p. 39.

NO_PANIC. “Escape and Panic in Buildings”—Architectural Basic Research in the Context of Security and Safety Research

Christa Illera¹, Matthias Fink¹, Harry Hinneberg¹, Karin Kath¹,
Nathalie Waldau², Andrea Rosič¹, and Gabriel Wurzer³

¹ Institute of Architecture and Design, Vienna University of Technology,
Karlsplatz 13/253-3, 1040 Vienna, Austria

e-mail: cillera@email.archlab.tuwien.ac.at

² Waldau Engineering, Hackhofergasse 5/11, 1190 Vienna, Austria

e-mail: office@ibw-wien.at

³ Institute of Architectural Sciences, Vienna University of Technology,
Treitlstrasse 3/259-1, 1040 Vienna, Austria

e-mail: gabriel.wurzer@tuwien.ac.at

Summary. The increasing number of reported fires or other catastrophes (see Table 1) occurring in large events leads to the interesting question of why preventive design-related and organizational measures have not been taken. It also confirms the need to rethink existing building codes and safety concepts, as well as inclusion of new ways to optimize buildings and event sites. This research project “KEINE_PANIK”—“NO_PANIC” deals with planning criteria in regards to orientation in public buildings (such as airports, train stations, meeting halls or areas, concert halls, stadiums, etc.) during high-stress situations and its influence on the right choice of evacuation routes. The potentials of simulation-data optimizing the safety of persons in buildings must be included to the planning process, the same as the results of the different research groups should be applied in the three dimensional procedure of architectural design.

1 Motivation

Recent series of catastrophes gave us reason to think about *crowd dynamics* under stress and panic. What puzzles us is that even so there is a long time of research of *pedestrian dynamics*, preventive measures concerning building and organizations of mass gathering have not caught yet. It is our opinion that it is necessary for architects and planners to investigate three dimensional space in terms of the interaction of crowds under spatial constraints.

Year	City	Location	Casualties
2006	Manila-Pasig	Philsports arena TV show	88 dead, 600 injured
2004	Buenos Aires	Nightclub	169 dead, 375 injured
2003	Chicago	Event hall	21 dead, 100 injured
	Rhode Island	Nightclub	96 dead, 187 injured
2001	Volendam, NL	Discotheque	10 dead, 130 injured
2000	Lissabon	Nightclub	7 dead, 65 injured
	Roskilde, DK	Rock festival	9 dead, 26 injured
1999	Innsbruck	Bergisel stadium	5 dead, 25 injured
1989	Sheffield	Hillsborough stadium	96 dead, 200 injured
1985	Brussels	Heysel stadium	38 dead, 400 injured

Table 1. Timeline of recent catastrophes.

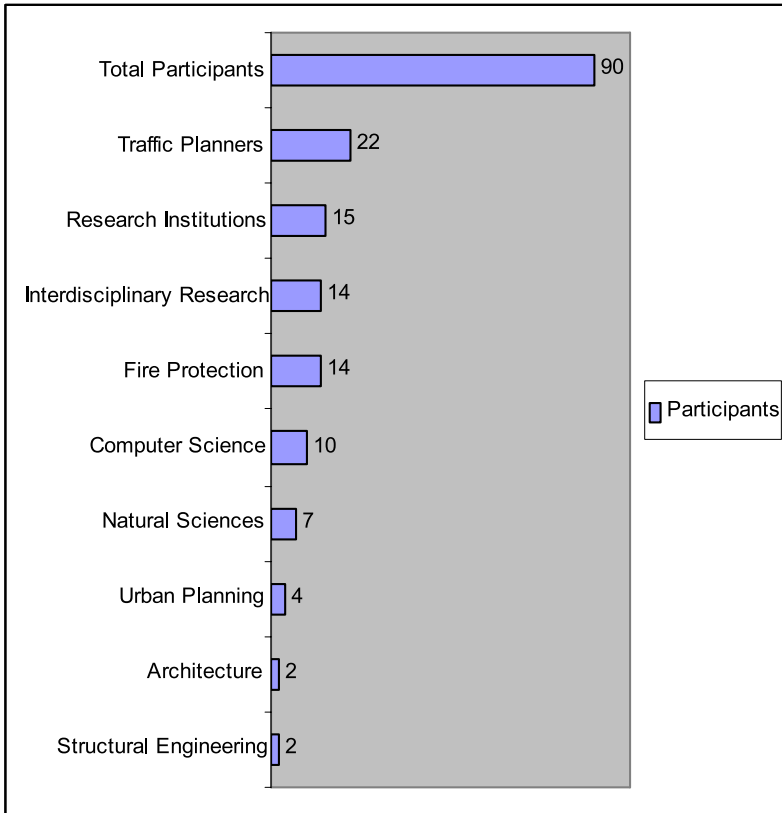


Fig. 1. Participants from PED 2005 in Vienna.

The number of participating architects in PED 2005 (see Fig. 1) clearly shows that egress planning is not a well-established research field in architectural sciences. Yet panic and stress originate in spaces, being the natural

action field of architects. We therefore argue for the need to translate the results from egress simulation and stress analysis into the language of architects and planners. It is their responsibility to consider these results in the planning process, and thus make building design safer.

2 The Five Dimensions of Architecture

As we have previously shown [1], architectural space can be described by five dimensions (also refer to Fig. 2):

- the first three dimensions (1D, 2D, 3D) build up the architectural form in space
- the fourth dimension, time, lets us perceive movements
- the fifth dimension describes the interaction between humans in time and space

Architectural solutions which try to mitigate the effects of panic must take into account all of these dimensions in order to work. For example, there is a recent debate whether people behave differently in a crowd than they do in free space, or as G. Keith Still puts it: “The ideas of a *group think* provokes heated debate among the psychologists. There are many psychological factors which influence human behavior, both in free space and in a crowd” [2]. Clearly, this takes the fourth and fifth dimension into account; however, it fails to include the actually implemented architecture.

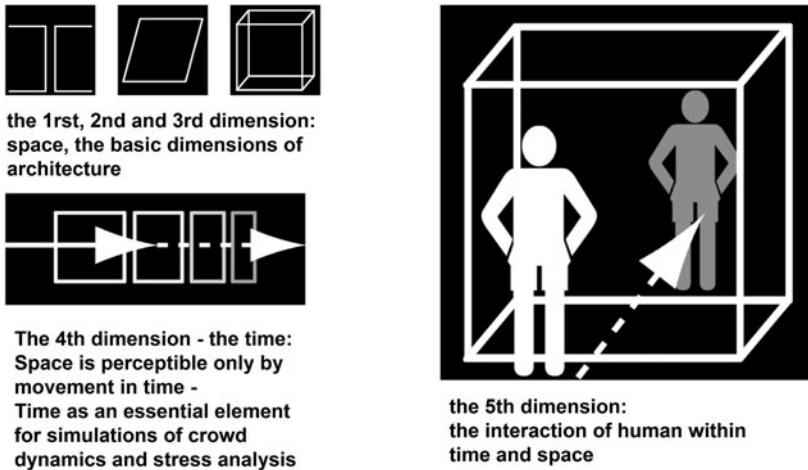


Fig. 2. The five dimensions of architecture.

3 Qualities vs. Quantities

Quantities in building design are easily measurable. This does, not apply to spatial qualities, which are difficult to name and complex to grasp. Quality factors from cognitive research and behavioral studies are the key to understanding user-specific aspects of building design.

As studies have shown [3], the experienced space is apparently perceived in the sequence ‘floor, wall, ceiling’ (see Fig. 3).

Spatial awareness and orientation within buildings is made possible by the five senses. Under stress and panic, there is a cognitive reduction [4] that acts on the evacuee. Even though exact data on the exact course of reduction of senses is still to be researched, we see a definitive decrease in cognitive ability as function of stress load (see Fig. 4a). People under pressure gradually lose four of their five senses, eventually leading to a tunnel vision with a reduced field of view (Fig. 4b). It is interesting to note that even healthy and young persons react like being mentally impaired in stress situations. As a matter of

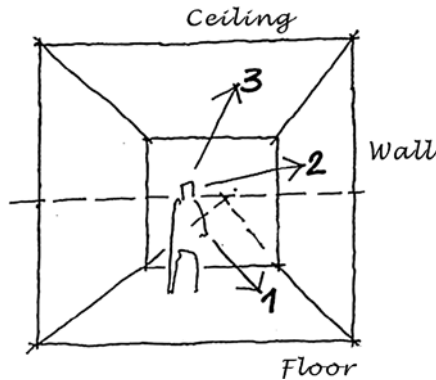


Fig. 3. Space is experienced in the sequence floor, wall, ceiling.

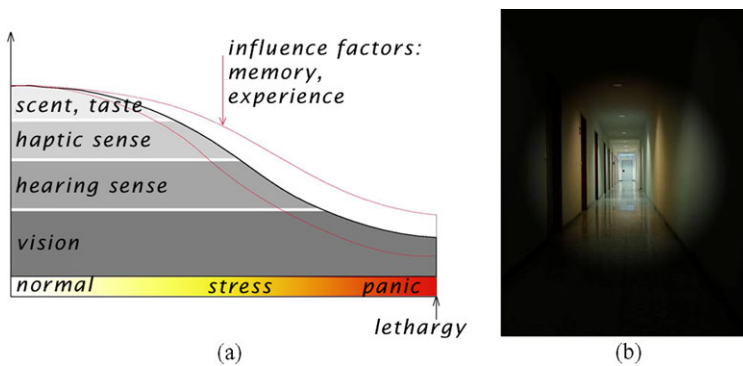


Fig. 4. a Pattern of cognitive reduction. b Tunnel vision.

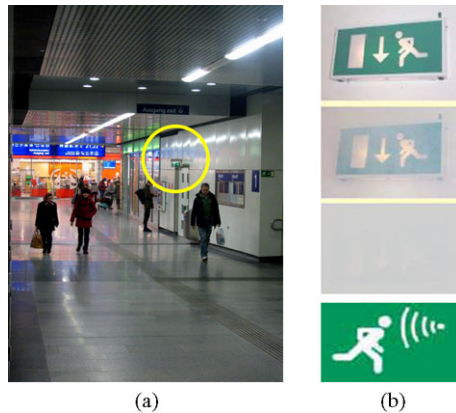


Fig. 5. **a** Spatial reality vs. escape signage. **b** “Little Green Man”.

fact, it is essential to make space intuitively perceivable, so that an evacuee can concentrate on simple, basic, understandable spatial structures.

4 Signage vs. Space

Deriving from the last section, we can say: If the signage is not supported by the architectural space, it will not be recognized in the case of stress or panic (see Fig. 5a). The space itself with all its dimensions tell the user how to flee and not the “little green man”, a small label mounted on the ceiling (see Fig. 5b). It can be assumed that especially in the case of panic humans are acting on instinct: the directionality of the space is clearly more compelling than the direction of the arrow. Furthermore, in the case of fire, smoke may seriously impair the visibility of such escape signage.

5 Towards Architectural Solutions that Support Egress

Every architectural measure concerning egress must be based on a clear and logical structuring of spaces as well as a intuitive sense of orientation originating in the building under consideration.

Figure 6 shows the example of such a solution: Taking into account the three dimensions, the staircase is clear and straight. To plan for the fourth dimension (crowd movement), the staircase is of reasonable width and has handles on either side. Finally, the fifth dimension is met by targeted lighting, aiding evacuees in path finding (crowd interaction under effects of tunnel vision). Consequently, the escape route becomes a bright sub-space within its parent space.



Fig. 6. Escape lighting for staircases.

It is, however, not enough to be safe—you must feel secure! Building codes, ordinances, and regulations prescribe design measures to ensure the safety of occupants entering and exiting buildings—again, however, only in terms of measurable dimensions such as escape route distances and width of door sizes. But the far more important are the qualitative design criteria regarding elements of architectural composition, which are rarely formulated. These qualities are what establish a sense—or feeling—of security as perceived by human beings by supporting a cognitive awareness of the correct escape route in emergency situations.

5.1 Avoiding Delays in Egress

Analysis shows that the perceived distance depends on number of intersections along the path [5]. Crossings delay orientation and exit ways with any number of intersections appear longer than equal-distant routes without any such intersections. This is due to the fact that exit routes with intersections contain more information, and therefore requires more time and effort to process. This of course means also a higher cognitive load for the user.

Furthermore, it was shown [6] that the human brain gets confused by frequent changes in direction or turnarounds. In consequence, orientation is delayed. Additionally, the uncertainty of an escape route that appears to run straight into a wall is stressful [7], as is shown in Fig. 7.

5.2 Avoiding Dualities

Duality means a perceptual ambiguity in terms of architectural elements. In the context of egress, dualities induced by multiple equivalent exits produce uncertainty in recognizing the escape route. It is usual that the exit sign shows into one direction while the space offers several possibilities—the signage is not supported by the space.

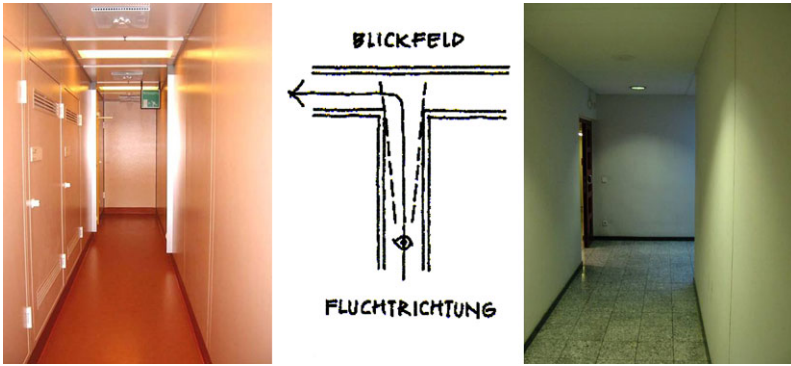


Fig. 7. Visual field of escape route.

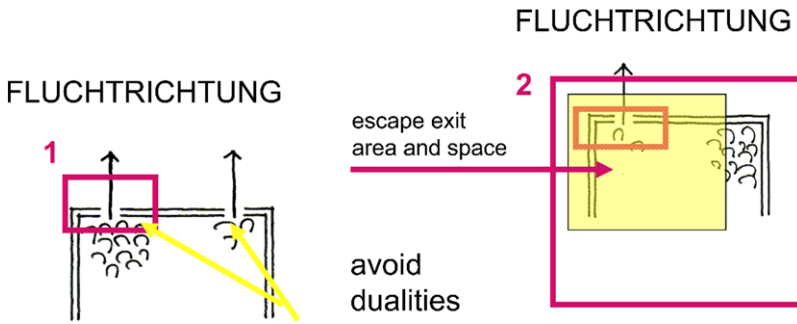


Fig. 8. Dualities: (left) phenomenon of the herd instinct (right) exits as *escape space*.

Another problem that can originate in exit dualities is the possibility to take the wrong exit. This is typically the case in smoke-filled rooms when in *herd instinct* [8] governs crowd behavior. The sketch in Fig. 8 (left) elaborates this situation: Width and number of the two exit doors is calculated according to regulations. Through herd instinct, evacuees will gather before one exit only. As a consequence, the envisioned egress rate cannot be achieved, or even worse, the taken exit is disadvantageous for the overall evacuation.

We thus argue for the need to plan for only one exit instead of more at different places (see Fig. 8, right) if regulations allow. We are convinced that this can reduce uncertainty and stress. Additionally, architects should not consider the exit as ‘an opening in a wall’ but as a whole area or an *escape space* where egress happens. Planning has to take the whole area into account, not only the doors.

Another type of exit duality is given by the human disposition towards light during stress situations, directly related to the tunnel vision phenomenon (see Fig. 9a): On the escape route, the view through a large, bright window communicates a safe and rapid way out of the building, and is generally more

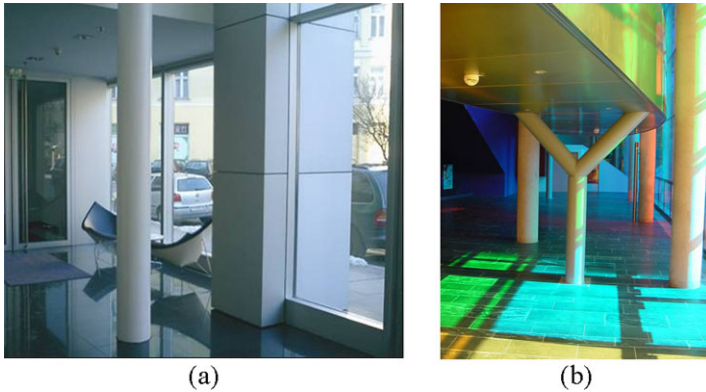


Fig. 9. **a** Emergency exits vs. openings to the exterior. **b** Light from openings attracts more attention than dark, occluded exit at the back.

tempting than a superficially added exit sign pointing to the darker interior. Of course, the design of exits should avoid such visual dualities along the escape route, as people who have jumped through safety-glass were seriously injured or even killed [9].

We must therefore consider all openings as *exits of choice* (see Fig. 9b). Since many emergency exit doors have resemblance to openings of a safe, they might be less attractive when comparing them with other exit choices. This applies even more when they are shut.

5.3 Architectural Elements for Managing Egress

Emergency exits require the architectural design of the entire surrounding, the so called “*escape space*” (see Fig. 8, right). Analysis has shown that an obstacle before the exit—such as a column—can control the speed of the flow [10]. From the architectural point of view, however, a column which stands in front of an exit is a clear nonsense. The fact that obstacles can control the speed of flow does not unbind the architect of coming up with a clever design for them. Such flow dividers, which we see not simply as ‘obstacle’ but rather as 3-dimensional architectural elements that can also be used for managing crowd flow, must have other functional meanings for the normal case of building use which is present in 99% of the time.

An depictive elaboration of architectural elements as obstacles is given in Fig. 10: A room without obstacles induces slower flow rate because of the formation of a bulk before the exit area (Fig. 10a). Adding a corridor-shaped obstacle produces raises the exit flow rate and can mitigate bulk formation (Fig. 10b) [11]. However, these examples are purely artificial. An architect might rather consider to build a column-shaped info-point before the exit area which is brightly lit and can be used by visitors to check mails (refer

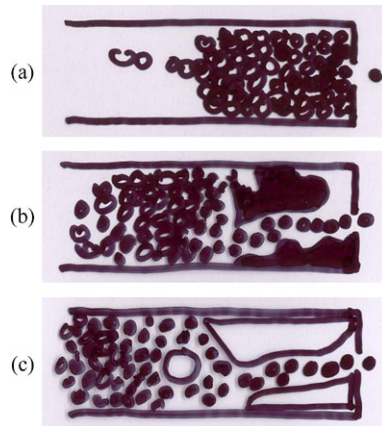


Fig. 10. Space **a** without obstacles, **b** with obstacles that server only egress purposes, **c** architectural elements used as obstacles.



Fig. 11. Architectural space vs. escape signage.

to Fig. 10c). Furthermore, two showcases near the opening could act as a corporate showroom for new products and be a corridor at the same time.

6 Conclusions

Panic and stress originate in spaces and spaces are the action field for architects. The valuable results of research to date must finally find its application in building design practice. Poorly designed spatial structures or figurations are not improved by superficial addition of signage, or as the Dutch information-designer Paul Mijksenaar commented: "Even the best signs can-

not cure sick buildings” [12]. Spatial reality clearly overrides escape signage (see Fig. 11).

Egress planning needs to be based on all dimensions of architecture, starting from three-dimensional space, going over temporality and ending in interaction between evacuees. We thus argue for the need of three-dimensional tools and thinking for the design of egress routes, rather than the now-common map-based approaches.

As our future contribution, we plan to develop design recommendations based on the results of pedestrian trans-disciplinary research as an instrument for planners and architects. Furthermore, we plan to develop tools based on our research that can support architects in the process of designing emergency spaces so that not only building safety is considered, but also the feeling of security of each individual user of the building can be raised. We are convinced that this is essential to lessen the impacts of stress and panic in egress situations.

References

1. C. Illera, *Trilogie der Fünf, 5 Dimensionen, 5 Prinzipien, 5 Phänomäne*, ISBN 3-85409-365-9, Vienna, 2003. Löcker.
2. G.K. Still, *Crowd Dynamics*, Ph.D. Thesis, University of Warwick, 2000.
3. K.-L. Spengemann, *Architektur Wahr-nehmen*, ISBN 3-924639-23-X, Bielefeld, 1993. K. Kerber.
4. N. Waldau, *Massenpanik in Gebäuden*, Diploma Thesis, Vienna University of Technology, Pages 101–112, 2002.
5. E.K. Sadalla, L.J. Staplin, The perception of traversed distance: Intersections. *Environment and Behavior*, Volume 12(1), Pages 65–69, 1980. Sage Publications.
6. E.K. Sadalla, L.J. Staplin, The perception of traversed distance. *Environment and Behavior*, Volume 12(2), Pages 167–182, 1980. Sage Publications.
7. G. Best, *Orientierung in großen Gebäuden*, In D. Canter, editor, *Architekturpsychologie. Theorie. Laboruntersuchungen. Feldarbeit. 12 Forschungsberichte*, Düsseldorf, 1973. Bertelsmann Fachverlag.
8. D. Helbing, I. Farkas, T. Vicsek, Simulating dynamic features of escape panic. *Nature*, Volume 407, Pages 487–490, 2000.
9. Mann nach Sturz durch Glasscheibe in Hamburg fast verblutet, *Hamburger Abendblatt*, 01.08.2006.
10. G. Still, Last Word, *Mind the gap*, *New Scientist*, March 20th 1999.
11. A. Johansson, D. Helbing, Pedestrian flow optimization with a genetic algorithm based on Boolean grids, In N. Waldau, P. Gattermann, H. Knoflacher, M. Schreckenberg, editors, *Pedestrian and Evacuation Dynamics 2005*, Vienna, 2005. Springer.
12. P. Mijksenaar, P. Westendorp, *Open Here: The Art of Instructional Design*, ISBN 0-500-28170-X, London, 1999. Thames and Hudson.

Was It Panic? An Overview About Mass-Emergencies and Their Origins All Over the World for Recent Years

Christian Rogsch¹, Michael Schreckenberg², Eric Tribble¹,
Wolfram Klingsch¹, and Tobias Kretz³

¹ Institute for Building Material Technology and Fire Safety Science, University of Wuppertal, Pauluskirchstr. 11, 42285 Wuppertal, Germany

e-mail: christian@rogsch.de, eric@tribble.ws, klingsch@uni-wuppertal.de

² Physics of Transportation and Traffic, University Duisburg-Essen, Lotharstr. 1, 47057 Duisburg, Germany

e-mail: schreckenberg@ptt.uni-due.de

³ PTV AG, Stumpfstraße 1, 76131 Karlsruhe, Germany

e-mail: Tobias.Kretz@ptv.de

Summary. Mass-emergencies are very popular in the news, whether we watch news on TV or read a newspaper. In most of these news we are able to read that people were fallen in panic or a mass-panic occurred. This is a simple, but often used explanation why people died in such situations. But is that the truth? If we look at selected mass-emergencies like Bergisel-Stadium we can see, that the loss of a shoe was the origin of this phenomenon, where five girls died. One pedestrian lost a shoe while he was walking to the exit. He stopped to put on his shoe, but because of the high density of pedestrians, the other pedestrian were not able to sidestep at this moment, thus they had to stop. The pedestrians behind them did not see the boy putting on his shoe and thus they pressed against the other pedestrians, just for fun. In this case, the phenomenon of behavior was not panic, we will call this crush with very local panic behavior.

Based on 127 mass-emergencies the authors want to show how often a real mass-panic occurs and what are the real origins of these mass-emergencies.

1 Introduction

Investigations about crowds and mass phenomena of human behavior have been performed since the 19th century [1, 2]. Several researchers in the field of engineering or sociology have written special papers (e.g. [3]) or books (e.g. [4, 5]) about the phenomenon of panic, but a complete definition of panic can not be found in the literature, thus the authors provide a survey of different definitions and the usage of the term “panic”.

2 What Is Panic?

Panic is a wide used term, which can be found in the field of human behavior and financial affairs. In this article we only investigate “panic” in the field of human behavior, not in the field of financial affairs. Because of the wide usage of this term, it is hard to find any definition of the term panic or panic attack, which is also sometimes used. Smelser [6] wrote about the definition of panic: “Precise referents of ‘panic’ are not consistently identifiable”. The first definition of panic can be found in the book of Park and Burgess [7] from 1921. They define “panic is the crowd in dissolution”. Furthermore the terms panic and fear are used in the same way, thus a differentiation of these terms is quite difficult. The following terms can also be used instead of panic by using an online thesaurus [8]: affright, alarm, apprehension, dread, fear, fearfulness, fright, funk, horror, terror, trepidation. In the following some definitions of the term panic or panic attack are listed. Based upon these definitions the authors describe their definition of panic, which is used in this investigation.

2.1 Different Definitions of Panic or Panic Attack

An actual definition of the term “panic attack” can be found in the “Fourth Edition of the Diagnostic and Statistical Manual of Mental Disorders” (DSM-IV) [9]:

“A *Panic Attack* is a discrete period in which there is the sudden onset of intense apprehension, fearfulness, or terror, often associated with feelings of impending doom. During these attacks, symptoms such as shortness of breath, palpitations, chest pain or discomfort, choking or smothering sensations, and fear of “going crazy” or losing control are present.” A panic attack occurs, if the following conditions are fulfilled: “A discrete period of intense fear or discomfort, in which four (or more) of the following symptoms developed abruptly and reached a peak within 10 minutes” [9]:

1. palpitations, pounding heart, or accelerated heart rate
2. sweating
3. trembling or shaking
4. sensations of shortness of breath or smothering
5. feeling of choking
6. chest pain or discomfort
7. nausea or abdominal distress
8. feeling dizzy, unsteady, lightheaded, or faint
9. derealization (feelings of unreality) or depersonalization (being detached from oneself)
10. fear of losing control or going crazy
11. fear of dying
12. paresthesias (numbness or tingling sensations)
13. chills or hot flushes

Panic is defined in several papers, books or in different online dictionaries, thus this is a short list of different “panic” definitions, which can be found:

- “A sudden, overpowering terror, often affecting many people at once.” [10]
- “a sudden overpowering fright; also: acute extreme anxiety” [11]
- “a sudden unreasoning terror often accompanied by mass flight ‘widespread panic in the streets’” [11]
- “A sudden strong feeling of fear that prevents reasonable thought or action.” [12]
- “a sudden overwhelming fear, with or without cause, that produces hysterical or irrational behavior, and that often spreads quickly through a group of persons or animals” [13]
- “an instance, outbreak, or period of such fear” [13]
- “Panic is a sudden terror which dominates thinking and often affects groups of people. Panics typically occur in disaster situations, for example, during a fire, and may endanger the overall health of the affected group. Architects and city planners increasingly try to accommodate the symptoms of panic, such as herd behavior, during design and planning, often using simulations to determine the best way to lead people to a safe exit.” [14]
- “In sociology, precipitate and irrational actions of a group are often referred to as panics (e.g. ‘sex panic’, ‘stock market panic’), see also hysteria.” [14]
- “Panic is a sudden fear which dominates or replaces thinking and often affects groups of people or animals. Panics typically occur in disaster situations, or violent situations (such as robbery, home invasion, a shooting rampage, etc.) which may endanger the overall health of the affected group.” [15]
- Panic is “a collective flight based on a hysterical belief”. [6]
- “Panic is the crowd in dissolution.” [7]
- Panic develops through the “linkage of a shock stimulus and four phases of human reaction to this stimulus”. [16]
- Panic is a “collective retreat from group goals into a state of extreme ‘privatization’”. [17]
- “In the literature the term ‘panic’ is used to refer to many things. Thus, one finds it applied to such divergent behavior as a single individual’s unrealistic anxieties to a group’s ill-coordinated activities; at times its referent ranges from paralysis of action to a wild outburst of flight. [...] For our purposes, panic can be conceived of as involving actual (or attempted) physical flight.” [18]
- “The introduction of any strong and irrelevant stimulus into a situation of any of the foregoing types will disrupt the normal course of interaction. Thus, the clamor of a fire engine outside the theater or auditorium will disrupt audience interaction. When such a stimulus is defined by the members of the situation as a source of danger, the situation may become a

panic situation. [...] Panic behavior is, thus, the antithesis of regimental behavior.” [19]

- “The word panic is often applied to a strictly individual, maladaptive reaction of flight, immobility, or disorganization stemming from intense fear. Individual panic frequently occurs as a unique individual response without triggering a similar reaction to others. Panic as collective behavior, however, is shared behavior.” [20]

A special note should be given to the Wikipedia definition [15], because it should be mentioned, that Wikipedia’s panic article factual accuracy is disputed. Furthermore it should be noticed, that Nolan [20] points out, that, contrary to LaPierre [19], “panic behavior (i.e., physical competition between participants) has typically not occurred in fire incident evacuations based upon interviews and questionnaires from survivors of major fire incidents where such actions might have been expected”. Thus, these examples show how difficult it is to define or use the term of panic today.

3 Definitions of Crush and Stampede

In this article, also definitions of “crush” and “stampede” are used, thus we want to give also a very short overview about different definitions of these terms:

- Crush
 - “a crowding together (as of people)” [21]
 - “a crowd of people pressing against one another” [21]
 - “to squeeze together into a mass” [22]
- Stampede
 - “a mass movement of people at a common impulse” [23]
 - “to cause to run away in a headlong panic” [24]
 - “to cause (as a group of people) to act on sudden or rash impulse” [24]
 - “A stampede is an act of mass impulse among herd animals or a crowd of people in which the herd (or crowd) collectively begins running with no clear direction or purpose”. [25]

If we have a close look at the definitions above, in one definition of stampede the term panic occurs [24], in another definition [23] it does not occur. Furthermore the Wikipedia article about Stampede [25] describes that the term “stampede” is “also known as crush or trampling”. Based on these different definitions it is difficult to find exact definitions of these terms, too.

3.1 Definitions Used in this Article

Based on the difficulties of different definitions above, we used the following definitions:

- *Panic*: People flight based on a sudden subjective or “infected” fear. People are moving imprudently. The cause of this movement can not be recognized by an outsider.
- *Crush*: People are moving and a stop occurs by external influences, e.g. barriers or narrowings, thus people are pressing against each other.
- *Stampede*: People are moving without possibility to stop.
- *Flight*: People leaving a place in “a normal way”. The death occurs by events of second order, e.g. hit by debris.

3.2 Panic, Stampede and Crush in the Media

Based upon the above definitions it is difficult to find a definition for “panic” which is used in the mass-media. If we compare the English and the German mass media, we find differences in the usage of the term “panic”:

- English media:
 - If the term “stampede” occurs, the term “panic” is normally not used. In this context, normally the cause of the incident is described in the article. If panic occurs, this is mentioned separately.
 - If people stumbled, the term “crush” is used.
- German media:
 - Only the terms panic (“Panik”) and mass panic (“Massenpanik”) are used. There is no use of synonyms for “crush” and “stampede”. “Stampede” exists as a word and is used, but only used for the movement of a group of big mammals (elephants, rhinos, zebras) into one and the same direction, ignoring vegetation or animals obstructing the path.

Based on this short overview the authors want to point out that the terms “panic”, “stampede” and “crush” are very language specific, thus one has to read articles in one’s native language and at least in one foreign language to ensure, that both language specific views are considered.

4 Experiments on Panic or Decision-Making Processes

In the last 65 years some experiments with real persons about panic or decision-making processes had been performed [26–28]. These experiments should help to understand the phenomenon of panic and how people decide in such situations. In detail, the experiments performed by French [26] and Mintz [27] will be discussed.

French [26] performed an “Experimental Study of Group Panic”. In this experiment, the behavior of specific groups (organized vs. unorganized) in a situation of fear was observed. “Eight organized groups composed of athletic teams were compared with eight unorganized groups composed of students

who were not acquainted with one another. Each group contained six members. Each group was left alone in a room and instructed to fill out a questionnaire while the doors of the room were locked without their knowledge. Then wood smoke came into the room and a siren was sounded. The behavior of the group varied from genuine panic to fairly complete skepticism or belief that the situation was a hoax.” The main result of these experiment was, that the organized groups were definitely more frightened than the unorganized groups, because:

1. “the members exhibited more social freedom and interdependence of behavior which led to more social facilitation and circular social stimulation”
2. “they were more frustrated in the previous situation”
3. “fewer members were currently taking courses in psychology and hence they lacked one possible frame of reference by which to judge the situation”
4. “two of the organized groups were more suggestible and less critical due to less education and more submissiveness to the prestige of the experimenter”

Mintz [27] study about “Non-Adaptive Group Behavior” was not as “dangerous” as that one performed by French [26]. Mintz [27] performed several experiments “with different groups, 15 to 21 subjects in each group. The subjects had the task of pulling cones out of a glass bottle; each subject was given a piece of string to which a cone was attached. Cooperation on the part of the subjects was required if the cones were to come out; the physical setup made it easy for “traffic jams” of cones to appear at the bottle neck. Only one could come out at a time; even a near-tie between two cones at the bottle neck prevented both from coming out because the narrow apex of the second cone, wedged into the bottle neck, blocked the path for the wide base of the cone ahead of it. The cones had to arrive at the bottle neck in order, one at a time.” The results of this experiments show that non-cooperative behavior is not the result of panic-driven emotional excitement, but that people adjust their behavior according to their expectations of the behavior of others and their perception of a challenging situation [29].

4.1 Discussion of the Experiments Performed by French and Mintz

The experiment of French [26] seems to produce a “real panic-like situation”, thus the results should be comparable with real mass-emergencies or disasters. The simulation of fire by using wood smoke and a siren seems to be a good idea, but the unknown is the influence of the locked door in this situation. It could be assumed that the participants discover the experimental setup, because the doors were locked without their knowledge. If anybody of the group members closed the door and the door lock gets broken, than the same situation could be in an other way realized by the group members.

The experiment by Mintz [27] is criticized mostly by Kelley et al. [28] and Brown [30]. Kelley et al. [28] complain about the loss of the danger effect. They point out that “his method cannot be considered to test the effect of danger” [28]. Furthermore they point out that based on the small monetary rewards “it is difficult to believe that the results from this situation shed much light on the behavior under conditions of high stress.” They furthermore point out that “the behavior of Mintz’s subjects do not seem to provide apt illustrations of his view that even under the press of the ‘panic’, individuals continue to act in a thoughtful manner”. Brown [30] points out that “no serious jams occurred even though Mintz instructed some subjects to make noise and do their best to ‘panic’ the others”.

It should be noticed that the mutual influence of group-belonging feelings and competitive behavior was pointed out by Tajfel [31, 32] in his famous minimal group experiments and later used as foundation for the theory of social identity. These experiments are also not discussed in this paper.

5 Different Mass-Emergencies in the Case of “Panic”

Based upon our definitions of the terms panic, crush, and stampede, we investigate 127 mass-emergencies from 1863–2007. Informations about listed mass-emergencies are taken from classical literature, The Library of the German Highschool of the Police, newspapers and TV-news like BBC, New York Times and Tagesschau (German TV-news), and web research (Wikipedia, Google, ...). If more than one definition is listed, the informations about this case are not precise in that way, that it was possible to find a clear definition of the human behavior. In those cases, further research with more literature sources should be helpful.

It should also be noticed, that the term “panic” is used in combination with other types of human behavior, like stampede or crush. In this cases, “panic” occurred mostly very local and very early. In that cases “local” means that only a few people who are located near to the causing event behave like “in panic”. “Early” means that the panic behavior occurs mostly in the first minute of the event. Later, people have realized the situation, thus no panic is involved in the case of flight or other human motion.

As it can be seen in the different definitions of panic above, it is quite hard to define those terms. The definitions about human behavior are based on our definitions above, but by using other definitions the results could be changed.

In total, 127 mass-emergencies are investigated (see Tables 2–5). The causes of these mass-emergencies are very different, an overview is given in Table 1.

A compressed list of human behavior in the investigated cases is shown in Table 6. A closer look to this table shows, that “real panic” occurred in the view of our definition 2 times. Furthermore the selected sources are often

Cause	Number of cases
Fire	19
Riot	12
No logical content	21
Organizational issue	34
Cupidity	11
Other/unknown	30
Sum	127

Table 1. Cause of mass-emergencies.

Date	Country	Town	Description in literature	New definition
1863-12-08	Chile	Santiago de Chile	no information	ambiguous
1881-12-18	Austria	Vienna	panic	crush
1883-06-16	Great Britain	Sunderland	crush	crush
1887-09-05	Great Britain	Exeter	panic	crush
1896-05-30	Russia	Moscow	no information	ambiguous
1903-08-10	France	Paris	panic, less informations	ambiguous
1903-12-30	USA	Chicago	panic	crush
1908-01-11	Great Britain	Barnsley	stampede	stampede/panic
1912-04-15	North Atlantic	Passenger Ship	panic	ambiguous, maybe panic
1913-12-24	USA	Michigan, Calumet	panic	crush/panic
1943-03-03	Great Britain	London	crush	crush
1946-03-09	Great Britain	Bolten	no information	ambiguous
1955-03-30	Chile	Santiago de Chile	no information	ambiguous
1964-05-24	Peru	Lima	no information	ambiguous
1968-06-23	Argentina	Buenos Aires	crush	crush
1970-11-01	France	Saint Laurent du Pont	stampede	crush
1971-01-02	Great Britain	Glasgow	crush	crush
1971-03-04	Brazil	Salvador	panic/stampede	stampede/panic
1973-04-12	Germany	Munich	no information	ambiguous
1973-08-02	Isle of Man	Douglas	stampede	crush
1974-02-17	Egypt	Cairo	no information	ambiguous
1976-12-17	Haiti	Port-au-Prince	panic	stampede/panic
1977-04-01	Germany	Hamburg	crush	crush
1977-05-01	Turkey	Istanbul	stampede	crush/panic

Table 2. Mass-emergencies from 1863–1977.

Date	Country	Town	Description in literature	New definition
1979-06-09	Germany	Hamburg	crush	crush
1979-08-01	Nigeria	?	panic	ambiguous
1979-09-16	Indonesia	Medan	crush	ambiguous
1979-12-03	USA	Ohio/Cincinnati	crush	crush
1981-02-08	Greece	Athens	crush	crush/stampede
1981-02-14	Ireland	Dublin	no information	ambiguous
1982-10-20	USSR	Moscow	stampede	crush/stampede
1982-11-18	Colombia	Santiago de Cali	stampede	ambiguous
1985-05-11	Great Britain	Bradford	no panic	no panic
1985-05-26	Mexico	Mexico City	crush	ambiguous
1985-05-29	Belgium	Brussels	panic	crush/panic/ stampede
1987-03-10	Libya	Tripoli	stampede	crush/stampede
1988-03-12	Nepal	Kathmandu	stampede	crush/stampede
1989-04-15	Great Britain	Sheffield	crush	crush
1990-07-02	Saudi Arabia	Mecca	stampede	stampede
1991-01-13	South Africa	Orkney	stampede	crush
1991-07-15	Kenya	Nairobi	stampede	ambiguous
1991-12-28	USA	New York City	stampede	crush
1993-01-01	China	Hong Kong	crush	crush
1993-10-30	USA	Madison/WI	crush	crush
1994-05-01	Liberia	Monrovia	no information	ambiguous
1994-05-25	Saudi Arabia	Mina	stampede	stampede
1994-09-27	Baltic Sea	Ferry	panic	ambiguous
1995-10-28	Azerbaijan	Underground in Baku	panic	stampede/panic
1995-12-23	India	Dabwali	stampede	crush/stampede
1996-04-11	Germany	Dusseldorf	panic	no panic
1996-04-19	Zimbabwe	Zimbabwe	stampede	ambiguous
1996-06-16	Zambia	Lusaka	stampede	ambiguous
1996-07-31	South Africa	Tembisa	stampede	ambiguous
1996-10-16	Guatemala	Guatemala City	stampede	crush
1997-04-15	Saudi Arabia	Mina	stampede	stampede
1997-07-28	Germany	Dusseldorf	no panic	no panic
1998-04-08	Saudi Arabia	Mena	stampede	stampede
1998-10-28	Sweden	Goeteborg	no information	ambiguous
1998-12-25	Peru	Lima	stampede/crush	crush
1999-01-11	Egypt	Alexandria	no information	ambiguous
1999-01-14	India	Sabarimala	no information	ambiguous
1999-05-30	Belarus	Minsk	no information	ambiguous
1999-12-04	Austria	Innsbruck Bergisel	panic	crush/panic

Table 3. Mass-emergencies from 1979–1999.

Date	Country	Town	Description in literature	New definition
2000-03-24	South Africa	Durban	stampede	crush/panic/ stampede
2000-04-16	Portugal	Lisbon	panic	panic
2000-04-23	Liberia	Monrovia	crush	crush
2000-05-26	Pakistan	Lahore	stampede	ambiguous
2000-06-05	Ethiopia	Addis Ababa	stampede	stampede/panic
2000-07-09	Zimbabwe	Harare	stampede	ambiguous
2000-07-30	Denmark	Roskilde	stampede	crush
2000-10-10	Mexico	Mexico City	panic	crush/stampede
2000-12-30	Brazil	Rio de Janeiro	panic	crush
2001-01-01	Netherlands	Volendam	panic	flight/panic/self- preservation
2001-01-26	Australia	Sidney	no panic	no panic/crush
2001-03-02	South Africa	Johannesburg	stampede	crush
2001-03-05	Saudi Arabia	Mecca	stampede	stampede
2001-03-16	Indonesia	Jakarta	stampede	ambiguous
2001-04-01	Pakistan	Pak Patten	stampede/panic	ambiguous, maybe stampede/panic
2001-04-11	South Africa	Johannesburg	stampede	crush
2001-04-29	Congo	Lubumbashi	stampede	stampede/panic
2001-05-06	Iran	Sari	no panic, riots	no panic
2001-05-09	Ghana	Accra	stampede	stampede/panic
2001-07-21	Japan	Kobe	stampede	crush
2001-08-08	India	Bangladesh	stampede	crush
2001-09-11	USA	New York City	panic	flight
2001-12-18	Brazil	Aracaju	no information	ambiguous
2001-12-21	Bulgaria	Sofia	no information	ambiguous
2002-03-11	Saudi Arabia	Mecca	stampede	crush
2003-02-11	Saudi Arabia	Mecca	stampede	stampede
2003-02-17	USA	Chicago	stampede	crush/panic/ stampede
2003-02-20	USA	Rhode Island	panic	crush
2003-05-14	Benin	Cotonou	crush	crush
2003-08-27	India	Nashik	stampede	crush/stampede
2004-01-23	India	Srirangam	stampede	ambiguous
2004-02-01	Saudi Arabia	Mecca	stampede	stampede
2004-02-05	China	Miyun	stampede	ambiguous
2004-03-13	Syria	Kameshli	stampede	ambiguous
2004-04-12	India	Lucknow	stampede	ambiguous, maybe stampede

Table 4. Mass-emergencies from 2000–2004.

Date	Country	Town	Description in literature	New definition
2004-05-04	India	Bangladesh	stampede	stampede
2004-09-01	Saudi Arabia	Jeddah	stampede	crush/stampede
2004-10-10	Togo	Lome	stampede	ambiguous
2004-11-20	Togo	Lome	stampede	ambiguous, maybe stampede
2004-12-30	Argentina	Buenos Aires	panic	crush
2005-01-25	India	Wai	panic/stampede	crush
2005-02-10	Great Britain	London	stampede	crush/stampede
2005-02-27	Burkina Faso	Ouagadougou	stampede	stampede
2005-03-25	Iran	Tehran	stampede	ambiguous, maybe stampede/panic
2005-04-06	India	Bangladesh	stampede	stampede
2005-04-23	Germany	Berlin	no information	ambiguous
2005-06-19	Kenya	Nairobi	stampede	ambiguous
2005-08-16	USA	Richmond	stampede/chaos	crush/panic/stampede
2005-08-31	Iraq	Bagdat	panic/stampede	stampede/panic
2005-09-09	Sri Lanka	Colombo Airport	stampede	panic
2005-12-18	India	Chennai	stampede	crush
2005-12-23	Slovenia	Ljubljana	no information	ambiguous
2006-01-12	Saudi Arabia	Mecca	stampede	stampede
2006-02-04	Philippines	Manila	stampede	crush/stampede
2006-04-09	Pakistan	Karachi	stampede	crush/stampede
2006-08-08	USA	San Diego	crush	crush
2006-08-20	Hungary	Budapest	panic	flight
2006-09-11	Yemen	Tiaz	stampede	ambiguous
2006-09-12	Yemen	Ibb	stampede	crush
2006-12-17	Pakistan	Jhok Utra	stampede	ambiguous
2007-04-30	Tunisia	Sfax	stampede	crush
2007-06-03	Zambia	Lusaka	stampede	ambiguous, maybe panic
2007-09-07	Zambia	Mpika	stampede	ambiguous
2007-09-13	Germany	Berlin	panic/chaos	crush/stampede

Table 5. Mass-emergencies from 2004–2007.

not precise enough to allow a definition of human behavior, thus 38 cases are described as “ambiguous”.

6 Conclusions

In this article the authors show how difficult it is to define the term “panic”. In different literature sources about human behavior in mass-emergencies statements about panic are very contrary, like Nolan [20] and LaPierre [19]. Furthermore an extended literature review about “panic definitions” is shown.

Category	Old	New
Crush	16	35
Crush/stampede	1	12
Crush/panic	0	3
Stampede	62	11
Stampede/chaos	1	0
Stampede/panic	4	8
Stampede/ambiguous	0	2
Panic	20	2
Panic/ambiguous	1	2
Panic/chaos	1	0
ambiguous	17	38
Stampede/crush/panic	4	4
Stampede/crush/ambiguous	0	2
Flight	0	2
Panic/flight/self-preservation	0	1
Sum	127	127

Table 6. Classification.

Based on this review, a definition of panic is “created”. This and other definitions are used to investigate 127 cases of mass-emergencies. The results show, that panic behavior in case of mass-emergencies does not as often occur as suggested.

Acknowledgements

The authors would like to acknowledge the German Highschool of the Police for using their library.

References

1. G. Le Bon. *The Crowd—A Study of the Popular Mind*. Batoche Books, Kitchener, 2001. Reprint of the 1896 ed.
2. L.E. Genevie, editor. *Collective Behavior and Social Movements*. F.E. Peacock Publishers, Itasca, 1978.
3. E.L. Quarantelli. The Sociology of Panic. Preliminary paper 283, Disaster Research Center, 2001.
4. J.M. Chertkoff and R.H. Kushigian. *Don't Panic—The Psychology of Emergency Egress and Ingress*. Praeger, New York, 1999.
5. A.R. Mawson. *Mass Panic and Social Attachment: The Dynamics of Human Behavior*. Ashgate, Aldershot, 2007.
6. N.J. Smelser. *Theory of Collective Behavior*. Routledge and Kegan Paul, London, 1970.

7. R.E. Park and E.W. Burgess. *Introduction to the Science of Sociology*. University of Chicago Press, Chicago, 1921.
8. <http://Answers.com>. Panic. Online, January 2009.
9. American Psychiatric Association. *Diagnostic and Statistical Manual of Mental Disorders: DSM-IV*, 4th edition. American Psychiatric Association, Washington, 1994.
10. The Free Dictionary. Panic. Online, January 2009.
11. Merriam Webster Online Dictionary. Panic. Online, January 2009.
12. Medical Online Dictionary. Panic. Online, January 2009.
13. <http://Dictionary.com>. Panic. Online, January 2009.
14. <http://KnowledgeRush.com>. Panic. Who is Panic? What is Panic? Where is Panic? Online, January 2009.
15. Wikipedia. Panic—Wikipedia, The Free Encyclopedia, 2009. [Online; accessed 26-January-2009].
16. P. Foreman. Panic theory. *Sociology and Social Research*, 37:295–304, 1953.
17. K. Lang and G.E. Lang. *Collective Dynamics*. Thomas Y. Crowell Company, New York, 1961.
18. E.L. Quarantelli. The behavior of panic participants. *Sociology and Social Research*, 41:187–194, 1957.
19. R.T. LaPierre. *Collective Behavior*. McGraw-Hill, New York, 1938.
20. D.P. Nolan. *Encyclopedia of Fire Protection*. Thomson Delmar Learning, London, 2006.
21. Merriam Webster Online Dictionary. Crush, noun. Online, January 2009.
22. Merriam Webster Online Dictionary. Crush, verb. Online, January 2009.
23. Merriam Webster Online Dictionary. Stampede, noun. Online, January 2009.
24. Merriam Webster Online Dictionary. Stampede, verb. Online, January 2009.
25. Wikipedia. Stampede—Wikipedia, The Free Encyclopedia, 2009. [Online; accessed 11-February-2009].
26. J.R.P. French, Jr. Experimental study of group panic. *Journal of the Elisha Mitchell Scientific Society*, 57(2):195–196, 1941.
27. A. Mintz. Non-adaptive group behavior. *The Journal of Abnormal and Social Psychology*, 46:150–159, 1951.
28. H.H. Kelley, J.C. Condry, Jr., A.E. Dahlke, and A.H. Hill. Collective behavior in a simulated panic situation. *Journal of Experimental Social Psychology*, 1:20–54, 1965.
29. Y. Vogiazou and M. Eisenstadt. Presence Based Play—Towards a Design for Large Group Social Interaction. In *Proceedings of the First International Conference on Appliance Design*, 2003.
30. R. Brown. *Social Psychology*. The Free Press, New York, 1965.
31. H. Tajfel. Experiments in intergroup discrimination. *Scientific American*, 223:96–102, 1970.
32. H. Tajfel and J.C. Turner. *The Social Identity Theory of Intergroup Behavior*, pages 7–24. Nelson-Hall, Chicago, IL, 1986.

Hierarchical Structure of the Mass and Group-Level Behaviors in Urban Rail Transfer Stations

Xiaolei Zou, Ruihua Xu, and Peng Gao

Department of Transportation Management Engineering, School of Transportation Engineering, Tongji University, 4800# CaoAn Road, Shanghai 201804, China
e-mail: zouxiaolei@mail.tongji.edu.cn

Summary. In Urban Rail Transit (URT) stations, safety problems and delays occur, because of the complicated passenger organization processes, space and facility layouts, mass composition and movement. This paper analyzed the structure of the mass as well as the features and behaviors of passenger groups in stations. First, we explored the passenger organization processes, the hierarchical structure of the space, the passenger service network and the hierarchical of the mass. Second, we showed a hierarchical model of the mass, and studied both individuals and groups in their features, behaviors and impact on safety and efficiencies of the crowd. Third, we built a process model to demonstrate mass behaviors. Last, we developed a simulation framework of URT station, based on the models and taking into considerations of passenger organization, train operation and space layout.

1 Introduction

Urban Rail Transit (URT) has become a primary transportation choice in cities worldwide. In some metropolises, such as London, Paris, New York and Tokyo, URT consists of more than 65% of public passenger transport. Take Shanghai for example, the contribution of URT in public transportation is about 25% today and it will be more than 40% in 2010. It means that in 2010, about 6,000,000 people will travel by urban rail every day and more than 300,000 will transfer at key stations with 60,000 trips generated in one rush hour in Shanghai.

Such a large passenger flow in a limited space and time frame could bring serious safety and efficiency issues. URT construction and operation organizations and research institutions in Shanghai have done some researches to find patterns in trip generation, passenger crowd movement in stations and the relationships among crowd, environment, passenger organization, and train operation.

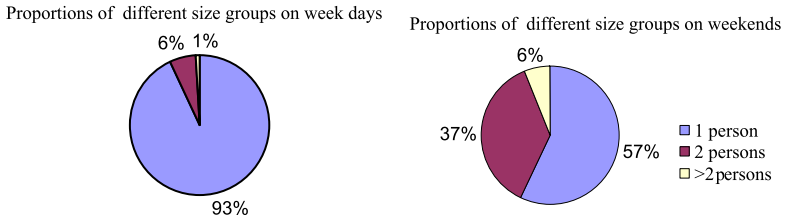


Fig. 1. Comparison of the proportion of different size groups in the same station between on weekdays and weekends.

In January 2008, we did a survey at People’s Square Station, the largest one in Shanghai. It sits on the intersection of three major metro lines. The focus is on the composition of passenger crowd, crowd movements, interactions of flows, and the impact of environment and passenger organizations on the behavior and distribution of passengers.

We found two major facts:

- (1) A large number of passengers take trips in groups with several others and group-level behaviors have great impacts on the whole mass. Observations in rush hours on both weekdays and weekends show that the proportions of grouping on weekends are much larger than that on weekdays. See Fig. 1. According to the survey, there are two kinds of groups, compact groups composed of friends and colleagues, and incompact groups formed by compact groups and individuals temporarily. On weekends, the impacts on the whole mass by compact groups are significant, while on weekdays it can be ignored. But the impacts of incompact groups on both weekdays and weekends should draw our attention.
- (2) The mass in URT stations is of a hierarchical structure generated by the passenger organization and service system. The mass consists of five hierarchies from macro to micro scope: mass, flows, sections, groups and individuals. The characteristics and behaviors of each are quite different but related.

We will investigate these facts in the following sections and try to draw a framework simulating the movements of the hierarchically structured mass in URT stations.

2 Hierarchical Structure of URT Station Space, Passenger Service Network and Mass

2.1 Passenger Organization Processes

Passenger organization processes can be classified into three categories: boarding, alighting and transfer as shown in Table 1. The stages enclosed with brackets are optional according to the ticketing and transfer set ups.

Passengers	Organization processes
Boarding	Entry → (Ticketing) → Entry Inspection → Waiting → Boarding → Departure
Alighting	Train arrival → Exit inspection → Exit
Transfer	Train arrival → (Exit inspection) → (Ticketing) → (Entry inspecting) → Waiting → Boarding → Departure

Table 1. Passenger organization processes.

2.2 Hierarchical Structure of URT Stations

Figure 2 is the layout of People’s Square Station. Three metro lines, No. 1, No. 2 and No. 8, intercross at this station. The station consists of five levels: concourse level 1, concourse level 2 and one platform for each metro line. Entries, exits, ticketing and inspection facilities are dispersed on level 1 and level 2. Staircases connect adjacent levels.

As People’s Square Station, most URT Stations can be split into several hierarchies from macro to micro scope: functional levels (entry/exit/passage, concourse, and platform levels), charge areas (paid and unpaid areas), functional areas (entry/exit, ticketing, inspection, staircase, passage and waiting areas) and facilities (entries, exits, ticket points, ticket gates, stairs, waiting points, etc.). The hierarchical structure of URT stations is determined by passenger organization processes.

2.3 Passenger Service Network

Functional areas can be classified into passenger service areas (ticketing, ticket inspection and waiting areas), transiting areas (entry/exit and staircase areas) and passage areas. Functional areas and passenger organizations can be described as a service network. Passengers accept service by routing and moving in the network.

Figure 3 shows the passenger service network for transfer in People’s Square Station. Passenger service areas are the nodes in black, transiting areas are in white, and passage areas are demonstrated as arrows. The nodes with the same function form a stage.

A network has a service capacity that is determined by those nodes or arrows with the least service capacities. Capacity of a node or arrow is determined by the largest number of people assembled in the area at the same time and the largest number of people served per unit time.

Each arrow has a weight that is determined by the length of the passage, the time spending in the passage and the capacity saturation of the following nodes and arrows.

Routing in the network is a procedure considering both capacity and weight.

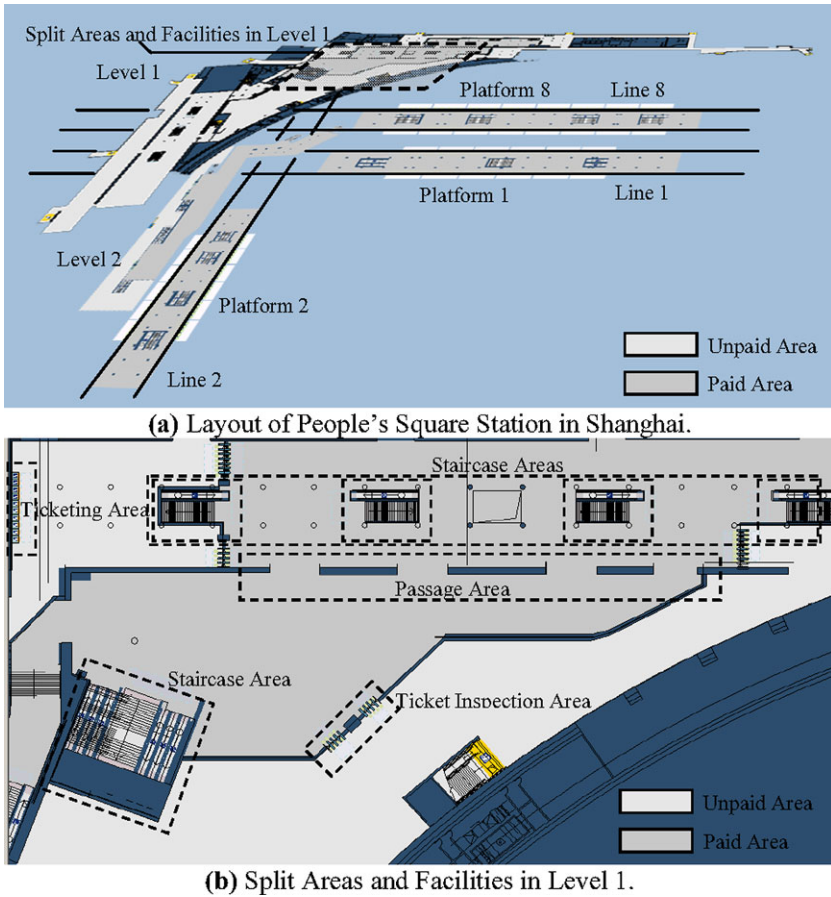


Fig. 2. Hierarchical structure of People's Square Station.

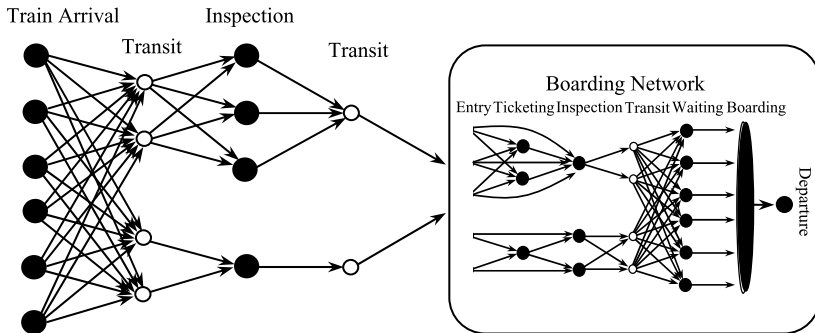


Fig. 3. Demonstration of transfer network structure.

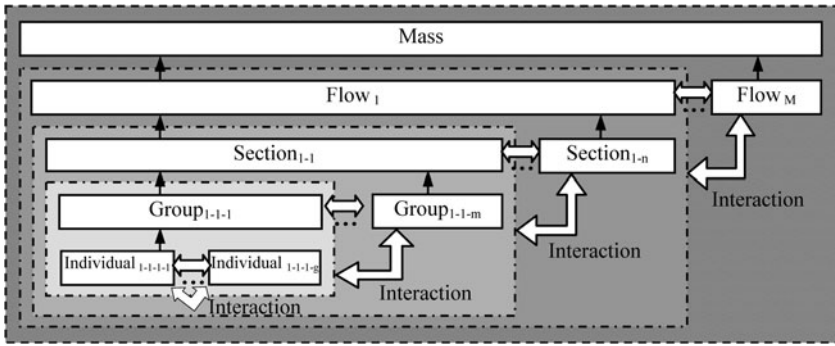


Fig. 4. The hierarchical structure of the mass.

2.4 The Hierarchical Structure of the Mass

A mass of passengers in a station has five hierarchies shown in Fig. 4: mass, flows, sections, groups and individuals. The relationship of the hierarchies can be described as following sets:

$$\begin{aligned}
 Mass &= \{Flow(i)|i \in N\}, \\
 Flow(i) &= \{Section(j)|j \in N\}, \\
 Section(j) &= \{Group(k)|k \in N\}, \\
 Group(k) &= \{Individual(g)|g \in N\}.
 \end{aligned}$$

Each hierarchy display unique patterns in its behaviors and all hierarchies interact with one another.

- (1) The mass in stations can be sorted into flows over different levels and areas. According to the organization processes, there are three types of main flows: boarding, alighting and transfer. Each type of main flow contains several flows distributed in the service network.
- (2) Each flow can be divided into several sections in accordance to the stages of organization process. Each section starts from one node of service area and ends before the node of the next service area in the route of the flow.
- (3) Each section contains many individuals and groups.

A demonstration of the mass in station is shown in Fig. 5.

In Fig. 5, the mass includes two kinds of main flows, boarding and alighting. Take the boarding for example, it can be divided into sections of Entry-Ticketing, Ticketing-Inspection, Inspection-Waiting, Waiting-Boarding, and Boarding-Departure. The boarding flow has several branches in some of its sections and many groups and individuals in sections.

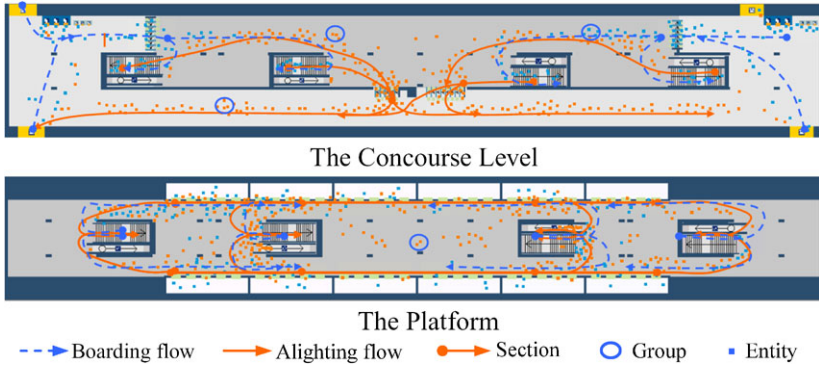


Fig. 5. Demonstration of the mass in station.

3 Analysis of the Features and Behaviors of Individuals and Groups

Individuals and Groups are at the bottom of the hierarchical structure of the Mass. And the movement and evolvement of the higher hierarchies are based on the features and behaviors of individuals and groups.

3.1 Individuals

(1) Human Physical Features

Two major human physical features, body dimension [1, 2] and mobility, are usually directly used to describe a simplified individual. By body dimension, the space occupied by an individual can be calculated. And by mobility, the speed, the acceleration and the movement of an individual can be tailed.

(2) Environmental Features

Environmental features constrain the reactions and behaviors of individuals and can trigger emergency evacuation. Environmental features refer to geometric structure (shape and size of space, layout of facilities), guidance information (signals, signs, guidance, alarm, illumination, etc.) and emergencies (failure and accident in train operation, fires, explosions, earthquakes, terrorist attacks, etc.). Geometric structure and guidance information affect the individuals relatively statically, while emergencies could evolve indefinitely and affect the individuals dynamically.

(3) Psychological and Sociological Features

Human beings have some basic psychological features, such as instinct, endurance, experience, and rationality. These features affect an individual's re-

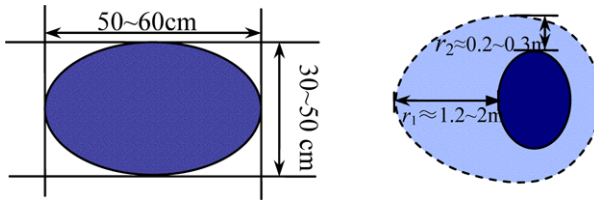


Fig. 6. Body dimension and personal space.

sponse to other individuals and environment, and in turn affect his/her decision making.

Individuals interact with others based on their sociological features. They intend to keep a personal space from others and realize self protection. As Fig. 6 shows, a personal space is larger than body dimension. An individual always expects to keep a larger space to move freely and safely. It needs a buffer distance in the front and a private distance around. The shape of a personal space can be demonstrated as an egg. The buffer distance r_1 is about a distance of two steps giving the individual enough time to react to adjust his direction and speed.¹ The private distance r_2 is about half of the width of the body dimension to keep away from others. The size and shape of a personal space change in different occasions.

(4) Individual Behaviors

Individual behaviors can be mainly classified into decision making and movement. People get information from both the environment and the crowd to compose cues. Individuals perceive cues and make decisions based on their psychological and sociological features. Then they act based on their decisions. Physical characteristics determine their movement and sociological characteristics promote the interaction among individuals. Some typical actions are: competing, queuing, herding, and lead-Following.

Behaviors of individuals can be simplified as a hierarchical structure modeled in Fig. 7. On top is a high level decision making that people make service routing on the constraints of service network. In the middle is a mid level decision making that people find path. At the bottom are the actions that people move and accept service.

Routing is a procedure involving both capacity and weight. The depth in each step of routing indicates the passengers' ability to judge rationally and comprehensively. In fact, most routes are not the optimum options. Passengers

¹ An individual needs a buffer distance r_1 equals the length of two steps plus a reaction distance to avoid collision. Assume the reaction time t_r is about 0.15–0.4 second, the speed of a passenger v is 1.0–1.3 meters per second, and the length of one step s is about 0.5–0.75 meter. Considering the difference of individuals, $r_1 = 2s + vt_r$ will fall in the range of [1.2, 2.0].

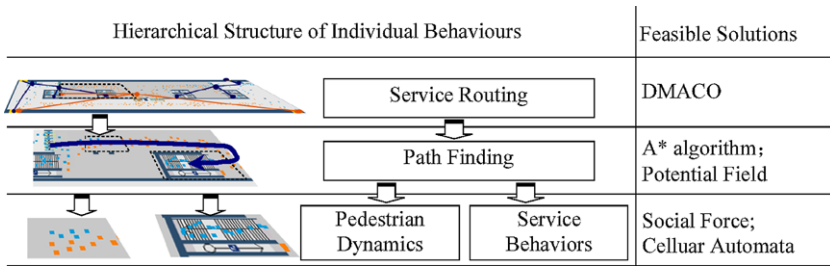


Fig. 7. A hierarchical structure of individual behaviors and feasible solutions.

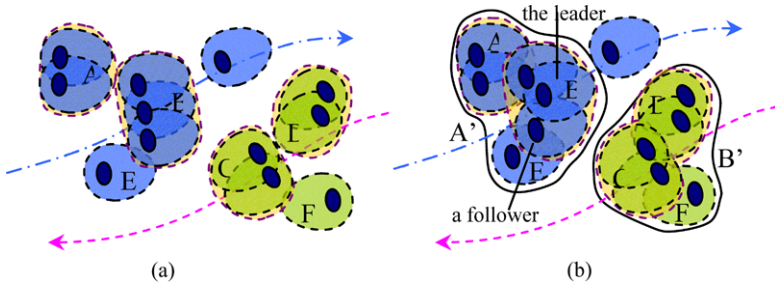


Fig. 8. Compact groups and incompact groups.

who are familiar with the station can think deeper and make global routings, but those who are not make judgments only by several consecutive nodes and make local routings. In a movement of crowd, routes are adjusted according to changes of conditions.

A route from an origin node to a destination node constitutes a way for a passenger to go through the whole organization process.

3.2 Groups

Features of Groups

(1) Composition

There are two types of groups, compact and incompact ones. According to the survey in People’s Square Station, compact groups mostly contain 2 persons. Incompact groups are made of compact groups and individuals in the same section and close to one another. Compact groups exist all the time in their service processes. Incompact groups exist temporarily when their members conflict with the groups in other flows to produce a stronger force to counteract the conflict pressure and go forward. As Fig. 8(b) shows, compact groups A and B and individual E composed an incompact group A'; compact groups C and D and individual F composed an incompact group B'.

(2) Relationships Within a Group

In a compact group, there is usually a leader and several followers, but sometimes this relationship is not so obvious and members make decisions together and behave equally. The relationships of members in a compact group are relatively steady. Members want to keep a coherent and steady walk and a relatively steady structure by communicating with one another.

In an incompact group, a sub group may act as a leader. But the process of decision making and behavior of the whole group is more like the process of collective behavior in vertebrates [3].

(3) Shapes and Areas

The shapes of groups are determined by the relationships and positions of group members. Shapes of compact groups are comparatively simple. Members in one group almost walk side by side in free space, such as group A, B and C in Fig. 8(a). When in a limited space or in a conflict with other flows, the group will be compressed, and the leader walks to the front, such as group D in Fig. 8(a) and groups in Fig. 9. Shapes of incompact groups are relatively complicated because incompact groups are always formed by compressing. These groups are shaped into various clusters as group A' and B' in Fig. 8(b).

Each group occupies a private space that is the union of personal spaces of all members. The function of private space is to keep a steady structure of members and to repel the disturbance from other individuals or groups. When a group is compressed, the area of its private space becomes smaller. Because a group has a trend to return to its originally balanced form, it produces a repellent force against the pressure that makes it transform.

(4) Mobility

Members in a group need to keep coherence. The inertia of a group is bigger than that of an individual. So groups usually move slower and the movement of a group is hard to be changed by an individual. The bigger a group is the greater inertia it has. When two groups in similar size walk towards each other, both will slow down to avoid conflict, and both transform. When groups in different sizes meet, the smaller ones are more likely to change form and speed.

Behaviors of Groups

(1) Interactions of Members

Different members play different roles in a group. A leader takes charge of decision making and organizing to lead all members to finish the service route

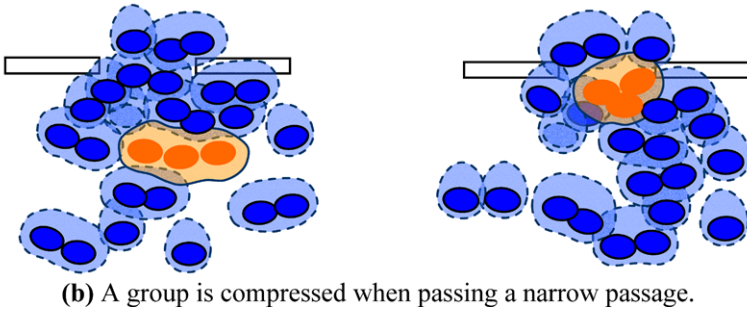
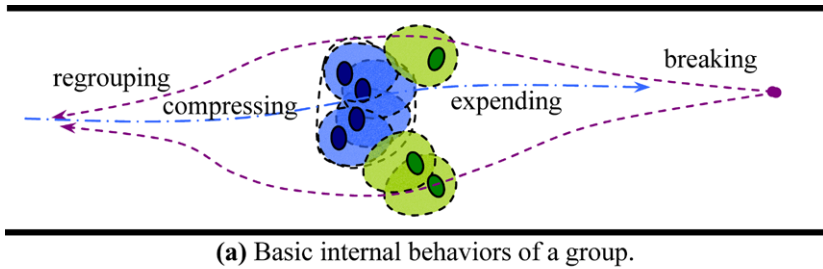


Fig. 9. Basic internal behaviors of a group.

quickly and safely. Followers follow the leader and keep balance with other members to compete with other groups.

Keeping balance with other members is an important factor to walk and finish the service route quickly, comfortably and safely. In order to keep balance, the group has four basic internal behaviors: compressing, expanding, breaking and regrouping as shown in Fig. 9.

Compressing takes place when a group conflicts with other groups or goes through a narrow passage, in order to keep the members together, go smoothly and avoid collision. When conflict disappears or the passage becomes wide enough, the group expand to resume the members' former positions and personal spaces. And by expanding, the members can repel other groups and individuals together.

When external pressure is too strong to endure and the group can not be compressed any more, it breaks and its members go through the narrow passage or the crowd separately. When members passed the conflict area, they regroup again.

(2) Interactions of Groups

Repulsion: Repulsion is a universally existing interaction that can keep distance between one group and other groups to avoid collision.

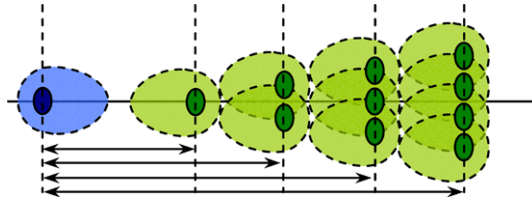


Fig. 10. Sketch of one individual meets different size groups.

Attraction: Attraction exists among groups in the same section of a flow in adjacent areas. It brings groups together and makes them move in the same route.

Combination: In a narrow space or a conflicting area, repulsion produces pressures that make groups compress or break and attraction combines the compressed and broken groups into incompact groups, as Fig. 8(b) and Fig. 12 shows. One incompact group is more powerful to push its way through its route.

The Impacts of Groups on the Crowd

(1) The Form and Mobility of Groups Make the Crowd Uneven

Groups occupy larger area with their irregular private spaces and move slower than individuals. Groups are hard to be drilled through by other groups or individuals. If groups slow down individuals, the individuals have to stop or yield. These may cause local congestions. An individual needs a longer distance to react and adjust its movement when it encounters groups as show in Fig. 10. Flows made of only individuals pass each other smoothly in opposite directions, while flows that made of both groups and individuals pass each other more unevenly. See Fig. 11.

(2) Groups Are More Powerful than Individuals in Conflicts

When flows come across one another, compact groups are compressed to form incompact groups. Incompact groups can generate group-level conflicts and produce greater opposite forces, which slow down the groups and individuals and form congestion in the conflicting area. If it happens in a narrow passage, the congestion would be even worse, as shown in Fig. 12.

(3) Breaking and Regrouping of Groups Disturb the Smooth Flow

Groups may break and regroup several times in conflicts along their route. Incompact groups break and regroup more frequently than compact groups. See Fig. 12. When groups break or regroup, their members disturb other groups and individuals and make the flow uneven.

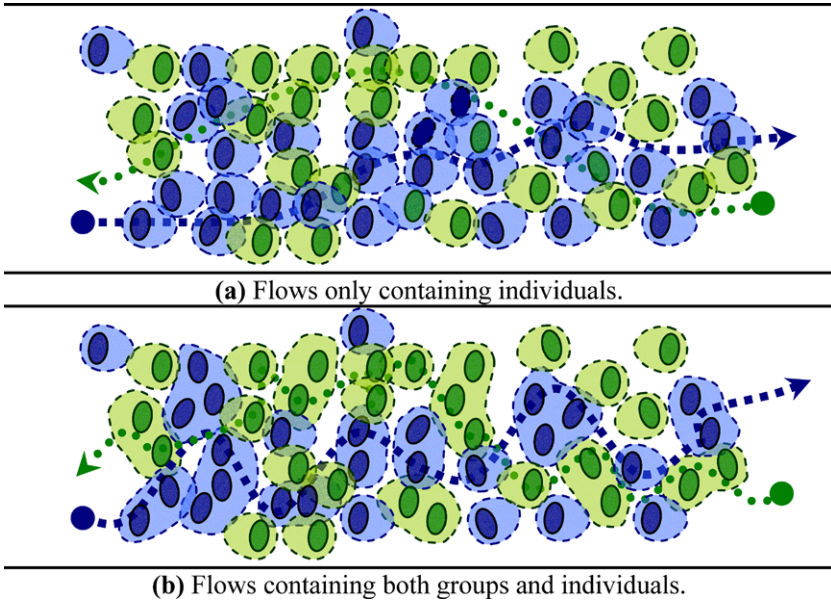


Fig. 11. Groups make the crowd uneven.

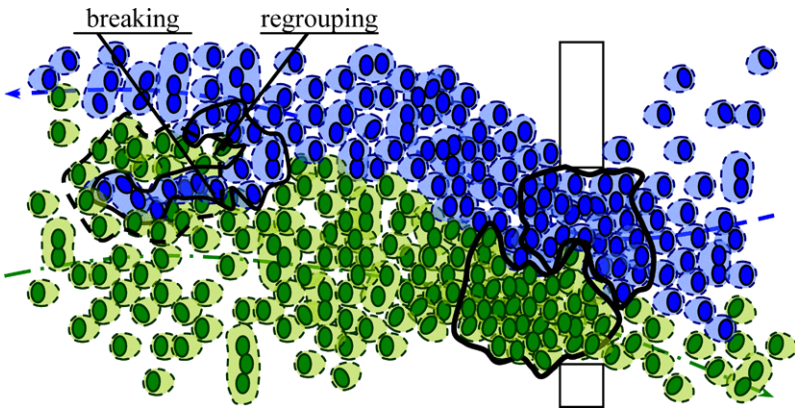


Fig. 12. Group-level conflict in narrow passage.

4 Process Modeling of the Mass and Simulation Framework Based on Group Level Behaviors

4.1 Process Modeling of the Mass

The relationships of all hierarchies can be described as a process model in Fig. 13. Group-level behaviors play an important role in this model. Train operation is the environment information. One element of a hierarchy is one agent.

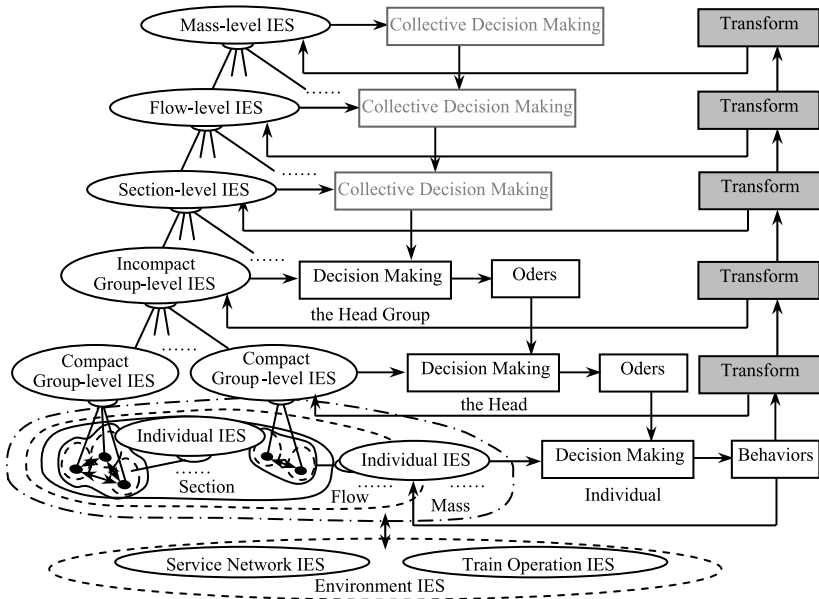


Fig. 13. A process model describing the behavior of the mass.

(1) Information Exchanging Space and Information Transmitting

We assume that each agent has an Information Exchanging Space (IES). The function of IES is to store the information from all members in an agent and provide a platform for members to exchange information. Table 2 shows the information stored in each hierarchy’s IES.

If a member wants to have a full view of the situation and make a rational decision, he can get information from a higher hierarchy via the IES of his agent. For example, if an individual wants to get information from the section he/she belongs to, he/she can send an application message to the IES of his/her own compact group, then the compact group sends the message to the IES of its incompact group, and the incompact group sends the message to IES of its section. The IES sends the information back to the individual through the opposite direction.

(2) Information Updating and Behaviors of All Hierarchies

All information should be updated in time. In the model, IES of every agent updates its information after it finishes behavior or transforms.

The behaviors of all hierarchies include decision making, order, movement, transform, etc. Table 3 shows the typical behaviors of different hierarchies. Collective decision making of mass, flow and section hierarchies is not covered here.

Hierarchies	Behaviors
Mass-level	Evacuating, Congesting
Flow-level	Interfering, Distributing, Converging, Splitting, and Intercrossing
Section-level	Intermiting, Resuming, Serving
Group-level	Compressing, Expending, Breaking, Regrouping, Repulsing, Attracting, and Combining
Individual	Percepting, Decision making (Routing, Path finding), Queing, Competing, Herding, Leading, Following, ...

Table 2. Contents of information exchanging spaces of different hierarchies.

Hierarchies	Items	Contents
Mass-level	Structure	Population, Flows, ...
Flow-level	Affiliation	Mass
Section-level	Structure	Flow ID, Route, Population, ...
Group-level	Affiliation	Flow
Individual	Structure	Section ID, Population, ...
information	Affiliation	Section
information	Mobility	Route, Speed, Direction, Location, ...
information	Structure	Group ID, Population, Head, Followers, Shape, Area, ...
Individual	Affiliation	Group
information	Mobility	Speed, Direction, Location, ...
	Personal Info	ID, Age, Gender, Experience, ...

Table 3. Typical behaviors of different hierarchies.

4.2 URT Station Mass Movement Simulation Framework

We built a simulation framework for URT station mass movement as shown in Fig. 14. Three levels of this framework are: database, models and modules.

(1) Database

A global database stores the data about space, facilities, passengers, train plans, and events and the results of simulation.

(2) Models

Models contain the hierarchical structure model of space and mass, the process model of the mass, individual behavior models and collective (group, section, flow and mass) behavior models. These models provide basic logics to process the data and do simulations.

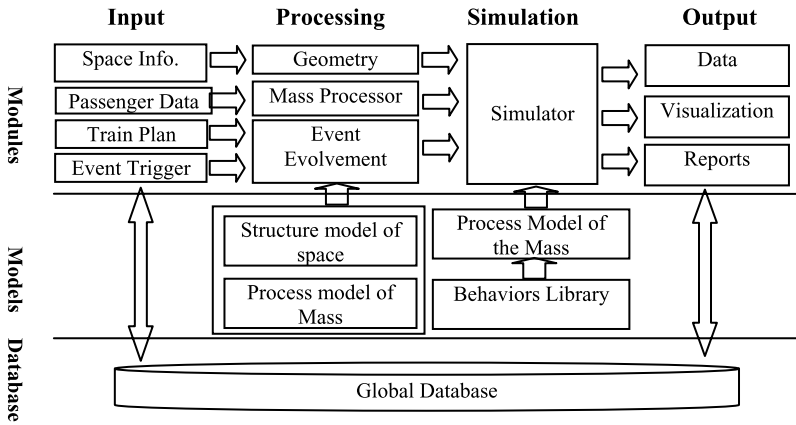


Fig. 14. Simulation framework.

(3) Modules

“Input” module reads data from the global database. “Processing” module translates the data to the format needed and creates an environment for simulation to run. “Simulation” module is the core module that simulates the movement and distribution of the mass in URT station based on the process and behavior models. “Output” module generates statistical data from simulation results, display simulating process by videos, pictures and reports.

5 Discussion

In this paper we have made a great effort on analysis of the hierarchical structure of URT station and the mass, and on top of it we studied group-level behaviors. Groups and their behaviors are discussed relatively less than flows and individuals in existing publications. Adding group level behaviors in the model should greatly improve the simulation.

The figures of the crowds are traced out from pictures in the survey in People’s Square Station. The analysis and conclusions are mostly qualitative. We have several thoughts on how to improve our study: (1) make more quantitative analysis; (2) study more URT Stations; (3) add computational models and algorithms into our existing simulation modules; (4) simplify the process model of the mass and improve calculation efficiency.

The group-level behaviors in other public spaces are similar to that in URT stations, and further study could also be used in simulation and evacuation studies for other public spaces.

Acknowledgements

This research is supported by the National Science Foundation of China, Grant Number 50478105. We are grateful to an anonymous referee for very helpful comments.

References

1. G. K. Still. Crowd dynamics on the simulation of the crowd for safety analysis, PhD Thesis, University of Warwick, 2000.
2. X. Pan. Computational modeling of human and social behaviors for emergency egress analysis, PhD Thesis, Department of Civil and Environmental Engineering, Stanford University, CA, 2006.
3. I.D. Couzin and J. Krause. Self-organization and collective behavior in vertebrates. *Advances in the Study of Behavior* 32, 1–75, 2003.

The Use of a Structure and Its Influence on Evacuation Behavior

Steve M.V. Gwynne and Dave Boswell

Hughes Associates, Inc., 3515 28th st #307, 80301 Boulder, USA

e-mail: sgwynne@haifire.com

Summary. A fire incident is just one event in the life of a building. The procedures employed to address a fire exist in an environment with other procedures. Given these facts, and the complexity of evacuee response, simulation tools must have the ability to simulate the building under a number of conditions and the interaction of the procedures in place. This would reduce the number of assumptions required of the engineer and produce a more reliable understanding of procedural effectiveness.

1 Introduction

Currently, egress models are employed to examine one mode of people movement; namely evacuation performance [1]. This excludes a significant influence upon the expected response of a population; i.e. how the building is used prior to the incident. In order to understand how people respond to an incident there is great value in understanding the other modes of people movement. Examining only a single mode also does not take into account that other modes of movement may exist simultaneously, even when an evacuation is taking place. For more robust simulation results, both of these key points need to be addressed.

2 Information Carried by the Individual

A fire does not occur in a contextual vacuum: the structure in which a fire occurs existed prior to the incident and is therefore likely to have a history that influences how people enter, use and leave the structure (see Fig. 1(b)). The building's use will therefore directly influence the performance of an evacuating population [2]. For instance, it will influence a population's initial distribution, their familiarity with the routes available, and their activities at the time of the incident. *The history of a building's use is stored in the experience and knowledge of the population* (see Fig. 1(a)).

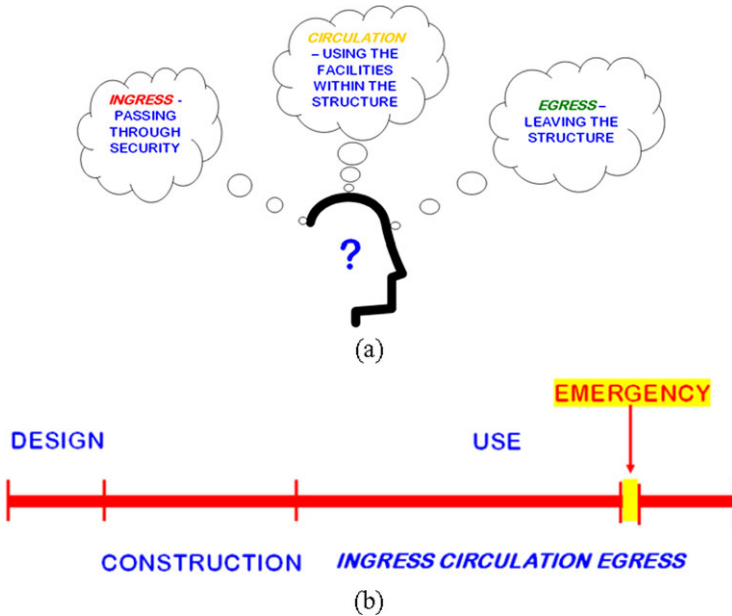


Fig. 1. **a** Experience of the individual. **b** Scenario is one event in the lifecycle of the building.

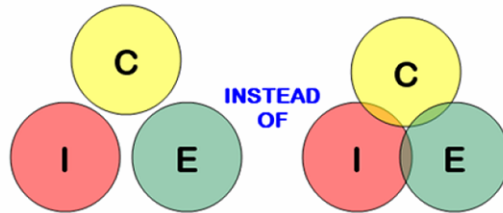
3 Procedures Employed

In recent times, the number and type of incident scenarios has increased significantly. This has been due, primarily, to the increased fear of terrorist attacks, post 9/11, particularly in high profile or vulnerable structures (e.g. tall structures, airports, etc.) [3]. It has therefore become necessary to increase the security measures present. Whereas previously security would have been primarily targeted at the prevention of crime and would have been relatively unobtrusive, current security levels have increased and have a much greater influence over the general movement of people.

These security developments will have a significant impact on the way that people use structures, in both non-emergency and emergency scenarios. In most cases, improved security is given precedence over the comfort level of people during non-emergency movement. Similarly, the impact of security changes upon the effectiveness of evacuation procedures is rarely examined; i.e. the effect of changes on ingress management/security upon circulation and egress (emergency or otherwise). Previous examples exist (e.g. Stardust, Dublin [4]) where the presence of security measures hindered the evacuation from an incident (see Fig. 2(a)). Given the increase in security measures over a short period of time, this hindrance will be increased and may not be addressed in typical egress analysis.

ICE		Scenario	
		Emergency	Non-Emergency
Phase of Movement	Ingress (I)	Crowd management, Fire Department Emergency	Security, Ticketed Access
	Circulation (C)	Ensuring initiation of response, disengagement of population from their pre-event activities	Providing information on facilities and services
	Egress (E)	Managing emergency evacuation	Leaving the building, crowd management

(a)



(b)

Fig. 2. a Phases of movement. b Coupling of these phases.

Several procedures can be employed at the same time during an incident. Members of a population may perform different (emergency/non-emergency) activities in the same space at the same time. Procedures can interact and influence the overall outcome. The effectiveness of one procedure is dependent on the performance of another. It is critical to understand these influences and take them into account when examining egress performance (see Fig. 2(b)).

The independent examination of security and evacuation procedural systems can have important consequences on the effectiveness of the procedures employed. For instance, if examined in isolation, security may be undermined in the event of a fire (security loopholes become apparent through the opening of emergency exits, for instance), and an evacuation from fire may be compromised by the constraints imposed by elevated levels of security (for instance, the presence of checkpoints and/or the reluctance of evacuees to enter previously secure areas).

For example, assume that a building is being used in a routine manner. Occupants are distributed about the space according to their activities and familiarity; for instance, in their office spaces, in cafeterias, etc. An incident occurs somewhere within the building, it is detected and an alarm sounds. The response of the population to this alarm cannot be guaranteed. Some occupants may continue to enter, leave and use the structure as normal. Others, although aware of the alarm, may be unwilling to leave; e.g. they may feel that the incident does not pose a threat. Other occupants will respond to the alarm; e.g. evacuate, collect belongings, etc. These are likely to evacuate the way that they entered the structure, especially in the absence of clear guidance. They are unlikely to breach established security points, even if it is part

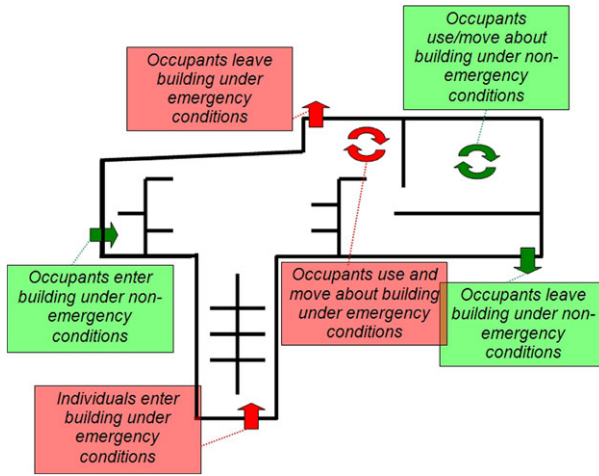


Fig. 3. The complexity of an actual incident.

of the emergency procedure. Eventually, emergency personnel will attend the scene and enter the structure. In this example, all three forms of movement (ingress, circulation and egress) are evident under both non-emergency and emergency conditions.

People do not respond uniformly to the non-emergency/emergency procedures. To assume that people do respond uniformly represents a gross simplification. People may interpret events differently, have access to different information, have different motivations, and may be subject to different procedures (security, evacuation, circulation), which in turn may interact, detracting from their effectiveness. This situation would be further compounded if several organizations occupied the same structure and applied different procedures.

4 Addressing the Situation

To examine the outcome of an incident it is important to understand/simulate all forms of people movement; be they due to the occupant experiences or the procedures employed. Simulation tools provide a mechanism by which to do this. Normally, these tools are applied to (or are able to address) a single mode of movement; e.g. evacuation, circulation etc. This misses the impact of the experience that the individual brings with them (e.g. familiarity, etc.) and the possibility of several procedures being performed simultaneously and then interacting.

The factors influencing occupant behavior should be simulated *temporally* (the experiences/knowledge of the evacuees) and *spatially* (the different procedures employed at the time). This has a number of benefits. It allows the engineer to better understand the initial conditions of an event (e.g. where people might be) and configure the scenario more accurately. The simulated

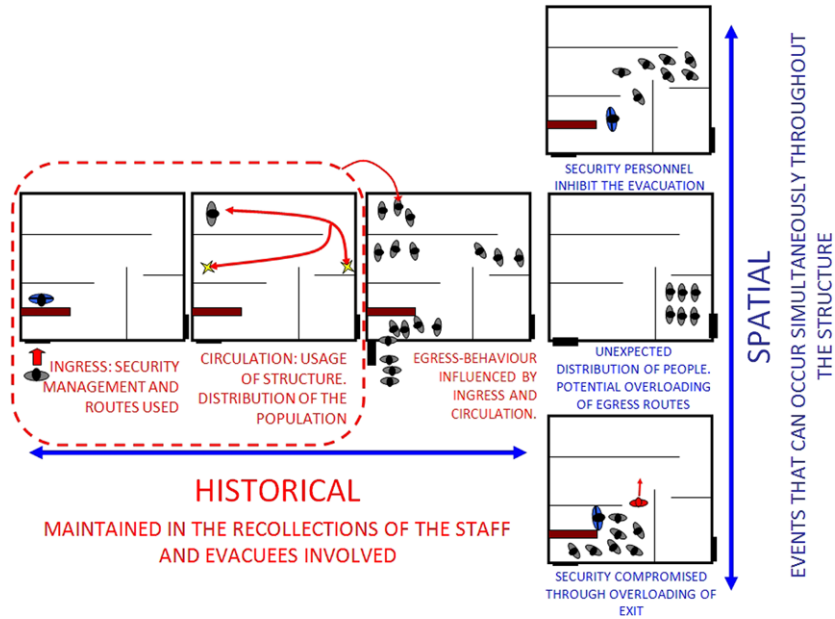


Fig. 4. The simulation of temporal and spatial conditions.

behavioral response of the occupants will be more realistic; i.e. it will be sensitive to their normal activities and knowledge levels. It will therefore require fewer estimates and assumptions from the engineer. The non-emergency and emergency procedures can be represented; i.e. a key factor in the response of occupants is included. A better understanding of procedural effectiveness is possible by considering both the information levels of the occupants and the impact that procedures can have upon each other. Therefore, two key parameters that influence evacuation performance (evacuee understanding and procedural effectiveness) can be taken into account, rather than assumed.

This requires a change in the capabilities of egress models. It will require models simulating conditions prior to the development of an incident (i.e. across the lifecycle of the building) and will require a broader range of behaviors during the incident. In situations where usage, scale and procedural complexity are a factor (e.g. airports, high-rise, etc.), this approach will:

- increase the accuracy of the results produced;
- highlight where there are shortfalls in the procedures;
- identify where occupant knowledge is not sufficient and where training/documentation can remedy this situation.

The suggested method simulates people movement within a structure as a highly coupled system, rather than as a set of disparate activities. The structure is treated as a system in which movement can take place under various conditions. The life-cycle of the structure will include three key modes

of people movement: Ingress; Circulation; and Egress. The movement components of the life-cycle (named after the acronym ICE) may be present at any time, especially in large or complex spaces. These may be present during non-emergency situations (e.g. daily movement) and during an emergency (e.g. the occurrence of a fire). In order to produce management procedures that are robust, the procedures should be sensitive to the other modes of movement.

The complexity that the ICE method suggests inevitably requires the use of simulation tools to investigate the relationship of the modes of people movement. Simulation tools may highlight the knock-on effect of changes to the security measures upon general circulation and upon emergency egress, and vice versa.

By adopting the simulation and engineering approach outlined here, the potential impact of changes in security (along with other procedures) upon emergency procedures will be better understood, and the loopholes in security more likely to be identified and avoided. The method should therefore avoid compromises in both safety and security. This, more integrated, approach allows the procedures in place (security, safety and general operation) to be cognizant of the other types of movement that might be present through a more systematic approach and through the application of sophisticated simulation tools.

5 Concluding Remarks

A fire is but one possible scenario that can occur in a building. It is possible to identify other (temporal or spatial) procedural factors that will influence the outcome of an emergency. If simulated, these factors allow the engineer to configure the scenario more accurately, assess the information levels of the evacuees and identify where procedural responses may interact, allowing a truer picture of their effectiveness to be established. It is therefore critical for models to simulate both FIRE and ICE in order to produce a more reliable assessment.

References

1. Kuligowski, E.D., and Peacock, R.D., Review of Building Evacuation Models, NIST TN 1471; NIST Technical Note 1471; p. 153, 2005.
2. Sime, J., *Escape Behaviour in Fire: 'Panic' or Affiliation?*, PhD Thesis, Department of Psychology, University of Surrey, 1984.
3. Final Report on the Collapse of the World Trade Center Towers, NIST, NCSTAR 1, September, 2005.
4. Fetherstonhaugh, N., and McCullagh, T., *They Never Came Home*, ISBN 1903582636, Merlin Publishing, 2006.

Part IV

Miscellaneous

Inhalation Injury of Lung and Heart After Inhalation of Toxic Substances

Herbert Löllgen¹ and Dieter Leyk^{2,3}

¹ Dept. and Clinic of Internal Medicine (Cardiology, Pneumology, Intensive Care Medicine), Sana-Klinikum Remscheid, University of Bochum, Burger Str. 211, 42859 Remscheid, Germany
e-mail: Herbert.Loellgen@gmx.de

² Department of Physiology and Anatomy, German Sport University Cologne, Cologne, Germany

³ Department IV—Military Ergonomics and Exercise Physiology, Central Institute of the Federal Armed Forces Medical Services Koblenz, Koblenz, Germany

Summary. The clinical manifestations of acute inhalation of toxic substances vary according to the particular injurious agents, concentration, length of exposure, and underlying pre-existing diseases in the subjects. Responses of lung and heart on acute and chronic irritant gases are discussed. The data mainly stem from occupational and environmental exposures. The effects of acute lung injury are demonstrated with special regard to carbon monoxide, hydrogen cyanide, and related substances observed in acute smoke inhalation. Clinical manifestations are illustrated. Most complications of fire exposures and death are due to inhalation injuries rather than by burn damages to the skin. Prevention can only be performed in fire fighters by means of protection masks. In case of intoxication during fire, e.g. in houses, smoke inhalation victims have to be treated according to symptoms and signs and toxic inhalants to be involved so far known. Oxygen supply, drugs to open airways (bronchodilators) and lung protection by corticosteroids are cornerstones in therapy. Victims have to be hospitalized as fast as possible. Evacuations of people in buildings also depend on physical fitness, age, weight and diseases of joints and bones.

1 Introduction

Inhalation of toxic agents is the main problem during fire in houses or open places as in occupational and environmental situations. This paper deals with irritant gases, toxic inhalants and their effects on heart and lung, acute smoke injury with heat and thermal injuries, as well as problems in firefighters and pedestrians exposed to smoke and fire.

Hydrogen	H ₂	asphyxia +	inflamm +
Helium	He	+	–
Methane	CH ₄	+	+
Ammonia	NH ₃	irritant	+
Acetylen	C ₂ H ₂	(blood*)	+
Hydrogen cyanide	HCN	(blood)	+
Nitrogen dioxide	NO ₂	+	–
Carbon monoxide	CO	(blood)	+

*Blood: Toxic effects via blood nerves and cells

Table 1. List of toxic inhalants (I) [11, 14].

Form aldehyde	CH ₂ O	irritant +	inflamm +
Hydrogen sulfide	H ₂ S	blood*	+
Hydrochloric acid	HCl	irritant	–
Carbon dioxide	CO ₂	blood	–
Nitrous gases	NO _x	irritant/blood	–
Salpetric acid	HNO ₃	irritant	–
<u>Sulfur dioxide</u>	SO ₂	irritant	–
Chlorine	Cl ₂	irritant	–
Sulfur carbonide	CS ₂	blood	+
<u>Sulfur acid</u>	H ₂ SO ₄	irritant	–
Ozone	O ₃	irritant	–

*Blood: Toxic effects via blood nerves and cells

Table 2. List of toxic inhalants (II) [12].

2 Toxic Agents

List of toxic inhalants is given in Tables 1 and 2 [12, 14]. Irritant means severe effects on the bronchial tree and lungs, asphyxia means imminent blockade of oxygen transport thus leading rapidly to death. Inflammation indicates severe lung disease due to acute or chronic mucosal irritation leading to bacterial or non-specific signs of inflammation [8]. “Blood” means that toxic effects are mediated via blood transport with secondary irritation or damage of the nervous system and cells of lung and heart. Mechanisms of injury are shown in Table 3 [1, 12, 14].

Agents that are water-soluble, are mainly dissolved in the upper respiratory tract causing direct irritation of conjunctival, mouth or tracheal mucosa. Irritant gases with relatively low water solubility penetrate more peripherally thus causing injury in the distal airways and alveoli. Effects on mucosa also depend on alkaline or acid composition of the inhalants, free radicals may also be involved (e.g. ozone, chlorine oxides of nitrogen) [1, 11, 14]. Figure 1 demonstrates the localized effects of respiratory irritants.

Irritants as mechanisms of injury act on manifold ways with direct injury of the mucosa in the respiratory tract replacing oxygen in inspired air thus leading to asphyxia or by toxic effects mediated by blood transport. Finally,

Toxic inhalant	Mechanism of injury
Irritants	
Ammonia (NH ₃)	Direct mucosal injury from alkaline burn
Chlorine (Cl ₂)	Direct mucosal injury from acid burn and free radical formation
Sulfur dioxide (SO ₂)	Low concentration exposure causes bronchoconstriction and increased mucous secretion. High concentration exposure causes acid burns
Asphyxiants	
Methane (CH ₄)	Replaces atmospheric oxygen
Carbon monoxide (CO)	Completes for oxygen-binding sites on hemoglobin
Systemic toxins	
Benzene (C ₆ H ₆)	Causes central nervous system toxicity and bone marrow suppression

Modified from Weiss et al., Clin. Chest Med., 1994

Table 3. Toxic inhalants according to mechanism of injury (modified from [12]).

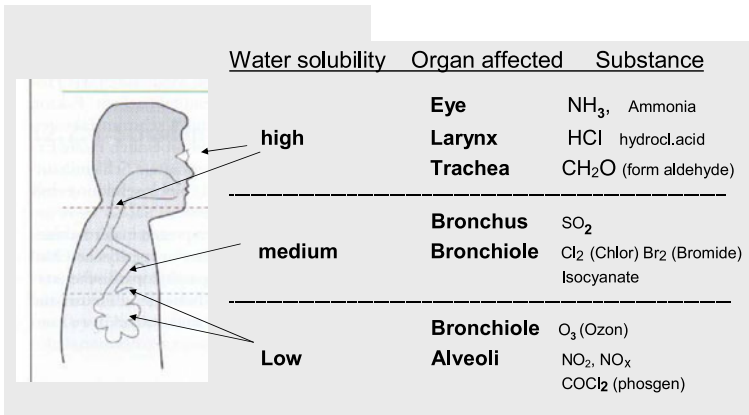


Fig. 1. Localized effects of respiratory irritants [12].

sources of exposure, physical properties and mechanisms of lung injury are summarized in Table 4. Manifestations of inhalation may appear by a variety of clinical symptoms and signs such as pneumonia, upper respiratory tract irritation, pulmonary edema or inflammation of the bronchi including obstruction of the bronchi resulting in asthma, cough or bronchitis and dyspnea [7, 11, 12].

3 Irritant Effects of Inhalant Noxious Agents

As an example of irritant effects, controlled studies of human exposures to single and combined action are shown in Figs. 2 and 3 [10]. These experiments in healthy young subjects clearly showed a decrease of oxygen content

Irritant gas	Sources of exposure	Water solubility	OSHA standard ceiling
Ammonia (NH ₃)	Agriculture, mining, plastic and explosive manufacturing	High	50.0 ppm
Chlorine (Cl ₂)	Paper and textile manufacturing, sewage treatment	Intermediate	1.0 ppm
Hydrogen chloride (HCl)	Dyes, fertilizers, textiles, rubber; thermal degradation of polyvinyl chloride	High	5.0 ppm
Oxides of nitrogen (NO, NO ₂ , N ₂ O ₄)	Agriculture, mining, welding, and manufacturing of dyes and lacquers	Low	5.0 ppm
Ozone (O ₃)	Welding, chemical industry, and high altitude transportation	Low	0.1 ppm
Phosgene (COCl ₂)	Firefighters, welders, paint strippers; chemical intermediates (isocyanates, pesticides, dyes, and pharmaceuticals)	Low	0.1 ppm
Sulfur dioxide (SO ₂)	Smelting, combustion of coal and oil, paper manufacturing, and food preparation	High	5.0 ppm

OSHA = Occupational Safety and Health Administration
Weiss et al., Clin. Chest Med., 1994.

Table 4. Sources of exposure, physical properties, and mechanism of lung injury of gaseous respiratory irritants (modified from [12]).

in blood after inhalation of these gases and an increase of airway resistance. Combination of several toxic gases (at MAK concentration) had no stronger effect than NO₂ alone. This underlines the pronounced toxic effect of NO₂ or NO_x. This gas also occurs in traffic situations. Acetylcholine as an unspecific provocative substance significantly increased bronchial reactivity after exposure to combined effect of irritant gases (Fig. 3). It should be kept in mind that recent investigations demonstrate an intermittent destruction on DNA in fire workers with rapid repair after end of exposure [6].

4 Ambient Air Pollution

In addition to irritant gases, ambient air pollution may also cause lung and heart injury [2, 5, 7, 12, 13]. Definitions are given in Table 5. Short term effects have been investigated in population studies in US and Europe with a significant effect on mortality either by lung or heart disease (Table 6) [2, 12, 13].

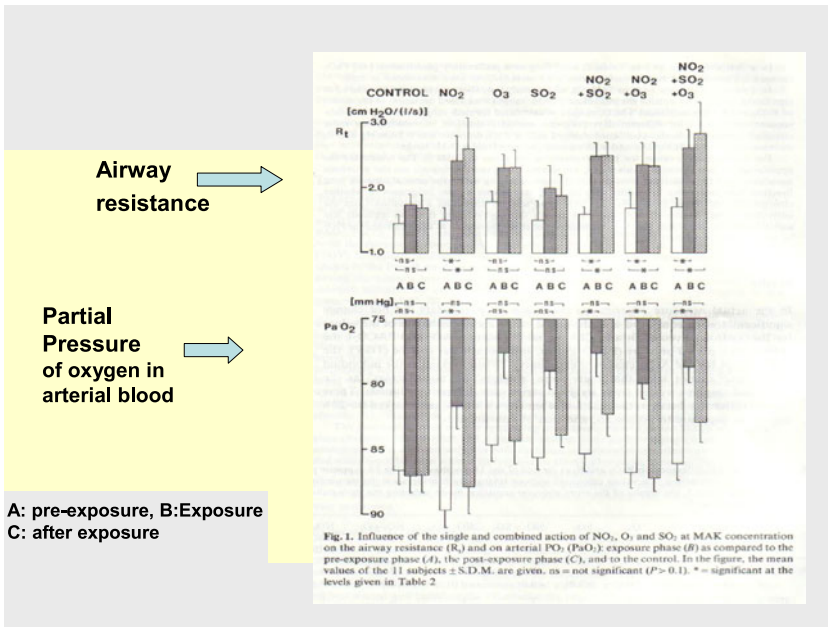


Fig. 2. Influence of single and combined action of NO_2 , O_3 , SO_2 , at MAK concentration on airway resistance (R_t) and arterial oxygen partial pressure (PaO_2) (modified from [6]).

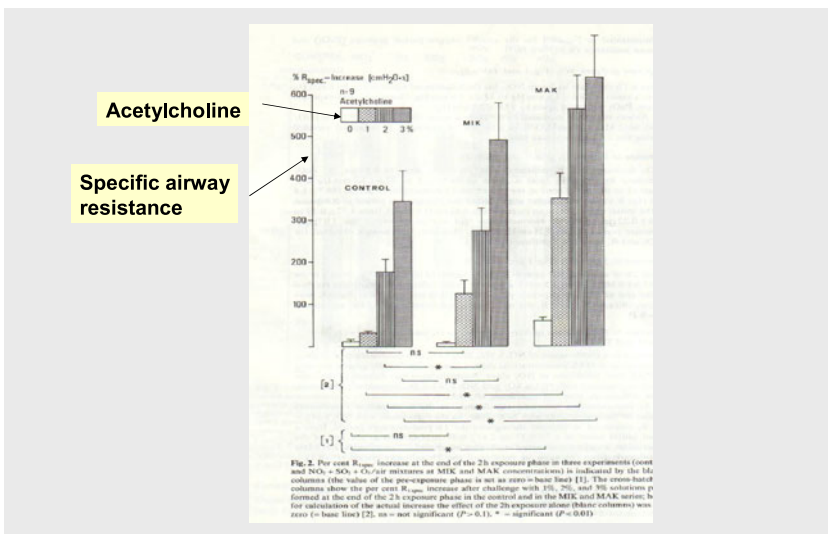


Fig. 3. Effects of non-specific irritants (acetylcholine) after 2 hours of exposure to combined irritants (NO_2 , SO_2 , O_3) [6].

Particular Matter: Definition

Mixture of **solid** and **liquid** particles suspended in air varying in size and chemical composition

Composition: Nitrates, sulfates from motor vehicle emissions, tire fragmentation and resuspension of road dust (so far up to thousands of chemicals identified)

Relevant components: Nitrogen oxides (NO_x), Carbon monoxides (CO), Sulfur dioxide (SO_2), and Ozone (O_3)

Table 5. Aspects of ambient air pollution.

NNMAPS-Study (US, 50 Mill. people) and APHEA-2* (Europe, 43 Mil. people): Average **mortality** rate was significantly associated with particle concentration the day before death

Each $10\text{-}\mu\text{g}/\text{m}^3$ elevation of PM_{10} increased all-cause mortality by 0.21 and cardiac mortality by 0.3 (US) and 0.60 and 0.69, respectively (Europe)

Besides, there are well-documented effects on cardiac morbidity and mortality in **long-term** effects of air pollution (Circulation 2004, Brook et al.)

*Horak, Atemw. Lungenkrkh, 2002

Table 6. Air pollution: short-term effects [3].

5 Acute Smoke Injury

The main problem during fire in houses or large buildings are acute lung injury due to smoke effects [6]. These effects are thermal injury and toxic effects as asphyxia, caustic burns or toxic effects via blood (see above). In the US, about 2 million people suffer thermal burns from fire per year and about 7,000–10,000 people die as a result of the injuries. Thermal injury is mostly limited to the upper airway region with swelling of the mucosa thus impeding respiration. With the water content of the inhaled agent increasing, inhaled steam causes thermal injury to the whole tracheo-bronchial tree. Steam has about 4,000 times higher heat carrying capacity compared to dry air. Acute smoke injury may further cause irritant effects, toxic effects and asphyxia depending on smoke composition [11]. In most situations, multiple toxic agents are involved the details of which are not always known. With ambient oxygen concentration less than 15%, unconsciousness and death do occur.

Main inhalants with asphyctic effects are carbon monoxide displacing oxygen from hemoglobin, cyanide, blocking oxygen transport via inhibition of cytochrome oxidase and hydrogen sulfide which inhibits cellular respiration by binding to cytochrome oxidase.

6 Clinical Manifestations

Clinical signs mostly are eye irritation, cough, dyspnea, hoarseness, stridor and wheezing [1, 8, 11, 14]. In-door evaluation can be done for carbon monoxide,

cyanide and later on lung function analysis. According to own experience, hospitalization is recommended for 48 to 72 hours depending on the suspected inhalant agent.

7 Medical Problems with Pedestrian Evacuation

Major problems with evacuation are physical fitness and lung function capacity. Both depend on endurance capacity of heart and lung, flexibility of the musculo-skeletal system, and local (muscular) endurance.

Today, most people have reduced fitness due to sedentary lifestyle and obesity. Degenerative joint diseases, especially in obese people, enhance difficulties to move rapidly and rush the stairs down. In addition to low level of fitness, manifest or suspected diseases such as coronary artery disease, hypertension or chronic obstructive lung disease with angina and/or dyspnea critically limit the speed of movement, especially in case of emergency. So limiting factors in movement on a staircase are musculoskeletal problems, overweight and limited physical fitness.

8 Medical Problems in Firefighters

Firefighters are examined regularly on an annual basis in Germany, the so-called G26 examination including an exercise test to screen for ischemia, hypertension and general fitness. Normal exercise capacity is 3/2.5 watts (male/female; m/f) per kg body weight below the age of 39 years and 2.1/1.8 watts (m/f) over 40 years. According to own experiences, reduced functional capacities in firefighters mainly depend on overweight, high blood pressure, smoking habits and lack of regular physical activity. Measurements of physiological demands during occupational situation results in sometimes high heart rates, even up to 190 bpm. This demonstrates the severity of firefighters' work load.

Physical demands for firefighters are:

- respiratory, i.e. self-containing breathing apparatus (Table 7),
- protective overall,
- microclimate, psychic effects due to claustrophobia and actual emergency situation,
- carrying heavy weight, especially when rescuing persons.

Especially the self containing breathing apparatus (SBCA) and the personal protective ensemble increase the physical and physiological demands for firefighters.

Respirators have a weight of about 3–5 kg, the resistance to breathing increases dead space ventilation thus impeding respiration.

Heart rate increases about 25% in simulation, but about 39% during fire exposition (Bruce-Low, 2007, UK)

$\text{VO}_{2\text{max}}$ was about 17% lower than control (43 vs. 52.2 ml/kg/min) during PPE and SCBA (Dreger, 2006, UK)

Tolerance time (TT): Passive recovery is not sufficient, with higher temperature $>30^{\circ}\text{C}$ and higher metabolic rate (Selkirk, 2004, Toronto)

TT decreased from 56 to 47 to 41 min. (Heavy) ... and 121 to 87 min for low work load, 35°C

Table 7. Personal protective ensemble (PPE) and self-containing breathing apparatus (SCBA) and heat, for further literature please contact the authors.

Therefore, good health and excellent physical fitness reduce the work load for fire fighters. Experiences from a large and severe action at the 9/11 catastrophe have been published recently [10]. Some of the firefighters engaged in this action reported longstanding symptoms of lung and bronchial diseases [3, 4, 9, 14].

9 Treatment of Smoke Inhalation

Therapy on stage after smoke inhalation consists of inhalation of bronchodilators and corticosteroids with repetition every 15 minutes for corticosteroids. In severe cases intravenous corticosteroids should be given. Immediate transport to hospital for intensive treatment is strongly recommended. Patients should stay for at least 24 to 48 hours due to late reaction on toxic agents causing late pulmonary edema [11].

10 Conclusion

Inhalation injuries are complex by nature. The great number of these agents with different injury mechanisms complicates prevention and treatment. For fire fighters, good physical fitness is the qualification for successful work, for self-protection and improved performance. Long-term medical observation and regular examinations after smoke exposure in patients **and** in fire fighters are strongly recommended.

Immediate therapy of inhalation injury on stage is state of the art in patients and fire fighters in case of injury, as well. Increased fitness in normal people and inhabitants or workers in large buildings may be life-saving in case of evacuation. Healthy life-style may also be helpful in such situations.

References

1. Brook RD, Franklin B, Cascio W, Hong Y, Howard G, Lipsett M, Luepker R, Mittleman M, Samet J, Smith SC, Tager I: Air pollution and cardiovascular disease. *Circulation* 109, 2004:2655–2671.
2. Hoffmann B, Moebus S, Möhlenkamp S, Stang A, Lehmann N, Dragano N, Schmermund A, Memmesheimer M, Mann K, Erbel R, Jöckel KH: Residential exposure to traffic is associated with coronary atherosclerosis. *Circulation* 116, 2007:489–496.
3. Horak F, Neuberger M, Kundi M, Frischer T, Studnicka M, Hauck H, Preining O: Gesundheitseffekte von Partikeln (Health effects of particular matter—first results of the AUHEP). *Atemw—Lungenkrankh* 28, 2002:291–292.
4. Kulkarni N, Pierse N, Rushton L, Grigg J: Carbon in airway macrophages and lung function in children. *New Engl. J. Med.* 355, 2006:21–30.
5. Mannino DM, Buist AS: Global burden of COPD: Risk factors, prevalence, and future trends. *Lancet* 370, 2007:765–773.
6. Nieding G, Wagner HM, Krekeler H, Löllgen H, Fries W, Beuthan A: Controlled studies of human exposure to single and combined action of NO₂, O₃, SO₂. *Int. Arch. Occup. Environ. Health* 43, 1979:195–210.
7. Nowak D: Inhalative Noxen: Toxisch irritative Gase und Aerosole (Inhalative Noxic Agents; Irritative toxic gases and aerosols) (in German). In: Vogelmeier C, Buhl R: *Pneumologische Notfälle (Pneumological Emergencies)* Wissenschaftliche Verlagsgesellschaft mbH, Stuttgart, 2004: 305–329.
8. Pope CA, Muhlestein JB, May HT, Renlund DG, Anderson JL, Horne BD: Ischemic heart disease events triggered by short-term exposure to fine particulate air pollution. *Circulation* 114, 2006:2443–2448.
9. Pope CA, Burnett RT, Thurston GD, Thun MJ, Calle EE, Krewski D, Godleski JJ: Cardiovascular mortality and long-term exposure to particulate air pollution. *Circulation* 109, 2004, 71–77.
10. Samet JM, Geyh AS, Utell MJ: The legacy of world trade center dust. *New Engl. J. Med.* 356, 2007:2233–2236.
11. Smidt U, Löllgen H, Nieding Gv, Krekeler: Early signs of chronic non-specific lung disease in dust exposed workers. *Bull. Physio-Path. Resp.* 11, 1973:52–55.
12. Weiss SM, Lakshminarayan S: Acute inhalation injury. *Clinics Chest Med.* 15, 1994:103–116.
13. Zanobetti A, Canner MJ, Stone PH, Schwartz J, Sher D, Eagan-Bengtson E, Gates KA, Hartley LH, Suh H, Gold DR: Ambient pollution and blood pressure in cardiac rehabilitation patients. *Circulation* 110, 2004:2184–2189.
14. www.anr.de, AG Notfallmedizin und Rettungswesen e.V. an der Ludwig-Maximilian-Universität München, 2005.

Quantitative Comparison of International Design Standards of Escape Routes in Assembly Buildings

Burkhard Forell¹, Ralf Seidenspinner², and Dietmar Hossler³

¹ Gesellschaft für Anlagen- und Reaktorsicherheit (GRS) mbH, Schwertnergasse 1, 50967 Cologne, Germany

e-mail: burkhard.forell@grs.de

² University of Wuppertal, Institute of Construction Management, Pauluskirchstraße 7, 42285 Wuppertal, Germany

e-mail: r.seidenspinner@baubetrieb.uni-wuppertal.de

³ Institute of Building Materials, Concrete Construction and Fire Protection, Braunschweig University of Technology, Beethovenstraße 52, 33106 Braunschweig, Germany

e-mail: d.hossler@tu-bs.de

Summary. The design standards for escape routes in assembly buildings are discussed by comparing the building codes and regulations of eight European countries, China, and USA. To quantify the results for the simple scenario of the evacuation of an assembly room, the travel times are calculated by flow capacity equations. For each country the results vary with the area of the assembly room. Among different countries there is a significant scatter of the results which varies by a factor of three. As the travel times are influenced by the design occupant densities which range from 0.5 to 4 p/m² for places of entertainment, a second comparison is made with a normalized density of 4 p/m². Here the results also scatter by a factor of three. The implications on occupant safety are discussed with regard to potential fire scenarios.

1 Introduction

Fires in places of assembly frequently lead to high death tolls. Due to the high occupant density and additional factors, places of entertainment like nightclubs and discotheques have been especially hit by severe fires over the last years. Well known incidents are the fires with 63 victims in a dance hall in Gothenburg (Sweden) (1988), 309 victims in a disco/dance hall in Luoyang (China) (2000), 100 victims in a concert hall in Warwick, RI (USA) (2003), and 194 victims in a disco/dance hall in Buenos Aires (Argentina) (2004). The incidents were caused by fast growing fires or fires which first developed undetected in a room adjacent to the assembly room. In many cases

the evacuation process was impaired by overcrowded occupancies and/or by blocked or badly-designed escape routes.

The vulnerability of assembly buildings to fires and other emergency situations widely depends on the required evacuation time to reach a safe area. The evacuation time is defined as pre-travel activity time plus travel time [1]

$$t_{\text{pre}} + t_{\text{trav}} = t_{\text{evac}}. \quad (1)$$

The pre-travel activity time t_{pre} very much depends on the specific scenario and many “soft” criteria which are not addressed in building codes. Therefore it is out of the scope of this study. The travel time t_{trav} is a function of the design of escape routes—especially the available escape route width per occupant. A commonly accepted number for the maximum evacuation time or the minimum available escape route width per occupant does not exist. Instead, every country has its own record of (fire) incidents and these incidents are rare from a statistical point of view. Therefore the national building codes are more or less affected by major incidents and provide a different level of safety to the occupants. The purpose of this study is to compare building codes of different countries and to quantify the results in terms of the travel time for a simple evacuation scenario. Because of the given incident record, the focus of this study is on places of entertainment.

In Table 1 the countries considered for this comparison are listed with the relevant regulations. The selection of countries is based on available information.

2 General Approach

The places of assembly (Fig. 1) are considered as a typical one-room situation on a first floor with predominately standing areas and relatively high occupant density. The typical bottleneck of the evacuation route is given by the exit doors. After the beginning of the evacuation process the congestion in front of the exit doors immediately develops. The safe area begins behind the exit doors. The travel time of an individual is given by the run-time plus the individual congestion time in front of the exit doors. For most occupants the run time is very short compared to the congestion time. For the last occupant to reach the safe area the travel time is given by the exit-flow time.

The travel time for the last occupant is implicitly given in every building code. To calculate this according to the approach described, the data for the

- minimum number of exit doors, n
- minimum width of each exit door, w_{min} ,
- design occupant load, N , and
- minimum increase of exit door/route width for every occupant

Country	Country code	Source, data
Austria	Aut	Gesetz betreffend Lage, Beschaffenheit, Einrichtung und Betrieb von Veranstaltungsstätten (Wiener Veranstaltungsstättengesetz), 1999
China	Chn	Code for life protection design of tall buildings, 2001, revised edition
England, Wales	GBr	Building Regulations 2000, Approved Document B
France	Fra	Code de la Construction et de l’Habitation
Germany	Deu	Musterverordnung über den Bau und Betrieb von Versammlungsstätten (MVStättV), ARGEBAU, 06-2005
Italy	Ita	Approvazione della regola tecnica di prevenzione incendi per la progettazione, costruzione ed esercizio dei locali di intrattenimento e di pubblico spettacolo, Decreto Ministeriale, 19.08.1996
Luxembourg	Lux	Precriptions de sécurité incendie Dispositions Generales “Bâtiments moyens”, ITM-CL 501.1 Dispositions Spécifiques “Salles de Spectacles”, ITM-CL 554.1
Sweden	Swe	Regelsamling för byggande—Boverkets byggregler (BBR). Code number: BFS 1993:57 med ändringar t.o.m. 2006:22. 01.07.2006
Switzerland	CHe	Brandschutzrichtlinie Flucht- und Rettungswege, VKF, AEAI, 26.03.2003
USA	USA	NFPA 101 Life Safety Code, 17.01.2003

Table 1. Countries and relevant building codes considered for this study.

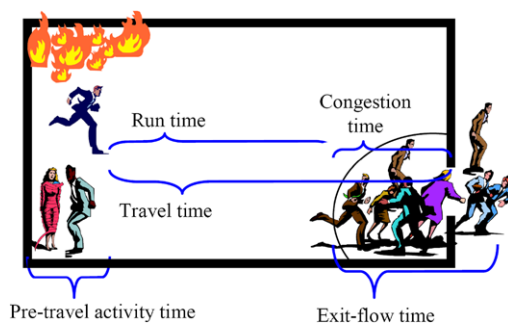


Fig. 1. Schematic illustration of the evacuation process.

is taken from each building code. The resulting relevant total exit door/route width w_{tot} is given either by

- the minimum number of exit doors times the minimum door width or by
- the design occupant load times the minimum increase of exit door/route width for every occupant.

For small places of assembly usually the first criterion becomes relevant while the second has to be taken for larger assemblies. Hence for each building code the travel time varies with the area A of the assembly room

$$t_{\text{trav}}(A) = N(A) \left/ \sum_{i=1}^n w_i \cdot F_i(w) \right. \quad (2)$$

where F_i is the specific flow of occupants through the exit door i which also depends on the given exit door width w .

3 Flow Capacity of Exits

The behavior of occupants passing bottlenecks and the resulting flow f [p/s] or specific flow F [p/(s m)] has been a field of research for decades [2–7]. For the purpose of this study we chose a simple approach accounting for the facts that

- for reasonable exit widths the specific flow F is relatively independent of the exit width w [2, 6], and
- for small exit widths the occurrence of bow behavior and jamming is increased and thus the specific flow $F(w)$ decreased [2–5].

According to the European Standard on spectator facilities [8] a minimum exit width of $w_{\text{min}} = 1.20$ m is proposed, a value that is also backed by work of [3] and [5] to prevent bow behavior and jamming in emergency situations. For these reasons, $w_{\text{min}} \geq 1.20$ m is considered as a reasonable exit width. In [8] the specific flow is given by

$$F_{w \geq 1.20 \text{ m}} = 1.39 \text{ p/(s m)}. \quad (3)$$

For $0.75 \text{ m} < w < 1.20 \text{ m}$ an empirical correlation is derived. In Fig. 2 the model approach is illustrated in comparison with data of Predtetschenski and Milinski [2] at optimum flow. To account for the bow behavior and jamming in emergency situations [3, 5], the decrease of F at $w < 1.20$ m is slightly more significant than given by P + M. The model approach is represented by

$$F_{0.75 \text{ m} < w < 1.20 \text{ m}} = -1.71w^2 + 4.12w - 1.08 \text{ [p/(s m)]}. \quad (4)$$

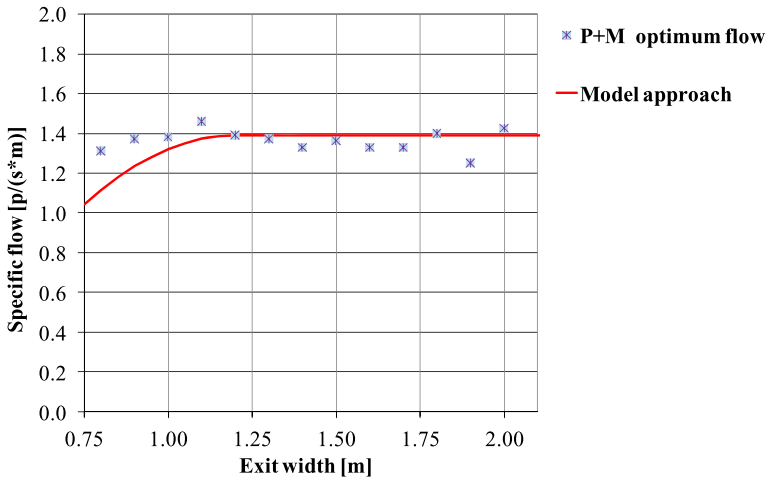


Fig. 2. Model approach for the specific flow F in comparison with data of Predtetschenski and Milinski [2] at optimum flow (projected area $0.13 \text{ m}^2/\text{p}$).

Table 2. Minimum exit door width w_{\min} .

Country	Min. exit width	Applies to
Austria	1.00 m	less than 120 occupants
China	1.40 m	for all assemblies
England, Wales	0.75 m	less than 60 occupants
France	0.90 m	less than 101 occupants
Germany	0.90 m	less than 200 occupants
Italy	0.90 m	less than 150 occupants
Luxembourg	0.90 m	less than 90 occupants
Sweden	1.20 m	for all assemblies
Switzerland	0.90 m	less than 200 occupants
USA	0.81 m	less than 162 occupants

4 Comparison of Raw Data

4.1 Minimum Width of Exit Doors

In Table 2 the minimum widths w_{\min} of exit doors are listed. Most countries allow small exit widths for assemblies with low number of occupants (N). Exceeding a certain number of occupants, door widths must be increased to a width larger than $w = 1.20 \text{ m}$ in all countries.

4.2 Design Occupant Load

The design occupant load is given by the assembly room area times the design occupant density. Table 3 illustrates that there is significant scatter of relevant design occupant densities from 0.5 to 4 p/m^2 .

Table 3. Design occupant density for places of entertainment.

Country	Occupant density	Applies to
Austria	300 p/m ²	Assembly and entertainment with flat standing areas
China	0.50 p/m ²	Places of entertainment
England, Wales	2.00 p/m ²	Amusement arcade, dance floor or hall, etc.
France	1.33 p/m ²	Dance clubs and places of entertainment
Germany	2.00 p/m ²	Assembly and entertainment with flat standing areas
Italy	0.70 p/m ²	Discotheques and entertainment
Luxembourg	3.00 p/m ²	Discotheques, ballrooms, multipurpose assemblies
Sweden	2.50 p/m ²	Dance occupancies
Switzerland	4.00 p/m ²	Discotheques, pop concerts with standing areas
USA	2.17 p/m ²	Assembly occupancies smaller than 929 m ²
	1.54 p/m ²	Concentrated use without fixed seating

Table 4. Design occupant density for places of entertainment.

Country	Increase	Average increase per one occupant
Austria	0.40 m / 60 p	0.67 cm
China	0.01 m / 1 p	1.00 cm
England, Wales	0.005 m / 1 p	0.50 cm for more than 220 occupants
France	–	not applicable
Germany	0.60 m / 100 p	0.60 cm
Italy	0.60 m / 50 p	1.20 cm
Luxembourg	0.01 m / 1 p	1.00 cm for the first 300 occupants
	0.0075 m / 1 p	0.75 cm for every occupant exceeding 300
Sweden	0.0067 m / 1 p	0.67 cm
Switzerland	0.60 m / 100 p	0.60 cm
USA	0.005 m / 1 p	0.50 cm

4.3 Increase of Exit Width per Occupant

In some countries the increase of exit width is by steps of 0.60 m (Deu, Ita, CHe) or 0.40 m (Aut) with respect to lane formation (Table 4).

In the other countries the increase is continuous per person. The average increase per occupant varies from 0.5 cm to 1.2 cm. However, the two countries with the largest increase per occupant (Chn, Ita) consider the smallest occupant density (Table 3).

5 Results

5.1 Exit Width Correlated with Assembly Room Area

The total exit width w_{tot} as a function of the assembly room area A for places of entertainment is given in Fig. 3. The required exit widths of different coun-

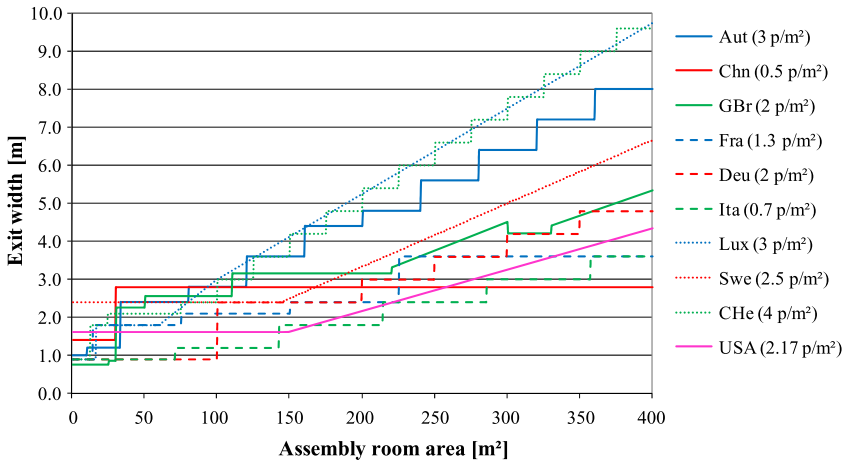


Fig. 3. Total exit width w_{tot} as a function of the assembly room area A .

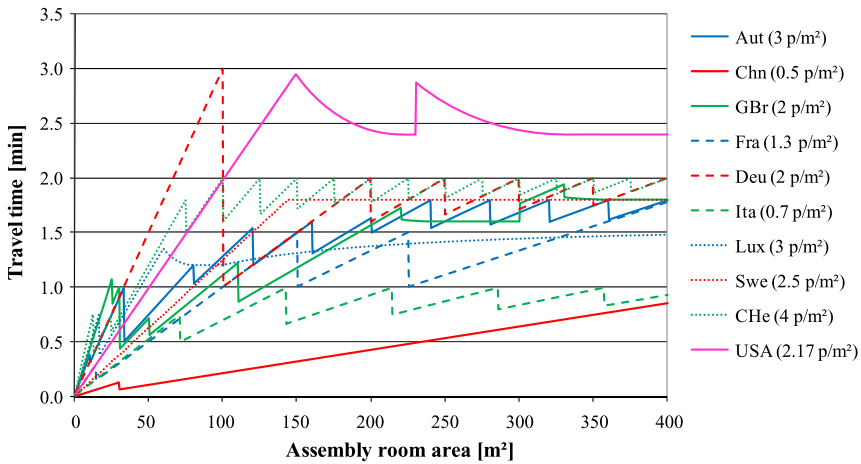


Fig. 4. Travel times t_{trav} as a function of the assembly room area A at design occupant density.

tries spread enormously. For large rooms the largest exit widths are needed according the Luxembourg and Swiss code.

5.2 Travel Times Correlated with Assembly Room Area at Design Occupant Density

The resulting travel times t_{trav} as a function of the assembly room area A for places of entertainment at design occupant density are given in Fig. 4. Generally, for each country it can be distinguished between small rooms where t_{trav} is determined from the minimum number of exit doors times the minimum



Fig. 5. a–c Illustrated densities of a 2 p/m^2 and b 4 p/m^2 compared with c a typical situation in a place of entertainment.

door width, and for large rooms where t_{trav} is determined from the design occupant load times the minimum increase of exit width for every occupant. With exception of Germany and USA the travel times for small rooms are shorter than for large rooms.

Maximum travel times peak at about three minutes (Deu, USA) where the majority of countries assume travel times ranging between one and two minutes. The average factor between minimum and maximum travel times for the same room area exceeds three. The travel time for China is the shortest because of the largest minimum exit width and the smallest design occupant density.

5.3 Travel Times Correlated with Assembly Room Area at Normalized Occupant Density of 4 p/m^2

The travel times in design conditions (Fig. 4) are largely influenced by the design occupant density that varies by a factor of eight for different countries. However, it is assumed that occupant behavior and willingness to form groups of high occupant densities is mostly the same in all countries. As 2 p/m^2 (Fig. 5a) is assumed to be too low for well-occupied places of entertainment (cf. Fig. 5c), a value of 4 p/m^2 (Fig. 5b) is taken for normal conditions. This value is also given by the Swiss code.

The resulting travel times t_{trav} as a function of the assembly room area A for places of entertainment at normalized density of 4 p/m^2 are given in Fig. 6. Except for Switzerland the travel times of all countries increased in these more realistic conditions. Maximum travel times peak above five minutes (Chn, Deu, Ita, USA). Other codes (Aut, Lux, Swe, CHe) provide travel times of less than three minutes. The average factor between minimum and maximum travel times for the same room area is about three.

6 Some Further Differences in the Codes

The travel times have been compared for a simple scenario. In some building codes additional provisions are required for assembly rooms in basements or

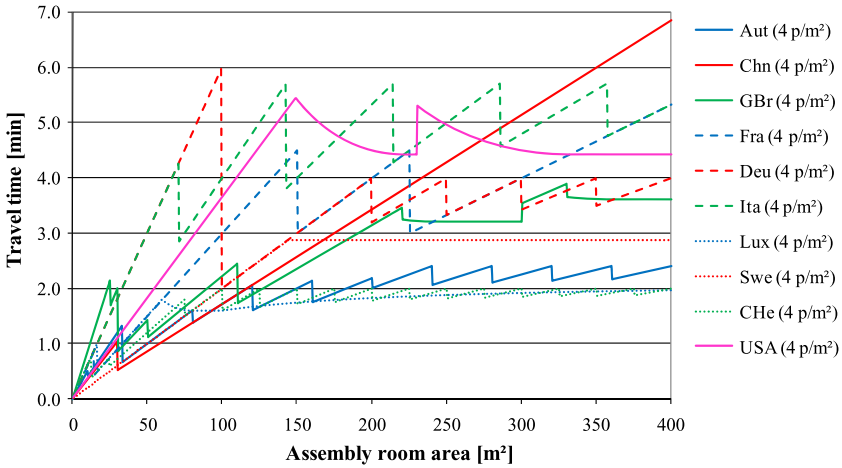


Fig. 6. Travel times t_{trav} as a function of the assembly room area A at normalized occupant density of 4 p/m^2 .

on elevated floors, e.g. increased exit width per occupant compared to the first floor situation. In many codes a distinction is made between horizontal escape route widths and staircase widths which have to be larger. This measure helps to prevent the staircase to become a dangerous bottleneck [2]. If more than one assembly room belongs to the same staircase, some codes add the overall number of occupants to determine the relevant staircase width, while other codes allow discounts with regard to the concept of staged evacuation. Another interesting point is the required redundancy of exit doors for assembly rooms. All building codes require two separate exits of an assembly room from a certain number of occupants (sometimes room area) on. In some codes a third or even a fourth exit door is required depending on the number of occupants.

Provisions for fire protection measures like smoke extraction and means of fire fighting significantly differ among the countries. To some extent these provisions are able to compensate the different means of escape.

7 Discussion

Short travel times during the egress of assembly rooms reduce the risk of injuries from fire incidents as well as the occurrence of crowd incidents. Concerning fire incidents, it was demonstrated [9, 10] that for large assembly rooms longer evacuation times are acceptable because of longer smoke filling times to pose unsafe conditions based on tenability criteria. Buildings fires occur with different fire growth rates that create different hazards. The longer the evacuation time, the more vulnerable is the place of assembly, i.e. the higher the possibility for a building fire to become critical and to exceed tenability

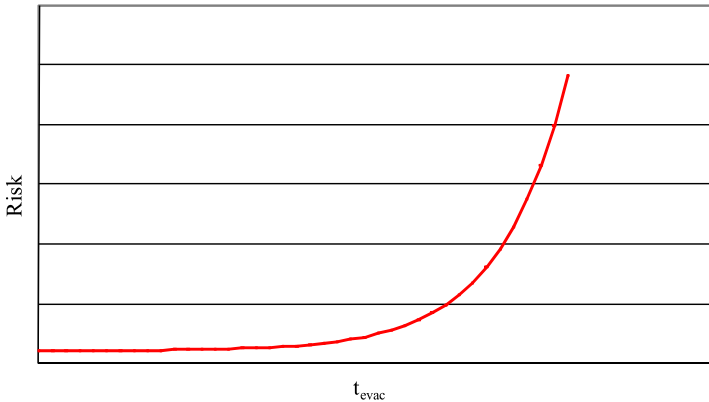


Fig. 7. Schematic relation between evacuation time and risk of being affected by an emergency.

criteria. The more a critical fire growth rate is exceeded, the more occupants are affected by a fire. The schematic relationship between evacuation time and the risk of an occupant of being affected by an emergency is illustrated in Fig. 7. It is not known how sensitive the risk is to a change of the evacuation time. However, based on sample calculations in [9] it is assumed that doubling the evacuation time (e.g. by double occupant density) increases the risk of emergencies in a place of assembly by a factor higher than two.

8 Conclusions

Requirements for escape route designs are based on historical experiences and political decisions and only to a small extent on scientific knowledge. It is believed that among fire protection infrastructure the means of escape decisively influence the occupant safety. Hence it must be considered that significant differences do exist in the occupant safety of similar assemblies in different countries.

Acknowledgements

The authors would like to thank Dieter Brein, Erica Ciapini, Gary Daniels, Jan Gerike, Daniel Nilsson, Monika Oswald, Frank Röhl, Lu Shouxiang, Eric Simha, and Karl Wallasch for providing the building codes and regulations and their help to interpret special requirements of different countries.

References

1. Draft International Standard ISO/WD 16738. Evaluation of behavior and movement of people (SC4_N487) 09-2004.
2. V.M. Predtetschenski, A.I. Milinski. *Personenströme in Gebäuden—Berechnungsverfahren für die Projektierung*. Müller, Köln–Braunsfeld, 1971 (also: *Planning for Foot Traffic in Buildings*. Amerind, New Delhi, India, 1978).
3. I. Peschl. Untersuchungen über das Benehmen von großen Menschenmengen bei der Strömung durch Türen und Engpässe in Panik- oder Gedrängesituationen. *VDI—Zeitschrift*, Vol. 113, pp. 13–16, 1971.
4. J.L. Pauls. Effective width model for evacuation flow in buildings. In: *Engineering Applications Workshop, Proceedings, Society of Fire Protection Engineers*, Boston, MA, 1980.
5. K. Müller. *Zur Gestaltung und Bemessung von Fluchtwegen für die Evakuierung von Personen aus Bauwerken auf der Grundlage von Modellversuchen*, Dissertation, University of Magdeburg, Germany, 1981.
6. S.P. Hoogendoorn, W. Daamen. Pedestrian behavior at bottlenecks. *Transportation Science*, Vol. 39, No. 2, pp. 147–159, 2005.
7. T. Kretz, A. Grünebohm, M. Schreckenberg. Experimental study of pedestrian flow through a bottleneck. *Journal of Statistical Mechanics*, P10014, 2006.
8. European Standard EN 13200. *Spectator facilities—Part 1: Layout criteria for spectator viewing area—Specification*. 2003.
9. B. Forell. Niveau der Personensicherheit von Versammlungsstätten—Nachweis nach VFDB-Leitfaden. In: *Proceedings of the 56th VFDB conference*, Leipzig, 21–23 May 2007, pp. 294–317. 2007.
10. D. Hosser, B. Forell, H. Janzen. Determination of critical fire growth coefficients for assembly rooms according to the German sample ordinance for places of assembly (MVStättV). Short report of [9], Internet publication <http://www.ibmb.tu-braunschweig.de/docpool/topics.php>. 2008.

Visualizing the Human Form for Simulation and Planning

Gabriel Wurzer

Institute of Architectural Sciences, Vienna University of Technology, Treitlstrasse 3/259-1, Vienna, Austria
e-mail: gabriel.wurzer@tuwien.ac.at

Summary. In pedestrian simulation, choosing the right visualization for the depiction of a simulated human is important. Recent taxonomies of visualization techniques for simulation can aid leverage a wide range of possible choices. Our work is to (1) narrow down these choices to the set of those applicable in pedestrian simulation, and (2) give a discussion over possible combinations of these visualization techniques.

1 Introduction

Visualization, as part of computer graphics, is driven by two forces: design and science. From the design point of view, one can speak of a visualization as “suitable”, “elaborate” etc.; the scientific part, on the other hand, is occupied with the correct mapping of the data onto a graphical representation. A good visualization includes the best of both worlds—it must be aesthetic as well as purposeful. Recent developments have tried to bring order into the vast field of visualization targeted at simulation by superimposing taxonomies and introducing design rationales to be used. There is, however, still lack of guidelines when it comes to specific problem areas, as it is in our case with the depiction of the human form for pedestrian simulation. This is a pity, since the simulated human is often the most central object in the simulation. Our contribution to the field of pedestrian simulation is therefore:

- the adoption of standards to aid with the depiction of human agents for simulation (see Sect. 3.1)
- to give a discussion over the combinability of visualization types (see Sect. 3.2)

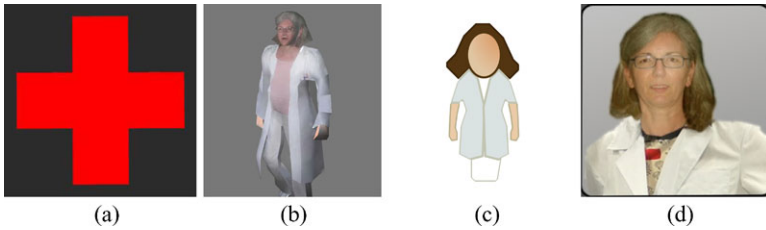


Fig. 1. Visualizing human form in multiple ways: **a** symbolic and 3D; **b** photorealistic and 3D; **c** iconic/stylized and 2D; **d** iconic/close-to-reality and 2D.

2 Background

We have based our work on the *VDI Standard 3633 Part 11 2003* “Simulation and Visualization” [1], which is a taxonomy that categorizes visualization from a graphical point of view. Eight categories are used for the classification of visualizations:

- *Dimension:* The number of dimensions used in the visualization. Can be either 1D, 2D, 2.5D or 3D.
- *Representation:* The form which the visualization uses to depict the information that is to be presented. Can be symbolic (using previously agreed symbols that do not have a relationship to the depicted information), iconic (using pictures that convey the meaning of the information they depict) or photo-realistic (a depiction that tries to show the information in a realistic way).
- *Display Format:* The presentational form which the visualization takes. Can be either font, table, chart, drawing, picture, virtual world or augmented reality.
- *Scale:* The measure of the geometrical coordinate system used. Can either be linear, logarithmic, exponential or none (in case there is no geometrical reference system for the visualization. Furthermore, it is possible that the axis of the geometrical coordinate system is used to form “categories” or clusters certain ranges.
- *Planar Geometrical Projection:* The transformation of objects in an n -dimensional space to a space of less dimensions. Can be perspective (for foreshortening), orthogonal/oblique (no foreshortening), or none if no projection is needed.
- *Temporal Dimension of Graphical Model:* The definition of the visualization with respect to a time axis. Can be continuous (a visualization which changes constantly), discrete (in steps) or none (if it does not change at all with time).
- *Time Mode within Representation:* In what temporal style the visualization is presented to the viewer. Can be as fixed-image (single picture), non-proportional full video (some arbitrary frames of video), or propor-

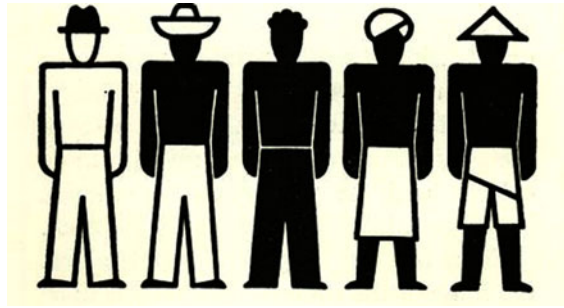


Fig. 2. Iconic symbols from the depictive language by Otto Neurath, using connotations to describe alternative interpretations of the symbol.

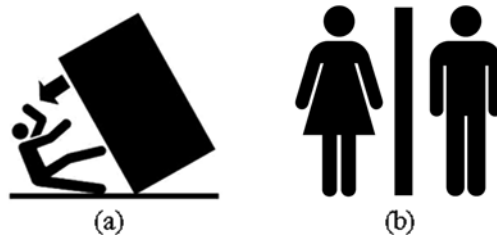


Fig. 3. **a** Iconic warning sign [5] versus **b** symbolic toilet sign.

tional full video (frames that are chronologically arranged, and played either in original speed, slower speed or faster speed).

- *Interaction:* The way in which the viewer can influence the visualization. Can be none, navigatable (e.g. start/stop), interaction with graphical model, interaction with simulation model or immersion (three-dimensional walkthrough with possibility to influence graphical model as well simulation model).

Apart from the VDI taxonomy, design science can give additional guidance when it comes to choosing the contents of a iconic or symbolic visualization. As most influential contribution, we see the depictive approach *IsoType* (International System of Typographic Picture Education, see Fig. 2) created by the Austrian philosopher and educator Otto Neurath [2]: Images that correspond closely to the subject or action they should describe are used to depict quantities and visualize actions (refer to Fig. 3a). Additional decorating symbols are used to describe alternatives of the same action or subject.

Catalogues of pictorial elements that are to be used in an environment are usually made into international standards—for example in the ISO 7001 norm “public information symbols” [3] for public spaces or the United States Department of Transportation pictogram language [4] for airports and train stations. Interestingly, pictorial norms do not clearly distinguish between symbolic images. For example, a warning sign might realistically depict hazard of

falling boxes using an iconic depiction (see Fig. 3a), while a toilet sign (see Fig. 3b) does not actually depict the act happening there but rather presents a predefined code (for obvious reasons).

3 Elaboration

The overall goal of this work is to give a depiction of the form of a simulated human in the context of simulation and planning. By depiction, we mean: to generate a graphical view, either in two or three dimensions, of a simulated human in his simulated environment: A two-dimensional map, an architectural model, or mixture of both. This environment is necessary because processes we would like to visualize cannot be understood without a visible reference to the space where they happen. Also, if the visualization is not anchored to a space, the visualization goal is likely not to depict the form of the simulated human, but other (relevant) variables such as queue lengths, inter-arrival times, and so on.

3.1 Discussion of the Criteria in the Taxonomy

Only a subset of visualization criteria in the VDI 3633/11 taxonomy have a reference to space or are able to depict form. As a matter of fact, they need to be rejected immediately, since they are not applicable to the scope of this work. These are, in detail:

- criteria with that less than 2D, such as: 1D visualization, symbolic representation through characters (e.g.: “bob”),
- display formats font, table/spreadsheet as well as display format chart,
- scale criteria (we assume a linear scale),
- interaction criteria (since the goal is depiction, not interaction), and
- orthogonal projection (we assume perspective projection)

Excluding all non-viable criteria from VDI 3633/11 yields a stripped-down version of the taxonomy given in Table 1, which includes all criteria applicable to the visualization of pedestrians.

3.2 Dependencies Between Criteria in the Taxonomy

If all criteria listed in Table 1 were independent, then visualizations could be switched even while the simulation executes. This is, however, not always the case; Table 2 lists a cross matrix of all categories compared for dependency, and clearly shows that there are interdependencies between them. Projection, for example, is strongly dependent on chosen dimension, in fact: only 3D dimension actually needs one.

Dimension	2D	2.5D	3D		
Re- presentation	symbolic/ abstract	iconic/ stylized	iconic/close to reality	photo- realistic	
Display format	drawing/ diagram	picture	virtual world	augmented reality	
Planar geometrical projection	none	oblique	perspective		
Temporal dimension of graphical model	discrete	continuous			
Time mode within presentation	fixed image	non- proportional full video	proportional full video/ slow motion	proportional full video/ real time	proportional full video/ fast motion

Table 1. Relevant criteria for the depiction of human form.

	Dimen- sion	Repre- sentation	Display format	Pro- jection	Temporal dimension	Time mode
Dimension	–	–	–	–	–	–
Representation	INDEP	–	–	–	–	–
Display format	DEP (1)	DEP (2)	–	–	–	–
Projection	DEP (3)	INDEP	DEP (4)	–	–	–
Temporal dimension	INDEP	INDEP	INDEP	INDEP	–	–
Time mode	INDEP	DEP (5)	DEP (6)	INDEP	DEP (7)	–

- (1) display format “virtual world” and “augmented reality” needs 3D as dimension
- (2) display format “drawing” is only compatible with representation “symbolic/abstract” and “iconic/stylized”, format “picture” only with “iconic/close-to-reality” and “photorealistic”
- (3) projection “none” is applicable to dimension “2D” and “2.5D”, oblique is for “2.5D” and “perspective” for “3D”
- (4) projection “none” not applicable for display format “virtual world” and “augmented reality”, and projection “oblique” not compatible with “augmented reality”
- (5) time mode “fixed image” is maybe impossible with representation “photorealistic”
- (6) display format “virtual world” is not compatible with time mode “fixed image”
- (7) time mode “fixed image” cannot work with temporal dimension “continuous”

Table 2. Dependence between criteria of taxonomy.

Interestingly, the subset {representation, dimension, temporal dimension} *is really independent*. Therefore, switching among those criteria would be possible. We have implemented a rather trivial demonstration that shows how switching between the two criteria representation (3D, 2.5D, 2D) and representation (symbolic/abstract, iconic/stylized, iconic/close-to-reality, photorealistic) would look like. A subset of the cases is given in Fig. 1:

- (a) the simulated human is depicted strictly as symbol. In this case, the agent is a doctor, therefore, the symbol is a red cross; the depiction is three-dimensional, although it could be argued that from the given perspective, the two-dimensional depiction would look quite the same
- (b) the simulated human is rendered as three-dimensional model with realistic textures, in a fully three-dimensional environment animation might be present, in order to enhance the realism of the figure
- (c) the agent is visualized as iconic image, in a stylized form; additional connotational symbols are present, such as the endoscope (for hinting at the action taken by the doctor—examination) or the hair (sex: female) the iconic image is presented in two dimensions
- (d) the visualization is again two-dimensional, however, a personalized image of the simulated doctor is given.

The currently most widely used depictive form in pedestrian dynamics software is in two-dimensional space, with the simulated human being represented symbolically. Furthermore, some packages provide a ‘post step’ in which the results of the simulation are presented in three-dimensional form, with animated characters and aesthetically pleasing graphics. We find that this is most problematic, since the depictive realism implicitly suggests that the simulation results are true. In fact, we would go as far as to claim that this is exactly what is intended—draw the critical mind away from the fact that what is depicted is just a simulation, and instead provide confidence in the reliability of the results.

4 Conclusion

In this paper, we have questioned why the depiction of human form, is often done in an ad-hoc, inconsiderate manner. Since human form is so central to pedestrian simulation, we have argued to use a widespread choice of depictive strategies rather than only those that are common now in the field.

To show that there is a broad choice of depictive strategies, we have adapted a visualization taxonomy for use in the context of pedestrian visualization. Since not all given taxonomic criteria made sense for use in this setting, we have produced a subset that encompass only the relevant criteria in Table 1.

Finally, the analysis of dependency (and thus switchability) between visualization choices (see Table 2) has shown that a switching is possible, but not

for all criteria. We have furthermore presented an example in which representation, dimension and temporal dimension are independent (see Fig. 1).

Our future work path is clearly laid out. We are to provide useful alternatives to realistic depiction, since this often provides confidence where there is rather need for critical questioning. These alternatives must foster the interpretation of simulation results and enhance the cognition of the user.

References

1. S. Wenzel, J. Bernhard, and J. Ulrich, A taxonomy of visualization techniques for simulation in production and logistics, in Proceedings of the 2003 Winter Simulation Conference, P. Chick, P.J. Sanchez, D. Ferrin, and D.J. Morrice, Editors, 2003.
2. P. Neurath, *Otto Neurath oder die Einheit von Wissenschaft und Gesellschaft*, ISBN 3-205-98127-8, Böhlau, Wien, 1994.
3. International Standardization Organization, ISO 7001 Graphical symbols—Public information symbols, Norm, 2007.
4. U.S. Department of Transportation, *Transportation Pictograms*, 1972.
5. N. Recchia, *Warning*, ISBN 0972563695, Mark Batty, New York, 2005.

A Real-Time Pedestrian Animation System

Christian Schulz, Michael Schultz, and Hartmut Fricke

Air Transport Technology and Logistics, Technische Universität Dresden, Hettner
Strasse 1-3, 01069 Dresden, Germany

e-mail: schulz@ifl.tu-dresden.de, schultz@ifl.tu-dresden.de, fricke@ifl.tu-dresden.de

Summary. The presented system clarifies possible connections between existing pedestrian simulations and human character animation. Crowd behavior control is separated from the local realization of the animation. A data-driven skeletal animation is indirectly controlled by a high level animation description. A mechanism is specified to transform behavior assignments into a continuous skeletal animation, which is used for an asynchronous visualization of virtual humans. A graphics hardware accelerated implementation shows the efficiency of the selected approach.

1 Introduction

A pedestrian simulation model will be more convincing if there is a realistic 3D visualization of virtual humans instead of the commonly used 2D particle representation. Speed and change in direction cannot be easily visually evaluated until animated characters are used. Applications in the field of computer graphics are focusing on a preferably good-looking visualization [1], but the realism of the behavior model is rather secondary. It is only crucial that the virtual crowd is credibly represented and animated. In contrast to that, pedestrian simulations are characterized by the quantitative correspondence to observations from the real world. To visualize the simulation, persons would normally be represented by a colored dot or a character-like rigid body. Combing the advantages of the various fields of virtual crowds would make it necessary to separate the visualization from the simulation process. Consequently, the presented graphical system offers a configurable interface to adapt to the needs of a custom pedestrian visualization instead of being tied to a specific simulation model. In this way a simulation developer can gain controlled access to sophisticated computer animation and rendering algorithms which are already widely spread in the game and film industries.

In the context of pedestrian animation several essential requirements can be defined. The first one is about the most basic form of animation: locomotion. Here, pedestrian movements are typically expressed as trajectories

on the ground. The whole body motion must be automatically generated. A constraint on simulation side would be that human trajectories have to be physically plausible to reproduce realistic animation. On top of or as a temporary replacement for locomotion there must be a mechanism to incorporate user-defined behavior, for example animation of a waiting pedestrian, head and eye movement, hand interactions or to take a seat. The challenge is to define the amount of impact on the behavior which comes from pedestrian simulation (more control) or animation (more visual realism). In reality every human has a unique appearance. For simulation purposes it is often sufficient to distinguish groups of individuals or to have at least a visual representation of certain kinds of important parameters of the individual. Therefore a variable appearance is a requirement. Furthermore, it is necessary to have real-time capabilities for immediate visual feedback. The graphics output should not be the limiting factor in simulation environments. Otherwise the system will not be well adopted. However, recent advances in graphics hardware facilitate displaying hundreds or thousands of characters in real-time. Finally, for an adequate integration of these graphics components into a crowd simulation environment, a well-designed software interface is a critical factor.

2 System Overview and Levels of Processing

The software architecture is primarily driven by a highly configurable animation pipeline with exchangeable processing models in each step (Fig. 1). Several layers of concerns are created to maximize decoupling of individual components. The representation as processing steps allows defining the inputs and outputs of each component more easily. The internal processing logic of a component is a black box system and therefore replaceable.

The central element of the system is the skeletal animation. The pedestrian simulation system is responsible for assembling this skeletal animation by using provided animation techniques. So-called Actions hide this complex functionality from the controller. Hence it is not the task of a behavior model to influence single orientations of skeletal joints. Being an open system, there

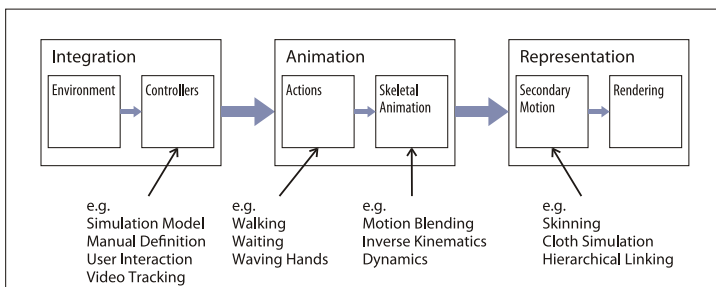


Fig. 1. Framework components.

is no default or any prescribed behavior model. The secondary motion, the actual visible animation, is entirely derived by the skeletal animation.

The environment (the virtual world) has only relevance for the controller, which solely takes the responsibility for any interactions. The environment definition could be adopted by the controller to add specific characteristics (e.g. a guidance system for pedestrians). For efficiency reasons and establishing common group behavior, a controller is responsible for a specific number of pedestrians. Simulation is not necessarily the only way to implement a controller. It would also be conceivable to do a manual definition (scripting), to insert a character controlled by user interaction or to use data generated by a video tracking system. Controllers need to produce a behavior description which can be converted to a skeletal animation. This has to be abstracted to allow for exchanging the internal technologies of the individual processing steps. Actions are based on human activities and not on techniques that are used for implementation. From the Actions point of view, the skeletal animation component is only a collection of techniques, which are facilitated for a generation and composition of an animation.

3 Skeletal Animation Generation

A skeletal animation system abstracts the virtual character to a small number of joints arranged in a tree structure, animated by changing root translation and joint orientations, instead of directly controlling possible tenth of thousands surface mesh vertices individually. In contrast to animation software in the field of computer graphics, skeletal animation determination may not influence the behavior of the person. It is not acceptable that different animation systems lead to a different simulation result. Though, for the sake of realistic animations, local deviations of the given constraints are possible.

Human perception is very sensitive to motion of other human beings. Even very small errors in an animation would be immediately recognized as unrealistic. The use of motion capture data seems to be an attractive approach, here the physics and kinetics of motion are already naturally included, but may be harder to control. Relevant information from an unlabeled motion sequence is extracted to be able to react on given input parameters in order to do an adequate clip selection and Motion Blending. Motion Graphs can help finding an optimal sequence, for an overview see [2]. Such data-driven methods are suitable for real-time applications. Since different approaches could be applied to solve those animation problems and every human activity would be implemented in a special way, a system extension point called Actions is provided. However, in order to make Actions development easier, common underlying operations are included as low-level animation techniques.

Next a Walk Action is described in greater detail [3, 4]. In our system, several discrete positions lead to a continuous motion sequence. Walking or running can be subdivided into several motion cycles. Clips are automatically

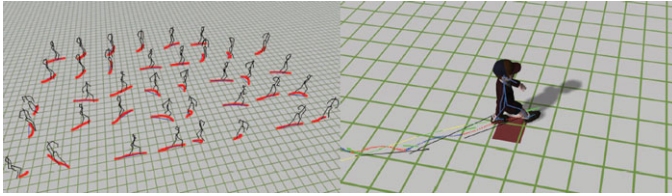


Fig. 2. Locomotion generation.

extracted from unlabeled motion capture data (Fig. 2). Raw data from a motion capture session, where arbitrary locomotion is performed, is already retargeted to a specific skeleton to have the possibility of (manual) adaption of the input material. Nevertheless, it is automatically detected which foot in the direction of locomotion is ahead, yielding a half walk cycle. The cycles must be locally aligned to allow for comparison. The reference direction is given by the previous cycle of the motion data. More (differing) cycles raise the quality of a motion generation and constraints can be better met. A cycle is characterized by its change in direction, time duration, path length and the resultant speed. It is the smallest non-divisible unit of an animation. Cycles are composed consecutively, additional overlappings are interpolated. Based on the previous skeletal animation and new position constraints, ideal parameters for a new walk cycle are calculated. A cycle nearest to the optimum is selected, globally transformed and possibly scaled in time. Special attention is given to the beginning and endings of the cycles, to have a proper alignment for a smooth transition. The system must be online capable so that position constraints for a cycle which extends into the future have to be estimated. In Fig. 2 (right) the square is a position constraint which updates every 300 ms. In this case, the position values are in continuous space, but a discrete position grid would be possible, too. The position update is also indicated by a color change of the solid line. The dotted trajectory (alternating red and blue colored curve) represents the generated animation cycles.

4 Behavior Model Integration

To make skeletal animation techniques more accessible, the concept of high-level Actions as parameterized models of low-level methods is utilized. A behavior model qualifies as an animation controller if it can produce an action-specific high-level animation description. The system should not be limited to a specific type of model. Animation itself is also a field of active research, so we cannot really make any definitive assumptions on what to expect from both sides. The ability to use several animation controllers in a single scenario would require a simulation model to deal with a dynamic environment.

The animation system is initially an incomplete framework. The data flow is given, but behavior and action models are user-defined. A high-level an-

imation description consists of a temporal sequence of base Actions, which deal with all joint orientations of a skeleton, and optional auxiliary Actions, which take the underlying result as the input for a custom blend operation. Every Action implementation can provide its own set of parameters as a requirement to be generated by the controller. Consequently, a behavior model actively controls the animation generation by forcing a timed sequence of parameterized activities. Adding a real-time visualization to a simulation system comes along with synchronization problems, since different time samplings must be handled. For a given time a controller will be asked to produce a valid state. This request can be arbitrary; it is only ensured that time is incremented. Controllers will use their own internal time discretization, but should not calculate too far over the requested point in time to ensure the online capability.

5 Implementation and Results

The implemented prototype consists of a mixture of a configurable graphical user interface (GUI) and a programmable interface (API) with defined extension points. The GUI is primarily employed for controlling simulation runs, setting model parameters and making design decisions. The API allows to connect external behavior models, program new Actions and to provide alternative implementations of animation algorithms. Underlying technologies are the Eclipse Rich Client Platform as a generic application framework, the Eclipse Modeling Framework for modeling scenario configurations, OpenGL for accessing graphics hardware, and Collada as the 3D data exchange format.

Many characters mean a massive amount of geometry and image data to process every frame. A CPU can not handle this task in real-time. Hence it is mandatory to perform expensive animation and rendering algorithms mainly on programmable graphics hardware. In contrast to that, behavior processing and action determination are better candidates for execution on CPUs due to their algorithmic complexity. Essentially, two system parts face each other. The simulation-driven part (behavior and actions) is sufficient for generating a continuous representation of the crowd scene. Then the render-driven part (animation generation and representation) is only responsible for realizing the given motion description, in case the character is currently visible.

This separation is not only useful to respect different time discretizations. It is also relevant in terms of performance considerations as it defers the actual skeletal animation generation. The required continuous determination of action only consists of a set of parameters for motion generation. The render-driven part can ask an Action to deliver the parameters for a certain point in time, which must be smaller than or equal to the simulated time. The Motion Blending (or any other animation technique) uses relative joint orientations to compose the animation. Afterwards the skeleton joints are transformed into global space. Secondary motions like Vertex Blending use



Fig. 3. Real-time visualization.

this information to animate the actual visible character mesh. The internal representation of the characters is not unique, as a small number of models are used by many parameterized character instances. As an example, a different coloration significantly varies the visual appearance, while it has a minimal impact on the performance of system and reduces creation efforts (Fig. 3).

The direct use of the OpenGL driver offers the greatest flexibility and performance potential as well as a complex and error-prone API. Nevertheless, it is necessary to implement the components on this low level, since current scene graph technologies and rendering engines typically do not support massive crowd scenes in particular.

6 Conclusion

The system is currently applied to pedestrian simulations in airport terminals and the visualization of trajectories extracted from video observations. Having a common visualization system eases combining, comparing, and validating pedestrian simulation models. A new issue occurs at high densities. According to the current situation of a virtual character, constraints on the animation must be raised to avoid collisions, reducing the possibility to produce visual realism. An adaptable action space could be defined to improve animation quality in situations with lower density. The separation of behavior and animation generation turns out to be very efficient. For performance reasons the use of several controllers in one scenario must be well thought out, at least it is the responsibility of the controller itself to cope with a dynamic environment.

Adding realistic animation to pedestrian simulation is definitely a rewarding investment. The importance of integrating better authoring methods should not be underestimated as it leads to a more usable system.

References

1. D. Thalmann and S.R. Musse. *Crowd Simulation*, Springer, Berlin, 2007.
2. L. Kovar. Automated methods for data-driven synthesis of realistic and controllable human motion. Ph.D. Thesis, University of Wisconsin-Madison, 2004.

3. S.I. Park, H.J. Shin, T.H. Kim, and S.Y. Shin. On-line motion blending for real-time locomotion generation. *Comput. Animat. Virtual Worlds* 15(3):125, 2004.
4. T. Kwon and S.Y. Shin. Motion modeling for on-line locomotion synthesis. *Proc. of ACM SIGGRAPH/Eurographics Symposium on Computer Animation*, 2005.

Modeling of Escape Routes According to Occupancy, Economy, and Level of Safety in Slovak Republic

Martin Lopusniak

Faculty of Civil Engineering, TU Košice, Vysokoškolská 4, Košice, Slovakia
e-mail: martin.lopusniak@tuke.sk

Summary. Fire safety is one of the six primary requirements in civil engineering projects. All of them are controlled by governmental authorities both in phase of design and execution. From the point of fire safety one of the most complicated requirement is to achieve safety evacuation of pedestrians. Due to different point of views between governmental institutions, fire safety engineers, and developers lots of projects get more expensive and complicated. The presented paper is based on an example of a building occupancy (hotel building) and their influence on the type of escape route based on Slovak condition. As a result of design and calculation two escape routes and their mutual comparison from different point of views is presented.

This work was supported by the grant project VEGA 1/0739/08 “Theoretical and experimental analysis of thermo-technical, acoustic and fire safety properties of glass systems for a well-founded construction project of multifunction glass system” funded by the Scientific Grant Agency of the Ministry of Education of Slovak Republic and the Slovak Academy of Sciences.

1 Building Description

The building is a hotel building located in Bojnice town. One part of the building consists of four floors, another part of five floors. The whole building has a basement, the ground plan is V-shaped with basic dimensions of 13.5 m × 47.1 m and 13.0 m × 33.7 m. The construction system is combined—cast-in-situ reinforced concrete frame and combination with supporting walls from ceramic blocks.

- On the basement in one part there are night-club, casino and public sanitary facilities located, in the other part kitchen operation with appartaining storerooms, dress rooms and sanitary facilities for employers, and a laundry.

- On 1st floor (equal to ground floor) rooms for hotel visitors (reception, cocktail lounge, saloon, restaurant, sanitary facilities) as well as rooms for hotel operations (kitchen, storerooms) are located.
- On 2nd and 3rd floor apartments are located.
- On 4th floor two flats and the hotel offices are located.

The building is located at the main town road, where it has its main entrance, too. It is connected to public services (water main, sewage system, gas line, and telephone).

According to the Act No. 94/2004 of Ministry of Interior of the Slovak republic [3] the building is classified as the B class building—building assigned on housing and accommodation.

2 Requirements for the Escape Routes

Occupancy of particular fire compartments is defined by:

- standard values on the basis of norm STN 73 0818—Person occupancy in buildings [1],
- if specific space is not defined in the standard, it is reflected with the value of space occupancy that is operatively or functionally identical with this space,
- alternatively to the two first approaches, multiply the designed number of occupancy, that is mentioned in the project by coefficient 1.5.

2.1 Calculations

The biggest problem of considering pedestrian evacuation shows the occupancy of particular spaces and especially for restaurant, multifunction saloon, casino and night club. The determined value of pedestrian occupancy based on the standard markedly oversteps the possibilities in mentioned spaces as well as in the project expected number of persons to be located in the given spaces.

The number of pedestrians seems to be a problem especially by finishing considerations of an all pedestrian evacuation from the building to the safety (open) space. In this case, the number of persons is countered from all spaces and this amount is under consideration of the escape route.

But the natural operating hotel mode does not allow parallel appearance of pedestrians in all spaces (this means that persons are located in the restaurant but not in the hotel room at the same time). Thus the logical end is that the spaces can not be fully engaged parallel in all hotel operations. It is evident that we can not exclude a situation like this and the standards directly do not mention the progress for situations like this. Thereby the responsibility is discretional on fire engineer who solves the fire safety and so he has to assume the risk problem which can be caused by pedestrian evacuation.

There is a possibility to solve a task by two basic ways [2, 3]:

- The maximum of persons in the considering building inclusive to the calculation of allowed evacuation time.
- Redistribution of number of persons according to fire engineer’s consideration.

In the first way, the number of evacuated persons unnaturally increases evacuation time as well as the requirements to the evacuation facilities (escape routes have to be widened, widened doors, eventually additional escape routes). See Tables 1, 2 and 3.

Alternative “A”

Evacuation route:	Partially protected escape route (PPER)
Number of evacuation route:	two
Point of evacuation:	Exit from building
Proposed kind of evacuation:	Synchronous
Number of evacuated persons:	662

Symbol	Description	Units
v_u	Speed of evacuation	(m/min)
E	Number of evacuated persons	(-)
s	Coefficient of evacuation condition	(-)
u	Number of escape units	(-)
l_u	Length of escape route	(m)
K_u	Capacity of escape route	(1/m)

Table 1. Symbol description.

Type	v_u	E	K_u	s	u	I_u
PPER	25	626	30	1	4	58

Table 2. Boundary condition for calculation for PPER.

Proposed time limit of evacuation (min)	t_u	$7.26 > 6$ Inconvenient	$t_{u,max}$	Times limit of evacuation (min)
Maximum length of evacuation route (m)	$I_{u,max}$	$16.11 < 58$ Inconvenient	I_u	Length of evacuation route (m)
Least number of escape unit	u_{min}	$5.18 > 4$ Inconvenient	u	Number of escape unit

Table 3. Result of calculation for PPER.

Type	v_u	E	K_u	s	u	I_u
PER	25	662	30	1	4	58

Table 4. Boundary condition for calculation for PER.

Proposed time limit of evacuation (min)	t_u	$7.26 < 10$ Convenient	$t_{u,max}$	Time limit of evacuation (min)
Maximum length of evacuation route (m)	$I_{u,max}$	$149.99 > 58$ Convenient	I_u	Length of evacuation route (m)
Least number of escape unit	u_{min}	$2.67 < 4$ Convenient	u	Number of escape unit

Table 5. Result of calculation for PER.

In the second way, the fire engineer exposes himself to the mentioned risk that if the situation which was not under consideration in the project is reached, grievous consequences on the health and in the worst case to loss on life can be happen. See Tables 1, 4 and 5.

Alternative “B”

Evacuation route:	Protected escape route (PER) type “A”
Number of evacuation route:	two
Point of evacuation:	Exit from building
Proposed kind of evacuation:	Synchronous
Number of evacuated persons:	662

3 Conclusion

The presented analysis shows the following results:

- safety evacuation of persons from the considered object can not be assured by partially protected escape route
- the safe evacuation of persons from the considered object can be assured by protected escape route
- planning protected escape route increases investment and working costs
- as alternative with considering of protected escape route it is allowed to use elevator
- both solutions remitted on impracticability and unreality of consideration with maximum persons occupancy in the spaces

The alternative with two partially protected escape routes does not allow fulfilling of requirements for the safety evacuation of persons from the object that are determined in the norm in the case of all three conditions. Too short evacuation time is a problem if the escape route is designed as a partially protected one. The big problem is too large number of evacuated persons

inside the building. For large numbers of evacuated persons it is not possible to ensure a safe evacuation by using partially protected escape routes or even unprotected escape routes. If the number of persons is larger than 400 it is expected and recommended the applying of protected escape routes.

The alternative of class “A” protected escape routes is shown as the most suitable. In this alternative the requirements determined by standard are fulfilled. Evacuation by protected escape route allows consideration with longer evacuation times. The possibility of longer evacuation times plays the key role also by considering the other two requirements (see Table 5). It is evident that this solution is indispensable for considerate a building like that.

Design of protected escape routes increases the investment for securing requirements on fire safety of constructions. Some limitedness of using fire stops (e.g. walls, doors) in the building interiors can be the disadvantage. Fulfilling the requirements on fire resistance leads to technically difficult solutions of fire stops that are later the limit of demanding interiors. Putting fire stops in places like receptions can cause disturbingly. The maintenance of fire stops may lead to increasing operation costs.

The problem of fire compartment occupancy is indirectly transferred to occupancy of escape routes. Despite the fact that in an object under consideration were two protected escape routes in both alternatives. The calculations assume that only one escape route is assessed with the full occupancy, the other one is not assessed. In this case the second escape route influences only the value of allowable escape time. In fact it can be possible to suppose that number of persons will be varying between both escape routes, even the alternative with the maximum occupancy of one escape route cannot be excluded.

References

1. STN 73 0818, 1982. Building fire protection—Building occupation.
2. J. Kucbel. Fire Safety in Buildings, Bratislava 1993. Vydavateľstvo a distribúcia technickej literatúry.
3. Ministry regulation No. 94/2004.

List of Participants

Mauro Atalla

United Technologies Research
Center, 411 Silver Lane, MS129-84,
06108 Ease Hatford, USA
AtallaMJ@utrc.utc.com

Maik Boltes

Jülich Supercomputing Centre,
FZ-Jülich GmbH, Leo-Brandt-Str.,
52425 Jülich, Germany
m.boltes@fz-juelich.de

Jason Averill

National Institute of Standards and
Technology, 100 Bureau Drive, Stop
8664, 20899-8664 Gaithersburg, USA
jason.averill@nist.gov

Cornelia Bönisch

PTV AG, Stumpfstr. 1,
76131 Karlsruhe, Germany
cornelia.boenisch@ptv.de

Monika Bartsch

Gregorstr. 3, 52066 Aachen,
Germany
monika.bartsch@gmx.net

Mario Campanella

Delft University of Technology,
Stevinweg 1, 2628 CN Delft,
The Netherlands
m.c.campanella@tudelft.nl

Dietmar Bauer

HCMT, arsenal research, Giefing-
gasse 2, 1210 Wien, Austria
dietmar.bauer@arsenal.ac.at

Sonic Chan

TU Dresden, Andreas-Schubert Str.
23, Zimmer 508, 01062 Dresden,
Germany
chan@vwi.tu-dresden.de

Noureddine Benichou

National Research Council of
Canada, 1200 Montreal Road,
Building M59, K1A0R6 Ottawa,
Canada
noureddine.benichou@nrc.gc.ca

Minjie Chen

TU Berlin, Strasse des 17. Juni 136,
10623 Berlin, Germany
minjie.chen@math.tu-berlin.de

Craig Childs

Accessibility Research Group, University College London, Chadwick Building, Gower Street, WC1E6Bt London, United Kingdom
craig.childs@ucl.ac.uk

Mohcine Chraibi

TU Hamburg Harburg, Washingtonallee 87b, 22111 Hamburg, Germany
mohcine.chraibi@tu-harburg.de

Arturo Cuesta

University of Cantabria, Avenida de los Castros s/n, 39005 Santander (Cantabria), Spain
cuestaar@unican.es

Winnie Daamen

Delft University of Technology, PO Box 5048, 2600 GA Delft, The Netherlands
w.daamen@tudelft.nl

Steven Deere

FSEG, University of Greenwich, School of CMS, Old Royal Naval College, 30 Park Row, SE109LS Greenwich, United Kingdom
s.deere@gre.ac.uk

Beatrice de Gelder

Tilburg University, Cognitive and Affective Neuroscience Lab, PO Box 90153, 5000 LE Tilburg, The Netherlands
degelder@uvt.nl

Cemalletin Demirel

BPK, Wahlerstr. 32, 40472 Düsseldorf, Germany
c.demirel@bpk-mail.de

Stéphane Donikian

INRIA, IRISA, Campus de Beaulieu, 35042 Rennes, France
donikian@irisa.fr

Burkhard Forell

Braunschweig University of Technology, Beethovenstr. 52, 38106 Braunschweig, Germany
b.forell@ibmb.tu-bs.de

Taku Fujiyama

University College London, Center for Transport Studies, Gower Street, WC1E6Bt London, United Kingdom
taku.fujiyama@ucl.ac.uk

Edwin Galea

FSEG, University of Greenwich, School of CMS, Old Royal Naval College, 30 Park Row, SE109LS Greenwich, United Kingdom
e.r.galea@gre.ac.uk

Peng Gao

School of Traffic and Transportation Engineering, Tongji University, CaoAn Road #4800, Campus JiaDing, 201804 Shanghai, China
tj-jt-gp@yahoo.com.cn

Georg Gecezek

Österreichisches Rotes Kreuz— Landesverband Wien, Nottendorfer Gasse 21, A-1030 Wien, Austria
georg.gecezek@w.rotekreuz.at

Ioakeim Georgoudas

Democratius University of Thrace, Department of Electrical and Computer Engineering, Laboratory of Electronics, GR-67100 Xanthi, Greece
igeorg@ee.duth.gr

Vladimir Grachev

Grachev & Partners / Sitis Ltd., 2,
Dolores Ibarruri str.,
620028 Ekaterinburg, Russia
vladimir.grachev@gppb.ru

Steven Gwynne

Hughes Associates, Inc., 3515 28th
st #307, 80301 Boulder, USA
sgwynne@haifire.com

Peter Harding

Manchester Metropolitan University,
Dept. of Computing and Maths,
John Dalton Building, Chester
Street, M15GD Manchester, United
Kingdom
p.harding@mmu.ac.uk

Karl Harrysson

Brandskyddslaget AB, Box 9196,
10273 Stockholm, Sweden
karl.harrysson@
brandskyddslaget.se

Christina Hartnack

BFT Cognos GmbH, Im Susterfeld
1, 52072 Aachen, Germany
christina.hartnack@
bft-cognos.de

Shota Hattori

Kozo Keikaku Engineering Inc.,
Honcho 4-38-13, 164-0012 Nakano,
Japan
shatto@kke.co.jp

Sven Hebben

TraffGo HT GmbH, Bismarckstr.
142a, 47047 Duisburg, Germany
kluepfel@traffgo-ht.com

Simo Heliövaara

Helsinki University of Technology,
System Analysis Laboratory,
P.O. Box 1100, 02015 HUT Espoo,
Finland
simo.heliovaara@tkk.fi

Colin Henein

Carleton University, 49 Newton St.,
K1S2S6 Ottawa, Canada
ped08@juicer.orange-carb.org

Stefan Hengst

PTV AG, Stumpfstr. 1,
76131 Karlsruhe, Germany
stefan.hengst@ptv.de

Neil Hitchen

ARUP Fire, 13 Fitzroy Street,
WIT4BQ London, United Kingdom
neil.hitchen@arup.com

Mario Höcker

Institut für Bauinformatik, Leibniz
Universität Hannover, Callinstr. 34,
30167 Hannover, Germany
hoecker@bauinf.uni-hannover.de

Christa Illera

Vienna University of Technology,
Karlsplatz 13, A-1040 Vienna,
Austria
cillera@
email.archlab.tuwien.ac.at

Gregor Jäger

FH Köln, Fakultät 09, Masterstu-
diengang Rettungsingenieurwesen,
Betzdorfer Str. 2, 50679 Köln,
Germany
gregor.jaeger@smail.fh-koeln.de

Anders Johansson

ETH Zürich, UNO D 11, Uni-
versitätsstr. 41, CH-8092 Zürich,
Switzerland
andersj@ethz.ch

Jens Kähler

BPK, Wahlerstr. 32,
40472 Düsseldorf, Germany
j.kaehler@bpk-mail.de

Ilya Karkin

SITIS Ltd., 2, Dolores Ibarruri str.,
620028 Ekaterinburg, Russia
ilya@sitis.ru

Lukas Kellenberger

FH Nordwestschweiz, Steinackerstr.
5, CH-5210 Windisch, Switzerland
lukas.kellenberger@fhnw.ch

Michael Kinsey

FSEG, University of Greenwich,
School of CMS, Old Royal Naval
College, 30 Park Row, SE109LS
Greenwich, United Kingdom
km44@gre.ac.uk

Hubert Kirchberger

Vienna University of Technology,
Inst. for Building Construction and
Technology, Karlsplatz 13/206-1,
A-1040 Vienna, Austria
hubert.kirchberger@tuwien.ac.at

Ekaterina Kirik

Institute of Computational Mod-
elling SB RAS, Akademgorodok,
660036 Krasnoyarsk, Russia
kirik@icm.krasn.ru

Uwe Kirsch

ETH Zürich, Wolfgang-Pauli-Str. 15,
CH-8093 Zürich, Switzerland
uwe.kirsch@ivt.baug.ethz.ch

Yasuhiro Kitakami

Kozo Keikaku Engineering Inc.,
Honcho 4-38-13, 164-0012 Nakano,
Japan
kitakami@kke.co.jp

Wolfram Klingsch

Bergische Universität Wuppertal,
Baustofftechnologie und Brand-
schutz, Pauluskirchstr. 11,
42285 Wuppertal, Germany
klingsch@uni-wuppertal.de

Hubert Klüpfel

TraffGo HT GmbH, Bismarckstr.
142a, 47047 Duisburg, Germany
kluepfel@traffgo-ht.com

Margrethe Kobes

Netherlands Institute for Safety
(NIFV/Nibra), PO Box 7010,
6801 HA Arnhem, The Netherlands
margrethe.kobes@nifv.nl

Rainer Könnecke

I.S.T. GmbH, Feuerbachstr. 19,
60325 Frankfurt, Germany
r.koennecke@ist-net.de

Timo Korhonen

VTT Technical Research Centre of
Finland, P.O. Box 1000,
FI-02044 VTT Espoo, Finland
timo.korhonen@vtt.fi

Michael Krabbe

Richard-Wagner-Str. 38,
41515 Grevenbroich, Germany
mikrabbe@t-online.de

Tobias Kretz

PTV AG, Stumpfstr. 1,
76131 Karlsruhe, Germany
tobias.kretz@ptv.de

Hua Kuang

Shanghai Institute of Applied Mathematics and Mechanics, Shanghai University, No. 149, Yangchang Road, 200072 Shanghai, China
khphy@hotmail.com

Erica Kuligowski

National Institute of Standards and Technology, 100 Bureau Drive, Stop 8664, 20899-8664 Gaithersburg, USA
erica.kuligowski@nist.gov

Gregor Lämmel

TU Berlin, Weichselstrasse 55, 12045 Berlin, Germany
laemmel@vsp.tu-berlin.de

Paolo Lino

Dipartimento di Elettrotecnica ed Elettronica, Politecnico di Bari, Via Re David 200, 70125 Bari, Italy
lino@deemail.poliba.it

Herbert Löllgen

Dept. and Clinic of Internal Medicine (Cardiology, Pneumology, Intensive Care Medicine), Sana-Klinikum Remscheid, Burger Str. 211, 42859 Remscheid, Germany
herbert.loellgen@gmx.de

Martin Lopusniak

TU Kosice, Vysokoskolska 4, 04200 Kosice, Slovakia
martin.lopusniak@tuke.sk

Rodrigo Machado Tavares

FSEG, University of Greenwich, School of CMS, Old Royal Naval College, 30 Park Row, SE109LS Greenwich, United Kingdom
rodrigotmj@gmail.com

Ralph Majer

Vitracom AG, Erbprinzenstr. 4-12, 76133 Karlsruhe, Germany
majer@vitracom.de

Sara Manzoni

University of Milano-Bicocca, Viale Sarca, 336, 20126 Milano, Italy
manzoni@disco.unimib.it

Bertrand Merminod

Ecole Polytechnique Fédérale de Lausanne, Bâtiment GC—Station 18, 1015 Lausanne, Switzerland
bertrand.merminod@epfl.ch

Frederik Meysel

Deutsches Zentrum für Luft- und Raumfahrt DLR e. V., Lilienthalplatz 7, 38108 Braunschweig, Germany
frederik.meysel@dlr.de

Alexandra Millonig

Department of Geoinformation and Cartography, TU Vienna, Gusshausstrasse 30, 1040 Wien, Austria
Alexandra.Millonig@arsenal.ac.at

Ruedi Müller

FH Nordwestschweiz, Steinackerstr. 5, CH-5210 Windisch, Switzerland
ruedi.mueller@fhnw.ch

Satish Narayanan

United Technologies Research Center, 411 Silver Lane, MS129-84, 06108 Ease Hatford, USA
Narayas@utrc.utc.com

Daniel Nilsson

Dep. of Fire Safety Engineering and Systems Safety, Lund University, Box 118, 22100 Lund, Sweden
daniel.nilsson@brand.lth.se

Katsuhiro Nishinari

Department of Aeronautics and
Astronautics, Faculty of Engineering,
The University of Tokyo, 7-3-1,
Hongo, 113-8656 Bunkyo-ku, Japan
tknishi@mail.ecc.u-tokyo.ac.jp

Itsuki Noda

AIST, 1-1-1 Umezono,
305-8568 Tsukuba, Japan
i.noda@aist.go.jp

**Alicia Guadalupe Ortega Ca-
marena**

Institute for Scientific Computing,
Hans-Sommer-Str. 65, 38106 Braun-
schweig, Germany
alicia.ortega@tu-bs.de

Monika Oswald

Vienna University of Technology,
Inst. for Building Construction and
Technology, Karlsplatz 13/206-1,
A-1040 Vienna, Austria
monika.oswald@tuwien.ac.at

Jin Hyoung Park

Wing Ship Technology, 171 Jang-
dong Yuseong, 305-343 Daejeon,
South Korea
jhpark@moeri.re.kr

Jake Pauls

Jake Pauls Consulting Services,
12507 Winexburg Manor Drive,
20906 Silver Spring, USA
bldguse@aol.com

Andrea Portz

Jülich Supercomputing Centre,
FZ-Jülich GmbH, Leo-Brandt-Str.,
52425 Jülich, Germany
a.portz@fz-juelich.de

David Purser

Hartfort Environmental Research,
1 Lowlands, AL9 5DY Hatfield,
United Kingdom
david-purser@ntlworld.com

Rebecca Rettner

BPK, Wählerstr. 32,
40472 Düsseldorf, Germany
r.rettner@bpk-mail.de

Christian Rogsch

Bergische Universität Wuppertal,
Baustofftechnologie und Brand-
schutz, Pauluskirchstr. 11,
42285 Wuppertal, Germany
christian@rogsch.de

Tobias Rupprecht

Bergische Universität Wuppertal,
Baustofftechnologie und Brand-
schutz, Pauluskirchstr. 11,
42285 Wuppertal, Germany
rupprecht@uni-wuppertal.de

Dmitry Samoshin

Academy of State Fire Service
of Russia, EMERCOM, 4, Borisa
Galushkina Street, 129366 Moscow,
Russia
info@fireevacuation.ru

Douglas Samuelson

Serco, 2650 Park Tower Drive,
Suite 800, 22180 Vienna, USA
Douglas.Samuelson@serco-na.com

Andreas Schadschneider

University of Cologne,
Institute of Theoretical Physics,
50937 Cologne, Germany
as@thp.Uni-Koeln.de

Henning Scheschonk

Meyer Werft, Industriegebiet Süd,
26871 Papenburg, Germany
henning.scheschonk@
meyerwerft.de

Bärbel Schlake

Westfälische-Wilhelms-Universität
Münster, Am Dill 60, 48163 Münster,
Germany
baerbelschlake@web.de

Volker Schneider

I.S.T. GmbH, Feuerbachstr. 19,
60325 Frankfurt, Germany
v.schneider@ist-net.de

Michael Schreckenber

University of Duisburg-Essen,
Physics of Transportation and
Traffic, 47057 Duisburg, Germany
schreckenber@ptt.uni-due.de

Michael Schultz

TU Dresden, Hettnerstr. 1-3,
01062 Dresden, Germany
schultz@ifl.tu-dresden.de

Christian Schulz

TU Dresden, Hettnerstr. 1-3,
01062 Dresden, Germany
christianschulz.net@
googlemail.com

Stefan Seer

arsenal research, Giefinggasse 2,
1210 Wien, Austria
stefan.seer@arsenal.ac.at

Armin Seyfried

Jülich Supercomputing Centre,
FZ-Jülich GmbH, Leo-Brandt-Str.,
52425 Jülich, Germany
a.seyfried@fz-juelich.de

Shrikant Sharma

Buro Happold, Camden Mill, Lower
Bristol Road, BA23DQ Bath, United
Kingdom
shrikant.sharma@burohappold.com

Marja-Liisa Siikonen

KONE Elevators Ltd., Keilasatama
3, FI-02150 Espoo, Finland
marja-liisa.siikonen@kone.com

Andrey Skochilov

SITIS Ltd., 2, Dolores Ibarruri str.,
620028 Ekaterinburg, Russia
skochilov@sitis.ru

Janne Sorsa

KONE Elevators Ltd., Keilasatama
3, FI-02150 Espoo, Finland
janne.sorsa@kone.com

Bernhard Steffen

Jülich Supercomputing Centre,
FZ-Jülich GmbH, Leo-Brandt-Str.,
52425 Jülich, Germany
b.steffen@fz-juelich.de

Chengyu Sun

College of Architecture and Urban
Planning, Tongji University, Si Ping
Road No. 1239, 200092 Shanghai,
China
ibund@126.com

Vincent Tabak

Buro Happold and Eindhoven
University of Technology, 30 Second
Avenue, BA23NN Bath, United
Kingdom
vtabak@yahoo.com

Masaki Tamada

Kozo Keikaku Engineering Inc.,
Honcho 4-38-13, 164-0012 Nakano,
Japan
tamada@kke.co.jp

Rolf Tilly

hhpberlin, Ingenieurgesellschaft für
Brandschutz mbH, Rotherstr. 19,
10245 Berlin, Germany
r.tilly@hhpberlin.de

Madeleine Togher

FSEG, University of Greenwich,
School of CMS, Old Royal Naval
College, 30 Park Row, SE109LS
Greenwich, United Kingdom

Akiyasu Tomoeda

The University of Tokyo, 7-3-1,
Hongo, 113-8656 Bunkyo-ku, Japan
tt67055@mail.ecc.u-tokyo.ac.jp

Jeffrey Tubbs

Arup, 1500 West Park, Suite 180,
01581 Westborough, USA
jeff.tubbs@arup.com

Juliette Venel

Laboratoire de Mathématique,
Université Paris Sud, Bâtiment 425,
91405 Orsay, France
juliette.venel@math.u-psud.fr

Peter Vortisch

PTV AG, Stumpfstr. 1,
76131 Karlsruhe, Germany
peter.vortisch@ptv.de

Nathalie Waldau

Ingenieurbüro Waldau, Sicken-
berggasse 13/3, 1190 Wien, Austria
office@ibw-wien.at

Jaroslav Was

AGH University of Sciences and
Technology, Al. Mickiewicza 30,
30-059 Krakow, Poland
jarek@agh.edu.pl

Nicolas Waterson

Mott MacDonald, St. Anne House,
20-26 Wellesley Road, CR92UL
Croydon, Surrey, United Kingdom
Nicholas.Waterson@mottmac.com

Yan Fang Wei

Shanghai Institute of Applied Math-
ematics and Mechanics, Shanghai
University, No. 149, Yangchang
Road, 200072 Shanghai, China
yanfangwei2007@hotmail.com

Andreas Winkens

Bergische Universität Wuppertal,
Baustofftechnologie und Brand-
schutz, Pauluskirchstr. 11,
42285 Wuppertal, Germany
winkens@uni-wuppertal.de

Christian Wittenzellner

AZT Risk & Technology GmbH,
Krausstr. 22, 85737 Ismaning,
Germany
christian.wittenzellner@
allianz.com

Gabriel Wurzer

TU Vienna, Treitlstr. 3/1,
1040 Vienna, Austria
wurzer@iemar.tuwien.ac.at

Yu Xue

College of Physical Science and
Engineering, Guangxi University,
530004 Nanning, China
yuxuegxu@gxu.edu.cn

Daichi Yanagisawa

The University of Tokyo, 7-3-1,
Hongo, 113-8656 Bunkyo-ku, Japan
tt66421@mail.ecc.u-tokyo.ac.jp

Takumi Yoshida

Nagoya Institute of Technology,
Gokiso-cho, Showa-ku,
466-8555 Nagoya City, Japan
sinsei_1384@hotmail.co.jp

Wei Zhu

Eindhoven University of Technology,
Vertigo 08.16, Den Dolech 2,
Postbus 513, 5600 MB Eindhoven,
The Netherlands
w.zhu@tue.nl

Xiaolei Zhu

School of Traffic and Transportation
Engineering, TongJi University,
CaoAn Road #4800, Campus
JiaDing, 201804 Shanghai, China
zouxiaolei@mail.tongji.edu.cn